BNL-107603-2015

RIKEN/RBRC Workshop
Multi-Hadron and Nonlocal Matrix Elements in Lattice QCD
February 5-6, 2015

Proceedings of RIKEN BNL Research Center Workshop

Volume 120

RBRC
RIKEN BNL Research Center

DISCLAIMER

This work was prepared as an account of work sponsored by an agency of the United States Government. Neither the United States Government nor any agency thereof, nor any of their employees, nor any of their contractors, subcontractors or their employees, makes any warranty, express or implied, or assumes any legal liability or responsibility for the accuracy, completeness, or any third party's use or the results of such use of any information, apparatus, product, or process disclosed, or represents that its use would not infringe privately owned rights. Reference herein to any specific commercial product, process, or service by trade name, trademark, manufacturer, or otherwise, does not necessarily constitute or imply its endorsement, recommendation, or favoring by the United States Government or any agency thereof or its contractors or subcontractors. The views and opinions of authors expressed herein do not necessarily state or reflect those of the United States Government or any agency thereof.

Notice: This manuscript has been authored by employees of Brookhaven Science Associates, LLC under Contract No. DE-SC0012704 with the U.S. Department of Energy. The publisher by accepting the manuscript for publication acknowledges that the United States Government retains a non-exclusive, paid-up, irrevocable, world-wide license to publish or reproduce the published form of this manuscript, or allow others to do so, for United States Government purposes.

Preface to the Series

The RIKEN BNL Research Center (RBRC) was established in 1997 at Brookhaven National Laboratory.* RBRC is funded by "Rikagaku Kenkyosho" (RIKEN, The Institute of Physical and Chemical Research) in Japan and the United States Department of Energy's Office of Science.

A Memorandum of Understanding between RIKEN and BNL, initiated in 1997, has been renewed in 2002, 2007 and 2012.

RBRC is dedicated to the study of strong interactions, including spin physics, lattice QCD and relativistic heavy ion physics through the nurturing of new generations of young physicists. The RBRC founding Director T.D. Lee and the second Director N. P. Samios conceived and implemented this vision, which has been maintained and further developed down to the present day.

The RBRC research program has theory, lattice gauge computing and high-energy experimental nuclear physics components. Recently, an astrophysics/cosmology component has been added. The RBRC Theory, Computing and Experimental Groups presently comprise 48 researchers. Positions include full-time RBRC Fellows, half-time joint RHIC Physics Fellows and full-time postdoctoral Research Associates. The RHIC Physics Fellows hold joint appointments with RHIC and other institutions, where they have tenure track positions. To date, RBRC has over 101 graduates (Fellows and Research Associates) of whom approximately 67 have already attained tenure at major research institutions worldwide.

In 2001 a RIKEN Spin Program (RSP) was initiated at RBRC. The research staff comprises joint appointments in theory and experiment between RBRC and RIKEN, including RSP Researchers, RSP Research Associates and Young Researchers. They are mentored by senior RBRC Scientists. A number of RIKEN junior Research Associates and Visiting Scientists also contribute to the program.

In support of the lattice gauge program at RBRC and elsewhere, a series of high-performance computers has been designed and built by researchers from Columbia University, IBM, BNL, RBRC and University of Edinburgh, with the U.S. DOE Office of Science providing infrastructure support at BNL. To date, the steps in this program have been: QCDSP (0.6 TFlops, 1998-2006), which was awarded the Gordon Bell Prize for price performance in 1998; QCDOC (10 TFlops, 2005-2012); QCDCQ (600 TFlops, 2011-present). Recent $K^{\circ} \rightarrow \pi\pi$ results were awarded the Ken Wilson Prize in 2012.

A very important activity of RBRC is its active Workshop series on Strong Interaction Physics, with each workshop focused on a specific physics problem. A list of proceedings of all past Workshops can be found on the RBRC website (http://www.bnl.gov/riken/proceedings.php). The talks from many of the recent workshops can be accessed from the link at the top of the Proceedings page. To date, about 119 Workshops have taken place; the full proceedings of most of the workshops from 2005 – 2014 are available at this link.

S. H. Aronson, Director
March 2015

* Work Performed under the auspices of U.S.D.O.E. Contract No. DE-SC0012704

Introduction

Nonperturbative QCD calculations of hadronic matrix elements are needed to understand the structure of the matter in our universe and to search for physics beyond the Standard Model. Numerical lattice gauge theory is uniquely suited for this task and has reached a remarkable level of precision. However, the types of observables that are accessible in a straightforward way are limited because lattice calculations are performed with imaginary time. Traditionally, lattice QCD determinations of hadronic matrix elements have been restricted to situations with at most one stable hadron in the initial and final states, and with a single insertion of a local current. This situation has been changing recently thanks to theoretical breakthroughs and pioneering numerical studies of new observables. At this workshop, the latest developments concerning multi-hadron systems and nonlocal matrix elements in lattice QCD were discussed:

- Lüscher's quantization condition relates the energy spectrum of two interacting particles in a finite volume to the scattering phase shifts. At this workshop, generalizations of Lüscher's quantization condition to three-particle systems, and to two-particle systems with long-range QED interactions were presented.

- Advanced numerical lattice QCD studies of hadronic resonances using the Lüscher method were shown, including coupled-channel scattering and near-threshold resonances.

- The Lellouch-Lüscher formula relates two-hadron matrix elements computed in a finite volume to the infinite-volume matrix elements. This workshop included presentations of the latest numerical lattice QCD calculations of the nonleptonic weak decay K ® π π, as well as new theoretical results extending the Lellouch-Lüscher formula to general multichannel 1 ® 2 transition matrix elements.

- Novel methods allowing the direct calculation of parton distribution functions in lattice QCD were discussed, and a one-loop calculation of the lattice-to-continuum matching required for these methods was presented.

- Lattice QCD calculations of nonlocal matrix elements relevant for rare kaon decays and for the K_L-K_S mass difference were shown. The inclusion of QED corrections in weak decays was discussed. Results from a new method for computing the hadronic light-by-light contribution to the muon anomalous magnetic moment were shown.

- Calculations of the binding energies and magnetic moments of light nuclei directly from lattice QCD were presented. The theoretical foundations of a potential-based method for studying multi-hadron interactions on the lattice were discussed, and an application of this method to charmed tetraquarks was shown.

Contents

Presentations:

Andria Agadjanov .....*Resonance form factors in lattice QCD*

Ziyuan Bai .....*Lattice QCD calculation of long distance contribution to epsilon_K*

Silas Beane.....*Charged particles scattering in a finite volume*

Raul Briceno .....*Hadronic transition processes in a finite volume*

Norman Christ .....*Computing the K_L-K_S mass difference using lattice QCD*

Zohreh Davoudi .....*Single-hadron states in a finite volume in the presence of QED interactions*

William Detmold .....*Nuclear matrix elements*

Takumi Doi .....*HAL QCD method for hadron interactions on the lattice*

Michael Engelhardt.....*Aspects of Lattice QCD calculations of transverse momentum-dependent parton distributions (TMDs)*

Xu Feng .....*K -> pi nu nubar decays on the lattice*

Anthony Francis .....*Ongoing search for the H-dibaryon in two-flavor lattice QCD*

Maxwell Hansen.....*Three particles in a box: Mapping the finite-volume spectrum to the S-matrix*

Yoichi Ikeda .....*Structure of charmed tetraquarks from LQCD*

Tomomi Ishikawa .....*Perturbative matching for quasi-PDFs between continuum and lattice*

Naruhito Ishizuka .....*K -> pi pi decay amplitudes from improved Wilson fermion*

Luchang Jin .....*Lattice calculation of the hadronic light by light contributions to the muon anomalous magnetic moment*

Christopher Kelly .....*Progress towards an ab initio, Standard Model calculation of direct CP-violation in K decays*

Daniel Mohler .....*Charmed-strange and bottom-strange positive parity mesons from Lattice QCD*

Antonin Portelli .....*K -> pi l+ l- decays on the lattice*

Jianwei Qiu .....*Extract collinear parton distributions from lattice QCD calculations*

Christopher Sachrajda ....*QED corrections to hadronic processes in lattice QCD*

Stephen Sharpe.....*Finite volume quantization conditions for multiparticle states*

Christian Shultz .....*Excited meson radiative transition matrix elements using distillation*

David Wilson .....*Resonances in coupled-channel scattering from lattice QCD*

Takeshi Yamazaki .....*Light nuclei from lattice QCD*

Agenda

List of Registered Participants

Additional RIKEN BNL Research Center Proceeding Volumes

Presentations

Resonance form factors in lattice QCD

Andria Agadjanov, University of Bonn

Brookhaven, February 5, 2015

AA, V. Bernard, U.-G. Meißner, A. Rusetsky, Nucl. Phys. B 886 (2014)

Outline

- Introduction: the $\Delta N \gamma^*$ transition
- Motivation
- Goals, results
- Outlook: the $B \to K^*$

Introduction

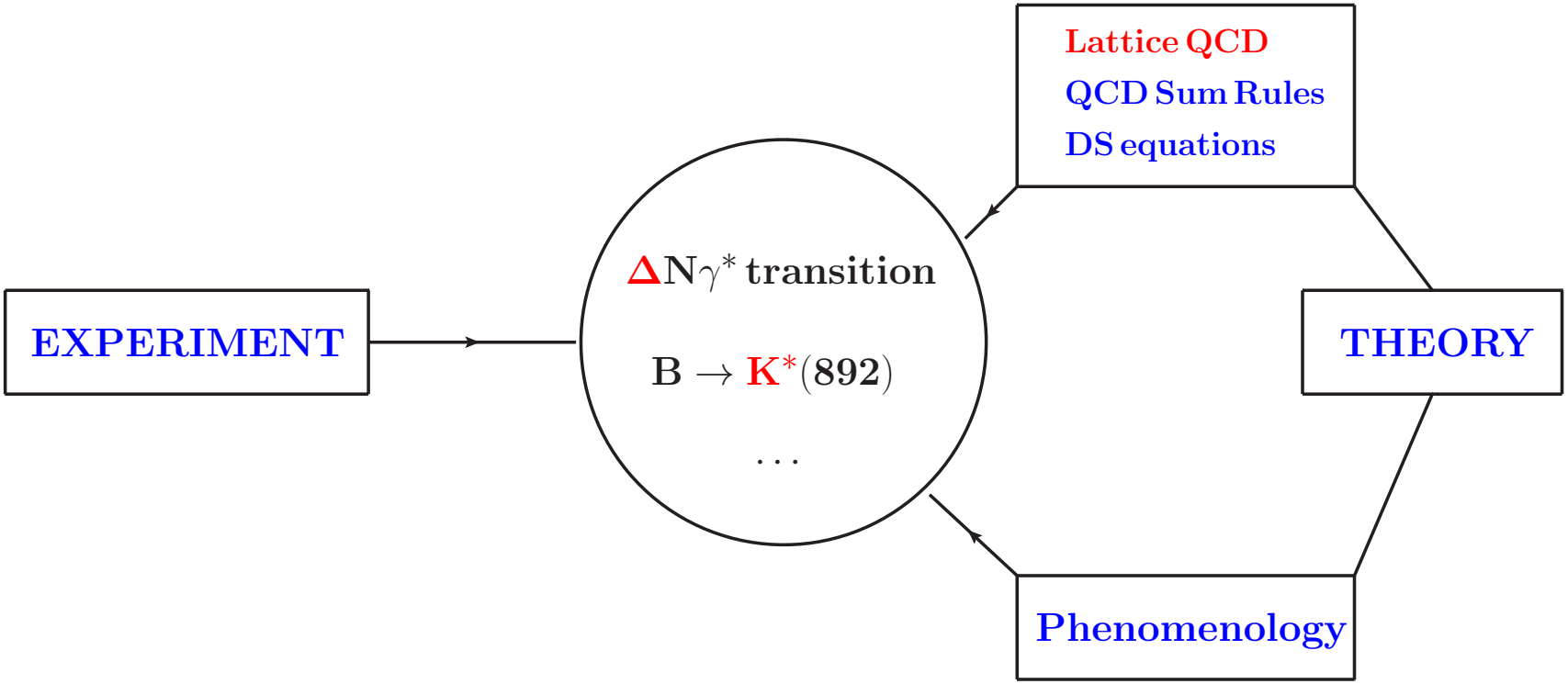

- $\gamma^* N \to \pi N$ near the $\Delta(1232)$: study of the hadron deformation
- $B \to K^*\gamma^*$, $B \to K^* l^+ l^-$ with $K^*(892) \to K\pi$: sensitive to NP

$\gamma^* N \to \Delta$

$$\gamma^* p \to \Delta^+(1232) \to p\pi^0 \quad (66\%)$$
$$\gamma^* p \to \Delta^+(1232) \to n\pi^+ \quad (33\%)$$
$$\gamma^* p \to \Delta^+(1232) \to p\gamma \quad (0.56\%)$$

$\hookrightarrow$ study of the de-excitation radiation pattern

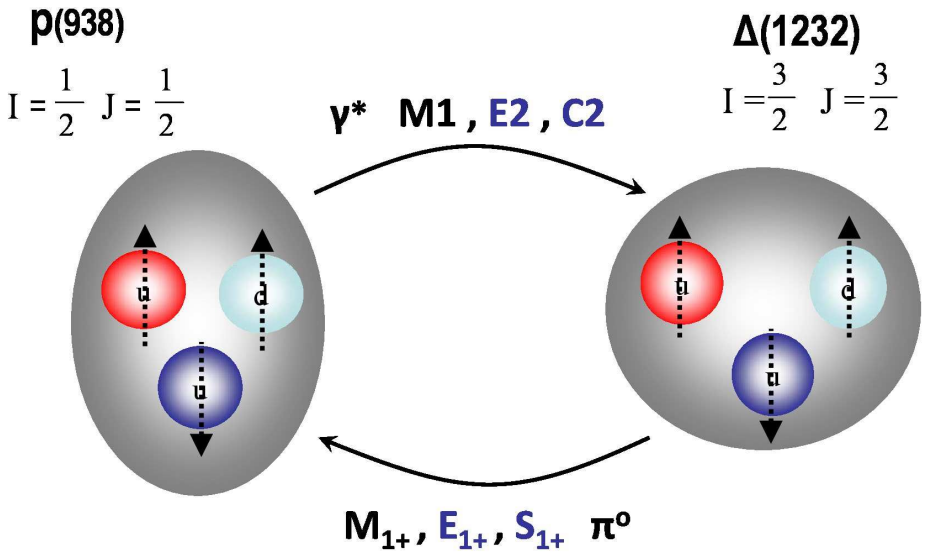

Spherical $\Rightarrow$ **M1**

Deformed $\Rightarrow$ **M1 , E2 , C2**

C. Alexandrou et al., Rev. Mod. Phys. **84** (2012) 1231

- The electromagnetic transition matrix element:

$$\langle \Delta(P,\lambda)|J_\mu(0)|N(Q,\epsilon)\rangle = \left(\frac{2}{3}\right)^{1/2} \bar{u}^\sigma(P,\lambda)\mathcal{O}_{\sigma\mu}u(Q,\epsilon)\,,$$

with the Lorentz-structure

$$\mathcal{O}_{\sigma\mu} = G_M(Q^2)K^{M1}_{\sigma\mu} + G_E(Q^2)K^{E2}_{\sigma\mu} + G_C(Q^2)K^{C2}_{\sigma\mu}$$

H. F. Jones and M. D. Scadron, Ann. Phys. **81** (1973) 1

$$\mathrm{EMR} \equiv \frac{\mathrm{Im}E_{1+}^{3/2}}{\mathrm{Im}M_{1+}^{3/2}} = -\frac{G_E(Q^2)}{G_M(Q^2)}, \quad \mathrm{CMR} \equiv \frac{\mathrm{Im}L_{1+}^{3/2}}{\mathrm{Im}M_{1+}^{3/2}} = -\frac{|\vec{Q}|}{2m_\Delta}\frac{G_C(Q^2)}{G_M(Q^2)}$$

$\hookrightarrow$ extracted from experiment calculated on the lattice $\hookleftarrow$

Experiment vs. theory

...notwithstanding its steady progress toward results with input parameters that approximate the real world, the numerical simulation of lattice-regularised QCD will not suffice. Approaches formulated in the continuum and inspired by, based upon, or connected directly with QCD are necessary.

C. D. Roberts arXiv:1501.06581 (2015)

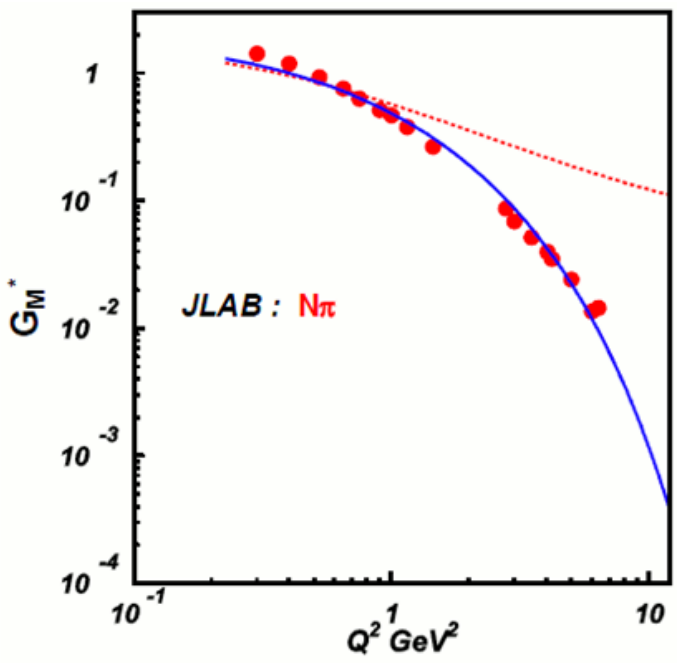

- $\gamma^* N \to \Delta$: infrared evolution of QCDs β-function

The values of EMR and CMR

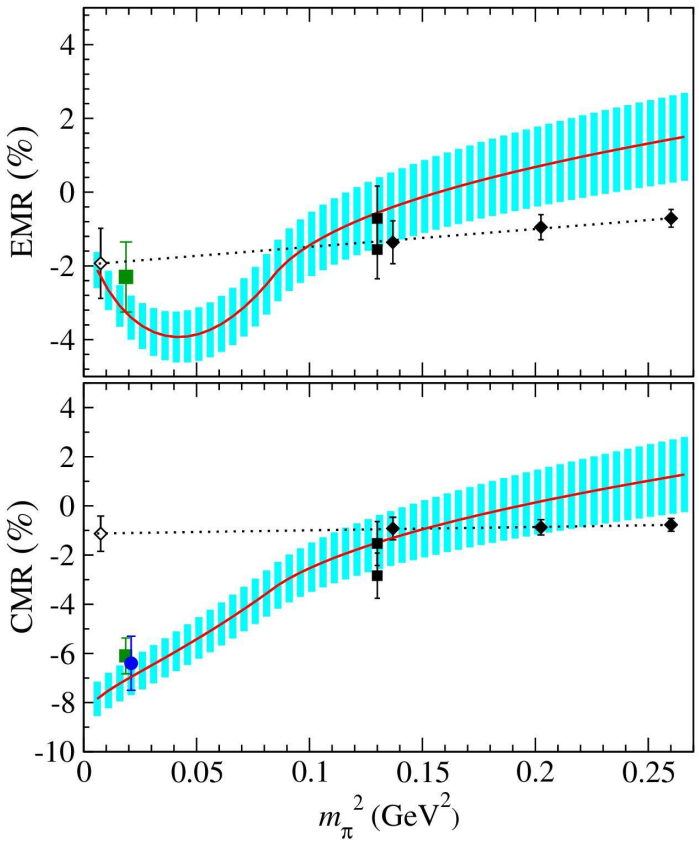

χEFT extrapolation of lattice results to the physical pion mass

V. Pascalutsa, M. Vanderhaeghen, Phys. Rev. D **73** (2006) 034003

- The Δ is treated as a stable particle!

Motivation

The largest conceptual question as we enter the chiral regime in full QCD, is how to fully incorporate the physical effect of the decay of the Δ into a pion and nucleon on the transition form factors.

C. Alexandrou et al., Phys. Rev. D **77** (2008) 085012

$\hookrightarrow$ seminal work on $K \to \pi\pi$ by

L. Lellouch and M. Lüscher, Commun.Math.Phys. **219**, 31 (2001)

• generalization of Lellouch-Lüscher method for matrix elements, involving resonances is needed

The framework: non-relativistic EFT

- Basic properties of the theory:
  - ▷ the total number of heavy particles is conserved
  - ▷ manifestly Lorentz-invariant formulation is possible
  - ▷ the theory is matched to the full QFT (e.g., ChPT).

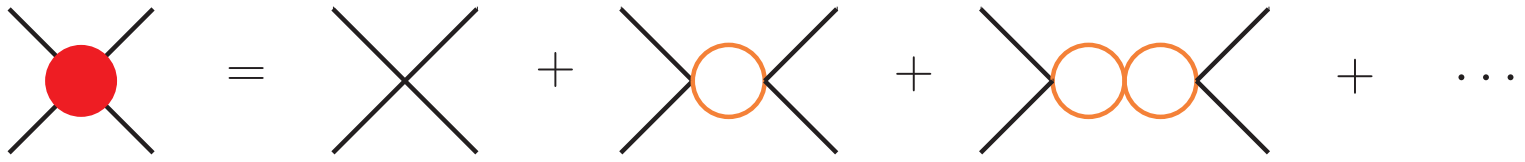

Bubble-chain diagrams

$$T \propto 1 + cJ + c^2 J^2 + \cdots = \frac{1}{1 - cJ}$$

- A bridge: finite volume spectrum $\leftrightarrow$ scattering sector

G. Colangelo, J. Gasser, B. Kubis, A. Rusetsky, Phys. Lett. B **638** (2006) 187

J. Gasser, B. Kubis, A. Rusetsky, Nucl. Phys. B **850** (2011) 96

Goals, results

- Previous work:

  D. Hoja, U.-G. Meißner, A. Rusetsky, JHEP 1004 (2010) 050

  V. Bernard, D. Hoja, U.-G. Meißner, A. Rusetsky, JHEP 1209 (2012) 023

  $\hookrightarrow$ scalar resonance form factor in the external scalar field (analog: $\Delta\Delta\gamma^*$)

- The $\Delta N\gamma^*$ transition:

  ▷ inclusion of *spin*;

  ▷ generalization to *transition* form factors.

Extraction of the form factors

- on the real energy axis $\rightarrow$ model-dependent

I. G. Aznauryan, V. D. Burkert and T. -S. H. Lee, arXiv:0810.099

D. Drechsel,O. Hanstein,S.S. Kamalov,L. Tiator, Nucl. Phys. A 645 (1999) 145

- at the resonance pole $\rightarrow$ *process-independent*

  ▷ definition of the resonance matrix element:

$$\langle P, \text{resonance}|J(0)|Q, \text{stable}\rangle = \lim_{P^2 \to s_R,\, Q^2 \to M^2} Z_R^{-1/2} Z^{-1/2} (s_R - P^2)(M^2 - Q^2) F(P, Q)$$

$\hookrightarrow$ analytic continuation to the pole is unavoidable

S. Mandelstam, Proc. Roy. Soc. Lond. A **233** (1955) 248.

- infinitely narrow resonances $\rightarrow$ identical results

$\hookrightarrow$ however, discrepancies in the results could be sizable:

R. L. Workman, L. Tiator and A. Sarantsev, Phys. Rev. C **87** (2013) 6, 068201

Kinematics

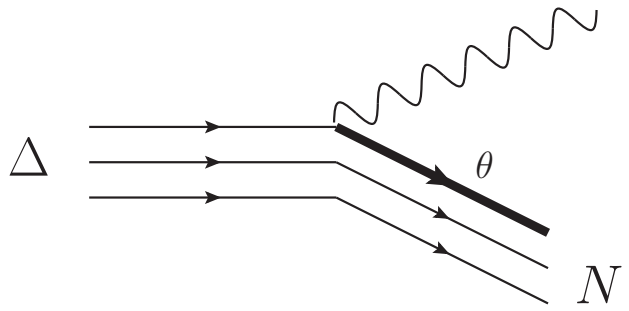

- The Δ is at rest $\mathbf{P} = 0$ and nucleon momentum $\mathbf{Q}$ along 3-axis.
- To perform the fit (*see below*): vary p, while $|\mathbf{Q}|$ fixed.
  - ▷ (partially) twisted boundary conditions;

  ↪ nucleon form factors: M. Göckeler et al., PoS LATTICE **2008** (2008) 138
  - ▷ asymmetric boxes $L \times L \times L'$. Alexandru, Döring
- *Note*: in practice, the case $\mathbf{P} \neq 0$ could be preferable.

Spin

- Spin-projecting local operators:

$$
\begin{aligned}
G_2 \qquad \mathcal{O}_{3/2}(t) &= \sum_{\mathbf{x}} \frac{1}{2}(1+\Sigma_3)\frac{1}{2}(1+\gamma_4)\frac{1}{\sqrt{2}}\left(\mathcal{O}^1(\mathbf{x},t) - i\Sigma_3\mathcal{O}^2(\mathbf{x},t)\right), \\
G_2 \qquad \mathcal{O}_{1/2}(t) &= \sum_{\mathbf{x}} \frac{1}{2}(1-\Sigma_3)\frac{1}{2}(1+\gamma_4)\frac{1}{\sqrt{2}}\left(\mathcal{O}^1(\mathbf{x},t) + i\Sigma_3\mathcal{O}^2(\mathbf{x},t)\right), \\
G_1 \qquad \tilde{\mathcal{O}}_{1/2}(t) &= \sum_{\mathbf{x}} \frac{1}{2}(1+\Sigma_3)\frac{1}{2}(1+\gamma_4)\mathcal{O}^3(\mathbf{x},t), \\
\bar{\psi}^{\mathbf{Q}}_{\pm 1/2}(t) &= \sum_{\mathbf{x}} e^{i\mathbf{Q}\mathbf{x}}\bar{\psi}(\mathbf{x},t)\frac{1}{2}(1\pm\Sigma_3)\frac{1}{2}(1+\gamma_4), \qquad \Sigma_3 = \mathrm{diag}(\sigma_3,\sigma_3)
\end{aligned}
$$

- Irreps G_1, G_2: no $S-P$–wave mixing (the P_{31} wave is small)

$$
p\cot\delta(p) = \frac{2}{\sqrt{\pi}L}\left\{\hat{Z}_{00}(1;q^2) \pm \frac{1}{\sqrt{5}q^2}\hat{Z}_{20}(1;q^2)\right\} \equiv -p\cot\phi(q), \qquad q = \frac{pL}{2\pi}
$$

$\hookrightarrow$ Lüscher eq. for the P_{33} wave: M. Göckeler, Phys. Rev. D **86** (2012) 094513

Lattice correlators

- The two-point functions:

$$
\begin{aligned}
\tilde{D}_{1/2}(t) &= \mathrm{Tr}\,\langle 0|\tilde{\mathcal{O}}_{1/2}(t)\bar{\tilde{\mathcal{O}}}_{1/2}(0)|0\rangle\,, \\
D_{1/2}(t) &= \mathrm{Tr}\,\langle 0|\mathcal{O}_{1/2}(t)\bar{\mathcal{O}}_{1/2}(0)|0\rangle\,, \\
D_{3/2}(t) &= \mathrm{Tr}\,\langle 0|\mathcal{O}_{3/2}(t)\bar{\mathcal{O}}_{3/2}(0)|0\rangle\,, \\
D^{\pm}_{\mathbf{Q}}(t) &= \mathrm{Tr}\,\langle 0|\psi^{\mathbf{Q}}_{\pm 1/2}(t)\bar{\psi}^{\mathbf{Q}}_{\pm 1/2}(0)|0\rangle.
\end{aligned}
$$

- The three-point functions:

$$
\begin{aligned}
\tilde{R}_{1/2}(t',t) &= \langle 0|\tilde{\mathcal{O}}_{1/2}(t')J^3(0)\bar{\psi}^{\mathbf{Q}}_{1/2}(t)|0\rangle\,, \\
R_{1/2}(t',t) &= \langle 0|\mathcal{O}_{1/2}(t')J^+(0)\bar{\psi}^{\mathbf{Q}}_{-1/2}(t)|0\rangle\,, \\
R_{3/2}(t',t) &= \langle 0|\mathcal{O}_{3/2}(t')J^+(0)\bar{\psi}^{\mathbf{Q}}_{1/2}(t)|0\rangle,
\end{aligned}
$$

where

$$
J^+(0) = \frac{1}{\sqrt{2}}\,(J^1(0) + iJ^2(0)).
$$

$\Longrightarrow$

- In the limit $t' \to +\infty$, $t \to -\infty$:

$$\mathcal{N}\frac{\mathrm{Tr}\,(\tilde{R}_{1/2}(t',t))}{\tilde{D}_{1/2}(t'-t)}\left(\frac{D^{+}_{\mathbf{Q}}(t')\tilde{D}_{1/2}(-t)\tilde{D}_{1/2}(t'-t)}{\tilde{D}_{1/2}(t')D^{+}_{\mathbf{Q}}(-t)D^{+}_{\mathbf{Q}}(t'-t)}\right)^{1/2} \quad \to \quad \langle 1/2|J^{3}(0)|1/2\rangle\,,$$

$$-\mathcal{N}\frac{\mathrm{Tr}\,(R_{1/2}(t',t))}{D_{1/2}(t'-t)}\left(\frac{D^{-}_{\mathbf{Q}}(t')D_{1/2}(-t)D_{1/2}(t'-t)}{D_{1/2}(t')D^{-}_{\mathbf{Q}}(-t)D^{-}_{\mathbf{Q}}(t'-t)}\right)^{1/2} \quad \to \quad \langle 1/2|J^{+}(0)|-1/2\rangle\,,$$

$$-\mathcal{N}\frac{\mathrm{Tr}\,(R_{3/2}(t',t))}{D_{3/2}(t'-t)}\left(\frac{D^{+}_{\mathbf{Q}}(t')D_{3/2}(-t)D_{3/2}(t'-t)}{D_{3/2}(t')D^{+}_{\mathbf{Q}}(-t)D^{+}_{\mathbf{Q}}(t'-t)}\right)^{1/2} \quad \to \quad \langle 3/2|J^{+}(0)|1/2\rangle,$$

where $\mathcal{N} = (4E\sqrt{m_N^2 + \mathbf{Q}^2})^{1/2}$.

$\|$

F_i, i=1, 2, 3

$\Rightarrow$ three $\Delta N\gamma^*$ form factors are separately projected out.

$\hookrightarrow$ similar procedure can be applied to fields with other spin

$\Delta N\gamma^*$ vertex

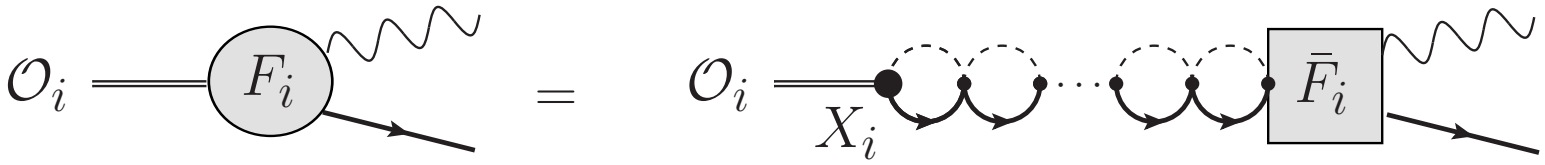

- ▷ The $F_i = F_i(p_n, |\mathbf{Q}|)$, i=1, 2, 3 $\rightarrow$ G_M, G_E, G_C form factors, are measured on *the lattice*.
- ▷ The $\bar{F}_i(p_n, |\mathbf{Q}|)$ are *volume-independent* irreducible amplitudes.

$$|\bar{F}_i(p_n, |\mathbf{Q}|)| = \underbrace{V^{1/2}\left(\frac{\cos^2\delta(p_n)}{|\delta'(p_n)+\phi'(q_n)|}\frac{p_n^2}{2\pi}\right)^{-1/2}}_{\text{LL factor}} |F_i(p_n, |\mathbf{Q}|)|$$

Real axis

- The $\bar{F}_i$ are related to the $\gamma^* N \to \pi N$ multipole amplitudes

$$\mathcal{A}_i(p, |\mathbf{Q}|) = e^{i\delta(p)} \cos\delta(p)\, \bar{F}_i(p, |\mathbf{Q}|)$$

$\hookrightarrow$ Watson's theorem

- $\mathcal{A}_i(p_A, |\mathbf{Q}|) = 0$ at $\delta(p_A) = \pi/2$? No!

$$\mathcal{A}_i(p, |\mathbf{Q}|) = \underbrace{\frac{e^{i\delta(p)}}{p^3} \sin\delta(p)}_{\text{potential}} \underbrace{p^3 \cot\delta(p)}_{\text{zero at } p^2 = p_A^2} \underbrace{\bar{F}_i(p, |\mathbf{Q}|)}_{\text{divereges at } p^2 = p_A^2}$$

$$\mathcal{A}_i(p_n, |\mathbf{Q}|) = e^{i\delta(p_n)}\, V^{1/2} \left(\frac{1}{|\delta'(p_n) + \phi'(q_n)|} \frac{p_n^2}{2\pi} \right)^{-1/2} |F_i(p_n, |\mathbf{Q}|)|$$

$\hookrightarrow$ LL equation for the photoproduction amplitude in the elastic region

- The $\mathcal{A}_i \leftrightarrow$ multipoles:

$$\tilde{\mathcal{A}}_{1/2} = -16\pi i E \sqrt{2} \frac{\sqrt{Q^2}}{|\mathbf{Q}|} S_{1+},$$
$$\mathcal{A}_{1/2} = -\frac{1}{2}(3E_{1+} + M_{1+})(-16\pi i E),$$
$$\mathcal{A}_{3/2} = \frac{\sqrt{3}}{2}(E_{1+} - M_{1+})(-16\pi i E).$$

- The narrow width approximation:

$$|\mathrm{Im}\, \mathcal{A}_i(p_A, |\mathbf{Q}|)| = \sqrt{\frac{8\pi}{p_A \Gamma}} |F_i^A(p_A, |\mathbf{Q}|)|,$$

$p = p_A$ - Breit-Wigner pole, $F_i^A(p_A, |\mathbf{Q}|) \to \Delta N \gamma^*$ form factors.

I. G. Aznauryan, V. D. Burkert and T. -S. H. Lee, arXiv:0810.099

Analytic continuation

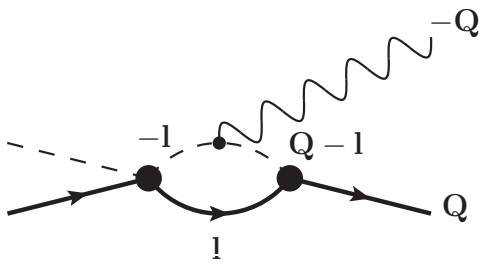

A potentially dangerous diagram in the $\bar{F}_i$

$$I = \frac{1}{V}\sum_{\mathbf{l}} \frac{1}{8w_1(\mathbf{l})w_2(-\mathbf{l})w_2(\mathbf{Q}-\mathbf{l})} \frac{1}{(w_1(\mathbf{l})+w_2(-\mathbf{l})-E_n)(w_1(\mathbf{l})+w_2(\mathbf{Q}-\mathbf{l})-Q^0)}$$

- After some transformations $\Rightarrow$

$$I = \underbrace{\frac{1}{V}\sum_{\mathbf{l}} \frac{1}{2E_n(\mathbf{l}^2-p_n^2)}}_{\propto\, p_n \cot\delta(p_n)} \frac{1}{2}\underbrace{\int_{-1}^{1} dy \frac{1}{2\hat{w}_2(\hat{w}_1+\hat{w}_2-Q^0)}}_{\text{polynomial in } p_n^2}$$

$$\hat{w}_1 = \sqrt{m_N^2+p_n^2}\,, \qquad \hat{w}_2 = \sqrt{M_\pi^2+p_n^2+\mathbf{Q}^2-2|\mathbf{Q}|p_n y}\,.$$

$\Rightarrow$ $p^2\, I$ is a low-energy polynomial in p^2

Complex plane

- The $\Delta N\gamma^*$ matrix elements, evaluated at the pole $p = p_R$:

$$F_i^R(p_R, |\mathbf{Q}|) = Z_R^{1/2}\, \bar{F}_i(p_R, |\mathbf{Q}|),$$

$$Z_R = \left(\frac{p_R}{8\pi E_R}\right)^2 \left(\frac{16\pi p_R^3 E_R^3}{w_{1R} w_{2R}(2p_R h'(p_R^2) + 3ip_R^2)}\right), \quad w_{iR} = \sqrt{m_i^2 + p_R^2},$$

$$p^3 \cot\delta(p) \doteq h(p^2) = -\frac{1}{a} + \frac{1}{2} rp^2 + \cdots, \quad h(p_R^2) = -ip_R^3$$

▷ The narrow width approximation ($p_R \to p_n$):

$$F_i^R(p_R, |\mathbf{Q}|) \to F_i^A(p_A, |\mathbf{Q}|) \quad \text{as} \quad p_R \to p_A\,!$$

$$F_i^R(p_n, |\mathbf{Q}|) = V^{1/2}\left(\frac{E_n}{2w_{1n}w_{2n}}\right)^{1/2} F_i(p_n, |\mathbf{Q}|)$$

$\hookrightarrow$ proper normalization of states

Prescription on the lattice

- Measure the $F_i(p, |\mathbf{Q}|)$ at different values of p with $|\mathbf{Q}|$ fixed.
- Real energy: extract the multipole amplitudes (*see above*).
- Extraction of the matrix elements at the resonance pole:
  1. fit the functions $p^3 \cot\delta(p)\, \bar{F}_i(p, |\mathbf{Q}|)$

$$p^3 \cot\delta(p)\, \bar{F}_i(p, |\mathbf{Q}|) = A_i(|\mathbf{Q}|) + p^2 B_i(|\mathbf{Q}|) + \cdots$$

  2. evaluate the resonance matrix elements by substitution

$$F_i^R(p_R, |\mathbf{Q}|) = i\, p_R^{-3}\, Z_R^{1/2} (A_i(|\mathbf{Q}|) + p_R^2 B_i(|\mathbf{Q}|) + \cdots)\,.$$

- No finite fixed points $\Rightarrow$ easier to measure than $\Delta\Delta\gamma^*$ vertex

$B \to K^*$ transitions

- A problem: long distance contributions.

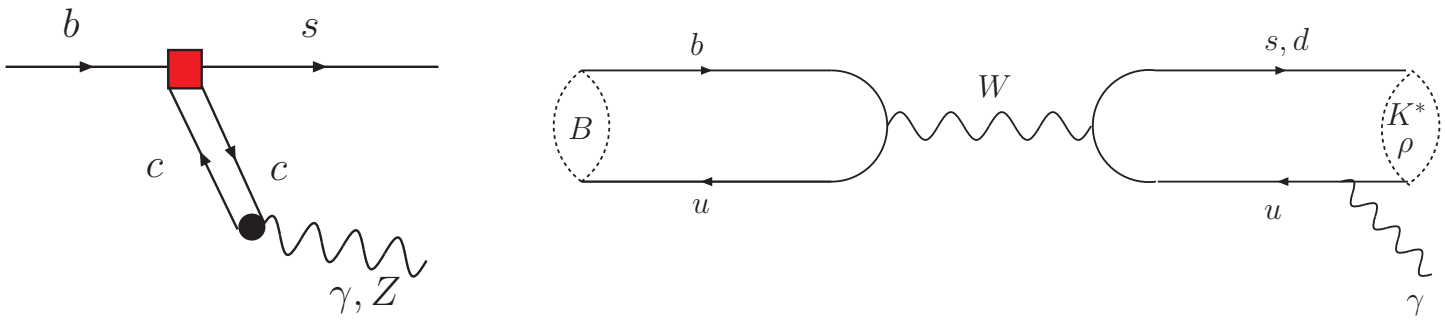

- Recent lattice measurement:

R. R. Horgan, Z. Liu, S. Meinel, M. Wingate, Phys. Rev. D **89**, 094501 (2014)

$\hookrightarrow$ consistent with LCSR determinations

- Related work: multichannel LL equation, kinematics.

R. A. Briceño, M.T. Hansen, A. Walker-Loud, arXiv:1406.5965 (2014)

Outlook

- Rigorous physical analysis of the problem.
- Extraction of the matrix elements at the pole: two-channel case.

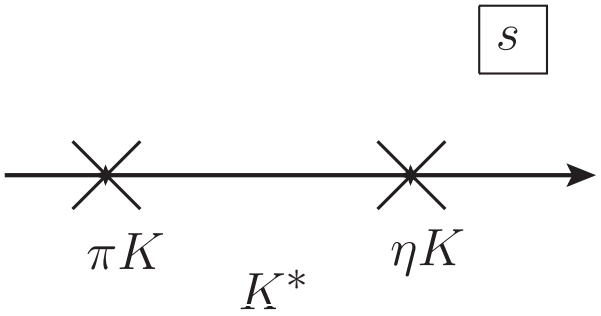

Thank you!

Finite fixed points ($\Delta\Delta\gamma^*$,...)

- The corresponding integral I: V. Bernard, et. al., JHEP 1209 (2012) 023

$$I = I_\infty + \frac{1}{32\pi E p}\left(1+\cot^2\delta(p)\right)\eta\phi'(\eta)\Big)\Big|_{p=p_n}, \quad \eta = \frac{pL}{2\pi}$$

- $p \to p_R$: $\quad Z_{00}(1;\eta_R^2) + i\pi^{3/2}\eta_R = 0 \to \exists\ \eta_R : |\mathrm{Im}\,\eta_R| < \infty$

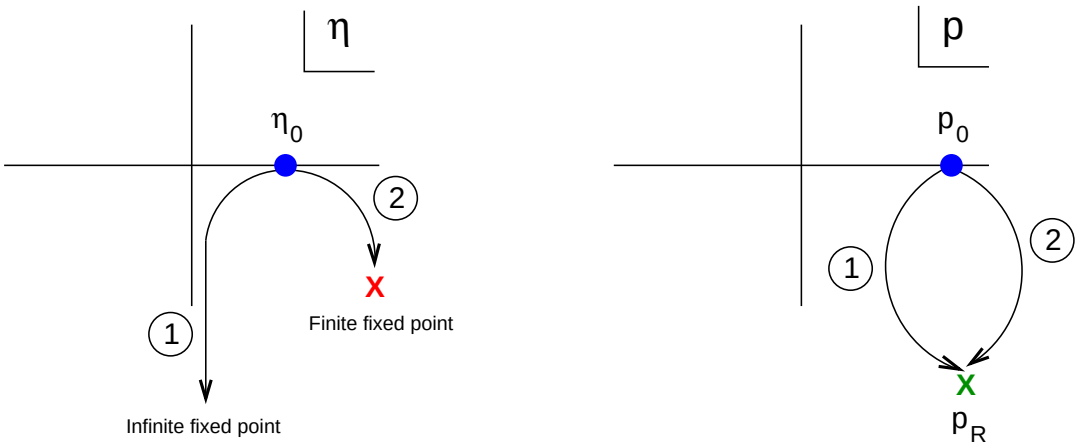

- Now, $\cot\phi(\eta)+i \propto \eta - \eta_R$ and $\phi(\eta) \propto \ln(\eta - \eta_R) \Rightarrow$

$$(\cot\phi(\eta) + i)\phi'(\eta) \to \mathrm{const} \neq 0$$

- Solution: perform the measurement at two energy levels

Lattice QCD calculation of long distance contribution to ϵ_K

Ziyuan Bai

Columbia University
RBC and UKQCD collaboration

February 5, 2015

Outline

- Introduction and theoretic background.
- Evaluation of Im $M_{0\bar{0}}$ and ϵ_K.
- Preliminary results and short distance correction.
- Outlook and summary.

Introduction

- One of the most important test of the Standard Model: CP violating observables ϵ_K, with the experimental value.

$$|\epsilon_K| = 2.228(11) \times 10^{-3}$$

- All previous attempt to calculate ϵ_K involve only the short distance part, (evaluating the kaon bag parameter B_K). The estimate of long distance contribution is a few percent, but not preceisely calculated.

- Previous method for the calculation of ΔM_K, with the technique of evaluating the space time integrated four point correlator, can also be used to calculate the long distance part of ϵ_K.

Introduction

- Our major challenge includes:

  1. different from the ΔM_K calculation, we focus on the CP violating part of kaon mixing. More operators and more diagrams to evaluate on lattice.

  2. In the ΔM_K calculation, all the diagrams are convergent. However, in our ϵ_K calculation, most of our four point diagrams have an $\log(a)$ ultraviolet divergence and therefore treatment of the divergence is required.

Theoretical background: $K^0 - \overline{K^0}$ mixing

- Let i, j stand for K^0 and $\overline{K^0}$, from the kaon mixing theory we obtain:
- dispersive part:

$$M_{ij} = \mathcal{P} \sum_{\alpha} \frac{\langle i|H_W|\alpha\rangle\langle\alpha|H_W|j\rangle}{m_K - E_\alpha}$$

- absorptive part:

$$\Gamma_{ij} = \sum_{\alpha} 2\pi \langle i|H_W|\alpha\rangle\langle\alpha|H_W|j\rangle \delta(m_K - E_\alpha)$$

- We have the ϵ_K:

$$\epsilon_K = \frac{exp(i\pi/4)}{\sqrt{2}\Delta M_K}(\mathrm{Im}\, M_{0\bar{0}} + 2\xi\, \mathrm{Re}\, M_{0\bar{0}})$$

$$\xi = \frac{\mathrm{Im}\, A_0}{\mathrm{Re}\, A_0}$$

Evaluation of $\mathrm{Im}\, M_{0\bar{0}}$

- Two types of diagram contribute to the $\Delta S = 2$, $K^0 - \overline{K^0}$ mixing process:

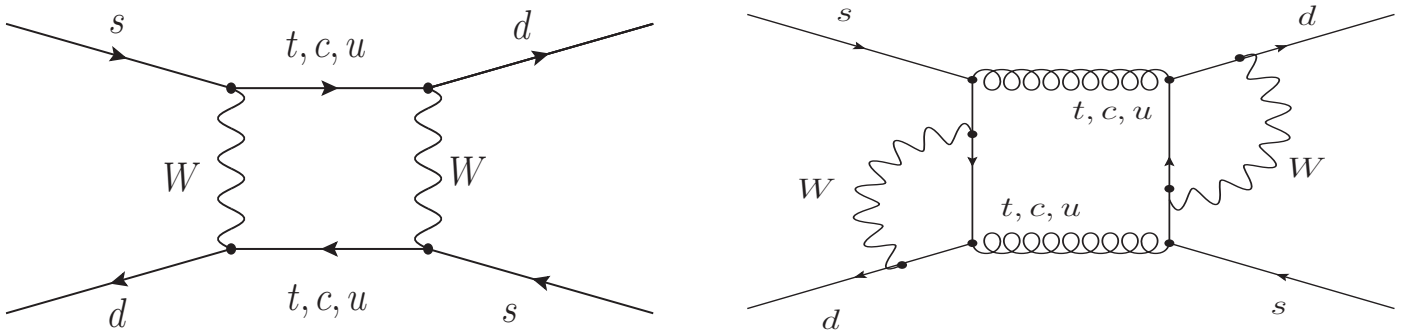

box topology disconnected topology

Figure : two types of $\Delta S = 2$ diagram

- Write the sum over three types of quark (u,c,t) into two terms ($\lambda_i = V_{id} V_{is}^*$, and $\lambda_u + \lambda_c + \lambda_t = 0$ has been used).
  The usual way is to eliminate up:

$$\sum_{i=u,c,t} \frac{\lambda_i \not{p}}{p^2 + m_i^2} = \lambda_c \left\{ \frac{\not{p}}{p^2 + m_c^2} - \frac{\not{p}}{p^2 + m_u^2} \right\} + \lambda_t \left\{ \frac{\not{p}}{p^2 + m_t^2} - \frac{\not{p}}{p^2 - m_u^2} \right\} \tag{1}$$

Evaluation of $\mathrm{Im}\, M_{0\bar{0}}$

- We choose to eliminate the **charm**.

$$\sum_{i=u,c,t} \frac{\lambda_i \not{p}}{p^2 + m_i^2} = \lambda_u \left\{ \frac{\not{p}}{p^2 + m_u^2} - \frac{\not{p}}{p^2 + m_c^2} \right\} + \lambda_t \left\{ \frac{\not{p}}{p^2 + m_t^2} - \frac{\not{p}}{p^2 - m_c^2} \right\} \tag{2}$$

- This choice has the following advantages:

1. Take the product of the two internal quark lines:
$\lambda_u \lambda_u$ term: has no imaginary parts (λ_u is real).
$\lambda_t \lambda_t$ term: pure perturbative.
Therefore, only focus on the $\lambda_u \lambda_t$ term.

2. Connected diagrams for the current-current operators don't have a pion intermediate state (all internal quark involve charm).

Evaluation of $\mathrm{Im}\, M_{0\bar{0}}$: $\Delta S = 1$ weak Hamiltonian

.

- We calculate $\langle \overline{K^0} | T H_W^{\Delta S=1}(x) H_W^{\Delta S=1}(y) | K^0 \rangle$ in four flavor theory. The $H_W^{\Delta S=1}$ is given by:

$$H_{eff}^{\Delta S=1} = \frac{G_F}{2} \left(\sum_{q,q'=u,c} V_{q's}^* V_{qd} \sum_{i=1,2} C_i Q_i^{q'q} - \lambda_t \sum_{i=3}^{6} C_i Q_i \right) \quad (3)$$

$$Q_1^{q',q} = \sum_{q,q'=u,c} V_{q',s}^* V_{q,d} (\bar{s}_i q_j')_{V-A} (\bar{q}_j d_i)_{V-A} \quad (4)$$

$$Q_2^{q',q} = \sum_{q,q'=u,c} V_{q',s}^* V_{q,d} (\bar{s}_i q_i')_{V-A} (\bar{q}_j d_j)_{V-A} \quad (5)$$

$$Q_3 = (\bar{s}_i d_i)_{V-A} \sum_{q=u,d,s,c} (\bar{q}_j q_j)_{V-A} \quad (6)$$

$$Q_4 = (\bar{s}_i d_j)_{V-A} \sum_{q=u,d,s,c} (\bar{q}_j q_i)_{V-A} \quad (7)$$

$$Q_5 = (\bar{s}_i d_i)_{V-A} \sum_{q=u,d,s,c} (\bar{q}_j q_j)_{V+A} \quad (8)$$

$$Q_6 = (\bar{s}_i d_j)_{V-A} \sum_{q=u,d,s,c} (\bar{q}_j q_i)_{V+A} \quad (9)$$

Evaluation of $\mathrm{Im}\, M_{0\bar{0}}$: 2nd order weak process.

- By multiplying two $H_W^{\Delta S=1}$, we get:

$$TH_W(x)H_W(y) = \frac{G_F^2}{2}\lambda_u\lambda_t \sum_{i=1}^{2}\sum_{j=1}^{6} C_i C_j Q_{i,j} \tag{10}$$

$$\begin{aligned} Q_{i,j} &= T\Big[2Q_i^{cc}(x)Q_j^{cc}(y) - Q_i^{uu}(x)Q_j^{cc}(y) - Q_i^{cc}(x)Q_j^{uu}(y) \\ &\quad -Q_i^{uc}(x)Q_j^{cu}(y) - Q_i^{cu}(x)Q_j^{uc}(y)\Big], (j=1,2) \\ Q_{i,j} &= T\left[(Q_i^{cc}(x) - Q_i^{uu}(y))Q_j(y) + Q_j(x)(Q_i^{cc}(y) - Q_i^{uu}(y))\right], (j=3,...,6) \end{aligned}$$

- The C_i are the Wilson Coefficient.
- As in the ΔM_K calculation, evaluate the integrated correlator:

$$\mathcal{A} = \frac{1}{2}\sum_{t_2=1}^{t_a}\sum_{t_1=t_a}^{t_b}\langle 0|T\left\{\overline{K}^0(t_f)H_W(t_2)H_W(t_1)\overline{K}^0(t_i)\right\}|0\rangle \tag{11}$$

Evaluation of $\mathrm{Im}\, M_{0\bar{0}}$

- After insertion of a complete set of intermediate states, we have:

$$\mathcal{A} = N_K^2 e^{-M_K(t_f - t_i)} \left\{ \sum_n \frac{\langle \bar{K}^0 | H_w | n \rangle \langle n | H_w | K^0 \rangle}{M_K - M_n} \left(-T + \frac{e^{(M_K - M_n)T} - 1}{M_K - M_n} \right) \right\} \quad (12)$$

- By doing a linear fit with T, we can find the $M_{0\bar{0}}$.
- Two different parts for the intermediate states $|n\rangle$:

  1. $E_n > m_K$: contribution to the exponential terms is highly suppressed, leaving only terms proportional to T, plus constant terms.

  2. $E_n < m_K$: their exponentially growing term should be identified and subtracted.

Evaluation of $\mathrm{Im}\, M_{0\bar{0}}$

- Four points diagrams:

type 1 type 2

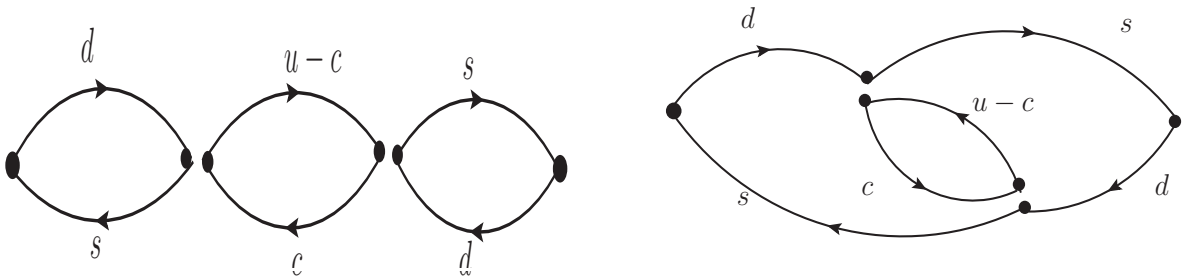

$i = 1, 2,\ j = 1, 2$

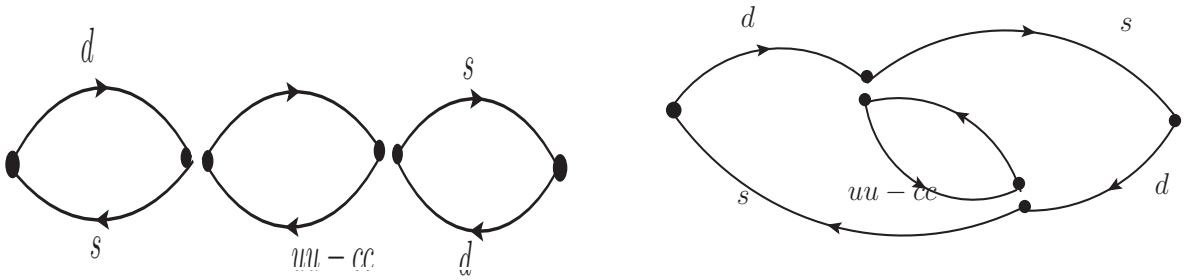

$i = 1, 2,\ j = 3, 4, 5, 6$

- In all these diagrams, the momentum in the internal quark lines are cutoff by a unphysical scale $\propto 1/a$ (inverse lattice spacing). The divergence piece should therefore be identified and corrected.

Evaluation of $\mathrm{Im}\, M_{0\bar{0}}$

- Four points diagrams.

type 3

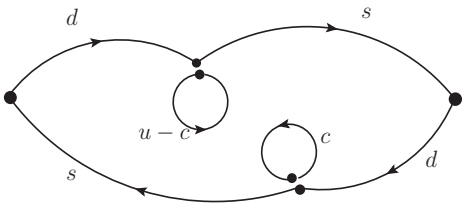

type 4

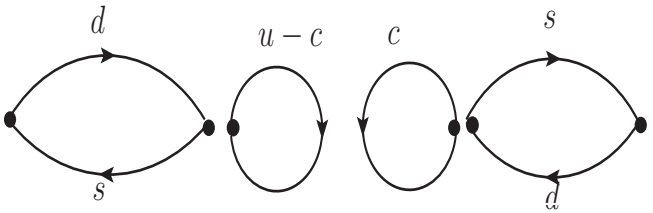

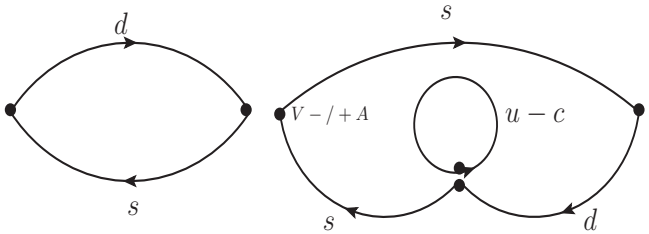

type 5

- Leave these to future work!

Simulation details

- $24^3 \times 64$ Iwasaki lattice, $m_\pi = 329$ MeV, and $m_K = 575$ MeV. quenched charm, $m_c = 0.363$ (949 MeV).
- Use wall source propagator for the kaon source and sink, and random volume source for the self loop.
- Use Lanczos algorithm with 300 eigenvectors.
- The main goal of this calculation:

  1. To understand the size of long distance contribution.

  2. Develop $\log(a)$ correction method.
- For the present analysis, we focus on type 1 and 2 diagrams :

  1. Smaller statistical noise.

  2. Short distance part easier to evaluate in continuum.

Short distance divergence

- For the case of ΔM_K calculation, our diagrams are convergent.

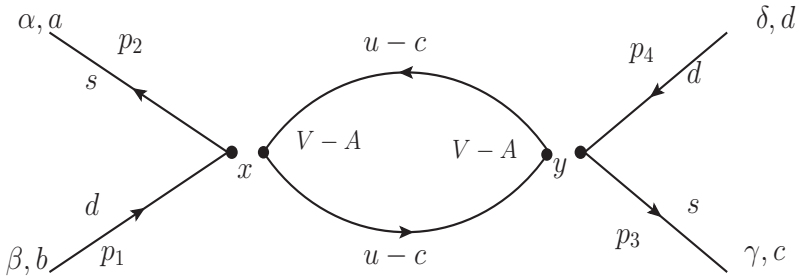

$$\int d^4p\gamma^\mu(1-\gamma^5)(\frac{\not p - m_u}{\not p^2+m_u^2} - \frac{\not p - m_c}{\not p^2+m_c^2})\gamma^\nu(1-\gamma^5)(\frac{\not p - m_u}{\not p^2+m_u^2} - \frac{\not p - m_c}{\not p^2+m_c^2}) \quad (13)$$

$$= \int d^4p\gamma^\mu(1-\gamma^5)\frac{\not p(m_c^2-m_u^2)}{(\not p^2+m_u^2)(\not p^2+m_c^2)}\gamma^\nu(1-\gamma^5)\frac{\not p(m_c^2-m_u^2)}{(\not p^2+m_u^2)(\not p^2+m_c^2)} \quad (14)$$

- We get this equation because the $V-A$ structure of the vertex made the m on the numerator disappear. And the final expression is not divergent when p is high.

Short distance divergence

- In the ϵ_K calculation, with both the two weak operator Q_1, Q_2, one of the internal quark lines is a single charm.

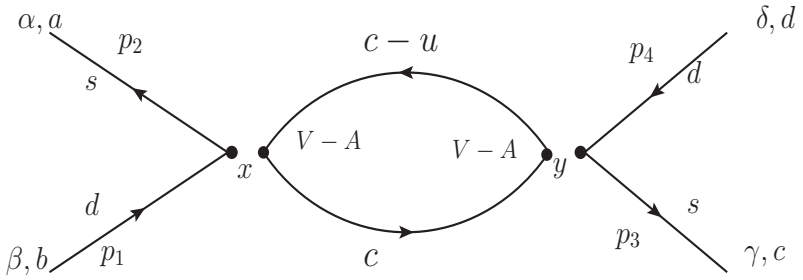

$$\int d^4p\gamma^\mu(1-\gamma^5)(\frac{\not p - m_c}{\not p^2+m_c^2} - \frac{\not p - m_u}{\not p^2+m_u^2})\gamma^\nu(1-\gamma^5)(\frac{\not p - m_c}{\not p^2+m_c^2}) \tag{15}$$

$$= \int d^4p\gamma^\mu(1-\gamma^5)\frac{\not p(m_c^2-m_u^2)}{(\not p^2+m_u^2)(\not p^2+m_c^2)}\gamma^\nu(1-\gamma^5)(\frac{\not p}{\not p^2+m_c^2}) \tag{16}$$

- Ultraviolet **logarithm** divergence, when the two weak vertex are close to each other. Cutoff by the unphysical scale $\propto 1/a$ on lattice. therefore the divergent part must be corrected.

Short distance divergence

- Gluonic penguin diagrams are also log divergent!

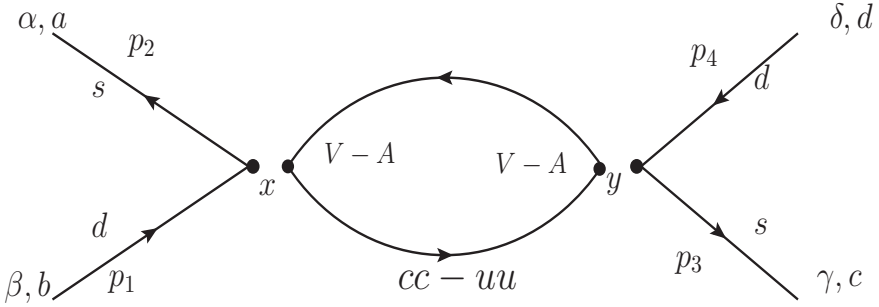

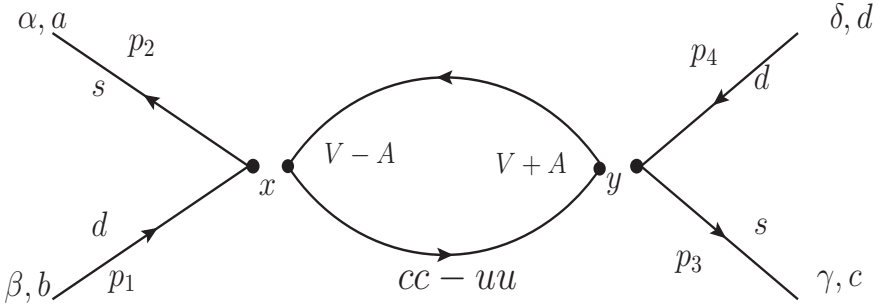

Short distance divergence: Rome-Southamption method

- Use a local operator $O_{LL} = (\bar{s}d)(\bar{s}d)$, to represent the short distance divergent part of $\langle \overline{K^0} | T H_W(x) H_W(y) | K^0 \rangle$
- Use Rome-Southamption method, work under momentum scale μ and find the coefficient $C_{i,j}^{lat}(\mu^2)$ that

$$\sum_{x,y} \langle \overline{K^0} | T Q_j(x) Q_j(y) | K^0 \rangle_{SD} = C_{i,j}^{lat}(\mu^2) \sum_x \langle \overline{K^0} | O_{LL}(x) | K^0 \rangle \tag{17}$$

- Then work in continuum under same μ, find the **physical** short distance part, which can be represented by a coefficient $C_{i,j}^{cont}(\mu^2)$. Finally, the correct correlator :

$$\mathcal{A} \to \mathcal{A} - C^{lat}(\mu^2) \sum_x \langle \overline{K^0} | O_{LL}(x) | K^0 \rangle + C^{cont}(\mu^2) \sum_x \langle \overline{K^0} | O_{LL}(x) | K^0 \rangle \tag{18}$$

Short distance divergence: Evaluation of C^{lat}

- To work out the coefficient C^{lat} on lattice, use the off-shell amputated Green function for our weak Hamiltonian and the O_{LL} operator, projected on the projection operator $P_{\alpha,\beta,\gamma,\delta}$:

$$\left(\Gamma^{amp}_{\alpha,\beta,\gamma,\delta}(p) - C^{lat}(\mu^2)\Gamma^{amp,SD}_{\alpha,\beta,\gamma,\delta}(p)\right) P_{\alpha,\beta,\gamma,\delta} = 0 \tag{19}$$

$$\Gamma_{\alpha\beta\gamma\delta}(p) = \langle s_\alpha(p_1)\bar{d}_\beta(p_2)\int d^4x_1 \int d^4x_2 H_W(x_1)H_W(x_2)s_\gamma(p_3)\bar{d}_\delta(p_4)\rangle. \tag{20}$$

$$\Gamma^{\mathrm{SD}}_{\alpha\beta\gamma\delta}(p) = \langle s_\alpha(p_1)\bar{d}_\beta(p_2)\int d^4x O_{LL}(x)s_\gamma(p_3)\bar{d}_\delta(p_4)\rangle. \tag{21}$$

- If the lattice momentum has relatively high scale, then the major contribution to $\Gamma_{\alpha\beta\gamma\delta}(p)$ is from short distance. Therefore C^{lat} can correctly represent the divergent part of our correlator.

Short distance divergence: Evaluation of C^{lat}

- choose momentum:
  $|p_1| = |p_2| = |p_3| = |p_4| = \mu, \quad |p_1 - p_2| = |p_3 - p_4| = \mu,$
  $p_1 + p_4 = p_2 + p_3$ (net momentum flow is 0).

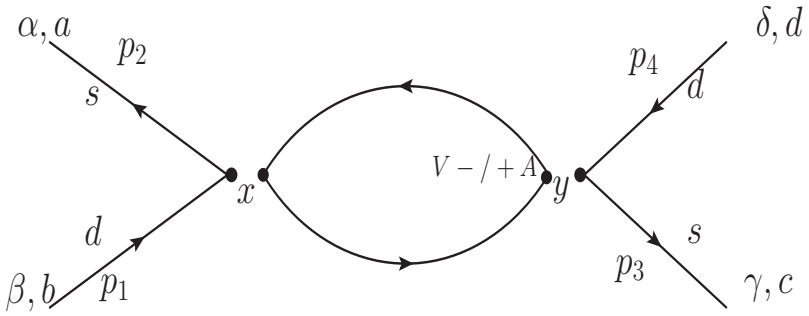

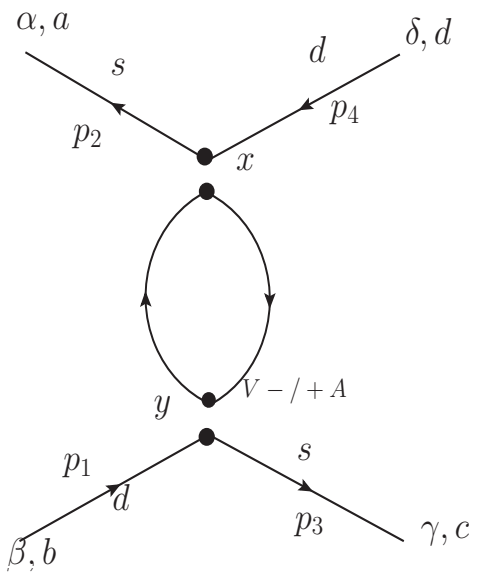

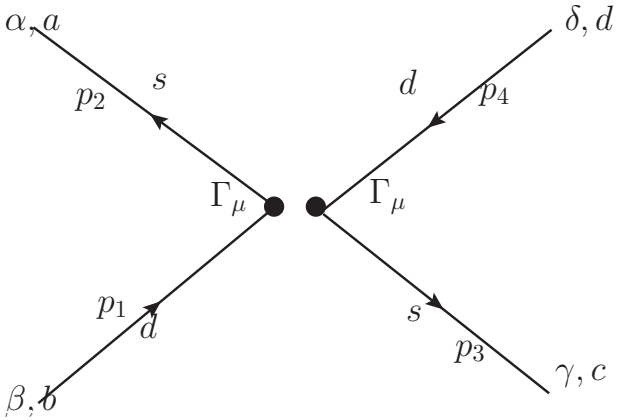

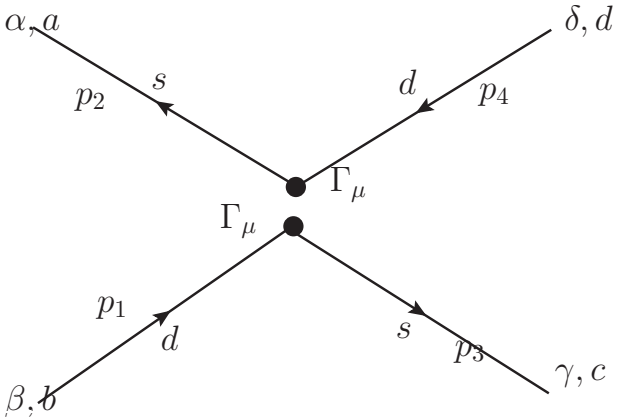

Short distance divergence: Evaluation of C^{lat}

- Use:

$$p_1 = \frac{2\pi}{La}(M, M, 0, 0), \quad p_2 = \frac{2\pi}{La}(M, 0, M, 0)$$
$$p_3 = \frac{2\pi}{La}(0, M, 0, M), \quad p_4 = \frac{2\pi}{La}(0, 0, M, M) \tag{22}$$

- To study the short distance divergence of our correlator, we impose a space-time cutoff R:

$$\Gamma_{\alpha\beta\gamma\delta}(p) = \langle s_\alpha(p_1)\bar{d}_\beta(p_2) \int d^4x_1 \int_{|x_1-x_2|^2<R^2} d^4x_2 H_W(x_1)H_W(x_2)s_\gamma(p_3)\bar{d}_\delta(p_4)\rangle. \tag{23}$$

- Small R dependence when $R \geq 5$: C^{lat} really represent short distance part!

cutoff	3	4	5	7	none
C_{11}^{lat}	0.1726	0.1881	0.1903	0.1905	0.1904
C_{22}^{lat}	0.0489	0.0520	0.0522	0.0522	0.0522

Table : $C_{i,j}^{lat}$: coefficient for Q_iQ_j.

Short distance divergence: Evaluation of C^{lat}

- Energy scale μ dependence of $C^{lat}(\mu^2)$:

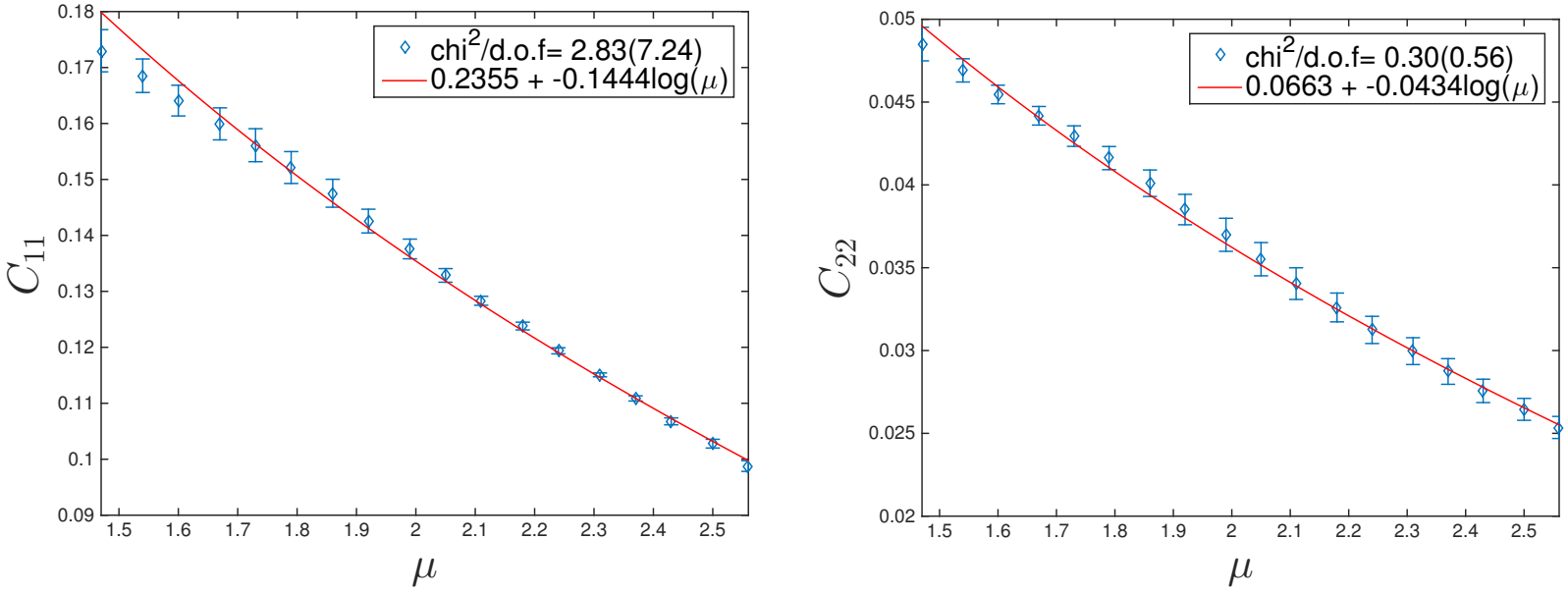

Figure : Short distance coefficients for energy scale $\mu = 1.41 GeV - 2.6 GeV$. Red line is a logarithm fit.

Preliminary results: Wilson coefficients

- We use the basis for operators (Q_1^{uu}, Q_2^{uu}, Q_3, Q_4, Q_5, Q_6). The Wilson coefficient for Q_i^{cc}, Q_i^{cu}, and Q_i^{uc} will be the same to Q_i^{uu} ($i = 1, 2$).
- We can find the Wilson coefficient in $\overline{MS}$ at $\mu = 2.15$ GeV:

$$C^{\overline{MS}} = \begin{pmatrix} -0.2967 & 1.1385 & 0.0217 & -0.0518 & 0.0102 & -0.0671 \end{pmatrix} \tag{24}$$

- Use NPR to find the lattice Wilson coefficient, renormalized at $\mu = 2.15$ GeV.

$$\sum_{i=1}^{6} C_i^{\overline{MS}} Q_i^{\overline{MS}} = \sum_{i=1}^{6} C_i^{lat} Q_i^{lat}, \tag{25}$$

$$C^{\overline{lat}} = \begin{pmatrix} -0.2373(1) & 0.6885(1) & 0.0113(8) & -0.0213(10) & 0.0085(8) & -0.0256(8) \end{pmatrix} \tag{26}$$

Preliminary results

- Integrated correlator before and after short distance correcton:

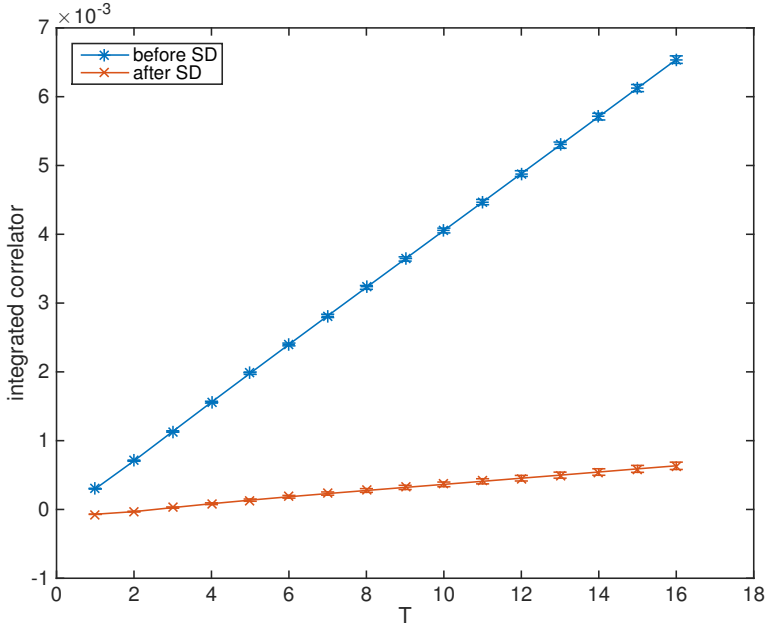

$Q_1 Q_1$

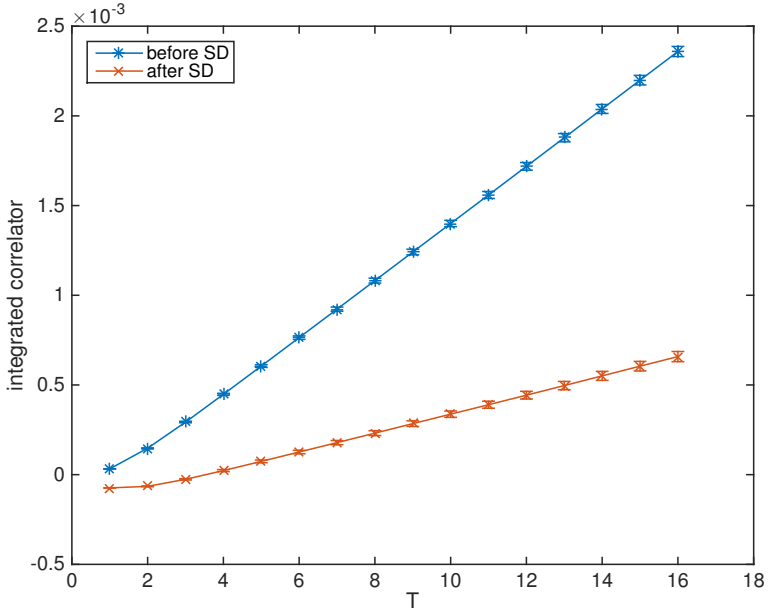

$Q_2 Q_2$

Figure : Integrated correlator, only $Q_1 Q_1$ and $Q_2 Q_2$ are plotted.

Preliminary results

- Different contribution to Im $M_{0\bar{0}}$, before and after subtraction of short distance contribution. Error comes from both the fitting of correlator and the Wilson coefficients.

	before	after		before	after
$Q_1 Q_1$	-0.7241(61)	-0.0786(59)			
$Q_1 Q_2$	0.9112(101)	0.0637(099)	$Q_2 Q_2$	-2.3472(281)	-0.7816(282)
$Q_1 Q_3$	0.1181(60)	0.0506(27)	$Q_2 Q_3$	-0.0190(21)	0.0242(22)
$Q_1 Q_4$	-0.0116(11)	0.0161(12)	$Q_2 Q_4$	0.2216(81)	0.1182(51)
$Q_1 Q_5$	-0.0681(048)	-0.0035(009)	$Q_2 Q_5$	0.3461(245)	0.2917(208)
$Q_1 Q_6$	0.1577(059)	0.0828(051)	$Q_2 Q_6$	0.0863(121)	0.2914(137)

Table : Imaginary part of $M_{0\bar{0}}$, before/ after subtraction of short distance contribution.

Preliminary results

- We therefore obtain the $\lambda_u \lambda_t$ contribution to $M_{0\bar{0}}$. Before the subtraction of short distance part:

$$M_{0\bar{0}} = (3.16(10) - 1.32(4)) \times 10^{-15} MeV$$

- After the subtraction of short distance part:

$$M_{0\bar{0}} = (-1.79(99) + 0.75(41)) \times 10^{-16} MeV$$

- To obtain correct results, we still need to calculate the **physical** short distance contribution in continuum and add them back.
- We can find the ϵ_K from:

$$\epsilon_k = \frac{exp(i\pi/4)}{\sqrt{2}\Delta M_K}(\mathrm{Im}\, M_{0\bar{0}} + 2\xi\, \mathrm{Re}\, M_{0\bar{0}}) \tag{27}$$

- The value for ξ can be obtained from lattice calculation of kaon to two pion A_0. Currently, we can set this term to 0, and we use the experimental value $\Delta M_K = 3.483(6) \times 10^{-12} MeV$.

Preliminary results

- The long distance contribution to $\lambda_u \lambda_t$ part of ϵ_K is:
- before short distance correction.

$$|\epsilon_K| = 2.69(8) \times 10^{-4},$$

- after short distance correction.

$$|\epsilon_K| = 1.52(84) \times 10^{-5},$$

- The experimental value(with all parts):

$$|\epsilon_K| = 2.228(11) \times 10^{-3}$$

- We have relatively large error on the ϵ_K after short distance subtraction, because there is huge cancellation between different contribution to ϵ_K, but the error is not cancelled.

Outlook and summary

- To obtain complete calculation of $\lambda_u \lambda_t$ part of ϵ_K, we have to:

  1. Find the correct short distance contribution from continuum for the box diagram topology, and add it back to our results. Then our type 1 and 2 diagrams for the box topology is complete.

  2. Include all the diagrams (type 3, 4, 5), do the corresponding NPR to remove the short distance artifact, and find the short distance contribution in continuum for the disconnected topology and add to our results.

  3. Work on a lattice with more physical kinematics, including lighter pion, unquenched charm, and larger physical volume.

Charged particles scattering in a finite volume

Silas Beane

BNL 2/5/2015

Outline

- Motivation
- Effective range theory / with Coulomb
- Review of A_1^+ QC in FV
- Coulomb in a FV w/ M.J.Savage, arXiv:1407.4846
- Conclusions

✦ Motivation

✓ Lattice QCD calculates scattering parameters

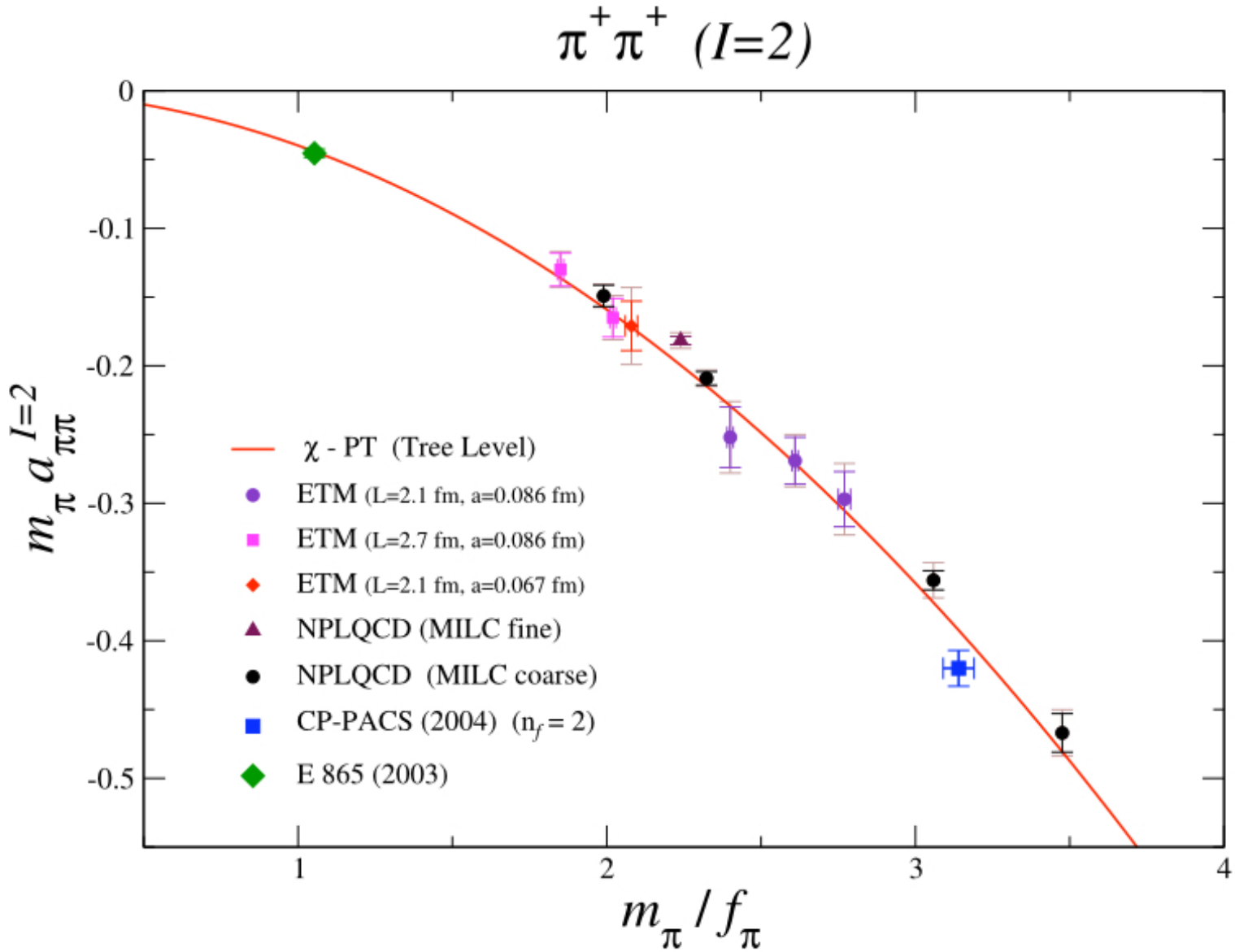

✓ $\alpha = 0$ phase shift prediction

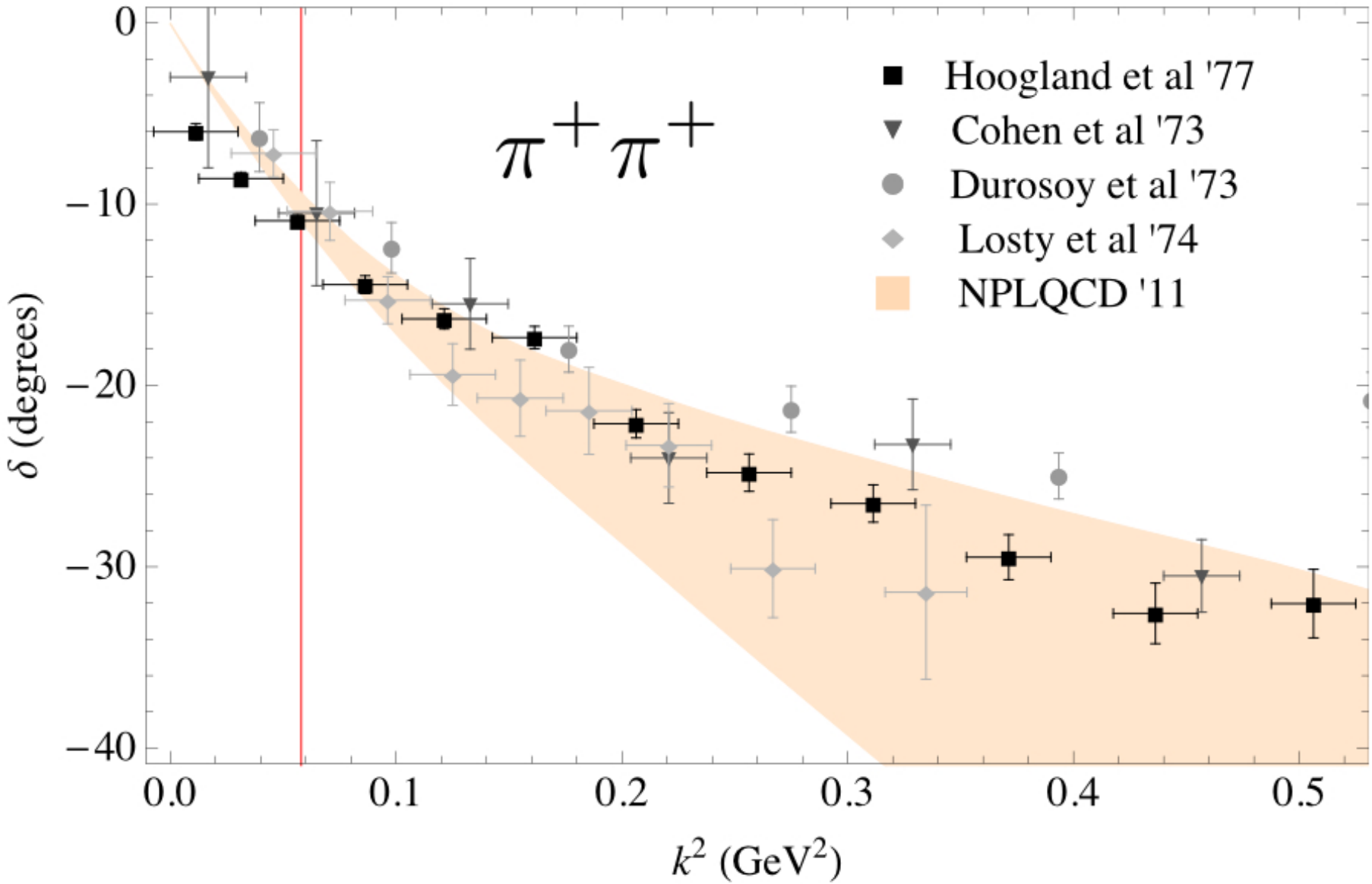

✓ Can one get proton-proton scattering *ab initio* ?

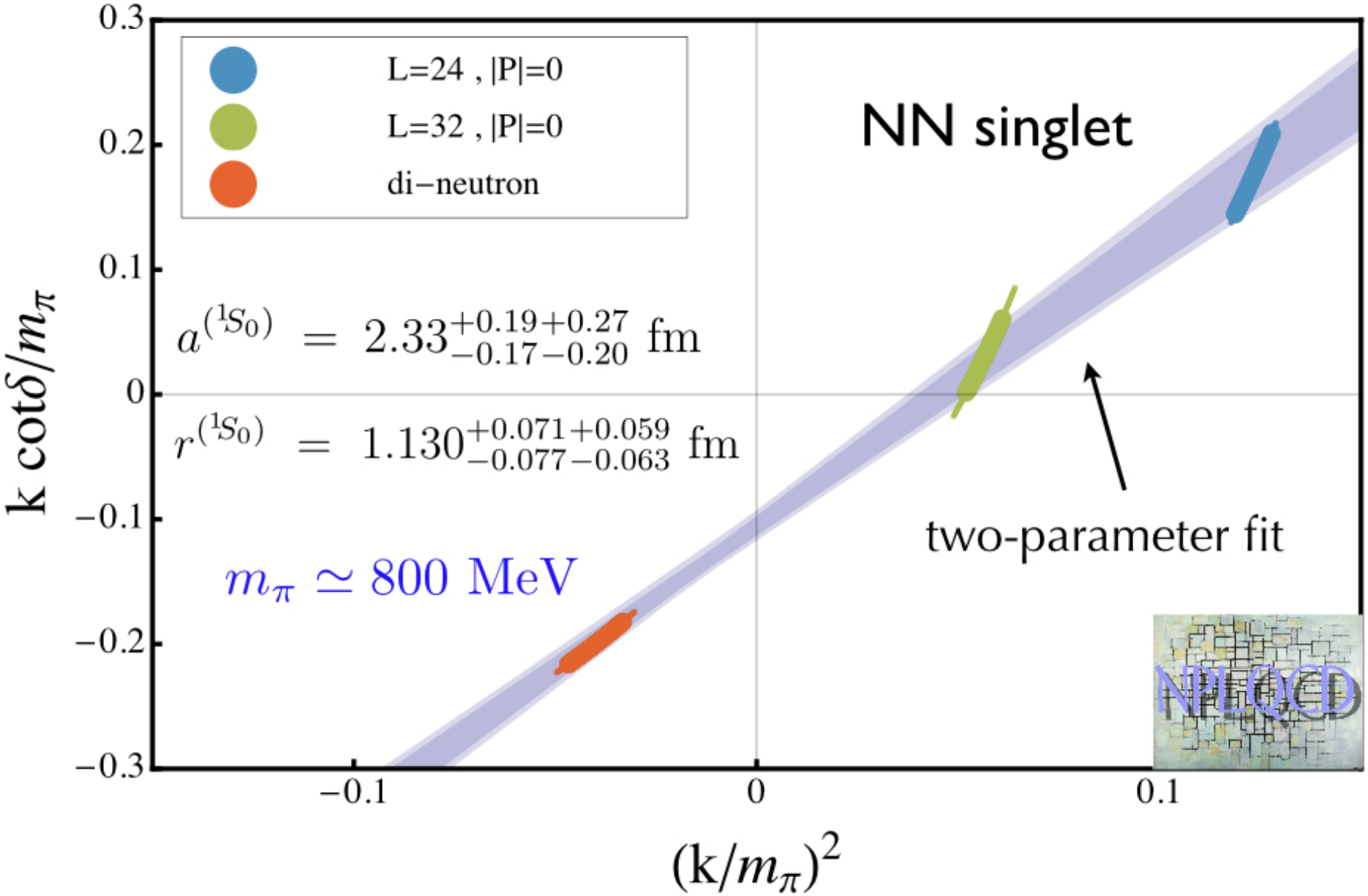

Di-neutron binding energy: world data

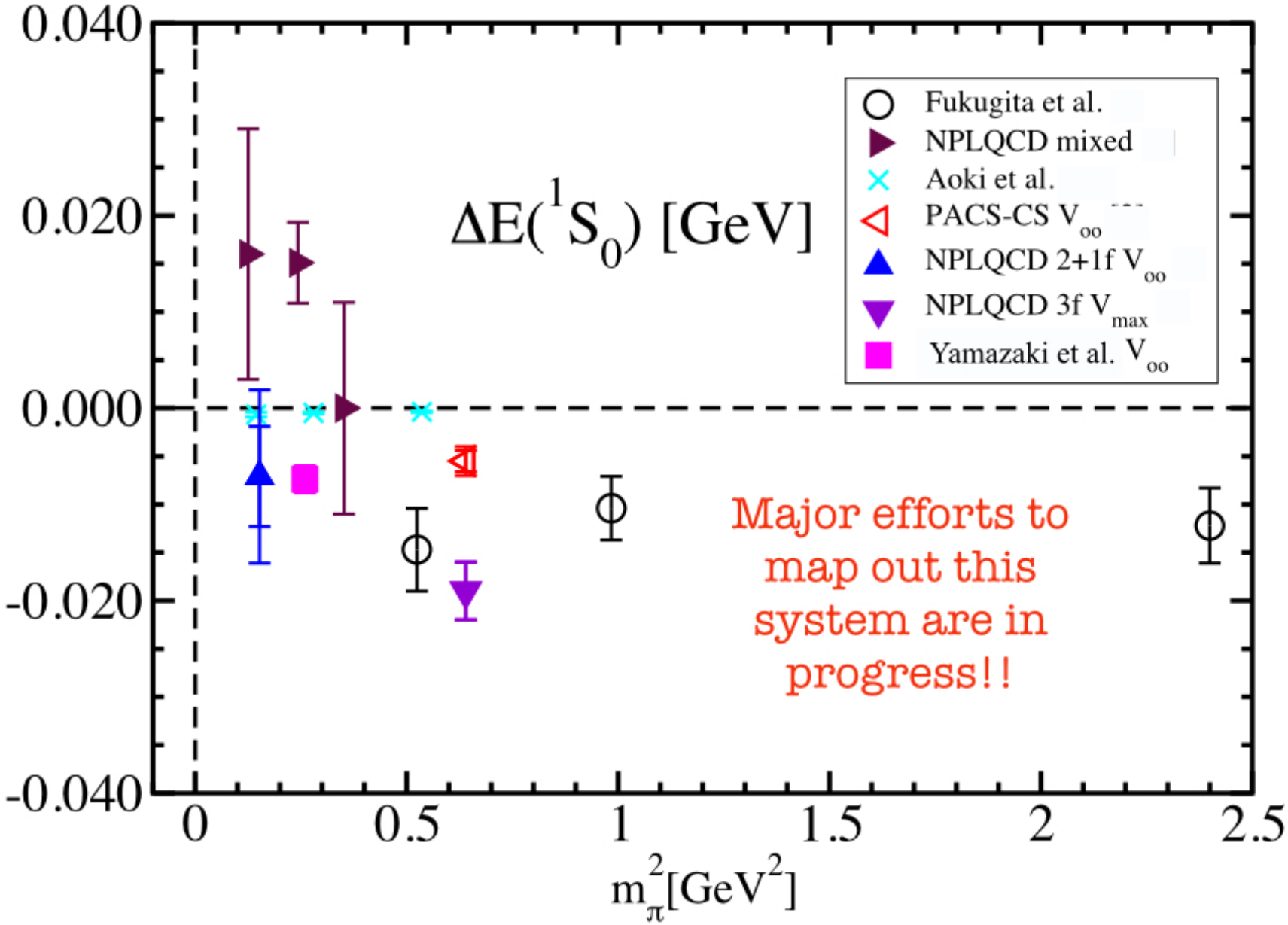

Di-neutron binding energy: world data

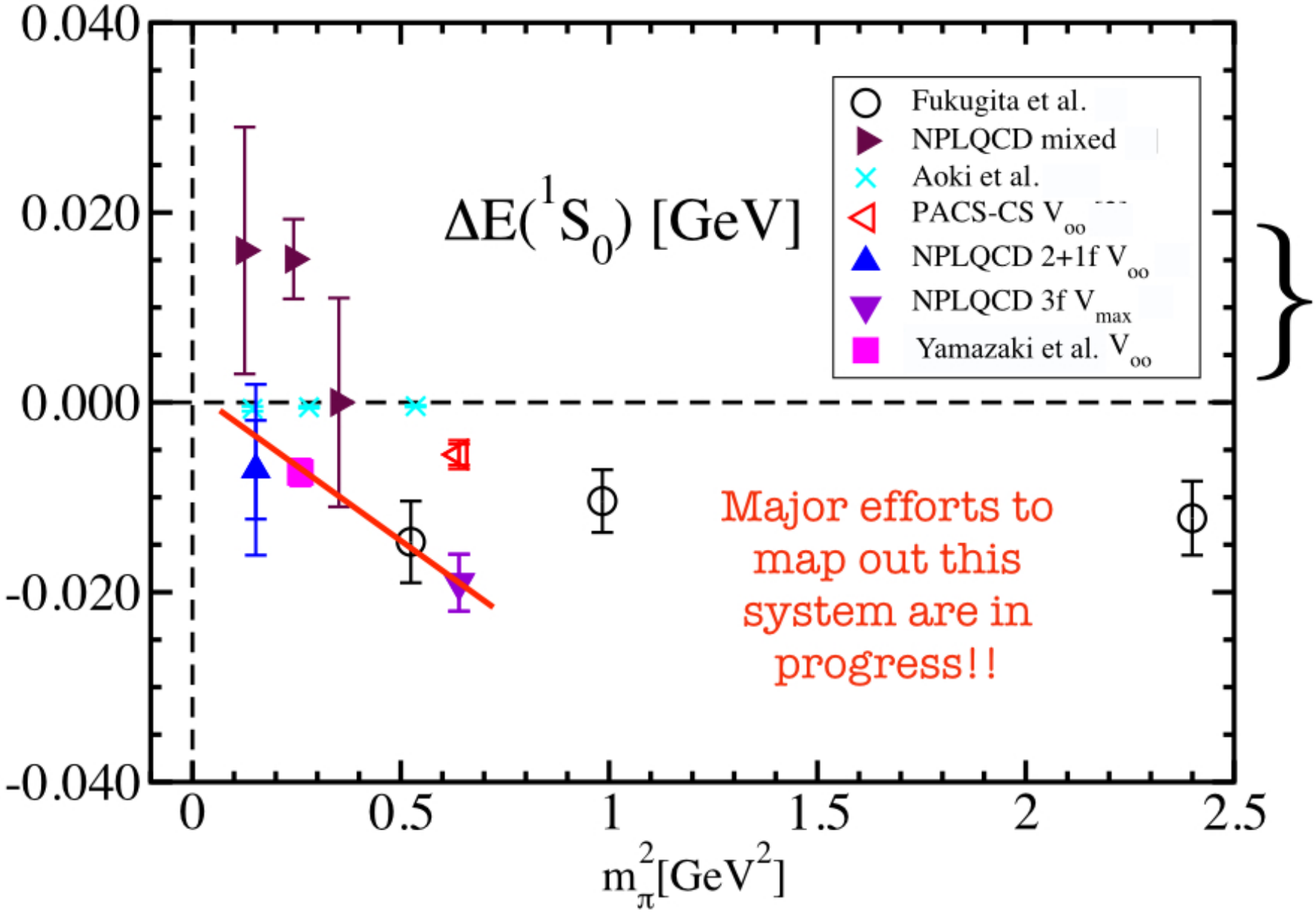

✦ Effective Range Theory (s-wave)

(Bethe, 1949)

✓ R is the range of the interaction

✓ $p \ll R^{-1}$ gives expansion of interaction in local operators:

$C(E^*) =$ 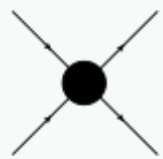 $= C_0 + C_2 M T^* + \ldots$

center-of-mass energy

$$E^* = 2M + \frac{p^2}{M} = 2M + T^*$$

✦ Effective Range Theory (s-wave)

(Bethe, 1949)

✓ R is the range of the interaction

✓ $p \ll R^{-1}$ gives expansion of interaction in local operators:

$C(E^*) =$ 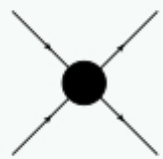 $= C_0 + C_2 M T^* + \ldots$

center-of-mass energy

$$E^* = 2M + \frac{p^2}{M} = 2M + T^*$$

✓ In practice, remove momentum dependence in EFT:

$$-\hat{\theta}\, \psi^T (\overleftarrow{\nabla} - \overrightarrow{\nabla})^2 \psi = 4M\, \hat{\theta} \left[i\partial_0 + \frac{\nabla^2}{4M} \right] \psi^T \psi \equiv 4M\, \hat{\theta}\, \mathcal{O}_{E^*} \psi^T \psi$$

✓ Scattering amplitude: interaction summed to all orders:

$T_S =$ 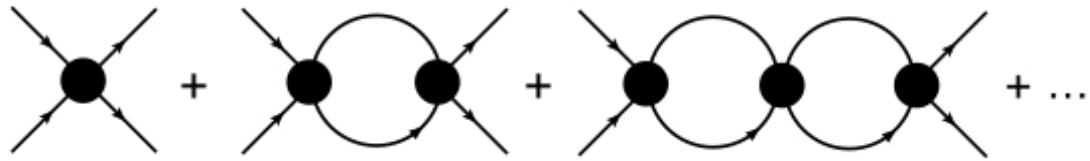

$$T_S = \frac{C(E^*)}{1 - C(E^*) J_0^\infty(E^*)} = -\frac{4\pi}{M} \frac{1}{p \cot\delta - ip}$$

✓ Matching achieved through renormalization ($\overline{MS}$):

$J_0^\infty(E^*) =$ 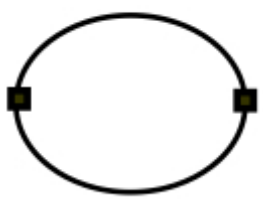 $= M \int \frac{d^3q}{(2\pi)^3} \frac{1}{p^2 - q^2 + i\epsilon}$ Green function

$$p \cot\delta = -\frac{1}{a} + \frac{1}{2} r_0 p^2 + \ldots$$

✓ Analytic structure of the scattering amplitude

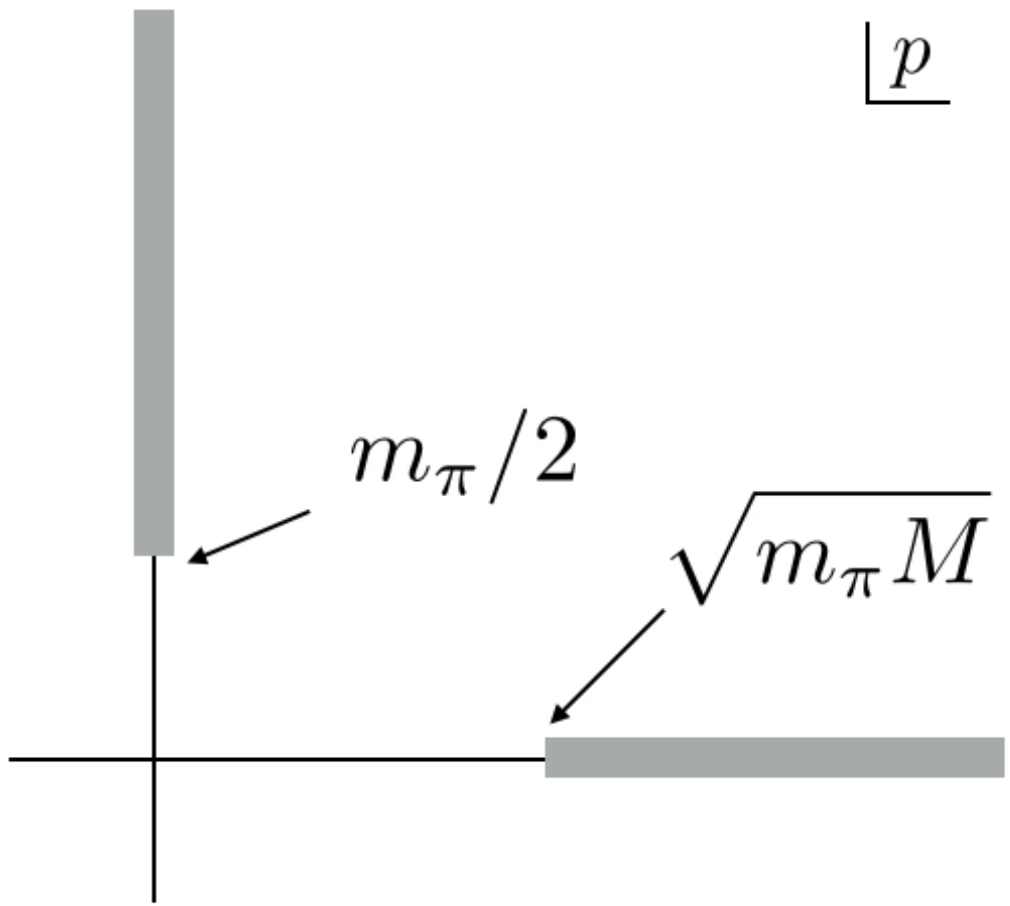

✓ Analytic structure of the scattering amplitude

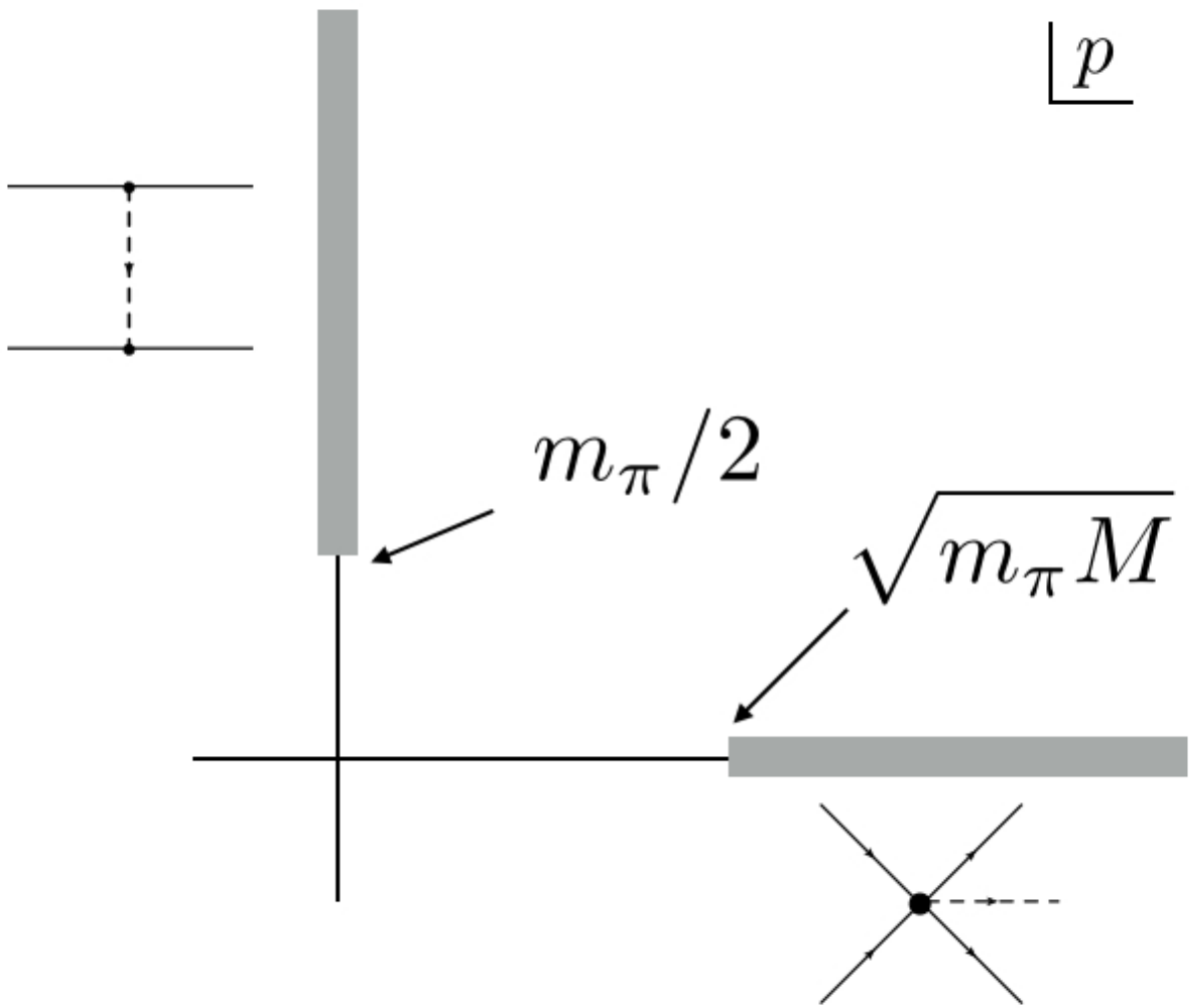

✓ Analytic structure of the scattering amplitude

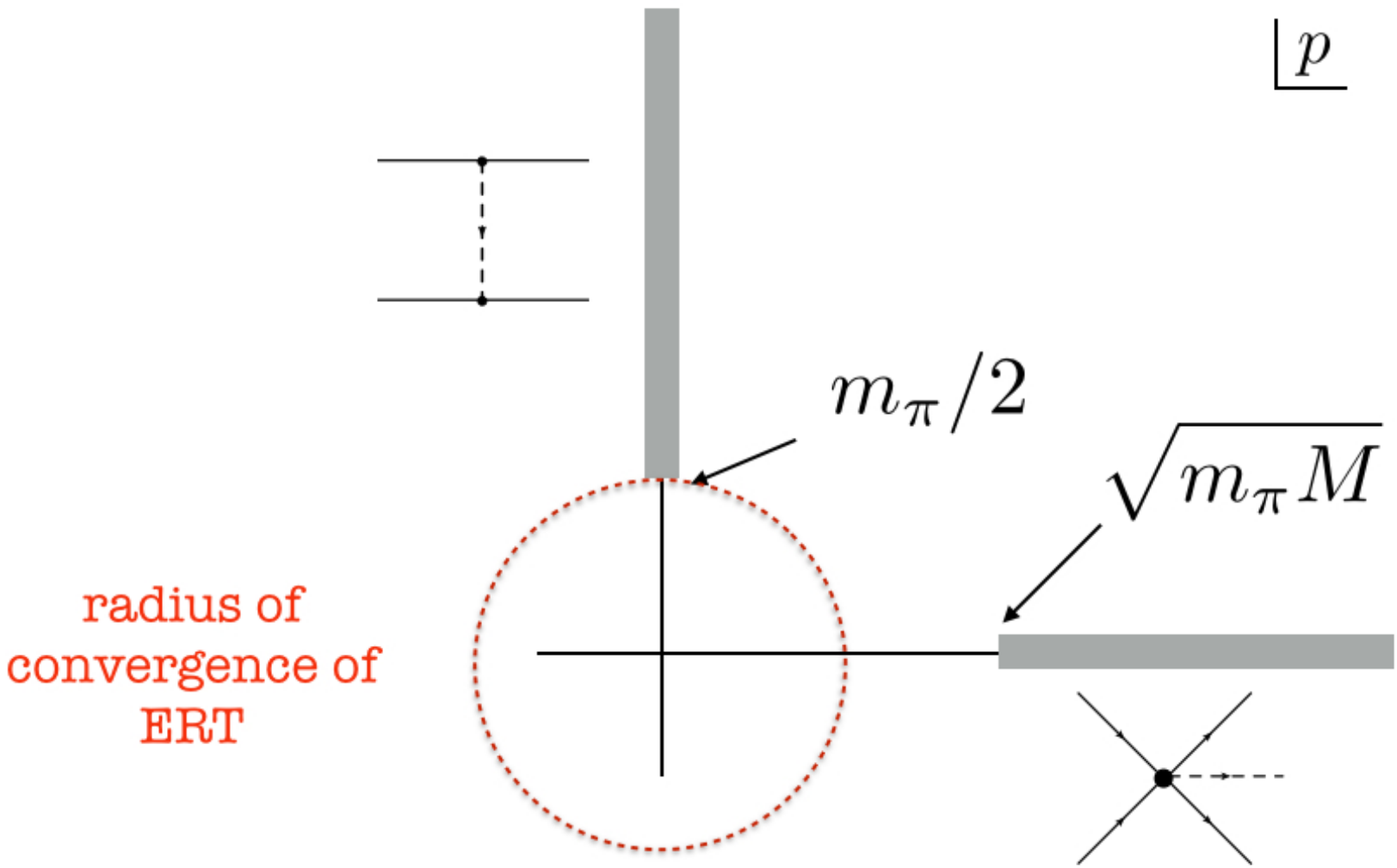

✦ Effective Range Theory with Coulomb

✓ Coulomb is enhanced in the infrared: (Bethe, 1949)

$$p \sim \alpha M \sim a_{\text{bohr}}^{-1}$$

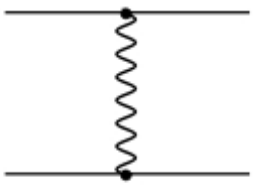

$$\frac{\alpha}{(\mathbf{p}-\mathbf{p}')^2} \sim \mathcal{O}(\alpha^{-1})$$

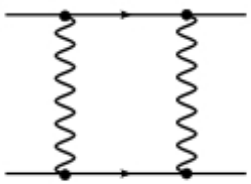

$$\int d^3\mathbf{k}dk_0 \frac{1}{\left(\frac{E}{2}+k_0-\frac{\mathbf{k}^2}{2M}+i\epsilon\right)} \frac{1}{\left(\frac{E}{2}-k_0-\frac{\mathbf{k}^2}{2M}+i\epsilon\right)} \frac{\alpha}{(\mathbf{k}-\mathbf{p})^2} \frac{\alpha}{(\mathbf{k}-\mathbf{p}')^2} \sim \mathcal{O}(\alpha^{-1})$$

Coulomb is non-perturbative

✦ Effective Range Theory with Coulomb

✓ Coulomb is enhanced in the infrared: (Bethe, 1949)

$$p \sim \alpha M \sim a_{\rm bohr}^{-1}$$

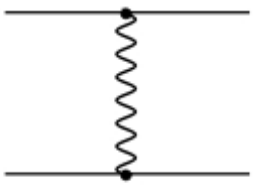

$$\frac{\alpha}{(\mathbf{p}-\mathbf{p}')^2} \sim \mathcal{O}(\alpha^{-1})$$

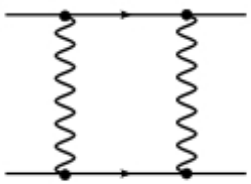

$$\int d^3\mathbf{k}dk_0 \frac{1}{\left(\frac{E}{2}+k_0-\frac{\mathbf{k}^2}{2M}+i\epsilon\right)} \frac{1}{\left(\frac{E}{2}-k_0-\frac{\mathbf{k}^2}{2M}+i\epsilon\right)} \frac{\alpha}{(\mathbf{k}-\mathbf{p})^2} \frac{\alpha}{(\mathbf{k}-\mathbf{p}')^2} \sim \mathcal{O}(\alpha^{-1})$$

Coulomb is non-perturbative

✓ Radiation is suppressed

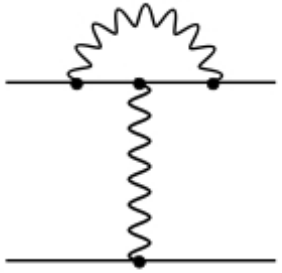

$$\sim \mathcal{O}(1)$$

✦ Effective Range Theory with Coulomb

✓ Coulomb ladders treated to all orders:

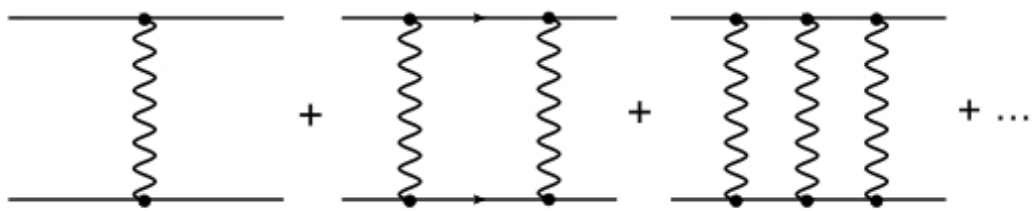

$$\sigma_0 = \arg\Gamma(1+i\eta)$$ is Coulomb phase shift

$$\boxed{T_{SC} = C^2_{\eta(p)} \frac{C(E^*)e^{i2\sigma_0}}{1 - C(E^*)J_0^\infty(E^*)} = -\frac{4\pi}{M}\frac{e^{2i\sigma_0}}{p\cot\delta - ip}}$$

$$C^2_{\eta(p)} = \frac{2\pi\eta(p)}{e^{2\pi\eta(p)} - 1} \qquad \eta \equiv \frac{\alpha M}{2p} \sim \frac{\alpha}{v} \sim 1$$

$$J_0^\infty(E^*) \;=\; M\int \frac{d^3q}{(2\pi)^3}\frac{C^2_{\eta(q)}}{p^2-q^2+i\epsilon}$$

QED "dressed" Green function

✓ Match to effective range parameters with $\overline{MS}$:

$$C^2_{\eta(p)}\, p\cot\delta + \alpha M h(\eta) \;=\; -\frac{1}{a_C} \;+\; \frac{1}{2}r_0 p^2 \;+\; \ldots$$

$$\downarrow$$

$$\ln\left(\frac{M\alpha}{p}\right) \;+\; \mathcal{O}(\alpha)$$

Removes non-analytic piece!

$$(pp: \quad a_c \;=\; -7.82 \text{ fm})$$

✓ Analytic structure of the scattering amplitude

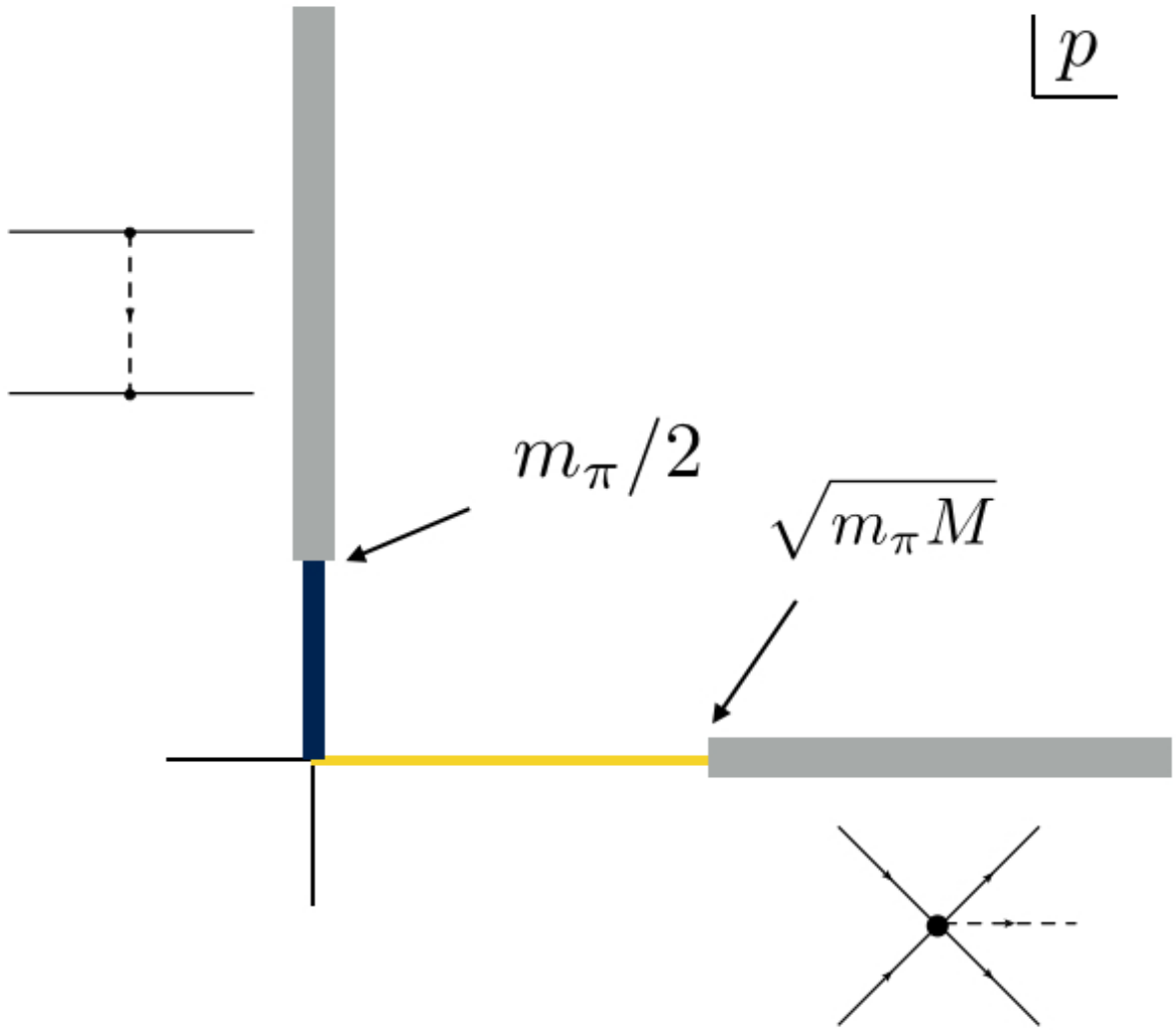

✓ Analytic structure of the scattering amplitude

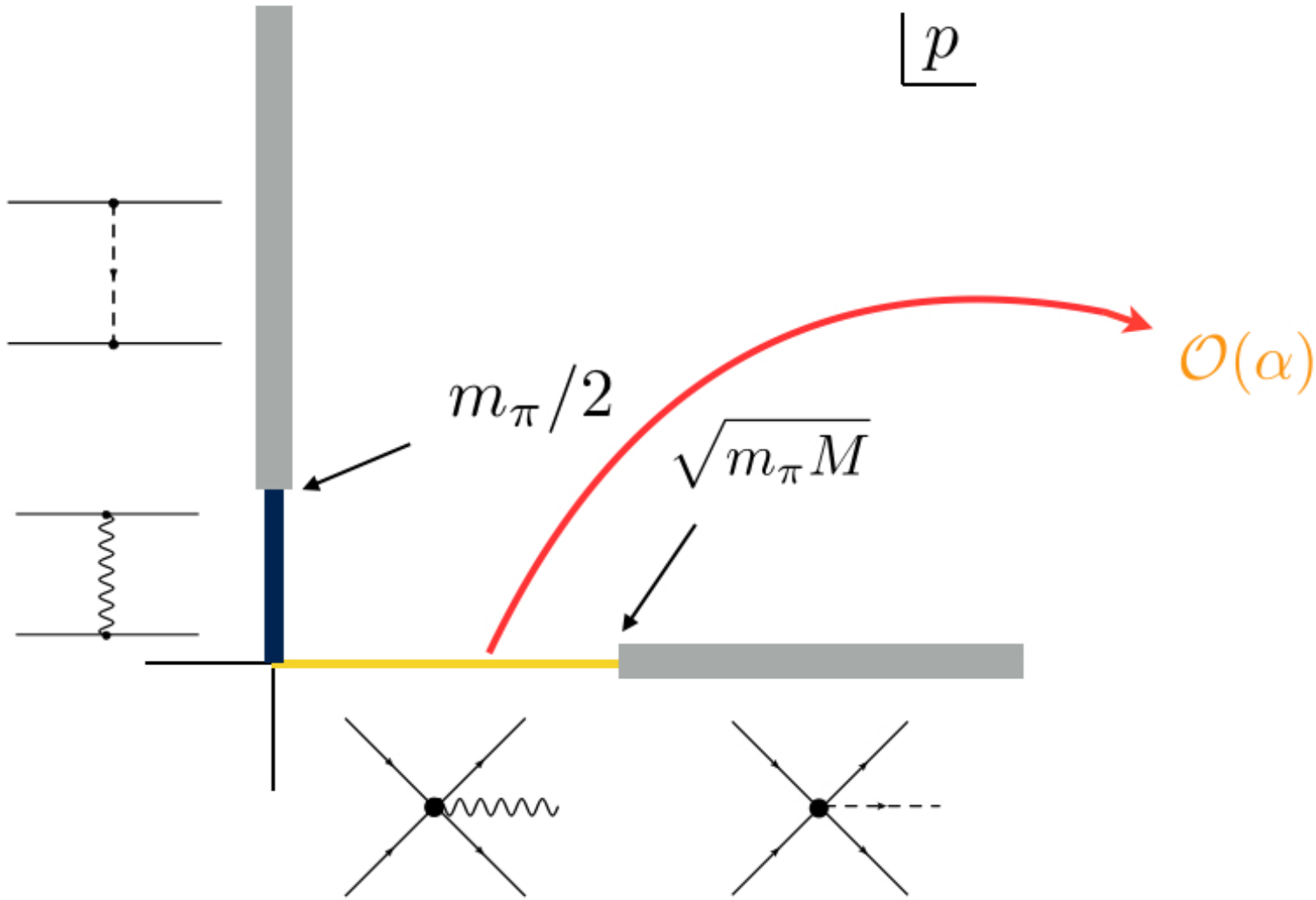

✓ Analytic structure of the scattering amplitude

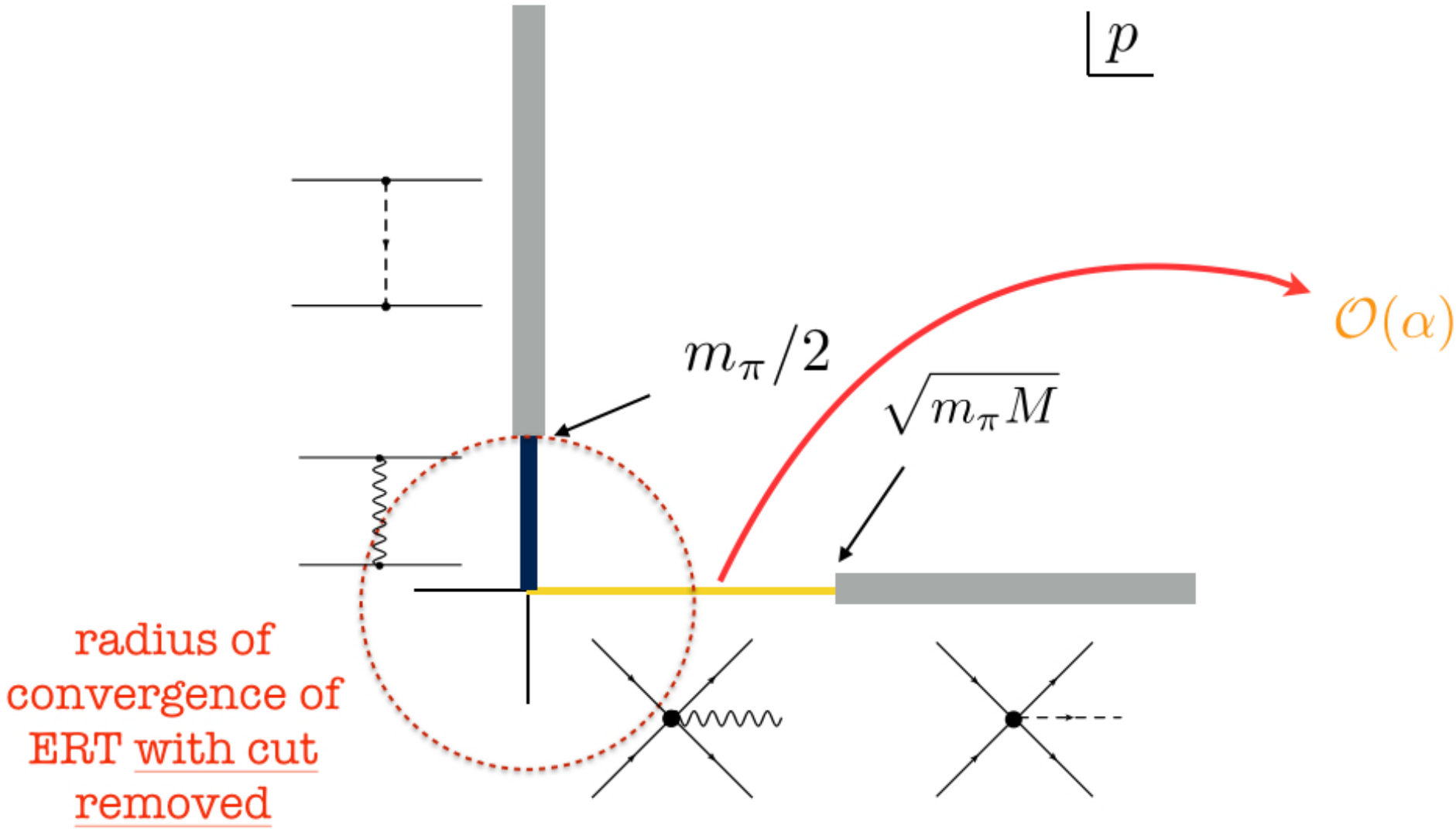

✦ Review of A_1^+ QC in FV

$b = 0,\ T = \infty,\ s - wave$

(Lüscher, 1990)

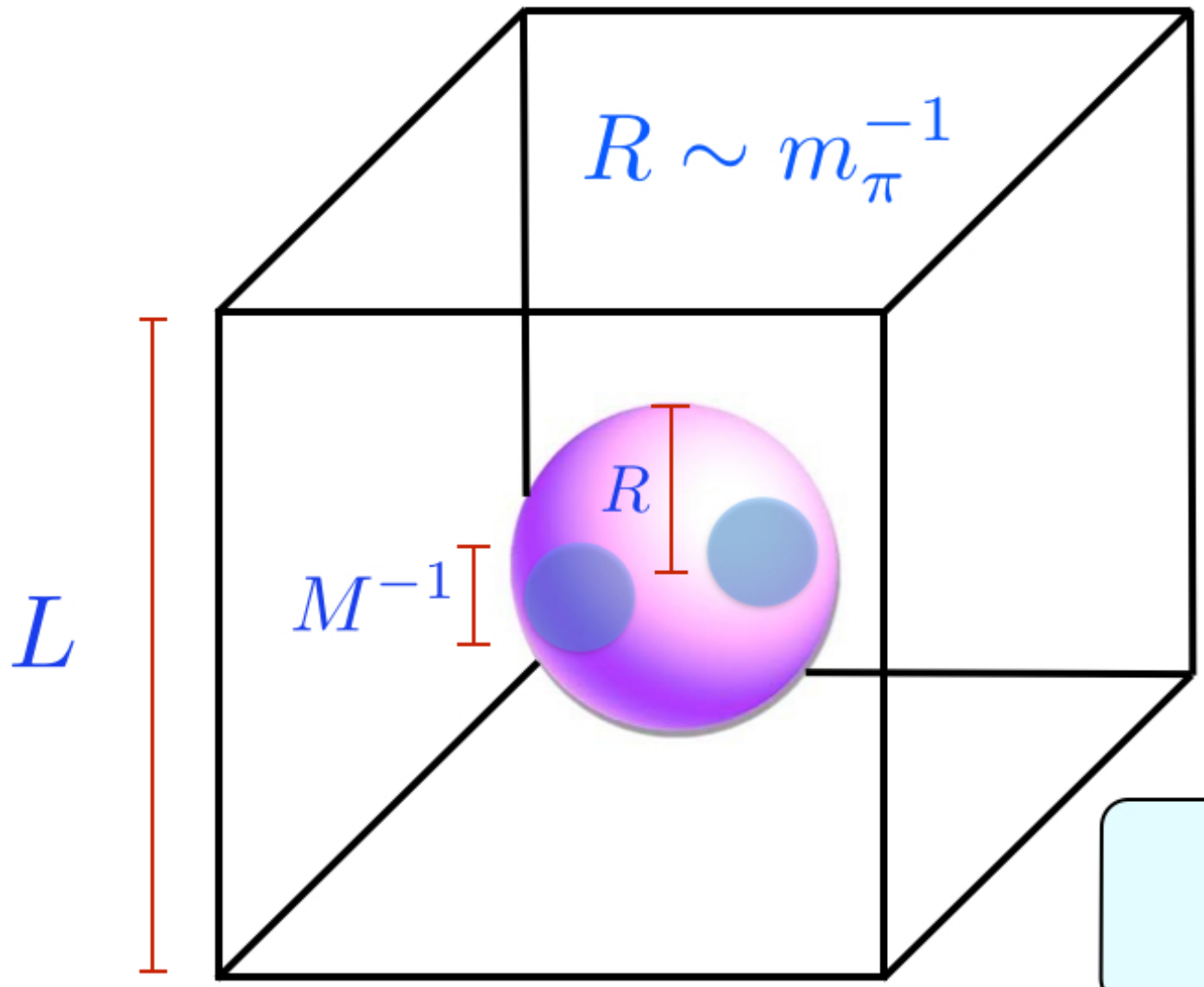

$$R < L/2$$

✓ Two-particle correlation function in FV

Source

Sink

$$S^\dagger \left[J_0^L(E^*) \; + \; C^L(E^*) \left(J_0^L(E^*)\right)^2 \; + \; C^L(E^*)^2 \left(J_0^L(E^*)\right)^3 \; + \; \ldots \right] S$$

$$= \; S^\dagger \frac{1}{1/J_0^L(E^*) - C^L(E^*)} S$$

Singularities of the correlation function

$$\boxed{\frac{1}{C^L(E^*)} \; = \; J_0^L(E^*)}$$

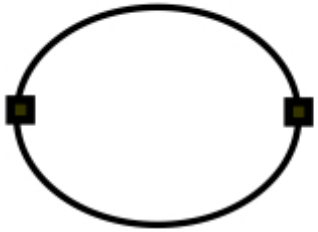

$$J_0^L(E^*) \; = \; -\frac{M}{4\pi^2 L} \sum_{\mathbf{n}}^{\Lambda_n} \frac{1}{|\mathbf{n}|^2 - \tilde{p}^2}$$

UV same as the continuum

✓ Quantization condition:

$$\boxed{p \cot \delta \;=\; \frac{1}{\pi L} \mathcal{S}(\tilde{p})} \;+\; \mathcal{O}\left(e^{-m_\pi L}\right)$$

Valid in QFT up to inelastic threshold

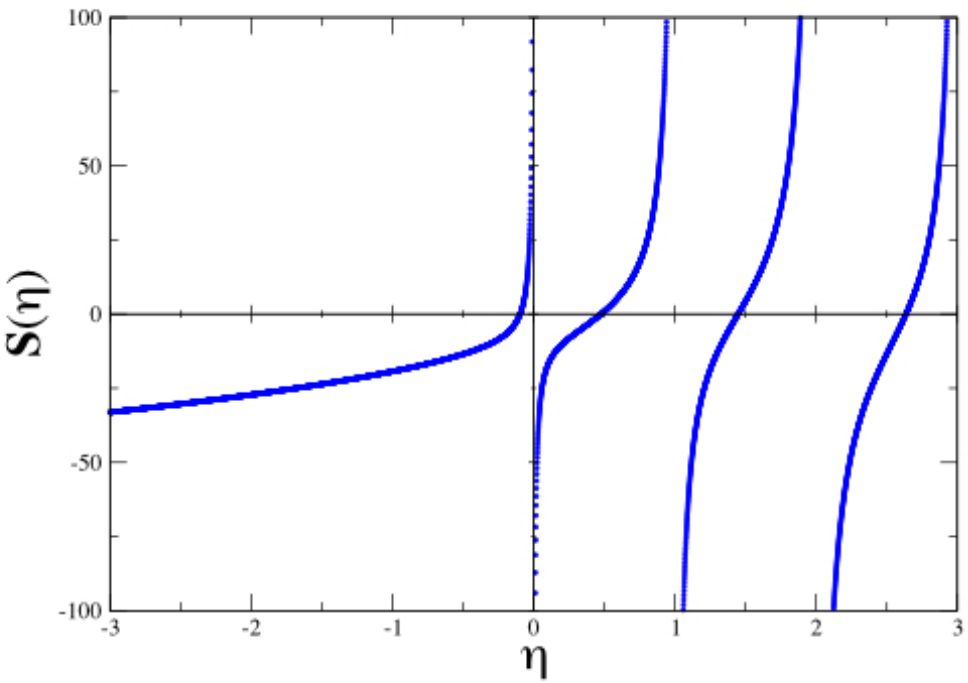

$$\mathcal{S}(x) \;\equiv\; \sum_{\mathbf{n}}^{\Lambda_n} \frac{1}{|\mathbf{n}|^2 - x^2} \;-\; 4\pi\Lambda_n$$

✓ Quantization condition in practice:

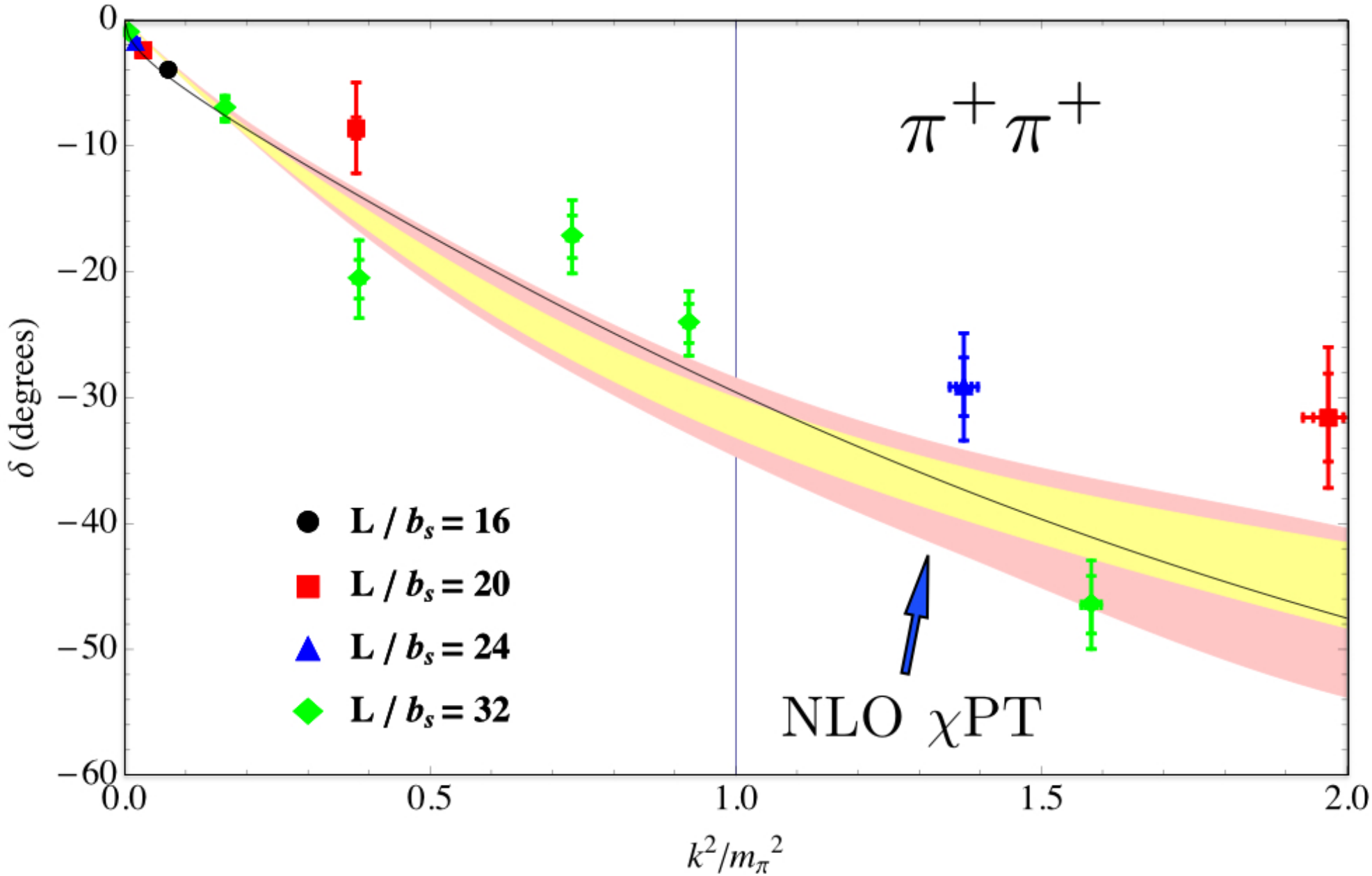

✦ A_1^+ QC in FV with Coulomb

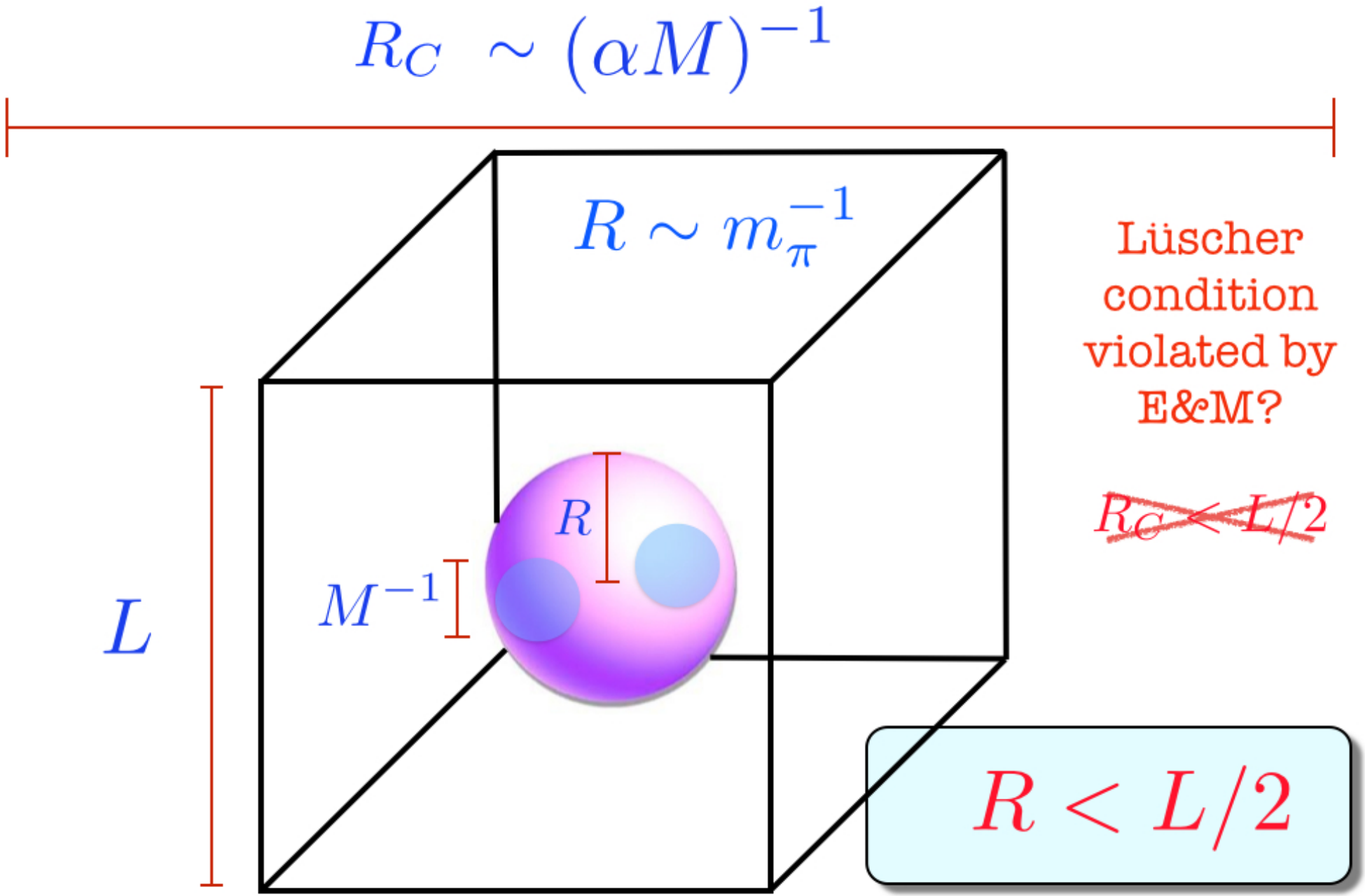

A prior there are many issues at FV…

- QED ill defined with PBCs — omit zero mode (ZD Talk)
- Increasingly complex integer sums .. many infrared problems
- Inelastic thresholds suppressed relative to Coulomb?
- Kinematics altered by power law effects
- Lack of universality

✓ Absence of zero mode: gap in momentum operator

$$p_{min} = \frac{2\pi}{L}$$

(ZD Talk)

$$L \to \infty$$

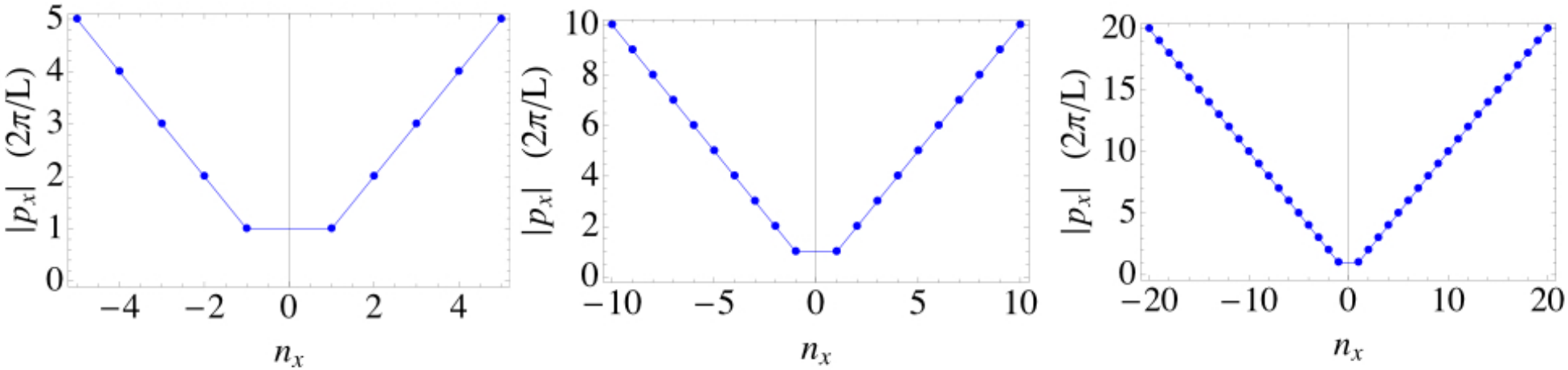

✓ Absence of zero mode: gap in momentum operator

$$p_{min} = \frac{2\pi}{L}$$

(ZD Talk)

$$L \to \infty$$

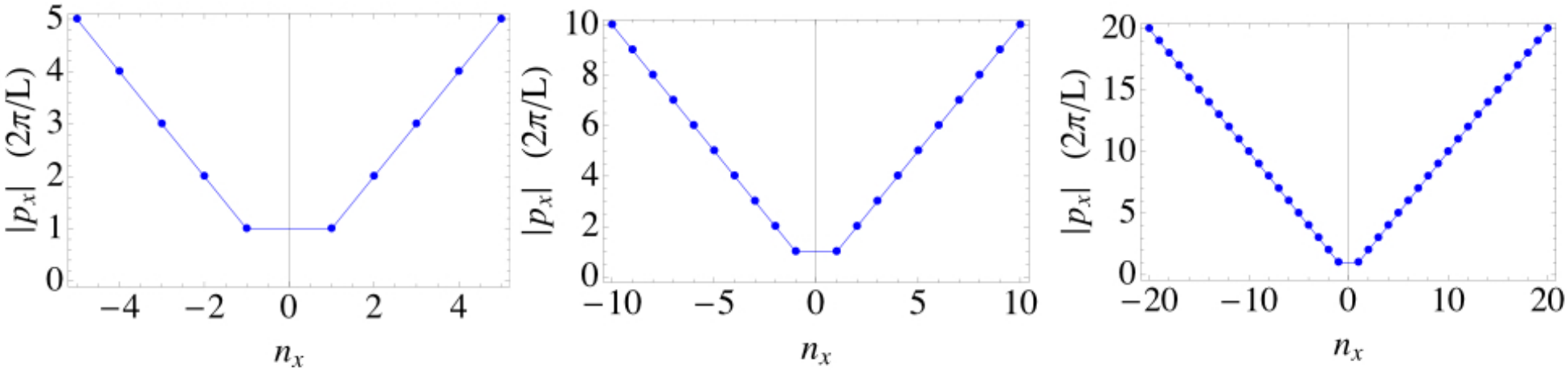

Gap is a good thing: $\eta \equiv \frac{\alpha M}{2p} \sim \alpha M L$

$\eta \ll 1$ if $1 \ll ML \ll 1/\alpha$

Coulomb is perturbative!

✓ Zero mode removed

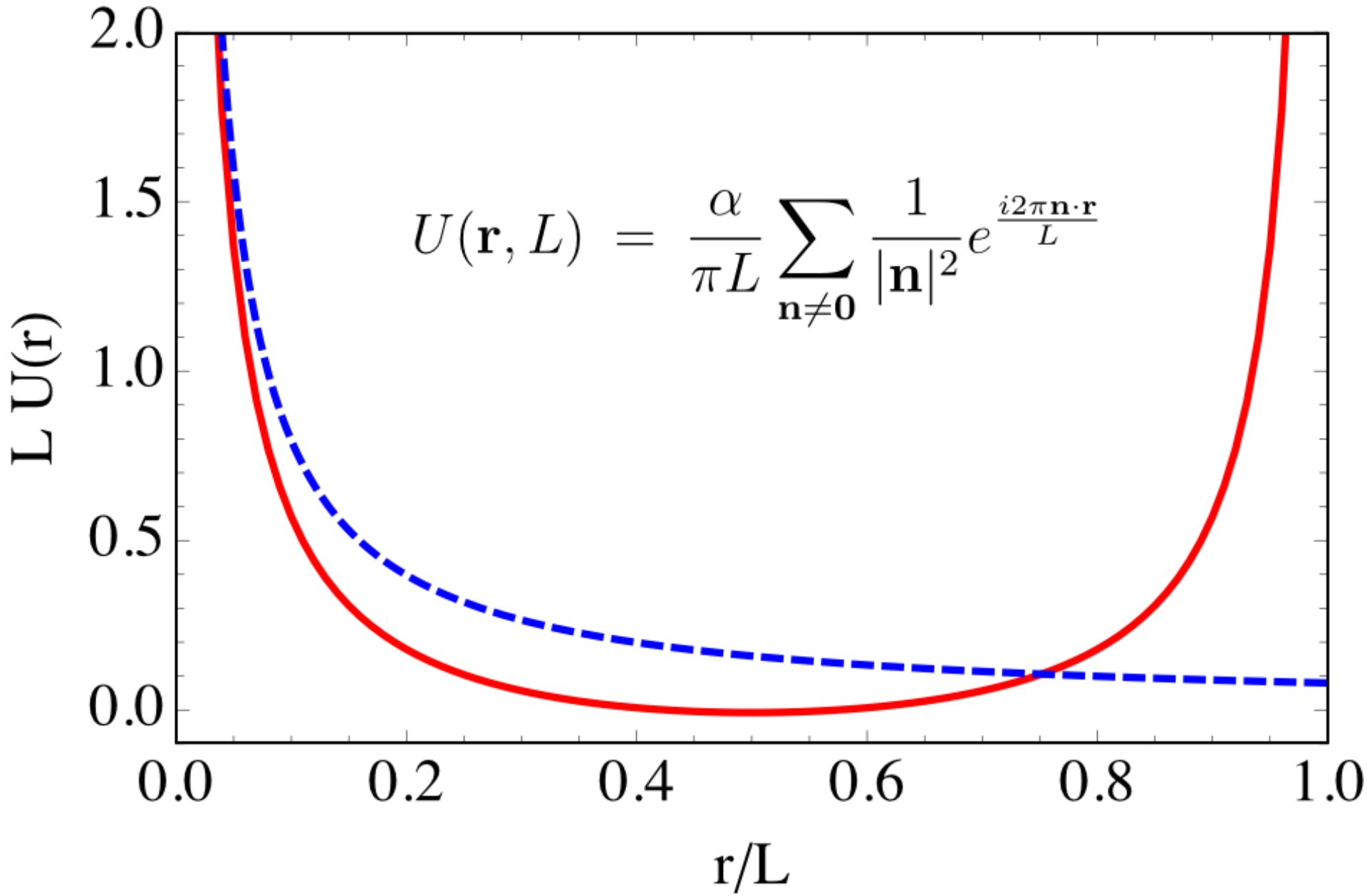

✓ Kinematics altered by power-law corrections:

$$E^* = 2M^L + T^{*L}$$

NRQED

$$p \cot \delta \quad \to -\frac{1}{a'_C} + \frac{1}{2} r'_0 M T^{*L} + r'_1 M^2 (T^{*L})^2 \; + \; \ldots$$

$$\frac{1}{a'_C} = \frac{1}{a_C} - \frac{\alpha \, r_0 M \, \mathcal{I}}{2\pi L} \; + \; \mathcal{O}(\alpha^2; \alpha/L^2)$$

$$r'_0 = r_0 + \frac{4 \, \alpha \, r_1 M \, \mathcal{I}}{\pi L} \; + \; \mathcal{O}(\alpha^2; \alpha/L^2)$$

Kinematically shifted effective range parameters

$$(\mathcal{I} = \pi c_1)$$

Source

Sink

$$= S^\dagger \frac{1}{1/J_0^L(E^*) - C^L(E^*)} S \quad \longrightarrow \quad \boxed{\frac{1}{C^L(E^*)} = J_0^L(E^*)}$$

$$J_0^\infty(E^*) =$$

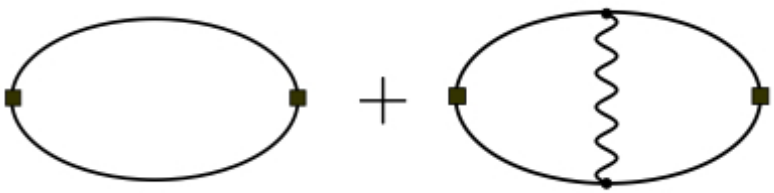

UV same as the continuum

$$- M \int \frac{d^3q}{(2\pi)^3} \frac{1}{q^2 - p^2} + 4\pi\alpha M^2 \int \frac{d^3q}{(2\pi)^3} \int \frac{d^3k}{(2\pi)^3} \frac{1}{q^2 - p^2} \frac{1}{k^2 - p^2} \frac{1}{|\mathbf{q} - \mathbf{k}|^2}$$

FV with PBCs

$$- \frac{M}{4\pi^2 L} \sum_{\mathbf{n}}^{\Lambda_n} \frac{1}{|\mathbf{n}|^2 - \tilde{p}^2} + \frac{\alpha M^2}{16\pi^5} \sum_{\mathbf{n}}^{\Lambda_n} \sum_{\mathbf{m} \neq \mathbf{n}}^{\infty} \frac{1}{|\mathbf{n}|^2 - \tilde{p}^2} \frac{1}{|\mathbf{m}|^2 - \tilde{p}^2} \frac{1}{|\mathbf{n} - \mathbf{m}|^2} \qquad \tilde{p} = Lp/2\pi$$

✓ Radiation *not* suppressed by α

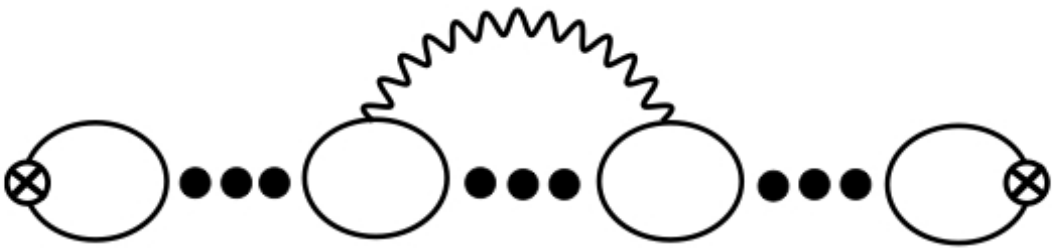

$$\sim \left(\sqrt{M/L}\right)^n$$

Infrared suppressed!

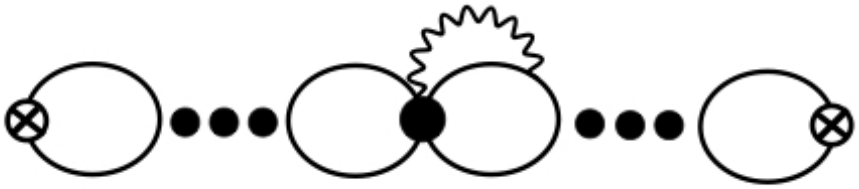

$$\delta C^{(FV)}(E^*) = -\alpha \left(\frac{4a_C^2 r_0}{L} \mathcal{I} + \ldots \right)$$

$$J_0^L \to J_0^L + (J_0^L)^2 \, \delta C^{(FV)}$$

$$(\mathcal{I} = \pi c_1)$$

Infrared suppressed but let's keep it..

✓ Quantization condition:

$$\boxed{-\frac{1}{a'_C} + \frac{1}{2} r'_0 p^2 + \ldots = \frac{1}{\pi L} \mathcal{S}^C(\tilde{p}) + \alpha M \left[\ln\left(\frac{4\pi}{\alpha M \mathrm{L}} \right) - \gamma_E \right]} + \ldots$$

Valid up to inelastic threshold!

$$\mathcal{S}^C(x) \equiv \mathcal{S}(x) - \frac{\alpha M L}{4\pi^3} \mathcal{S}_2(x) + \frac{\alpha\, M a_C^2 r_0}{\pi^2 L^2} \mathcal{I}\left[\mathcal{S}(x)\right]^2$$

$$\mathcal{S}_2(x) \equiv \sum_{\mathbf{n}}^{\Lambda_n} \sum_{\mathbf{m} \neq \mathbf{n}}^{\infty} \frac{1}{|\mathbf{n}|^2 - x^2} \frac{1}{|\mathbf{m}|^2 - x^2} \frac{1}{|\mathbf{n} - \mathbf{m}|^2} - 4\pi^4 \ln \Lambda_n$$

✓ Note the breakdown of universality

+ ... contains infrared suppressed, subleading QED, and 1/M effects

✓ Define a scale-dependent scattering length:

$$\frac{1}{a(\mu)} \equiv \frac{4\pi}{MC(0;\mu)} = \frac{1}{a_C} + \alpha M \left[\ln\left(\frac{2\mu}{\alpha M}\right) - \gamma_E \right]$$

$\overline{MS}_{FV}$

exhibits the impossibility of separating QCD and QED contributions

$$p \cot \bar{\delta}(p,\mu) \equiv -\frac{1}{a(\mu)} + \frac{1}{2} r_0 p^2 + \ldots$$

✓ Alternate form of QC:

$$p \cot \bar{\delta}'(p, 2\pi/L) \equiv -\frac{1}{a'(2\pi/L)} + \frac{1}{2} r_0' p^2 + \ldots = \frac{1}{\pi L} \mathcal{S}^C(\tilde{p})$$

leading QED effects from distance scales $> L$ are removed

Approximate formulas

✓ Ground state energy level:

$$\Delta E_0^C = \frac{4\pi\, a_C}{M\, L^3}\left\{1 - \left(\frac{a_C}{\pi\, L}\right)\mathcal{I} + \left(\frac{a_C}{\pi\, L}\right)^2 \left[\mathcal{I}^2 - \mathcal{J}\right] + \ldots\right\}$$

$$- \frac{2\alpha\, a_C}{L^2\pi^2}\left\{\mathcal{J} + \left(\frac{a_C}{\pi\, L}\right)\left[\mathcal{K} - \mathcal{I}\mathcal{J} - \tilde{\mathcal{R}}/2\right]\right.$$

$$+ \left(\frac{a_C}{\pi\, L}\right)^2 \left[\tilde{\mathcal{R}}\mathcal{I} + \mathcal{I}^2\mathcal{J} - 2\mathcal{J}^2 - 2\mathcal{I}\mathcal{K} + \mathcal{L} - \mathcal{R}_{24}\right]$$

$$\left. + \frac{a_C r_0 \pi^2}{L^2}\mathcal{I} + \ldots\right\}$$

geometric constants: $\mathcal{I}, \mathcal{J}, \mathcal{K}, \mathcal{L}, \mathcal{R}, \mathcal{R}_{24}$

$$\tilde{\mathcal{R}} \equiv \mathcal{R} - 4\pi^4\left[\ln\left(\frac{4\pi}{\alpha M L}\right) - \gamma_E\right]$$

✓ First excited energy level:

$$\Delta E_1^C = \frac{4\pi^2}{ML^2} - \frac{12\tan\overline{\delta}'}{ML^2}\left(1 + c_1'\tan\overline{\delta}' + c_2'\tan^2\overline{\delta}' + \ldots\right)$$
$$+ \frac{9\alpha}{4\pi \mathrm{L}}\left(1 + c_{1\alpha}'\tan\overline{\delta}' + \left(c_{2\alpha}' + \frac{8}{3}\log(\alpha M L)\right)\tan^2\overline{\delta}' + \ldots\right)$$

geometric constants: $c_1', c_2', c_{1\alpha}', c_{2\alpha}'$

$$\frac{9\alpha}{4\pi \mathrm{L}} \xrightarrow[\mathrm{L} = 10\ \mathrm{fm}]{} \sim 100\ \mathrm{keV}$$

Coulomb effects are very small!

Bound state

✓ Bound state QC with binding momentum κ :

$$-\frac{1}{a_C} - \frac{1}{2} r_0 \kappa^2 = -\kappa - \alpha M \left(\gamma_E + \log\left(\frac{\alpha M}{4\kappa}\right) \right) - \frac{\alpha M}{2\pi\kappa L}(1-\kappa r_0)\mathcal{I}$$

$$\boxed{B^C = \frac{\kappa_0^2}{M} - \frac{2\alpha\kappa_0}{1-\kappa_0 r_0}\left[\gamma_E + \log\left(\frac{\alpha M}{4\kappa_0}\right)\right] - \frac{\alpha}{\pi L}\mathcal{I} + \ldots}$$

Bound state

✓ Bound state QC with binding momentum κ :

$$-\frac{1}{a_C} - \frac{1}{2} r_0 \kappa^2 \;=\; -\kappa - \alpha M \left(\gamma_E + \log\left(\frac{\alpha M}{4\kappa}\right) \right) \;-\; \frac{\alpha M}{2\pi\kappa L}(1-\kappa r_0)\mathcal{I}$$

$$\boxed{B^C \;=\; \frac{\kappa_0^2}{M} \;-\; \frac{2\alpha\kappa_0}{1-\kappa_0 r_0}\left[\gamma_E \;+\; \log\left(\frac{\alpha M}{4\kappa_0}\right)\right] \;-\; \frac{\alpha}{\pi L}\mathcal{I} \;+\; \ldots}$$

✓ Two contributions in the *compact* limit:

$$\delta M_{BS}^{(FV)} \;=\; 2\delta M^{(FV)} - \delta B^C \;=\; 2\left(\frac{\alpha}{2\pi L}\mathcal{I}\right) + \frac{\alpha}{\pi L}\mathcal{I} \;+\; \ldots \;=\; \boxed{\frac{2\alpha}{\pi L}\mathcal{I}} + \;\ldots$$

2(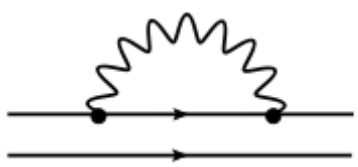) + 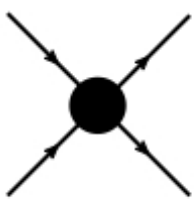

✓

Summary

- Electromagnetism essential for *ab initio* nuclear physics
- QED in a FV with PBCs is consistent without zero mode
- Two particle QC is tricky: violates Lüscher condition
- There is hierarchy of scales that allows perturbative treatment of Coulomb
- It would be very interesting to look at a simple system in lattice QCD.. $\pi^+\pi^+$?

Hadronic transition processes in a finite volume

Raúl Briceño
rbriceno@jlab.org

Jefferson Lab

RB, Hansen & Walker-Loud (2014)
RB & Hansen (to appear, 2015)

BNL, Feb. 2015

Transition amplitudes

(e.g., radiative neutron capture [np-to-dγ])

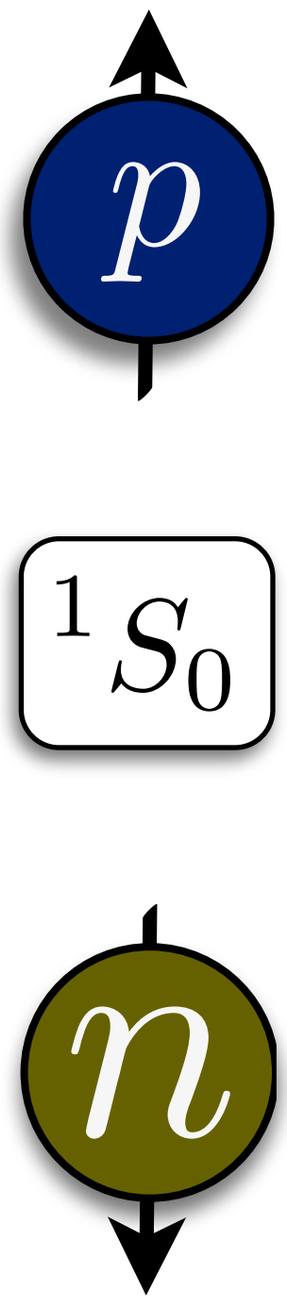

Transition amplitudes

(e.g., radiative neutron capture [np-to-dγ])

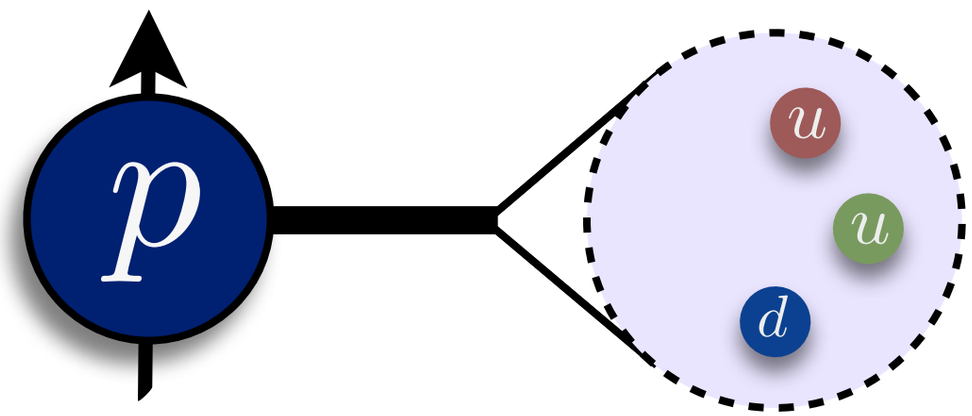

$^1S_0$

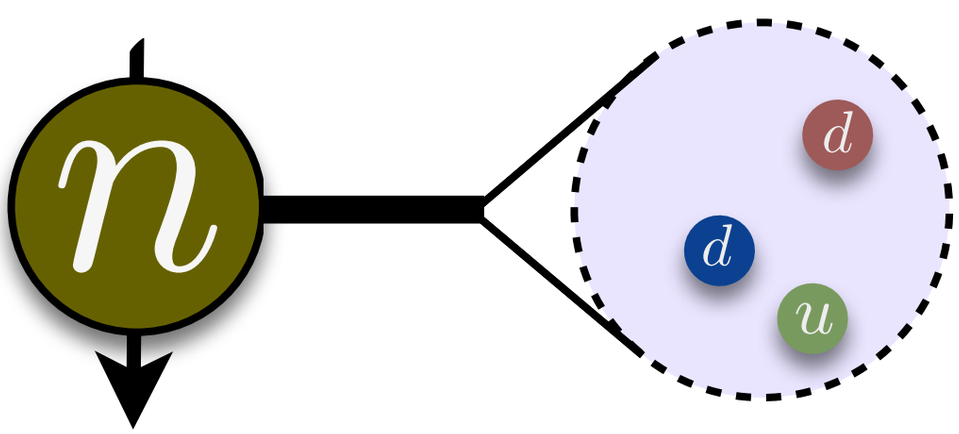

Transition amplitudes

(e.g., radiative neutron capture [np-to-dγ])

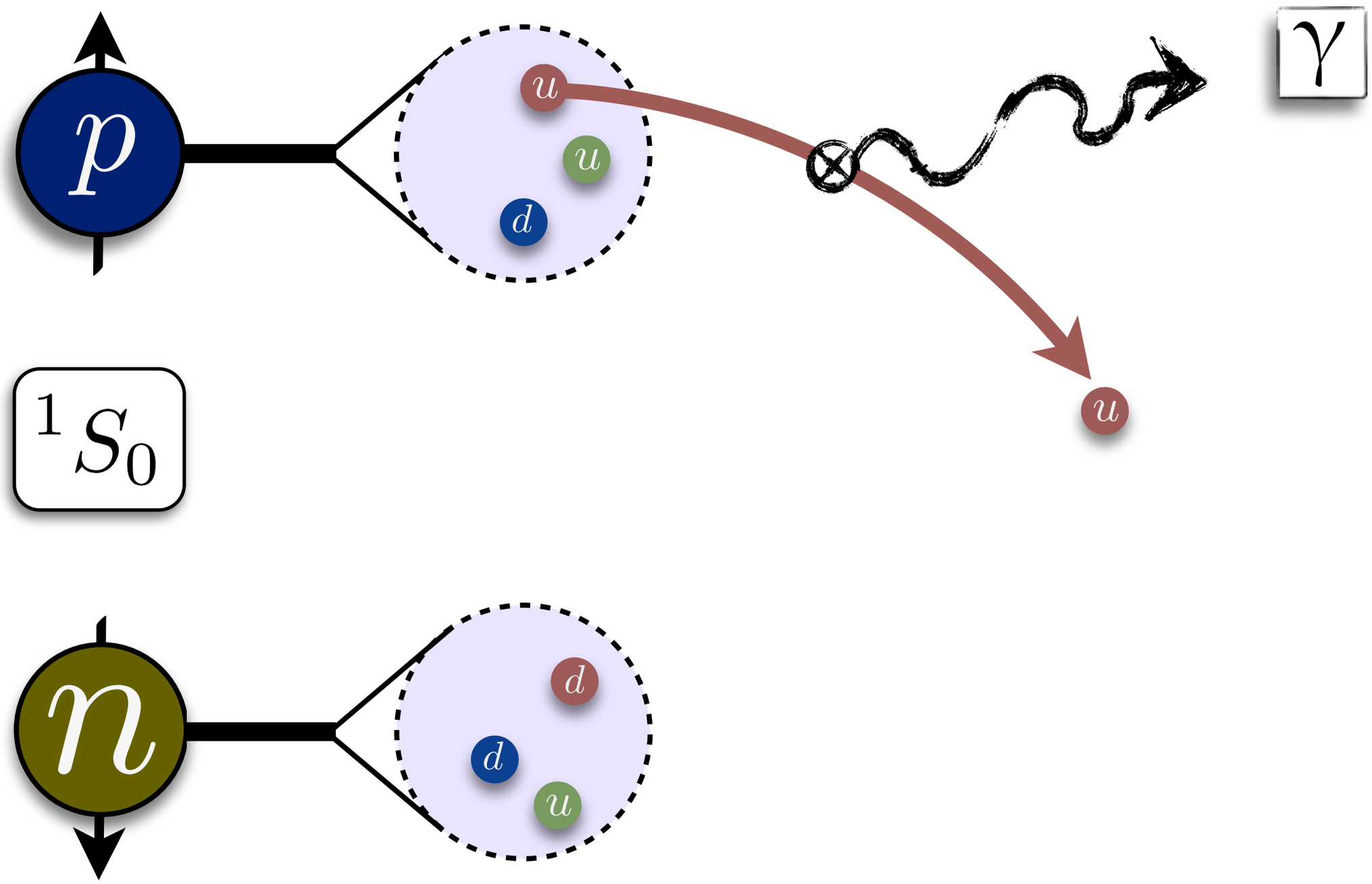

Transition amplitudes

(e.g., radiative neutron capture [np-to-dγ])

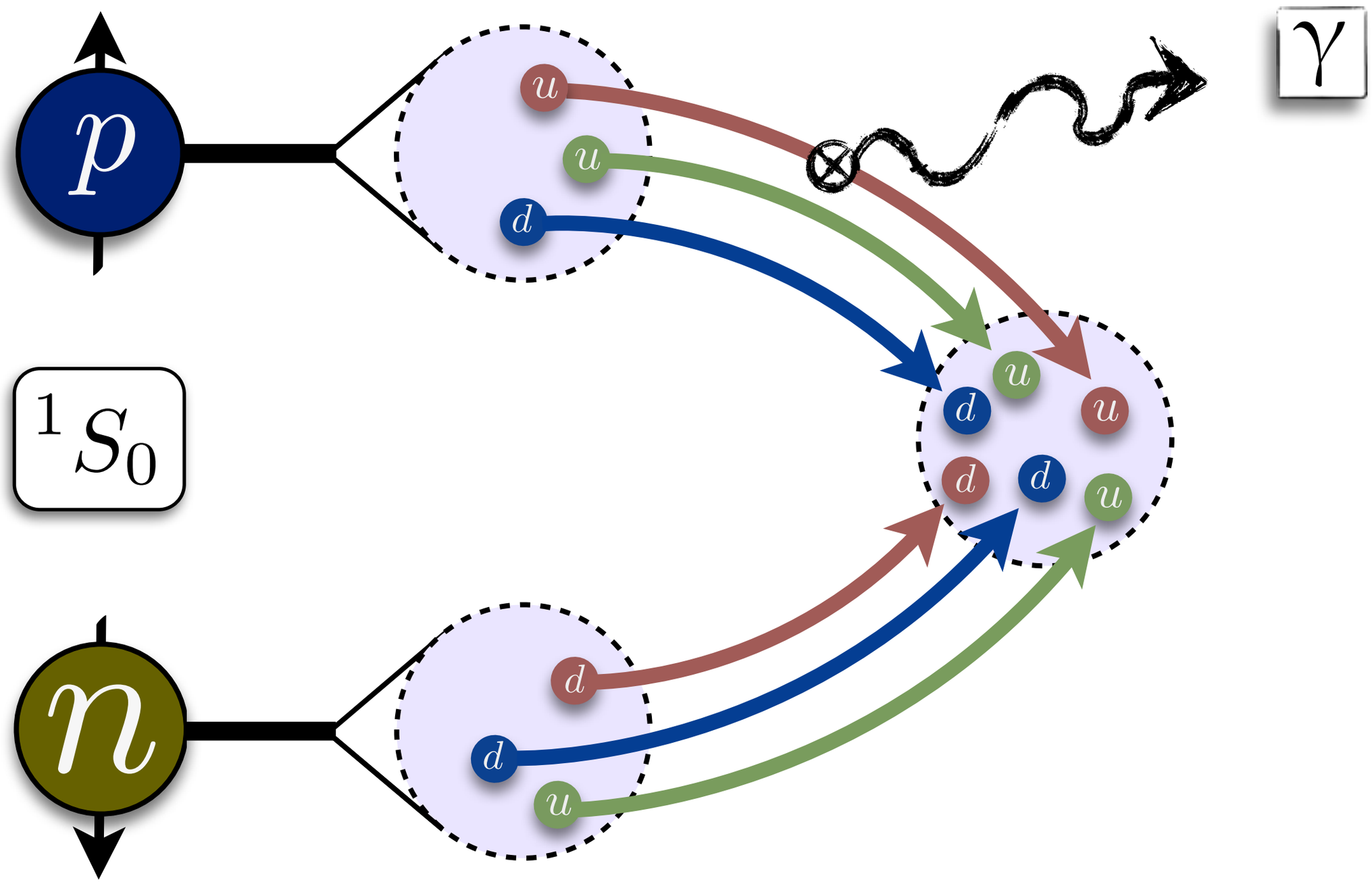

Transition amplitudes

(e.g., radiative neutron capture [np-to-dγ])

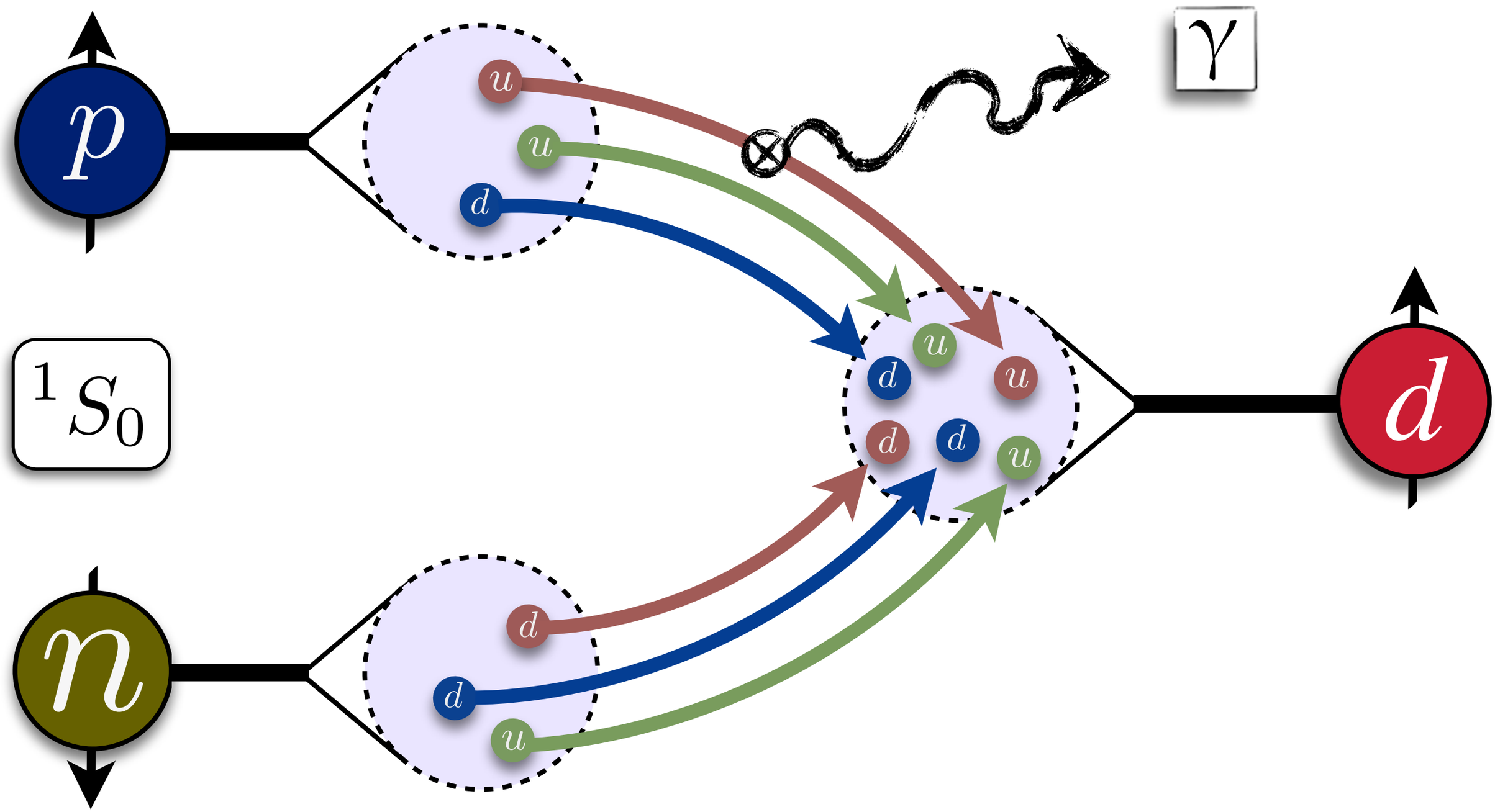

Transition amplitudes

(other applications)

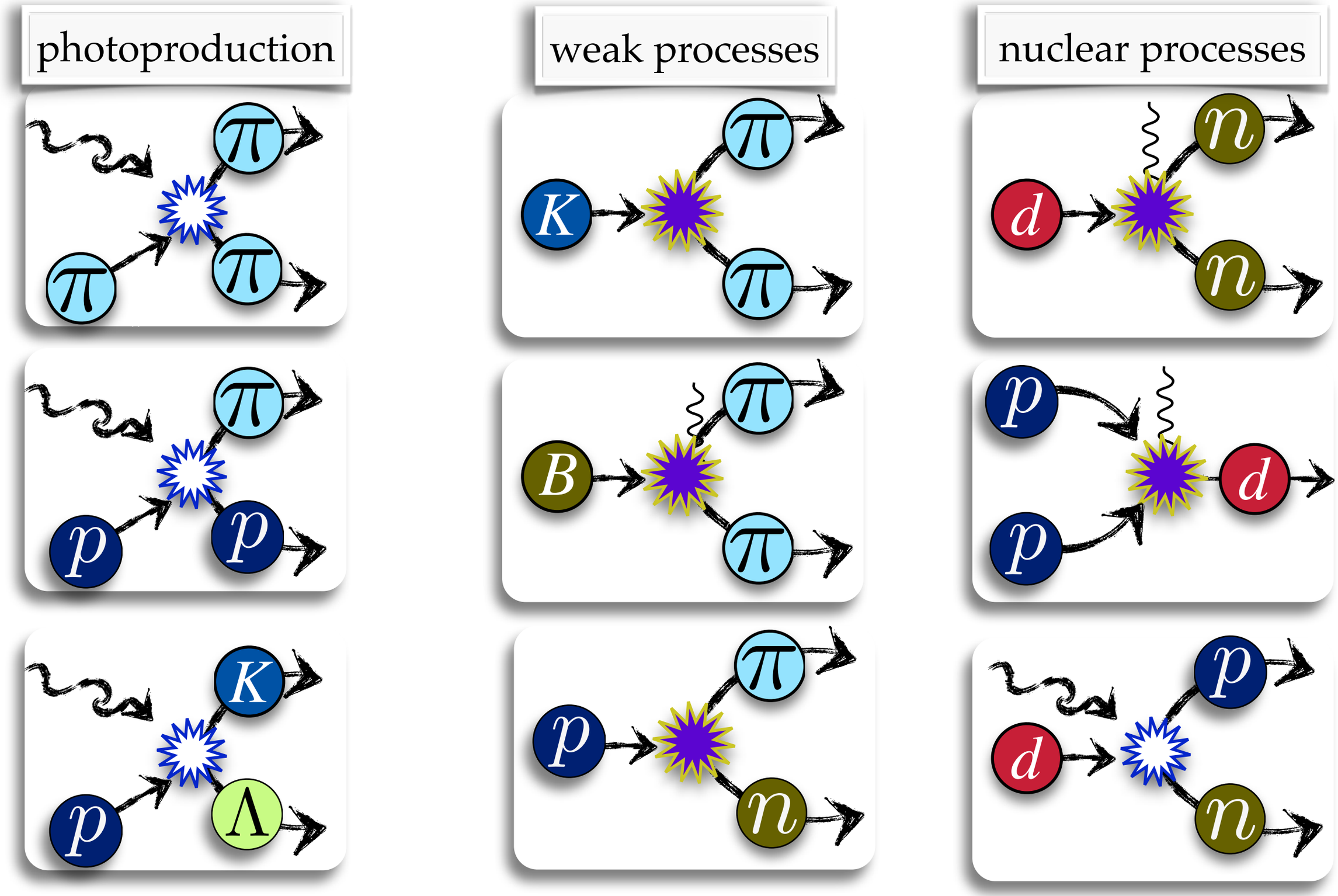

Main results

RB, Hansen & Walker-Loud (2014)
RB & Hansen (2015)

Transition amplitudes

- 0-to-2 with intrinsic spin:

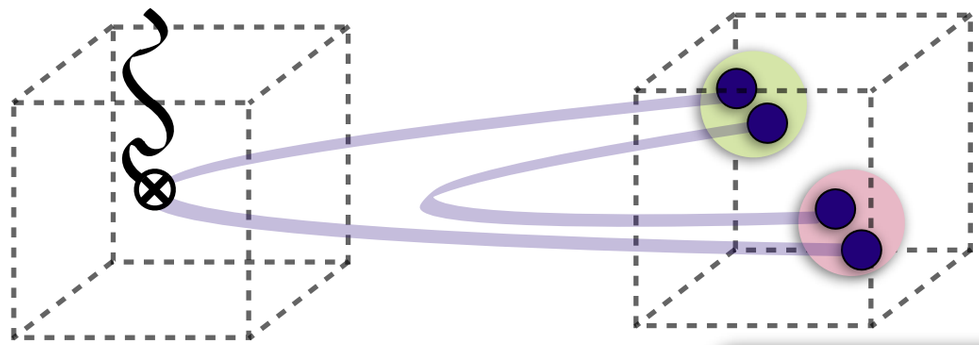

RB & Hansen (2015)

- 1-to-2 with intrinsic spin:

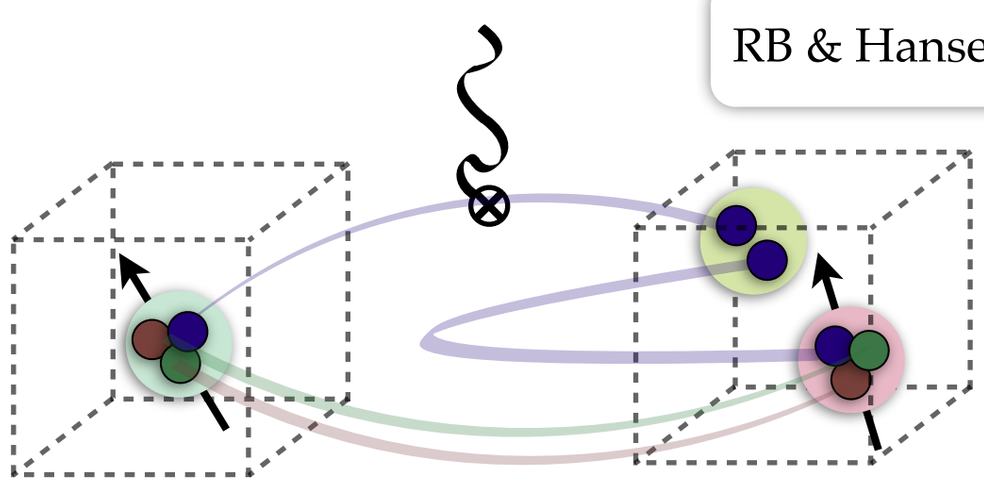

RB, Hansen & Walker-Loud (2014) / RB & Hansen (2015)

- 2-to-2 with intrinsic spin:

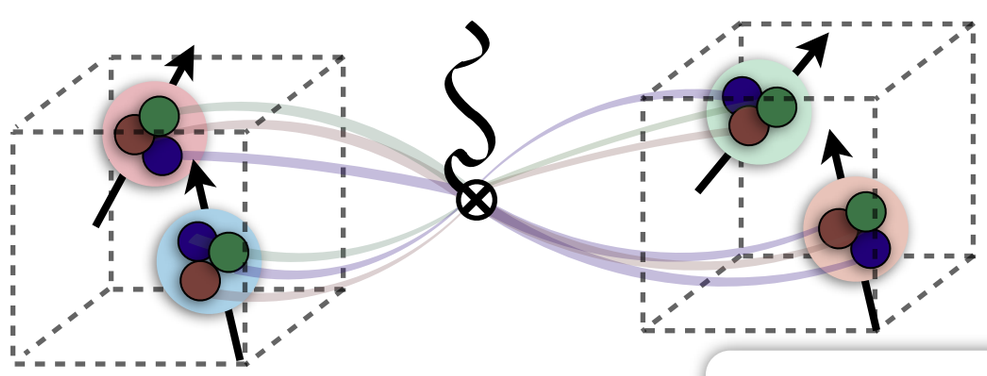

RB & Hansen [in preparation]

Transition amplitudes

- 0-to-2 with intrinsic spin:

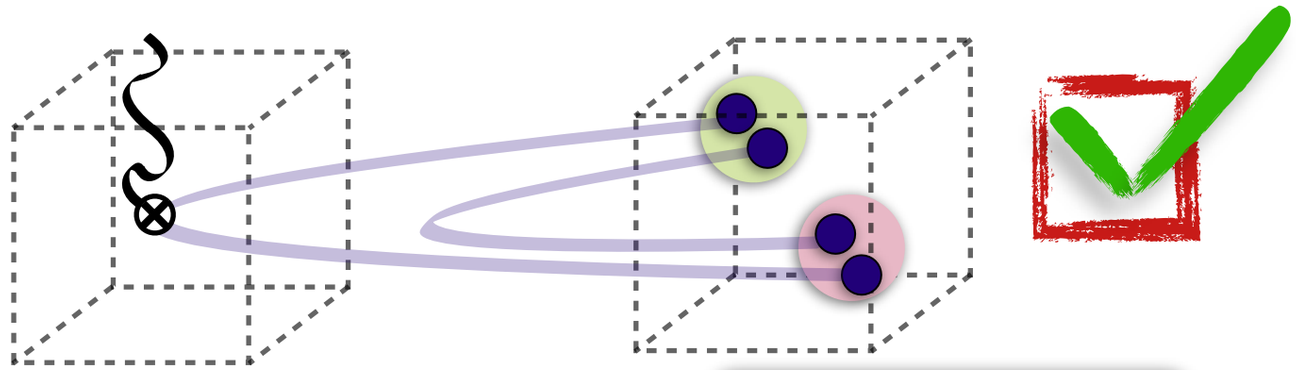

RB & Hansen (2015)

- 1-to-2 with intrinsic spin:

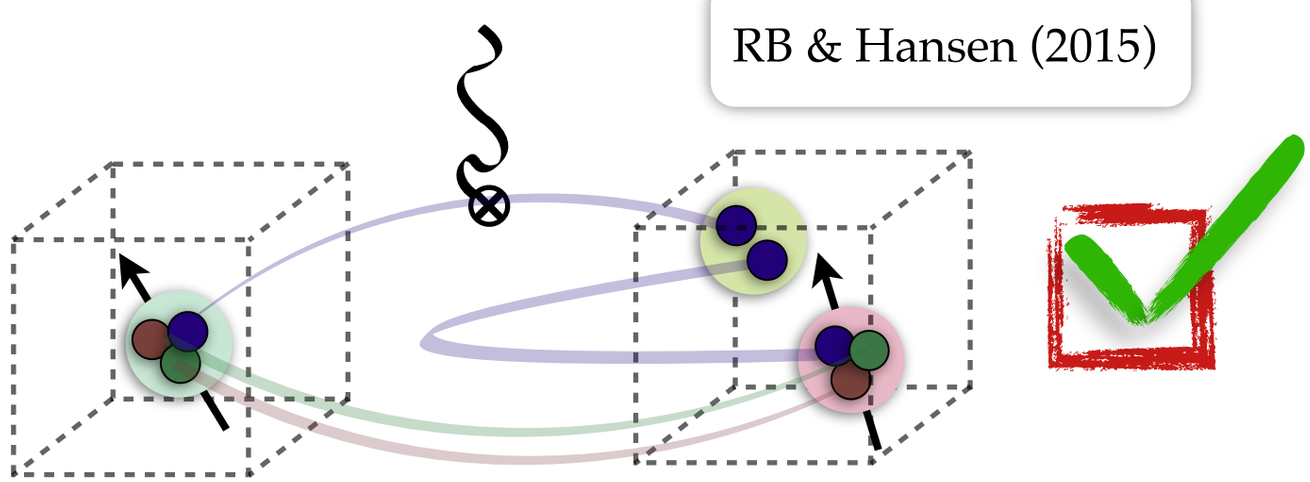

RB, Hansen & Walker-Loud (2014) / RB & Hansen (2015)

- 2-to-2 with intrinsic spin:

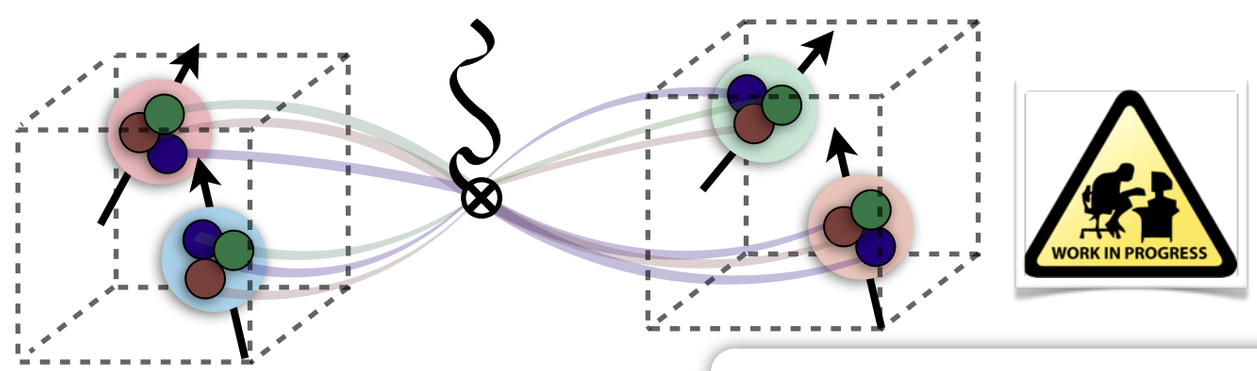

RB & Hansen [in preparation]

Transition amplitudes

- 0-to-2 with intrinsic spin:

RB & Hansen (2015)

- 1-to-2 with intrinsic spin:

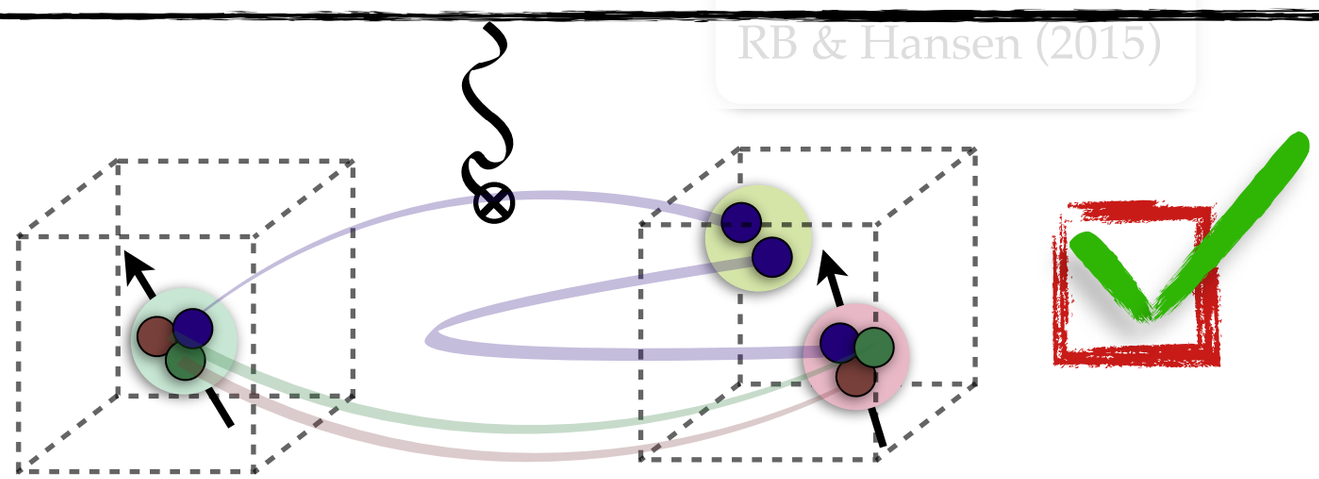

RB, Hansen & Walker-Loud (2014) / RB & Hansen (2015)

- 2-to-2 with intrinsic spin:

Transition Amplitudes

$$|\langle E'_n, \mathbf{P}', L|\widetilde{\mathcal{J}}_A(0, \mathbf{P}-\mathbf{P}')|E_0, \mathbf{P}, L, 1\rangle| = \frac{1}{\sqrt{2E_0}}\sqrt{\mathcal{H}_A^{\text{in}}\ \mathcal{R}(E'_n, \mathbf{P}')\ \mathcal{H}_A^{\text{out}}}$$

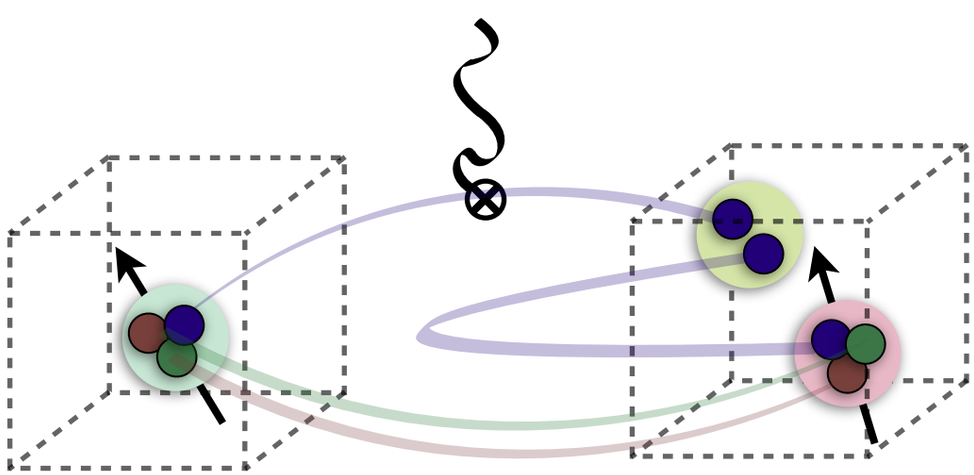

RB, Hansen & Walker-Loud (2014)

RB & Hansen (2015)

Transition Amplitudes

$$|\langle E'_n, \mathbf{P}', L|\widetilde{\mathcal{J}}_A(0, \mathbf{P}-\mathbf{P}')|E_0, \mathbf{P}, L, 1\rangle| = \frac{1}{\sqrt{2E_0}}\sqrt{\mathcal{H}_A^{\text{in}}\ \mathcal{R}(E'_n, \mathbf{P}')\ \mathcal{H}_A^{\text{out}}}$$

final state

external current

initial state

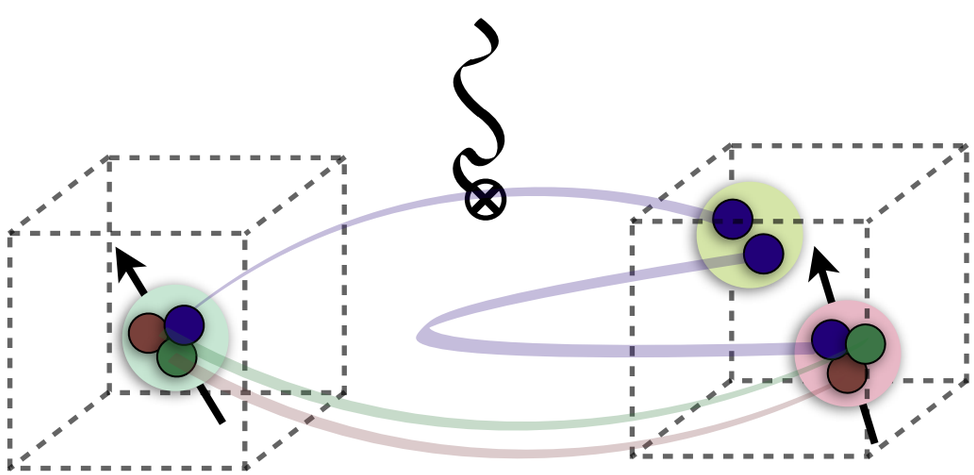

RB, Hansen & Walker-Loud (2014)

RB & Hansen (2015)

Transition Amplitudes

$$|\langle E'_n, \mathbf{P}', L|\widetilde{\mathcal{J}}_A(0, \mathbf{P}-\mathbf{P}')|E_0, \mathbf{P}, L, 1\rangle| = \frac{1}{\underline{\sqrt{2E_0}}}\sqrt{\mathcal{H}_A^{\text{in}}\ \mathcal{R}(E'_n, \mathbf{P}')\ \mathcal{H}_A^{\text{out}}}$$

energy of initial particle

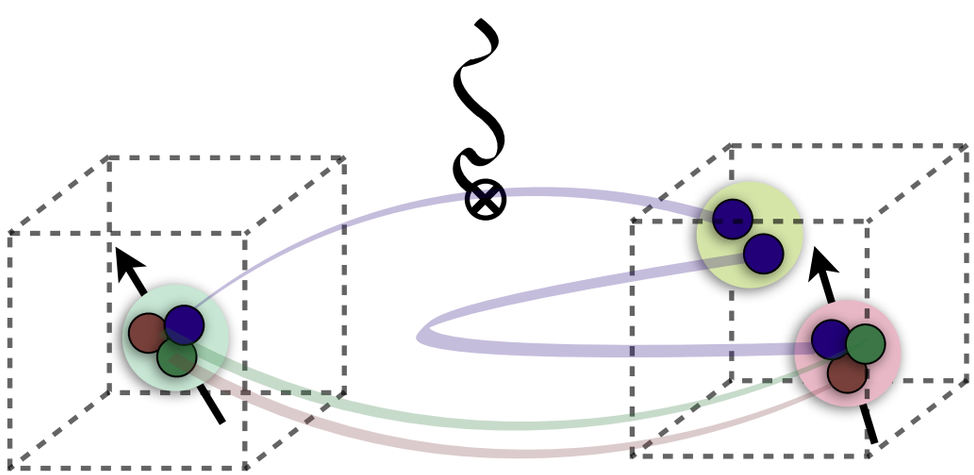

RB, Hansen & Walker-Loud (2014)

RB & Hansen (2015)

Transition Amplitudes

$$|\langle E'_n, \mathbf{P}', L|\widetilde{\mathcal{J}}_A(0, \mathbf{P}-\mathbf{P}')|E_0, \mathbf{P}, L, 1\rangle| = \frac{1}{\sqrt{2E_0}}\sqrt{\underline{\mathcal{H}_A^{\text{in}}}\ \mathcal{R}(E'_n, \mathbf{P}')\ \underline{\mathcal{H}_A^{\text{out}}}}$$

fully dressed, on-shell infinite volume transition amplitude!

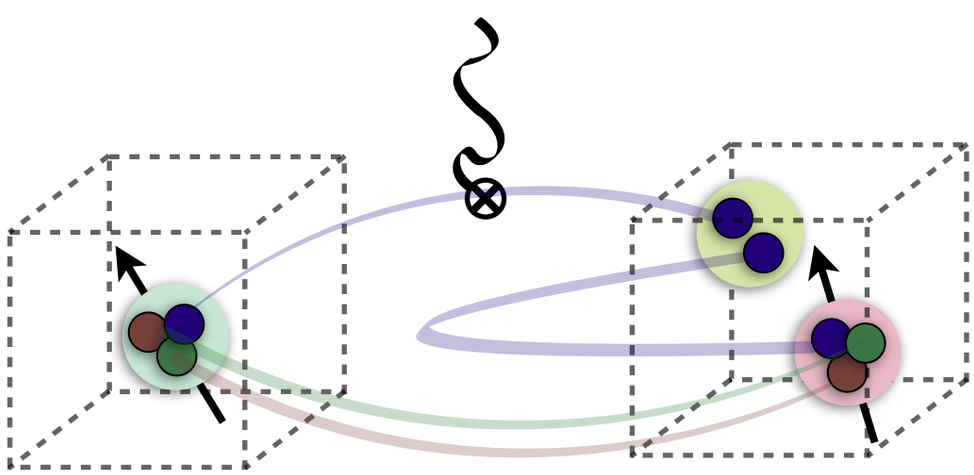

RB, Hansen & Walker-Loud (2014)

RB & Hansen (2015)

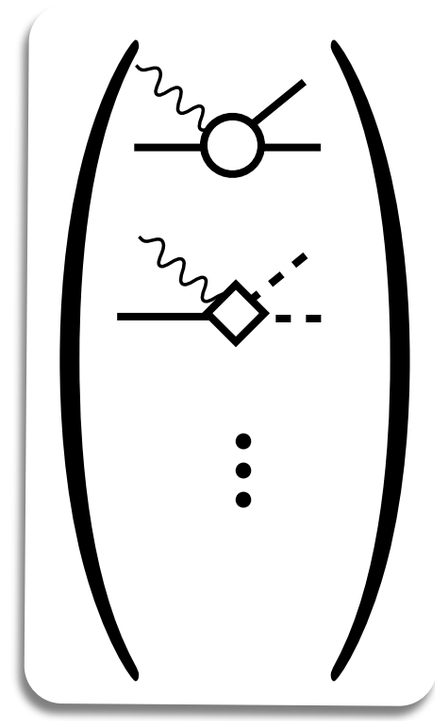

a vector in the space of open channels

Transition Amplitudes

$$|\langle E'_n, \mathbf{P}', L|\widetilde{\mathcal{J}}_A(0, \mathbf{P}-\mathbf{P}')|E_0, \mathbf{P}, L, 1\rangle| = \frac{1}{\sqrt{2E_0}}\sqrt{\mathcal{H}_A^{\text{in}}\ \mathcal{R}(E'_n, \mathbf{P}')\ \mathcal{H}_A^{\text{out}}}$$

fully dressed, on-shell infinite volume transition amplitude!

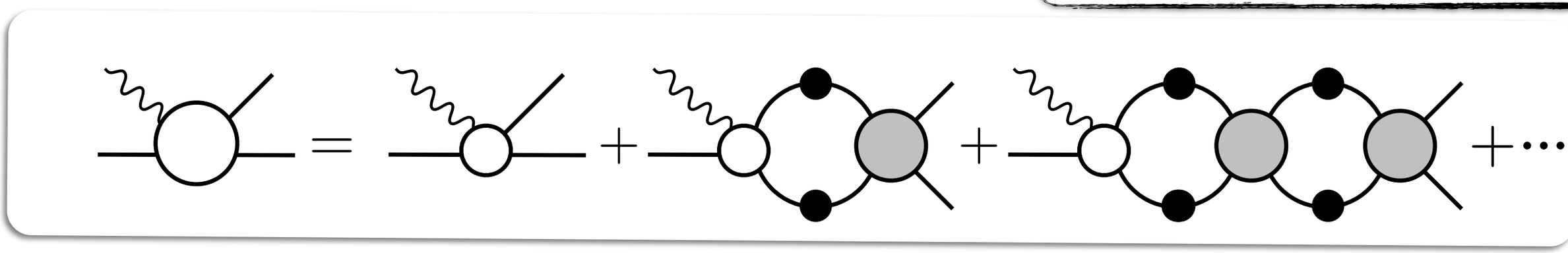

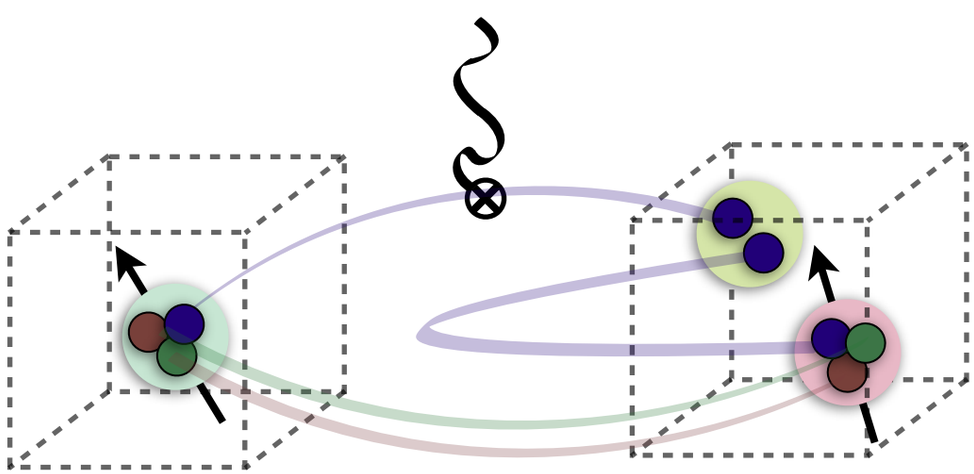

RB, Hansen & Walker-Loud (2014)

RB & Hansen (2015)

Transition Amplitudes

$$|\langle E'_n, \mathbf{P}', L|\widetilde{\mathcal{J}}_A(0, \mathbf{P}-\mathbf{P}')|E_0, \mathbf{P}, L, 1\rangle| = \frac{1}{\sqrt{2E_0}}\sqrt{\mathcal{H}_A^{\text{in}}\ \underline{\mathcal{R}(E'_n, \mathbf{P}')}\ \mathcal{H}_A^{\text{out}}}$$

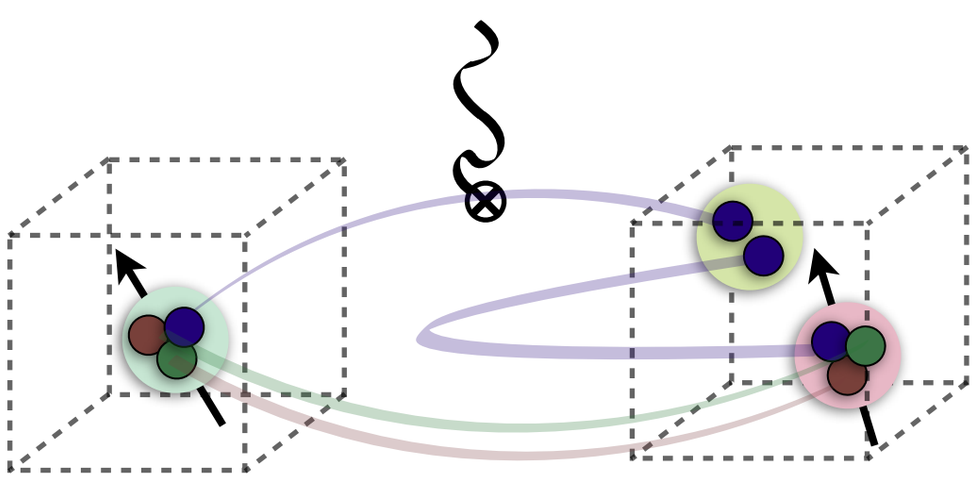

RB, Hansen & Walker-Loud (2014)

RB & Hansen (2015)

two-particle propagator residue, depends on energy, phase shifts and derivative of phase shifts

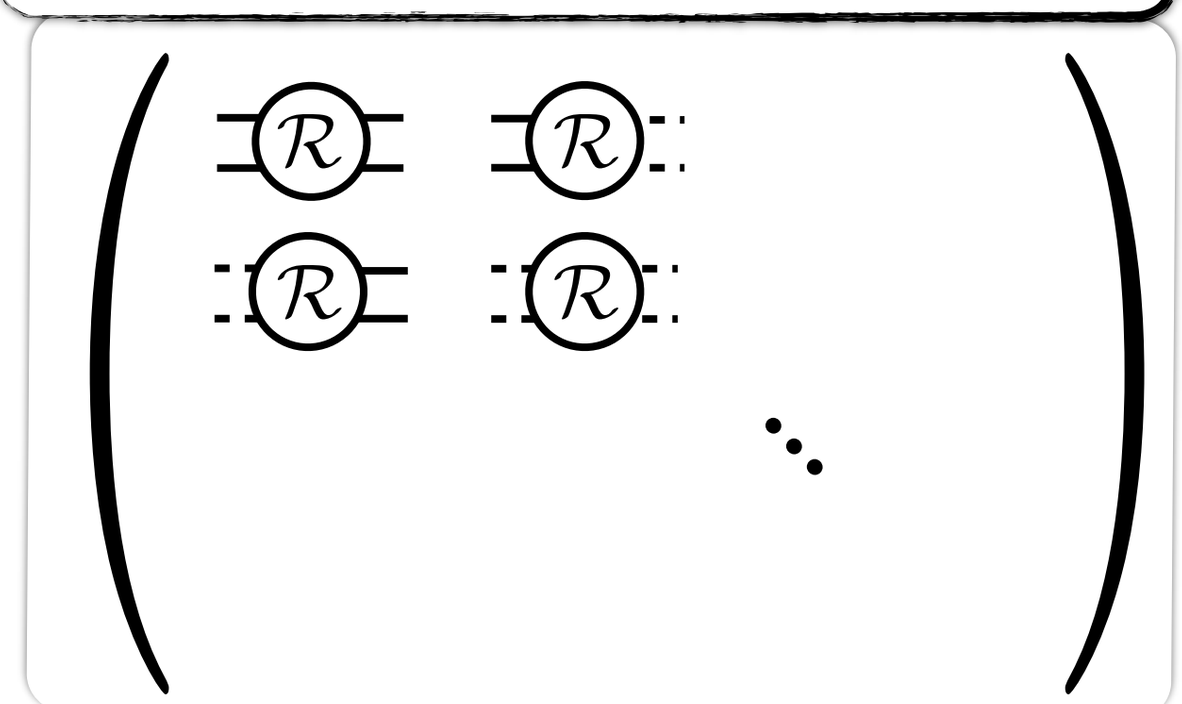

a matrix in the space of open channels

Transition Amplitudes

$$|\langle E'_n, \mathbf{P}', L|\widetilde{\mathcal{J}}_A(0, \mathbf{P}-\mathbf{P}')|E_0, \mathbf{P}, L, 1\rangle| = \frac{1}{\sqrt{2E_0}}\sqrt{\mathcal{H}_A^{\text{in}}\ \mathcal{R}(E'_n, \mathbf{P}')\ \mathcal{H}_A^{\text{out}}}$$

- Model independent & non-perturbative
- Universal: lattice QCD, lattice EFT, cold atoms, etc.
- Arbitrary quantum numbers for two particles
- General volumes and boundary conditions: periodic, anti-periodic , or any linear combination on any rectangular prism
- "Just a mapping": between finite/infinite volume physics. Not a one-to-one, but rather a one-to-many.

RB, Hansen & Walker-Loud (2014)

RB & Hansen (2015)

Lüscher formalism

- Lüscher (1986), (1991)
- Rummukainen and Gottlieb (1995)
- Bedaque (2004)
- Li and Liu (2004)
- Feng, Li, and Liu (2004)
- Christ, Kim, and Yamazaki (2005)
- Kim, Sachrajda, and Sharpe (2005)
- Bernard, Lage, Meissner, and Rusetsky (2008)
- Ishizuka (2009)
- Bour, Koenig, Lee, Hammer, and Meissner (2011)
- Gockeler, Horsley, Lage, Meissner, Rakow, Rusetsky, Schierholz, Zanotti (2012)
- Hansen and Sharpe (2012)
- **RB** and Davoudi (2012)
- Li and Liu (2013)
- **RB**, Davoudi, and Luu (2013)
- **RB**, Davoudi, Luu and Savage (2013)
- **RB** (2014)
- ...

Lellouch-Lüscher formalism

- Lellouch & Lüscher (2000)
- Lin, G. Martinelli, C. T. Sachrajda (2001)
- Christ, Kim, and Yamazaki (2005)
- Kim, Sachrajda, and. Sharpe (2005)
- Hansen and Sharpe (2012)
- Agadjanov, V. Bernard, Meissner, Rusetsky (2013)
- **RB**, Hansen & Walker-Loud (2014)
- **RB** & Hansen (2015)
- ...

Transition Amplitudes

$$|\langle E'_n, \mathbf{P}', L|\widetilde{\mathcal{J}}_A(0, \mathbf{P}-\mathbf{P}')|E_0, \mathbf{P}, L, 1\rangle| = \frac{1}{\sqrt{2E_0}}\sqrt{\mathcal{H}_A^{\text{in}}\ \mathcal{R}(E'_n, \mathbf{P}')\ \mathcal{H}_A^{\text{out}}}$$

summarizes everything previously done and more!

Lellouch-Lüscher formalism

- Lellouch & Lüscher (2000)
- Lin, G. Martinelli, C. T. Sachrajda (2001)
- Christ, Kim, and Yamazaki (2005)
- Kim, Sachrajda, and. Sharpe (2005)
- Hansen and Sharpe (2012)
- Agadjanov, V. Bernard, Meissner, Rusetsky (2013)
- **RB**, Hansen & Walker-Loud (2014)
- **RB** & Hansen (2015)

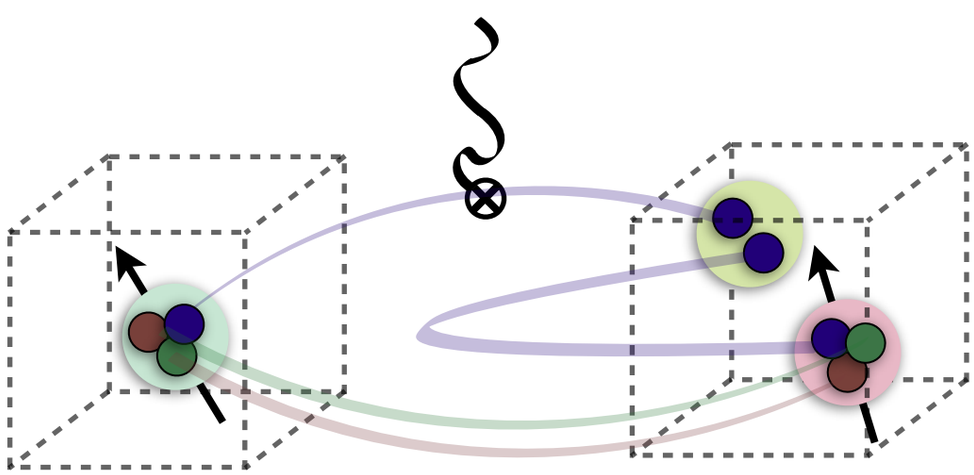

RB, Hansen & Walker-Loud (2014)

RB & Hansen (2015)

Transition Amplitudes

$$\frac{\langle E'_n, \mathbf{P}', L|\widetilde{\mathcal{J}}_{A_1}(0, \mathbf{P}-\mathbf{P}')|E_0, \mathbf{P}, L, 1\rangle}{\langle E'_n, \mathbf{P}', L|\widetilde{\mathcal{J}}_{A_2}(0, \mathbf{P}-\mathbf{P}')|E_0, \mathbf{P}, L, 1\rangle} = \frac{\mathcal{X}^\dagger\ \mathcal{R}(E'_n, \mathbf{P}')\ \mathcal{H}^{\text{out}}_{A_1}}{\underline{\mathcal{X}^\dagger}\ \mathcal{R}(E'_n, \mathbf{P}')\ \mathcal{H}^{\text{out}}_{A_2}}$$

a generic vector in the space of open channels and angular momentum

Absolute sign of matrix elements is unphysical, but relative sign is determinable

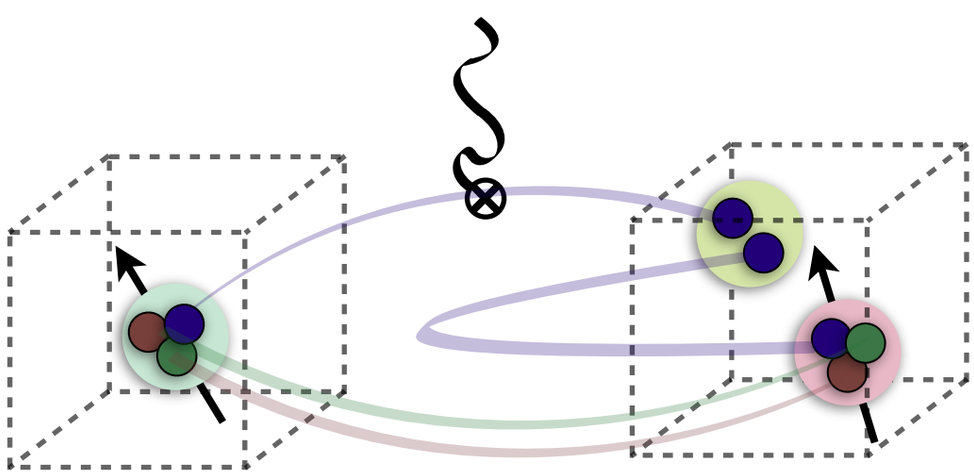

RB, Hansen & Walker-Loud (2014)

RB & Hansen (2015)

Transition amplitudes

(other applications)

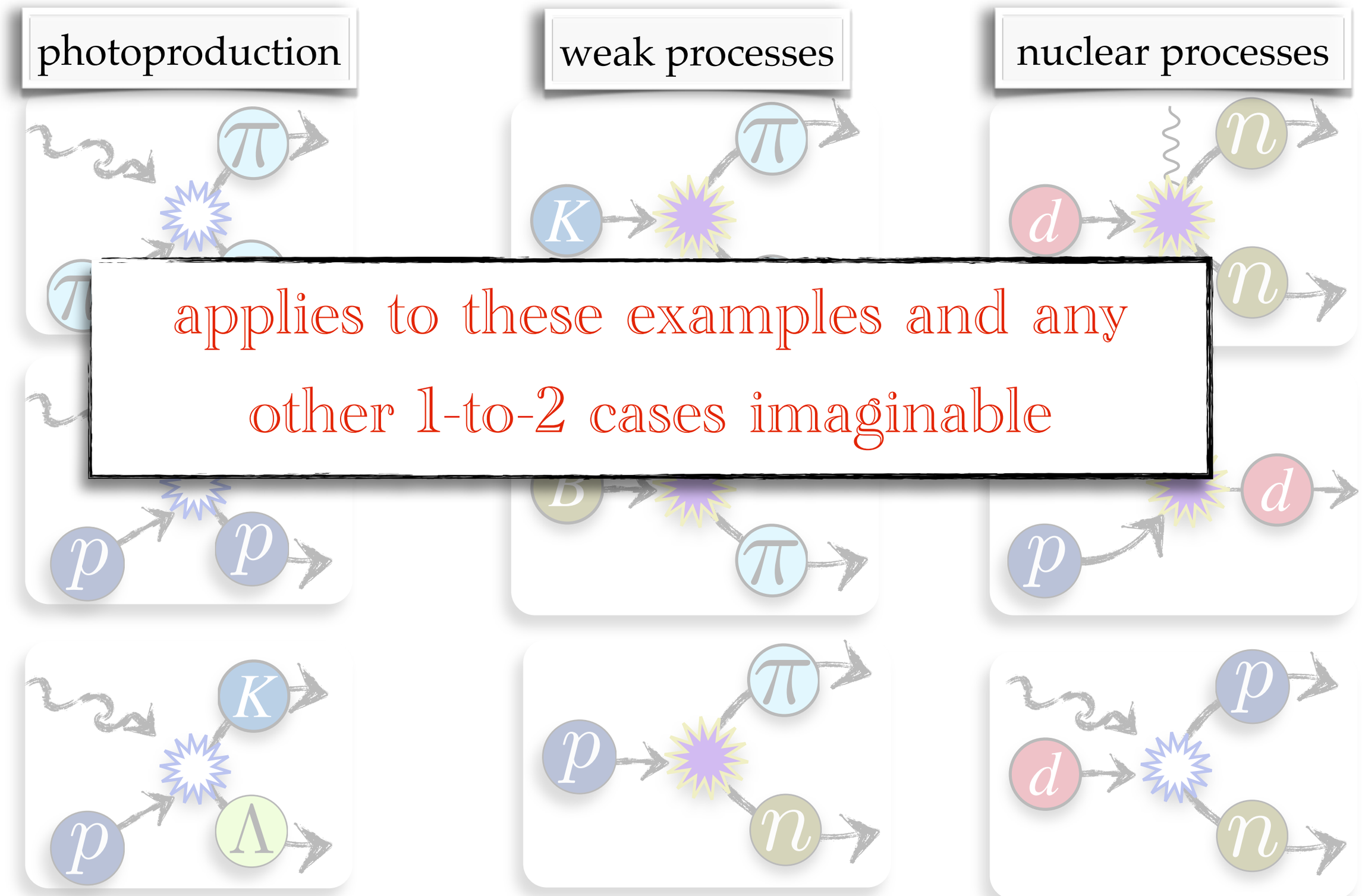

applies to these examples and any

other 1-to-2 cases imaginable

a sketch of the derivation

for 0-to-2 and 1-to-2 processes

à la mode de Kim, Sachrajda, and Sharpe (2005)

Two-point function

$$C_L(x_4 - y_4, \mathbf{P}) \equiv \int_L d\mathbf{x} \int_L d\mathbf{y}\; e^{-i\mathbf{P}\cdot(\mathbf{x}-\mathbf{y})} \Big[\langle 0|T\mathcal{A}(x)\mathcal{B}^\dagger(y)|0\rangle\Big]_L$$

1. Evaluate two-point correlation function using:

- Complete set of states
- Feynman diagrams

2. Match:

- Spectrum
- Overlap matrix elements

Two-point function

$$C_L(x_4 - y_4, \mathbf{P}) \equiv \int_L d\mathbf{x} \int_L d\mathbf{y}\; e^{-i\mathbf{P}\cdot(\mathbf{x}-\mathbf{y})} \Big[\langle 0|T\mathcal{A}(x)\mathcal{B}^\dagger(y)|0\rangle\Big]_L$$

Using complete set of states:

$$\begin{aligned} &C_L(x_4 - y_4, \mathbf{P}) \\ &\quad = \int_L d\mathbf{x} \int_L d\mathbf{y}\; e^{-i\mathbf{P}\cdot(\mathbf{x}-\mathbf{y})} \sum_n \Big[\langle 0|\mathcal{A}(x_4,\mathbf{x})|E_n,\mathbf{P},L\rangle\Big]_L \Big[\langle E_n,\mathbf{P},L|\mathcal{B}^\dagger(y_4,\mathbf{y})|0\rangle\Big]_L \\ &\quad = L^6 \sum_n e^{-E_n(x_4-y_4)} \Big[\langle 0|\mathcal{A}(0)|E_n,\mathbf{P},L\rangle\Big]_L \Big[\langle E_n,\mathbf{P},L|\mathcal{B}^\dagger(0)|0\rangle\Big]_L . \end{aligned}$$

assuming finite volume states are normalized to 1

Two-point function

Using Feynman diagrams:

$$\int \frac{dP_0}{2\pi} e^{iP_0(x_0-y_0)} \Bigg\{$$

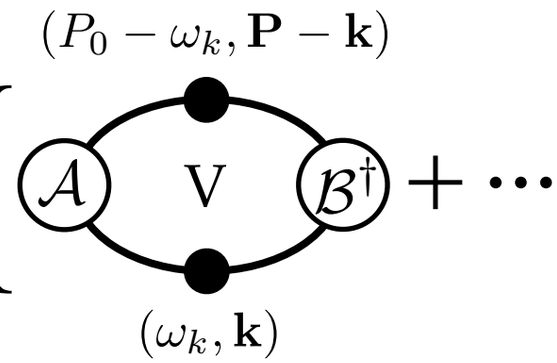

$$+ \cdots \Bigg\}$$

- λ = helicity
- This holds for any particle with spin
- **The particle must be stable**
- Consequence of:
  - relativity
  - helicity conservation

Single body propagator with arbitrary spin:

smooth and finite

$$[$$

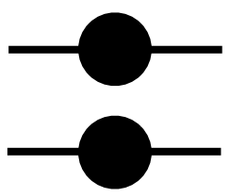

$$]_{\lambda\alpha,\lambda'\alpha'} = \left[\frac{\delta_{\lambda,\lambda'}\delta_{\alpha,\alpha'}}{(4\omega_k\omega_{Pk})(E-\omega_k-\omega_{Pk}+i\epsilon)} + \cdots \right]$$

Two-point function

Using Feynman diagrams:

$$\int \frac{dP_0}{2\pi} e^{iP_0(x_0-y_0)} \Bigg\{$$

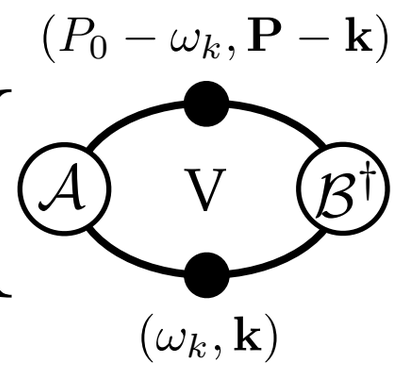

$$+ \cdots \Bigg\}$$

On-shell states can sample boundaries of your volume and lead to power law volume dependence

Matrices in *angular momentum / open channel* space

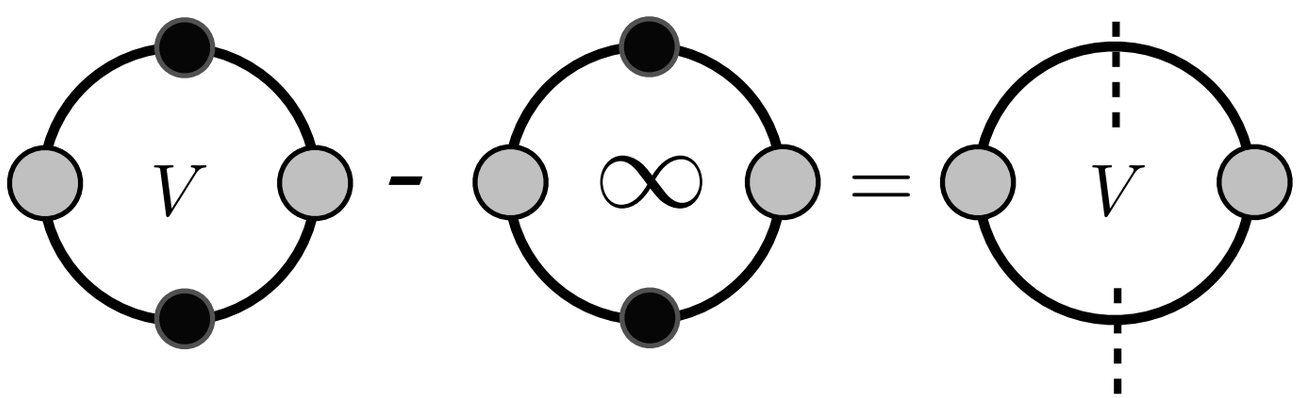

$$= -L\ F(P,L)\ R$$

Two-point function

Using Feynman diagrams:

$$\int \frac{dP_0}{2\pi} e^{iP_0(x_0-y_0)} \Big\{$$

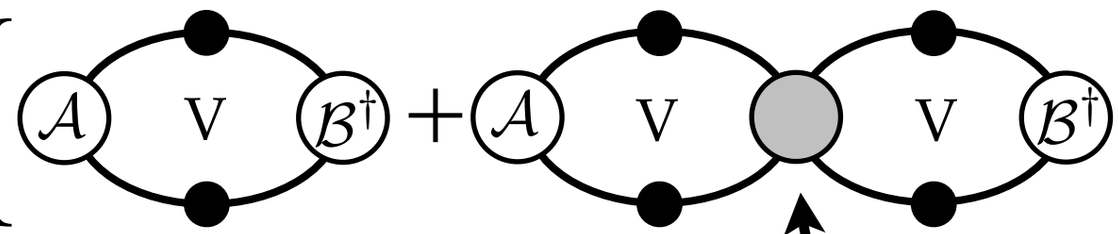

$$\Big\}$$

Bethe-Salpeter kernel

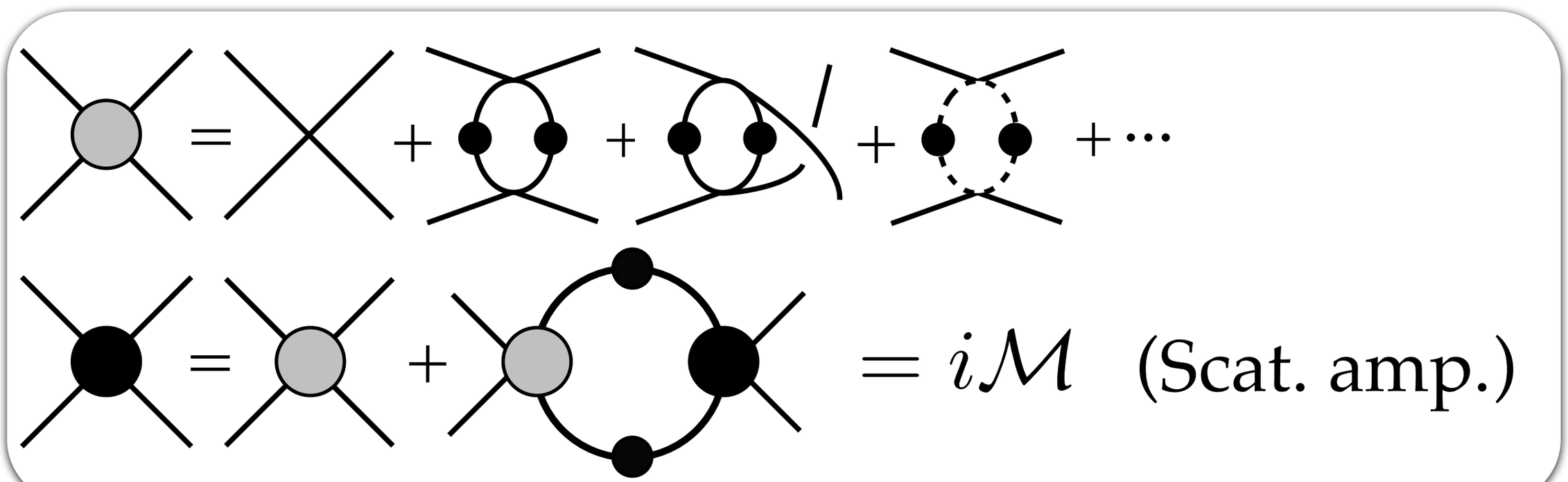

Two-point function

Using Feynman diagrams:

$$\int \frac{dP_0}{2\pi} e^{iP_0(x_0-y_0)} \Big\{$$

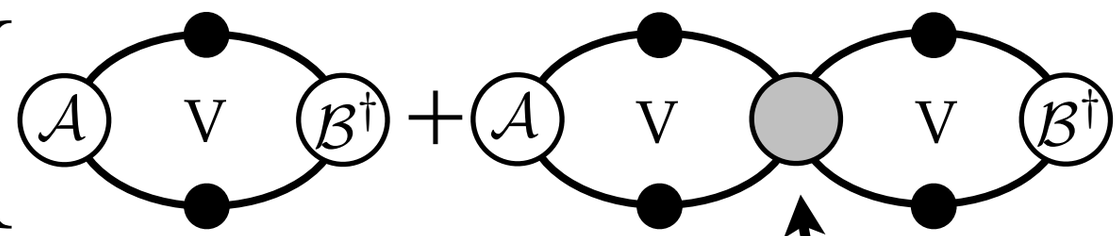

$$+ \cdots \Big\}$$

Bethe-Salpeter kernel

Generalization to two-particle multichannels:

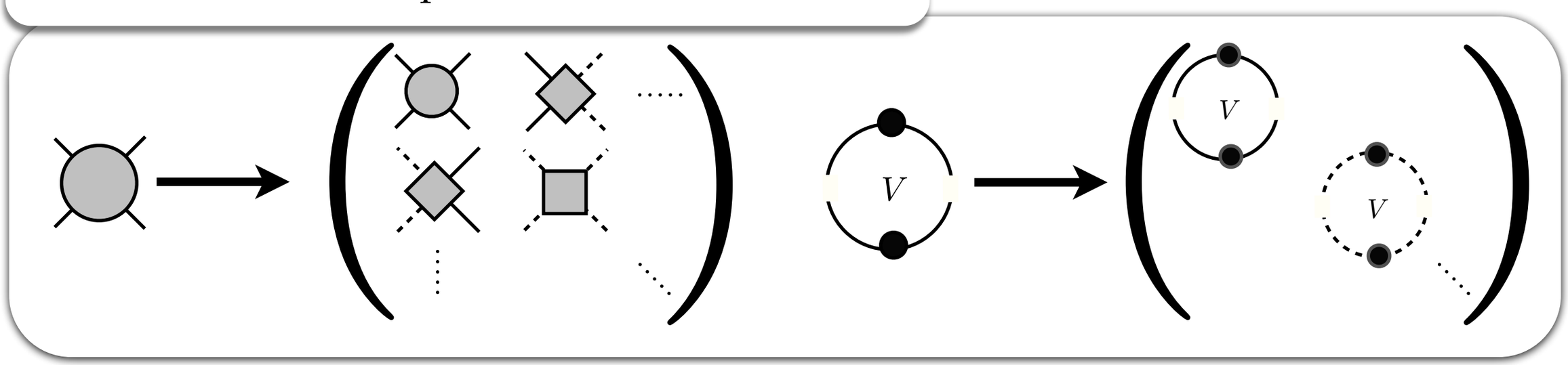

Two-point function

Using Feynman diagrams:

$$\int \frac{dP_0}{2\pi} e^{iP_0(x_0-y_0)} \Big\{$$

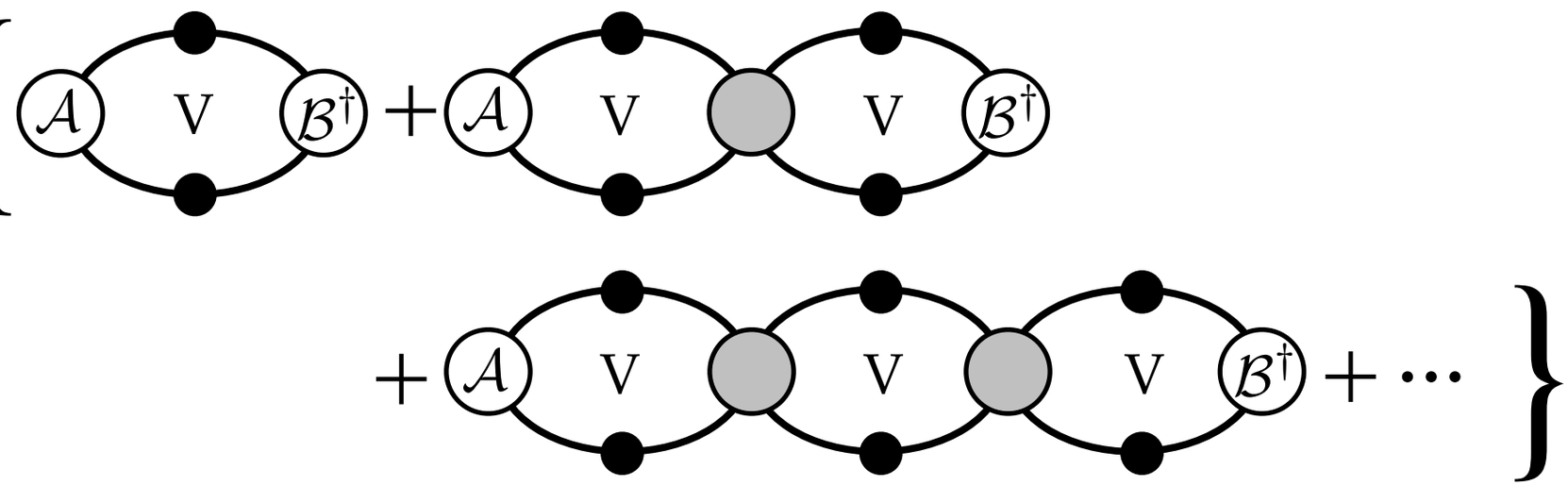

$$\Big\}$$

$$= L^3 \int \frac{dP_0}{2\pi} e^{iP_0(x_0-y_0)} \left\{ C_\infty(P) - A(P) \frac{1}{F^{-1}(P,L) + \mathcal{M}(P)} B^\dagger(P) \right\}$$

$\langle 0|\mathcal{A}(0)|E, \mathbf{P}, \{J\}, \text{in}\rangle$

$\langle E, \mathbf{P}, \{J'\}, \text{out}|\mathcal{B}^\dagger(0)|0\rangle$

asymptotic infinite volume, two-particle states

Two-point function

Using Feynman diagrams:

$$\int \frac{dP_0}{2\pi} e^{iP_0(x_0-y_0)} \Big\{$$

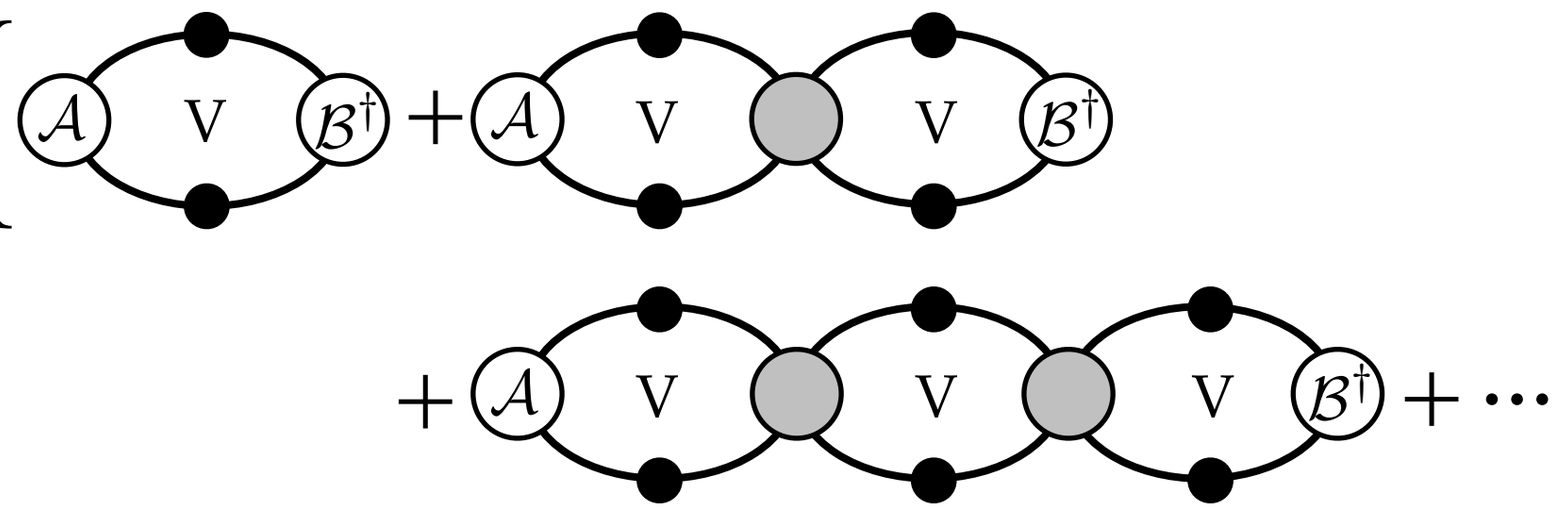

$$\Big\}$$

$$= L^3 \int \frac{dP_0}{2\pi} e^{iP_0(x_0-y_0)} \left\{ C_\infty(P) - A(P) \frac{1}{F^{-1}(P,L) + \mathcal{M}(P)} B^\dagger(P) \right\}$$

poles satisfy: $\det[F^{-1}(P,L) + \mathcal{M}(P)] = 0$

generalization of Lüscher formalism for arbitrary spin, multichannel, two-particle systems **[RB (2014)]**

Lüscher formalism

- Lüscher (1986), (1991)
- Rummukainen and Gottlieb (1995)
- Bedaque (2004)
- Li and Liu (2004)
- Feng, Li, and Liu (2004)
- Christ, Kim, and Yamazaki (2005)
- Kim, Sachrajda, and. Sharpe (2005)
- Bernard, Lage, Meissner, and Rusetsky (2008)
- Ishizuka (2009)
- Bour, Koenig, Lee, Hammer, and Meissner (2011)
- Gockeler, Horsley, Lage, Meissner, Rakow (2012)
- Hansen and Sharpe (2012)
- **RB** and Davoudi (2012)
- Li and Liu (2013)
- **RB**, Davoudi, and Luu (2013)
- **RB**, Davoudi, Luu and Savage (2013)
- **RB** (2014)
- ...

summarizes everything previously done and more!

poles satisfy: $\det[F^{-1}(P,L) + \mathcal{M}(P)] = 0$

generalization of Lüscher formalism for arbitrary spin, multichannel, two-particle systems **[RB (2014)]**

Two-point function

Using Feynman diagrams:

$$\int \frac{dP_0}{2\pi} e^{iP_0(x_0-y_0)} \Big\{$$

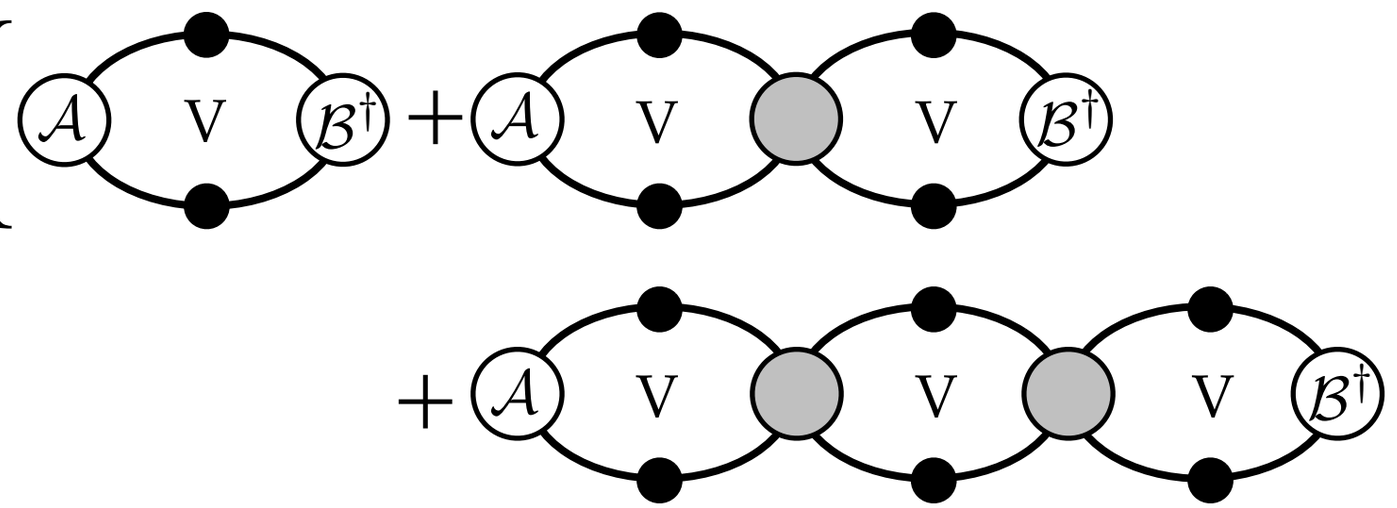

$$\Big\}$$

$$= L^3 \int \frac{dP_0}{2\pi} e^{iP_0(x_0-y_0)} \left\{ C_\infty(P) - A(P) \frac{1}{F^{-1}(P,L) + \mathcal{M}(P)} B^\dagger(P) \right\}$$

Residue matrix: $\mathcal{R}_{\{J\},\{J'\}}(E_n, \mathbf{P}) \equiv \lim_{P_4 \to iE_n} \left[-(iP_4 + E_n) \frac{1}{F^{-1}(P,L) + \mathcal{M}(P)} \right]_{\{J\},\{J'\}}$

$$|E, \mathbf{P}, \{J\}, \text{in}\rangle \equiv |E, \mathbf{P}, a, J, M, l, S, s_1^a, s_2^a, \text{in}\rangle$$

Two-point function

Using Feynman diagrams:

$$\int \frac{dP_0}{2\pi} e^{iP_0(x_0-y_0)} \Big\{$$

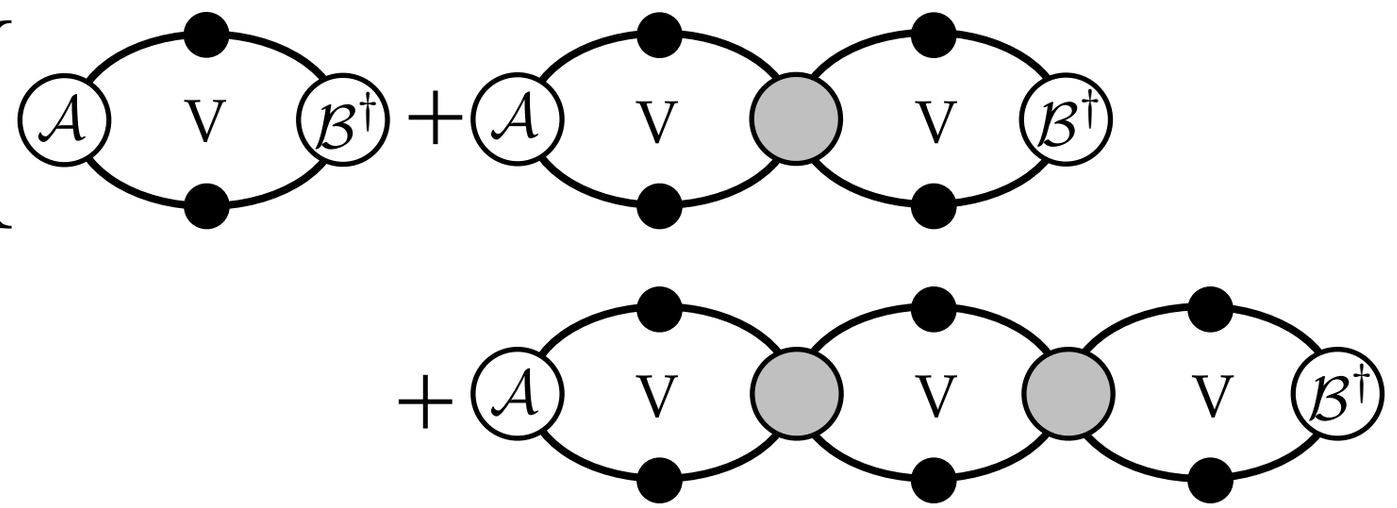

$$\Big\}$$

$$= L^3 \int \frac{dP_0}{2\pi} e^{iP_0(x_0-y_0)} \left\{ C_\infty(P) - A(P) \frac{1}{F^{-1}(P,L) + \mathcal{M}(P)} B^\dagger(P) \right\}$$

$$= \sum_n e^{-E_n(x_4-y_4)} L^3 \langle 0|\mathcal{A}(0)|E_n, \mathbf{P}, \{J\}, \text{in}\rangle \Big[\mathcal{R}_{\{J\},\{J'\}}(E_n, \mathbf{P})\Big] \langle E_n, \mathbf{P}, \{J'\}, \text{out}|\mathcal{B}^\dagger(0)|0\rangle$$

mimics the outer product of finite volume states

Master equation

Equating both representation of the correlation functions:

$$\Big[\langle 0|\mathcal{A}(0)|E_n,\mathbf{P},L\rangle\Big]_L\Big[\langle E_n,\mathbf{P},L|\mathcal{B}^\dagger(0)|0\rangle\Big]_L = \frac{1}{L^3}\langle 0|\mathcal{A}(0)|E_n,\mathbf{P},\{J\},\mathrm{in}\rangle\Big[\mathcal{R}_{\{J\},\{J'\}}(E_n,\mathbf{P})\Big]\langle E_n,\mathbf{P},\{J'\},\mathrm{out}|\mathcal{B}^\dagger(0)|0\rangle$$

"Relating finite volume and infinite volume states"

Master equation

Equating both representation of the correlation functions:

$$\boxed{\begin{aligned}&\Big[\langle 0|\mathcal{A}(0)|E_n,\mathbf{P},L\rangle\Big]_L\Big[\langle E_n,\mathbf{P},L|\mathcal{B}^\dagger(0)|0\rangle\Big]_L = \\ &\qquad\qquad \frac{1}{L^3}\langle 0|\mathcal{A}(0)|E_n,\mathbf{P},\{J\},\mathrm{in}\rangle\Big[\mathcal{R}_{\{J\},\{J'\}}(E_n,\mathbf{P})\Big]\langle E_n,\mathbf{P},\{J'\},\mathrm{out}|\mathcal{B}^\dagger(0)|0\rangle\end{aligned}}$$

"Relating finite volume and infinite volume states"

Similarly, can study three-point function:

$$\int \frac{dP_{i,0}}{2\pi}\frac{dP_{f,0}}{2\pi}e^{iP_{i,0}(x_{f,0}-y_0)}e^{iP_{f,0}(y_0-x_{i,0})}\Bigg\{$$

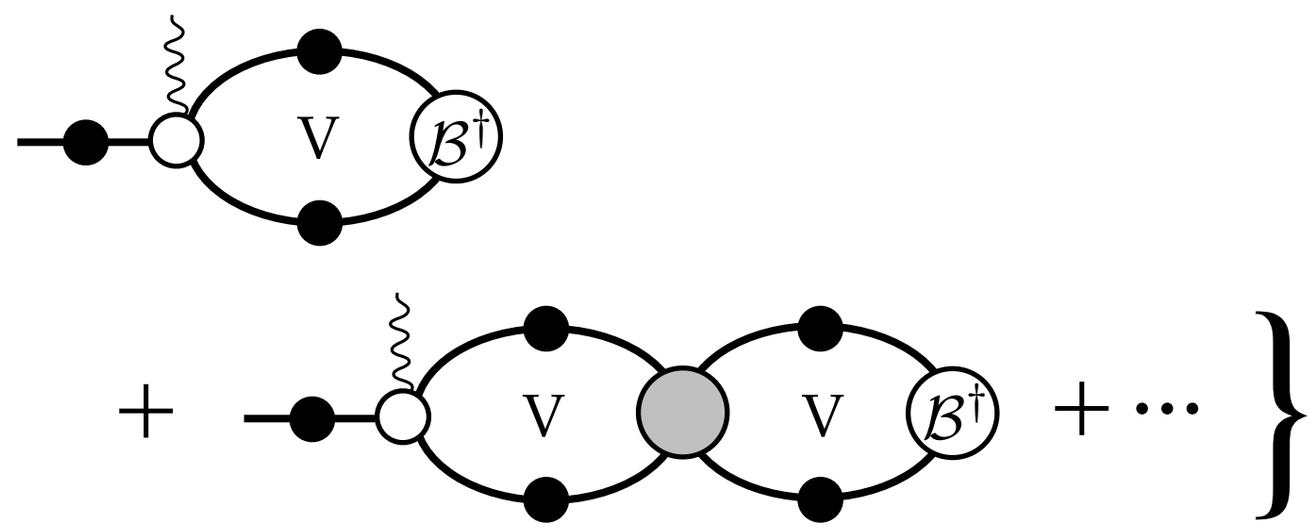

Alternatively, one can use clever choices for $\mathcal{A}(0),\ \mathcal{B}^\dagger(0)$

1-to-2 transitions

Using clever choices for $\mathcal{A}(0),\ \mathcal{B}^\dagger(0)$

$$\Big[\langle 0|\mathcal{A}(0)|E_n,\mathbf{P},L\rangle\Big]_L\Big[\langle E_n,\mathbf{P},L|\mathcal{B}^\dagger(0)|0\rangle\Big]_L = \frac{1}{L^3}\langle 0|\mathcal{A}(0)|E_n,\mathbf{P},\{J\},\text{in}\rangle\Big[\mathcal{R}_{\{J\},\{J'\}}(E_n,\mathbf{P})\Big]\langle E_n,\mathbf{P},\{J'\},\text{out}|\mathcal{B}^\dagger(0)|0\rangle$$

$$\mathcal{B}^\dagger(0) = \frac{1}{\sqrt{2E_0'L^3}}\mathcal{J}_A(0)a^\dagger_{E_0',\mathbf{P}'}\,,\quad \mathcal{A}(0) = \frac{1}{\sqrt{2E_0'L^3}}a_{E_0',\mathbf{P}'}\mathcal{J}_A^\dagger(0)$$

and some massaging...

$$|\langle E_n,\mathbf{P},L|\widetilde{\mathcal{J}}_A(0,\mathbf{P}'-\mathbf{P})|E_0',\mathbf{P}',L,1\rangle| = \frac{1}{\sqrt{2E_0'}}\sqrt{\mathcal{H}_A^{\text{in}}\ \mathcal{R}(E_n,\mathbf{P})\ \mathcal{H}_A^{\text{out}}}$$

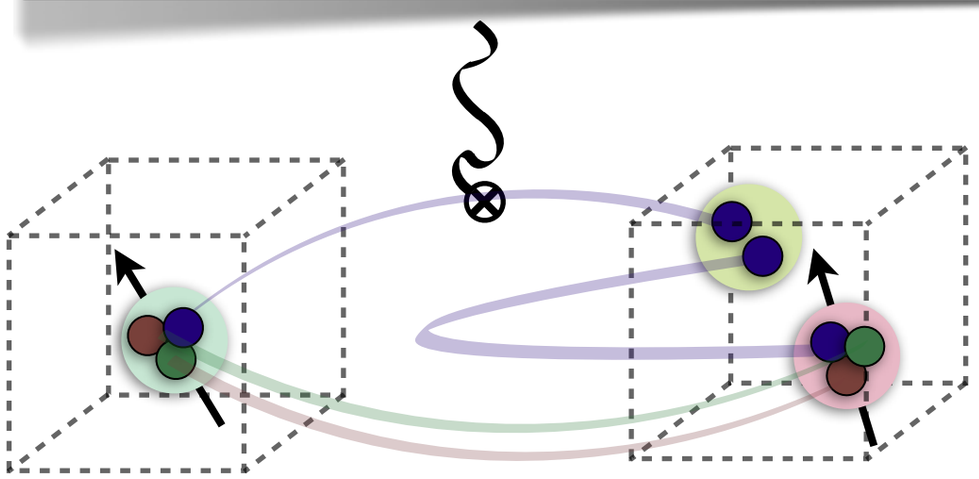

Subducing this equation onto cubic irreps is straightforward, once one understands how to subduce the two-body quantization condition

0-to-2 transitions

Using clever choices for $\mathcal{A}(0),\ \mathcal{B}^\dagger(0)$

$$\Big[\langle 0|\mathcal{A}(0)|E_n,\mathbf{P},L\rangle\Big]_L\Big[\langle E_n,\mathbf{P},L|\mathcal{B}^\dagger(0)|0\rangle\Big]_L = \frac{1}{L^3}\langle 0|\mathcal{A}(0)|E_n,\mathbf{P},\{J\},\text{in}\rangle\Big[\mathcal{R}_{\{J\},\{J'\}}(E_n,\mathbf{P})\Big]\langle E_n,\mathbf{P},\{J'\},\text{out}|\mathcal{B}^\dagger(0)|0\rangle$$

$$\mathcal{B}^\dagger(0)=\mathcal{J}_A(0)\,,\quad \mathcal{A}(0)=\mathcal{J}_A^\dagger(0)$$

and some massaging...

$$\Big|\langle E_n,\mathbf{P},L|\widetilde{\mathcal{J}}_A(0,-\mathbf{P})|0\rangle\Big| = \sqrt{\mathcal{V}^{\text{in}}_{A,\{J\}}\Big[L^3\mathcal{R}_{\{J\},\{J'\}}(E_n,\mathbf{P})\Big]\mathcal{V}^{\text{out}}_{A,\{J'\}}}$$

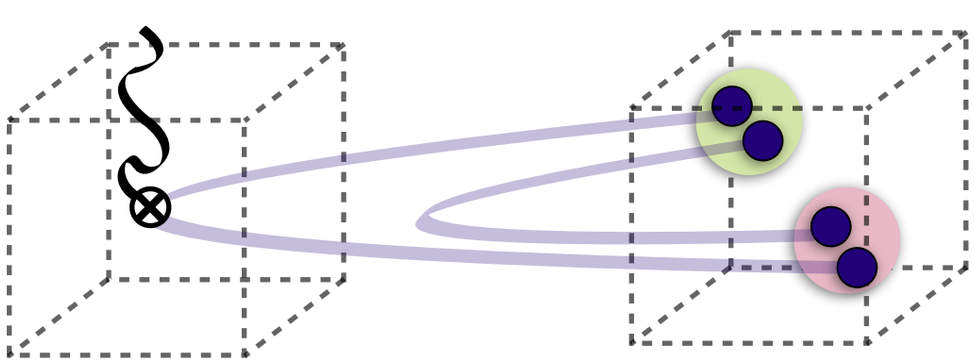

Subducing this equation onto cubic irreps is straightforward, once one understands how to subduce the two-body quantization condition

Examples: X-to-ππ

X -to-ππ could stand for:

- πγ*-to-ππ, B-to-ππll, D-to-ππll, ...

in the ϱ-channel

let's ignore partial wave mixing for now...

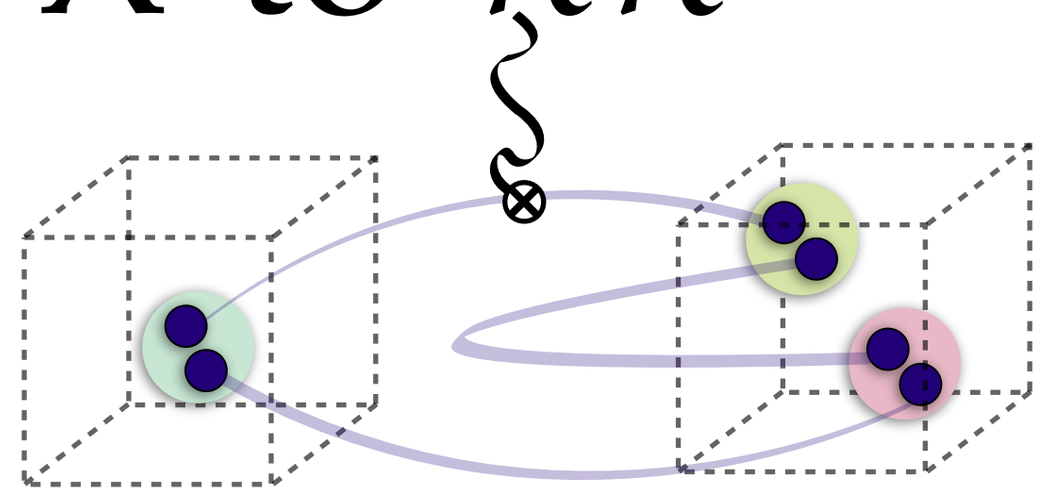

$$\frac{|\mathcal{H}_{X\to\pi\pi}|^2}{|\langle\pi\pi,n|\mathcal{J}|X\rangle_L|^2} = \frac{32\pi E_X\ E^*_{\pi\pi,n}}{q^*_{\pi\pi,n}}\ \left.\frac{\partial(\delta_P+\phi^{\mathbf{d}})}{\partial P_0}\right|_{P_0=E_{\pi\pi,n}}$$

Examples: X-to-ππ

X -to-ππ could stand for:

- πγ*-to-ππ, B-to-ππll, D-to-ππll, ...

in the ϱ-channel

let's ignore partial wave mixing for now...

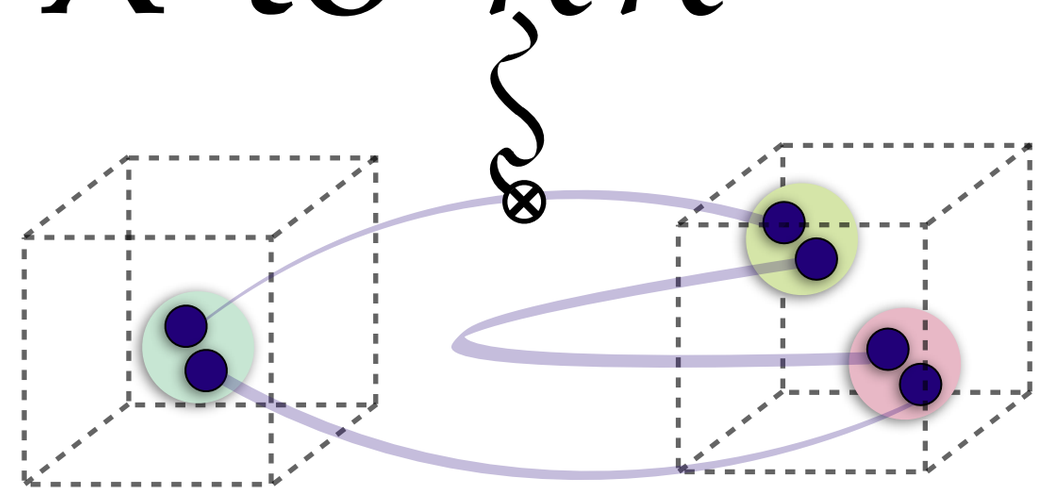

$$\frac{|\mathcal{H}_{X\to\pi\pi}|^2}{|\langle\pi\pi,n|\mathcal{J}|X\rangle_L|^2} = \frac{32\pi E_X\ E^*_{\pi\pi,n}}{q^*_{\pi\pi,n}}\ \left.\frac{\partial(\delta_P+\phi^{\mathbf{d}})}{\partial P_0}\right|_{P_0=E_{\pi\pi,n}}$$

$$\frac{|\mathcal{H}_{X\to\pi\pi}|^2}{|\langle\pi\pi,n|\mathcal{J}|X\rangle_L|^2} = 4E_X\frac{E^2_{\pi\pi,n}}{\nu_n}L^3$$

free limit

Examples: X-to-ππ

X -to-ππ could stand for:

- πγ*-to-ππ, B-to-ππll, D-to-ππll, ...

in the ϱ-channel

let's ignore partial wave mixing for now...

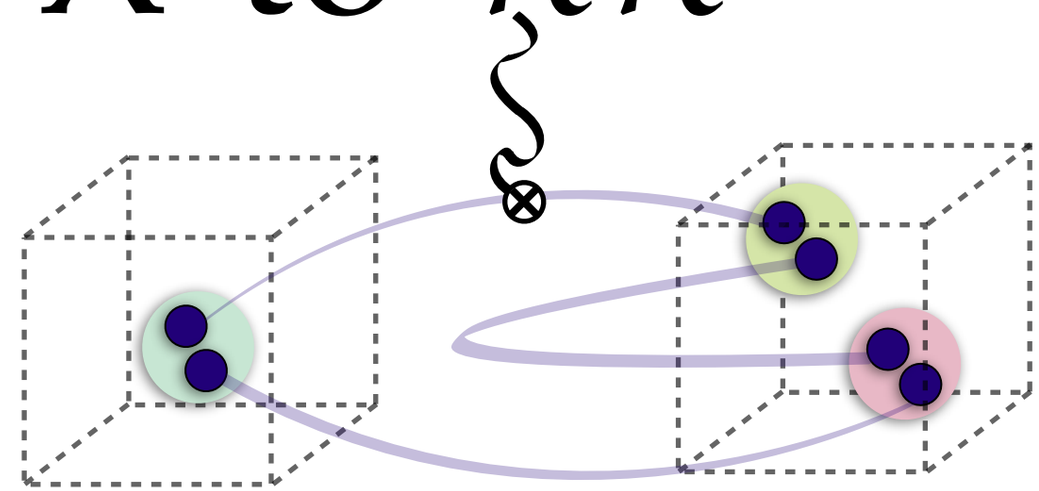

$$\frac{|\mathcal{H}_{X\to\pi\pi}|^2}{|\langle\pi\pi,n|\mathcal{J}|X\rangle_L|^2} = \frac{32\pi E_X\ E^*_{\pi\pi,n}}{q^*_{\pi\pi,n}}\ \left.\frac{\partial(\delta_P+\phi^{\mathbf{d}})}{\partial P_0}\right|_{P_0=E_{\pi\pi,n}}$$

$$\frac{|\mathcal{H}_{X\to\pi\pi}|^2}{|\langle\pi\pi,n|\mathcal{J}|X\rangle_L|^2} = 4E_X\frac{E^2_{\pi\pi,n}}{\nu_n}L^3$$

free limit

$$\frac{|\mathcal{H}_{X\to\pi\pi}|^2}{|\langle\pi\pi,n|\mathcal{J}|X\rangle_L|^2} = 2E_X\frac{32\pi E_\rho}{q^*_\rho\Gamma_\rho}\left[1+\mathcal{O}(\Gamma_\rho/m_\rho)\right]$$

narrow-width limit

Million dollar question...

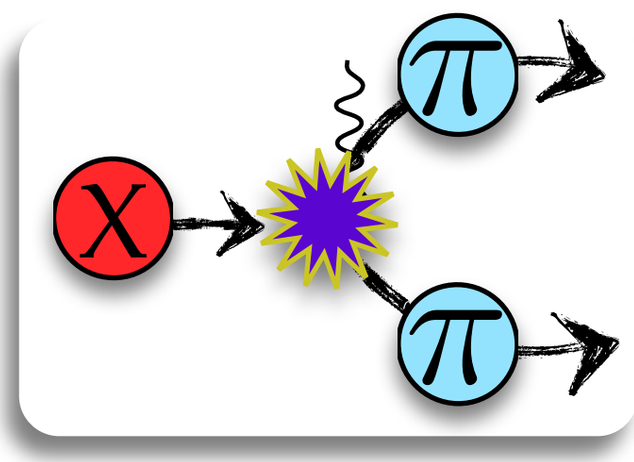

V.S.

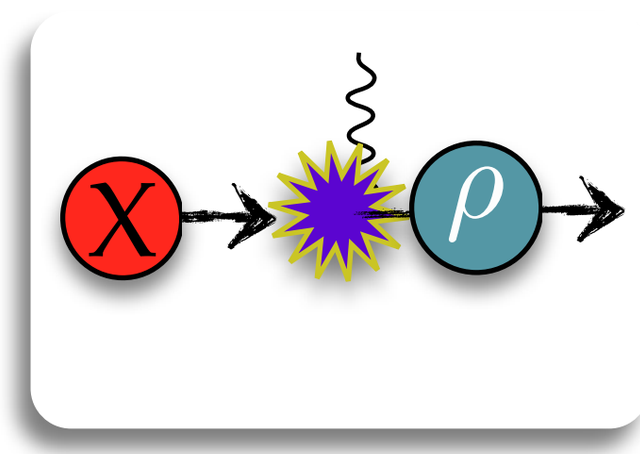

X-to-$\pi\pi$

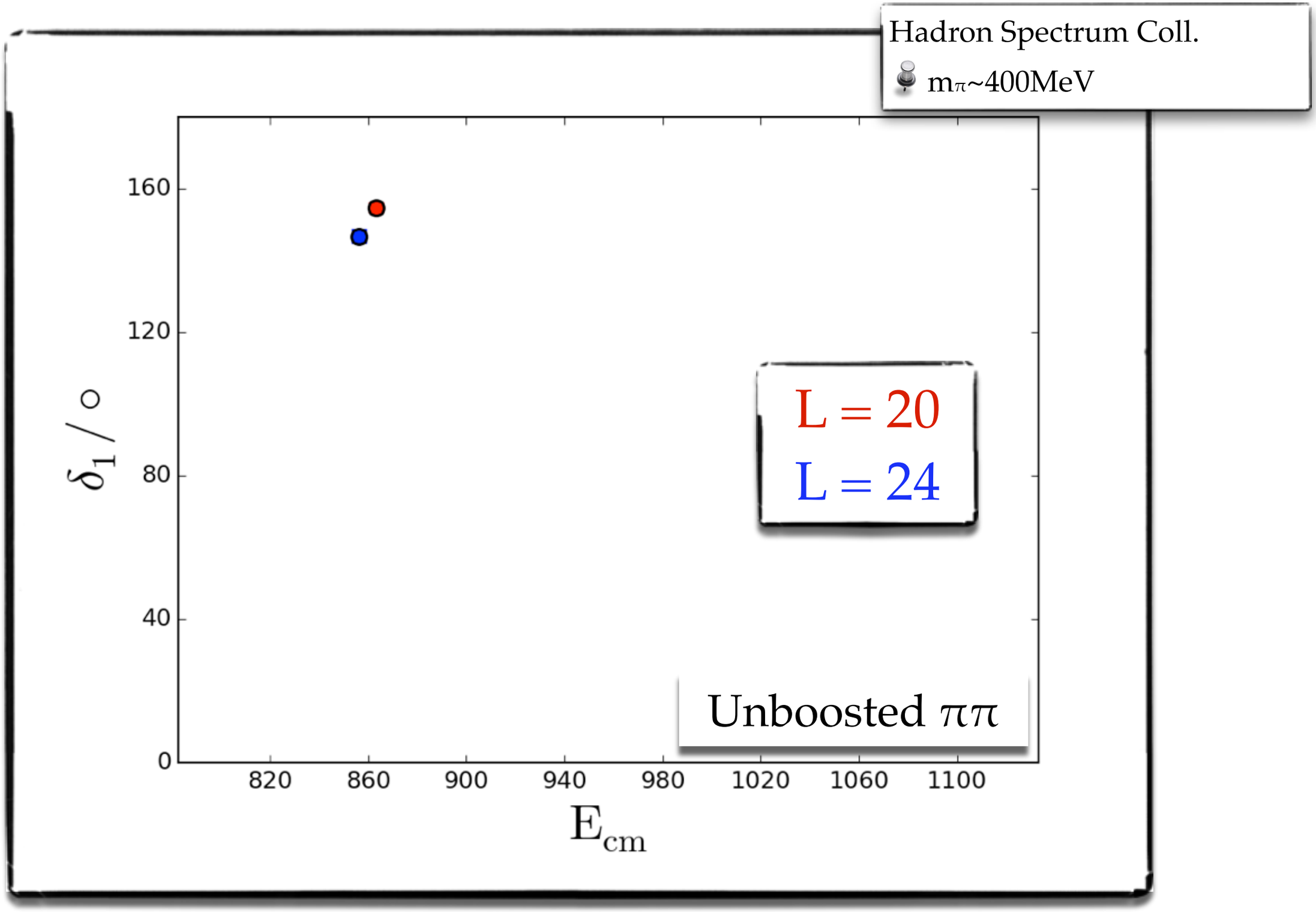
Hadron Spectrum Coll.
m_π~400MeV
L = 20
L = 24
Unboosted $\pi\pi$
δ_1 / °
0
40
80
120
160
820
860
900
940
980
1020
1060
1100
E_{cm}

X-to-$\pi\pi$

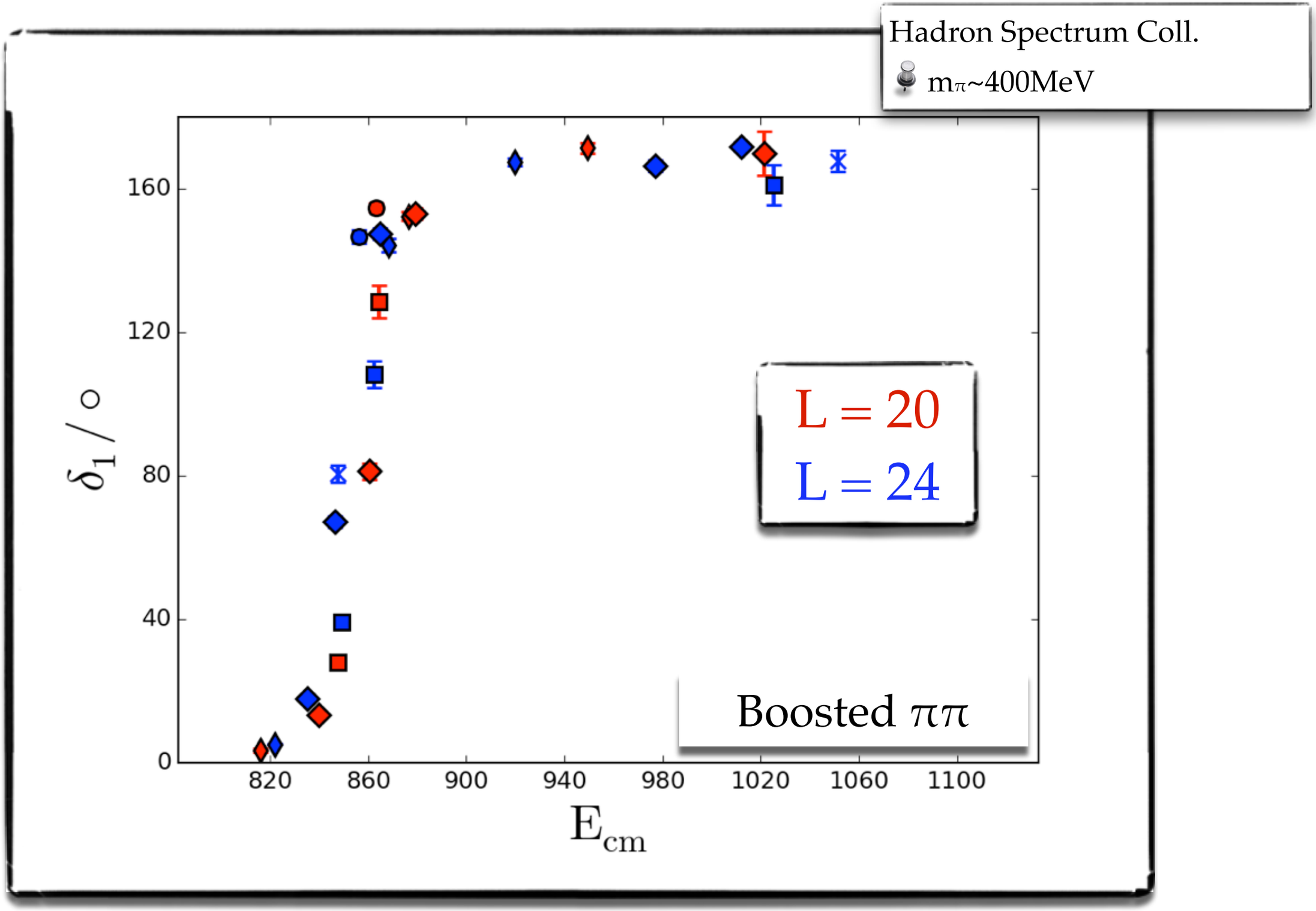
Hadron Spectrum Coll.
m_π~400MeV
L = 20
L = 24
Boosted $\pi\pi$
δ_1 / °
E_{cm}
0
40
80
120
160
820
860
900
940
980
1020
1060
1100

X-to-ππ

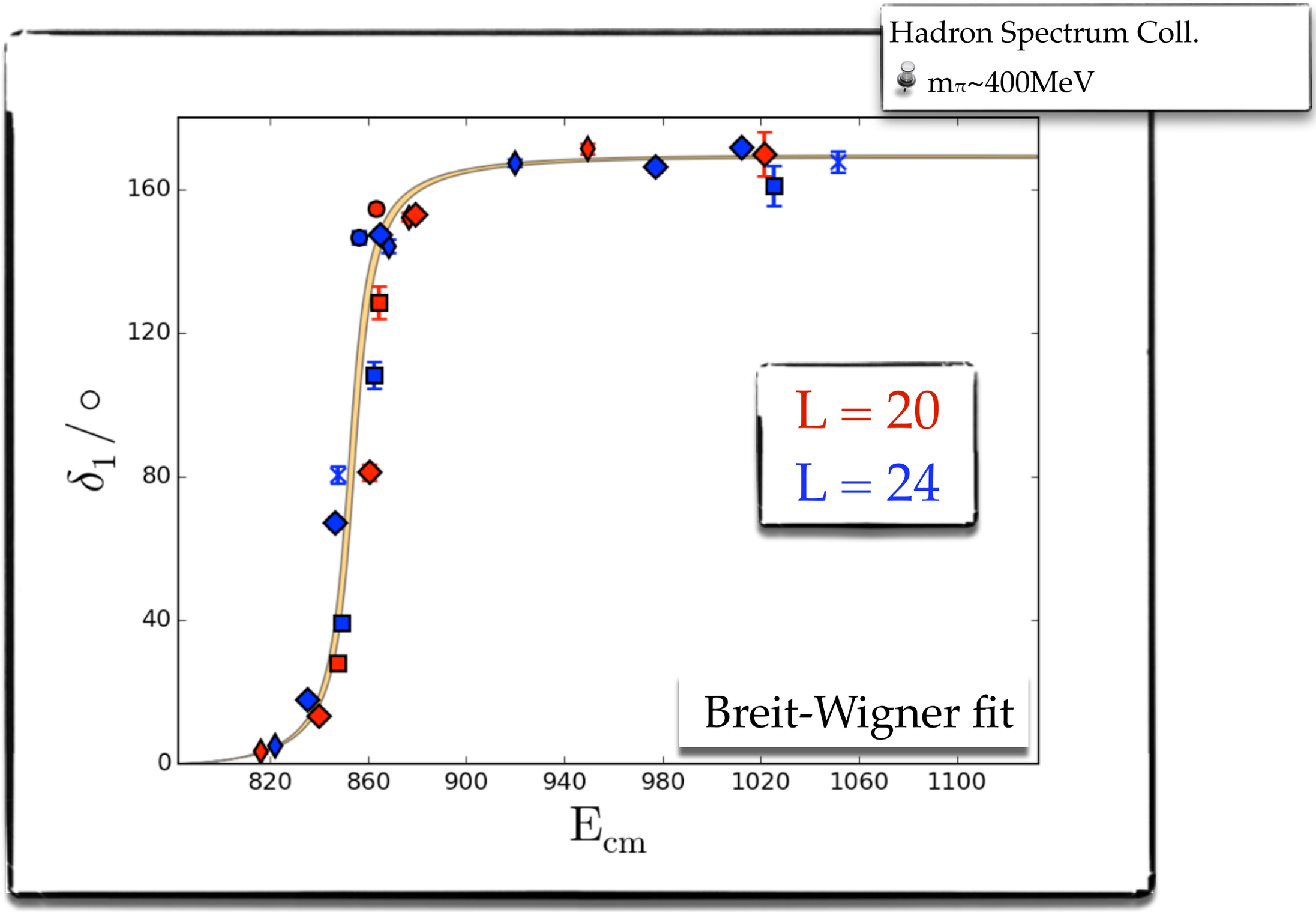
Hadron Spectrum Coll.
mπ~400MeV
L = 20
L = 24
Breit-Wigner fit
δ1 / °
Ecm
0
40
80
120
160
820
860
900
940
980
1020
1060
1100

X-to-$\pi\pi$

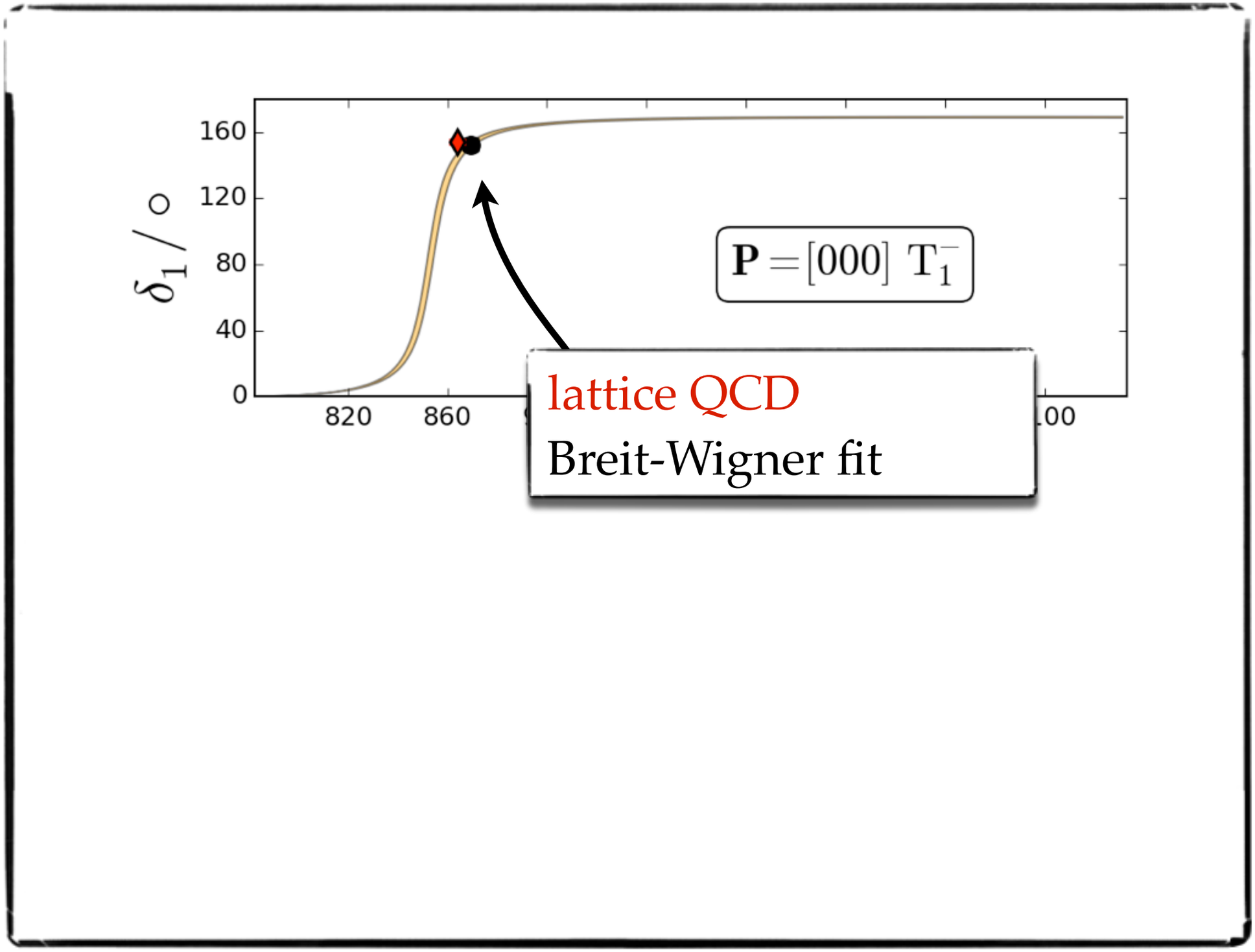
160
120
80
40
0
δ_1 / °
820
860
$\mathbf{P} = [000]\ \mathrm{T}_1^-$
lattice QCD
Breit-Wigner fit

X-to-$\pi\pi$

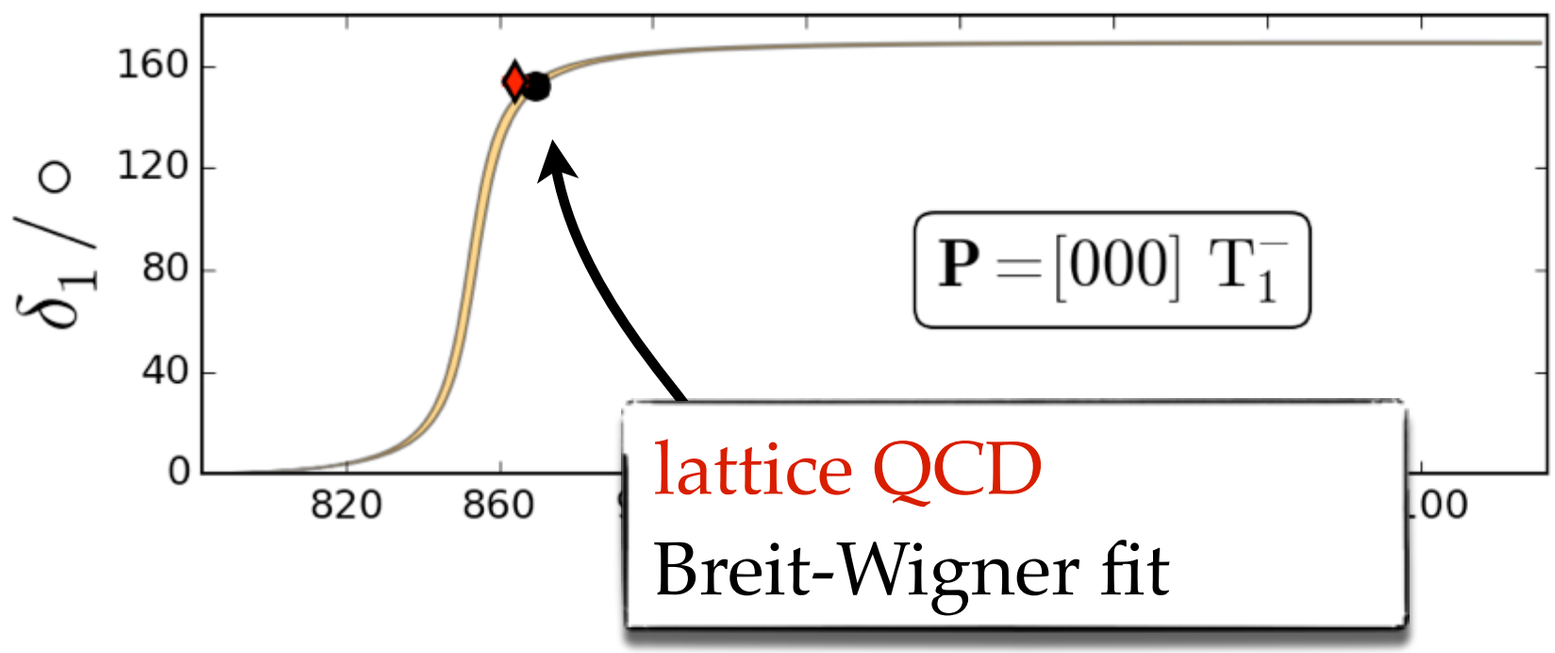

Note: there is an ambiguity as to which energy level is chosen: lattice QCD vs. "model"

X-to-$\pi\pi$

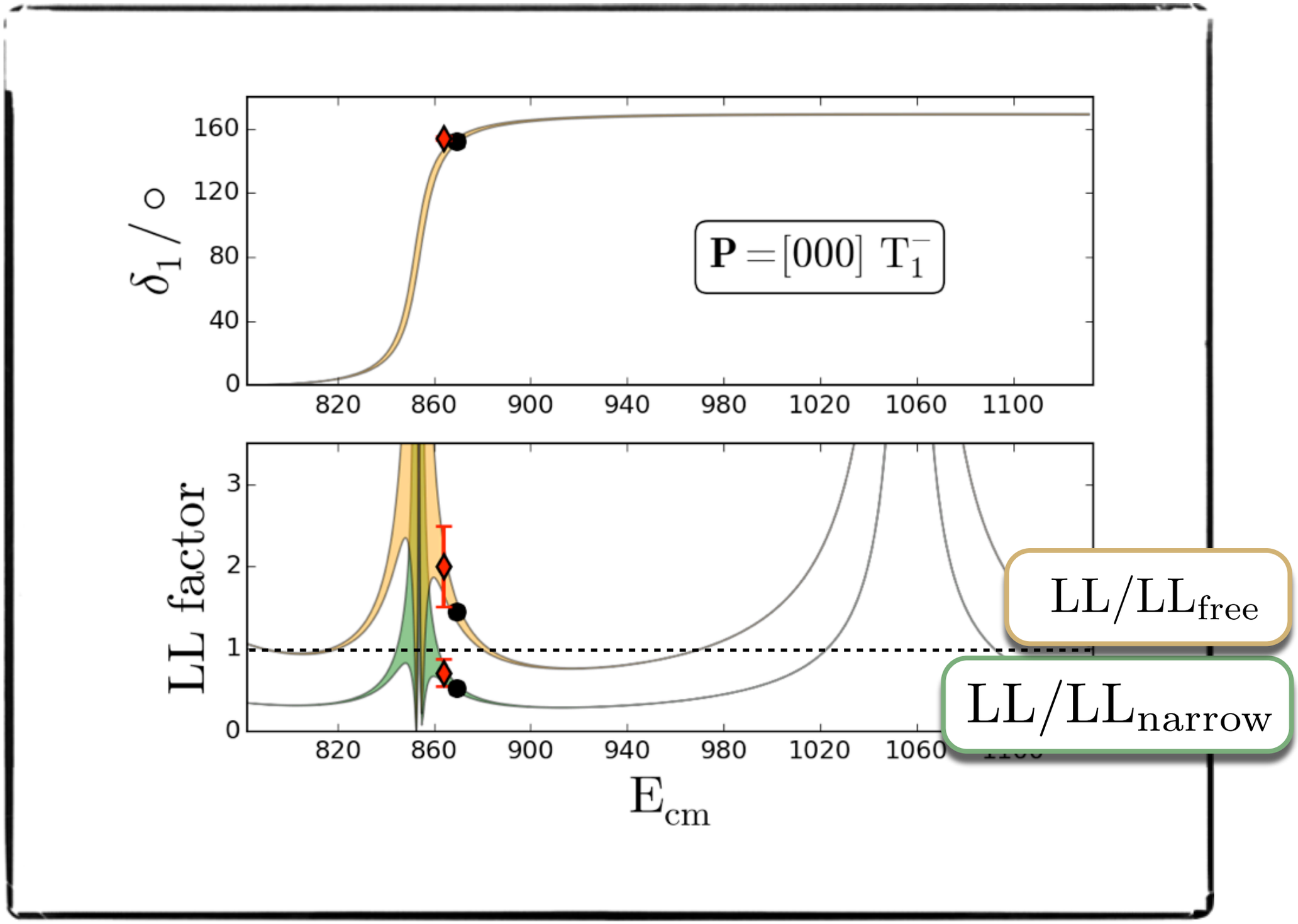
δ_1 / °
160
120
80
40
0
820
860
900
940
980
1020
1060
1100
$\mathbf{P} = [000]\ \mathrm{T}_1^-$
LL factor
3
2
1
0
E_{cm}
$\mathrm{LL}/\mathrm{LL}_{\mathrm{free}}$
$\mathrm{LL}/\mathrm{LL}_{\mathrm{narrow}}$

X-to-$\pi\pi$

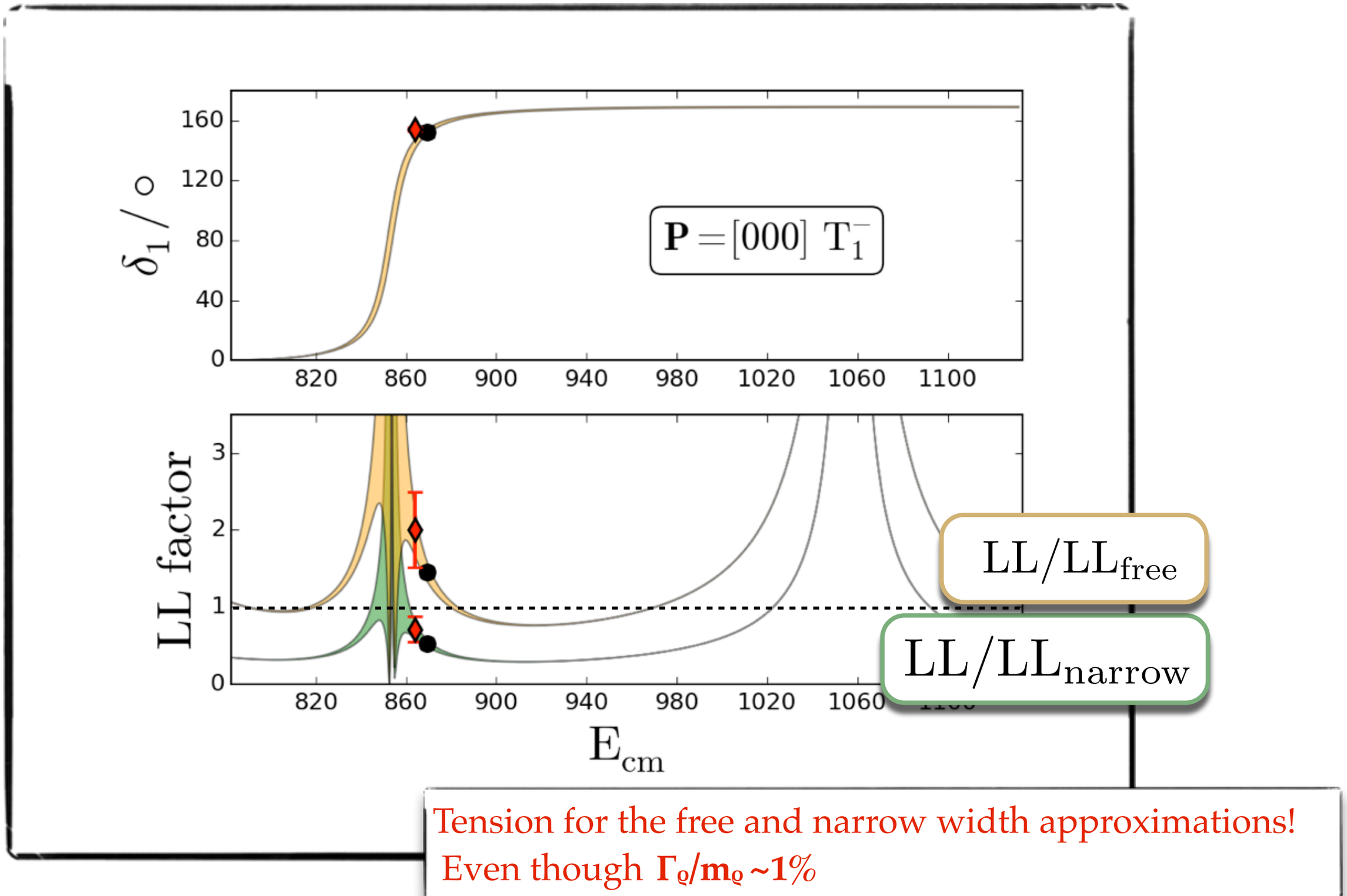
δ_1 / °
160
120
80
40
0
820
860
900
940
980
1020
1060
1100
$\mathbf{P} = [000]\ \mathrm{T}_1^-$
LL factor
3
2
1
0
$\mathrm{LL}/\mathrm{LL}_{\mathrm{free}}$
$\mathrm{LL}/\mathrm{LL}_{\mathrm{narrow}}$
E_{cm}
Tension for the free and narrow width approximations!
Even though $\Gamma_\varrho/m_\varrho \sim 1\%$

X-to-ππ

Consider the following parametrization:

$$\mathcal{H}_{X\to\pi\pi} = F_{X\to\rho}(E^*, Q^2)\frac{\sqrt{E^*\Gamma(E^*)}}{m_\rho^2 - E^{*2} - iE^*\Gamma(E^*)}\sqrt{\frac{16\pi E^*}{q^*}}$$

energy-dependent amplitude

Intuitive picture:

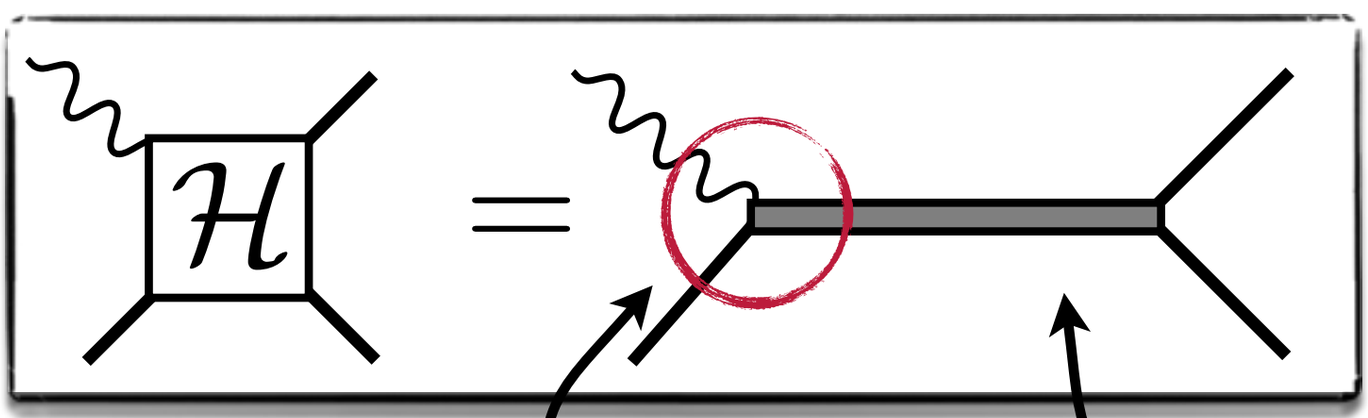

current couples to incoming state to create an "off-shell" ϱ-meson

the ϱ-meson propagates and decays to two pions

X-to-$\pi\pi$

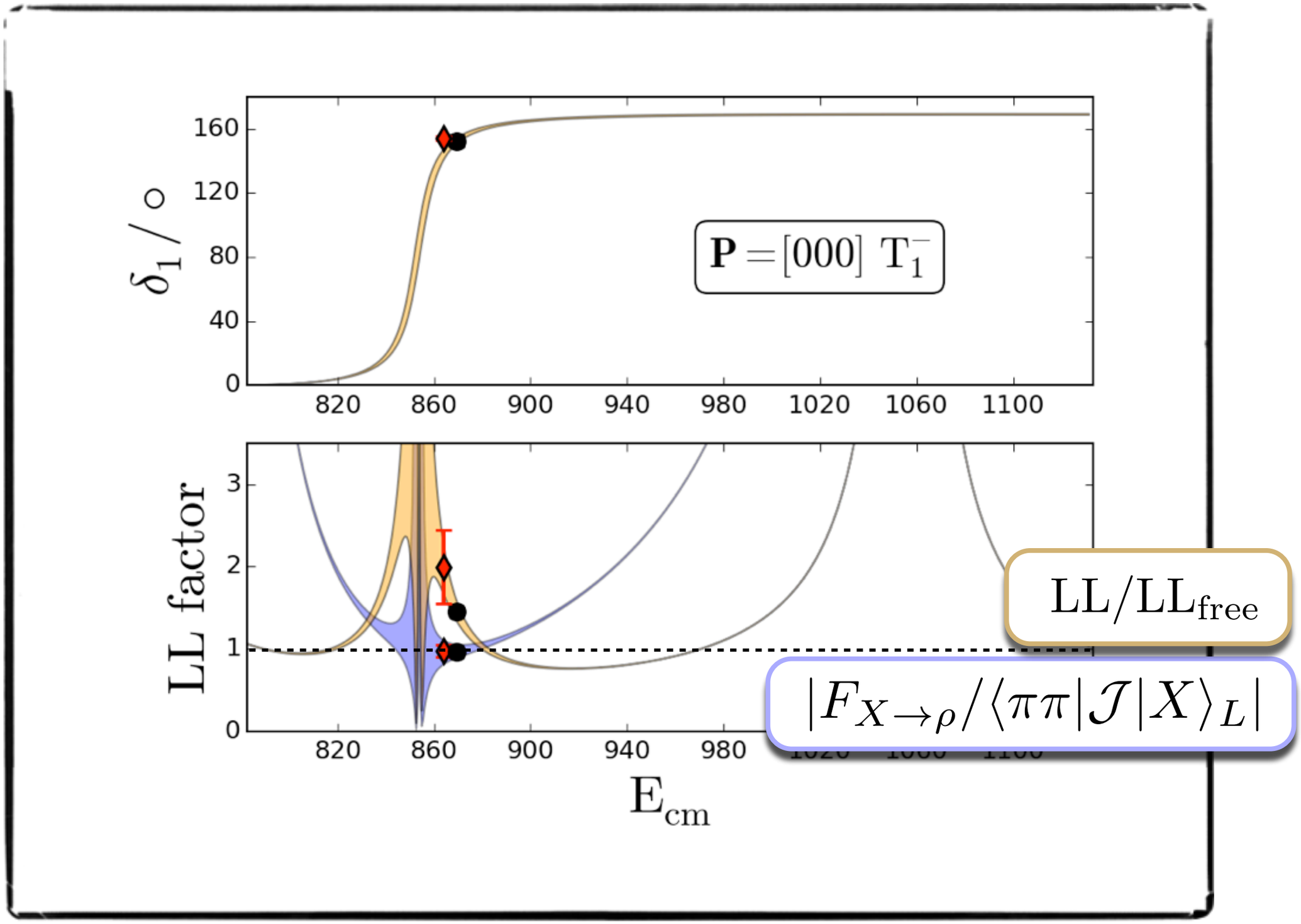
δ_1 / °
160
120
80
40
0
820
860
900
940
980
1020
1060
1100
$\mathbf{P} = [000]\ \mathrm{T}_1^-$
LL factor
3
2
1
0
820
860
900
940
980
E_{cm}
$\mathrm{LL}/\mathrm{LL}_{\mathrm{free}}$
$|F_{X\to\rho}/\langle\pi\pi|\mathcal{J}|X\rangle_L|$

X-to-$\pi\pi$

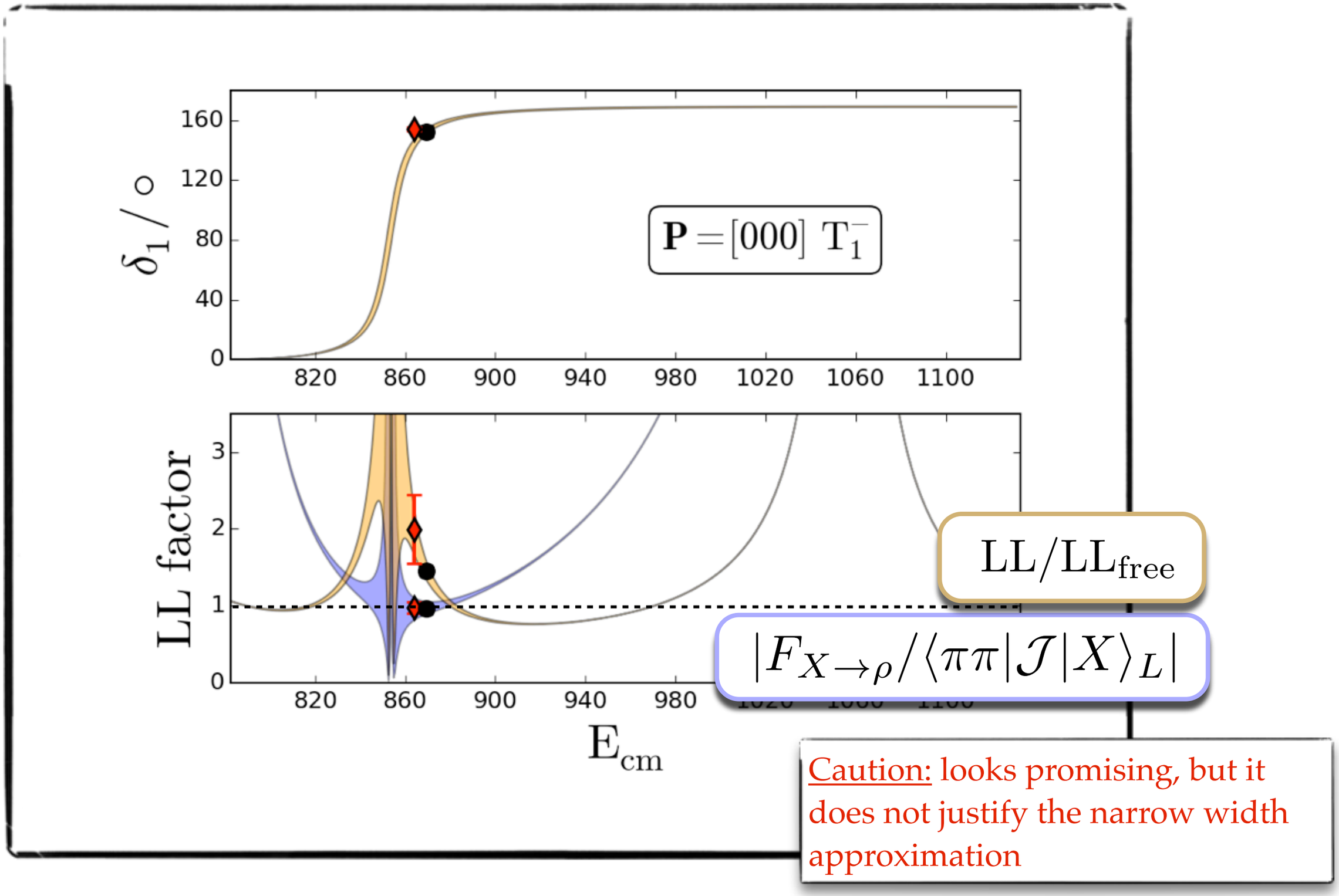
δ_1 / °
160
120
80
40
0
820
860
900
940
980
1020
1060
1100
$\mathbf{P} = [000]\ \mathrm{T}_1^-$
LL factor
3
2
1
0
E_{cm}
$\mathrm{LL}/\mathrm{LL}_{\mathrm{free}}$
$|F_{X\to\rho}/\langle\pi\pi|\mathcal{J}|X\rangle_L|$
Caution: looks promising, but it does not justify the narrow width approximation

X-to-$\pi\pi$

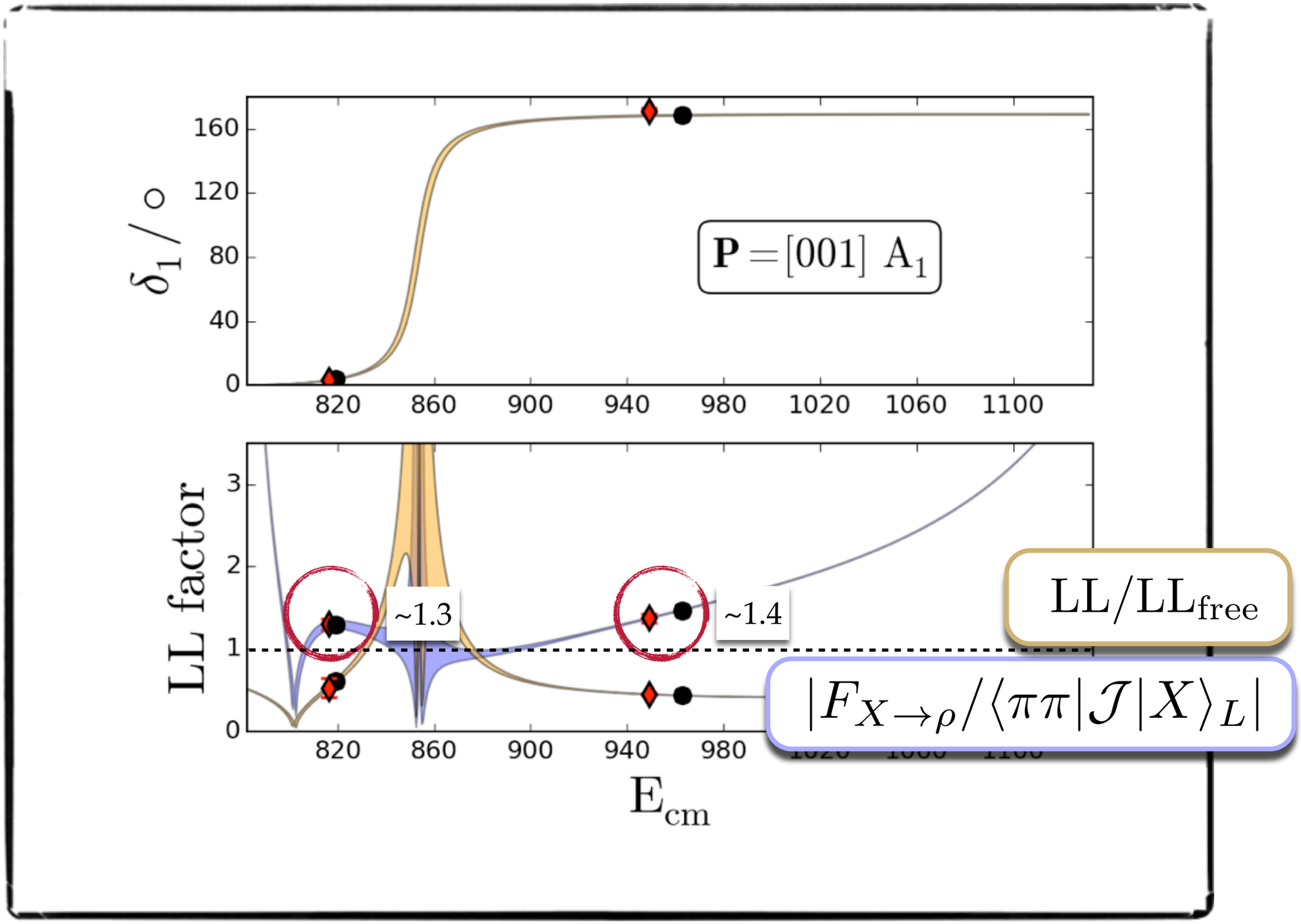
δ_1 / °
160
120
80
40
0
820
860
900
940
980
1020
1060
1100
$\mathbf{P} = [001]\ \mathrm{A}_1$
LL factor
3
2
1
0
~1.3
~1.4
E_{cm}
LL/LL$_{\mathrm{free}}$
$|F_{X\to\rho}/\langle\pi\pi|\mathcal{J}|X\rangle_L|$

X-to-$\pi\pi$

Conclusion: if precision is what you're seeking, the finite volume formalism is your best hope!

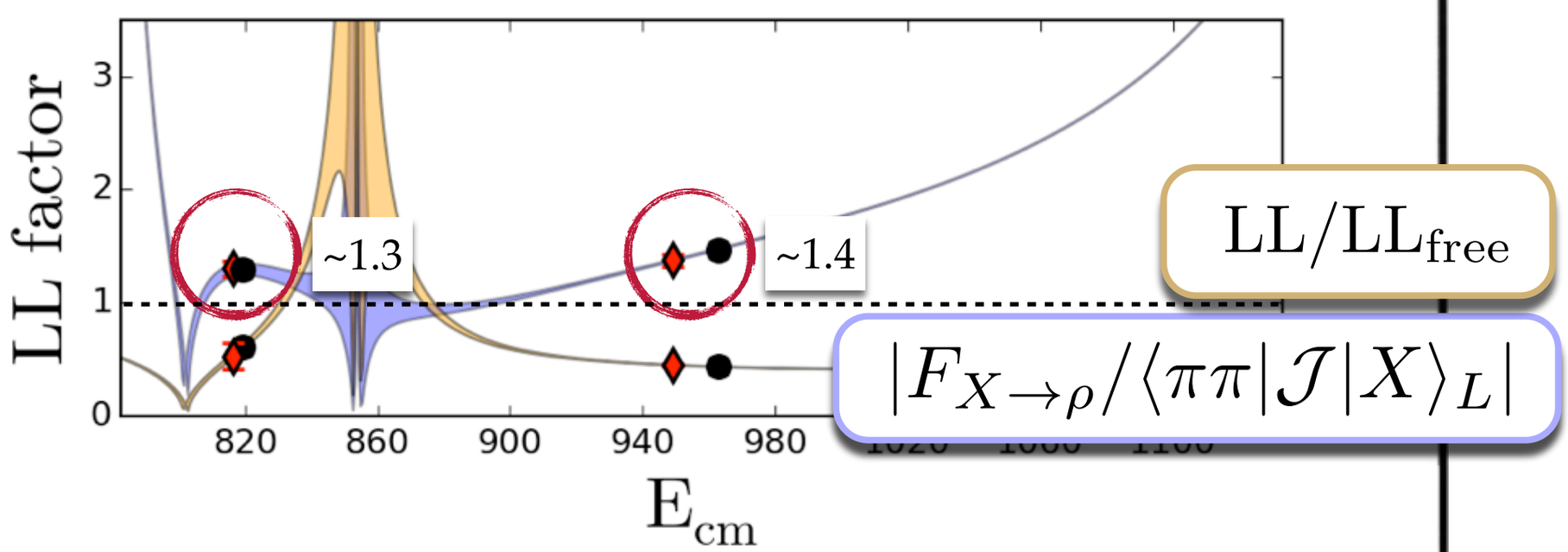

Final comments

Partial wave mixing and coupled channels:

David Wilson

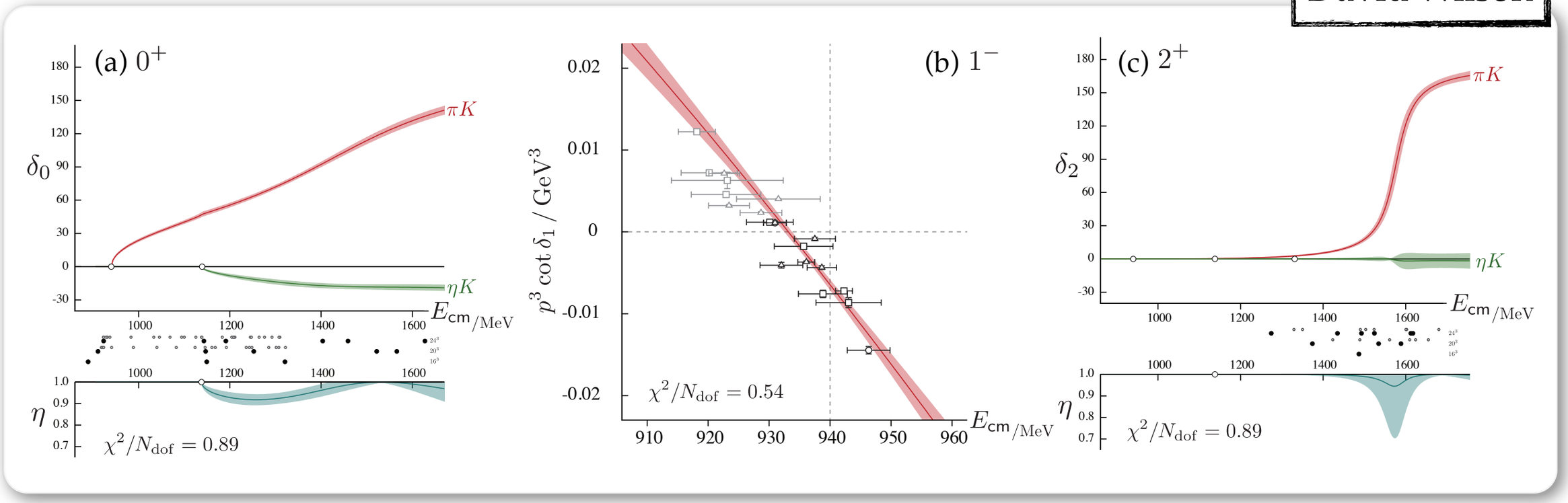

Matrix elements of not just ground states:

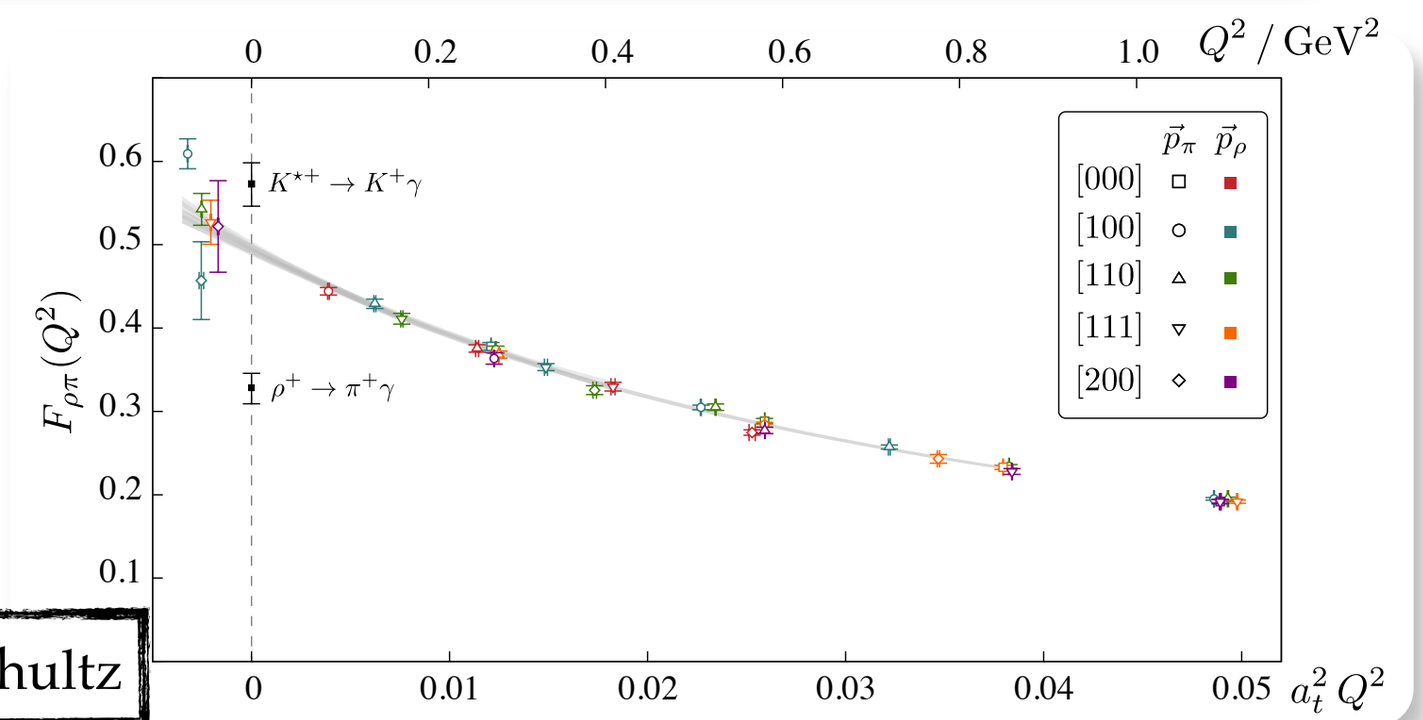

Christian Shultz

What the future holds!

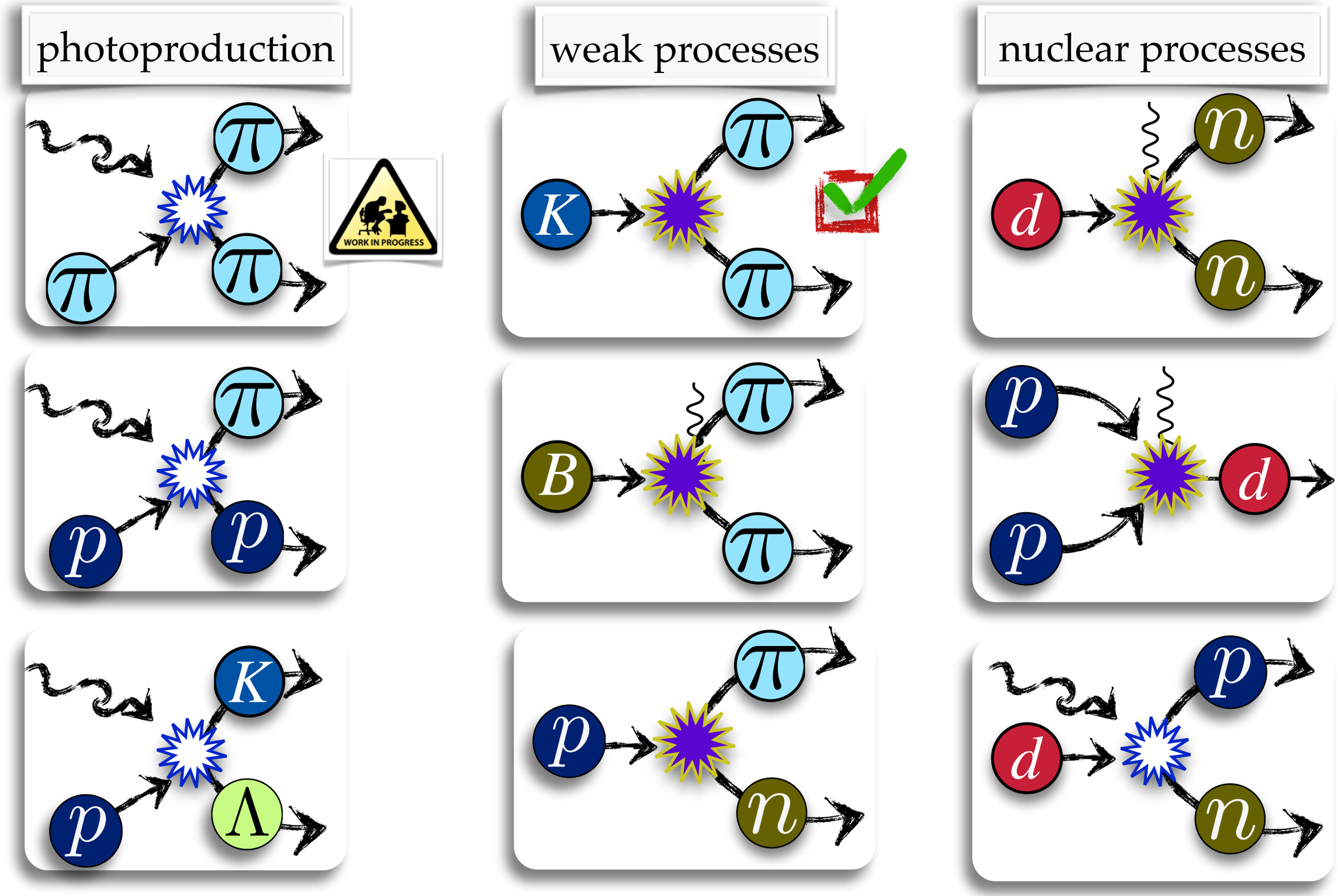

Computing the $K_L - K_S$ mass difference using lattice QCD

Multi-Hadron and Nonlocal Matrix Elements in Lattice QCD

February 6, 2015

Norman H. Christ

Columbia University

RBC and UKQCD Collaborations

Outline

- The $K_L - K_S$ mass difference
- Current lattice capability
- The $K_L - K_S$ mass difference from Euclidean space
- Finite volume correction
- Numerical experiments

RBC Collaboration

- BNL
  - Chulwoo Jung
  - Taku Izubuchi (RBRC)
  - Christoph Lehner
  - Amarjit Soni
- RBRC
  - Chris Kelly
  - Tomomi Ishikawa
  - Shigemi Ohta (KEK)
  - Sergey Syrityn
- Connecticut
  - Tom Blum
- Columbia
  - Ziyuan Bai
  - Xu Feng
  - Norman Christ
  - Luchang Jin
  - Robert Mawhinney
  - Greg McGlynn
  - David Murphy
  - Daiqian Zhang

UKQCD Collaboration

- Edinburgh
  - Peter Boyle
  - Julien Frison
  - Nicolas Garron (Plymouth)
  - Jamie Hudspith
  - Karthee Sivalingam
  - Oliver Witzel
- Southampton
  - Shane Drury
  - Jonathan Flynn
  - Tadeusz Janowski
  - Andreas Juttner
  - Andrew Lawson
  - Edwin Lizarazo
  - Andrew Lytle (Mumbai)
  - Marina Marinkovic (CERN)
  - Antonin Portelli
  - Chris Sachrajda
  - Matthew Spraggs
  - Tobi Tsang

Physics Context

$K^0 - \overline{K}^0$ mixing

- ΔS=1 weak interactions allow $\overline{K}^0$ and K^0 to mix.

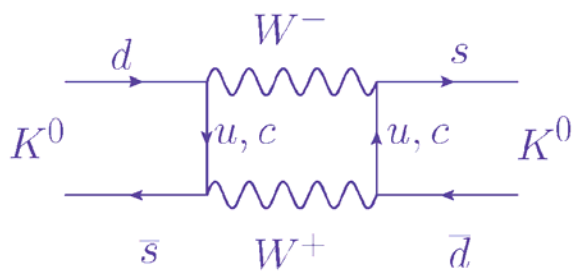

- New eigenstates are approximately:

$$K_+ = \frac{1}{\sqrt{2}}(K^0 + \overline{K}^0) \qquad K_- = \frac{1}{\sqrt{2}}(K^0 - \overline{K}^0)$$

- Small mass difference: ΔM_K = 3.483(6) x 10^{-12} MeV
- Effective $\frac{\alpha_{EM}}{\Lambda^2}(\bar{s}d)(\bar{s}d)$ operator would give ΔM_K = 3 x 10^{-12} MeV for Λ = 1000 TeV

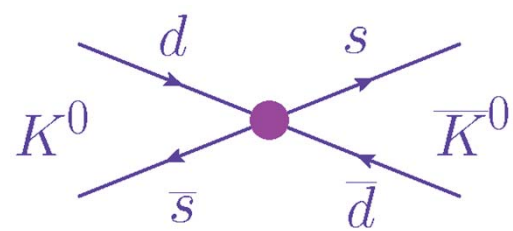

$K^0 - \bar{K}^0$ mixing: Indirect CP Violation

- CP violation leads to K_L and K_S states which are not CP eigenstates:

$$K_S = \frac{K_+ + \bar{\epsilon} K_-}{\sqrt{1 + |\bar{\epsilon}|^2}} \qquad K_L = \frac{K_- + \bar{\epsilon} K_+}{\sqrt{1 + |\bar{\epsilon}|^2}}$$

- Here $\bar{\varepsilon}$ is closely related to $\epsilon_K = \bar{\epsilon} + i \frac{\mathrm{Im} A_0}{\mathrm{Re} A_0}$

- Where $|\varepsilon_K| = (2.228 \pm 0.011) \times 10^{-3}$

$K^0 - \overline{K}^0$ Mixing

- Time evolution of $K^0 - \overline{K}^0$ system given by familiar Wigner-Weisskopf formula:

$$i\frac{d}{dt}\begin{pmatrix} K^0 \\ \overline{K}^0 \end{pmatrix} = \left\{ \begin{pmatrix} M_{00} & M_{0\bar{0}} \\ M_{\bar{0}0} & M_{\bar{0}\bar{0}} \end{pmatrix} - \frac{i}{2}\begin{pmatrix} \Gamma_{00} & \Gamma_{0\bar{0}} \\ \Gamma_{\bar{0}0} & \Gamma_{\bar{0}\bar{0}} \end{pmatrix} \right\} \begin{pmatrix} K^0 \\ \overline{K}^0 \end{pmatrix}$$

where:

$$\Gamma_{ij} = 2\pi \sum_{\alpha} \int_{2m_\pi}^{\infty} dE \langle i|H_W|\alpha(E)\rangle\langle\alpha(E)|H_W|j\rangle \delta(E - m_K)$$

$$M_{ij} = \sum_{\alpha} \mathcal{P} \int_{m_\pi}^{\infty} dE \frac{\langle i|H_W|\alpha(E)\rangle\langle\alpha(E)|H_W|j\rangle}{m_K - E}$$

$K^0 - \overline{K}^0$ Mixing

- CP violating: $p \sim m_t$

$$\bar{\epsilon} = \frac{i}{2}\left\{\frac{\mathrm{Im}\,M_{0\bar{0}} - \frac{i}{2}\mathrm{Im}\,\Gamma_{0\bar{0}}}{\mathrm{Re}\,M_{0\bar{0}} - \frac{i}{2}\mathrm{Re}\,\Gamma_{0\bar{0}}}\right\}$$

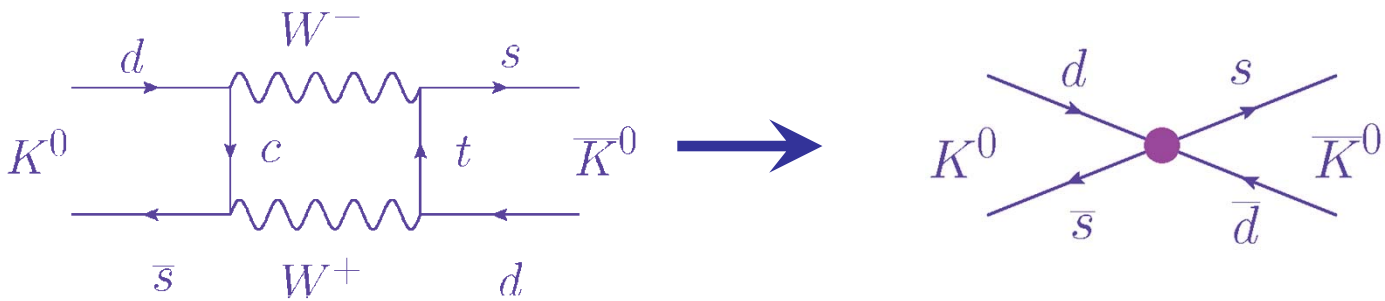

- CP conserving: $p \leq m_c$

$$m_{K_S} - m_{K_L} = 2\mathrm{Re}\{M_{0\bar{0}}\}$$

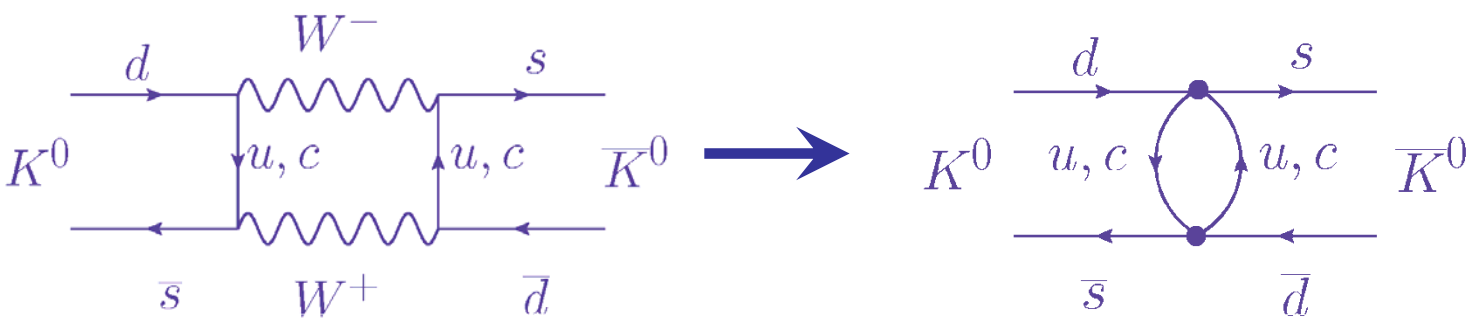

$K^0 - \overline{K}^0$ Mixing

- CP violating: $p \sim m_t$

$$\overline{\epsilon} = \frac{i}{2}\left\{\frac{\mathrm{Im}\,M_{0\overline{0}} - \frac{i}{2}\mathrm{Im}\,\Gamma_{0\overline{0}}}{\mathrm{Re}\,M_{0\overline{0}} - \frac{i}{2}\mathrm{Re}\,\Gamma_{0\overline{0}}}\right\}$$

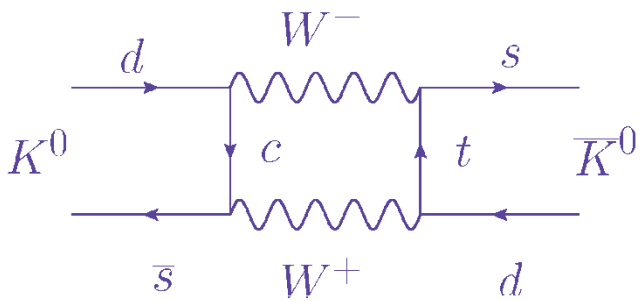

Long distance part is a small but important contribution: following talk of Ziyuan Bai

- CP conserving: $p \leq m_c$

$$m_{K_S} - m_{K_L} = 2\mathrm{Re}\{M_{0\overline{0}}\}$$

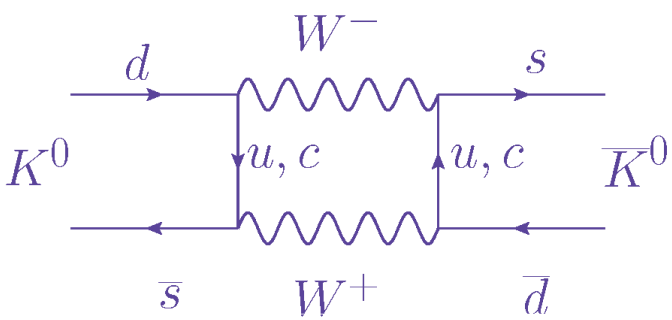

Long distance part is large. QCD perturbation theory fails at the 30% level.

Lattice QCD in 2015

Current state-of-the-art

- Use chiral fermions: Mobius DWF
- Physical m_π=135 MeV and L = 4 – 6 fm.
- Generate 48^3 x 96 and 64^3 x 128.
- Many complex ingredients:
  - Highly optimized code (64 threads, SPI comms., wide-vector FP)
  - Sophisticated algorithms (deflation, FG $(\Delta t)^3$ integrator, multigrid)
  - Complex measurement strategies (NPR, G-parity BC, 5-pt functions, all-mode-averaging)
- Complete set of measurements took 5.3 hours on a 32-rack BG/Q machine (sustains 1 Pflops)

Simple state-of-the-art example: f_π

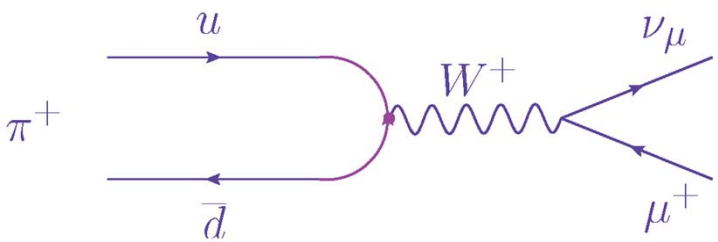

$$\langle 0|\bar{d}\gamma^5\gamma^\mu u|\pi^+(\vec{p})\rangle = f_\pi \frac{p^\mu}{\sqrt{4E_\pi(\vec{p})}}$$

$$f_\pi = N \sum_{\vec{r}} \frac{\langle A^0(\vec{r},t)\, O_\pi(t=0)\rangle}{\langle O_\pi^\dagger(t)\, O_\pi(t=0)\rangle^{\frac{1}{2}}} e^{m_\pi t/2}$$

- 2012 (elaborate chiral fit): $f_\pi = 127(3)_{\text{stat}}(3)_{\text{sys}}$ MeV
- 2013 (m_π=135 MeV): $f_\pi = 130.0(0.3)_{\text{stat}}$ MeV (40 configs.)
- Experiment: $f_\pi = 130.4(0.04)(0.2)$ MeV

ΔM_K from Euclidean space

ΔM_K from Euclidean space

- Replace $W^{\pm}$ exchange by four-Fermi operator:

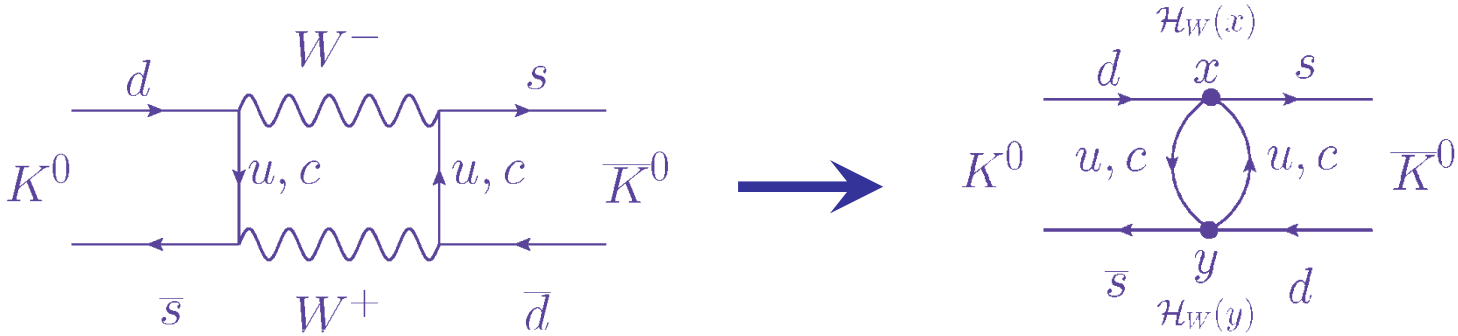

- Use 4-flavor theory incorporating GIM cancellation
- Amplitude is regular when the two weak operators collide: $x \rightarrow y$
- This long distance calculation is self-contained with no subtraction or perturbative correction needed!

ΔM_K from Euclidean space

- Start with $H = H_{\mathrm{QCD}} + H_{\mathrm{W}}$
- Calculate:

$$\langle K_\pm | e^{-\left(H_{\mathrm{QCD}}+H_{\mathrm{W}}\right)t} | K_\pm \rangle = e^{-\left(M_K+\Delta M_{K_\pm}\right)t} + \ldots$$

$$= e^{-M_K t}\left(1 + \Delta M_{K_\pm} t\right) + \ldots$$

- The … terms include |0>, $|\pi>$ and $|\pi\,\pi>$ states with energy below M_K
- These fall with increasing t exponentially less rapidly that the term of interest!

ΔM_K from Euclidean space

- Evaluate standard, Euclidean, 2nd order $\overline{K}^0 - K^0$ amplitude:

$$\mathcal{A} = \langle 0|T\left(K^0(t_f)\frac{1}{2}\int_{t_a}^{t_b} dt_2 \int_{t_a}^{t_b} dt_1 H_W(t_2) H_W(t_1) K^{0\dagger}(t_i)\right)|0\rangle$$

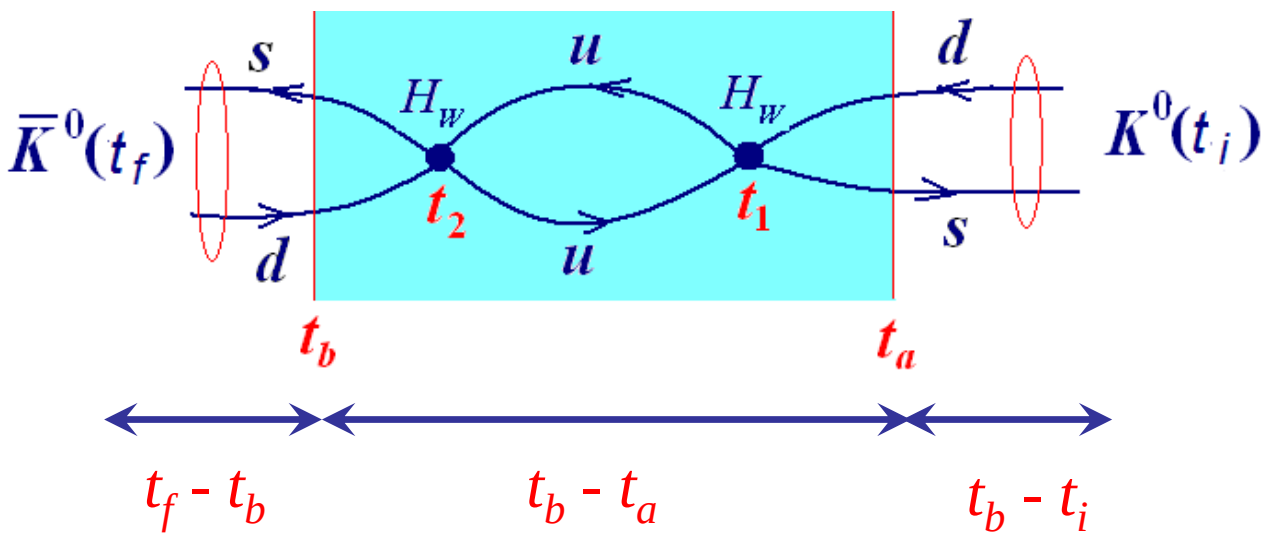

Interpret Lattice Result

1. 2.

$$\mathcal{A} = N_K^2 e^{-M_K(t_f-t_i)} \sum_n \frac{\langle \overline{K}^0 | H_W | n \rangle \langle n | H_W | K^0 \rangle}{M_K - E_n} \left(-(t_b - t_a) - \frac{1}{M_K - E_n} + \frac{e^{(M_K - E_n)(t_b - t_a)}}{M_K - E_n} \right)$$

1. Δm_K^{FV}
2. Uninteresting constant
3. Growing or decreasing exponential:

   $E_n < m_K$ must be removed!

3.

- Finite volume correction:

$$M_{K_L} - M_{K_S} = 2 \sum_n \frac{\langle \overline{K}^0 | H_W | n \rangle \langle n | H_W | K^0 \rangle}{M_K - E_n} + 2 \frac{d(\phi + \delta_0)}{dk}\bigg|_{m_K} |\langle n_0 | H_W | K^0 \rangle|^2 \cot(\phi + \delta_0)\big|_{M_K}$$

N.H. Christ, X. Feng, G. Martinelli, C.T. Sachrajda

Finite volume correction

- Exploit Kim, Sachrajda and Sharpe arXiv:hep-lat/0507006

$$\Delta_{\rm FV}\left\{\left\langle T\left(K^0(0)\int_{-\infty}^{\infty}H_W(t_1)dt_1\int_{-\infty}^{\infty}H_W(t_2)dt_2\int d^4x\,\overline{K}^0(x)e^{iqx}\right)\right\rangle\right\}\left(\frac{(q^2+M_K^2)}{i}\right)^2$$

$=$

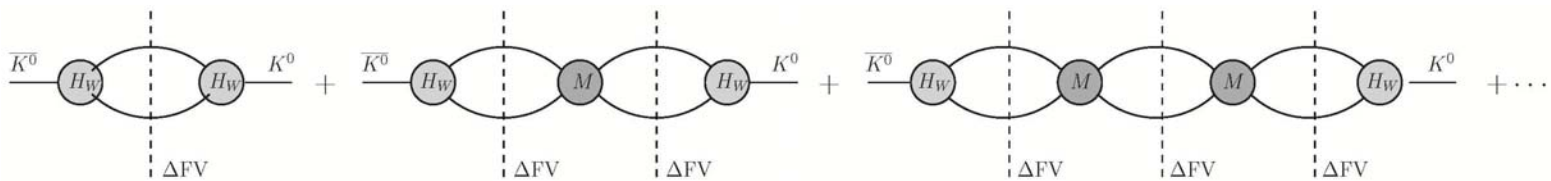

$$= \langle\overline{K}^0|H_W|(\pi\pi)^{in}\rangle F\frac{1}{1+\frac{i}{2}MF}\langle(\pi\pi)^{out}|H_W|K^0\rangle$$

$$= \frac{qM_K\pi}{2}\left|\langle\overline{K}^0|H_W|(\pi\pi)^{in}\rangle\right|\left(\cot(\phi+\delta)+i\right)\left|\langle(\pi\pi)^{out}|H_W|K^0\rangle\right|$$

$$M_{K_L}-M_{K_S}=2\sum_n\frac{\langle\overline{K}^0|H_W|n\rangle\langle n|H_W|K^0\rangle}{M_K-E_n}+2\frac{d(\phi+\delta_0)}{dk}\bigg|_{m_K}|\langle n_0|H_W|K^0\rangle|^2\cot(\phi+\delta_0)\big|_{M_K}$$

N.H. Christ, X. Feng, G. Martinelli, C.T. Sachrajda

Numerical Experiments

Choice of weak operators

- Use four-Fermi operators in the four-flavor theory:

$$Q_1^{qq'} = (\overline{q}_i d_i)_{V-A} (\overline{q}'_j s_j)_{V-A} \qquad Q_2^{qq'} = (\overline{q}_i d_j)_{V-A} (\overline{q}'_j s_i)_{V-A}$$

$$\mathcal{H}_W = \frac{G_F}{2} \sum_{q,q'=u,c} V_{qd} V_{q's}^* \left(C_1 Q_1^{qq'} + C_2 Q_2^{qq'} \right)$$

- Use Rome-Southampton NPR and 4-flavor RI/SMOM / $\overline{\text{MS}}$-NDR matching from Lehner and Sturm
- Assume Cabibbo unitarity:

$0 = \lambda_u + \lambda_c + \lambda_t \approx \lambda_u + \lambda_c$ where $\lambda_q = V_{qd} V_{qs}^*$

Lattice setup

- Must include charm quark (GIM *u–c* cancellation)
- Three calculations performed:

Jianglei Yu
- – $16^3 \times 32$, m_p = 420 MeV, types 1 & 2 (arXiv:1212.5931)
- – $24^3 \times 64$, m_p = 330 MeV, all graphs (arXiv:1406.0916)

Ziyuan Bai
- – $32^3 \times 64$, m_p = 170 MeV, all graphs

Type 1

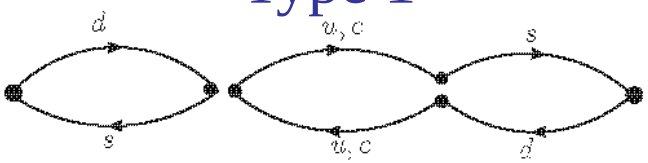

Type 2

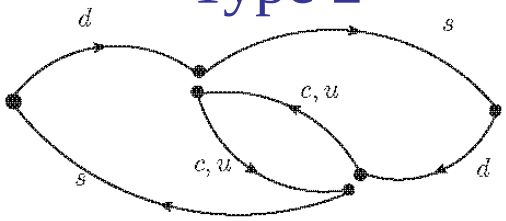

Type 3

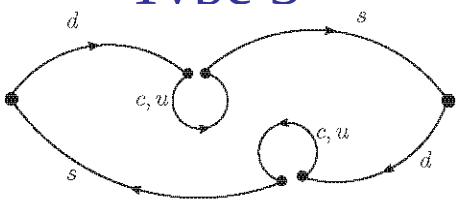

Type 4

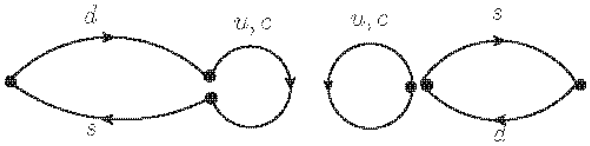

Exponentially growing terms

- The vacuum, π^0 and η require special treatment:
  - Calculate $\langle$ X | H_W | K^0 $\rangle$ directly and subtract, X = $|0\rangle$, π^0, η
  - Fit the exponential time dependence in the 4-point function
  - Adjust $c_s\, \bar{s}\, d$ or $c_p\, \bar{s}\, \gamma^5 d$ terms to completely remove two unwanted states.

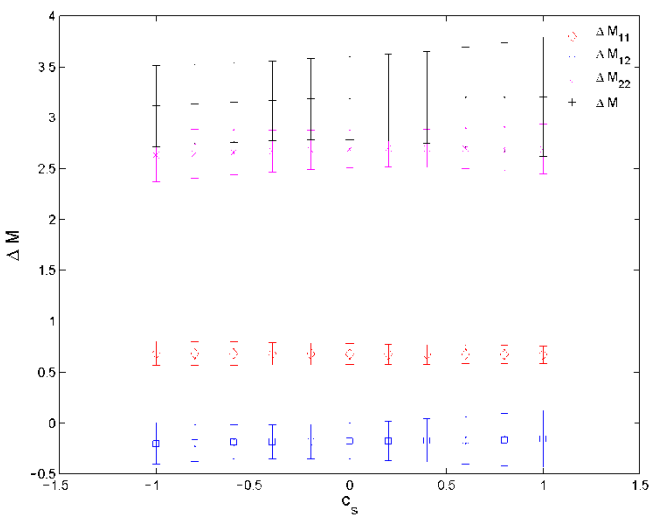

vary c_s

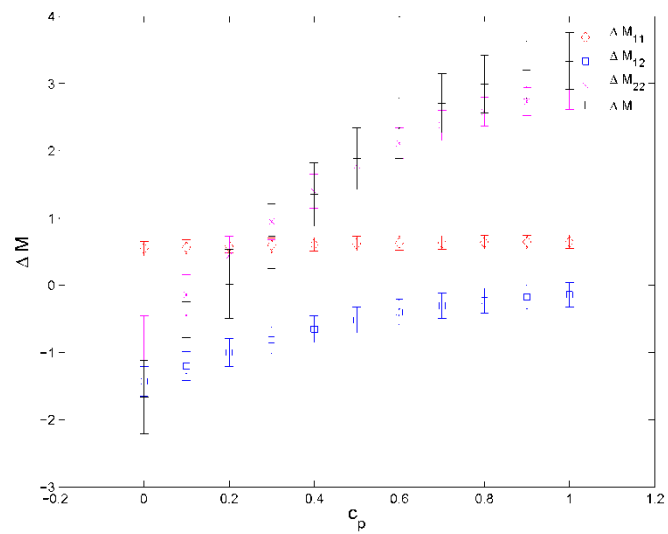

vary c_p

Remove extra η contribution

- Calculate $\langle\ \eta\ |\ H_W\ |\ K^0\ \rangle$ directly and remove
- Has an ~10% effect on the result

PRL **105,** 241601 (2010) PHYSICAL REVIEW LETTERS week ending 10 DECEMBER 2010

η and η' Mesons from Lattice QCD

N. H. Christ,[1] C. Dawson,[2] T. Izubuchi,[3,4] C. Jung,[3] Q. Liu,[1] R. D. Mawhinney,[1] C. T. Sachrajda,[5] A. Soni,[3] and R. Zhou[6]

(RBC and UKQCD Collaborations)

[1]*Physics Department, Columbia University, New York, New York 10027, USA*
[2]*Department of Physics, University of Virginia, 382 McCormick Road, Charlottesville, Virginia 22904-4714, USA*
[3]*Brookhaven National Laboratory, Upton, New York 11973, USA*
[4]*RIKEN-BNL Research Center, Brookhaven National Laboratory, Upton, New York 11973, USA*
[5]*School of Physics and Astronomy, University of Southampton, Southampton SO17 1BJ, United Kingdom*
[6]*Physics Department, University of Connecticut, Storrs, Connecticut 06269-3046, USA*
(Received 24 February 2010; published 8 December 2010)

The large mass of the ninth pseudoscalar meson, the η', is believed to arise from the combined effects of the axial anomaly and the gauge field topology present in QCD. We report a realistic, 2 + 1-flavor, lattice QCD calculation of the η and η' masses and mixing which confirms this picture. The physical eigenstates show small octet-singlet mixing with a mixing angle of $\theta = -14.1(2.8)^\circ$. Extrapolation to the physical light quark mass gives, with statistical errors only, $m_\eta = 573(6)$ MeV and $m_{\eta'} = 947(142)$ MeV, consistent with the experimental values of 548 and 958 MeV.

DOI: 10.1103/PhysRevLett.105.241601 PACS numbers: 12.38.Gc, 11.15.Ha, 11.30.Rd, 14.40.Be

The relatively large mass of the ninth pseudoscalar meson, the η', provides a significant challenge for quantum chromodynamics (QCD), the component of the standard model which describes the interactions of quarks and gluons. On a naive classical level, there are nine conserved axial-vector currents. Given the vacuum breaking of the symmetries which these currents generate, this should diagrams to decrease exponentially with increasing time separation. For mesons this falloff roughly matches the exponential time dependence of the massive, Euclidean-space meson propagator, and good numerical signals can be seen over a large range of times. For terms in which the source and sink of the meson propagator are not joined by quark propagators, the needed exponential decrease comes

$$\eta' = \frac{1}{\sqrt{3}}\left(\bar{u}u + \bar{d}d + \bar{s}s\right)$$

$$\eta = \frac{1}{\sqrt{6}}\left(\bar{u}u + \bar{d}d - 2\bar{s}s\right)$$

$$\frac{\left|\langle\eta|H_W|K^0\rangle\right|^2}{M_K - M_\eta}\left(-(t_b - t_a) - \frac{1}{M_K - M_\eta} + + \frac{e^{(M_K - M_\eta)(t_b - t_a)}}{M_K - M_\eta}\right)$$

Lattice results
(Jianglei Yu)

- N_f=2+1, 24^3 x 64, m_π = 330 MeV, $m_c^{\overline{MS}}$(2 GeV) = 949 MeV
- Incorporate GIM cancellation

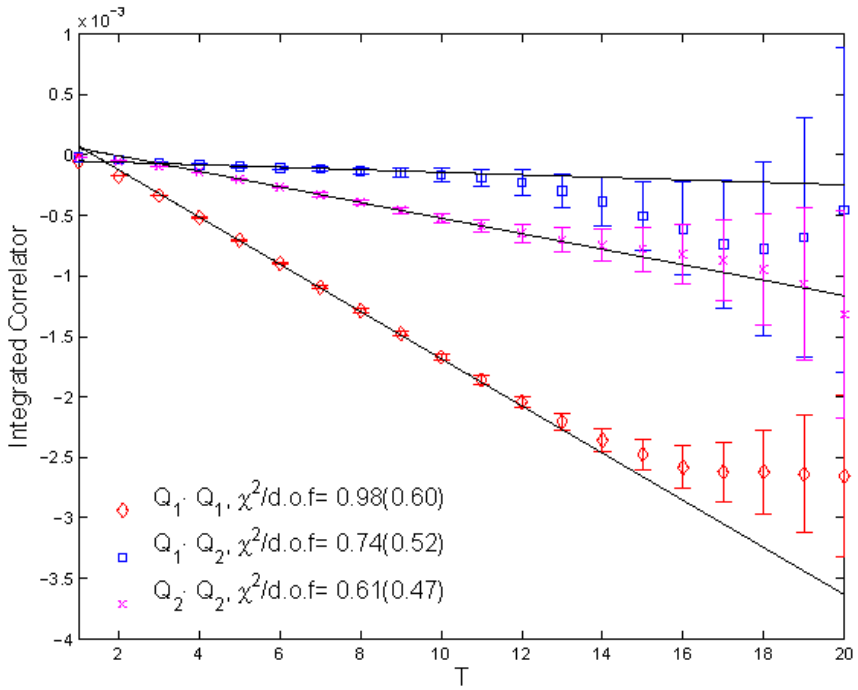

- Large statistics (800 configurations, 64 measurements each).

Results

Δ_K	T_{min}	$Q_1 \cdot Q_1$	$Q_1 \cdot Q_2$	$Q_2 \cdot Q_2$	ΔM_K
7	6	0.754(42)	-0.16(15)	2.70(18)	3.30(34)
	7	0.755(42)	-0.18(15)	2.66(18)	3.23(34)
	8	0.751(42)	-0.18(15)	2.62(19)	3.18(35)

x 10^{-12} MeV

Diagrams	$Q_1 \cdot Q_1$	$Q_1 \cdot Q_2$	$Q_2 \cdot Q_2$	ΔM_K
Type 1,2	1.485(80)	1.567(38)	3.678(56)	6.730(96)
All	0.754(42)	-0.16(15)	2.70(18)	3.30(34)

x 10^{-12} MeV

- Unphysical, m_π = 330 MeV
- Active charm but $m_c\, a = 0.55$
- 80^2 x 96 x 192, 1/a=3.0 GeV calculations planned!

- Result:
  ΔM_K = 3.30(34) 10^{-12} MeV
- ΔM_K^{expt} = 3.483(6) 10^{-12} MeV
- Agreement fortuitous!

New m_π = 170 MeV calculation
(Ziyuan Bai)

- N_f=2+1, 32^3 x 64, 1/a=1.37 GeV
- Charm: m_c = 592 and 750 MeV

M_K	M_π	M_η	$E_{\pi\pi,I=0}$	$E_{\pi\pi,I=2}$
492.8(2)	171.9(2)	496(32)	335.8(13)	346.8(7)

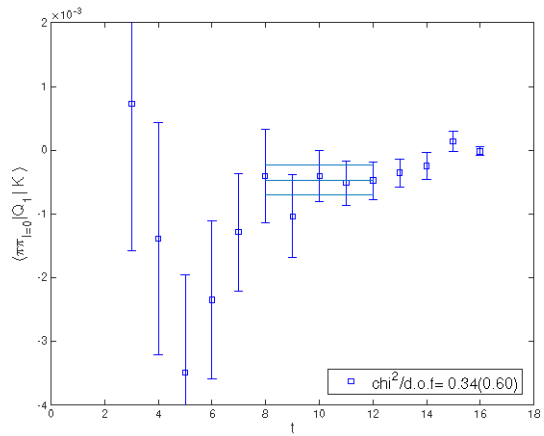

Q1

m_η

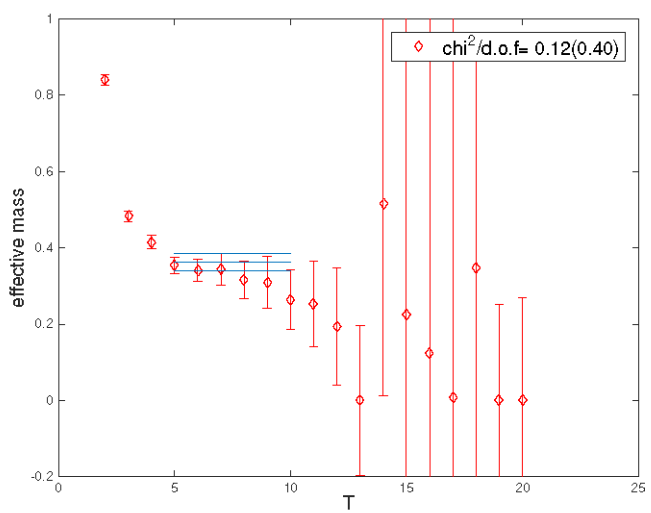

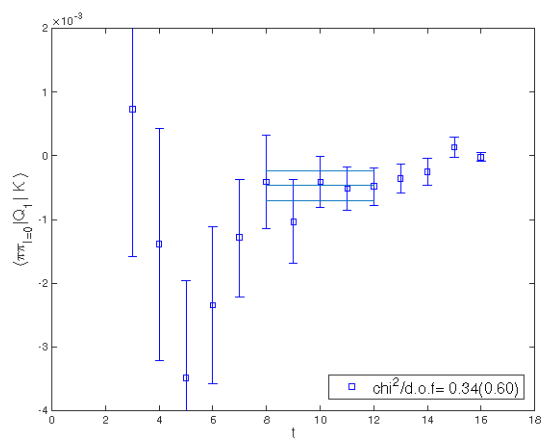

Q2

m_π = 170 MeV results

(Ziyuan Bai)

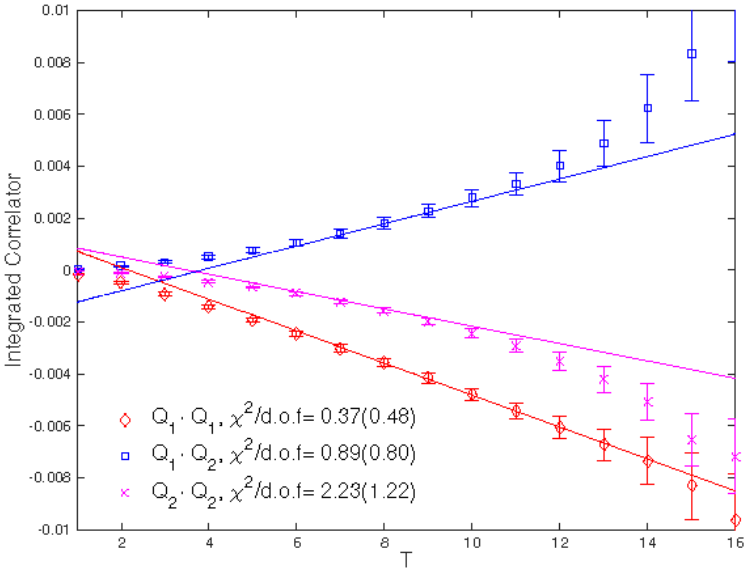

	ΔM_K x 10^{+12}
Types 1-4	5.76(73)
Types 1-2	4.19(15)
η	0
π	0.27(14)
$\pi\pi$, I=0	-0.097(49)
$\pi\pi$, I=2	-6.56(6) x 10^{-4}
Δ_{FV}	0.029(19)

- Use m_c = 750 MeV, fit for t ≥ 8
- Disconnected contribution small
- $\pi\pi$ contribution ~2% and FV correction ~0.5%

Outlook

- The $K_L - K_S$ mass difference in the standard model (and beyond) is a practical target for lattice QCD.
- A result with controlled 15-20% errors should be possible in ~2 years, as soon as $1/a \geq 3$ GeV ensembles become available.
- Sub-percent accuracy possible in 5-10 years!
- An exciting time for lattice QCD:
  - $K \to \pi\pi$, ΔI=3/2 and 1/2, ε'
  - $m_{K_L} - m_{K_S}$ and ε_K
  - $K^0 \to \pi^0 \bar{l} l$, $K^\pm \to \pi^\pm \bar{\nu}\nu$
  - Quark effects on g_μ - 2 at $O(\alpha^3)$

BNL WORKSHOP ON MULTI-HADRON AND NONLOCAL MATRIX ELEMENTS IN LATTICE QCD
FEBRUARY 5-6, 2015

SINGLE-HADRON STATES IN A FINITE VOLUME IN THE PRESENCE OF QED INTERACTIONS

ZOHREH DAVOUDI
MIT

IN COLLABORATION WITH MARTIN J. SAVAGE
PHYS. REV. D 90, 054503 (2014)

PHOTO COURTESY OF
SHUTTERSTOCK/ISCATEL

QED IS SPECIAL IN A FINITE VOLUME

GAUSS'S LAW + PERIODICITY ?

Hilf and Polley, Phys. Lett. B 131, 412 (1983)
Duncan, Eichten and Thacker, Phys. Rev. Lett. 76, 3894 (1996)
Hayakawa and Uno, Prog. Theor. Phys. 120, 413 (2008)

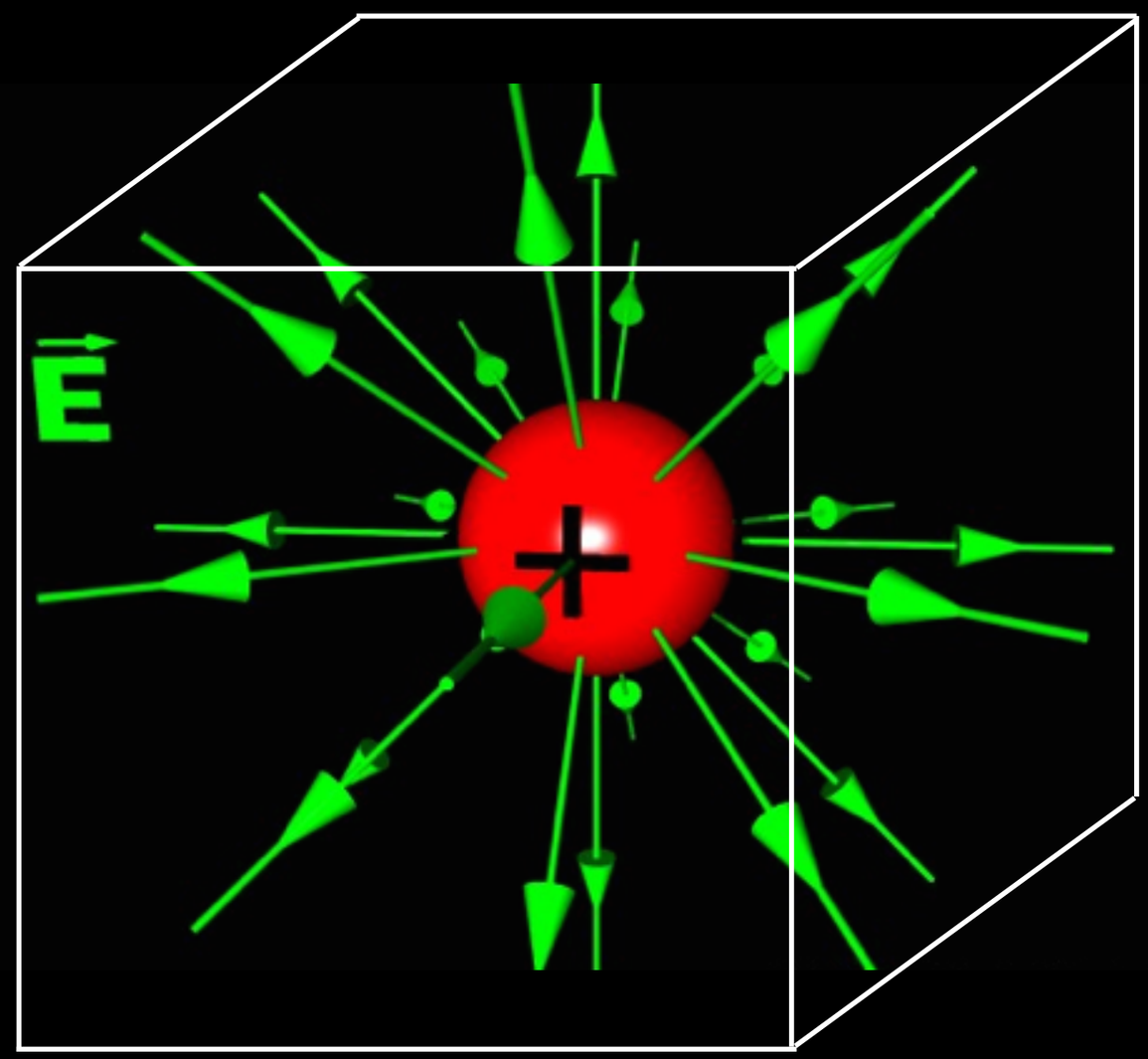

PHOTO COURTESY OF
YVES PELLETIER
(YPELLETIER@NCF.CA)

QED IS SPECIAL IN A FINITE VOLUME

GAUSS'S LAW + PERIODICITY ?

Hilf and Polley, Phys. Lett. B 131, 412 (1983)
Duncan, Eichten and Thacker, Phys. Rev. Lett. 76, 3894 (1996)
Hayakawa and Uno, Prog. Theor. Phys. 120, 413 (2008)

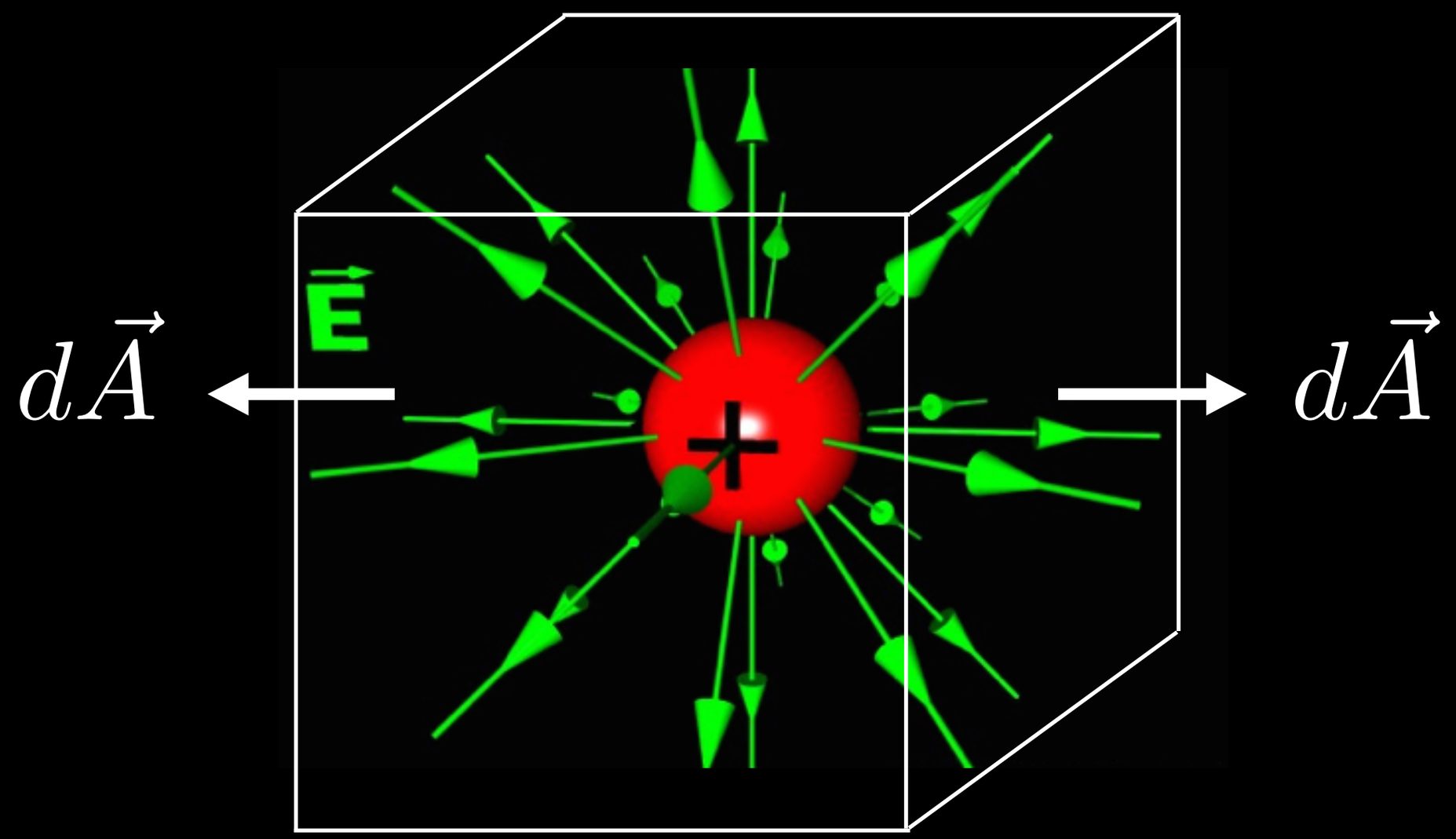

PHOTO COURTESY OF
YVES PELLETIER
(YPELLETIER@NCF.CA)

QED IS SPECIAL IN A FINITE VOLUME

$$\delta S = \int d^4x \; \left[\partial_\mu F^{\mu\nu}(x) - eQ\,\overline{\psi}(x)\gamma^\nu\psi(x)\right]\delta\left(A_\nu(x)\right)$$

$$= \int dt \; \frac{1}{L^3}\sum_{\mathbf{q}} \delta\left(\tilde{A}_\nu(t,\mathbf{q})\right)\int_{\mathrm{L}^3} d^3\mathbf{x}\; e^{i\mathbf{q}\cdot\mathbf{x}} \; \left[\partial_\mu F^{\mu\nu}(t,\mathbf{x}) - eQ\,\overline{\psi}(t,\mathbf{x})\gamma^\nu\psi(t,\mathbf{x})\right]$$

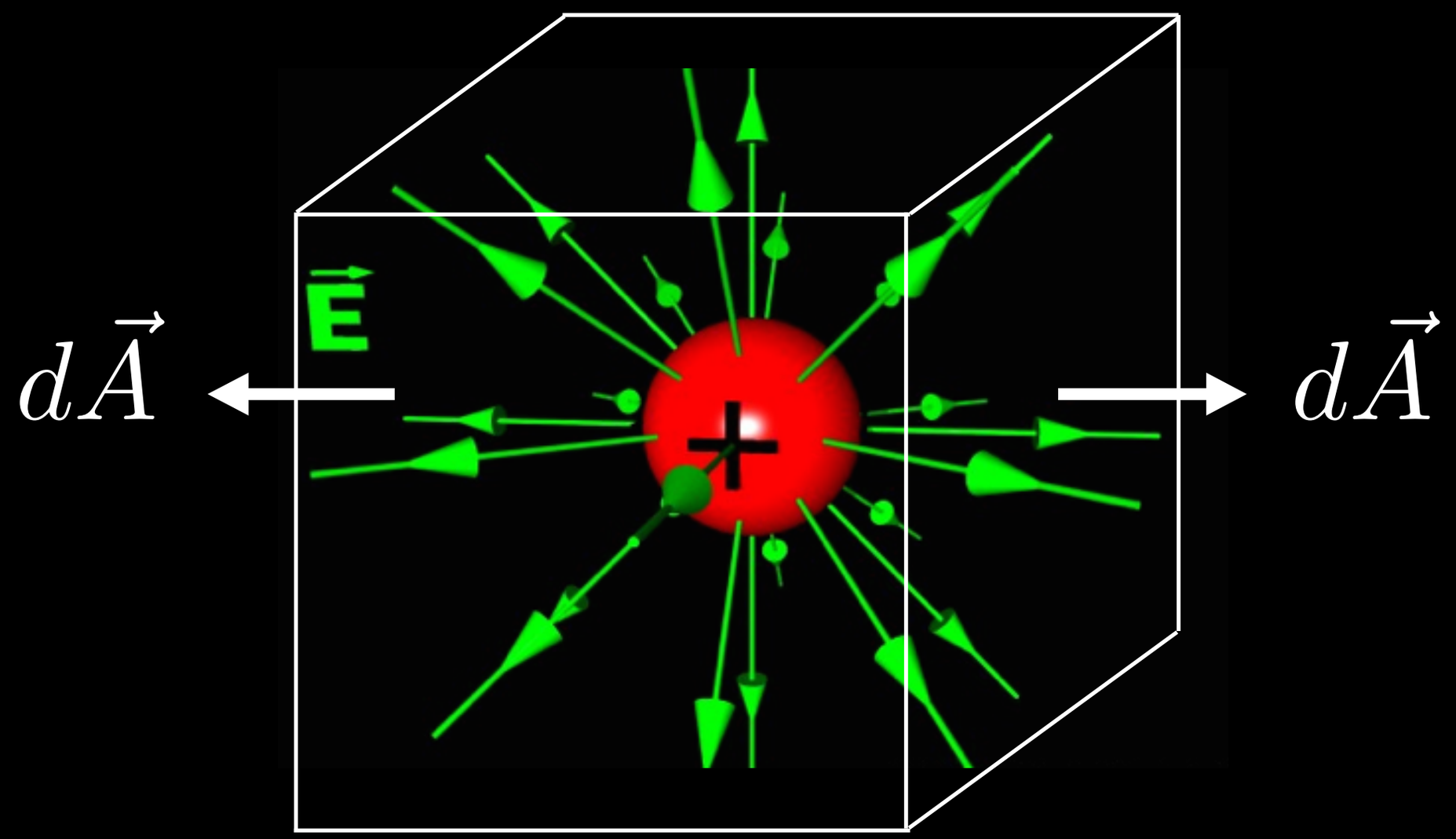

PHOTO COURTESY OF
YVES PELLETIER
(YPELLETIER@NCF.CA)

QED IS SPECIAL IN A FINITE VOLUME

$$\delta S = \int d^4x \; \left[\partial_\mu F^{\mu\nu}(x) - eQ\,\overline{\psi}(x)\gamma^\nu\psi(x)\right]\delta\left(A_\nu(x)\right)$$

$$= \int dt\,\frac{1}{L^3}\sum_{\mathbf{q}}\delta\left(\tilde{A}_\nu(t,\mathbf{q})\right)\int_{\mathrm{L}^3} d^3\mathbf{x}\; e^{i\mathbf{q}\cdot\mathbf{x}}\;\left[\partial_\mu F^{\mu\nu}(t,\mathbf{x}) - eQ\,\overline{\psi}(t,\mathbf{x})\gamma^\nu\psi(t,\mathbf{x})\right]$$

$$\mathbf{q}=0 \;\rightarrow\; \partial_\mu F^{\mu\nu} = j^\nu \;\rightarrow \int \mathbf{E}\cdot d\mathbf{A} = \int dV\, j^0 = eQ$$

GAUSS'S LAW

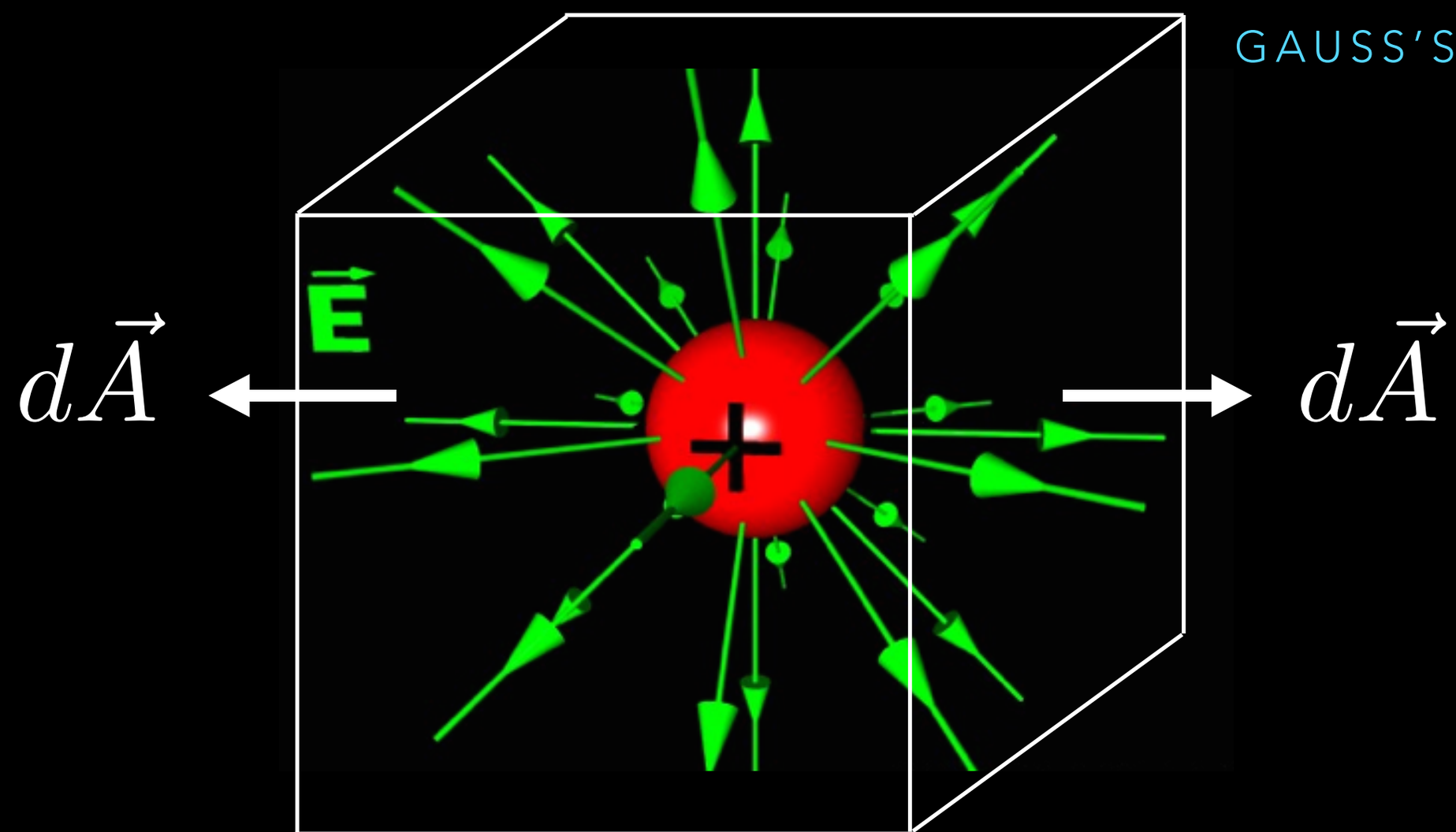

PHOTO COURTESY OF
YVES PELLETIER
(YPELLETIER@NCF.CA)

QED IS SPECIAL IN A FINITE VOLUME

SOLUTION: ADD A UNIFORM BACKGROUND CHARGE/CURRENT DENSITY

$$\mathcal{L}^{QED} \to \mathcal{L}^{QED} - b^\nu A_\nu \qquad (j^\nu \to j^\nu + b^\nu)$$

REQUIRING $\int dV\ b^0 = -eQ$ RESTORES GAUSS'S LAW.

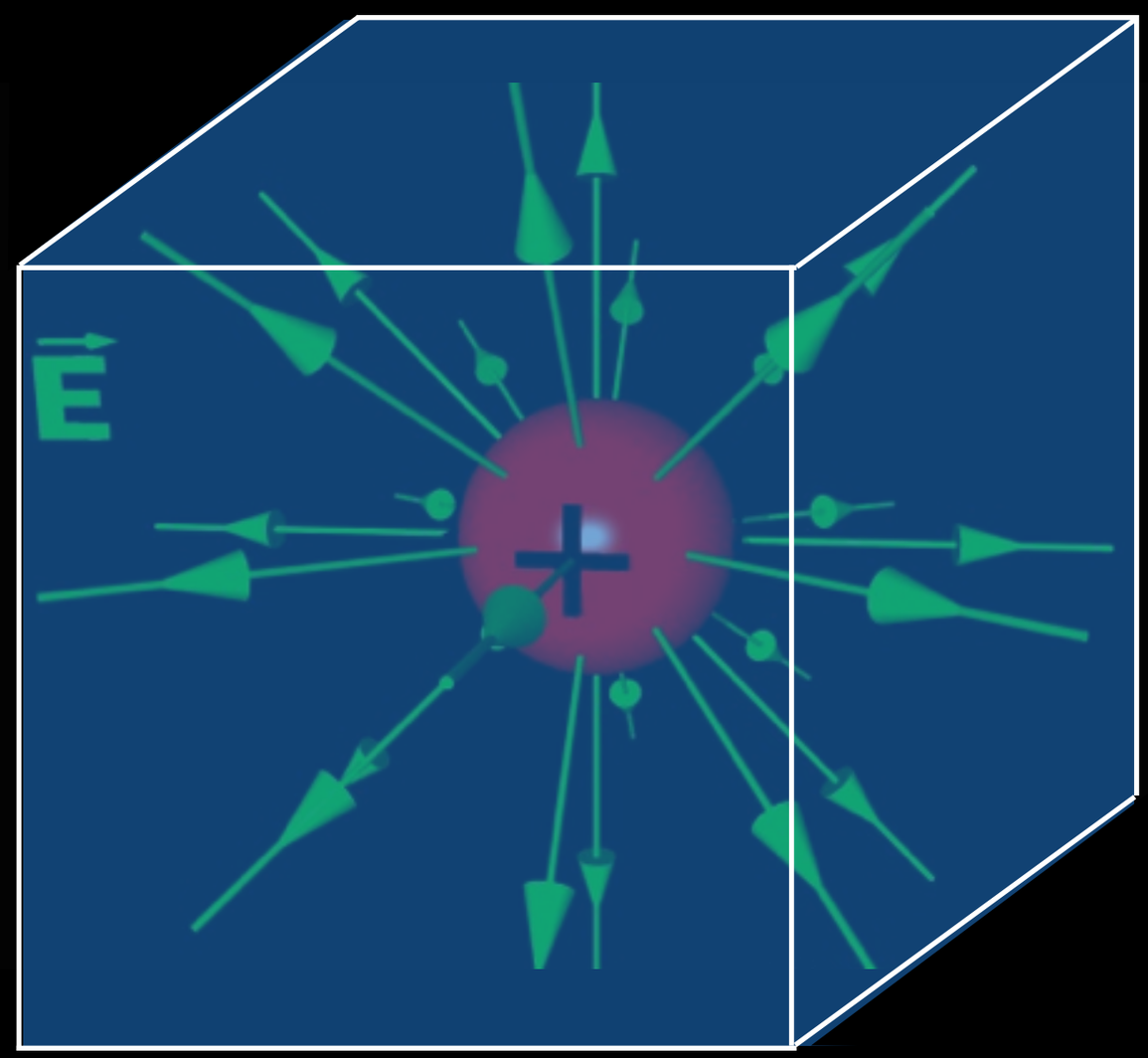

QED IS SPECIAL IN A FINITE VOLUME

HOW DO WE IMPLEMENT THIS?

$$\mathcal{L}^{QED} \to \mathcal{L}^{QED} - b^\nu A_\nu$$

$$\frac{\delta S}{\delta b^\nu} = 0 \;\to\; -\int dt d^3x \; A_\nu(\mathbf{x}, t) = 0 \;\to\; \boxed{\widetilde{A}_\nu(\mathbf{q} = 0; t) = 0}$$

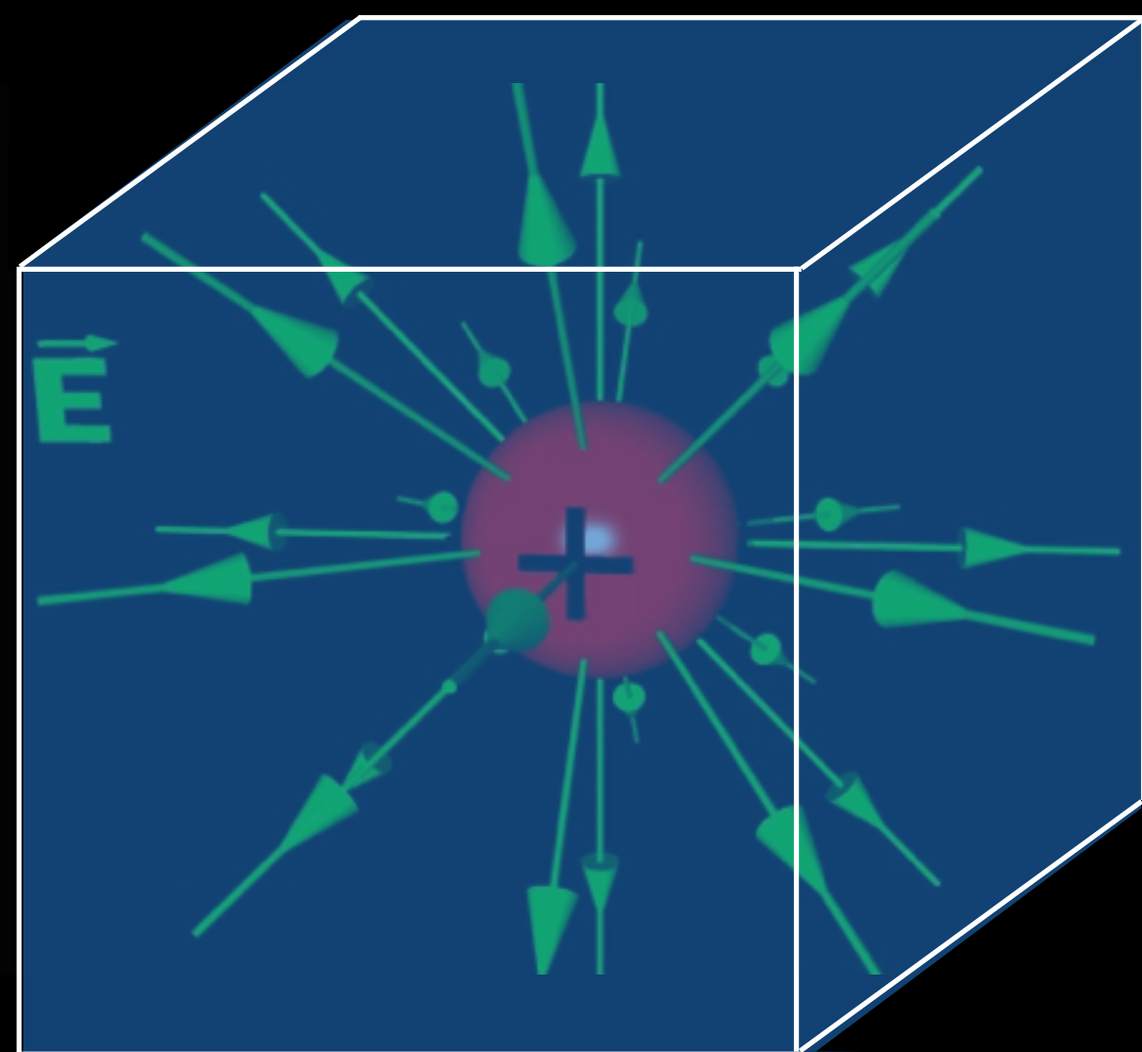

REMOVE THE PHOTON ZERO MODE

QED IS SPECIAL IN A FINITE VOLUME

COULOMB POTENTIAL OF A POINT CHARGE
WITHOUT THE UNIFORM CHARGE DENSITY

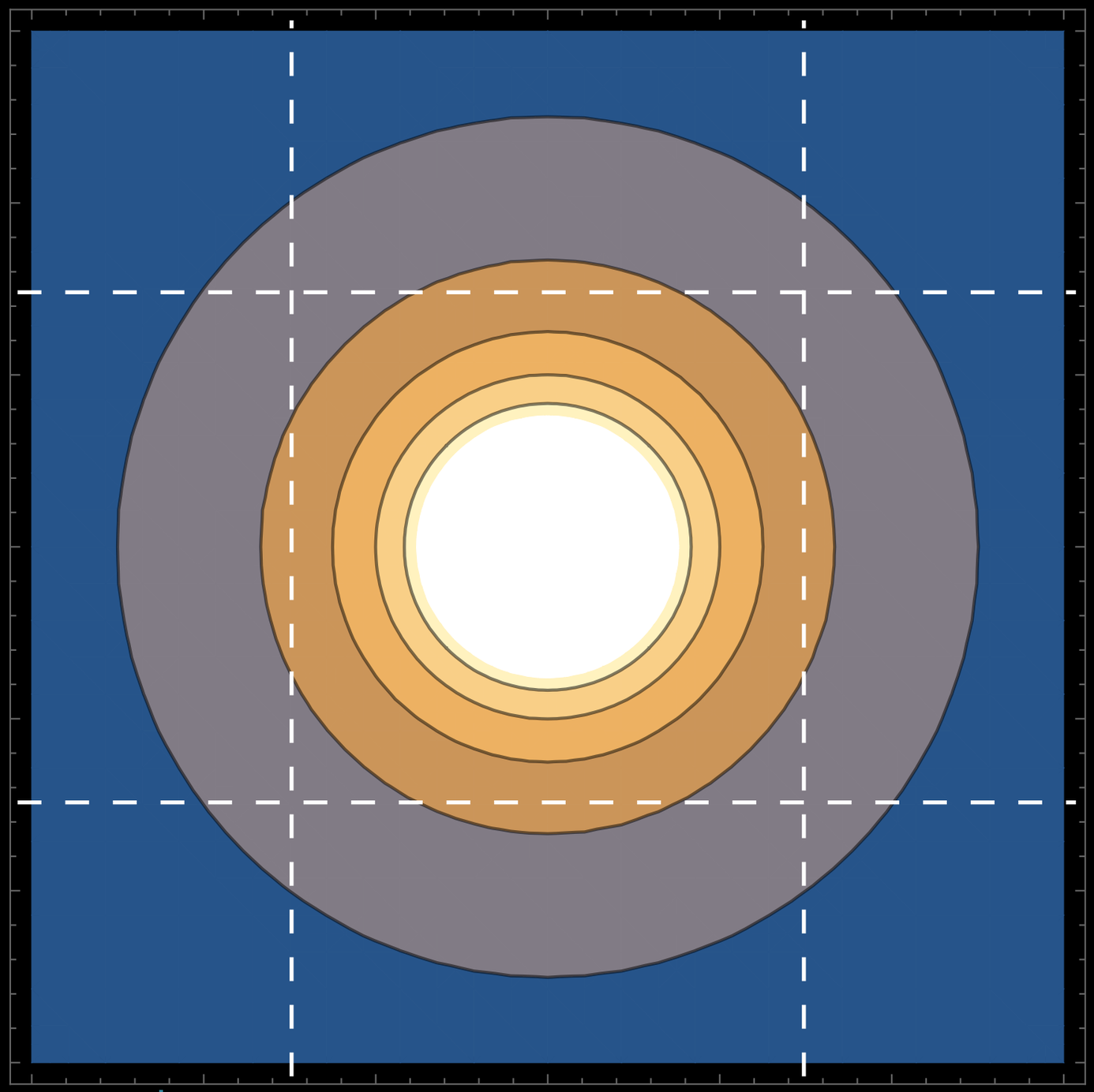

x-y plane

QED IS SPECIAL IN A FINITE VOLUME

COULOMB POTENTIAL OF A POINT CHARGE **WITH** THE UNIFORM CHARGE DENSITY

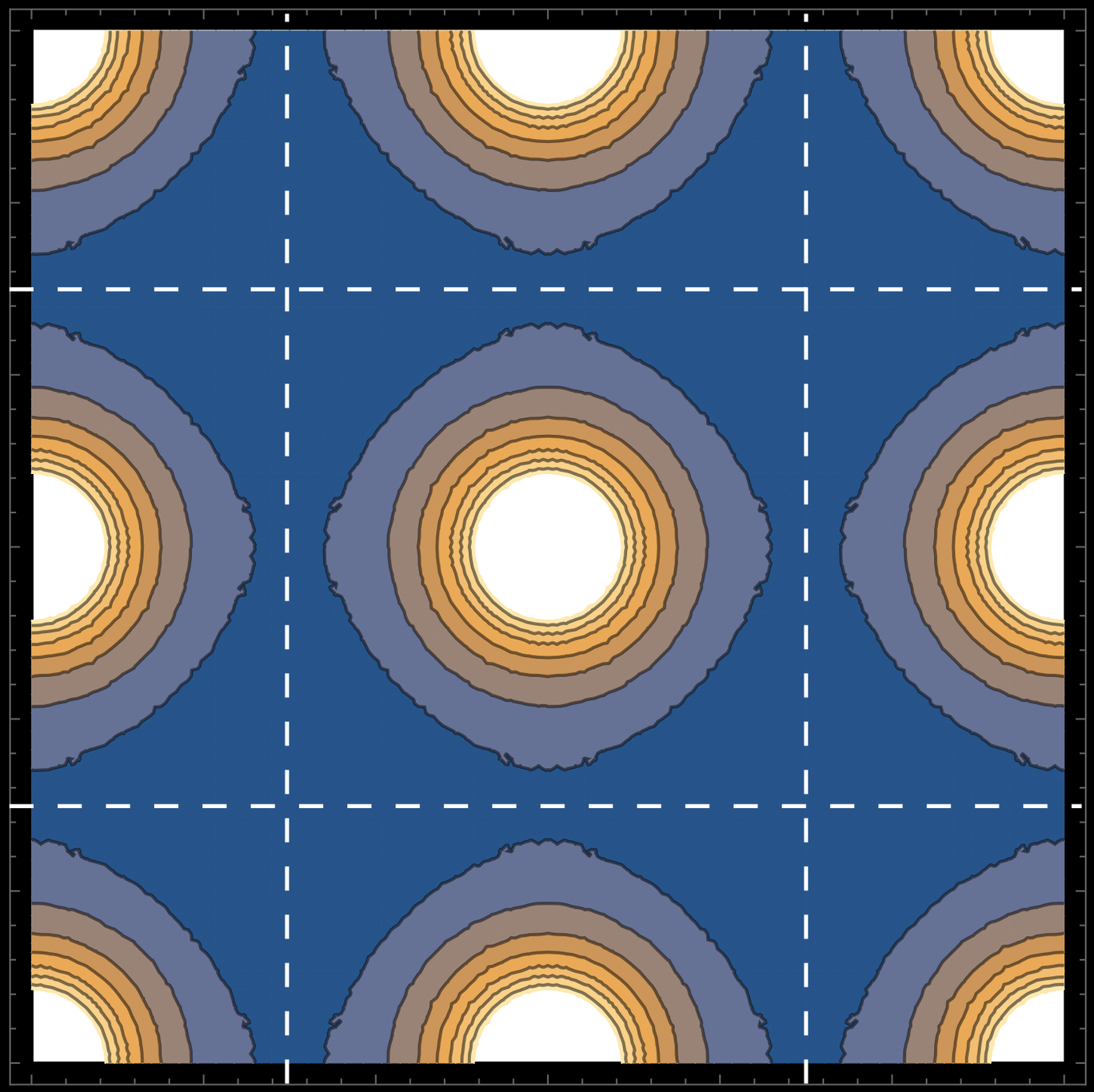

x-y plane

PREVIOUS INVESTIGATIONS OF QED FINITE-VOLUME EFFECTS ON MASSES

- VECTOR-DOMINANCE MODELS
  Bardeen, Bijnens and Gerard, Phys. Rev. Lett. 62, 1343 (1989)
  Duncan, at al., Phys. Rev. Lett. 76, 3894 (1996)
  Blum, et al., Phys. Rev. D 76, 114508 (2007)
- CHIRAL PERTURBATION THEORY
  Hayakawa and Uno, Prog. Theor. Phys. 120, 413 (2008)
  Blum, et al., Phys. Rev. D 82, 094508 (2010)
  Thomas, Lang and Young (2014), nucl-th:1406.4579
- SCALAR AND SPINOR QED
  Borsanyi, et al., arXiv:1406088.

CURRENT WORK

ZD, Martin J. Savage, Phys. Rev. D 90, 054503 (2014)

- SYSTEMATICALLY INCLUDING COMPOSITENESS CONTRIBUTIONS
- THE FIRST COMPLETE $\mathcal{O}\left(\frac{1}{L^4}\right)$ CALCULATION
- COMPLETELY GENERAL: APPLICABLE TO HADRONS AND NUCLEI

A CLASSICAL EXAMPLE: CHARGED SPHERE IN A FINITE VOLUME

SELF ENERGY

$$U(R,L) = \frac{1}{2}\int d^3r\, d^3r' \rho\, V(\mathbf{r}-\mathbf{r}')$$

$$\rho = \frac{eQ}{\frac{4}{3}\pi R^3}$$

$$V(\mathbf{r}-\mathbf{r}') = \frac{eQ}{4\pi|\mathbf{r}-\mathbf{r}'|}$$

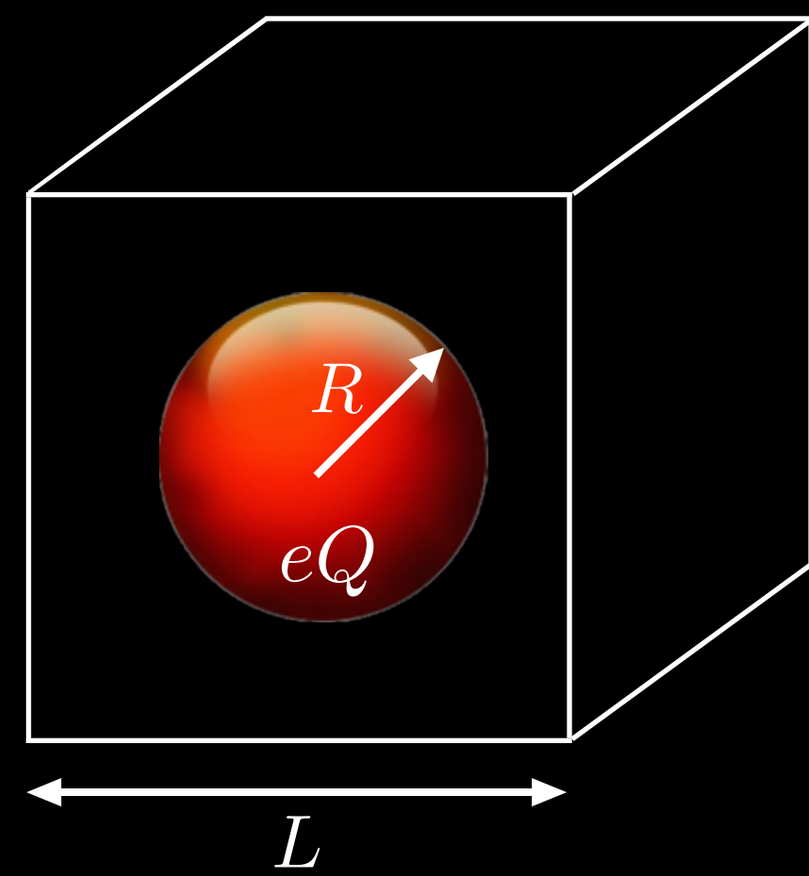

A CLASSICAL EXAMPLE: CHARGED SPHERE IN A FINITE VOLUME

SELF ENERGY

$$U(R,L) = \frac{1}{2}\int d^3r\, d^3r' \rho\, V(\mathbf{r}-\mathbf{r}')$$

$$\rho = \frac{eQ}{\frac{4}{3}\pi R^3}$$

$$V(\mathbf{r}-\mathbf{r}') = \frac{eQ}{4\pi|\mathbf{r}-\mathbf{r}'|}$$

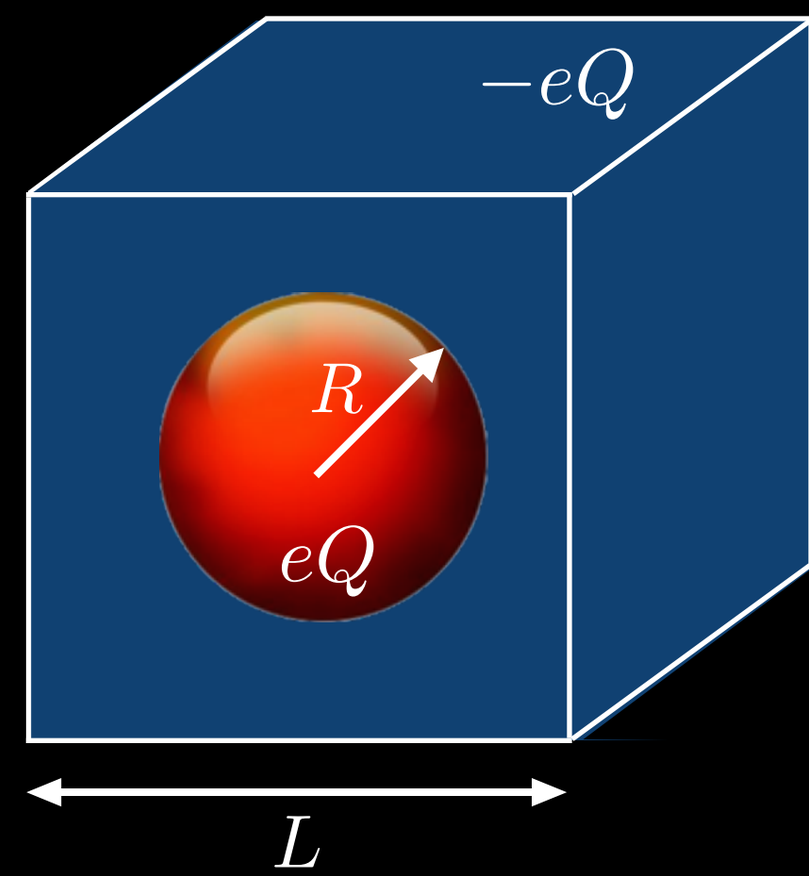

A CLASSICAL EXAMPLE: CHARGED SPHERE IN A FINITE VOLUME

SELF ENERGY

$$U(R,L) = \frac{1}{2}\int d^3r\, d^3r' \rho\, V(\mathbf{r}-\mathbf{r}')$$

$$\rho = \frac{eQ}{\frac{4}{3}\pi R^3}$$

$$V(\mathbf{r}-\mathbf{r}') = \frac{eQ}{4\pi|\mathbf{r}-\mathbf{r}'|}$$

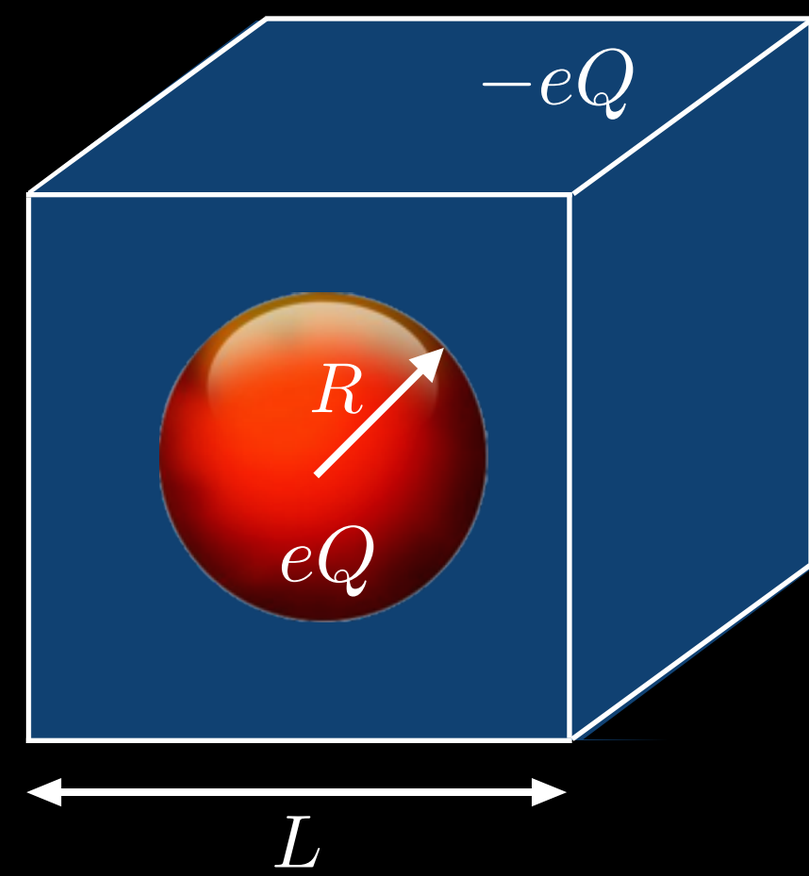

ZERO MODE REMOVED

$$V(\mathbf{r}-\mathbf{r}') = \frac{1}{L^3}\sum_{\mathbf{k}\in\frac{2\pi\mathbf{n}}{L},\mathbf{n}\neq\mathbf{0}} \frac{e^{i\mathbf{k}\cdot(\mathbf{r}-\mathbf{r}')}}{\mathbf{k}^2} = V^{(\infty)}(\mathbf{r}-\mathbf{r}') + \sum_{\mathbf{m}\neq\mathbf{0}}\int \frac{d^3k}{(2\pi)^2}\frac{e^{i\mathbf{k}\cdot(\mathbf{r}-\mathbf{r}')}}{\mathbf{k}^2}e^{i\mathbf{k}\cdot\mathbf{m}L}$$

POISSON RE-SUMMATION
(NOT EXACTLY: INCLUDE THE ZERO MODE BUT INTRODUCE AN IR REGULATOR. SUBTRACT OFF THE IR DIVERGENCE AT THE END.)

A CLASSICAL EXAMPLE: CHARGED SPHERE IN A FINITE VOLUME

SELF ENERGY

$$U(R,L) = \frac{1}{2}\int d^3r\, d^3r' \rho\, V(\mathbf{r}-\mathbf{r}')$$

$$\rho = \frac{eQ}{\frac{4}{3}\pi R^3}$$

$$V(\mathbf{r}-\mathbf{r}') = \frac{eQ}{4\pi|\mathbf{r}-\mathbf{r}'|}$$

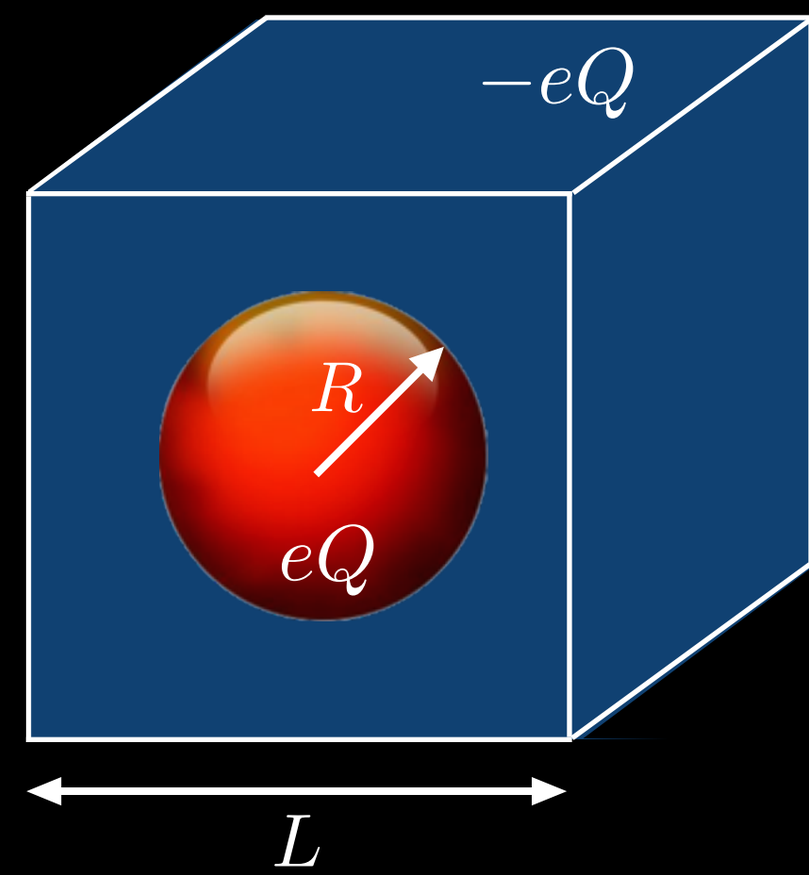

EXPANSION IN R/L

$$U(R,L) = \frac{3}{5}\frac{(Qe)^2}{4\pi R} + \frac{(Qe)^2}{8\pi L}\, c_1 + \frac{(Qe)^2}{10L}\left(\frac{R}{L}\right)^2 + \cdots$$

$$c_1 = -2.83729$$

A CLASSICAL EXAMPLE: CHARGED SPHERE IN A FINITE VOLUME

SELF ENERGY

$$U(R,L) = \frac{1}{2}\int d^3r\, d^3r' \rho\, V(\mathbf{r}-\mathbf{r}')$$

$$\rho = \frac{eQ}{\frac{4}{3}\pi R^3}$$

$$V(\mathbf{r}-\mathbf{r}') = \frac{eQ}{4\pi|\mathbf{r}-\mathbf{r}'|}$$

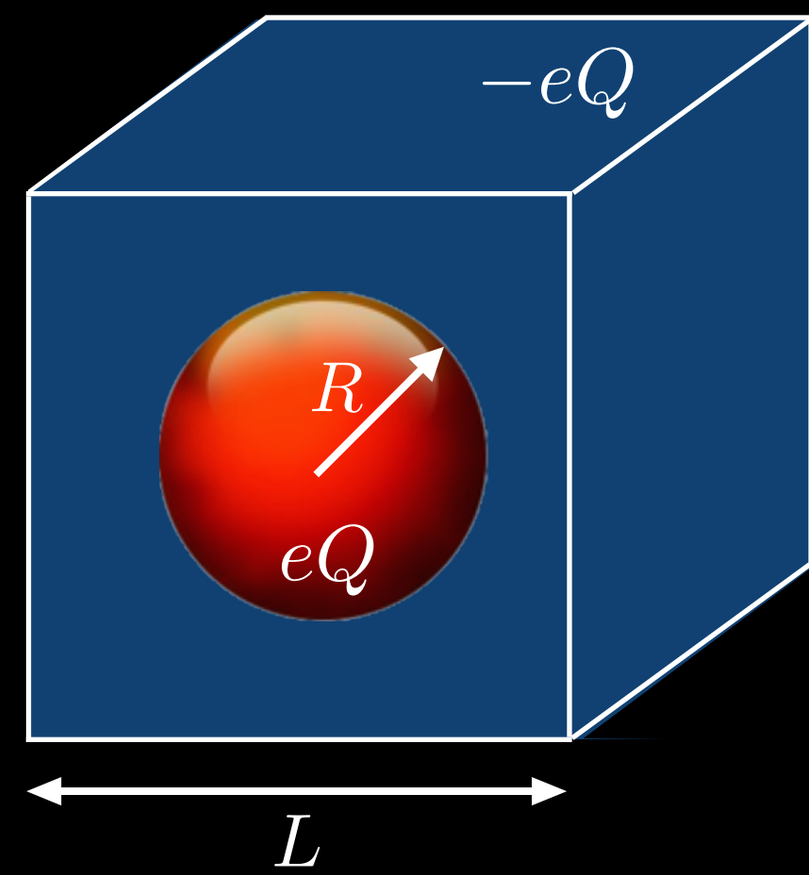

EXPANSION IN R/L

$$U(R,L) = \frac{3}{5}\frac{(Qe)^2}{4\pi R} + \frac{(Qe)^2}{8\pi L}\, c_1 + \frac{(Qe)^2}{10L}\left(\frac{R}{L}\right)^2 + \cdots$$

INDEPENDENT OF R

$$\frac{(Qe)^2}{6L^3}\langle r^2\rangle \text{ with } \langle r^2\rangle = \frac{3}{5}R^2$$

A NON-RELATIVISTIC EFFECTIVE FIELD THEORY APPROACH

HEAVY-FIELD FORMALISM

Isgur and Wise, Phys. Lett. B 232, 113 (1989)

Isgur and Wise, Phys. Lett. B 237, 527 (1990)

Jenkins and Manohar, Phys. Lett. B 255, 558 (1991)

Thacker and Lepage, Phys.Rev. D 43, 196 (1991)

Labelle (1992), hep-ph/9209266.

Manohar, Phys. Rev. D 56, 230 (1997)

Luke and Savage, Phys. Rev. D 57, 413 (1998)

Hill and Paz, Phys. Rev. Lett. 107, 160402 (2011)

Chen, Rupak and Savage, Nucl. Phys. A 653, 386 (1999)

COMPOSITE SPIN-0 PARTICLES

NR-QED LAGRANGIAN

$$\mathcal{L}_\phi = \phi^\dagger \left[iD_0 + \frac{|\mathbf{D}|^2}{2m_\phi} + \frac{|\mathbf{D}|^4}{8m_\phi^3} + \frac{e\langle r^2\rangle_\phi}{6}\nabla\cdot\mathbf{E} + 2\pi\tilde{\alpha}_E^{(\phi)}|\mathbf{E}|^2 + 2\pi\tilde{\beta}_M^{(\phi)}|\mathbf{B}|^2 + iec_M\frac{\{D^i,(\nabla\times\mathbf{B})^i\}}{8m_\phi^3} + \cdots \right]\phi$$

$$D_0 = \partial_0 + ieQA_0$$

$$\mathbf{D} = \vec{\nabla} - ieQ\mathbf{A}$$

MATCHING

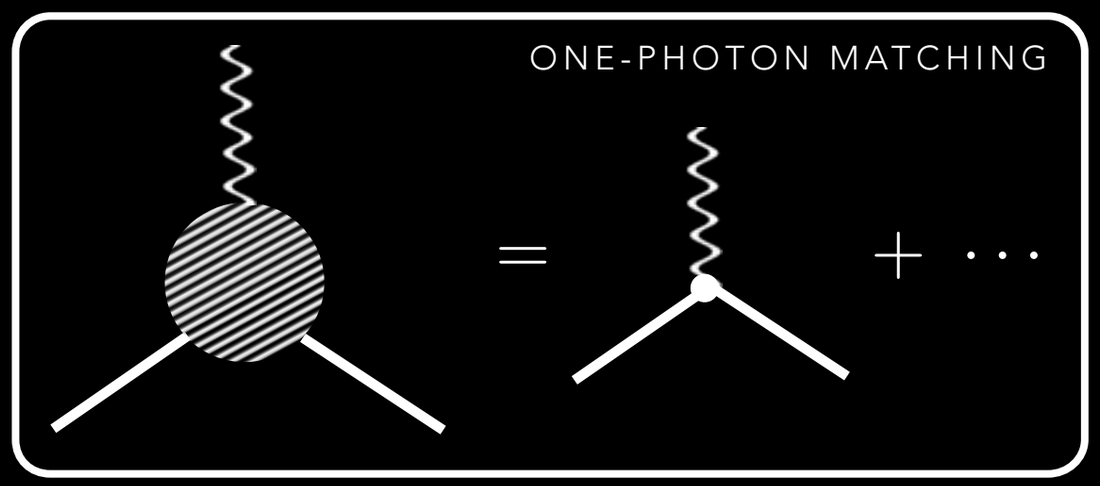

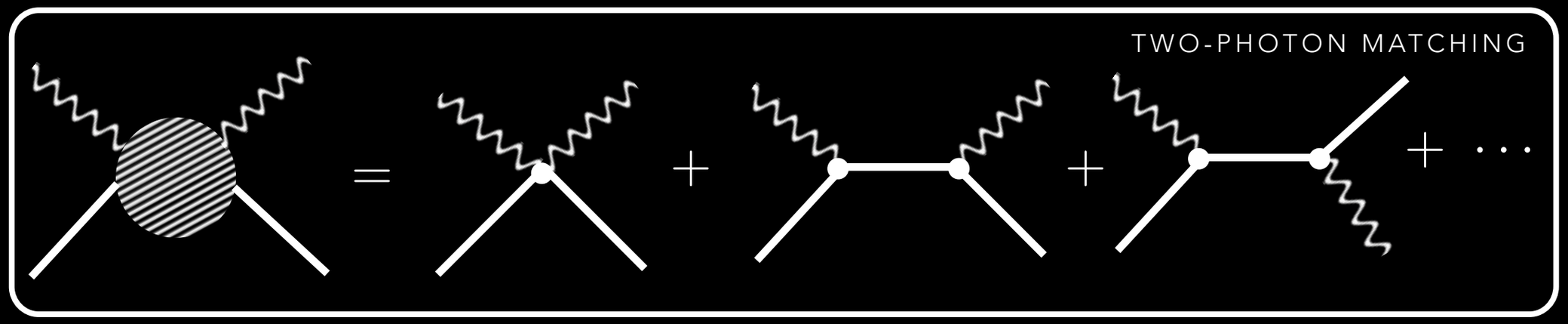

$$\tilde{\alpha}_E^{(\phi)} = \alpha_E^{(\phi)} - \frac{\alpha_e Q}{3m_\phi}\langle r^2\rangle_\phi$$

$$\tilde{\beta}_M^{(\phi)} = \beta_M^{(\phi)}$$

$$c_M = \frac{2}{3}m_\phi^2\langle r^2\rangle_\phi$$

COMPOSITE SPIN-0 PARTICLES

PROPAGATOR

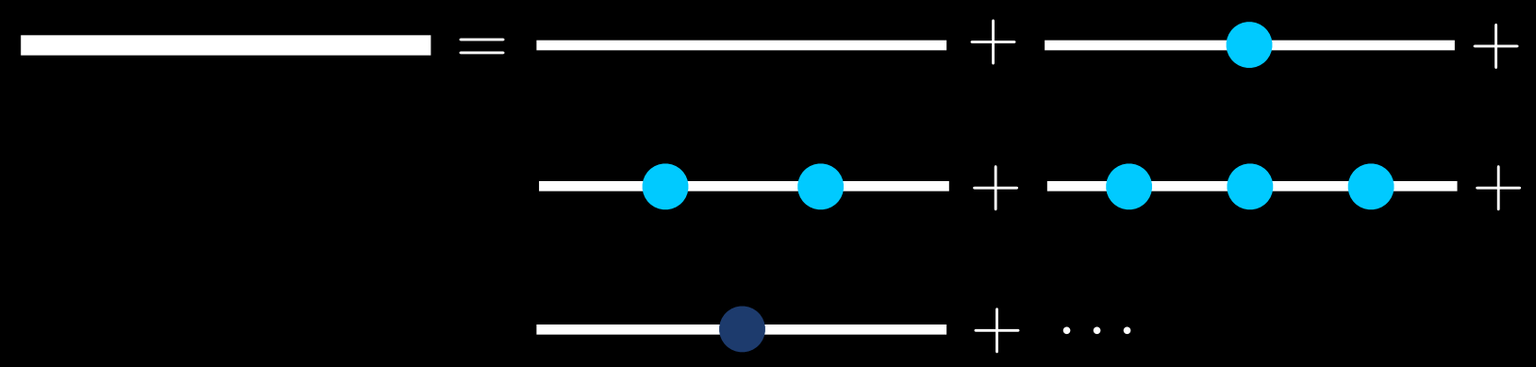

$$\mathcal{O}\left(\frac{1}{m_\phi}\right)$$

$$\mathcal{O}\left(\frac{1}{m_\phi^2}, \langle r^2 \rangle_\phi\right)$$

$$\mathcal{O}\left(\frac{1}{m_\phi^3}, \frac{\langle r^2 \rangle_\phi}{m_\phi}, \alpha_E, \beta_M\right)$$

VERTICES

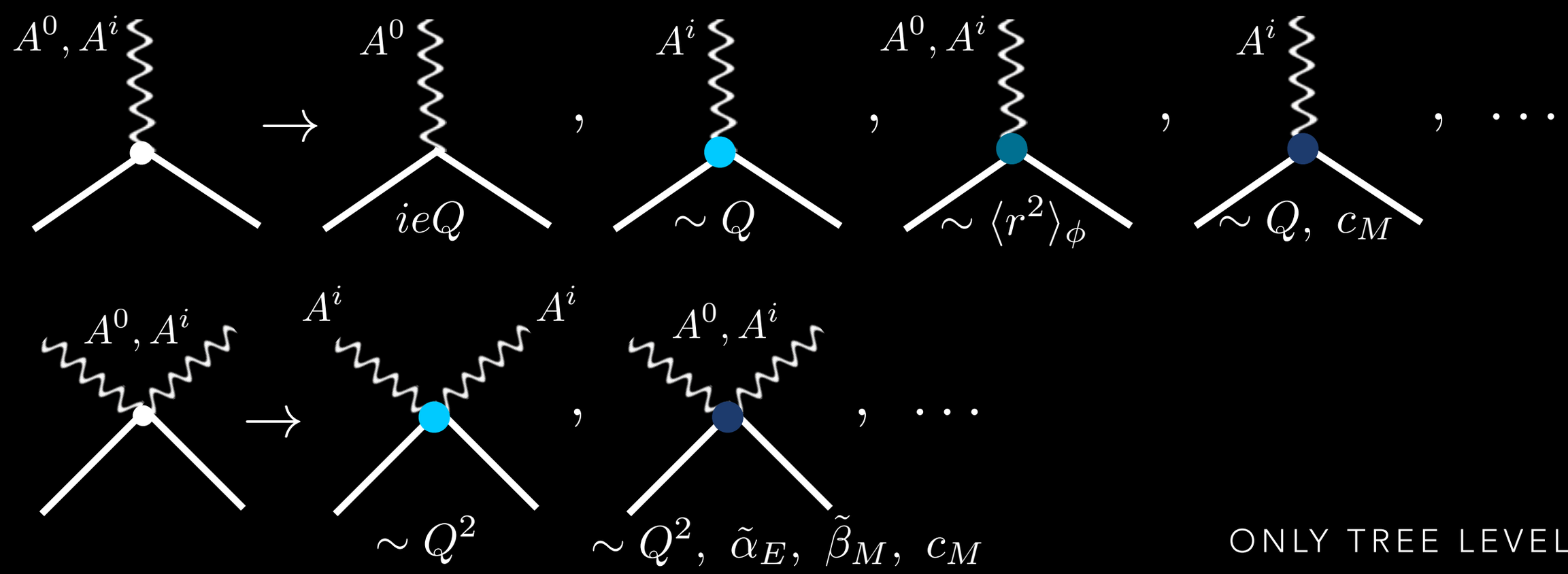

ONLY TREE LEVEL

COMPOSITE SPIN-0 PARTICLES

WHAT IS $\delta m_\phi = m_\phi^V - m_\phi^\infty$?

LEADING ORDER

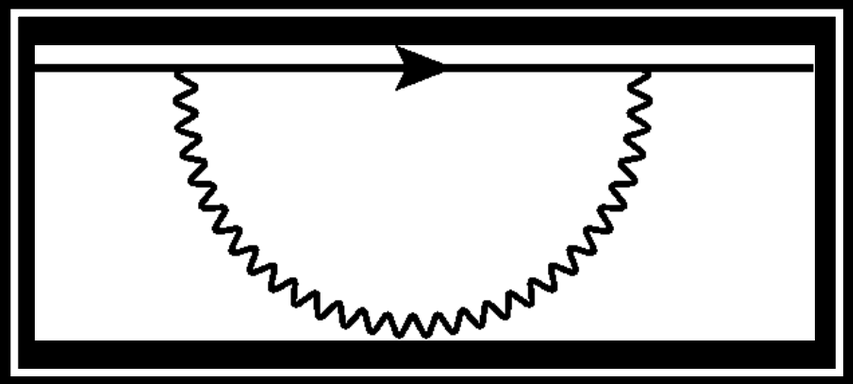

$$\delta m_\phi^{(\mathrm{LO})} = \frac{\alpha_e Q^2}{2\mathrm{L}}\, c_1$$

NEXT-TO-LEADING ORDER

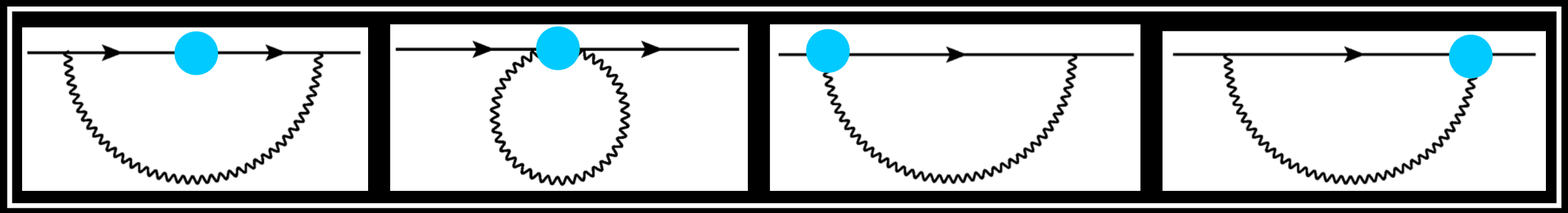

Also by:
Hayakawa and Uno, Prog. Theor. Phys. 120, 413 (2008)
Borsanyi, et al., arXiv:1406088.

$$\delta m_\phi^{(\mathrm{NLO})} = \frac{\alpha_e Q^2}{m_\phi L^2}\, c_1$$

$$\hat{\sum_{\mathbf{n}\neq\mathbf{0}}} \frac{1}{|\mathbf{n}|^2} = \pi c_1, \quad \hat{\sum_{\mathbf{n}\neq\mathbf{0}}} \frac{1}{|\mathbf{n}|} = c_1 = -2.83729, \quad \hat{\sum_{\mathbf{n}\neq\mathbf{0}}} 1 = -1, \hat{\sum_{\mathbf{n}\neq\mathbf{0}}} |\mathbf{n}| = c_{-1} = -0.266596.$$

COMPOSITE SPIN-0 PARTICLES

WHAT IS $\delta m_\phi = m_\phi^V - m_\phi^\infty$?

NEXT-TO-NEXT-TO-LEADING ORDER

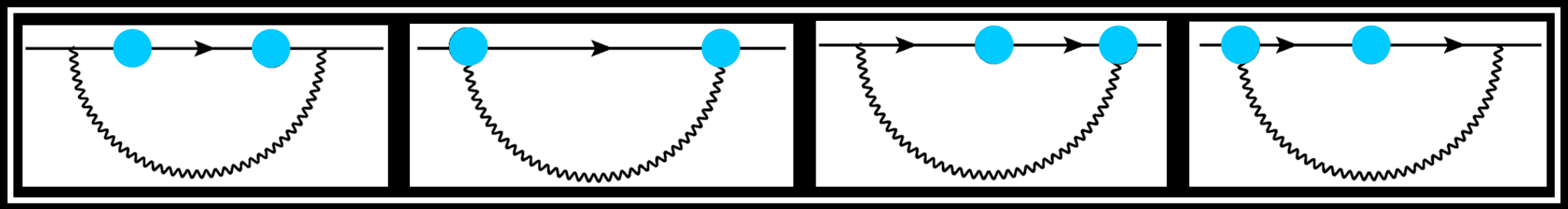

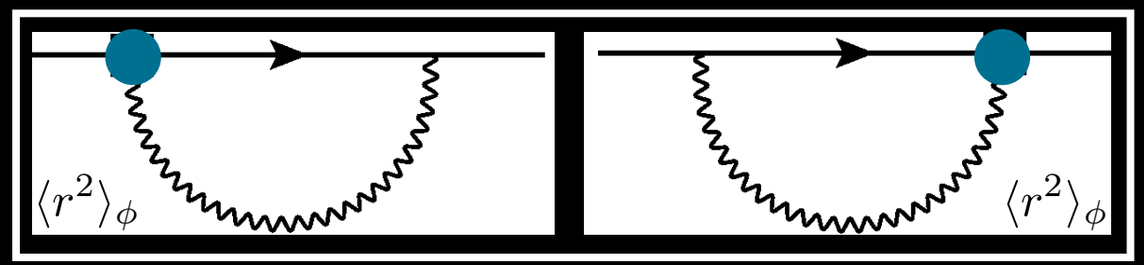

$$\delta m_\phi^{(\mathrm{N^2LO})} = \frac{2\pi\alpha_e Q}{3L^3} \langle r^2 \rangle_\phi$$

NEXT-TO-NEXT-TO-NEXT-T0-LEADING ORDER

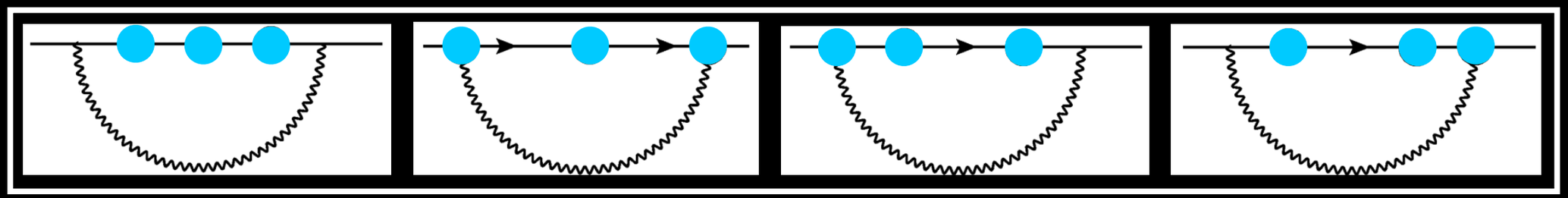

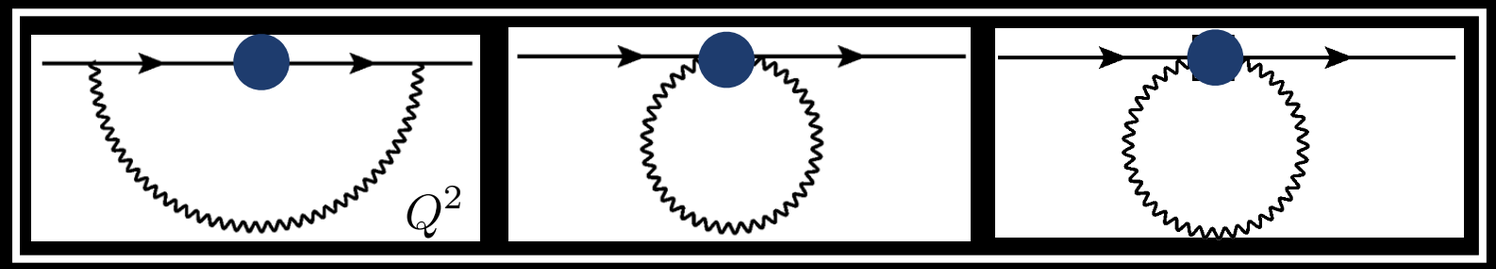

$$\delta m_\phi^{(\mathrm{N^3LO})} = -\frac{4\pi^2}{L^4}\left(\alpha_E^{(\phi)} + \beta_M^{(\phi)}\right) c_{-1} + \frac{4\pi^2\alpha_e Q}{3m_\phi L^4} \langle r^2 \rangle_\phi \, c_{-1}$$

VOLUME-DEPENDENCE OF KAON AND PION MASSES

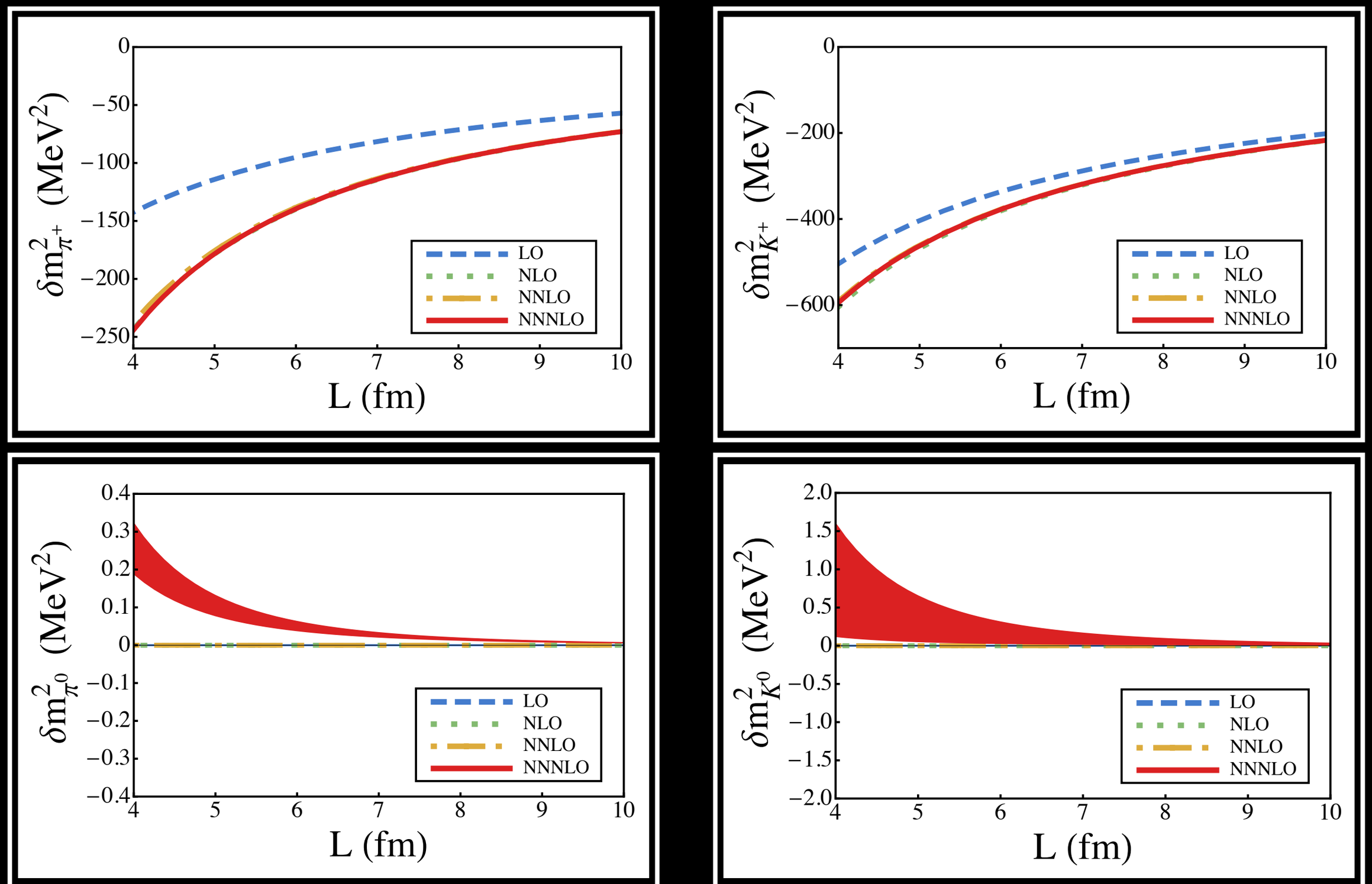

COMPOSITE SPIN-1/2 PARTICLES

NR-QED LAGRANGIAN

$$\mathcal{L}_\psi = \psi^\dagger[iD_0 + \frac{|\mathbf{D}|^2}{2M_\psi} + \frac{|\mathbf{D}|^4}{8M_\psi^3} + c_F\frac{e}{2M_\psi}\sigma\cdot\mathbf{B} + c_D\frac{e}{8M_\psi^2}\nabla\cdot\mathbf{E} + ic_S\frac{e}{8M_\psi^2}\sigma\cdot(\mathbf{D}\times\mathbf{E}-\mathbf{E}\times\mathbf{D}) +$$

$$2\pi\tilde{\alpha}_E^{(\psi)}|\mathbf{E}|^2 + 2\pi\tilde{\beta}_M^{(\psi)}|\mathbf{B}|^2 + iec_M\frac{\{D^i,(\nabla\times\mathbf{B})^i\}}{8M_\psi^3} + \cdots]\psi$$

MATCHING

$$c_F = Q + \kappa_\psi + \mathcal{O}(\alpha_e)$$

$$c_D = Q + \frac{4}{3}M_\psi^2\langle r^2\rangle_\psi + \mathcal{O}(\alpha_e)$$

$$c_S = 2c_F - Q$$

$$c_M = (c_D - c_F)/2$$

$$\tilde{\alpha}_E^{(\psi)} = \alpha_E^{(\psi)} - \frac{\alpha_e}{4M_\psi^3}\left(Q^2+\kappa_\psi^2\right) - \frac{\alpha_e Q}{3M_\psi}\langle r^2\rangle_\psi$$

$$\tilde{\beta}_M^{(\psi)} = \beta_M^{(\psi)} + \frac{\alpha_e Q^2}{4M_\psi^3}$$

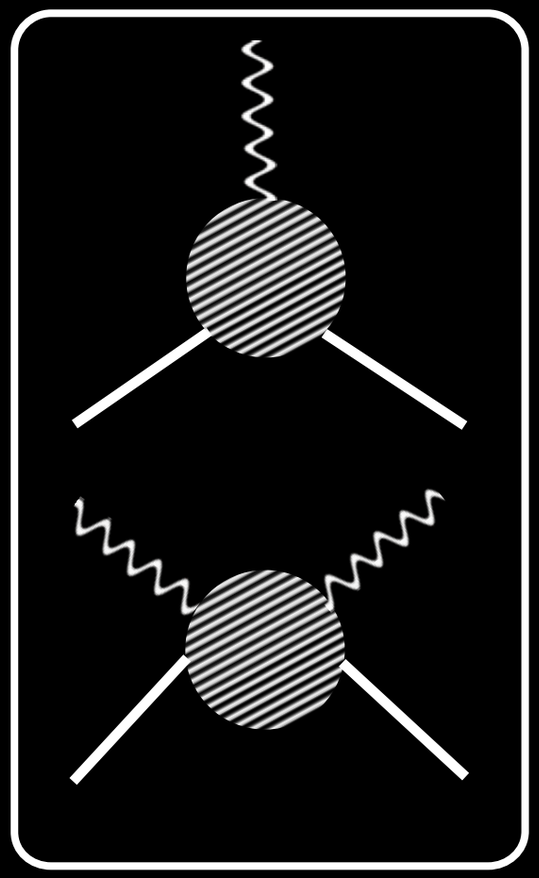

COMPOSITE SPIN-1/2 PARTICLES

WHAT IS $\delta M_\psi = M_\psi^V - M_\psi^\infty$?

NEW CONTRIBUTIONS:

NNLO

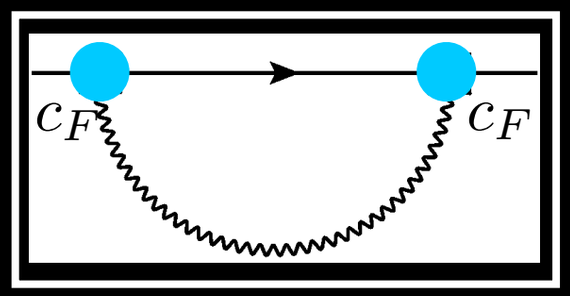

NNNLO

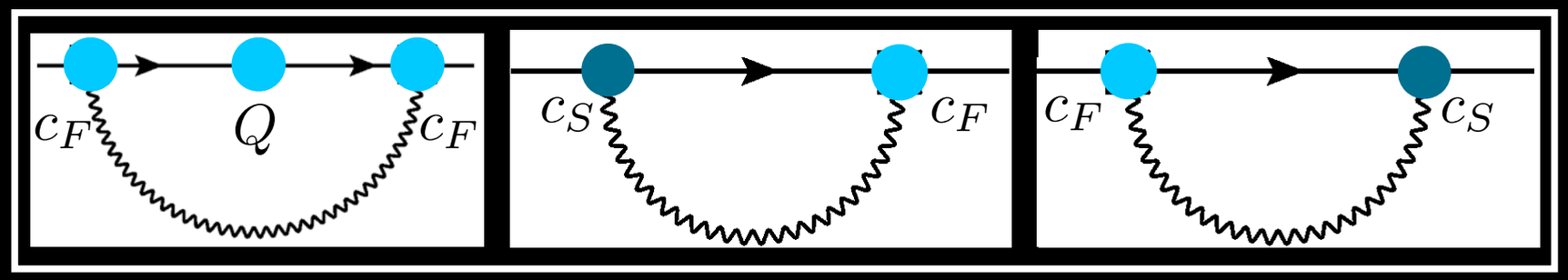

RESULT

$$\delta M_\psi = \frac{\alpha_e Q^2}{2L} c_1 + \frac{\alpha_e Q^2}{M_\psi L^2} c_1 + \frac{2\pi\alpha_e Q}{3L^3}\langle r^2\rangle_\psi + \frac{\pi\alpha_e}{M_\psi^2 L^3}\left[\frac{1}{2}Q^2 + (Q+\kappa_\psi)^2\right]$$

$$-\frac{4\pi^2}{L^4}\left(\tilde{\alpha}_E^{(\psi)} + \tilde{\beta}_M^{(\psi)}\right)c_{-1} + \frac{\pi^2\alpha_e Q}{M_\psi^3 L^4}\left(\frac{4}{3}M_\psi^2\langle r^2\rangle_\psi - \kappa_\psi\right)c_{-1} - \frac{\alpha_e\pi^2}{M_\psi^3 L^4}\kappa_\psi(Q+\kappa_\psi)c_{-1}$$

COMPOSITE SPIN-1/2 PARTICLES

WHAT IS $\delta M_\psi = M_\psi^V - M_\psi^\infty$?

NEW CONTRIBUTIONS:

NNLO

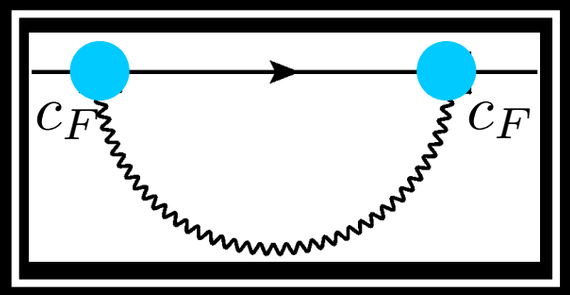

NNNLO

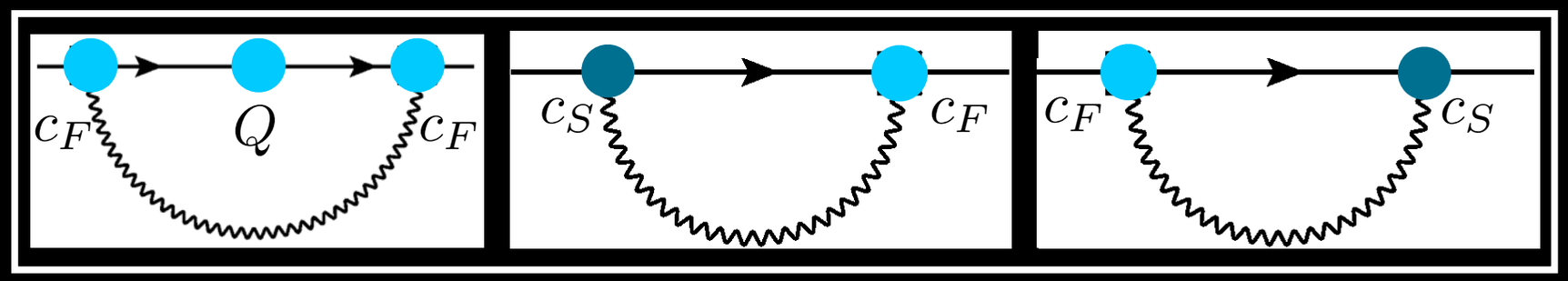

RESULT

$$\delta M_\psi = \frac{\alpha_e Q^2}{2L} c_1 + \frac{\alpha_e Q^2}{M_\psi L^2} c_1 + \frac{2\pi\alpha_e Q}{3L^3}\langle r^2\rangle_\psi + \frac{\pi\alpha_e}{M_\psi^2 L^3}\left[\frac{1}{2}Q^2 + (Q+\kappa_\psi)^2\right]$$

$$-\frac{4\pi^2}{L^4}\left(\tilde{\alpha}_E^{(\psi)} + \tilde{\beta}_M^{(\psi)}\right)c_{-1} + \frac{\pi^2\alpha_e Q}{M_\psi^3 L^4}\left(\frac{4}{3}M_\psi^2\langle r^2\rangle_\psi - \kappa_\psi\right)c_{-1} - \frac{\alpha_e\pi^2}{M_\psi^3 L^4}\kappa_\psi(Q+\kappa_\psi)c_{-1}$$

VOLUME-DEPENDENCE OF PROTON AND NEUTRON MASSES

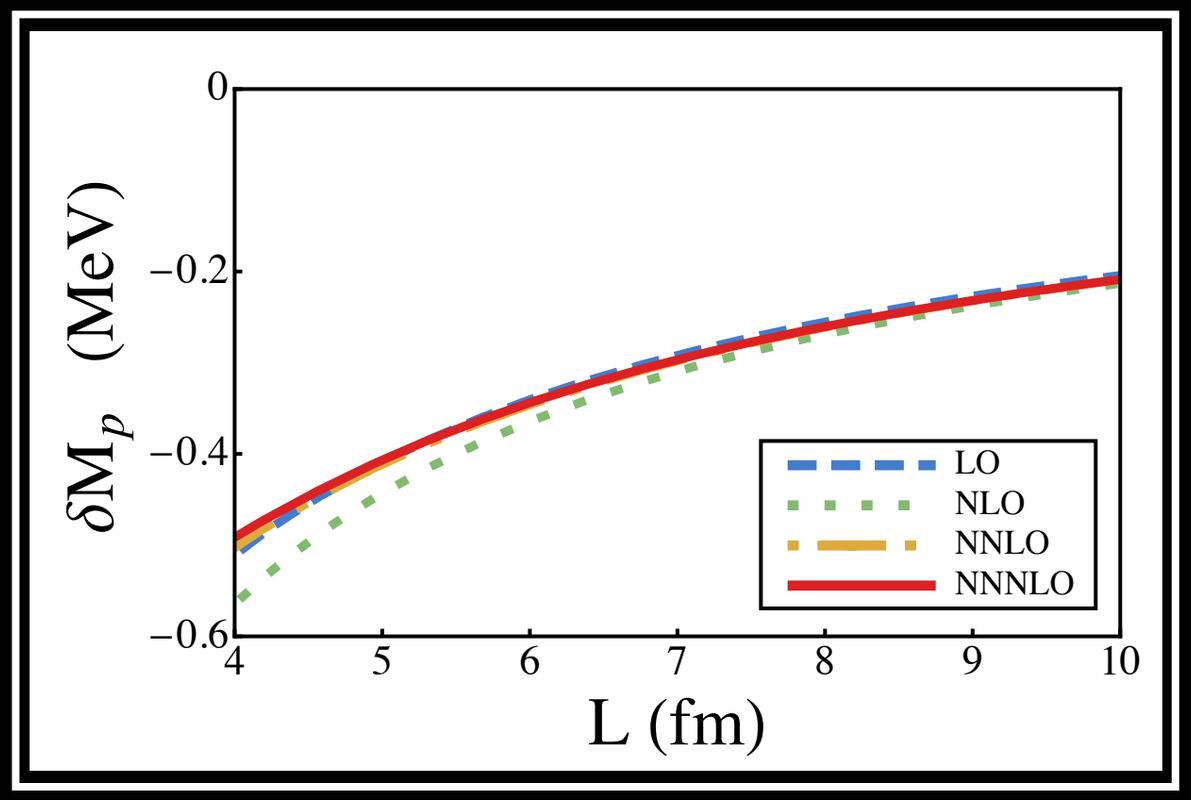

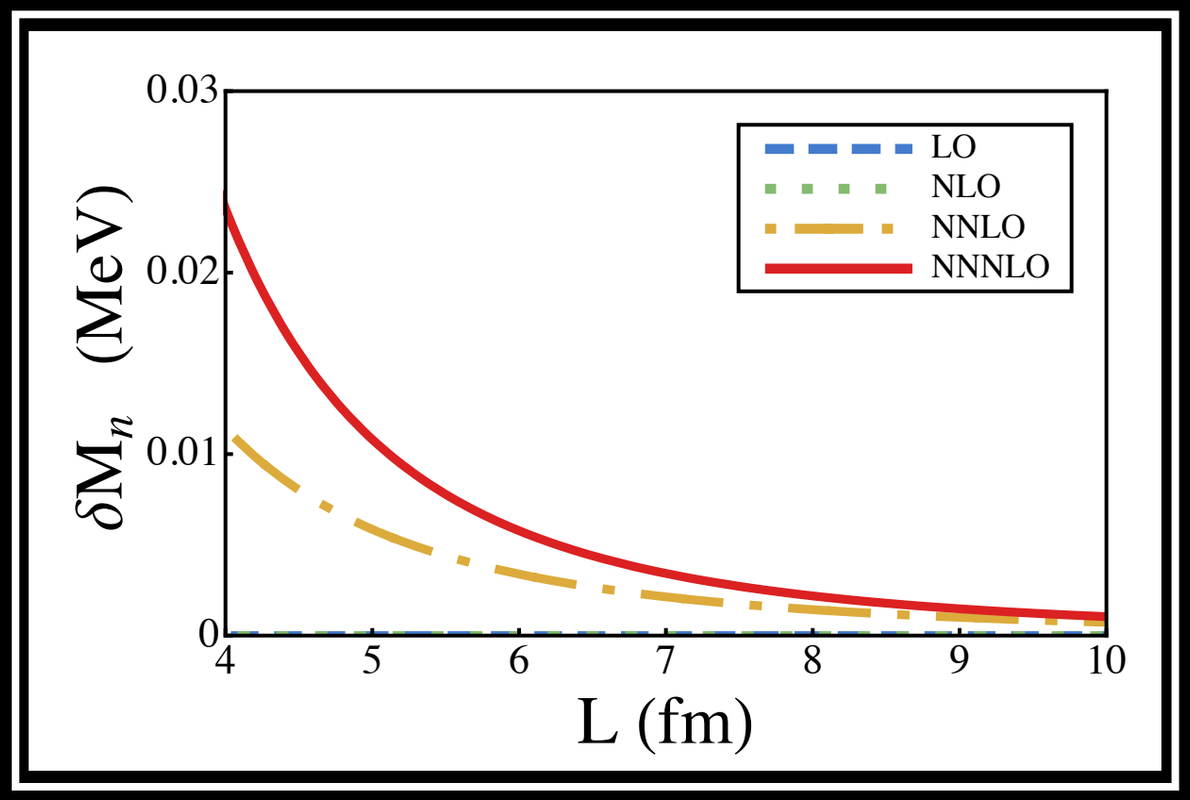

VOLUME-DEPENDENCE OF LIGHT NUCLEI: DEUTERON AND HELIUM-4

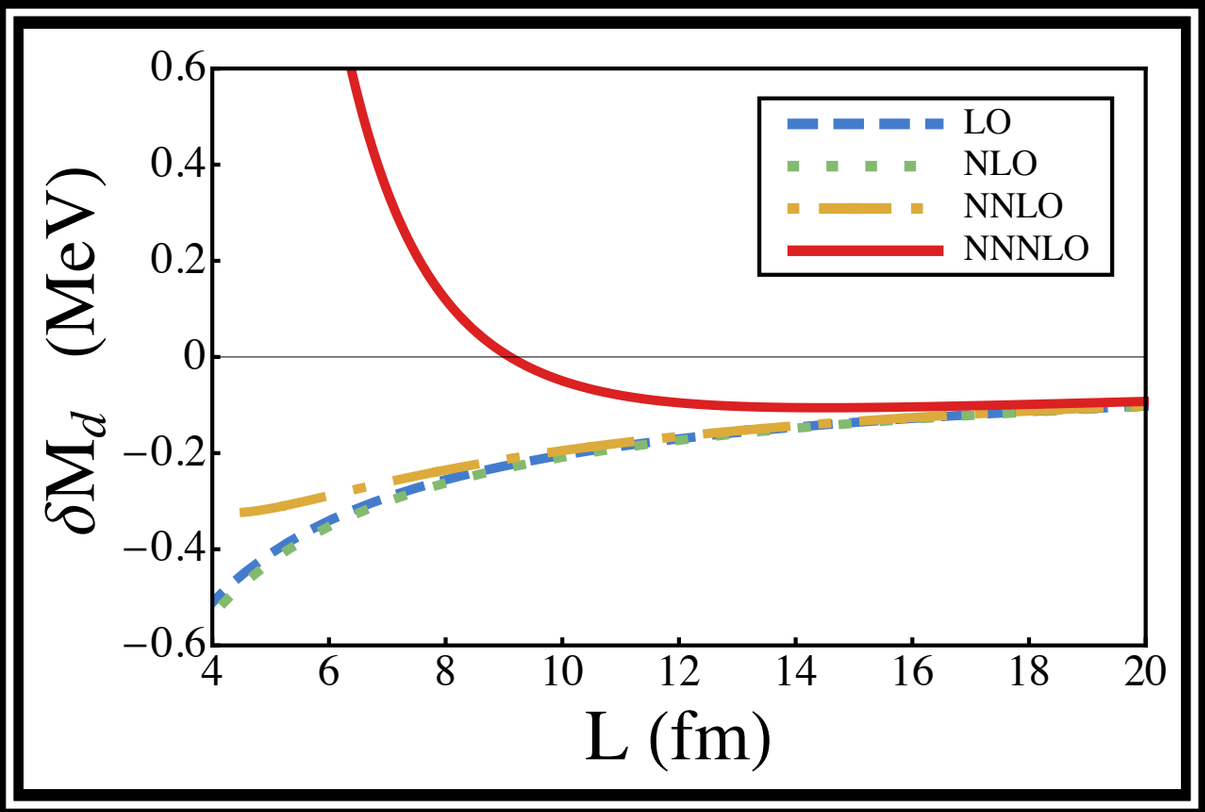

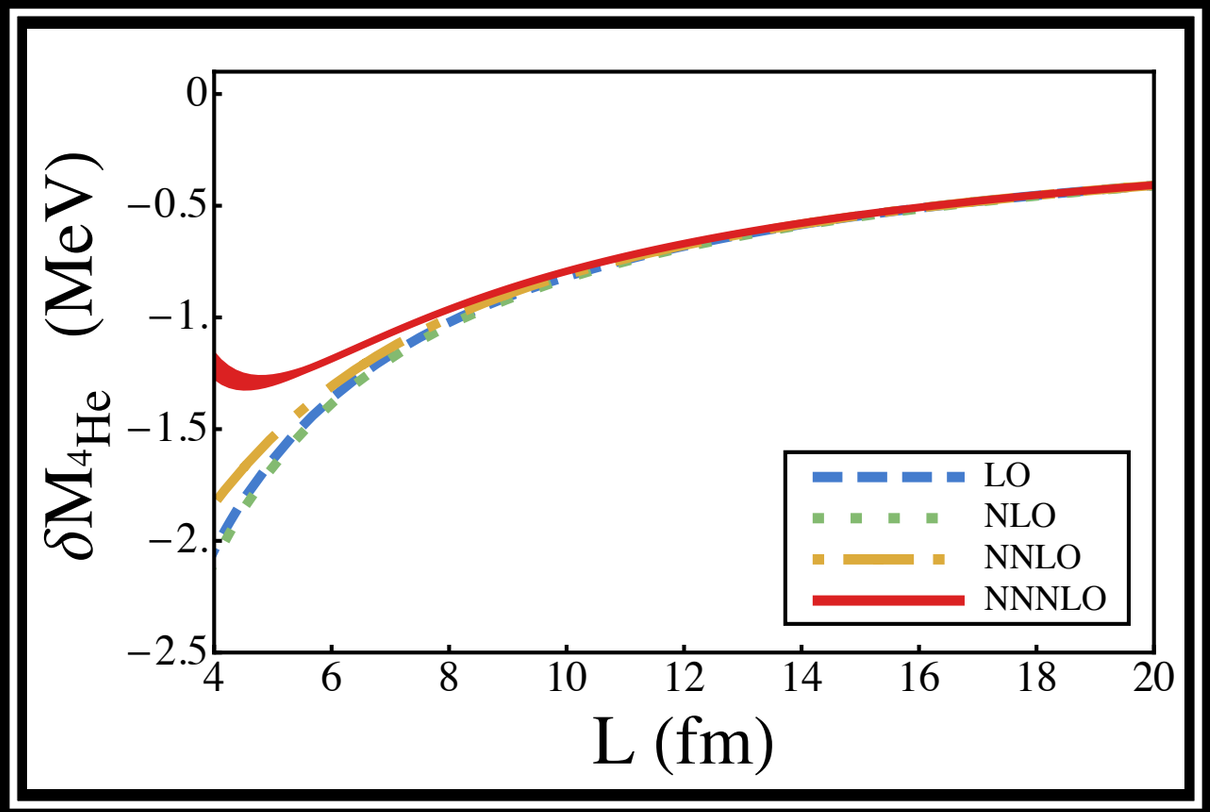

MAGNETIC MOMENT OF MUON

FINITE-VOLUME CORRECTIONS TO κ_μ?

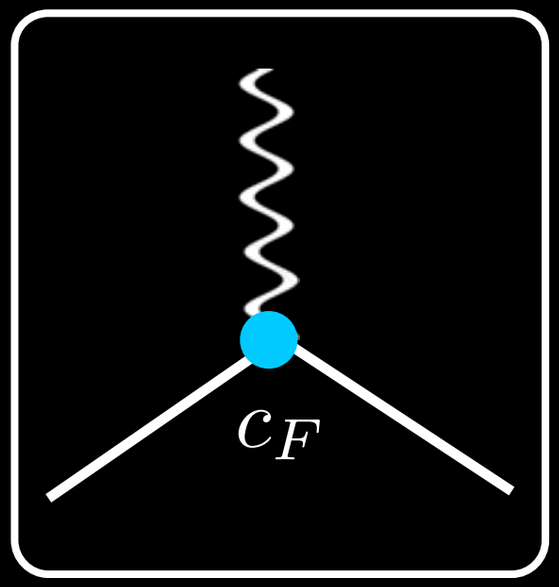

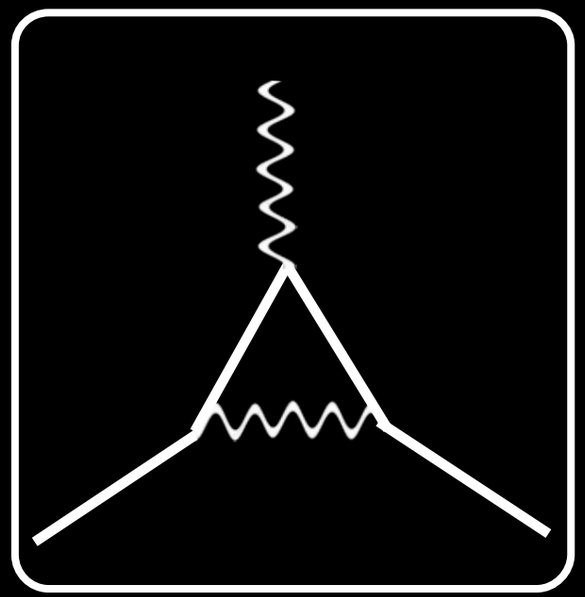

NR-QED $\times \left(\sqrt{\frac{E}{M_\mu}}\right)^2$ $\longrightarrow$ QED

RESULT

$$\kappa_\mu \equiv \frac{g_\mu - 2}{2} = \frac{\alpha_e}{2\pi}\left[1 + \frac{\pi c_1}{M_\mu \mathrm{L}} + \mathcal{O}\left(\frac{1}{M_\mu^2 \mathrm{L}^2}\right)\right]$$

$1\mathrm{ppm}$ PRECISION REQUIRES $\sim (60\ \mathrm{nm})^3$ VOLUMES!!

WHY SHOULD WE CONTROL FINITE-VOLUME EFFECTS IN SINGLE-HADRON SECTOR?

- MASS SPLITTING IN HADRONIC MULTIPLETS e.g. Blum, et al., Phys. Rev. D 82, 094508 (2010) Divitiis, et al., Phys. Rev. D 87, 114505 (2013)

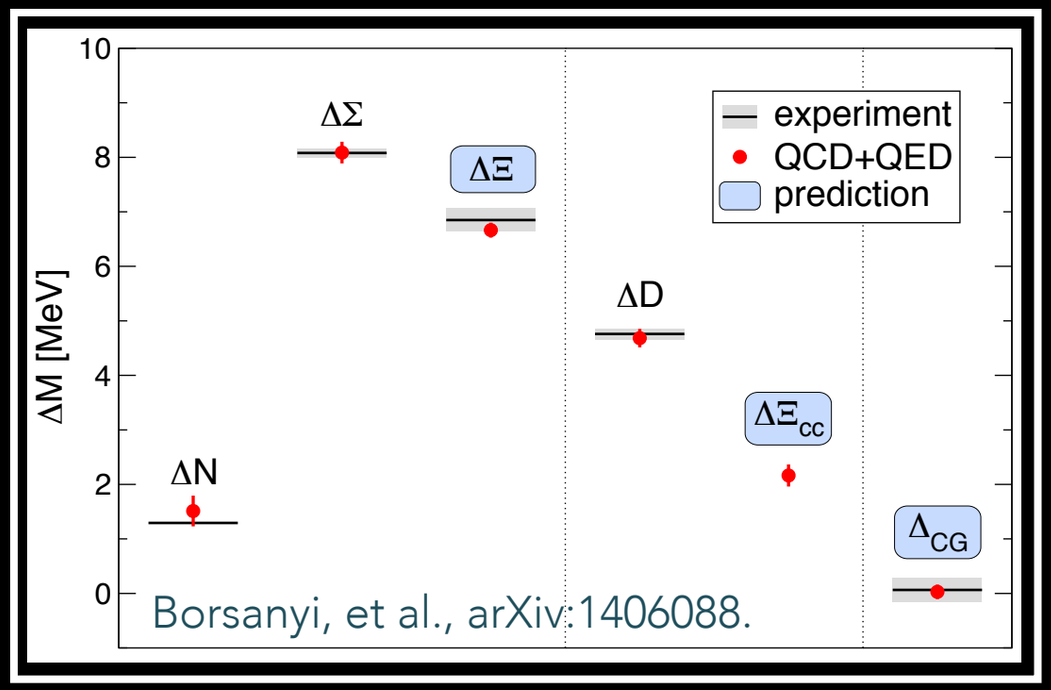

- SINGLE-HADRON MATRIX ELEMENTS e.g. Corrasco, et al., arXiv:1502.0025 (2015)

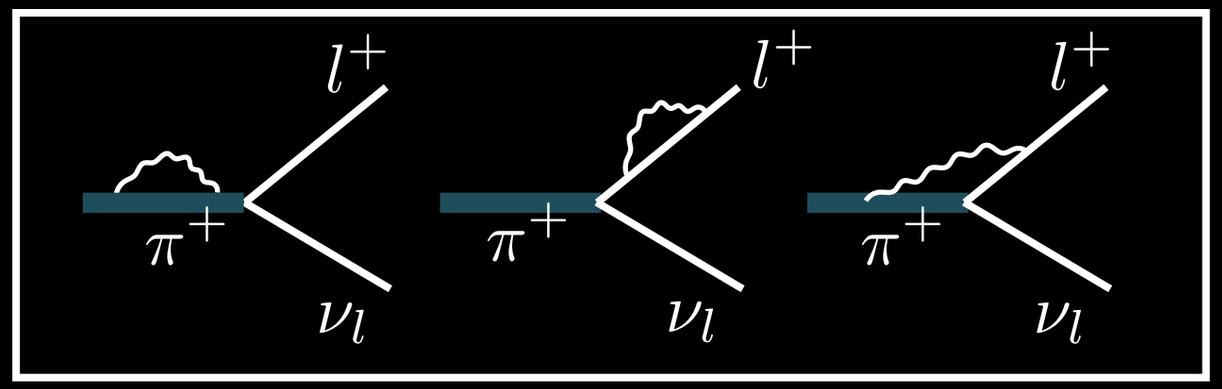

- HADRONIC CONTRIBUTIONS TO MUON $g-2$ e.g. Blum, et al., Phys. Rev. Lett. 114, 012001 (2014)

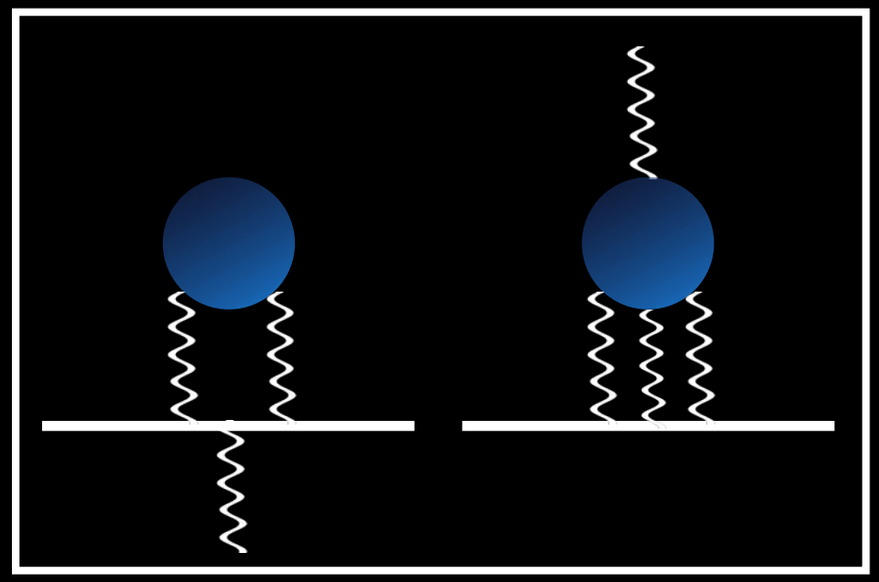

- MULTI-HADRON PROCESSES WITH QED Beane and Savage, Phys. Rev. D 90, 074511 (2014)

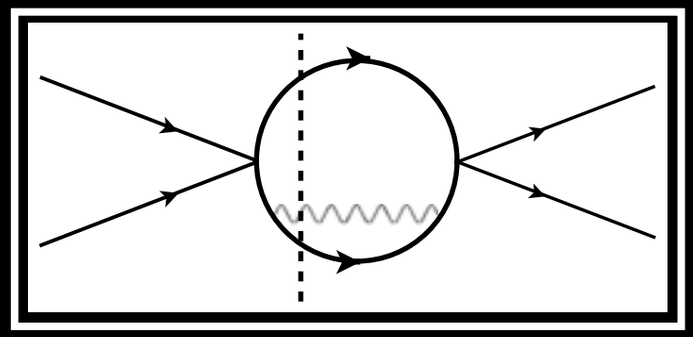

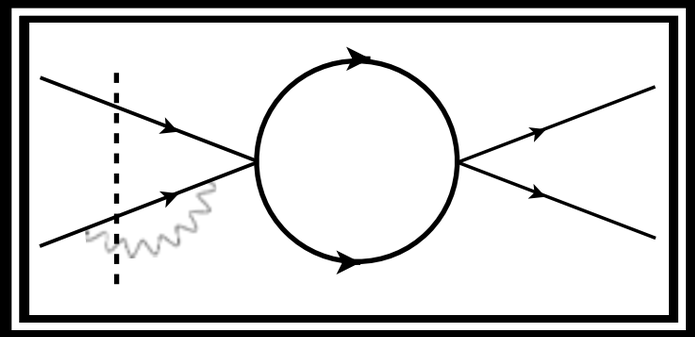

CONCLUSION

- ELIMINATION OF ZERO MODE GIVES RISE TO A SENSIBLE QED IN A FINITE VOLUME.

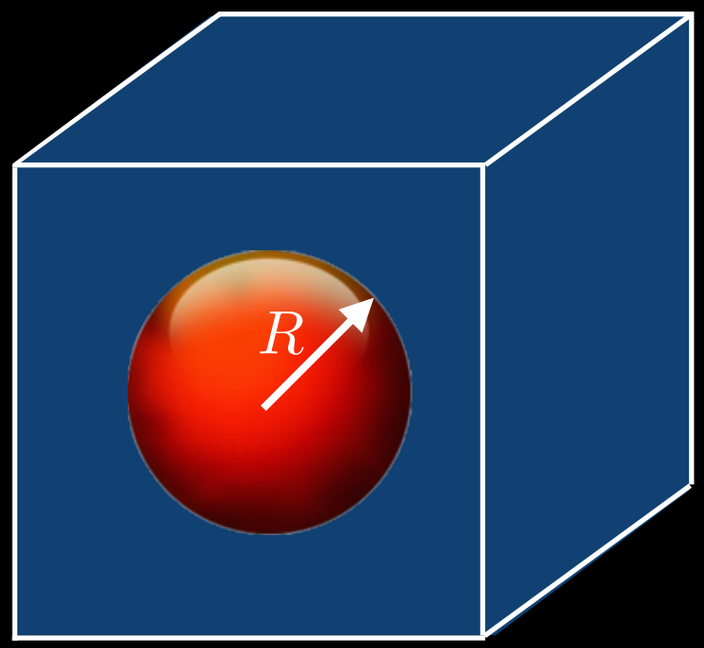

- CHARGED PARTICLES ARE LARGELY AFFECTED BY THE FINITE BOUNDARY OF THE VOLUME.

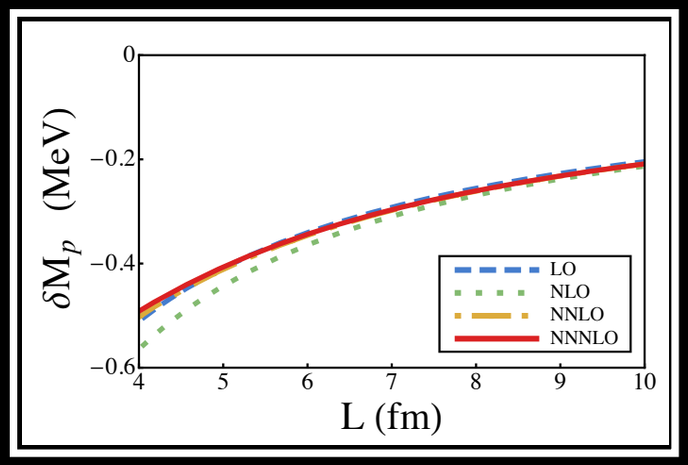

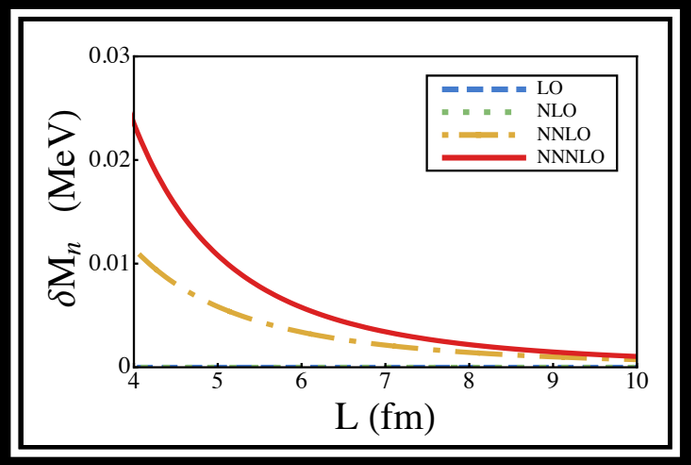

- NREFT IS A SIMPLE AND GENERAL FORMALISM TO STUDY FINITE-VOLUME QED EFFECTS.

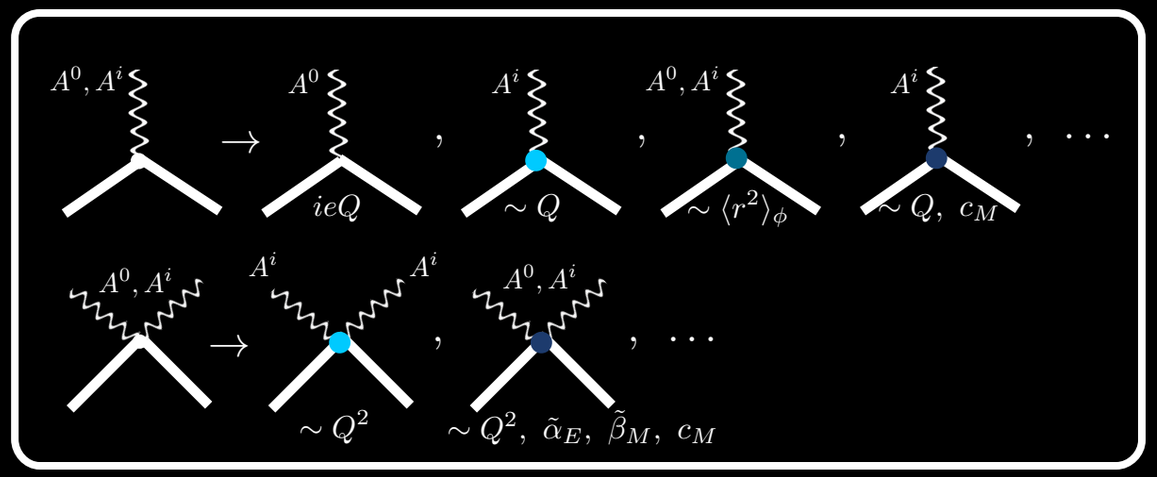

- THE DIRECT EVALUATION OF MUON MAGNETIC MOMENT TO REQUIRED PRECISION REQUIRES UNFEASIBLY LARGE VOLUMES.

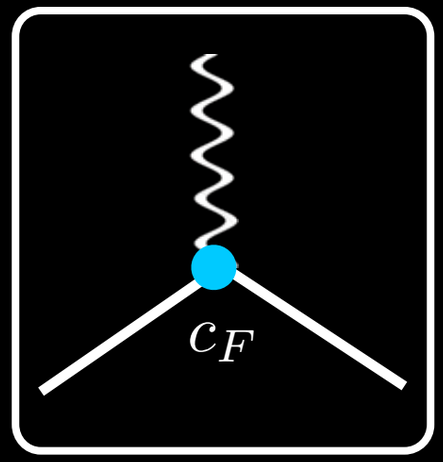

- NEUTRAL PARTICLES RECEIVE CORRECTIONS TO THEIR MASSES DUE TO THEIR MAGNETIC MOMENT (IF ANY) AND THEIR POLARIZABILITIES.

THANK YOU

Nuclear matrix elements

William Detmold, MIT

The intensity frontier

- Seek new physics through quantum effects
- Precise experiments
  - Sensitivity to probe the rarest interactions of the SM
  - Look for effects where there is no SM contribution
- Major focus of HEP experimental program over next decade
  - Dark matter direct detection
  - Neutrino physics
  - Charged lepton flavour violation
  - Proton decay, neutron-antineutron oscillations…

Dark matter direct detection

- Search for DM in multiple ways
  - Look for astronomical signals of annihilation
  - Try to produce it at particle colliders
  - Direct detection: wait for DM passing by to hit a nucleus
- Detection rate/bounds depends on
  - Dark matter properties/dynamics
  - Probability for interaction with nucleus: nuclear matrix elements

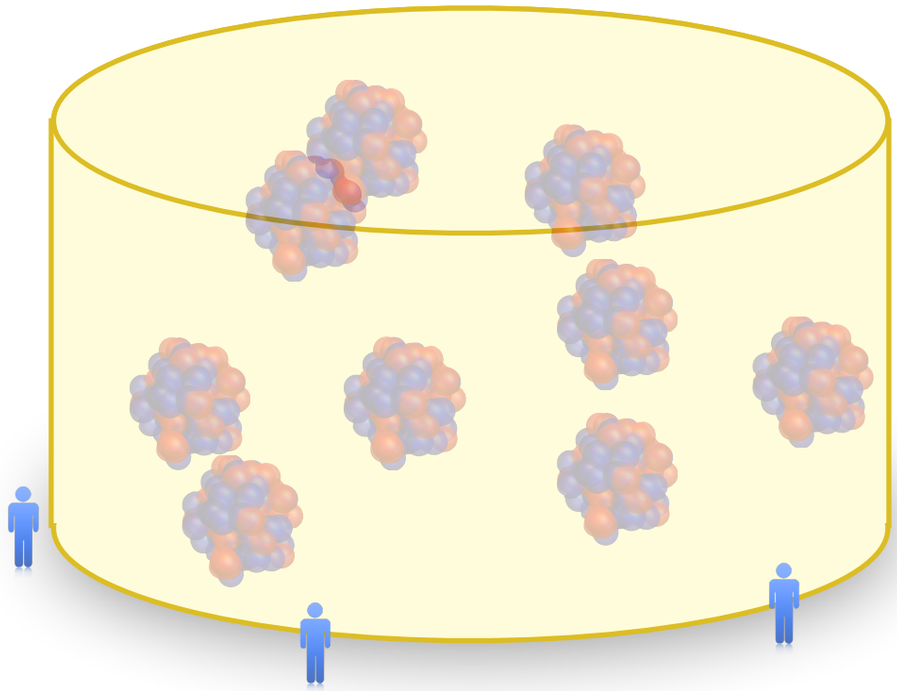

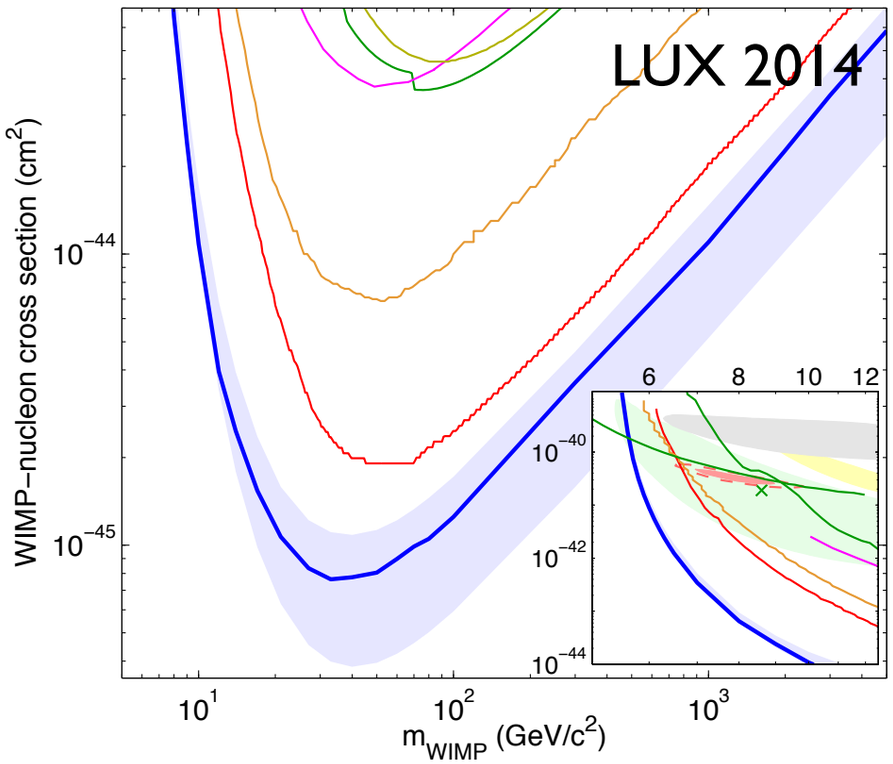

The intensity frontier

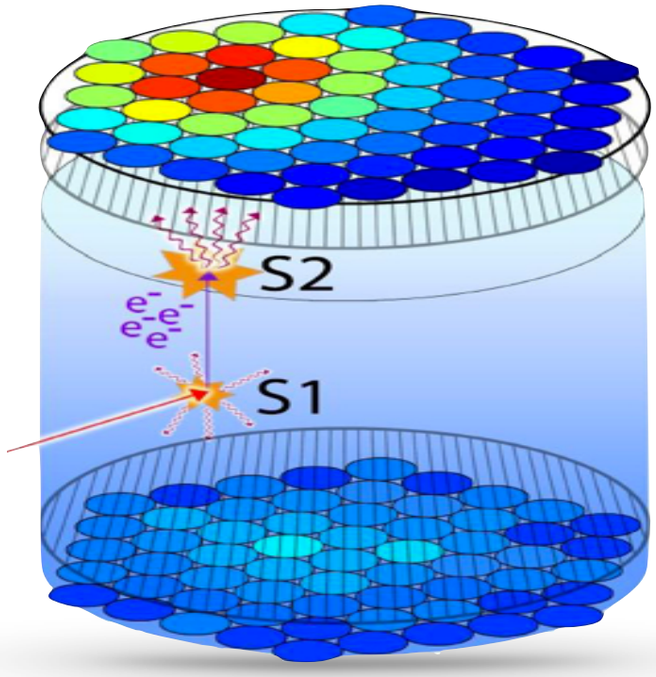

- Dark matter detection: nuclear recoils as signal
  Nuclear matrix elements of exchange current
- μ2e expt: search for charged lepton flavour violation via μ→e conversion in field of Al nucleus

😍 Positive signals would be unambiguous

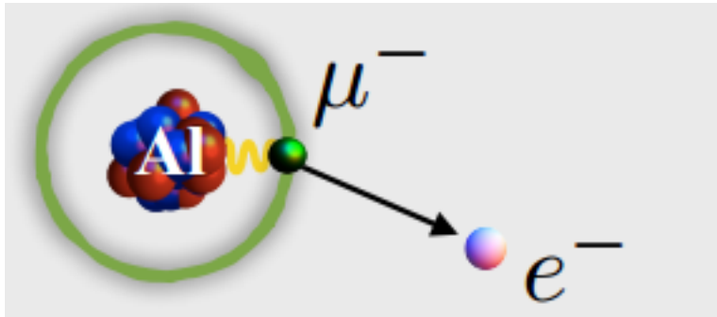

- However <u>need</u> precise nuclear matrix elements with fully quantified uncertainties to discern underlying dynamics
- Also relevant for experimental design and backgrounds

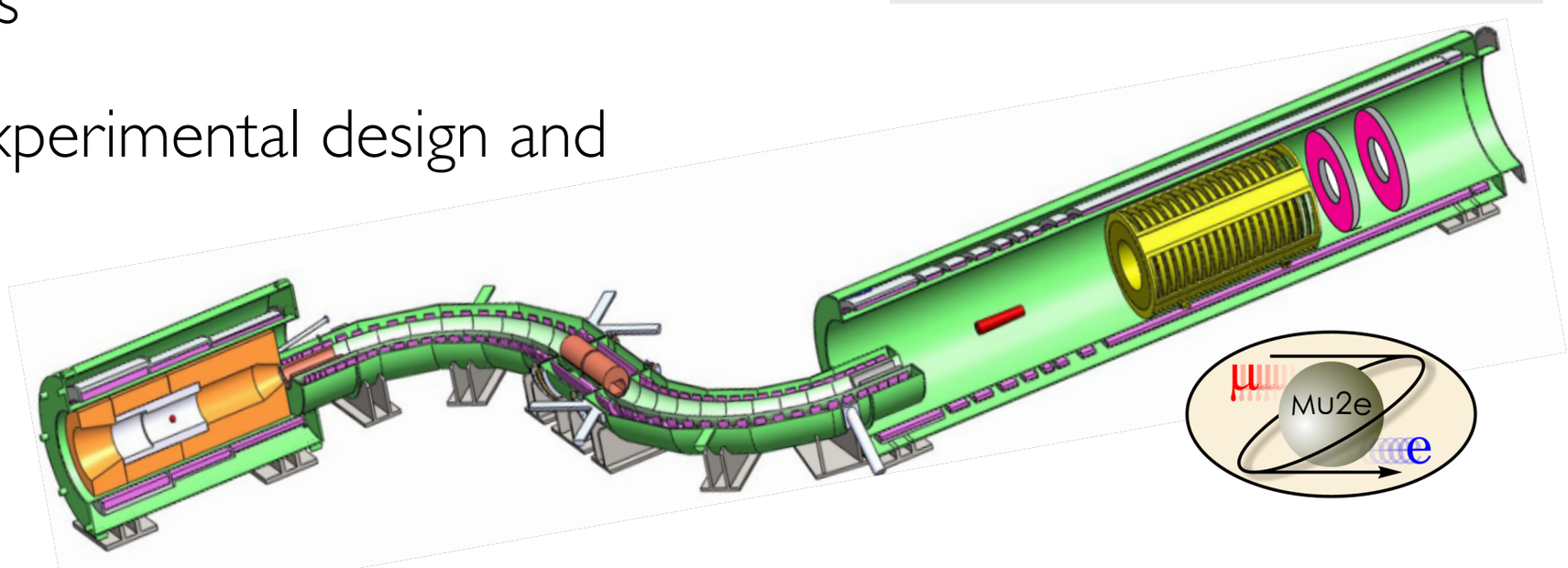

Neutrino oscillations and mass hierarchy

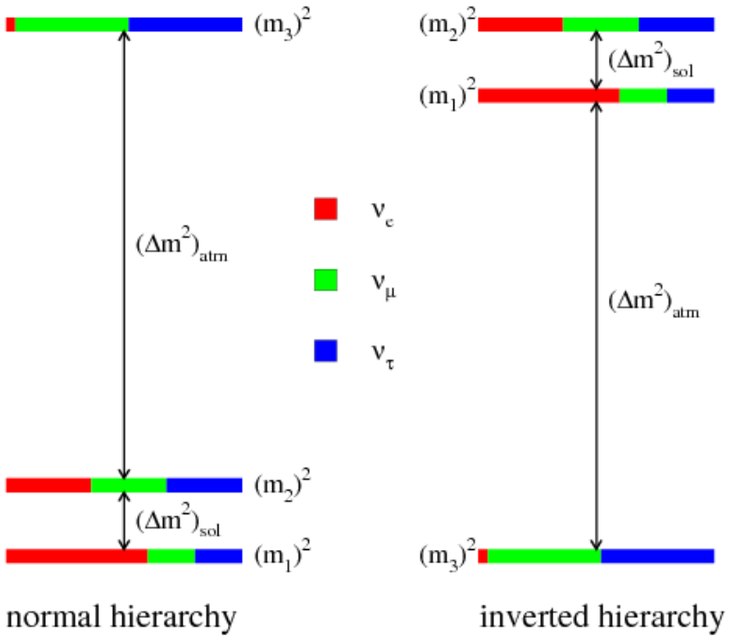

Neutrino oscillations and mass hierarchy

- Long-baseline neutrino beams: further constrain neutrino oscillation parameters and determine mass hierarchy

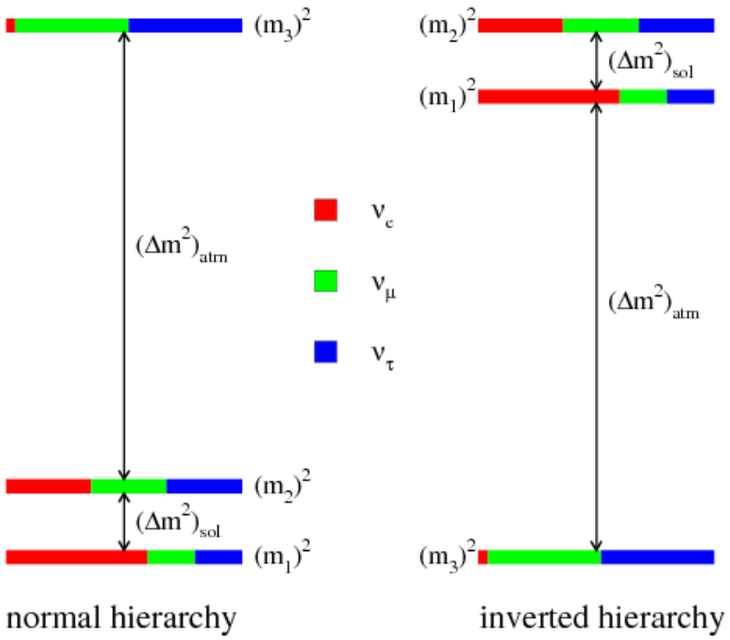

Neutrino oscillations and mass hierarchy

- Long-baseline neutrino beams: further constrain neutrino oscillation parameters and determine mass hierarchy
- Targets are nuclei (C, Fe, Si, Ar, Ge, Xe, Pb, CH_x, H_2O, steel)

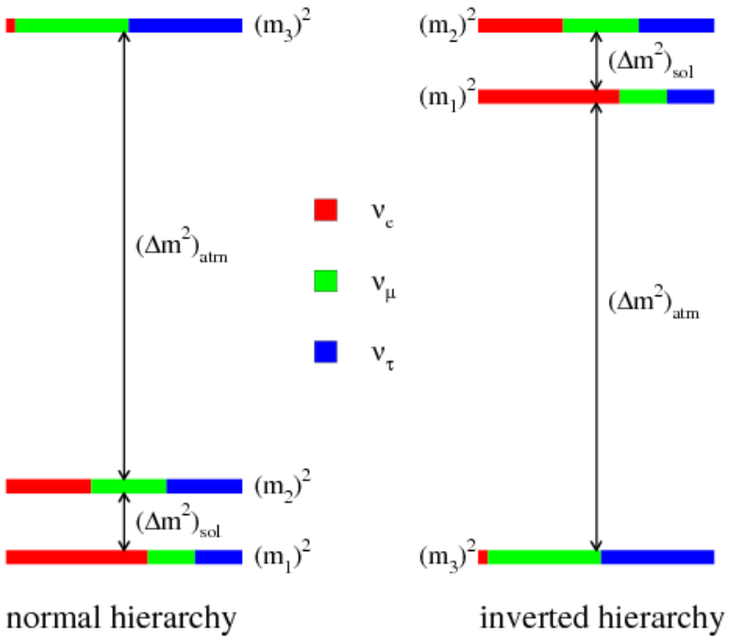

Neutrino oscillations and mass hierarchy

- Long-baseline neutrino beams: further constrain neutrino oscillation parameters and determine mass hierarchy
- Targets are nuclei (C, Fe, Si, Ar, Ge, Xe, Pb, CH_x, H_2O, steel)
- Future LBNE/O/F requires knowing energies/fluxes to high accuracy
  - Depends on nuclear axial & transition form factors and neutrino-nucleus DIS

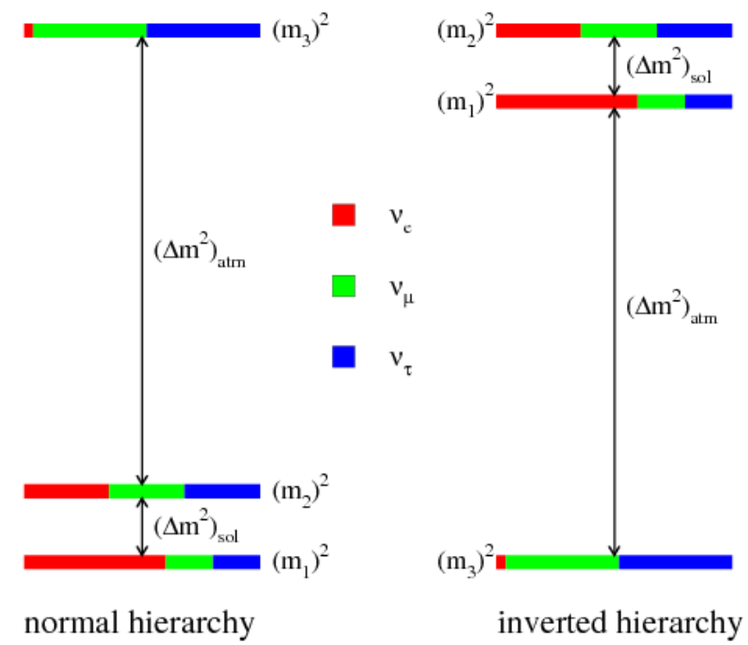

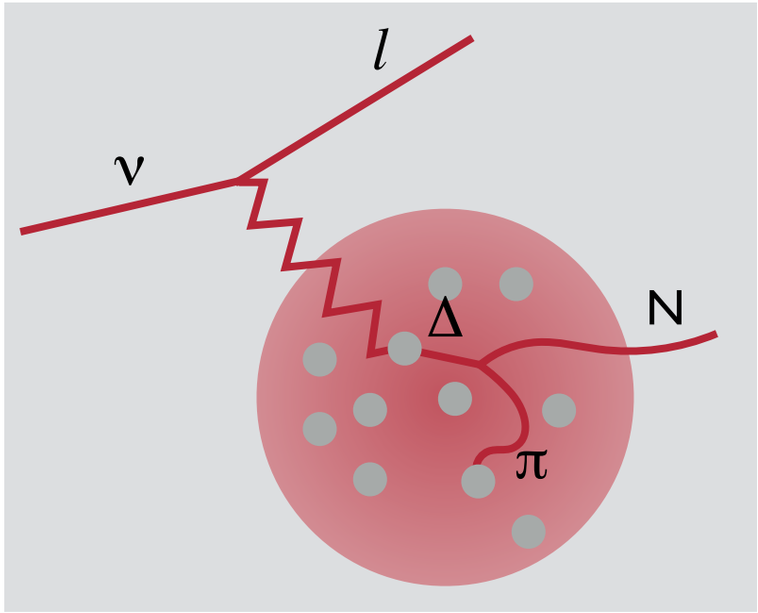

Neutrino oscillations and mass hierarchy

- Long-baseline neutrino beams: further constrain neutrino oscillation parameters and determine mass hierarchy
- Targets are nuclei (C, Fe, Si, Ar, Ge, Xe, Pb, CH_x, H_2O, steel)
- Future LBNE/O/F requires knowing energies/fluxes to high accuracy
  - Depends on nuclear axial & transition form factors and neutrino-nucleus DIS
  - Current knowledge produces significant uncertainty in determination of oscillation parameters
    [INT workshop 2013]

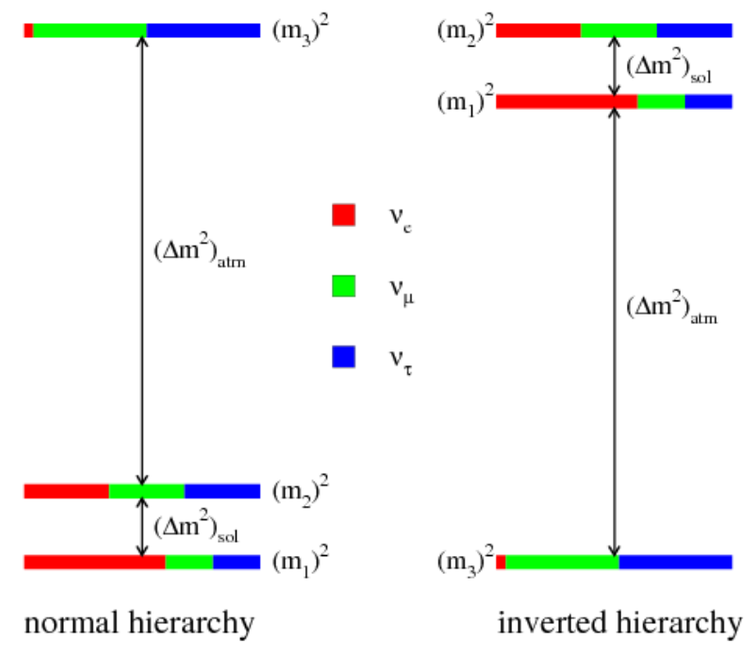

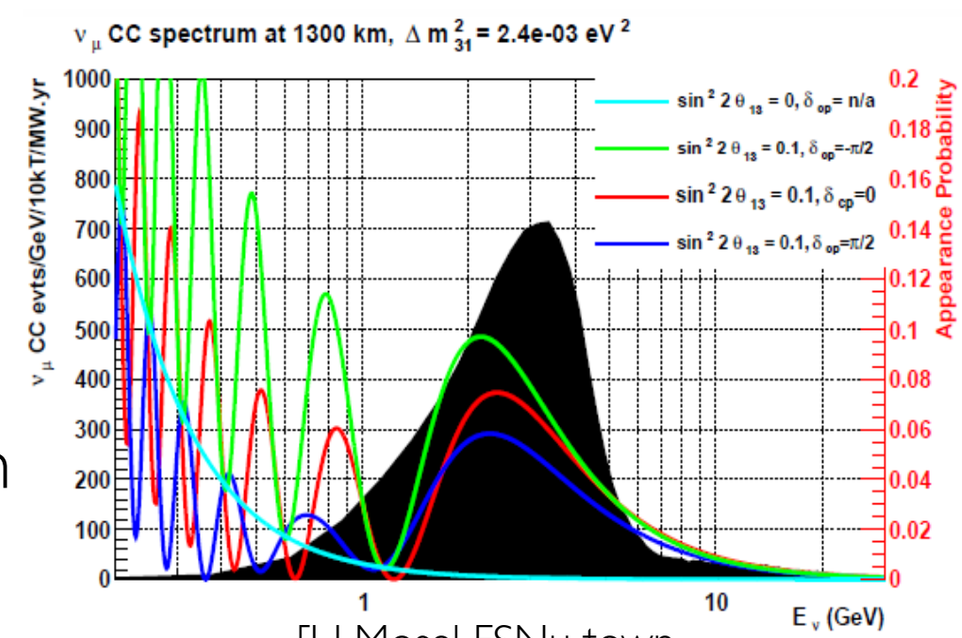

[U Mosel FSNu town

$0\nu\beta\beta$ decay

0νββ decay

- Certain nuclei allow observable ββ decay

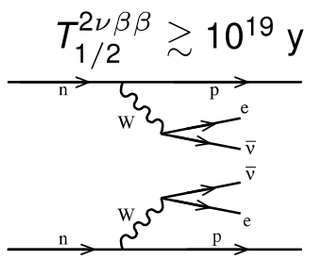

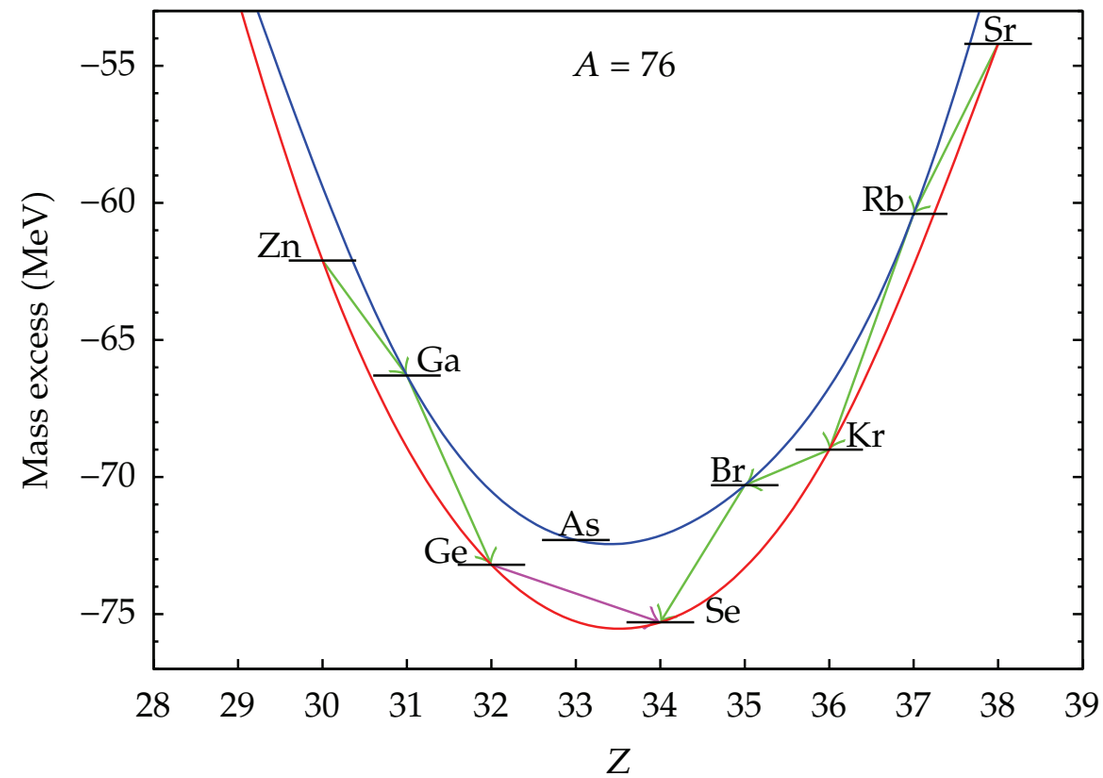

0νββ decay

- Certain nuclei allow observable ββ decay

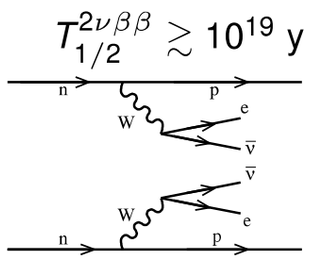

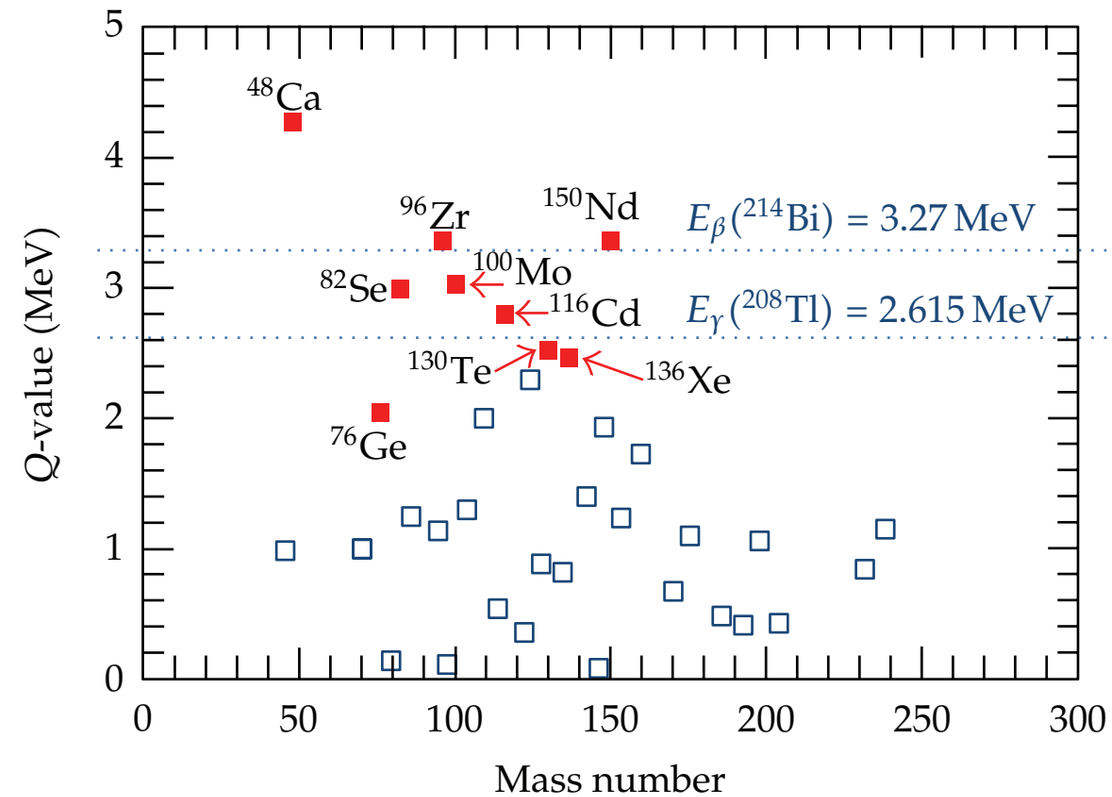

0νββ decay

- Certain nuclei allow observable ββ decay

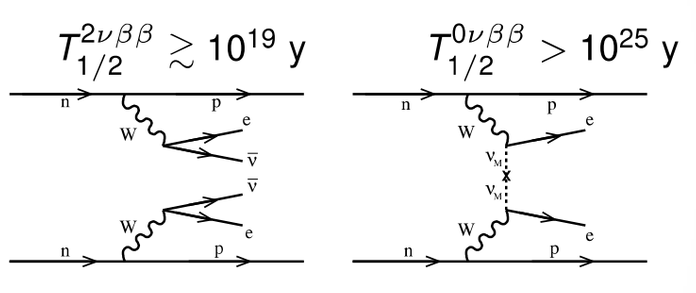

- If neutrinos are massive Majorana fermions 0νββ decay is possible

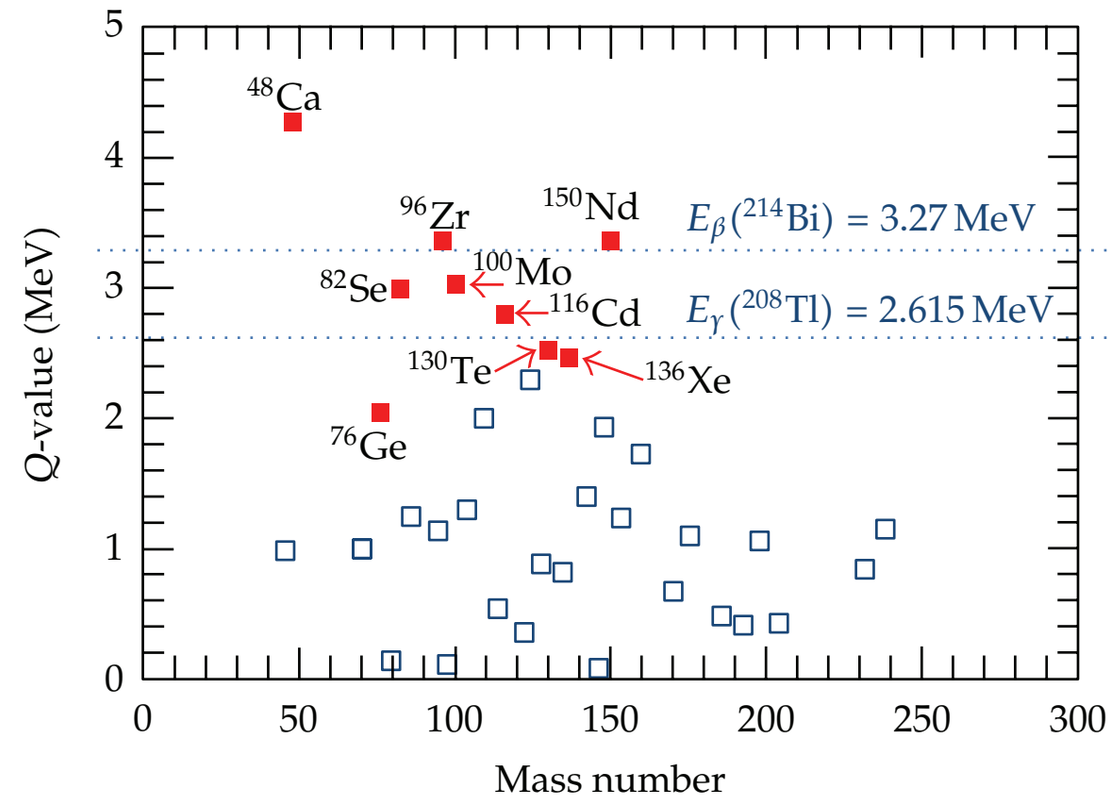

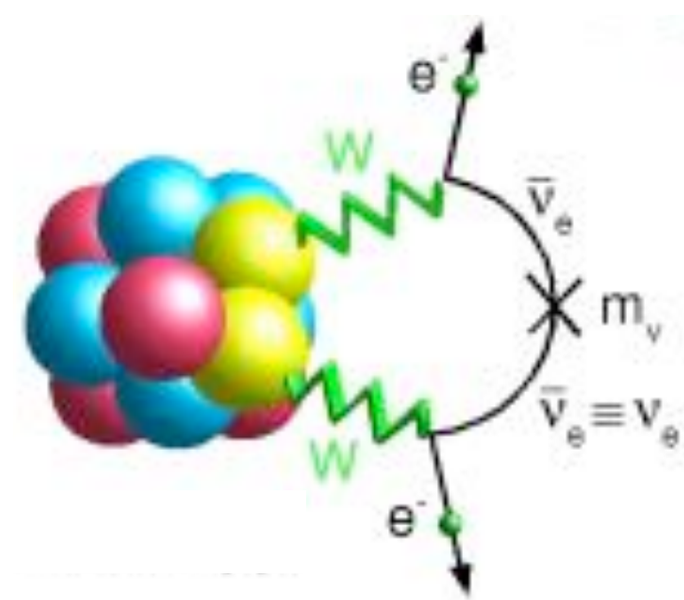

0νββ decay

- Certain nuclei allow observable ββ decay

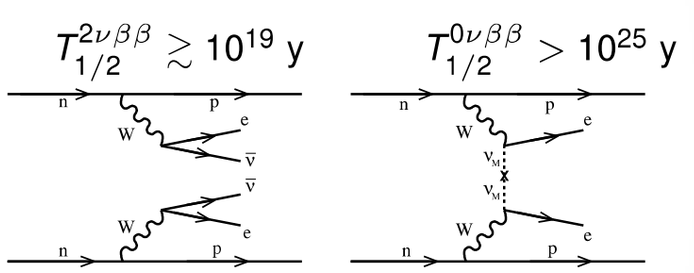

- If neutrinos are massive Majorana fermions 0νββ decay is possible

- Half-life depends critically on the nuclear matrix elements of two weak currents!

$$\left(T_{1/2}^{0\nu\beta\beta}(0^+ \rightarrow 0^+)\right)^{-1} = G_{01}\left|M^{0\nu\beta\beta}\right|^2\left(\frac{\langle m_\nu \rangle}{m_e}\right)^2$$

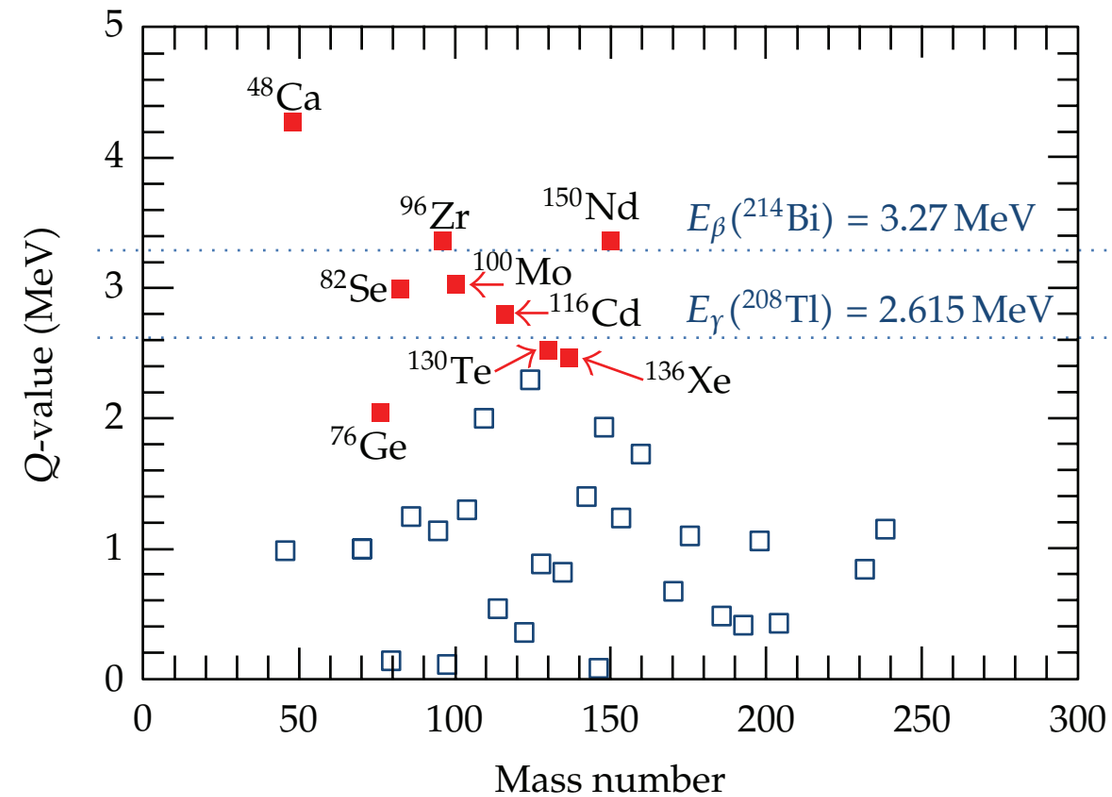

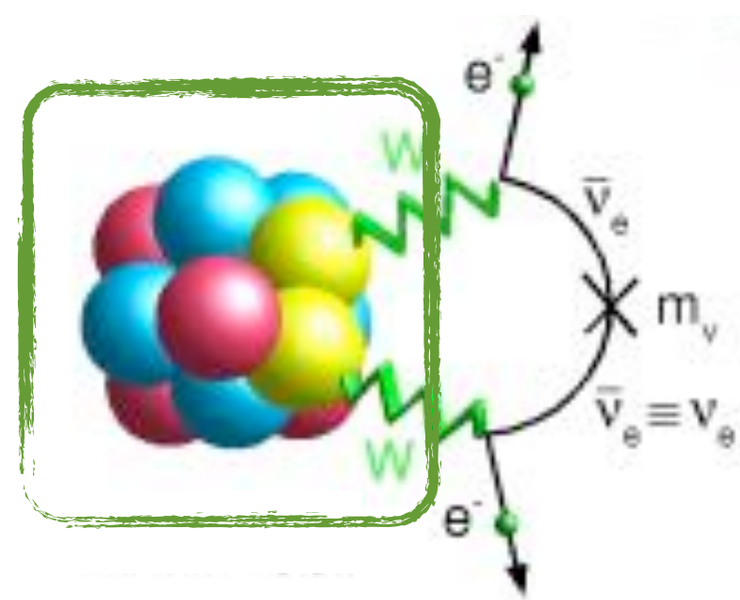

0νββ decay nuclear matrix elements

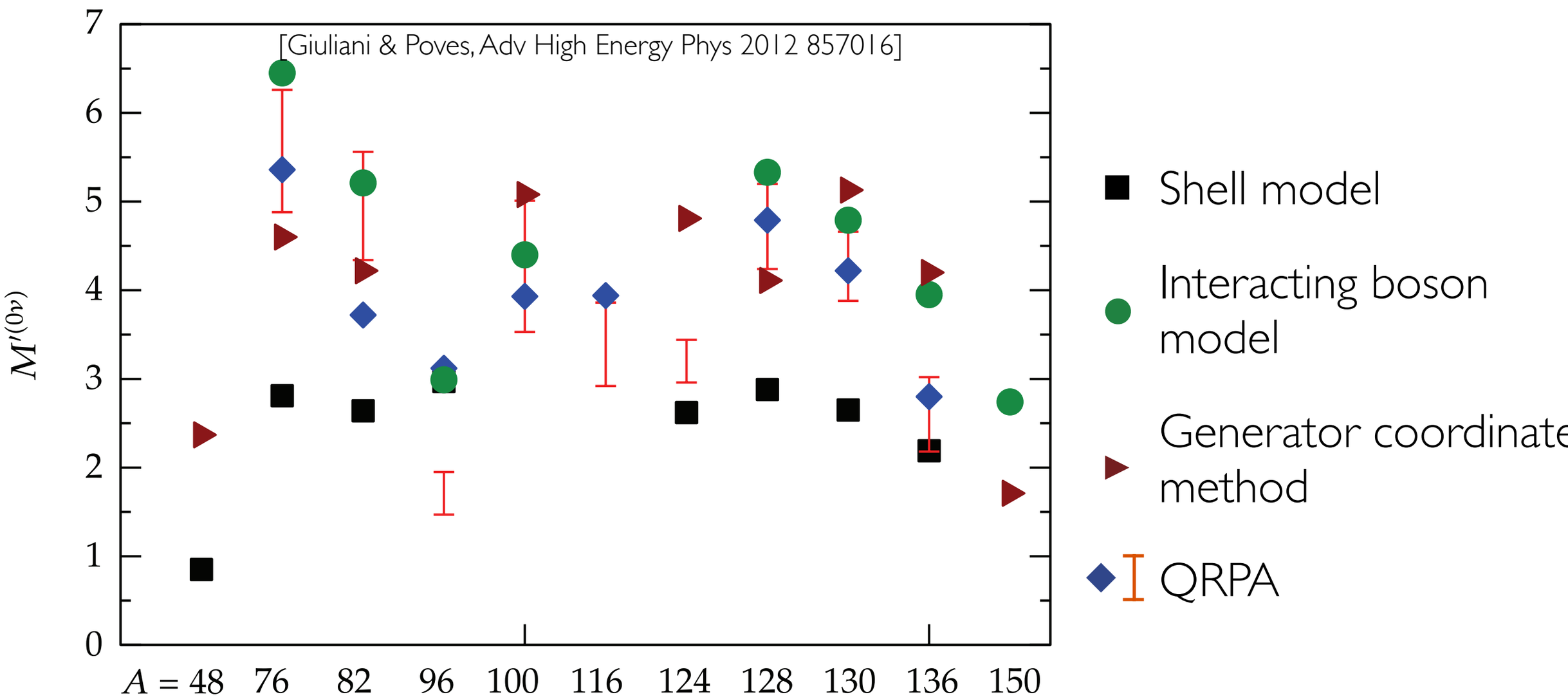

- Large spread of calculations
- Is the spread representative of the true uncertainty?

Nuclear uncertainties

- How well do we know nuclear matrix elements?

😢 Stark example of problems: Gamow-Teller transitions in nuclei

  - Well measured for large range of nuclei (30<A<60)
  - Many nuclear structure calcs (QRPA, shell-model,…) – spectrum well described
  - Matrix elements systematically off by 20–30%
  - "Correct" by "quenching" axial charge in nuclei ...

[Martinez-Pinedo et al., Phys. Rev. C53, 2602 (1996)]

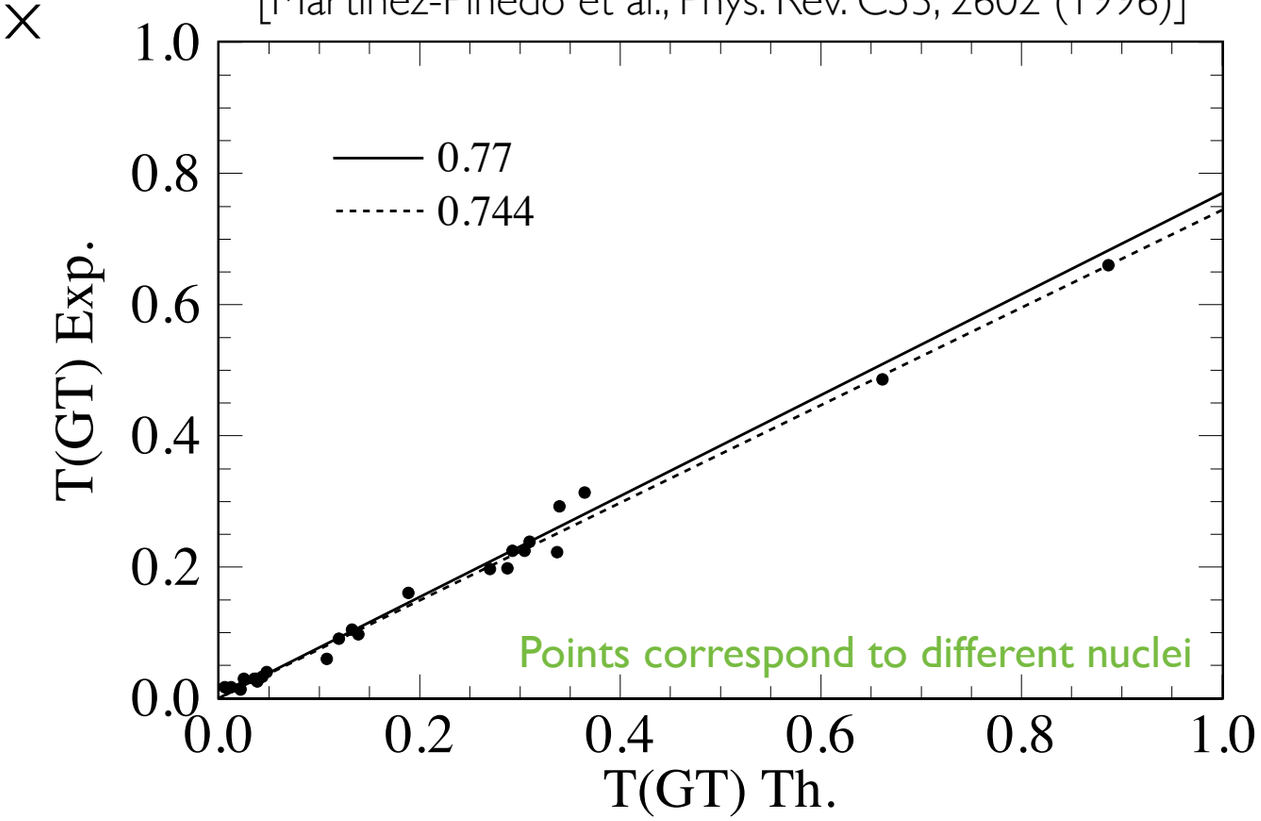

$$T(GT) \sim \sqrt{\sum_f \langle \boldsymbol{\sigma} \cdot \boldsymbol{\tau} \rangle_{i \to f}}$$

$$\langle \boldsymbol{\sigma\tau} \rangle = \frac{\langle f || \sum_k \boldsymbol{\sigma}^k \boldsymbol{t}_\pm^k || i \rangle}{\sqrt{2J_i + 1}}$$

Nuclear theory at the intensity frontier

- Definitive need for precision determinations of nuclear matrix elements
  - Must be based on the Standard Model
  - Must have fully quantified uncertainties
  - Timeframe and precision goals set by experiment
- Current state is far from this
- *Nuclear physics is the new flavour physics!*
  - Develop appropriate tools

Precision nuclear physics

- ***We need to develop the tools for precision predictions***
- Exploit effective degrees of freedom
- Establish quantitative control through linkages between different methods
  - QCD forms a foundation determines few body interactions & matrix elements
  - Match existing EFT and many body techniques onto QCD

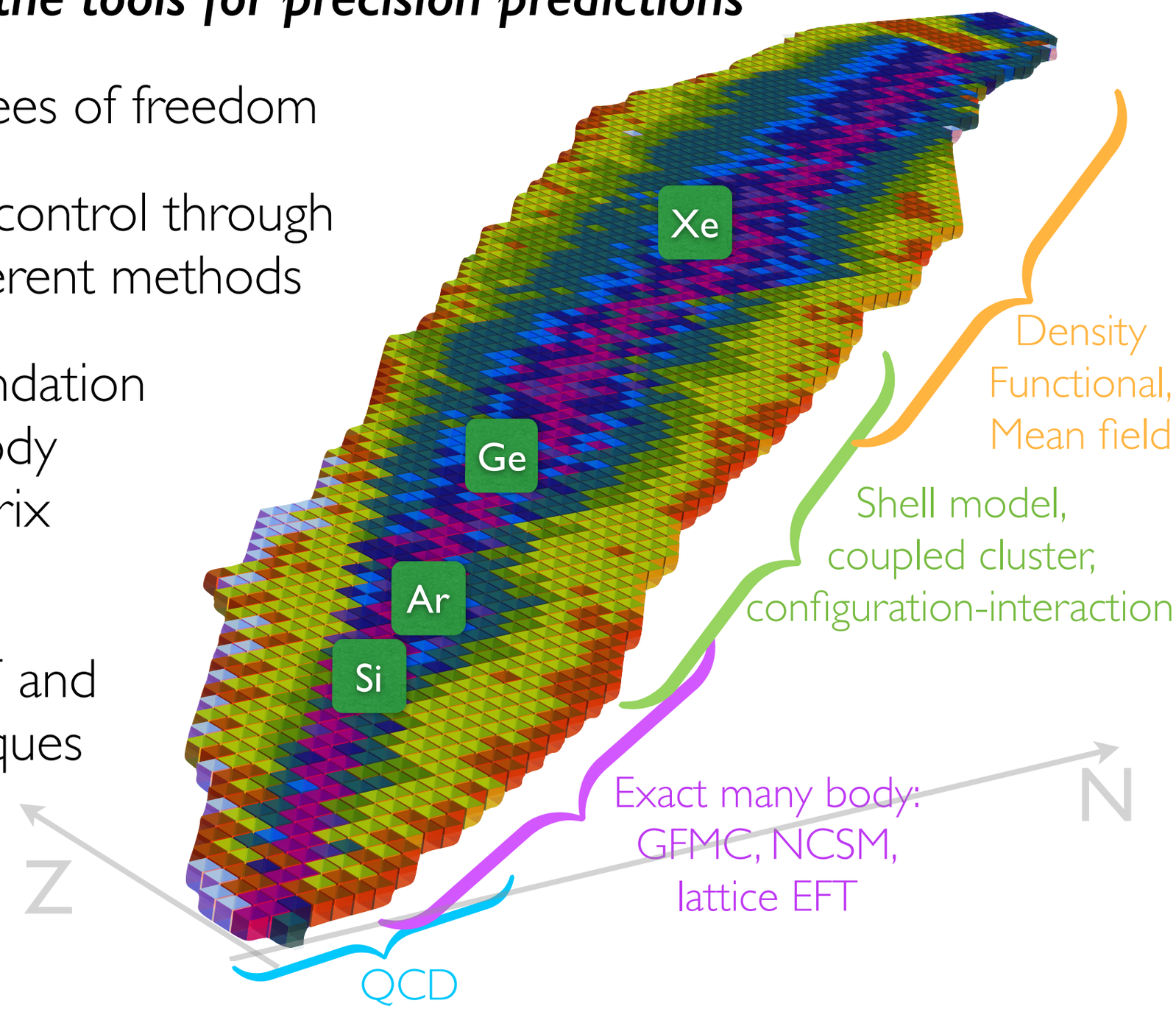

Nuclear Spectra

QCD for Nuclei

- QCD (+EW) describes nuclei
  - Can compute the mass of any nucleus ... in principle
- In practice: a hard problem
- Multiple exponentially difficult challenges
  - Physics at multiple scales
  - Noise: probabilistic method so statistical uncertainty grows exponentially with A
  - Contraction complexity grows factorially
- Large nuclei are challenging, A=2,3,4 are feasible

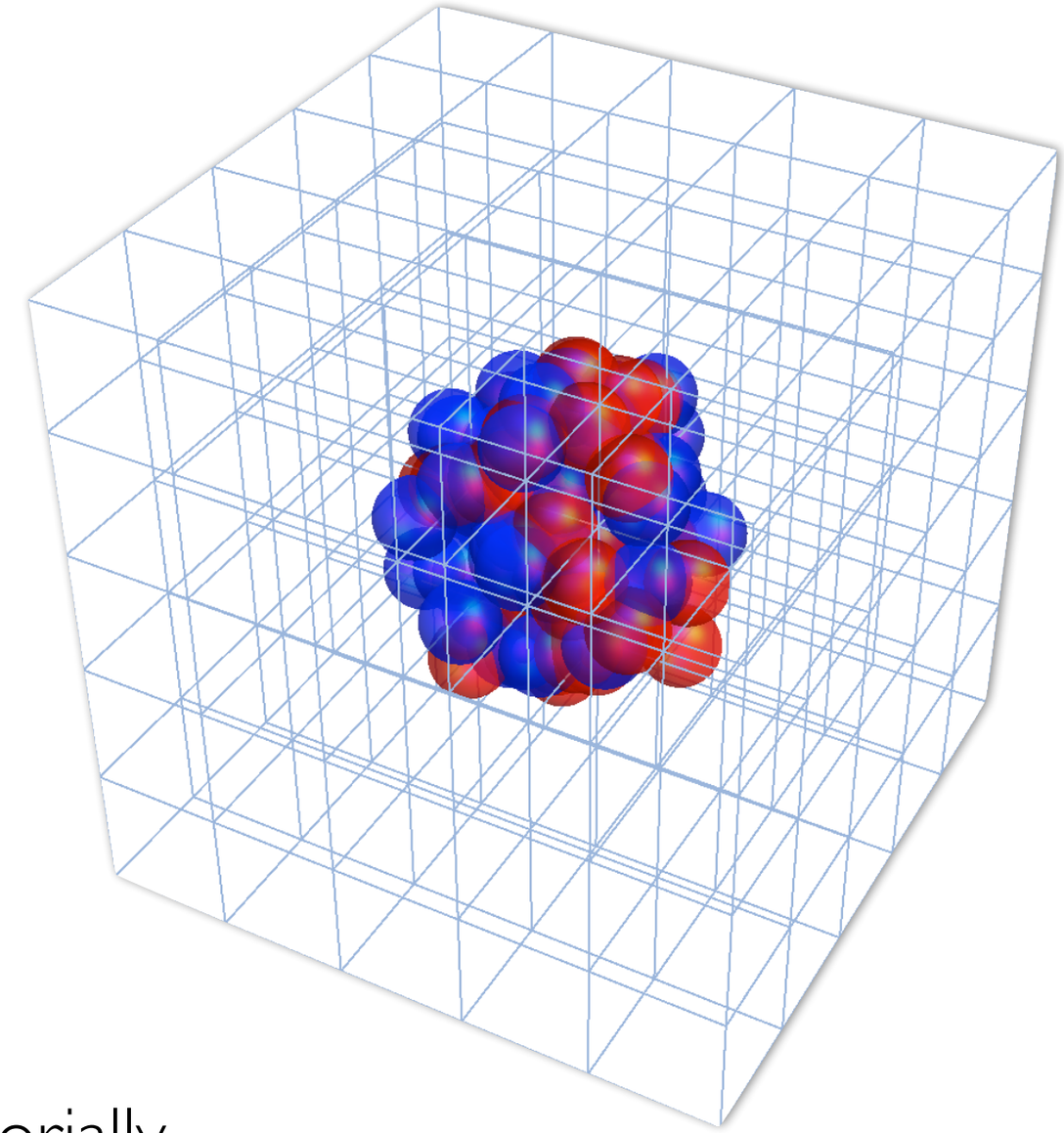

- Quarks need to be tied together in all possible ways
  - $N_{\text{contractions}} = N_u! N_d! N_s!$

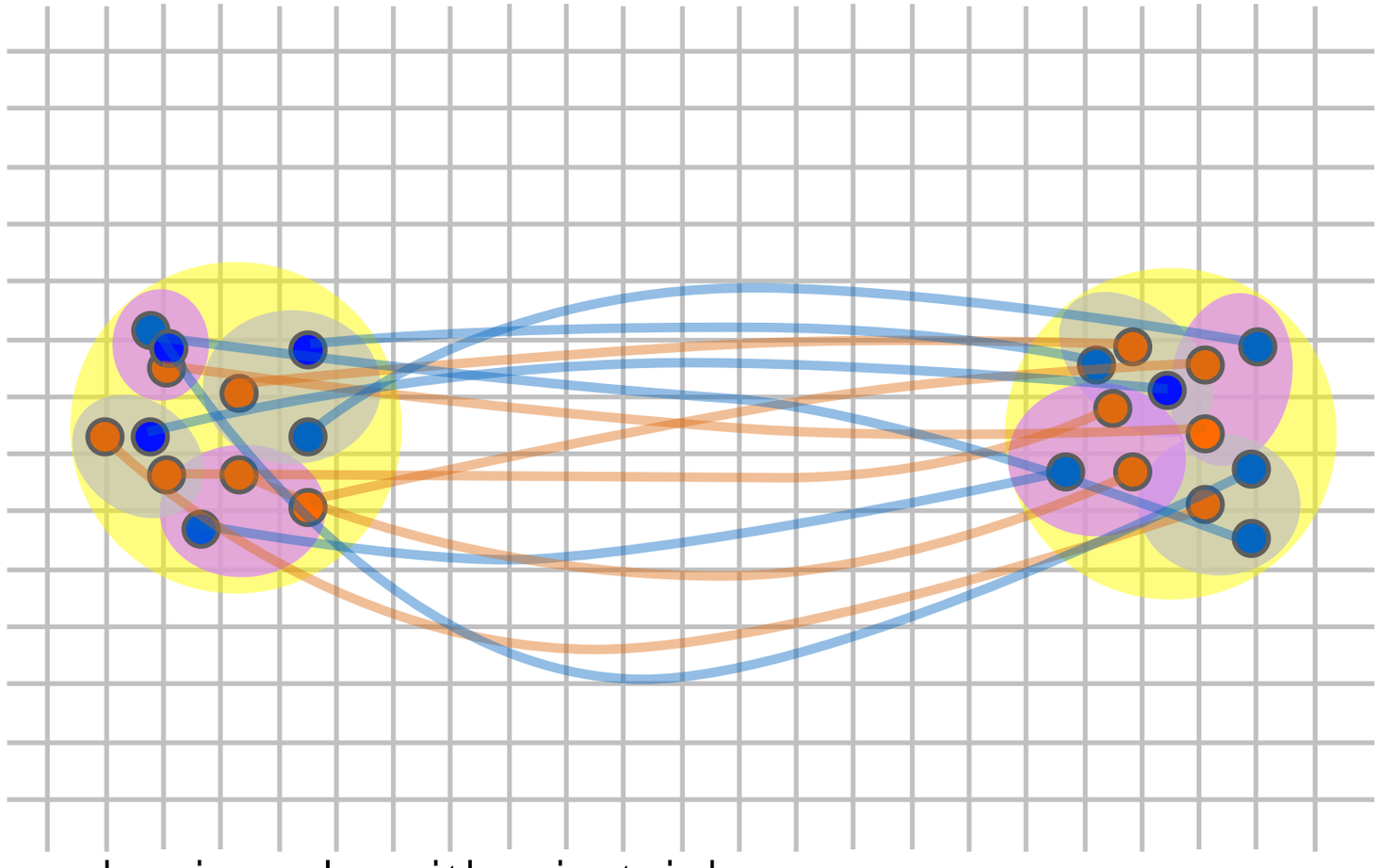

- Managed using algorithmic trickery [WD & Savage Doi & Endres, WD & Orginos, Günther&Varnhorst]
  - Study up to N=72 pion systems, A=5/28 nuclei

Light nuclei

- Light hypernuclear spectrum @ 800 MeV

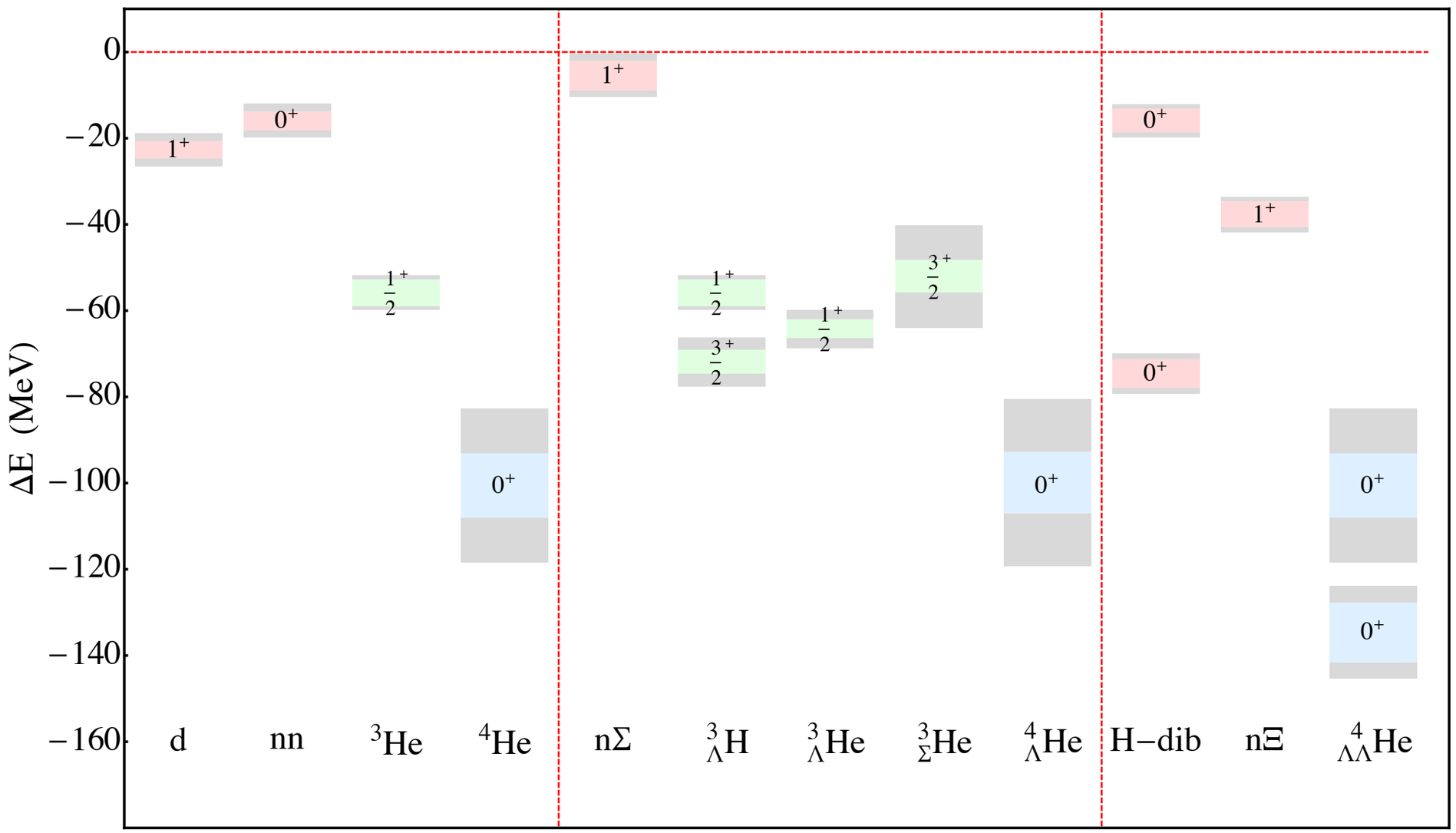

See also talks in previous session

[NPLQCD Phys.Rev. D87 (2013), 034506]

Heavy quark universe

[Barnea et al. 1311.4966 to appear in PRL]

- Combining LQCD and nuclear EFT (pionless EFT)
- For heavy quarks, even spectroscopy requires QCD matching:

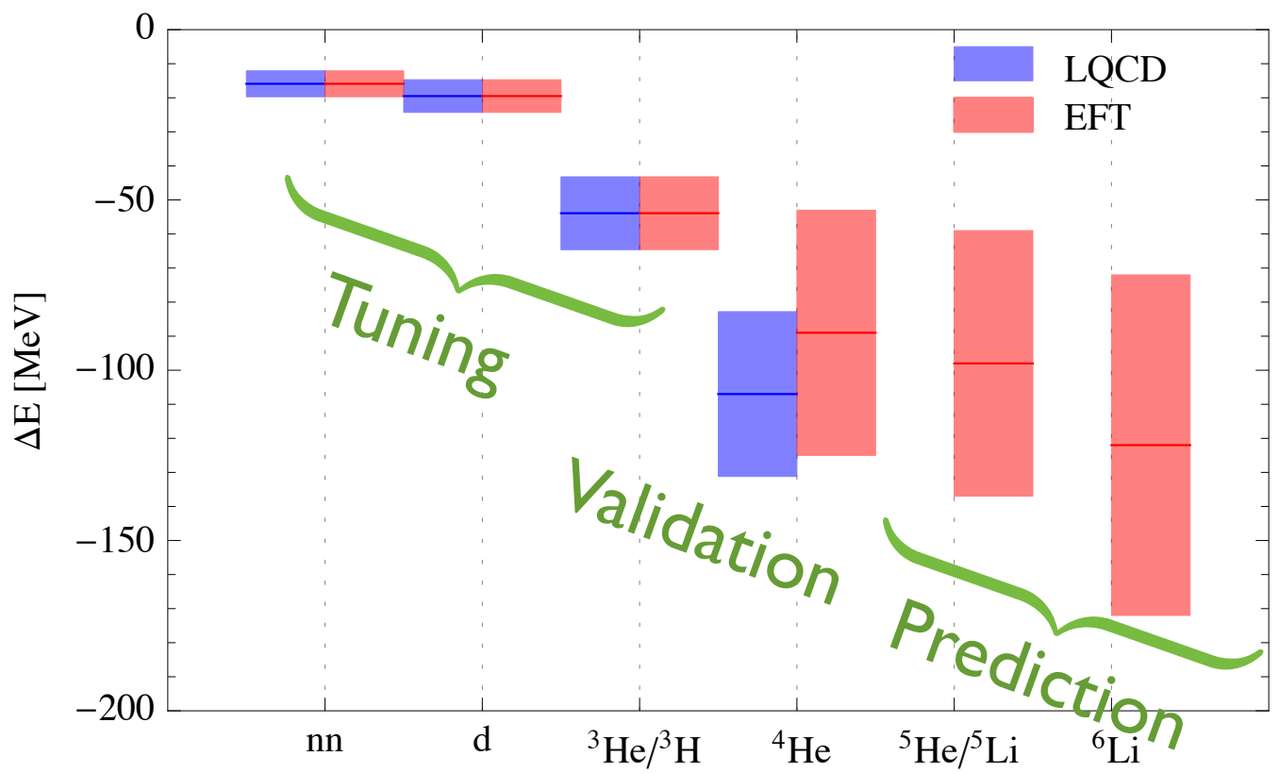

In a world @ m_π = 800 MeV

- Equally important for matrix elements

Nuclear Structure

External currents and nuclei

External currents and nuclei

- Current-nucleus interaction
  - Born approximation – interacts with a single nucleon

$$\sigma \sim |A \ \langle N|J|N\rangle|^2$$

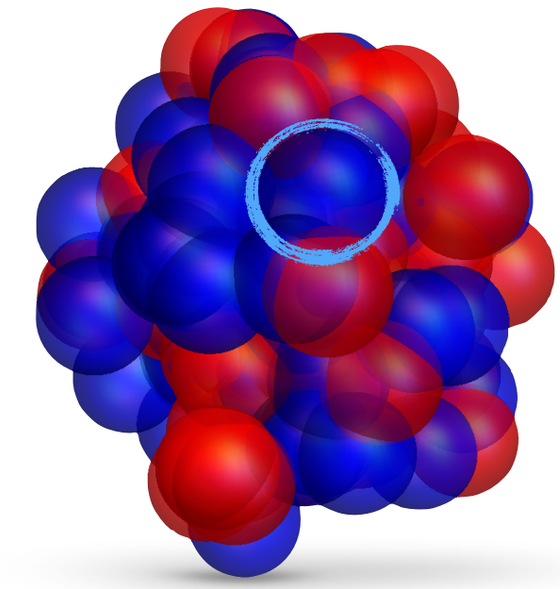

External currents and nuclei

- Current-nucleus interaction
  - Born approximation – interacts with a single nucleon

$$\sigma \sim |A \langle N|J|N\rangle|^2$$

known from expt/LQCD

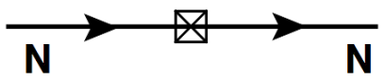

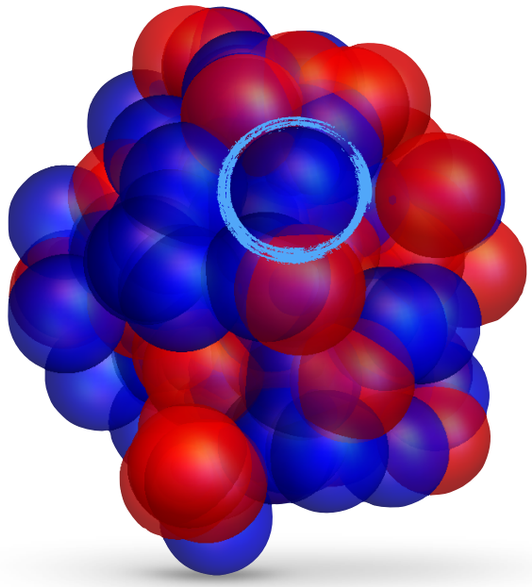

External currents and nuclei

- Current-nucleus interaction
  - Born approximation – interacts with a single nucleon

$$\sigma \sim |A \, \langle N|J|N\rangle|^2$$

known from expt/LQCD

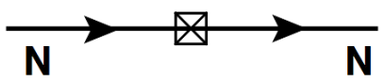

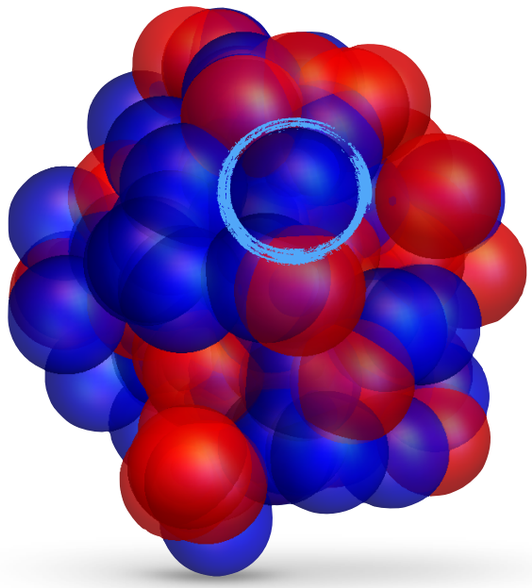

  - Interact non-trivially with multiple nucleons

$$\sigma \sim |A \, \langle N|J|N\rangle + \alpha \, \langle NN|J|NN\rangle + \ldots|^2$$

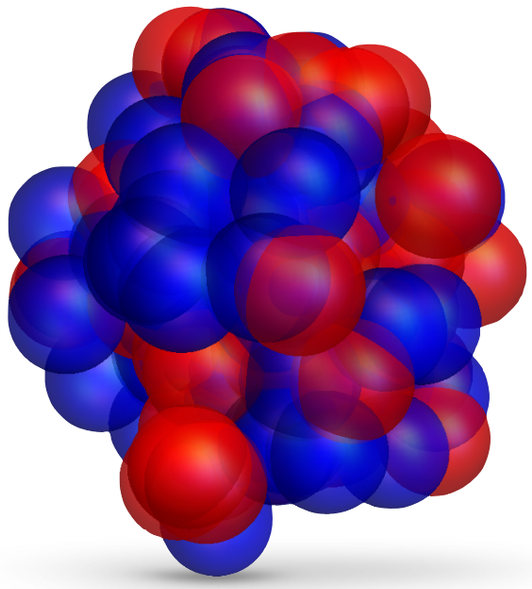

External currents and nuclei

- Current-nucleus interaction
  - Born approximation – interacts with a single nucleon

$$\sigma \sim |A \langle N|J|N\rangle|^2$$

known from expt/LQCD

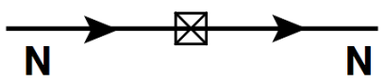

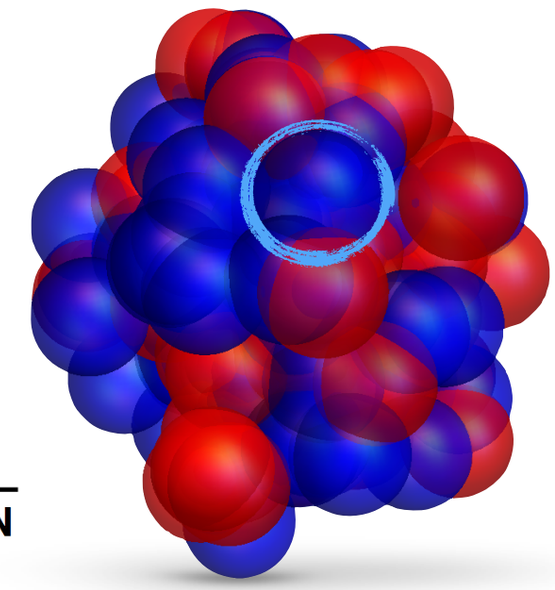

  - Interact non-trivially with multiple nucleons

$$\sigma \sim |A \langle N|J|N\rangle + \alpha \langle NN|J|NN\rangle + \ldots|^2$$

unknown/poorly known!

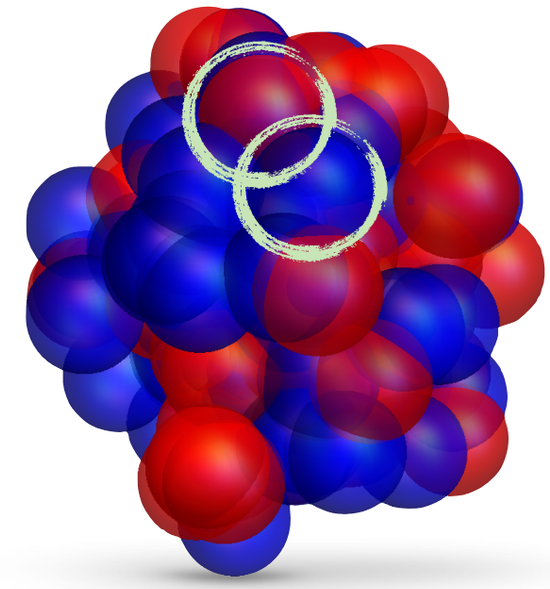

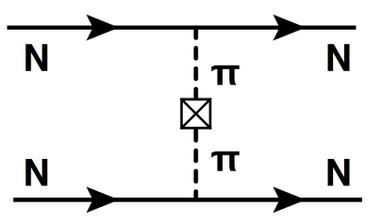

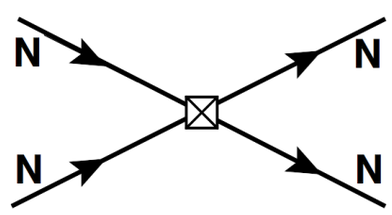

External currents and nuclei

- Current-nucleus interaction
  - Born approximation – interacts with a single nucleon

$$\sigma \sim |A \langle N|J|N\rangle|^2$$

known from expt/LQCD

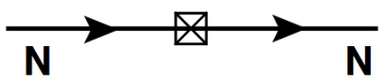

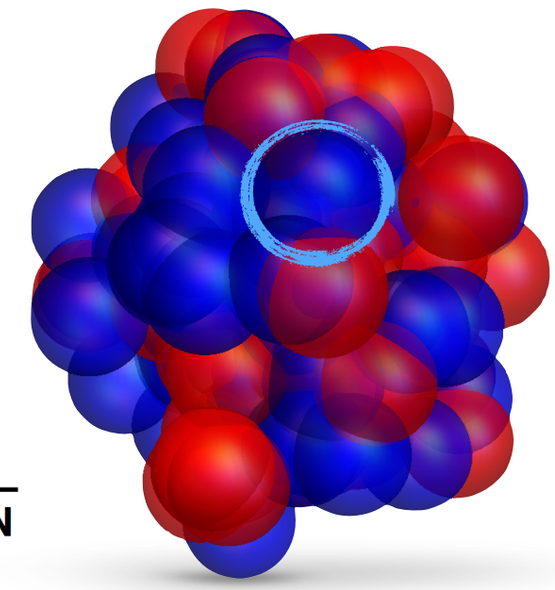

  - Interact non-trivially with multiple nucleons

$$\sigma \sim |A \langle N|J|N\rangle + \alpha \langle NN|J|NN\rangle + \ldots|^2$$

unknown/poorly known!

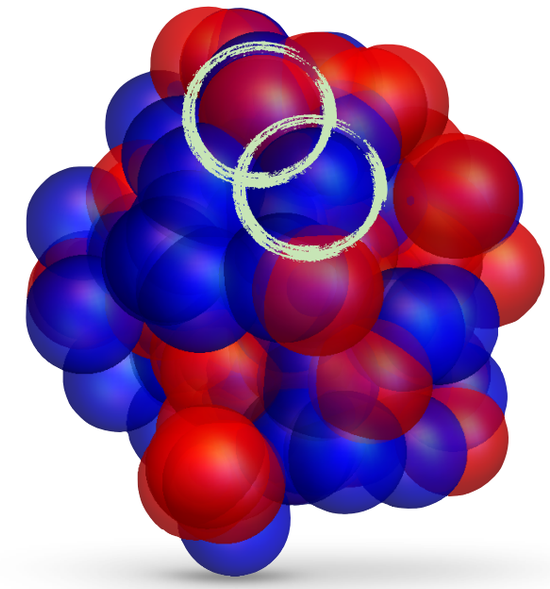

- Second term may be significant
  - May shift cross sections
  - May scale differently with Z and A
  - Leads to significant uncertainty

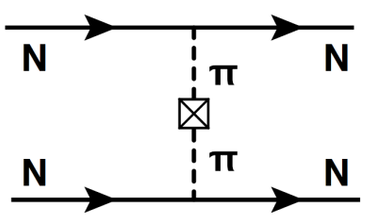

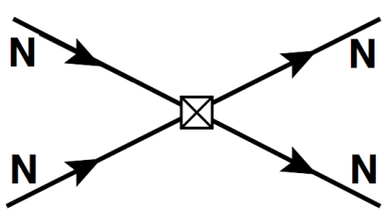

Nuclear matrix elements

- For deeply bound nuclei, use the techniques as for single hadron matrix elements

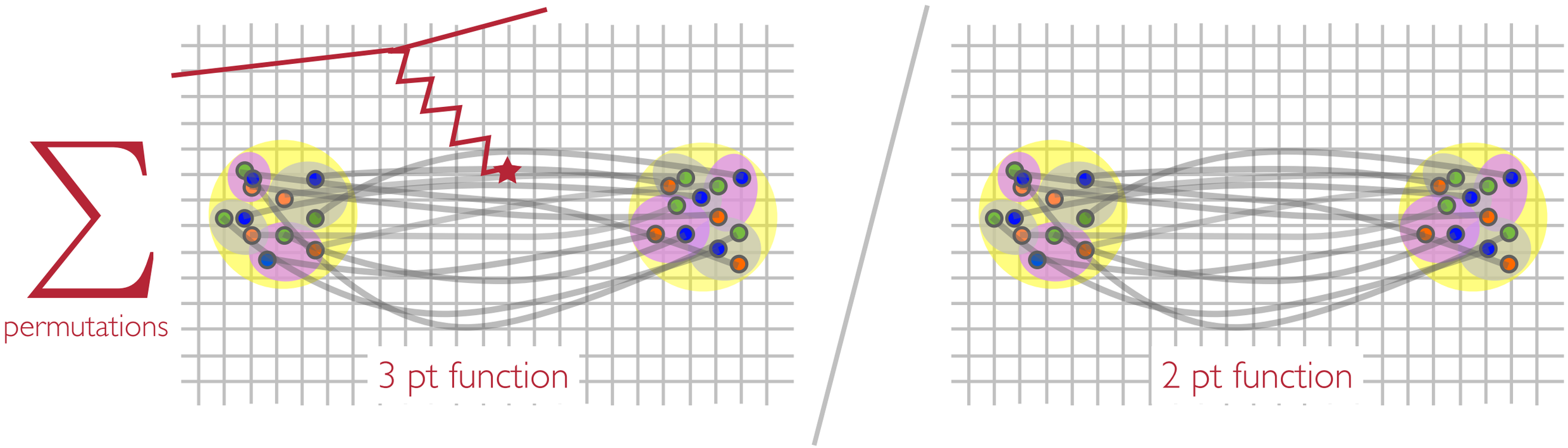

  - At large separations gives ground-state matrix element of current

- For near threshold states and scattering states need to be careful with volume effects

- Calculations of matrix elements of currents in light nuclei just beginning for A<5

Multi-pion matrix elements

- Perturbatively interacting multi-hadron systems
  [WD & M Flynn arXiv:1412.3895]

- External current (no momentum injection)

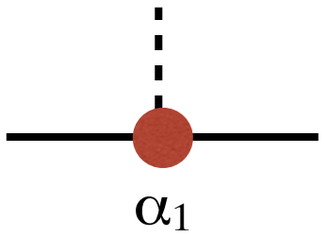

$$J = \sum_{\mathbf{k}} \alpha_1 h^\dagger_{\mathbf{k}} h_{\mathbf{k}} + \sum_{\mathbf{k},\mathbf{Q},\mathbf{p}} \alpha_2 h^\dagger_{\frac{\mathbf{Q}}{2}+\mathbf{k}} h^\dagger_{\frac{\mathbf{Q}}{2}-\mathbf{k}} \, h_{\frac{\mathbf{Q}}{2}+\mathbf{p}} \, h_{\frac{\mathbf{Q}}{2}-\mathbf{p}}$$

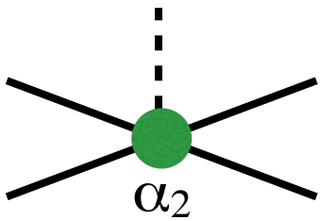

- Matrix element of current J in n boson state in finite volume

$$\begin{aligned}
\langle n|J|n\rangle \;=\; & n\alpha_1 + \frac{n\alpha_1 a^2}{\pi^2 L^2}\binom{n}{2}\mathcal{J} + \frac{\alpha_2}{L^3}\binom{n}{2} \\
& + \frac{2n\alpha_1 a^3}{\pi^3 L^3}\binom{n}{2}\left\{\mathcal{K}\binom{n}{2} - \left[\mathcal{I}\,\mathcal{J} + 4\mathcal{K}\binom{n-2}{1} + \mathcal{K}\binom{n-2}{2}\right]\right\} - \frac{2\alpha_2 a}{\pi L^4}\binom{n}{2}\mathcal{I} \\
& + \frac{n\alpha_1 a^4}{\pi^4 L^4}\left[3\mathcal{I}^2\mathcal{J} + \mathcal{L}\left(186 - \frac{241n}{2} + \frac{29}{2}n^2\right) + \mathcal{J}^2\left(\frac{n^2}{4} + \frac{3n}{4} - \frac{7}{2}\right)\right. \\
& \left. + \mathcal{I}\,\mathcal{K}(4n-14) + \mathcal{U}(32n-64) + \mathcal{V}(16n-32)\right] + \mathcal{O}(1/L^5)\,.
\end{aligned}$$

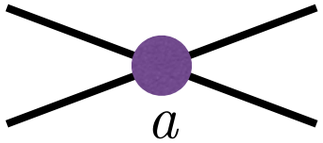

- Compare with FV lattice calculations to extract α_1 and α_2 (previous calculation with HW Lin for <x> operator)

Background field method

- Hadron/nuclear two-point functions are modified in presence of fixed eternal fields
- Eg: fixed B field: modified exponential behaviour

$$E(\mathbf{B}) \;=\; M \;+\; \frac{|Q\,e\,\mathbf{B}|}{2M} \;-\; \boldsymbol{\mu}\cdot\mathbf{B} \\ -\; 2\pi\beta_{M0}\;|\mathbf{B}|^2 - 2\pi\beta_{M2}T_{ij}B_iB_j + \ldots$$

- QCD spectroscopy with multiple fields enable extraction of coefficients of response
  - Eg: magnetic moments, polarisabilities, …
  - Not restricted to simple EM fields (axial, twist-2,…)

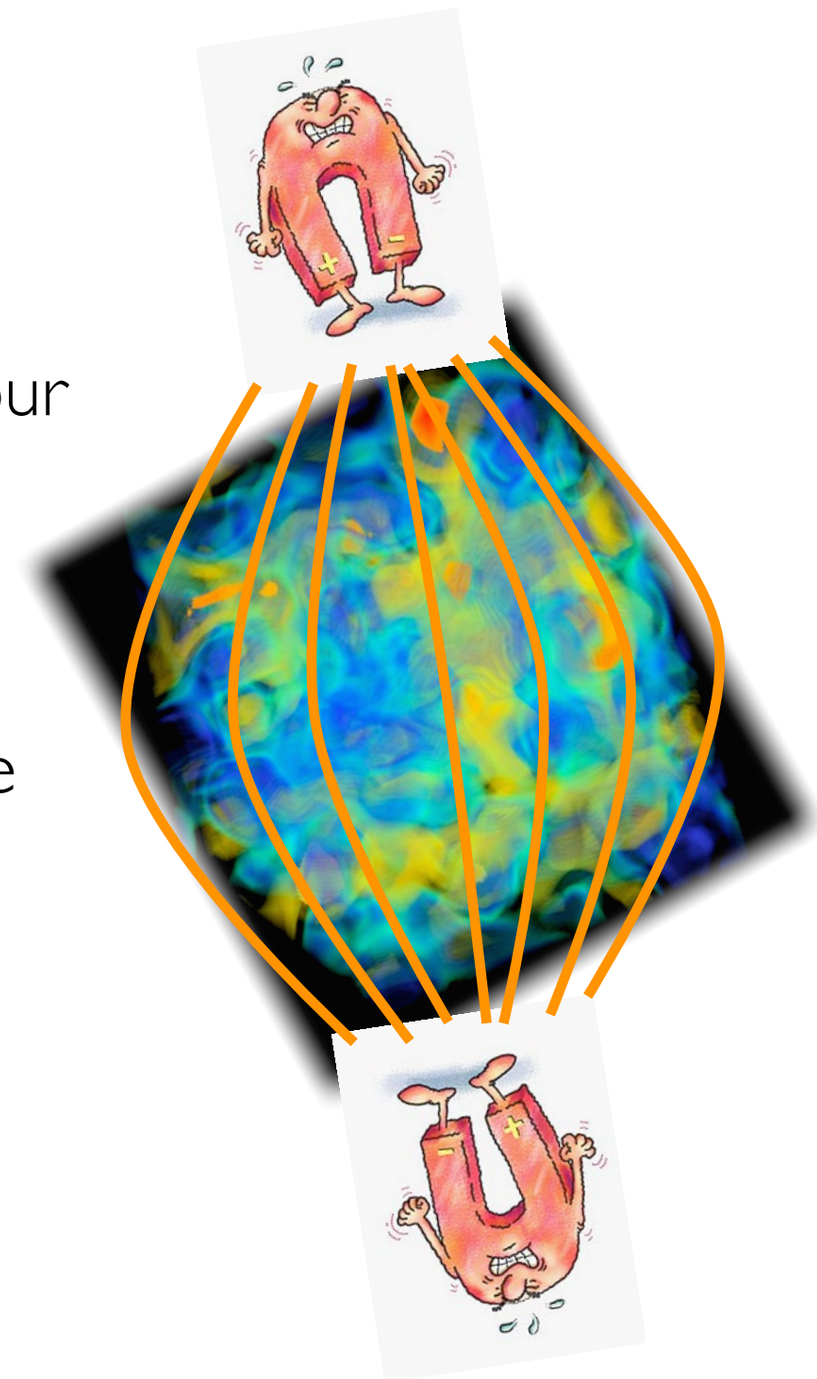

Nuclear magnetic moments

- Magnetic moments from spin splittings

$$\delta E^{(B)} \equiv E^{(B)}_{+j} - E^{(B)}_{-j} = -2\mu|\mathbf{B}| + \gamma|\mathbf{B}|^3 + \ldots$$

- Extract splittings from ratios of correlation functions

$$R(B) = \frac{C^{(B)}_{j}(t)\; C^{(0)}_{-j}(t)}{C^{(B)}_{-j}(t)\; C^{(0)}_{j}(t)} \xrightarrow{t\to\infty} Ze^{-\delta E^{(B)} t}$$

- Careful to be in single exponential region of each correlator

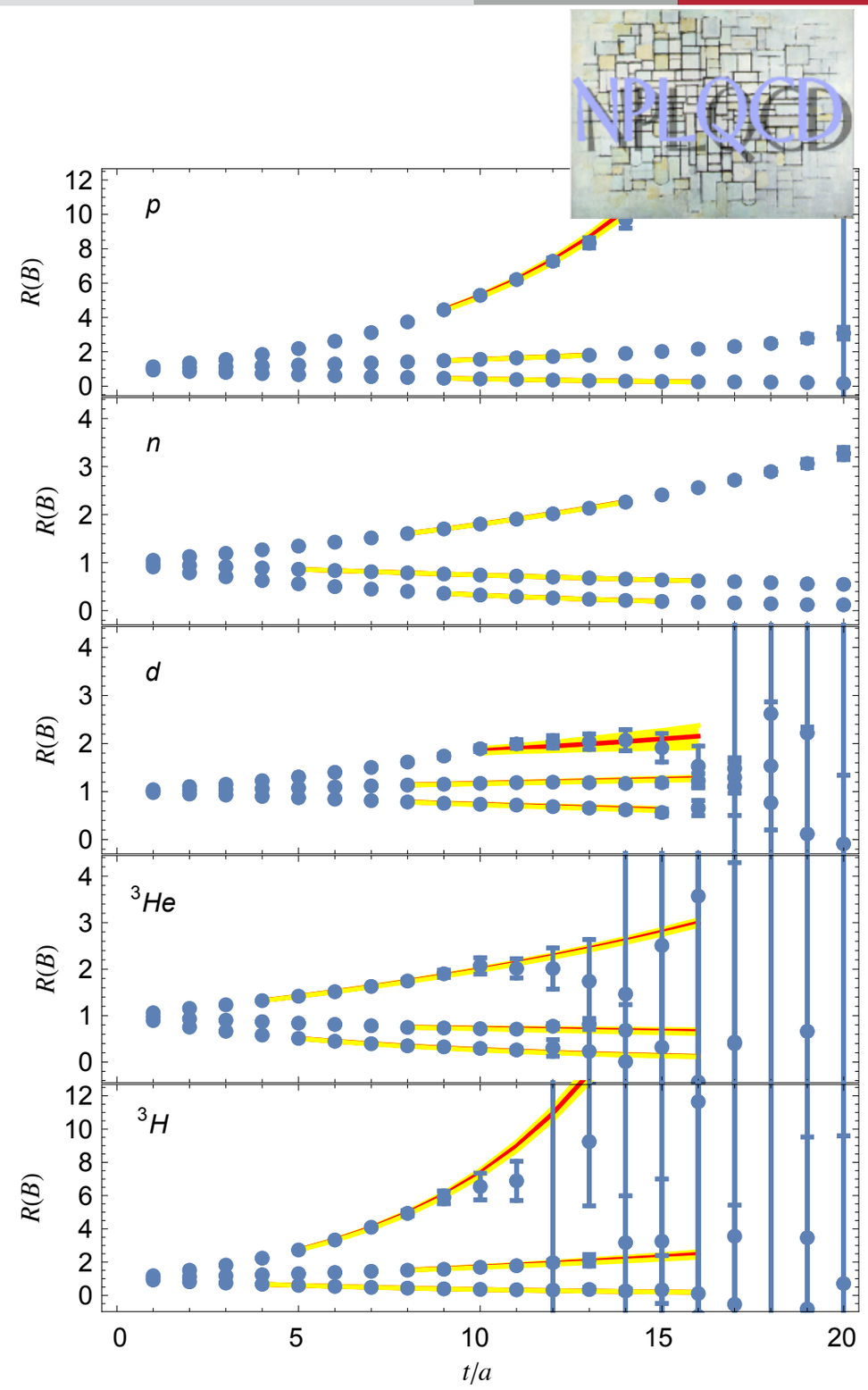

[NPLQCD 1409.3556, PRL to appear]

Nuclear magnetic moments

Energy shift vs B

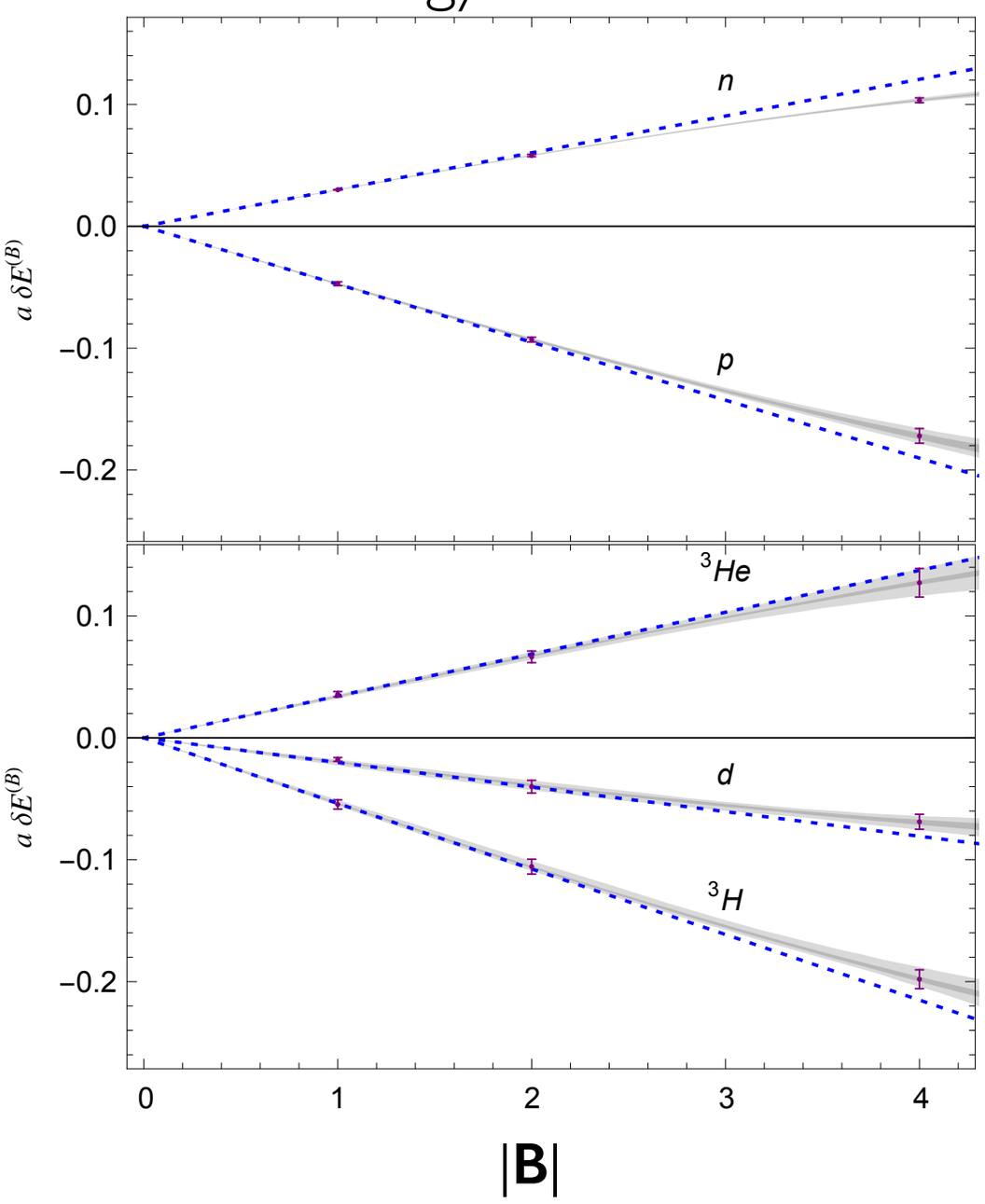

[NPLQCD 1409.3556, PRL to appear]

Nuclear magnetic moments

Energy shift vs B

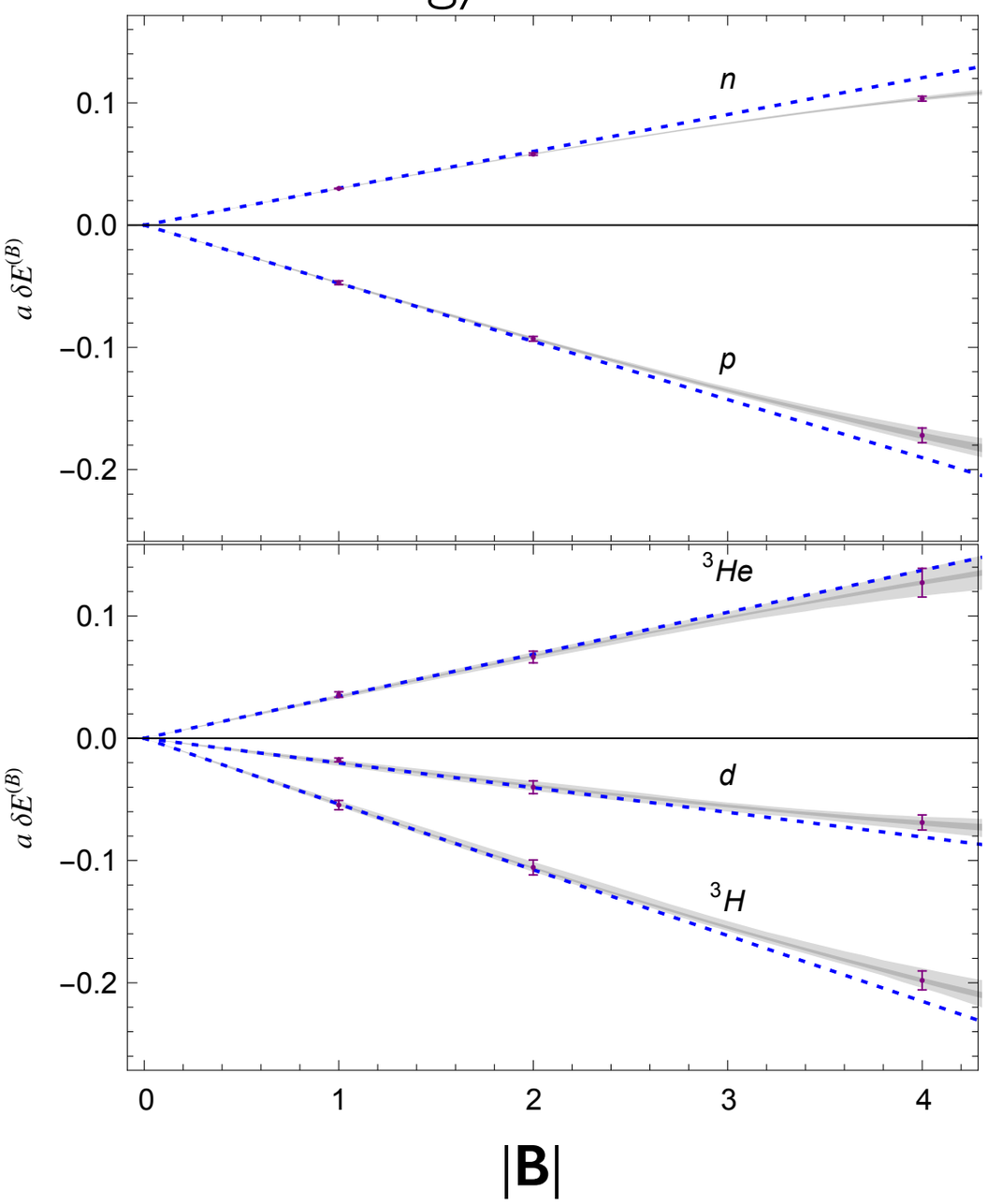

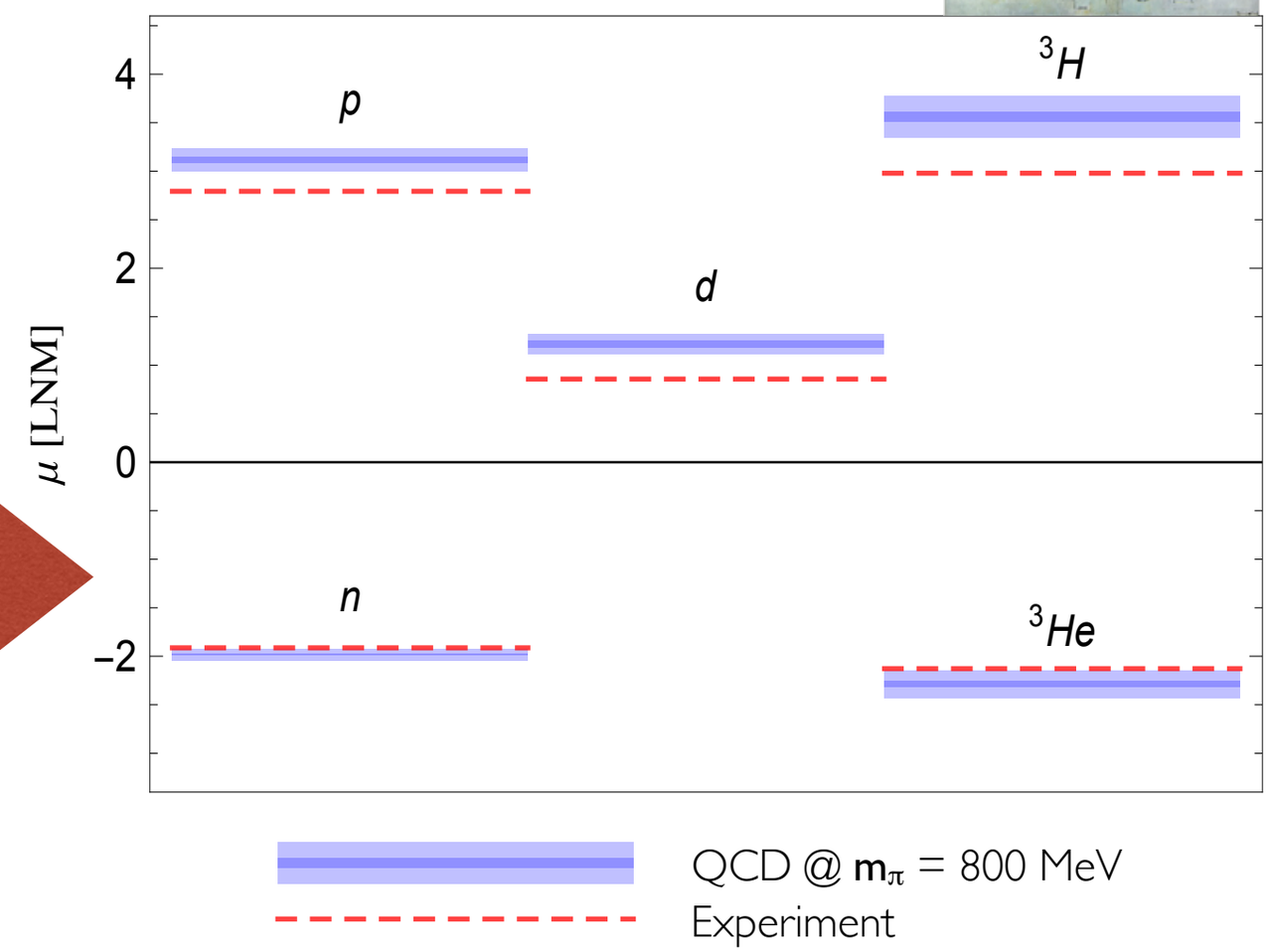

	n	p	d	3	3
μ	-1.98(1)(2)	3.21(3)(6)	1.22(4)(9)	-2.29(3)(12)	3.56(5)(18)

In units of appropriate nuclear magnetons (heavy M_N)

[NPLQCD 1409.3556, PRL to appear]

Nuclear magnetic moments

- Numerical values are surprisingly interesting
- Shell model expectations

$$\mu_d = \mu_p + \mu_n$$
$$\mu_{^3\mathrm{H}} = \mu_p$$
$$\mu_{^3\mathrm{He}} = \mu_n$$

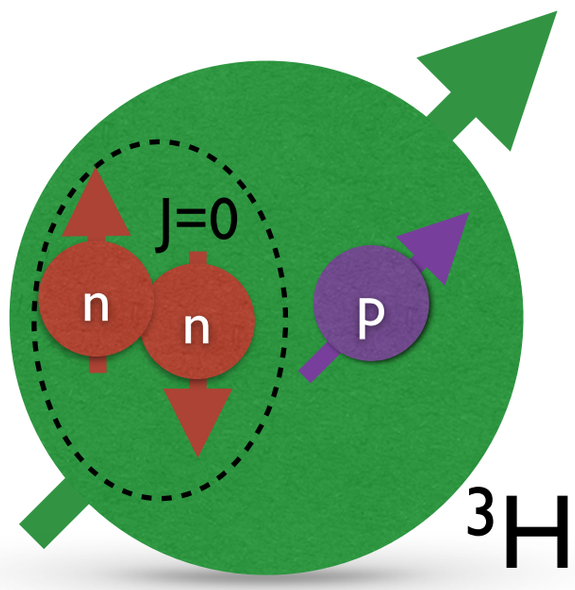

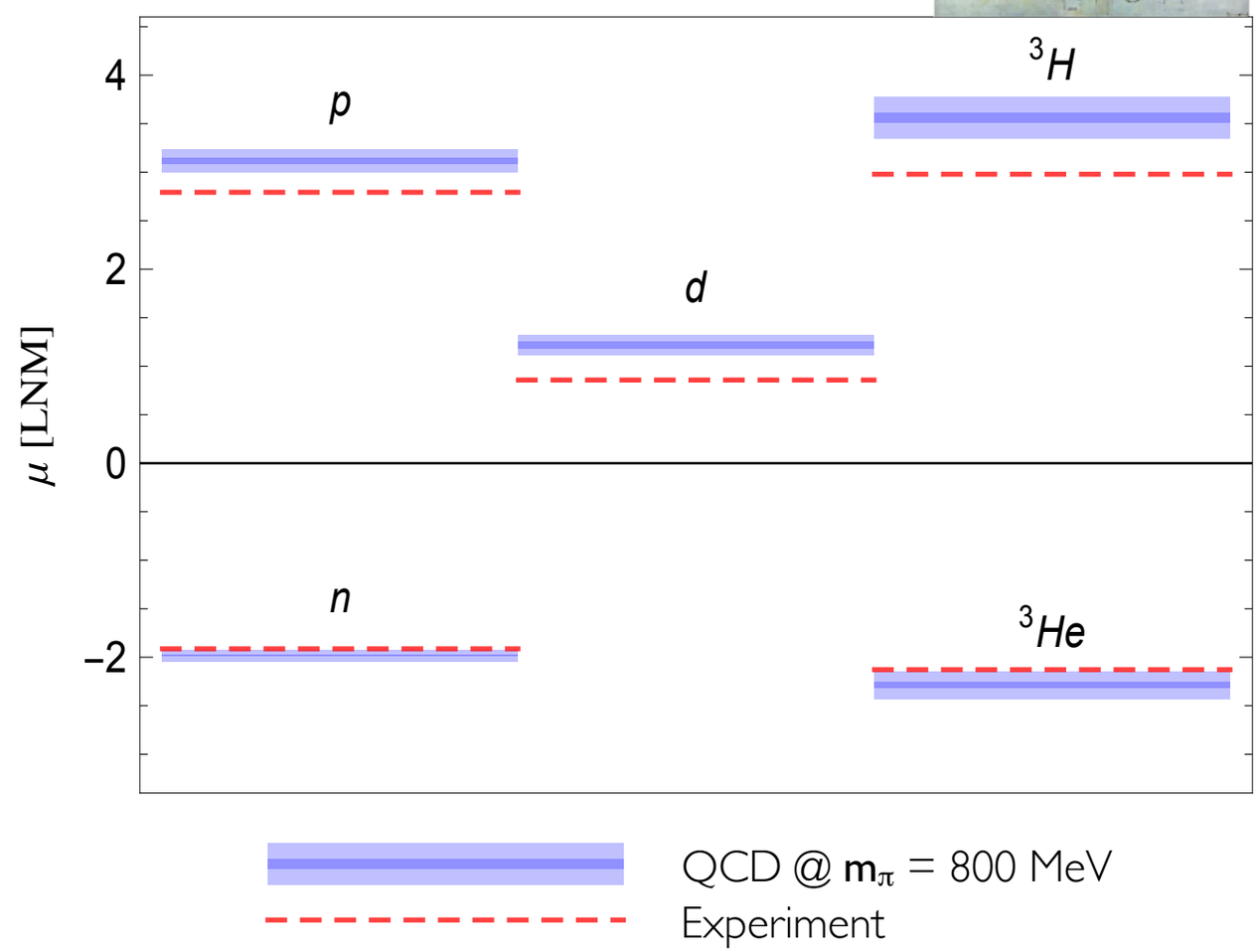

- Lattice results appear to suggest heavy quark nuclei are shell-model like!

	n	p	d	3	3
μ	-1.98(1)(2)	3.21(3)(6)	1.22(4)(9)	-2.29(3)(12)	3.56(5)(18)

In units of appropriate nuclear magnetons (heavy M_N)

[NPLQCD 1409.3556, PRL to appear]

Nuclear magnetic moments

- Numerical values are surprisingly interesting
- Shell model expectations

$$\mu_d = \mu_p + \mu_n$$
$$\mu_{^3\mathrm{H}} = \mu_p$$
$$\mu_{^3\mathrm{He}} = \mu_n$$

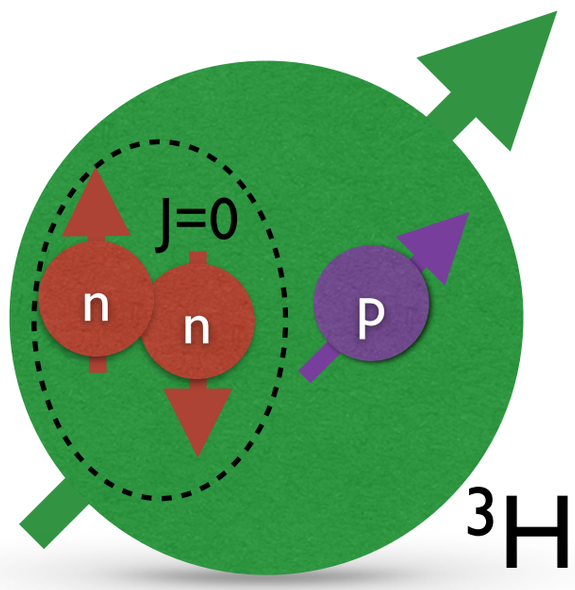

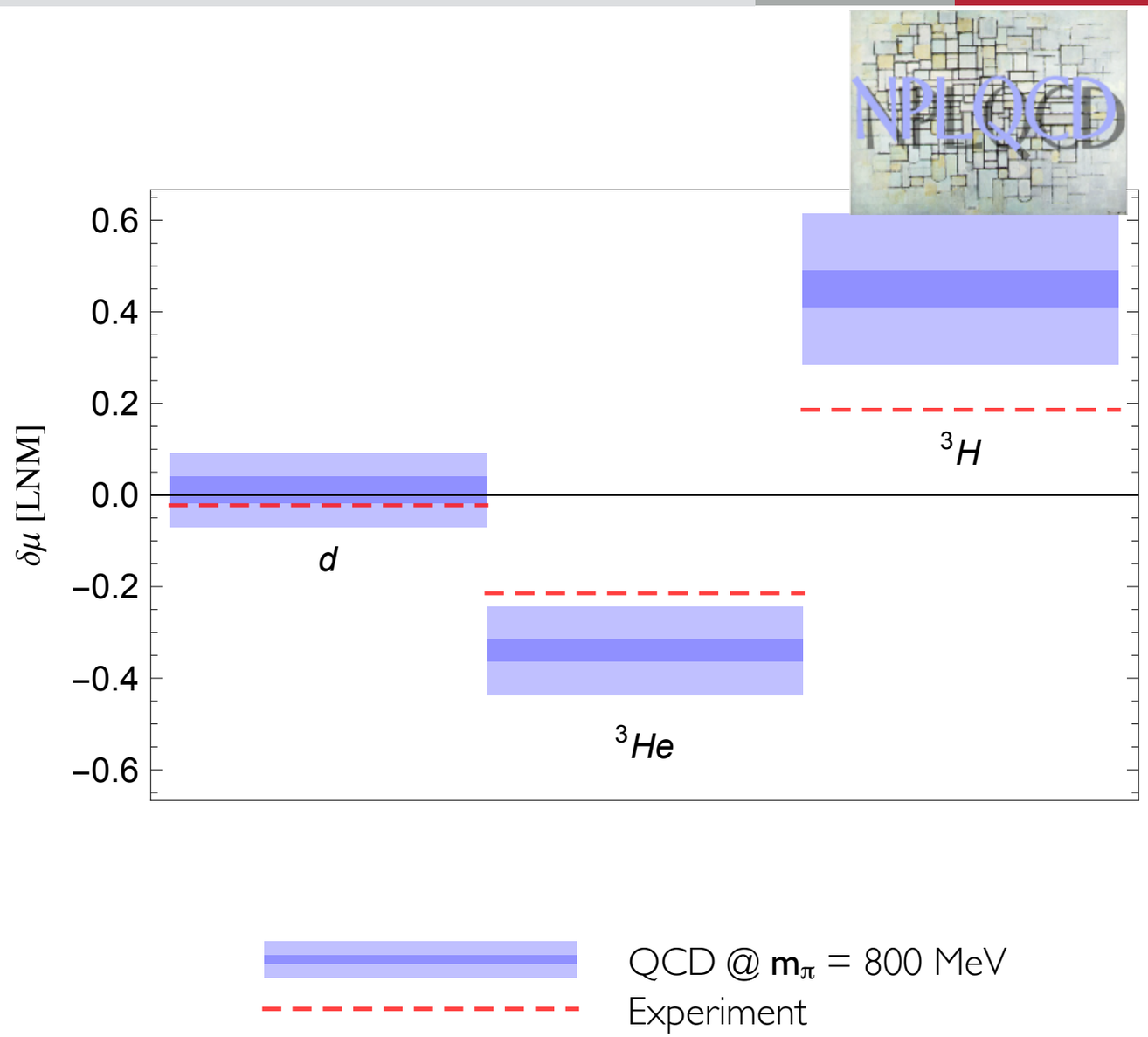

- Lattice results appear to suggest heavy quark nuclei are shell-model like!

	d	3	3
δμ	0.01(3)(7)	-0.34(2)(9)	0.45(4)(16)

Difference from NSM expectation

[NPLQCD 1409.3556, PRL to appear]

Nuclear sigma terms

- One possible DM interaction is through scalar exchange

$$\mathcal{L} = \frac{G_F}{2} \sum_q a_S^{(q)} (\overline{\chi}\,\chi)(\overline{q}\,q)$$

- Accessible via Feynman-Hellman theorem
- At hadronic/nuclear level

$$\mathcal{L} \to G_F\, \overline{\chi}\chi \left(\frac{1}{4}\langle 0|\overline{q}q|0\rangle\, \mathrm{Tr}\left[a_S\Sigma^\dagger + a_S^\dagger\Sigma\right] + \frac{1}{4}\langle N|\overline{q}q|N\rangle N^\dagger N \mathrm{Tr}\left[a_S\Sigma^\dagger + a_S^\dagger\Sigma\right] - \frac{1}{4}\langle N|\overline{q}\tau^3 q|N\rangle \left(N^\dagger N \mathrm{Tr}\left[a_S\Sigma^\dagger + a_S^\dagger\Sigma\right] - 4N^\dagger a_{S,\xi} N\right) + \ldots\right)$$

- Contributions:

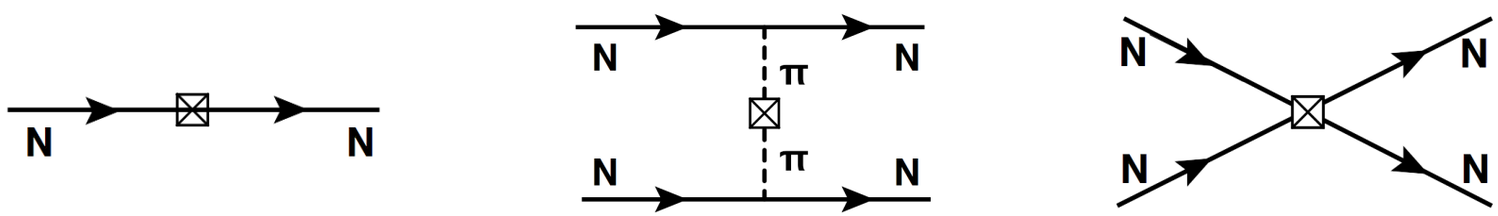

Nuclear sigma terms

- Previous work suggested scalar dark matter couplings to nuclei have O(50%) uncertainty arising from MECs [Prezeau et al 2003]
- Quark mass dependence of nuclear binding energies bounds such contributions

$$\delta\sigma_{Z,N} = \frac{\langle Z, N(\mathrm{gs})|\ \bar{u}u + \bar{d}d|Z, N(\mathrm{gs})\rangle}{A\ \langle N|\ \bar{u}u + \bar{d}d|N\rangle} - 1 = -\frac{1}{A\sigma_N}\frac{m_\pi}{2}\frac{d}{dm_\pi}B_{Z,N}$$

- Lattice calculations + physical point suggest such contributions are O(10%) or less for light nuclei (A<4)

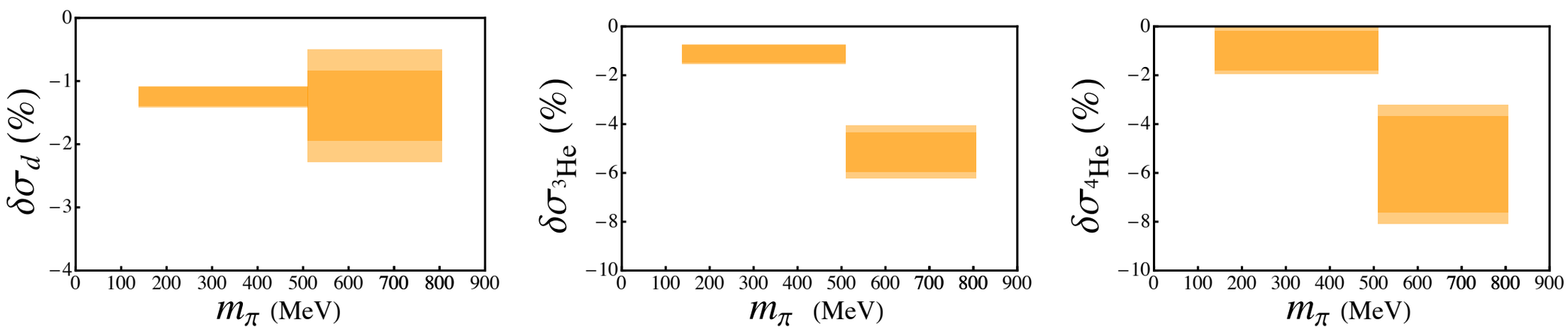

[NPLQCD PRD to appear]

QCD for nuclear physics

- Nuclei are under serious study directly from QCD
  - Spectroscopy of light nuclei and exotic nuclei (strange, charmed, …)
  - Nuclear properties/matrix elements
- Prospect of a quantitative connection to QCD makes this a very exciting time for nuclear physics
  - Critical role in current and upcoming intensity frontier experimental program
- Learn many interesting things about nuclear physics along the way

fin

HAL QCD method for hadron interactions on the lattice

Takumi Doi

(Nishina Center, RIKEN)

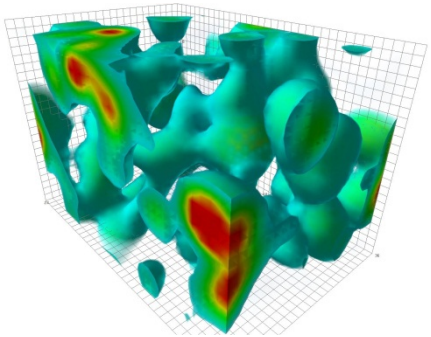

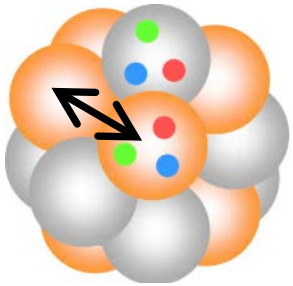

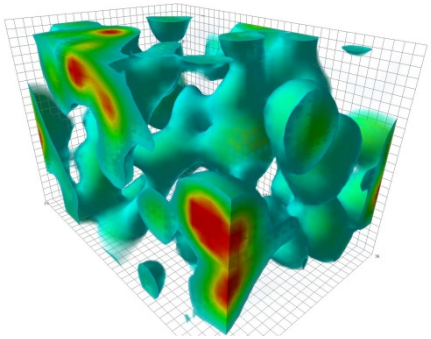

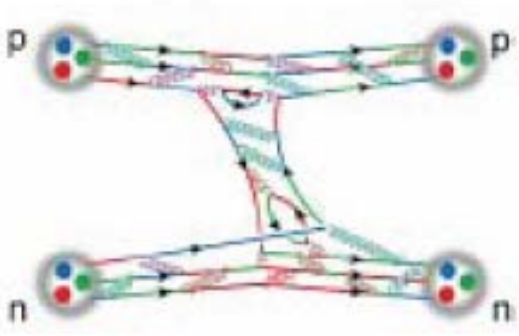

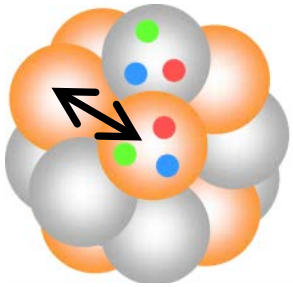

- **<u>Outline</u>**
  - Introduction
  - Theoretical framework of HAL QCD method
    - Challenges in multi-baryons
    - NBS wave functions & E-indep “potential”
  - Numerical results
  - Prospects toward physical point

Motivation:
Nuclear Physics and Astrophysics from Lat QCD

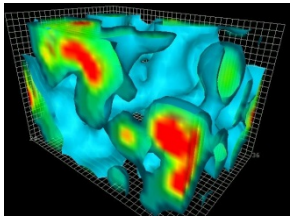

QCD Vacuum

Baryon

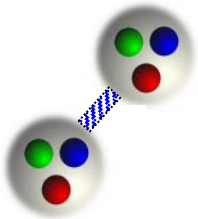

Few-Body

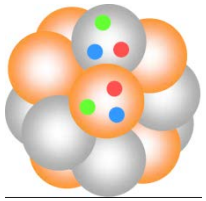

Nuclei

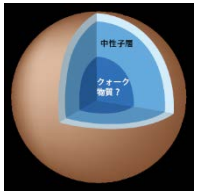

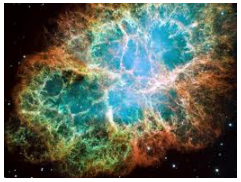

Neutron Star / Supernova

Standard Model

1st-principle lat calc.

Nuclear Forces

Ab-initio nuclear calc.

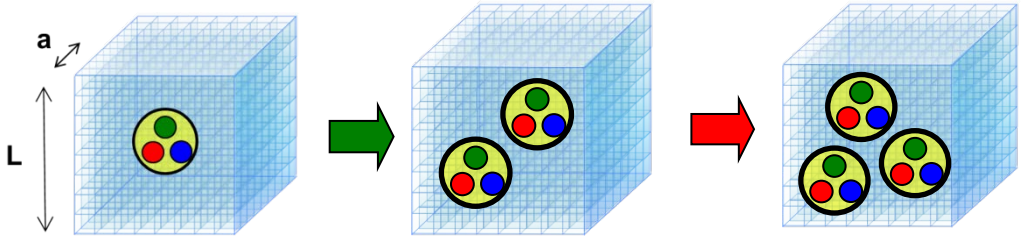

1st-principle lat calc.

Lattice QCD predictions play a crucial role

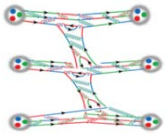

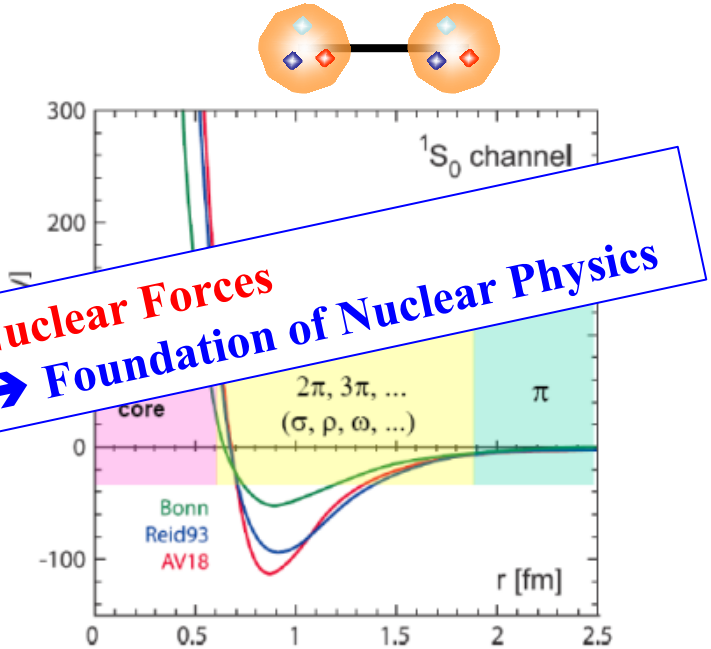

Nuclear Forces
➔ **Foundation of Nuclear Physics**

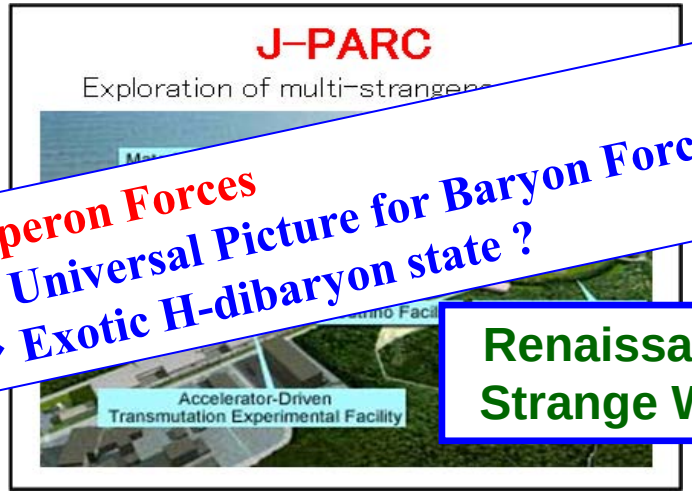

Hyperon Forces
➔ **Universal Picture for Baryon Forces**
➔ **Exotic H-dibaryon state ?**

Renaissance in Strange World !

Three-Baryon Forces
➔ **Paradigm Shift in Unstable Nuclei ?**
➔ **Nucleosynthesis**

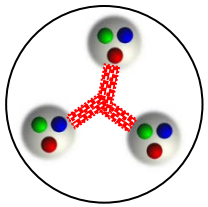

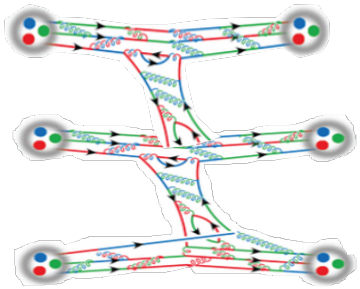

EoS of Dense Matter
➔ **Neutron Star**

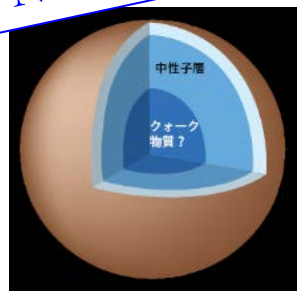

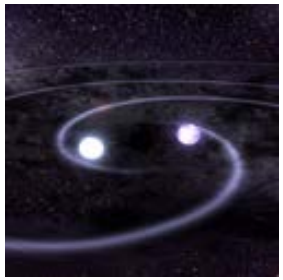

Exotics w/ charm ➔ Y. Ikeda's talk

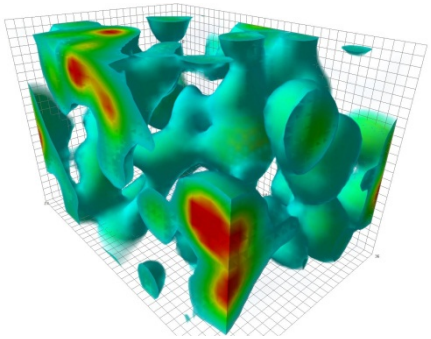

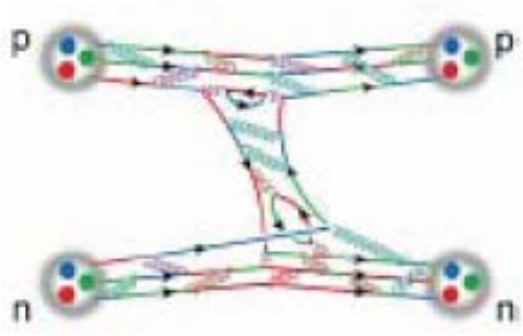

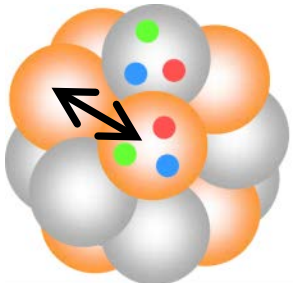

- **<u>Outline</u>**
  - Introduction
  - Theoretical framework of HAL QCD method
    - Challenges in multi-baryons
    - NBS wave functions & E-indep “potential”
  - Numerical results
  - Prospects toward physical point

Interactions on the Lattice

- Luscher's method (& Light nuclei)
  - Phase shift & B.E. from temporal correlation in finite V
  - (Probe interactions in indirect way)

M.Luscher, CMP104(1986)177
CMP105(1986)153
NPB354(1991)531

- HAL QCD method
  - "Potential" from spacial (& temporal) correlation
  - (Probe interactions in direct way)
  - Phase shift & B.E by solving Schrodinger eq in infinite V

Ishii-Aoki-Hatsuda, PRL99(2007)022001, PTP123(2010)89
HAL QCD Coll., PTEP2012(2012)01A105

Luscher's formula: Scatterings on the lattice

- Consider Schrodinger eq at asymptotic region

$$(\nabla^2 + k^2)\psi_k(\boldsymbol{r}) = mV_k(\boldsymbol{r})\psi_k(\boldsymbol{r})$$

$$V_k(\boldsymbol{r}) = 0 \text{ for } r > R$$

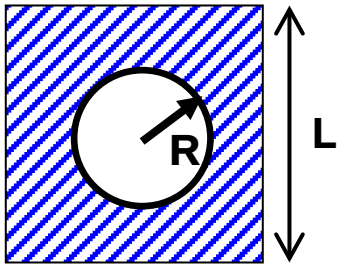

  - (periodic) Boundary Condition in finite V
    ➔ constraint on energies of the system
  - Energy E ➔ phase shift (at E)

$$k \cot \delta_{\mathbf{E}} = \frac{2}{\sqrt{\pi} L} Z_{00}(1; q^2), \quad q = \frac{kL}{2\pi}, \quad E = 2\sqrt{m^2 + k^2}$$

Large V: $$\Delta E = E - 2m = -\frac{4\pi \mathbf{a}}{mL^3}\left[1 + c_1 \frac{a}{L} + c_2 \left(\frac{a}{L}\right)^2 + \mathcal{O}(\frac{1}{L^3})\right]$$

- Calculate the energy spectrum of NN on (finite V) lattice
  - Temporal correlation in Euclidean time ➔ energy

$$G(t) = \langle 0|\mathcal{O}(t)\overline{\mathcal{O}}(0)|0|\rangle = \sum_n A_n e^{-E_n t} \to A_0 e^{-E_0 t} \quad (t \to \infty)$$

The Challenges

- Signal / Noise issue

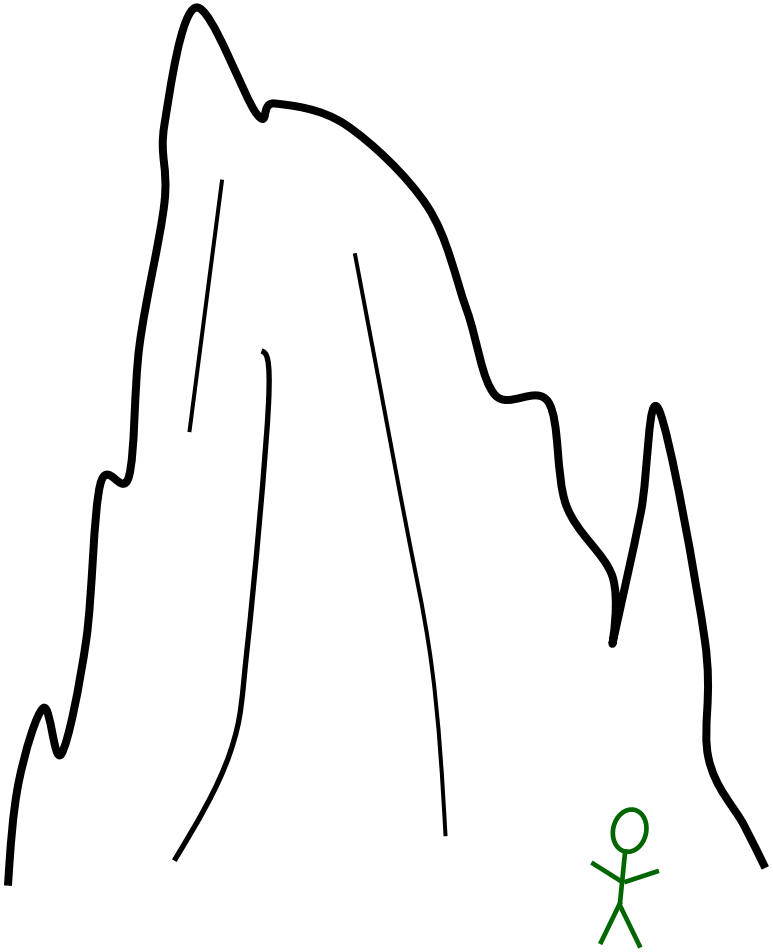

Challenges in multi-baryons on the lattice

- Signal / Noise estimate

Parisi, Lepage(1989)

In usual LQCD calc.,
G.S. saturation is necessary by t ➔ ∞

– pion

$$\frac{\text{Signal}}{\text{Noise}} \sim \frac{\exp(-m_\pi t)}{\sqrt{\exp(-2m_\pi t)}} \sim \boxed{\text{const.}}$$

– nucleon

$$\frac{\text{Signal}}{\text{Noise}} \sim \frac{\exp(-m_N t)}{\sqrt{\exp(-3m_\pi t)}} \sim \boxed{\exp[-(m_N - 3/2m_\pi)t]}$$

$$\frac{\text{Signal}}{\text{Noise}} \sim \boxed{\exp[-\mathbf{A}(m_N - 3/2m_\pi)t]}$$

(for mass number = A)

Challenges in multi-baryons on the lattice

- Signal / Noise estimate

Parisi, Lepage(1989)

  – S/N gets worse
  for larger mass number A & light quark mass & $t \to \infty$

$$S/N \sim \exp[-\mathbf{A} \times (\mathbf{m_N} - \mathbf{3/2m_\pi}) \times \mathbf{t}]$$

Variational method ?

  – Larger spectral density
  ➔ larger t required

$$\Delta E \simeq \frac{\vec{p}^2}{m_N} \simeq 15\mathrm{MeV} \quad \text{for } L = 10\mathrm{fm}$$
$$\longrightarrow t \gg 100 \times (0.1\mathrm{fm}/a)$$

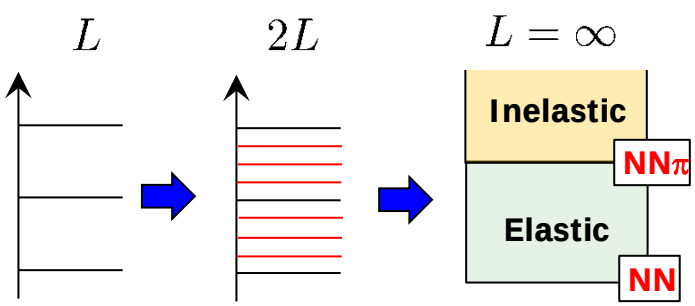

G.S. saturation becomes more and more difficult for larger V & lighter mass

$S/N \sim 10^{-42}$!?

Luscher's formula: Scatterings on the lattice

- Consider Schrodinger eq at asymptotic region

$$(\nabla^2 + k^2)\psi_k(\boldsymbol{r}) = mV_k(\boldsymbol{r})\psi_k(\boldsymbol{r})$$

$$V_k(\boldsymbol{r}) = 0 \text{ for } r > R$$

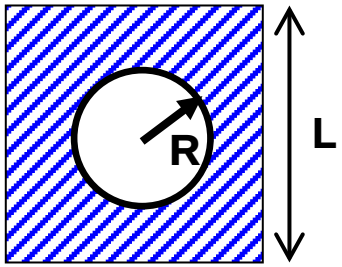

  - (periodic) Boundary Condition in finite V
    ➔ constraint on energies of the system
  - Energy E ➔ phase shift (at E)

$$k \cot \delta_{\mathbf{E}} = \frac{2}{\sqrt{\pi} L} Z_{00}(1; q^2), \quad q = \frac{kL}{2\pi}, \quad E = 2\sqrt{m^2 + k^2}$$

Large V: $$\Delta E = E - 2m = -\frac{4\pi \mathbf{a}}{mL^3}\left[1 + c_1 \frac{a}{L} + c_2 \left(\frac{a}{L}\right)^2 + \mathcal{O}\left(\frac{1}{L^3}\right)\right]$$

G.S. Saturation required

- Calculate the energy spectrum of (finite V) lattice
  - Temporal correlation in Euclidean time ➔ energy

$$G(t) = \langle 0|\mathcal{O}(t)\overline{\mathcal{O}}(0)|0|\rangle = \sum_n A_n e^{-E_n t} \to A_0 e^{-E_0 t} \quad (t \to \infty)$$

Further Challenges in multi-baryons on Lat

Is energy the only quantity from which we can extract interactions ?

- Phase shift:
  - Obtained at only one (or several) energies (➔ we have to repeat the calc w/ different V, etc.)

- Coupled channel
  - Unknown: 2 phases shifts + 1 mixing parameter (for 2x2) Obtained on Lat: 2 energies
  - ➔ "Parametrize" E-dependence

S. He et al., JHEP07(2005)011
Hansen-Sharpe, PRD86(2012)016007
J. Dudek et al., PRL113(2014)182001

- Many-body forces
  - Embedded in E in inefficient way
  - 2-body: ~ $1/L^3$, 3-body: ~$1/L^6$, 4-body: ~$1/L^9$

$$\Delta E = E - 2m = -\frac{4\pi \mathbf{a}}{mL^3}\left[1 + c_1\frac{a}{L} + c_2\left(\frac{a}{L}\right)^2 + \mathcal{O}(\frac{1}{L^3})\right]$$ (for 2-body)

(the situation may be better for bound states)

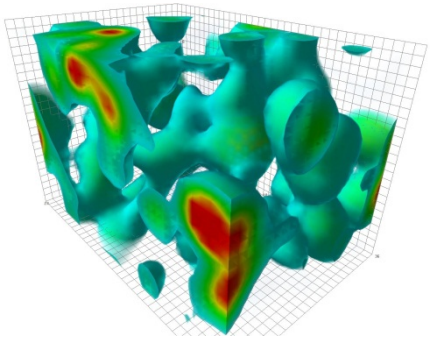

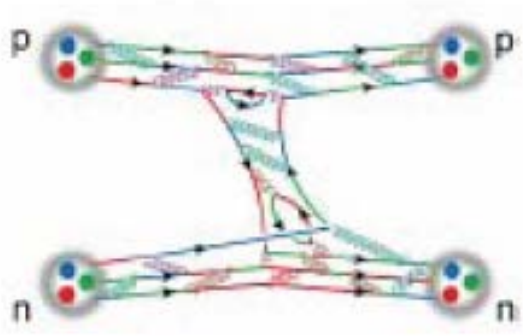

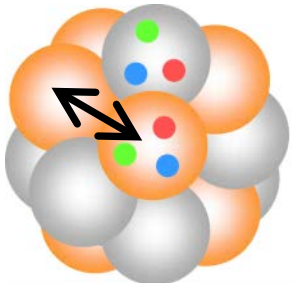

- **<u>Outline</u>**
  - Introduction
  - Theoretical framework of HAL QCD method
    - Challenges in multi-baryons
    - NBS wave functions & E-indep “potential”
  - Numerical results
  - Prospects toward physical point

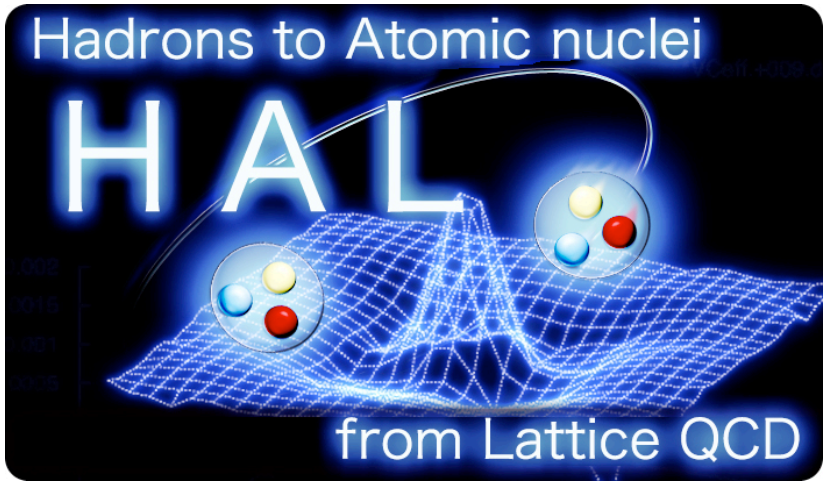

Hadrons to Atomic nuclei from Lattice QCD (HAL QCD Collaboration)

S. Aoki, T. Iritani (YITP)
B. Charron (Univ. of Tokyo)
T. Doi, T.Hatsuda, Y. Ikeda, V. Krejcirik (RIKEN)
F. Etminan (Univ. of Birjand)
T. Inoue (Nihon Univ.)
N. Ishii, K. Murano (RCNP)
T. Miyamato, H. Nemura, K. Sasaki, M. Yamada (Univ. of Tsukuba)

HAL QCD method for 2-body elastic scatt.

- Potential is constructed so as to reproduce the NN phase shifts (or, S-matrix)

- Nambu-Bethe-Salpeter (NBS) wave function

$$\psi(\vec{r}) = \langle 0|N(\vec{x}+\vec{r})N(\vec{x})|2N, W\rangle$$

$$W = 2\sqrt{m^2+k^2}$$

$$(\nabla^2 + k^2)\psi(\vec{r}) = 0, \quad r > R$$

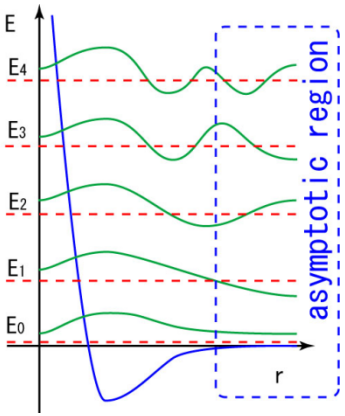

– Wave function ⇔ phase shifts

$$\psi(r) \simeq A\frac{\sin(kr - l\pi/2 + \delta(k))}{kr}$$

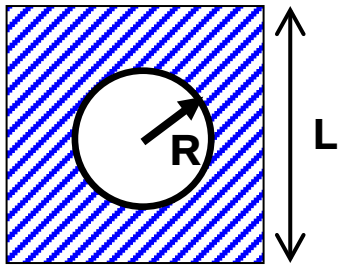

M.Luscher, NPB354(1991)531
C.-J.Lin et al., NPB619(2001)467
CP-PACS Coll., PRD71(2005)094504
Ishizuka, Pos LAT2009 (2009) 119
Aoki-Hatsuda-Ishii PTP123(2010)89
S.Aoki et al., PRD88(2013)014036

Asymptotic form of BS wave function

[C.-J.D.Lin et al., NPB619,467(2001)]

For simplicity, we consider BS wave function of two pions

$$\psi_{\vec{q}}(\vec{x}) \equiv \langle 0 | N(\vec{x})\, N(\vec{0}) | N(\vec{q}) N(-\vec{q}), in \rangle$$

complete set

$$1 = \int \frac{d^3 p}{(2\pi)^3 2E_N(\vec{p})} |N(\vec{p})\rangle\langle N(\vec{p})| + \cdots$$

$$= \int \frac{d^3 p}{(2\pi)^3 2E_N(\vec{p})} \langle 0 | N(\vec{x}) | N(\vec{p}) \rangle \langle N(\vec{p}) | N(\vec{0}) | N(\vec{q}) N(-\vec{q}), in \rangle + I(\vec{x})$$

$$Z^{1/2} e^{i\vec{p}\cdot\vec{x}}$$

$$disc. + Z^{1/2} \frac{T(\vec{p};\vec{q})}{m_N^2 - \left(2E_N(\vec{q}) - E_N(\vec{p})\right)^2 + \vec{p}^{\,2} - i\varepsilon}$$

$$= Z\left(e^{i\vec{q}\cdot\vec{x}} + \frac{1}{(2\pi)^3} \int \frac{d^3 p}{2E_N(\vec{p})} \frac{T(\vec{p};\vec{q})}{4E_N(\vec{q}) \cdot \left(E_N(\vec{p}) - E_N(\vec{q}) - i\varepsilon\right)} e^{i\vec{p}\cdot\vec{x}} \right)$$

Integral is dominated by the on-shell contribution $E_N(\vec{p}) \approx E_N(\vec{q})$

➔ T-matrix becomes the on-shell T-matrix

$$T^{(s-wave)}(s) = \frac{E(\vec{q})}{2|\vec{q}|}(-i)\left(e^{2i\delta_0(s)} - 1\right)$$

$$= Z\left(e^{i\vec{q}\cdot\vec{x}} + \frac{1}{2i}\left(e^{2i\delta_0(s)} - 1\right) \frac{e^{iqr}}{qr} \right) + \cdots$$

The asymptotic form

$$\boxed{\psi_{\vec{q}}(\vec{x}) = Z e^{i\delta_0(s)} \frac{\sin\left(qr + \delta_0(s)\right)}{qr} + \cdots \quad \text{(s-wave)}}$$

This is analogous to a non-rela. wave function

“Potential” as a representation of S-matrix

- Consider the wave function at “interacting region”

$$(\nabla^2 + k^2)\psi(\boldsymbol{r}) = m\int d\boldsymbol{r}' U(\boldsymbol{r},\boldsymbol{r}')\psi(\boldsymbol{r}'), \quad r < R$$

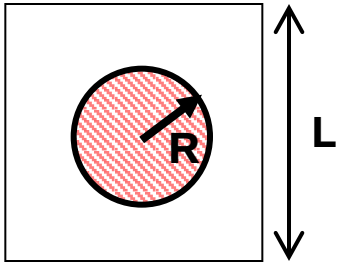

Probe interactions in “direct” way

  - U(r,r’): faithful to the phase shift by construction
    - U(r,r’): NOT an observable, but well defined
    - U(r,r’): E-independent, while non-local in general

Proof of Existence of E-independent potential

$V_W(\boldsymbol{r})\psi_W(\boldsymbol{r}) = (E_W - H_0)\psi_W(\boldsymbol{r})$ **[START] local but E-dep pot. (L^3xL^3 dof)**

- We consider the linear-indep wave functions and define

$$\mathcal{N}_{W_1W_2} = \int d\boldsymbol{r}\overline{\psi_{W_1}(\boldsymbol{r})}\psi_{W_2}(\boldsymbol{r})$$

- We define the non-local potential

$$U(\boldsymbol{r},\boldsymbol{r}') = \sum_{W_1,W_2}^{W_{\rm th}} (E_{W_1} - H_0)\psi_{W_1}(\boldsymbol{r})\mathcal{N}^{-1}_{W_1W_2}\overline{\psi_{W_2}(\boldsymbol{r}')}$$

- The above potential trivially satisfy Schrodinger eq.

$$\begin{aligned}\int d\boldsymbol{r}'U(\boldsymbol{r},\boldsymbol{r}')\psi_W(\boldsymbol{r}') &= \int d\boldsymbol{r}' \sum_{W_1,W_2}^{W_{\rm th}} (E_{W_1} - H_0)\psi_{W_1}(\boldsymbol{r})\mathcal{N}^{-1}_{W_1W_2}\overline{\psi_{W_2}(\boldsymbol{r}')}\psi_W(\boldsymbol{r}') \\ &= \sum_{W_1,W_2}^{W_{\rm th}} (E_{W_1} - H_0)\psi_{W_1}(\boldsymbol{r})\mathcal{N}^{-1}_{W_1W_2}\mathcal{N}_{W_2W} \\ &= (E_W - H_0)\psi_W(\boldsymbol{r})\end{aligned}$$

Intuitive understanding

[GOAL] non-local but E-indep pot. (L^3xL^3 dof)

c.f. Krolikowski-Rzewuski, Nuovo Cimento, 4, 1212 (1956)

“Potential” as a representation of S-matrix

- Consider the wave function at “interacting region”

$$(\nabla^2 + k^2)\psi(\boldsymbol{r}) = m\int d\boldsymbol{r}' U(\boldsymbol{r},\boldsymbol{r}')\psi(\boldsymbol{r}'), \quad r < R$$

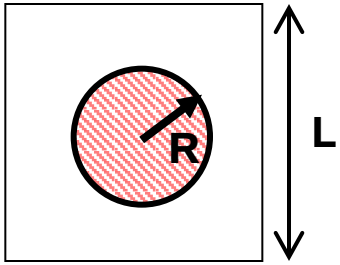

Probe interactions in “direct” way

  - U(r,r’): faithful to the phase shift by construction
    - U(r,r’): NOT an observable, but well defined
    - U(r,r’): E-independent, while non-local in general
  - Phase shifts at all E (below inelastic threshold) obtained by solving Scrodinger eq in infinite V
    - Non-locality ➔ derivative expansion

Okubo-Marshak(1958)

$$U(\vec{r},\vec{r'}) = \underbrace{V_c(r)}_{\text{LO}} + \underbrace{S_{12}V_T(r)}_{\text{LO}} + \underbrace{\vec{L}\cdot\vec{S}V_{LS}(r)}_{\text{NLO}} + \underbrace{\mathcal{O}(\nabla^2)}_{\text{NNLO}}$$

Check on convergence: K.Murano et al., PTP125(2011)1225

Control the E-dependence of phase shifts

Taming of S/N issue w/ E-indep potential

- Original (t-indep) HAL QCD method

$$R(\boldsymbol{r},t) \equiv C_{NN}(\boldsymbol{r},t)/C_N(t)^2 = \sum_i A_{W_i}\psi_{W_i}(\boldsymbol{r})e^{-(W_i-2m)t}$$

$$\begin{aligned}
\int d\boldsymbol{r}' U(\boldsymbol{r},\boldsymbol{r}')\psi_{W_0}(\boldsymbol{r}') &= (E_{W_0}-H_0)\psi_{W_0}(\boldsymbol{r}) \\
\int d\boldsymbol{r}' U(\boldsymbol{r},\boldsymbol{r}')\psi_{W_1}(\boldsymbol{r}') &= (E_{W_1}-H_0)\psi_{W_1}(\boldsymbol{r}) \\
\int d\boldsymbol{r}' U(\boldsymbol{r},\boldsymbol{r}')\psi_{W_2}(\boldsymbol{r}') &= (E_{W_2}-H_0)\psi_{W_2}(\boldsymbol{r})
\end{aligned}$$

G.S. saturation necessary

- New (t-dep) HAL QCD method
  - All equations can be combined in

$$\int d\boldsymbol{r}' U(\boldsymbol{r},\boldsymbol{r}')R(\boldsymbol{r}',t) = (-\frac{\partial}{\partial t} + \frac{1}{4m}\frac{\partial^2}{\partial t^2} - H_0)R(\boldsymbol{r},t)$$

Relativistic correction

G.S. saturation in R(r,t) NOT necessary

Extract the signal from excited states

N.Ishii et al. (HAL QCD Coll.) PLB712(2012)437

E-indep of potential U(r,r') ➔ *(excited) scatt states share the same U(r,r')*

*They are **not contaminations**, **but signals***

➔ **Time-dependent Schrodinger Eq.**

$$2\sqrt{m^2+k_n^2} = E_n = -\frac{\partial}{\partial t}$$

$$\left(-\frac{\partial}{\partial t} + \frac{1}{4m}\frac{\partial^2}{\partial t^2} - H_0\right) R(\boldsymbol{r},t) = \int d\boldsymbol{r}' U(\boldsymbol{r},\boldsymbol{r}') R(\boldsymbol{r}',t)$$

$$R(\boldsymbol{r},t) \equiv C_{NN}(\boldsymbol{r},t)/C_N(t)^2$$

Ground State (G.S.) saturation is NOT necessary !

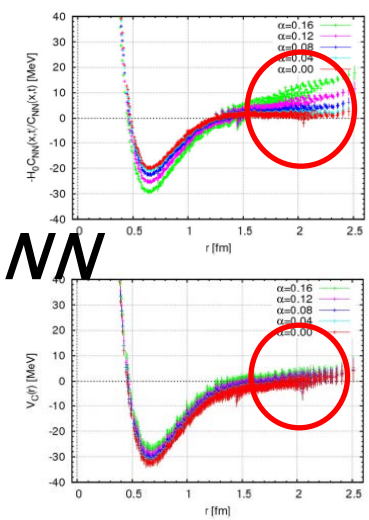

[OLD] "contaminations" from excited states

[NEW] "signals" from excited states

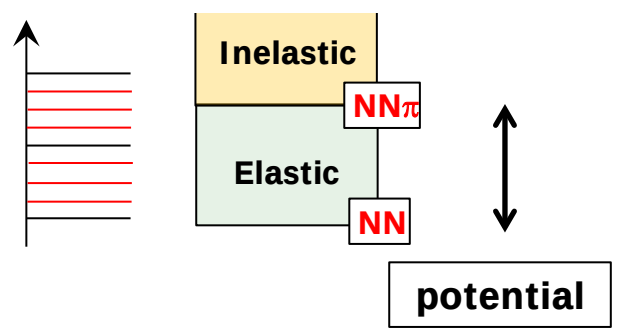

N.B. Inelastic scattering suppression still necessary

Coupled Channel

(beyond inelastic threshold)

- Asymptotic behavior of NBS wave func

Ex.) A + B ⇄ C + D

$$\psi_{AB}(\boldsymbol{r},\boldsymbol{k}) = 1/\sqrt{Z_A Z_B}\cdot\langle 0|\phi_A(\boldsymbol{x}+\boldsymbol{r})\phi_B(\boldsymbol{x})|W\rangle$$
$$\psi_{CD}(\boldsymbol{r},\boldsymbol{q}) = 1/\sqrt{Z_C Z_D}\cdot\langle 0|\phi_C(\boldsymbol{x}+\boldsymbol{r})\phi_D(\boldsymbol{x})|W\rangle$$

$$|W\rangle = c_{AB}|AB,W\rangle_{\text{in}} + c_{CD}|CD,W\rangle_{\text{in}}$$

$$W = \sqrt{m_A^2+k^2}+\sqrt{m_B^2+k^2} = \sqrt{m_C^2+q^2}+\sqrt{m_D^2+q^2}$$

$$\psi^l_{AB}(r,k) = c_{AB}\left[j_l(kr)+\frac{k}{4\pi}H_l^{AB,AB}(k,k)(n_l(kr)+ij_l(kr))\right]+c_{CD}\left[\frac{k}{4\pi}H_l^{AB,CD}(k,q)(n_l(kr)+ij_l(kr))\right]$$
$$\psi^l_{CD}(r,q) = c_{CD}\left[j_l(qr)+\frac{q}{4\pi}H_l^{CD,CD}(q,q)(n_l(qr)+ij_l(qr))\right]+c_{AB}\left[\frac{q}{4\pi}H_l^{CD,AB}(q,k)(n_l(qr)+ij_l(qr))\right]$$

where

$$H^{AB,AB(CD)}(\boldsymbol{k};\boldsymbol{k}(\boldsymbol{q})) = \frac{1}{2W}T^{AB,AB(CD)}(k_A,k_B;k_A,k_B(q_C,q_D))$$
$$H^{CD,AB(CD)}(\boldsymbol{q};\boldsymbol{k}(\boldsymbol{q})) = \frac{1}{2W}T^{CD,AB(CD)}(q_C,q_D;k_A,k_B(q_C,q_D))$$

S.Aoki et al. (HAL Coll.), Proc. Jpn. Acad. Ser. B87(2011)

Coupled Channel

- T-matrix parametrization by unitarity

$$T_l^{I,J}(W) = \frac{8\pi W}{p_I}\left[O(W)\begin{pmatrix} e^{i\delta_l^1(W)}\sin\delta_l^1(W) & 0 \\ 0 & e^{i\delta_l^2(W)}\sin\delta_l^2(W)\end{pmatrix}O^{-1}(W)\right]^{I,J}$$

$$O(W) = \begin{pmatrix} \cos\theta(W) & -\sin\theta(W) \\ \sin\theta(W) & \cos\theta(W)\end{pmatrix} \qquad (p_1 = k, p_2 = q)$$

- Asymptotic behavior ←→ $\delta_l^1(W), \delta_l^2(W), \theta(W)$

$$\begin{pmatrix}\psi_{AB}(r,k)\\ \psi_{CD}(r,q)\end{pmatrix} \simeq \begin{pmatrix} j_l(kr) & 0 \\ 0 & j_l(qr)\end{pmatrix}\begin{pmatrix} c_{AB}\\ c_{CD}\end{pmatrix}$$
$$+ \begin{pmatrix} n_l(kr)+ij_l(kr) & 0 \\ 0 & n_l(qr)+ij_l(qr)\end{pmatrix} O(W)\begin{pmatrix} e^{i\delta_l^1(W)}\sin\delta_l^1(W) & 0 \\ 0 & e^{i\delta_l^2(W)}\sin\delta_l^2(W)\end{pmatrix} O^{-1}(W)\begin{pmatrix} c_{AB}\\ c_{CD}\end{pmatrix}$$

- → Coupled channel potentials can be defined

$$(E_{k_i}^{AB} - H_0^{AB})\psi_{AB}(\boldsymbol{r},k_i) = \int d\boldsymbol{r}' U_{AB,AB}(\boldsymbol{r},\boldsymbol{r}')\psi_{AB}(\boldsymbol{r}',k_i) + \int d\boldsymbol{r}' U_{AB,CD}(\boldsymbol{r},\boldsymbol{r}')\psi_{CD}(\boldsymbol{r}',q_i)$$
$$(E_{q_i}^{CD} - H_0^{CD})\psi_{CD}(\boldsymbol{r},q_i) = \int d\boldsymbol{r}' U_{CD,AB}(\boldsymbol{r},\boldsymbol{r}')\psi_{AB}(\boldsymbol{r}',k_i) + \int d\boldsymbol{r}' U_{CD,CD}(\boldsymbol{r},\boldsymbol{r}')\psi_{CD}(\boldsymbol{r}',q_i)$$

Coupled Channel

S.Aoki et al. (HAL Coll.), PRD87(2013)034512

- Proof of Existence of E-indep potential

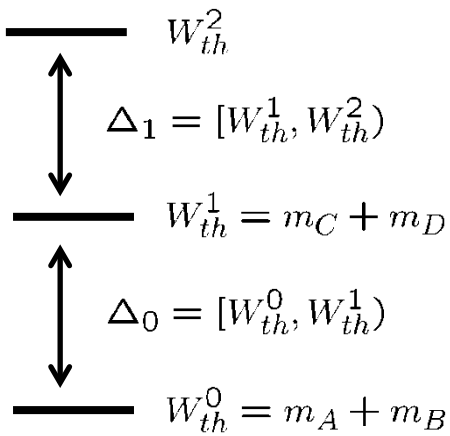

NBS wave func.

$$\begin{aligned}
\psi_{AB,AB}(\boldsymbol{r}) &= 1/\sqrt{Z_A Z_B} \cdot \langle 0|\phi_A(\boldsymbol{x}+\boldsymbol{r})\phi_B(\boldsymbol{x})|AB, W\rangle_{\text{in}} \\
\psi_{AB,CD}(\boldsymbol{r}) &= 1/\sqrt{Z_A Z_B} \cdot \langle 0|\phi_A(\boldsymbol{x}+\boldsymbol{r})\phi_B(\boldsymbol{x})|CD, W\rangle_{\text{in}} \\
\psi_{CD,AB}(\boldsymbol{r}) &= 1/\sqrt{Z_C Z_D} \cdot \langle 0|\phi_C(\boldsymbol{x}+\boldsymbol{r})\phi_D(\boldsymbol{x})|AB, W\rangle_{\text{in}} \\
\psi_{CD,CD}(\boldsymbol{r}) &= 1/\sqrt{Z_C Z_D} \cdot \langle 0|\phi_C(\boldsymbol{x}+\boldsymbol{r})\phi_D(\boldsymbol{x})|CD, W\rangle_{\text{in}}
\end{aligned}$$

Vector of NBS

$$\Psi_{XY} = (\psi_{AB,XY}, \psi_{CD,XY})^T, \quad (XY = AB \text{ or } CD) \quad \text{for } W \in \Delta_1$$

$$\Psi_{XY} = (\psi_{AB,XY}, \psi_{CD,XY})^T, \quad (XY = AB \text{ only}) \quad \text{for } W \in \Delta_0$$

Norm

$$\mathcal{N} = \begin{pmatrix} \mathcal{N}_{AB,AB}(\Delta_0,\Delta_0) & \mathcal{N}_{AB,AB}(\Delta_0,\Delta_1) & \mathcal{N}_{AB,CD}(\Delta_0,\Delta_1) \\ \mathcal{N}_{AB,AB}(\Delta_1,\Delta_0) & \mathcal{N}_{AB,AB}(\Delta_1,\Delta_1) & \mathcal{N}_{AB,CD}(\Delta_1,\Delta_1) \\ \mathcal{N}_{CD,AB}(\Delta_1,\Delta_0) & \mathcal{N}_{CD,AB}(\Delta_1,\Delta_1) & \mathcal{N}_{CD,CD}(\Delta_1,\Delta_1) \end{pmatrix} \qquad \mathcal{N}_{XY,X'Y'} = (\Psi_{XY}, \Psi_{X'Y'})$$

E-indep pot.

$$U = \sum (E - H_0)\Psi\mathcal{N}^{-1}\overline{\Psi}$$

- Generalization to A+B ←→ C+D+E, etc. possible
  - 2-body relativistic, otherwise non-rela approx. necessary

Extension to multi-particle systems (n>=3)

S.Aoki et al. (HAL Coll.), PRD88(2013)014036

- Unitarity of S-matrix

$$T^\dagger - T = iT^\dagger T$$

Hyper-spherical func in D=3(n-1) dim

$$T([\boldsymbol{q}^A]_n, [\boldsymbol{q}^B]_n) = \sum_{[L],[K]} T_{[L][K]}(Q_A, Q_B) Y_{[L]}(\Omega_{Q_A}) \overline{Y_{[K]}(\Omega_{Q_B})}$$

$$[L] = L, M_1, M_2, \ldots$$

diagonalization

$$T_{[L][K]}(Q, Q) = \sum_{[N]} U_{[L][N]}(Q) T_{[N]}(Q) U^\dagger_{[N][K]}(Q)$$

$$(Q = Q_A = Q_B)$$

$$T_{[L]}(Q) = -\frac{2n^{3/2}}{mQ^{3n-5}} \boxed{e^{i\delta_{[L]}(Q)} \quad \sin\delta_{[L]}(Q)}$$

c.f. R.B. Newton (1974) for n = 3

Similar formula to 2-body system
(w/ diagonalization matrix U which includes dynamics)

(non-rela approx.)

Extension to multi-particle systems (n>=3)

S.Aoki et al. (HAL Coll.), PRD88(2013)014036

- NBS wave function

$$\psi_\alpha([\boldsymbol{x}]) = {}_{\text{in}}\langle 0|\phi([\boldsymbol{x}])|\alpha\rangle_{\text{in}} = {}_{\text{in}}\langle 0|N(\vec{x}_1)N(\vec{x}_2)\cdots N(\vec{x}_n)|\alpha\rangle_{\text{in}}$$

Lippmann-Schwinger eq.

$$\psi_\alpha([\boldsymbol{x}]) = {}_{\text{in}}\langle 0|\phi([\boldsymbol{x}])|\alpha\rangle_0 + \int d\beta \frac{{}_{\text{in}}\langle 0|\phi([\boldsymbol{x}])|\beta\rangle_0 T_{\beta\alpha}}{E_\alpha - E_\beta + i\epsilon}$$

Expansion w/ hyper-coordinate

$$\psi(\boldsymbol{R}, \boldsymbol{Q}_A) = \sum_{[L],[K]} \psi_{[L][K]}(R, Q_A) Y_{[L]}(\Omega_R) \overline{Y_{[K]}(\Omega_{Q_A})}$$

$$\psi_{[L],[K]}(R, Q_A) \propto \sum_{[N]} U_{[L][N]}(Q_A) \boxed{e^{i\delta_{[N]}(Q_A)} \frac{\sin(Q_A R - \Delta_L + \delta_{[N]}(Q_A))}{(Q_A R)^{(D-1)/2}}} U^\dagger_{[N][K]}(Q_A)$$

Similar asymptotic behavior to 2-body system

(non-rela approx.)
(no bound state in subsystem assumed)

c.f. Finite V spectrum, n=3 only, relativistic: Hansen-Sharpe, arXiv:1408.5933

Prescription in HAL QCD method

Lattice QCD

NBS wave func.

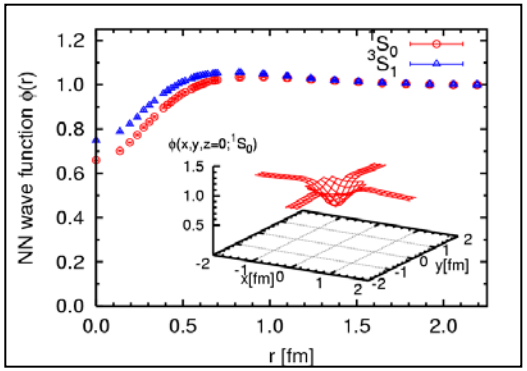

Lat Nuclear Force

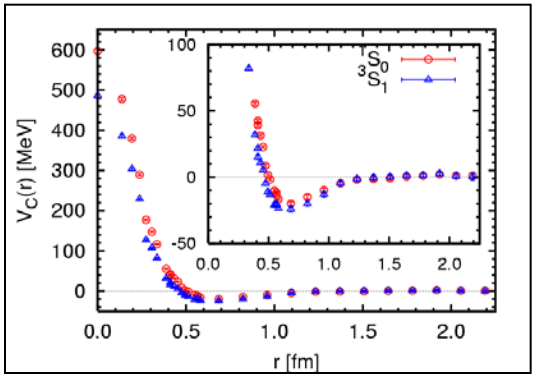

$$\psi_{NBS}(\vec{r}) = \langle 0|N(\vec{r})N(\vec{0})|N(\vec{k})N(-\vec{k}), in\rangle \simeq e^{i\delta_l(k)}\sin(kr - l\pi/2 + \delta_l(k))/(kr)$$

(at asymptotic region)

$$(k^2/m_N - H_0)\,\psi(\vec{r}) = \int d\vec{r}'\,U(\vec{r},\vec{r}')\psi(\vec{r}')$$

Lat potential is faithful to phase shift by construction

Analog to …

Scattering Exp.

Phase shifts

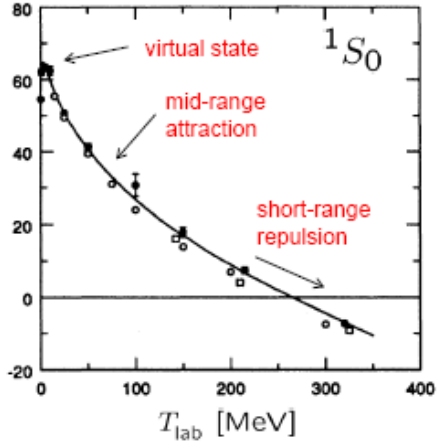

Phen. Potential

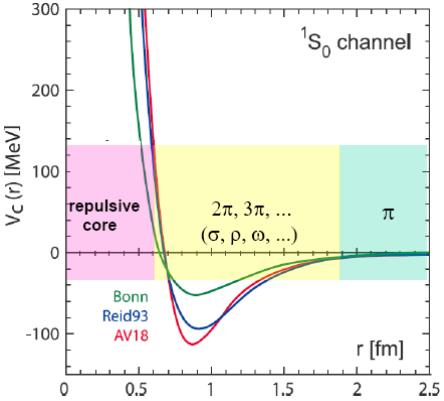

A few remarks on the Lattice Potential

- Potential is NOT an observable and is not unique:
  They are, however, phase-shift equivalent potentials.
  - Choosing the pot. ⇔ choosing the "scheme" (sink op.)

- Potential approach has some benefits:
  - Convenient to understand physics
  - Essential to study many-body

$$Lat \rightarrow \boxed{\delta_E \rightarrow U(\boldsymbol{r})} \rightarrow \text{many-body}$$

$$\boxed{Lat \rightarrow \begin{matrix} \rightarrow & \rightarrow \\ \delta_E & \leftarrow \end{matrix} U(\boldsymbol{r})} \rightarrow \text{many-body}$$

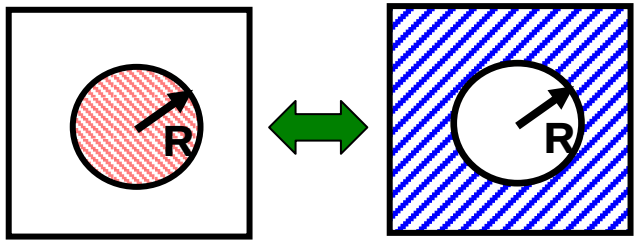

  - Phase shifts at various E obtained
    ➔ Coupled channel straightforward
  - Finite V artifact better under control
  - Excited states better under control

Luscher's method vs. HAL method

I = 2 ππ system

Beautiful Agreement !

Best S/N on the lattice
G.S. saturation can be achieved in this case

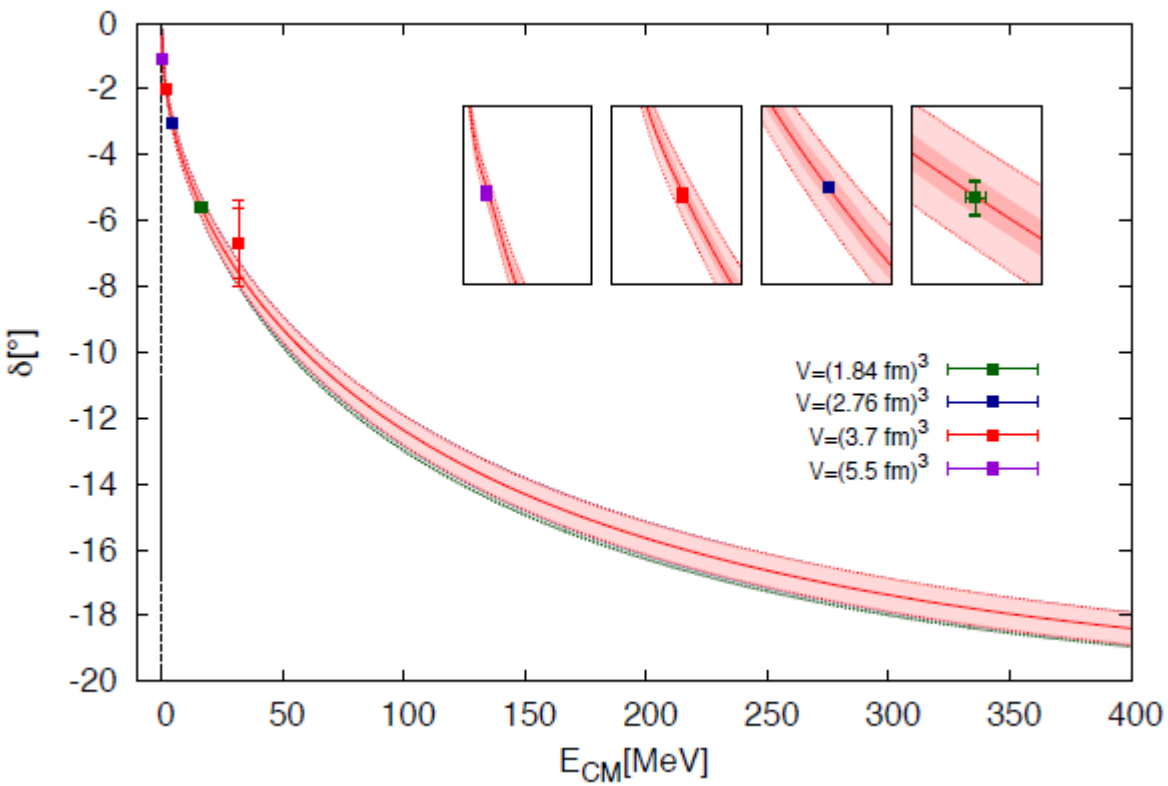

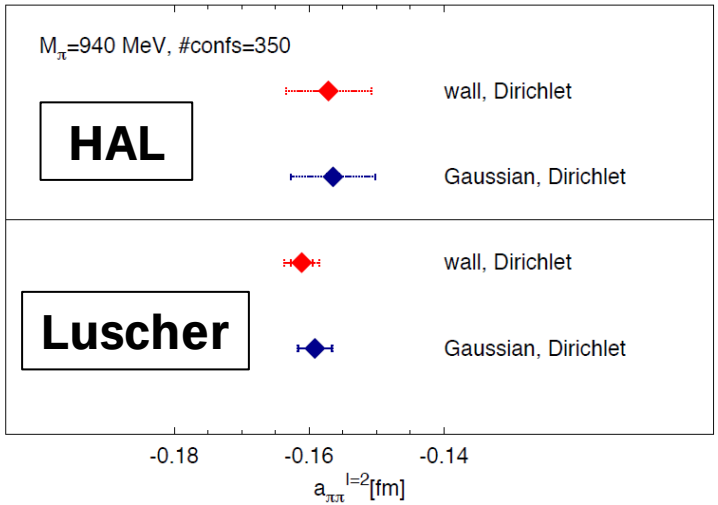

(HAL = "time-dependent" HAL method)

Kurth et al., JHEP1312(2013)015

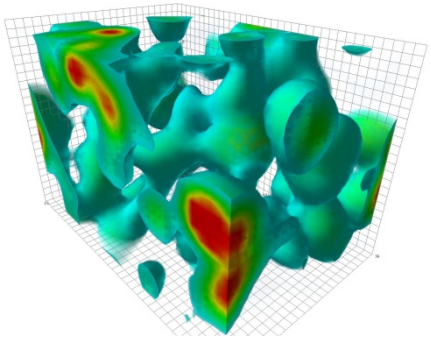

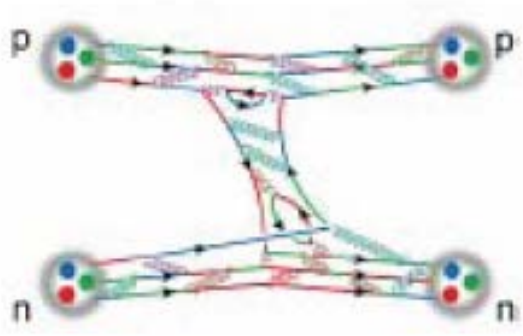

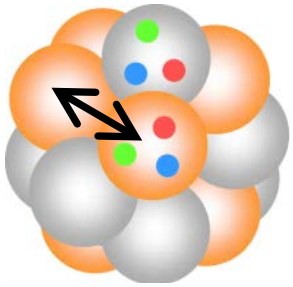

- **<u>Outline</u>**
  - Introduction
  - Theoretical framework of HAL QCD method
    - Challenges in multi-baryons
    - NBS wave functions & E-indep “potential”
  - Numerical results
    - Unified Contraction Algorithm (UCA)
    - NN, YN/YY (H-dibaryon), NNN
  - Prospects toward physical point

Challenges in multi-baryons on the lattice (2)

- Enormous computational cost for correlators
  - # of Wick contraction (permutation)

$$N_{\rm perm} = N_u! \times N_d! \sim [\,(\tfrac{3}{2}A)!\,]^2$$ for mass number A

(🡐 can be reduced by 2^A by inner-baryon exchange)

  - # of color / spinor contractions

$$N_{\rm loop} = \underbrace{6^A}_{\text{(color)}} \cdot \underbrace{4^A}_{\text{(spinor)}} \quad \text{or} \quad 6^A \cdot 2^A$$

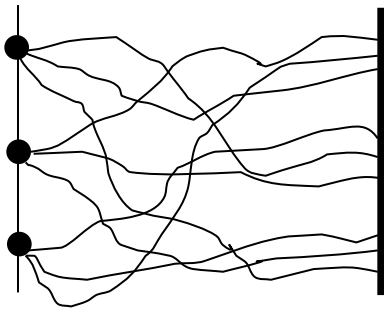

  - Total cost: $N_{\rm perm} \times N_{\rm loop}$
    - ^{2}H : 9 x 144 = 1 x 10^3
    - ^{3}H : 360 x 1728 = 6 x 10^5
    - ^{4}He : 32400 x 20736 = 7 x 10^8

c.f. T.Yamazaki et al., PRD81(2010)111504

$N_{\rm perm} = 1107$ for ^{4}He in the isospin limit

Solution: **Unified contraction algorithm**

TD, M.Endres, Comput. Phys. Comm.184(2013)117

- Traditional algorithm

color/spinor contractions (ξ')

$$\Pi^{2N} \simeq \langle qqqqqq(t)\bar{q}(\xi_1')\bar{q}(\xi_2')\bar{q}(\xi_3')\bar{q}(\xi_4')\bar{q}(\xi_5')\bar{q}(\xi_6')(t_0)\rangle \times \mathrm{Coeff}^{2N}(\xi_1', \cdots, \xi_6')$$

Permutations

color ϵ_{abc}, spinor $(C\gamma_5)$, etc.

- New algorithm

[impose the same spacial label at source]

  – Permutation applies to color/spinor indices at "Coeff"

Permuted Sum

$$\Pi^{2N} \simeq \langle qqqqqq(t)\bar{q}(\xi_1')\bar{q}(\xi_2')\bar{q}(\xi_3')\bar{q}(\xi_4')\bar{q}(\xi_5')\bar{q}(\xi_6')(t_0)\rangle \times \mathrm{Coeff}^{2N}(\xi_1', \cdots, \xi_6')$$

Sum over color/spinor unified list

  – **Permutation DONE beforehand**
    - (Wick contraction and color/spinor contractions are unified)
  – Significant improvement

$\times 192$ for $^3\mathrm{H}/^3\mathrm{He}$, $\times 20736$ for $^4\mathrm{He}$, $\times 10^{11}$ for $^8\mathrm{Be}$ (x add'l. speedup)

See also subsequent works: Detmold et al., PRD87(2013)114512
Gunther et al., PRD87(2013)094513

(1) NN potential on the lattice (positive parity)

$^{2S+1}L_J$

- "di-neutron" channel $^1S_0$ ➔ central force
- "deuteron" channel $^3S_1$–$^3D_1$ ➔ central & tensor force

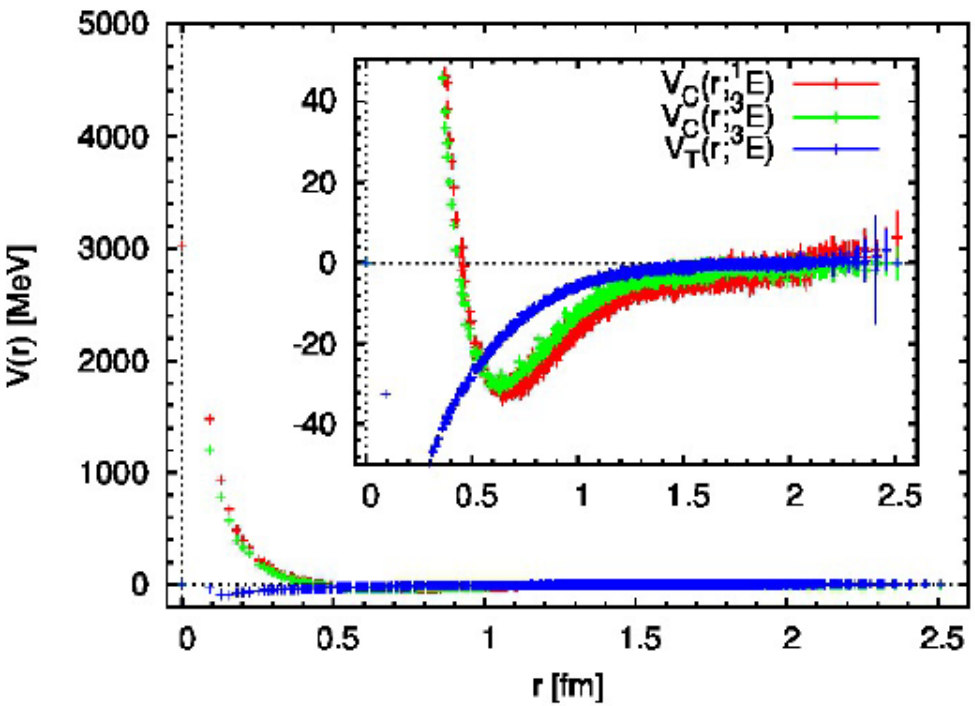

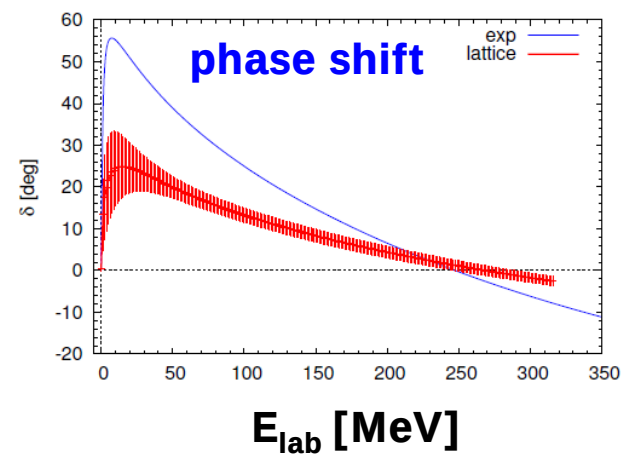

Not Bound $a(^1S_0) = 1.6(1.1)$ fm

Nf=2+1 clover (PACS-CS), 1/a=2.2GeV, L=2.9fm, mπ=0.7GeV, m_N=1.6GeV

N.Ishii et al. (HAL QCD Coll.) PLB712(2012)437

Quark mass dependence

Central in $^1S_0$

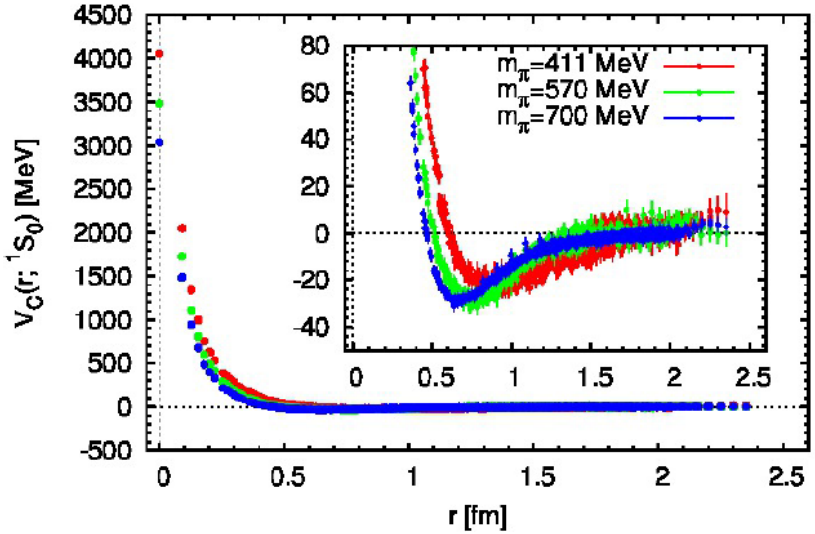

$^3S_1$-$^3D_1$ channel

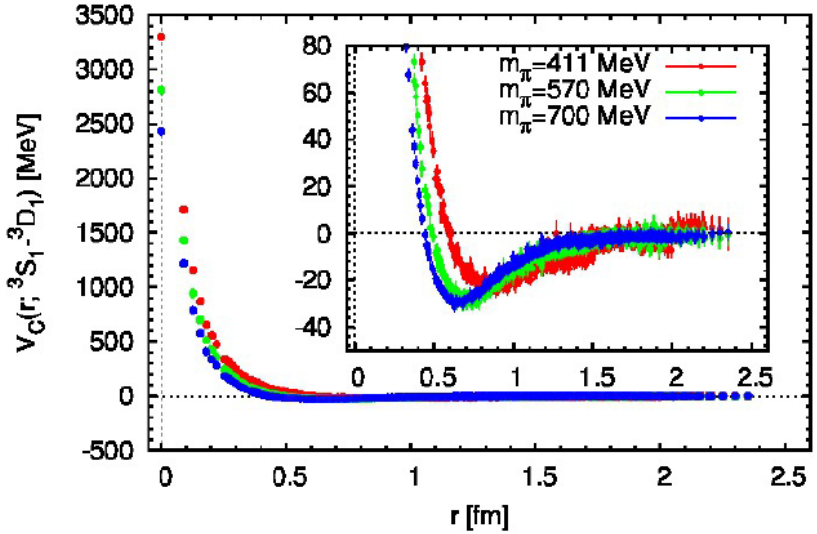

Central

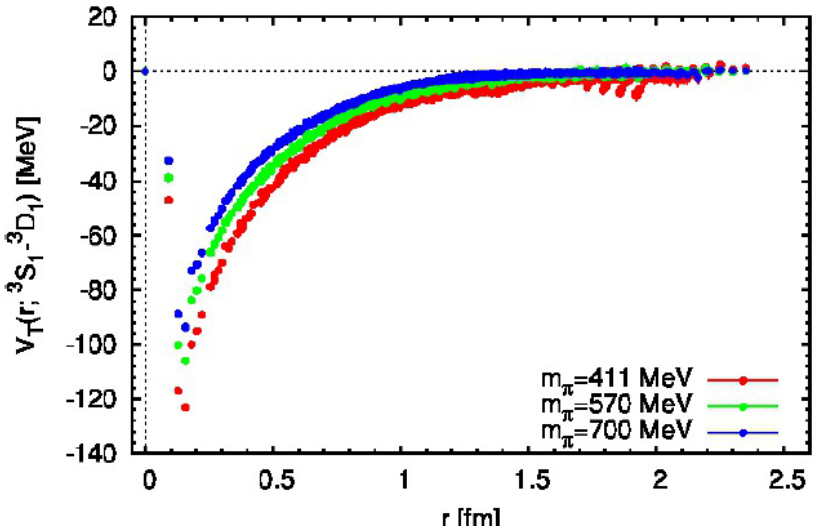

Tensor

<u>Lighter mass</u> corresponds to…

- **Longer interaction range**
- **Larger Repulsive Core**
- **Stronger Tensor Force**

N.Ishii @ Lat2012

Hyperon Forces

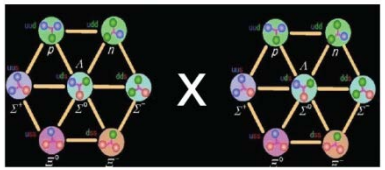

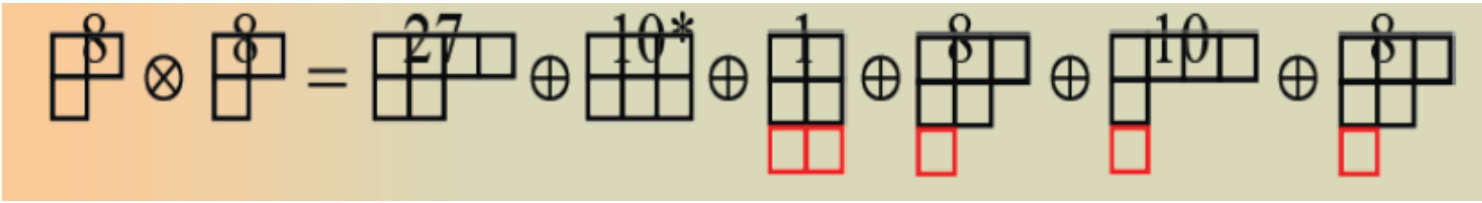

8 X 8 = 27 + 8s + 1 + 10* + 10 + 8a

symmetric

anti-symmetric

NN channel

SU(3) study

(2) BB potentials

a=0.12fm, L=3.9fm,
m(PS)= 0.47-1.2GeV

$^1S_0$

$^3S_1-^3D_1$

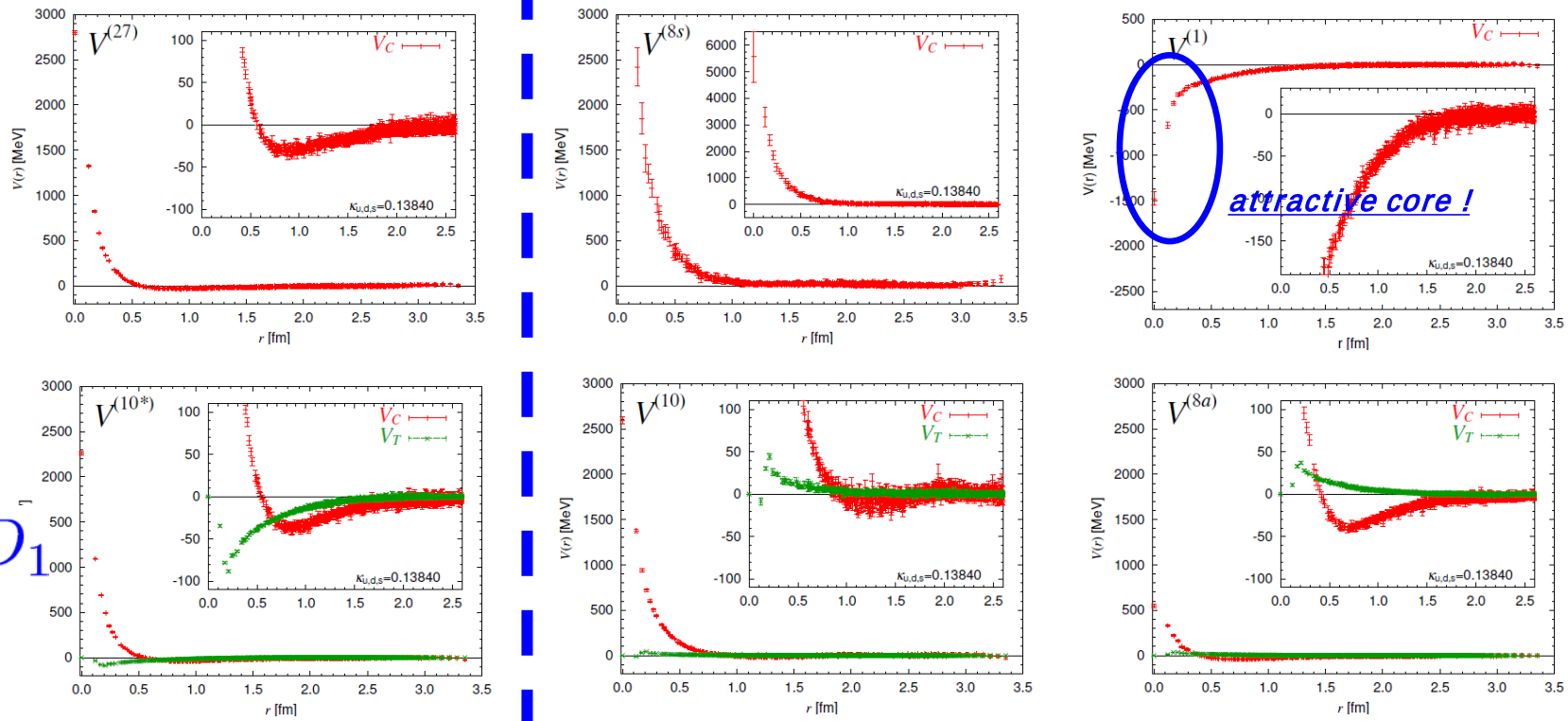

27,10*:
Same as NN

8s,10:
strong repulsive core

1s: deep attractive pocket
8a: weak repulsive core

Repulsive core
← Pauli principle !

T.Inoue et al. (HAL QCD Coll.), NPA881(2012)28

Also seen in SU(2)c , Takahashi et al.,, PRD82(2010)094506
Charmonium-N, Kawanai-Sasaki, PRD82(2010)091501
Meson-baryon, Y.Ikeda et al., arXiv:1111.2663

M.Oka et al., NPA464(1987)700

H-dibaryon (uuddss, I=0, $^1S_0$)

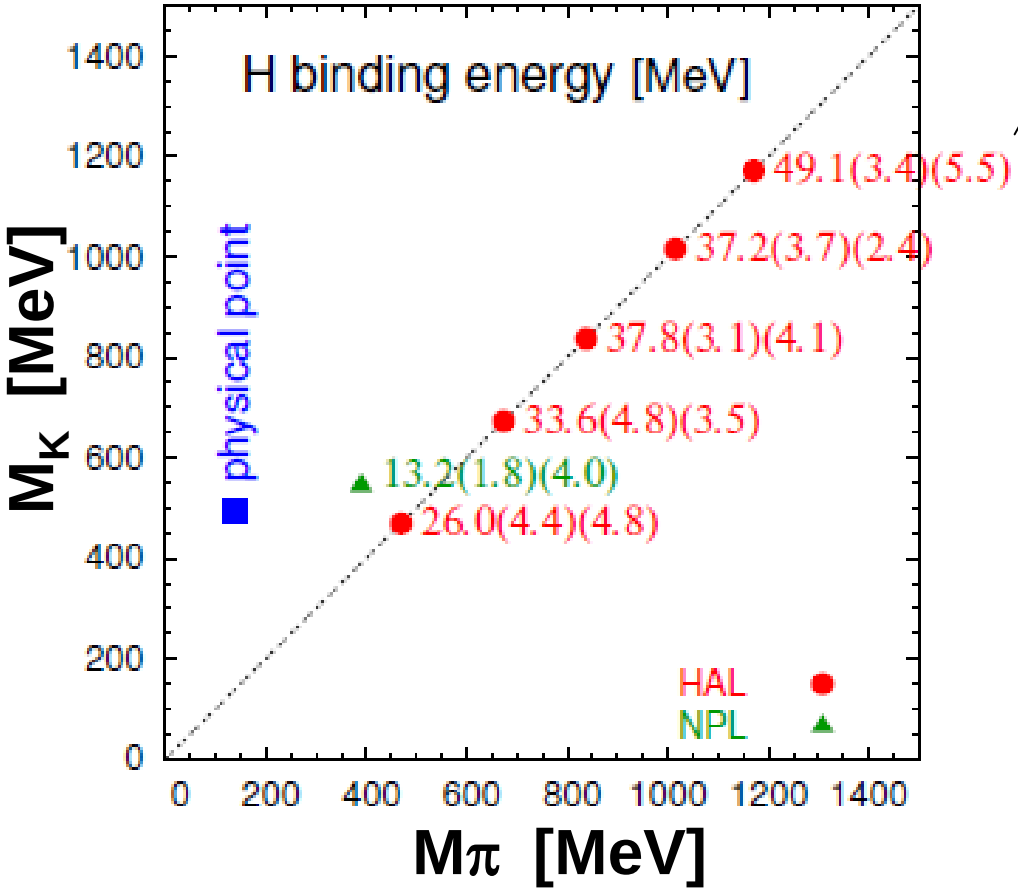

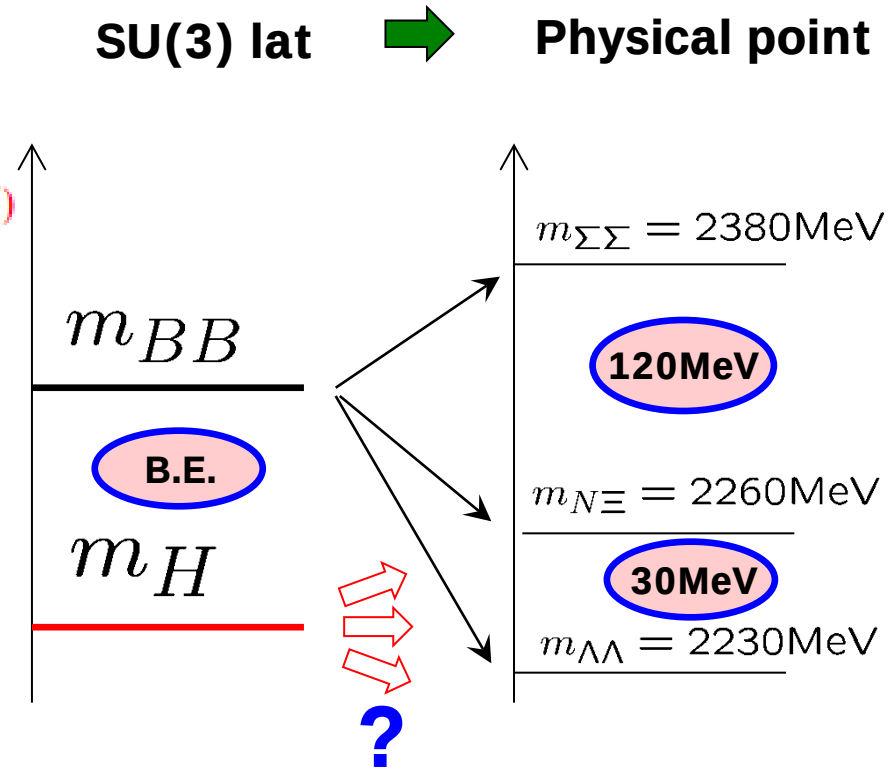

Coupled channel study is essential

$\Lambda\Lambda$–$N\Xi$–$\Sigma\Sigma$

Beane et al. (NPLQCD Coll.) PRL106(2011)162001

Inoue et al. (HAL QCD Coll.) PRL106(2011)162002

Coupled channel formalism in HAL

$\Lambda\Lambda - N\Xi - \Sigma\Sigma$

$\Lambda\Lambda$ and $N\Xi$ phase shifts

Esb1 : m_π= 701 MeV | **Esb2 : m_π= 570 MeV** | **Esb3 : m_π= 411 MeV**

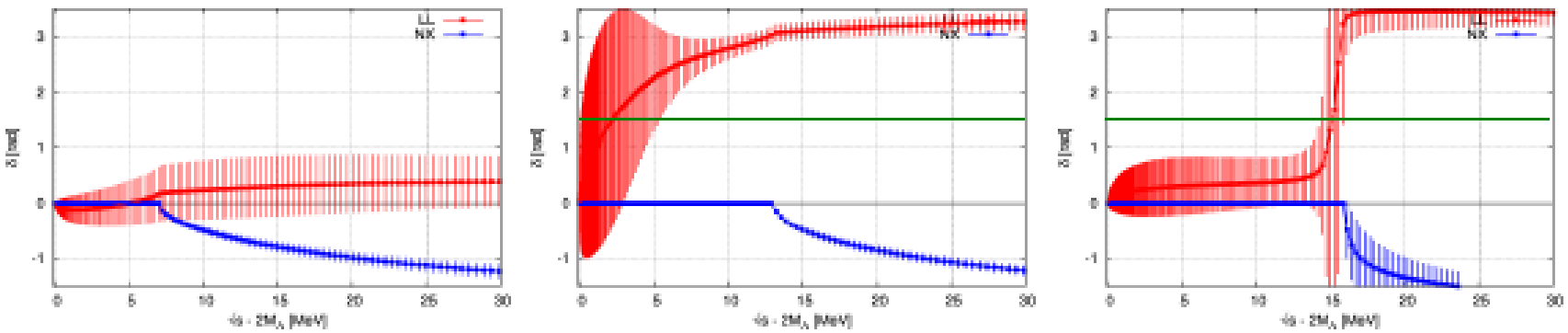

Preliminary!

In unit of MeV	Esb 1	Esb 2	Esb 3
π	701±1	570±2	411±2
K	789±1	713±2	635±2
m_π/m_K	0.89	0.80	0.65
N	1585±5	1411±12	1215±12
Λ	1644±5	1504±10	1351± 8
Σ	1660±4	1531±11	1400±10
Ξ	1710±5	1610± 9	1503± 7

u,d quark masses lighter

- Esb1:
  - Bound H-dibaryon
- Esb2:
  - H-dibaryon is near the $\Lambda\Lambda$ threshold
- Esb3:
  - The H-dibaryon resonance energy is close to $N\Xi$ threshold..

- We can see the clear resonance shape in $\Lambda\Lambda$ phase shifts for Esb2 and 3.
- The "binding energy" of H-dibaryon from $N\Xi$ threshold becomes smaller as decreasing of quark masses.

[K. Sasaki]

Frontier in Hadron-Hadron Interactions
⇒Three-Nucleon Forces (3NF)

What is 3NF ?

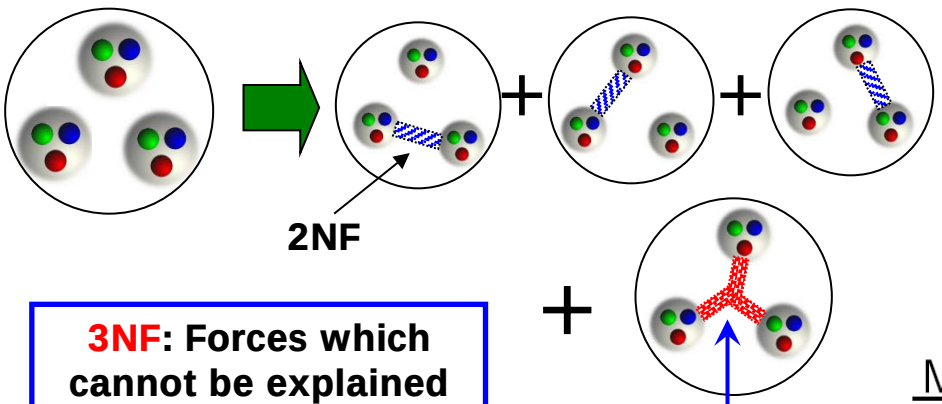

3NF: Forces which cannot be explained by pair-wise 2NF

- *EoS of high density matter*
- *Neutron rich nuclei / Nucleosynthesis*
- *B.E. of light nuclei*

Neutron Star

（Densest system in the Universe）

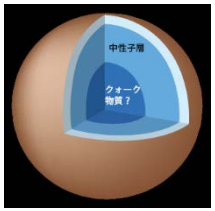

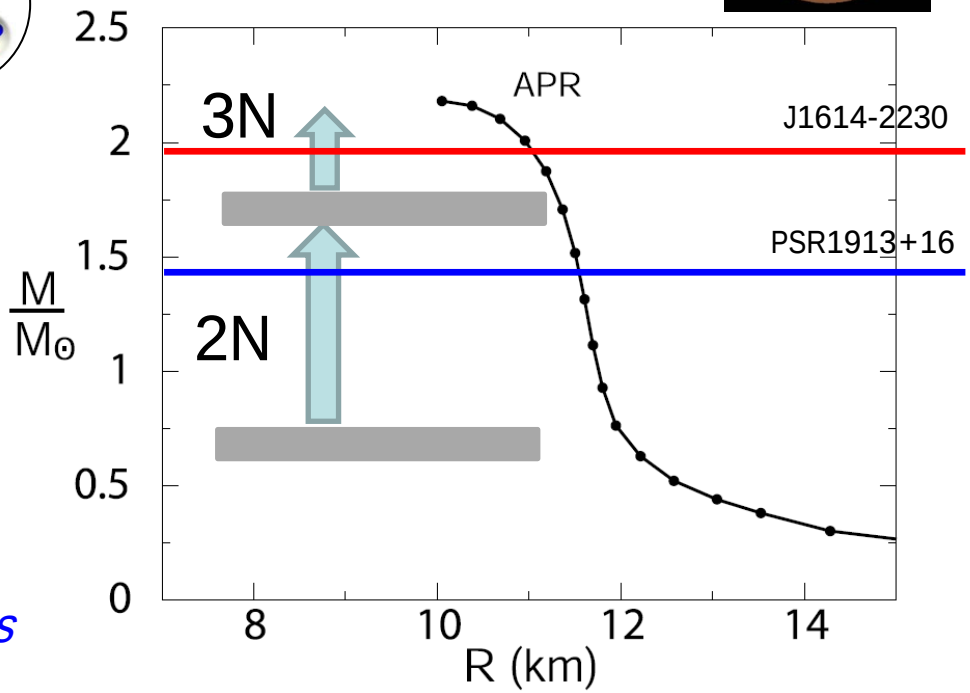

Short-range repulsive 3NF is required

Can we understand it from QCD ?

(3) 3N-forces (3NF) on the lattice

T.D. et al. (HAL QCD Coll.) PTP127(2012)723
+ t-dep method updates etc.

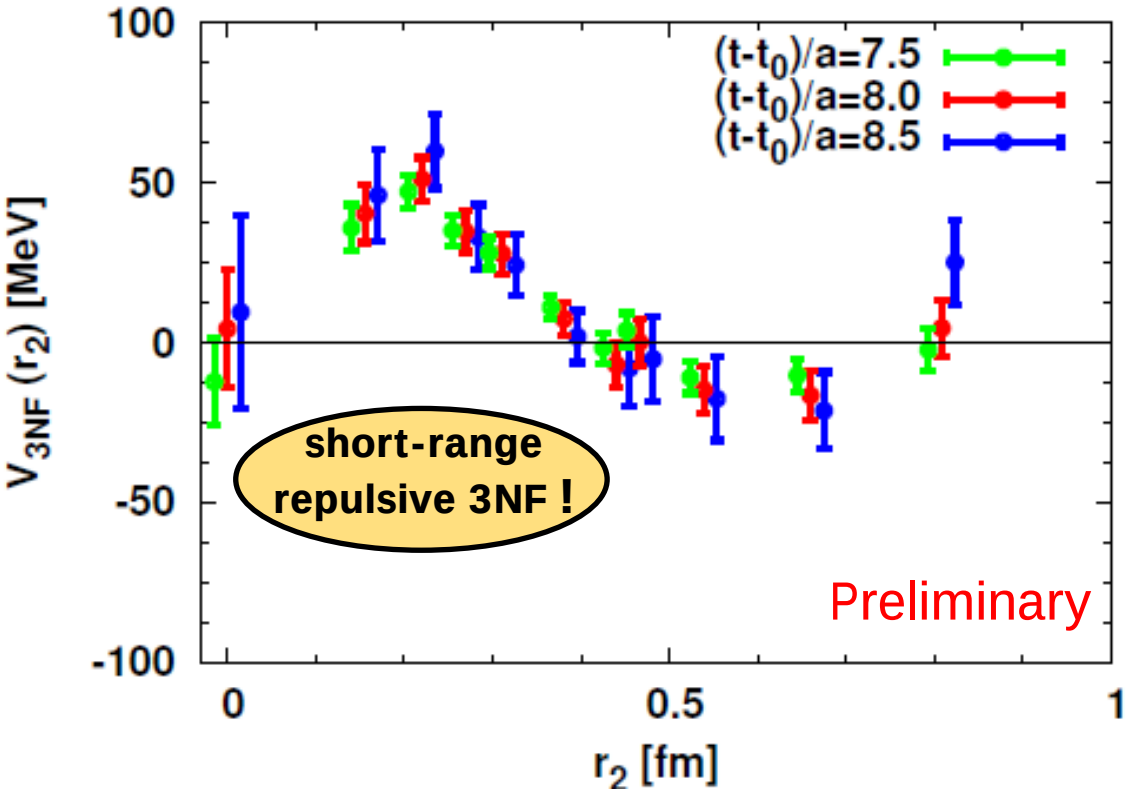

Triton channel

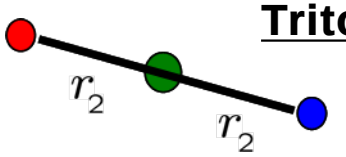

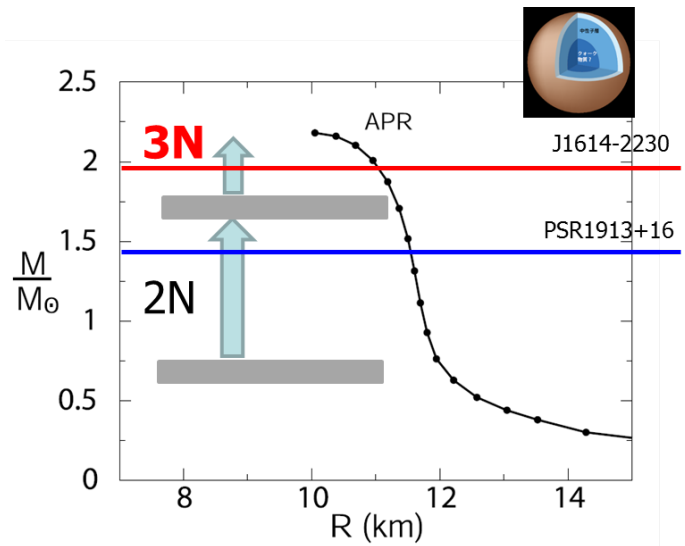

Nf=2 clover (CP-PACS), 1/a=1.27GeV,
L=2.5fm, $m\pi$=1.1GeV, m_N=2.1GeV

(3) 3N-forces (3NF) on the lattice

T.D. et al. (HAL QCD Coll.) PTP127(2012)723

+ t-dep method updates etc.

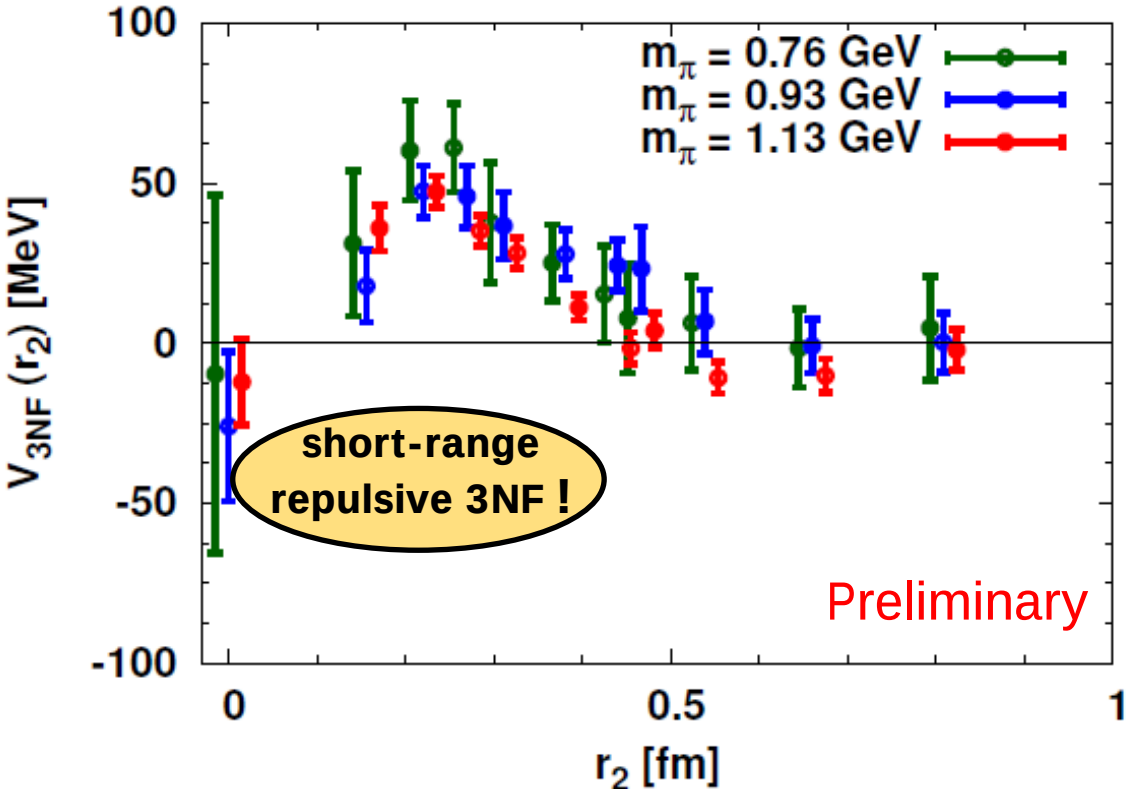

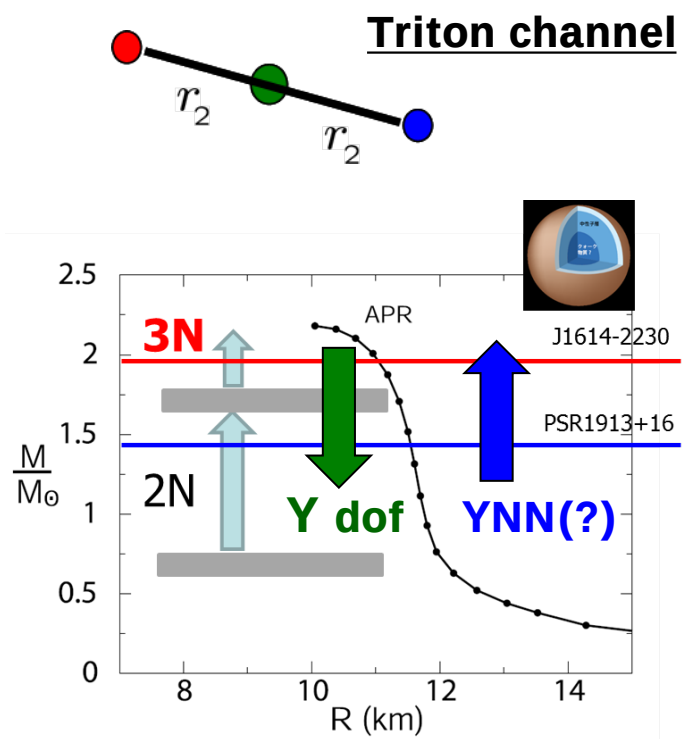

Nf=2 clover (CP-PACS), 1/a=1.27GeV,
L=2.5fm, m_π=0.76-1.1GeV, m_N=1.6-2.1GeV

How about other geometries ?

How about YNN, YYN, YYY ?

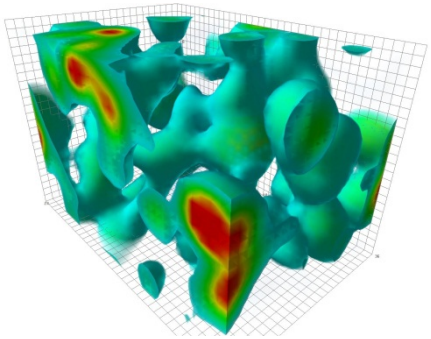

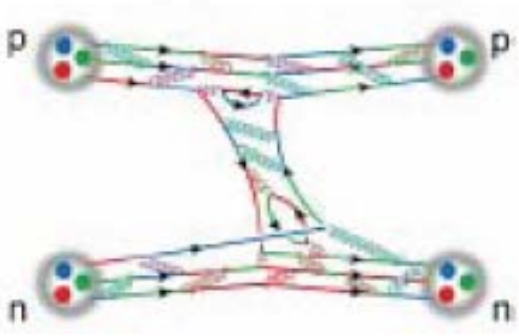

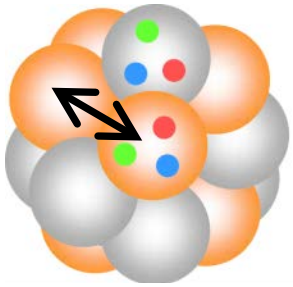

- **<u>Outline</u>**
  - Introduction
  - Theoretical framework of HAL QCD method
    - Challenges in multi-baryons
    - NBS wave functions & E-indep “potential”
  - Numerical results
  - Prospects toward physical point

Towards realistic potential

- **Physical mass point, Infinite V limit, continuum limit**
  - Physical mπ crucial for OPEP, chiral extrapolation won't work

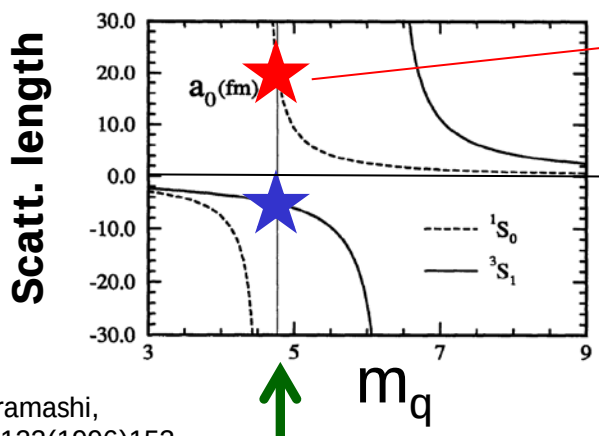

Y.Kuramashi, PTPS122(1996)153

Phys. point

$a_0(^1S_0) \sim 20\text{fm}$

"Unitary Region"

➔ m_q

We are here

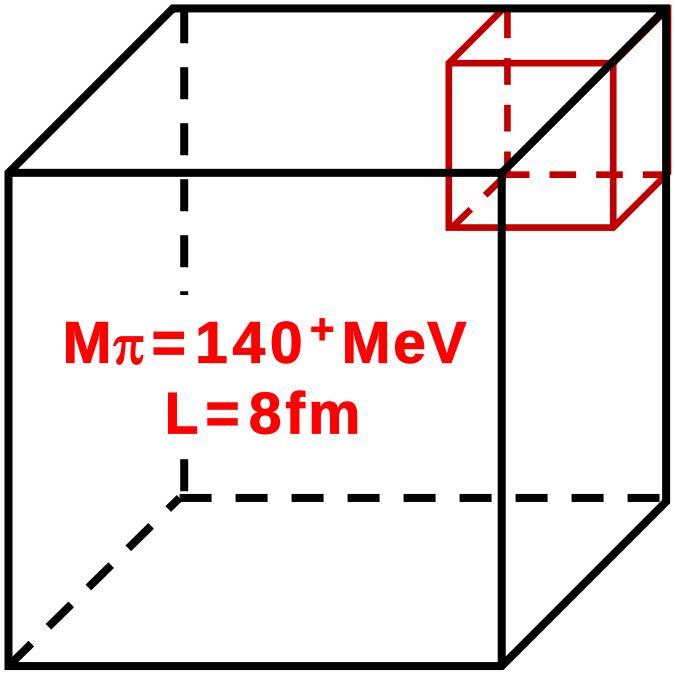

Mπ>=400MeV
L=3fm

K computer

Summary and Prospects

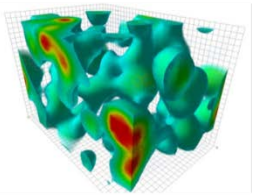

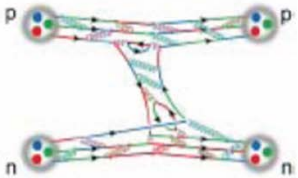

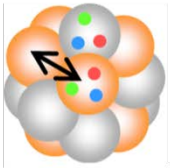

- HAL QCD method
  - Asymptotic behavior of NBS wave functions
  - Energy-independent potential
    - Avoid S/N issue by ground state saturation (t-dep HAL method)
    - Extended to coupled channel systems, many-body forces
- Lattice QCD results for NN, **YN/YY**, NNN, etc.
  - Intriguing physics even at heavy quark masses
- Toward physical quark mass point:
  - Unified Contraction Algorithm: breakthrough in comput. cost

➔ Realistic hadron interactions
➔ Nuclear Physics on the Lattice !

Aspects of Lattice QCD calculations of transverse momentum-dependent parton distributions (TMDs)

Michael Engelhardt
New Mexico State University

In collaboration with:
B. Musch, P. Hägler, J. Negele, A. Schäfer
T. Bhattacharya, R. Gupta, B. Yoon
S. Syritsyn, A. Pochinsky, J. R. Green, S. Meinel

Fundamental TMD correlator

$$\widetilde{\Phi}^{[\Gamma]}_{\text{unsubtr.}}(b, P, S, \ldots) \equiv \frac{1}{2}\langle P, S|\ \bar{q}(0)\ \Gamma\ \mathcal{U}[0, \ldots, b]\ q(b)\ |P, S\rangle$$

$$\Phi^{[\Gamma]}(x, k_T, P, S, \ldots) \equiv \int \frac{d^2 b_T}{(2\pi)^2} \int \frac{d(b \cdot P)}{(2\pi) P^+} \exp\left(ix(b \cdot P) - i b_T \cdot k_T\right) \frac{\widetilde{\Phi}^{[\Gamma]}_{\text{unsubtr.}}(b, P, S, \ldots)}{\widetilde{\mathcal{S}}(b^2, \ldots)}\Bigg|_{b^+=0}$$

- "Soft factor" $\widetilde{\mathcal{S}}$ required to subtract divergences of Wilson line $\mathcal{U}$
- $\widetilde{\mathcal{S}}$ is typically a combination of vacuum expectation values of Wilson line structures
- Here, will consider only ratios in which soft factors cancel

Gauge link structure motivated by SIDIS

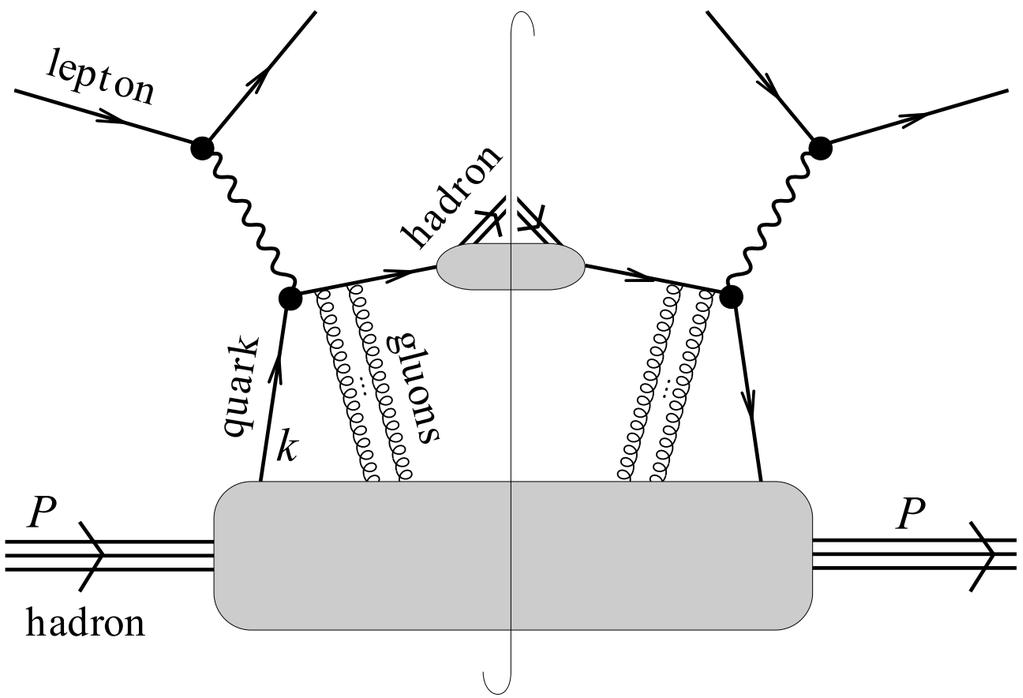

$l + H(P) \longrightarrow l' + h(P_h) + X$

Gauge link structure:

In matrix element $\widetilde{\Phi}^{[\Gamma]}_{\text{unsubtr.}}(b, P, S, \ldots) \equiv$

$\frac{1}{2}\langle P, S|\ \bar{q}(0)\ \Gamma\ \mathcal{U}[0, \ldots, b]\ q(b)\ |P, S\rangle$

Staple-shaped gauge link $\mathcal{U}[0, \eta v, \eta v + b, b]$

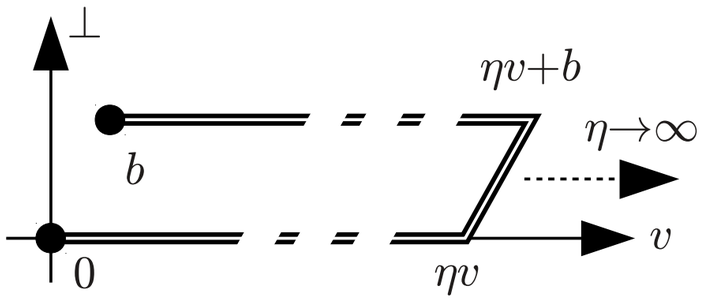

incorporates SIDIS final state effects

Gauge link structure motivated by SIDIS

Staple-shaped links incorporate SIDIS final state effects:

- Gauge link roughly follows direction of ejected quark, (close to) light cone
- Effective resummed description of gluon exchanges between ejected quark and remainder of nucleon in evolving final state
- Beyond tree level: Rapidity divergences suggest taking staple direction slightly off the light cone. Approach of Aybat, Collins, Qiu, Rogers makes v space-like. Parametrize in terms of Collins-Soper parameter

$$\hat{\zeta} \equiv \frac{P \cdot v}{|P||v|}$$

Light-like staple for $\hat{\zeta} \to \infty$. Perturbative evolution equations for large $\hat{\zeta}$.

Fundamental TMD correlator

$$\widetilde{\Phi}^{[\Gamma]}_{\text{unsubtr.}}(b, P, S, \ldots) \equiv \frac{1}{2}\langle P, S|\ \bar{q}(0)\ \Gamma\ \mathcal{U}[0, \eta v, \eta v + b, b]\ q(b)\ |P, S\rangle$$

$$\Phi^{[\Gamma]}(x, k_T, P, S, \ldots) \equiv \int \frac{d^2 b_T}{(2\pi)^2} \int \frac{d(b \cdot P)}{(2\pi) P^+} \exp\left(ix(b \cdot P) - i b_T \cdot k_T\right) \frac{\widetilde{\Phi}^{[\Gamma]}_{\text{unsubtr.}}(b, P, S, \ldots)}{\widetilde{\mathcal{S}}(b^2, \ldots)} \Bigg|_{b^+=0}$$

- "Soft factor" $\widetilde{\mathcal{S}}$ required to subtract divergences of Wilson line $\mathcal{U}$
- $\widetilde{\mathcal{S}}$ is typically a combination of vacuum expectation values of Wilson line structures
- Here, will consider only ratios in which soft factors cancel

Decomposition of Φ into TMDs

All leading twist structures:

$$\Phi^{[\gamma^+]} = f_1 - \left[\frac{\epsilon_{ij} k_i S_j}{m_H} f_{1T}^{\perp}\right] \text{odd}$$

$$\Phi^{[\gamma^+\gamma^5]} = \Lambda g_1 + \frac{k_T \cdot S_T}{m_H} g_{1T}$$

$$\Phi^{[i\sigma^{i+}\gamma^5]} = S_i h_1 + \frac{(2k_i k_j - k_T^2 \delta_{ij}) S_j}{2m_H^2} h_{1T}^{\perp} + \frac{\Lambda k_i}{m_H} h_{1L}^{\perp} + \left[\frac{\epsilon_{ij} k_j}{m_H} h_1^{\perp}\right] \text{odd}$$

TMD Classification

All leading twist structures:

$q \rightarrow$ H $\downarrow$	U	L	T
U	f_1		$h_1^\perp$
L		g_1	$h_{1L}^\perp$
T	$f_{1T}^\perp$	g_{1T}	h_1 $h_{1T}^\perp$

$\longleftarrow$ Boer-Mulders (T-odd)

$\uparrow$ Sivers (T-odd)

Decomposition of $\widetilde{\Phi}$ into amplitudes

$$\widetilde{\Phi}^{[\Gamma]}_{\text{unsubtr.}}(b, P, S, \hat{\zeta}, \mu) \equiv \frac{1}{2}\langle P, S|\ \bar{q}(0)\ \Gamma\ \mathcal{U}[0, \eta v, \eta v + b, b]\ q(b)\ |P, S\rangle$$

Decompose in terms of invariant amplitudes; at leading twist,

$$\begin{aligned}
\frac{1}{2P^+}\widetilde{\Phi}^{[\gamma^+]}_{\text{unsubtr.}} &= \widetilde{A}_{2B} + i m_H \epsilon_{ij} b_i S_j \widetilde{A}_{12B} \\
\frac{1}{2P^+}\widetilde{\Phi}^{[\gamma^+\gamma^5]}_{\text{unsubtr.}} &= -\Lambda \widetilde{A}_{6B} + i[(b\cdot P)\Lambda - m_H(b_T \cdot S_T)]\widetilde{A}_{7B} \\
\frac{1}{2P^+}\widetilde{\Phi}^{[i\sigma^{i+}\gamma^5]}_{\text{unsubtr.}} &= i m_H \epsilon_{ij} b_j \widetilde{A}_{4B} - S_i \widetilde{A}_{9B} \\
&\quad - i m_H \Lambda b_i \widetilde{A}_{10B} + m_H[(b\cdot P)\Lambda - m_H(b_T\cdot S_T)] b_i \widetilde{A}_{11B}
\end{aligned}$$

(Decompositions analogous to work by Metz et al. in momentum space)

Fourier-transformed TMDs

$$\tilde{f}(x, b_T^2, \ldots) \equiv \int d^2k_T \, \exp(ib_T \cdot k_T) f(x, k_T^2, \ldots)$$

$$\tilde{f}^{(n)}(x, b_T^2, \ldots) \equiv n! \left(-\frac{2}{m_H^2} \partial_{b_T^2} \right)^n \tilde{f}(x, b_T^2, \ldots)$$

In limit $|b_T| \to 0$, recover k_T-moments:

$$\tilde{f}^{(n)}(x, 0, \ldots) \equiv \int d^2k_T \left(\frac{k_T^2}{2m_H^2} \right)^n f(x, k_T^2, \ldots) \equiv f^{(n)}(x)$$

ill-defined for large k_T, so will not attempt to extrapolate to $b_T = 0$, but give results at finite $|b_T|$.

In this study, only consider first x-moments (accessible at $b \cdot P = 0$), rather than scanning range of $b \cdot P$:

$$f^{[1]}(k_T^2, \ldots) \equiv \int_{-1}^{1} dx \, f(x, k_T^2, \ldots)$$

$\longrightarrow$ Bessel-weighted asymmetries (Boer, Gamberg, Musch, Prokudin, JHEP 1110 (2011) 021)

Relation between Fourier-transformed TMDs and invariant amplitudes $\widetilde{A}_i$

Invariant amplitudes directly give selected x-integrated TMDs in Fourier (b_T) space (showing just the ones relevant for Sivers, Boer-Mulders shifts), up to soft factors:

$$\tilde{f}_1^{[1](0)}(b_T^2, \hat{\zeta}, \ldots, \eta v \cdot P) \;=\; 2\widetilde{A}_{2B}(-b_T^2, 0, \hat{\zeta}, \eta v \cdot P)/\widetilde{S}(b^2, \ldots)$$

$$\tilde{f}_{1T}^{\perp[1](1)}(b_T^2, \hat{\zeta}, \ldots, \eta v \cdot P) \;=\; -2\widetilde{A}_{12B}(-b_T^2, 0, \hat{\zeta}, \eta v \cdot P)/\widetilde{S}(b^2, \ldots)$$

$$\tilde{h}_1^{\perp[1](1)}(b_T^2, \hat{\zeta}, \ldots, \eta v \cdot P) \;=\; 2\widetilde{A}_{4B}(-b_T^2, 0, \hat{\zeta}, \eta v \cdot P)/\widetilde{S}(b^2, \ldots)$$

Generalized shifts

Form ratios in which soft factors, (Γ-independent) multiplicative renormalization factors cancel

Boer-Mulders shift:

$$\langle k_y \rangle_{UT} \equiv m_H \frac{\tilde{h}_1^{\perp[1](1)}}{\tilde{f}_1^{[1](0)}} = \left. \frac{\int dx \int d^2k_T \, k_y \Phi^{[\gamma^+ + s^j i\sigma^{j+}\gamma^5]}(x, k_T, P, \ldots)}{\int dx \int d^2k_T \, \Phi^{[\gamma^+ + s^j i\sigma^{j+}\gamma^5]}(x, k_T, P, \ldots)} \right|_{s_T=(1,0)}$$

Average transverse momentum of quarks polarized in the orthogonal transverse ("T") direction in an unpolarized ("U") hadron; normalized to the number of valence quarks. "Dipole moment" in $b_T^2 = 0$ limit, "shift".

Issue: k_T-moments in this ratio singular; generalize to ratio of Fourier-transformed TMDs at *nonzero* b_T^2,

$$\langle k_y \rangle_{UT}(b_T^2, \ldots) \equiv m_H \frac{\tilde{h}_1^{\perp[1](1)}(b_T^2, \ldots)}{\tilde{f}_1^{[1](0)}(b_T^2, \ldots)}$$

(remember singular $b_T \to 0$ limit corresponds to taking k_T-moment). "Generalized shift".

Generalized shifts from amplitudes

Now, can also express this in terms of invariant amplitudes:

$$\langle k_y \rangle_{UT}(b_T^2, \ldots) \equiv m_H \frac{\tilde{h}_1^{\perp[1](1)}(b_T^2, \ldots)}{\tilde{f}_1^{[1](0)}(b_T^2, \ldots)} = m_H \frac{\widetilde{A}_{4B}(-b_T^2, 0, \hat{\zeta}, \eta v \cdot P)}{\widetilde{A}_{2B}(-b_T^2, 0, \hat{\zeta}, \eta v \cdot P)}$$

Analogously, Sivers shift (in a polarized hadron):

$$\langle k_y \rangle_{TU}(b_T^2, \ldots) = -m_H \frac{\widetilde{A}_{12B}(-b_T^2, 0, \hat{\zeta}, \eta v \cdot P)}{\widetilde{A}_{2B}(-b_T^2, 0, \hat{\zeta}, \eta v \cdot P)}$$

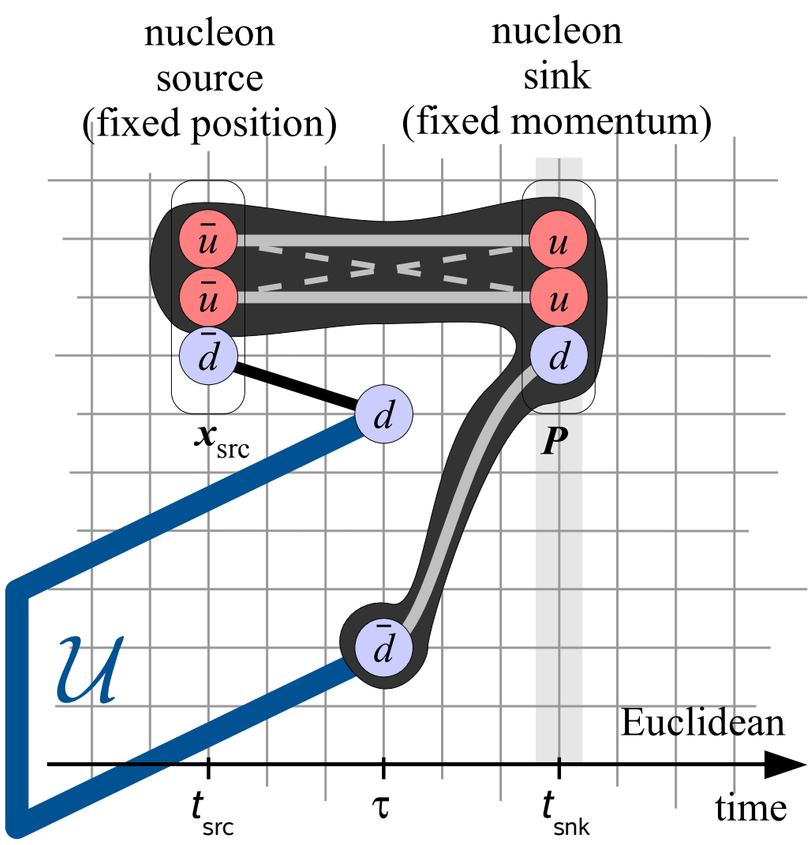

Lattice setup

- Evaluate directly $\widetilde{\Phi}^{[\Gamma]}_{\text{unsubtr.}}(b, P, S, \hat{\zeta}, \mu)$

  $\equiv \frac{1}{2}\langle P, S|\ \bar{q}(0)\ \Gamma\ \mathcal{U}[0, \eta v, \eta v + b, b]\ q(b)\ |P, S\rangle$

- Euclidean time: Place entire operator at one time slice, i.e., b, ηv purely spatial
- Since generic b, v space-like, no obstacle to boosting system to such a frame!
- Parametrization of correlator in terms of $\widetilde{A}_i$ invariants permits direct translation of results back to original frame; form desired $\widetilde{A}_i$ ratios.
- Use variety of P, b, ηv; here $b \perp P$, $b \perp v$ (lowest x-moment, kinematical choices/constraints)
- Extrapolate $\eta \to \infty$, $\hat{\zeta} \to \infty$ numerically.

Challenges

- The limit $\hat{\zeta} \to \infty$: Approaching the light cone
- Discretization effects, soft factor cancellation on the lattice in TMD ratios
- Progress toward the physical pion mass

Approaching the light cone (with a pion)

Results: Boer-Mulders shift (pion)

Dependence on staple extent; sequence of panels at different $|b_T|$

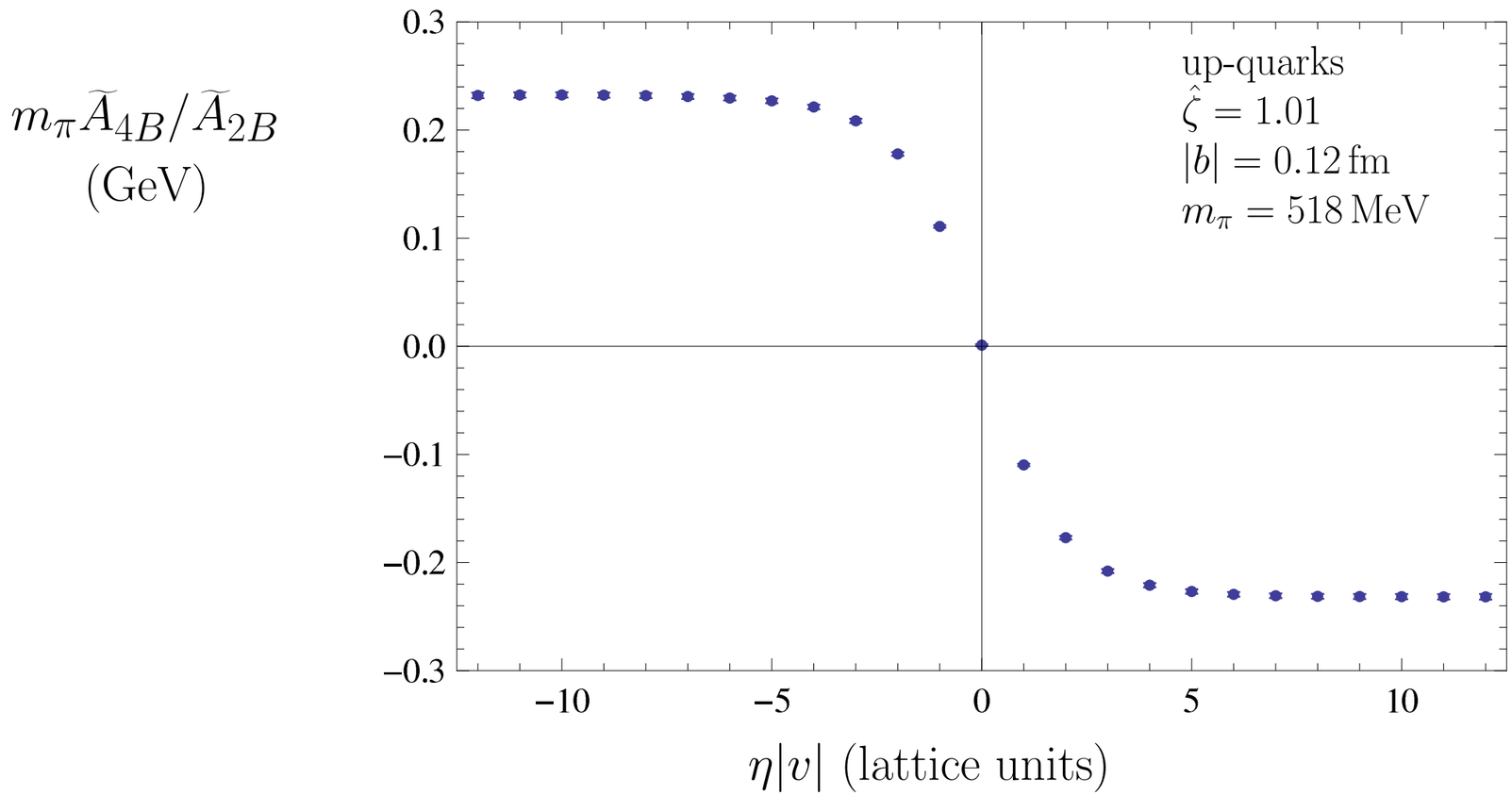

Results: Boer-Mulders shift (pion)

Dependence on staple extent; sequence of panels at different $|b_T|$

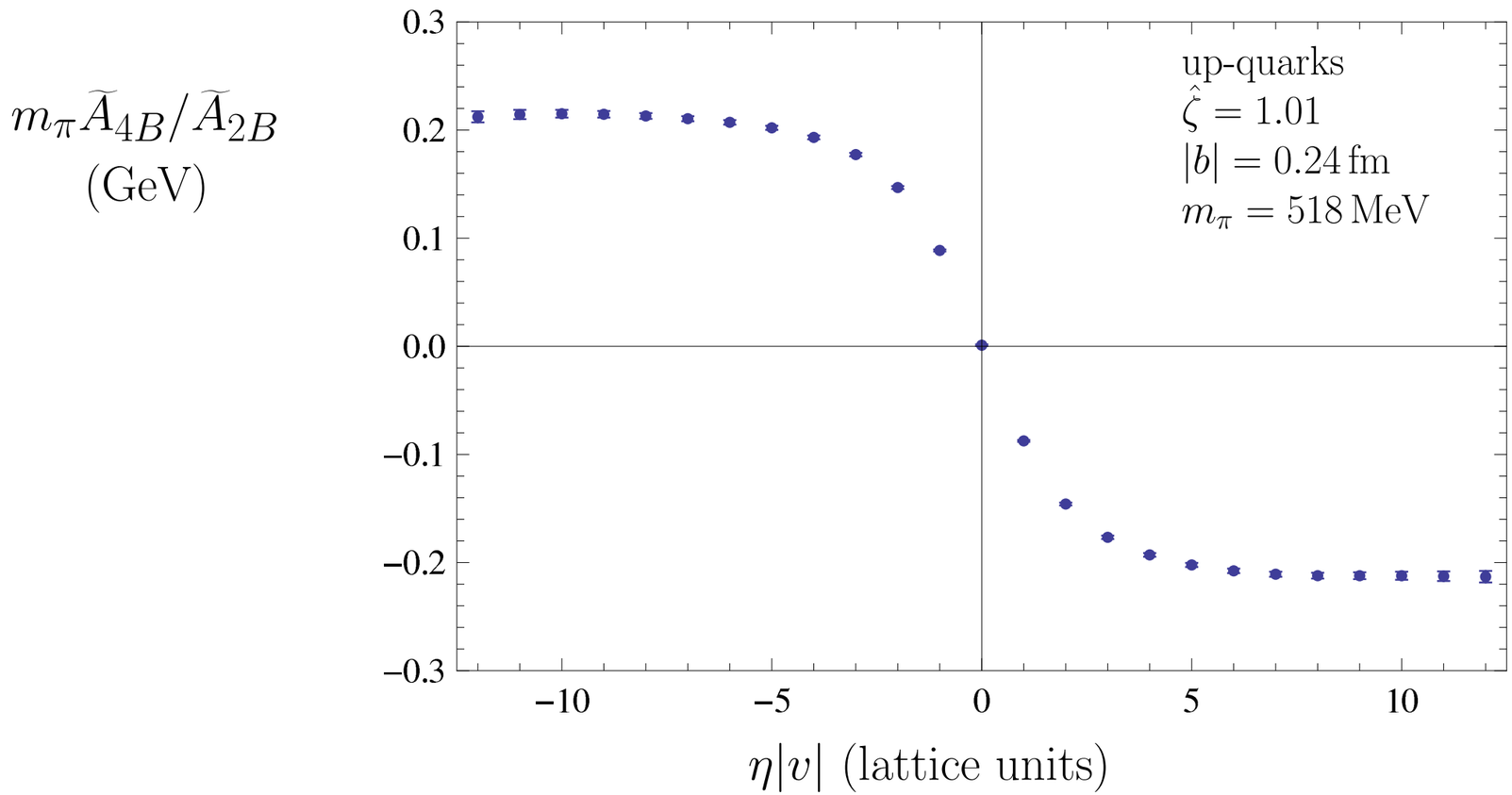

Results: Boer-Mulders shift (pion)

Dependence on staple extent; sequence of panels at different $|b_T|$

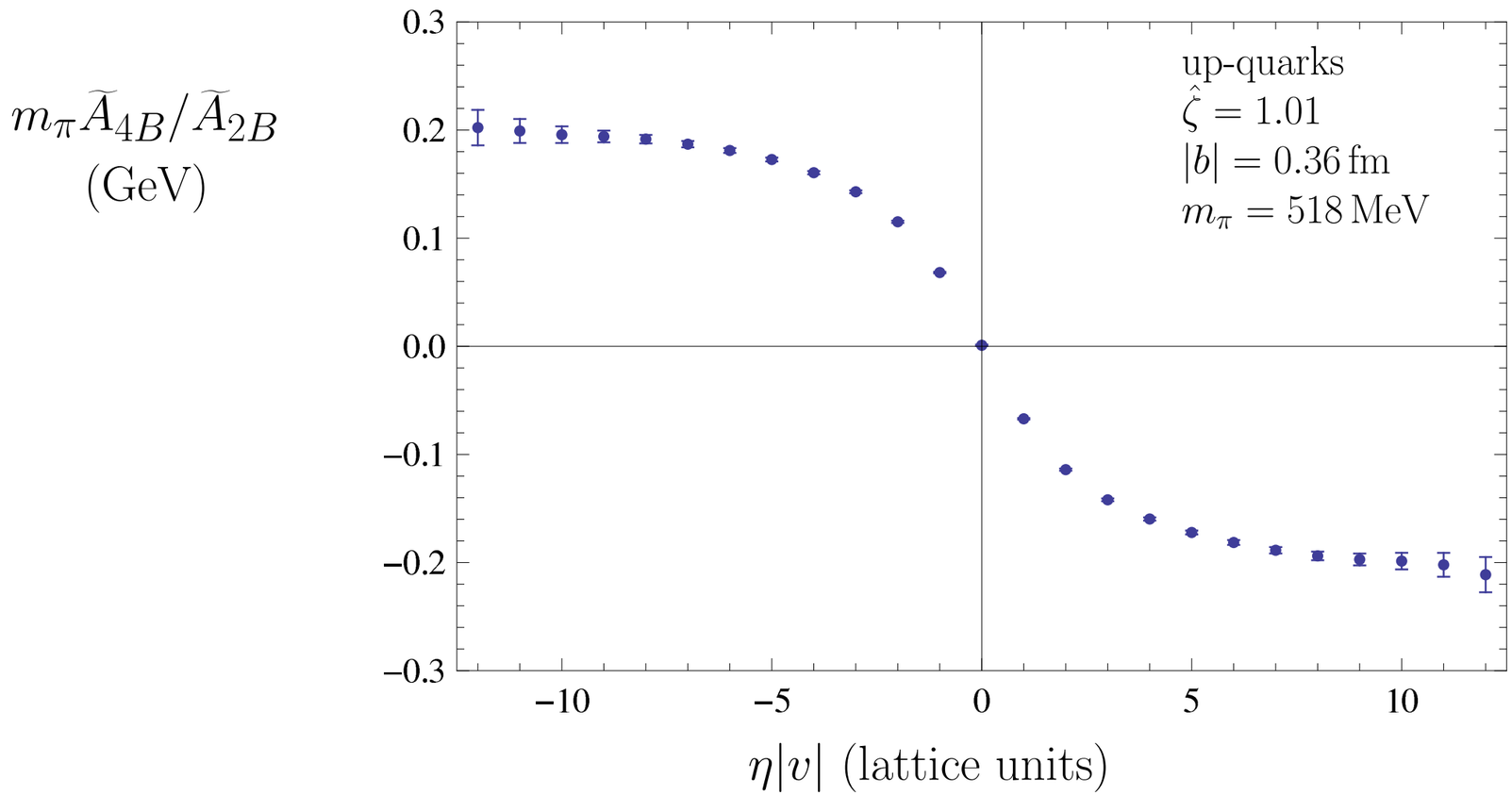

Results: Boer-Mulders shift (pion)

Dependence on staple extent; sequence of panels at different $|b_T|$

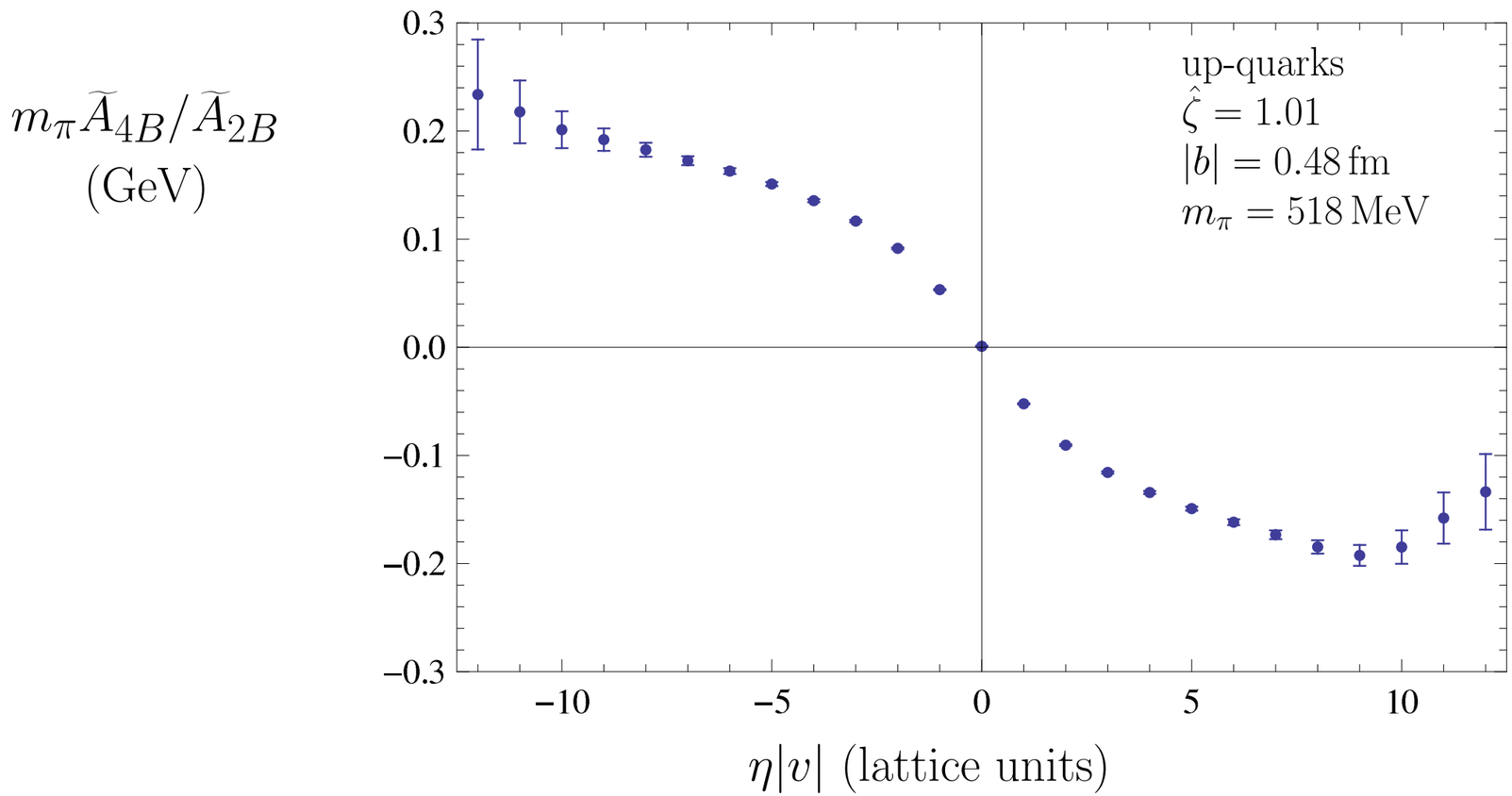

Results: Boer-Mulders shift (pion)

Dependence of SIDIS limit on $|b_T|$

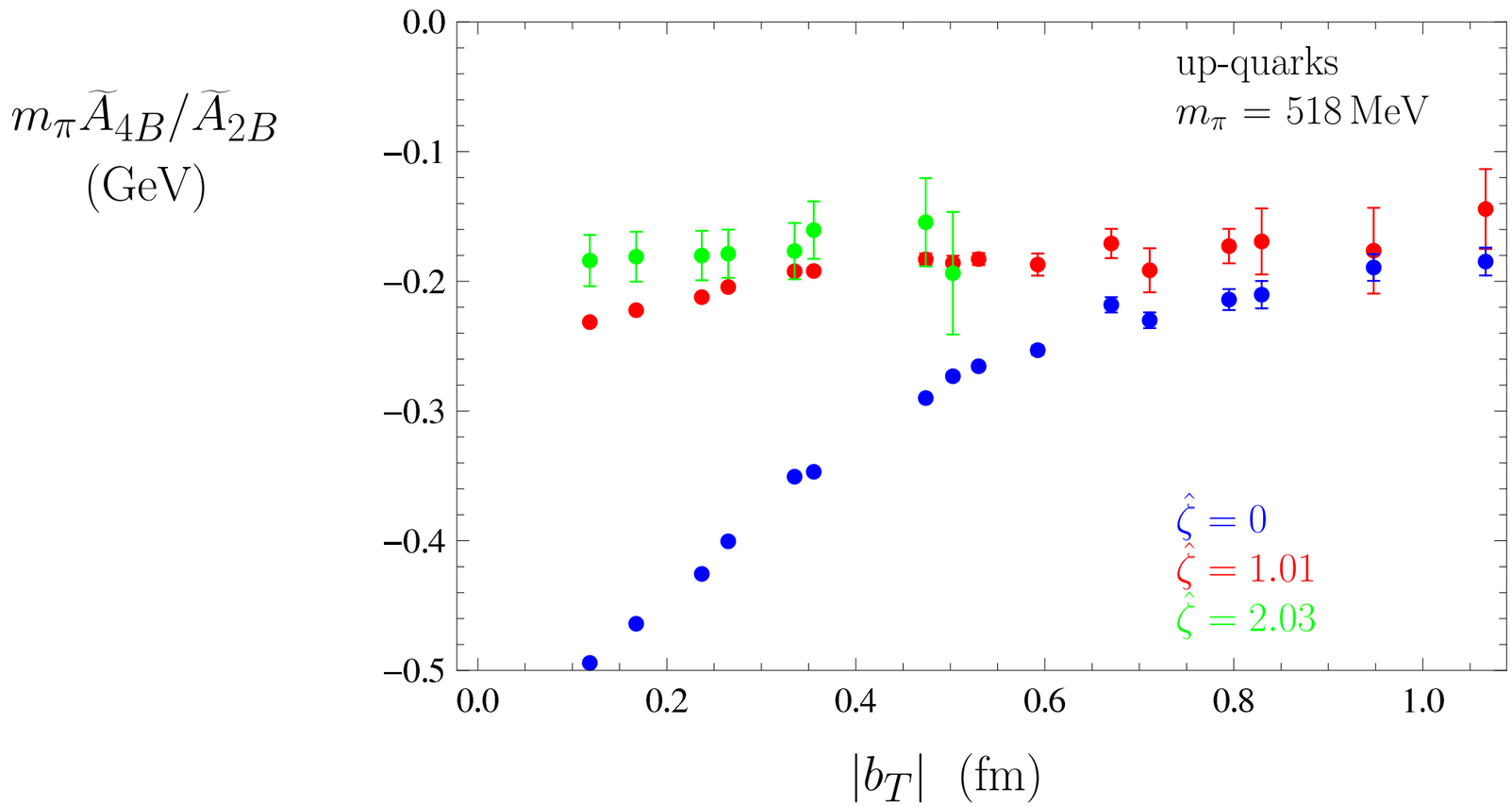

Results: Boer-Mulders shift (pion)

Dependence of SIDIS limit on $\hat{\zeta}$

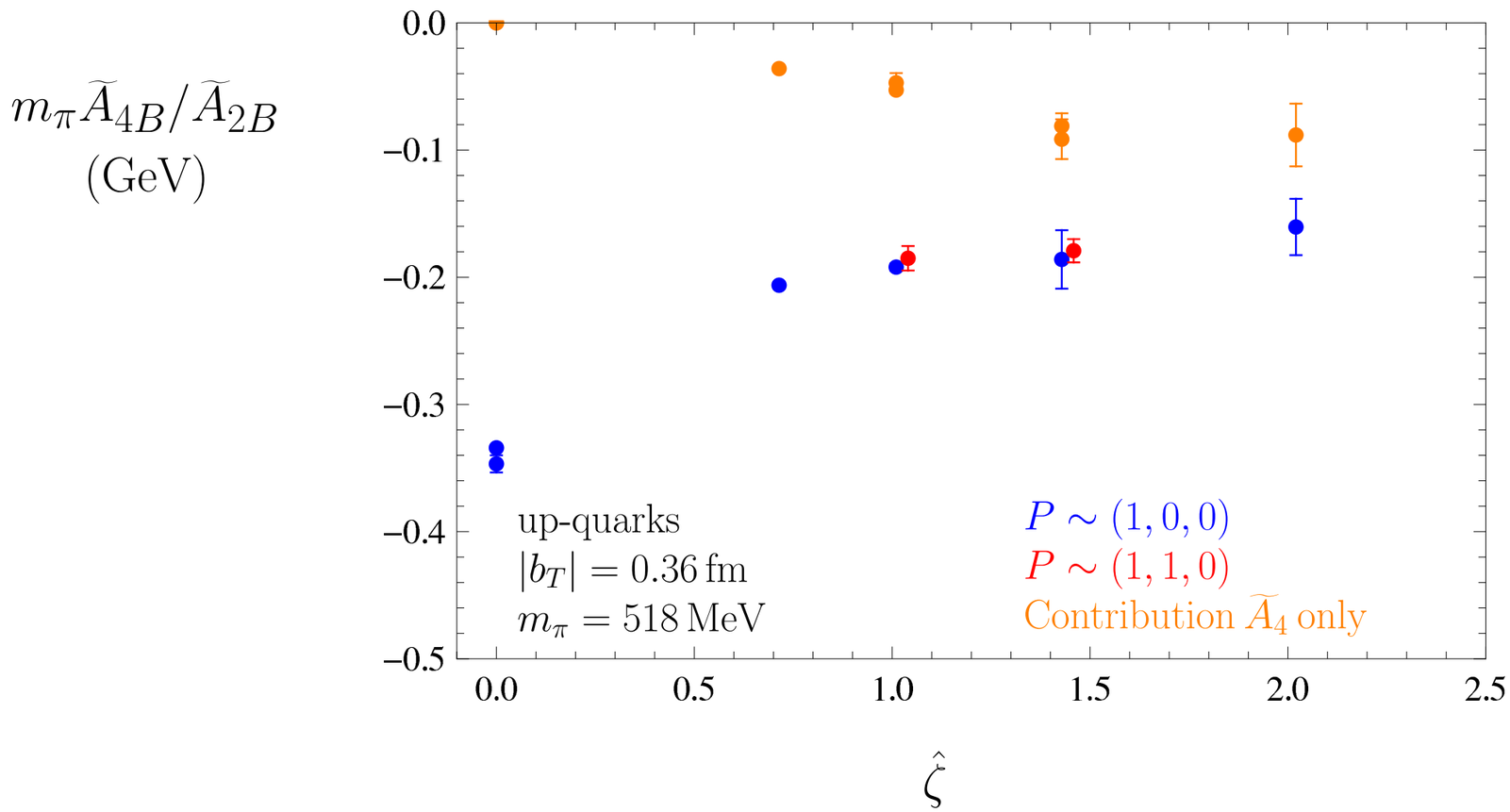

Results: Boer-Mulders shift (pion)

Dependence of SIDIS limit on $\hat{\zeta}$

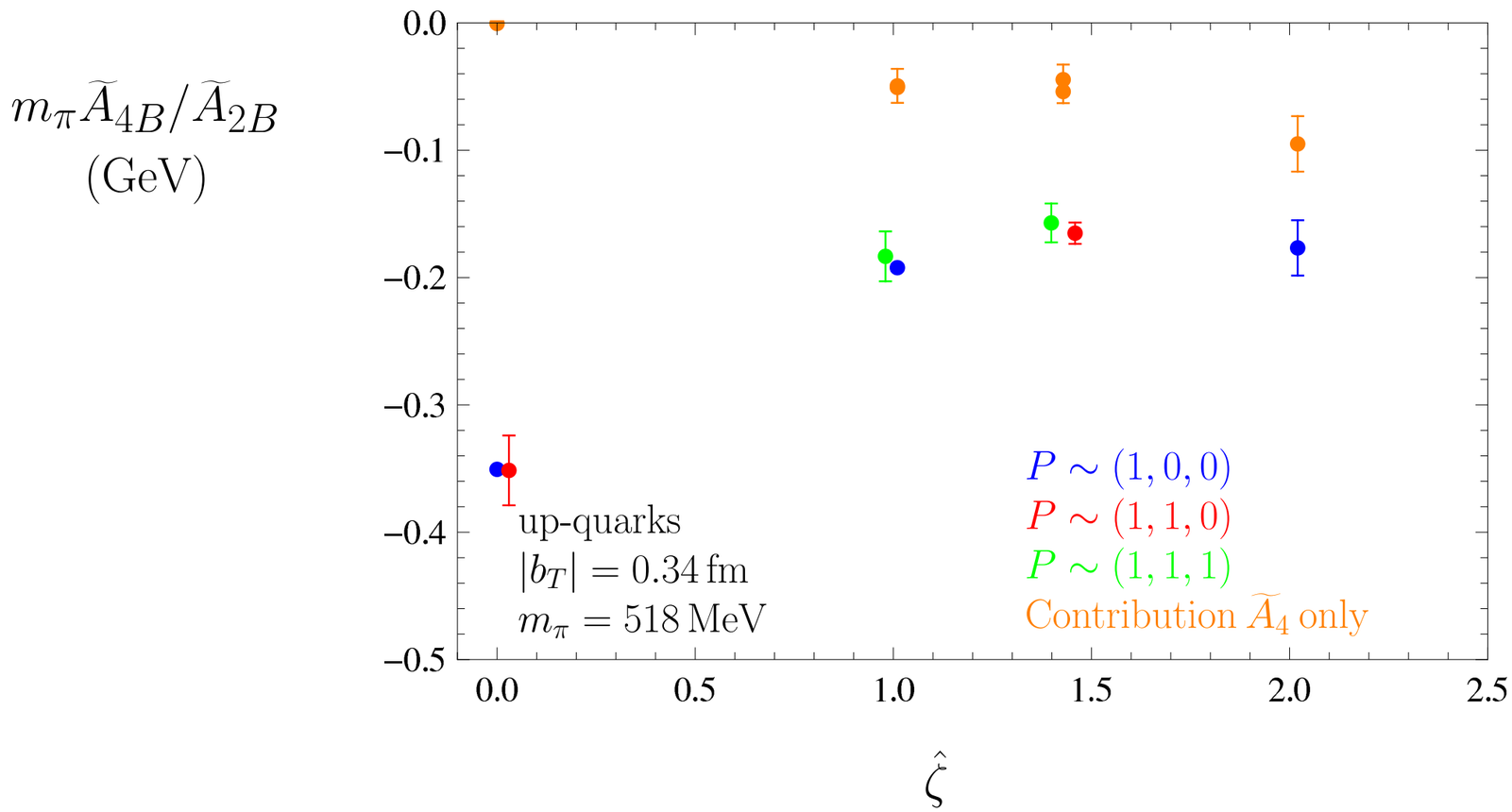

Results: Boer-Mulders shift (pion)

Dependence of SIDIS limit on $\hat{\zeta}$

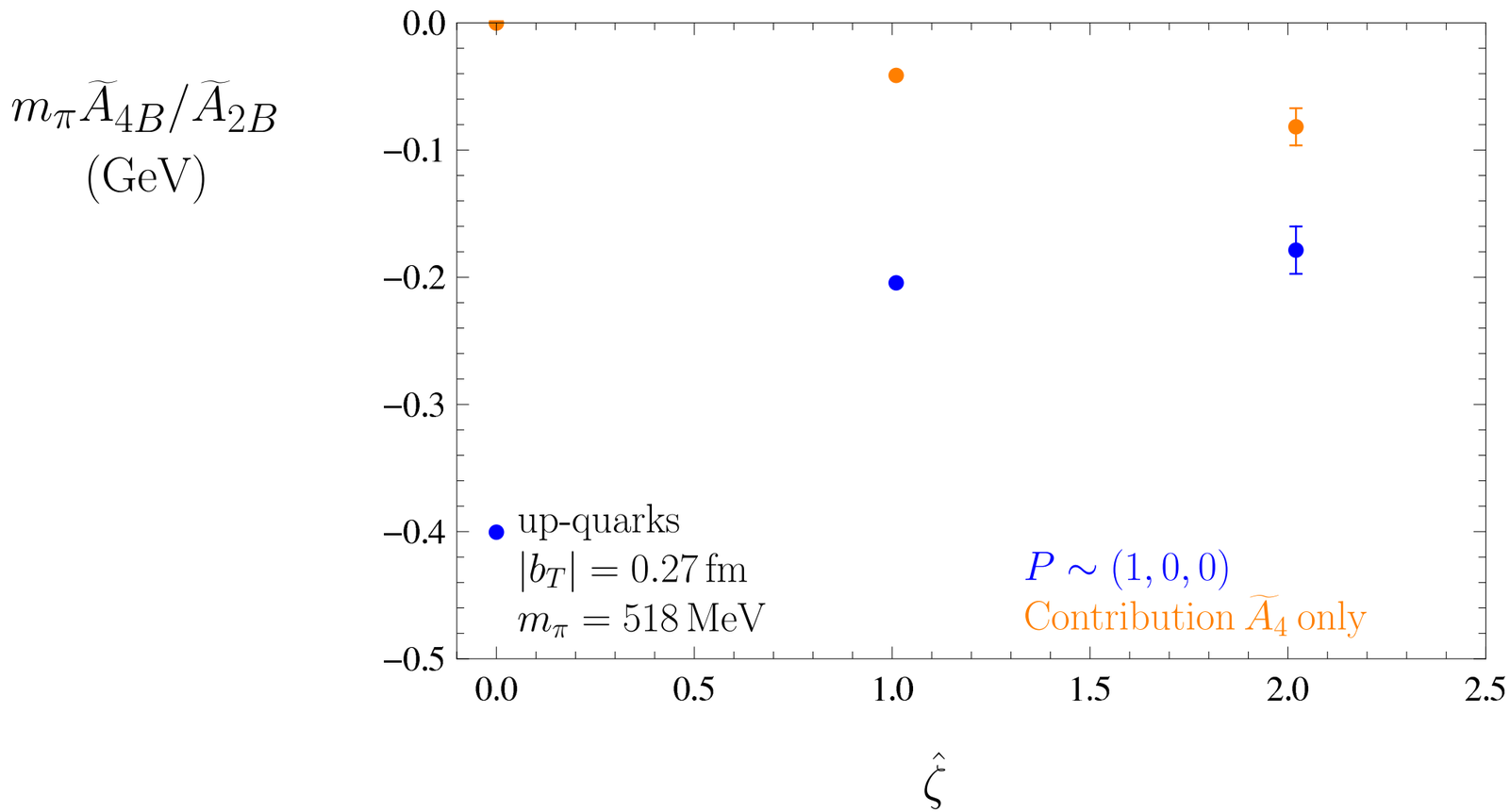

Results: Boer-Mulders shift (pion)

Dependence of SIDIS limit on $\hat{\zeta}$; fit function $a + b/\hat{\zeta}$

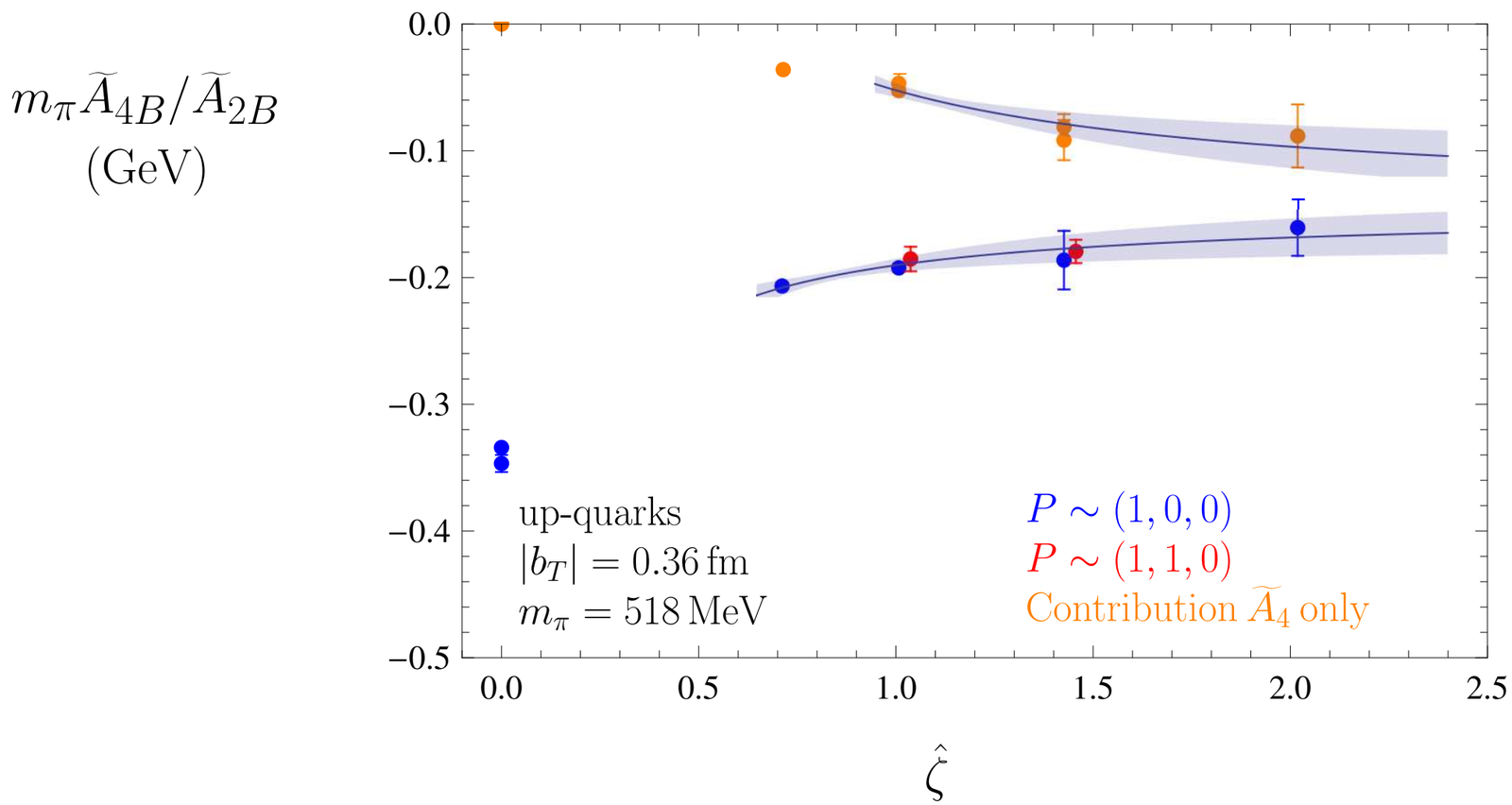

Results: Boer-Mulders shift (pion)

Dependence of SIDIS limit on $\hat{\zeta}$; fit function $a + b/\hat{\zeta}$

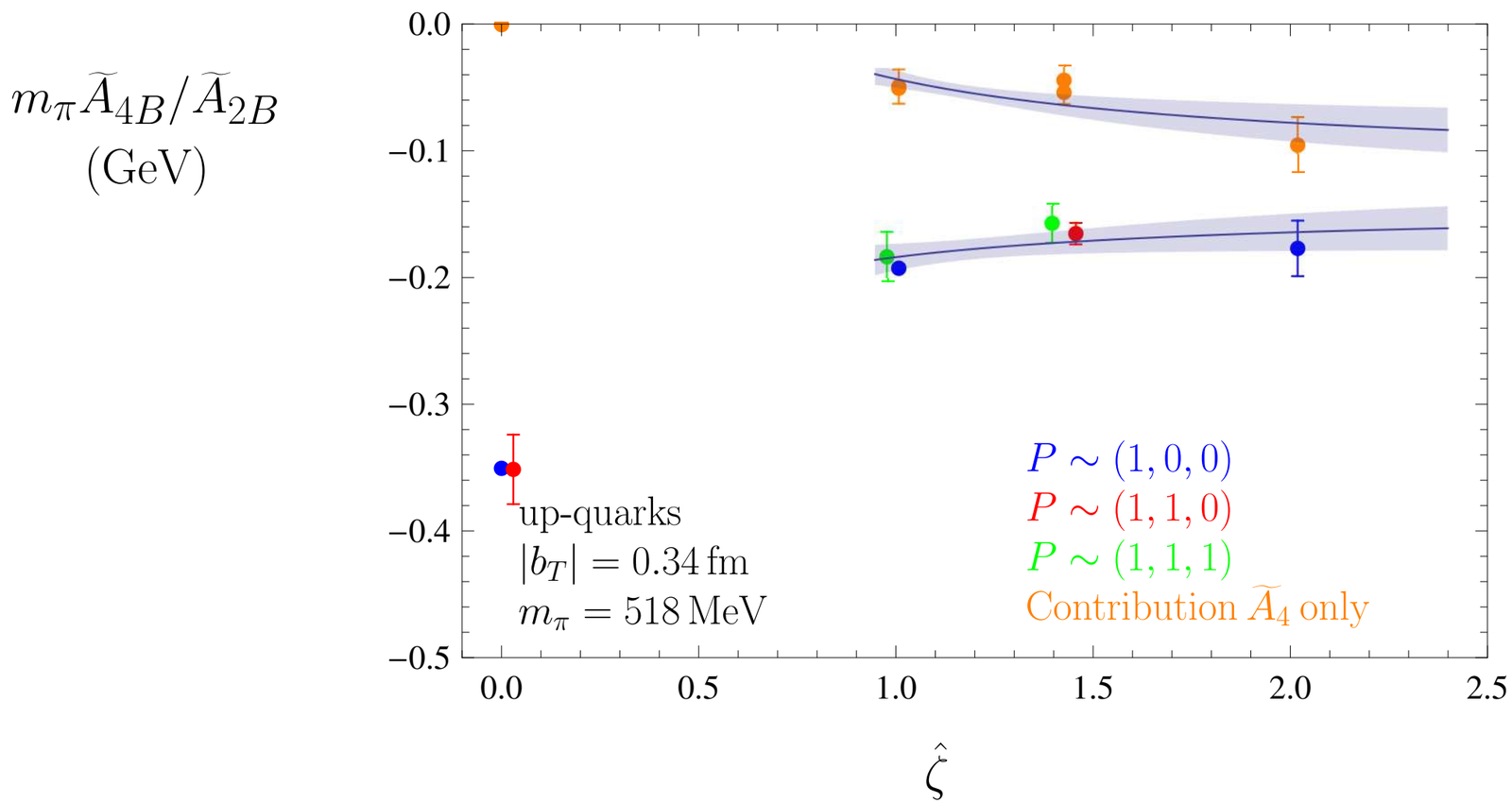

Results: Boer-Mulders shift (pion)

Extrapolation of SIDIS limit to $\hat{\zeta} \to \infty$

	Fit function	Full BM ratio (GeV)	Contribution $\widetilde{A}_4$ only (GeV)	Combined fit (GeV)	RMS deviation of combined fit (GeV)
$\lvert b_T \rvert = 0.36\,\mathrm{fm}$	$a + b/\hat{\zeta}$	-0.146(26)	-0.141(36)	-0.145(25)	0.00755
$\lvert b_T \rvert = 0.36\,\mathrm{fm}$	$a + b/\hat{\zeta}^2$	-0.166(16)	-0.110(22)	-0.148(15)	0.01695
$\lvert b_T \rvert = 0.34\,\mathrm{fm}$	$a + b/\hat{\zeta}$	-0.145(33)	-0.112(33)	-0.128(29)	0.01466
$\lvert b_T \rvert = 0.34\,\mathrm{fm}$	$a + b/\hat{\zeta}^2$	-0.157(19)	-0.084(19)	-0.121(16)	0.02315

up-quarks
$m_\pi = 518\,\mathrm{MeV}$

Discretization effects:

Comparison of

RBC/UKQCD DWF ensemble ($m_\pi = 297\,\mathrm{MeV}$, $a = 0.084\,\mathrm{fm}$)

with clover ensemble ($m_\pi = 317\,\mathrm{MeV}$, $a = 0.114\,\mathrm{fm}$)
produced by K. Orginos and JLab collaborators

Results: Sivers shift

Dependence on staple extent; sequence of panels at different $|b_T|$

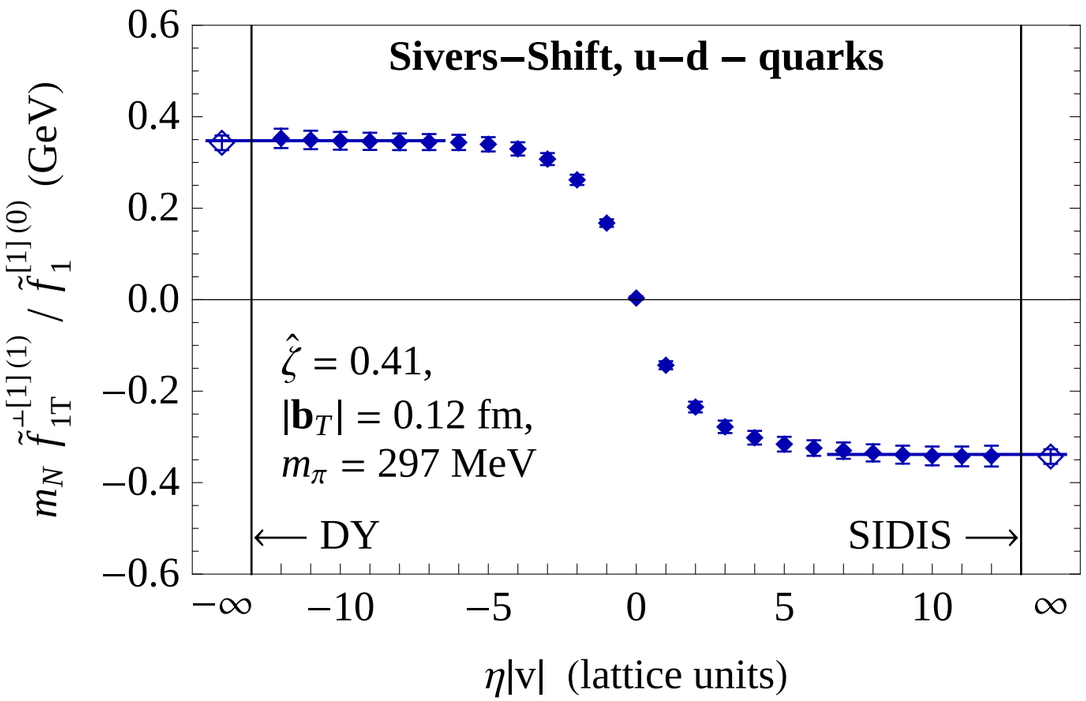

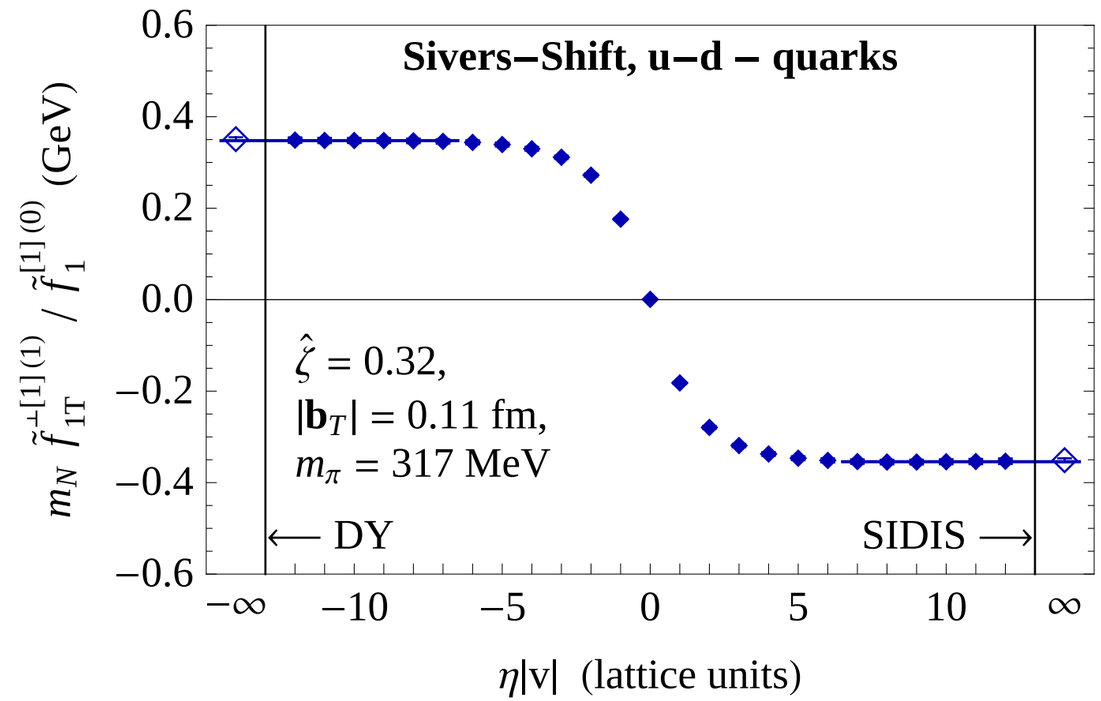

Results: Sivers shift

Dependence on staple extent; sequence of panels at different $|b_T|$

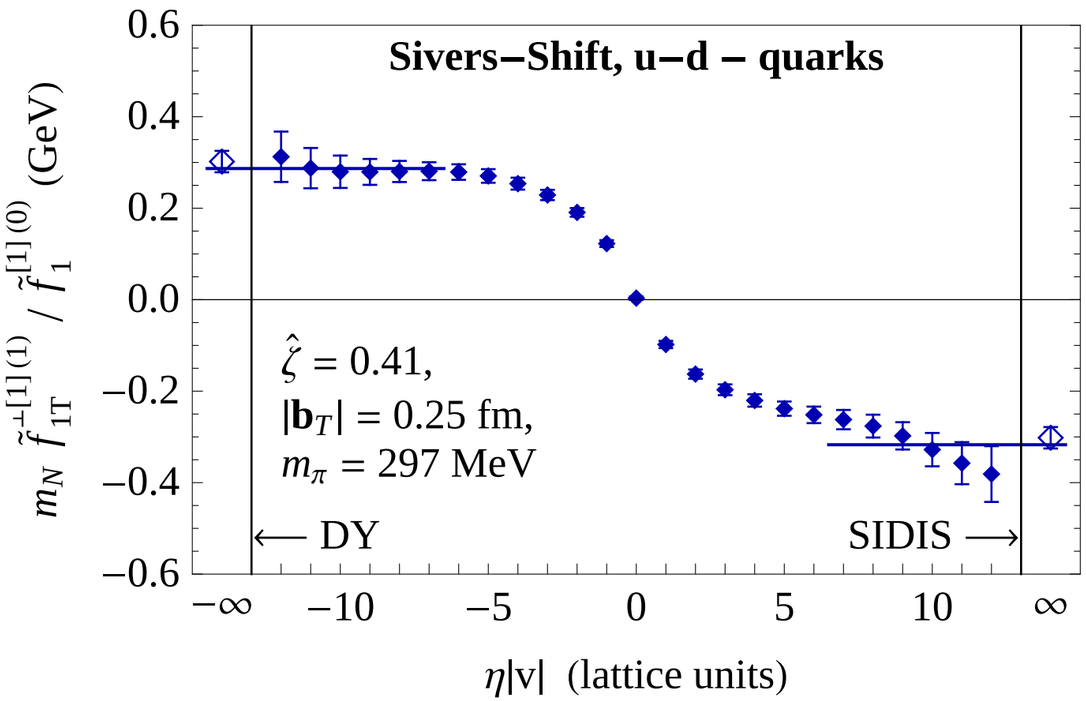

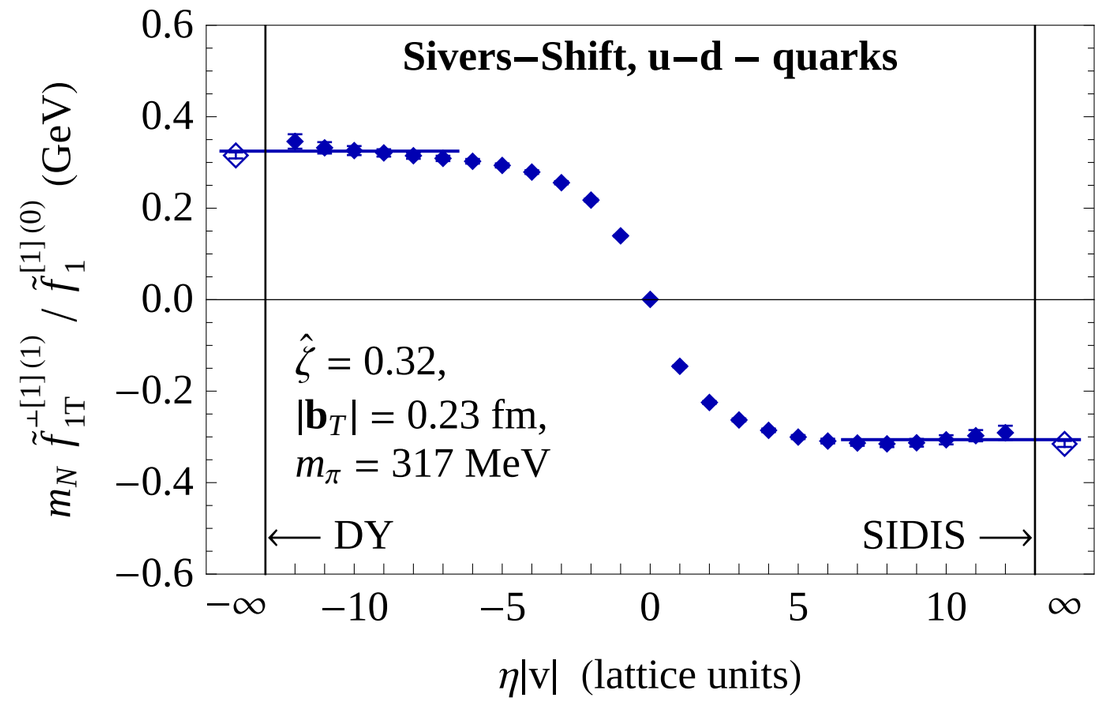

Results: Sivers shift

Dependence on staple extent; sequence of panels at different $|b_T|$

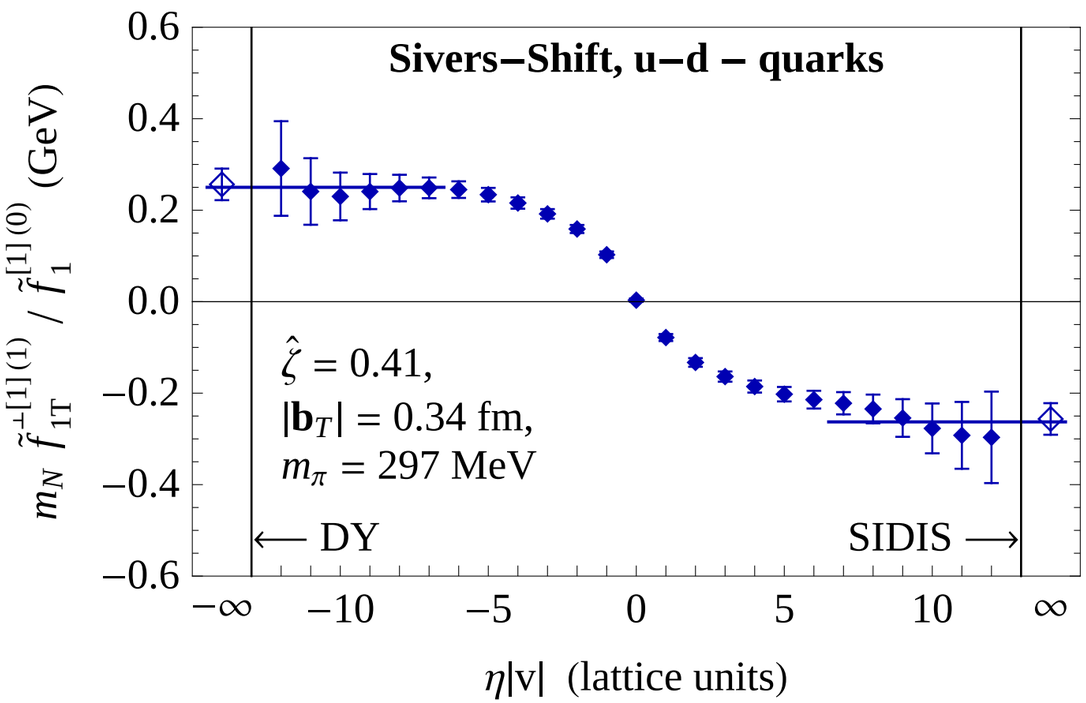

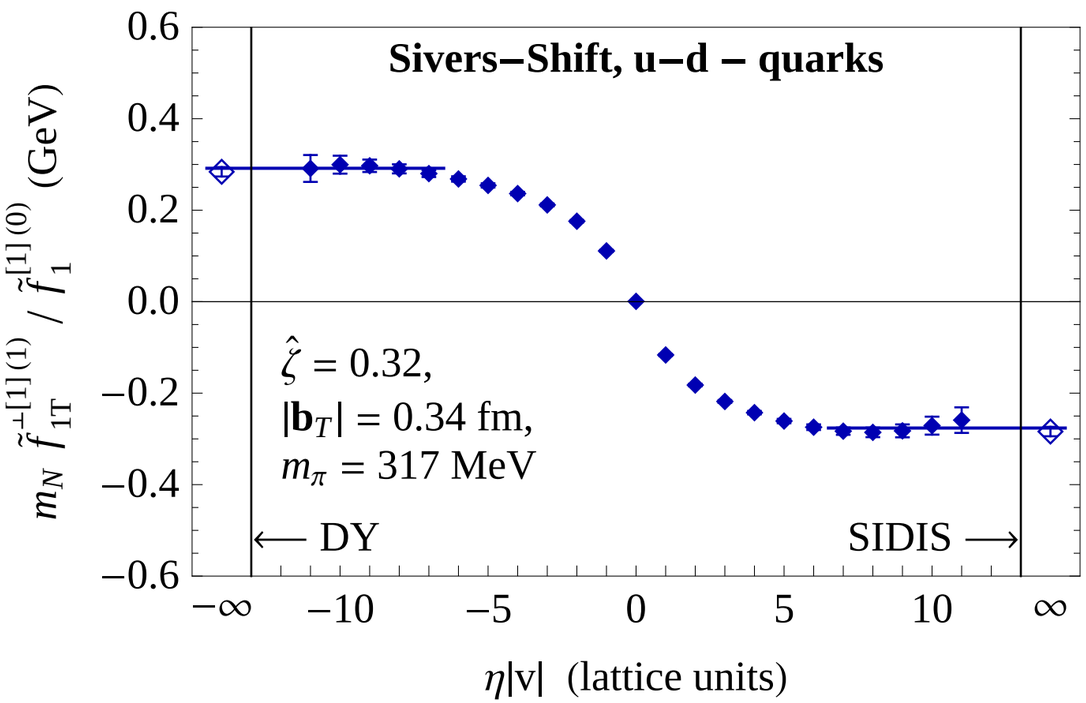

Results: Sivers shift

Dependence of SIDIS limit on $|b_T|$

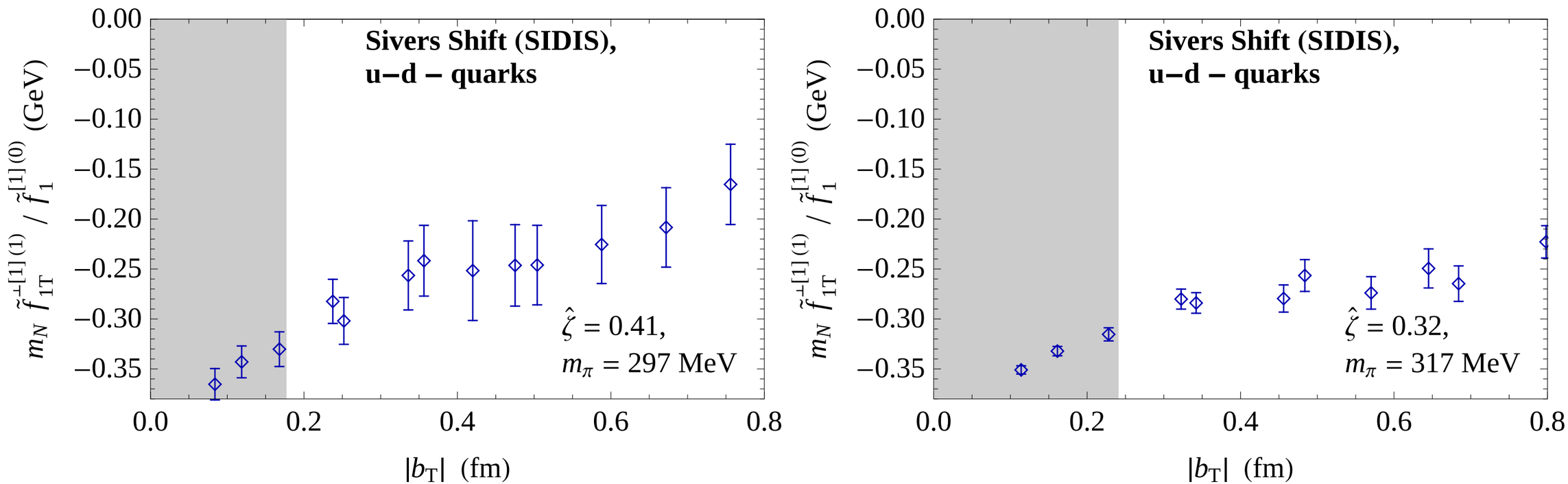

Results: Sivers shift

Dependence of SIDIS limit on $\hat{\zeta}$

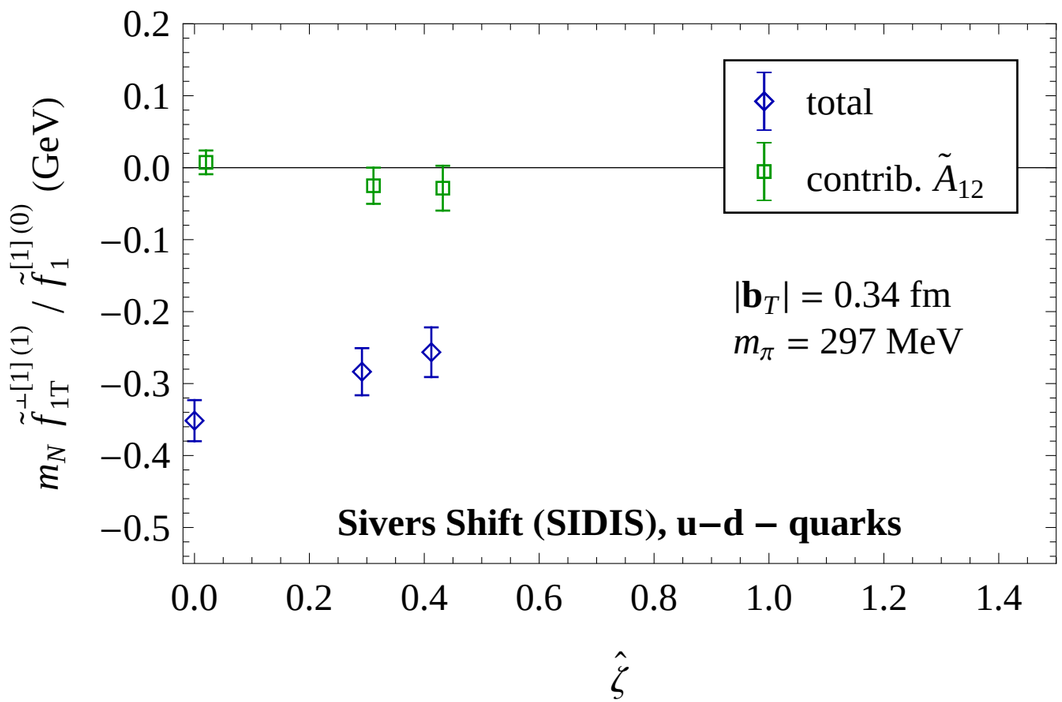

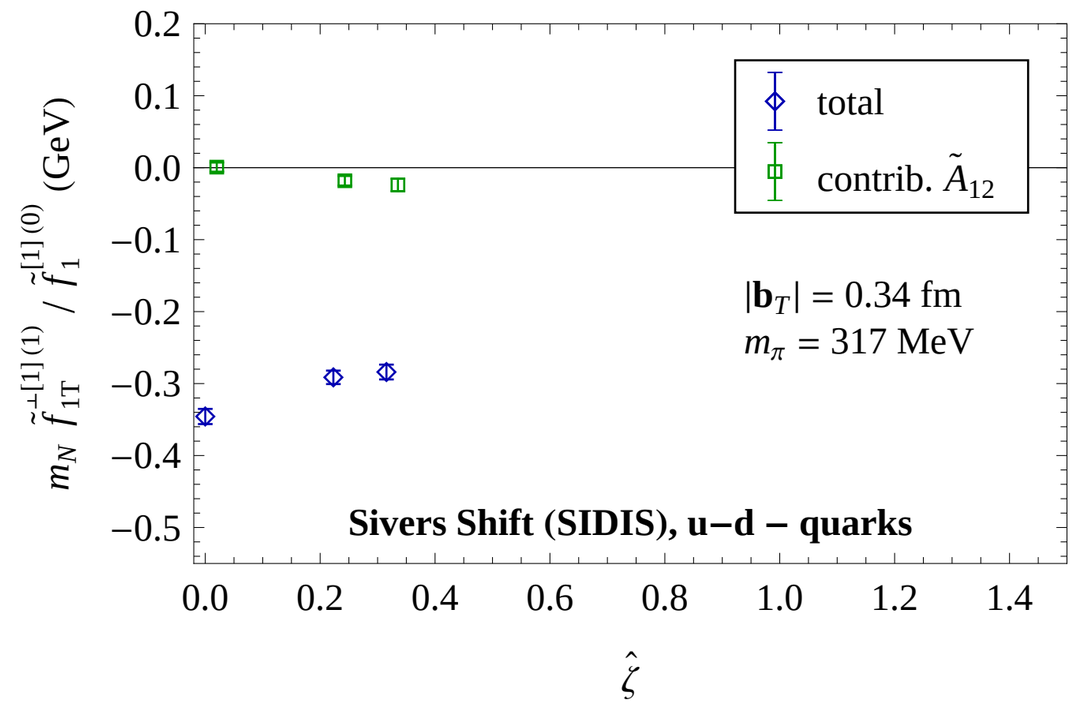

Results: Boer-Mulders shift

Dependence on staple extent

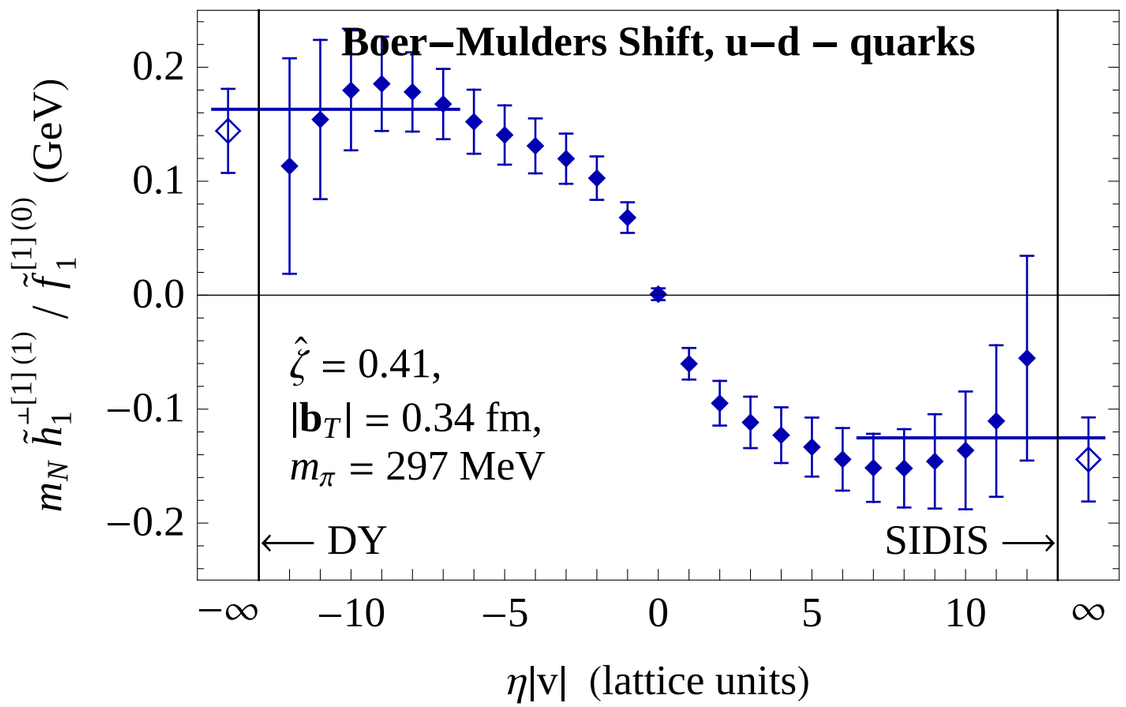

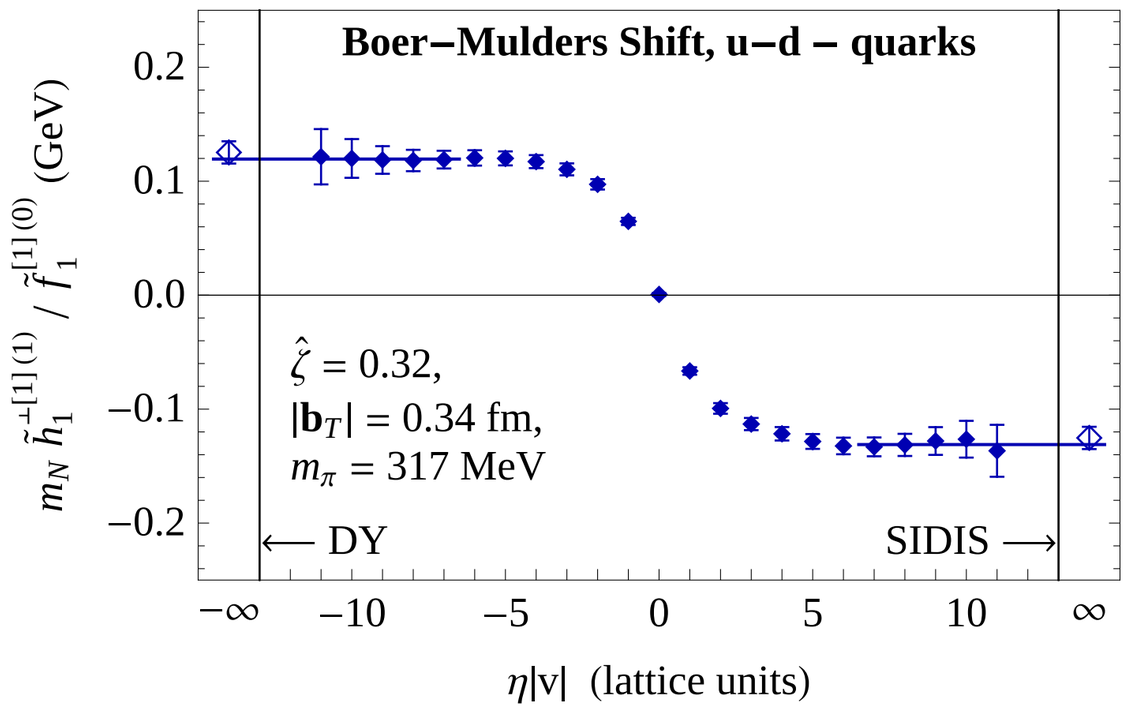

Results: Boer-Mulders shift

Dependence of SIDIS limit on $|b_T|$

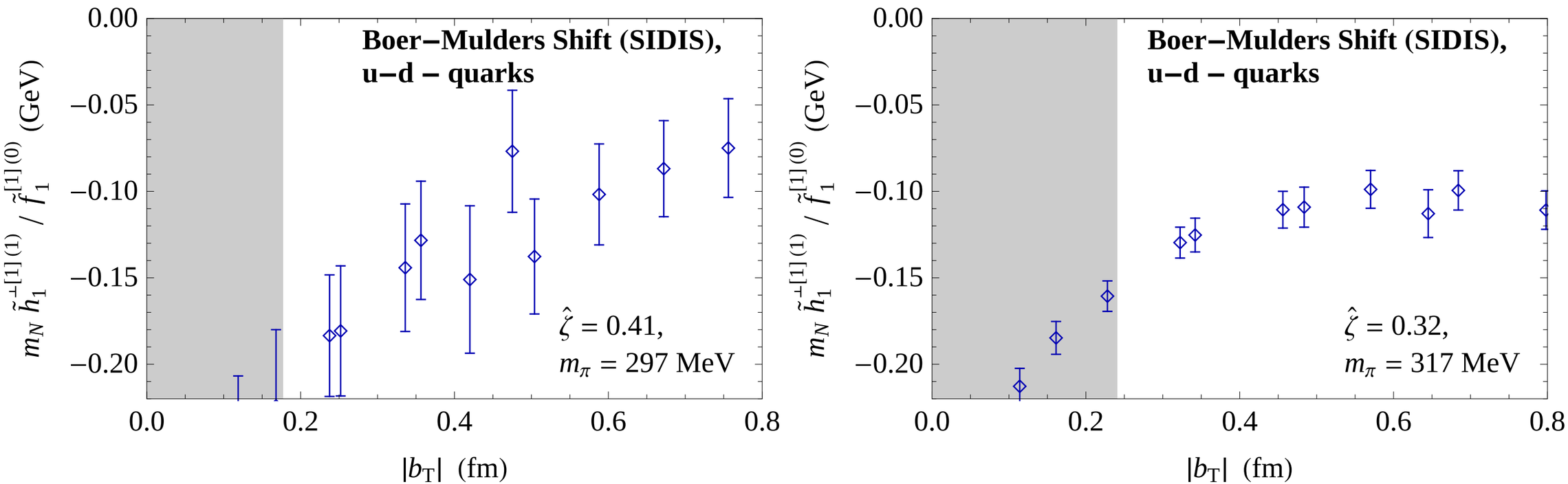

Results: Boer-Mulders shift

Dependence of SIDIS limit on $\hat{\zeta}$

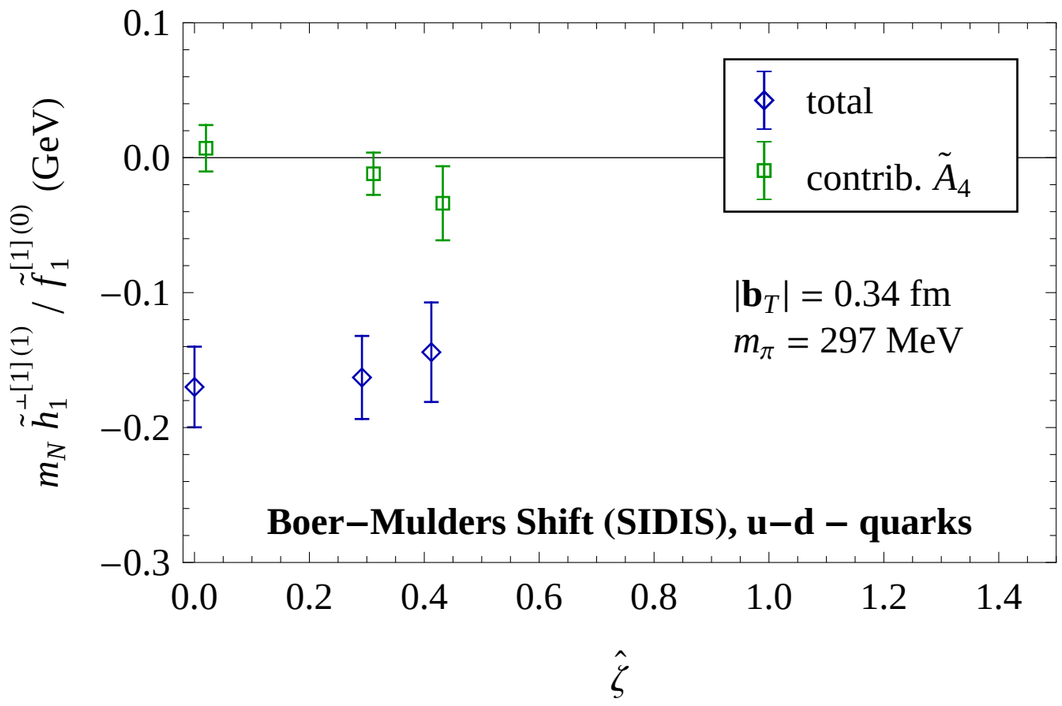

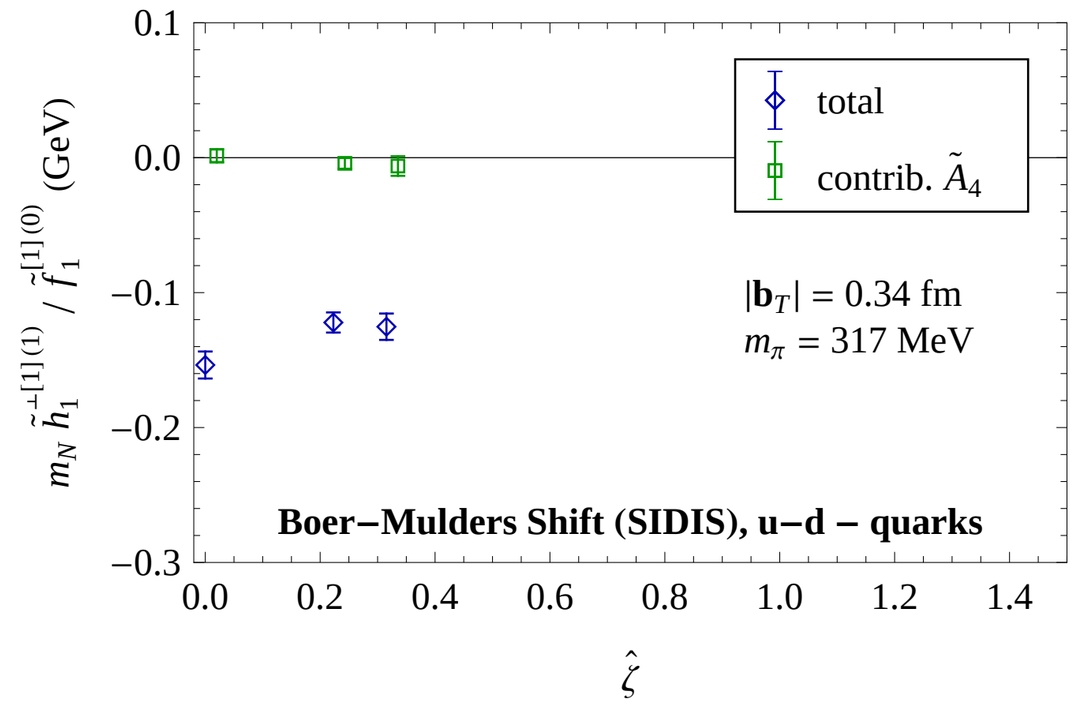

Dependence on the pion mass

Results: Sivers shift

Dependence on staple extent; sequence of panels at different $|b_T|$

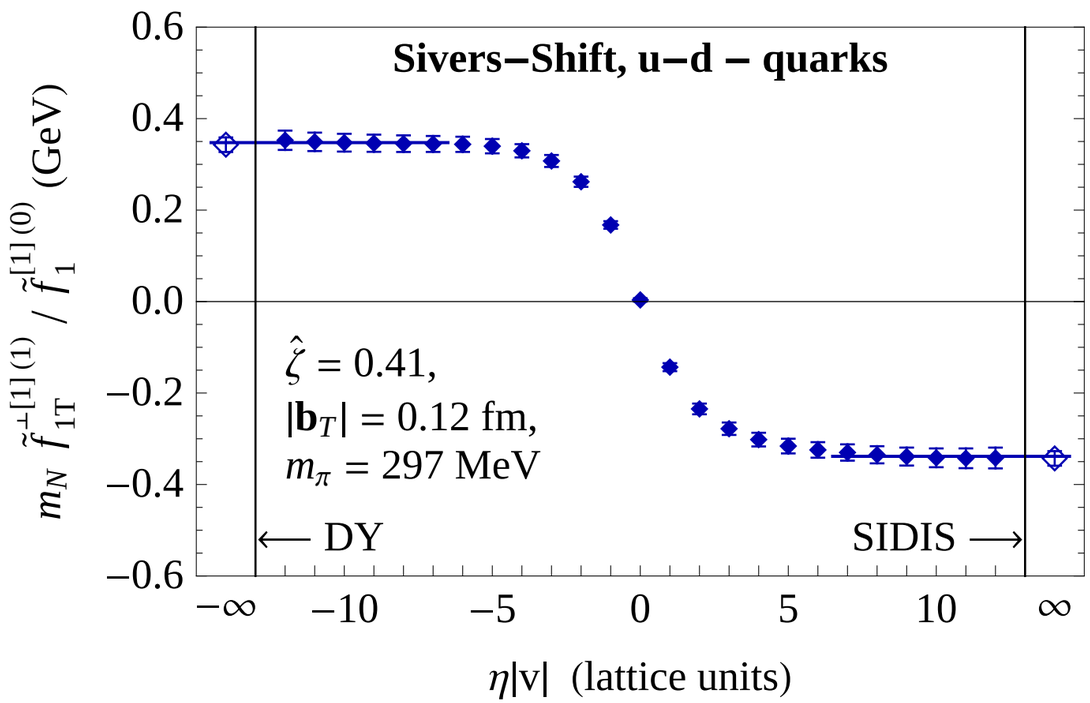

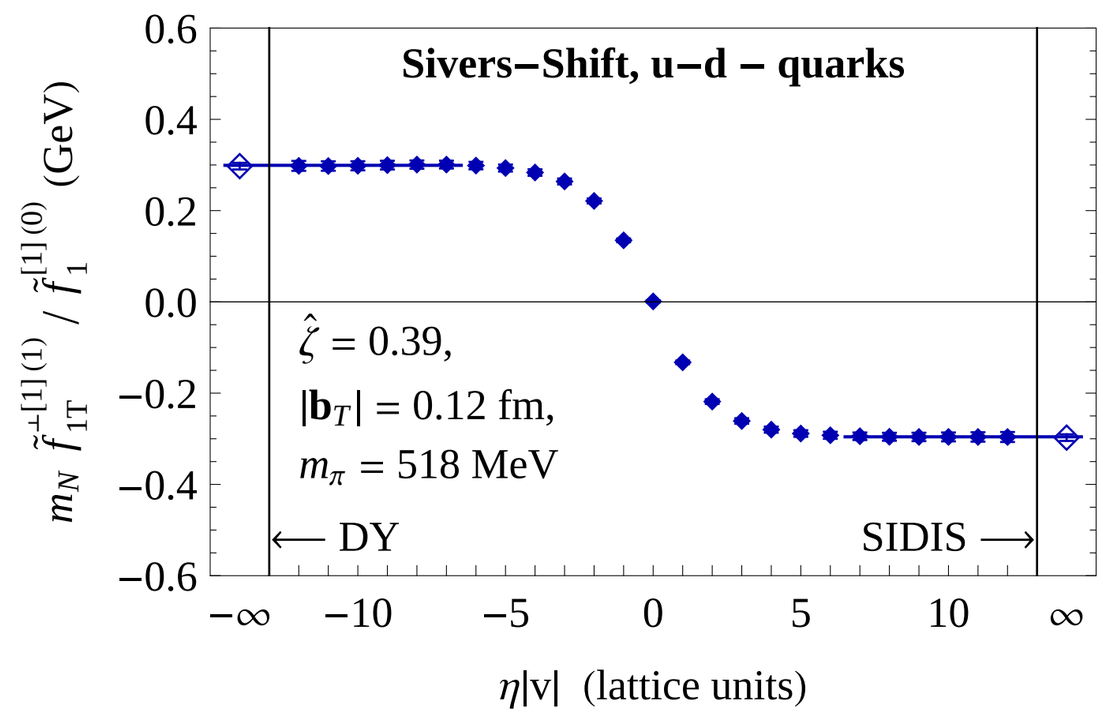

Results: Sivers shift

Dependence on staple extent; sequence of panels at different $|b_T|$

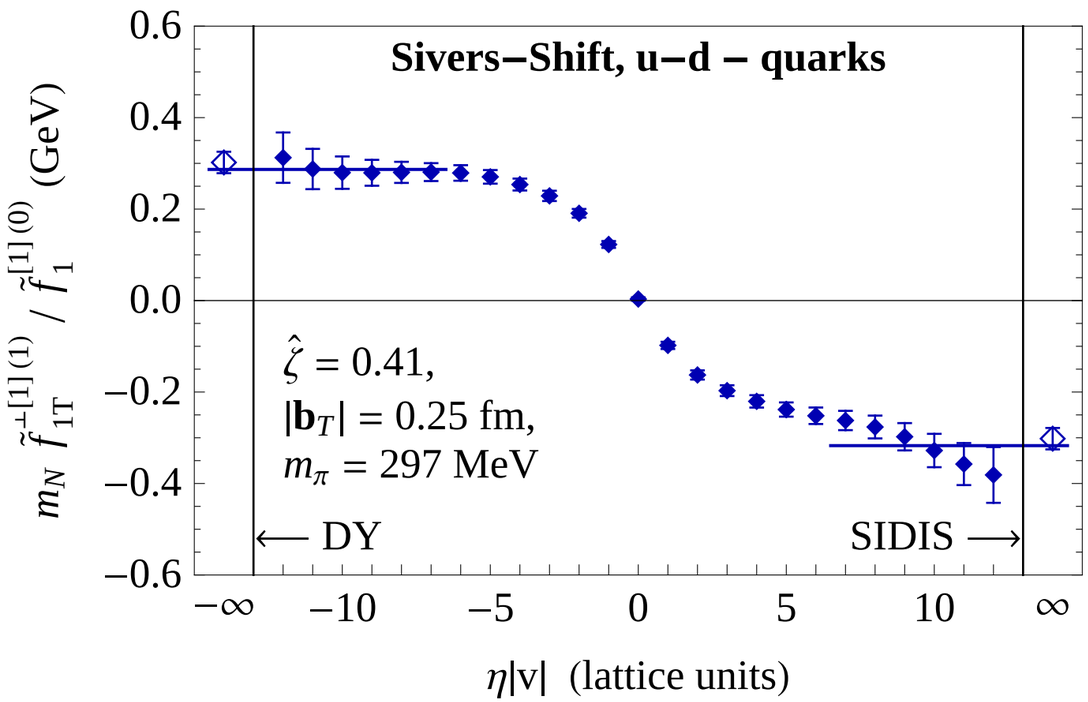

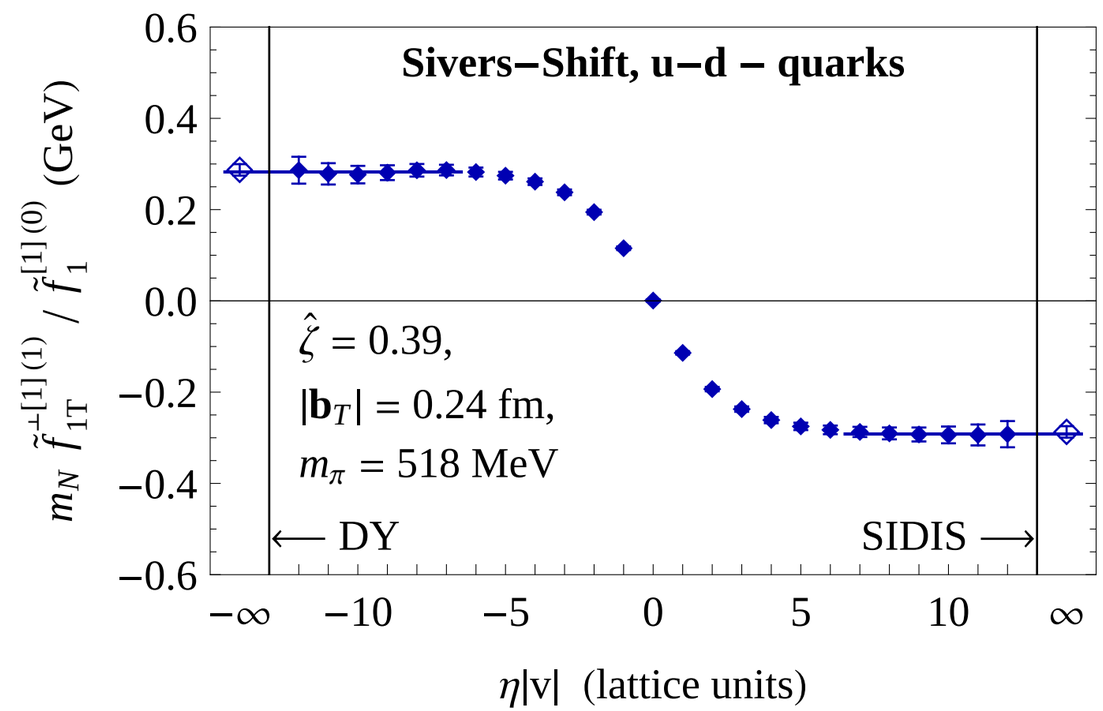

Results: Sivers shift

Dependence on staple extent; sequence of panels at different $|b_T|$

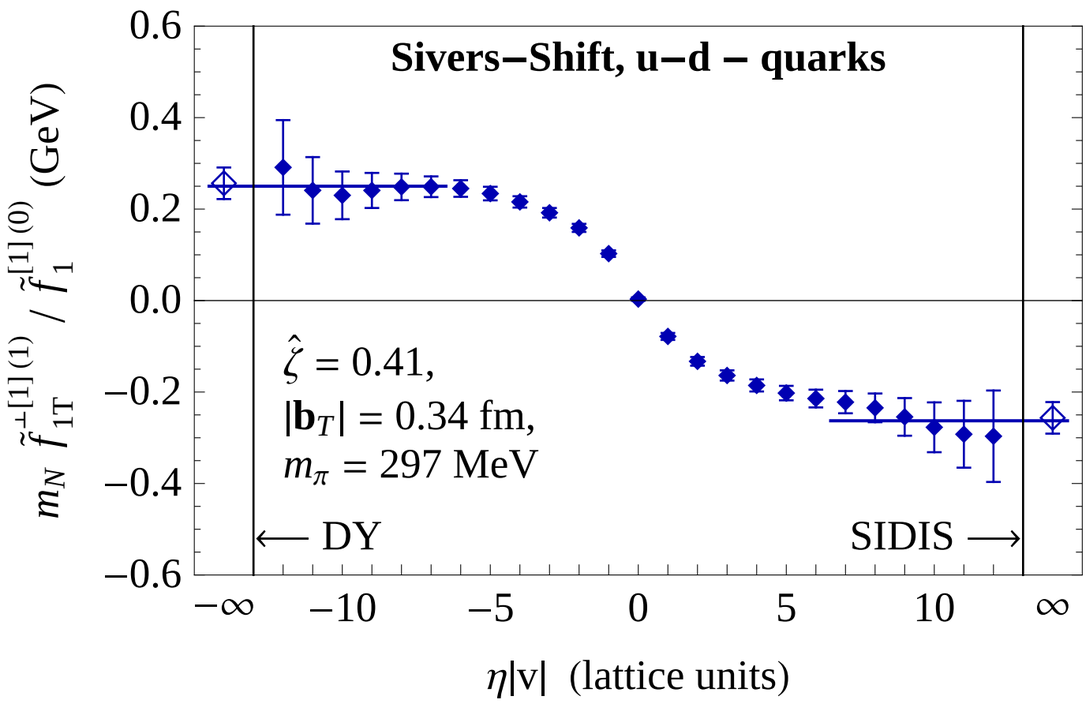

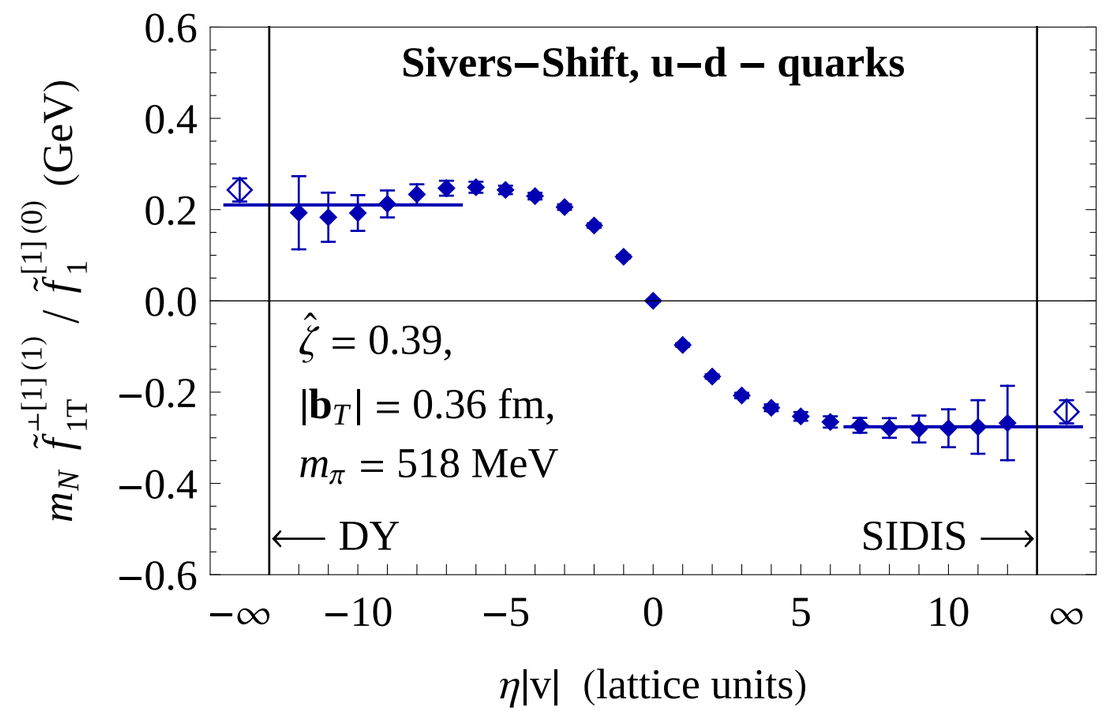

Results: Sivers shift

Dependence of SIDIS limit on $|b_T|$

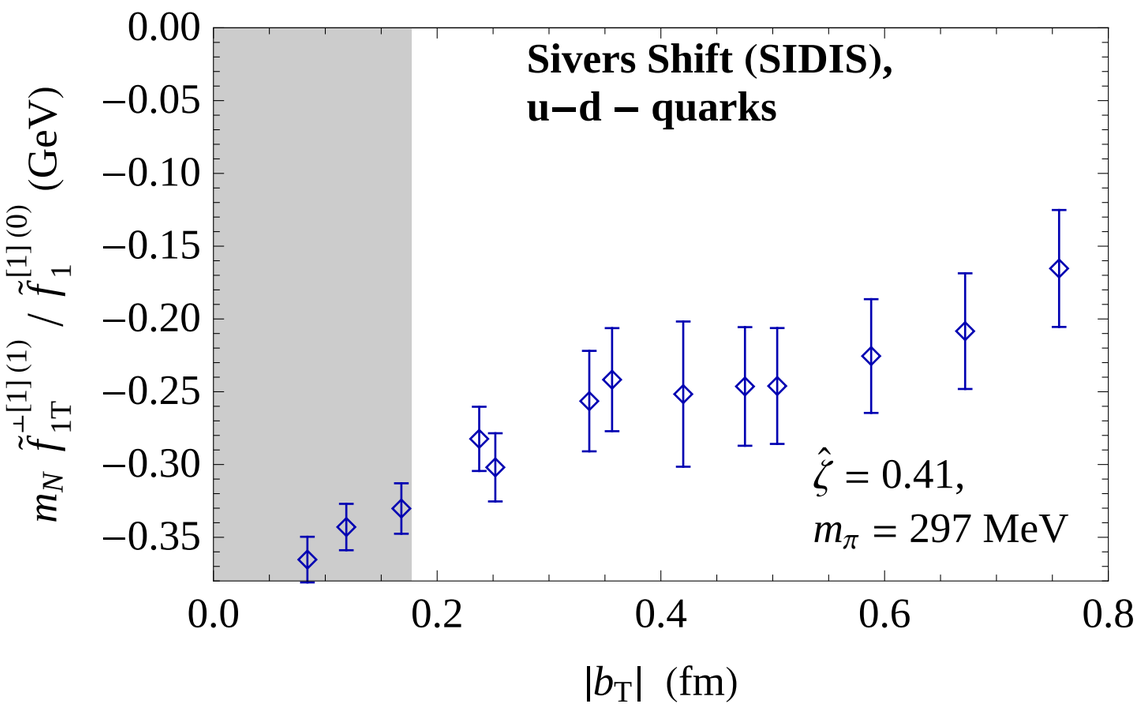

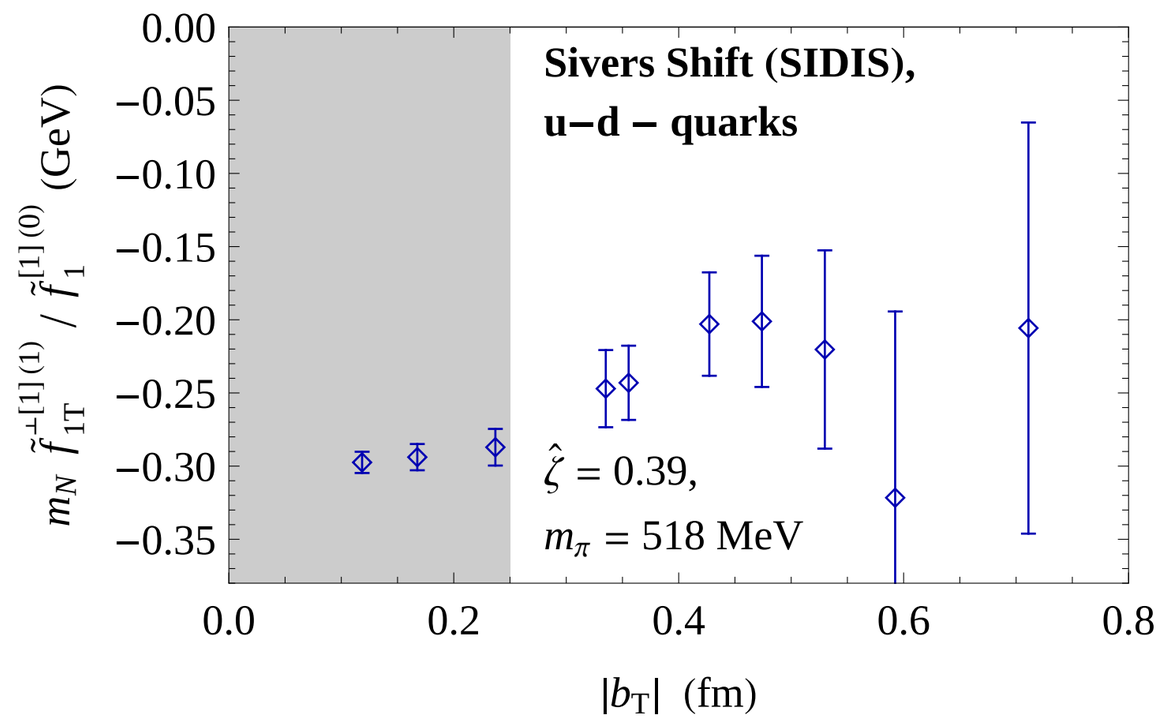

Results: Sivers shift

Dependence of SIDIS limit on $\hat{\zeta}$

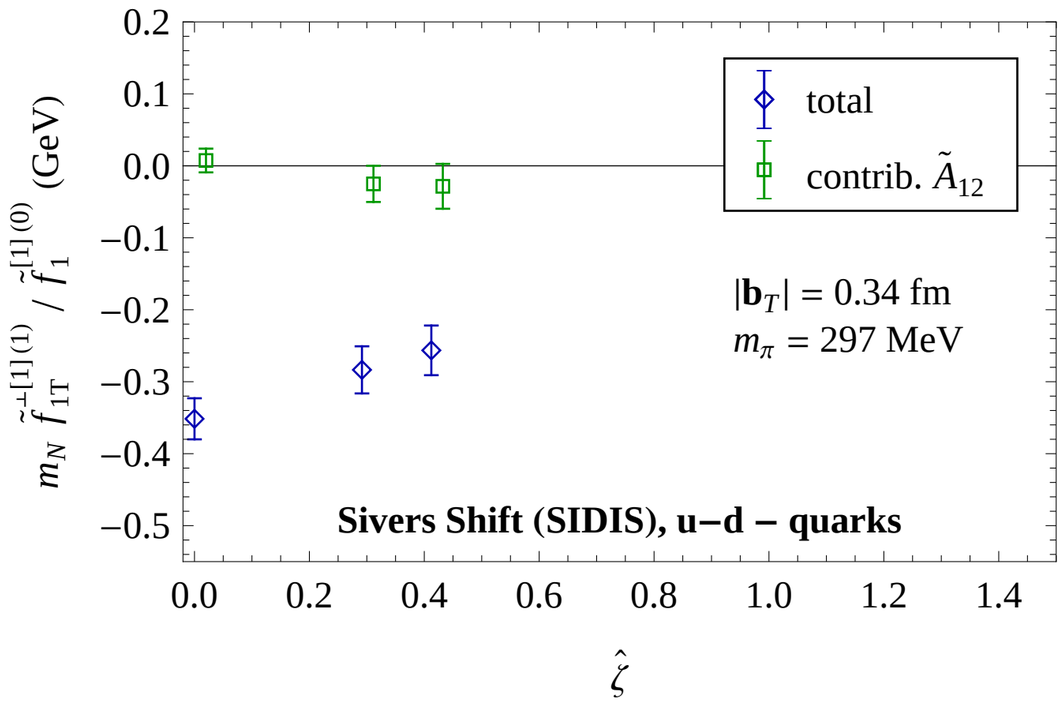

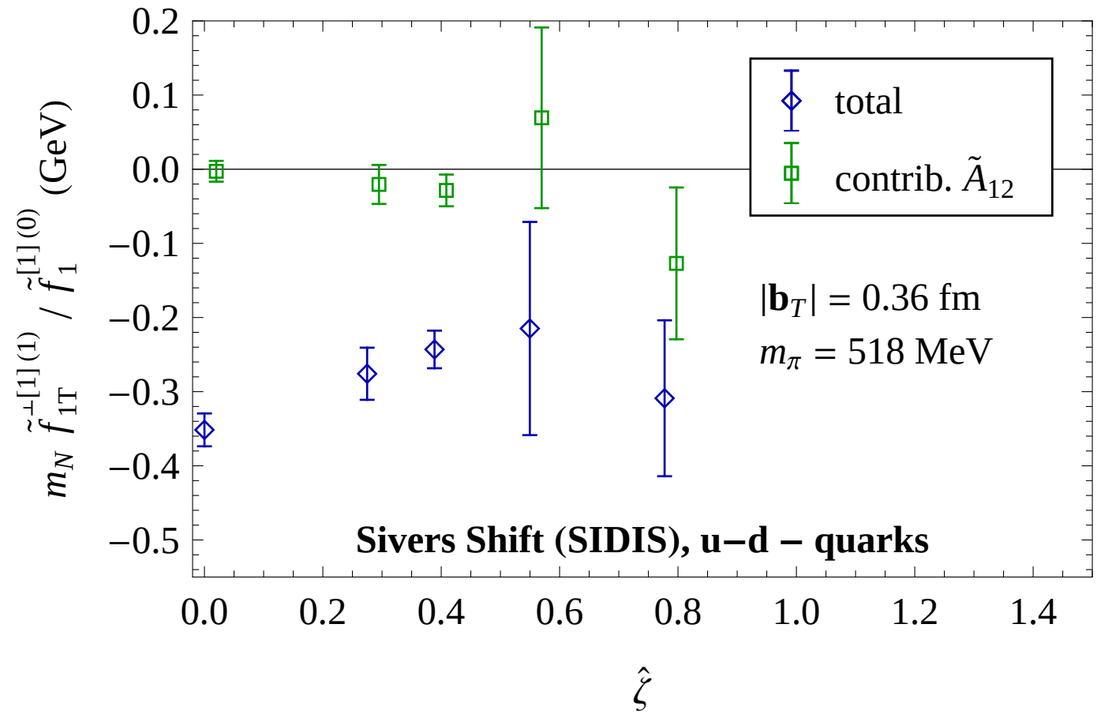

Results: Boer-Mulders shift

Dependence on staple extent

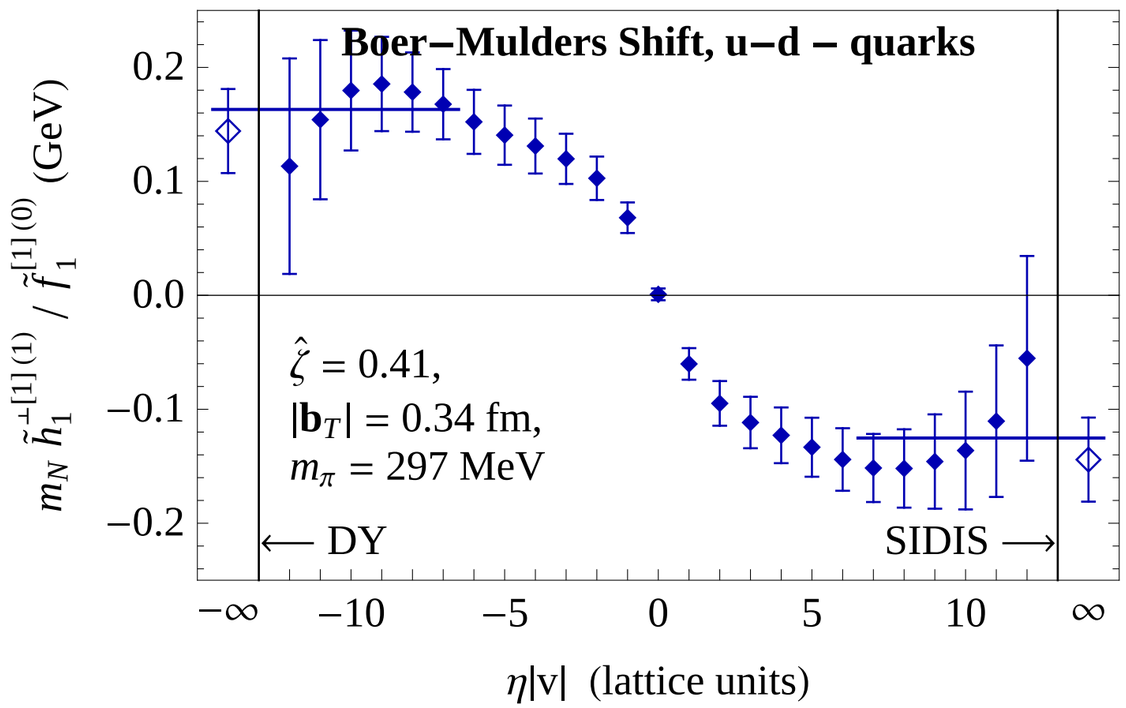

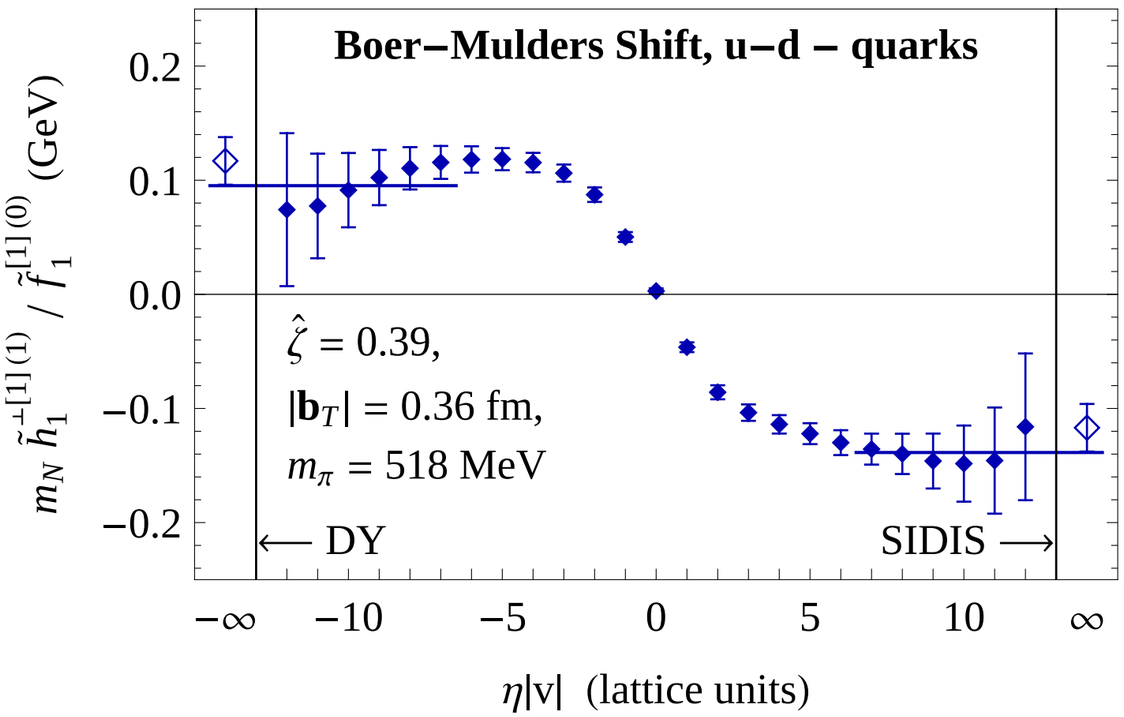

Results: Boer-Mulders shift

Dependence of SIDIS limit on $|b_T|$

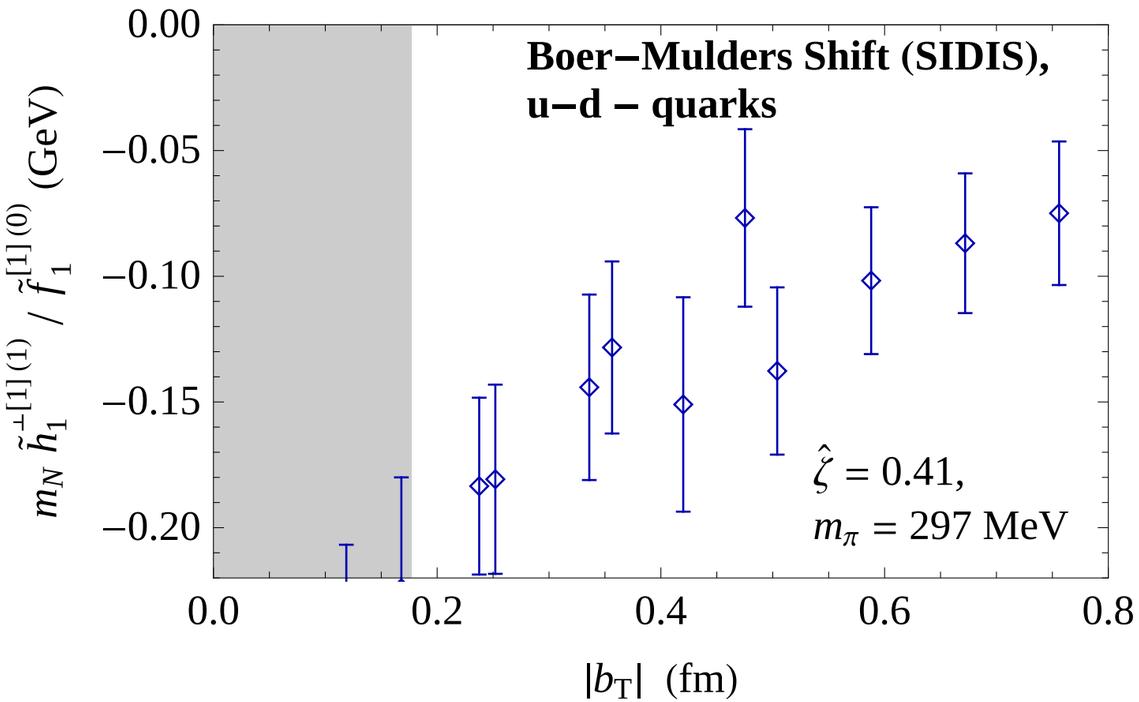

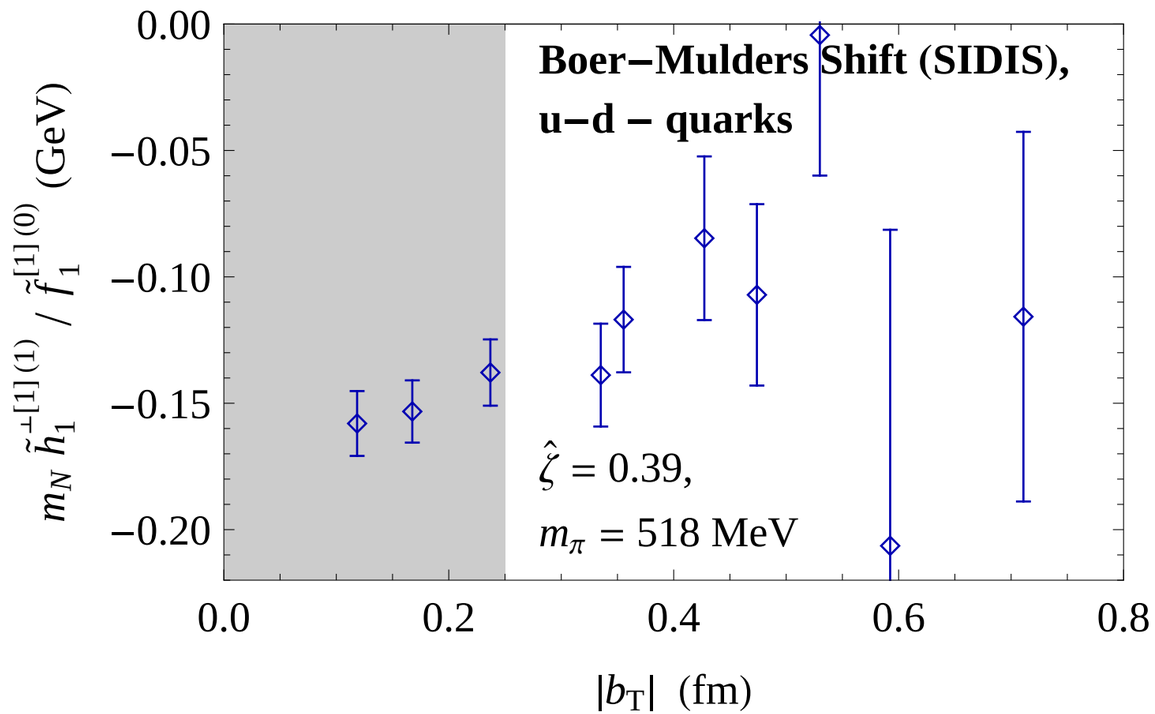

Results: Boer-Mulders shift

Dependence of SIDIS limit on $\hat{\zeta}$

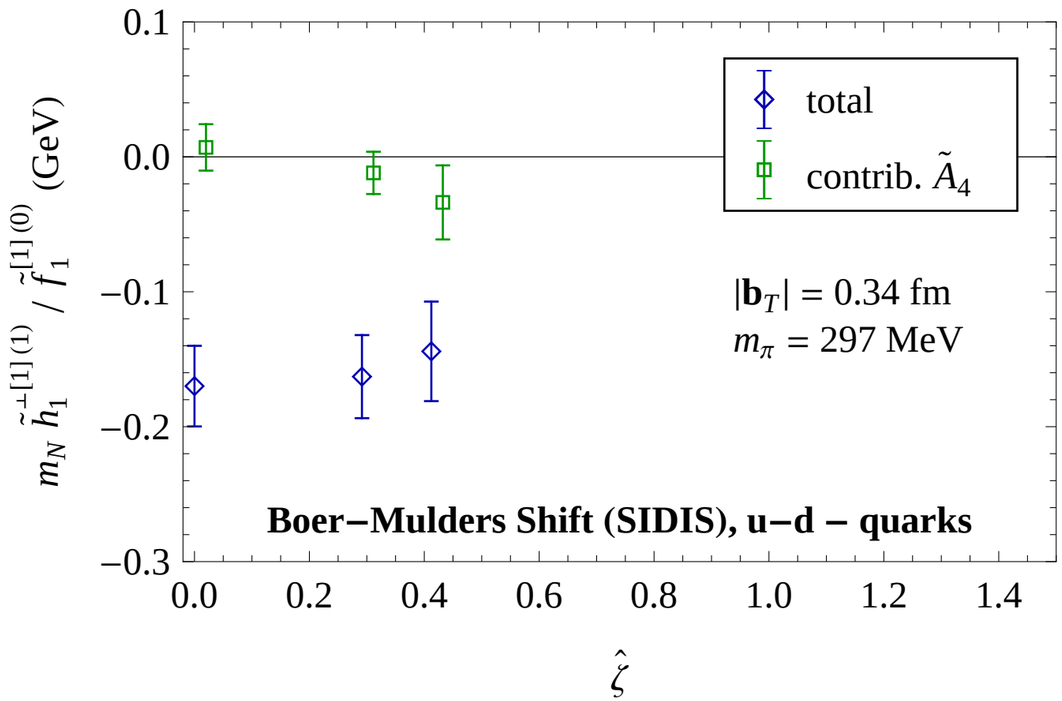

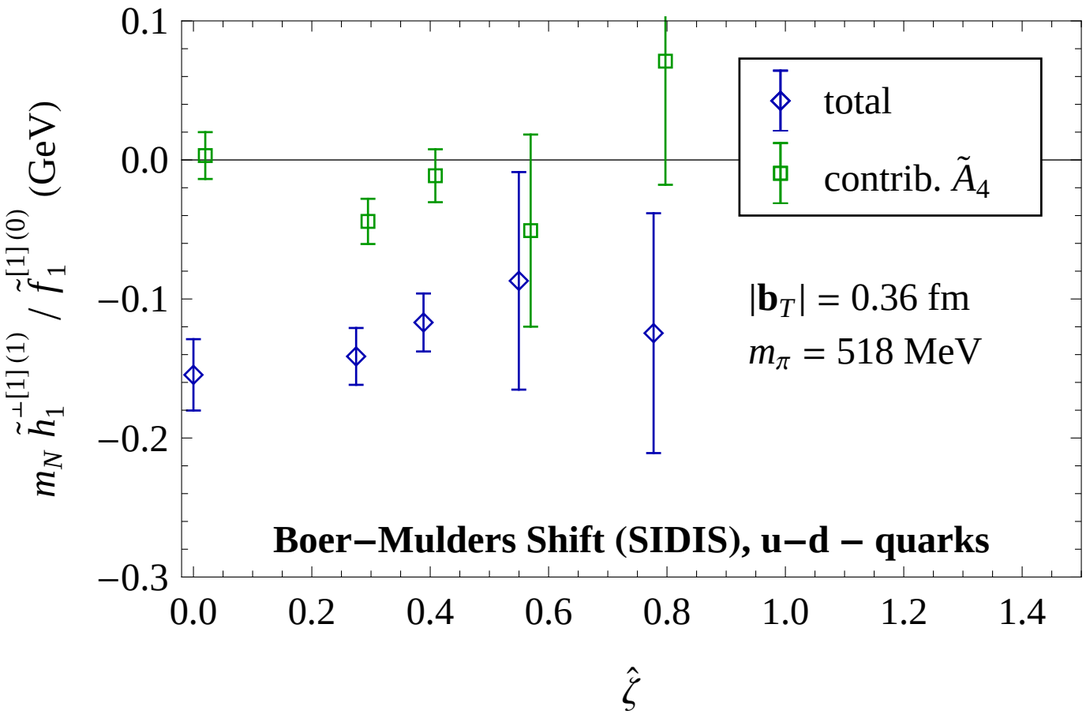

Progressing toward the physical pion mass

Production completed, analysis pending: RBC/UKQCD DWF ensemble at 170 MeV pion mass

2015 production: RBC/UKQCD DWF ensemble at the physical pion mass

Results: Sivers shift summary

Dependence of SIDIS limit on $\hat{\zeta}$

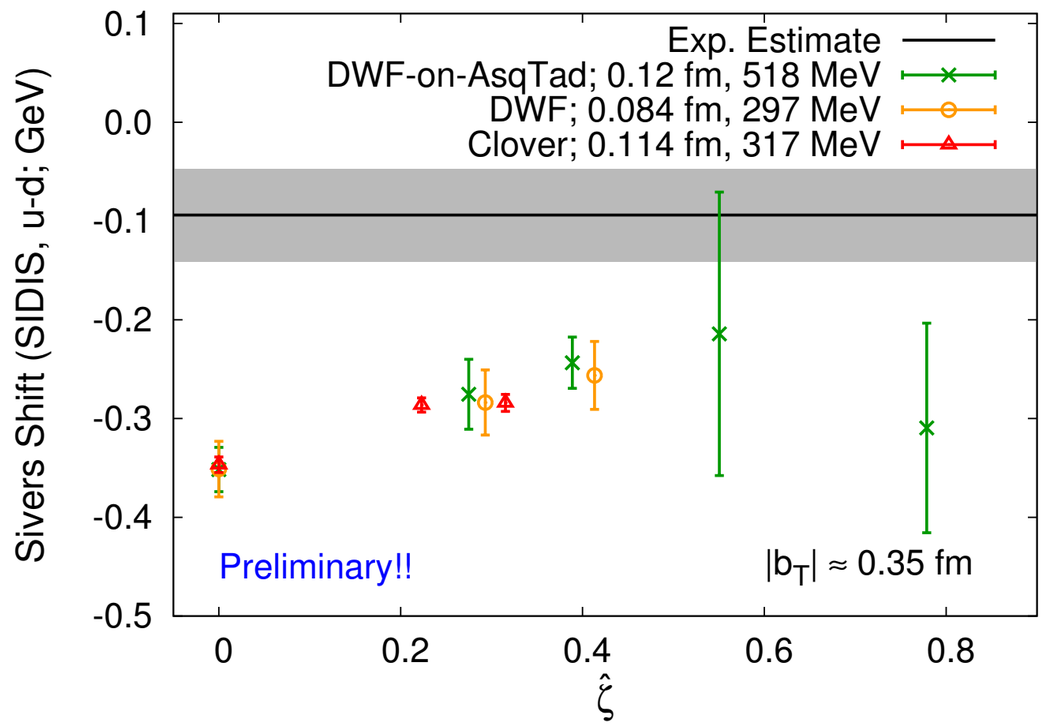

Experimental value from global fit to HERMES, COMPASS and JLab data,
M. Echevarria, A. Idilbi, Z.-B. Kang and I. Vitev, Phys. Rev. D 89 (2014) 074013

Conclusions and Outlook

- Continued exploration of TMDs using bilocal quark operators with staple-shaped gauge link structures; exploration of challenges posed by $\hat{\zeta} \to \infty$ limit, discretization effects, physical limit.
- To avoid soft factors, multiplicative renormalization constants, considered appropriate ratios of Fourier-transformed TMDs ("shifts").
- These observables show no statistically significant variation under the considered changes of action, lattice spacing and pion mass, except at very short distances.
- Analysis underway on an RBC/UKQCD 170 MeV pion mass ensemble, production on an RBC/UKQCD ensemble at physical pion mass in preparation.
- Generalization to mixed transverse momentum / transverse position observables (Wigner functions) will give direct access to quark orbital angular momentum; production underway.

Accessing Bjorken-x dependence

(Fourier transform of) unpolarized distribution, up quarks, normalized to unity at $l \cdot P = 0$

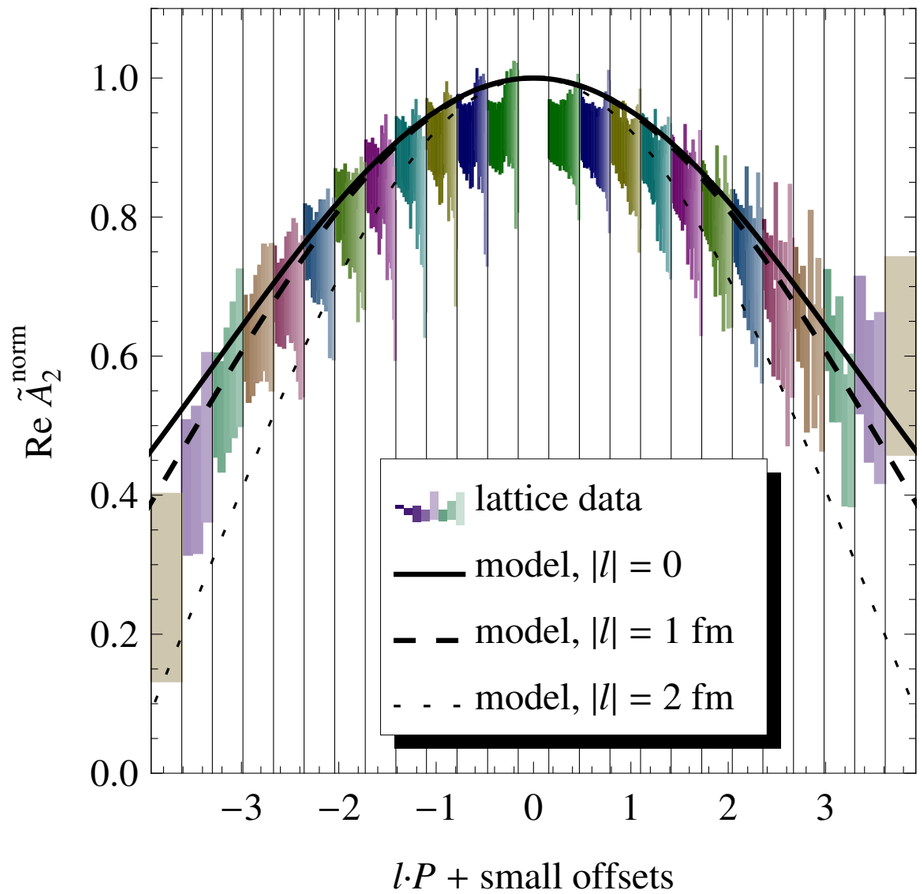

From: B. Musch, P. Hägler, J. Negele and A. Schäfer, Phys. Rev. **D 83** (2011) 094507.

Lattice: $m_\pi = 625\,\text{MeV}$
Model curves: Spectator diquark model

$l \cdot P$: Variable Fourier conjugate to Bjorken x

Relation to Ji Large Momentum Effective Theory (LaMET)

Phenomenology

Lattice QCD

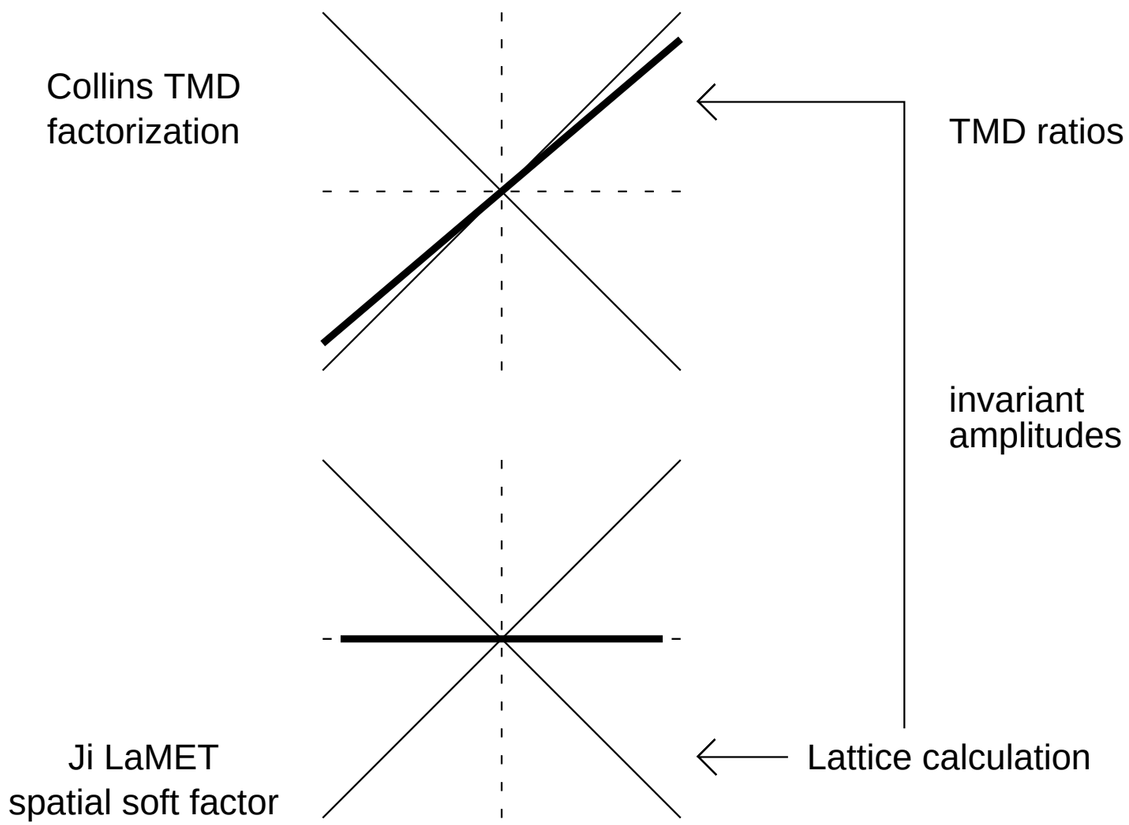

$K \to \pi\nu\bar{\nu}$ decays on the lattice

Xu Feng (Columbia University)

in collaboration with N. H. Christ, A. Portelli and C. T. Sachrajda on behalf of RBC-UKQCD collaboration

February 6, 2015

Phenomenological background

Three decay modes in $K \to \pi\nu\bar{\nu}$

Top-quark (short-distance) contributions dominate in $K \to \pi\nu\bar{\nu}$

- $K^+ \to \pi^+\nu\bar{\nu}$
  - t-quark contribution much larger than c-quark, but $\lambda_t \ll \lambda_c$
  - this compensation makes c-quark important in $A(K^+ \to \pi^+\bar{\nu}\nu)$

$$A^t : A^c : A^u = 68\% : 29\% : 3\%$$ [Cirigliano et.al. Rev. Mod. Phys.]

- $K_L \to \pi^0\nu\bar{\nu}$, CP violating decay
  - $\text{Im}\,\lambda_c \ll \text{Re}\,\lambda_c \Rightarrow A^c$ suppressed, $\text{Im}\,\lambda_u = 0 \Rightarrow A^u = 0$
- $K_S \to \pi^0\nu\bar{\nu}$, similar as K^+ decay, but too difficult in experiment

Only $K^+ \to \pi^+\nu\bar{\nu}$ might be interesting for a non-perturbative calculation

Charm quark contribution, LD or SD dominated?

- A^c is about 29%, if LD dominated, then very interesting for us
- unfortunately, not likely the case
  - Inami & Lim's function for charm quark contribution

$$X^B(x_c) = x_c(-1 - \ln(x_c)), \quad X^Z(x_c) = x_c(-3/4 - \ln(x_c)/4), \quad x_c = \frac{m_c^2}{M_W^2}$$

  - $m_c \ll M_W \Rightarrow \ln(x_c) = -8.28$, log term dominated
  - in log term, most contribution from SD?
- QCD perturbation theory [hep-ph/0603079], charm quark contribution P_c, LO $\rightarrow$ NNLO, uncertainty from varying μ_c 26% $\rightarrow$ 9.8% $\rightarrow$ 2.4%

$$P_c = 0.369 \pm 0.036_{\text{theory}} \pm 0.033_{m_c} \pm 0.009_{\alpha_s} \quad \text{NLO}$$
$$P_c = 0.375 \pm 0.009_{\text{theory}} \pm 0.031_{m_c} \pm 0.009_{\alpha_s} \quad \text{NNLO}$$

Charm quark contribution is likely SD dominated

SM error budget for $K^+ \to \pi^+ \nu\bar{\nu}$

- SM branching ratio for $K^+ \to \pi^+ \nu\bar{\nu}$ [Brod, et.al. 1009.0947]

$$\mathrm{Br}[\mathrm{K}^+ \to \pi^+ \nu\bar{\nu}] = (7.81^{+0.80}_{-0.71\text{para}} \pm 0.29_{\text{theory}}) \times 10^{-11}$$

- parametric error $\sim 10\%$ comes from the input parameters, including

$$\mathrm{CKM}: \ (|V_{cb}| : 56\%,\ \bar{\rho} : 21\%,\ \bar{\eta} : 4\%) \quad \mathrm{others} : 19\%$$

- theory error $\sim 4\%$ dominated by LD contribution $\delta P_{c,u}$
- χPT [hep-ph/0503107] $\delta P_{c,u} = 0.04 \pm 0.02 \Rightarrow$ Br enhanced by 6%
- 6% is comparable to 10%, especially in the future uncertainties in CKM matrix elements may be reduced

Important to determine LD contribution accurately

Lattice methodology

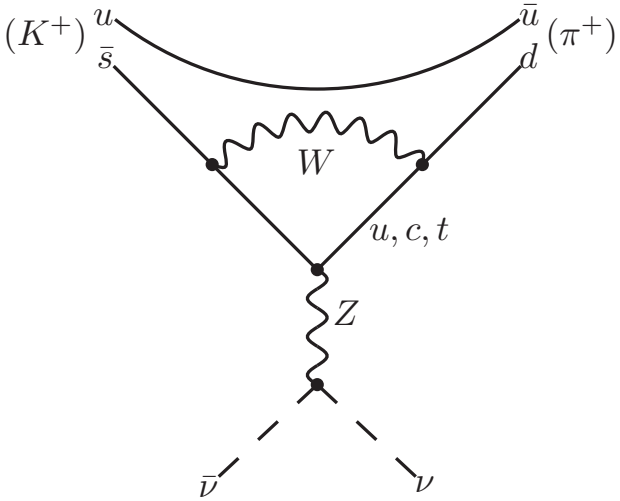

Z-exchange

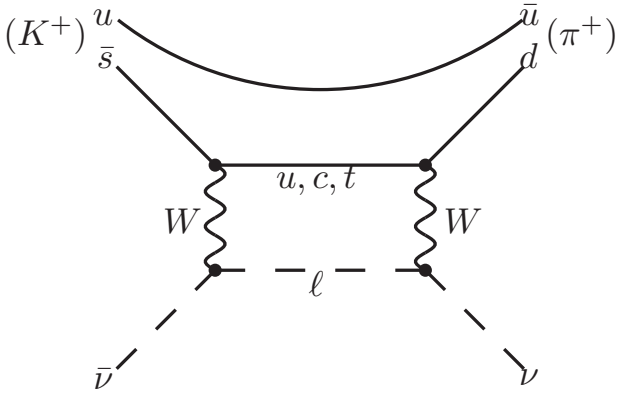

W-box

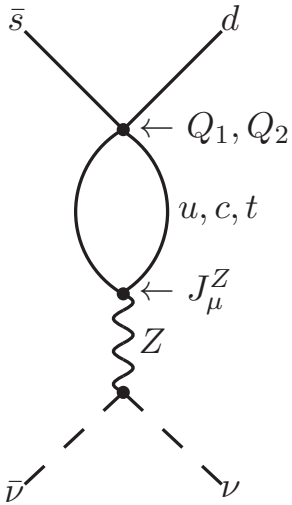

$\int d^4x \, \langle \pi | T[Q_{1,2}(x) J_\mu^Z(0)] | K \rangle$

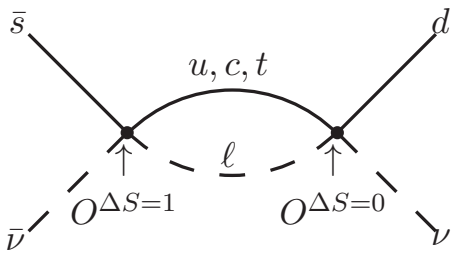

$\int d^4x \, \langle \pi\nu\bar{\nu} | T[O^{\Delta S=1}(x) O^{\Delta S=0}(0)] | K \rangle$

Non-local matrix element

We are going to calculate the non-local matrix element

$$\mathcal{T}^{W,\ell} = \int d^4x \, \langle \pi^+, \nu, \bar{\nu} | \, T[\overbrace{\bar{s}\gamma^\alpha(1-\gamma_5)q \times \bar{\nu}_\ell \gamma_\alpha (1-\gamma_5)\ell(x)}^{O^{\Delta S=1}} \underbrace{\bar{\ell}\gamma^\beta(1-\gamma_5)\nu_\ell \times \bar{q}\gamma_\beta(1-\gamma_5)d(0)}_{O^{\Delta S=0}}] | K^+ \rangle \Big|_{q=u-c}$$

The (anti-)neutrino states are given by

$$\langle \nu_l(\mathbf{p}_\nu) | \bar{\nu}_l(x) | 0 \rangle = \bar{u}(p_\nu) e^{ip_\nu x}, \quad \langle \bar{\nu}_l(\mathbf{p}_{\bar{\nu}}) | \nu_l(0) | 0 \rangle = v(p_{\bar{\nu}}) e^{ip_{\bar{\nu}} 0}$$

Separate the hadronic and leptonic parts in $T^{W,\ell}$

$$\mathcal{T}^{W,\ell} = \int d^4x \, \overbrace{\langle \pi^+ | \, T \, [\bar{s}\gamma_\alpha(1-\gamma_5)q(x) \, \bar{q}\gamma_\beta(1-\gamma_5)d(0)] \, | K^+ \rangle}^{H_{\alpha\beta}\text{: hadronic part}} \times \underbrace{\bar{u}(p_\nu)\gamma^\alpha(1-\gamma_5)S_\ell(x,0)\gamma^\beta(1-\gamma_5)v(p_{\bar{\nu}}) \, e^{ip_\nu x}}_{\bar{u}(p_\nu)\Gamma^{\alpha\beta}v(p_{\bar{\nu}})\text{: leptonic part}}$$

Lorentz structure

For simplicity we may write

$$\mathcal{T}^{W,\ell} = H_{\alpha\beta}\, \bar{u}(p_\nu)\Gamma^{\alpha\beta} v(p_{\bar{\nu}}) \tag{1}$$

Due to the chiral property of the spinors $\bar{u}(p_\nu)$ and $v(p_{\bar{\nu}}) \Rightarrow$

$$\mathcal{T}^{W,\ell} = T^\mu(p_K, p_\nu, p_{\bar{\nu}})\, \bar{u}(p_\nu)\gamma_\mu(1-\gamma_5)v(p_{\bar{\nu}})$$

Massless neutrinos smplifies the structure of $T^\mu = F^\ell(p_K, p_\nu, p_{\bar{\nu}})p_K^\mu$

$$\mathcal{T}^{W,\ell} = F^\ell(p_K, p_\nu, p_{\bar{\nu}})\, \bar{u}(p_\nu)\not{p}_K(1-\gamma_5)v(p_{\bar{\nu}}) \tag{2}$$

Combining Eq. (1) and (2), we have

$$H_{\alpha\beta}\, \bar{u}(p_\nu)\Gamma^{\alpha\beta} v(p_{\bar{\nu}}) = F^\ell(p_K, p_\nu, p_{\bar{\nu}})\bar{u}(p_\nu)\not{p}_K(1-\gamma_5)v(p_{\bar{\nu}})$$

It can be shown that

$$F^\ell(p_K, p_\nu, p_{\bar{\nu}}) = \frac{H_{\alpha\beta}\, \mathrm{Tr}[\Gamma^{\alpha\beta}\not{p}_{\bar{\nu}}\not{p}_K(1-\gamma_5)\not{p}_\nu]}{\mathrm{Tr}[\not{p}_K(1-\gamma_5)\not{p}_{\bar{\nu}}\not{p}_K(1-\gamma_5)\not{p}_\nu]}$$

Short summary of procedures

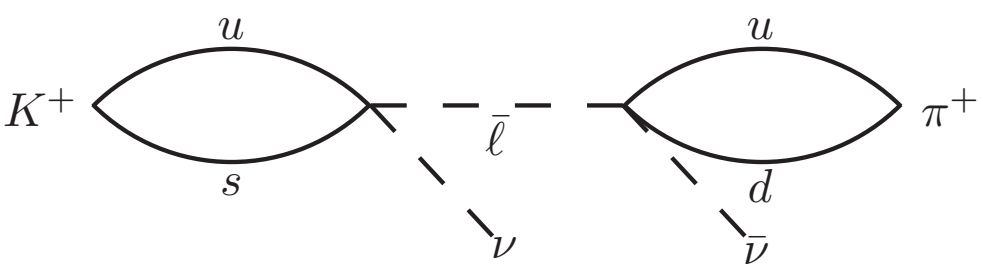

Type 1

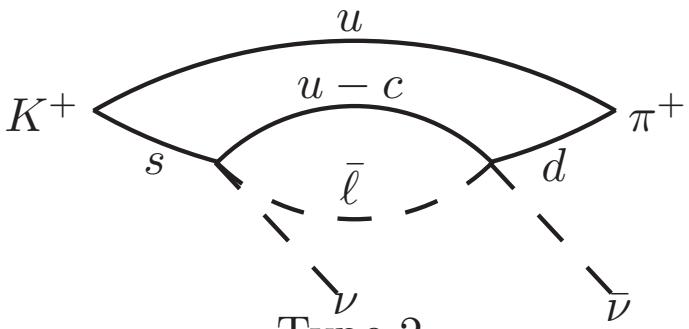

Type 2

- hadronic $H_{\alpha\beta}$ can be calculated from a 4-point correlation function
- leptonic $\Gamma^{\alpha\beta}$ involves a lepton propagator, here we use overlap fermion
- then form factor $F^{\ell}(p_K, p_\nu, p_{\bar{\nu}})$ can be determined
- the decay amplitude for the W-box diagrams can be written as

$$A = G_F^2 V_{us}^* V_{ud} \sum_{\ell=e,\mu,\tau} F^{\ell}(p_K, p_\nu, p_{\bar{\nu}}) p_K^{\mu} \bar{u}(p_\nu)\gamma_\mu(1-\gamma_5)v(p_{\bar{\nu}})$$

Lattice results

Lattice setup

- $16^3 \times 32 \times 16$ domain wall fermion on Iwasaki gauge action
- $m_\pi = 420$ MeV, $m_K = 540$ MeV
- $a^{-1} = 1.729$ GeV, m_c chosen so that $m_c^{\overline{MS}}(2\text{ GeV})$=863 MeV
- every 10 of 8000 configurations are measured
- collinear decay: momentum $\mathbf{p}_K = (0,0,0)$, $\mathbf{p}_\pi = (-p,-p,-p)$, $\mathbf{p}_\nu = \mathbf{p}_{\bar{\nu}} = (p/2, p/2, p/2)$, p is chosen to satisfy $m_K = E_\pi + E_\nu + E_{\bar{\nu}}$

Minkowski vs Euclidean

Generic feature of non-local matrix element in 2nd order weak interaction

$$\begin{aligned}\mathcal{T}^M &= i\int dt\,\langle f|T[O^{\Delta S=1}(t)O^{\Delta S=0}(0)]|K\rangle \\ &= \sum_{n_s}\frac{\langle f|O^{\Delta S=1}|n_s\rangle\langle n_s|O^{\Delta S=0}|K\rangle}{E_{n_s}-E_f+i\epsilon}-\sum_{n}\frac{\langle f|O^{\Delta S=0}|n\rangle\langle n|O^{\Delta S=1}|K\rangle}{E_K-E_n+i\epsilon}\end{aligned} \tag{3}$$

In Euclidean space

$$\begin{aligned}\mathcal{T}^E &= \sum_{t=-T_a}^{T_b}\langle f|T[O^{\Delta S=1}(t)O^{\Delta S=0}(0)]|K\rangle \\ &= \sum_{n_s}\frac{\langle f|O^{\Delta S=1}|n_s\rangle\langle n_s|O^{\Delta S=0}|K\rangle}{E_{n_s}-E_f}\left(1-e^{(E_f-E_{n_s})T_b}\right) \\ &\quad -\sum_{n}\frac{\langle f|O^{\Delta S=0}|n\rangle\langle n|O^{\Delta S=1}|K\rangle}{E_K-E_n}\left(1-e^{(E_K-E_n)T_a}\right)\end{aligned} \tag{4}$$

Removing exp growing contamination, $\mathcal{T}^E \Rightarrow \mathcal{T}^M$ (see A. Portelli's talk)

Double integration

Double integration as shown in $K_L - K_S$ mass diff (N. Christ's talk)

$$\sum_{t_1=t_a}^{t_b}\sum_{t_2=t_a}^{t_b}\langle f|T[O^{\Delta S=1}(t_1)O^{\Delta S=0}(t_2)]|K\rangle\, e^{m_K t_2}e^{-m_f t_2}$$
$$= \sum_{n_s}\frac{\langle f|O^{\Delta S=1}|n_s\rangle\langle n_s|O^{\Delta S=0}|K\rangle}{E_{n_s}-E_f}\left(T-\frac{1-e^{(E_f-E_{n_s})T}}{E_{n_s}-E_f}\right)$$
$$-\sum_{n}\frac{\langle f|O^{\Delta S=0}|n\rangle\langle n|O^{\Delta S=1}|K\rangle}{E_K-E_n}\left(T+\frac{1-e^{(E_K-E_n)T}}{E_K-E_n}\right) \quad (5)$$

Here $T = t_b - t_a + 1$ is defined as size of the integral window

Remove exp., and fit with $a + bT$, the slope b is what we want

In this talk, we use the double integration to gain more precision

Type 1 diagram

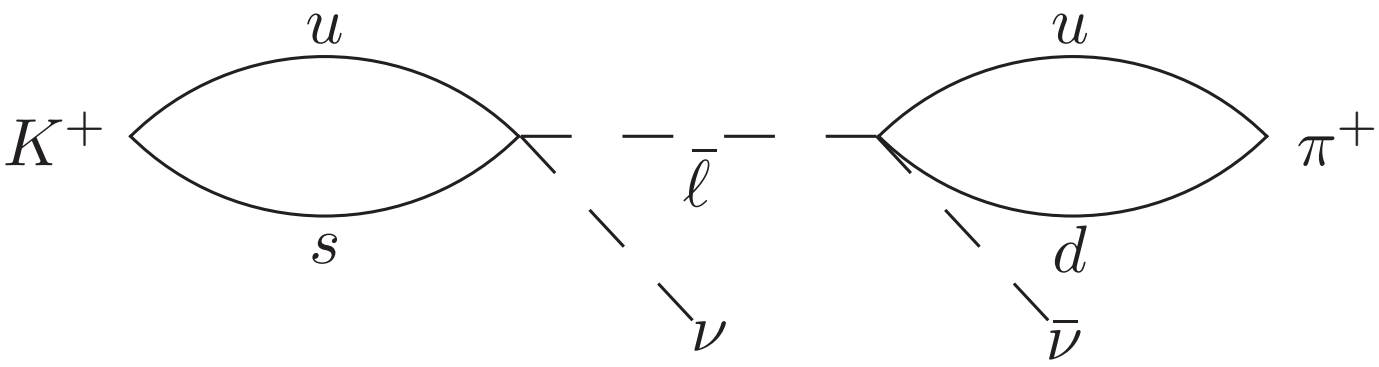

Type 1 diagram, unintegrated matrix element

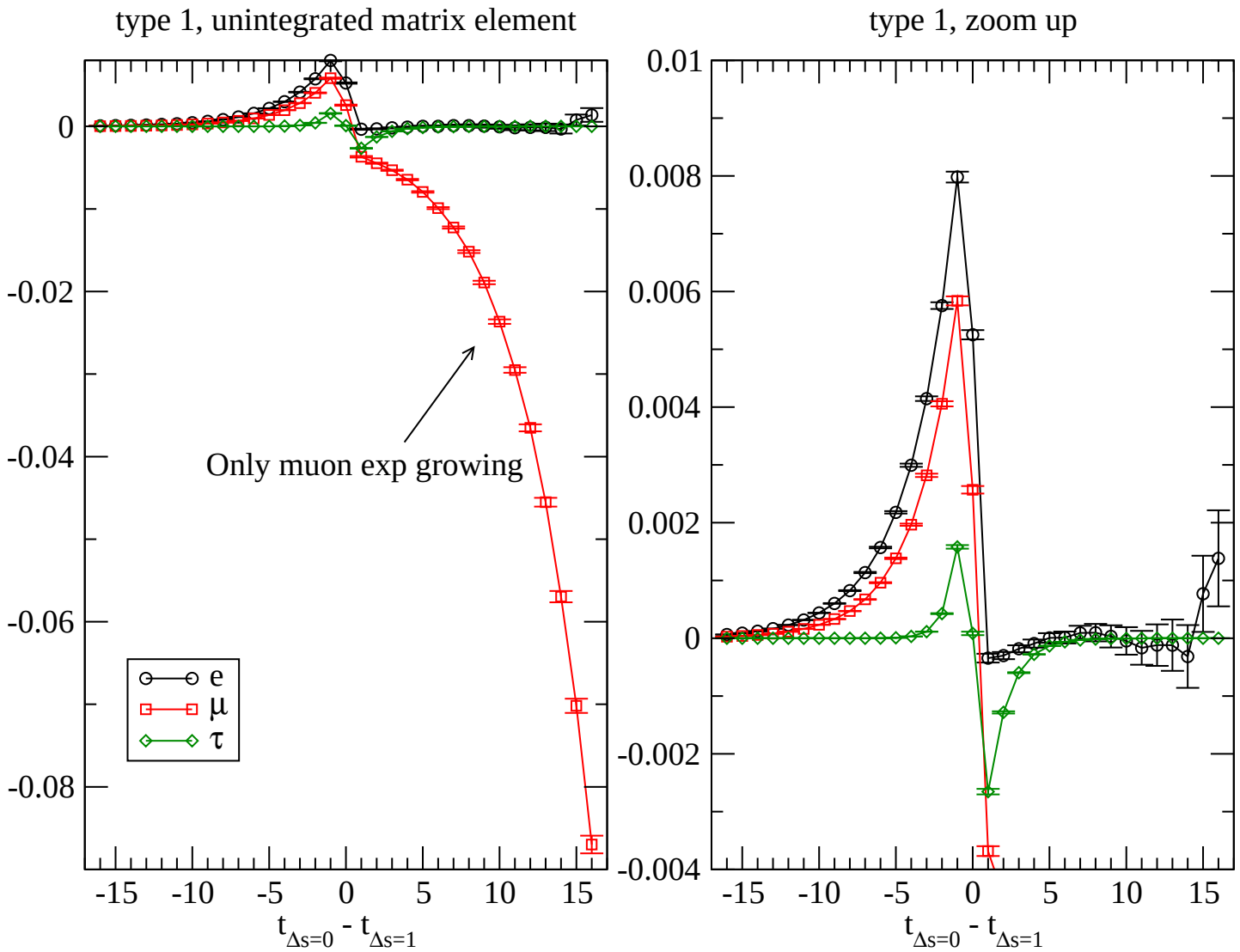

- e mode: no exp growing contamination due to helicity suppression
- τ mode: no exp growing contamination since tau is heavy

Integrated matrix element

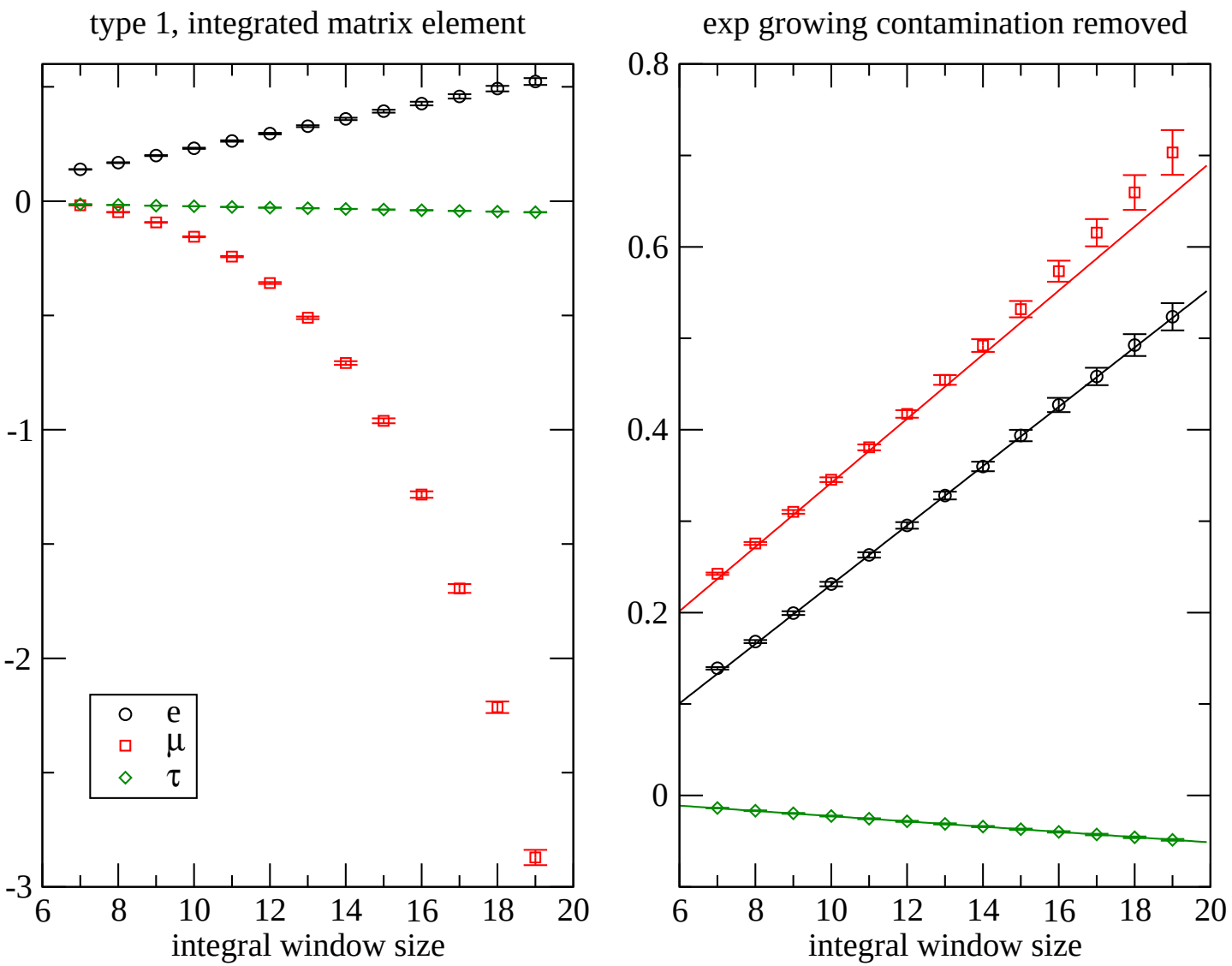

Right figure: the slope of the curve gives the $F^{\ell}(p_K, p_\nu, p_{\bar{\nu}})$

F^ℓ for type 1 diagram

F^ℓ	lattice	model
e	$3.244(90) \times 10^{-2}$	$3.352(12) \times 10^{-2}$
μ	$3.506(77) \times 10^{-2}$	$3.511(13) \times 10^{-2}$
τ	$-2.871(70) \times 10^{-3}$	$-2.836(10) \times 10^{-3}$

- vacuum state dominance model assuming only single-lepton contribution in the intermediate state

$$f_K f_\pi \bar{u}(p_\nu) \not{p}_K (1-\gamma_5) \frac{\not{q}}{q^2 - m_\ell^2} \not{p}_\pi (1-\gamma_5) v(p_{\bar{\nu}})$$
$$= f_K f_\pi \frac{2q^2}{q^2 - m_\ell^2} \bar{u}(p_\nu) \not{p}_K (1-\gamma_5) v(p_{\bar{\nu}})$$

with $q = p_K - p_\nu = p_\pi + p_{\bar{\nu}}$

- in the above table, model values are given by $Z_A^{-2} f_K f_\pi \frac{2q^2}{q^2 - m_\ell^2}$

Type 2 diagram

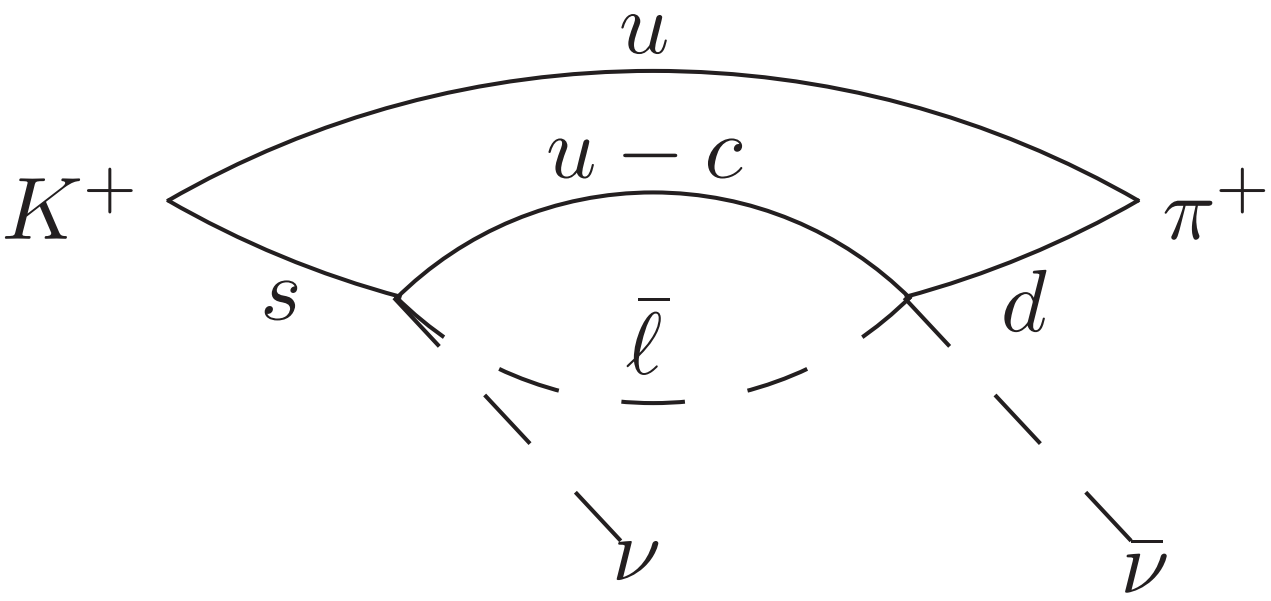

Type 2 diagram, left: unintegrated, right: integrated

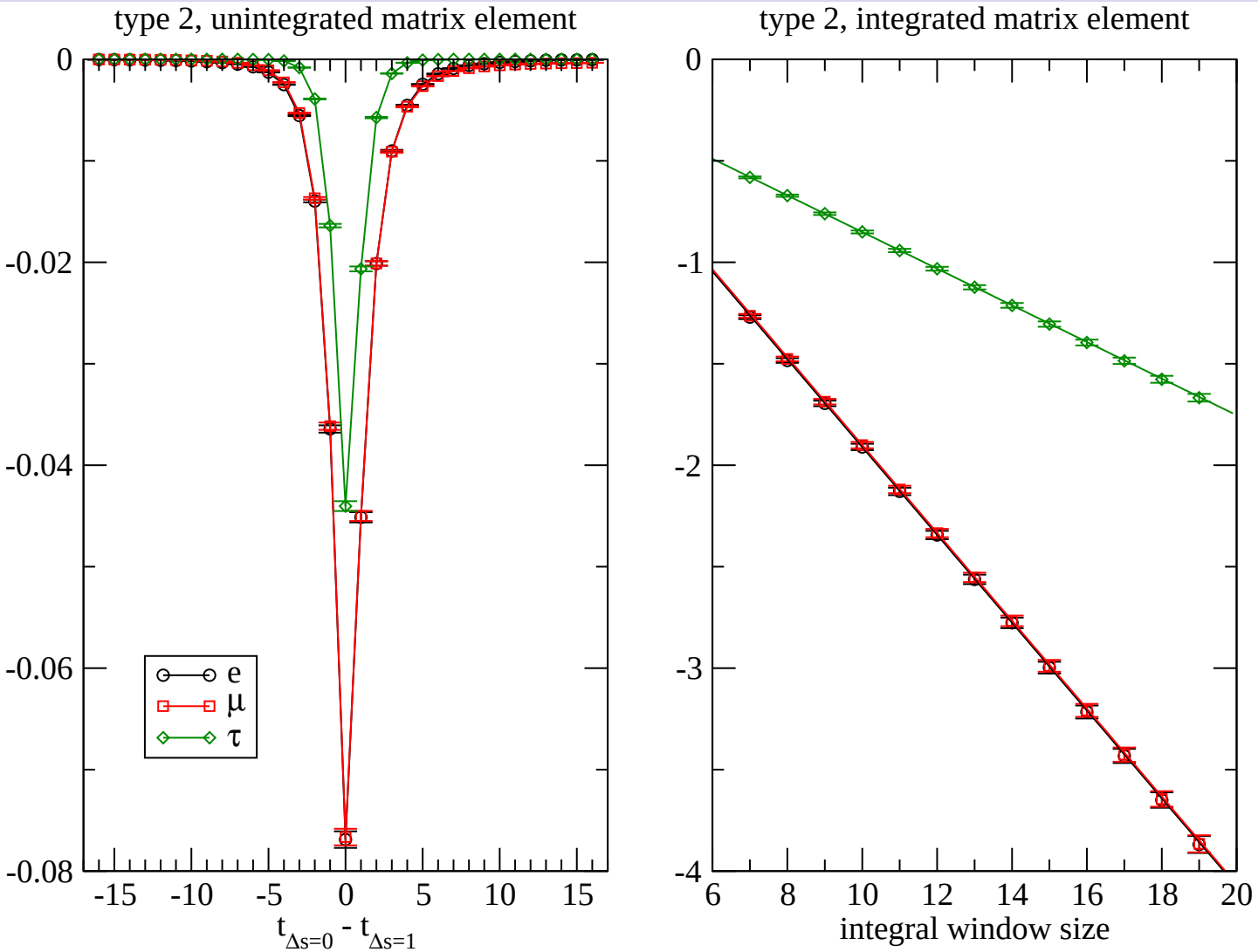

intermediate state is given by $\ell + \pi^0$, since pion is heavy, we don't observe significant exponential growing effects

SD divergence in type 2 diagram

- loop integral for type 2 diagram is log divergent (also in Z. Bai's case)
- in the physical world, the SD divergence is cut off by physical M_W
- in the lattice calculation it is cut off by an energy scale $\Lambda_{lat} \sim \frac{1}{a}$
- correction can be made through $A - A_{SD}^{lat} + A_{SD}^{cont} =$

$$\int d^4x \langle f|T\{O_1(x)O_2(0)\}|K\rangle - \langle f|C^{lat}(\mu^2)O_{SD}|K\rangle + \langle f|C^{cont}(\mu^2)O_{SD}|K\rangle \quad (6$$

- $C^{lat}(\mu^2)$ is determined non-perturbatively using RI/MOM approach
- $C^{cont}(\mu^2)$ can be calculated perturbatively, not yet done

Preliminary results

- type 1 diagram

F^ℓ	lattice	model
e	$3.244(90) \times 10^{-2}$	$3.352(12) \times 10^{-2}$
μ	$3.506(77) \times 10^{-2}$	$3.511(13) \times 10^{-2}$
τ	$-2.871(70) \times 10^{-3}$	$-2.836(10) \times 10^{-3}$

- type 2 diagram before subtraction

F^ℓ	lattice
e	$-2.164(31) \times 10^{-1}$
μ	$-2.164(31) \times 10^{-1}$
τ	$-9.03(14) \times 10^{-2}$

- type 2 diagram after subtraction, using $C^{lat}(\mu^2)$

F^ℓ	$\mu^2 = (2\ \text{GeV})^2$	$\mu^2 = (3\ \text{GeV})^2$
e	$-1.400(31) \times 10^{-1}$	$-1.849(31) \times 10^{-1}$
μ	$-1.402(31) \times 10^{-1}$	$-1.850(31) \times 10^{-1}$
τ	$-4.13(14) \times 10^{-2}$	$-6.68(14) \times 10^{-2}$

Conclusion

- so far we focus on the discussion of the W-box diagram
- in the final result, it should be W-box + Z-exchange
- type 1 diagram, single-lepton state dominates the contribution, excited states very highly suppressed (OZI rule)
- type 2 diagram, contribution (before sub.) 6 times larger than type 1, (after sub.) 4-5 times larger
- ChPT [hep-ph/0503107] consider type 1 diagram as $O(p^2)$ contribution and type 2 as $O(p^4)$, thus type 2 $\ll$ type 1
- for type 2 diagram, correct cont. SD contribution need to be included
- since type 2 diagram involve $\ell + \pi^0$, FV effects need to be esitmated

Ongoing search for the H-dibaryon in two-flavor lattice QCD

Anthony Francis* **Jeremy Green** **Parikshit Junnarkar**
Chuan Miao **Thomas Rae** **Hartmut Wittig**

Multi-Hadron and Nonlocal Matrix Elements in Lattice QCD
06.02.2015

YORK UNIVERSITÉ UNIVERSITY
HELMHOLTZ GEMEINSCHAFT
Helmholtz-Institut Mainz
PRISMA Cluster of Excellence

Outline

Why the H-dibaryon?
- Experimental constraints
- The lattice perspective
- A laboratory system

Our ongoing search
- Local six-quark interpolating operators
- All-mode averaging
- Lattice results
- Extending the basis
- Hint of a bound state

Summary

Why the H-dibaryon?

Quark bag model: A stable dibaryon

VOLUME 38, NUMBER 5 PHYSICAL REVIEW LETTERS 31 JANUARY 1977

Perhaps a Stable Dihyperon*

R. L. Jaffe†
Stanford Linear Accelerator Center, Stanford University, Stanford, California 94305, and Department of Physics and Laboratory of Nuclear Science,‡ Massachusetts Institute of Technology, Cambridge, Massachusetts 02139
(Received 1 November 1976)

In the quark bag model, the same gluon-exchange forces which make the proton lighter than the $\Delta(1236)$ bind six quarks to form a stable, flavor-singlet (with strangeness of -2) $J^P=0^+$ dihyperon (H) at 2150 MeV. Another isosinglet dihyperon (H^*) with $J^P=1^+$ at 2335 MeV should appear as a bump in $\Lambda\Lambda$ invariant-mass plots. Production and decay systematics of the H are discussed.

TABLE I. Quantum numbers and masses of S-wave dibaryons.

$SU(6)_{cs}$ representation	C_6	J	$SU(3)_f$ representation	Mass in the limit $m_s=0$ (MeV)
490	144	0	$\underline{1}$	1760
896	120	1,2	$\underline{8}$	1986
280	96	1	$\underline{10}$	2165
175	96	1	$\underline{10}^*$	2165
189	80	0,2	$\underline{27}$	2242
35	48	1	$\underline{35}$	2507
1	0	0	$\underline{28}$	2799

- Stable dibaryon with: $I=0,\ S=-2,\ J^P=0^+$
- Proposed in 1976:
  - deep binding $\rightarrow$ exp. excluded
  - shallow binding $\rightarrow$ possible
- Interesting question for lattice QCD

Experimental constraints: The "Nagara"-event

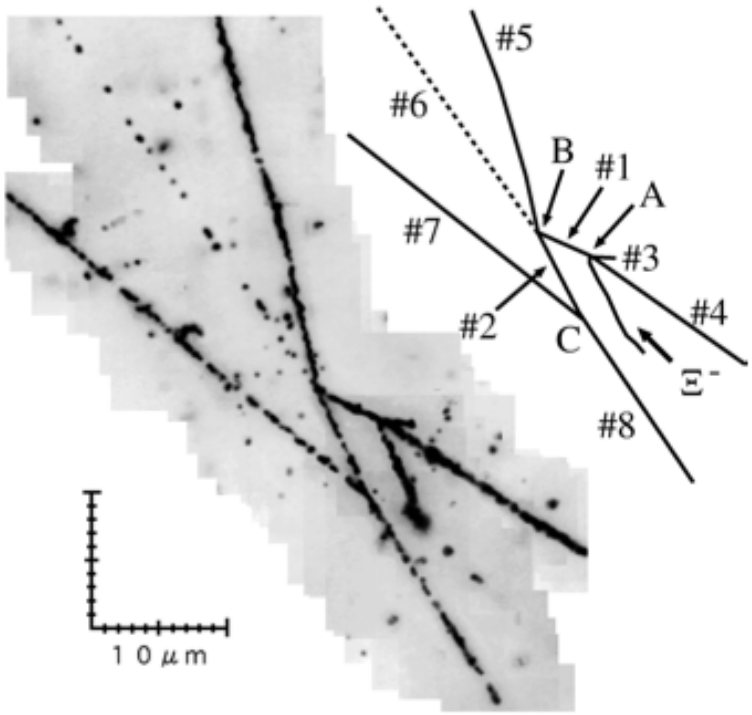

FIG. 2. Photograph and schematic drawing of NAGARA event. See text for detailed explanation.

(H. Takahashi *et al.*, PRL **87**, 212502 (2001))

"Nagara"-event at KEK (2001):

- discovery of a ${}^{6}_{\Lambda\Lambda}\mathrm{He}$ double hypernucleus

$$E_{\Lambda\Lambda} = 6.91 \pm 0.16\mathrm{MeV}.$$

- strong constraint on the existence of the H-dibaryon, since

$$m_H \overset{!}{>} 2m_\Lambda - B_{\Lambda\Lambda}$$

- i.e. its binding energy E_H must be smaller than $E_{\Lambda\Lambda}$
- due to the absence of ${}^{6}_{\Lambda\Lambda}\mathrm{He} \to {}^{4}\mathrm{He} + H$

The lattice perspective

- Shallow binding $E_H < 7\text{MeV}$ is a challenge for lattice QCD
- But: H is a good *stepping stone calculation* for lattice multi-hadron systems and lattice nuclear physics
- Number of Wick contractions required goes like $N = \prod_i^{N_f} N_{q_i}!$
  - The $H = udsuds$ has $N = 2!2!2! = 8$ Wick contraction terms
  - Can be done even by brute force
  - Ideal test-bed for advanced contraction algorithms
- No antiquarks in the operator $\Rightarrow$ No need for all-to-all propagators (counter example: $\pi\pi$-systems)
- Rule of thumb: Operators with heavy quarks are less noisy

The H-dibaryon as a laboratory: $\Delta\Delta$ from WASA@COSY

ABC Effect in Basic Double-Pionic Fusion --- Observation of a new resonance?

WASA-at-COSY Collaboration (P. Adlarson (Uppsala U.) *et al.*) Show all 123 authors

Apr 2011

Phys.Rev.Lett. 106 (2011) 242302
DOI: 10.1103/PhysRevLett.106.242302
e-Print: arXiv:1104.0123 [nucl-ex] | PDF

Abstract (arXiv)
We report on a high-statistics measurement of the basic double pionic fusion reaction $pn \to d\pi^0\pi^0$ over the energy region of the so-called ABC effect, a pronounced low-mass enhancement in the $\pi\pi$-invariant mass spectrum. The measurements were performed with the WASA detector setup at COSY. The data reveal the ABC effect to be associated with a Lorentzian shaped energy dependence in the integral cross section. The observables are consistent with a resonance with $I(J^P) = 0(3^+)$ in both pn and $\Delta\Delta$ systems. Necessary further tests of the resonance interpretation are discussed.

Evidence for a New Resonance from Polarized Neutron-Proton Scattering

WASA-at-COSY Collaboration (P. Adlarson (Uppsala U.) *et al.*) Show all 109 authors

Feb 27, 2014 - 6 pages

Phys.Rev.Lett. 112 (2014) 202301
(2014-05-23)
DOI: 10.1103/PhysRevLett.112.202301
e-Print: arXiv:1402.6844 [nucl-ex] | PDF
Experiment: WASA-COSY

Abstract (APS)

Exclusive and kinematically complete high-statistics measurements of quasifree polarized n→p scattering have been performed in the energy region of the narrow resonancelike structure d* with I(JP)=0(3+), M≈2380 MeV, and Γ≈70 MeV observed recently in the double-pionic fusion channels pn→dπ0π0 and pn→dπ+π-. The experiment was carried out with the WASA detector setup at COSY having a polarized deuteron beam impinged on the hydrogen pellet target and utilizing the quasifree process d→p→np+pspectator. This allowed the np analyzing power, Ay, to be measured over a broad angular range. The obtained Ay angular distributions deviate systematically from the current SAID SP07 NN partial-wave solution. Incorporating the new Ay data into the SAID analysis produces a pole in the D33−G33 waves in support of the d* resonance hypothesis.

- Evidence of a resonance (dibaryon?) in the $\Delta\Delta$ channel at COSY
- Here we have $\Delta\Delta = uuuuuu$ with $6! = 720$ Wick contraction terms
- Much harder for lattice $\Rightarrow$ Gain experience with *udsuds*

Rcent lattice calculations

- Past lattice efforts have found a bound H-dibaryon at $M_\pi > M_\pi^{\mathrm{phys.}}$
- It is not clear yet if it is bound or unbound at the physical point

Group	Method	N_f	N_{vol}	$M_\pi[\mathrm{MeV}]$	$B_H[\mathrm{MeV}]$
HALQCD	B-B potentials	3	1	1171	49.1(3.4)(5.5)
			3	1015	37.2(3.7)(2.4)
			1	837	37.8(3.1)(4.1)
			1	672	33.6(4.8)(3.5)
			1	469	26(4.4)(4.8)
NPLQCD	2pt	3	3	806	74.6(3.3)(3.4)
		2+1	4	390	13.2(1.8)(4.0)
			1	230	-0.6(8.9)(10.3)

- Our search so far has been focused on $N_f = 2$ ensembles with $M_\pi = 451$MeV and $M_\pi = 1$GeV $\rightarrow$ here only $M_\pi = 1$GeV shown

Our ongoing search

Local six-quark interpolating operators

We use six parity-projected quarks to form six-quark interpolating operators of the form:

$$[abcdef] = \epsilon^{ijk}\epsilon^{lmn}(b_i^T C\gamma_5 P_+ c_j)(e_l^T C\gamma_5 P_+ f_m)(a_k^T C\gamma_5 P_+ d_n),$$

In the case $m_u = m_d$, two operators can be formed in this way that couple to the H-dibaryon:

$$H^{\mathbf{1}} = \frac{1}{48}\left([sudsud] - [udusds] - [dudsus]\right)$$
$$H^{\mathbf{27}} = \frac{1}{48\sqrt{3}}\left(3[sudsud] + [udusds] + [dudsus]\right),$$

these belong to the singlet and 27-plet irreps of flavour $SU(3)_f$.

Contractions using a blocking algorithm

An efficient way to contract the six-quark operators into correlation functions is to use a blocking algorithm:

- Form blocks of three propagators contracted into a color-singlet at the source

$$B(\alpha_1, \xi_1', \xi_2', \xi_3') = \epsilon_{c_1,c_2,c_3}(C\gamma_5 P_+)_{\alpha_2\alpha_3} S_l(\xi_1, \xi_1') S_l(\xi_2, \xi_2') S_s(\xi_3, \xi_3')$$

- Then sum over all permutations when contracting at the sink

$$[sudsud] = (C\gamma_5 P_+)_{\alpha\beta} \times \epsilon_{c_1',c_2',c_3'}\epsilon_{c_4',c_5',c_6'}(C\gamma_5 P_+)_{\alpha_2'\alpha_3'}(C\gamma_5 P_+)_{\alpha_5'\alpha_6'}$$
$$\sum_{\sigma_u,\sigma_d,\sigma_s} B(\alpha, \xi'_{\sigma_u(1)}, \xi'_{\sigma_d(2)}, \xi'_{\sigma_s(3)}) B(\beta, \xi'_{\sigma_u(4)}, \xi'_{\sigma_d(5)}, \xi'_{\sigma_s(6)})$$

Boosting the calculation: All-mode averaging

- Computing the propagator is the most costly part of the calculation
- AMA: Reduce the precision of propagator on multiple source locations $\Rightarrow$ correct the introduced bias via

$$\mathcal{O} = \mathcal{O}_{x_0}^{\text{high prec.}} - \mathcal{O}_{x_0}^{\text{low prec.}} + \frac{1}{N_{\Delta x}} \sum_{\Delta x} \mathcal{O}_{x_0+\Delta x}^{\text{low prec.}}$$

- Depending on the ensemble we gain a factor $\sim 1.5 - 2$ in speed

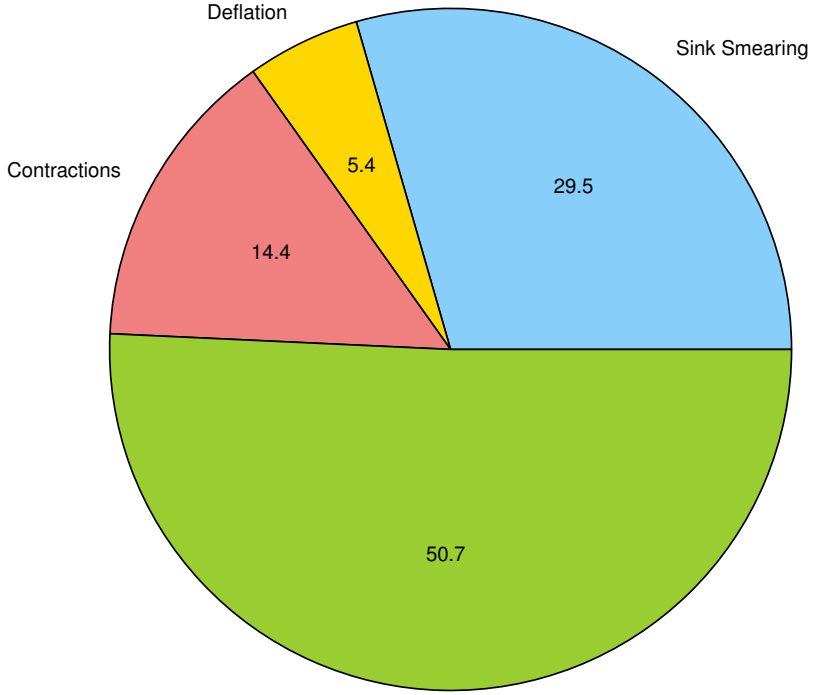

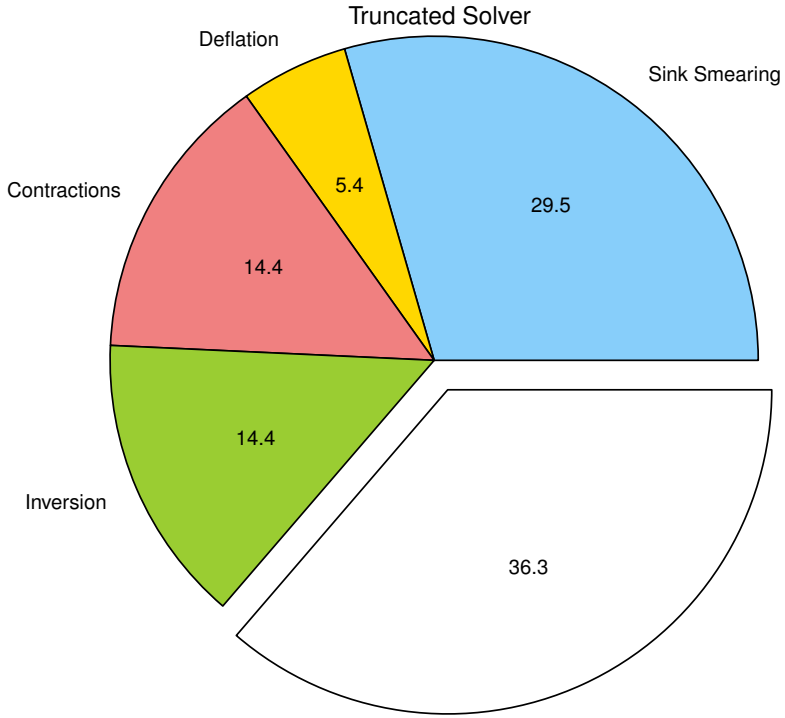

Results: E1 ensemble

- $L = 32,\ T = 64$ at $a = 0.063$fm
- $M_\pi = 1$GeV and $M_\pi L = 10$
- $N_{\mathrm{conf}} = 168$
- One high precision/low precision propagator solves for AMA bias
- $N_{src} = 128$ with low precision solves
- Double statistics using P_+ and P_- for the forward/backward propagating states
- In total this makes:

$$168 \times 128 \times 2 = 43008 \text{ measurements}$$

- $\kappa_s = \kappa_{ud}$ implies no mixing between the singlet and 27-plet irreps
- Multiple sets of smearing $\Rightarrow$ GEVP for ground state determination

Results: Effective masses

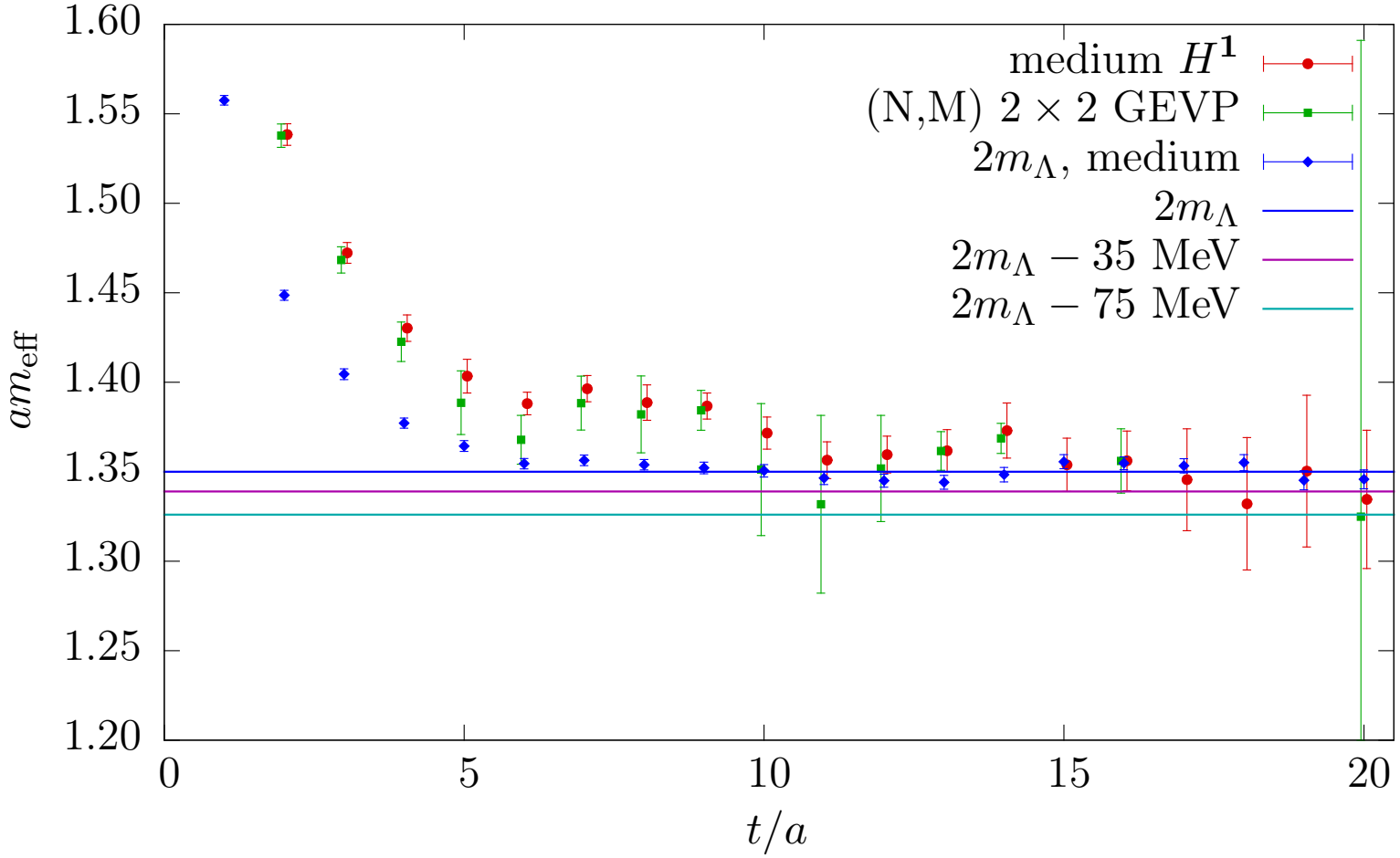

- At this point: No bound state seen with local six-quark operators

Results: Extending the basis

This was the status of our study using local six-quark operators, as presented at Lat'14. Possible issues:

- Insufficient statistics? Finite volume effects?
- Quenched strange quark

But, most importantly,

- we used only $\langle qqqqqq(x), \bar{q}\bar{q}\bar{q}\bar{q}\bar{q}\bar{q}(0)\rangle$ operators

Now, we extend our analysis and

- include $\langle qqq(x)qqq(y), \bar{q}\bar{q}\bar{q}\bar{q}\bar{q}\bar{q}(0)\rangle$ operators,
- more specifically, we compute the $SU(3)_f$ singlet combination:

$$H^1 = -\frac{1}{\sqrt{3}}\Lambda\Lambda + \Sigma\Sigma + \frac{2}{\sqrt{3}}\Xi N$$

Results: Hint of a bound state

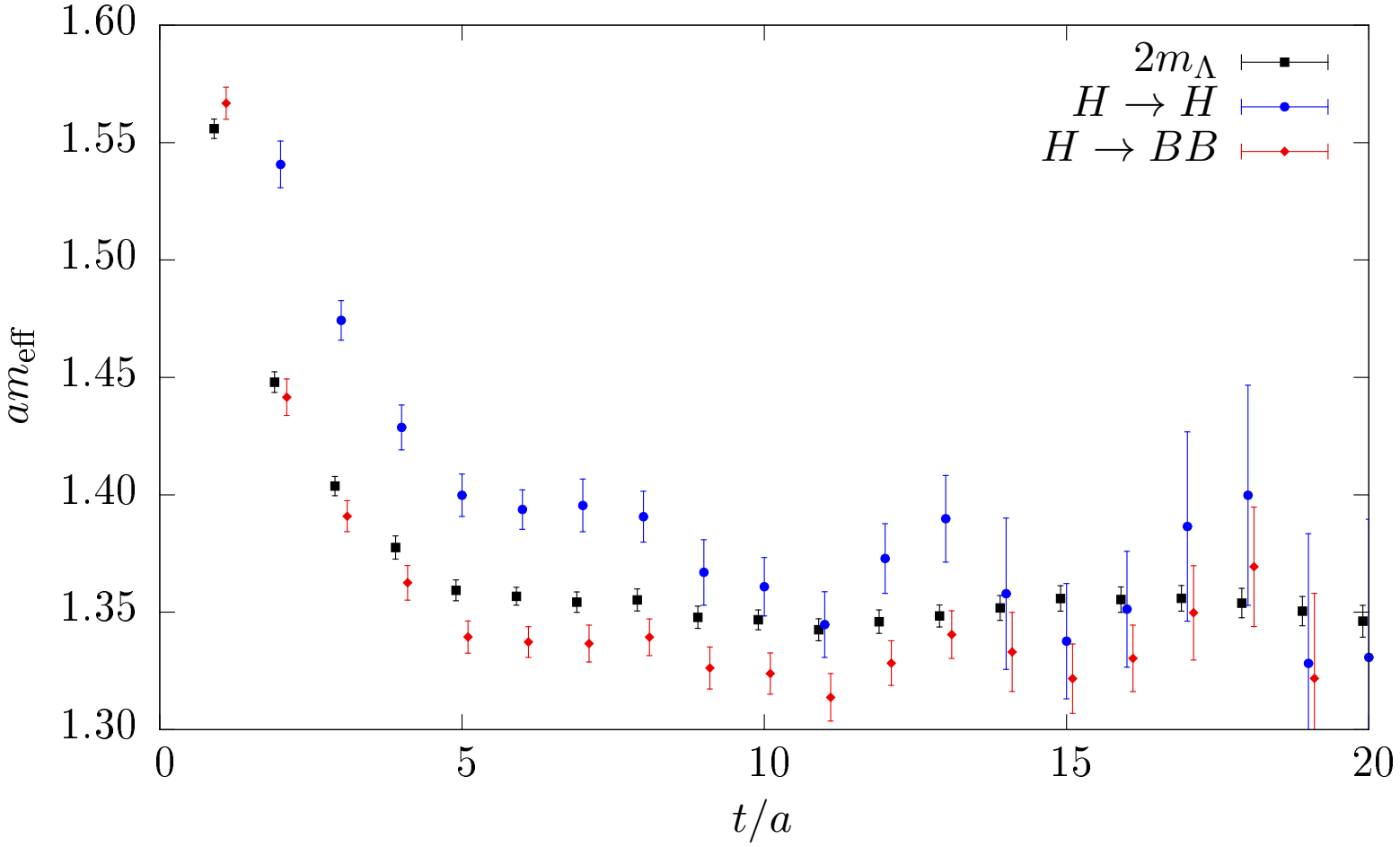

- At this point: Hint of a bound state using the new operators
- Next step, combine both analyses (combined fit? Matrix Prony?)

Summary

Summary

Status

- H-dibaryon is an interesting challenge for lattice QCD
- Laboratory system for learning to do e.g. the $\Delta\Delta$ or nuclear physics
- On our heavy ($M_\pi = 1\text{GeV}$) lattice we
  - calculated $\langle qqqqqq(x), \bar{q}\bar{q}\bar{q}\bar{q}\bar{q}\bar{q}(0)\rangle$ operators
  - extended our basis to $\langle qqq(x)qqq(y), \bar{q}\bar{q}\bar{q}\bar{q}\bar{q}\bar{q}(0)\rangle$ operators

  $\Rightarrow$ Hint of bound state

Outlook

- Combine analyses to determine ground state
- Reduce the mass (again) to $M_\pi = 451\text{MeV}$ (E5) and further to $M_\pi = 270$ (F7)

Lots to do!

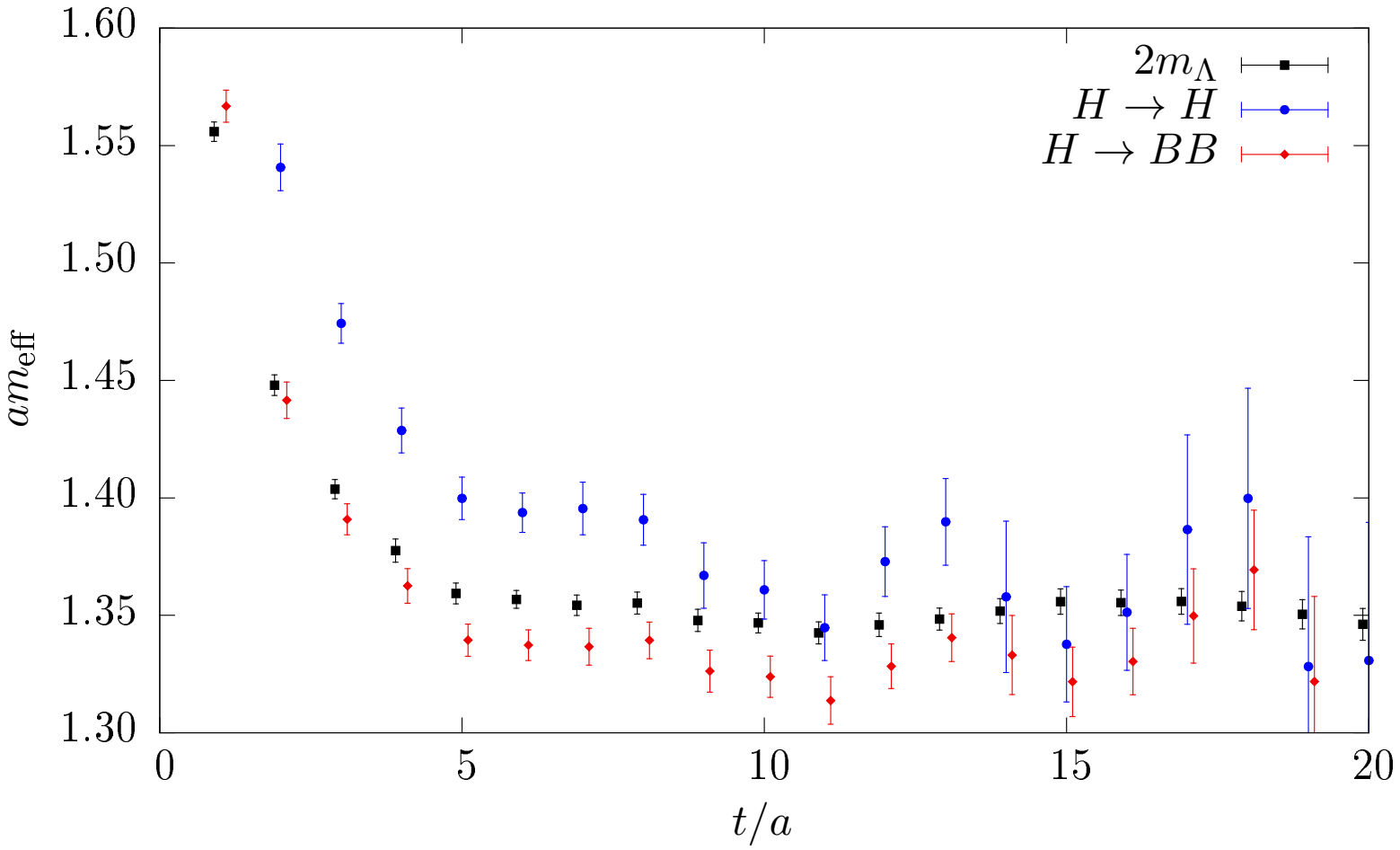
1.60
1.55
1.50
1.45
1.40
1.35
1.30
$am_{\rm eff}$
0
5
10
15
20
t/a
$2m_\Lambda$
$H \to H$
$H \to BB$

Three particles in a box: Mapping the finite-volume spectrum to the S-matrix

Maxwell T. Hansen

Institut für Kernphysik and HIM, JG-Universität Mainz

February 5th, 2014

MTH and Stephen R. Sharpe, arXiv:1408.5933, 2014
(published in PRD)

The three-particle quantization condition is a necessary first step for using LQCD to investigate...

resonances decaying to three or more hadrons

$\omega(782) \to \pi\pi\pi$ $\qquad$ $N(1440) \to N\pi\pi$

three-body forces

$\pi\pi\pi \to \pi\pi\pi$ $\qquad$ $NNN \to NNN$

The three-particle quantization condition is a necessary first step for using LQCD to investigate...

weak decays coupling to three or more hadrons

$K \to \pi\pi\pi$ $\quad$ $D \to \pi\pi$ $\quad$ $D \to K\overline{K}$

(couples to $\pi\pi\pi\pi$)

Need QCD scattering amplitudes to relate finite-volume lattice matrix elements to physical decay amplitudes

Lellouch, L. & Lüscher, M.
Commun. Math. Phys. 219, 31-44 (2001)

Outline

Two particle review

Three particle quantization condition

Relation to scattering amplitude

Conclusion

Particle content

Single scalar, mass m

all results for identical scalars

Relativistic field theory

$\mathbb{Z}_2$ **symmetry**

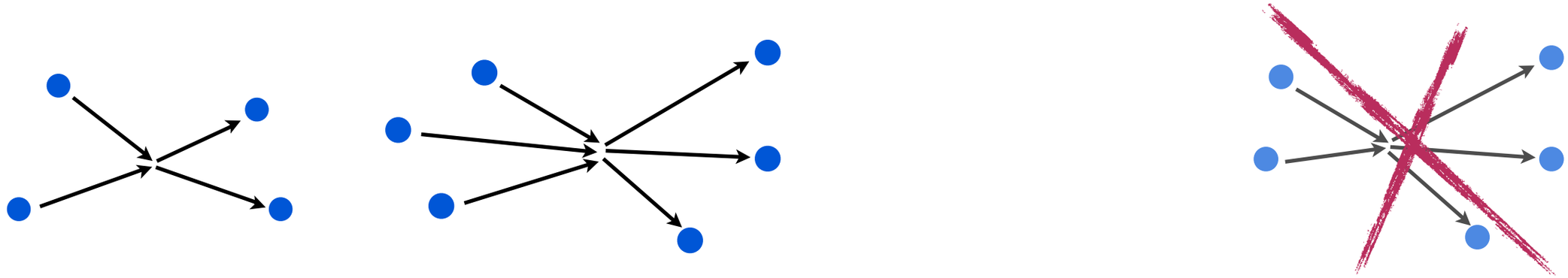

(For pions in QCD this is G-parity)

Include all vertices

with even number of legs

Finite volume

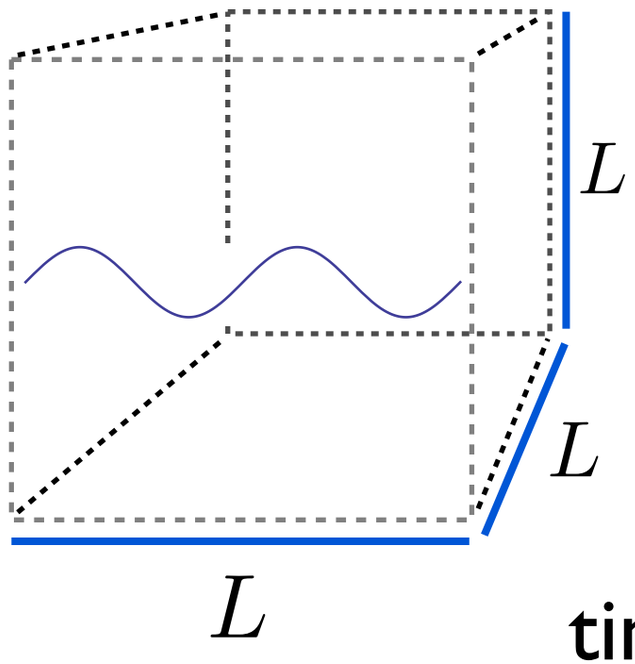

cubic, spatial volume (extent L)

periodic boundary conditions

$\vec{p} \in (2\pi/L)\mathbb{Z}^3$

time direction **infinite** and **Minkowski**

Take L large enough to ignore e^{-mL}

dropped throughout!

Take space to be continuous

lattice spacing set to zero

Two particles in a box

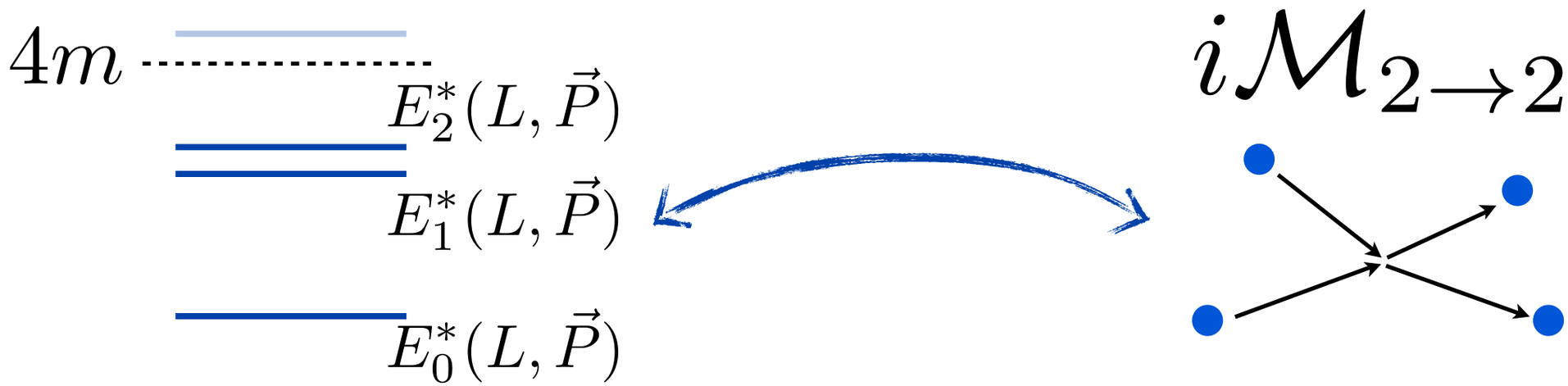

$$C_L(E,\vec{P}) \equiv \int_L d^4x\, e^{i(Ex^0 - \vec{P}\cdot\vec{x})} \langle 0|\mathrm{T}\sigma(x)\sigma^\dagger(0)|0\rangle$$

Require $E^* < 4m$ **even-particle quantum numbers**

Calculate $C_L(E,\vec{P})$ to all orders in perturbation theory and determine condition of divergence.

Following Kim, Sachrajda and Sharpe. *Nucl. Phys.* B727, 218-243 (2005)

Two particles in a box

1

$C_L(E, \vec{P}) =$

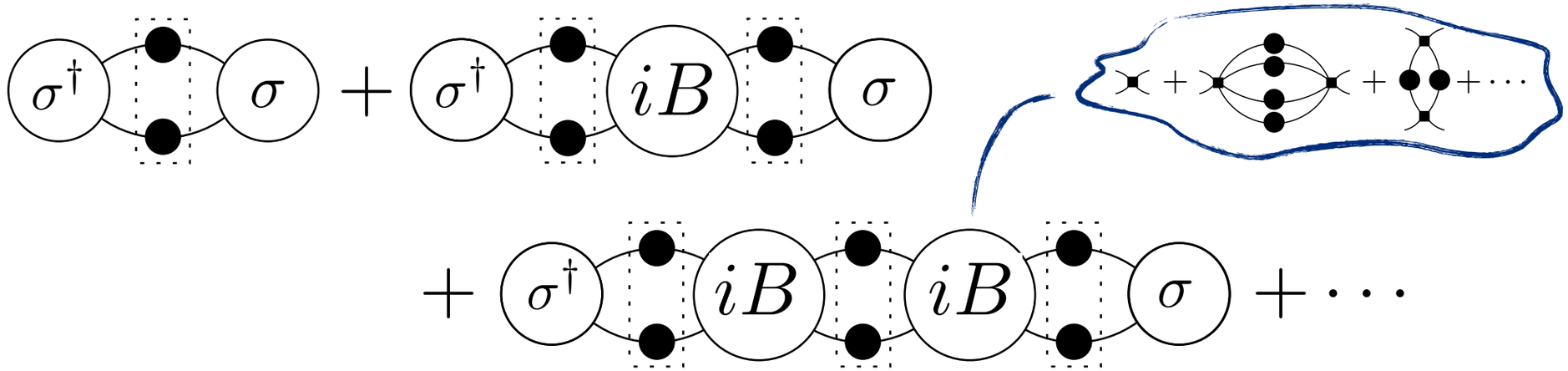

Two particles in a box

1

$C_L(E,\vec{P}) =$

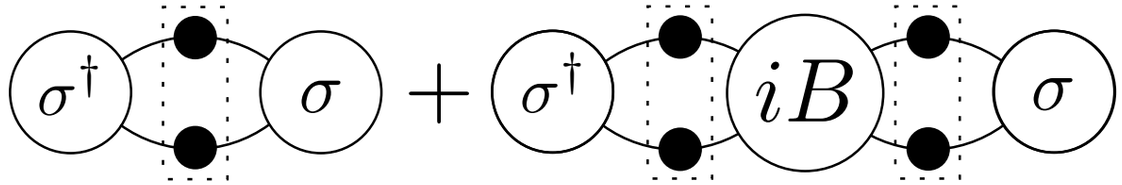

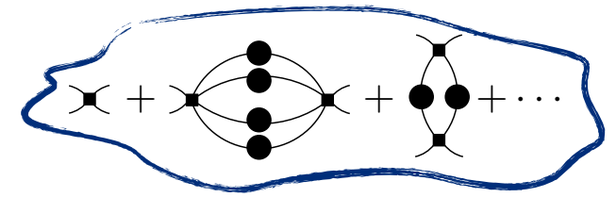

2

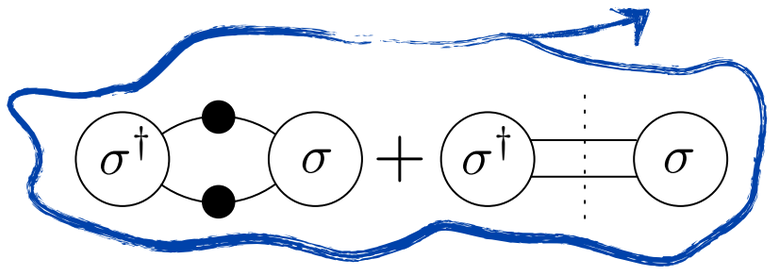

$+$

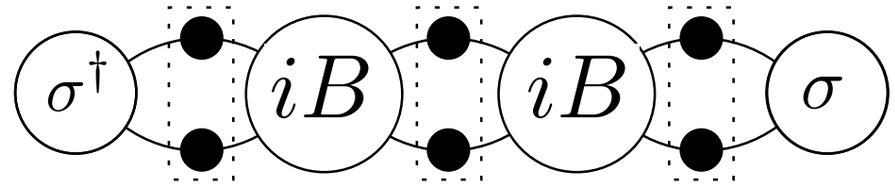

$+ \cdots$

Two particles in a box

1

$$C_L(E,\vec{P}) =$$

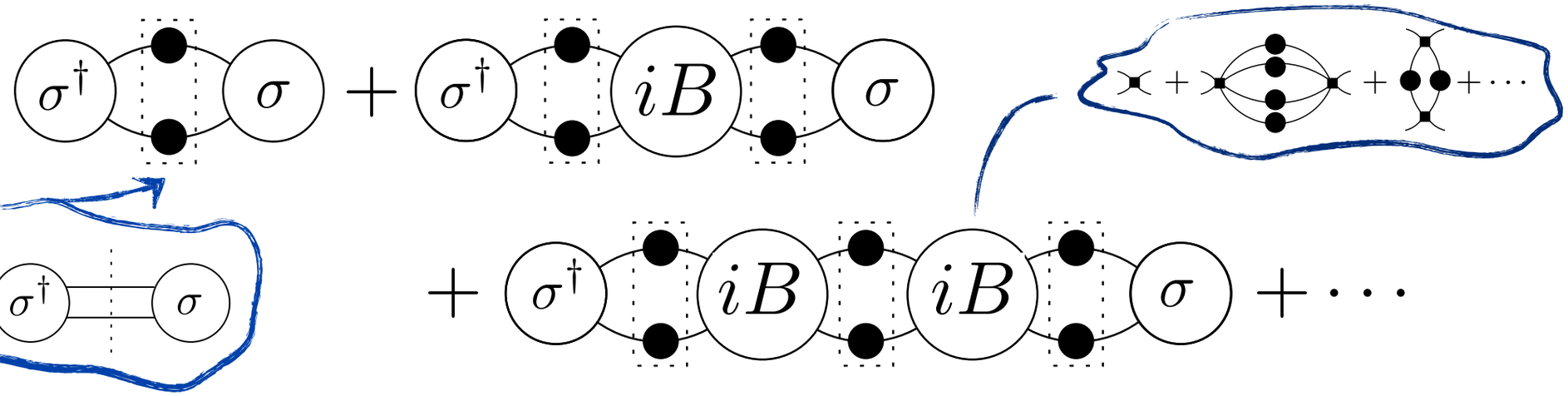

2

$$C_L(E,\vec{P}) = C_\infty(E,\vec{P})$$

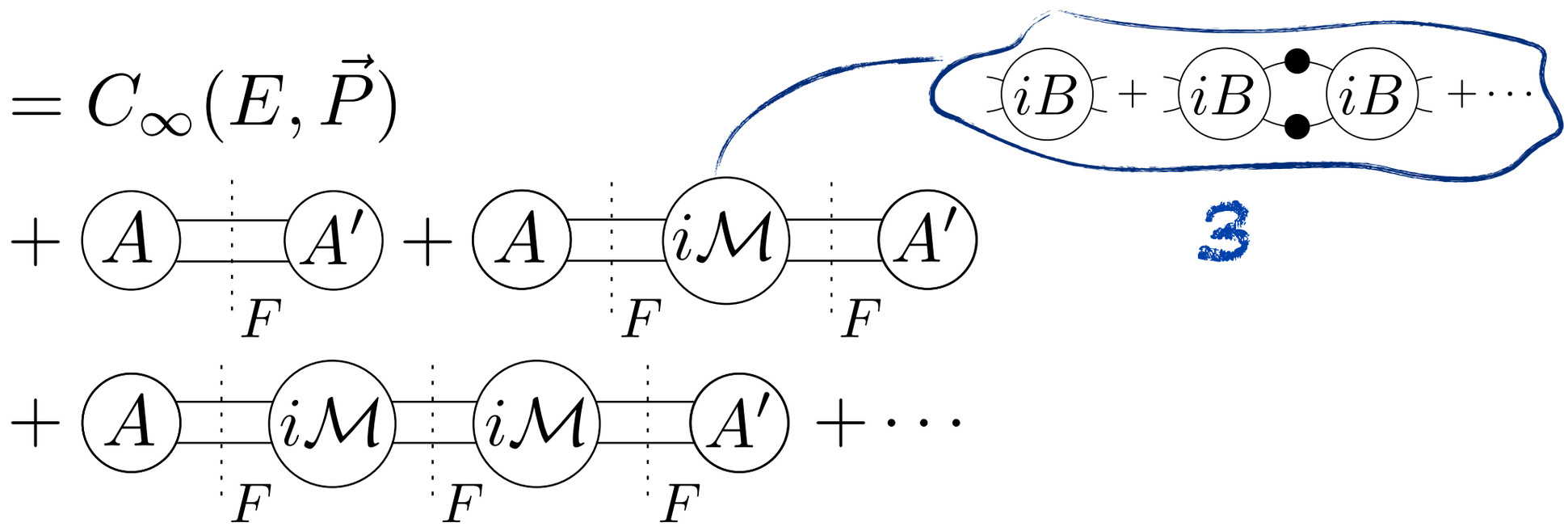

3

Two particles in a box

1

$$C_L(E,\vec{P}) =$$

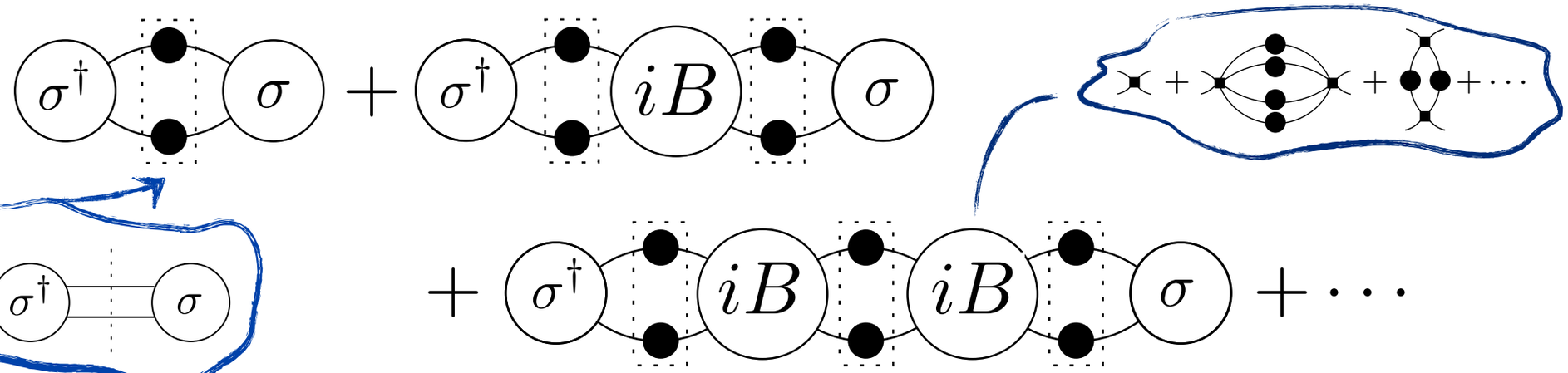

2

$$C_L(E,\vec{P}) = C_\infty(E,\vec{P})$$

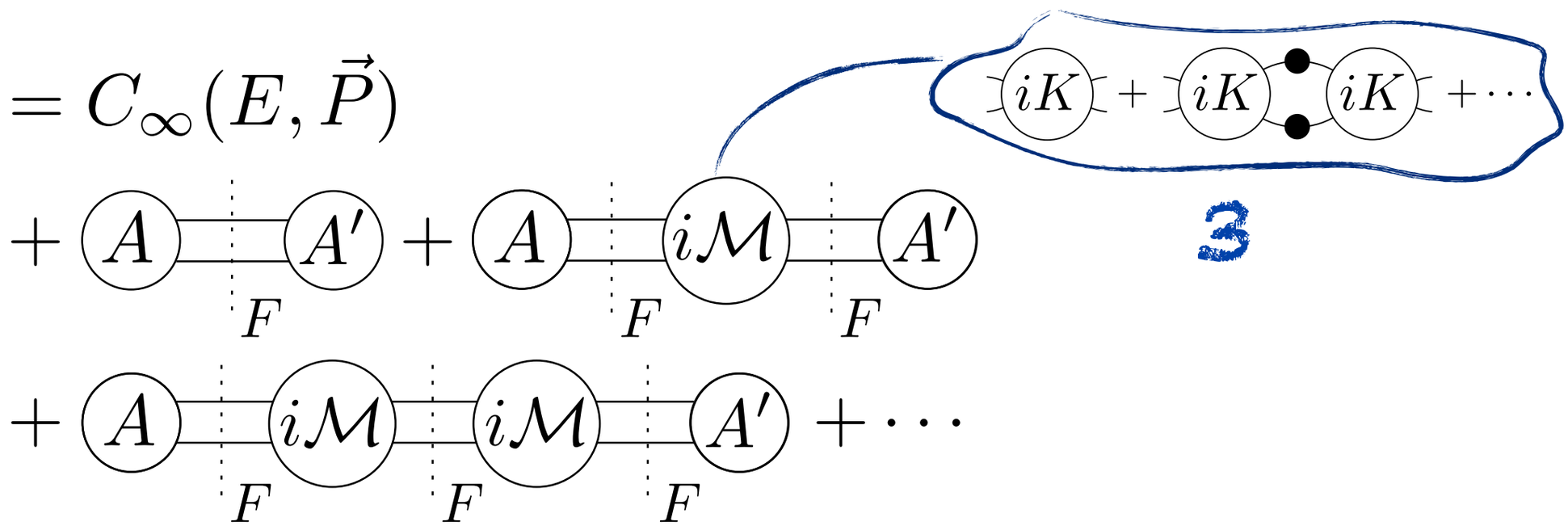

3

4

$$C_L(E,\vec{P}) = C_\infty(E,\vec{P}) + A' iF \frac{1}{1 - i\mathcal{M}_{2\to 2} iF} A$$

Two-particle result

At fixed $(L, \vec{P})$, finite-volume spectrum is all solutions to

$$\Delta_{L,P}(E) = \det[1 - i\mathcal{M}_{2\to 2} iF] = 0$$

diagonal matrix in angular momentum space

kinematic (related to Lüscher Zeta function)

$F \equiv$ 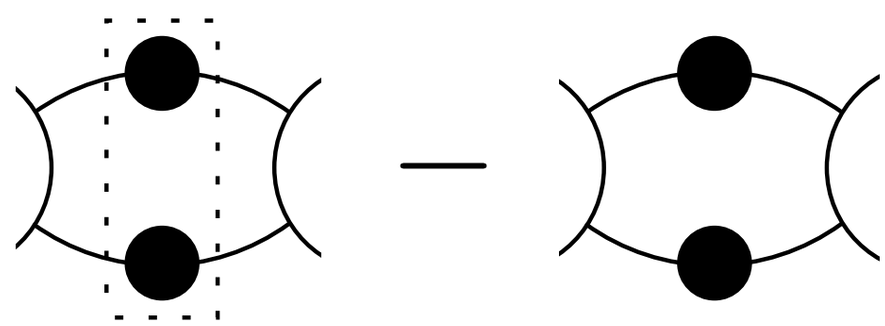

Two-particle result

$$\Delta_{L,P}(E) = \det[1 - i\mathcal{M}_{2\to 2} iF] = 0$$

...is it useful?

At low energies, s-wave dominates

$$[\mathcal{M}^s_{2\to 2}(E^*_n)]^{-1} = -F^s(E_n, \vec{P}, L)$$

$$F^s(E, \vec{P}, L) \equiv \frac{1}{2}\left[\frac{1}{L^3}\sum_{\vec{k}} - \int \frac{d^3k}{(2\pi)^3}\right] \frac{1}{2\omega_k 2\omega_{P-k}(E - \omega_k - \omega_{P-k} + i\epsilon)}$$

Two-particle result

Note also, equation is real

$$[\mathcal{M}^s_{2\to 2}(E^*_n)]^{-1} = -F^s(E_n, \vec{P}, L)$$

$$\boxed{p_n \cot\delta^s(p_n) - i\cancel{p}_n = -16\pi E^*_n \,\mathrm{Re}F^s - i\cancel{p}_n}$$

This can also be seen by **replacing i-epsilon with principal value** everywhere in derivation.

$$\mathcal{M}_{2\to 2} \longrightarrow \mathcal{K}_{2\to 2} \qquad\qquad F \longrightarrow \mathrm{Re}\, F$$

Important for three-particle case

Now, three particles in a box

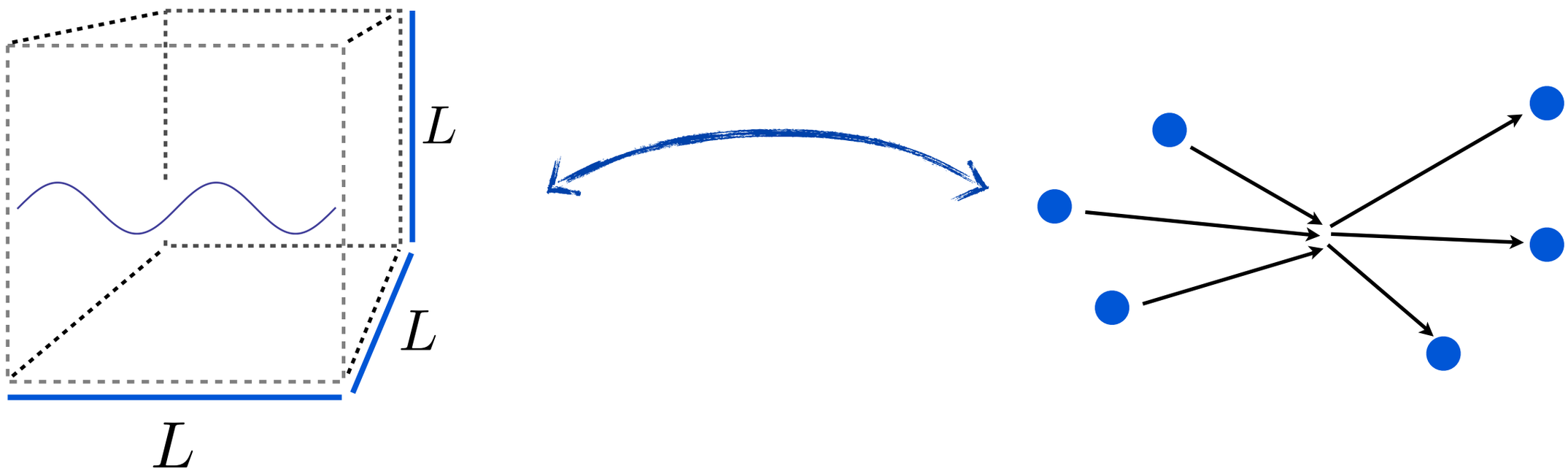

Three particles in a box

$$C_L(E,\vec{P}) \equiv \int_L d^4x\, e^{i(Ex^0-\vec{P}\cdot\vec{x})}\langle 0|\mathrm{T}\sigma(x)\sigma^\dagger(0)|0\rangle$$

Require $m < E^* < 5m$

odd-particle quantum numbers

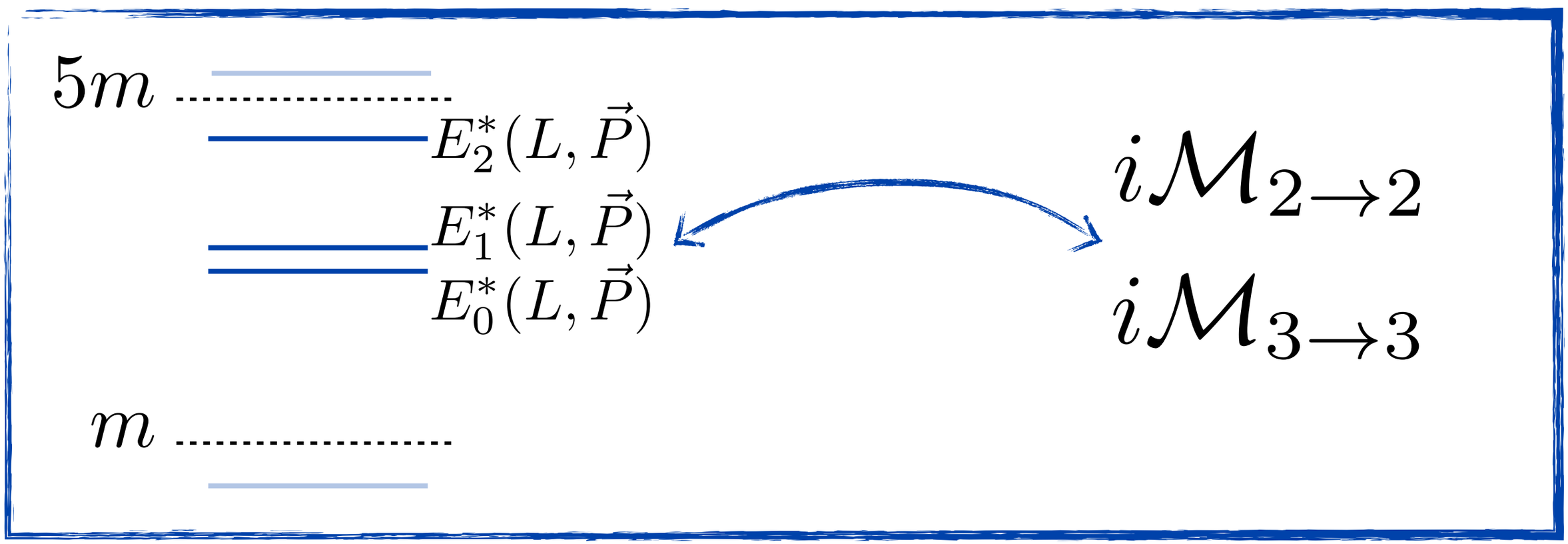

Assume no two-particle bound state

New skeleton expansion

$C_L(E,\vec{P}) \overset{?}{=}$ 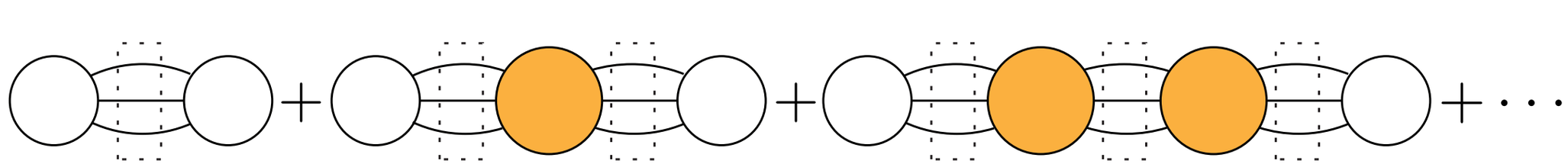

(propagators still fully dressed)

No! We also need diagrams like

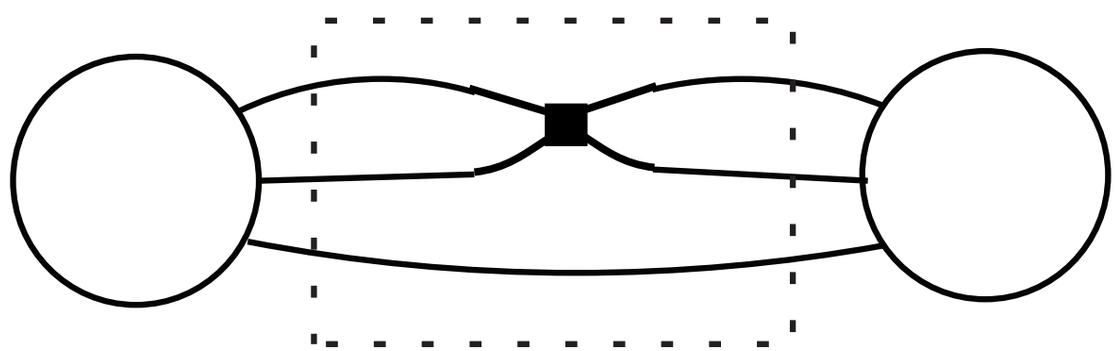

(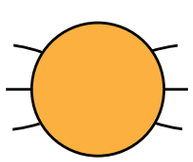 **should only contain connected diagrams)**

New skeleton expansion

$C_L(E, \vec{P}) =$

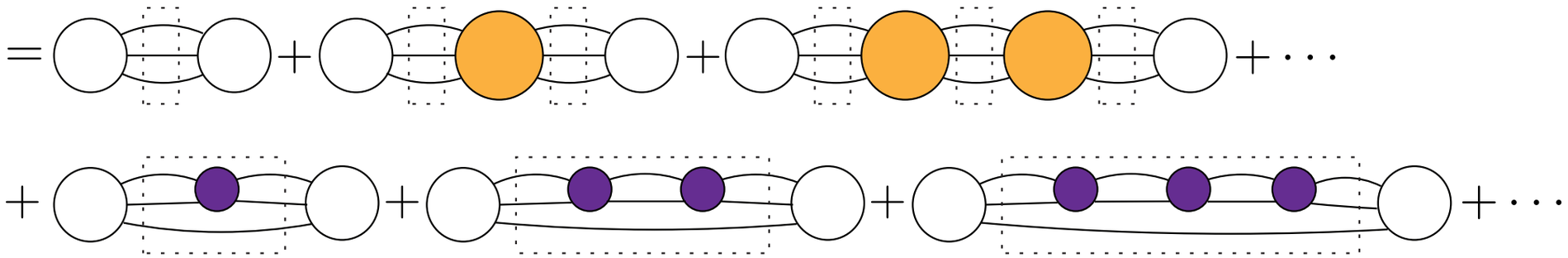

Kernel definitions:

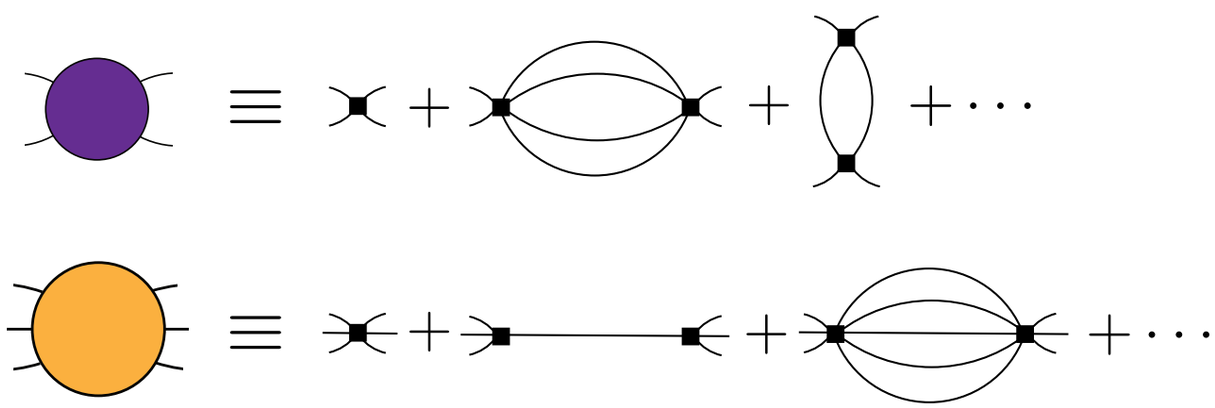

New skeleton expansion

$C_L(E, \vec{P}) =$

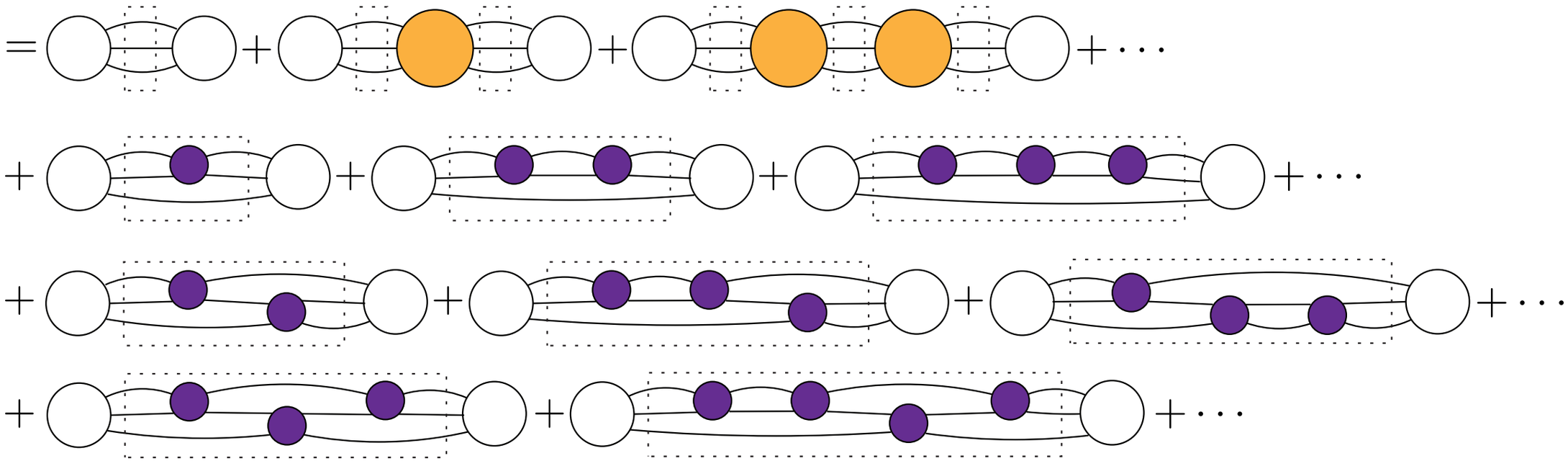

Kernel definitions:

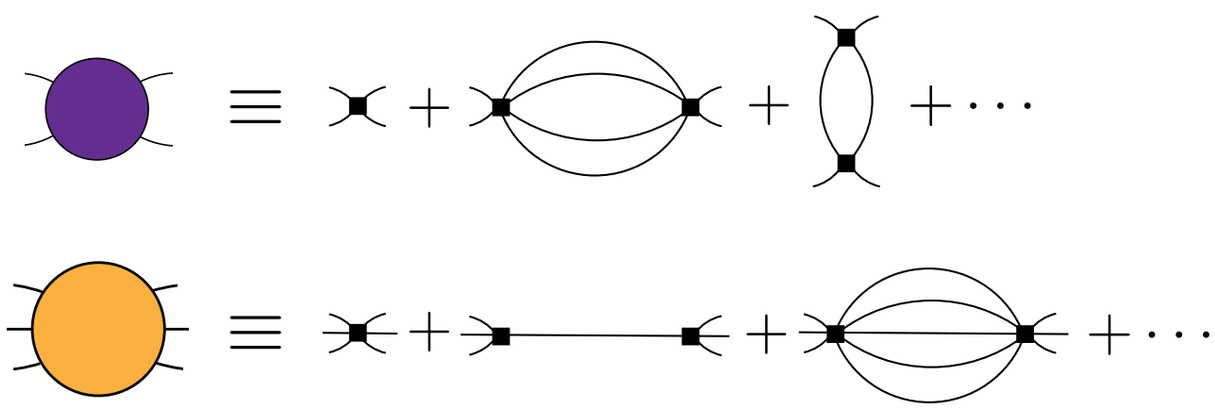

New skeleton expansion

$C_L(E, \vec{P}) =$

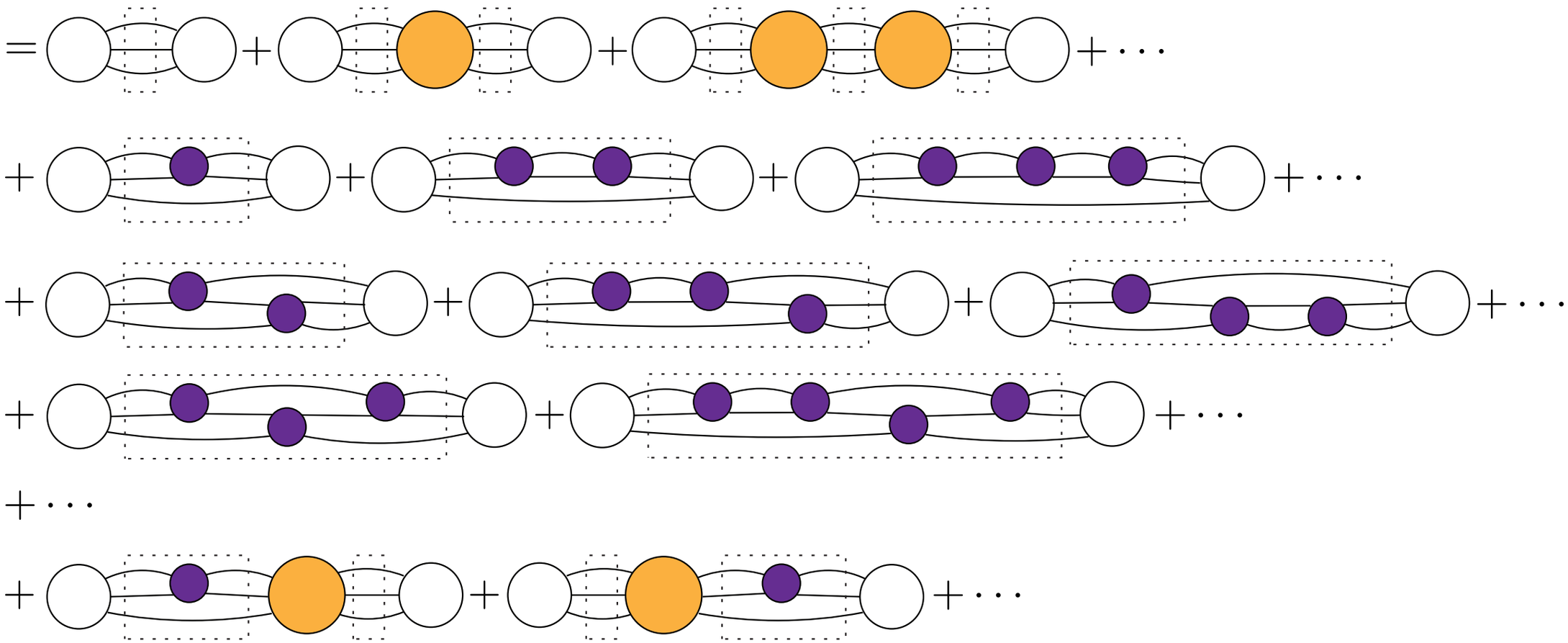

Kernel definitions:

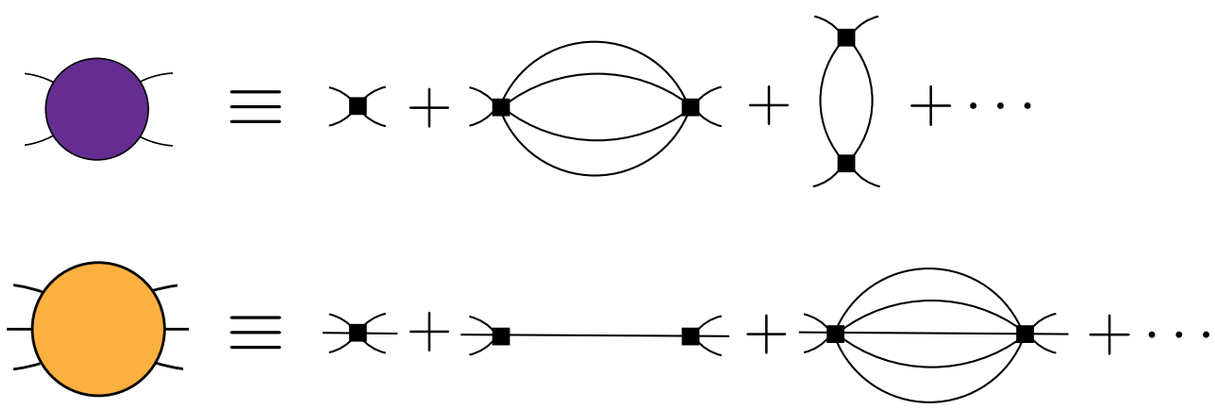

New skeleton expansion

$C_L(E, \vec{P}) =$

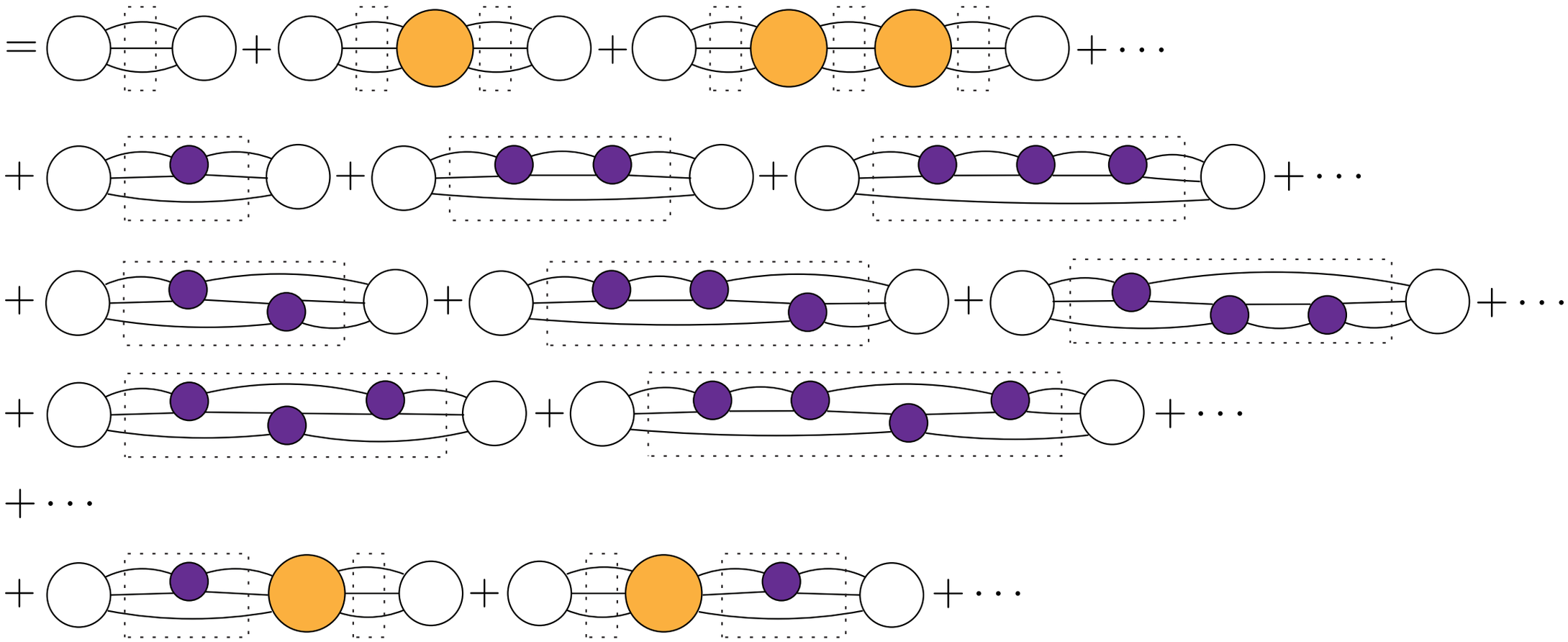

Compare to two-particle skeleton expansion

$C_L(E, \vec{P}) =$

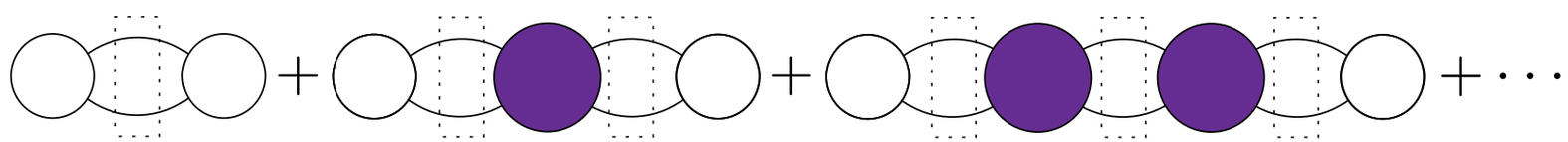

What is new here?

1. Degrees of freedom are different

two particles

two-particle angular momentum

three particles

$\vec{k}$ + **two-particle angular momentum**

Our result only depends on finite-volume $\vec{k}$

$$\vec{k} = \frac{2\pi}{L}\vec{n}$$

integer vector

What is new here?

2. Three particle divergences

Three particle observable $i\mathcal{M}_{3\to 3}$

contains the diagram

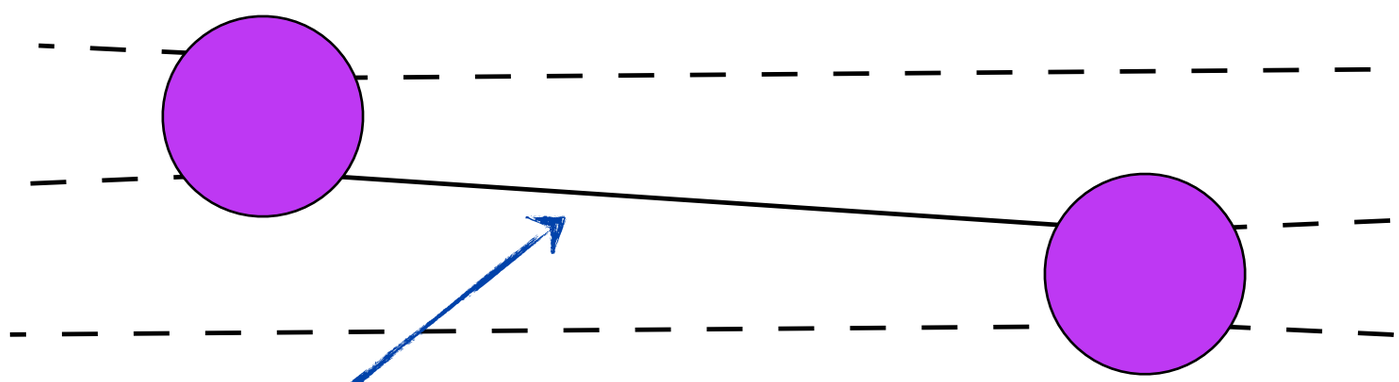

Certain external momenta put this on-shell → $i\mathcal{M}_{3\to 3}$ **has singularities**

What is new here?

2. Three particle divergences

Define $i\mathcal{M}_{\mathrm{df},3\to3}$

$$\equiv i\mathcal{M}_{3\to3} - \left[i\mathcal{M}_{2\to2} S i\mathcal{M}_{2\to2} + \int i\mathcal{M}_{2\to2} S i\mathcal{M}_{2\to2} S i\mathcal{M}_{2\to2} + \cdots \right]$$

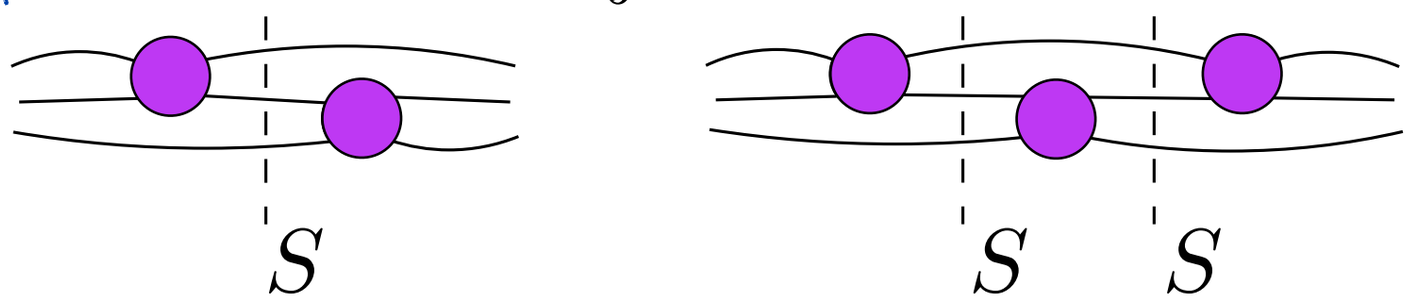

only on-shell amplitudes here

infinite series built with factors of $Si\mathcal{M}_{2\to2}$

This subtraction emerges naturally in our finite-volume analysis

What is new here?

3. Must now worry about sum crossing two-particle unitary cusp

two-particle scattering (real part)

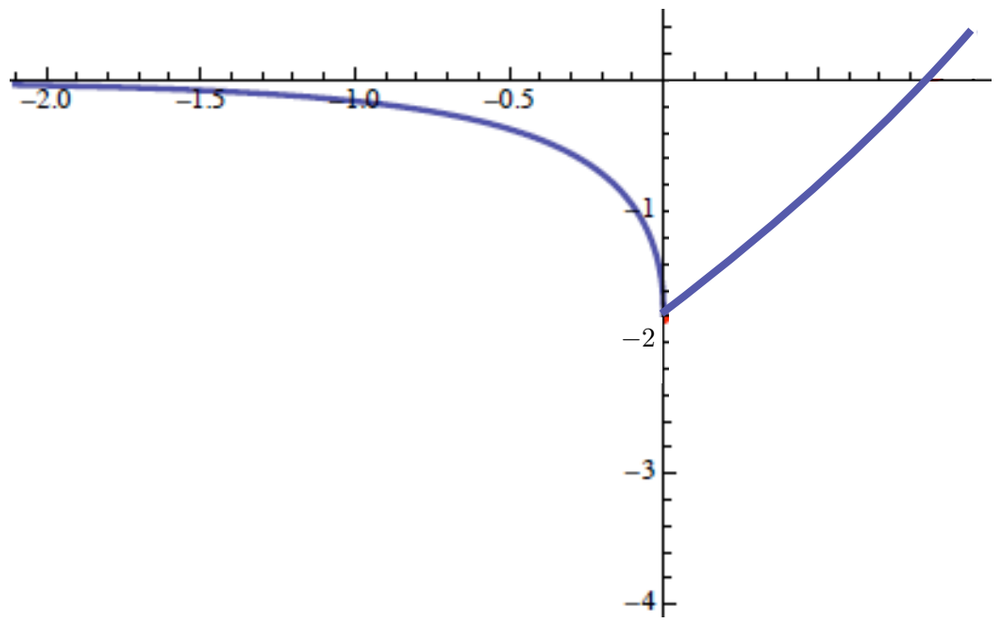

depends on k

two particle energy

$$\frac{1}{L^3}\sum_{\vec{k}}$$

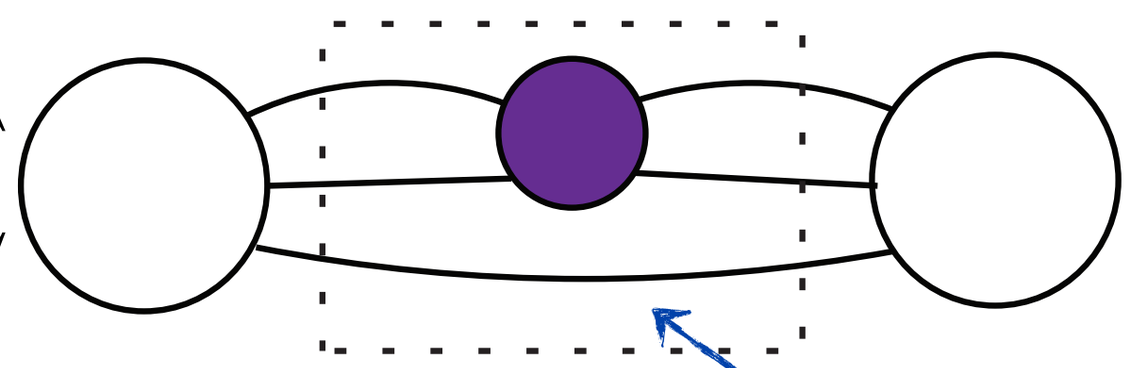

k

What is new here?

3. Must now worry about sum crossing two-particle unitary cusp

To remove cusp

$i\epsilon$ prescription → principal value $\widetilde{\mathrm{PV}}$

Analytically continue principal value below threshold then interpolate to prescription-free subthreshold form

Polejaeva, K. and Rusetsky, A. *Eur. Phys. J.* A48 (2012) 67

What is new here?

3. Must now worry about sum crossing two-particle unitary cusp

To remove cusp

$i\epsilon$ prescription → principal value $\widetilde{\mathrm{PV}}$

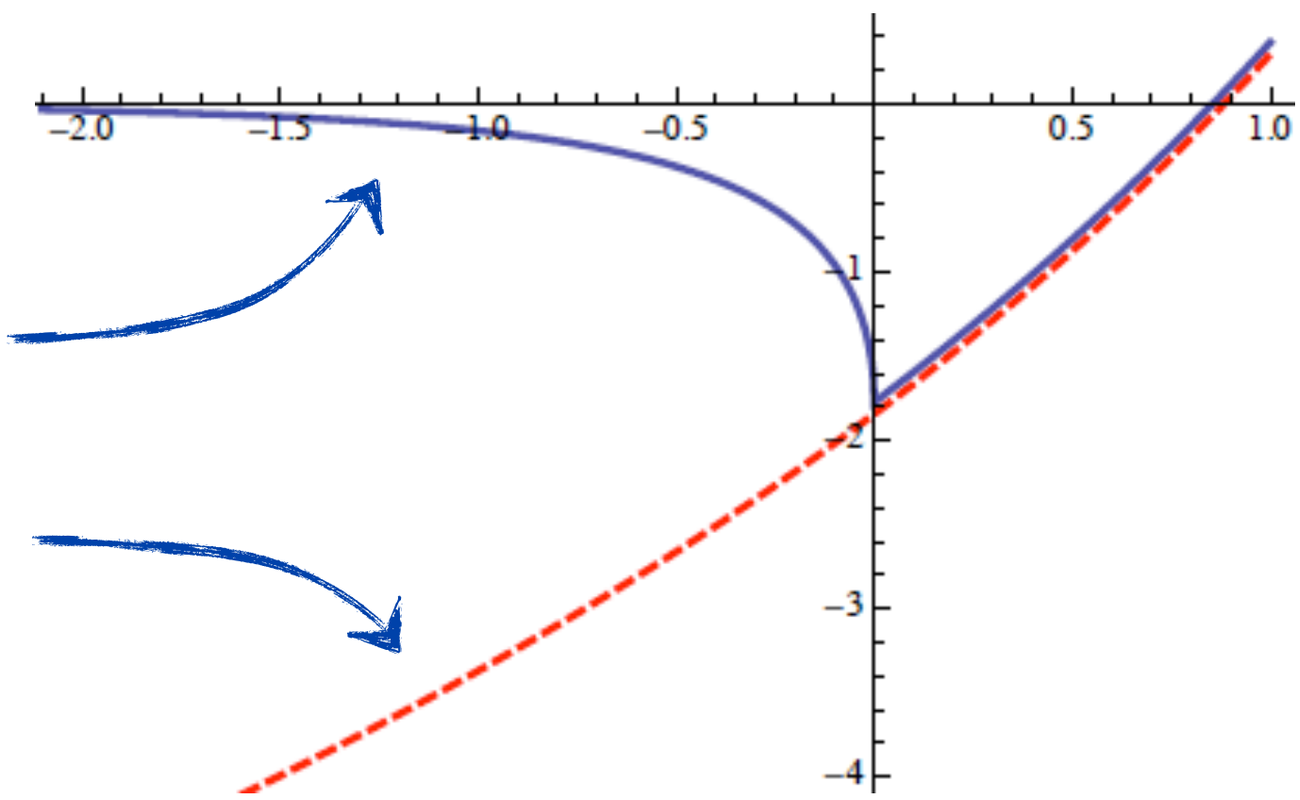

standard definition

modification $\widetilde{\mathrm{PV}}$

What is new here?

3. Must now worry about sum crossing two-particle unitary cusp

$i\mathcal{M}_{2\to 2} =$ 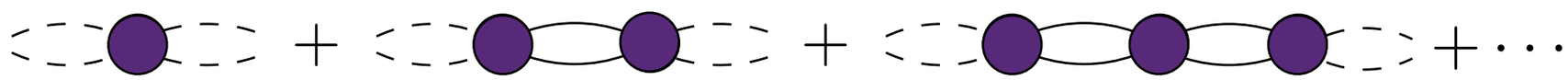

has cusp

$i\mathcal{K}_{2\to 2} =$ 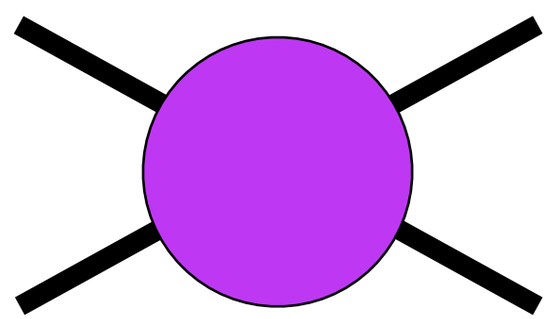 $=$

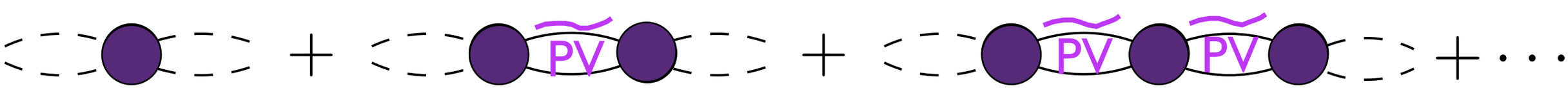

has no cusp

What is new here?

3. Must now worry about sum crossing two-particle unitary cusp

$$i\mathcal{M}_{2\to 2} \longrightarrow i\mathcal{K}_{2\to 2}$$

$$i\mathcal{M}_{\mathrm{df},3\to 3} \qquad i\mathcal{K}_{\mathrm{df},3\to 3}$$

We relate these infinite-volume quantities to the finite-volume spectrum

Three-particle result

$$C_L(E,\vec{P}) = C_\infty(E,\vec{P}) + A_3' i F_3 \frac{1}{1 - i\mathcal{K}_{\mathrm{df},3\to3}\ iF_3} A_3$$

$$iF_3 \equiv \frac{iF}{2\omega L^3}\left[\frac{1}{3} + \frac{1}{1 - i\mathcal{M}_{L,2\to2}\ iG}\ i\mathcal{M}_{L,2\to2}\ iF\right]$$

$$i\mathcal{M}_{L,2\to2} \equiv i\mathcal{K}_{2\to2}\frac{1}{1 - iFi\mathcal{K}_{2\to2}}$$

Three-particle result

$$C_L(E,\vec{P}) = C_\infty(E,\vec{P}) + A_3' iF_3 \frac{1}{1 - i\mathcal{K}_{\mathrm{df},3\to3}\, iF_3} A_3$$

sum-integral difference

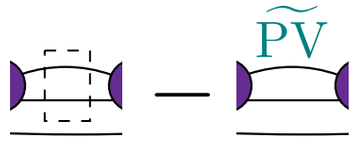

$$iF_3 \equiv \frac{iF}{2\omega L^3}\left[\frac{1}{3} + \frac{1}{1 - i\mathcal{M}_{L,2\to2}\, iG}\, i\mathcal{M}_{L,2\to2}\, iF\right]$$

encodes switches

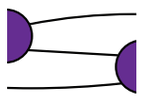

$$i\mathcal{M}_{L,2\to2} \equiv i\mathcal{K}_{2\to2}\frac{1}{1 - iFi\mathcal{K}_{2\to2}}$$

sum of all two-particle loops (with summed momenta)

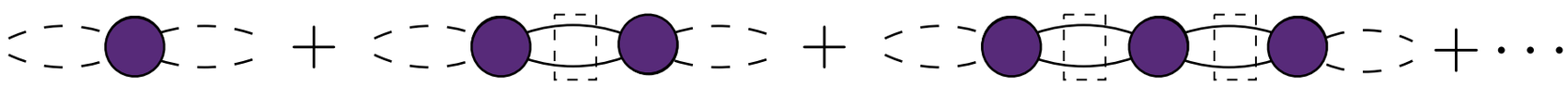

Three-particle result

$$C_L(E,\vec{P}) = C_\infty(E,\vec{P}) + A_3' i F_3 \frac{1}{1 - i\mathcal{K}_{\mathrm{df},3\to3}\; iF_3} A_3$$

row matrices column

all in $\vec{k}, \ell, m$ space

$$iF_3 \equiv \frac{iF}{2\omega L^3}\left[\frac{1}{3} + \frac{1}{1 - i\mathcal{M}_{L,2\to2}\; iG}\; i\mathcal{M}_{L,2\to2}\; iF\right]$$

$$i\mathcal{M}_{L,2\to2} \equiv i\mathcal{K}_{2\to2}\frac{1}{1 - iFi\mathcal{K}_{2\to2}}$$

Three-particle result

$$C_L(E,\vec{P}) = C_\infty(E,\vec{P}) + A_3' iF_3 \frac{1}{1 - i\mathcal{K}_{\mathrm{df},3\to3}\ iF_3} A_3$$

no poles **no poles** **no poles**

$C_L(E,\vec{P})$ **diverges whenever** $iF_3 \dfrac{1}{1 - i\mathcal{K}_{\mathrm{df},3\to3}\ iF_3}$ **diverges**

$$iF_3 \equiv \frac{iF}{2\omega L^3}\left[\frac{1}{3} + \frac{1}{1 - i\mathcal{M}_{L,2\to2}\ iG}\ i\mathcal{M}_{L,2\to2}\ iF\right]$$

$$i\mathcal{M}_{L,2\to2} \equiv i\mathcal{K}_{2\to2}\frac{1}{1 - iFi\mathcal{K}_{2\to2}}$$

Three-particle result

At fixed $(L, \vec{P})$, finite-volume spectrum is all solutions to

$$\Delta_{L,P}(E) = \det\left[1 - \underline{i\mathcal{K}_{\mathrm{df},3\to3}}\,\underline{iF_3}\right] = 0$$

matrix in space $\vec{k}, \ell, m$

depends on kinematics and two-particle scattering

Three-particle result

$$\Delta_{L,P}(E) = \det\left[1 - i\mathcal{K}_{\mathrm{df},3\to3} iF_3\right] = 0$$

...is it useful?

truncate in angular momentum to reduce to finite matrices ✓

need relation between $i\mathcal{M}_{3\to3}$ **and** $i\mathcal{K}_{\mathrm{df},3\to3}$

need to explore parametrizations of $i\mathcal{K}_{\mathrm{df},3\to3}$

Threshold expansion

At weak coupling, perturbatively study finite-volume shift from threshold

$$E = 3m + \mathcal{O}(1/L^3)$$ ← **finite-volume shift**

We find…

$$E = 3m + \frac{12\pi a}{mL^3}\left[1 + A\frac{a}{L} + B\frac{a^2}{L^2}\right] + C_1\frac{1}{L^6} - \frac{\mathcal{K}_{\mathrm{df},3\to3,\mathrm{thresh}}}{48m^3L^6} + C_2\frac{\log(mL)}{L^6}$$

A, B, C_2 **agree unambiguously with earlier work**

Beane, S., Detmold, W. & Savage, M. *Phys. Rev.* D76 (2007) 074507
Tan, S. Phys. Rev. A78 (2008) 013636

$$C_1 - \frac{\mathcal{K}_{\mathrm{df},3\to3,\mathrm{thresh}}}{48m^3}$$ **related to non-relativistic contact interaction**

Relating $i\mathcal{K}_{\mathrm{df},3\to3}$ to $i\mathcal{M}_{3\to3}$

$C_L(E,\vec{P}) =$

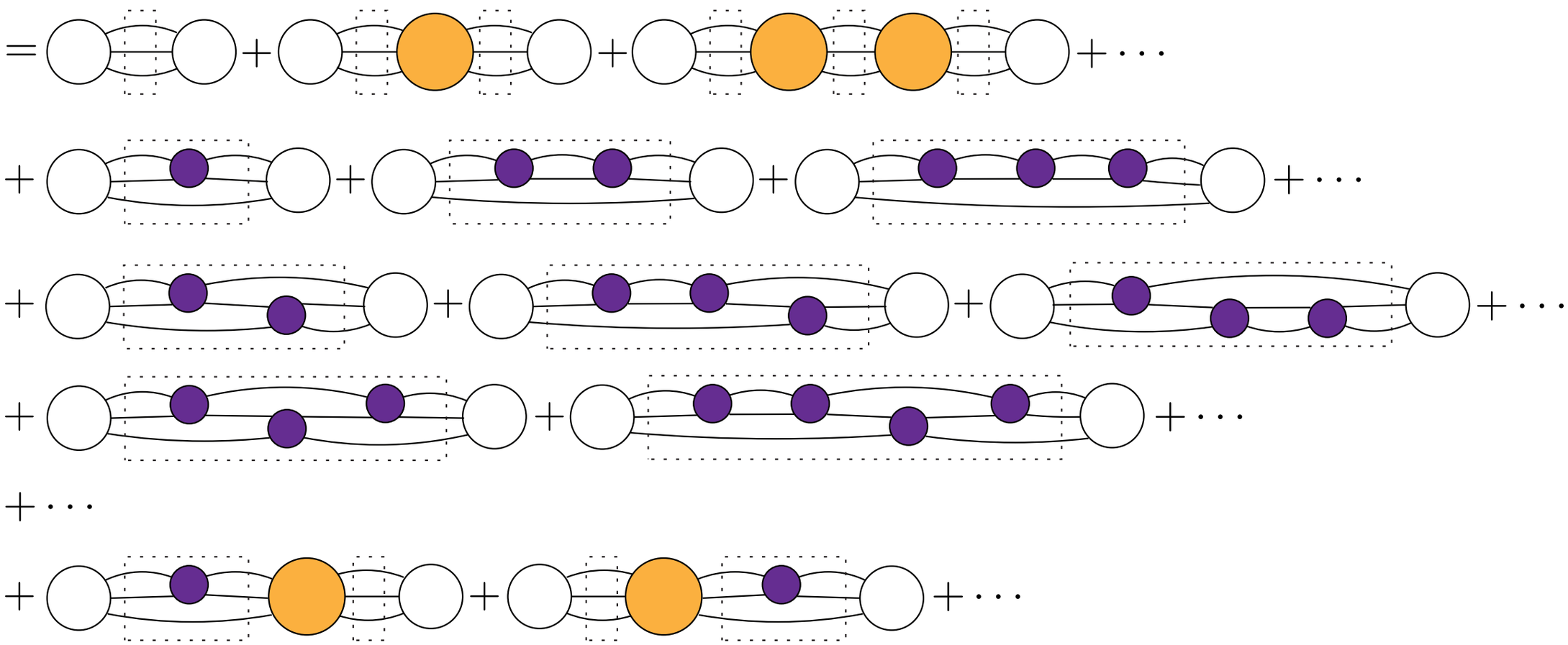

First we modify $C_L(E,\vec{P})$ to define $i\mathcal{M}_{L,3\to3}$

Relating $i\mathcal{K}_{\mathrm{df},3\to3}$ to $i\mathcal{M}_{3\to3}$

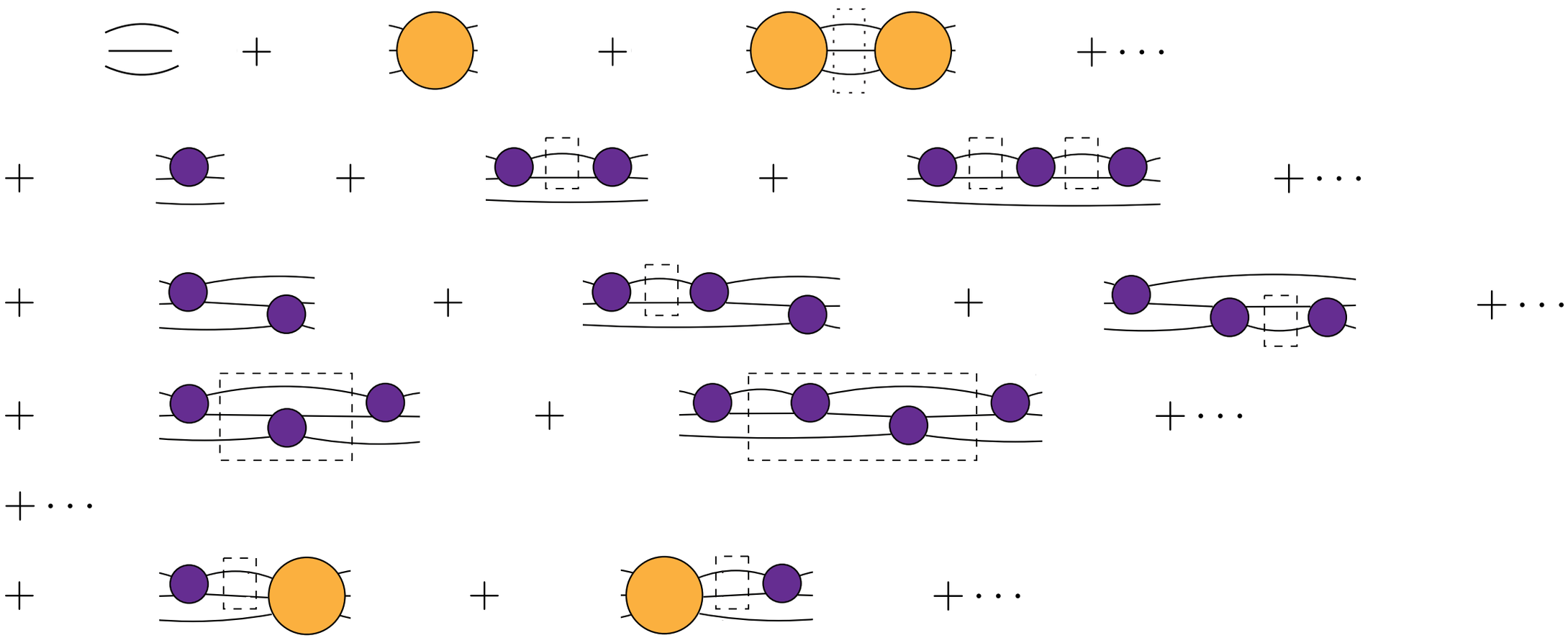

First we modify $C_L(E,\vec{P})$ to define $i\mathcal{M}_{L,3\to3}$

1. Amputate interpolating fields

Relating $i\mathcal{K}_{\mathrm{df},3\to3}$ to $i\mathcal{M}_{3\to3}$

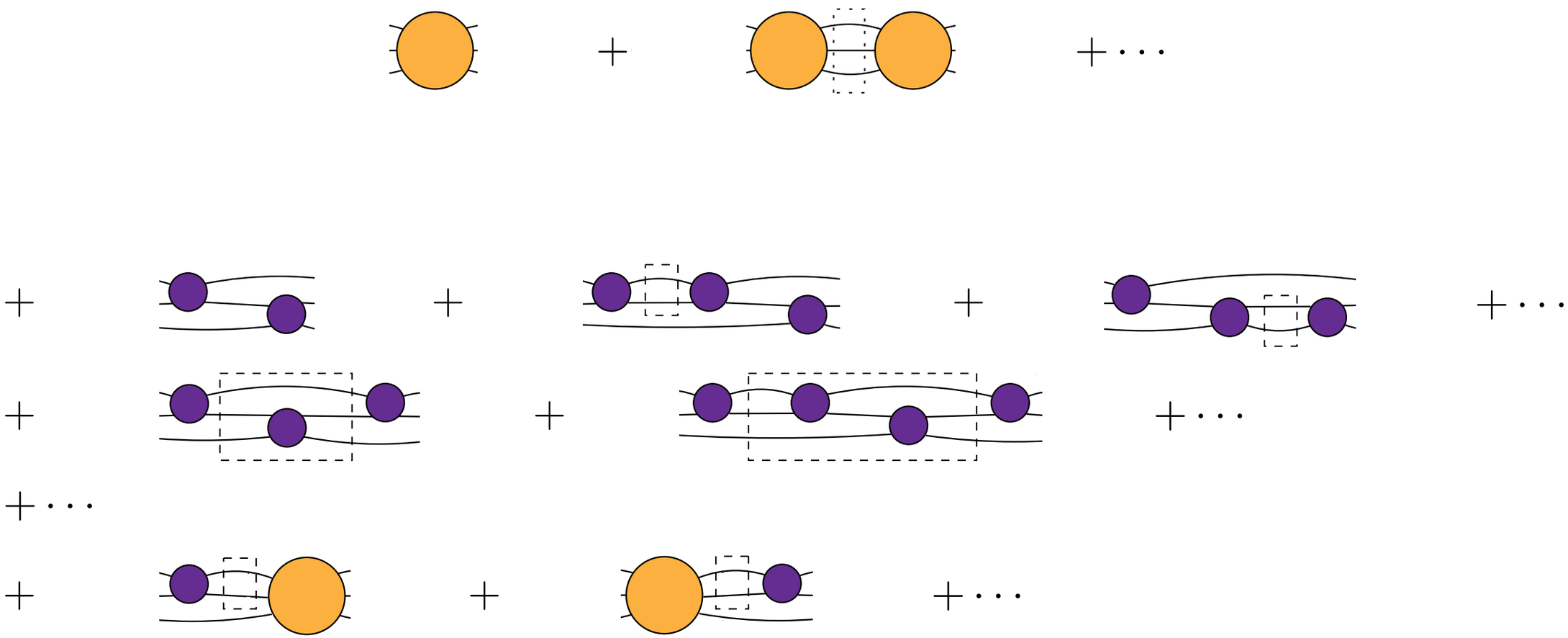

First we modify $C_L(E,\vec{P})$ to define $i\mathcal{M}_{L,3\to3}$

2. Drop disconnected diagrams

Relating $i\mathcal{K}_{\mathrm{df},3\to3}$ to $i\mathcal{M}_{3\to3}$

$i\mathcal{M}_{L,3\to3} \equiv \mathcal{S}\Big\{$

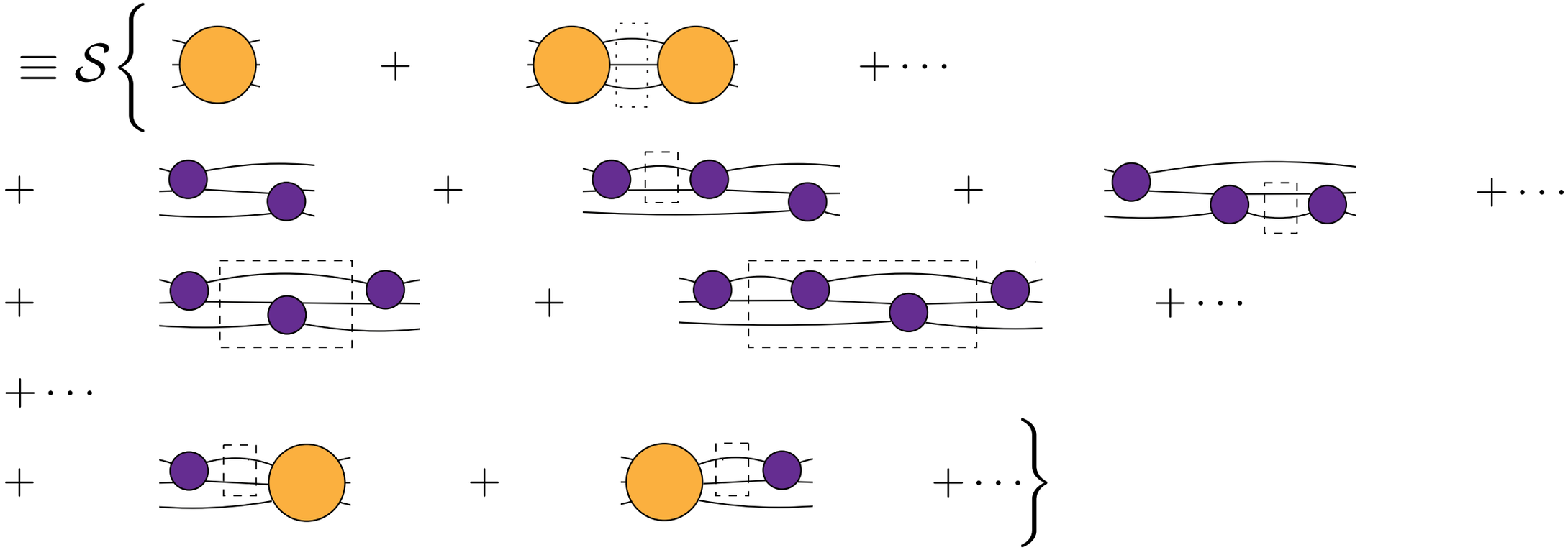

First we modify $C_L(E,\vec{P})$ to define $i\mathcal{M}_{L,3\to3}$

3. Symmetrize

Relating $i\mathcal{K}_{\mathrm{df},3\to3}$ to $i\mathcal{M}_{3\to3}$

$i\mathcal{M}_{L,3\to3} \equiv \mathcal{S}\Big\{$

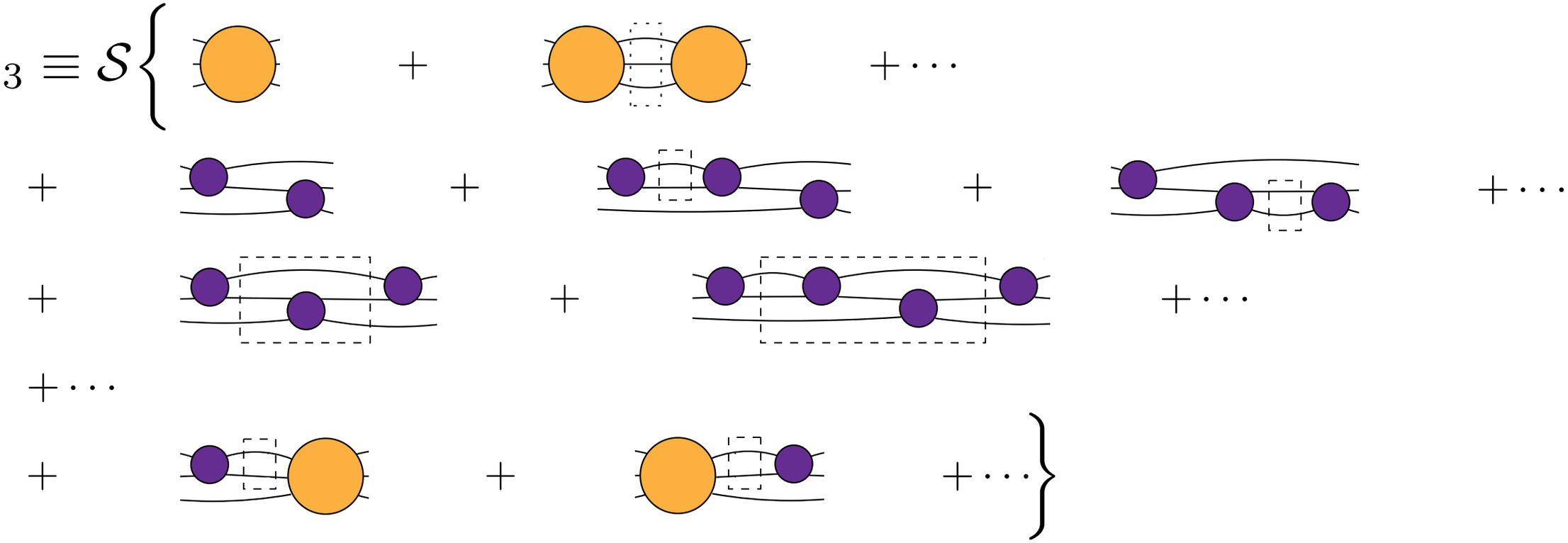

$\Big\}$

Replacing all loop momentum sums with i-epsilon prescription integrals would give physical three-to-three scattering amplitude

Relating $i\mathcal{K}_{\mathrm{df},3\to3}$ to $i\mathcal{M}_{3\to3}$

We find a simple form for $i\mathcal{M}_{L,3\to3}$

$$i\mathcal{M}_{L,3\to3} = i\mathcal{D}_L + \mathcal{S}\left[\mathcal{L}_L \; i\mathcal{K}_{\mathrm{df},3\to3} \frac{1}{1 - iF_3 \; i\mathcal{K}_{\mathrm{df},3\to3}} \; \mathcal{R}_L\right]$$

$$i\mathcal{D}_L \equiv \mathcal{S}\left[\frac{1}{1 - i\mathcal{M}_{L,2\to2} \; iG} \; i\mathcal{M}_{L,2\to2} \; iG \; i\mathcal{M}_{L,2\to2}[2\omega L^3]\right]$$

$$iF_3 \equiv \frac{iF}{2\omega L^3}\left[\frac{1}{3} + \frac{1}{1 - i\mathcal{M}_{L,2\to2} \; iG} \; i\mathcal{M}_{L,2\to2} \; iF\right]$$

$$\equiv \frac{iF}{2\omega L^3}\mathcal{L}_L \equiv \mathcal{R}_L \frac{iF}{2\omega L^3}$$

Relating $i\mathcal{K}_{\mathrm{df},3\to3}$ to $i\mathcal{M}_{3\to3}$

We find a simple form for $i\mathcal{M}_{L,3\to3}$

$$i\mathcal{M}_{L,3\to3} = i\mathcal{D}_L + \mathcal{S}\left[\mathcal{L}_L \; i\mathcal{K}_{\mathrm{df},3\to3} \frac{1}{1 - iF_3 \; i\mathcal{K}_{\mathrm{df},3\to3}} \; \mathcal{R}_L\right]$$

Complete analysis with infinite volume limit

$$i\mathcal{M}_{3\to3} = \lim_{L\to\infty} \Big|_{i\epsilon} \; i\mathcal{M}_{L,3\to3}$$

$$i\mathcal{M}_{L,3\to3} = i\mathcal{D}_L + \mathcal{S}\left[\mathcal{L}_L \; i\mathcal{K}_{\mathrm{df},3\to3} \frac{1}{1 - iF_3 \; i\mathcal{K}_{\mathrm{df},3\to3}} \; \mathcal{R}_L\right]$$

Recall $i\mathcal{M}_{\mathrm{df},3\to3}$

$$\equiv i\mathcal{M}_{3\to3} - \left[i\mathcal{M}_{2\to2} S i\mathcal{M}_{2\to2} + \int i\mathcal{M}_{2\to2} S i\mathcal{M}_{2\to2} S i\mathcal{M}_{2\to2} + \cdots\right]$$

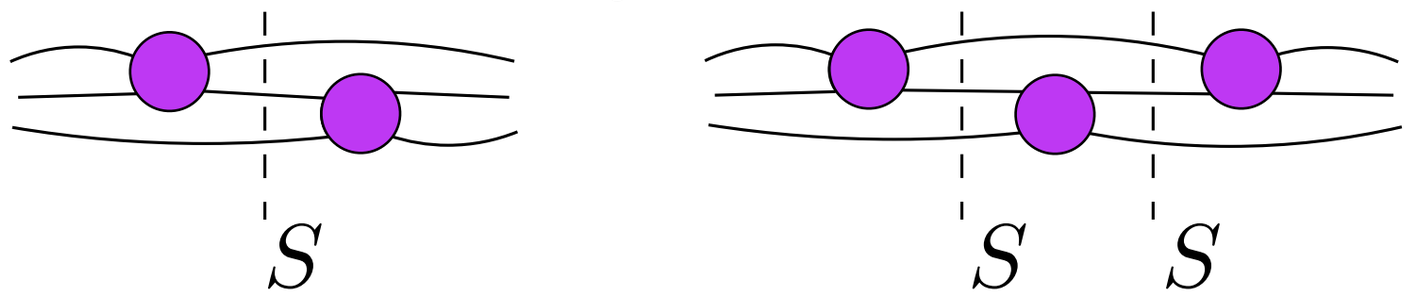

It reappears here… $i\mathcal{M}_{df,3\to3} \equiv \lim_{L\to\infty} \Big|_{i\epsilon} \left[i\mathcal{M}_{L,3\to3} - i\mathcal{D}_L\right]$

$$i\mathcal{D}_L \equiv \mathcal{S}\left[\frac{1}{1 - i\mathcal{M}_{L,2\to2} \; iG} \; i\mathcal{M}_{L,2\to2} \; iG \; i\mathcal{M}_{L,2\to2}[2\omega L^3]\right]$$

encodes switches

Relating $i\mathcal{K}_{\mathrm{df},3\to3}$ to $i\mathcal{M}_{3\to3}$

$$i\mathcal{M}_{L,3\to3} = i\mathcal{D}_L + \mathcal{S}\left[\mathcal{L}_L \; i\mathcal{K}_{\mathrm{df},3\to3} \frac{1}{1 - iF_3 \; i\mathcal{K}_{\mathrm{df},3\to3}} \; \mathcal{R}_L\right]$$

$$i\mathcal{M}_{3\to3} = \lim_{L\to\infty} \Big|_{i\epsilon} \; i\mathcal{M}_{L,3\to3}$$

Gives integral equation relating $i\mathcal{K}_{\mathrm{df},3\to3}$ to $i\mathcal{M}_{3\to3}$

Completes formal story (for the setup considered!)

Relation only depends on on-shell scattering quantities

Summary

Presented work relating finite-volume spectrum and three-to-three scattering.

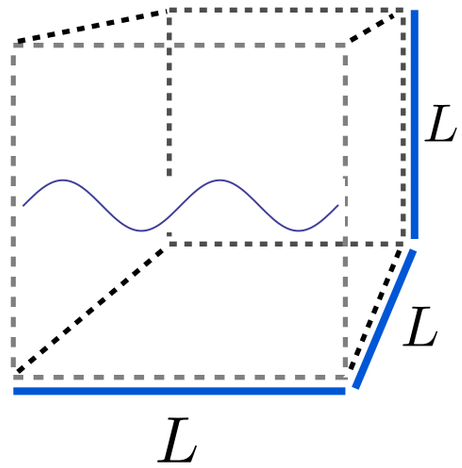

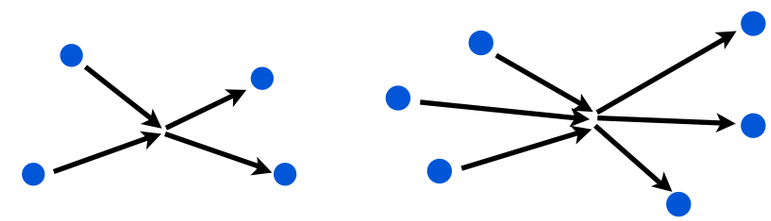

Necessary first step for extracting any decay or scattering amplitude with more than two hadrons from Lattice QCD.

Future work and Applications

Generalize Lellouch-Lüscher method, to extract three-particle weak decays

$$K \longrightarrow \pi\pi\pi$$

Include non-identical, non-degenerate and spin-half particles

Extend mapping to four-particle states

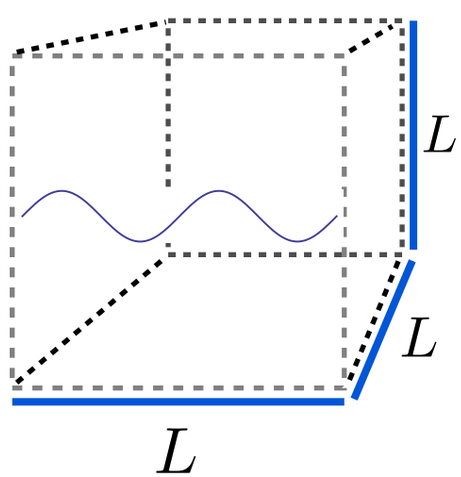

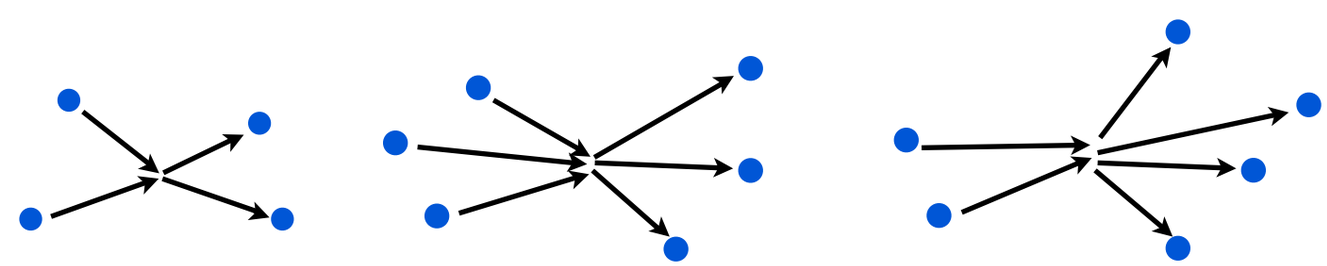

Isotropic approximation

Following two particle case, suppose $\mathcal{K}_{\mathrm{df},3\to3}$ can be approximated to be isotropic (only depends on E^*)

$$\mathcal{K}_{\mathrm{df},3\to3}(E_n^*) = -[F_{3,\mathrm{iso}}(E_n, \vec{P}, L)]^{-1}$$

$$F_{3,\mathrm{iso}} \equiv \sum_{\vec{k},\vec{p}} F_{3;k,p}$$

$$iF_3 \equiv \frac{iF}{2\omega L^3}\left[\frac{1}{3} + \frac{1}{1 - i\mathcal{M}_{L,2\to2}\, iG}\, i\mathcal{M}_{L,2\to2}\, iF\right]$$

Three-particle result

At fixed $(L, \vec{P})$ the finite-volume spectrum $E_1, E_2, \cdots$ is the set of solutions to

$$\Delta_{L,P}(E) = \det[1 - i\widetilde{\mathcal{K}}_{df,3\to3} iF_3] = 0$$

where

$$iF_3 \equiv \frac{1}{2\omega L^3}\left[-(2/3)iF_{\widetilde{\mathrm{PV}}} + \frac{1}{[iF_{\widetilde{\mathrm{PV}}}]^{-1} - [1 - i\widetilde{\mathcal{K}}_{2\to2} iG]^{-1} i\widetilde{\mathcal{K}}_{2\to2}}\right]$$

$$iF_{\widetilde{\mathrm{PV}};k,k'} \equiv \delta_{k,k'}\frac{1}{2}\left[\frac{1}{L^3}\sum_{\vec{a}} - \widetilde{\mathrm{PV}}\int_{\vec{a}}\right]\frac{iQ(\vec{a}^*)Q^*(\vec{a}^*)}{2\omega_a 2\omega_{P-k-a}(E - \omega_k - \omega_a - \omega_{P-k-a})}$$

$$iG_{k,p} \equiv \frac{1}{2\omega_p L^3}\frac{iQ(\vec{p}^*)Q^*(\vec{k}^*)}{2\omega_{P-p-k}(E - \omega_p - \omega_k - \omega_{P-p-k})}$$

$$Q_{\ell,m}(\vec{k}^*) \equiv \sqrt{4\pi}Y_{\ell,m}(\hat{k}^*)(k^*/q^*)^\ell$$

with $\omega_k^2 = \vec{k}^2 + m^2$ and $q^{*2} = (1/4)[E^2 - \vec{P}^2] - m^2$

Additional Material Concerning Differences Between Two- and Three-Particle Quantization

New skeleton expansion

$C_L(E, \vec{P}) =$

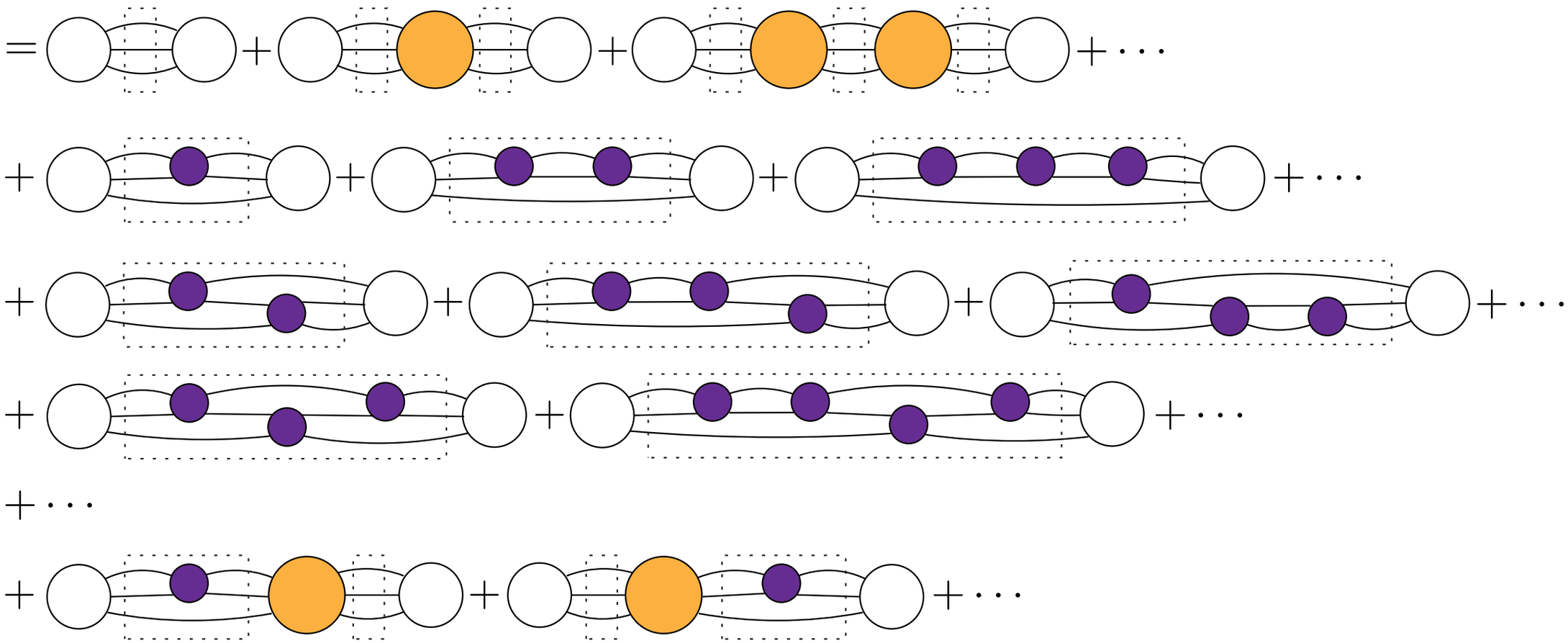

Here I will only give first parts of derivation.

This is to illustrate certain points, needed to understand the final result.

First Part: Sum "no-switch" diagrams

$C_L^{(1)} \equiv$ 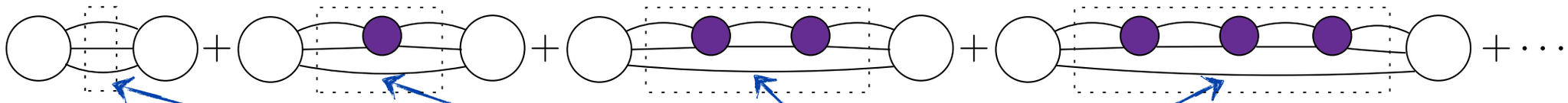

call the bottom momentum k

important finite-volume corrections only arise from $k^0 = \omega_k$

$C_L^{(1)} = \frac{1}{L^3} \sum_{\vec{k}} \frac{1}{2\omega_k} \Big\{$ 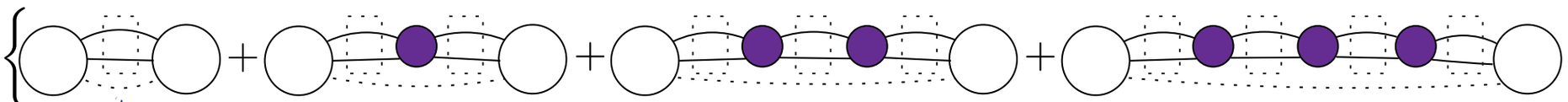 $\Big\}$

bottom propagator replaced with $1/(2\omega_k)$

First Part: Sum "no-switch" diagrams

$C_L^{(1)} \equiv$ 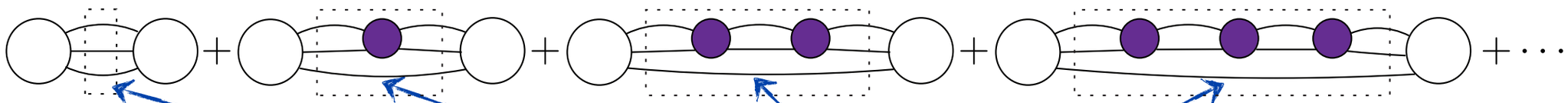

call the bottom momentum k

important finite-volume corrections only arise from $k^0 = \omega_k$

$C_L^{(1)} = \frac{1}{L^3}\sum_{\vec{k}} \frac{1}{2\omega_k}\Big\{$ 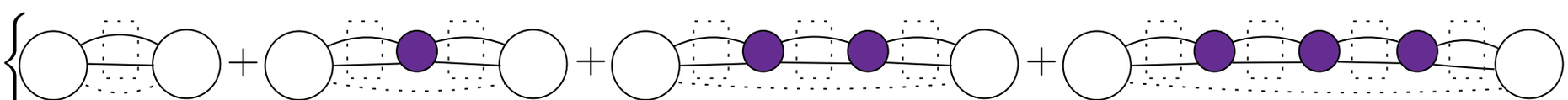 $\Big\}$

bottom propagator replaced with $1/(2\omega_k)$

Next substitute 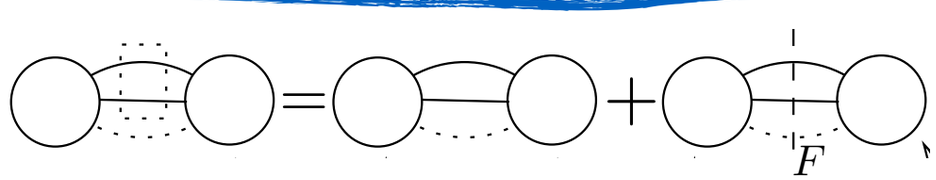 and regroup by F-cuts

$C_L^{(1)} = \frac{1}{L^3}\sum_{\vec{k}}\Big\{$ 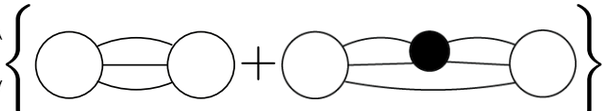 $\Big\}$

$+ \frac{1}{L^3}\sum_{\vec{k}} \frac{1}{2\omega_k}\Big\{$ 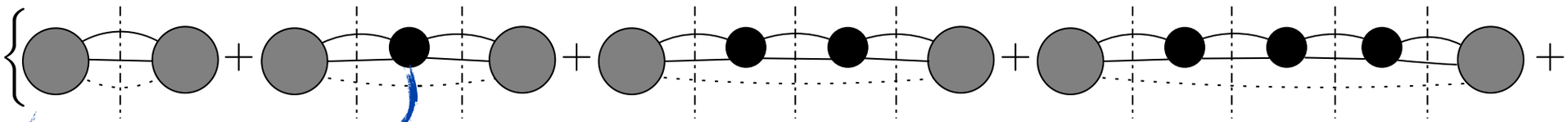 $\Big\}$

$=$ 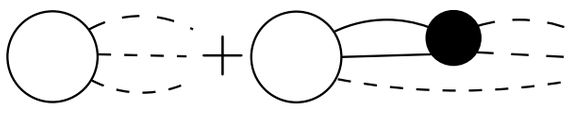

$=$ 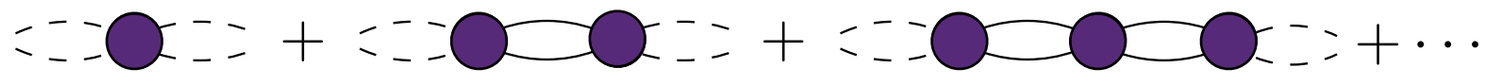

$= i\mathcal{M}_{2\to 2}$

First Part: Sum "no-switch" diagrams

$C_L^{(1)} \equiv$ 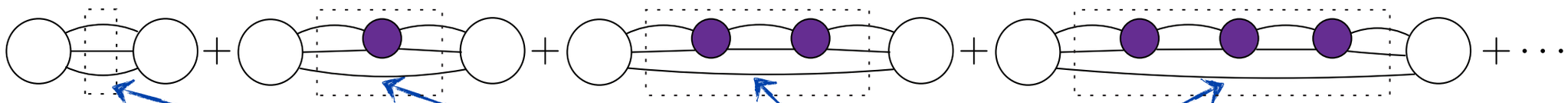

call the bottom momentum k

important finite-volume corrections only arise from $k^0 = \omega_k$

$C_L^{(1)} = \frac{1}{L^3}\sum_{\vec{k}} \frac{1}{2\omega_k}\Big\{$ 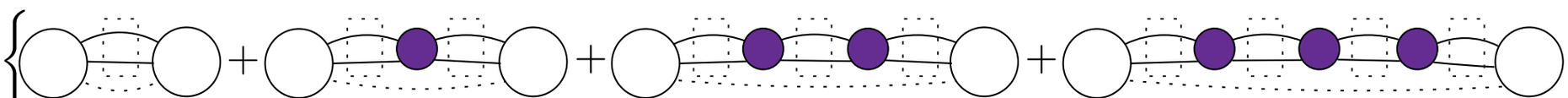 $\Big\}$

bottom propagator replaced with $1/(2\omega_k)$

Next substitute 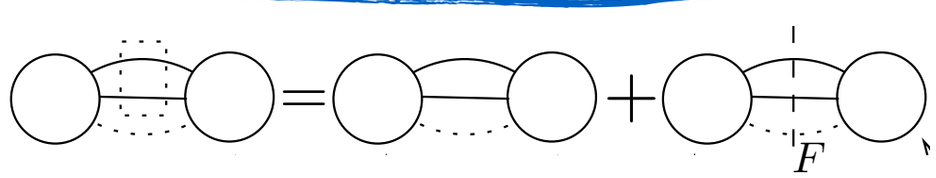 and regroup by F-cuts

$C_L^{(1)} = \frac{1}{L^3}\sum_{\vec{k}}\Big\{$ 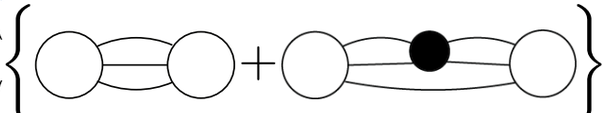 $\Big\}$ **Can this be replaced with an integral?** **No!**

$+ \frac{1}{L^3}\sum_{\vec{k}} \frac{1}{2\omega_k}\Big\{$ 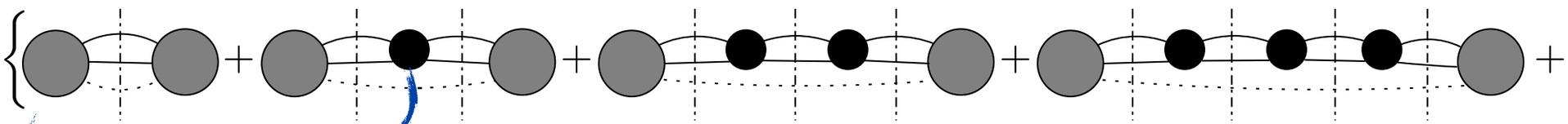 $\Big\}$

$=$ 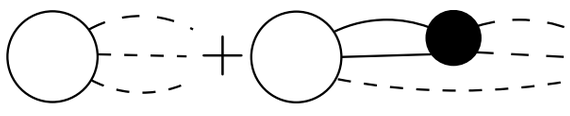

$=$ 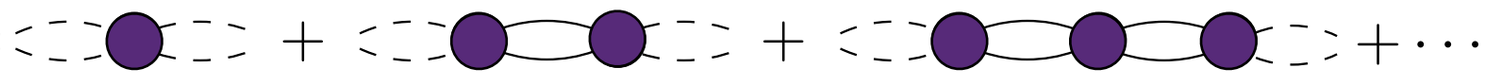

$= i\mathcal{M}_{2\to 2}$

Main Lesson Number 1: Cusp effects

$$\frac{1}{L^3}\sum_{\vec{k}} f(\vec{k}) = \int_{\vec{k}} f(\vec{k}) + \mathcal{O}(e^{-mL})$$

only holds if $f(\vec{k})$ is an infinitely differentiable function with width $\sim m$.

$C_\infty^{(1)}(\vec{k}) \equiv$

has a unitary cusp at threshold

$$(E-\omega_k)^2 - (\vec{P}-\vec{k})^2 = 4m^2$$

To remove cusp

$i\epsilon$ prescription → principal value $\widetilde{\mathrm{PV}}$

(analytically continue below threshold, then interpolate to standard subthreshold form)

Polejaeva, K. and Rusetsky, A. *Eur. Phys. J.* A48 (2012) 67

$$C_L^{(1)} = \frac{1}{L^3}\sum_{\vec{k}}\Big\{$$ 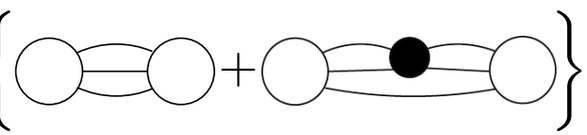 $$\Big\}$$

Can this be replaced with an integral? No!

$$+\frac{1}{L^3}\sum_{\vec{k}}\frac{1}{2\omega_k}\Big\{$$ 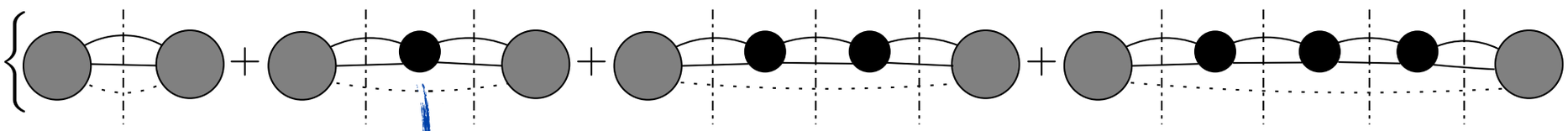 $$+\cdots\Big\}$$

$$=$$ 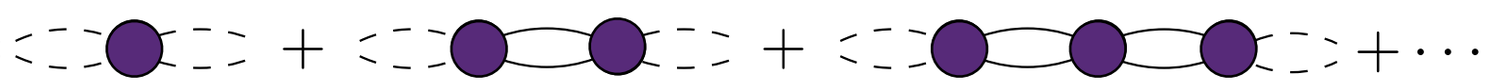 $$+\cdots$$

$$= i\mathcal{M}_{2\to 2}$$

$$C_L^{(1)} = \frac{1}{L^3}\sum_{\vec{k}}$$

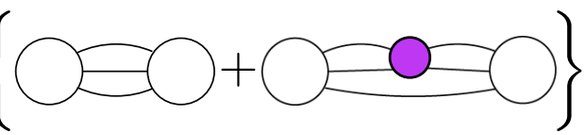

But if we change pole prescription, then we can make the replacement

$$+\frac{1}{L^3}\sum_{\vec{k}}\frac{1}{2\omega_k}$$

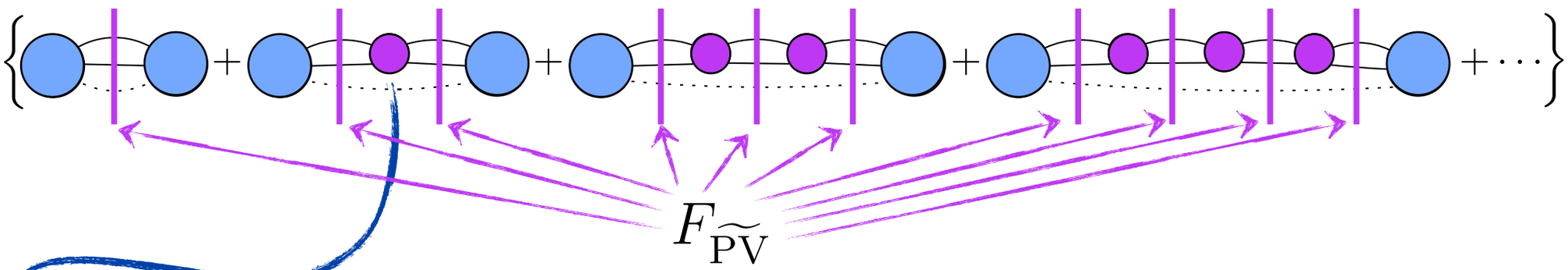

$$= i\widetilde{\mathcal{K}}_{2\to 2}$$

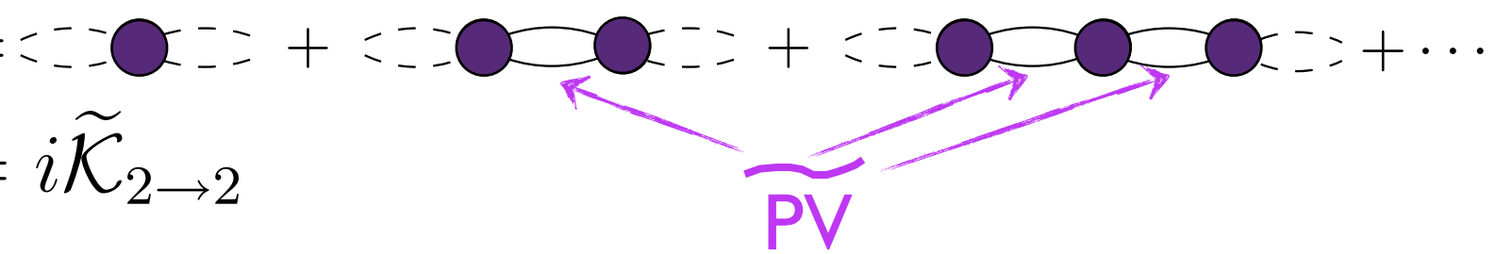

All three-particle poles now have principal-value prescription

Deduce

$$C_L^{(1)} = \widetilde{C}_\infty^{(1)} +$$

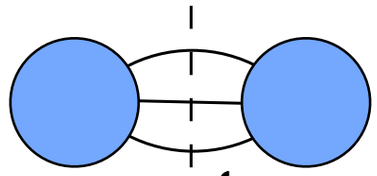

$$[\mathcal{A}] \equiv \frac{iF_{\widetilde{\mathrm{PV}}}}{2\omega L^3} \frac{1}{1 + \widetilde{\mathcal{K}}_{2\to 2} F_{\widetilde{\mathrm{PV}}}}$$

think of this as a new cut,
like F it puts neighbors on-shell

Deduce

$$C_L^{(1)} = \widetilde{C}_\infty^{(1)} +$$ 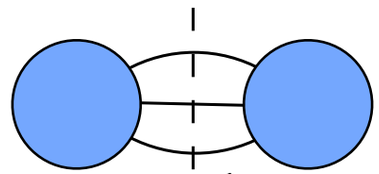

$$[\mathcal{A}] \equiv \frac{iF_{\widetilde{\mathrm{PV}}}}{2\omega L^3} \frac{1}{1+\widetilde{\mathcal{K}}_{2\to 2} F_{\widetilde{\mathrm{PV}}}}$$

think of this as a new cut, like F it puts neighbors on-shell

Main Lesson Number 2: Matrix structure

Finite volume residue terms (such as 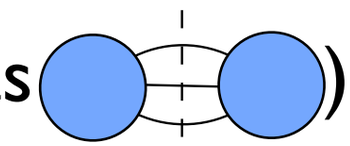) are of the form:

(row vector)x(matrix)x(column vector), acting on product space

[finite-volume momentum]x[angular momentum]

For example, $[\mathcal{A}]$ is built from

$$F_{\widetilde{\mathrm{PV}};k',\ell',m';k,\ell,m} \equiv \delta_{k',k}\, F_{\widetilde{\mathrm{PV}};\ell',m';\ell,m}(E-\omega_k, \vec{P}-\vec{k}) \qquad \vec{k}=\vec{k}' \in (2\pi/L)\mathbb{Z}^3$$

$$\widetilde{\mathcal{K}}_{2\to 2;k',\ell',m';k,\ell,m} \equiv \delta_{k',k}\, \widetilde{\mathcal{K}}_{2\to 2;\ell',m';\ell,m}(E-\omega_k, \vec{P}-\vec{k})$$

Deduce

$$C_L^{(1)} = \widetilde{C}_\infty^{(1)} + \quad \mathcal{A} \qquad [\mathcal{A}] \equiv \frac{iF_{\widetilde{\mathrm{PV}}}}{2\omega L^3} \frac{1}{1 + \widetilde{\mathcal{K}}_{2\to 2} F_{\widetilde{\mathrm{PV}}}}$$

think of this as a new cut,
like F it puts neighbors on-shell

Main Lesson Number 2: Matrix structure

Finite volume residue terms (such as) are of the form:

(row vector)x(matrix)x(column vector), acting on product space

[finite-volume momentum]x[angular momentum]

Observe that $\vec{k}, \ell, m$ parametrizes three particles with fixed $(E, \vec{P})$

Second part: Sum "one-switch" diagrams

$C_L^{(2)} =$ 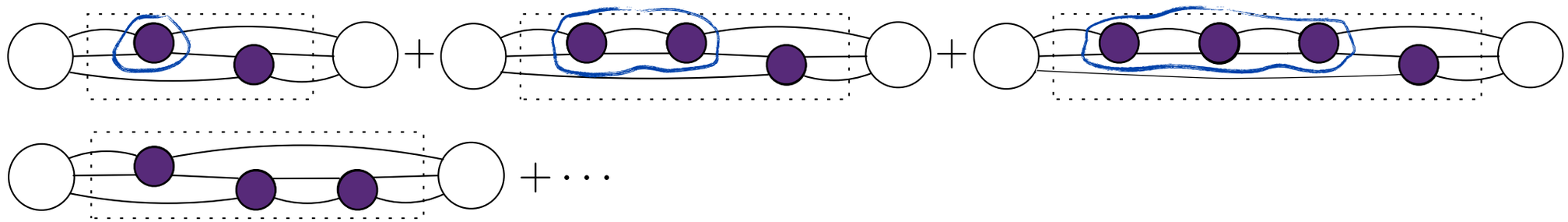

In this case we have two "spectator-momenta"
(momenta that do not appear in two-particle loops)

$C_L^{(2)} = \widetilde{C}_\infty^{(2)} +$ 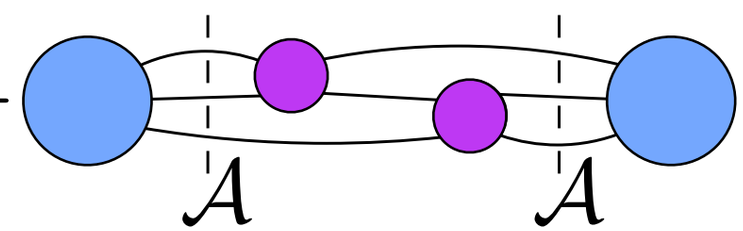

$+ \cdots$

stands for terms that modify endcaps of $C_L^{(1)}$

Between $\mathcal{A}$ factors we have first contribution to three-to-three scattering

$i\widetilde{\mathcal{K}}^{(2,\mathrm{unsym})}_{3\to 3;k',\ell',m';k,\ell,m} \equiv$ 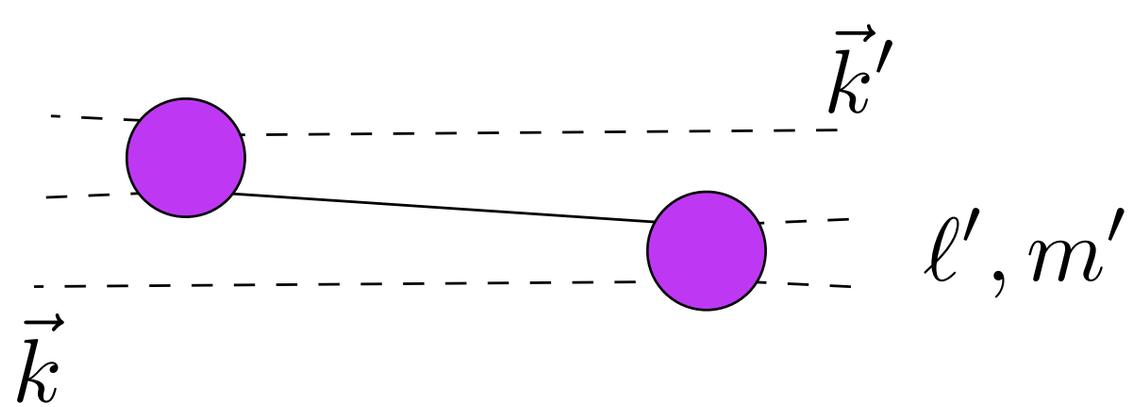

Main Lesson Number 3: On-shell divergences

Certain external moment put the intermediate propagator on-shell

$$i\widetilde{\mathcal{K}}^{(2,\mathrm{unsym})}_{3\to3;k',\ell',m';k,\ell,m} \equiv$$

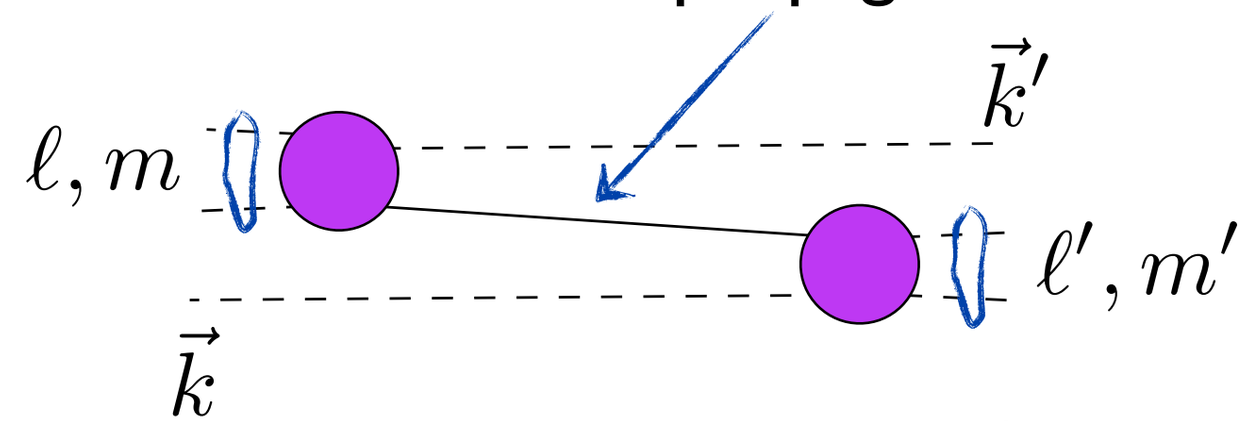

This implies that this diagram, and indeed also the full

$i\widetilde{\mathcal{K}}_{3\to3}$ **has physical singularities above threshold**

nothing to do with bound states

This is a problem because K-matrix is symmetric in external momenta

$$i\widetilde{\mathcal{K}}_{3\to3;k',\ell',m';k,\ell,m} \overset{!}{\supset}$$

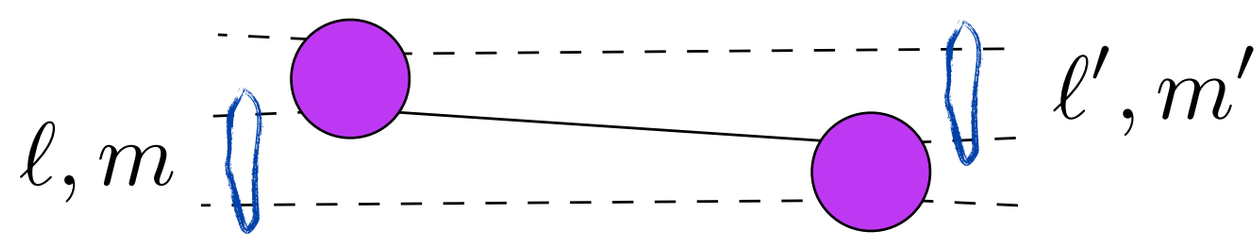

But this would demand decomposing a singular function in $Y_{\ell,m}$

The decomposition is not valid!

Resolution: Introduce

$$i\widetilde{\mathcal{K}}^{(2,\mathrm{unsym})}_{df,3\to3} \equiv i\widetilde{\mathcal{K}}^{(2,\mathrm{unsym})}_{3\to3} - i\widetilde{\mathcal{K}}_{2\to2} S i\widetilde{\mathcal{K}}_{2\to2}$$

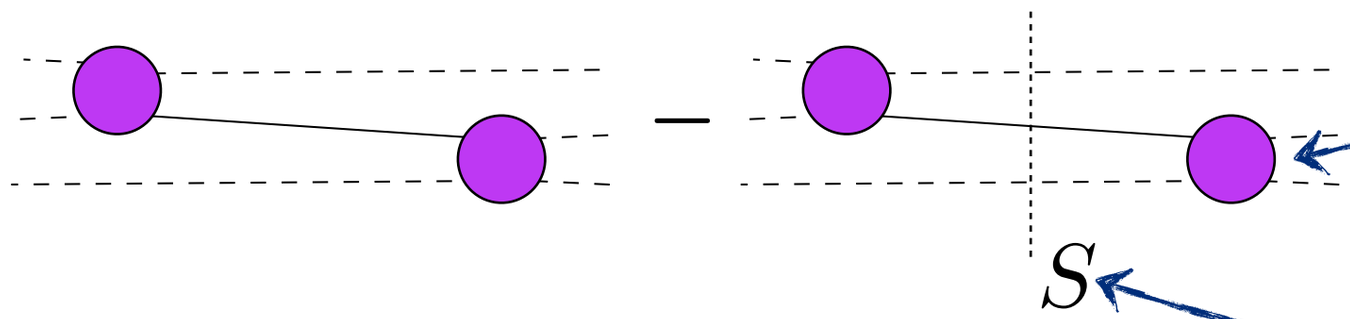

on-shell

represents simple kinematic pole factor

$i\widetilde{\mathcal{K}}_{df,3\to3}$ is finite:

Can decompose in harmonics and truncate expansion at low energies

The approach of separating out singularities like this was first suggested over 40 years ago (Rubin et al. *PR 146-6* (1966))

It makes sense to recover singularity-free quantity from finite-volume spectrum.
Then add singular terms back in.

This pattern of separating out singularities persists to all orders

Define

$$i\widetilde{\mathcal{K}}_{df,3\to3} \equiv i\widetilde{\mathcal{K}}_{3\to3} - \left[i\widetilde{\mathcal{K}}_{2\to2} S i\widetilde{\mathcal{K}}_{2\to2} + \int i\widetilde{\mathcal{K}}_{2\to2} S i\widetilde{\mathcal{K}}_{2\to2} S i\widetilde{\mathcal{K}}_{2\to2} + \cdots \right]$$

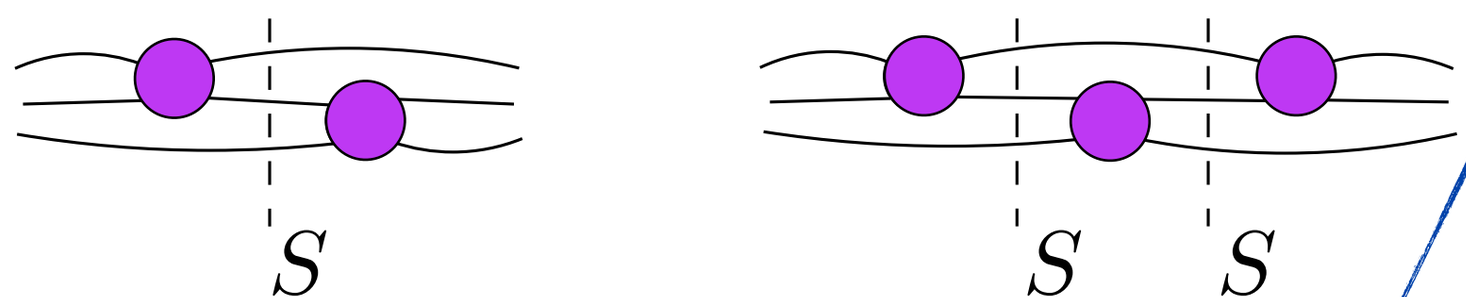

only on-shell amplitudes here

infinite series built with factors of $S i\widetilde{\mathcal{K}}_{2\to2}$

Definition arises from analyzing all two-to-two diagrams

$$i\widetilde{\mathcal{K}}_{df,3\to3;k',\ell',m';k,\ell,m}$$

is the natural observable to extract from the finite-volume spectrum

Review Lessons

1. Need modified principal value to remove cusp effects

2. In the three particle case, all matrices act on product space
[finite-volume momentum]x[angular momentum]
In other words, they have indices $\vec{k}, \ell, m$

needed to describe three particles

3. Singularities in $i\widetilde{\mathcal{K}}_{3\to 3}$ invalidate decomposition in $Y_{\ell,m}$
Resolution is to introduce $i\widetilde{\mathcal{K}}_{df,3\to 3}$

$i\widetilde{\mathcal{K}}_{df,3\to 3} \equiv i\widetilde{\mathcal{K}}_{3\to 3} -$

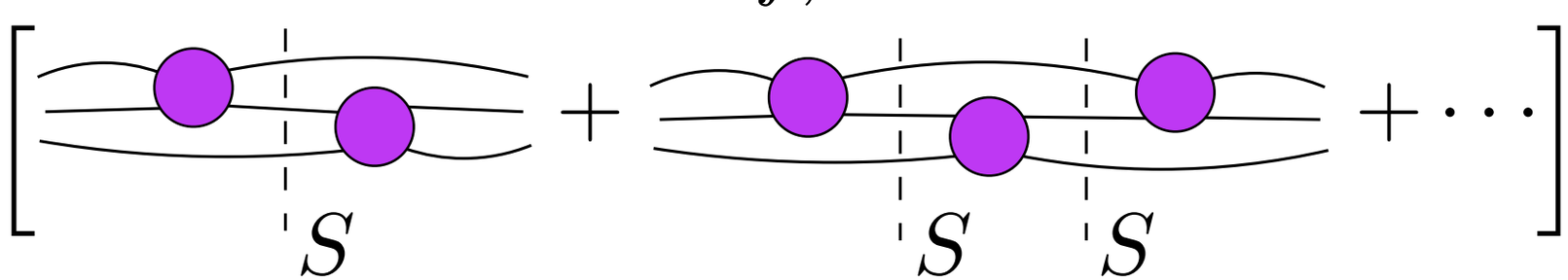

This object arises naturally in finite-volume analysis.

Intro- and Two-Particle Material

What can we extract from LQCD?

We are trying to evaluate a difficult integral numerically

$$\langle T\phi_1 \cdots \phi_n \rangle = \int \mathcal{D}\phi \, e^{iS} \, \phi_1 \cdots \phi_n$$

What can we extract from LQCD?

We are trying to evaluate a difficult integral numerically

$$\langle T\phi_1 \cdots \phi_n \rangle_{\text{Euc, latt, fv}} = \int \prod_i^N d\phi_i \, e^{-S} \, \phi_1 \cdots \phi_n$$

To do so we have to make three compromises

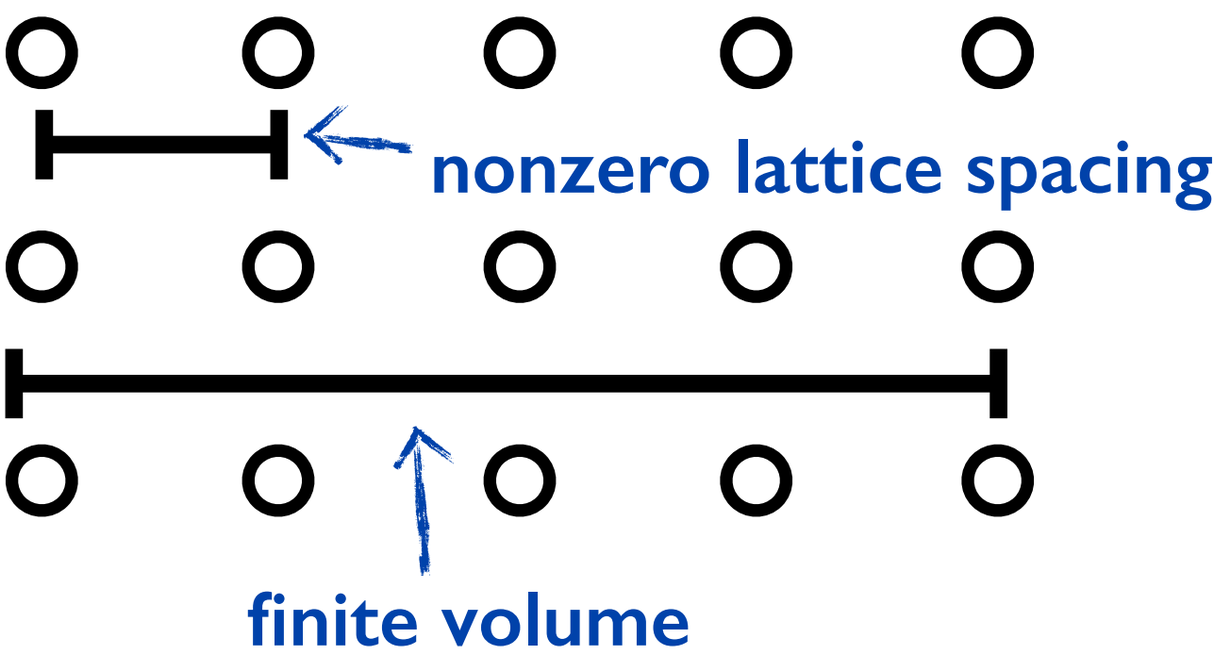

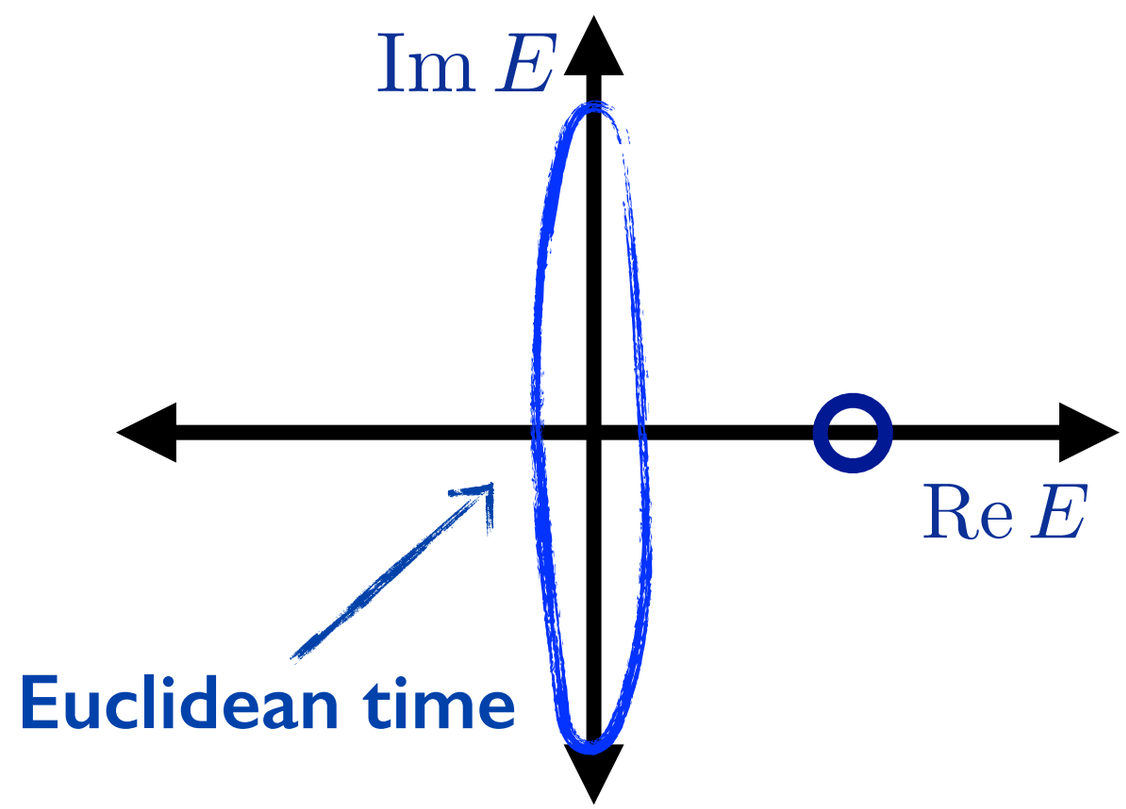

What can we extract from LQCD?

Not possible to directly calculate

$\langle \pi\pi | \pi\pi \rangle$

$\langle \pi\pi\pi | \pi\pi\pi \rangle$

$\langle K\pi\pi | \mathcal{J} | B \rangle$

$\langle \pi\pi | \mathcal{H} | K \rangle$

$\langle \pi\pi | \mathcal{J} | \pi \rangle$

$\langle K\pi | \mathcal{J} | B \rangle$

What can we extract from LQCD?

Not possible to directly calculate

$\langle \pi\pi | \pi\pi \rangle$

$\langle \pi\pi\pi | \pi\pi\pi \rangle$

$\langle K\pi\pi | \mathcal{J} | B \rangle$

$\langle \pi\pi | \mathcal{H} | K \rangle$

$\langle \pi\pi | \mathcal{J} | \pi \rangle$

$\langle K\pi | \mathcal{J} | B \rangle$

multi-particle in- and outstates

What can we extract from LQCD?

Not possible to directly calculate

$\langle \pi\pi | \pi\pi \rangle$ $\langle \pi\pi\pi | \pi\pi\pi \rangle$

$\langle \pi\pi | \mathcal{H} | K \rangle$ $\langle \pi\pi | \mathcal{J} | \pi \rangle$ $\langle K\pi\pi | \mathcal{J} | B \rangle$ $\langle K\pi | \mathcal{J} | B \rangle$

multi-particle in- and outstates

$\langle \pi\pi | \pi\pi \rangle =$ Amputate and put on-shell $\langle 0 | \tilde{\pi}(p')\tilde{\pi}(k') \; \tilde{\pi}(p)\tilde{\pi}(k) | 0 \rangle$

$\langle \pi\pi | \mathcal{H} | K \rangle =$ Amputate and put on-shell $\langle 0 | \tilde{\pi}(p')\tilde{\pi}(k') \; \mathcal{H}(x) \; \tilde{K}(P) | 0 \rangle$

Requires Minkowski momenta and infinite-volume

In 1991 **M. Lüscher** found a method to circumvent this issue and extract $\pi\pi \to \pi\pi$ scattering from LQCD.

Lüscher, M. *Nucl. Phys* B354, 531-578 (1991)

His key insight was to **use finite-volume as a tool**.

He gave a mapping between **finite-volume spectrum** and **elastic pion scattering amplitude**.

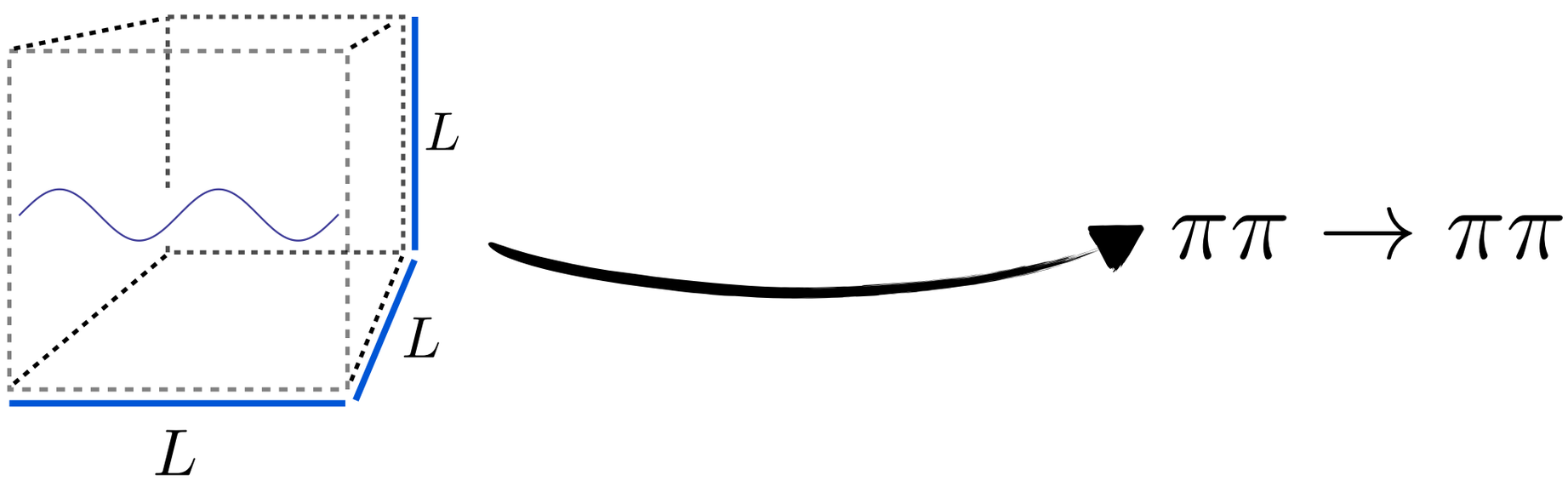

Lüscher's method has led to a large body of work extracting phase shifts from Lattice QCD.

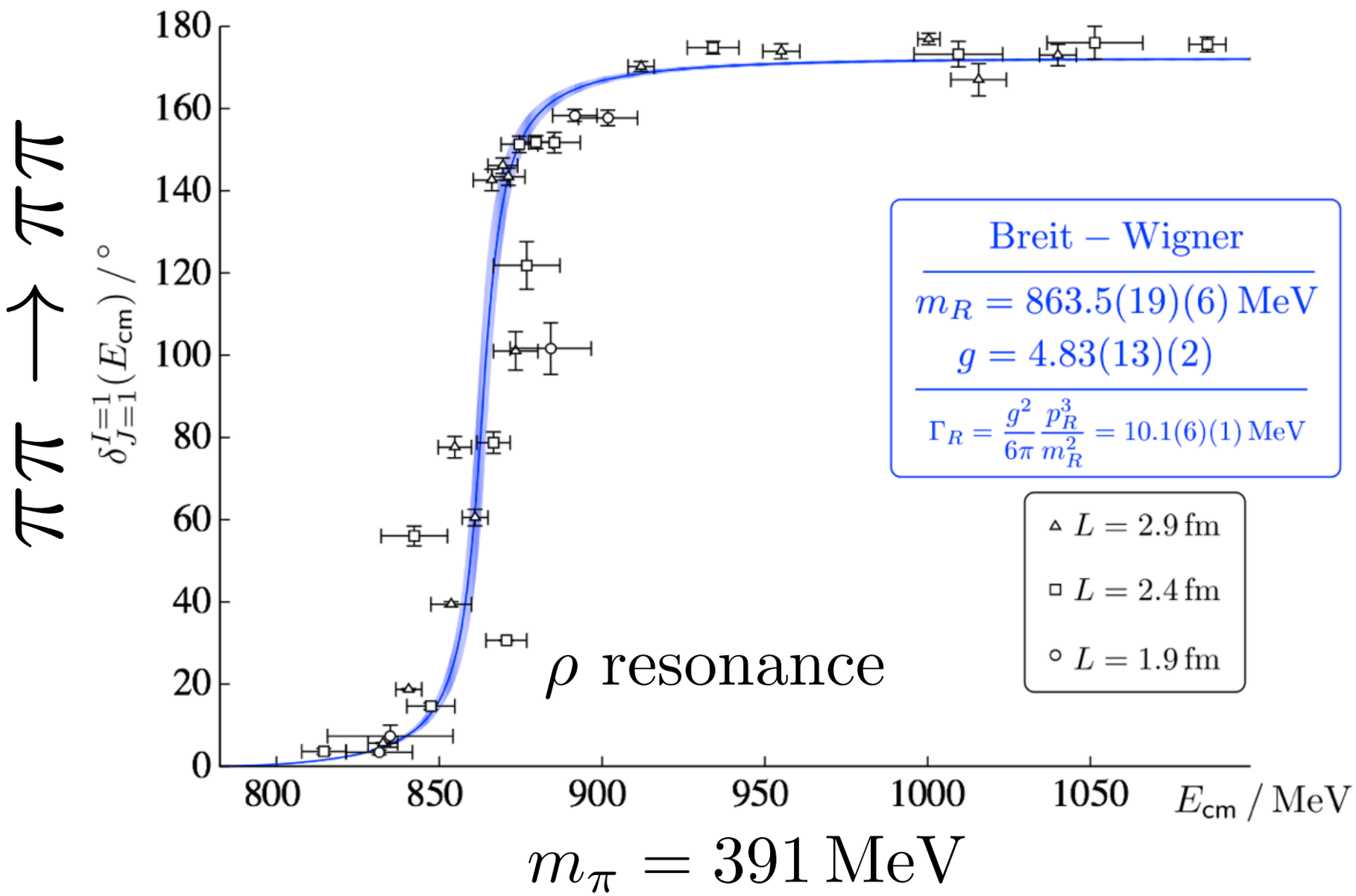

from Dudek, Edwards, Thomas in *Phys.Rev.* D87 (2013) 034505

However, there is **no general method** for extracting scattering amplitudes involving **more than two hadrons**.

As a result LQCD cannot investigate...

However, there is **no general method** for extracting scattering amplitudes involving **more than two hadrons**.

As a result LQCD cannot investigate...

resonances which decay into more than two hadrons

$$\omega(782) \to \pi\pi\pi \qquad N(1440) \to N\pi\pi$$

three-body forces

$$\pi\pi\pi \to \pi\pi\pi \qquad NNN \to NNN$$

However, there is **no general method** for extracting scattering amplitudes involving **more than two hadrons**.

As a result LQCD cannot investigate...

weak decays coupled to channels containing more than two hadrons

$K \to \pi\pi\pi$ $\quad$ $D \to \pi\pi$ $\quad$ $D \to K\overline{K}$

(couples to $\pi\pi\pi\pi$)

Need strong scattering to relate lattice weak matrix elements to physical decay amplitudes

Lellouch, L. & Lüscher, M.
Commun. Math. Phys. 219, 31-44 (2001)

In recent years important progress has been made towards extracting three-particle scattering.

Polejaeva, K. and Rusetsky, A. *Eur. Phys. J.* A48 (2012) 67
Briceno, R. A. and Davoudi, Z. *Phys. Rev.* D87 (2013) 094507

However a relativistic, model-independent method is still unknown.

This is the focus of today's talk.

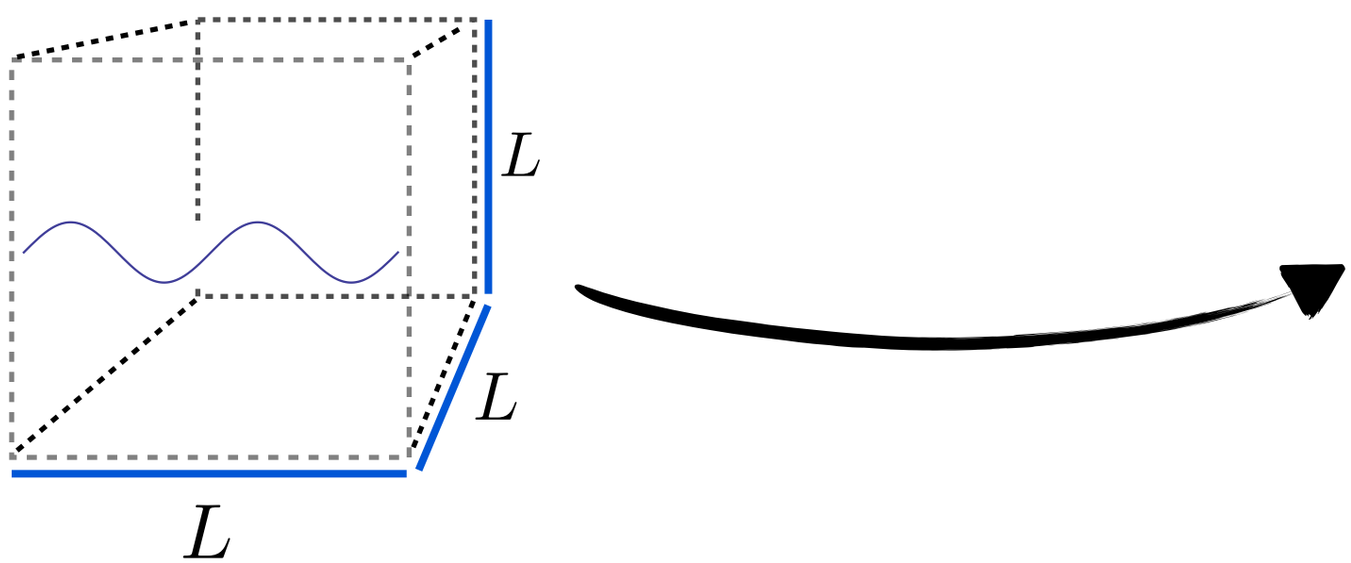

$$\pi\pi \to \pi\pi$$
$$\pi\pi\pi \to \pi\pi\pi$$

Outline

Detailed set-up

Two particles in a box

Three particles in a box

Conclusion

Particle content

Single scalar, mass m

all results for identical scalars

Relativistic field theory

$\mathbb{Z}_2$ **symmetry**

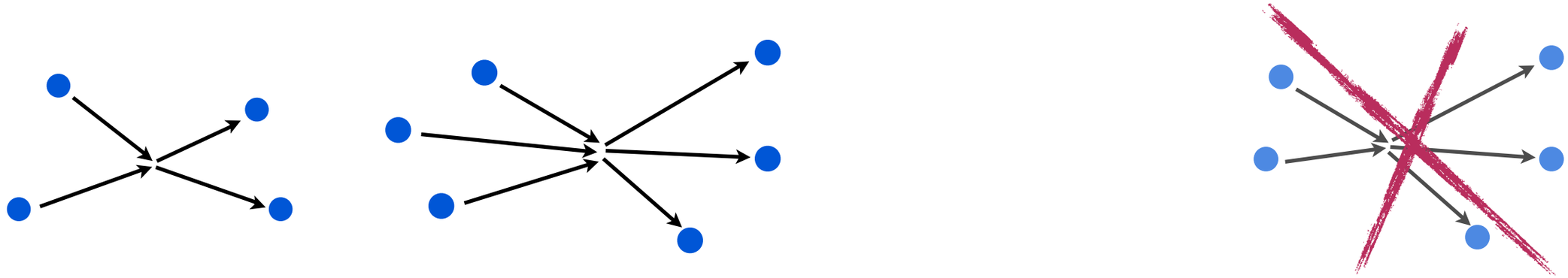

(For pions in QCD this is G-parity)

Include all vertices

with even number of legs

Finite volume

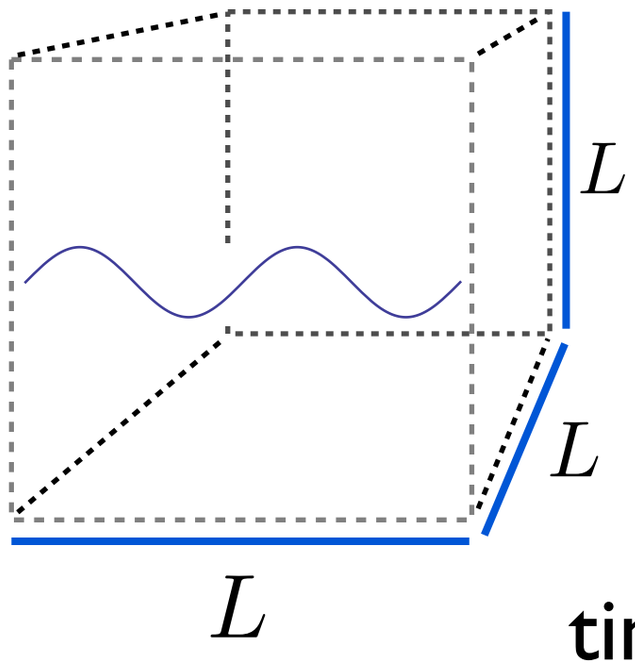

cubic, spatial volume (extent L)

periodic boundary conditions

$$\vec{p} \in (2\pi/L)\mathbb{Z}^3$$

time direction **infinite** and **Minkowski**

Take L large enough to ignore e^{-mL}

dropped throughout!

Take space to be continuous

lattice spacing set to zero

Finite volume

Infinite volume

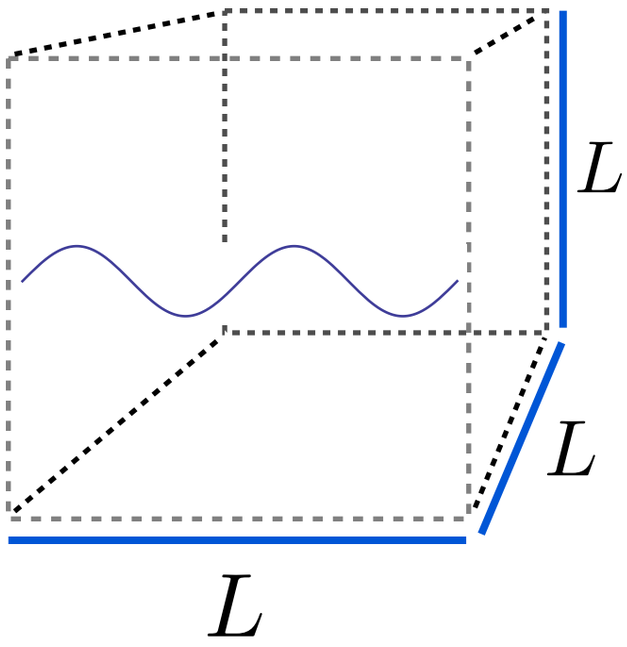

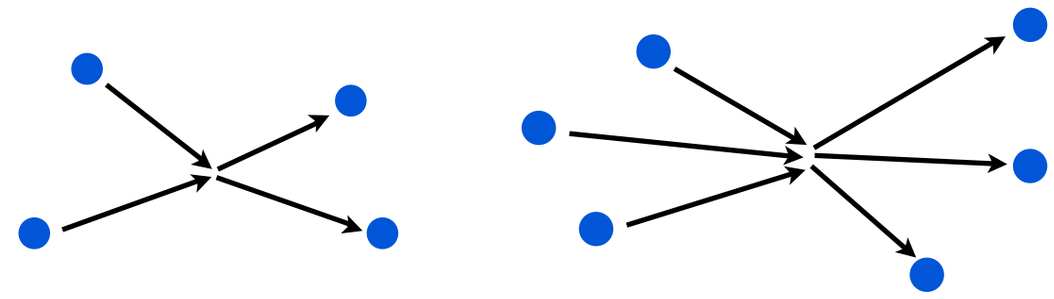

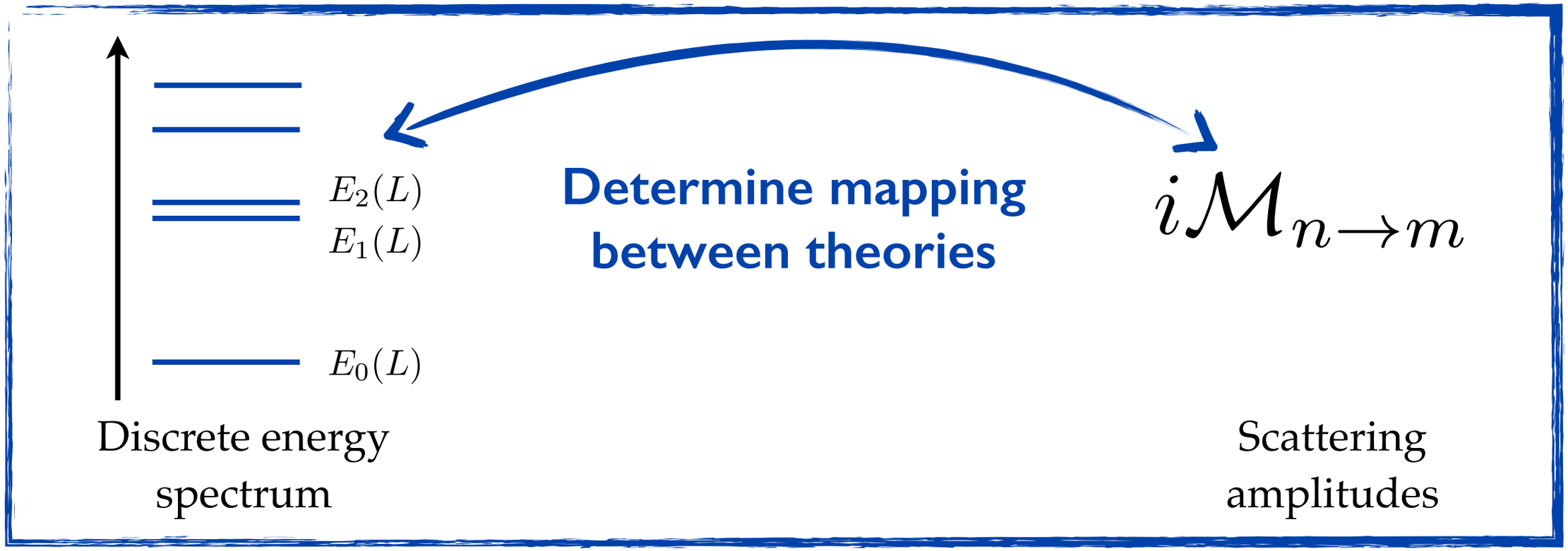

Determine relation using finite-volume correlator

$$C_L(E,\vec{P}) \equiv \int_L d^4x\, e^{i(Ex^0 - \vec{P}\cdot\vec{x})} \langle 0|\mathrm{T}\sigma(x)\sigma^\dagger(0)|0\rangle$$

Determine relation using finite-volume correlator

$$C_L(E,\vec{P}) \equiv \int_L d^4x\, e^{i(Ex^0 - \vec{P}\cdot\vec{x})} \langle 0|\mathrm{T}\sigma(x)\sigma^\dagger(0)|0\rangle$$

energy E, momentum $\vec{P} = (2\pi/L)\vec{n}_P$

CM energy $E^{*2} \equiv E^2 - \vec{P}^2$

interpolating field

Determine relation using finite-volume correlator

$$C_L(E,\vec{P}) \equiv \int_L d^4x\, e^{i(Ex^0 - \vec{P}\cdot\vec{x})} \langle 0|\mathrm{T}\sigma(x)\sigma^\dagger(0)|0\rangle$$

energy E, momentum $\vec{P} = (2\pi/L)\vec{n}_P$

CM energy $E^{*2} \equiv E^2 - \vec{P}^2$

interpolating field

At fixed $L, \vec{P}$, poles in C_L give finite-volume spectrum

We calculate $C_L(E,\vec{P})$ to all orders in perturbation theory and determine condition of divergence.

First, two particles in a box

$$C_L(E,\vec{P}) \equiv \int_L d^4x\, e^{i(Ex^0 - \vec{P}\cdot\vec{x})} \langle 0|\mathrm{T}\sigma(x)\sigma^\dagger(0)|0\rangle$$

Require $E^* < 4m$ **even-particle quantum numbers**

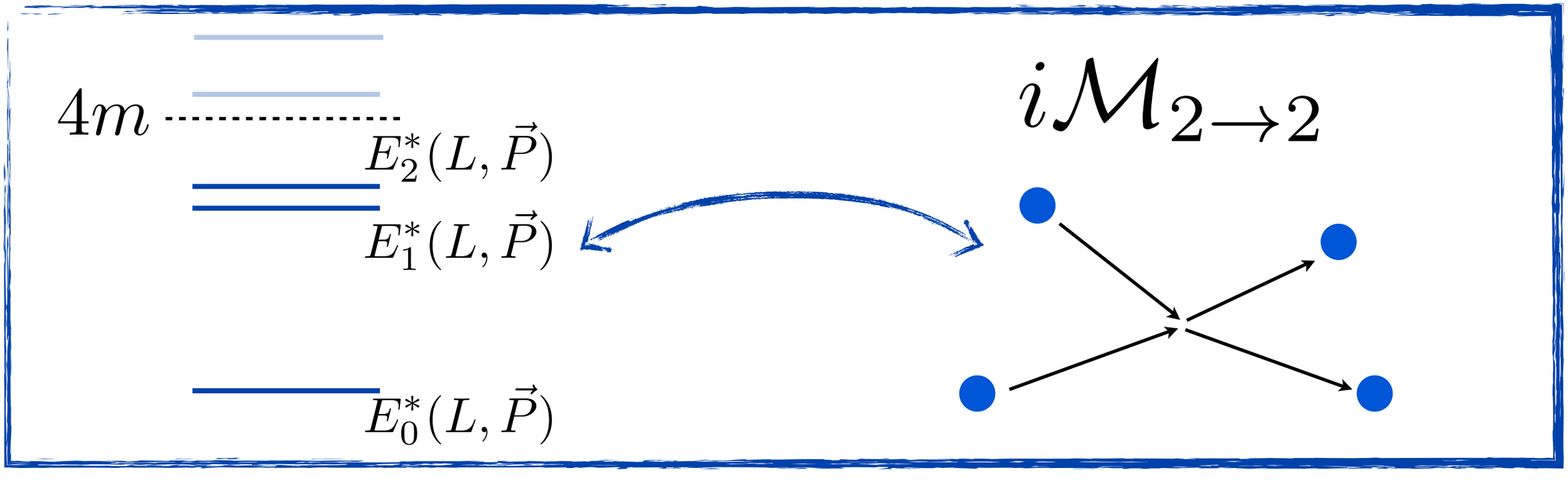

Derivation from Kim, Sachrajda and Sharpe. *Nucl. Phys.* B727, 218-243 (2005)

$$C_L(E,\vec{P}) \equiv$$

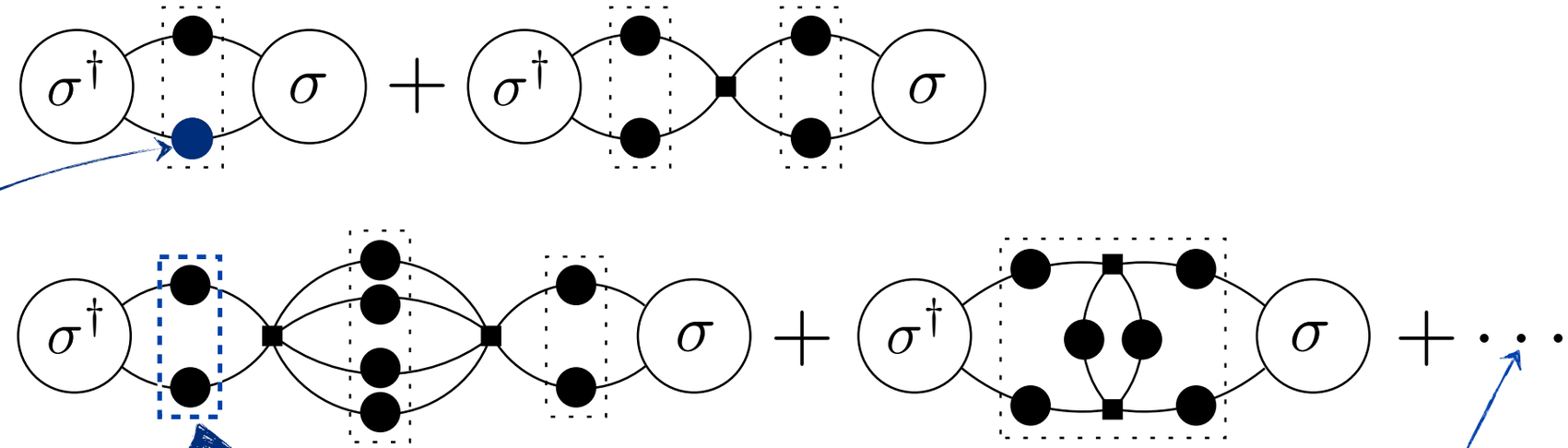

fully dressed propagators

infinite set of terms
no assumed suppression

spatial loop momenta are summed

$$\frac{1}{L^3} \sum_{\vec{k}\in(2\pi/L)\mathbb{Z}^3} \int \frac{dk^0}{2\pi}$$

$$C_L(E,\vec{P}) \equiv$$

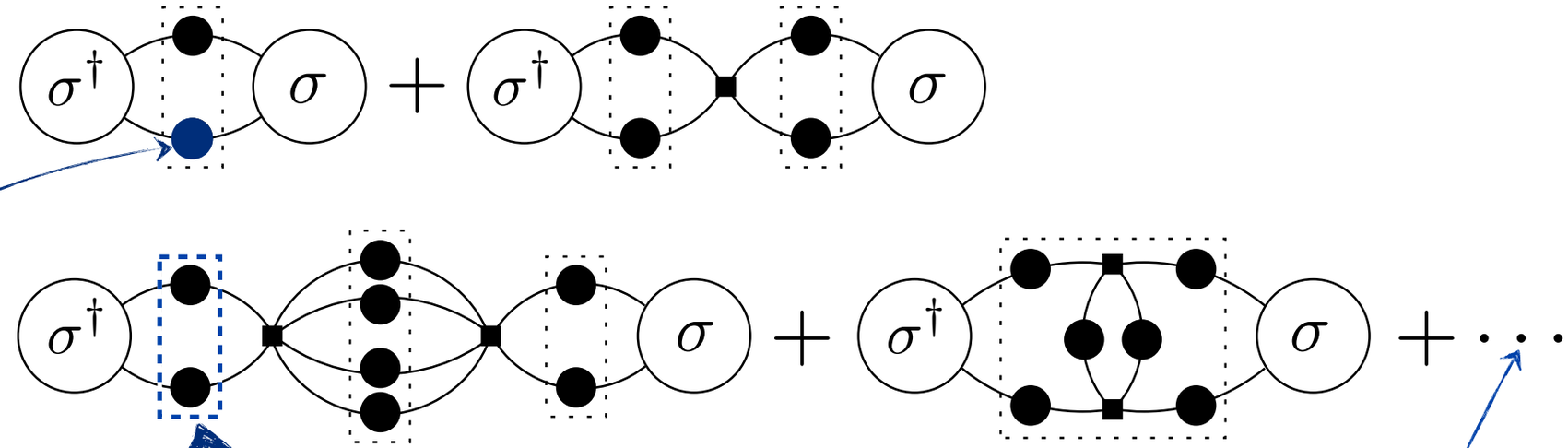

fully dressed propagators

infinite set of terms
no assumed suppression

spatial loop momenta are summed

$$\frac{1}{L^3}\sum_{\vec{k}\in(2\pi/L)\mathbb{Z}^3}\int\frac{dk^0}{2\pi}$$

Key observation:

If particles in summed loops cannot all go on shell, then replace

$$\frac{1}{L^3}\sum_{\vec{k}} \longrightarrow \int\frac{d^3k}{(2\pi)^3}$$

difference is order

$$e^{-mL}$$

$C_L(E, \vec{P}) \equiv$

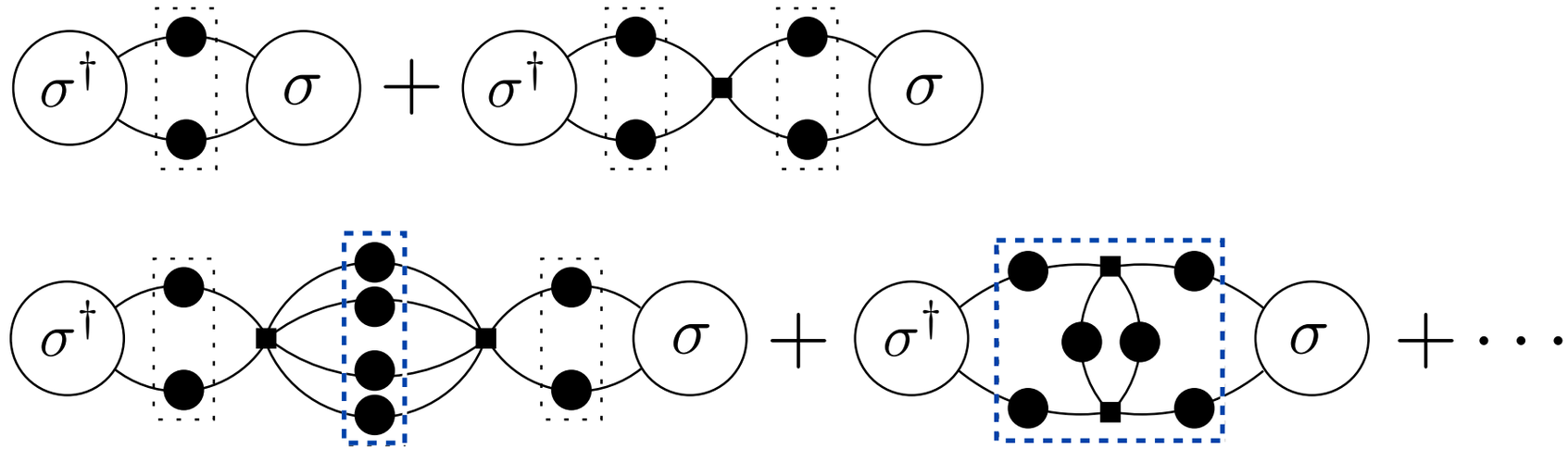

$$\frac{1}{L^3}\sum_{\vec{k}} \longrightarrow \int_{\vec{k}} \equiv \int \frac{d^3k}{(2\pi)^3}$$

Since $E^* < 4m$, **only two** particles with total momentum $(E, \vec{P})$ **can go on-shell**

$$C_L(E,\vec{P}) =$$

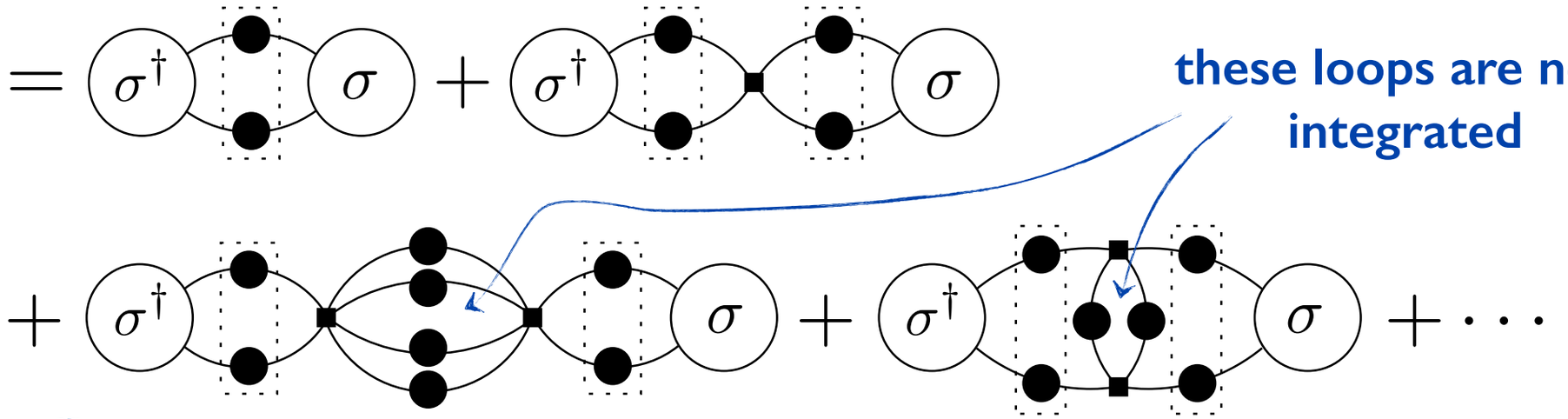

these loops are now integrated

$C_L(E,\vec{P}) =$

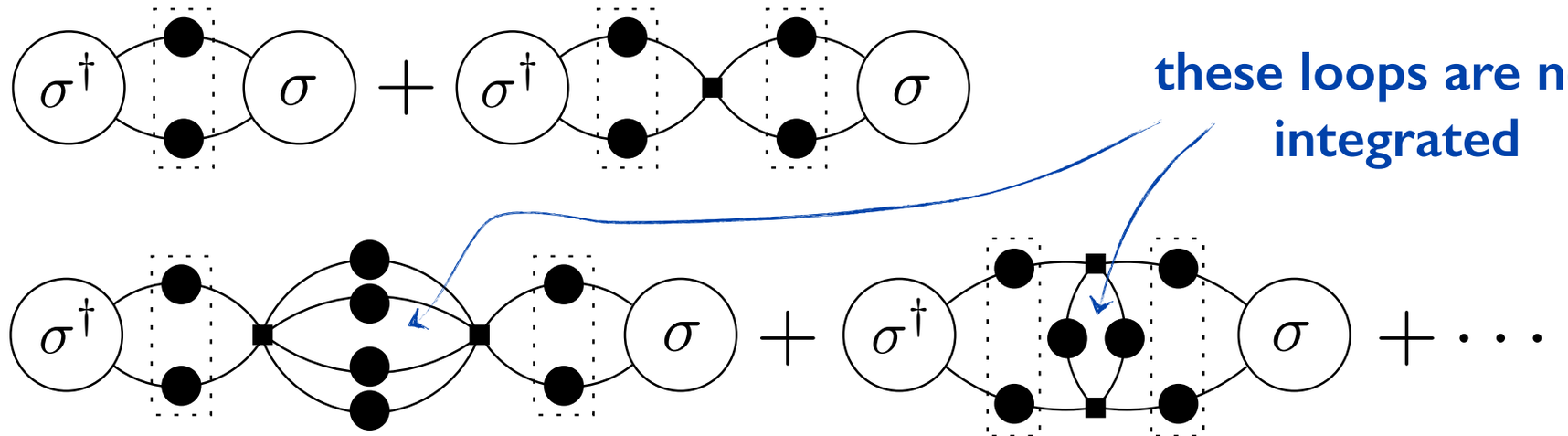

these loops are now integrated

$C_L(E,\vec{P}) =$

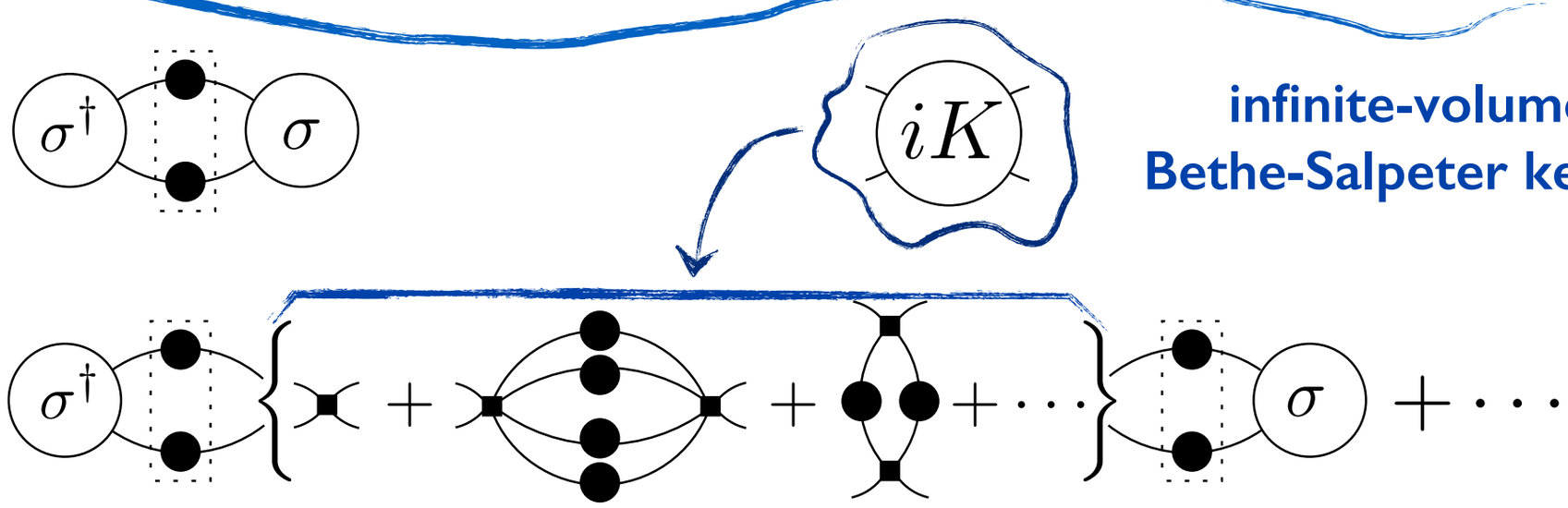

infinite-volume Bethe-Salpeter kernel

$C_L(E,\vec{P}) =$

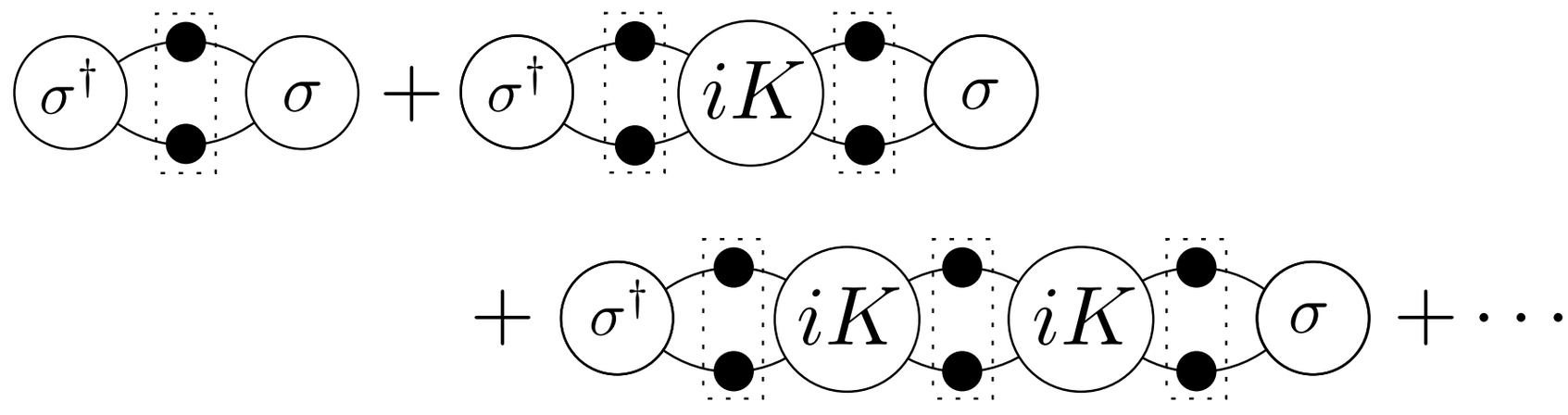

$C_L(E,\vec{P}) =$ 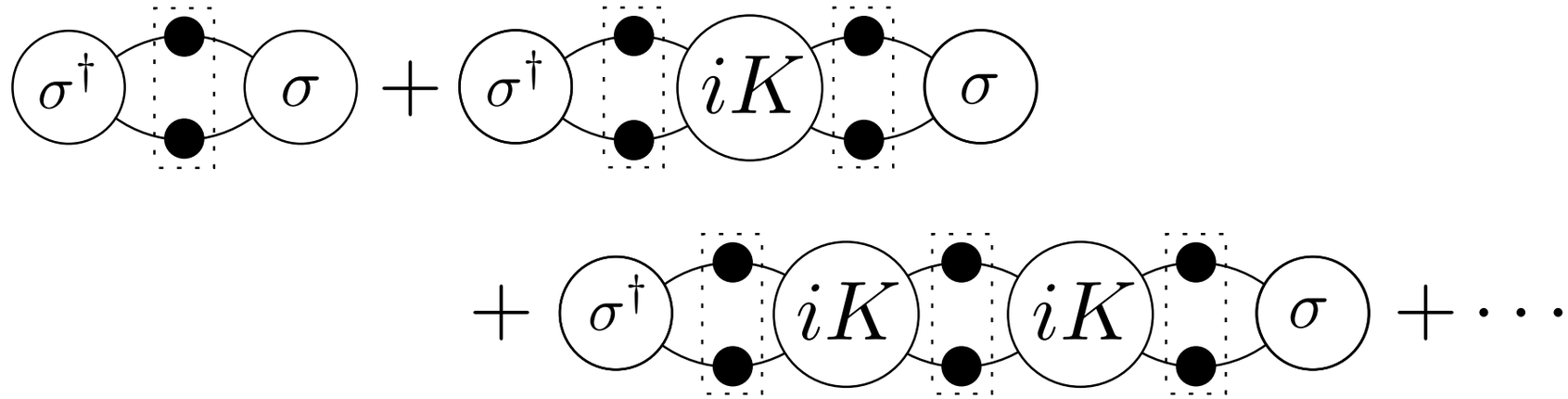

Next we introduce an important identity

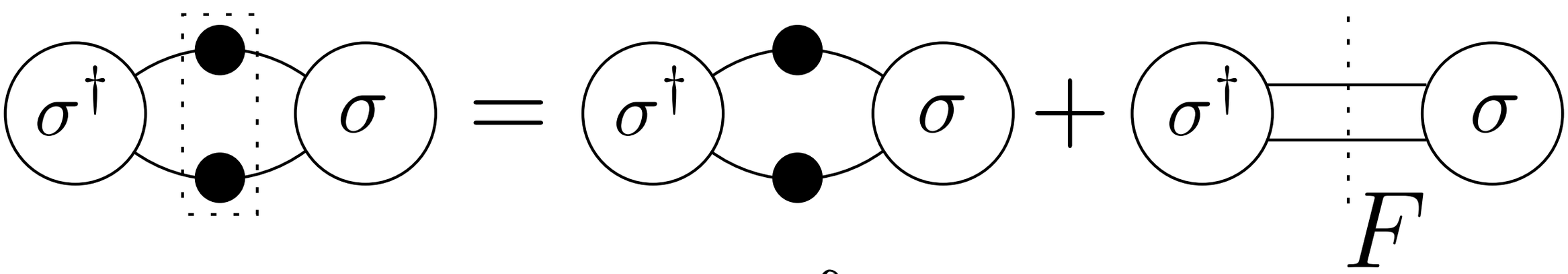

$$\frac{1}{L^3}\sum_{\vec{k}} \qquad \int_{\vec{k}}$$

contains all power-law corrections

$$C_L(E,\vec{P}) =$$

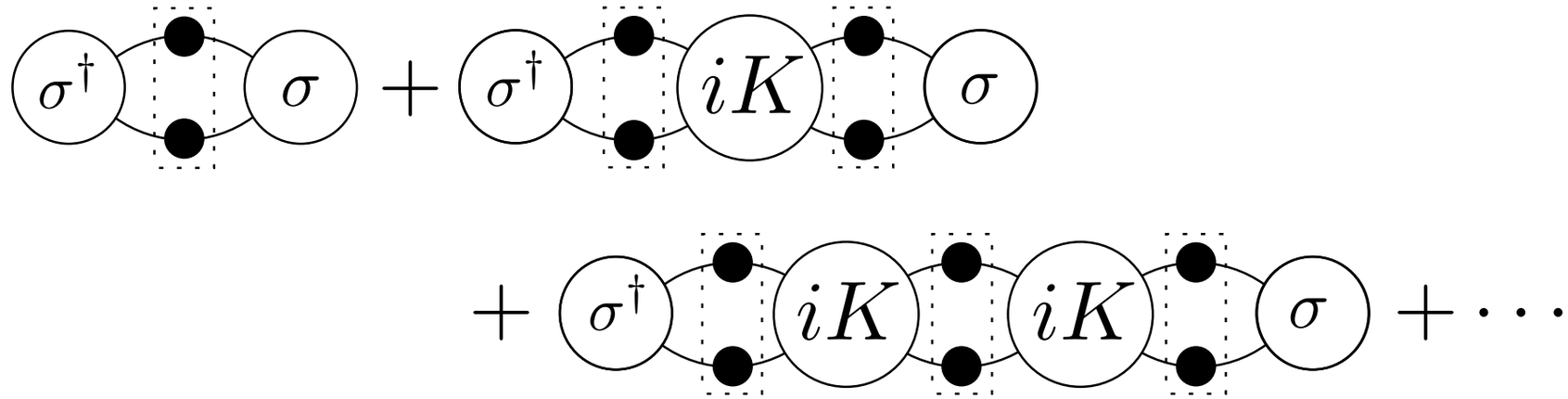

Next we introduce an important identity

off-shell **on-shell**

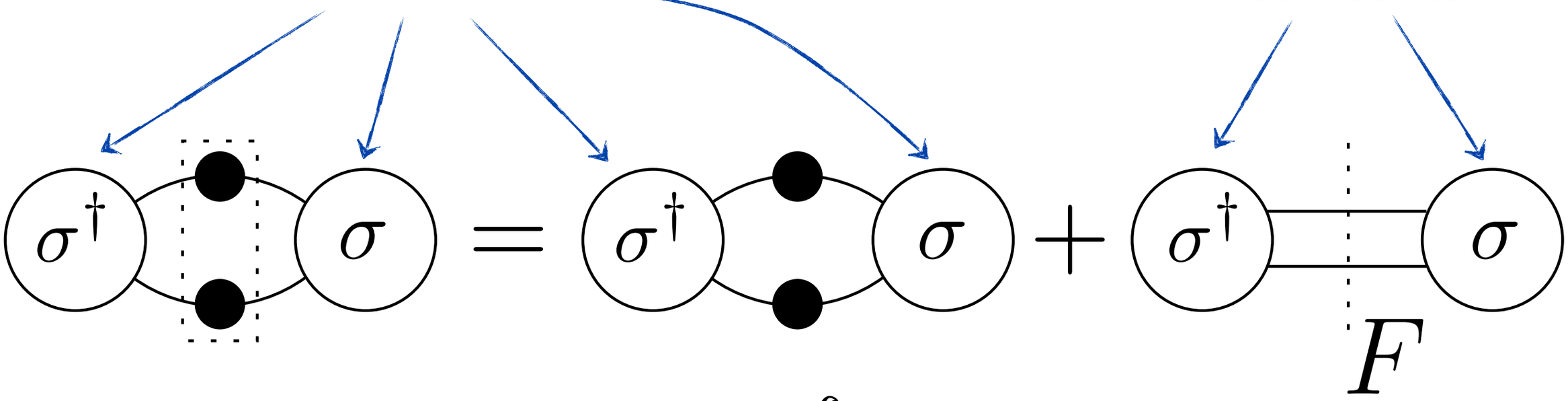

$$\frac{1}{L^3}\sum_{\vec{k}} \qquad \int_{\vec{k}}$$

contains all power-law corrections

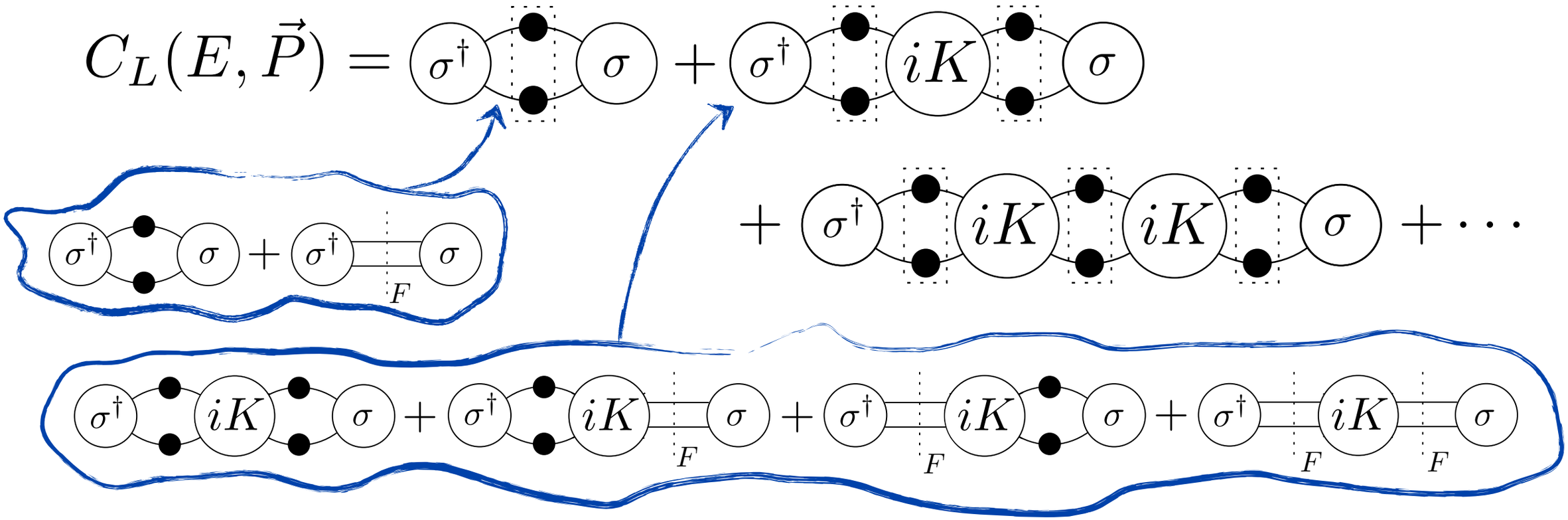
$C_L(E,\vec{P}) =$
$\sigma^\dagger$
σ
iK
F
$+ \cdots$

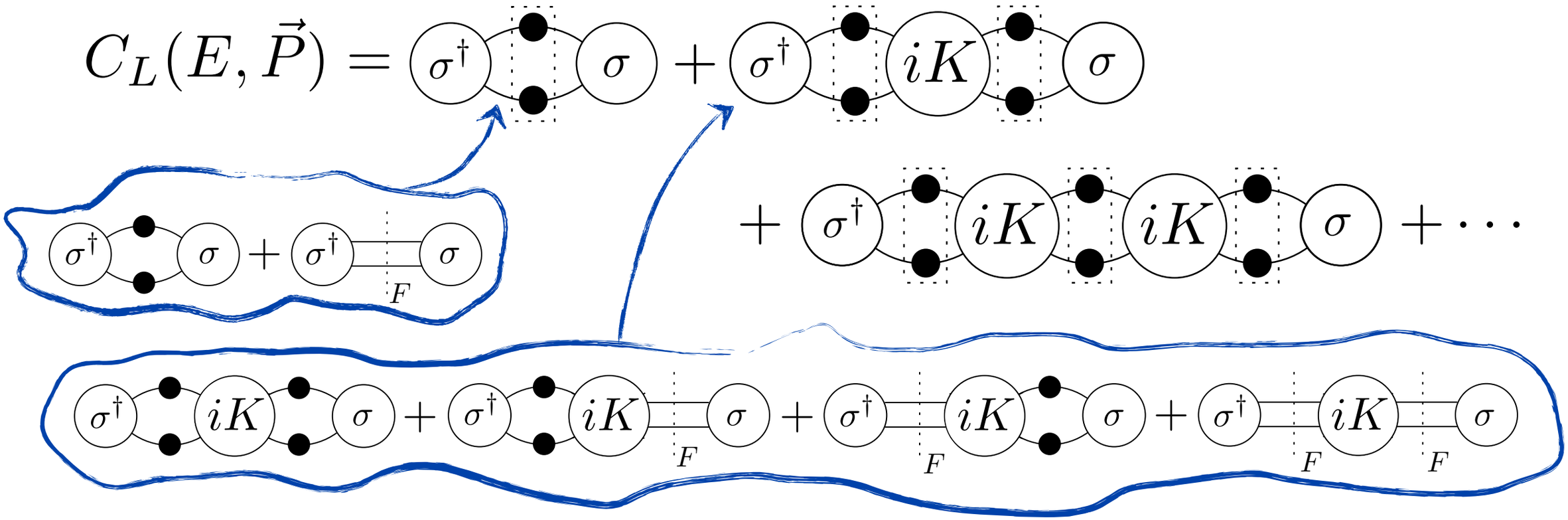

Now regroup by number of F cuts

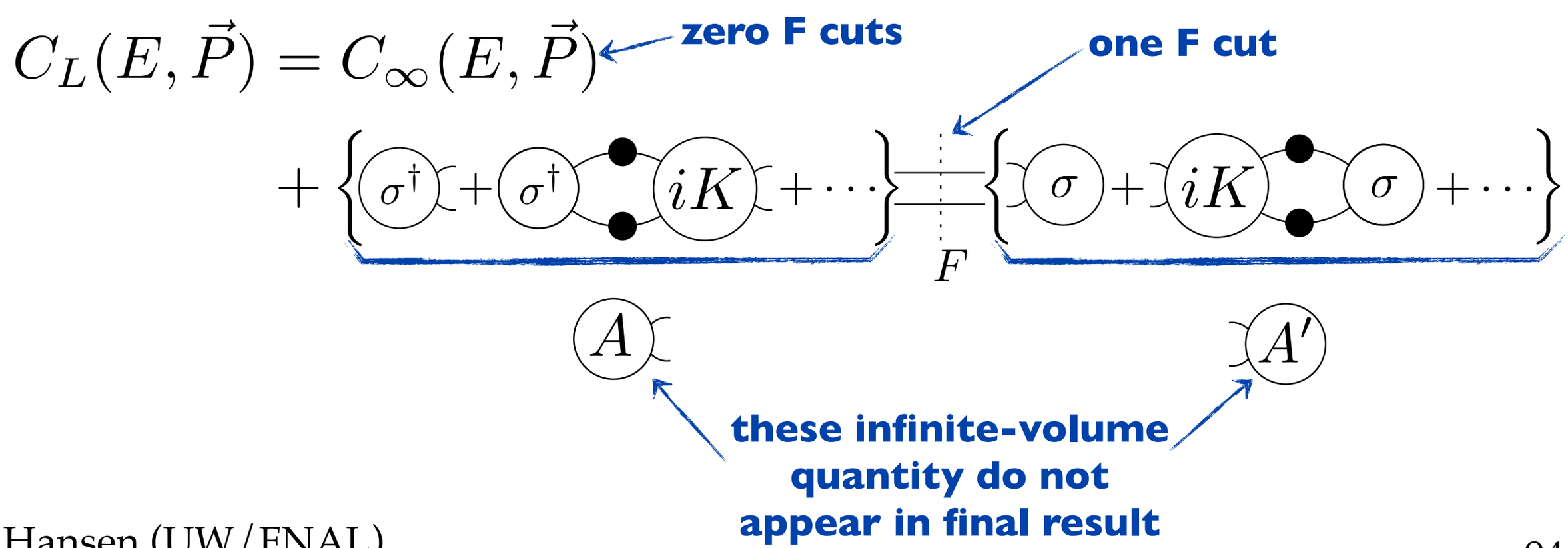

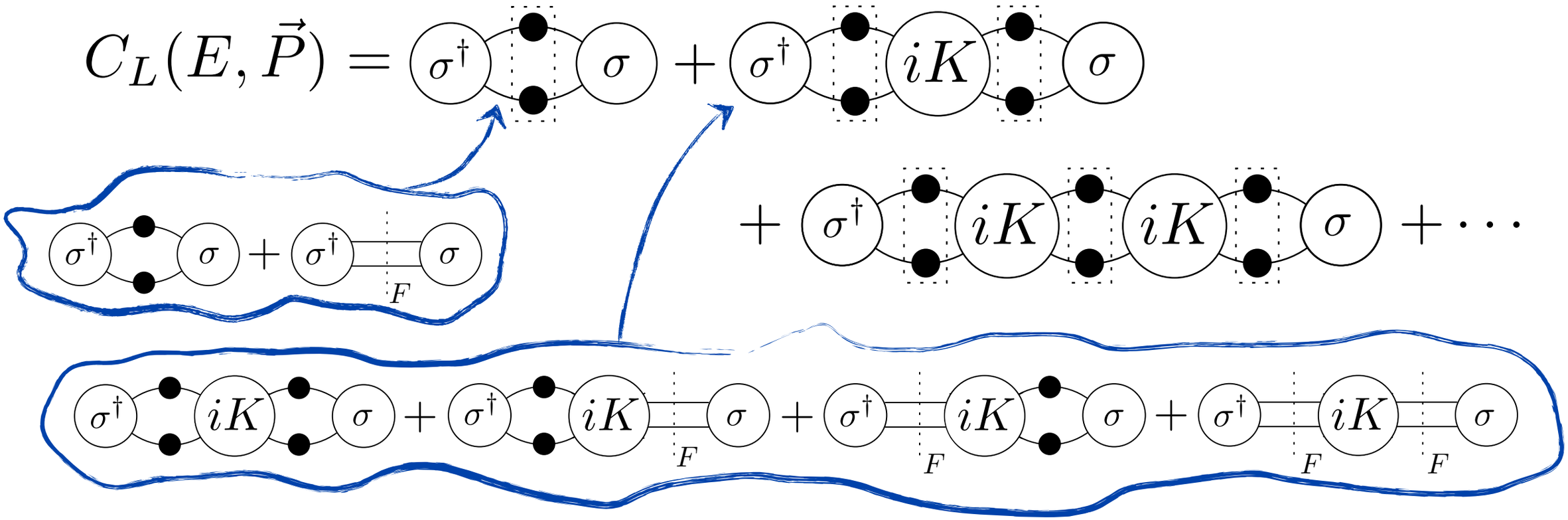

Now regroup by number of F cuts

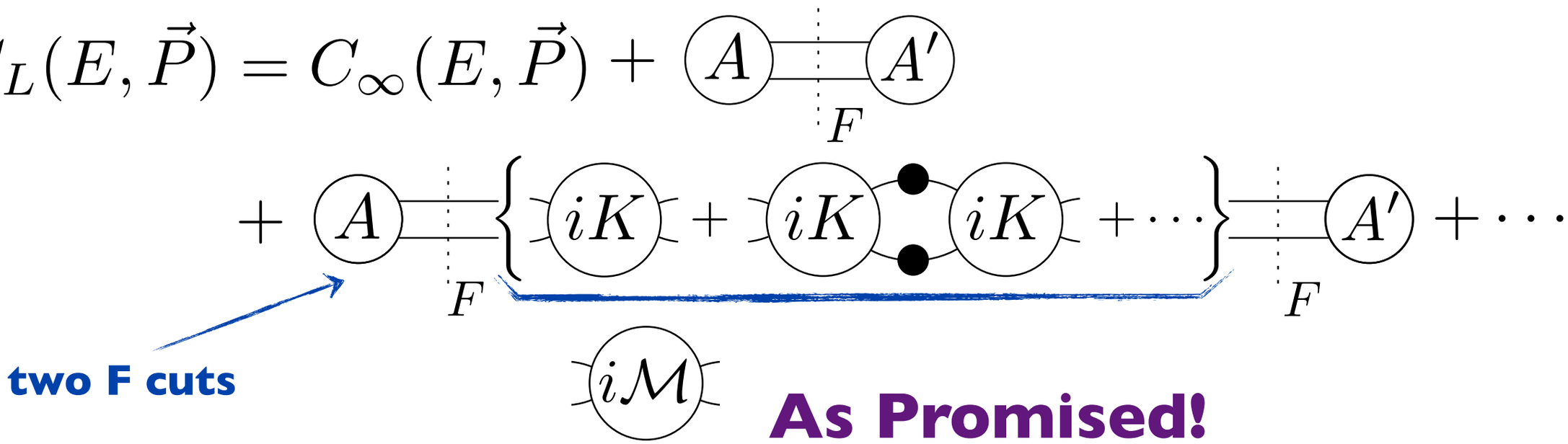

As Promised!
infinite-volume on-shell two-to-two scattering amplitude

$$C_L(E,\vec{P}) = C_\infty(E,\vec{P})$$

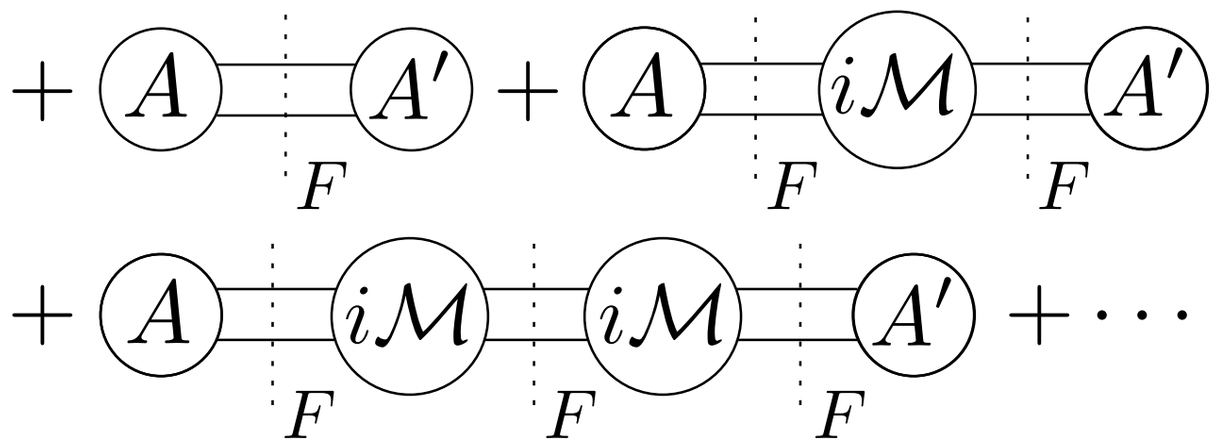

$$C_L(E,\vec{P}) = C_\infty(E,\vec{P}) + \sum_{n=0}^{\infty} A' iF [i\mathcal{M}_{2\to 2} iF]^n A$$

$$C_L(E,\vec{P}) = C_\infty(E,\vec{P})$$

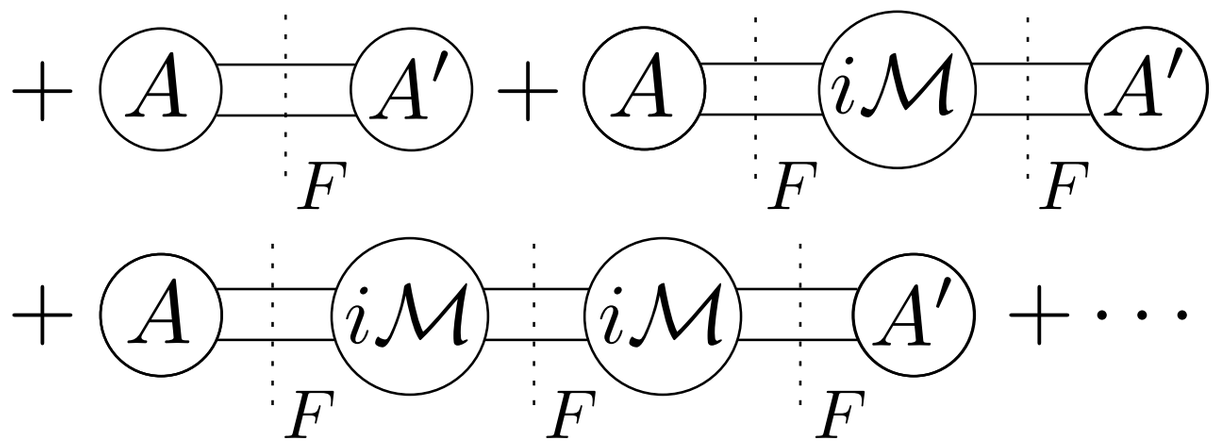

$$+ \cdots$$

$$C_L(E,\vec{P}) = C_\infty(E,\vec{P}) + \sum_{n=0}^{\infty} A' iF [i\mathcal{M}_{2\to 2} iF]^n A$$

$$C_L(E,\vec{P}) = C_\infty(E,\vec{P}) + A' iF \frac{1}{1 - i\mathcal{M}_{2\to 2} iF} A$$

no poles **no poles** **no poles**

$C_L(E,\vec{P})$ **diverges whenever** $iF \dfrac{1}{1 - i\mathcal{M}_{2\to 2} iF}$ **diverges**

Two-particle review

1

$C_L(E,\vec{P}) =$ 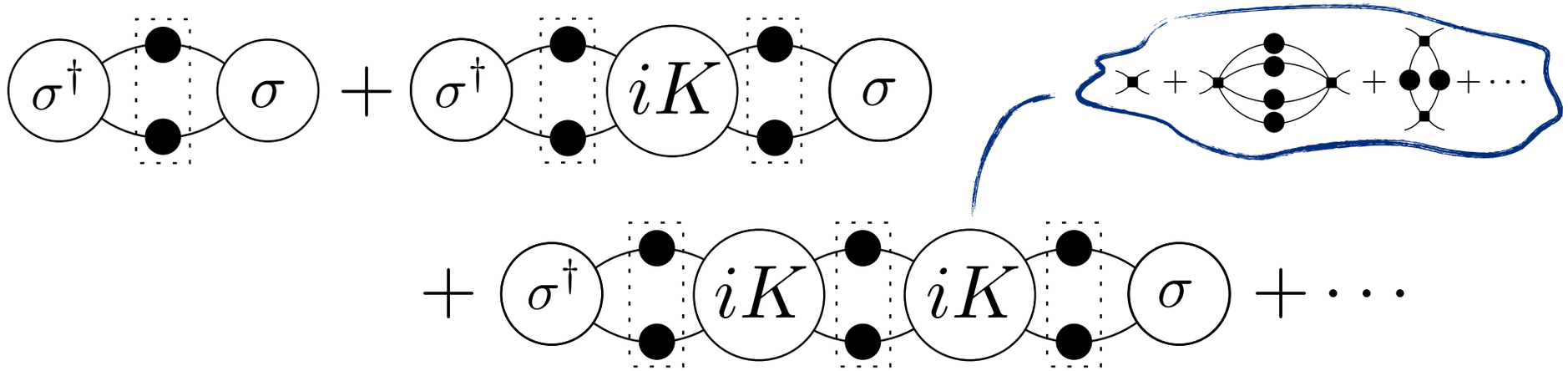

Two-particle review

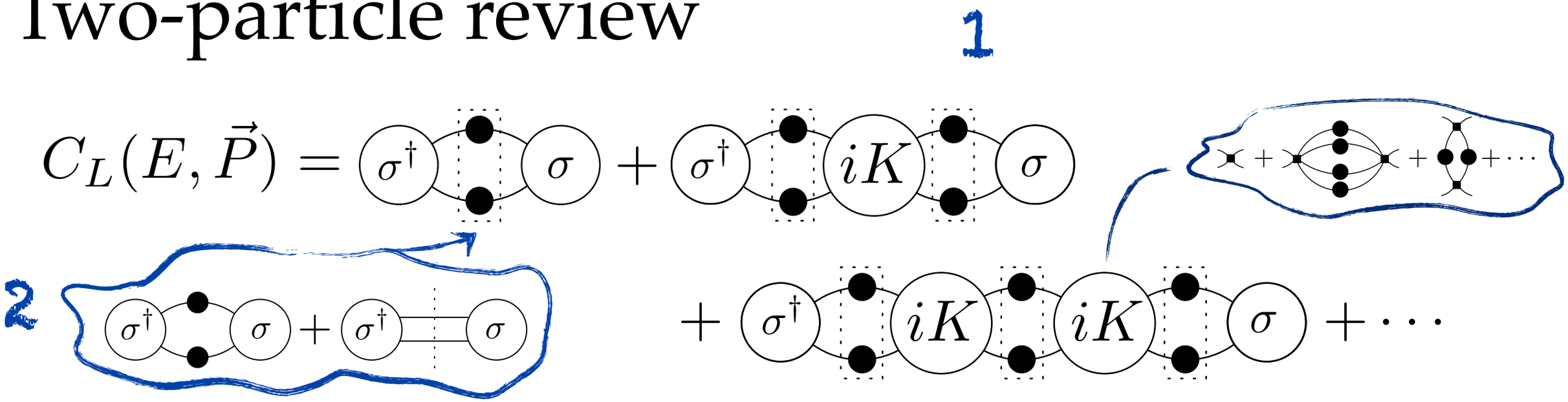

Two-particle review

1

$$C_L(E,\vec{P}) =$$

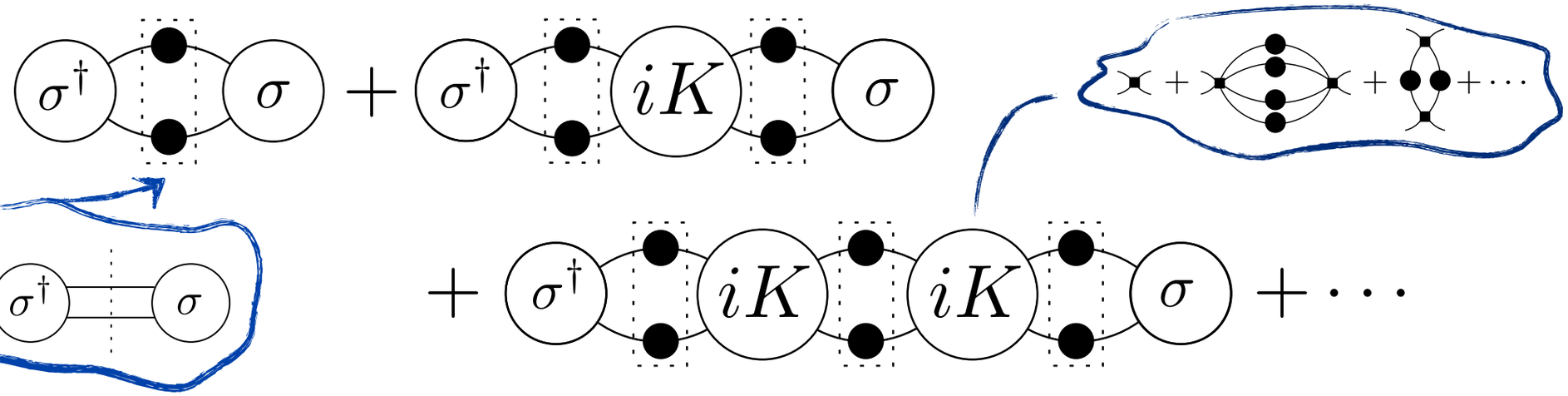

2

$$C_L(E,\vec{P}) = C_\infty(E,\vec{P})$$

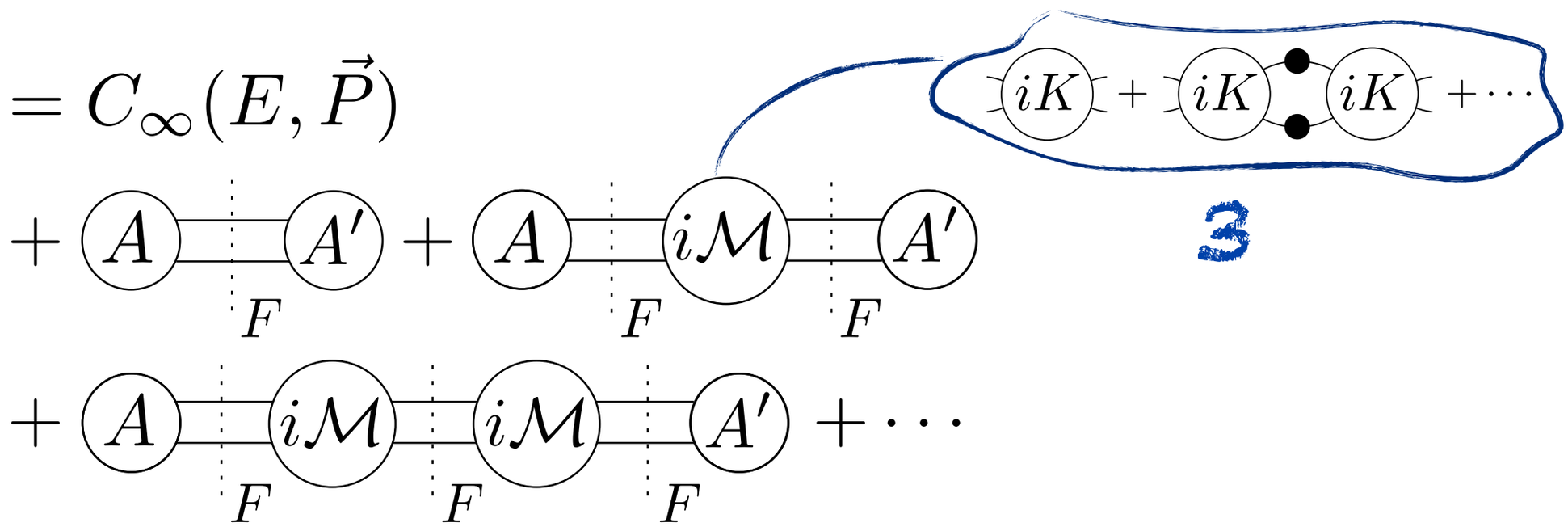

3

Two-particle review

1

$$C_L(E,\vec{P}) =$$

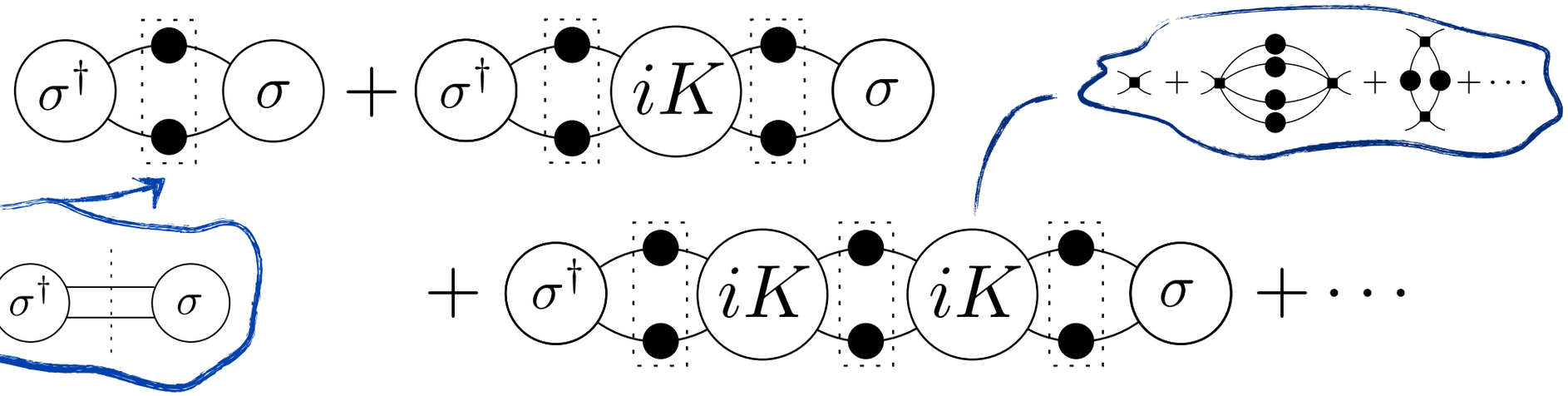

2

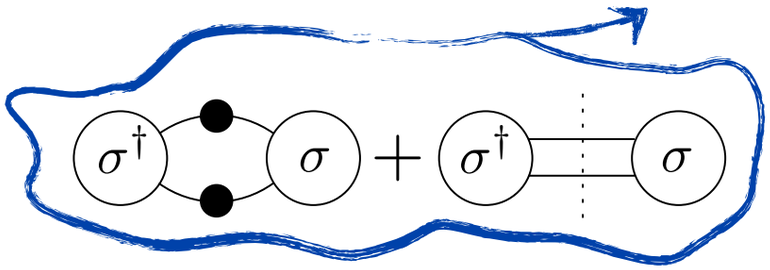

$$C_L(E,\vec{P}) = C_\infty(E,\vec{P})$$

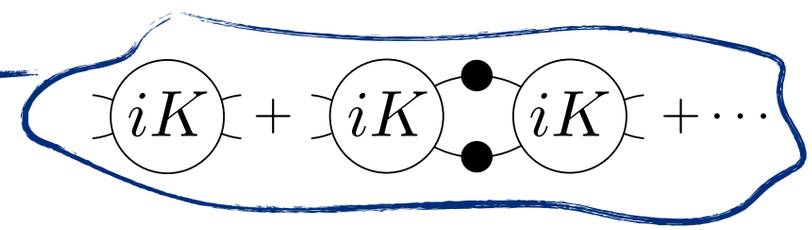

3

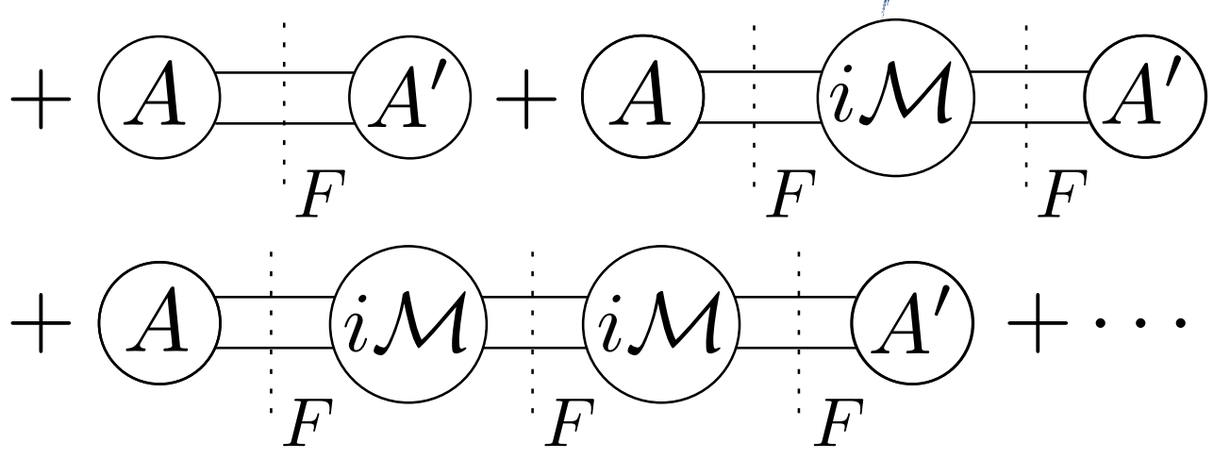

4

$$C_L(E,\vec{P}) = C_\infty(E,\vec{P}) + A' iF \frac{1}{1 - i\mathcal{M}_{2\to 2} iF} A$$

Two-particle result

At fixed $(L, \vec{P})$, finite-volume spectrum is all solutions to

$$\Delta_{L,P}(E) = \det[1 - i\mathcal{M}_{2\to 2} iF] = 0$$

diagonal matrix in angular momentum space

kinematic (related to Lüscher Zeta function)

$F \equiv$ 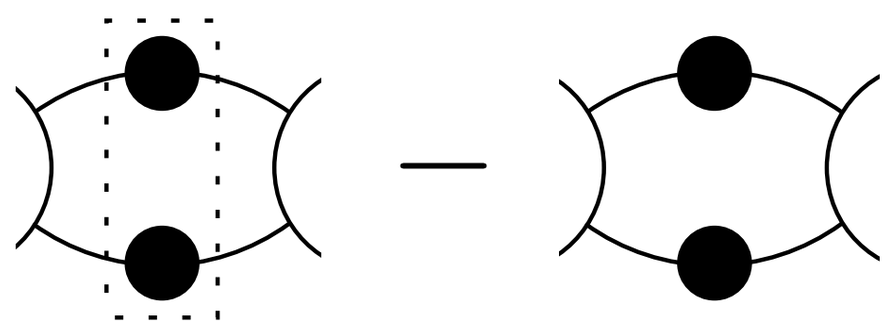

Two-particle result

$$\Delta_{L,P}(E) = \det[1 - i\mathcal{M}_{2\to 2} iF] = 0$$

...is it useful?

At low energies, s-wave dominates

$$[\mathcal{M}^s_{2\to 2}(E^*_n)]^{-1} = -F^s(E_n, \vec{P}, L)$$

$$F^s(E, \vec{P}, L) \equiv \frac{1}{2}\left[\frac{1}{L^3}\sum_{\vec{k}} - \int \frac{d^3k}{(2\pi)^3}\right] \frac{1}{2\omega_k 2\omega_{P-k}(E - \omega_k - \omega_{P-k} + i\epsilon)}$$

Two-particle result

Note also, equation is real

$$[\mathcal{M}^s_{2\to 2}(E^*_n)]^{-1} = -F^s(E_n, \vec{P}, L)$$

$$\boxed{p_n \cot\delta^s(p_n) - i\cancel{p}_n = -16\pi E^*_n \,\mathrm{Re}F^s - i\cancel{p}_n}$$

This can also be seen by **replacing i-epsilon with principal value** everywhere in derivation.

$$\mathcal{M}_{2\to 2} \longrightarrow \mathcal{K}_{2\to 2} \qquad\qquad F \longrightarrow \mathrm{Re}\, F$$

Important for three-particle case

$$p_n \cot \delta(p_n) = -16\pi E_n^* \mathrm{Re} F$$

$$\mathcal{M}^s_{2\to 2}(E) = \frac{16\pi E}{p \cot \delta(p) - ip}$$

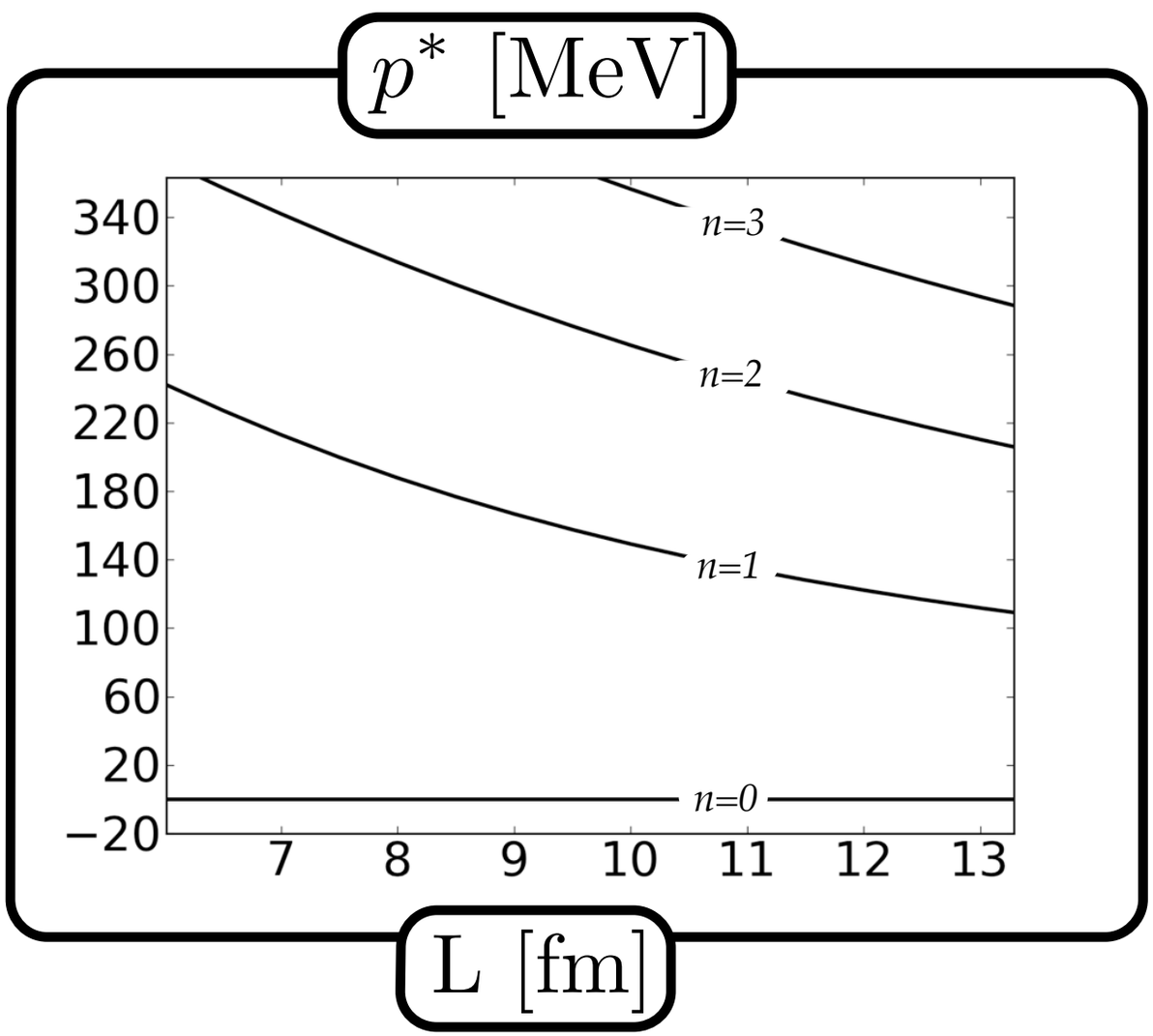

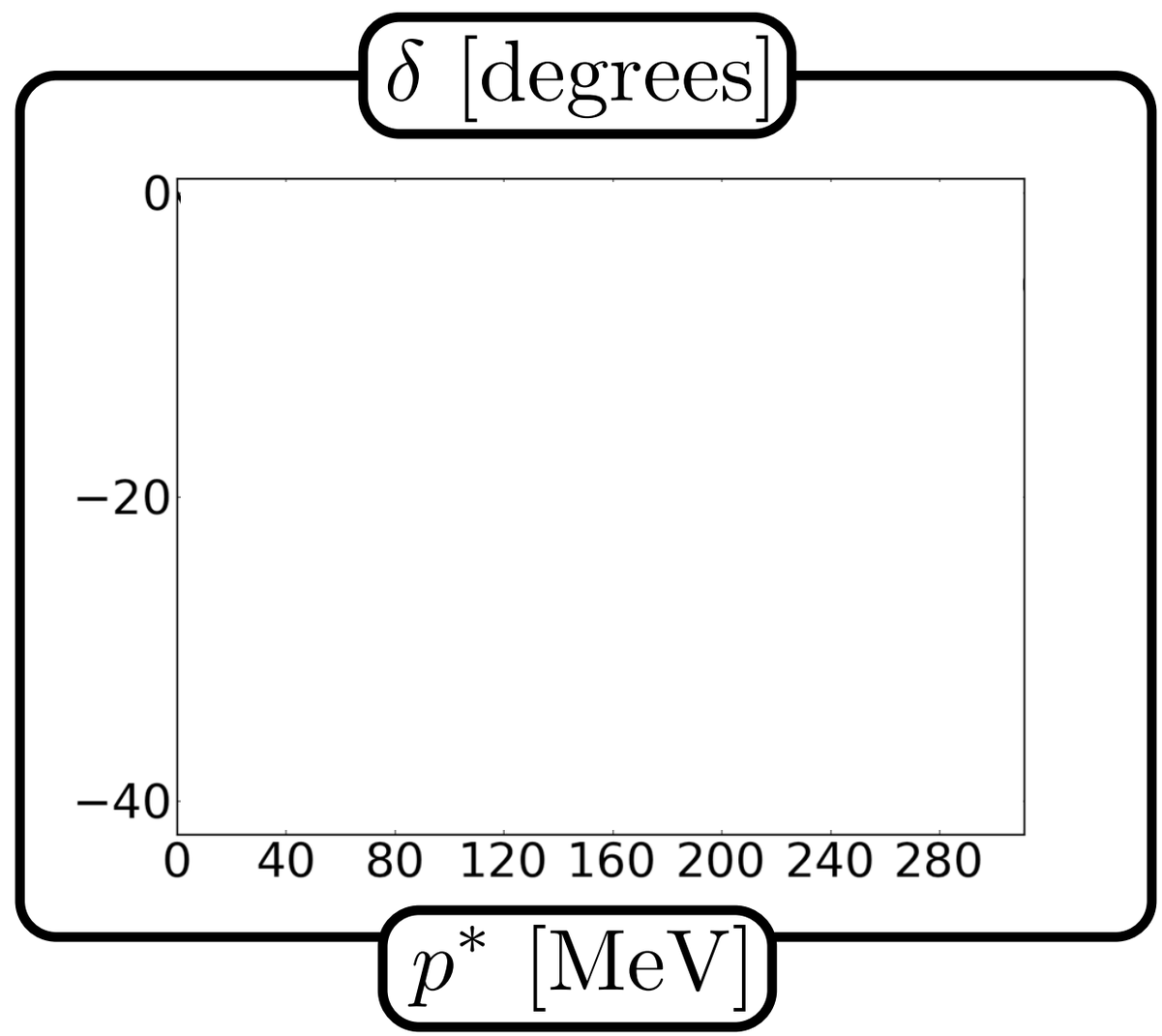

$$p_n \cot \delta(p_n) = -16\pi E_n^* \mathrm{Re} F$$

$$\mathcal{M}^s_{2\to 2}(E) = \frac{16\pi E}{p \cot \delta(p) - ip}$$

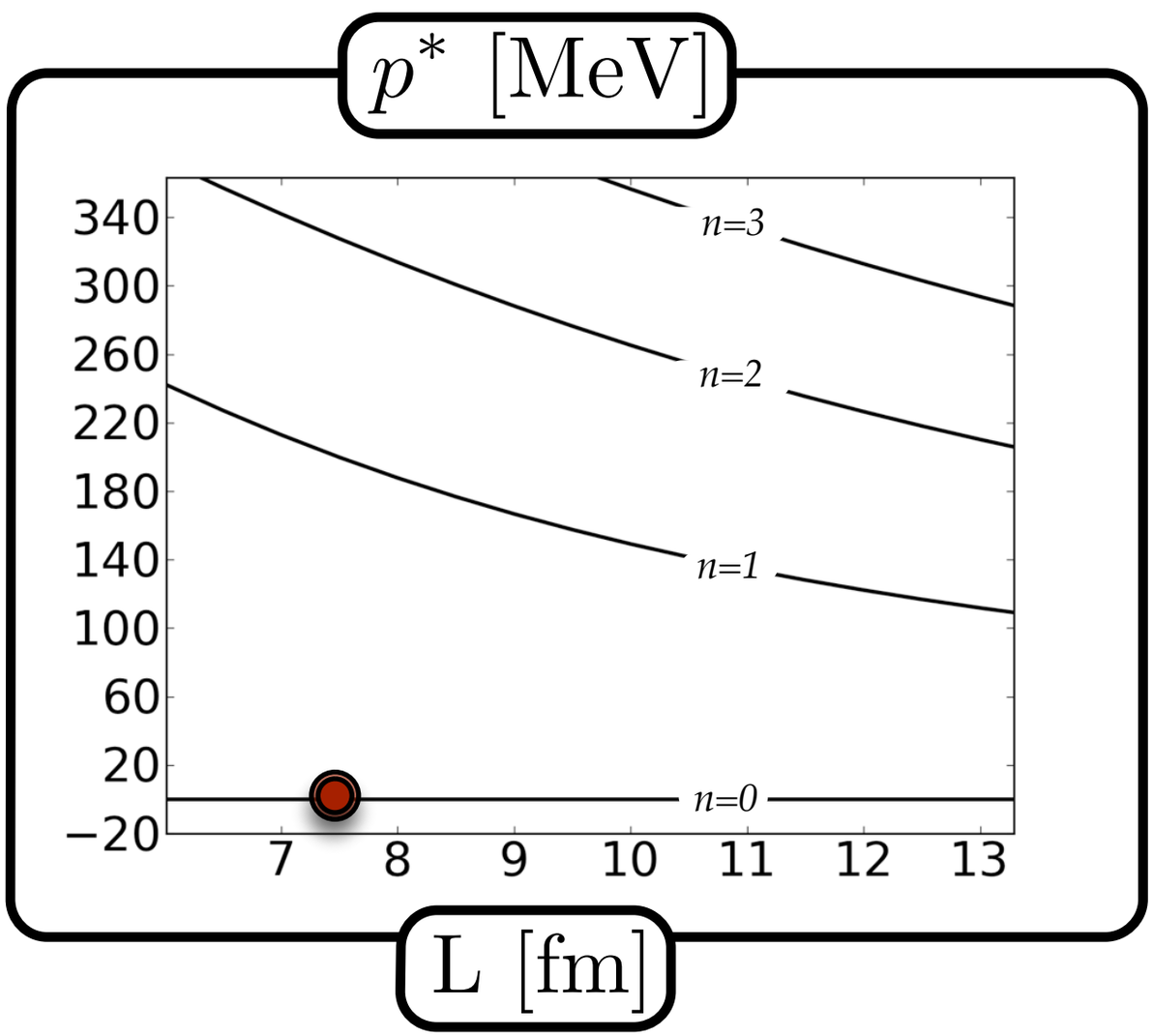

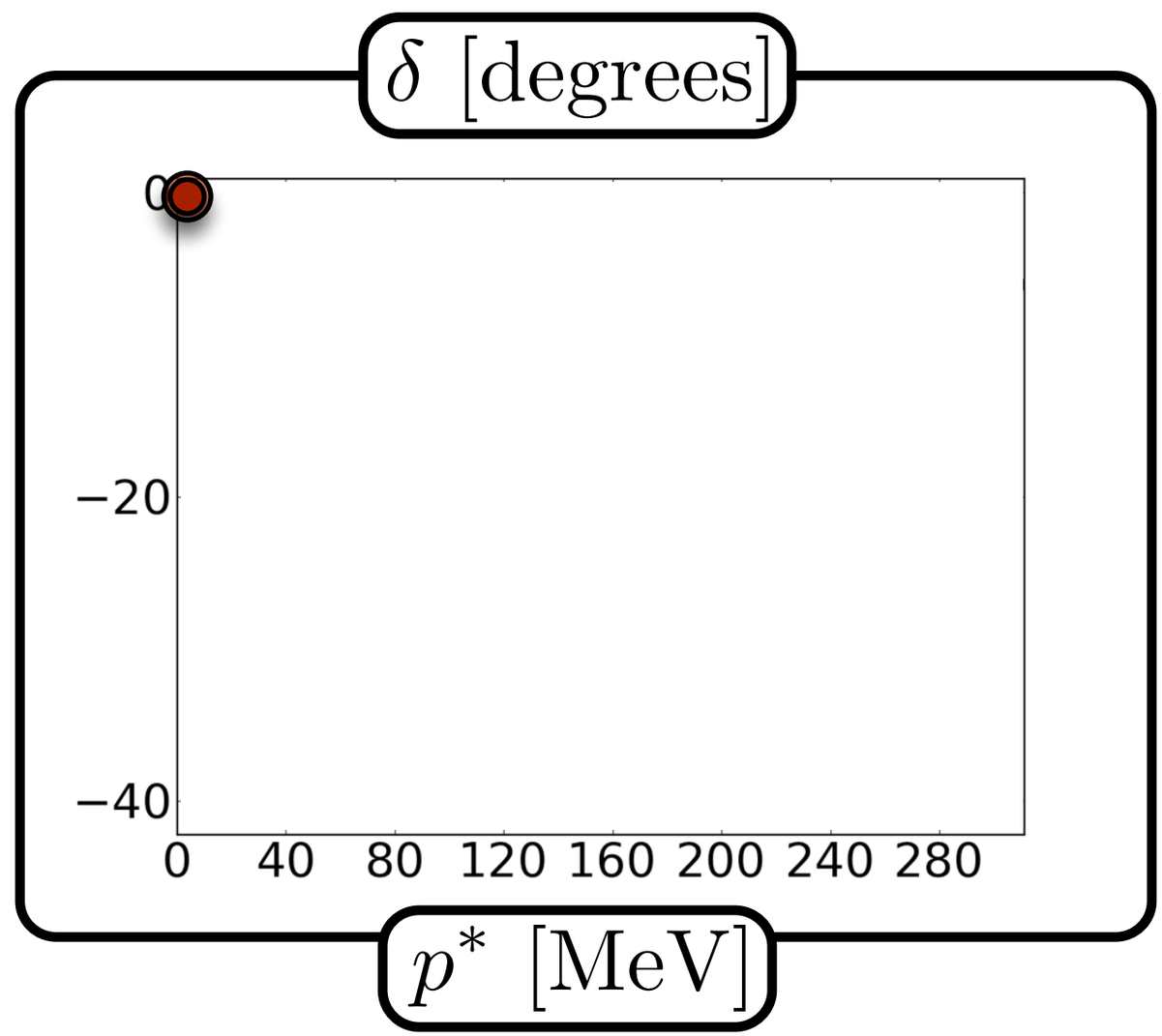

$$p_n \cot \delta(p_n) = -16\pi E_n^* \mathrm{Re} F$$

$$\mathcal{M}^s_{2\to 2}(E) = \frac{16\pi E}{p \cot \delta(p) - ip}$$

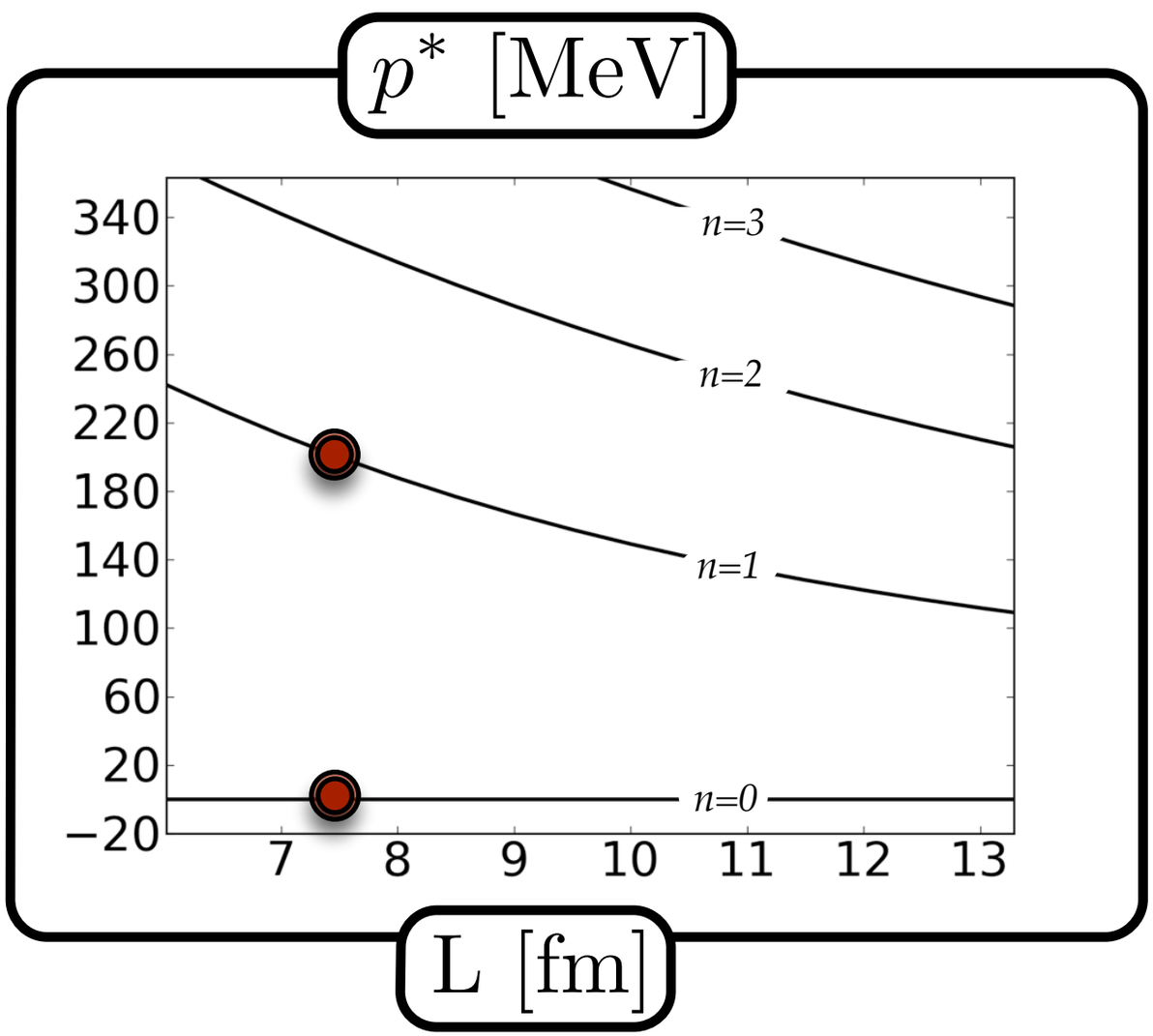

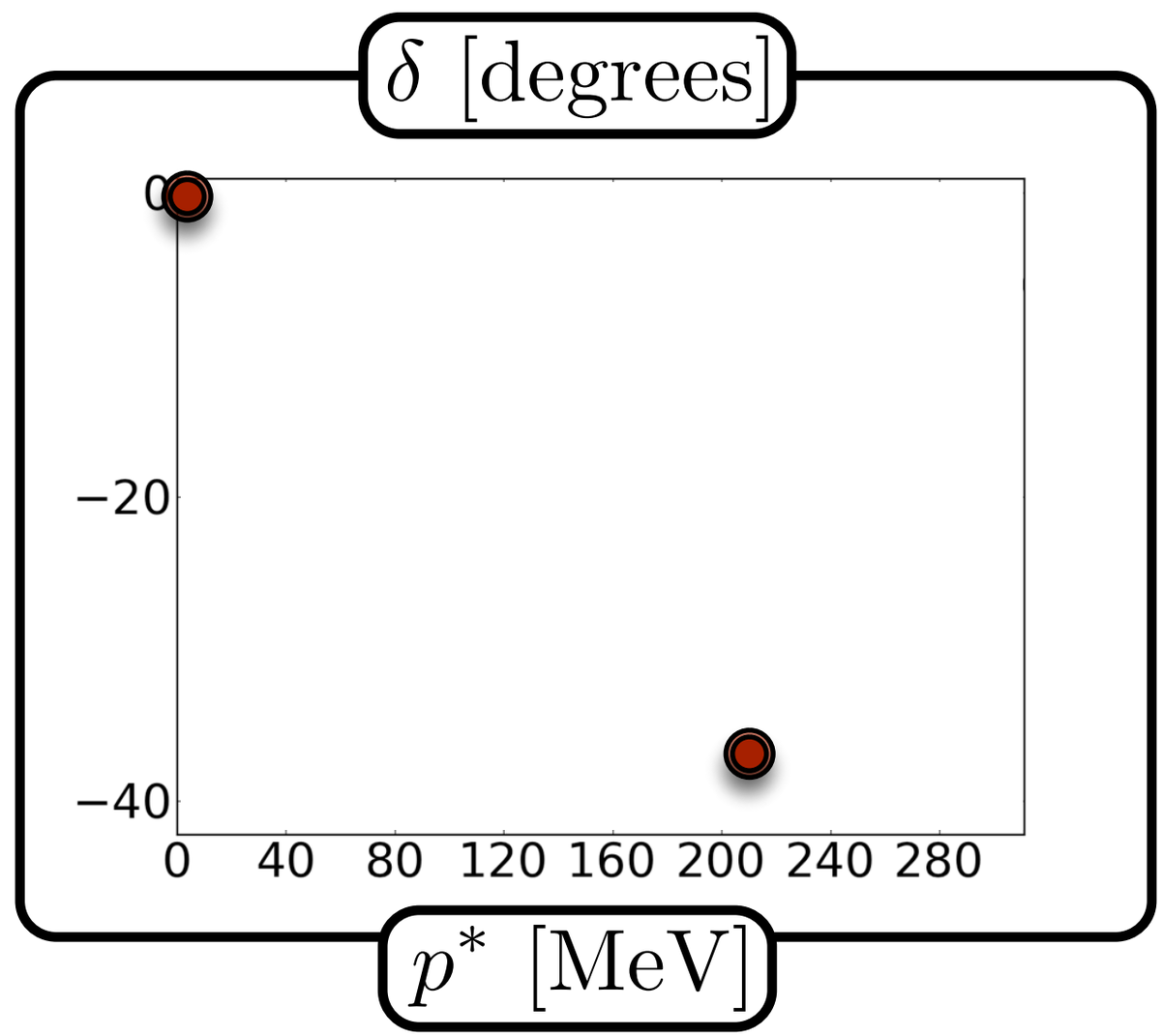

$$p_n \cot \delta(p_n) = -16\pi E_n^* \mathrm{Re} F$$

$$\mathcal{M}^s_{2\to 2}(E) = \frac{16\pi E}{p \cot \delta(p) - ip}$$

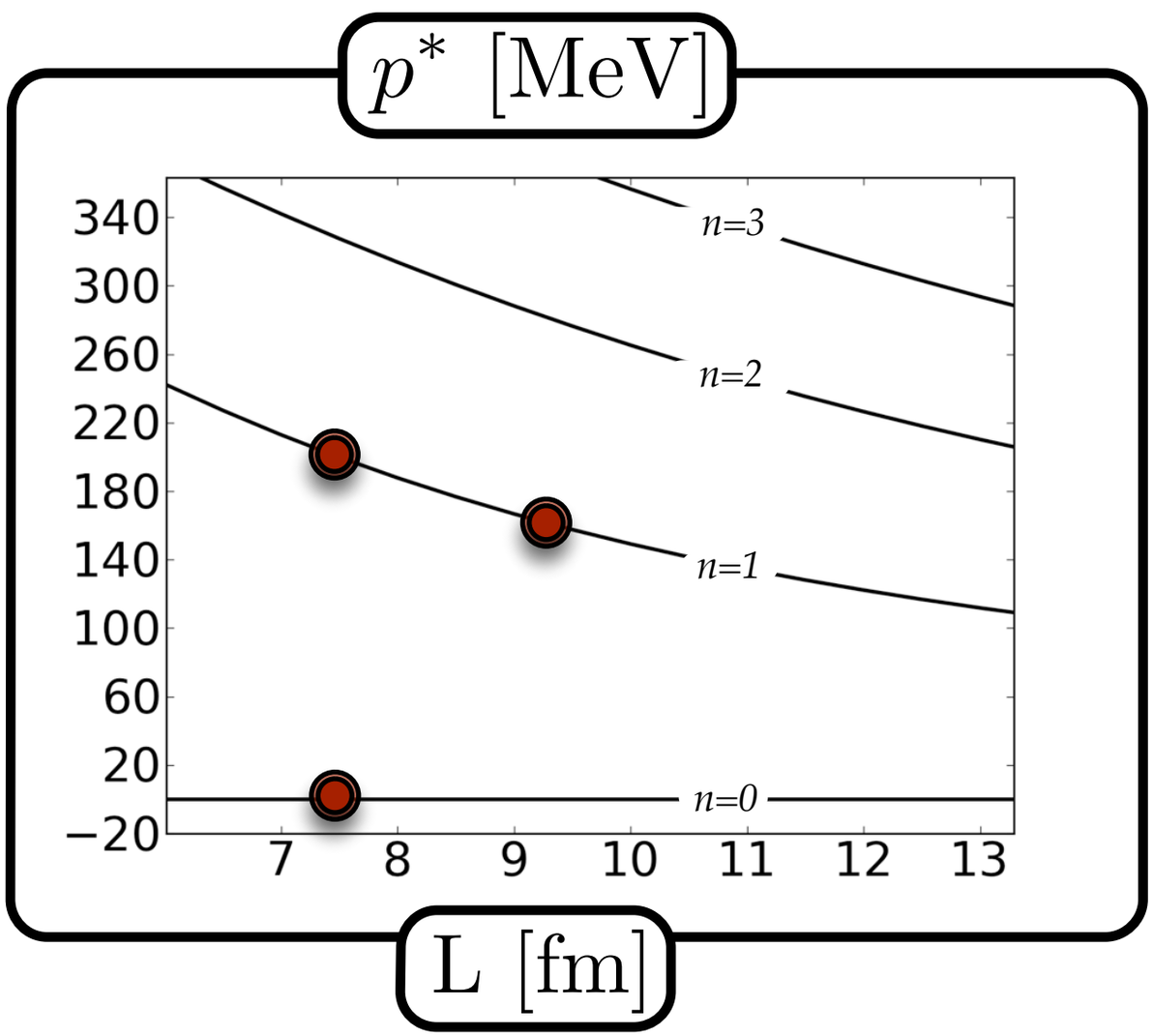

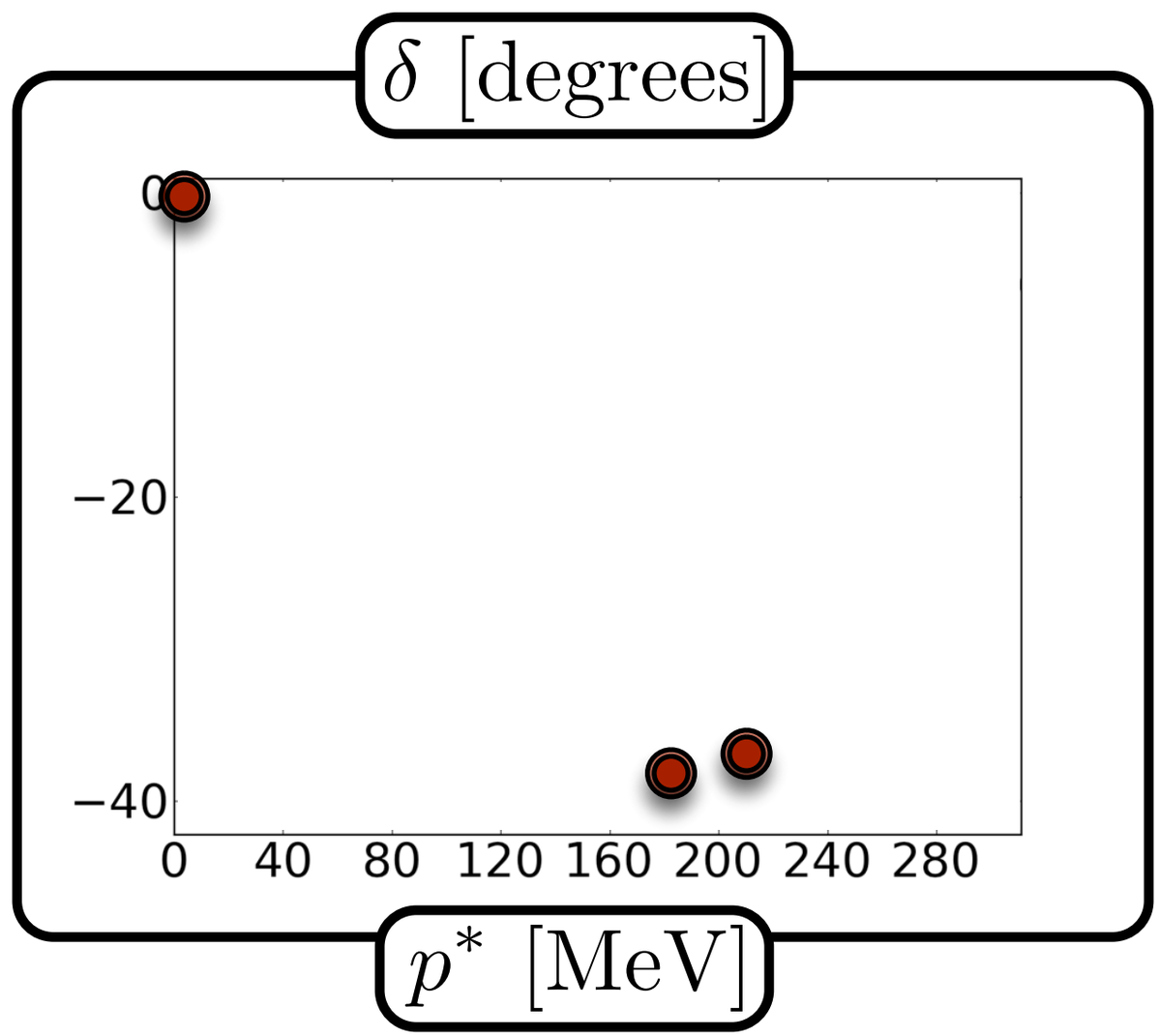

$$p_n \cot \delta(p_n) = -16\pi E_n^* \mathrm{Re} F$$

$$\mathcal{M}^s_{2\to 2}(E) = \frac{16\pi E}{p \cot \delta(p) - ip}$$

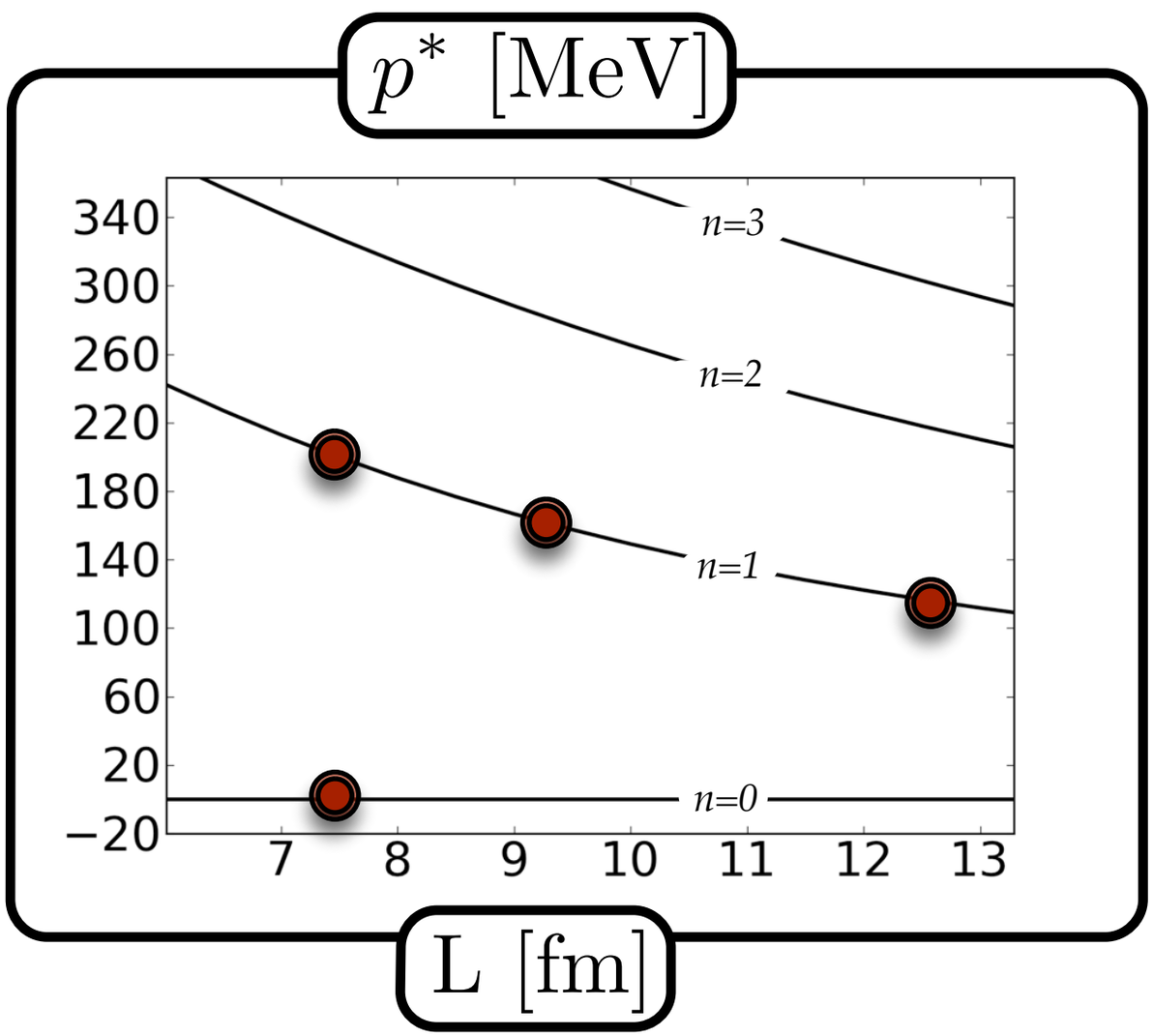

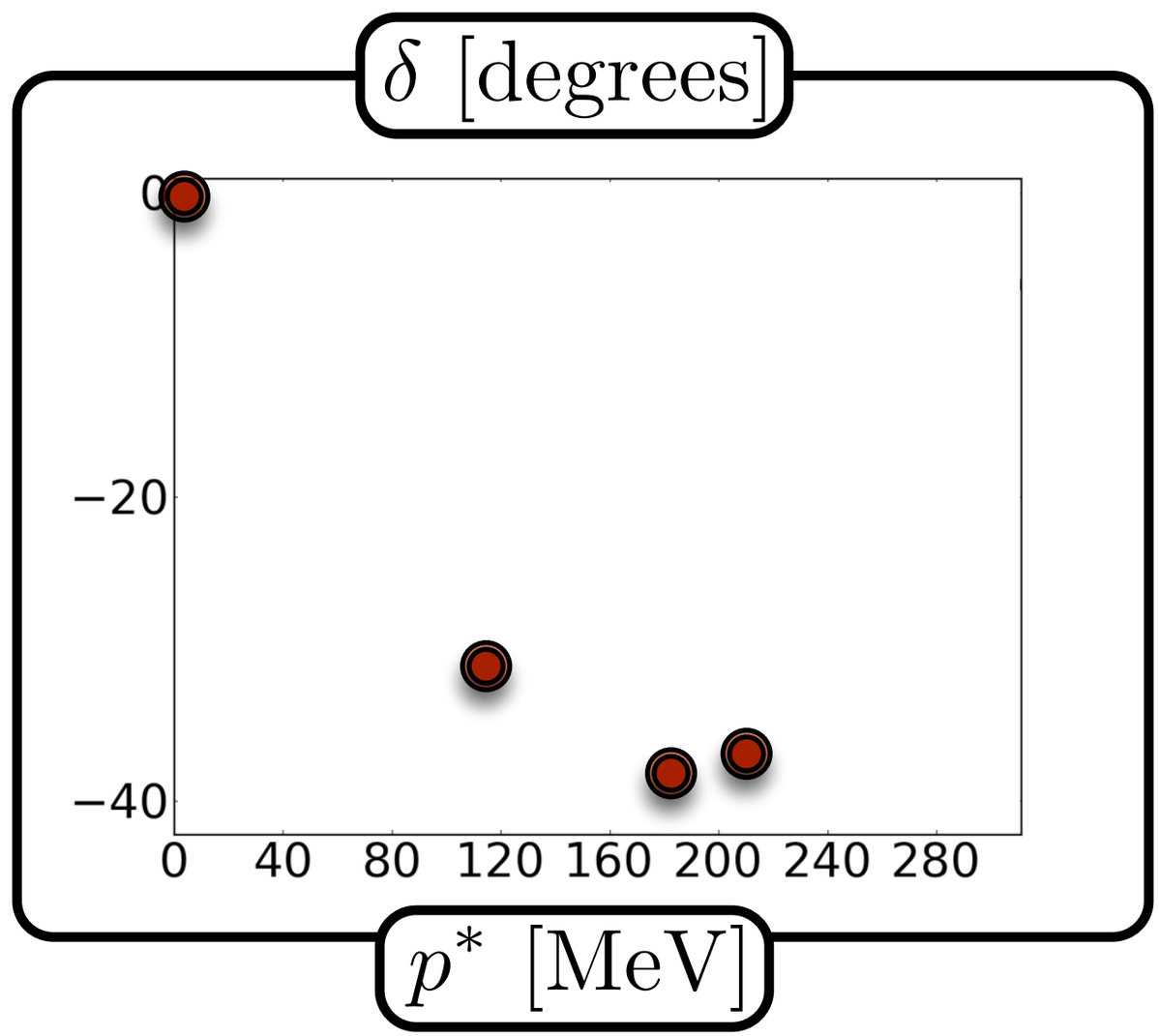

$$p_n \cot \delta(p_n) = -16\pi E_n^* \mathrm{Re} F$$

$$\mathcal{M}^s_{2\to 2}(E) = \frac{16\pi E}{p \cot \delta(p) - ip}$$

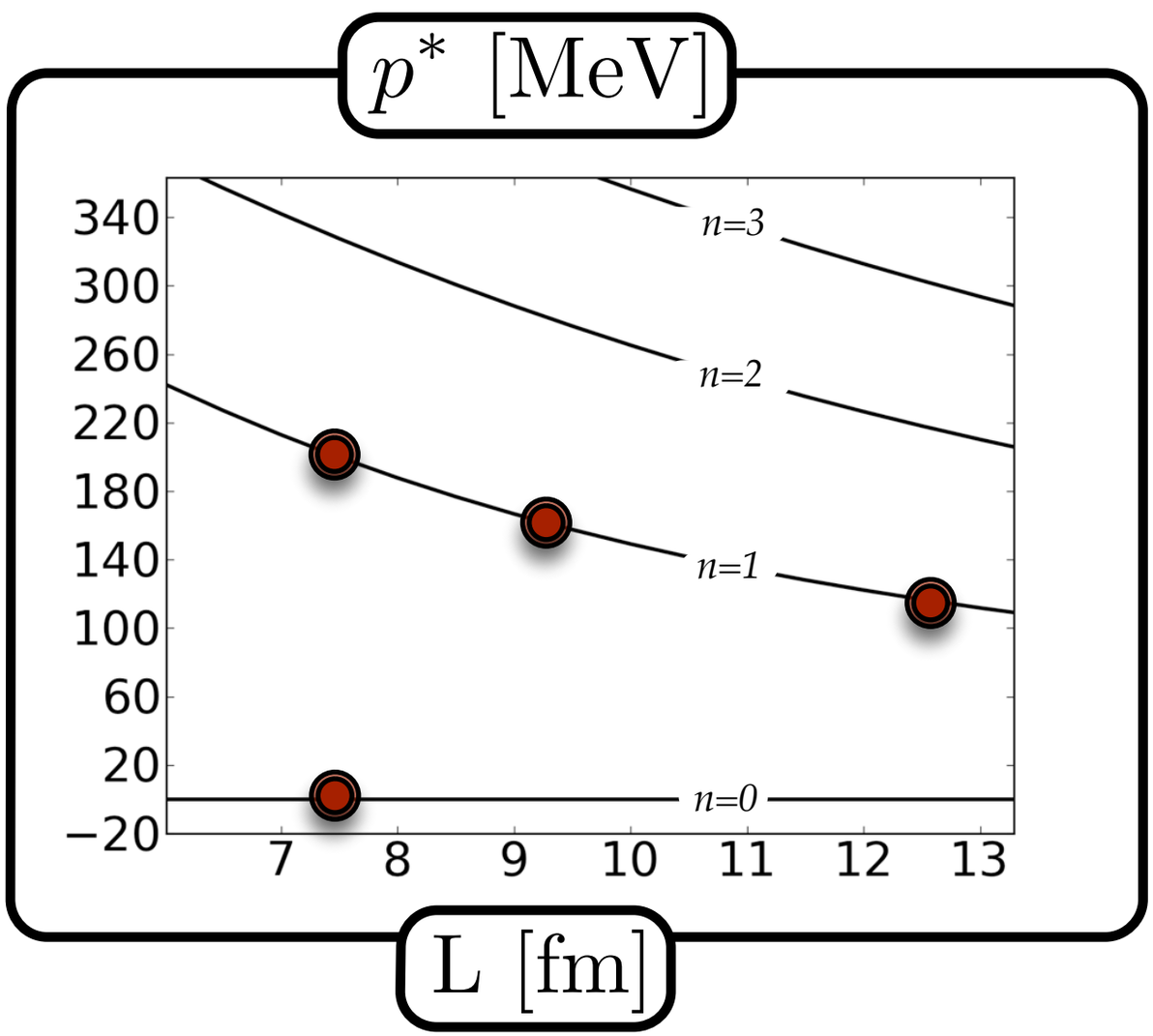

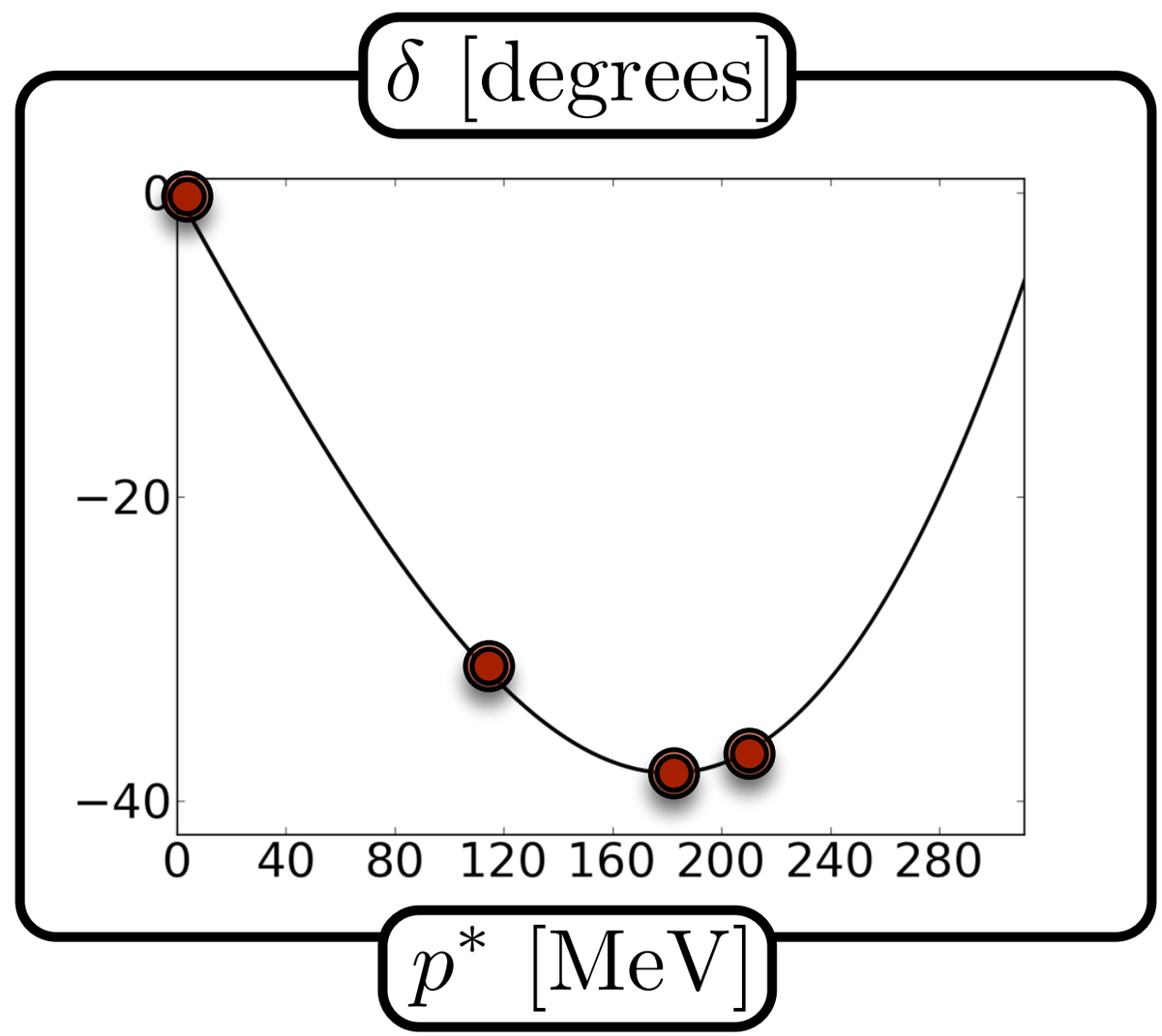

$$p_n \cot \delta_{J=1}(p_n) = -16\pi E_n^* \,\mathrm{Re}\, F_{10;10}(E_n, \vec{P}, L)$$

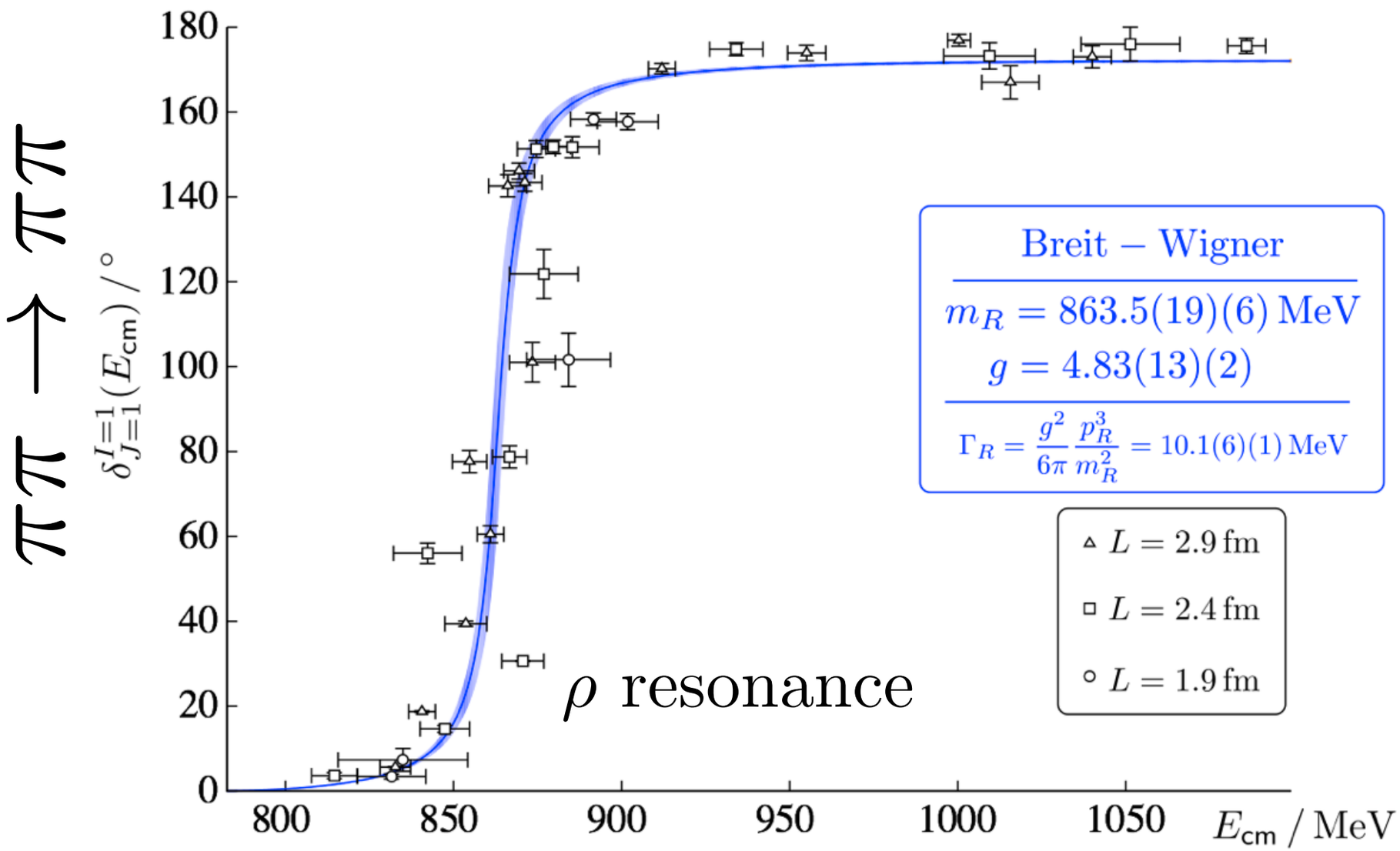

$m_\pi = 391$ MeV

from Dudek, Edwards, Thomas in *Phys.Rev*. D87 (2013) 034505

Scattering of multiple two-particle channels

$$\pi\pi \to \overline{K}K \qquad \pi K \to \eta K$$

Make following replacements

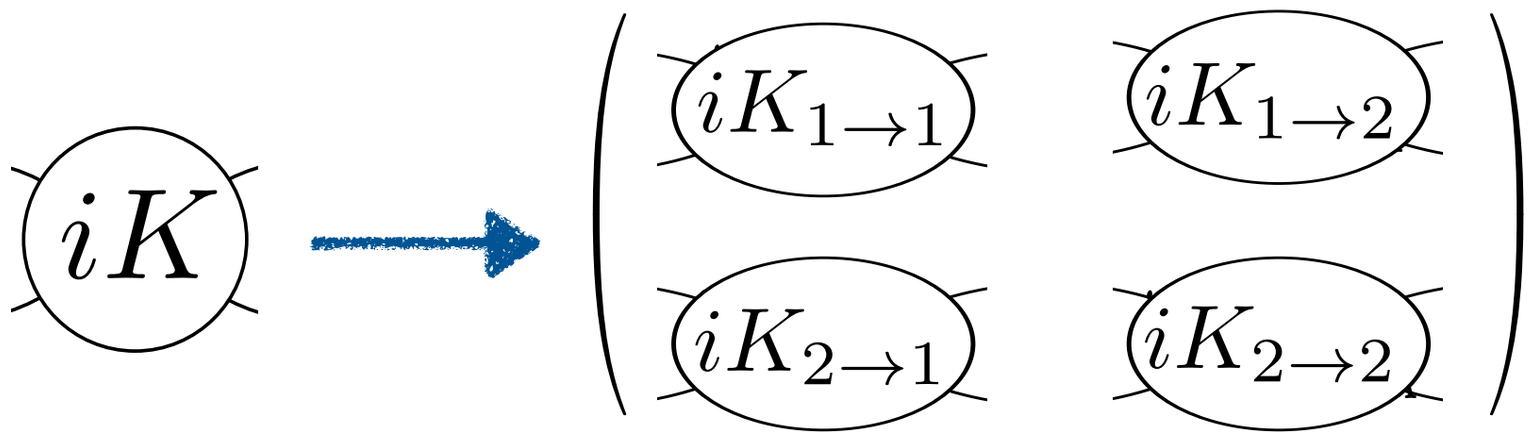

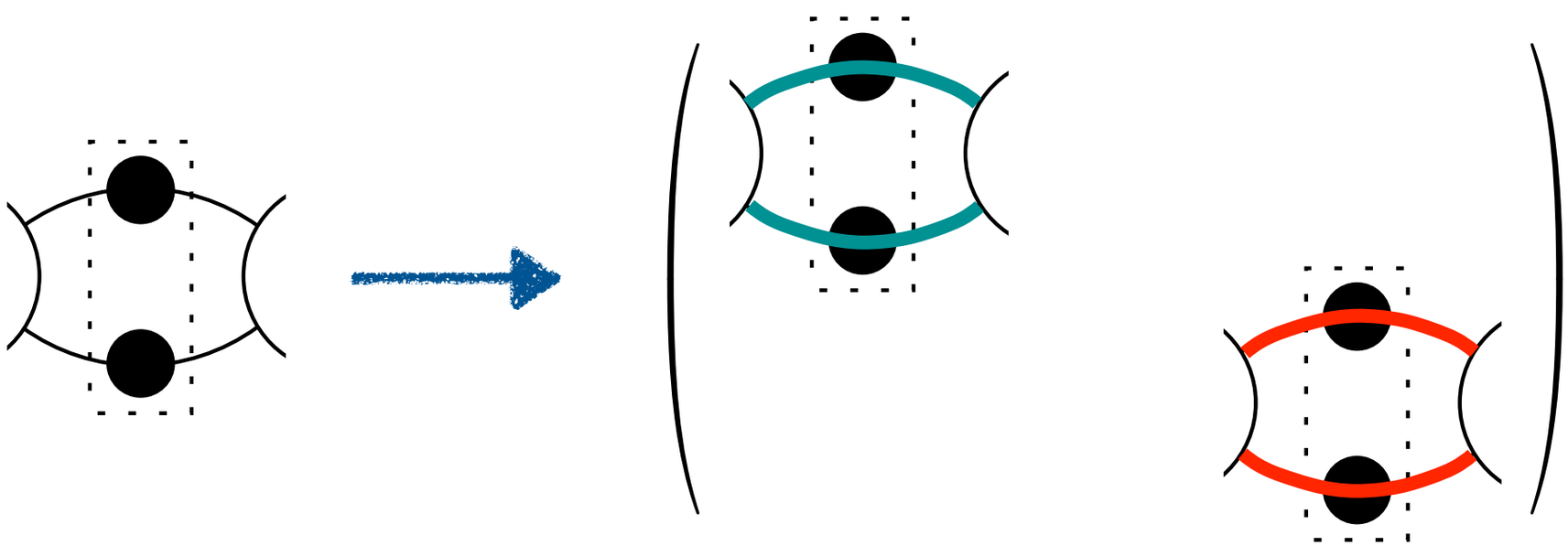

Scattering of multiple two-particle channels

$$\pi\pi \to \overline{K}K \qquad \pi K \to \eta K$$

One finds

$$\det\left[1 - \begin{pmatrix} i\mathcal{M}_{1\to1} & i\mathcal{M}_{1\to2} \\ i\mathcal{M}_{2\to1} & i\mathcal{M}_{2\to2} \end{pmatrix} \begin{pmatrix} iF_1 & 0 \\ 0 & iF_2 \end{pmatrix}\right] = 0$$

M. Lage, U.-G. Meißner, and A. Rusetsky, Phys.Lett., B681, 439 (2009)
V. Bernard, M. Lage, U.-G. Meißner, and A. Rusetsky, JHEP, 1101, 019 (2011)
M. Döring, U.-G. Meißner, E. Oset, and A. Rusetsky, Eur.Phys.J., A47, 139 (2011)
MTH, S. R. Sharpe, *Phys.Rev. D86* (2012) 016007
R. A. Briceño, Z. Davoudi, *Phys.Rev. D88* (2013) 094507

Already implemented in LQCD calculation

$$\pi K \to \eta K$$

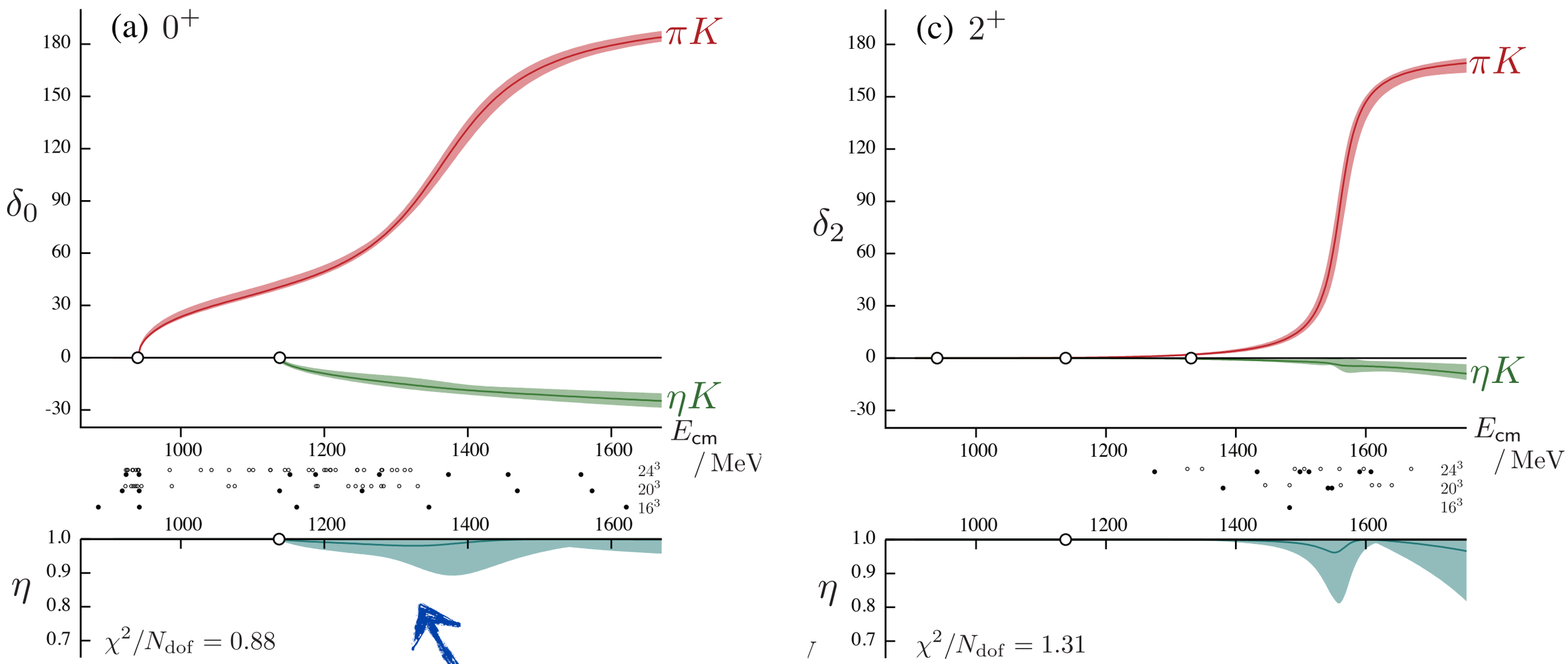

$$\mathcal{M}(\pi K \to \eta K) \sim \sqrt{1-\eta^2}$$

from Dudek, Edwards, Thomas, Wilson in arXiv:1406:4158

Structure of Charmed Tetraquarks from LQCD

Yoichi Ikeda

(RIKEN, Nishina Center)

RIKEN NiSHiNA CENTER

HAL QCD (Hadrons to Atomic nuclei from Lattice QCD)

Sinya Aoki (YITP, Kyoto Univ.)
Takumi Doi, Tetsuo Hatsuda, Yoichi Ikeda, Vojtech Krejcirik (RIKEN)
Takashi Inoue (Nihon Univ.)
Noriyoshi Ishii, Keiko Murano (RCNP, Osaka Univ.)
Hidekatsu Nemura, Kenji Sasaki,
Masanori Yamada, Takaya Miyamoto (Univ. Tsukuba)

Hadrons to Atomic nuclei HAL from Lattice QCD

"Multi-Hadron and Nonlocal Matrix Elements in Lattice QCD"
@BNL, 5-6Feb. 2015.

Spectrum of charmonium(-like) system

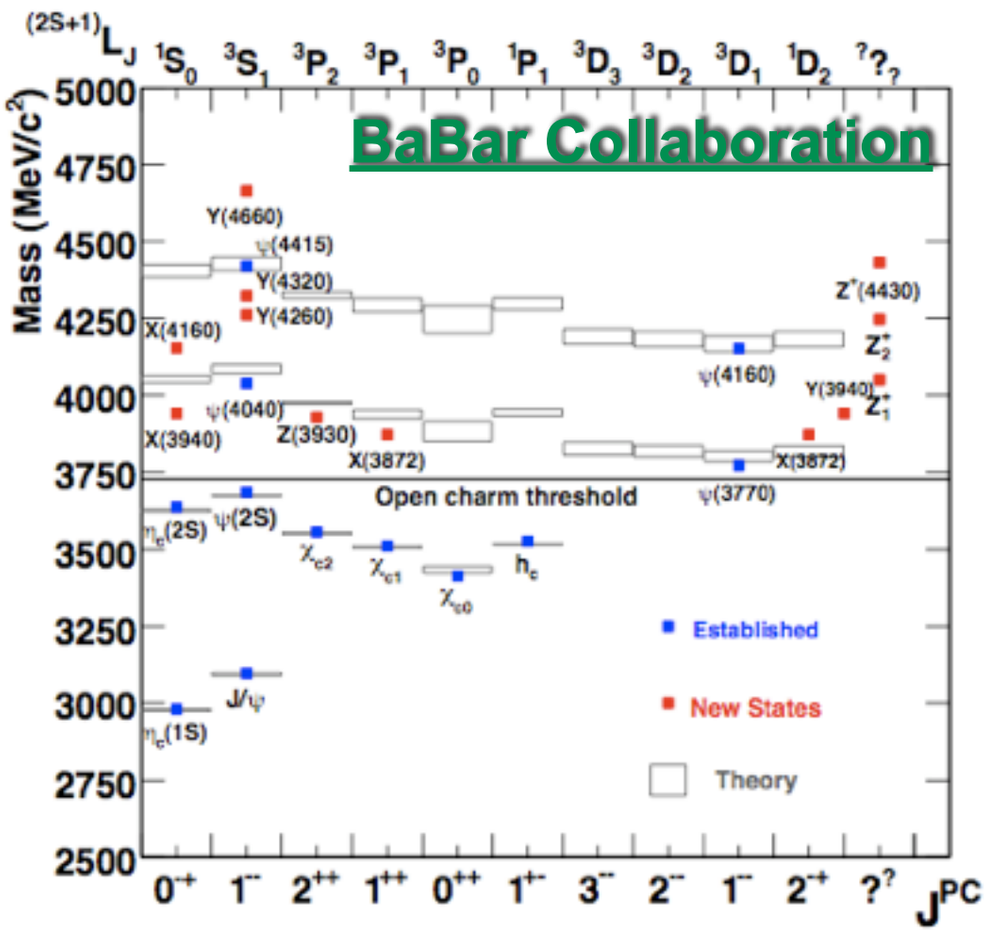

- Quark potential models well describe mass spectra below open charm threshold

  Godfrey, Isgur, PRD 32 (1985).
  Barnes, Godfrey, Swanson, PRD 72 (2005).

- "NEW" charmonium-like (X, Y, Z) states:
  ➡ not within quark model spectrum
  ➡ candidates of exotic hadrons

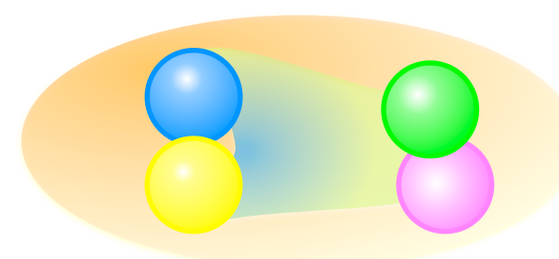

- "Other" exotic candidates (expected from quark models):
  ➡ doubly charmed tetra-quark, but experimentally not observed so far

Our target: tetra-quark channels

- "Tetraquark" Tcc ($ccu^{bar}d^{bar}$) is manifest 4-quark channel
- "Charged" charmonium-like states ($cc^{bar} + \pi^{+/-}$) require at least 4 quarks

Key dynamics involving heavy quarks

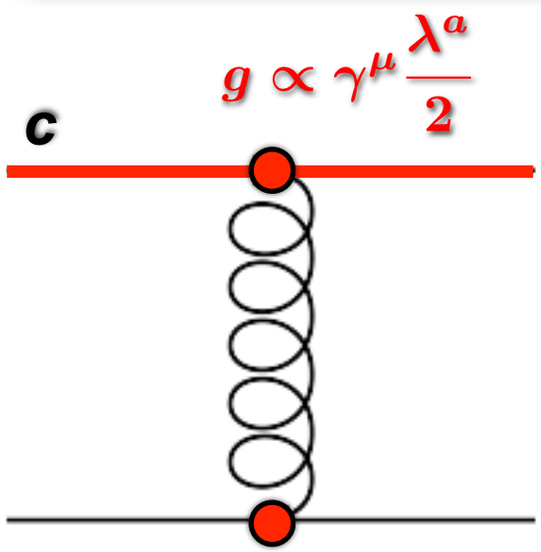

$$\sim \bar{c}\gamma^\mu \frac{\lambda^a}{2} c A^a$$

➡ color magnetic + color electric forces

magnetic interactions << electric interactions

➡ magnetic gluon coupling is suppressed by $O(1/m_c)$

✓ Heavy quark spin symmetry

- **Color magnetic interaction : mass splitting**

$$V_{ij}^{\mathrm{CMI}} \propto -\frac{(\vec{\lambda}(i)\cdot\vec{\lambda}(j))(\vec{\sigma}(i)\cdot\vec{\sigma}(j))}{M_i M_j}$$

H. J. Lipkin, PLB172, 242 (1986).

➡ I=0 [ud]-diquark correlation (good diquark) --> Tcc bound state?

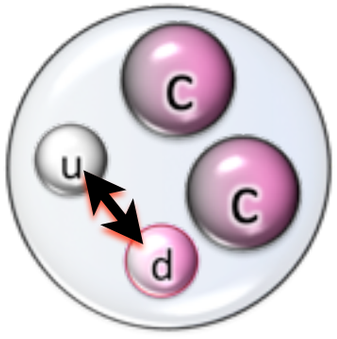

- **Color electric interaction : threshold**

- Zc(3900) is near threshold resonance?
- $J^P = 1^+$ seems most probable
- $D^{bar}D^*$ molecule? cc^{bar} + meson cloud?

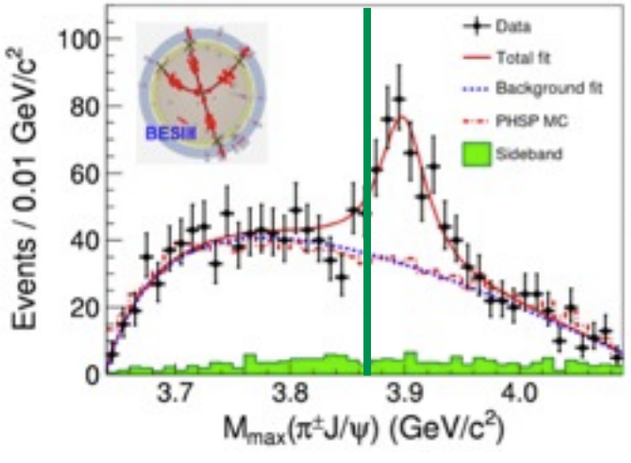

BESIII Coll., PRL110 (2013).

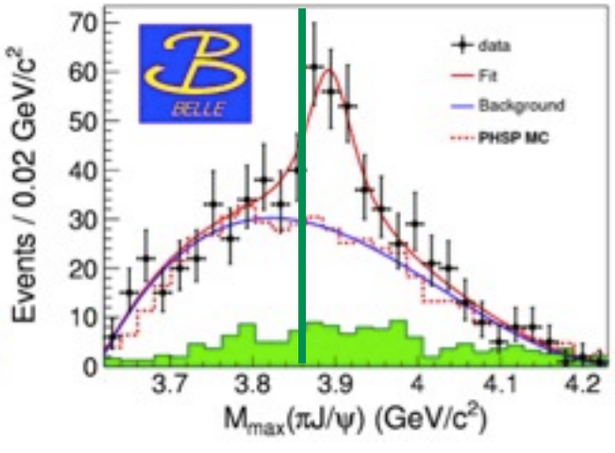

Belle Coll., PRL110 (2013).

Contents

- Introduction
- HAL QCD method to define (coupled-channel) potentials
- Tcc in $I(J^P)=0,1(1^+)$ channels [DD* single-channel]
- Zc(3900) in $I(J^P)=1(1^+)$ [$\pi J/\Psi$-$\rho\eta_c$-$D^{bar}D^*$ coupled-channel]
- Summary

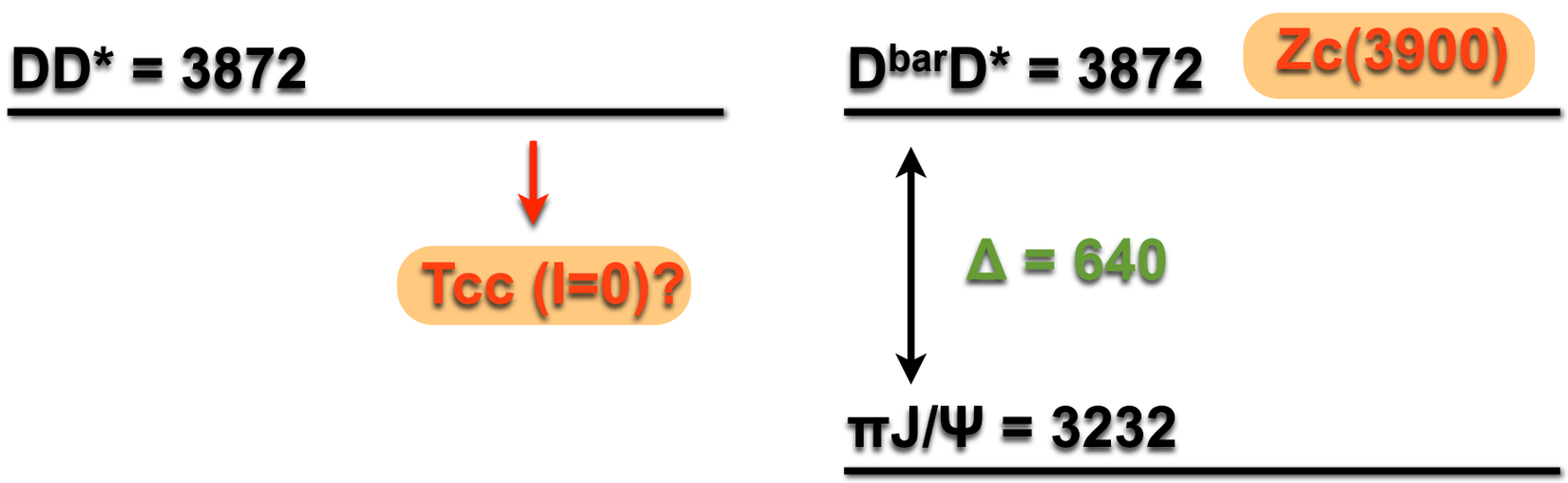

Two identical methods for scattering

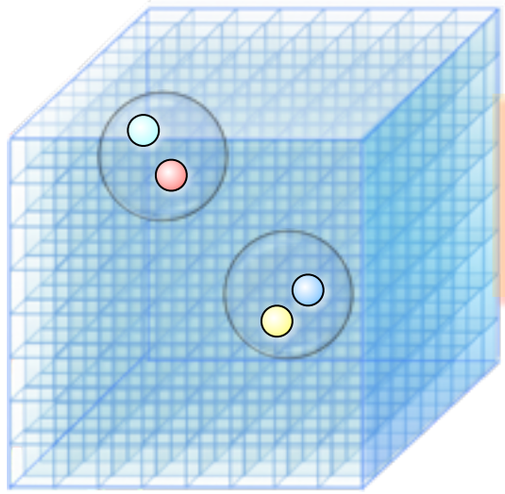

- ***Lüscher's finite size formula***

  interaction energy --> phase shift

  Lüscher, NPB354, 531 (1991).

- ***Scattering parameters***

$$k\cot\delta(k) = \frac{1}{a} - \frac{1}{2}r_e k^2 + \cdots$$

Two identical methods for scattering

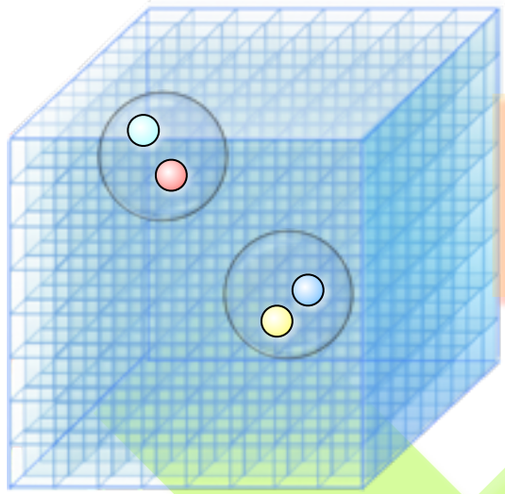

- ***Lüscher's finite size formula***

  interaction energy --> phase shift

  Lüscher, NPB354, 531 (1991).

- ***Scattering parameters***

$$k\cot\delta(k) = \frac{1}{a} - \frac{1}{2}r_e k^2 + \cdots$$

- **Guaranteed to be the same**

  Kurth et al., JHEP 1312 (2013) 015.

- ***NBS wave function***

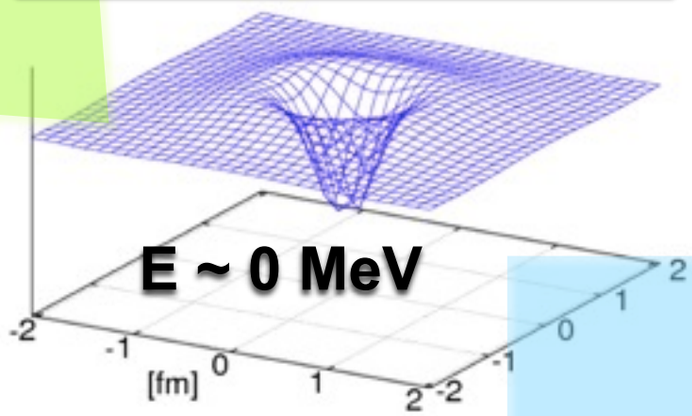

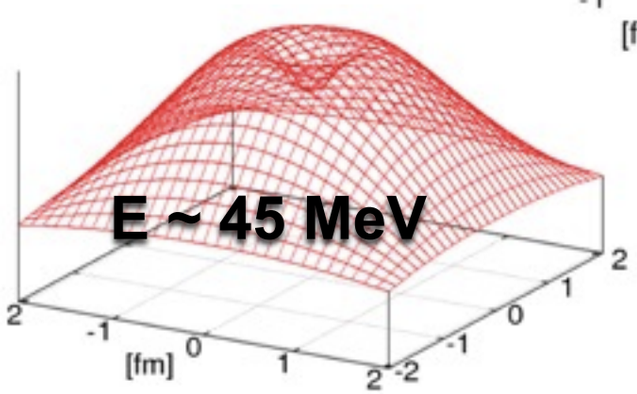

Ishii, Aoki, Hatsuda, PRL99, 02201 (2007).

Aoki, Hatsuda, Ishii, PPTP123, 89 (2010).

- ***Energy-independent potential***

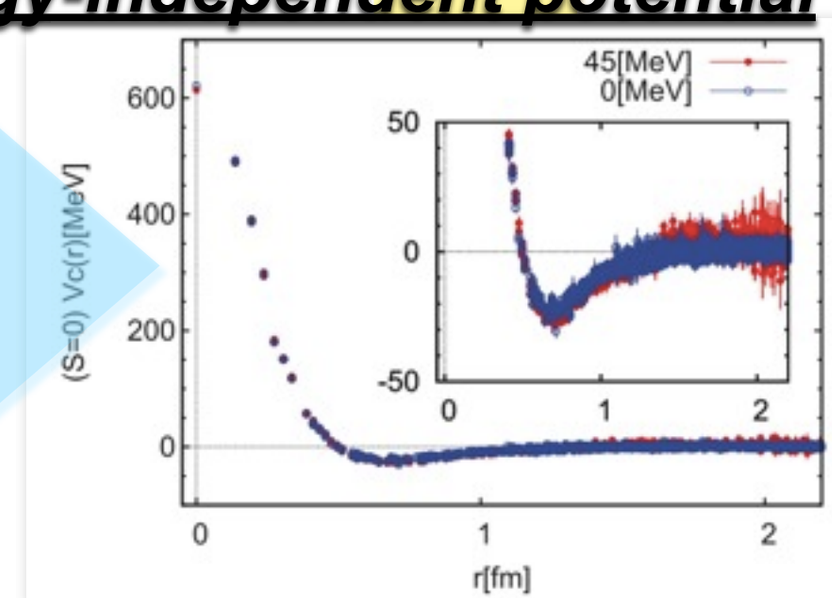

Two identical methods for scattering

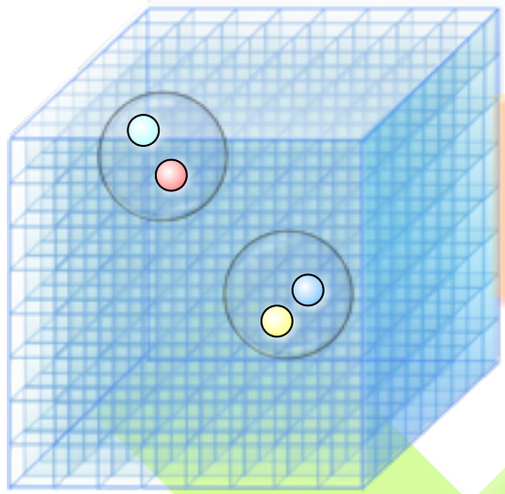

- ***Lüscher's finite size formula***

  interaction energy --> phase shift

  Lüscher, NPB354, 531 (1991).

- ***Scattering parameters***

$$k\cot\delta(k) = \frac{1}{a} - \frac{1}{2}r_e k^2 + \cdots$$

- **Guaranteed to be the same**

  Kurth et al., JHEP 1312 (2013) 015.

- ***NBS wave function***

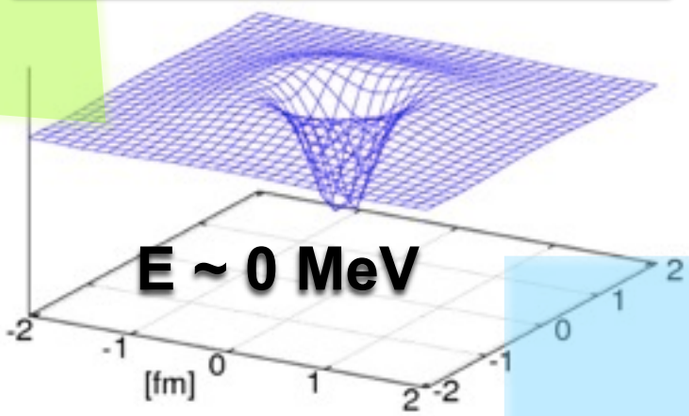

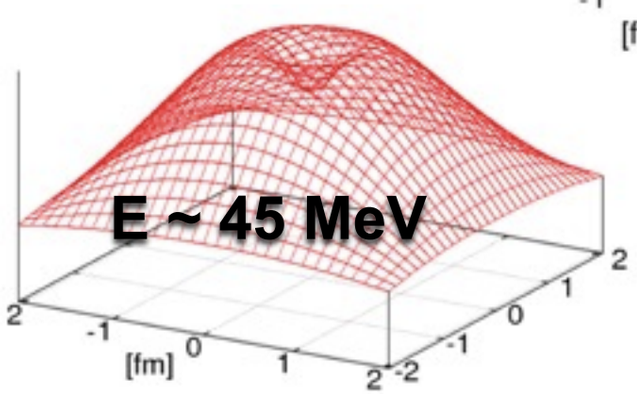

Ishii, Aoki, Hatsuda, PRL99, 02201 (2007).

Aoki, Hatsuda, Ishii, PPTP123, 89 (2010).

- ***Energy-independent potential***

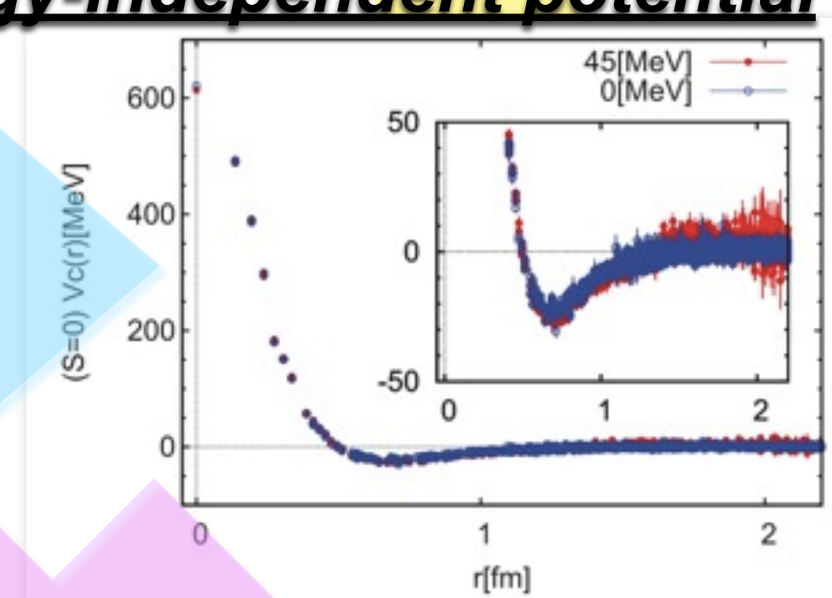

✓ **LQCD potentials can be applied to...**

properties of hadrons & nuclei, construction of EOS, etc.

Resonance from LQCD

T-matrix in formal scattering theory (N/D method)

$$T^{-1}(\sqrt{s}) = V^{-1} + \frac{1}{2\pi}\int_{s_+}^{\infty} ds' \frac{\rho(s')}{s'-s}$$

Interaction part is not determined within scattering theory

➡ **interactions faithful to phase shift from LQCD**

Resonance from LQCD

T-matrix in formal scattering theory (N/D method)

$$T^{-1}(\sqrt{s}) = V^{-1} + \frac{1}{2\pi}\int_{s_+}^{\infty} ds' \frac{\rho(s')}{s'-s}$$

Interaction part is not determined within scattering theory

➡ **interactions faithful to phase shift from LQCD**

Analyticity of T-matrix is uniquely determined

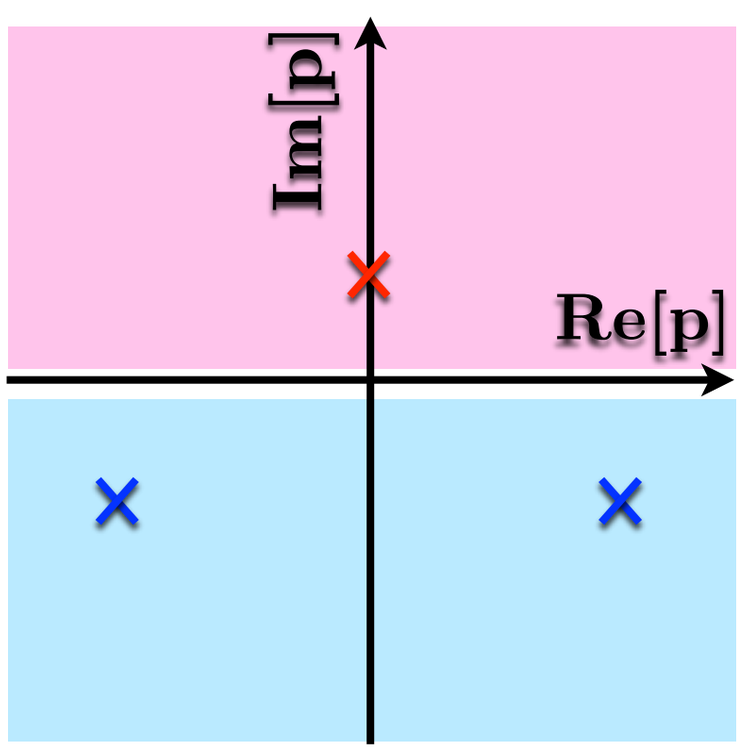

Bound states (physical sheet, 1st)

- binding energy --> T-matrix pole position
- coupling --> residue of pole

Resonance/Virtual states (unphysical sheet, 2nd)

- Analytic continuation of T-matrix
- resonance energy --> T-matrix pole position
- coupling --> (complex) residue of pole?

“Potentials” in QCD

Hadron 4pt functions & Nambu-Bethe-Salpeter (NBS) wave function

$$\psi^{ab}(\vec{r},\tau) = \sum_{\vec{x}} \langle 0|\phi_1^a(\vec{x}+\vec{r},\tau)\phi_2^a(\vec{x},\tau)\mathcal{J}^{b\dagger}(\tau=0)|0\rangle$$
$$= \sum_n A_n^b \exp\left[-W_n\tau\right]\sqrt{Z_1^a}\sqrt{Z_2^a}\psi_n^a(\vec{r})$$

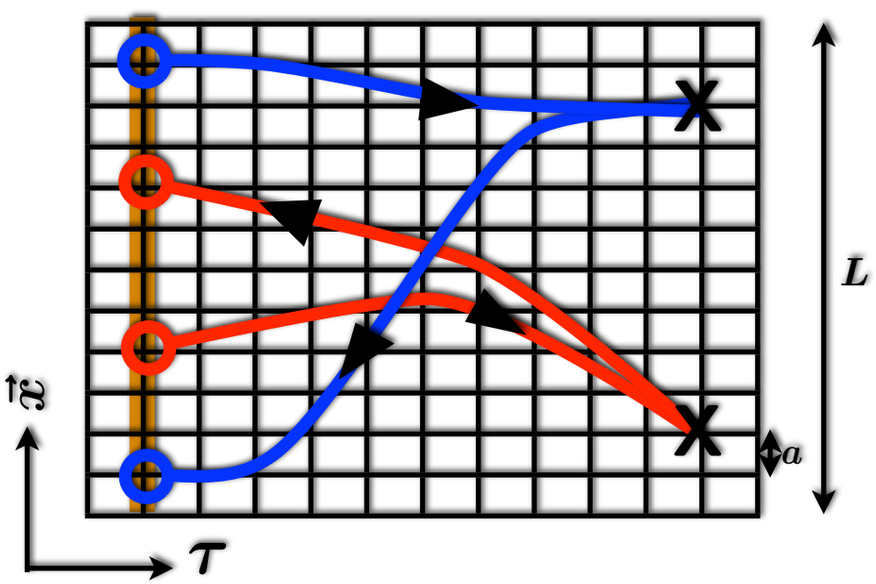

- Helmholtz eq. of NBS wave func.

$$(\nabla^2 + (\vec{k}^a)^2)\psi^a_{W(\vec{k})}(\vec{r}) = 0 \quad (|\vec{r}| > R)$$

$$\psi^{(l)}_{W(\vec{k})}(r) \sim \frac{e^{i\delta_l(k)}}{kr}\sin\left(kr + \delta_l(k) - l\pi/2\right)$$

- NBS wave func. in QFT ~ wave func. in Q.M.

- Coupled-channel potential matrix (faithful to phase shifts)

$$\left(\nabla^2 + (\vec{k}^a)^2\right)\psi^a_n(\vec{r}) = 2\mu^a \sum_b \int d\vec{r}' U^{ab}(\vec{r},\vec{r}')\psi^b_n(\vec{r}')$$

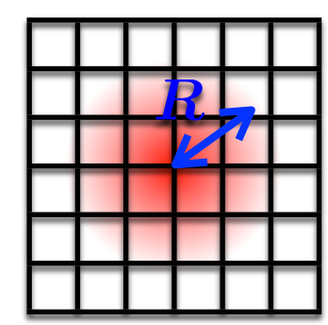

Aoki et al. [HAL QCD Coll.], Proc. Jpn. Acad., Ser. B, 87 (2011); PTEP 2012, 01A105 (2012).

- Coupled-channel potentials are energy-independent (non-local in general)

HAL QCD method

✓ **Definition of energy-independent coupled-channel potentials :**

Aoki, Hatsuda, Ishii, PTP123, 89 (2010).

$$\psi_n(\vec{r}) = \langle 0|\phi_1^a(\vec{r}+\vec{x})\phi_2^a(\vec{x})|W_n; J^P\rangle$$

$$\left(\nabla^2 + (\vec{k}^a)^2\right)\psi_n^a(\vec{r}) = 2\mu \sum_b \int d\vec{r}' U^{ab}(\vec{r},\vec{r}')\psi_n^b(\vec{r}')$$

✓ **Extract energy-independent potential from time-dependent Schrödinger-type eq.**

Ishii et al.(HAL QCD), PLB712, 437(2012).

$$R^{ab}(\vec{r},\tau) \equiv \psi^{ab}(\vec{r},\tau)\frac{e^{(m_1^a+m_2^a)\tau}}{\sqrt{Z_1^a}\sqrt{Z_2^a}} \qquad \delta = \frac{m_1^a - m_2^a}{m_1^a + m_2^a} \qquad \Delta^{ac} = \frac{e^{(m_1^a+m_2^a)t}}{e^{(m_1^c+m_2^c)t}}$$

$$\left[-\partial_\tau + \nabla^2/2\mu^a + \partial_\tau^2/8\mu^a + \mathcal{O}(\delta^2)\right]R^{ab}(\vec{r},\tau) = \sum_c \int d\vec{r}' \Delta^{ac} U^{ac}(\vec{r},\vec{r}')R^{cb}(\vec{r}',\tau)$$

✤ **Since energy-independent potential can produce all scattering states, single-state saturations in simulations is not required**

✓ **Velocity expansion:**

$$U(\vec{r},\vec{r}') = V(\vec{r},\nabla)\delta(\vec{r}-\vec{r}')$$

$$\Rightarrow V(\vec{r},\nabla) = \underbrace{V_C(\vec{r})}_{\text{(LO)}} + \underbrace{\vec{L}\cdot\vec{S}V_{LS}(\vec{r})}_{\text{(NLO)}} + \mathcal{O}(\nabla^2)$$

✓ **Calculate observable: phase shift, binding energy, pole position, ...**

Tcc in $I(J^P)=0,1(1^+)$

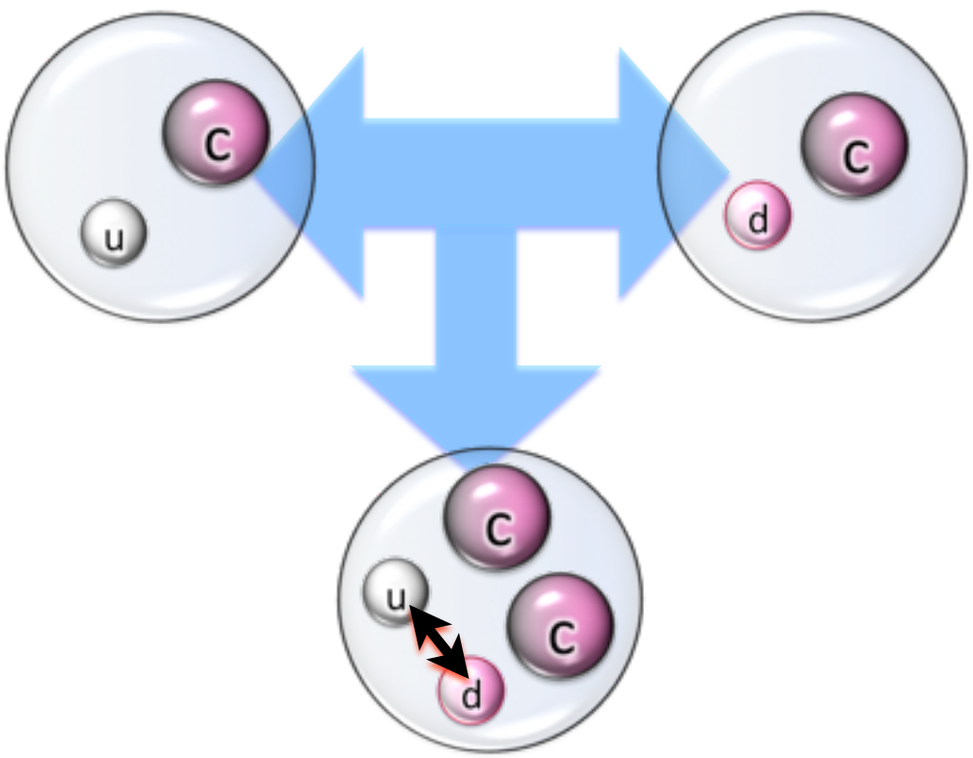

Asymptotic states : DD* (s-wave)

Lattice QCD Setup

N_f=2+1 full QCD configurations generated by PACS-CS Coll.

PACS-CS Coll., S. Aoki et al., PRD79, 034503, (2009).

- Iwasaki gauge & O(a)-improved Wilson quark actions
- a=0.0907(13) fm --> L~2.9 fm (32^3 x 64)

Light meson mass [conf.1, conf.2, conf.3] (MeV)

M_π=699(1), 572(2), 411(2) [PDG:135 (π^0)]

M_K=787(1), 714(1), 635(2) [PDG:498 (K^0)]

Tsukuba-type Relativistic Heavy Quark (RHQ) action for charm quark

S. Aoki et al., PTP109, 383 (2003)

➡ remove leading cutoff errors $O(m_c a)$, $O(\Lambda_{QCD} a)$, ...

- We are left with $O((a\Lambda_{QCD})^2)$ error (~ a few %)
- We employ RHQ parameters tuned by Namekawa et al.

Y. Namekawa et al., PRD84, 074505 (2011)

Charmed meson mass [conf.1, conf.2, conf.3] (MeV)

$M_{\eta c}$=3024(1), 3005(1), 2988(2) [PDG:2981]

$M_{J/\psi}$=3142(1), 3118(1), 3097(2) [PDG:3097]

M_D=1999(1), 1946(1), 1902(3) [PDG:1865 (D^0)]

M_{D^*}=2159(4), 2099(6), 2048(12) [PDG:2007 (D^{*0})]

S-wave DD* in I=1 : "bad" diquark

Y. Ikeda et al. (HAL QCD), PLB729, 85 (2014).

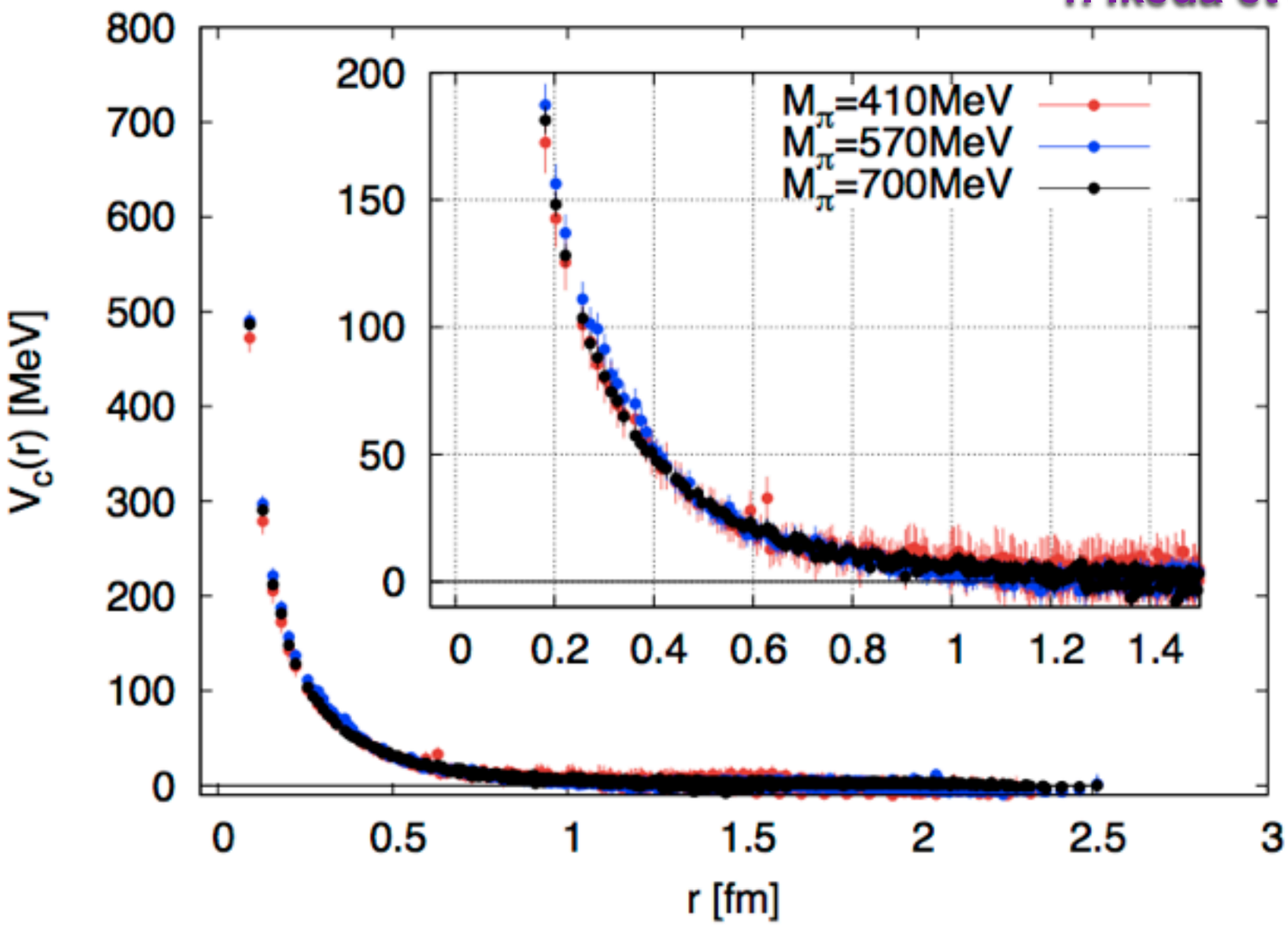

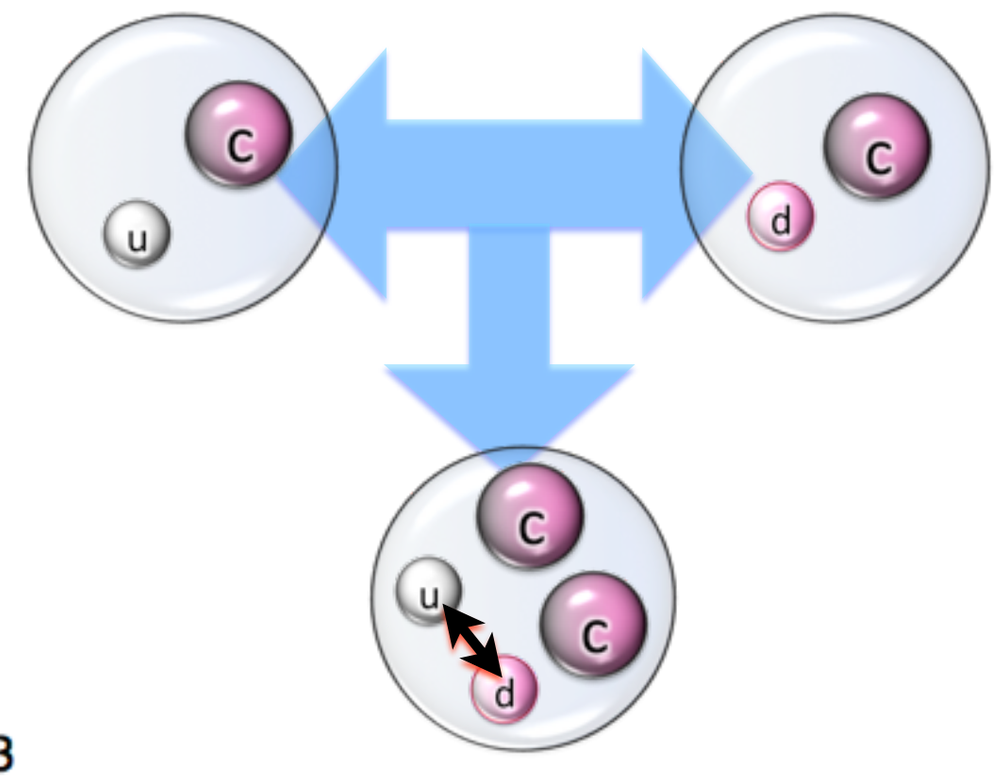

- **Repulsive s-wave potentials of DD***
- **Weak quark mass dependence**
- **It is unlikely to form bound state even at physical point**

S-wave DD* in I=0 : "good" diquark

Y. Ikeda et al. (HAL QCD), PLB729, 85 (2014).

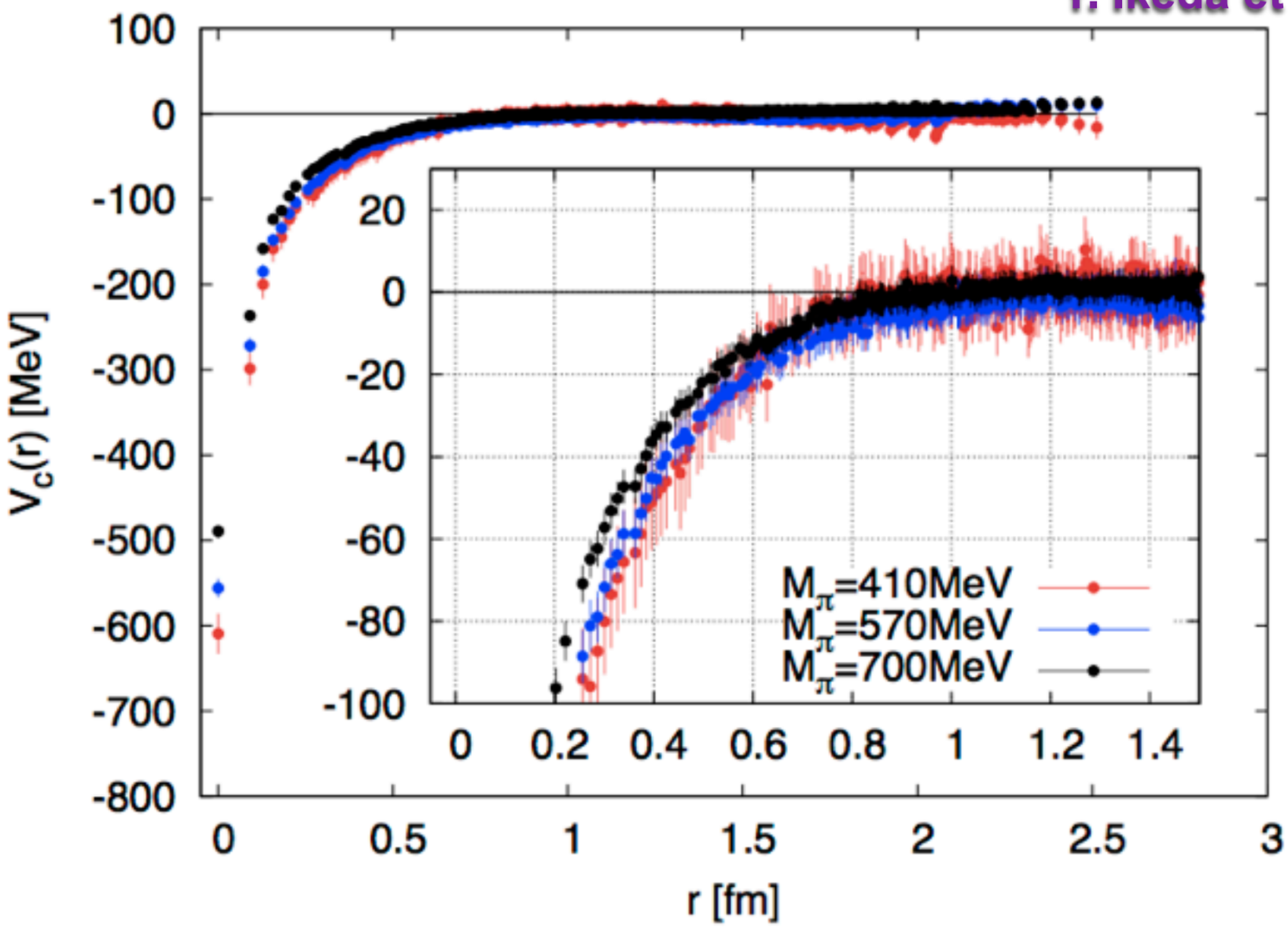

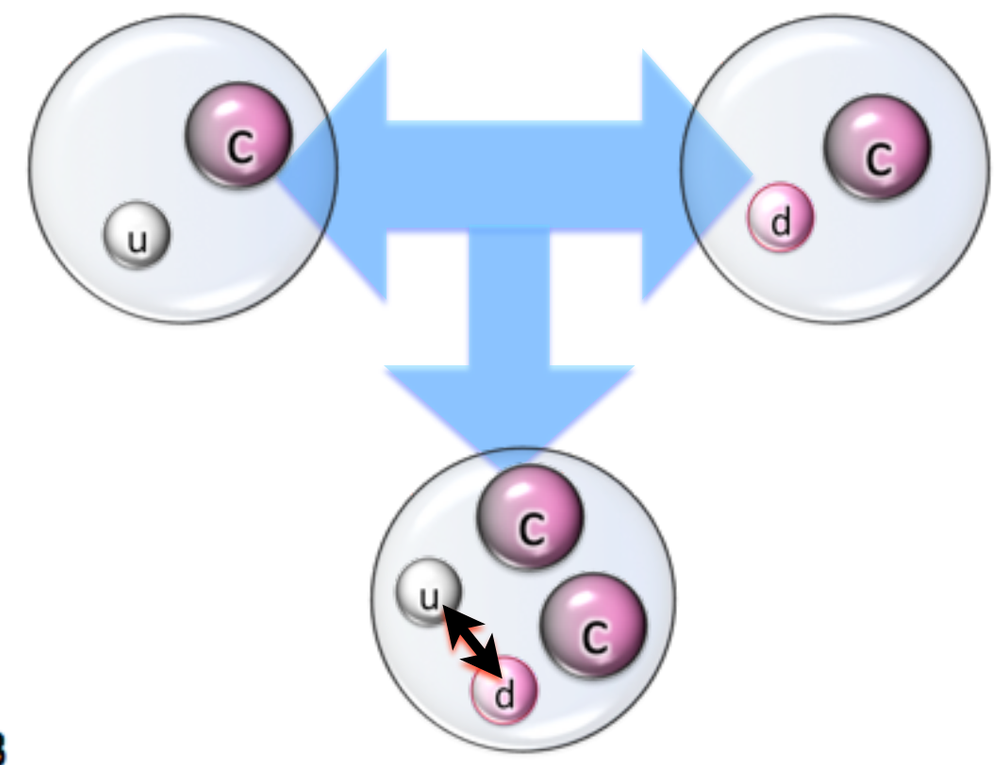

- **Attractive S-wave potentials**
- **Attraction increases, as m_q decreases**
- **Check whether bound T_{cc} exist or not --> phase shift analysis**

S-wave phase shifts : Tcc in I=0

Y. Ikeda et al. (HAL QCD), PLB729, 85 (2014).

- solve Schrödinger equation --> phase shifts

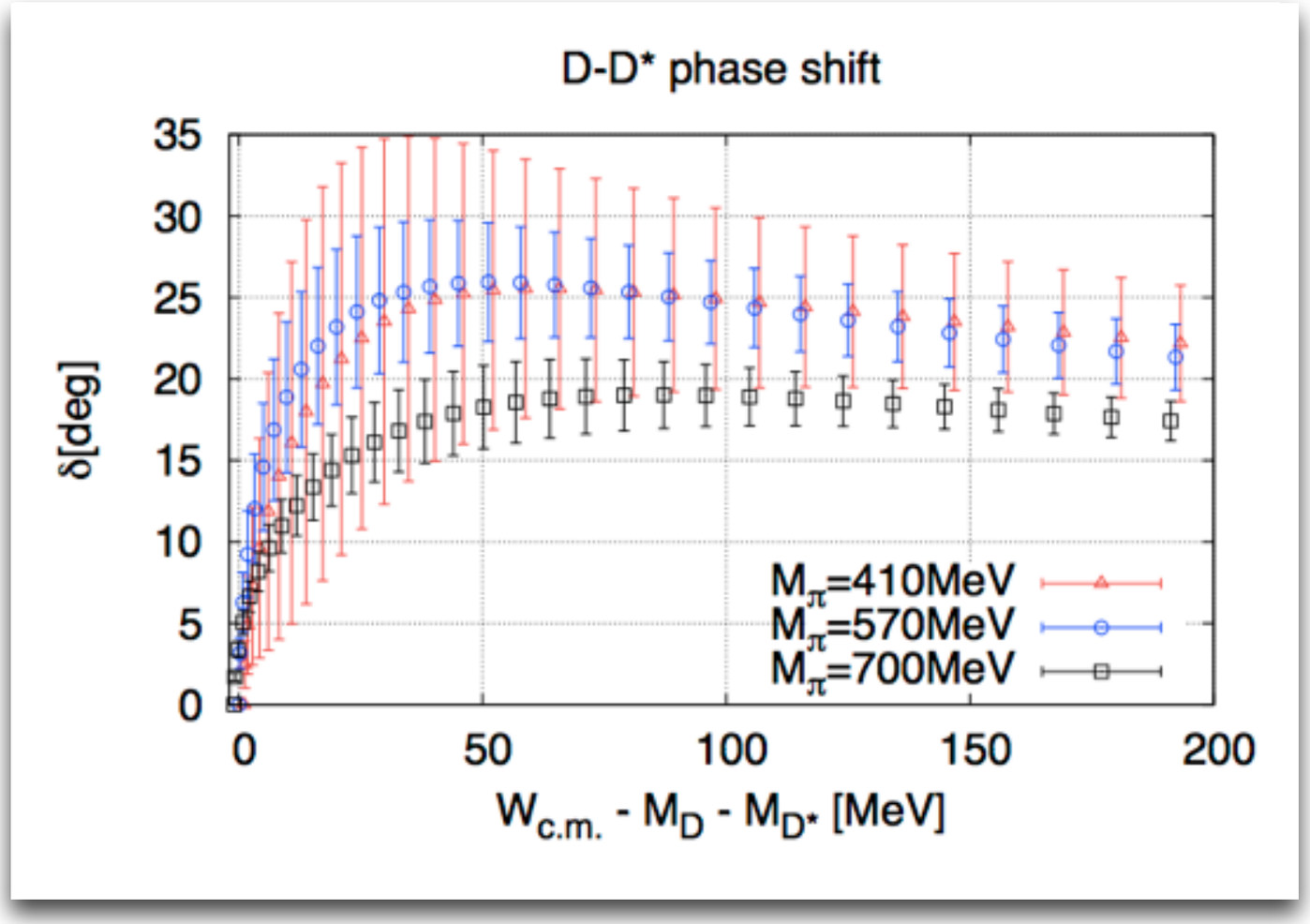

- Attraction is not sufficiently strong to generate bound state
- Rapid increase at threshold of DD* phase shift --> effect of virtual state?

➡ examine pole position

I=0 DD* T-matrix on complex energy plane

- **Pole search w/ LQCD potential@m_π=410MeV**

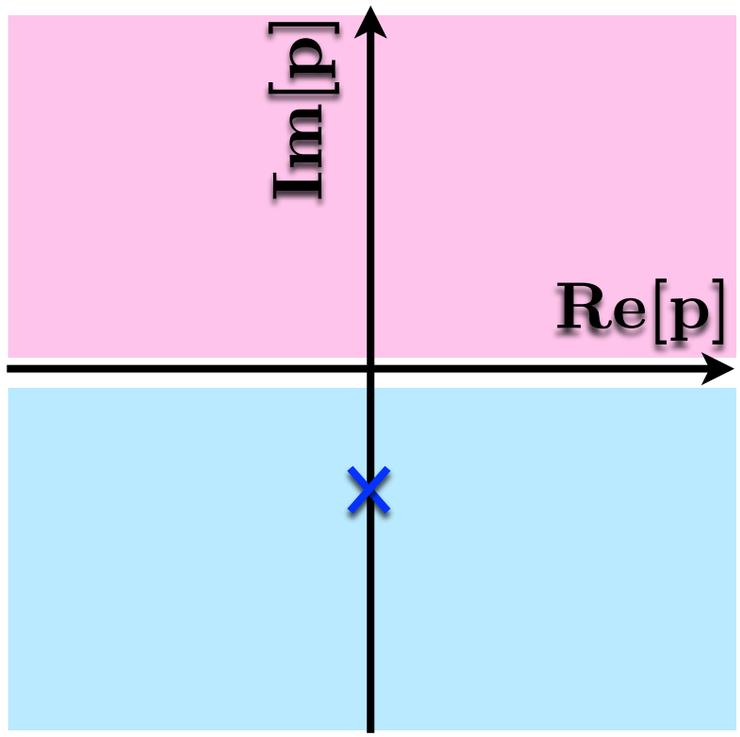

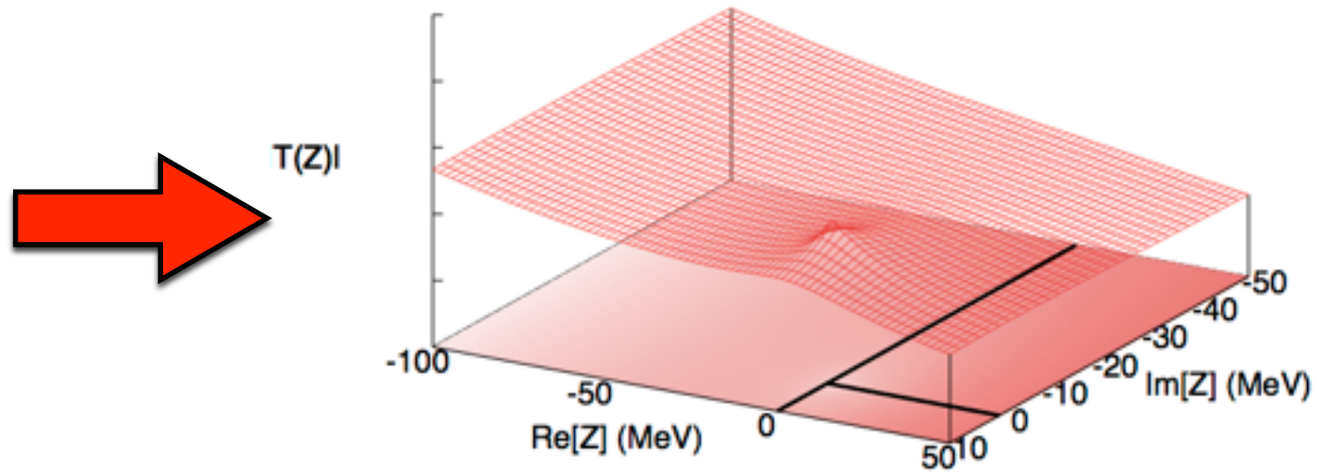

❖ **Analytic continuation**

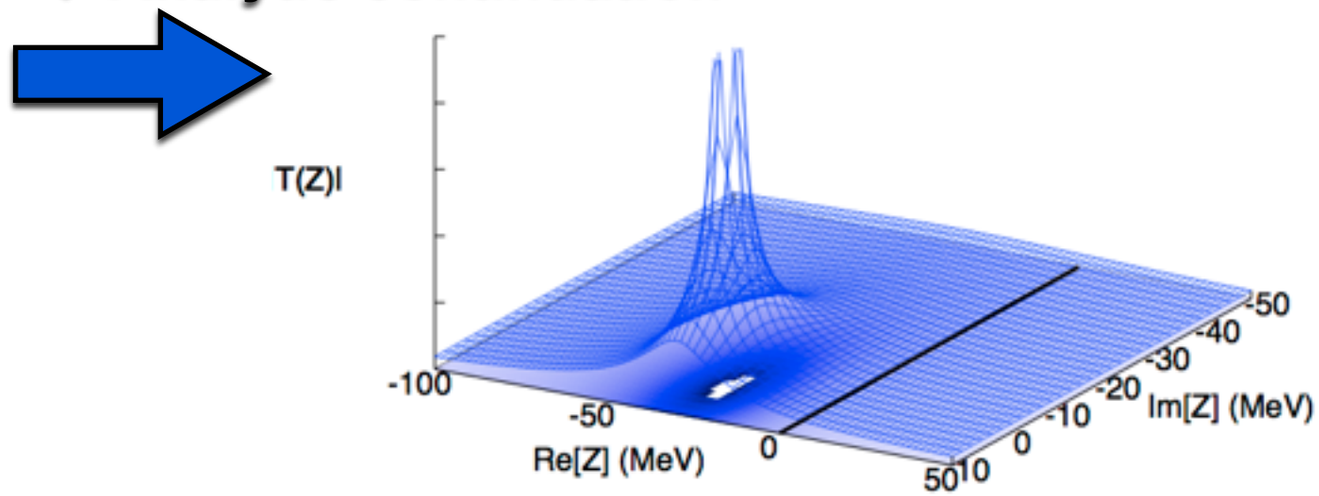

- **Virtual pole on the DD* unphysical energy plane**

➡ **threshold cusp of the amplitude**

➡ **rapid increase of scattering phase shift**

Zc(3900) in $I^G(J^P)=1^+(1^+)$

BESIII Coll., PRL110, 252001, (2013).

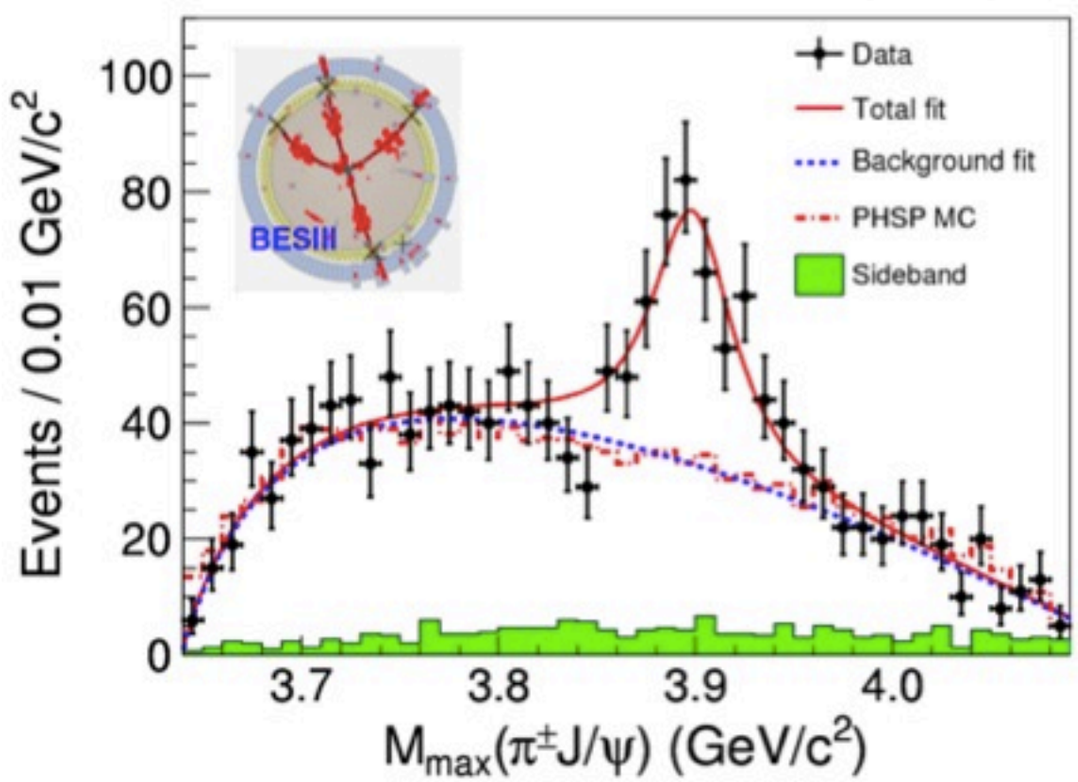

Belle Coll., PRL110, 252002, (2013).

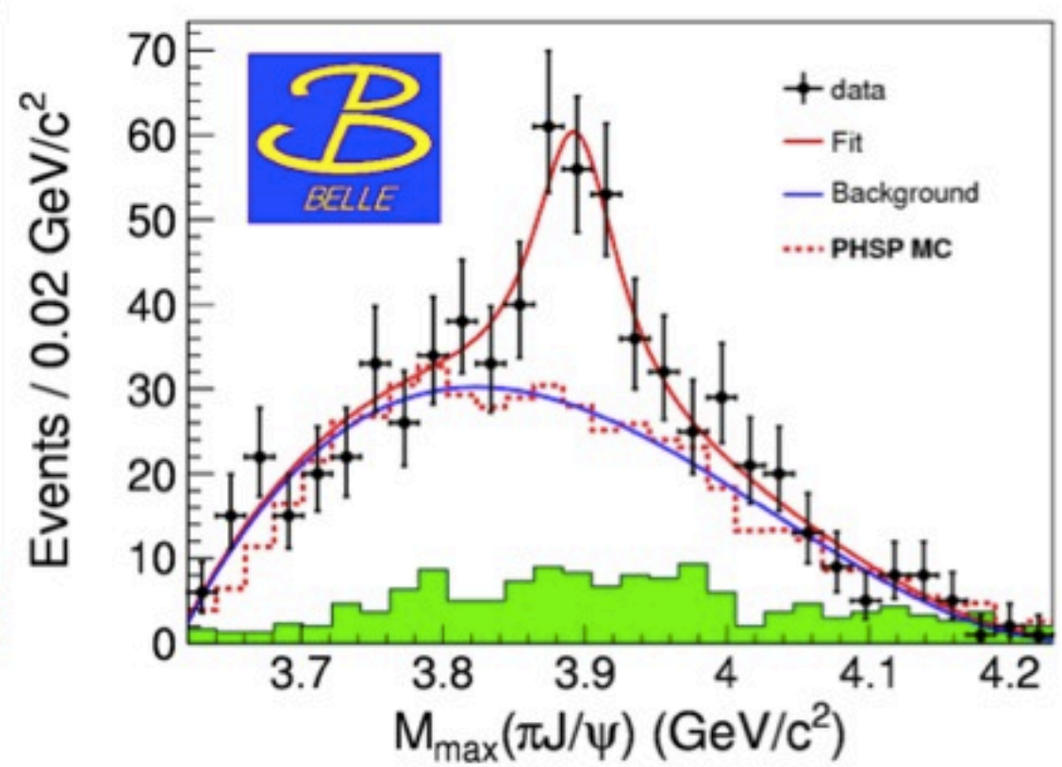

Lattice QCD setup

- N_f=2+1 full QCD configurations (PACS-CS) w/ L=2.9fm

  S. Aoki et al. (PACS-CS Coll.), PRD79, 034503, (2009).

- Tsukuba-type RHQ action for charm quark

  S. Aoki et al., PTP109, 383 (2003)

  Y. Namekawa et al., PRD84, 074505 (2011)

Light meson mass (MeV)

M_π= 411(2) [PDG:135 (π^0)]

M_ρ= 895(14) [PDG:775]

Charmed meson mass (MeV)

$M_{\eta c}$= 2988(2) [PDG:2981]

$M_{J/\Psi}$= 3097(2) [PDG:3097]

M_D= 1902(3) [PDG:1865 (D^0)]

M_{D^*}= 2048(12) [PDG:2007 (D^{*0})]

Thresholds in $I^G J^P$=1^+1^+ channel

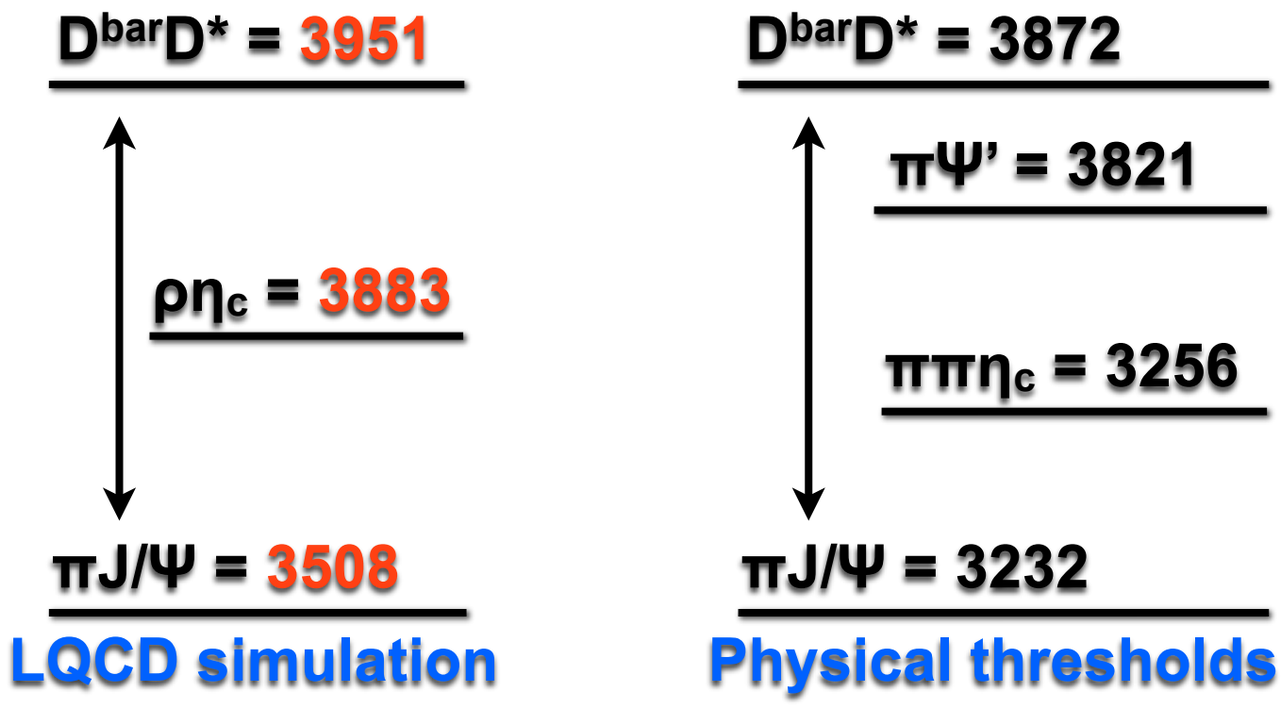

- $M_{\pi\Psi'}$ > $M_{D^{bar}D^*}$ due to heavy pion mass
- $\rho \to \pi\pi$ decay not allowed in our setup

- S-wave $\pi J/\Psi$ - $\rho\eta_c$ - $D^{bar}D^*$ coupled-channel analysis is performed

Potential matrix ($\pi J/\Psi$ - $\rho\eta_c$ - $D^{bar}D^*$)

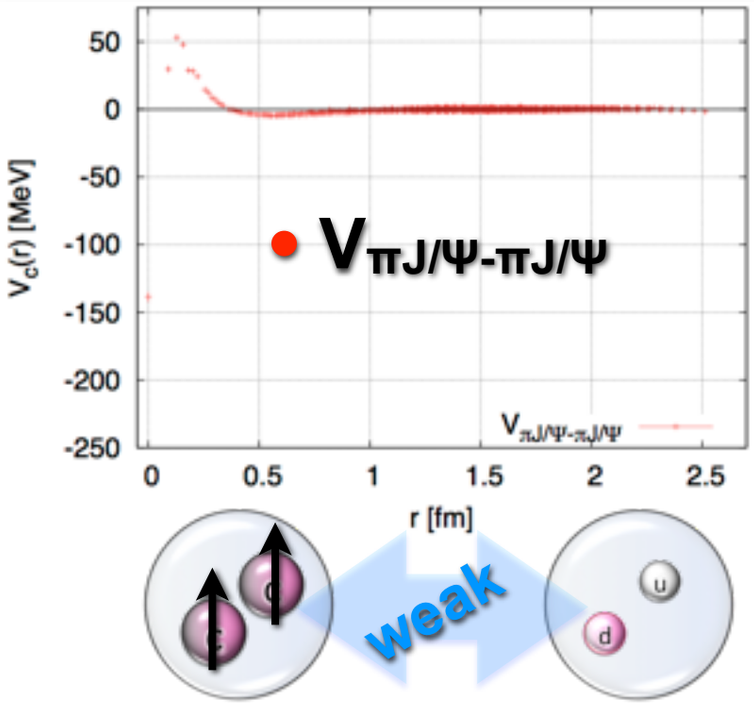

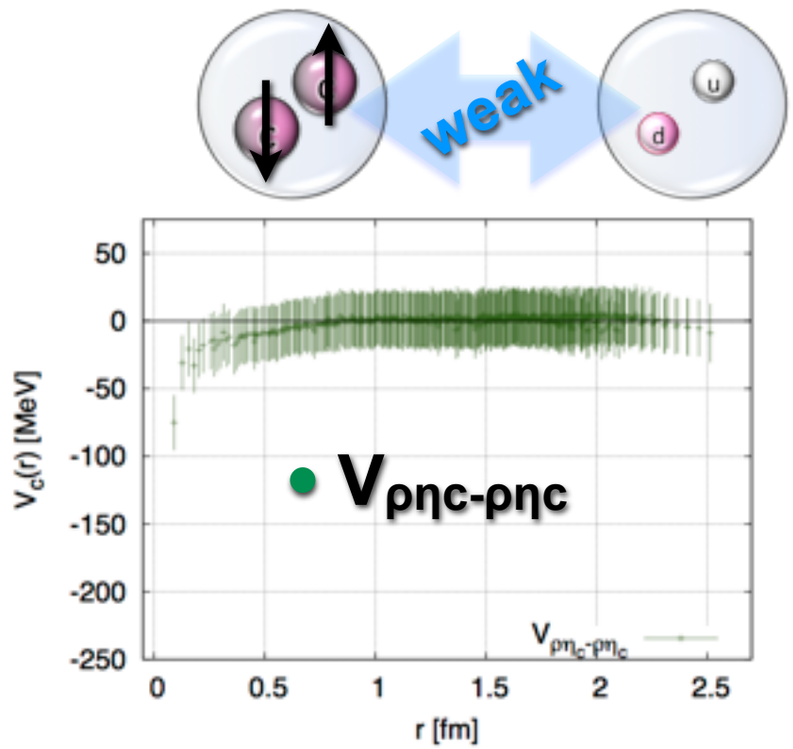

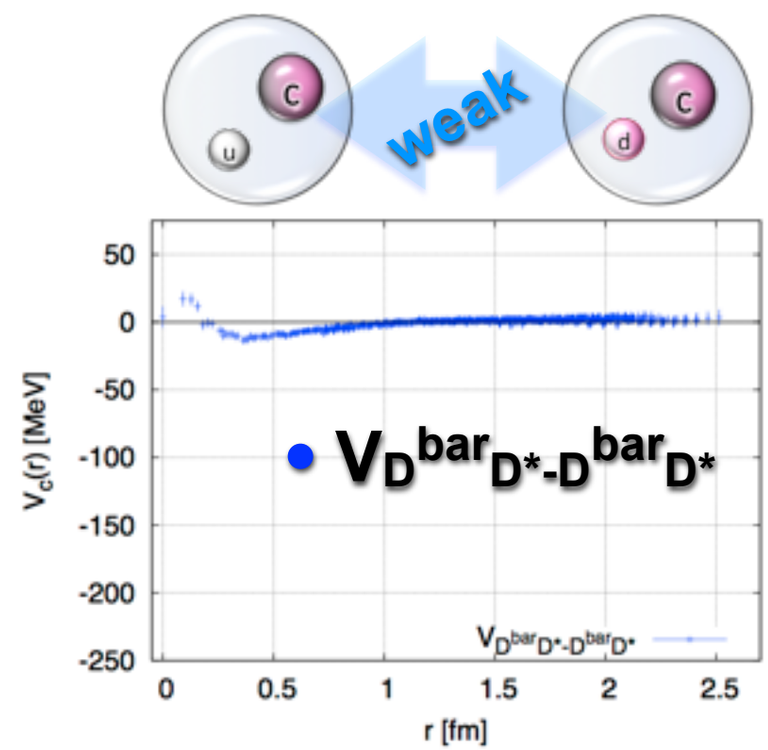

- **All diagonal potentials are weak**

  ➡ **no bound $D^{bar}D^*$**

Potential matrix ($\pi J/\Psi$ - $\rho\eta_c$ - $D^{bar}D^*$)

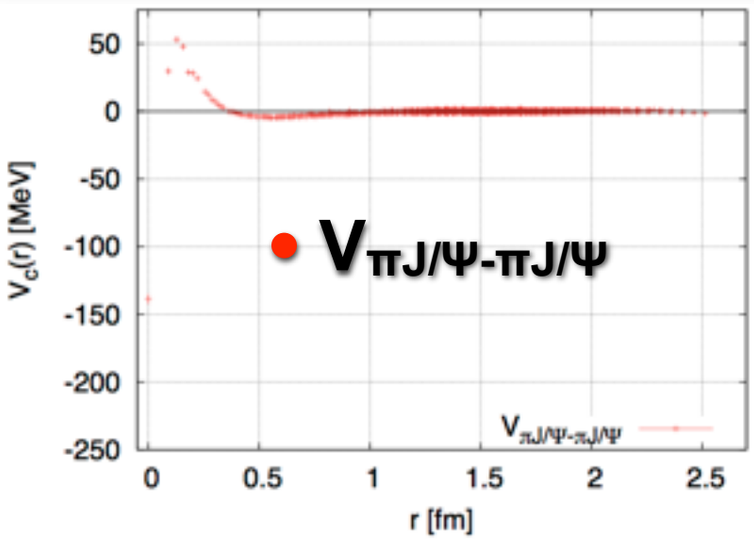

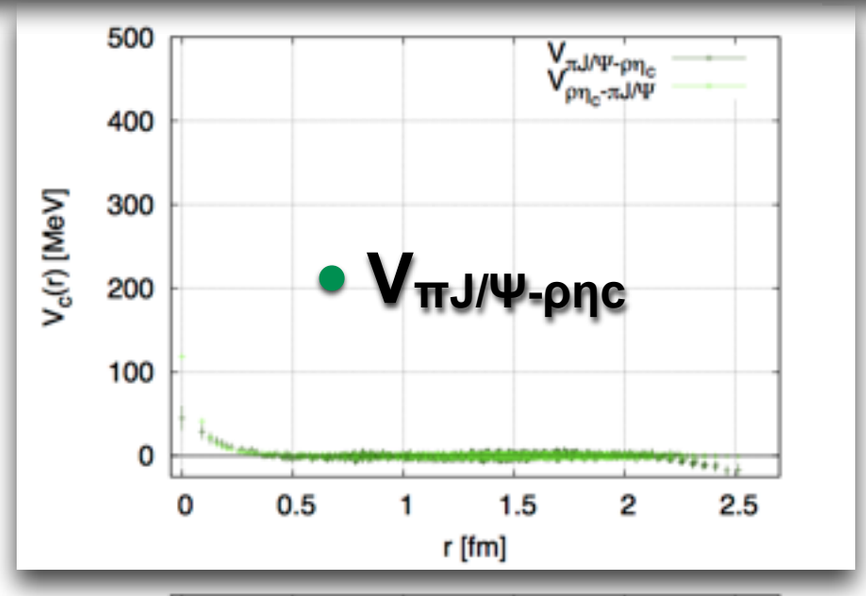

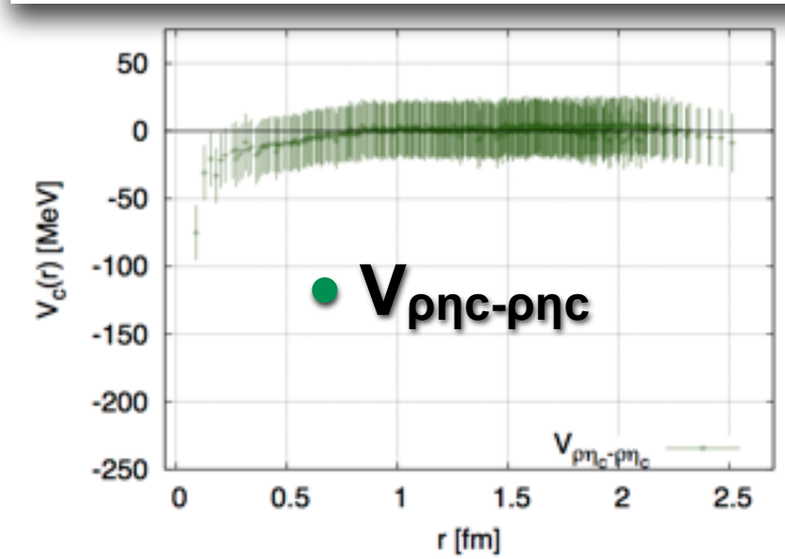

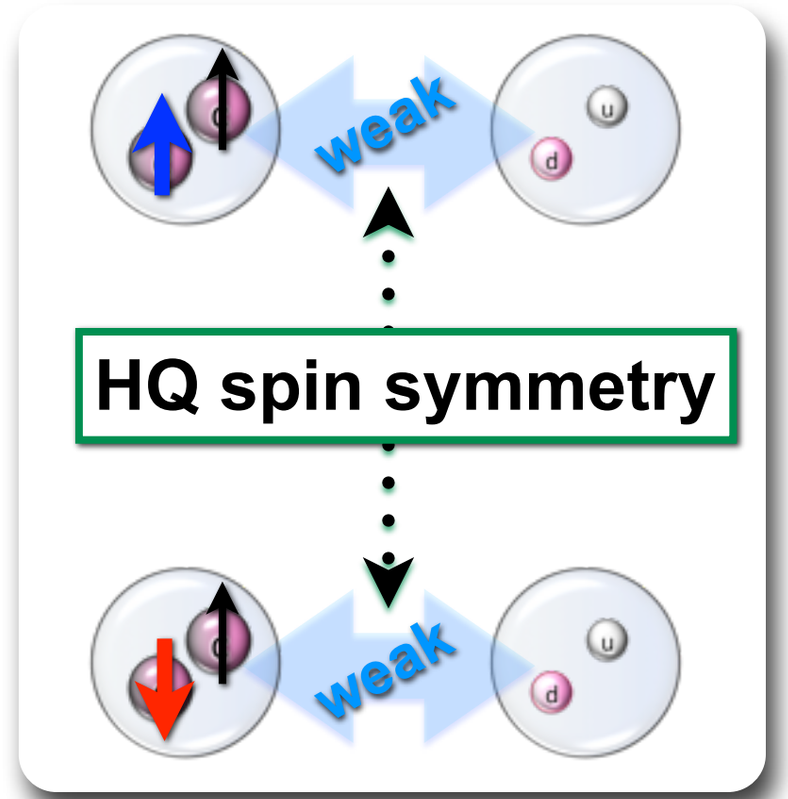

- **Weak charm spin-flip potential**

➡ **heavy quark spin symmetry**

(charm quark spin-flip amplitude is suppressed)

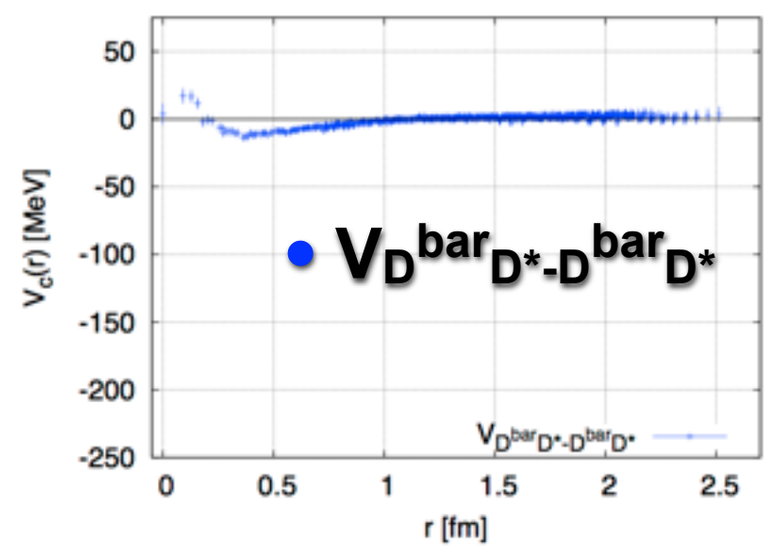

Potential matrix ($\pi J/\Psi$ - $\rho\eta_c$ - $D^{bar}D^*$)

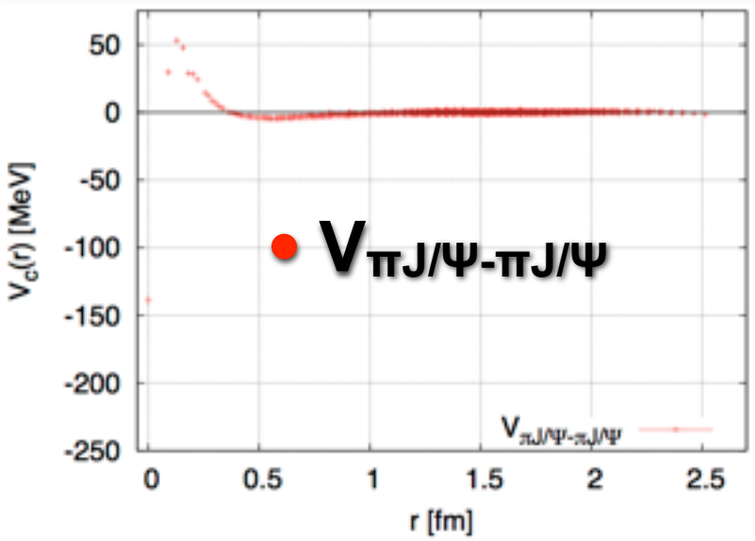

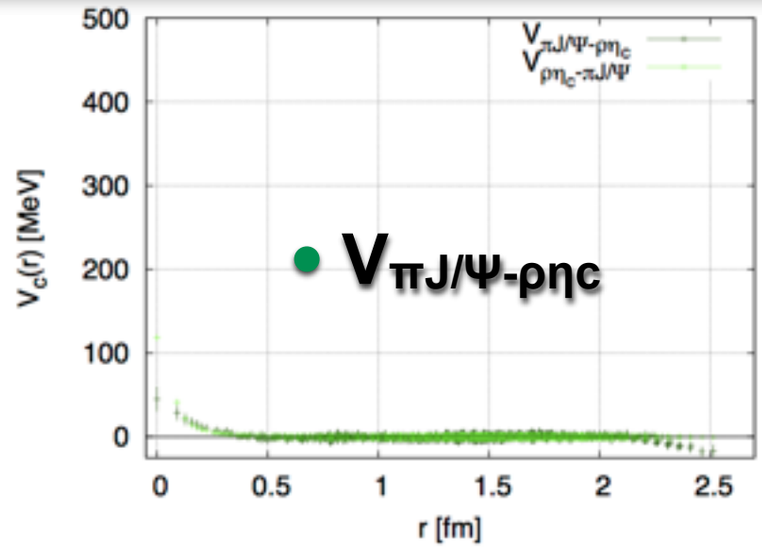

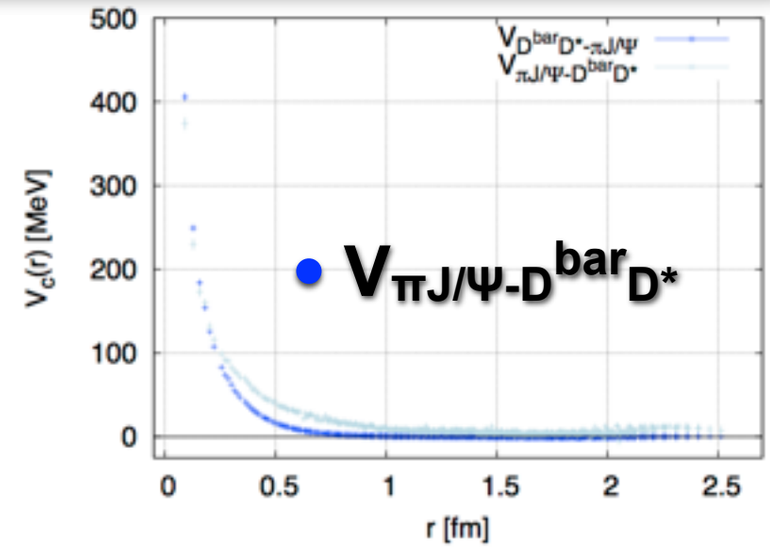

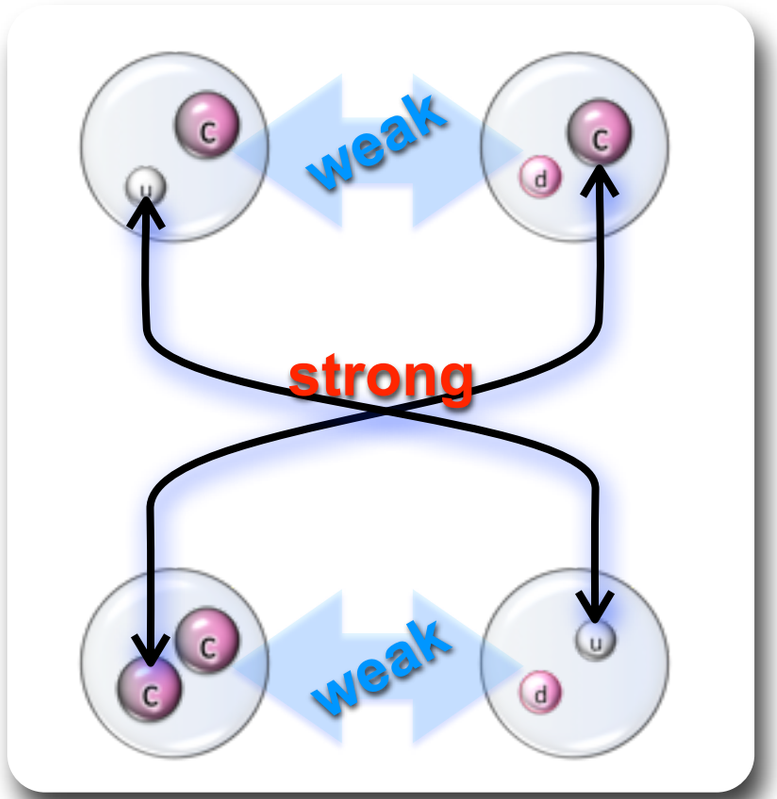

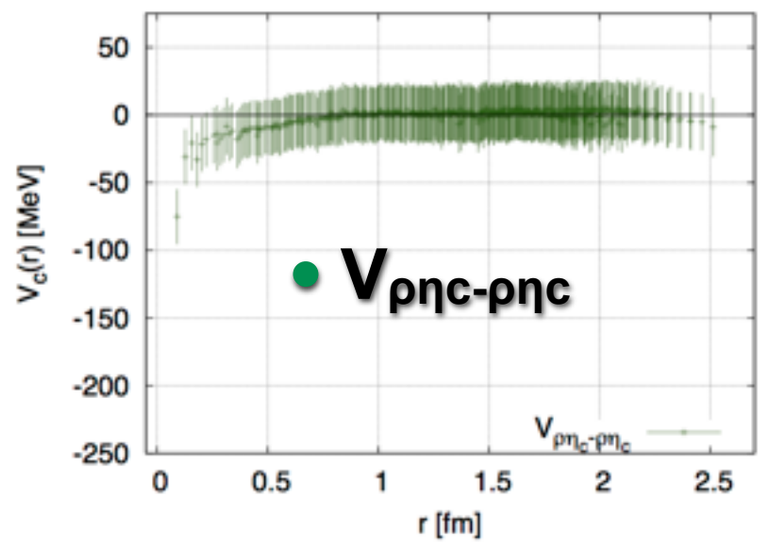

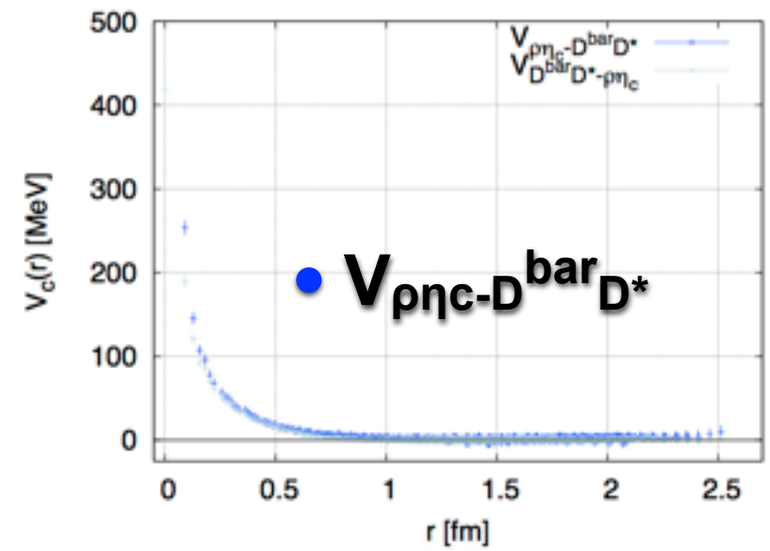

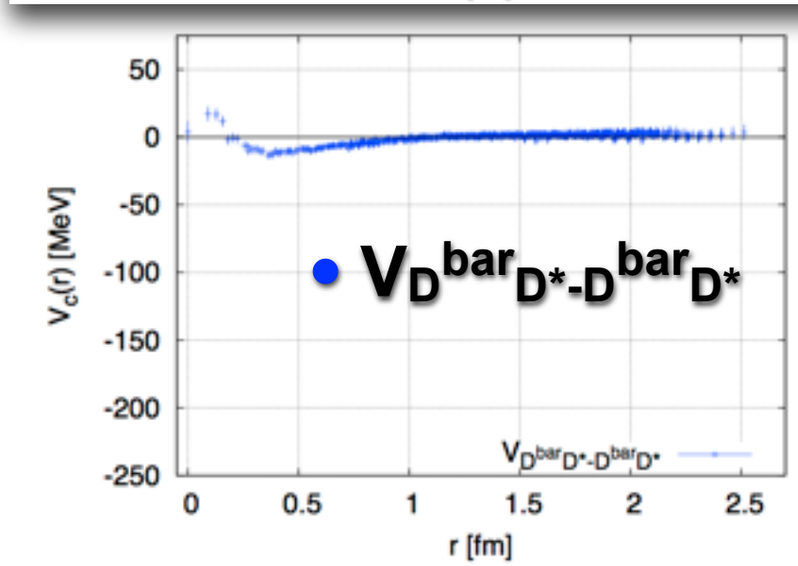

- **Strong off-diagonal $D^{bar}D^*$ potentials**
  - ✓ strong charm-quark-exchange interactions

Potential matrix ($\pi J/\Psi$ - $\rho\eta_c$ - $D^{bar}D^*$)

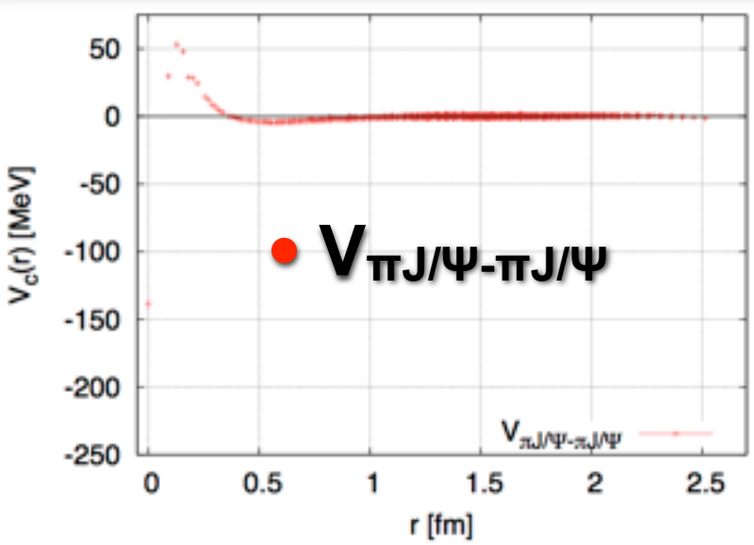

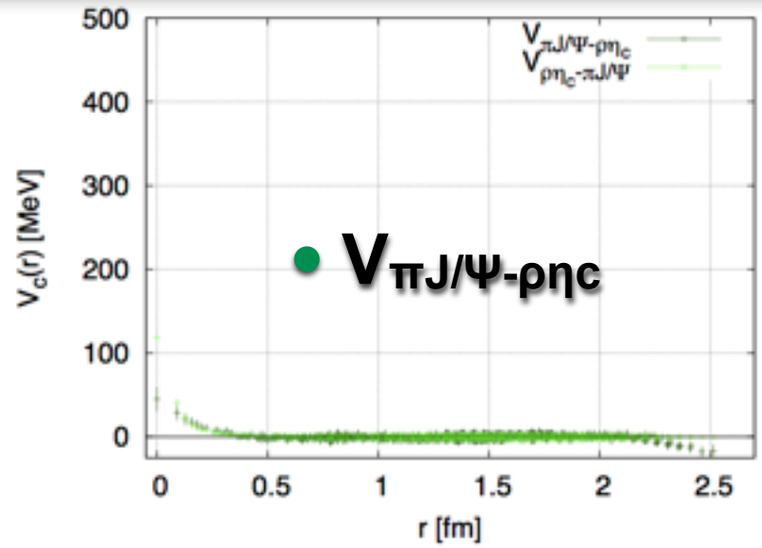

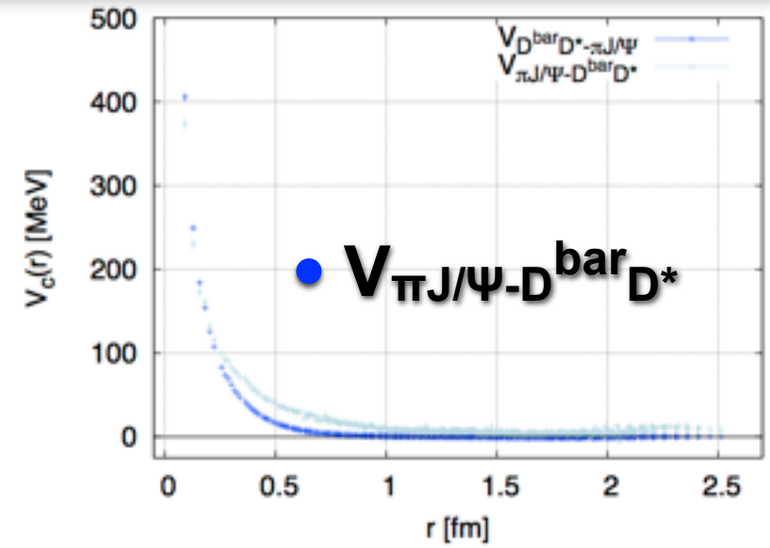

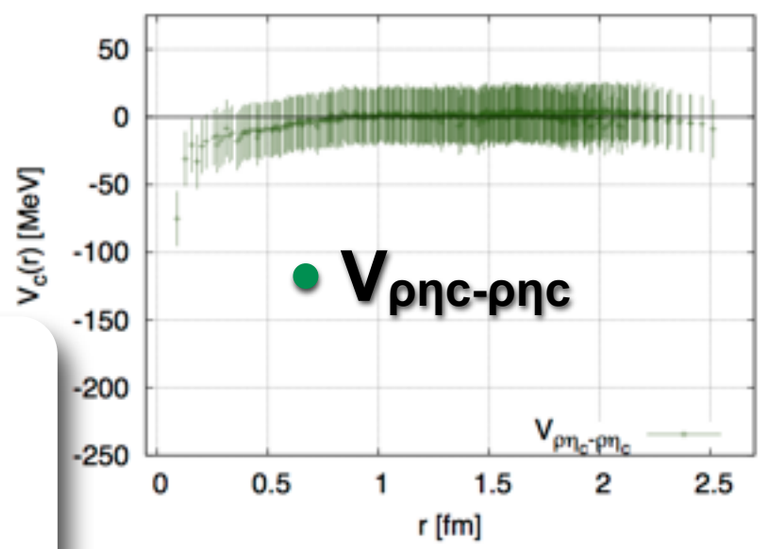

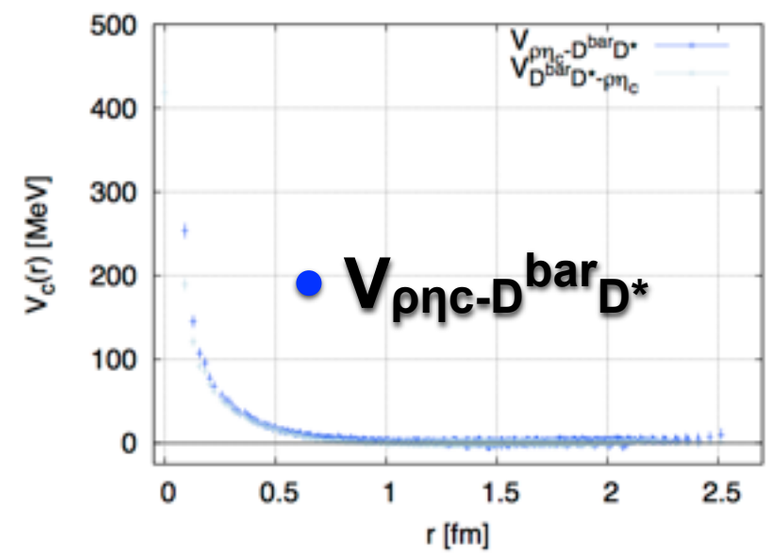

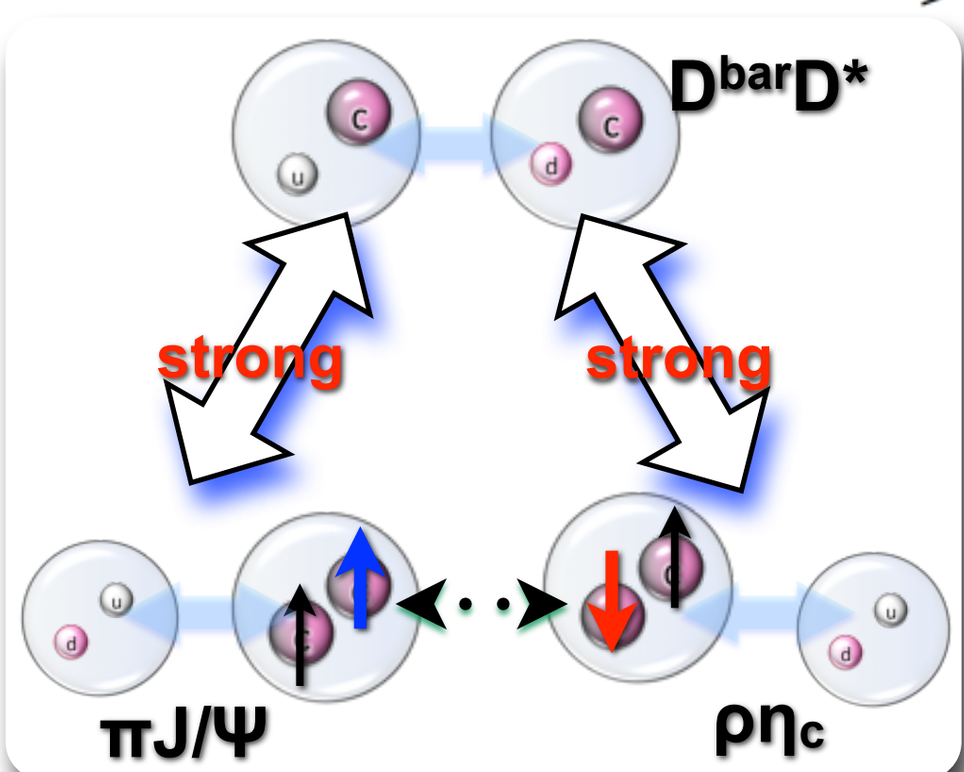

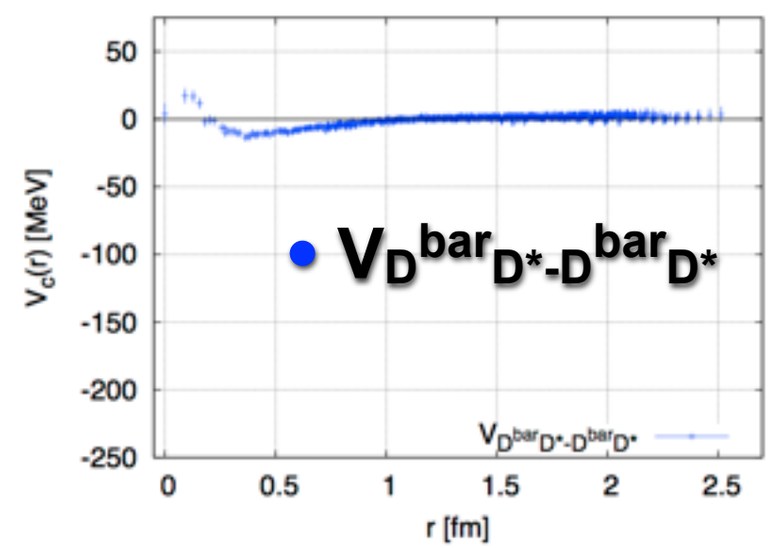

Invariant mass spectra of πJ/Ψ & $D^{bar}D^*$

- πJ/Ψ invariant mass (m_π=410MeV)

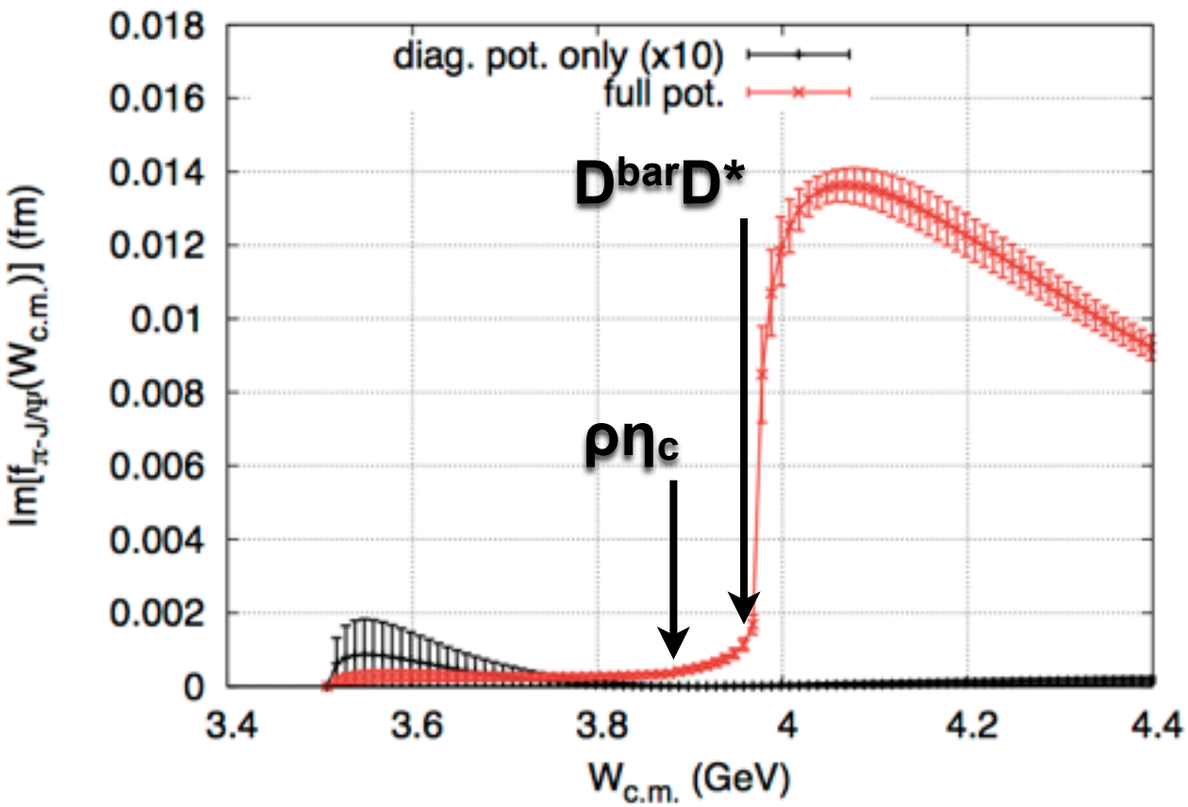

- $D^{bar}D^*$ invariant mass (m_π=410MeV)

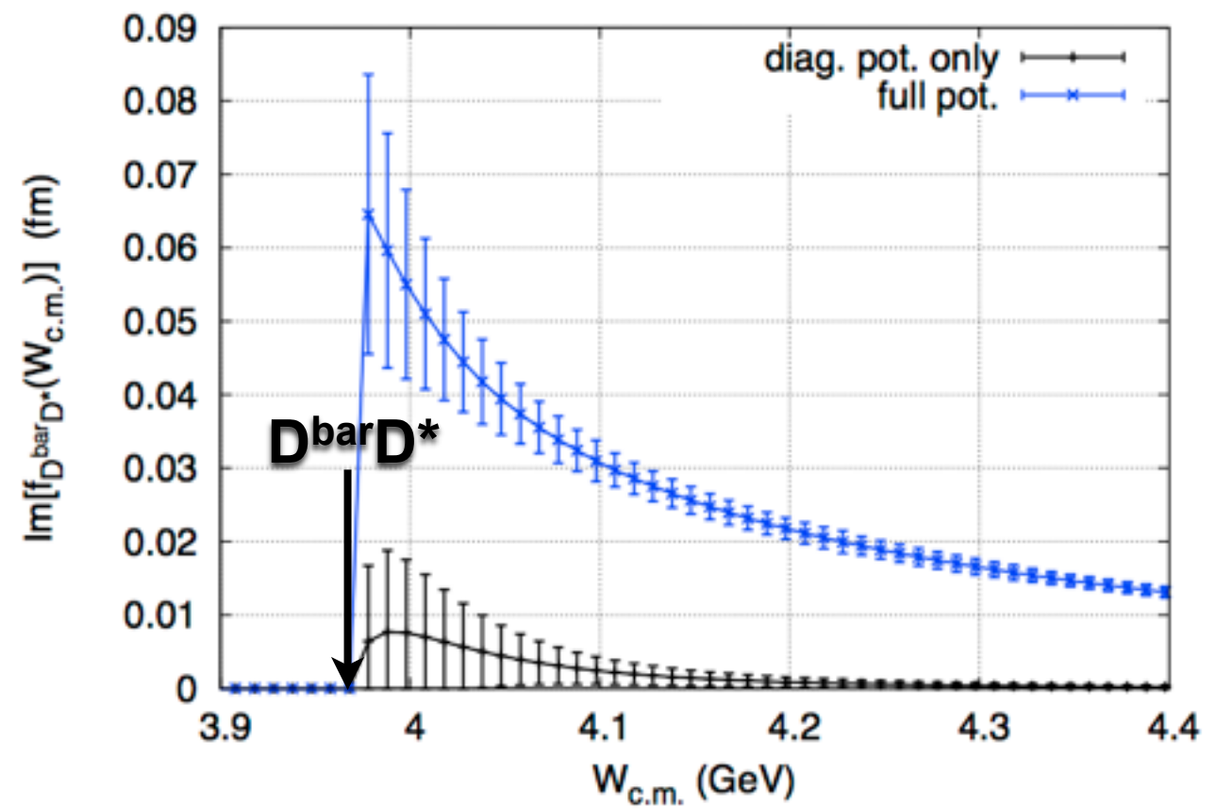

✓ enhancement near $D^{bar}D^*$ threshold due to large πJ/Ψ-$D^{bar}D^*$ coupling

- peak in πJ/Ψ invariant mass
- sharp enhancement in $D^{bar}D^*$ invariant mass

LQCD results & EXP. results

- **πJ/Ψ invariant mass (m_π=410MeV)**

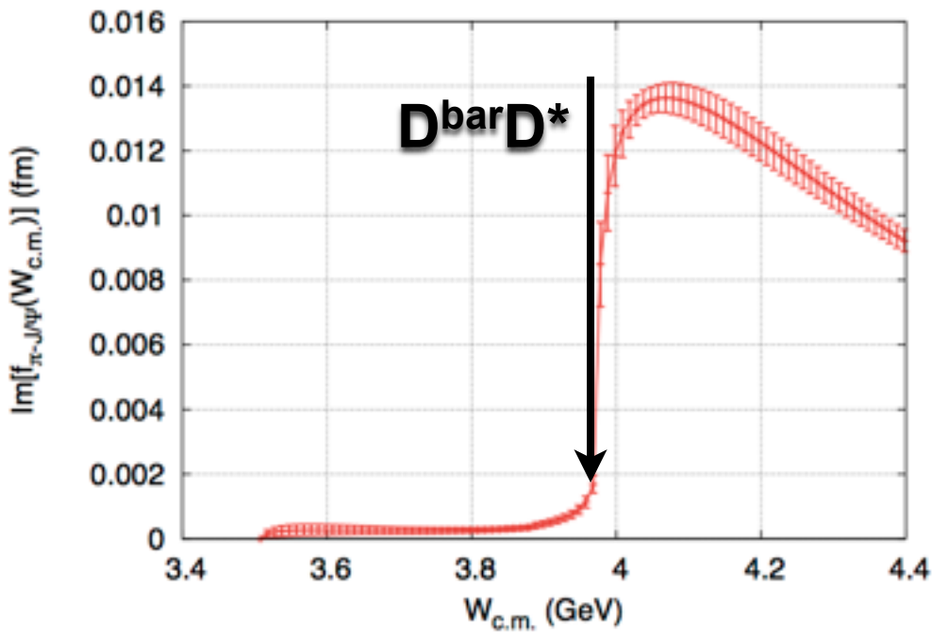

- **$D^{bar}D^*$ invariant mass (m_π=410MeV)**

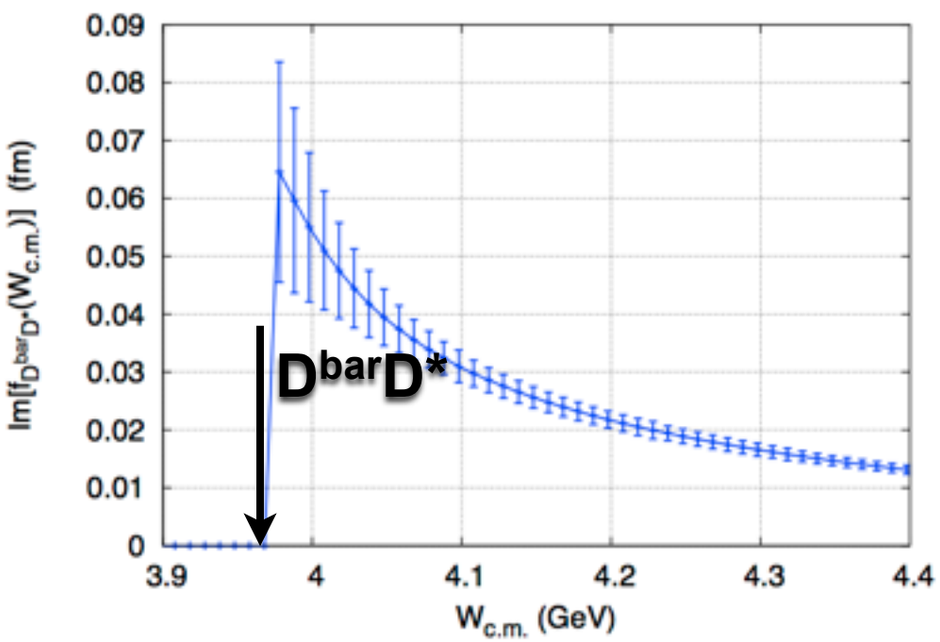

- **e^+e^- --> π(πJ/Ψ) @ 4.26GeV**

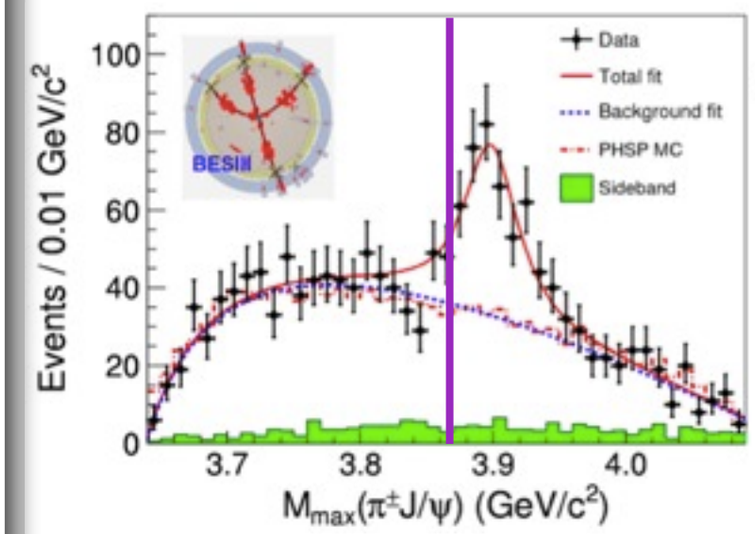

BESIII Coll., PRL110 (2013).

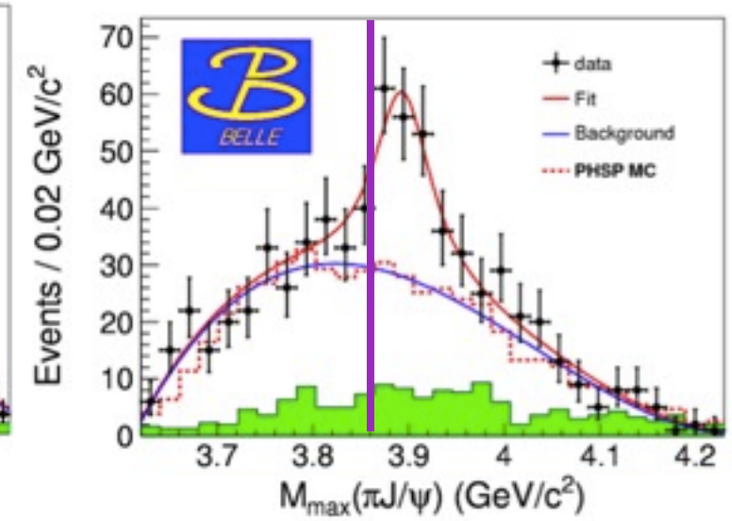

Belle Coll., PRL110 (2013).

- **e^+e^- --> $\pi^{+/-}$ $(D^{bar}D^*)^{-/+}$**

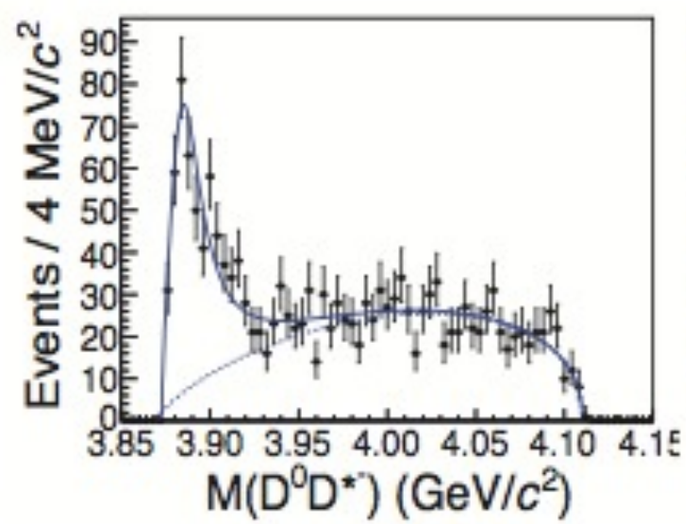

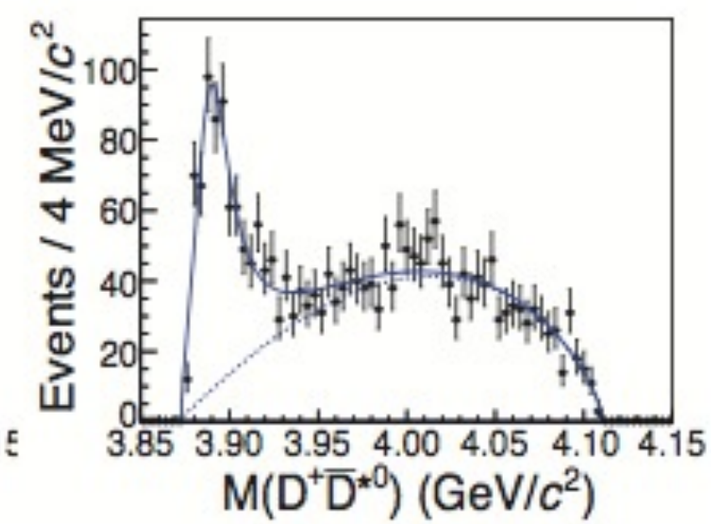

BESIII Coll., PRL112 (2014).

✔ **We observe similar line shapes of πJ/Ψ & $D^{bar}D^*$ inv. mass**

Pole search ($\pi J/\Psi$:2nd, $\rho\eta_c$:2nd, $D^{bar}D^*$:2nd)

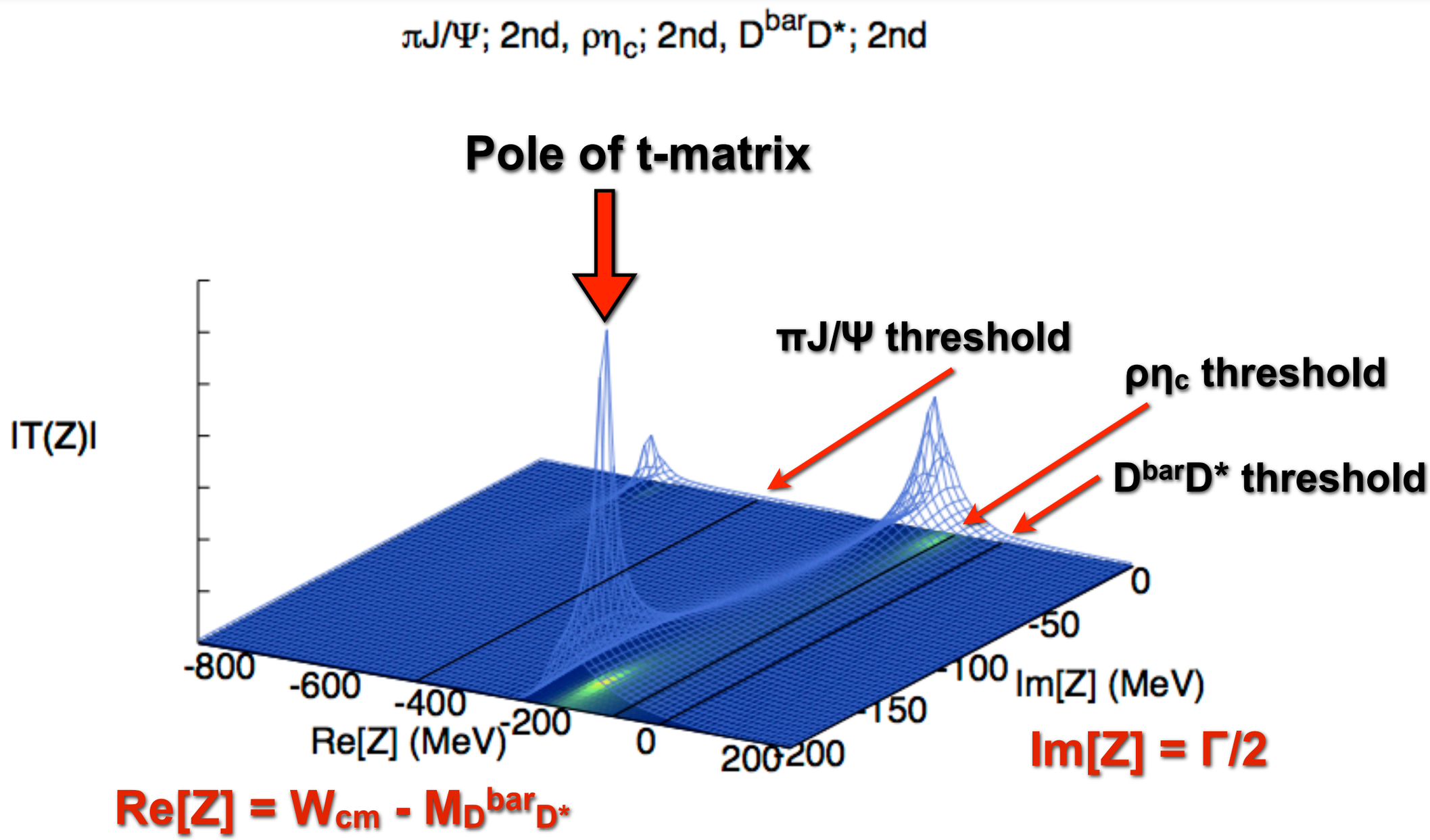

- ✓ Pole for Zc(3900) on the most adjacent complex energy plane is found
- ✓ Origin of enhancement in 2-body invariant mass near $D^{bar}D^*$ threshold

Summary

✤ Applications of HAL QCD method to tetra-quarks, Tcc & Zc(3900)

- T_{cc} search on the lattice@m_π=410--700MeV
  - ➡ T_{cc} is not bound for m_π>400MeV (T_{bb} is already bound)
  - ➡ sizable correlation of diquarks is found
    - I=0 good diquark channel : attractive
    - I=1 bad diquark channel : repulsive
- Zc(3900) in $I^G(J^P)=1^+(1^{+)}$ channel on the lattice@m_π=410MeV
  - ➡ Large channel coupling between $\pi J/\Psi$-$D^{bar}D^*$ is a key
  - ➡ Heavy quark spin symmetry is seen in c.c. potentials
    - Zc(3900) is neither simple $D^{bar}D^*$ molecule nor J/Ψ + π-cloud
    - pole on complex energy plane is found (w/ relatively large width)

see also, S. Prelovsek et al., PRD91, 014504 (2015).

✤ Physical point simulation is the next step

Backup

Potential matrix ($\pi J/\Psi$ - $\rho\eta_c$ - $D^{bar}D^*$)

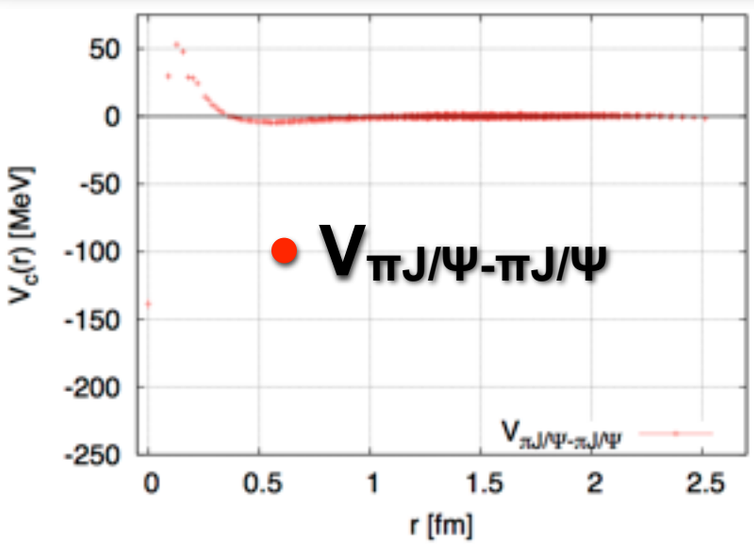

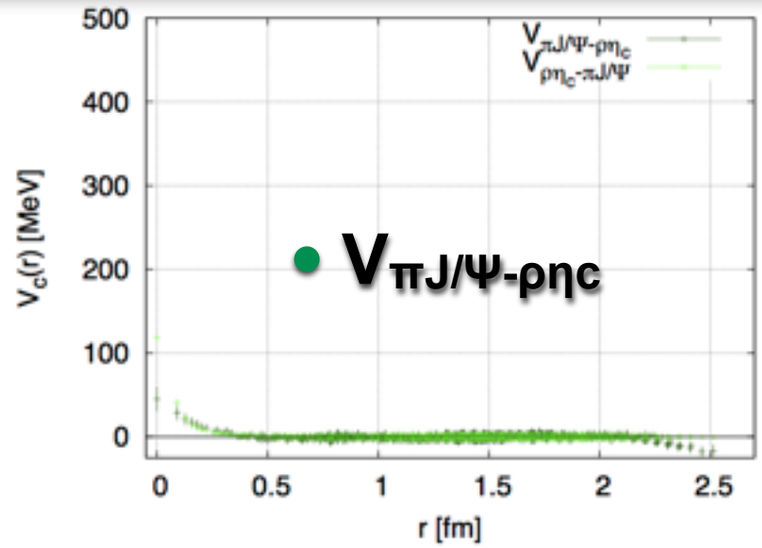

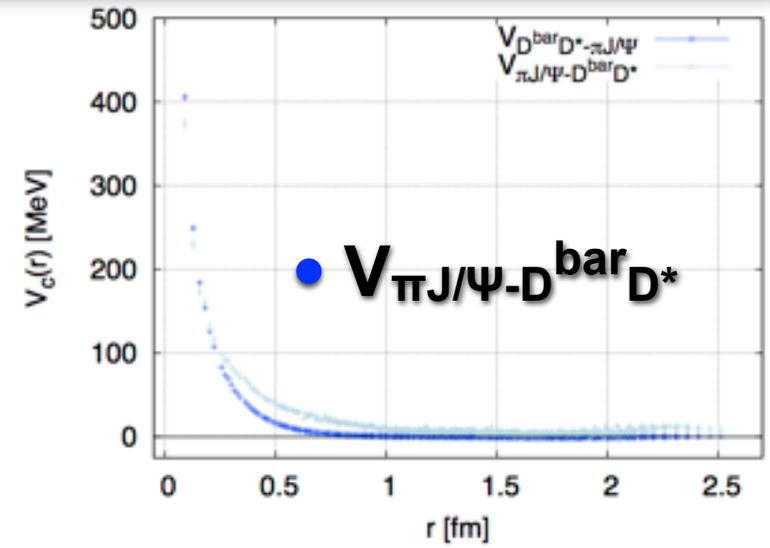

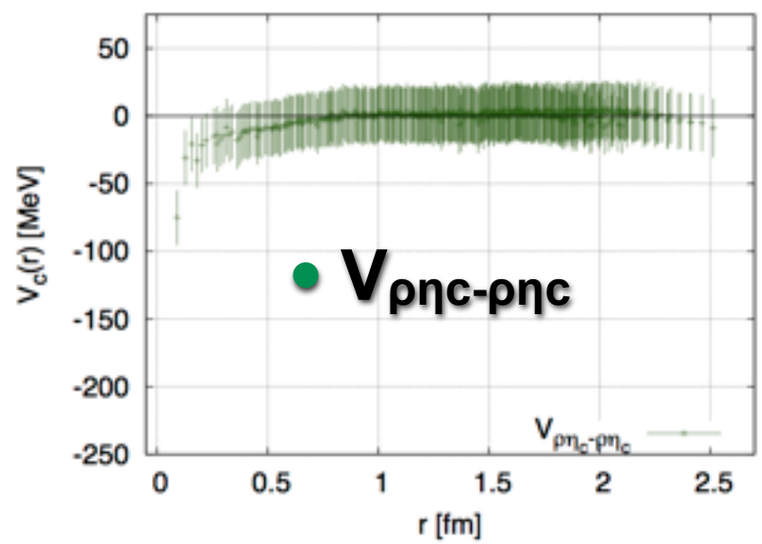

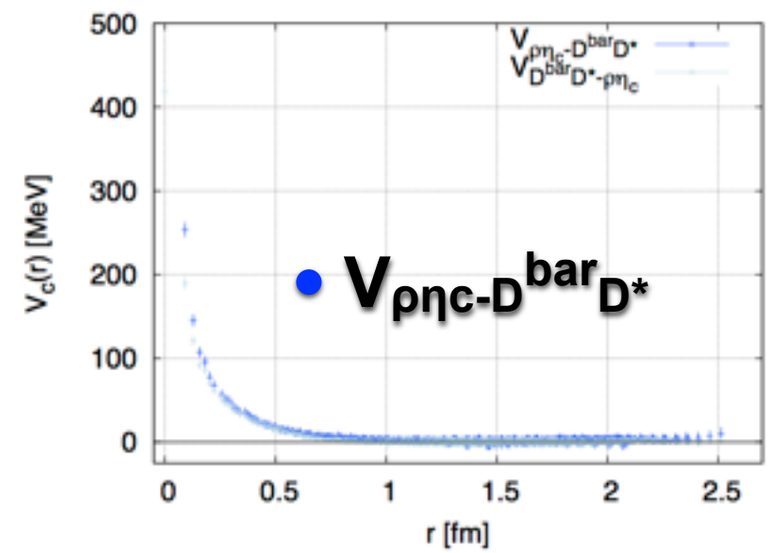

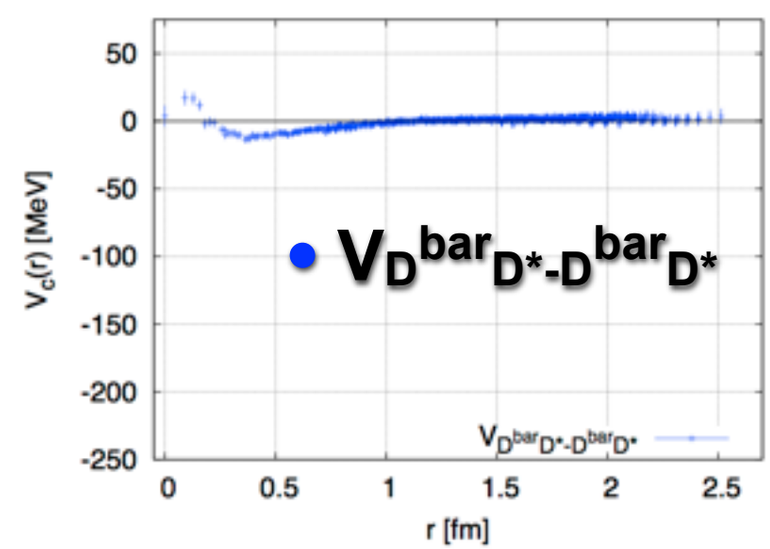

- **<u>Strong off-diagonal $D^{bar}D^*$ potentials</u>**
  - ✓ **heavy quark spin symmetry**
  - ✓ **strong charm-quark-exchange interactions**

➡ $V_{DbarD^*-\pi J/\Psi} \sim V_{DbarD^*-\rho\eta c} >> V_{\pi J/\Psi-\rho\eta c}$

2-body invariant mass spectra

- πJ/Ψ invariant mass (m_π=410MeV)

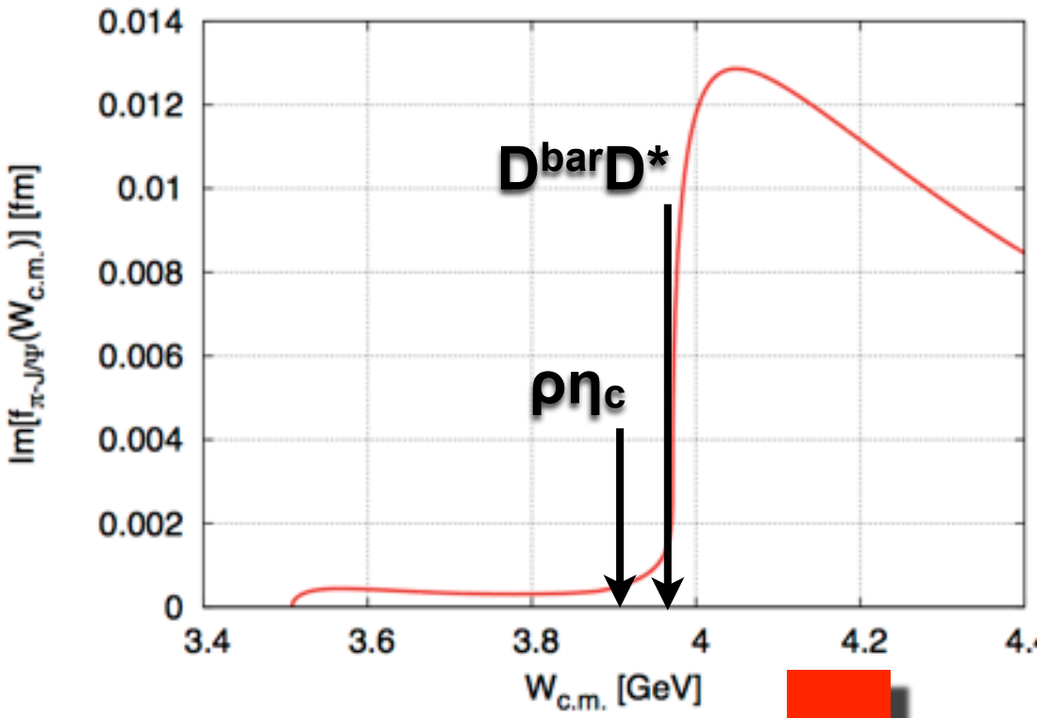

- $D^{bar}D^*$ invariant mass (m_π=410MeV)

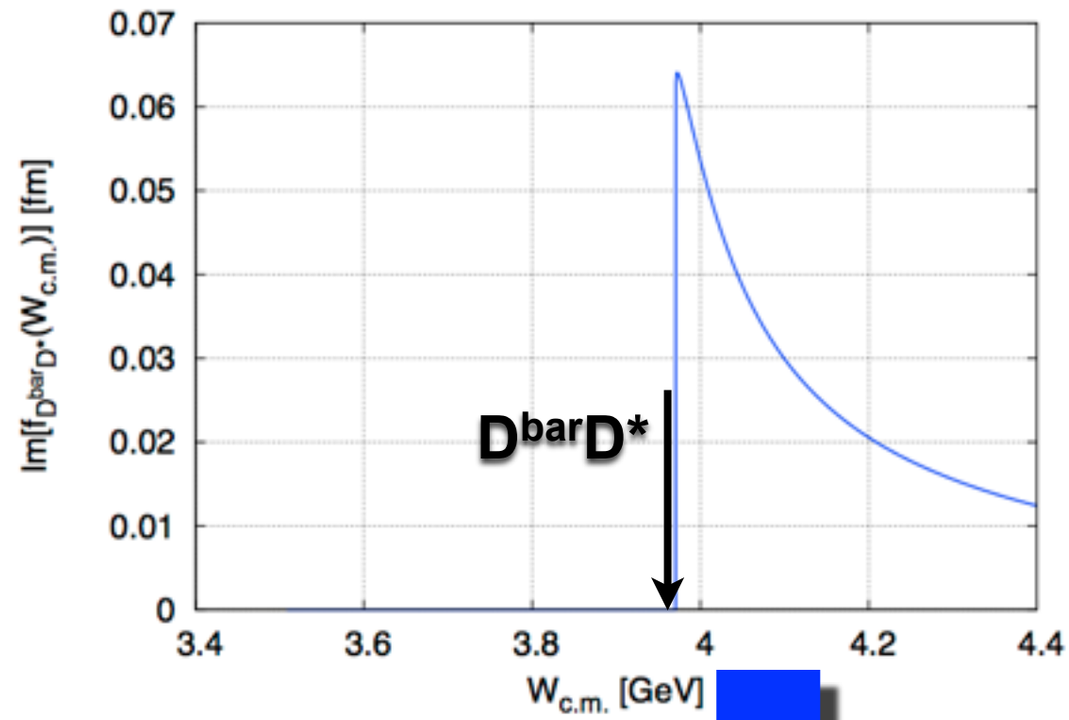

off-diagonal potentials V_{ij}=0

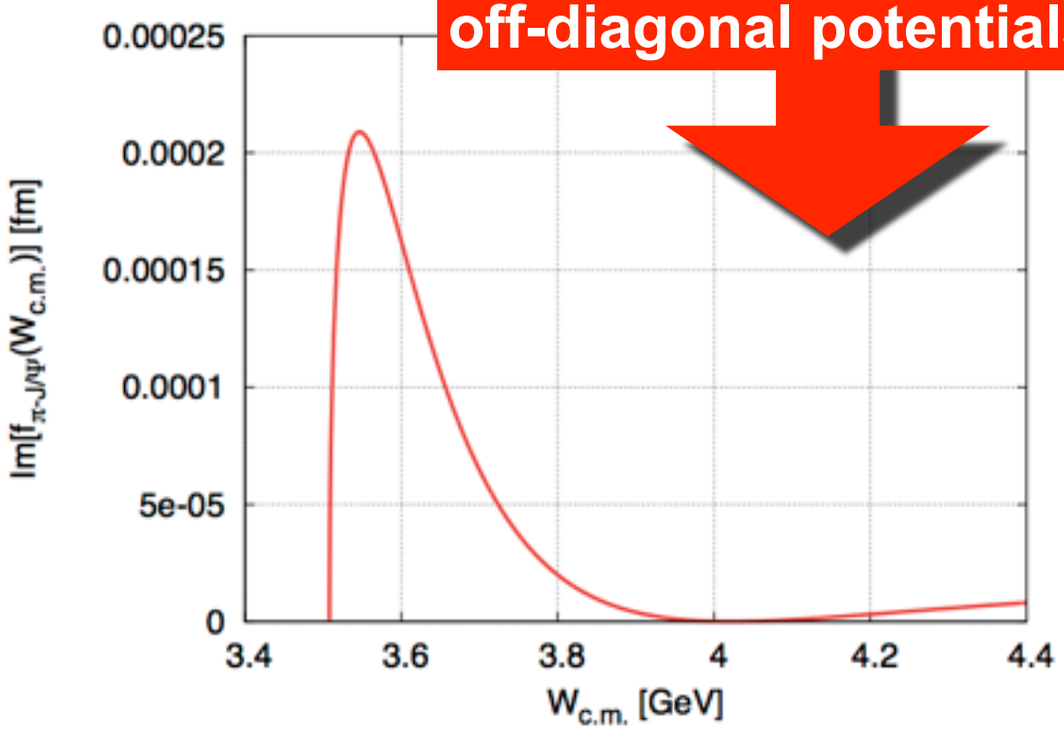

off-diagonal potentials V_{ij}=0

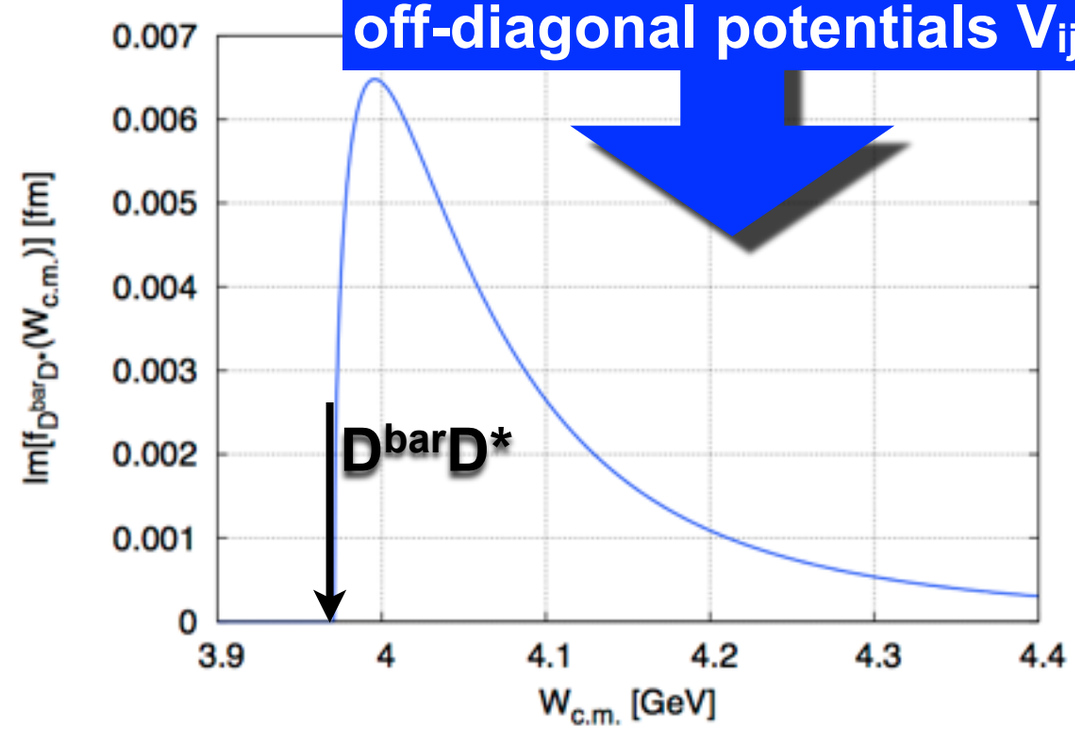

Backup

Tcc bound state

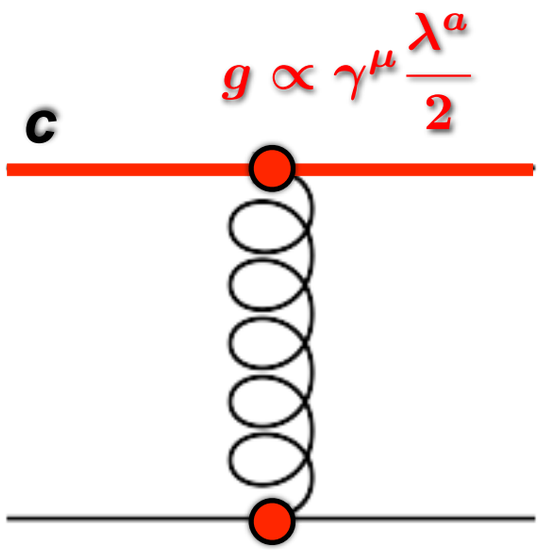

$$\sim \bar{c}\gamma^\mu \frac{\lambda^a}{2} c A^a$$ = color magnetic + color electric forces

- **Color magnetic interaction (CMI)** : hadron mass splitting

$$V_{ij}^{\mathrm{CMI}} \propto -\frac{\left(\vec{\lambda}(i)\cdot\vec{\lambda}(j)\right)\left(\vec{\sigma}(i)\cdot\vec{\sigma}(j)\right)}{M_i M_j}$$

- Color-spin matrix elements : $\langle v_{ij}\rangle = -\langle\left(\vec{\lambda}(i)\cdot\vec{\lambda}(j)\right)\left(\vec{\sigma}(i)\cdot\vec{\sigma}(j)\right)\rangle$

$\langle v_{ij}\rangle$	C=1	C=8	C=3	C=6^{bar}
S=0	-16	2	-8	4
S=1	16/3	-2/3	8/3	-4/3

- C=3, S=0 (I=0) : -8
- C=6^{bar}, S=1 (I=0) : -4/3
- C=3, S=1 (I=1) : 8/3
- C=6^{bar}, S=0 (I=1) : 4

attractive

repulsive

- CMI proportional to $1/M_i$: strongly attractive u^{bar}d^{bar}-diquark pair

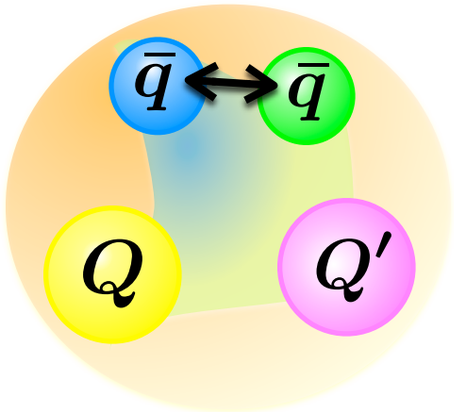

➡ Possibility of bound $T_{QQ'}$

H. J. Lipkin, PLB172, 242 (1986).

Zc(3900) : experimental observations (I)

BESIII Coll., PRL110, 252001, (2013).

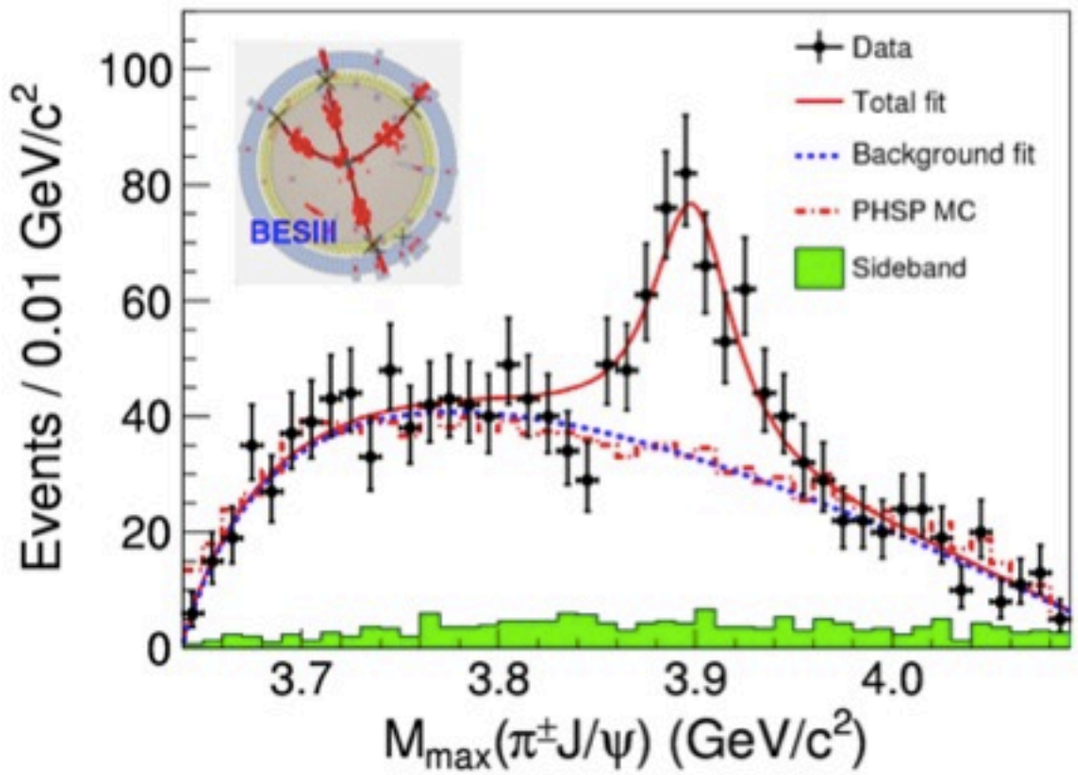

Belle Coll., PRL110, 252002, (2013).

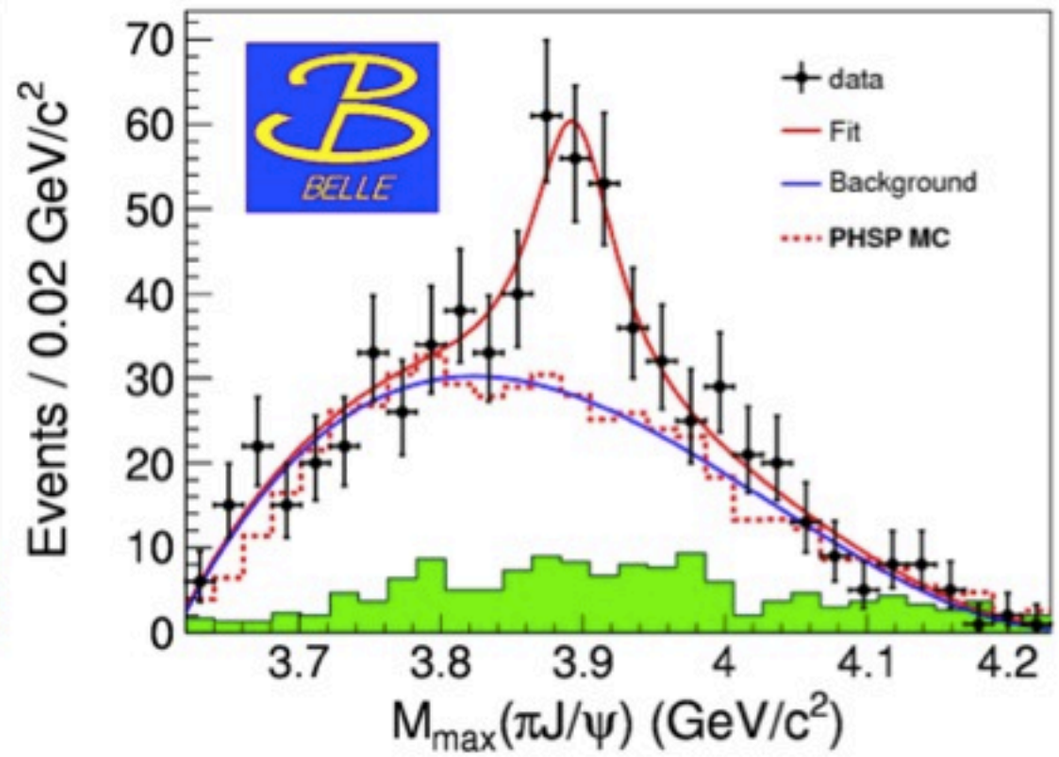

- Zc(3900) is observed in $\pi^{\pm}J/\Psi$ invariant mass
- Zc(3900) is charged state --> at least 4-quark?
- Isospin of Zc(3900) must be $I^G=1^+$
- M ~ 3900, Γ ~ 60 MeV from BW line shape
- Peak confirmed by CLEO Coll.

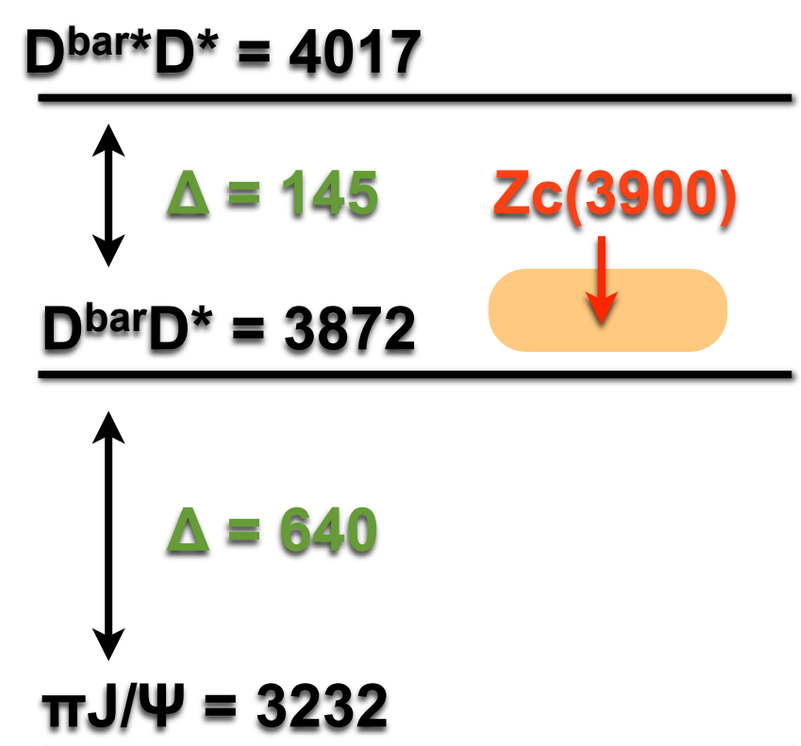

Zc(3900) : experimental observations (II)

- **What about J^P?**
  : $e^+e^- \to \pi^{+/-} (D^{bar}D^*)^{-/+}$ [$\pi^{+/-}$ Zc(3900)$^{-/+}$]

BESIII Coll., PRL112, 022001, (2014).

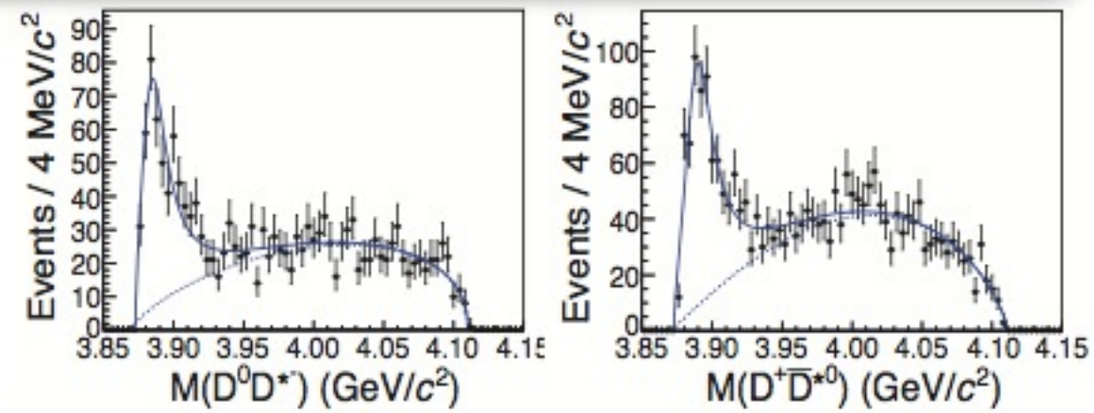

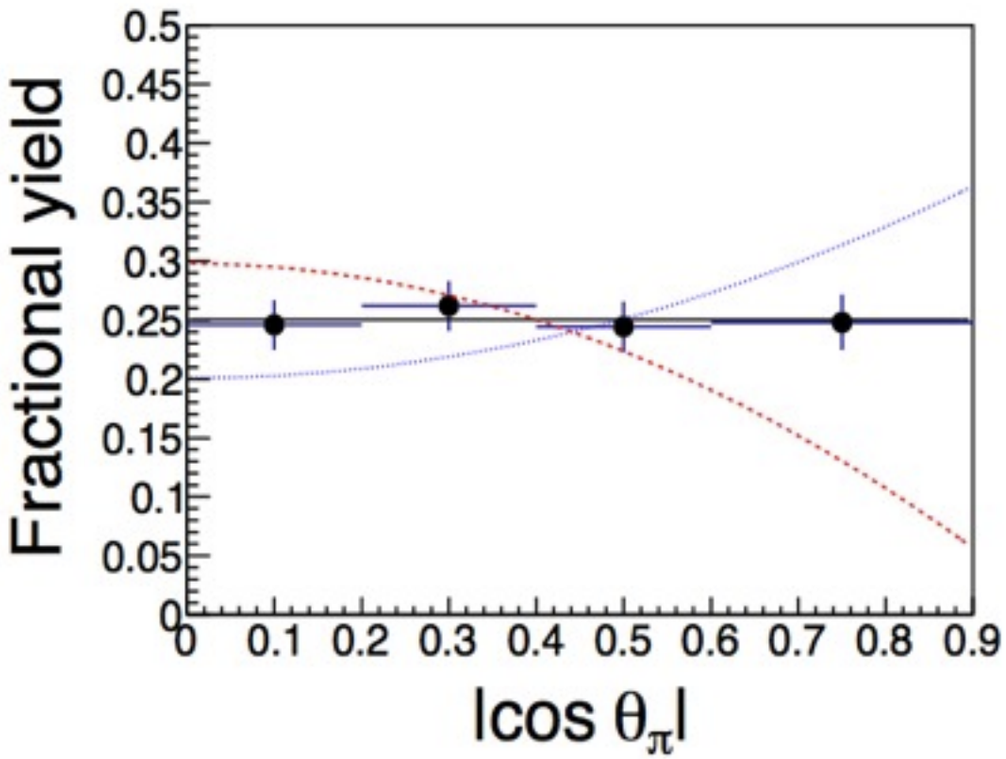

J^P of Zc(3900)$^{-/+}$

- **0^- : P-wave (J_z=1)--> $\sin^2\theta_\pi$**
- **0^+ : forbidden due to parity cons.**
- **1^- : P-wave --> $1+\cos^2\theta_\pi$**
- **1^+ : S/D-wave --> flat dist.**

- **What about coupling?**

Partial width of Zc(3900)$^{-/+}$

$$\frac{\Gamma(Z_c(3900) \to \bar{D}D^*)}{\Gamma(Z_c(3900) \to \pi J/\Psi)} \simeq 6.2$$

Zc(3900)$^{-/+}$ by BESIII analysis

- **$I^G J^P$=1^+1^+**
- **large coupling to $D^{bar}D^*$**
  --> consistent with small width
- **just above $D^{bar}D^*$ threshold**

S-wave $D^{bar}D^*$ molecule???

Zc(3900) : models

- **Tetraquark picture : diquark-antidiquark model** Maiani et al., PRD71 (2005).

  ➡ diquark mass is unknown (fixed to reproduce X(3872))

  ✓ M=3882 MeV, $J^P=1^+$ (S-wave $D^{bar}D^*$ channel)

$$\frac{\Gamma^{\mathrm{Model}}(Z_c(3882) \to \bar{D}D^*)}{\Gamma^{\mathrm{Model}}(Z_c(3882) \to \pi J/\Psi)} = \frac{4(\mathrm{MeV})}{29(\mathrm{MeV})}$$

Maiani et al., PRD87 (2013).

- **Molecule picture :**
  - πJ/Ψ + π-cloud M.B. Voloshin, PRD87 (2013) 9, 091501.
  - **Zc(3900) pole + $D^{bar}D^*$ cloud :** Wang et al., PRL111 (2013).

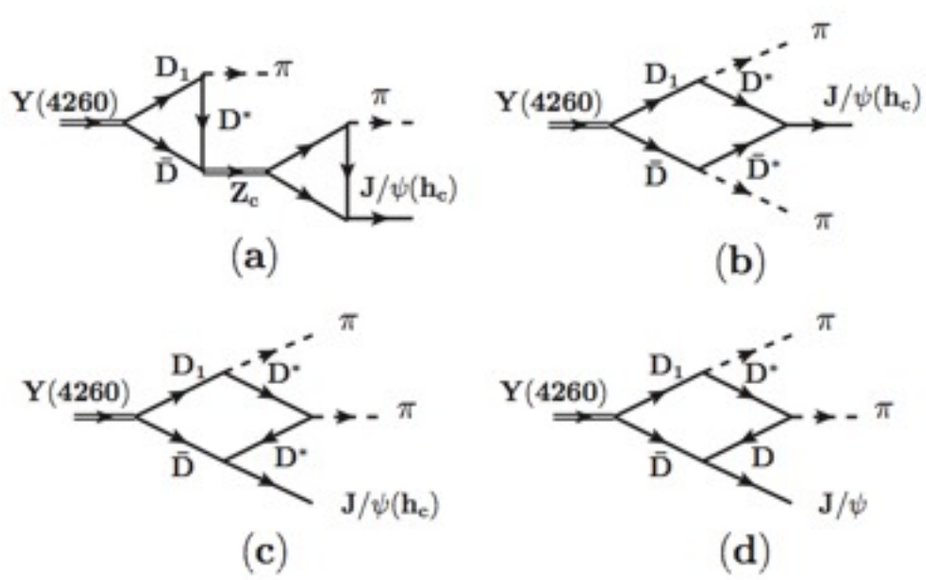

➡ Y(4260) is assumed to be bound state of $DD_1(2420)$

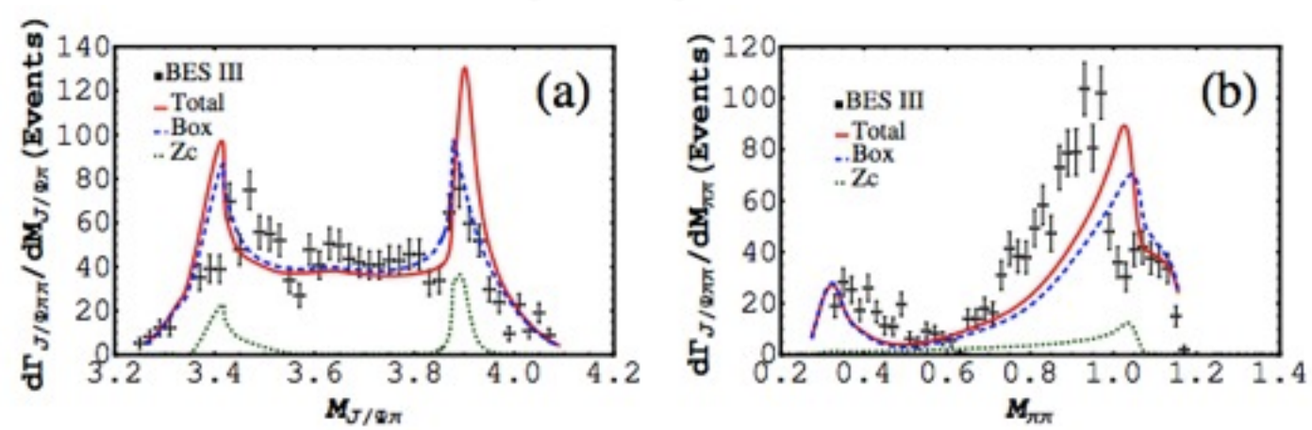

Zc(3900) : models for decay process

- **Zc(3900) pole + $D^{bar}D^*$ cloud :**

Wang et al., PRL111 (2013).

➡ **Y(4260) is assumed to be bound state of $DD_1(2420)$**

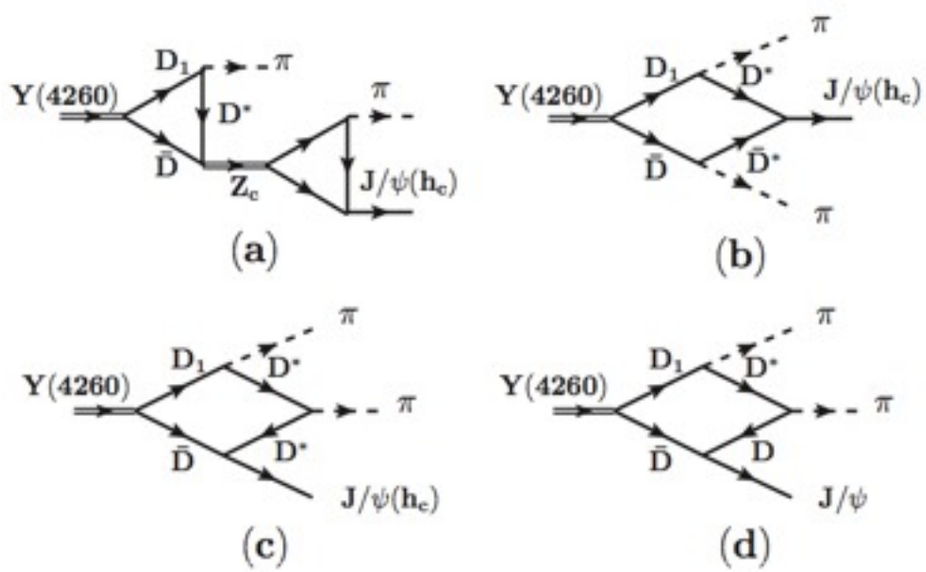

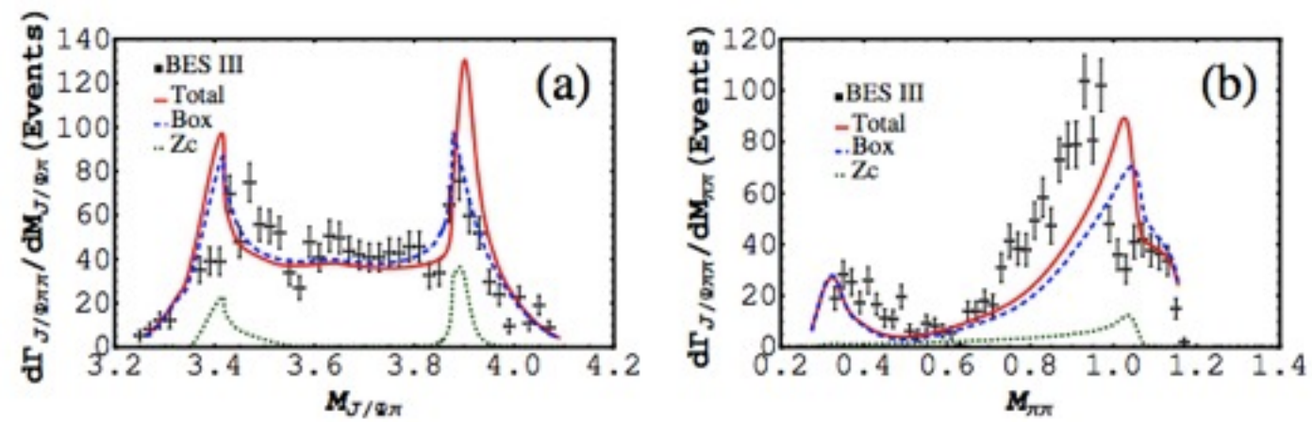

- **No Zc(3900) pole : initial-state pion exchange mechanism**

Chen-Liu-Matsuki, PRD88 (2013).

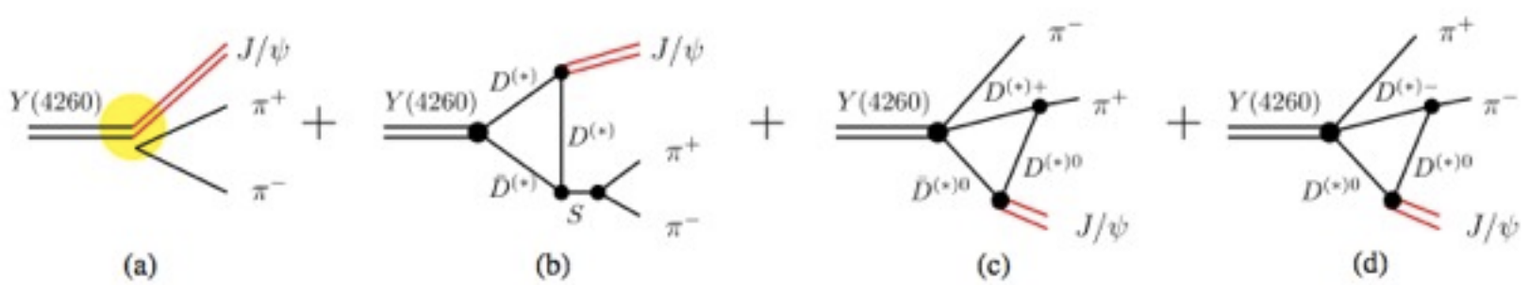

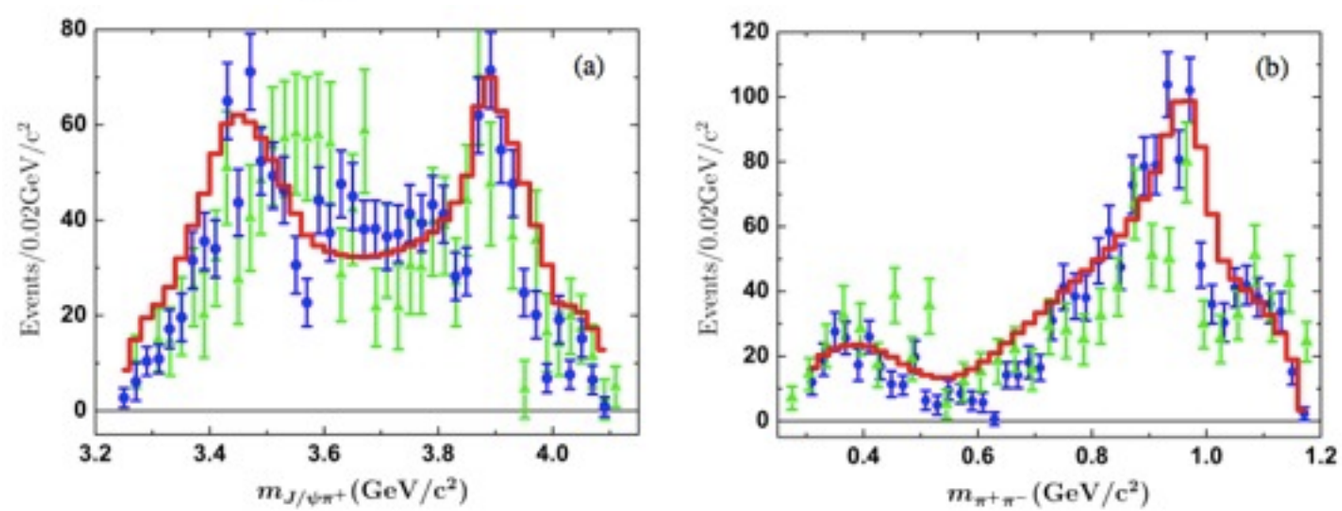

Perturbative matching for quasi-PDFs between continuum and lattice

Tomomi Ishikawa (RBRC)

tomomi@quark.phy.bnl.gov

Collaborators:
Jianwei Qiu (BNL)
Shinsuke Yoshida (RIKEN/BNL)

Multi-Hadron and Nonlocal Matrix Elements in Lattice QCD
RIKEN BNL Research Center Workshop
February 5-6, 2015 at Brookhaven National Laboratory

normal-PDFs v.s. quasi-PDFs

- normal-PDFs

$$q(x,\mu) = \int \frac{d\xi^-}{2\pi} e^{-ixP^+\xi^-} \langle \mathcal{N}(P)|O(\xi^-)|\mathcal{N}(P)\rangle,$$
$$O(\xi^-) = \overline{\psi}(\xi^-)\gamma^+ U_+(\xi^-,0)\psi(0)$$

- $\xi^\pm = (t \pm z)/\sqrt{2}$: light-cone coordinate
- Time-dependent. ⇨ It cannot be calculated on the lattice directly.

- quasi-PDFs [Ji (2013)]

$$\widetilde{q}(\tilde{x},\mu,P_z) = \int \frac{d\delta z}{2\pi} e^{-i\tilde{x}P_z\delta z} \langle \mathcal{N}(P_z)|\widetilde{O}(\delta z)|\mathcal{N}(P_z)\rangle,$$
$$\widetilde{O}(\delta z) = \overline{\psi}(\delta z)\gamma^z U_z(\delta z,0)\psi(0)$$

- P_z may not be infinite.
- Time-independent. It is computable on the lattice.

Lattice quasi-PDFs, so far

- Non-local matrix element

$$\langle \mathcal{N}(P_z)|O(\delta z)|\mathcal{N}(P_z)\rangle$$

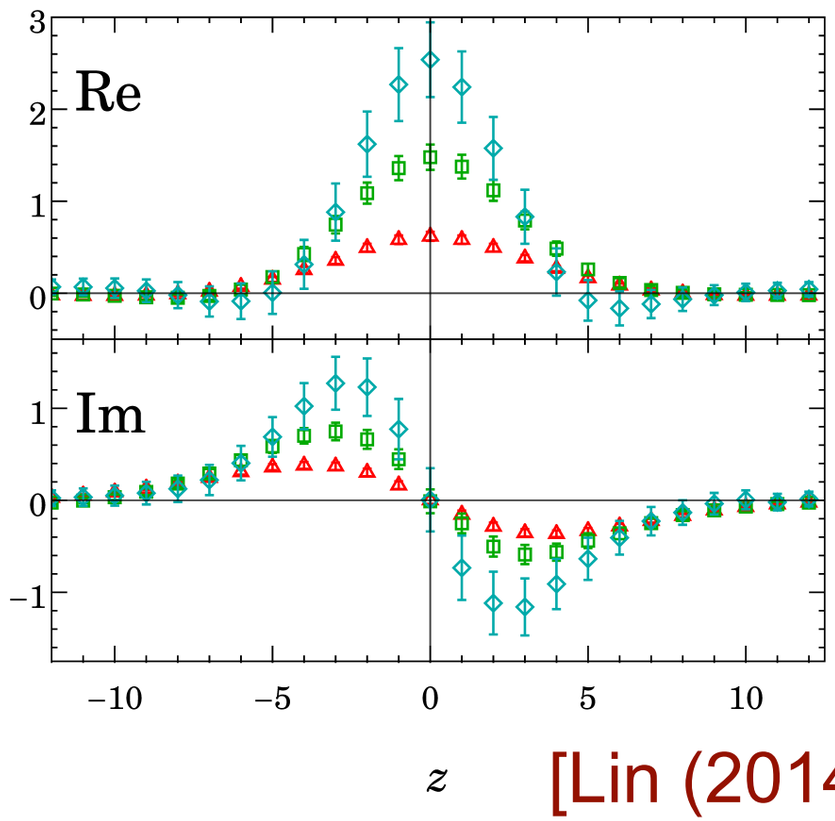

[Lin (2014)]

FIG. 1. The real (top) and imaginary (bottom) parts of the nonlocal isovector matrix element h of Eq. 3 computed on a lattice with the nucleon momentum P_z (in units of $2\pi/L$) = 1 (red triangles), 2 (green squares), 3 (cyan diamonds).

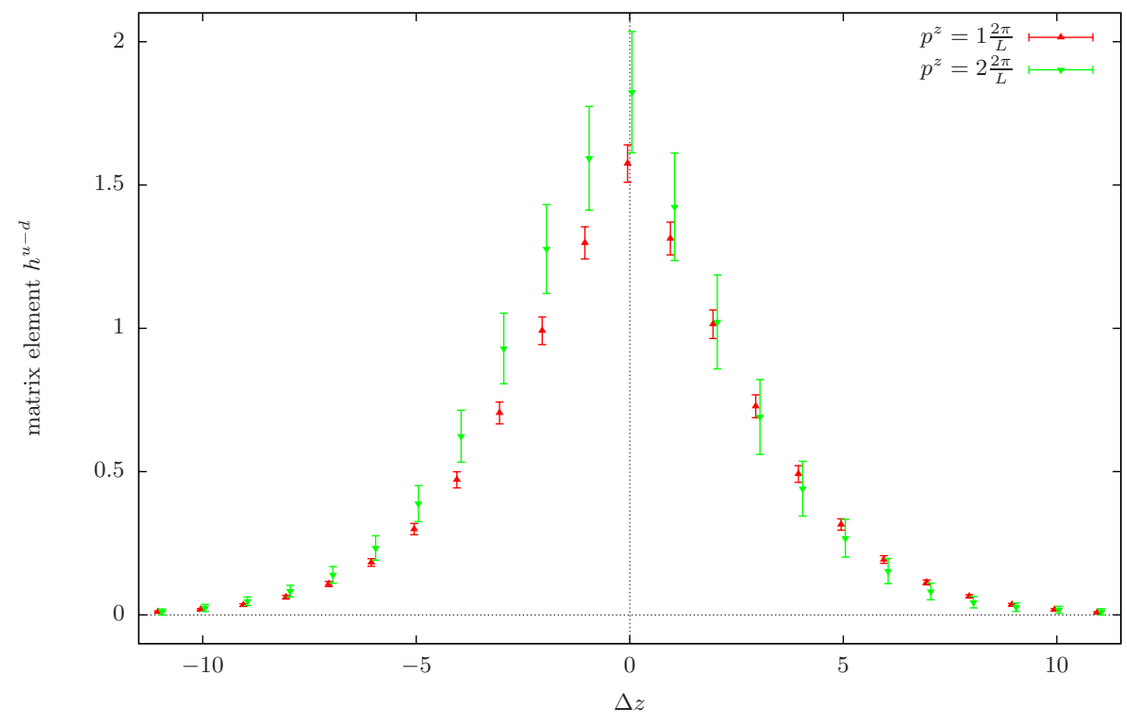

Figure 4: Real part of the matrix element for the first two momenta with 1000 measurements.

[Wiese (2014)]

Matching between continuum and lattice has not been implemented.

Matching overview

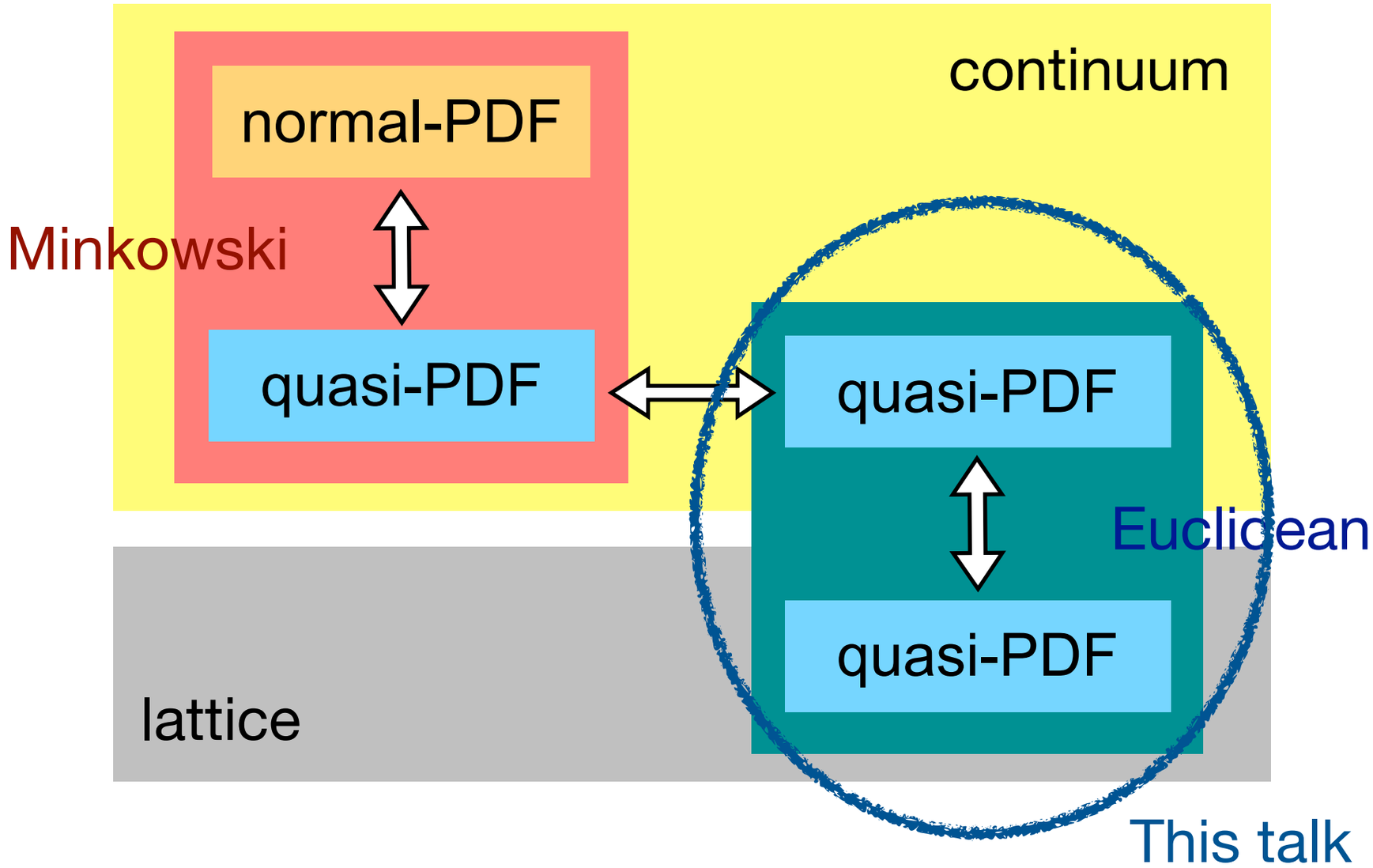

- Matching in continuum Minkowski space has been done.

[Ji (2013), Xiong et. al. (2013), Ma and Qiu (2014)]

- Minkowski and Euclidean space should be equivalent in quasi-PDF.

Momentum space v.s. Coordinate space

$$\widetilde{q}(\tilde{x},\mu,P_z) = \int \frac{d\delta z}{2\pi} e^{-i\tilde{x}P_z\delta z} \langle \mathcal{N}(P_z)|\widetilde{O}(\delta z)|\mathcal{N}(P_z)\rangle,$$
$$\widetilde{O}(\delta z) = \overline{\psi}(\delta z)\gamma^z U_z(\delta z, 0)\psi(0)$$

- Matching in momentum space

$$\widetilde{q}_{\rm cont}(\tilde{x},\mu,P_z) \quad \Longleftrightarrow \quad \widetilde{q}_{\rm latt}(\tilde{x},a^{-1},P_z)$$

  - z-component of the momentum is restricted to be P_z .
  - Loop-momentum becomes 3-dimensional.

- Matching in coordinate space

$$\widetilde{O}_{\rm cont}(\delta z) \quad \Longleftrightarrow \quad \widetilde{O}_{\rm latt}(\delta z)$$

  - There is no restriction on momenta.

Momentum space v.s. Coordinate space

- momentum space

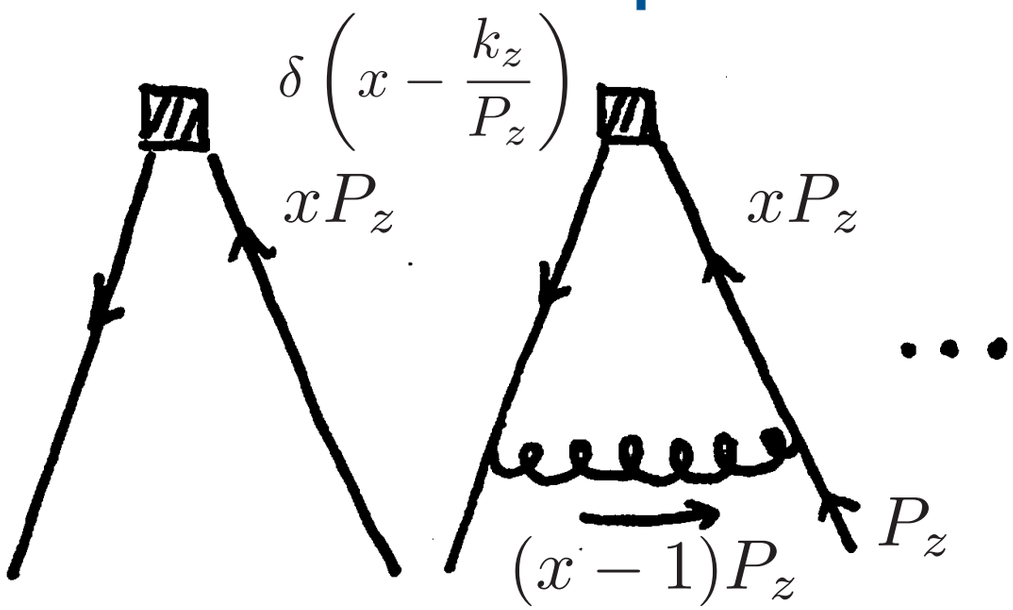

- z-component of the momentum is restricted to be xP_z .
- Loop-momentum becomes 3-dimensional.

Shinsuke Yoshida is working on this.

- coordinate space

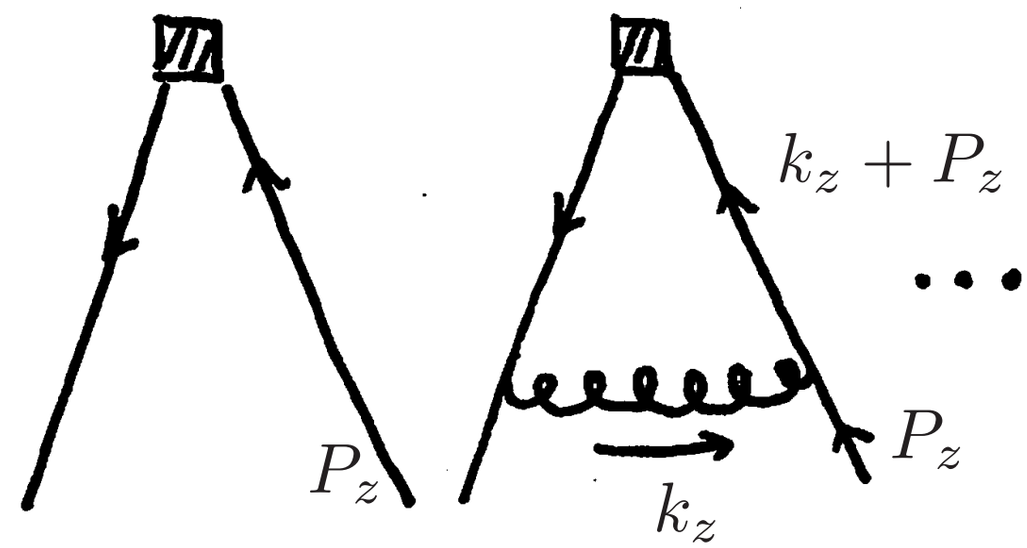

- No restriction on momentum.
- Loop-momentum is 4-dimensional.

This talk

Covariant gauge v.s. Axial gauge

$$\widetilde{O}(\delta z) = \overline{\psi}(\delta z)\gamma^z U_z(\delta z, 0)\psi(0)$$

- Axial gauge $A_z(x) = 0$

  - It looks convenient, because $U_z(\delta z, 0) = 1$

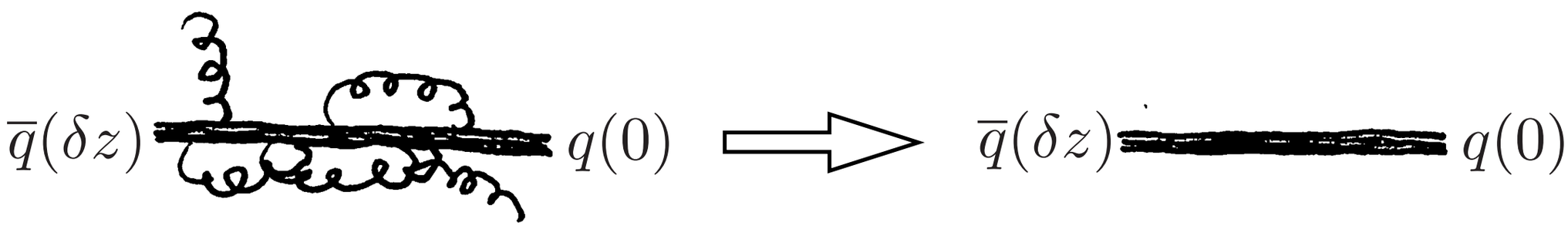

  - No free lunch, because gluon propagators introduce complication.

$$G_{\mu\nu}(k) = \frac{1}{k^2}\left(\delta_{\mu\nu} - \frac{\delta_{\mu,z}k_\nu + k_\mu\delta_{\nu,z}}{k_z} + \frac{k_\mu k_\nu}{k_z^2}\right).$$

  - Spurious pole exists. Pole prescription is required in many cases. $k_z \longrightarrow 0$

Feynman rules in covariant gauge

$$\widetilde{O}(\delta z) = \overline{\psi}(\delta z)\gamma^z U_z(\delta z, 0)\psi(0)$$

- Tree, one-gluon, two-gluon (at one-loop level)

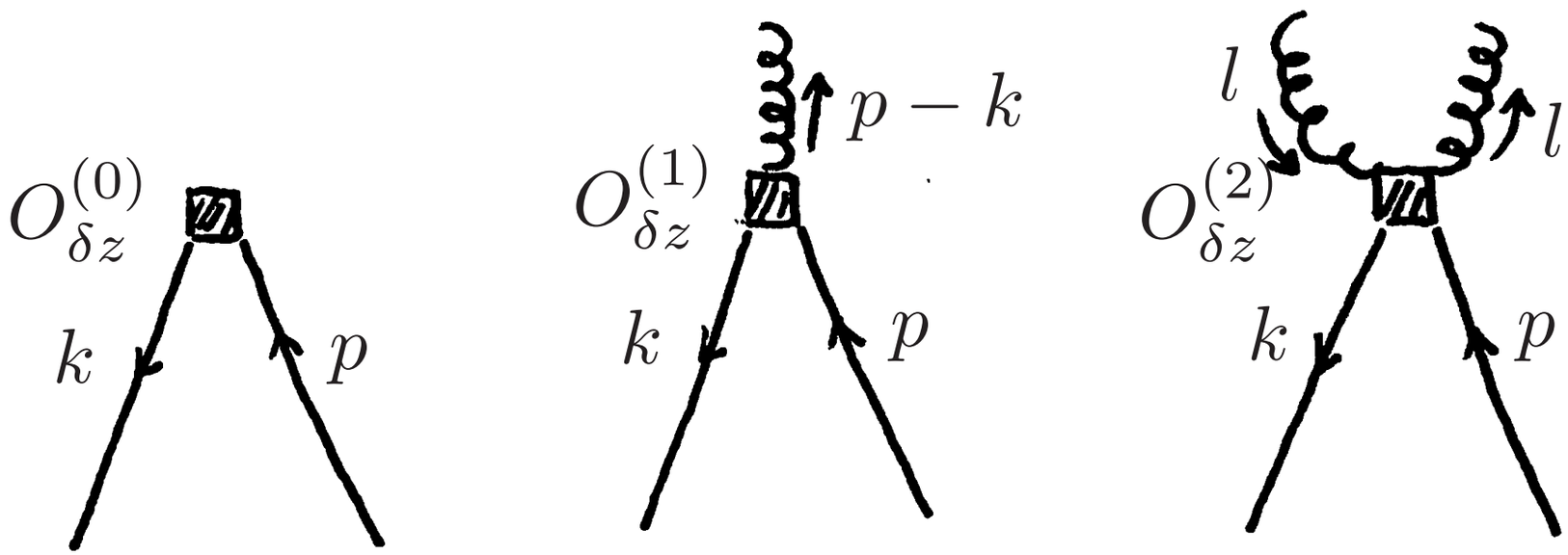

$$O^{(0)}_{\delta z}(p,k) = \gamma_z \delta(p-k) e^{-ip_z \delta z}$$

$$O^{(1)}_{\delta z}(p,k) = ig\gamma_z \frac{e^{-ip_z\delta z} - e^{-ik_z\delta z}}{i(p-k)_z}$$

There is no pole.

$$O^{(2)}_{\delta z}(p,k,l) = -g^2\gamma_z\delta(p-k)e^{-ip_z\delta z}\left(\frac{1-e^{il_z\delta z}}{l_z^2} - \frac{\delta z}{il_z}\right)$$

Diagrams at 1-loop

$\langle P|O(\delta z)|P\rangle_0 = e^{-iP_z\delta z}$

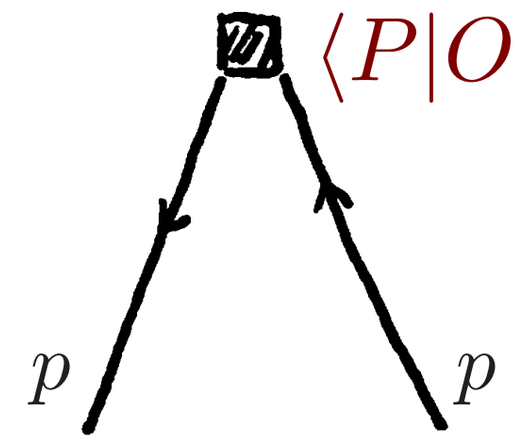

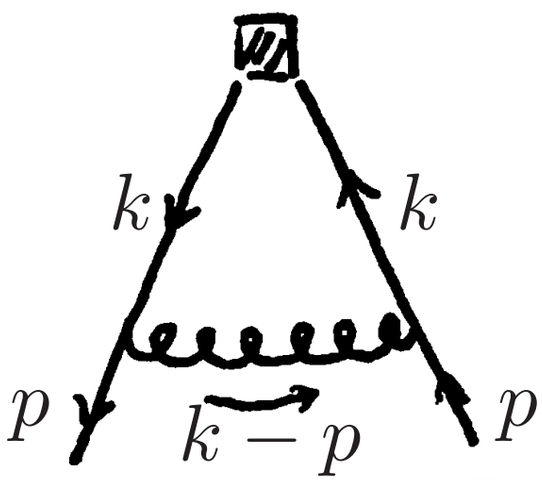

$\delta\Gamma_0(p)e^{-iP_z\delta z}$

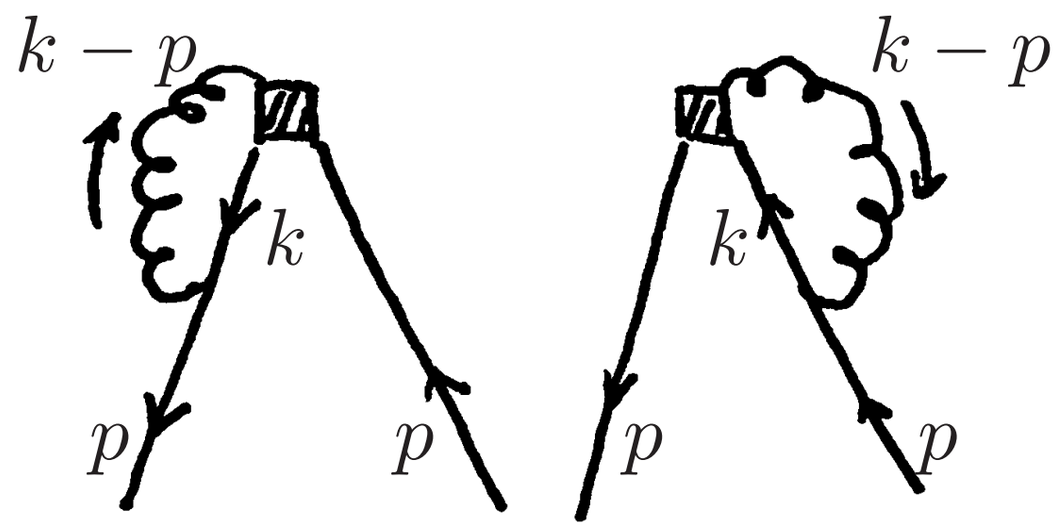

$\delta\Gamma_1(p)e^{-iP_z\delta z}$

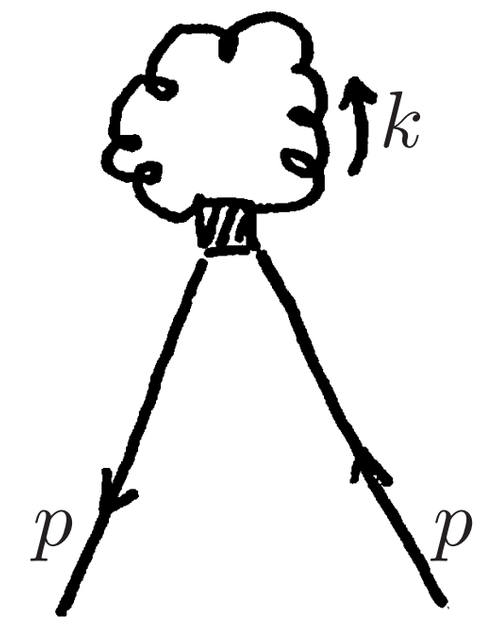

$\delta\Gamma_2 e^{-iP_z\delta z}$

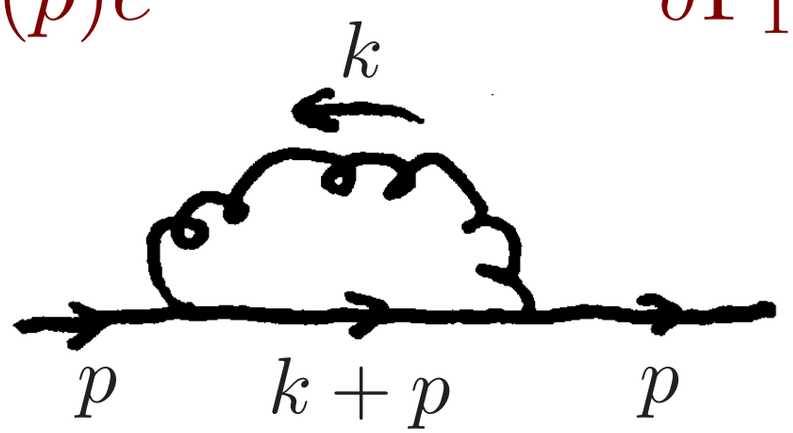

$\Sigma_{\mathrm{RS}}(p)$

$\Sigma_{\mathrm{TP}}(p)$ (only in lattice)

Momentum dependent v.s. independent

$$\langle P|\widetilde{O}(\delta z)|P\rangle_{\rm cont} = Z(\delta z, P)\langle P|\widetilde{O}(\delta z)|P\rangle_{\rm latt}$$

- Momentum dependence ?

- The difference of momentum dependence between continuum and lattice is related to UV-divergences in loop integral. $\int dk f(k,p)$

When the loop-integral involves UV-log divergence at most,

$$\int_{-\pi/a}^{\pi/a} dk \underbrace{\left[f^{\rm latt}(k,p+\Delta p) - f^{\rm latt}(k,p)\right]}_{\text{no UV-divergence}} \xrightarrow[a\to 0]{} \int_{-\infty}^{\infty} dk \left[f^{\rm cont}(k,p+\Delta p) - f^{\rm cont}(k,p)\right]$$

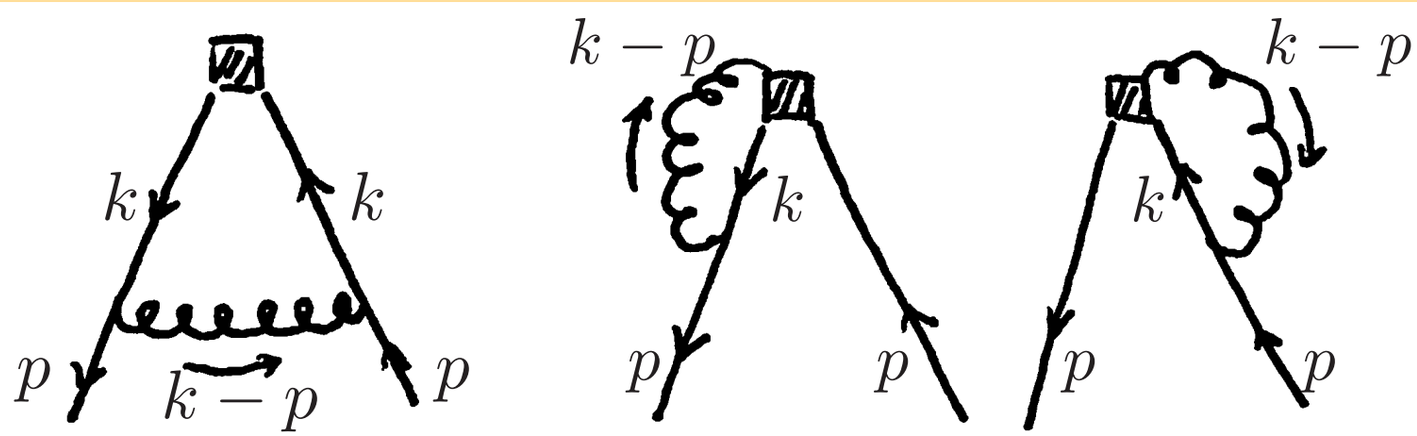

Common momentum dependence between continuum and lattice.

Momentum dependent v.s. independent

Momentum dependence

- $\delta\Gamma_2$ has UV-linear divergence, but external momentum is not involved in the loop integral.

continuum

$$\delta\Gamma_2 = -g^2 C_F \int_k \frac{1}{k^2}\left(\frac{1-e^{ik_z\delta z}}{k_z^2} - \frac{\delta z}{ik_z}\right)$$

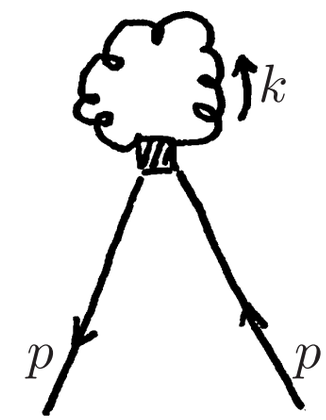

same as on the lattice

Common momentum dependence between continuum and lattice.

$$\delta\Gamma_0(p=0) \quad \delta\Gamma_1(p=0)$$

tree-level

$e^{-iP_z\delta z}$

$$\frac{\langle P|\widetilde{O}(\delta z)|P\rangle_{\rm cont}}{\langle P|\widetilde{O}(\delta z)|P\rangle_0} = 1 + g^2\mathcal{A}_{\rm cont}(\delta z) + g^2\mathcal{B}(\delta z, P)$$

$$\frac{\langle P|\widetilde{O}(\delta z)|P\rangle_{\rm latt}}{\langle P|\widetilde{O}(\delta z)|P\rangle_0} = 1 + g^2\mathcal{A}_{\rm latt}(\delta z) + g^2\mathcal{B}(\delta z, P)$$

common.
vanished
in the matching.

$$\langle P|\widetilde{O}(\delta z)|P\rangle_{\rm cont} = Z(\delta z, \cancel{P})\langle P|\widetilde{O}(\delta z)|P\rangle_{\rm latt}$$

1-loop in continuum

- Divergence structure (P=0)

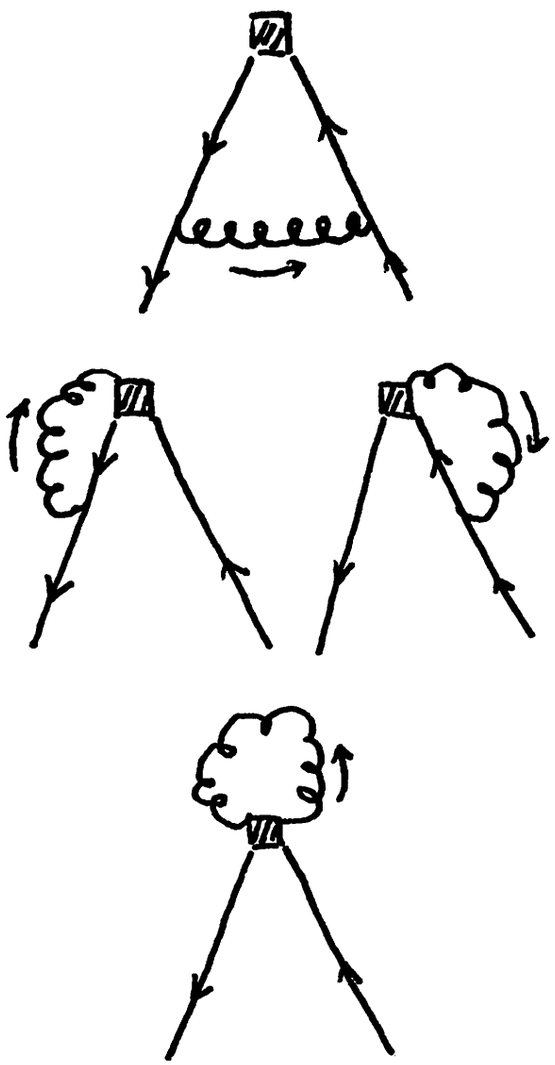

$$\delta\Gamma_0 = \frac{1}{8\pi^2}\left(\mathrm{Ei}(-k_\perp) - (2+k_\perp)e^{-k_\perp}\right)\Big|_{\lambda|\delta z|}^{\mu|\delta z|} \xrightarrow[\delta z\to 0]{} \frac{1}{8\pi^2}\ln\frac{\mu}{\lambda}$$

$$\delta\Gamma_1 = \frac{1}{4\pi^2}\left(\ln(k_\perp) - \mathrm{Ei}(-k_\perp) + e^{-k_\perp}\right)\Big|_{\lambda|\delta z|}^{\mu|\delta z|} \xrightarrow[\delta z\to 0]{} 0$$

$$\delta\Gamma_2 = \frac{1}{4\pi^2}\left(\ln(k_\perp) - \mathrm{Ei}(-k_\perp) - k_\perp\right)\Big|_{\lambda|\delta z|}^{\mu|\delta z|} \xrightarrow[\delta z\to 0]{} 0$$

Linear divergence

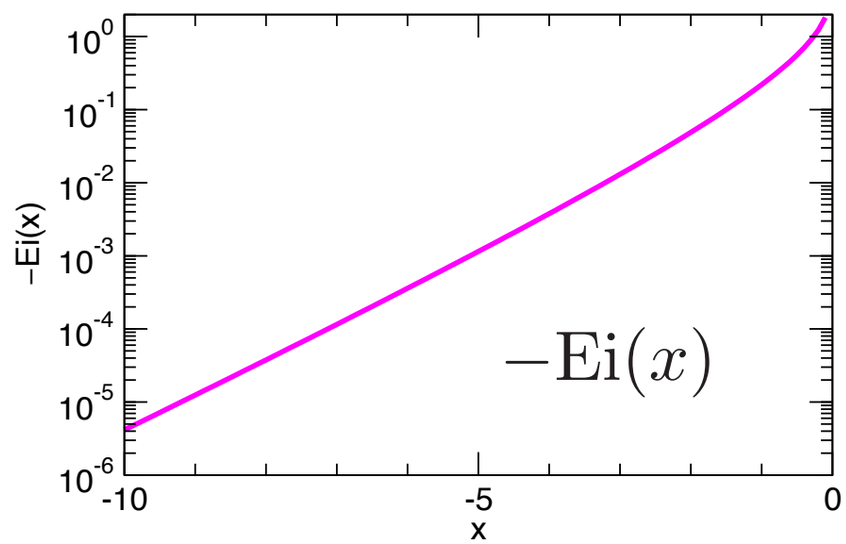

$$\mathrm{Ei}(x) = -\int_{-x}^{\infty} dt\,\frac{e^{-t}}{t}$$

: exponential integral

- Local case ($\delta z \to 0$) can be safely reproduced.
- Linear divergence from the tad-pole like diagram.
- UV(μ) and IR(λ) regulators are introduced in $\perp = (t, x, y)$ direction.

Back to the Axial gauge

- 1-loop correction

$$\delta\Gamma + \left.\frac{\partial\Sigma(p)}{\partial\,\not{p}}\right|_{p=0} = \underbrace{\begin{aligned}&+g^2C_F\int_k\frac{1}{k^4}\left(1-\frac{4k_z^2}{k^2}e^{-ik_z\delta z}\right)\\&-g^2C_F\int_k\frac{1}{k^2}\left(\frac{1-e^{ik_z\delta z}}{k_z^2}-\frac{\delta z}{ik_z}\right)\end{aligned}}_{\text{same as Feynman gauge}}\underbrace{+\,g^2C_F\int_k\frac{1}{k^2}\frac{\delta z}{ik_z}}_{\text{extra part}}$$

- The extra term includes a spurious pole.
- The spurious pole needs a prescription to be dealt with:

$$\int_k\frac{1}{k^2}\frac{1}{k_z}=\int_{k_\perp}\frac{1}{k_\perp^2}\int_{k_z}\frac{1}{k_z}.$$

$$\boxed{\frac{1}{k_z}\longrightarrow\frac{1}{2}\left(\frac{1}{k_z-i\epsilon}+\frac{1}{k_z+i\epsilon}\right)}$$

- Do not use axial gauge to avoid the pole prescription ambiguity.

1-loop matching

- 1-loop matching coefficients

  - UV cut-off is set to be $\mu = a^{-1}$.

  - Naive fermion is used.
  (not practical, but OK.)

$$\delta\Gamma_{\rm cont} - \delta\Gamma_{\rm latt} \equiv \frac{g^2}{16\pi^2} C_F \gamma_z \delta\gamma$$

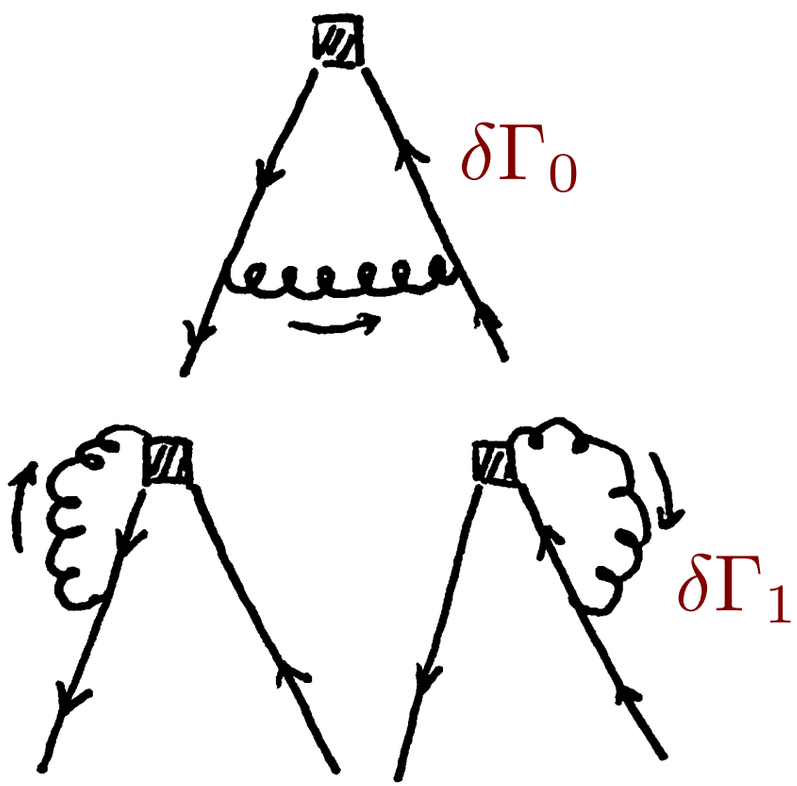

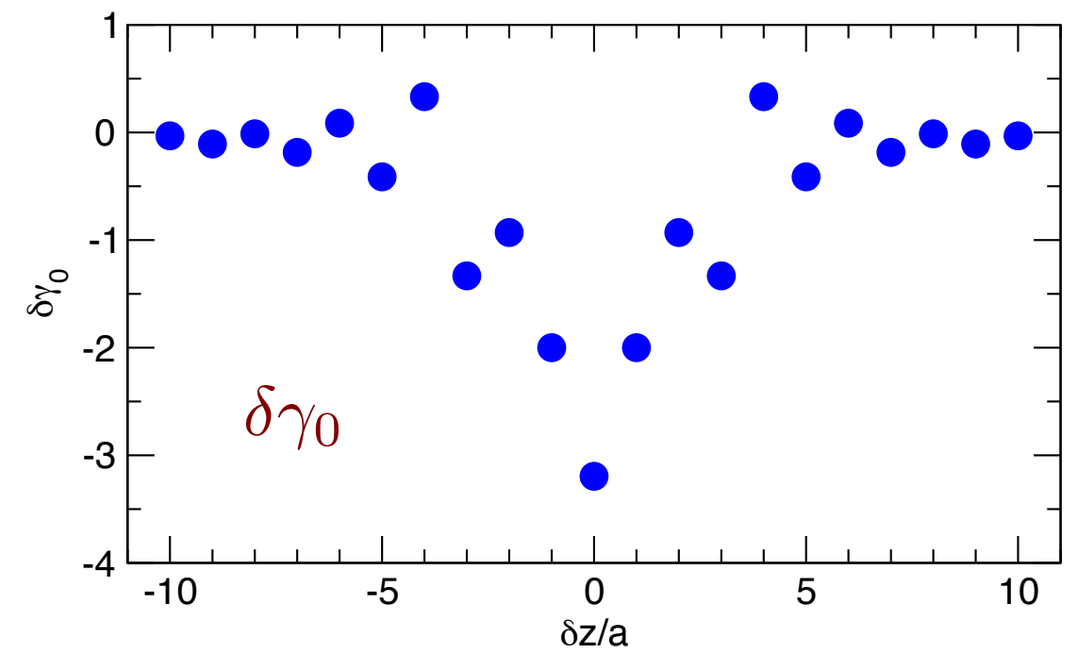

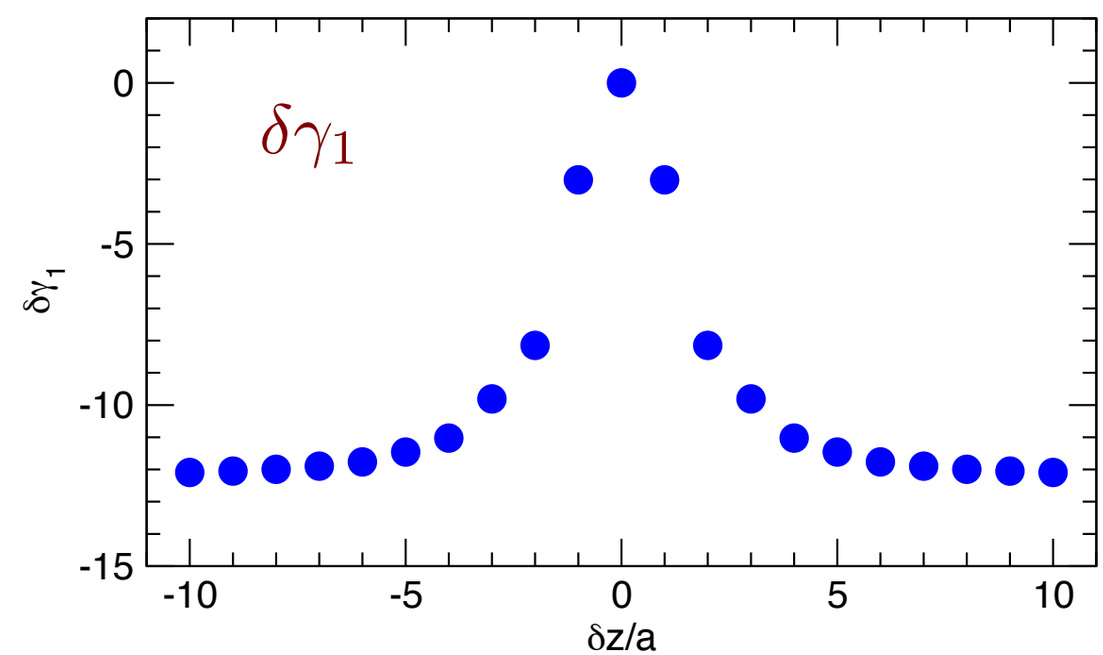

1-loop matching

- 1-loop matching coefficients

$$\delta\Gamma_{\rm cont} - \delta\Gamma_{\rm latt} \equiv \frac{g^2}{16\pi^2} C_F \gamma_z \delta\gamma$$

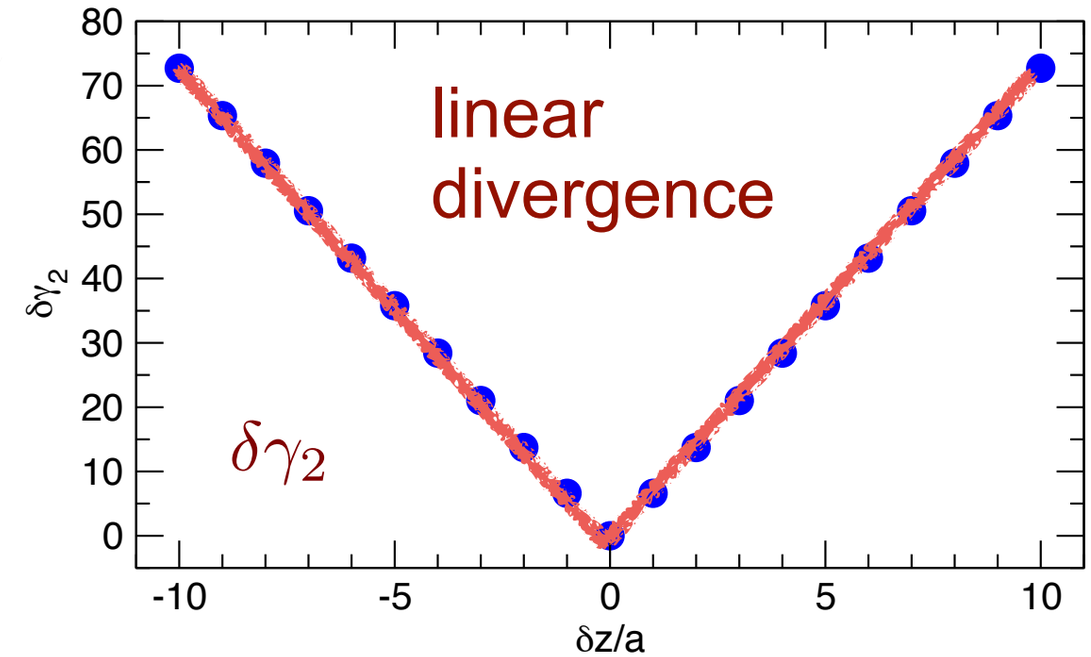

- There is a mismatch in linear divergence between continuum and lattice.
- The linear divergence should be subtracted, otherwise the continuum limit cannot be taken.

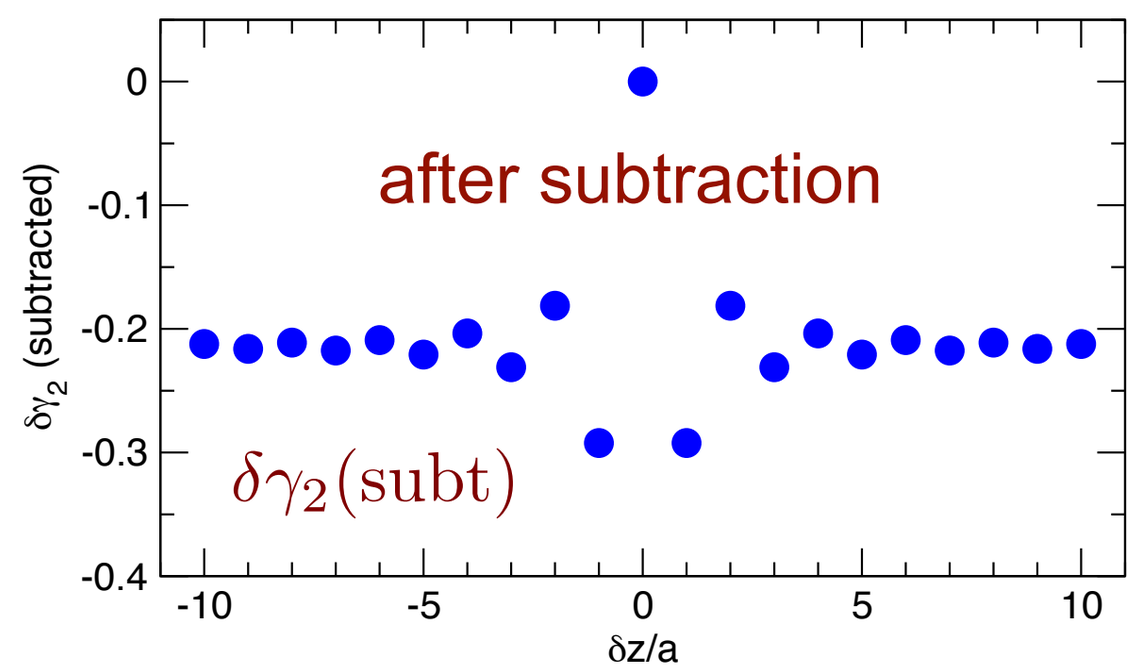

1-loop matching

- 1-loop matching coefficients

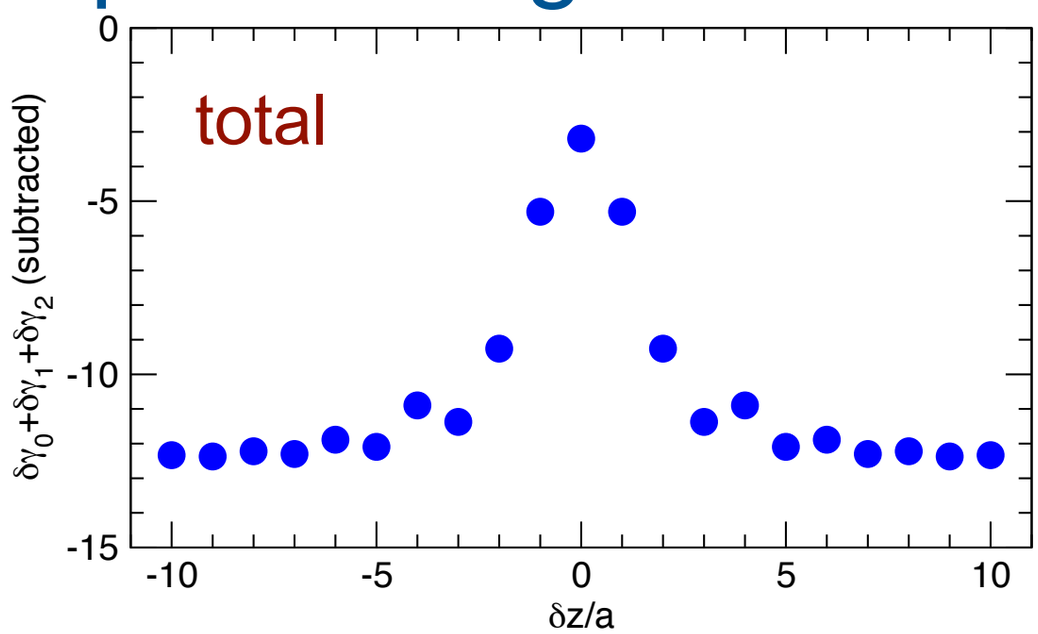

$$\delta\Gamma_{\rm cont} - \delta\Gamma_{\rm latt} \equiv \frac{g^2}{16\pi^2} C_F \gamma_z \delta\gamma$$

Wave function part is not included.
(It is the same as usual local operator case.)

- Comments

- MF-improvement should be used in the actual matching factor.
- Other lattice actions and link smearings can be easily implemented.
- In the Large Momentum Effective Theory (Ji's context), non-perturbative subtraction of the linear divergence would be required, once $O(1/P_z^2)$ correction is included.
(Mixing with lower dimensional operators cannot be treated perturbatively.)

Summary and outlook

- 1-loop perturbative matching factor of quasi-PDFs between continuum and lattice is discussed.
- Matching method in coordinate space is applied in this talk.
- When axial gauge is used, there is a prescription ambiguity to deal with a spurious pole.
- External momentum dependence is common between continuum and lattice, which results in momentum independent matching factor.
- Linear divergent behavior can be seen. This linear divergent should be subtracted, otherwise continuum limit cannot be taken.
- We are preparing numerical simulations of the quasi-PDFs.

$K \to \pi\pi$ decay amplitudes from improved Wilson fermion

at BNL 2015/02/05

N. Ishizuka , K.I. Ishikawa, A. Ukawa, T. Yoshie

We present our results of $K \to \pi\pi$ decay amplitudes for both $\Delta I = 1/2$ and $3/2$.

- $N_f = 2+1$ improved Wilson fermion

  $a = 0.091\,\mathrm{fm}$, $La = 2.91\mathrm{fm}$

  $m_\pi = 280\mathrm{MeV}$ ($m_K \sim 2 \times m_\pi$)

  Decay process : $K(\mathbf{0}) \to \pi(\mathbf{0})\pi(\mathbf{0})$

1. Introduction

Long-standing problems of the Lattice QCD
in the neutral K meson system :

- Understanding $\Delta I = 1/2$ rule
- Calculation of ϵ'/ϵ from SM. → Precise verification of SM . Possibility of the beyond SM.

We need calculates two decay amplitudes :

$$A_I = \langle K|H|\pi\pi; I\rangle \quad (I = 0, 2)$$

issues :

(1) relation between the amplitude on the lattice (Euclid)
and that in the continuum (Minkowski).

: solved by Lellouch and Lüscher

Lellouch and Lüscher, Math.Phys.219(2001)31.

(2) large fluctuation from the dis-connected diagram.

Calculations has been unsuccessful for a long time.

First calculation of the K decay amplitudes decay for $\Delta I = 1/2$:

RBC-UKQCD

$N_f = 2+1$ Domain wall fermion , $a = 0.114\,\mathrm{fm}$

- $m_\pi = 422\,\mathrm{MeV}$, $La = 1.8\,\mathrm{fm}$ PRD84(2011)114503
- $m_\pi = 330\,\mathrm{MeV}$, $La = 2.7\,\mathrm{fm}$ LAT2011 [arXiv:1110.2143]

For the Wilson fermion, operator renormalization for parity odd part of $\Delta S = 1$ op. :

$$Q_i^{\overline{\mathrm{MS}}}(\mu) = \sum_j Z_{ij}(\mu)\,\overline{Q}_j^{\mathrm{Lat}} \quad (i, j = 1, 2, \cdots 10)$$

$$\overline{Q}_j^{\mathrm{Lat}} = Q_j - \alpha_j P \ , \ \underline{P = \bar{s}\gamma_5 d}$$

P does not give finite contributions in the continuum.
This is not true for the Wilson fermion.

$Z_{ij}(\mu)$: same form as for the chiral sym. preserved case

(from *CPS* symmetry)

The calculation of the amplitudes is also possible with Wilson fermion,
if we subtract the lower dimensional operator with a renormalization condition :

$$\alpha_j = \langle 0|Q_j|K\rangle / \langle 0|P|K\rangle$$

Calculation cost : Wilson fermion << Domain wall fermion

Statistical improvement is expected by using Wilson fermion.

2. Method

Parameter

$N_f = 2+1$ improved Wilson fermion + Iwasaki gauge action

$32^3 \times 64$, $a = 0.091\,\mathrm{fm}$, $La = 2.91\mathrm{fm}$

$m_\pi = 275.7(15)\,\mathrm{MeV}$, $m_K = 579.8(13)\,\mathrm{MeV}$

$m_K \sim 2 \times m_\pi \quad (m_K - 2 \cdot m_\pi = 28.3\,\mathrm{MeV})$

Decay process : $K(\mathbf{0}) \to \pi(\mathbf{0})\pi(\mathbf{0})$

Configurations :

PACS-CS (original) : 2,000 MD step

New : 10,000 MD step

# of conf. = 480 (every 25 MD step)

Our preliminary results
have been presented at Lat2013 and Lat2014.

arXiv:1311.0958, arXiv:1410.8237.

Time correlation function

$$G^I(Q_i)(t) = \frac{1}{T}\sum_{\delta=0}^{T-1} \langle 0|\, W_K(t_K+\delta)\, \overline{Q}_i(t+\delta)\, W^I_{\pi\pi}(t_\pi+\delta)\, |0\rangle$$

(: periodic BC. in time)

$$t_K = 24\ ,\ t_\pi = 0\ ,\ t = \mathrm{run}$$

$$\overline{Q}_i = Q_i - \alpha_i P$$

$$P = \bar{s}\gamma_5 d$$

$$\alpha_i = \langle 0|Q_i|K\rangle / \langle 0|P|K\rangle$$

$W_K(t)\,,\, W^I_{\pi\pi}(t)$: Wall source for K and $\pi\pi$ with the iso-spoin I

(: used with Coulomb gauge fixing at time slice of the wall sources)

Note our convention : $K^0 = -\bar{s}\gamma_5 d$

Calculation of quark loop at weak operators

Quark contractions :

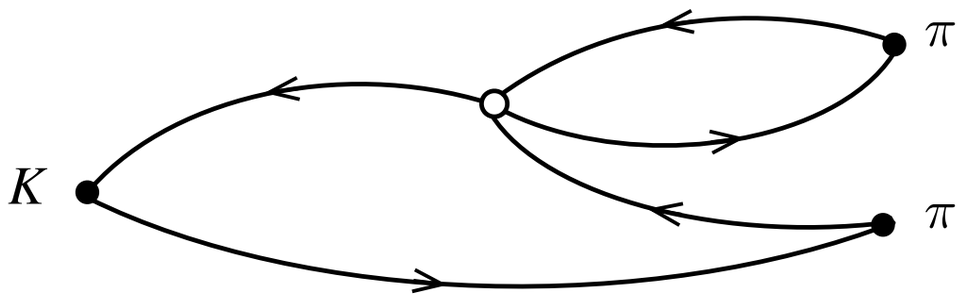

type1

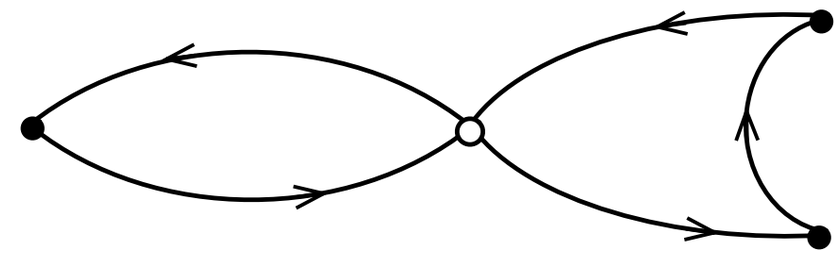

type2

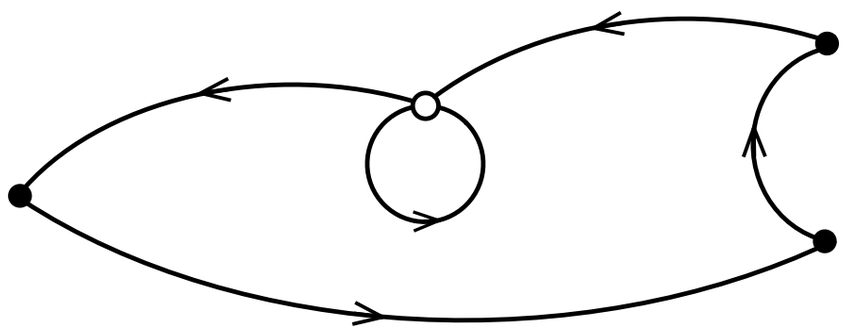

type3

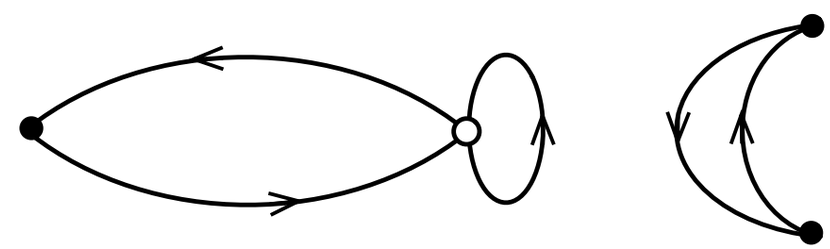

type4

Calculation of Quark loop :

Stochastic method

+ Hopping parameter expansion technique (HPE)

+ Truncated solver method (TSM)

(G.S.Bali et.al, Comp.Phys.Comm. 181(2010)1570.)

Hopping parameter expansion technique (HPE)

Wilson fermion :

$$S^W = \bar{\psi}\, W\, \psi = \bar{\psi}\,(M - D)\,\psi = \bar{\psi}\, M(1 - \overline{D})\,\psi \qquad \left(\overline{D} = M^{-1} D \right)$$

$$(M\psi)(x) = [\,1 - \kappa C_{SW}(\sigma \cdot F(x))/2\,]\,\psi(x)$$

$$(D\psi)(x) = \kappa \sum_{\mu} \left[\, (1-\gamma_\mu) U_\mu(x)\psi(x+\mu) \,+\, (1+\gamma_\mu) U_\mu^\dagger(x-\mu)\psi(x-\mu) \,\right]$$

Quark propagator :

$$Q = W^{-1} = (1-\overline{D})^{-1} M^{-1} = \sum_{n=0}^{\infty} \overline{D}^{\,n} M^{-1} = \sum_{n=0}^{k-1} \overline{D}^{\,n} M^{-1} + \overline{D}^{\,k} W^{-1} \qquad (\text{ for any } k\ )$$

$$= M^{-1} + \overline{D} M^{-1} + \overline{D}^{\,2} M^{-1} + \overline{D}^{\,3} M^{-1} + \overline{D}^{\,4} W^{-1} \qquad (\text{ for } k = 4\ )$$

Quark loop :

$$Q(x,x) = \left[\, M^{-1} + \cancel{\overline{D} M^{-1}} + \overline{D}^{\,2} M^{-1} + \cancel{\overline{D}^{\,3} M^{-1}} + \overline{D}^{\,4} W^{-1} \right] (x,x)$$

$$= \left[\, M^{-1} + \overline{D}^{\,2} M^{-1} + \overline{D}^{\,4} W^{-1} \right] (x,x)$$

Calculation of the quark loop by the stochastic method

$$Q(\mathbf{x},t;\mathbf{x},t) = \frac{1}{N_R} \sum_{i=1}^{N_R} \xi_i^*(\mathbf{x},t)\, S_i(\mathbf{x},t) \qquad \left(\delta^3(\mathbf{x}-\mathbf{y}) = \lim_{N_R \to \infty} \frac{1}{N_R} \sum_{i=1}^{N_R} \xi_i^*(\mathbf{x},t)\, \xi_i(\mathbf{y},t) \right)$$

$$S_i(\mathbf{x},t) = \sum_{\mathbf{y}} \left[\, M^{-1} + \overline{D}^{\,2} M^{-1} + \overline{D}^{\,4} W^{-1} \right] (\mathbf{x},t;\mathbf{y},t)\ \xi_i(\mathbf{y},t)$$

Truncated solver method (TSM)

$$Q(\mathbf{x},t;\mathbf{x},t) = \frac{1}{N_R}\sum_{i=1}^{N_R} \xi_i^*(\mathbf{x},t)\ \left[S_i(\mathbf{x},t) - S_i^T(\mathbf{x},t)\right] + \frac{1}{N_T}\sum_{i=N_R+1}^{N_T+N_R} \xi_i^*(\mathbf{x},t)\, S_i^T(\mathbf{x},t)$$

$$S_i(\mathbf{x},t) = \sum_{\mathbf{y}} \left[\ M^{-1} + \overline{D}^{\,2} M^{-1} + \overline{D}^{\,4} W^{-1}\right](\mathbf{x},t;\mathbf{y},t)\ \xi_i(\mathbf{y},t)$$

$S_i^T(\mathbf{x},t)$: with W^{-1} calculated with a loose stopping condition

$N_R = 1$ tor. $< 10^{-14}$ (tor. $= |WW^{-1} - \xi|/|\xi|$)

$N_T = 5$ tor. $< 1.2 \times 10^{-6}$

2. Results

Effect of TSM

$$Q(\mathbf{x},t;\mathbf{x},t) = \frac{1}{N_R}\sum_{i=1}^{N_R} \xi_i^*(\mathbf{x},t)\ \left[S_i(\mathbf{x},t) - S_i^T(\mathbf{x},t)\right] + \frac{1}{N_T}\sum_{i=N_R+1}^{N_T+N_R} \xi_i^*(\mathbf{x},t)\, S_i^T(\mathbf{x},t)$$

$$(\ N_R = 1\ ,\ N_T = 5\ )$$

$$S_i(\mathbf{x},t) = \sum_{\mathbf{y}} \left[\ M^{-1} + \overline{D}^{\,2} M^{-1} + \overline{D}^{\,4} W^{-1}\right](\mathbf{x},t;\mathbf{y},t)\ \xi_i(\mathbf{y},t)$$

$G^{I=0}(Q_2)$ at $t = 9$

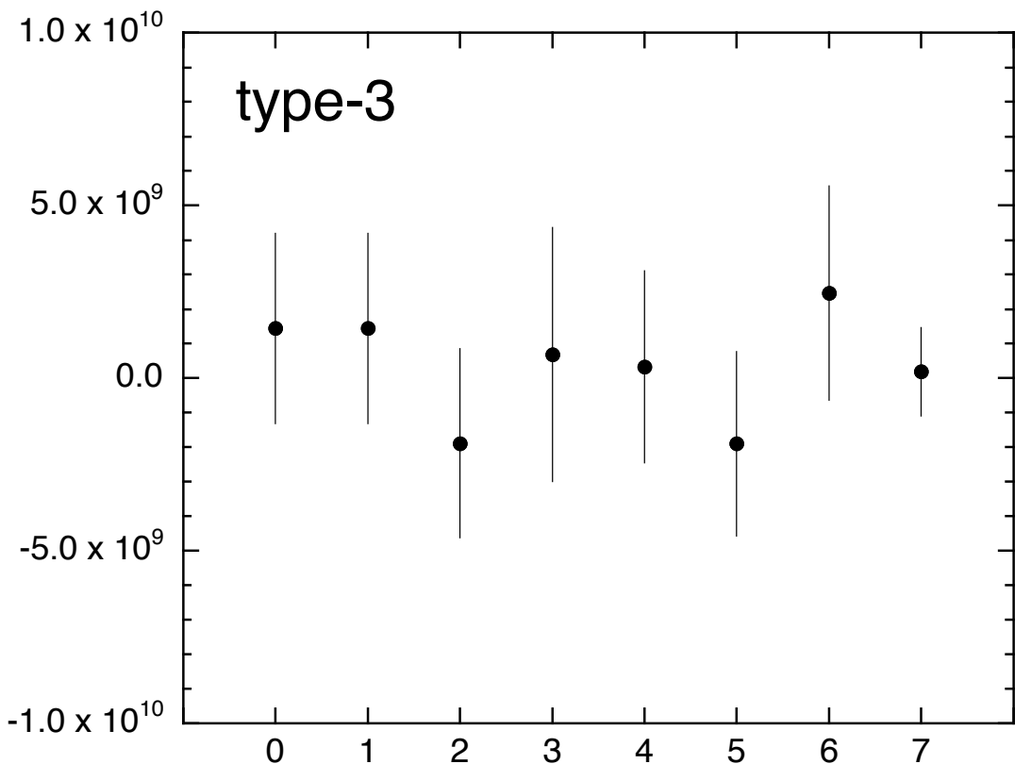

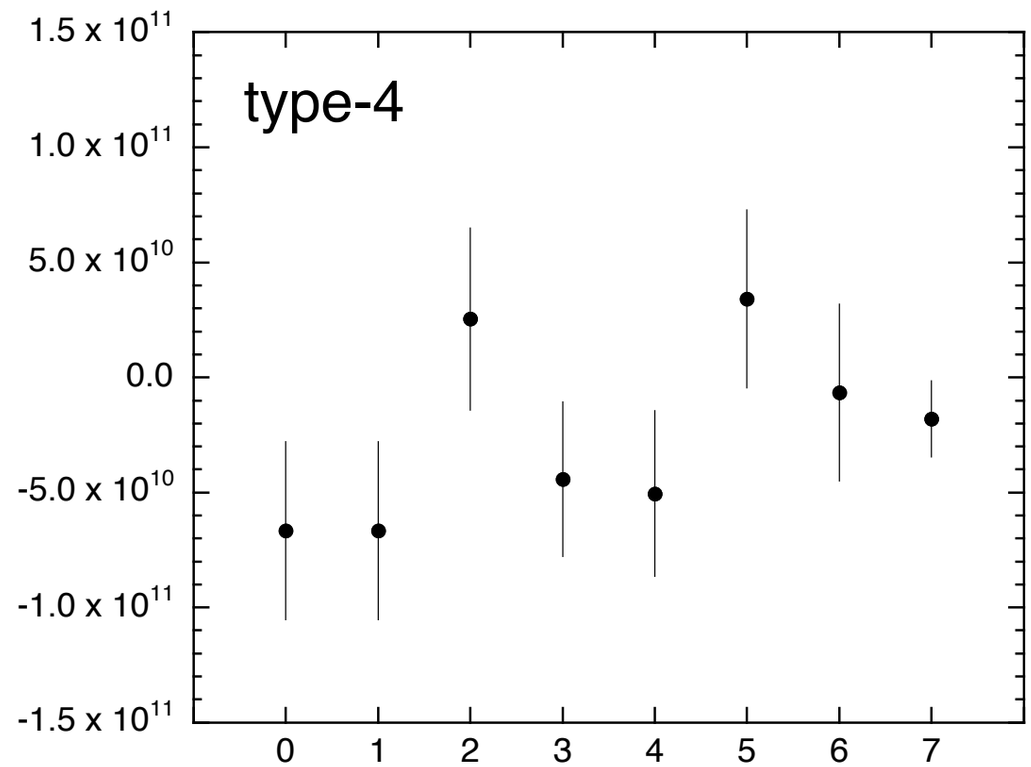

$$x = 0\ :\quad Q(\mathbf{x},t;\mathbf{x},t) = \xi_i^*(\mathbf{x},t) S_i(\mathbf{x},t) \qquad \text{for } i = 1$$

$$x = 1\ :\quad Q(\mathbf{x},t;\mathbf{x},t) = \xi_i^*(\mathbf{x},t) S_i^T(\mathbf{x},t) \qquad \text{for } i = 1$$

$$x = 2\cdots 6\ :\quad Q(\mathbf{x},t;\mathbf{x},t) = \xi_i^*(\mathbf{x},t) S_i^T(\mathbf{x},t) \qquad \text{for } i = 2\cdots 6$$

$$x = 7\ :\quad Q(\mathbf{x},t;\mathbf{x},t) = \frac{1}{6}\sum_{i=1}^{6} \xi_i^*(\mathbf{x},t) S_i^T(\mathbf{x},t)$$

$G^{I=0}(Q_6)$ at $t = 9$

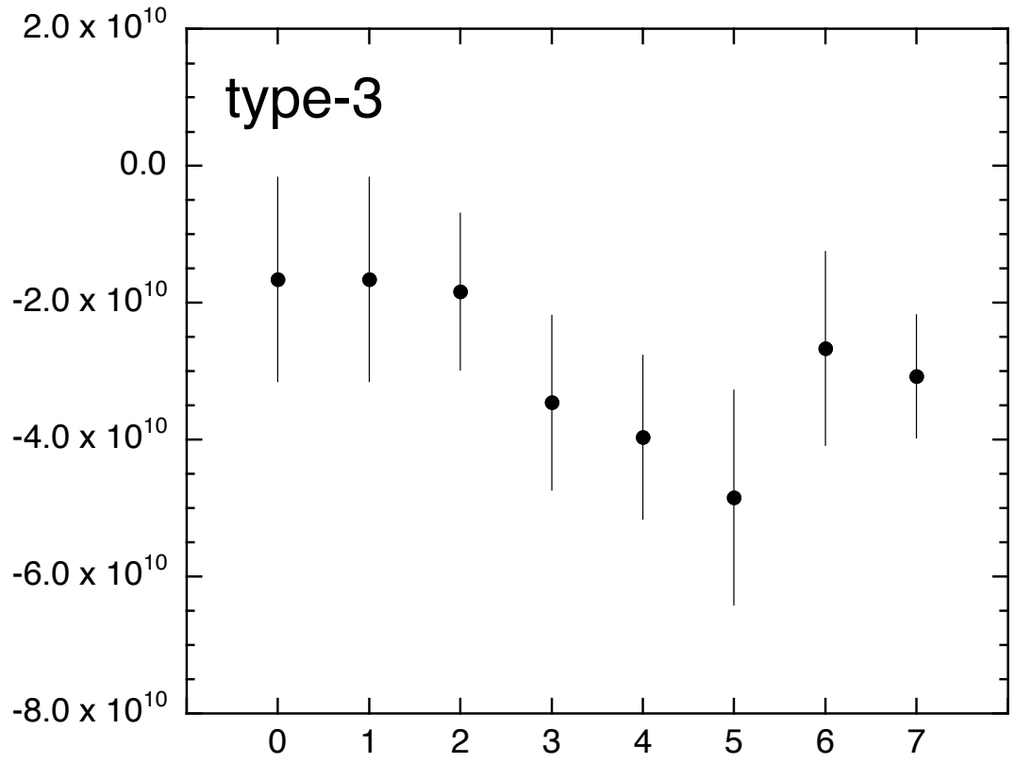

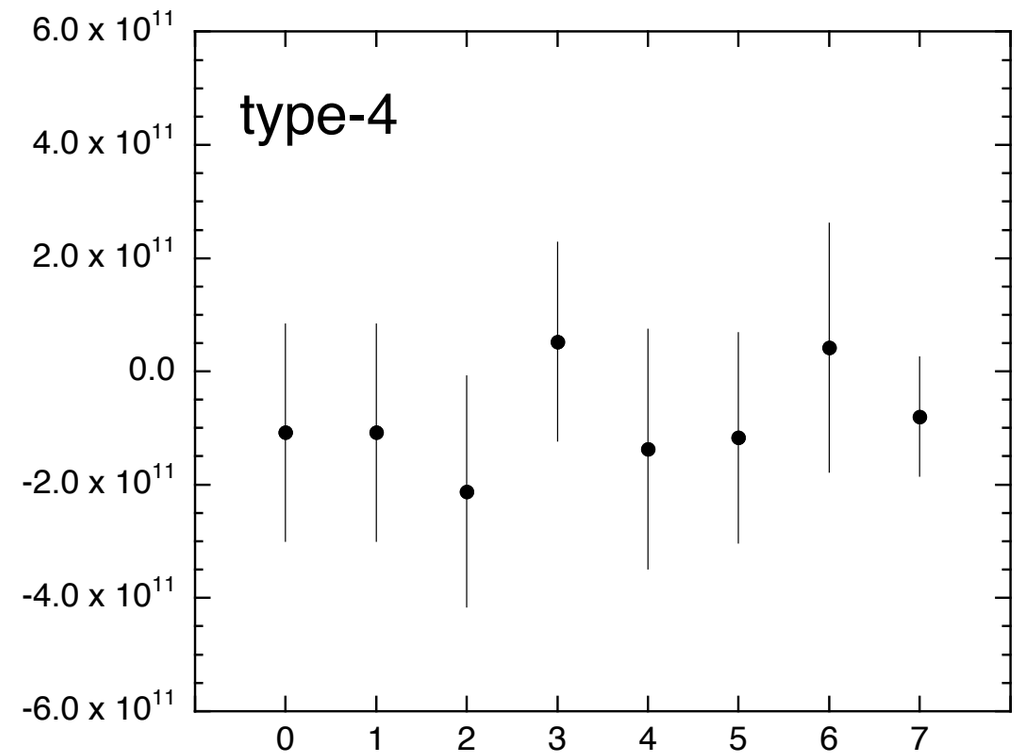

$$
\begin{aligned}
x = 0 \;&:\quad Q(\mathbf{x},t;\mathbf{x},t) = \xi_i^*(\mathbf{x},t) S_i(\mathbf{x},t) \qquad \text{for } i = 1 \\
x = 1 \;&:\quad Q(\mathbf{x},t;\mathbf{x},t) = \xi_i^*(\mathbf{x},t) S_i^T(\mathbf{x},t) \qquad \text{for } i = 1 \\
x = 2\cdots 6 \;&:\quad Q(\mathbf{x},t;\mathbf{x},t) = \xi_i^*(\mathbf{x},t) S_i^T(\mathbf{x},t) \qquad \text{for } i = 2\cdots 6 \\
x = 7 \;&:\quad Q(\mathbf{x},t;\mathbf{x},t) = \frac{1}{6}\sum_{i=1}^{6} \xi_i^*(\mathbf{x},t) S_i^T(\mathbf{x},t)
\end{aligned}
$$

The correction terms are negligible.

We use x=7 for calculations of the decay amplitudes.

$G^{I=0}(Q_2)$ from type-3 and type-4 $(\, t_K = 24\,,\, t_\pi = 0\,,\, Q(t) : \mathrm{run}\,)$

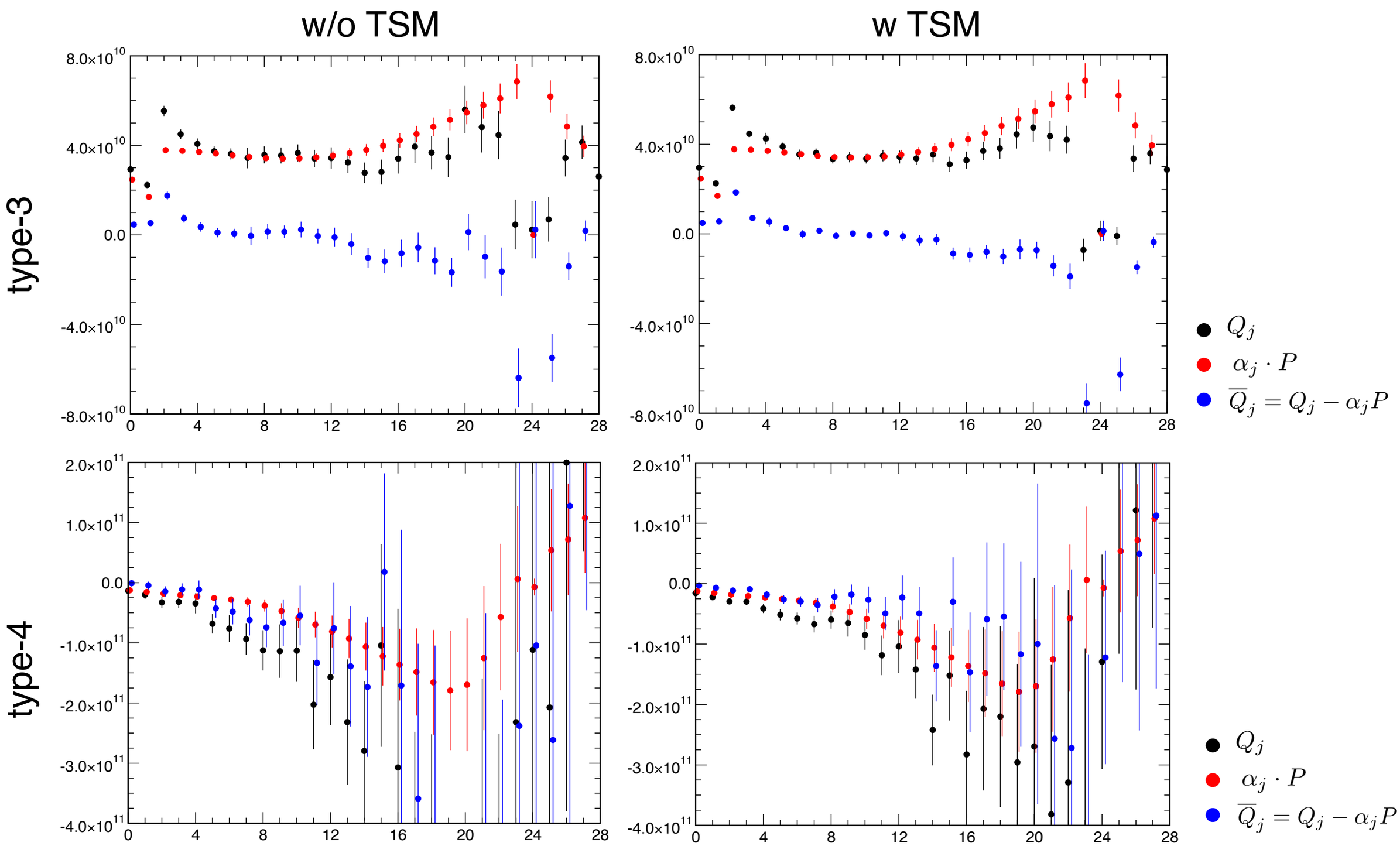

TSM reduces the statistical error

$G^{I=0}(Q_2)$ $(t_K = 24 , t_\pi = 0 , Q(t) : \mathrm{run})$

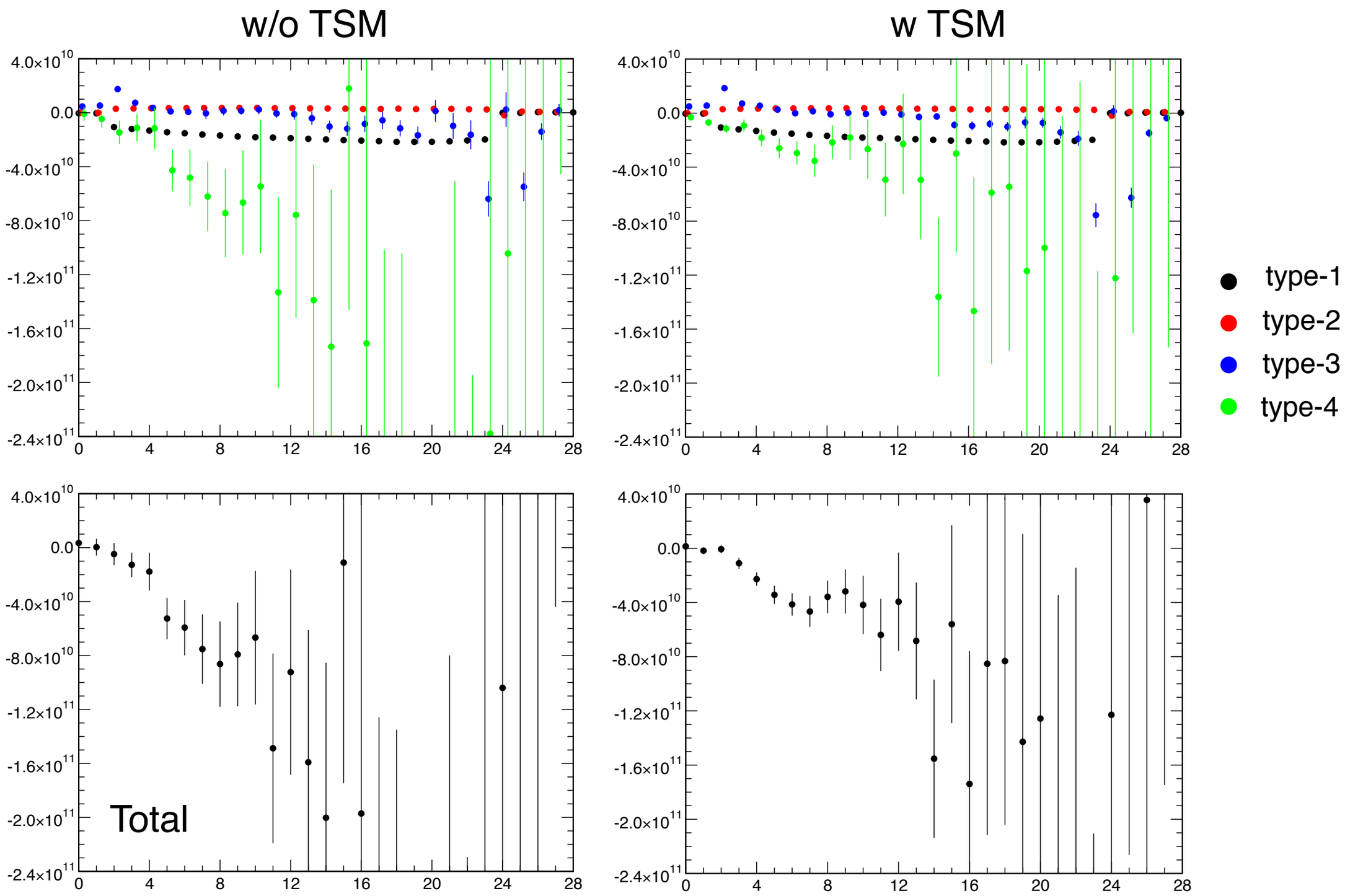

type-4 is large !!

type-4 ~ type-1

$G^{I=0}(Q_6)$ from type-3 and type-4 $(\, t_K = 24\,,\, t_\pi = 0\,,\, Q(t) : \mathrm{run}\,)$

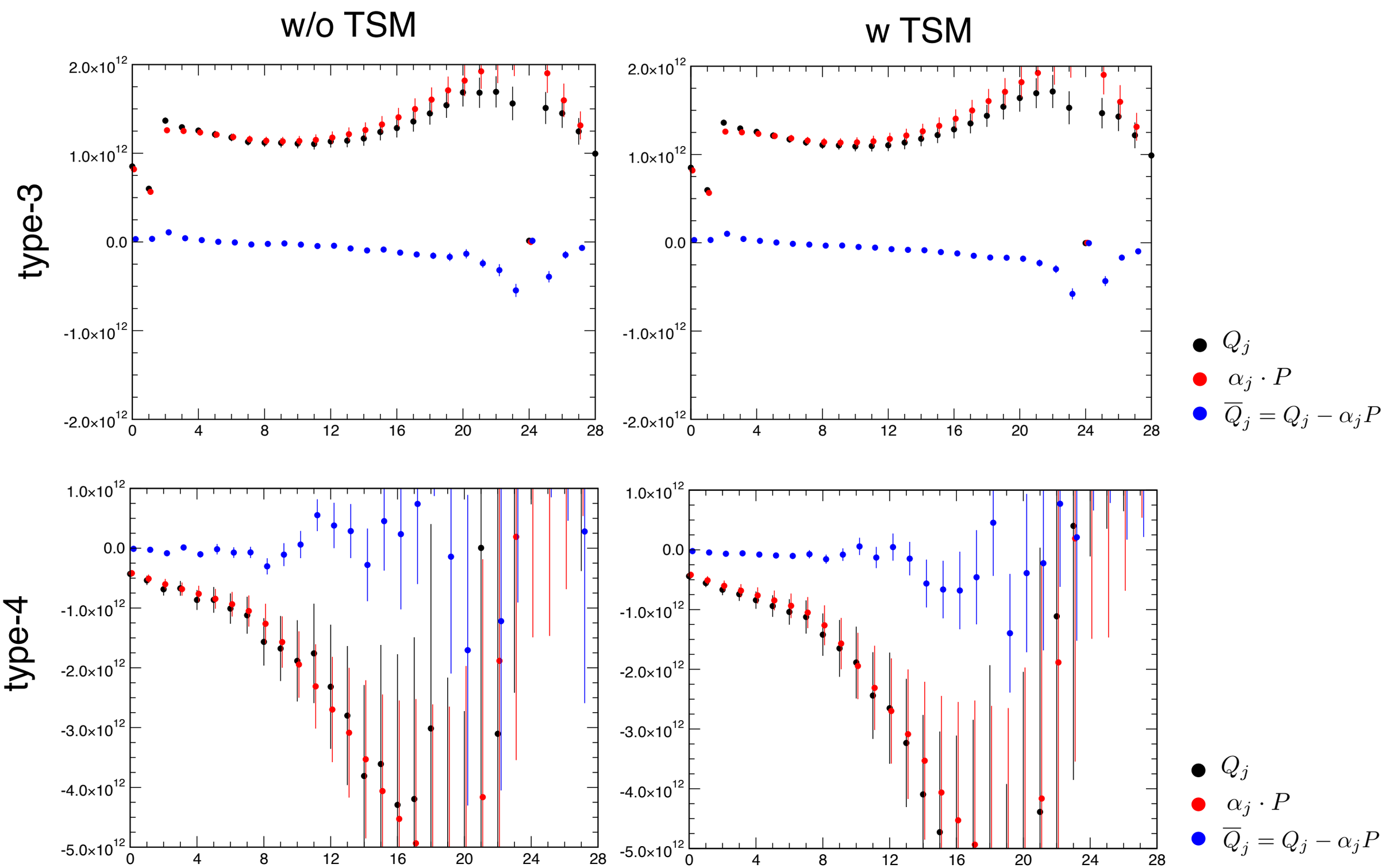

$G^{I=0}(Q_6)$ ($t_K = 24$, $t_\pi = 0$, $Q(t)$: run)

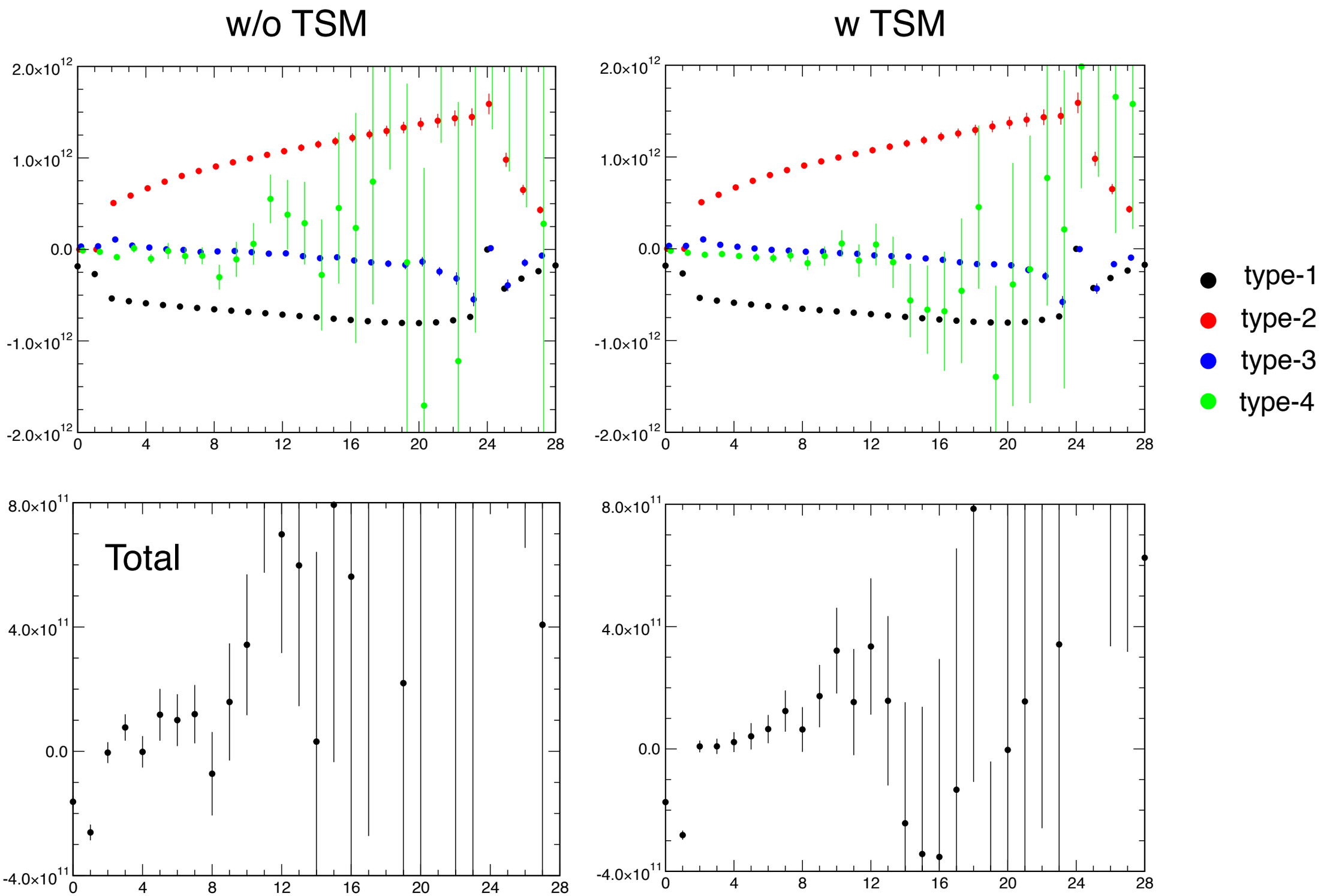

Large cancelation between type-1 and type-2.

Time correlation function of $\pi\pi \to \pi\pi$

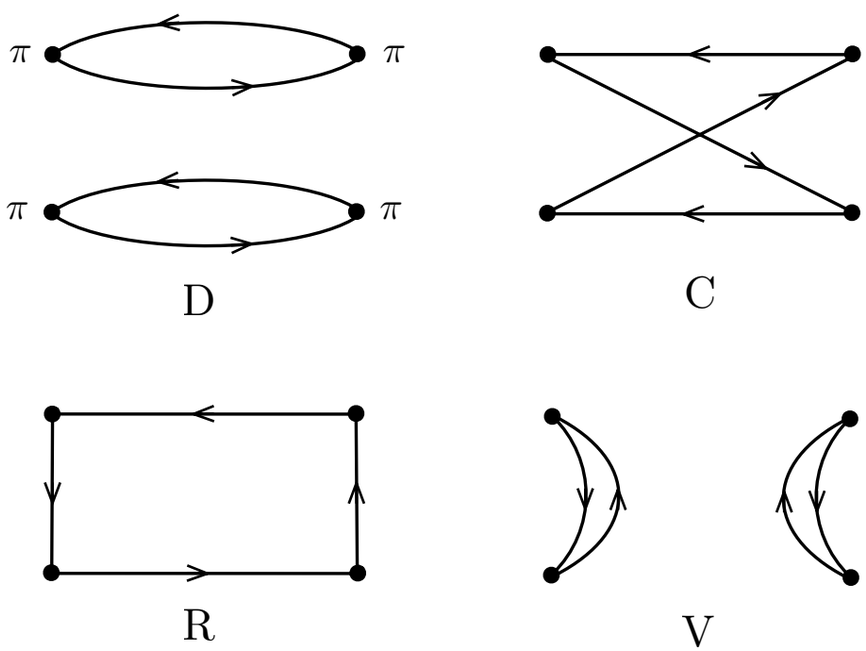

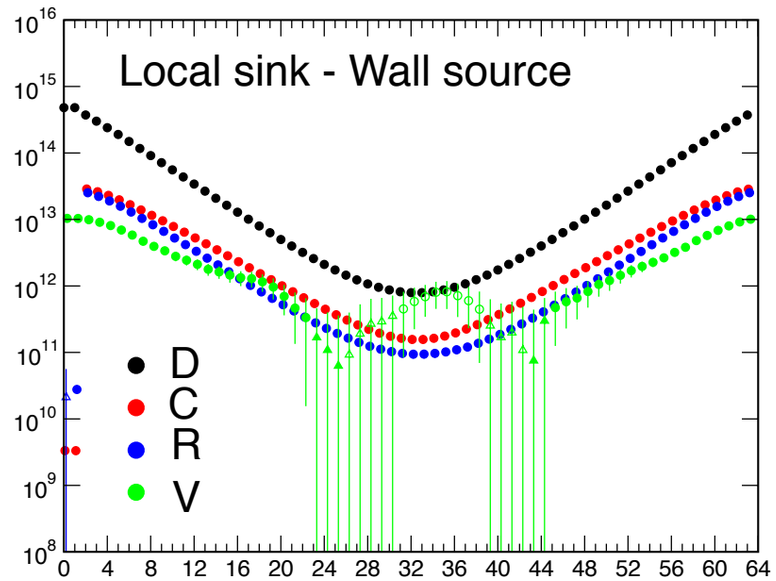

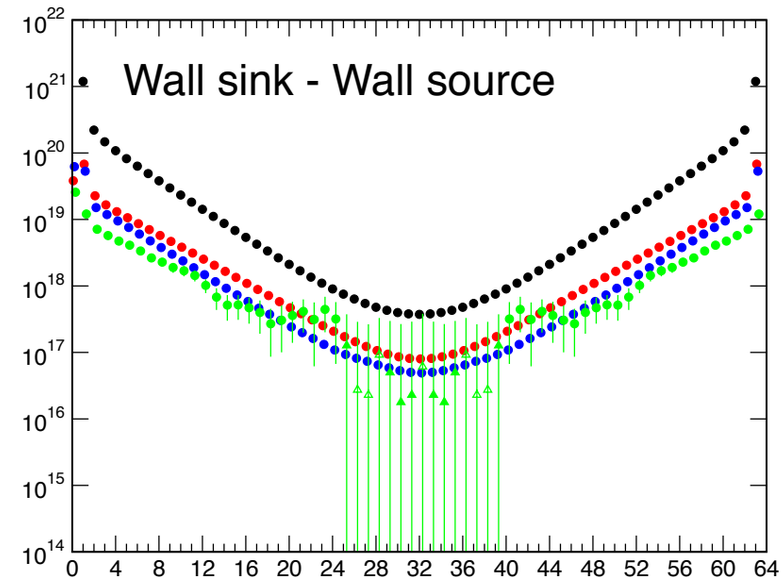

$$G(t) = A^I \cdot \left(\mathrm{e}^{-E^I_{\pi\pi} t} + \mathrm{e}^{-E^T_{\pi\pi}(T-t)} \right) + C^I$$

C^I : around-the-world effect

Effective mass of LW

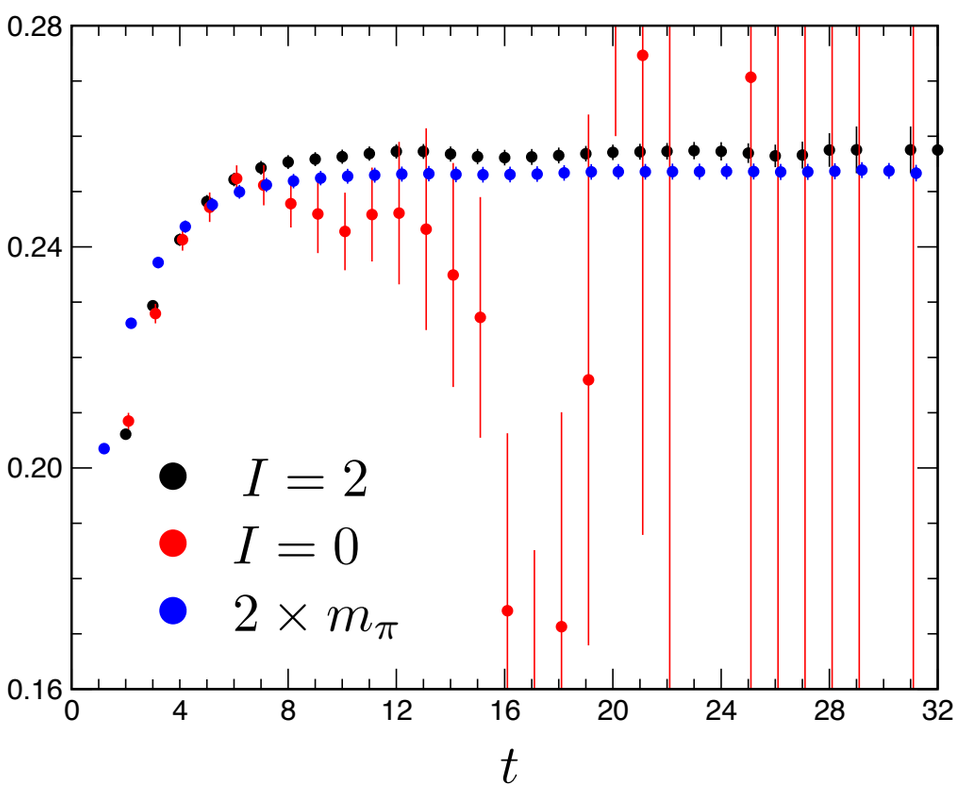

$2 \times m_\pi = 0.2535(14)$

$E^{I=2}_{\pi\pi} = 0.2567(14)$ (from LW)

$N^{I=2}_{\pi\pi} = \langle 0 | W^{I=2}_{\pi\pi} | \pi\pi; I=2 \rangle = 1.5852(85) \times 10^{10}$

$t = [9, 32]$ (from WW)

$E^{I=0}_{\pi\pi} = 0.2499(83)$ (from LW)

$N^{I=0}_{\pi\pi} = \langle 0 | W^{I=0}_{\pi\pi} | \pi\pi; I=0 \rangle = 1.552(42) \times 10^{10}$

$t = [9, 12]$ (from WW)

Extraction of the amplitudes

Effective amplitude :

$$M^I(Q_i)(t) = G^I(Q_i)(t) \cdot F^I_{LL}/(N_K N^I_{\pi\pi}) \cdot \mathrm{e}^{m_K(t_K - t) + E^I_{\pi\pi}(t - t_\pi)} \times \underline{(-1)}$$

(for our convention of $K^0 = -\bar{s}\gamma_5 d$)

$$\longrightarrow \quad M^I(Q_i) = \langle K | \overline{Q}_i | \pi\pi; I \rangle \quad \text{for } t_K \gg t \gg t_\pi$$

$$(\ t_K = 24 \, , \, t_\pi = 0 \, , \, t : \text{run} \ )$$

$$N_K = \langle 0 | W_K | K \rangle \qquad E^I_{\pi\pi} \ : \ \text{energy of } |\pi\pi; I\rangle$$

$$N^I_{\pi\pi} = \langle 0 | W^I_{\pi\pi} | \pi\pi; I \rangle$$ (from K and $\pi\pi$ correlation function)

Lellouch - Lüscher factor :

$$(F^I_{LL})^2 = \langle K | K \rangle \cdot \langle \pi\pi; I | \pi\pi; I \rangle / V^2$$

$$= (4\pi) \left(\frac{(E^I_{\pi\pi})^2 m_K}{p^3} \right) \left(p \frac{\partial \delta^I(p)}{\partial p} + q \frac{\partial \phi(q)}{\partial q} \right)$$

$$E^I_{\pi\pi} = 2\sqrt{p^2 + m_\pi^2}$$

$$q = pL/(2\pi)$$

$$\tan \phi(q) = -\pi^{3/2} q / Z_{00}(1 : q^2)$$

$$Z_{00}(s : q^2) = \frac{1}{\sqrt{4\pi}} \sum_{\mathbf{n} \in \mathbb{Z}^3} (n^2 - q^2)^{-s}$$

for *I=0* stat. of SC. phase is not enough.

the factor for non-interacting case is used.

for *I=2* the factor is estimated, neglecting the cubic term of

$$\delta^I(p) = a \cdot p + \mathrm{O}(p^3)$$

$$F^{I=2}_{LL} / F^{\text{free}}_{LL} = 0.9254(64)$$

Effective amplitudes $(t_K = 22, 24, 26 \, , \, t_\pi = 0 \, , \, Q(t) : \mathrm{run} \,)$

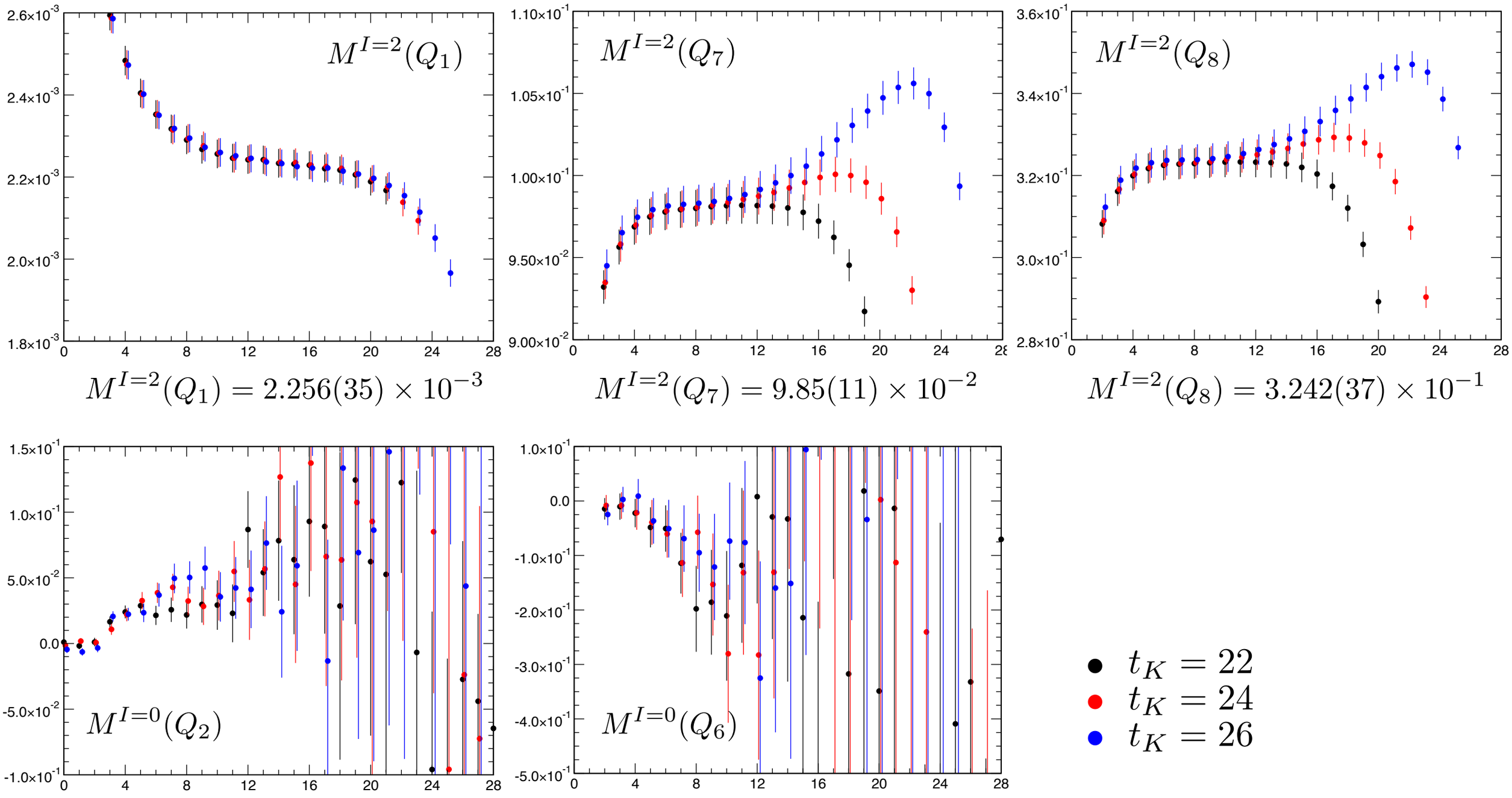

$M^{I=2}(Q_1) = 2.256(35) \times 10^{-3}$ $\quad$ $M^{I=2}(Q_7) = 9.85(11) \times 10^{-2}$ $\quad$ $M^{I=2}(Q_8) = 3.242(37) \times 10^{-1}$

$M^{I=0}(Q_2) = 3.55(1.43) \times 10^{-2}$ $\quad$ $M^{I=0}(Q_6) = -1.96(1.06) \times 10^{-1}$

The around-the-world effect for two pion state can be avoided for the time range t=[9,12].

Physical decay amplitudes

From the lattice to the continuum :

$$Q_i^{\overline{\rm MS}}(\mu) = \sum_j Z_{ij}(\mu)\, \overline{Q}_j^{\rm Lat} \qquad (\ i,j = 1,2,\cdots 10\ )$$

with perturbative renormalization factor (1 loop).

Y. Taniguchi, JHEP04(2012)143.

matching point : $\mu = 1/a$

(also $\mu = \pi/a$ to estimate higher order effect)

Coefficient function : G. Bychalla, A.J.Buras, M.E. Lautenbacher, RMP 68(1996)125.

$$H = \sum_i C_i(\mu) Q_i^{\overline{\rm MS}}(\mu) = \frac{G_F}{\sqrt{2}} V_{ud}^* V_{us} \sum_i \left(z_i(\mu) + \tau y_i(\mu)\right) Q_i^{\overline{\rm MS}}(\mu)$$

Physical decay amplitudes :

$$A_I = \langle K|H|\pi\pi; I\rangle = \sum_{ij} C_i(\mu) Z_{ij}(\mu) M^I(Q_j)$$

$M^I(Q_i)$: matrix element on the lattice

Physical decay amplitudes

	$\mu = 1/a$	$\mu = \pi/a$	RBC-UKQCD		Exp
$a\,(\mathrm{fm})$	0.091		0.114	0.114	
$m_\pi\,(\mathrm{MeV})$	280		330	422	140
$\mathrm{ReA}_2\,(\times 10^{-8}\,\mathrm{GeV})$	2.426(38)	2.460(38)	2.668(14)	4.911(31)	1.479(4)
$\mathrm{ReA}_0\,(\times 10^{-8}\,\mathrm{GeV})$	60(36)	56(32)	31.1(45)	38.0(82)	33.2(2)
$\mathrm{Re}A_0/\mathrm{Re}A_2$	25(15)	23(13)	12.0(17)	7.7(17)	22.45(6)
$\mathrm{ImA}_2\,(\times 10^{-12}\,\mathrm{GeV})$	−1.14(13)	−0.7457(83)	−0.6509(34)	−0.5502(40)	
$\mathrm{ImA}_0\,(\times 10^{-12}\,\mathrm{GeV})$	−67(56)	−52(48)	−33(15)	−25(22)	
$\mathrm{Re}(\epsilon'/\epsilon)\,(\times 10^{-3})$	0.8(25)	0.9(25)	2.0(17)	2.7(26)	1.66(23)

(used $|\epsilon^{\mathrm{EXP}}| = 2.22 \times 10^{-3}$)

- Stat. error of our A_0 is much larger than those of RBC-UKQCD at $m_\pi = 330\,\mathrm{MeV}$

  They used a different two-pion operator from ours
  and set the fitting range closer to the operator.

- Matching point dependence is very large for ImA_2 .
- Enhancement of $\Delta I = 1/2$ process is seen.
- Further improvement of statistics is necessary for ϵ'/ϵ .

arXiv:1110.2143 (RBC-UKQCD)

$m_\pi = 330\,\mathrm{MeV}$

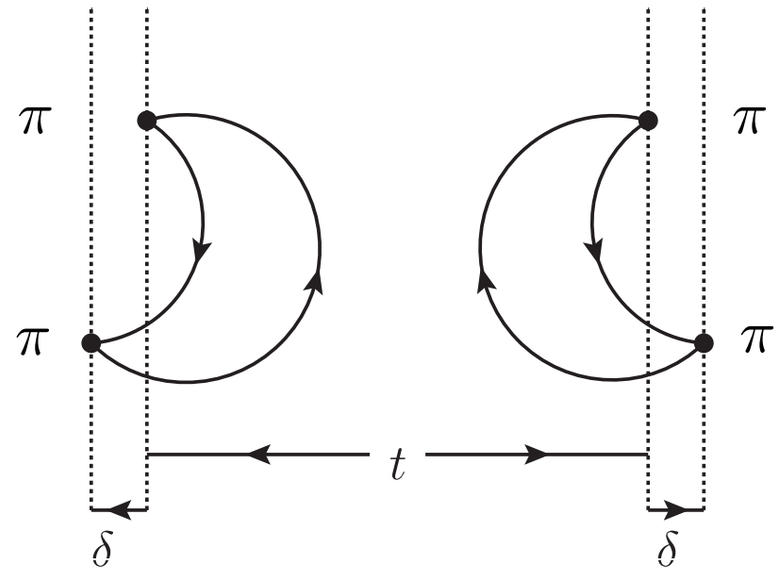

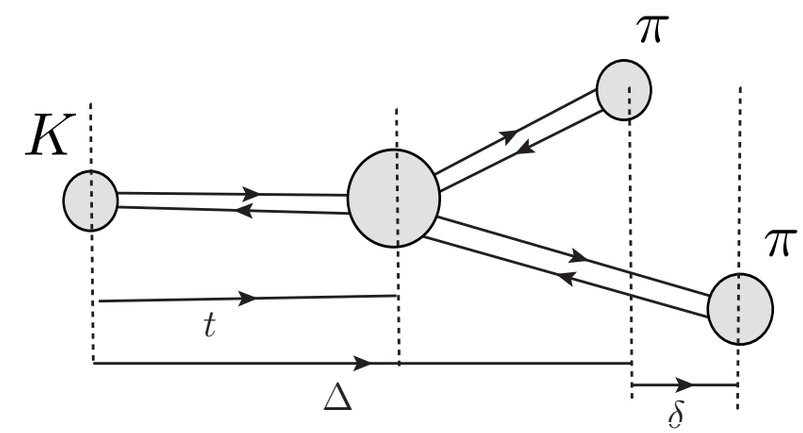

effective mass of $\pi\pi \to \pi\pi \ (I=0)$

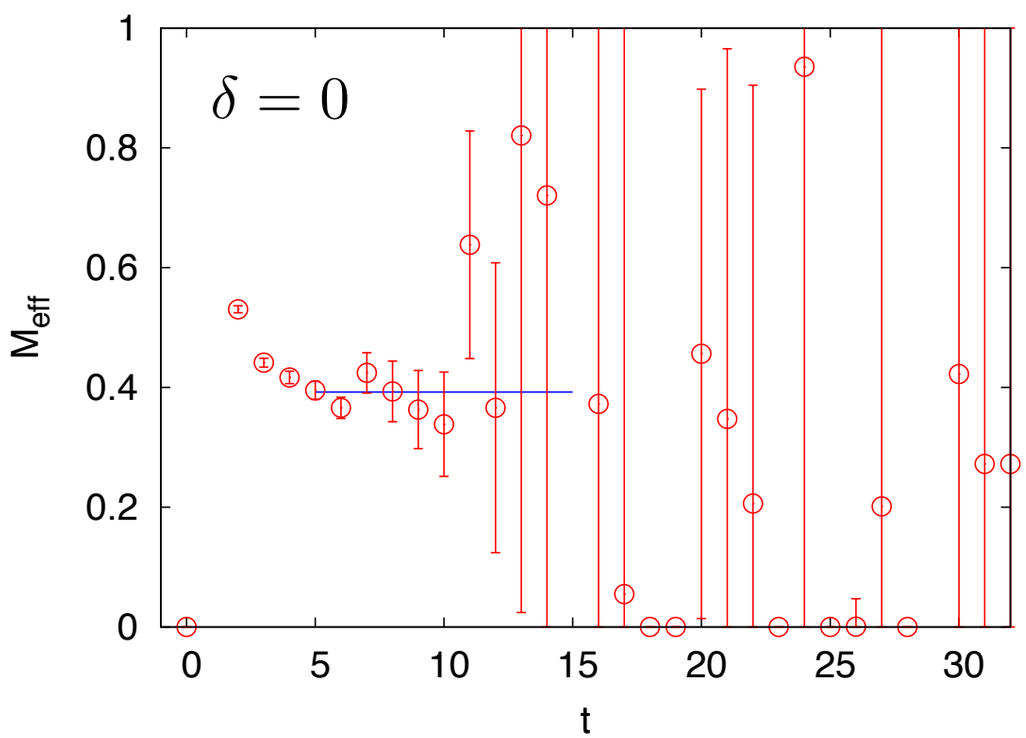

$E = 0.3922(126)$

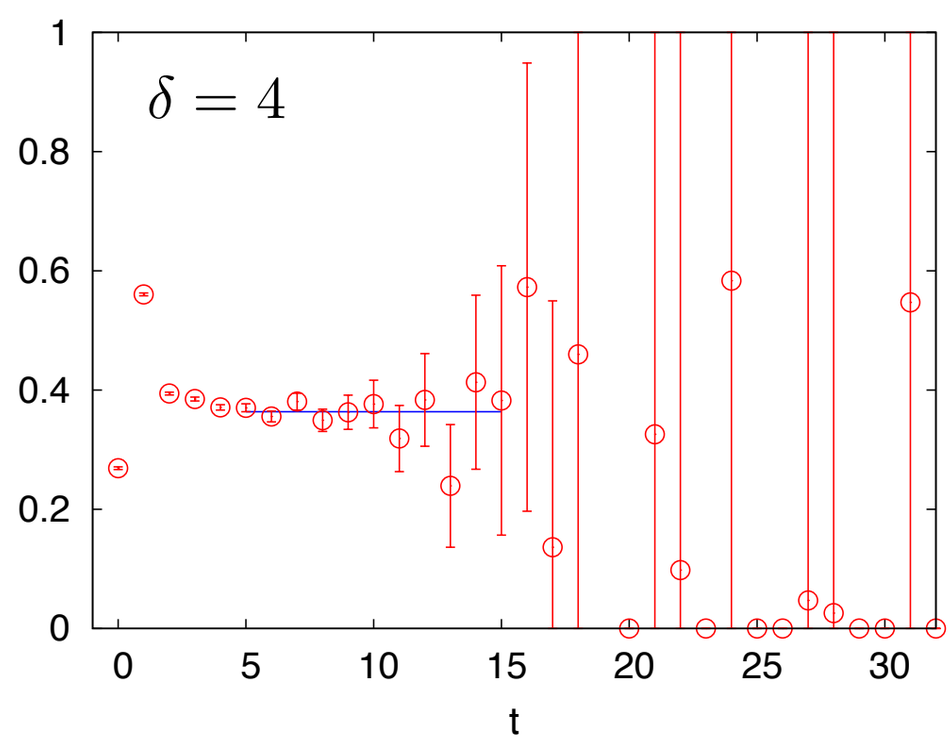

$E = 0.3639(55)$

Error is reduced by taking non-zero δ .

Reason ?

Contribution of the matrix element on the lattice

$\mu = 1/a$

i	$\mathrm{Re}A_2$ (GeV)	$\mathrm{Im}e A_2$ (GeV)
1	$-1.887(29) \times 10^{-08}$	0
2	$4.330(68) \times 10^{-08}$	0
7	$1.053(12) \times 10^{-10}$	$2.772(32) \times 10^{-13}$
8	$-2.722(31) \times 10^{-10}$	$-1.670(19) \times 10^{-12}$
9	$-1.140(18) \times 10^{-12}$	$3.762(59) \times 10^{-13}$
10	$3.771(59) \times 10^{-10}$	$-1.756(27) \times 10^{-13}$
Total	$2.426(38) \times 10^{-08}$	$-1.192(14) \times 10^{-12}$

i	$\mathrm{Re}A_0$ (GeV)	$\mathrm{Im}e A_0$ (GeV)
1	$-4(11) \times 10^{-08}$	0
2	$6.8(28) \times 10^{-07}$	0
3	$-1.25(65) \times 10^{-08}$	$-2.5(13) \times 10^{-11}$
4	$5.3(20) \times 10^{-08}$	$6.6(25) \times 10^{-11}$
5	$1.5(59) \times 10^{-09}$	$1.7(68) \times 10^{-12}$
6	$-8.4(46) \times 10^{-08}$	$-1.03(56) \times 10^{-10}$
7	$2.58(19) \times 10^{-10}$	$6.81(50) \times 10^{-13}$
8	$-6.26(45) \times 10^{-10}$	$-3.84(28) \times 10^{-12}$
9	$1.02(48) \times 10^{-11}$	$-3.4(16) \times 10^{-12}$
10	$0.0(14) \times 10^{-11}$	$-0.1(64) \times 10^{-13}$
Total	$6.0(36) \times 10^{-07}$	$-6.7(56) \times 10^{-11}$

$$A_I = \langle K|H|\pi\pi; I\rangle \ = \sum_i \bar{A}_i$$

$$\bar{A}_i = \sum_j C_j(\mu) Z_{ji}(\mu) M^I(Q_i)$$

$M^I(Q_i)$: bare matrix element on the lattice

5. Summary

We calculate $K \to \pi\pi$ decay amplitudes
for the process $K(\mathbf{0}) \to \pi(\mathbf{0})\pi(\mathbf{0})$ at $m_\pi = 280\mathrm{MeV}$ ($m_K \sim 2 \times m_\pi$)

- $N_f = 2+1$ improved Wilson fermion with
  Non-perturbative subtraction of the lower dimensional operator .
- Calculation of quark loop by
  Stochastic method with HPE and TSM

We found :

- TSM is an efficient method.
- For Q_2 , the contribution of type-4 (OZI-suppression diag.) is large.
  type-4 ~ type-1 (: Wilson fermion ?)
- Stat. error of our A_0 is much larger than those of RBC-UKQCD.
  Improvement of the *K* and *ππ* operator is necessary.
- Matching point dependence is very large for ImA_2 .
  Non-perturbative renormalization factor is needed.
- Enhancement of $\Delta I = 1/2$ process is seen.
  $\mathrm{Re}A_0/\mathrm{Re}A_2 = 25 \pm 15$
- Further improvement of statistics is necessary for ϵ'/ϵ .
  Improvement of the *K* and *ππ* operator is necessary.

Back-up

Comparison with PRL 110,152001(2013) by RBC-UKQCD

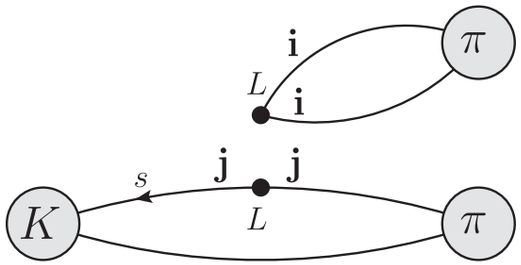

Contraction ①.

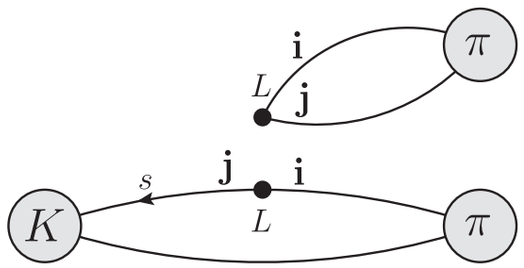

Contraction ②.

$$\mathrm{Re}A_2 = (\ (1)\ +\ (2)\ )$$
$$\mathrm{Re}A_0 = (\ 2\times(1)\ -\ (2)\ )$$

RBC-UKQCD

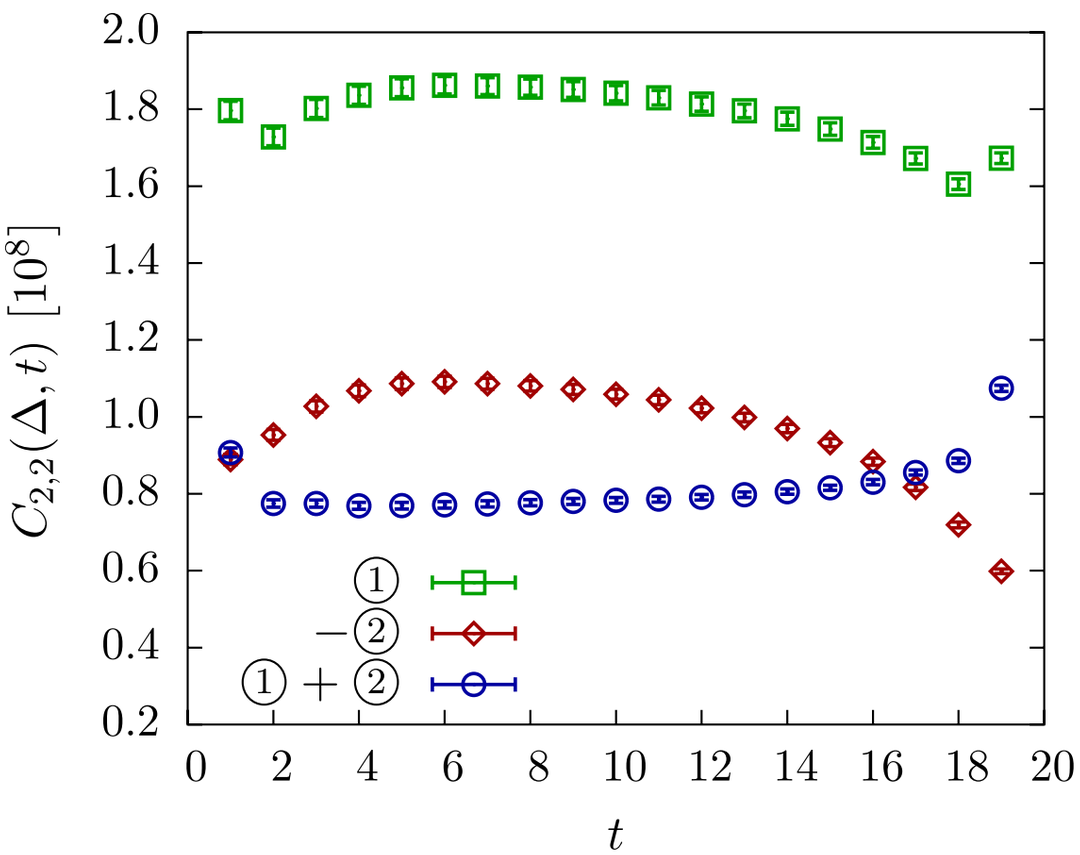

$m_\pi = 330\,\mathrm{MeV}$
$t_K = 0\,,\ t_\pi = 20$

Ours

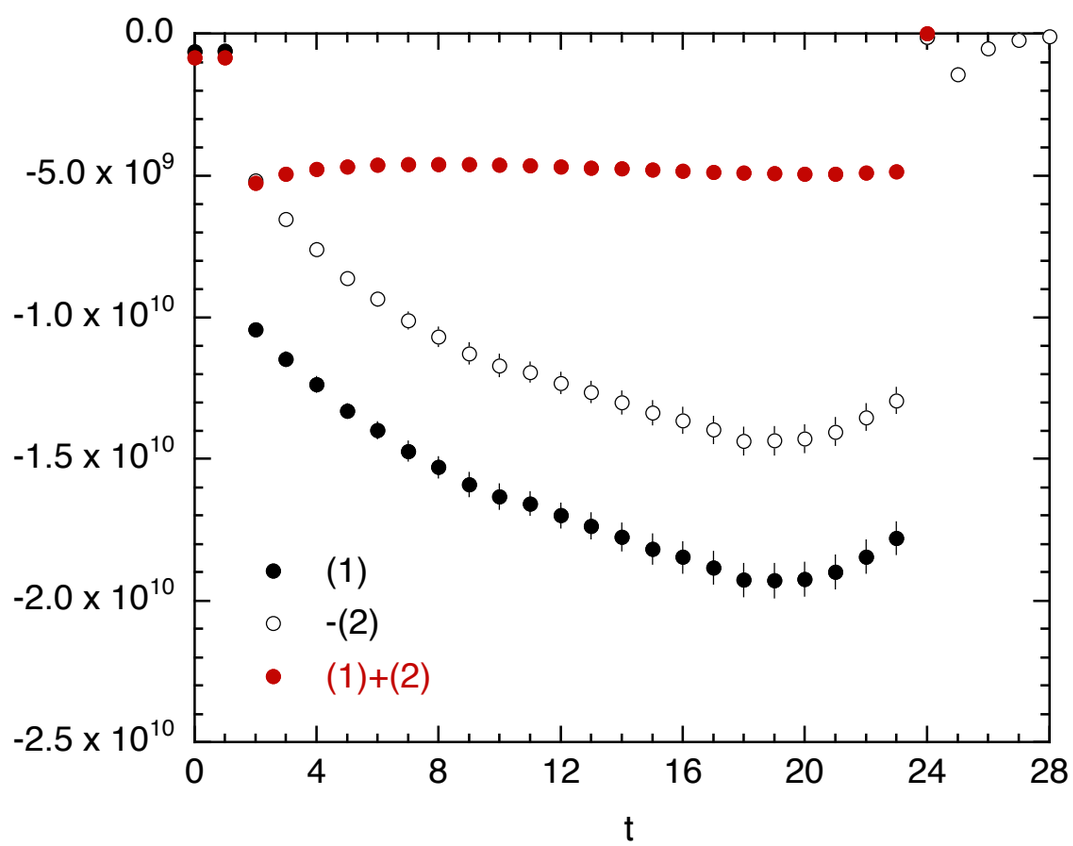

$m_\pi = 280\,\mathrm{MeV}$
$t_\pi = 0\,,\ t_K = 24$

Note our convention : $K^0 = -\bar{s}\gamma_5 d$

Lattice Calculation of the Hadronic Light by Light Contributions to the Muon Anomalous Magnetic Moment

by Luchang Jin

Columbia University / RBC Collaboration

Tom Blum (UConn)
Norman Christ (Columbia)
Masashi Hayakawa (Nagoya)
Taku Izubuchi (BNL/RBRC)
Christoph Lehner (BNL)
Norikazu Yamada (KEK)

Multi-Hadron and Nonlocal Matrix Elements in Lattice QCD

Brookhaven National Laboratory

2015.02.06

$$\boldsymbol{\mu}_\mu = -g_\mu \frac{e}{2m_\mu} \mathbf{s}_\mu \tag{1}$$

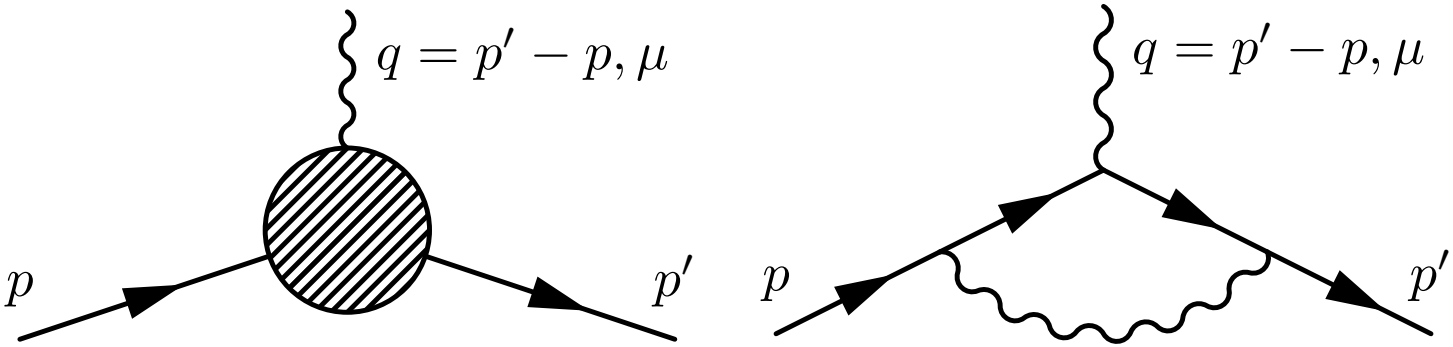

Figure 1. (L) Muon Vertex Function Diagram (R) Schwinger Term Diagram.

$$\bar{u}(p')\Gamma^\mu(p',p)u(p) = \bar{u}(p')\left[F_1(q^2)\gamma_\mu + i\frac{F_2(q^2)}{4m}[\gamma_\mu,\gamma_\nu]q_\nu\right]u(p) \tag{2}$$

$$F_2(0) = \frac{g_\mu - 2}{2} \equiv a_\mu \tag{3}$$

Figure 2. The headstone of Julian Schwinger at Mt Auburn Cemetery in Cambridge, MA.

BNL E821 (0.54 ppm) and Standard Model Prediction

	Value $\pm$ Error	Reference
Experiment (0.54 ppm)	116592089 ± 63	E821, The $g-2$ Collab. 2006
Standard Model	116591828 ± 50	arXiv:1311.2198
Difference (Exp $-$ SM)	261 ± 78	
HVP LO	6949 ± 43	Hagiwara et al. 2011
Hadronic Light by Light	105 ± 26	Glasgow Consensus, 2007

Table 1. Standard model theory and experiment comparison [in units 10^{-11}]

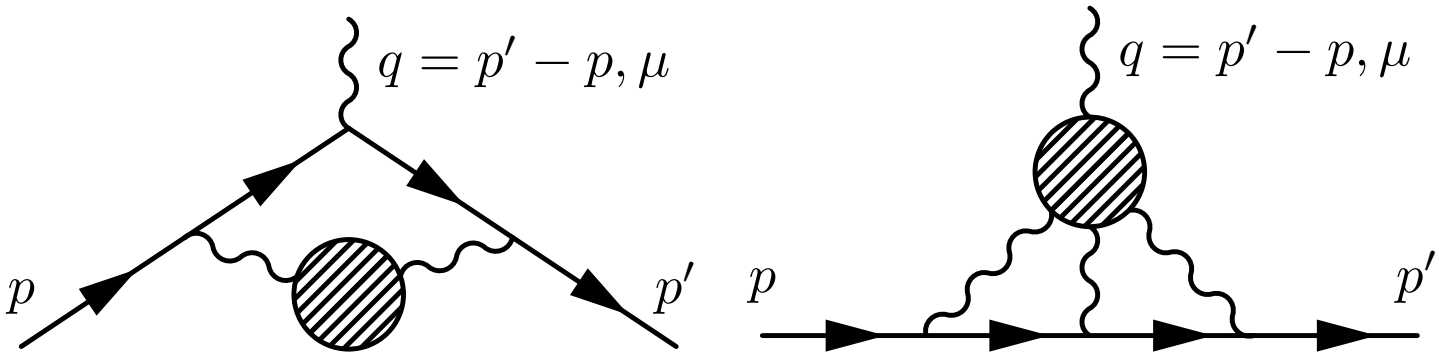

Figure 3. (L) Vaccum polarization diagram. (R) Light by light diagram.

There is 3.3σ deviation!

Future Fermilab E989 (0.14 ppm)

Figure 4. The 50-foot-wide Muon g-2 electromagnet being driven north on I-355 between Lemont and Downers Grove, Illinois, shortly after midnight on Thursday, July 25, 2013. *Credit: Fermilab.*

Almost 4 times more accurate then the previous experiment.

- In this talk, we focus on the calculation of connected light by light amplitude on lattice.
- This subject is started by T. Blum, S. Chowdhury, M. Hayakawa, T. Izubuchi more than 5 years ago. Phys. Rev. Lett. 114, 012001 (2015).

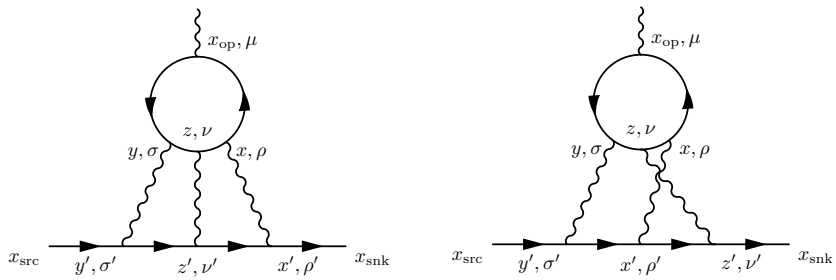

Figure 5. Light by Light diagrams. There are 4 other possible permutations.

$$
\begin{aligned}
\mathcal{M}_\mu^{\rm LbL} \;=\; & -(-ie)^6 \sum_{x,y,z} \left\langle \sum_q \mathrm{tr}[\gamma_\mu S_q(x_{\rm op},x)\gamma_\rho S_q(x,z)\gamma_\nu S_q(z,y)\gamma_\sigma S_q(y,x_{\rm op})] \right\rangle_{\rm QCD} \\
& \cdot \sum_{x',y',z'} G_{\rho\rho'}(x;x')G_{\sigma\sigma'}(y;y')G_{\nu\nu'}(z;z') \\
& \cdot \Big[S(x_{\rm snk},x')\gamma_{\rho'}S(x',z')\gamma_{\nu'}S(z',y')\gamma_{\sigma'}S(y',x_{\rm src}) \\
& + S(x_{\rm snk},z')\gamma_{\nu'}S(z',x')\gamma_{\rho'}S(x',y')\gamma_{\sigma'}S(y',x_{\rm src}) \\
& + \text{other 4 permutations} \Big]
\end{aligned}
\tag{4}
$$

Outline

1. Muon Anomalous Magnetic Moment
2. BNL E821 (0.54 ppm) and Standard Model Prediction
3. **Lattice QED Schwinger Term as an Example**
   i. Stochastic Photon
   ii. Exact Photon
   iii. Finite Volume
   iv. Discretization Errors
4. Stochastic Photon Light by Light
5. Point Source Photon Light by Light
6. Current Status and Outlook

We would like to do a standard Euclidean-space lattice calculation with a muon source and sink, well separated in Euclidean time.

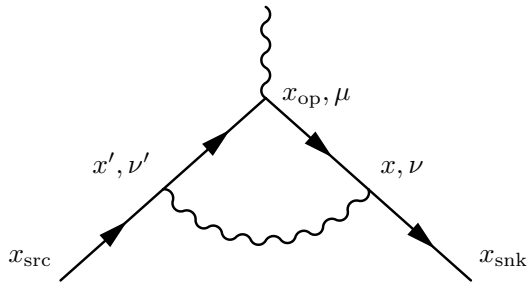

Figure 6. Schwinger term diagram.

$$\begin{aligned} \mathcal{M}_\mu^{\text{1-loop}} &= (-ie)^2 \sum_{x,x'} S(x_{\rm snk}, x)\gamma_\nu S(x, x_{\rm op})\gamma_\mu S(x_{\rm op}, x')\gamma_{\nu'} S(x', x_{\rm src}) \\ &\cdot \; G_{\nu\nu'}(x, x') \end{aligned} \tag{5}$$

Naively, the sum would require $\mathcal{O}(\text{Volume}^2)$ computation, which is not affordable. We discuss two strategies:

- Calculate the sum stochastically.
- Fast Fourier Transformation.

Both approaches make the problem $\mathcal{O}(\text{Volume})$.

Evaluate the photon propagator with N stochastic sample.

$$G_{\mu\nu}(x,y) \approx \frac{1}{M}\sum_{m=1}^{M} A_\nu^m(x)A_{\nu'}^m(y) \tag{6}$$

$$A_\mu^m(x) = \frac{1}{\sqrt{V}}\sqrt{2}\mathrm{Re}\sum_k \frac{\epsilon_\mu^m(k)}{\sqrt{|k^2|}}e^{i\,k\cdot x} \qquad \frac{1}{M}\sum_{m=1}^{M} \epsilon_\mu^m(k)\epsilon_\nu^{m*}(k') \approx \delta_{\mu\nu}\delta_{kk'} \tag{7}$$

$$\begin{aligned}\mathcal{M}_\mu^{\text{1-loop}} &= (-ie)^2\frac{1}{M}\sum_{m=1}^{M} \\ &\cdot \left[\sum_x S(x_{\text{snk}},x)\gamma_\nu A_\nu^m(x)S(x,x_{\text{op}})\right]\gamma_\mu\left[\sum_{x'} S(x_{\text{op}},x)\gamma_{\nu'}A_{\nu'}^m(x')S(x',x_{\text{src}})\right]\end{aligned} \tag{8}$$

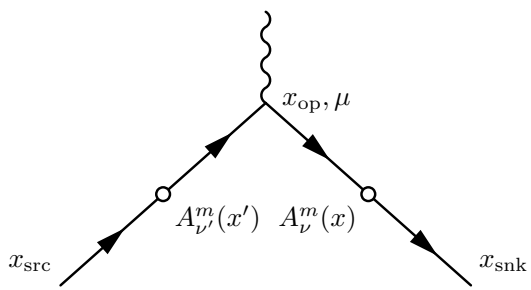

Figure 7. Schwinger term diagram calculated with stochastic photon.

$$G_{\mu\nu}(x;y) \;=\; \frac{1}{V}\sum_k \frac{\delta_{\mu\nu}}{k^2} e^{i\,k\cdot(x-y)} \tag{9}$$

$$\begin{aligned}\mathcal{M}_\mu^{\text{1-loop}} \;&=\; (-ie)^2 \frac{1}{V}\sum_k \frac{\delta_{\nu\nu'}}{k^2} \\ &\cdot\; \left[\sum_x S(x_{\text{snk}},x)\gamma_\nu e^{i\,k\cdot x} S(x,x_{\text{op}})\right]\gamma_\mu \left[\sum_{x'} S(x_{\text{op}},x')\gamma_{\nu'} e^{-i\,k\cdot x'} S(x',x_{\text{src}})\right]\end{aligned} \tag{10}$$

Evaluate the expression in brackets with Fast Fourier Transformation.

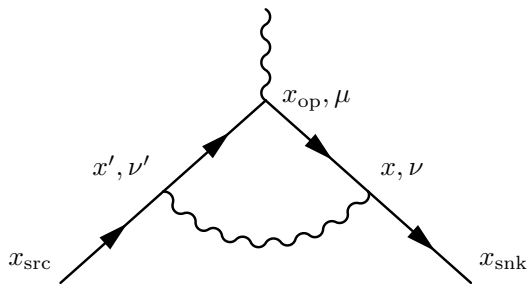

Figure 8. Schwinger term diagram calculated with exact photon.

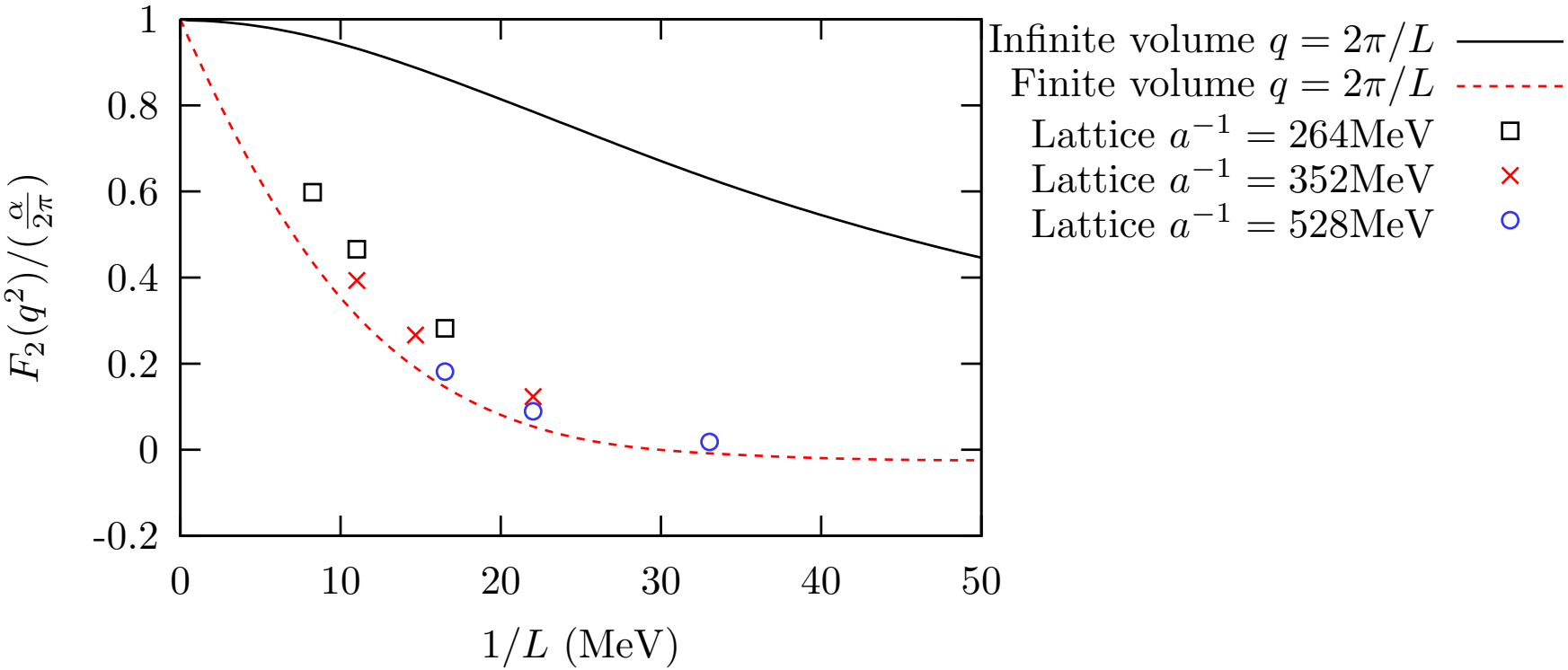

Figure 9. Finite volume effects on F_2. The data points are obtained using exact photon method.

- The solid line represents the continuum result in infinite volume and momentum transfer $q = 2\pi / L$. The dashed line represents the continuum result in L^3 volume and momentum transfer $q = 2\pi / L$.
- Lattice sizes are $32^3 \times 128$, $24^3 \times 96$, $16^3 \times 64$ with $L_s = 8$ and $t_{\rm snk} - t_{\rm op} = t_{\rm op} - t_{\rm src} = T / 4$.
- Muon mass is $m_\mu = 106\text{MeV}$. a is the lattice spacing.

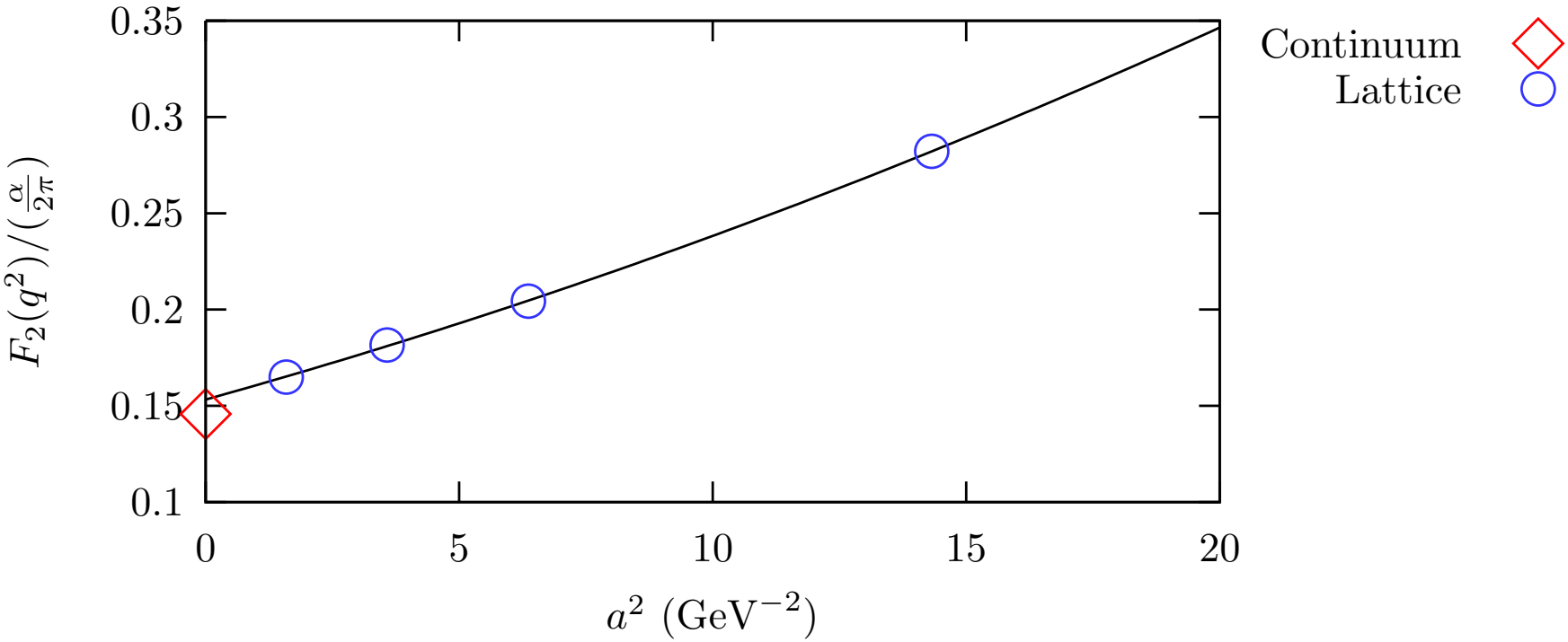

Figure 10. Discretization errors on F_2. The data points are obtained using exact photon method.

- $m_\mu L = 6.4$ and lattice sizes are $32^3 \times 128$, $24^3 \times 96$, $16^3 \times 64$, $12^3 \times 48$ with $L_s = 8$ and $t_{\rm snk} - t_{\rm op} = t_{\rm op} - t_{\rm src} = T/4$.
- $q = 2\pi/L$ is the momentum of the external photon.
- The line is 2nd order polynomial obtained by fitting the results from lattice calculations.
- Muon mass is $m_\mu = 106\text{MeV}$. a is the lattice spacing. An a^4 term is visible.

Outline

1. Muon Anomalous Magnetic Moment
2. BNL E821 (0.54 ppm) and Standard Model Prediction
3. Lattice QED with Schwinger Term as an Example
4. **Stochastic Photon Light by Light**
   i. Evaluation Formula
   ii. QED Cost Comparison
   iii. QED Excited States
   iv. QED Finite Volume
   v. QCD Model Value
   vi. QCD Excited States
5. Point Source Photon Light by Light
6. Current Status and Outlook

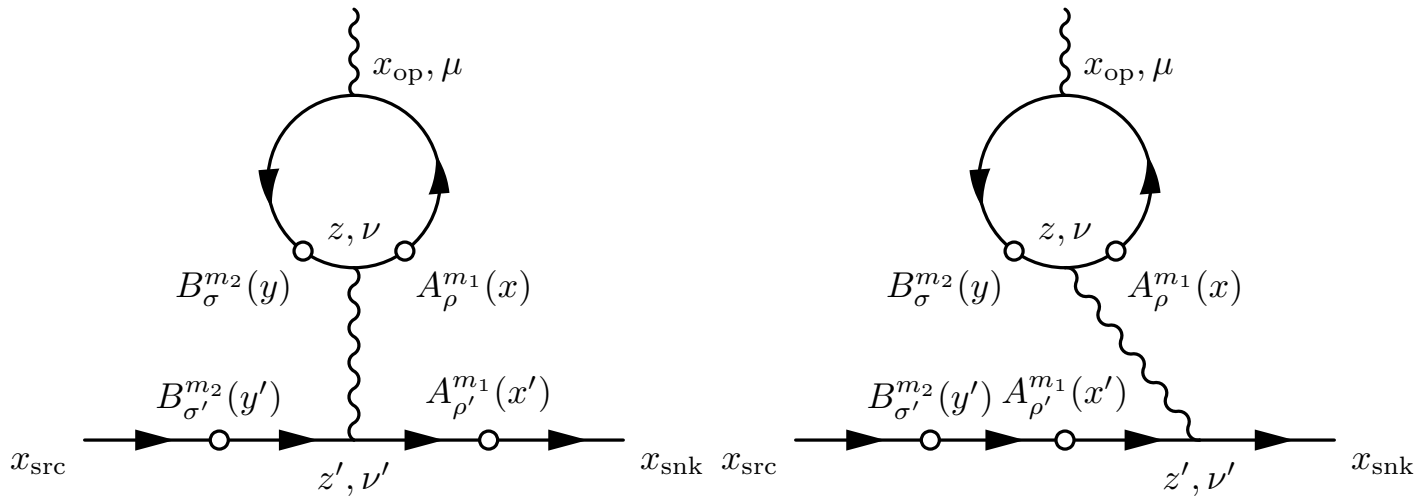

Figure 11. Light by Light diagrams calculated with one exact photon and two stochastic photon. There are 4 other possible permutations.

- $M = 12$ stochastic photon fields for both A and B.
- $S = 18$ random wall sources for the external local current.

Computation Cost

- $2 \times S \times M$ times inversion for the quark loop.
- $8 \times M^2$ times inversion for muon line.
- Statistics is roughly proportional to $S \times M^2$.
- Cost grows as $\mathcal{O}(\text{Volume})$ not $\mathcal{O}(\text{Volume}^2)$.

Stochastic Photon Light by Light - Evaluation Formula

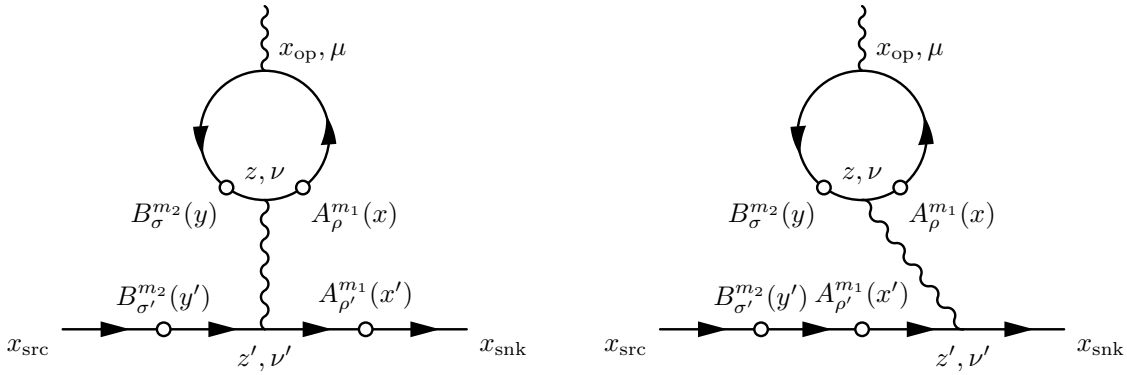

$$
\begin{aligned}
= \; & -(-ie)^6 \frac{1}{M^2} \sum_{m_1, m_2 = 1}^{M} \frac{1}{V} \sum_k \frac{\delta_{\nu\nu'}}{k^2} \\
\cdot \; & \sum_z \left\langle \sum_q \mathrm{tr} \left\{ \gamma_\mu \left[\sum_x S_q(x_{\rm op}, x) \gamma_\rho A^{m_1}_\rho(x) S_q(x, z) \right] \gamma_\nu e^{i k \cdot z} \left[\sum_y S_q(z, y) \gamma_\sigma B^{m_2}_\sigma(y) S_q(y, x_{\rm op}) \right] \right\} \right\rangle_{\rm QCD} \\
\cdot \; & \sum_{z'} \left\{ \left[\sum_{x'} S(x_{\rm snk}, x') \gamma_{\rho'} A^{m_1}_{\rho'}(x') S(x', z') \right] \gamma_{\nu'} e^{-i k \cdot z'} \left[\sum_{y'} S(z', y') \gamma_{\sigma'} B^{m_2}_{\sigma'}(y') S(y', x_{\rm src}) \right] \right. \\
& + S(x_{\rm snk}, z') \gamma_{\nu'} e^{-i k \cdot z'} \left[\sum_{x'} S(z', x') \gamma_{\rho'} A^{m_1}_{\rho'}(x') \left(\sum_{y'} S(x', y') \gamma_{\sigma'} B^{m_2}_{\sigma'}(y') S(y', x_{\rm src}) \right) \right] \\
& \left. + \text{other 4 permutations} \right\}
\end{aligned}
\tag{11}
$$

- QED test: Replace quark loop by muon loop.

Lattice Size	$t_{\rm sep}$	$m_\mu a$	$\frac{F_2 \pm \mathrm{Err}}{(\alpha/\pi)^3}$	$N \times S \times M^2$ confs	$\frac{\sqrt{\mathrm{Var}}}{(\alpha/\pi)^3}$
$16^3 \times 64$	32	0.2	0.2228 ± 0.0046	$548 \times 18 \times 12^2$	5.5
$16^3 \times 64$	32	0.2	0.1962 ± 0.0368	$1024 \times 18 \times 1^2$	5.0
$16^3 \times 64$ (point src)	32	0.2	0.232 ± 0.033	$1508 \times 12 \times 6^2$	28.4
$16^3 \times 64$	32	0.1	0.1666 ± 0.0069	$88 \times 18 \times 12^2$	3.3
$16^3 \times 64$ ($\mathbf{p}_1 = 0$)	32	0.1	0.2278 ± 0.0265	$285 \times 36 \times 24^2$	64.4

Figure 12. M stands for the number of stochastic A or B fields, S stands for the number of random wall sources that we use to calculate the external current. The calculation is repeated N times. $\sqrt{\mathrm{Var}} = \mathrm{Err} \times \sqrt{N \times S \times M^2}$ stands for the projected variance deduced from to the statistical uncertainty of the averaged result and the total number of samples.

- Average over different combinations of A, B electromagnetic field helps reducing the statistical errors.
- Random wall source at the location of the external current works very well.
- Using symmetric kinematics significantly reduces the statistical error as both the initial and the final state are the lowest energy state possible. For muon, we use anti-periodic boundary condition in z direction and set the momenta of initial and final state to be $\pm\pi/L$.

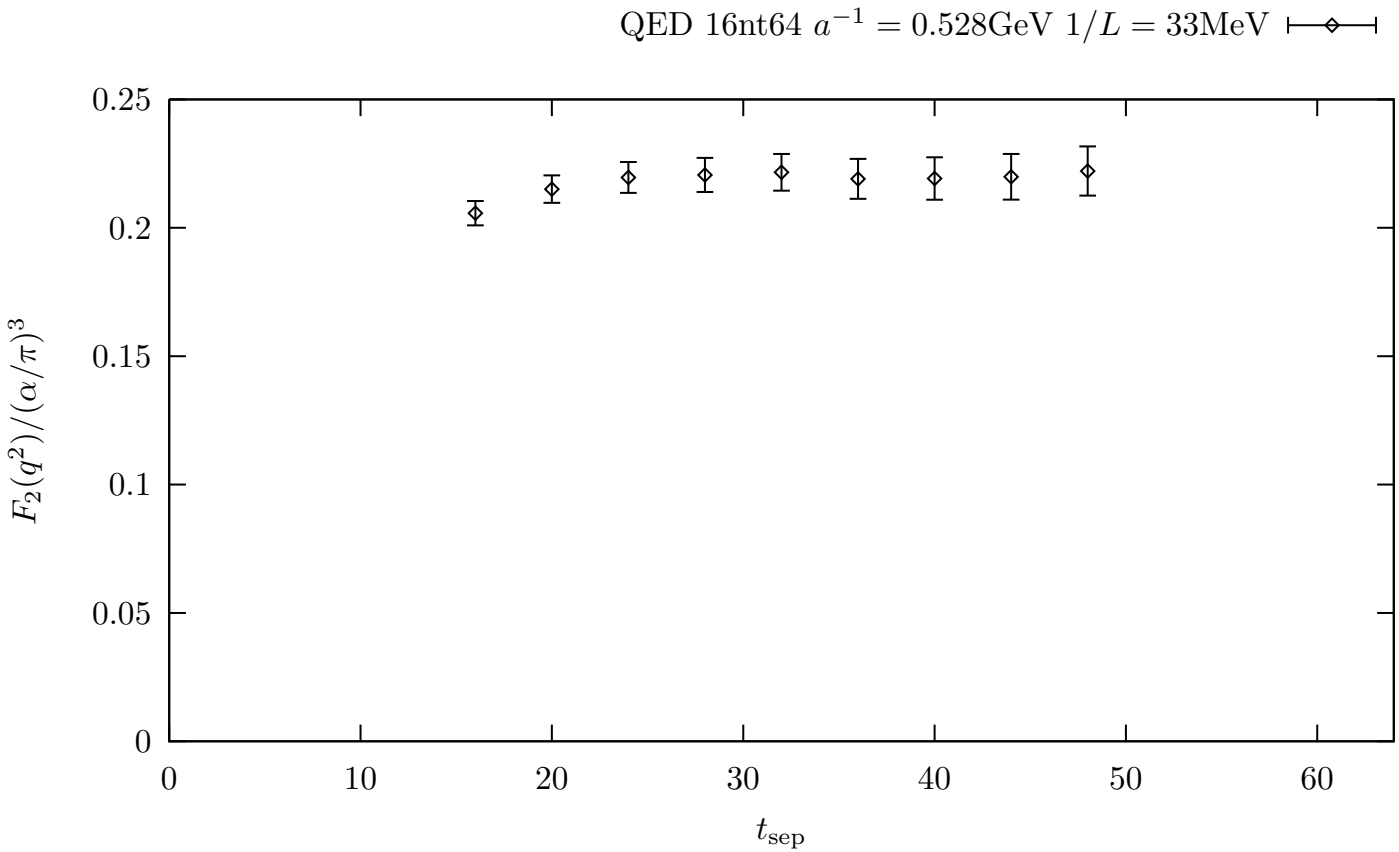

Figure 13. Excited effects on F_2.

- We have good control of the excited state effects.
- The simulations were done in L^3 volume and momentum transfer $q = 2\pi / L$.
- Muon mass is $m_\mu = 106\text{MeV}$. a is the lattice spacing.

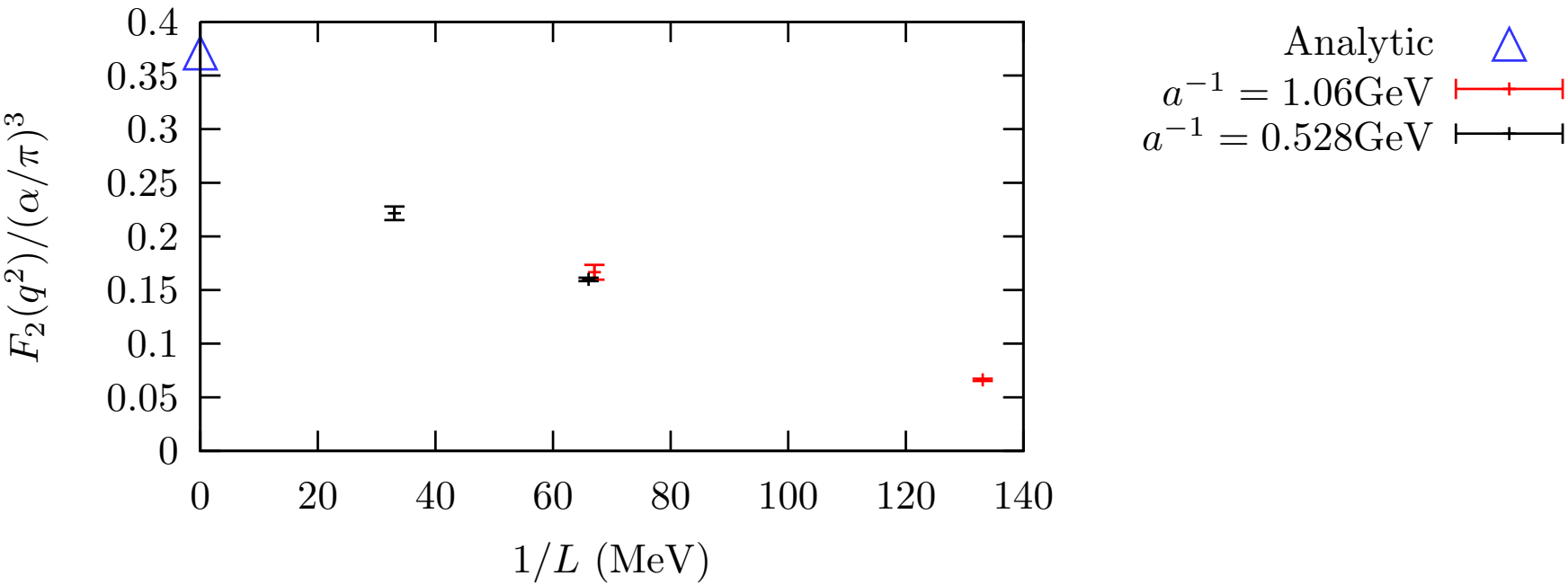

Figure 14. Finite volume effect on F_2.

- Lattice sizes are $16^3 \times 64$, $8^3 \times 32$ with $L_s = 8$ and $t_{\rm snk} - t_{\rm op} = t_{\rm op} - t_{\rm src} = T/4$.
- The simulations were done in L^3 volume and momentum transfer $q = 2\pi/L$.
- Muon mass is $m_\mu = 106\text{MeV}$. a is the lattice spacing.

	Model	Subtraction
$\frac{F_2 \pm \mathrm{Err}}{(\alpha/\pi)^3}$	0.08 ± 0.02	0.29 ± 0.06

Table 2. Hadronic Light by Light Estimates, values were also shown in section 2.

- Model: Glasgow Consensus, 2007
- Subtraction: Using the experimental $g-2$ value, E821, The $g-2$ Collab. 2006 and subtract the theoretical values of other contributions.
- First lattice attempt: T. Blum, S. Chowdhury, M. Hayakawa, T. Izubuchi, Phys. Rev. Lett. 114, 012001 (2015).

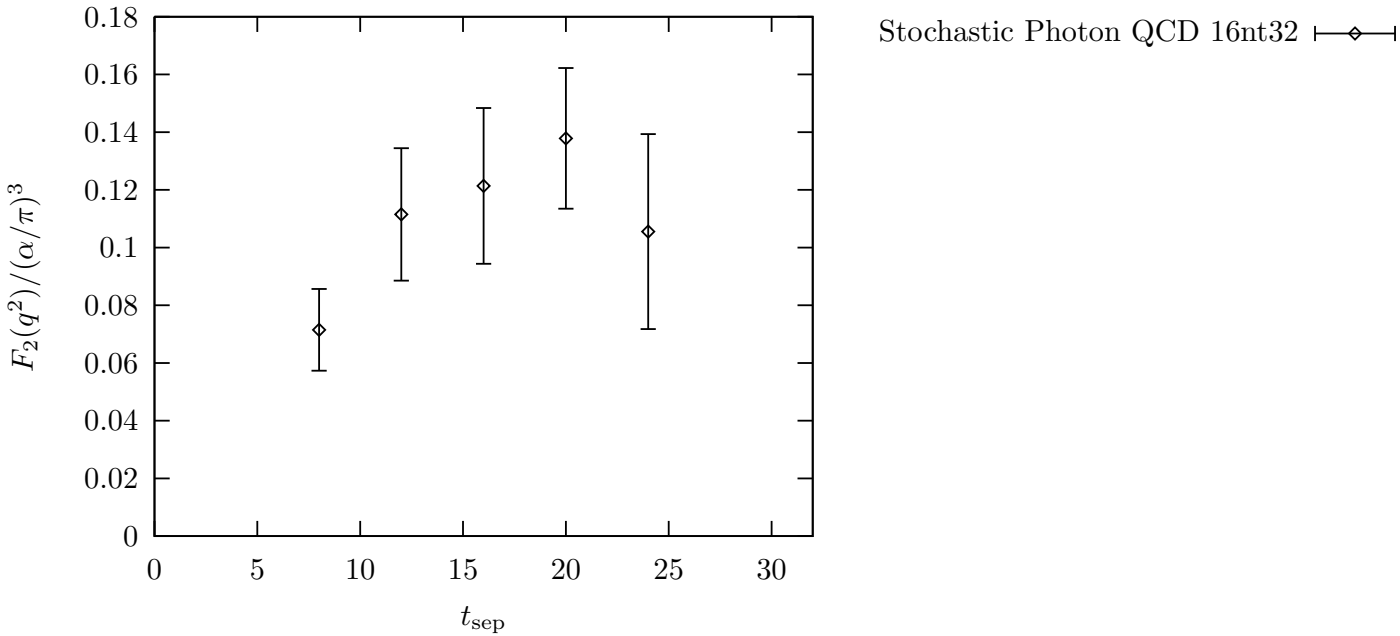

Figure 15. Excited effects on F_2. $16^3 \times 32$ lattice, with $a^{-1} = 1.747\text{GeV}$, $m_\pi = 424\text{MeV}$, $m_K = 613\text{MeV}$, $m_\mu = 332\text{MeV}$.

Outline

1. Muon Anomalous Magnetic Moment
2. BNL E821 (0.54 ppm) and Standard Model Prediction
3. Lattice QED with Schwinger Term as an Example
4. Stochastic Photon Light by Light
5. **Point Source Photon Light by Light**
   i. Comparison
   ii. Formula
   iii. Features
   iv. Distribution 16I
   v. Distribution 32ID
6. Current Status and Outlook

Point Source Photon Light by Light - Comparison

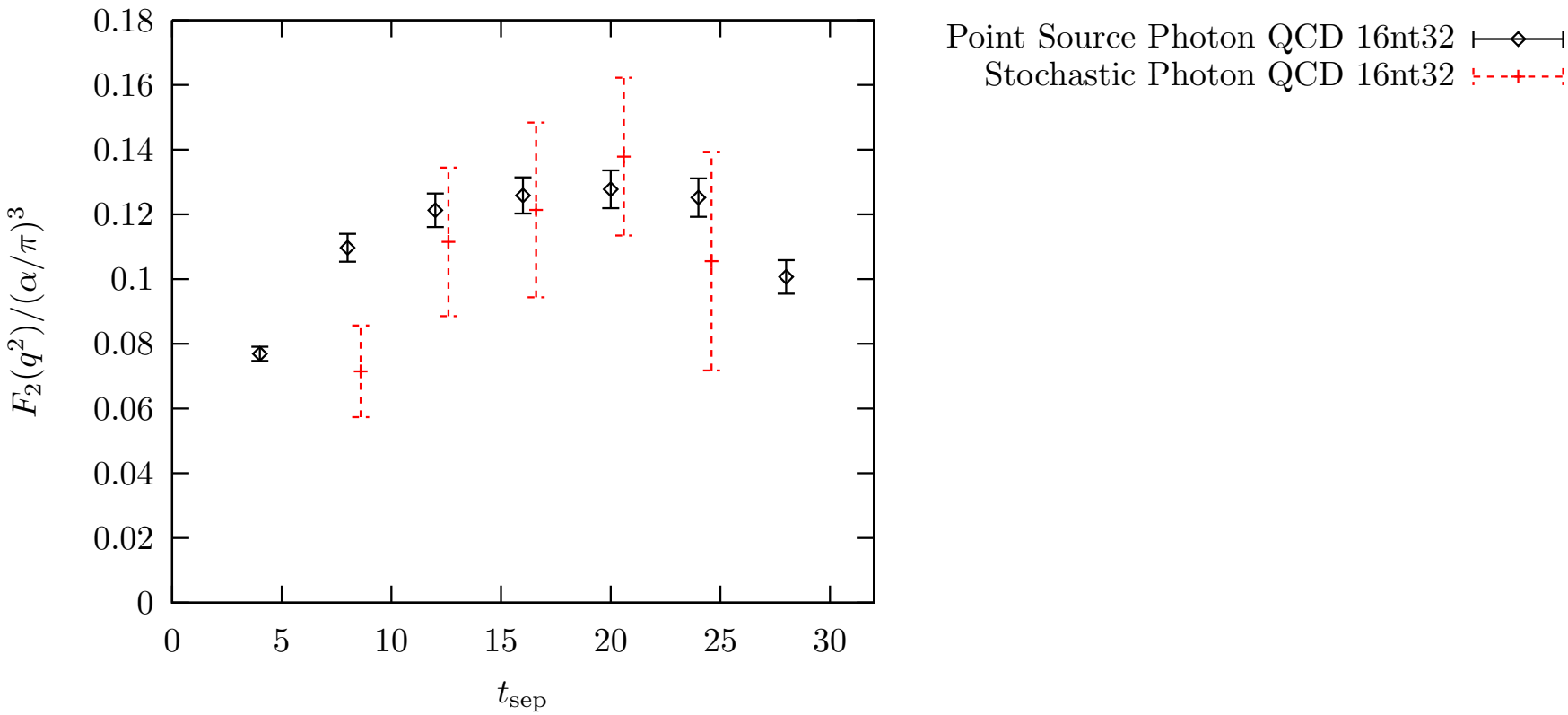

Figure 16. Excited effects on F_2. $16^3 \times 32$ lattice, with $a^{-1} = 1.747\text{GeV}$, $m_\pi = 424\text{MeV}$, $m_\mu = 332\text{MeV}$. Here we compare the new point source method with the old stochastic photon method.

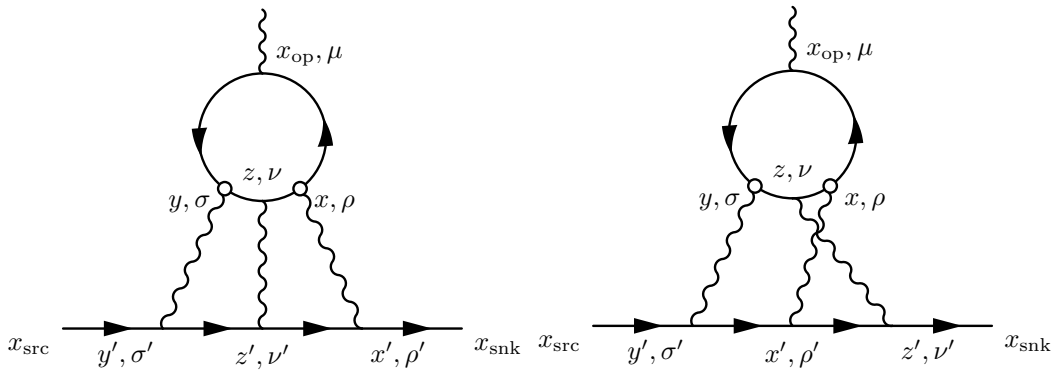

Figure 17. Light by Light diagrams. There are 4 other possible permutations.

$$\begin{aligned}\mathcal{M}_\mu^{\rm LbL}(\mathbf{q}) &= e^{i\mathbf{q}\cdot\mathbf{x}_{\rm op}}\mathcal{M}_\mu^{\rm LbL}(\mathbf{q}; x_{\rm op}) \\ &= \sum_{x,y}\sum_{z} F_{\mathbf{q}}(x, y; z, x_{\rm op}) \qquad (12)\\ &= \sum_{r}\left[\sum_{z, x_{\rm op}} F'_{\mathbf{q}}(x_{\rm ref}, r; z, x_{\rm op})\right] \qquad (13)\end{aligned}$$

$$x_{\rm ref} = \frac{x+y}{2} \qquad r = y - x \qquad (14)$$

$$F'_{\mathbf{q}}(x_{\rm ref}, r; z, x_{\rm op}) = F_{\mathbf{q}}(x, y; z, x_{\rm op}) \qquad (15)$$

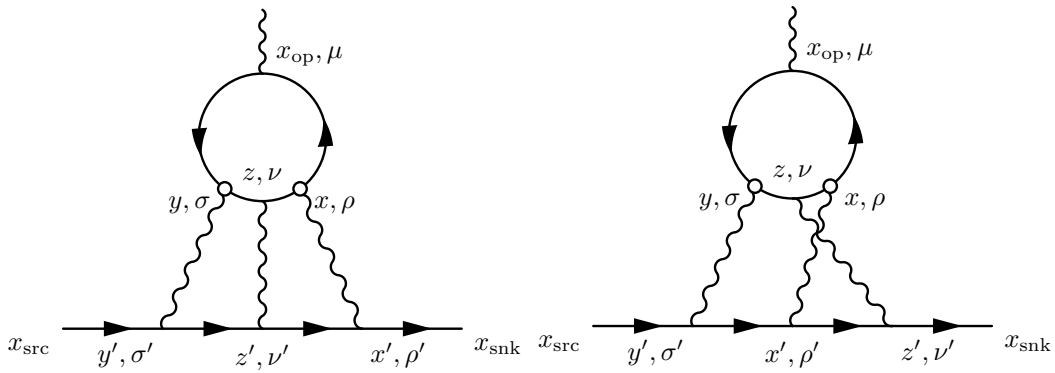

Figure 18. Light by Light diagrams. There are 4 other possible permutations.

$$
\begin{aligned}
F_{\mathbf{q}}(x, y; z, x_{\rm op}) \;=\; & e^{i\mathbf{q}\cdot\mathbf{x}_{\rm op}} \lim_{t_{\rm src}\to-\infty, t_{\rm snk}\to+\infty} e^{E_{\mathbf{q}/2} t_{\rm sep}} \\
& \cdot \sum_{\mathbf{x}_{\rm snk}, \mathbf{x}_{\rm src}} e^{-i\mathbf{q}/2\cdot\mathbf{x}_{\rm src}} e^{-i\mathbf{q}/2\cdot\mathbf{x}_{\rm snk}} (-)(-ie)^6 \\
& \cdot \left\langle \sum_q \mathrm{tr}(\gamma_\mu S_q(x_{\rm op}, x)\gamma_\rho S_q(x, z)\gamma_\nu S_q(z, y)\gamma_\sigma S_q(y, x_{\rm op})) \right\rangle_{\rm QCD} \\
& \cdot \sum_{x', y', z'} G_{\rho\rho'}(x, x') G_{\sigma\sigma'}(y, y') G_{\nu\nu'}(z, z') \\
& \cdot [\, S(x_{\rm snk}, x')\gamma_{\rho'} S(x', z')\gamma_{\nu'} S(z', y')\gamma_{\sigma'} S(y', x_{\rm src}) \\
& + S(x_{\rm snk}, z')\gamma_{\nu'} S(z', x')\gamma_{\rho'} S(x', y')\gamma_{\sigma'} S(y', x_{\rm src}) \\
& + \text{other 4 permutations}] \qquad (16)
\end{aligned}
$$

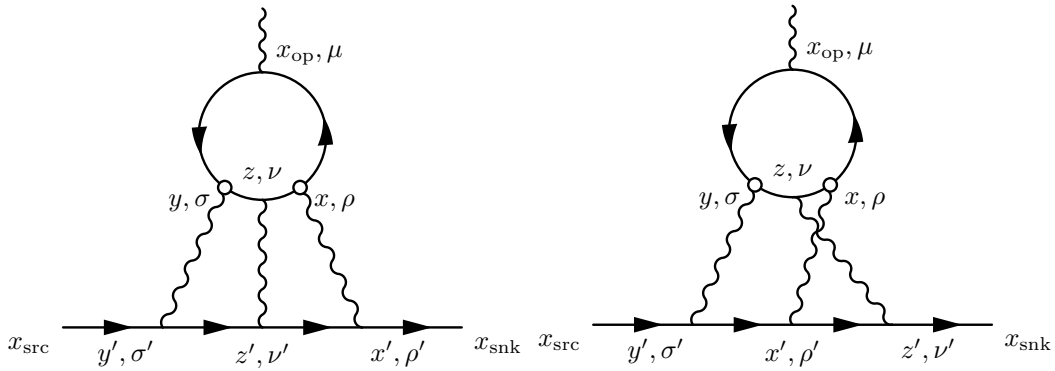

Figure 19. Light by Light diagrams. There are 4 other possible permutations.

- M^2 statistics: We use two point source propagators to calculate the QCD four point function. We can calculate M point source propagators and calculate the QCD four point function with $M(M-1)/2$ combinations.
- Importance sampling: We use importance sampling when choosing the M points. So we calculate the region that contribute to the noise the most with the highest frequency but lowest weight.
- Exact short distance: We can calculate all the short distance part of the sum without using the Monte Carlo technique.
- Conserved current: In order to make the loop integral converge, the external photon need to couple to conserved current, while all the three internal photons may couple to local currents.

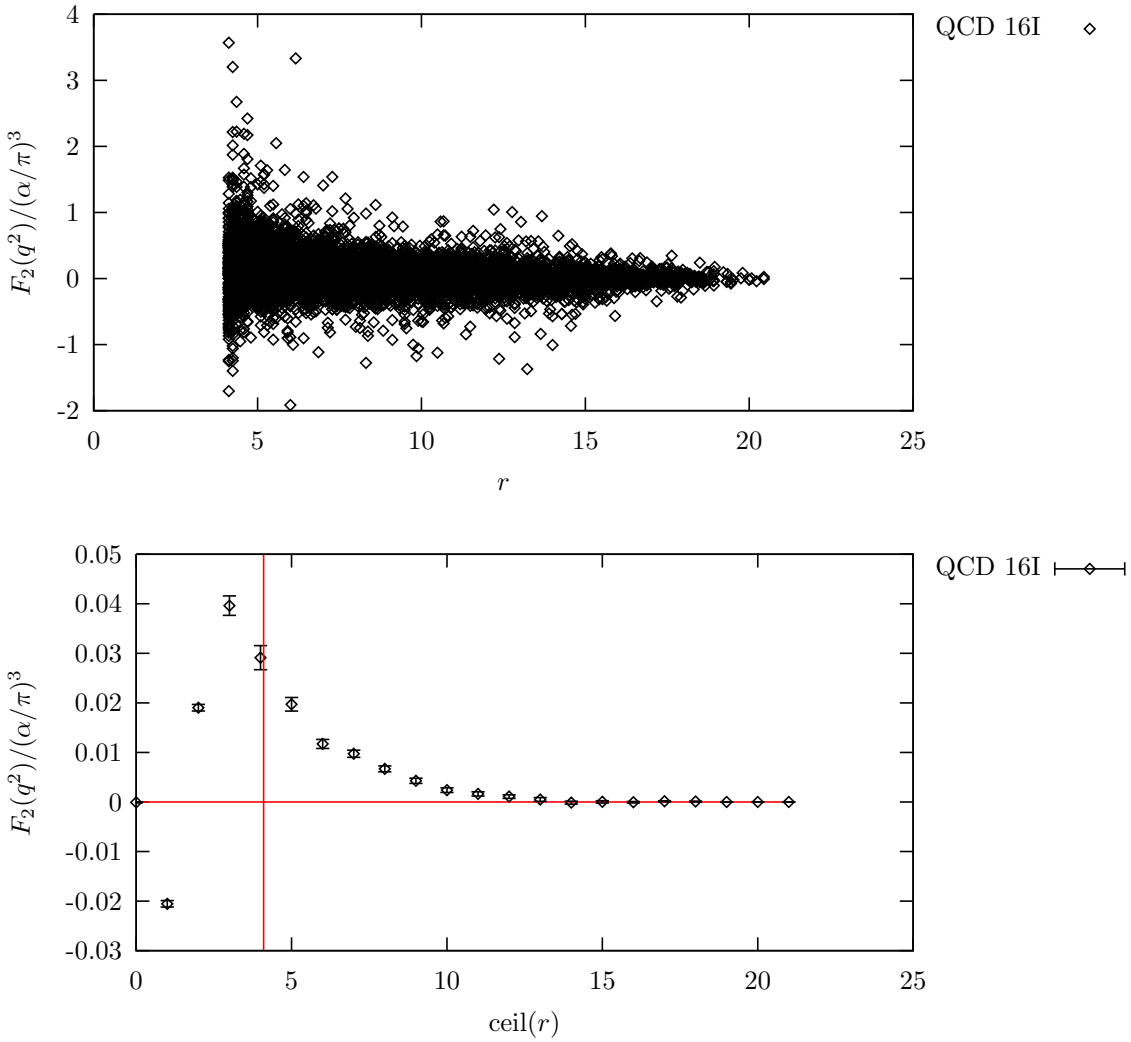

Figure 20. $16^3 \times 32$ lattice, with $a^{-1} = 1.747\text{GeV}$, $m_\pi = 424\text{MeV}$, $m_\mu = 332\text{MeV}$.

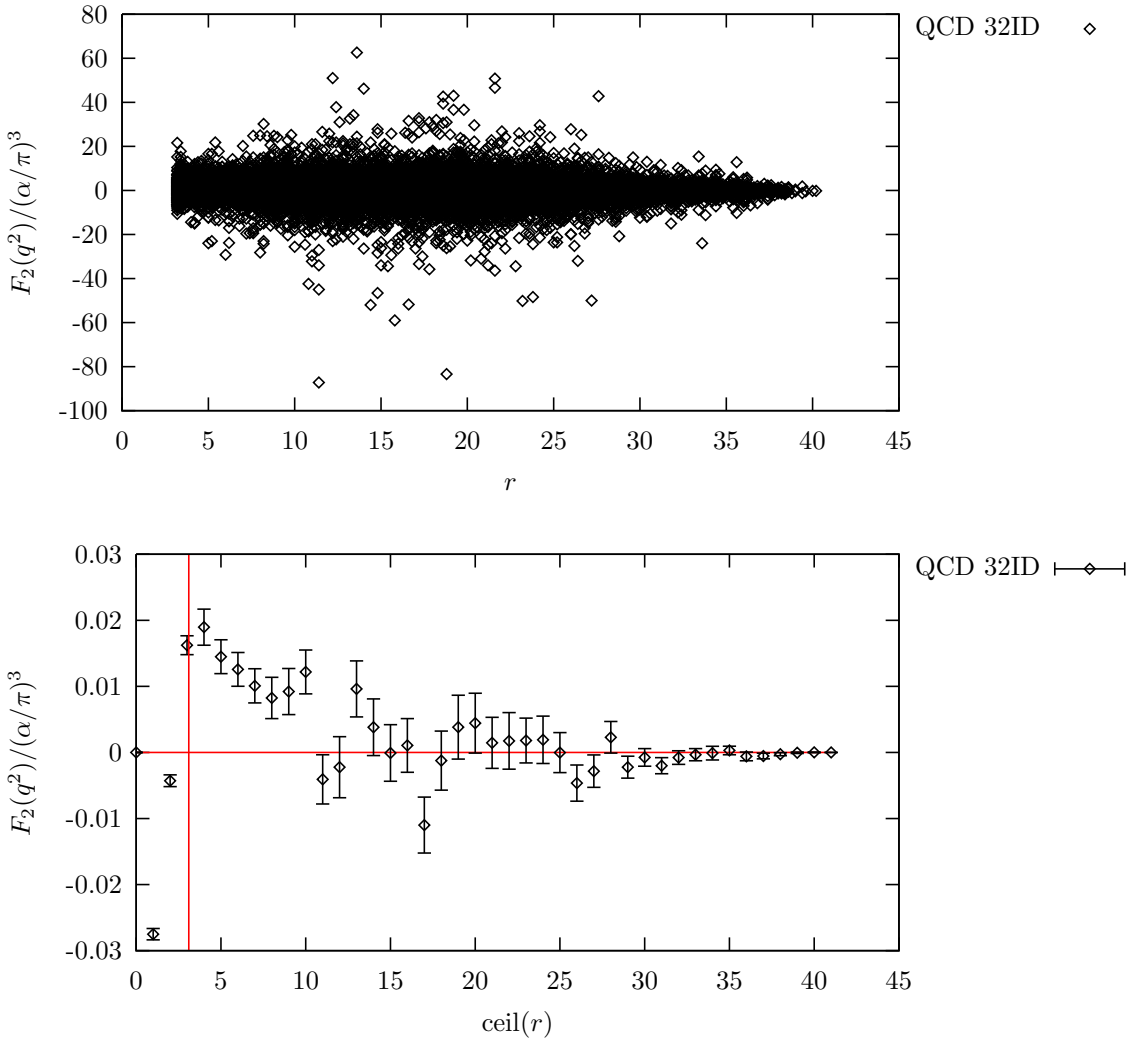

Figure 21. $32^3 \times 64$ lattice, with $a^{-1} = 1.371\,\mathrm{GeV}$, $m_\pi = 171\,\mathrm{MeV}$, $m_\mu = 134\,\mathrm{MeV}$.

Outline

1. Muon Anomalous Magnetic Moment
2. BNL E821 (0.54 ppm) and Standard Model Prediction
3. Lattice QED with Schwinger Term as an Example
4. Stochastic Photon Light by Light
5. Point Source Photon Light by Light
6. **Current Status and Outlook**

Label	size	$\frac{2\pi}{m_\mu L}$	m_π/GeV	#qcdtraj	t_{sep}	$\frac{F_2 \pm \mathrm{Err}}{(\alpha/\pi)^3}$	$\frac{\mathrm{Cost}}{\mathrm{BG/Q\ rack\ days}}$
16I	$16^3 \times 32$	2.07	0.423	8	16	0.1248 ± 0.0047	0.31
24I	$24^3 \times 64$	1.38	0.423	5	32	0.2436 ± 0.0181	0.85
24I-L	$24^3 \times 64$	1.74	0.333	5	32	0.1676 ± 0.0091	0.85
32ID	$32^3 \times 64$	2.00	0.171	47	32	0.0693 ± 0.0218	10

Table 3. Central values and errors. $a^{-1} = 1.747\mathrm{GeV}$. Muon mass and pion mass ratio is fixed at physical value. #prop is the number of propagator calculated for the loop.

- We plan to follow this with a calculation with a physical pion mass and a $6\mathrm{fm}$ volume with either $a = 0.18\mathrm{fm}$ or $a = 0.12\mathrm{fm}$ depending on the computer time needed.
- Possible strategies for the calculation of all disconnected diagrams are being developed and we hope to begin numerical experiments this year.

Thank You!

Progress towards an *ab initio*, Standard Model calculation of direct CP-violation in K decays

Christopher Kelly
(RBC & UKQCD Collaboration)

Multi-Hadron and Nonlocal Matrix Elements in Lattice QCD Workshop, Friday February 6th 2015

RIKEN BNL Research Center

BROOKHAVEN NATIONAL LABORATORY

Baryogenesis

$$\eta = \frac{n_B - n_{\bar{B}}}{n_\gamma} = 6.14(25) \times 10^{-10}$$

- The Universe is matter dominated, but why?
- Most likely explanation is existence of baryogenesis mechanism.
- Sackarov conditions (1967):
  - B-number violation
  - Non-thermal interactions (e.g. during a phase transition)
  - C and CP violation.
- Amount of CP-violation in Standard Model far too small to account for observed value.
- Most BSM theories introduce additional direct CP-violation but a precise SM value does not yet exist which could be compared to experiment.

$\mathbf{K} \to \pi\pi$ Decays

- Direct CP-violation first observed in K→ππ decays.
- Two types of decay:

$$\begin{array}{lll} \Delta I = 3/2 \ : K^+ & \to (\pi^+\pi^0)_{I=2} & \text{with amplitude} \quad A_2 \\ \Delta I = 1/2 \ : \ K^0 & \to (\pi^+\pi^-)_{I=0} & \text{with amplitude} \quad A_0 \\ \qquad\qquad K^0 & \to (\pi^0\pi^0)_{I=0} & \end{array}$$

- Direct CP-violation:

$$\epsilon' = \frac{i\omega e^{i(\delta_2-\delta_0)}}{\sqrt{2}}\left(\frac{\mathrm{Im}A_2}{\mathrm{Re}A_2} - \frac{\mathrm{Im}A_0}{\mathrm{Re}A_0}\right)$$

where

$\omega = \mathrm{Re}A_2/\mathrm{Re}A_0$ and δ_I are ππ scattering phase shifts.

- ϵ' is highly sensitive to BSM sources of CPV.
- Strong interactions very important – origin of the ΔI=1/2 rule: preference to decay to I=0 final state.

[arXiv:1212.1474]

Lattice determination

MSbar renormalization matrix using NPR and perturbative matching at high scale

$$\mathcal{A}_I = \sum_{i=1}^{7}\sum_{j=1}^{10} \mathcal{F}\frac{G_F}{\sqrt{2}} V_{us}^* V_{ud}[z_i(\mu) + \tau y_i(\mu)] Z_{ij}(\mu) \langle (\pi\pi)_I | Q_j(\mu) | K \rangle$$

Lellouch-Luscher factor relates finite to inf. vol.

MSbar perturbative Wilson coeffs for Weak effective theory

10 Weak effective four-quark operators (7 independent)

$$\tau = -\frac{V_{ts}^* V_{td}}{V_{us}^* V_{ud}} = 0.0014606 + 0.00060408i$$

This imaginary part is responsible for the CP-violation! (everything else is pure-real)

$\Delta I=3/2$ Calculation

- Original physical measurement [Phys.Rev.Lett. 108 (2012) 141601]

$$\mathrm{Re}(A_2) = 1.38(5)_{\mathrm{stat}}(26)_{\mathrm{sys}} \times 10^{-8}\ \mathrm{GeV}$$
$$\mathrm{Im}(A_2) = -6.54(46)_{\mathrm{stat}}(120)_{\mathrm{sys}} \times 10^{-13}\ \mathrm{GeV}$$

20% sys error dominated by 15% discretization error

- Calculation has now been repeated on RBC & UKQCD 48^3x96 and 64^3x128 Mobius DWF ensembles with (5 fm)^3 volumes and a=0.114 fm, a=0.084 fm.
- Make full use of eigCG and AMA to translate over all timeslices. Obtain 0.7-0.9% stat errors on all bare matrix elements!

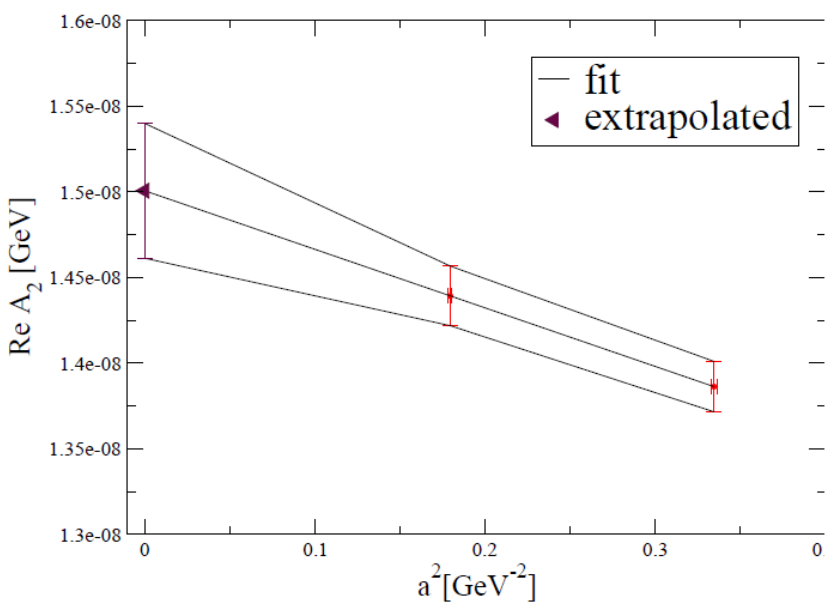

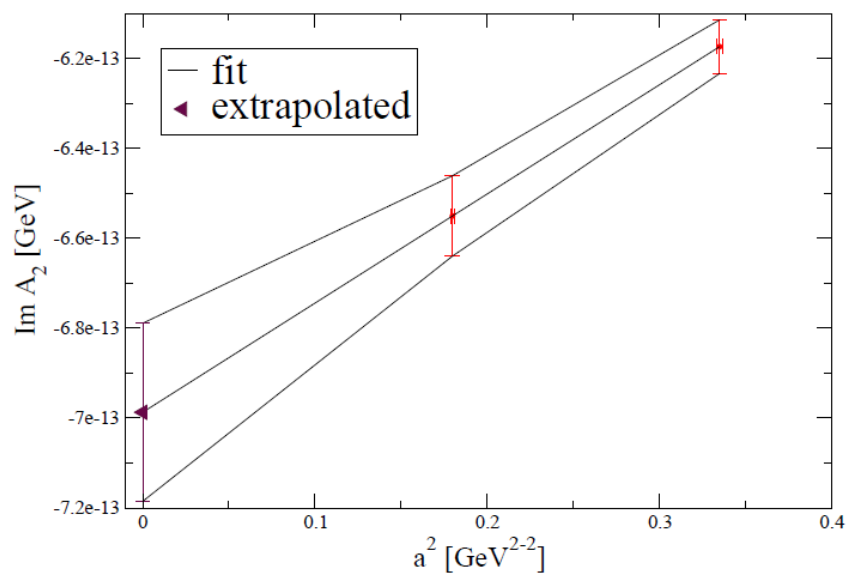

- New results published Monday: [arXiv:1502.00263]

$$\mathrm{Re}(A_2) = 1.50(4)_{\mathrm{stat}}(14)_{\mathrm{sys}} \times 10^{-8}\ \mathrm{GeV}$$
$$\mathrm{Im}(A_2) = -6.99(20)_{\mathrm{stat}}(84)_{\mathrm{sys}} \times 10^{-13}\ \mathrm{GeV}$$

10%, 12% total errors on Re, Im!

Systematic errors in $\mathrm{Im}A_2/\mathrm{Re}A_2$	48^3	64^3	cont
NPR (nonperturbative)	0.1%	0.1%	0.1%
NPR (perturbative)	7.6 %	6.7 %	7.6 %
Finite volume corrections	3.5 %	3.5 %	3.5 %
Unphysical kinematics	1.8 %	4.6%	4.6%
Wilson coefficients	12.0 %	10.5 %	12.0%
Derivative of the phase shift	0	0	0
Total	14.7%	13.7%	15.3%

TABLE XIII: Systematic error breakdown for $\mathrm{Im}A_2/\mathrm{Re}A_2$.

- Systematic error completely dominated by perturbative error on NPR and Wilson coefficients.
- Future considerations:
    - Higher order PT calculation of NPR and Wilson coeffs.
    - Step-scaling NPR to higher energy scale.

$\Delta I=1/2$ Calculation

- A_0 is significantly more difficult than A_2 for two reasons:

1) Disconnected diagrams

- $\pi\pi$ has same quantum numbers as vacuum, hence there are disconnected diagrams of the form:

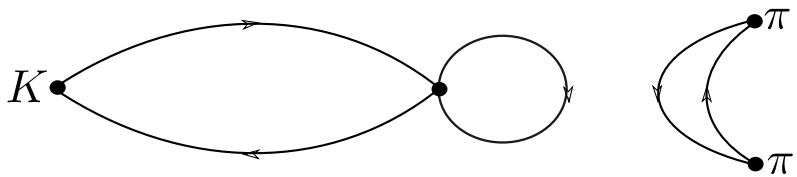

- These are extremely noisy and dominate stat error.
- We use A2A method with O(1000) exact low modes and stochastic high modes with spin, color and flavor dilution.
- Disconnected diagram evaluated for all lattice sites for maximum statistical resolution.

2) Obtaining Physical Kinematics

- Physical decay is energy conserving but lattice ground-state comprises two stationary pions (after explicit vacuum subtraction for I=0): $2\,E_\pi << m_K$
- Avoid multi-exponential fits by modifying spatial BCs to remove stationary pion state.
- Must measure $K^0 \to \pi^0\pi^0$ and $K^0 \to \pi^+\pi^-$ with I=0 final state. Boundary conditions must therefore:
  - Conserve isospin such that I=0 state can be isolated.
  - Give momentum to both charged and neutral pions.
- In I=2 calculation we used twisted BCs applied to the d-quark, but this satisfies neither of the above conditions.
- Instead, we use G-parity BCs:

$$\hat{G} = \hat{C} e^{i\pi \hat{I}_y} \quad : \quad \hat{G}|\pi^\pm\rangle = -|\pi^\pm\rangle$$
$$\hat{G}|\pi^0\rangle = -|\pi^0\rangle$$

- As a boundary condition:
  $\pi^i(x+L) = \hat{G}\pi^i(x) = -\pi^i(x)$

→ Discretized lattice momenta
$|p| \in (\pi/L,\, 3\pi/L,\, 5\pi/L \ldots)$
Moving ground-state

Demonstration

- 16^3x32 DWF+Iwasaki a^{-1} = 1.73(3) GeV with 420 MeV pion test configurations with GPBC in 0,1,2 directions.

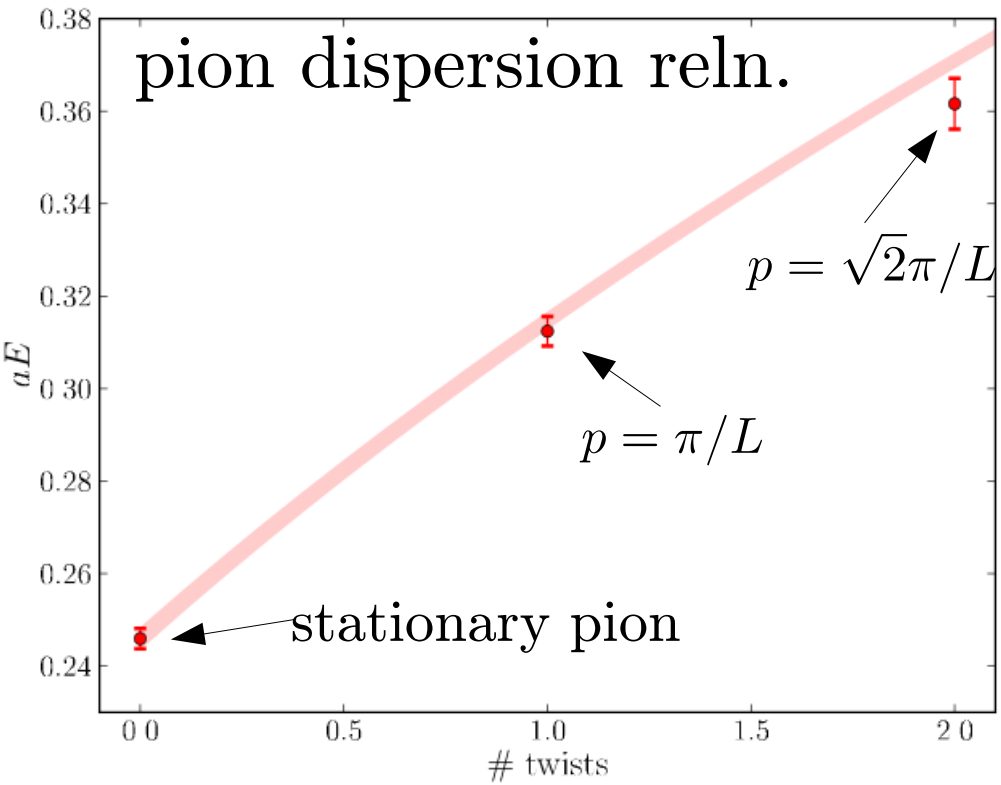

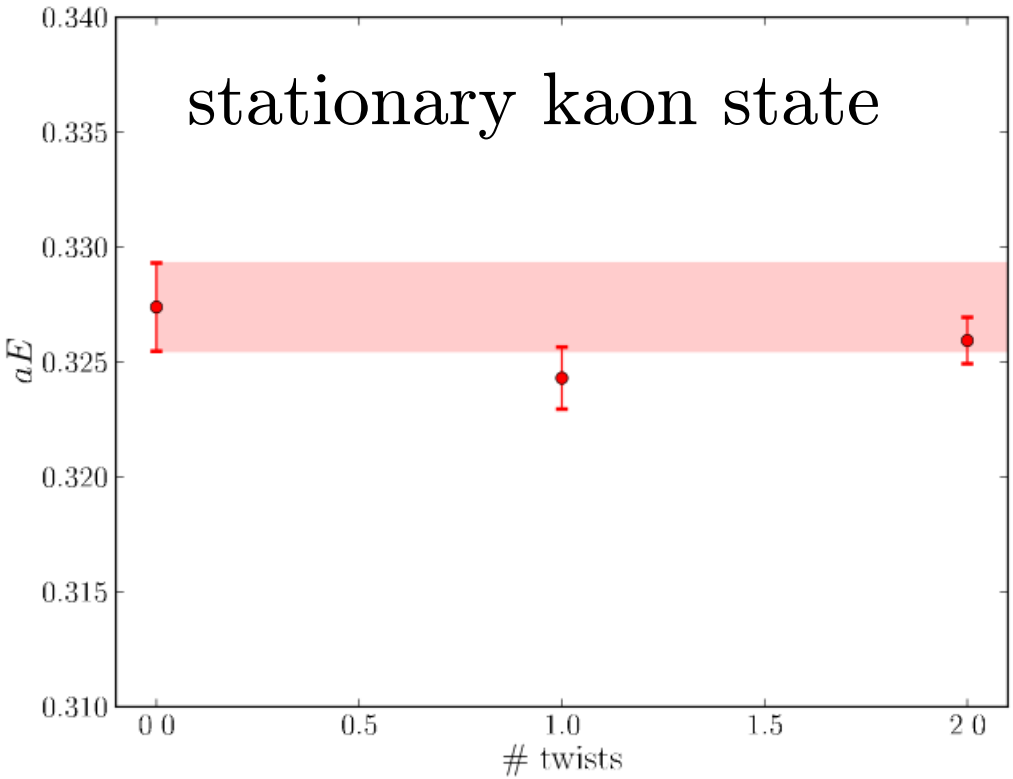

Direct comparison of ΔI=3/2 amplitudes between GPBC and twisted BCs, both in 3 directions, on 16^3 ensembles

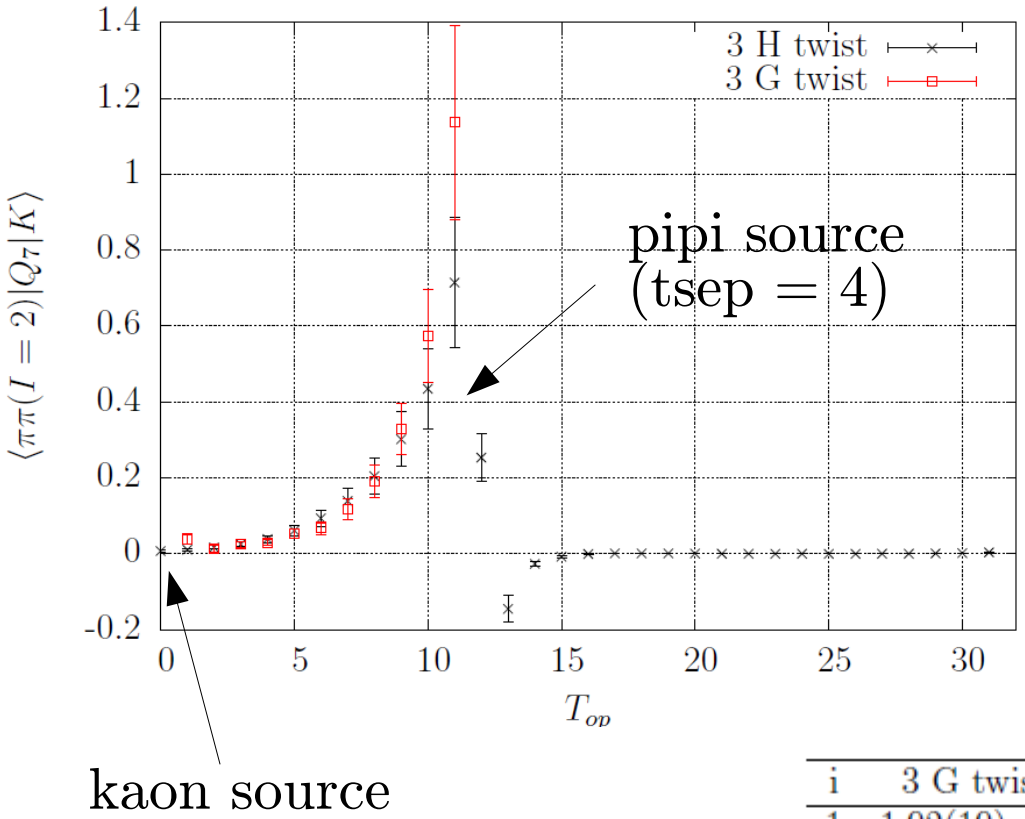

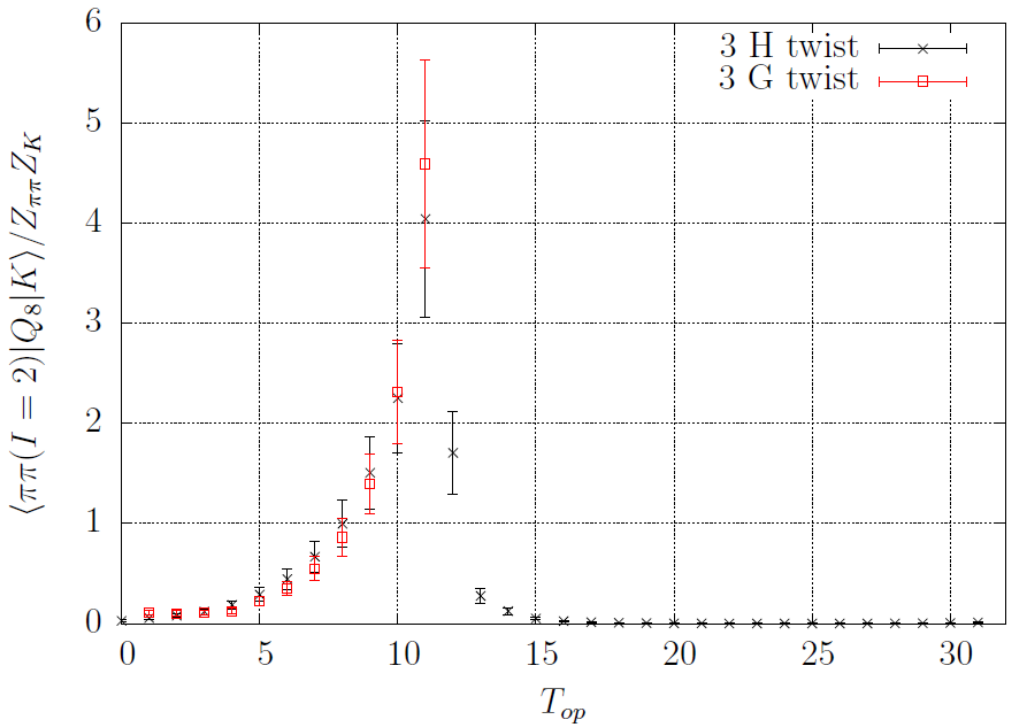

i	3 G twist	3 H twist
1	1.92(19)e-03	2.10(12)e-03
7	6.41(45)e-03	6.03(32)e-03
8	2.98(16)e-02	2.91(15)e-02

Table 7: Fitting results of $\frac{\langle\pi\pi|Q_i|K\rangle}{Z_K Z_{\pi\pi} e^{-E_{\pi\pi}\Delta_T}}$. Fitting range [4:8].

	3 G twist	3 H twist
$E_{\pi\pi(I=2)}$	0.922(25)	0.955(27)

Table 8: Fitting results of pipi(I=2)

Preliminary Results

Physical Ensemble

- To-date generated 988 configs (~688 thermalized).
- Utilizing USQCD 512-node BG/Q machine.

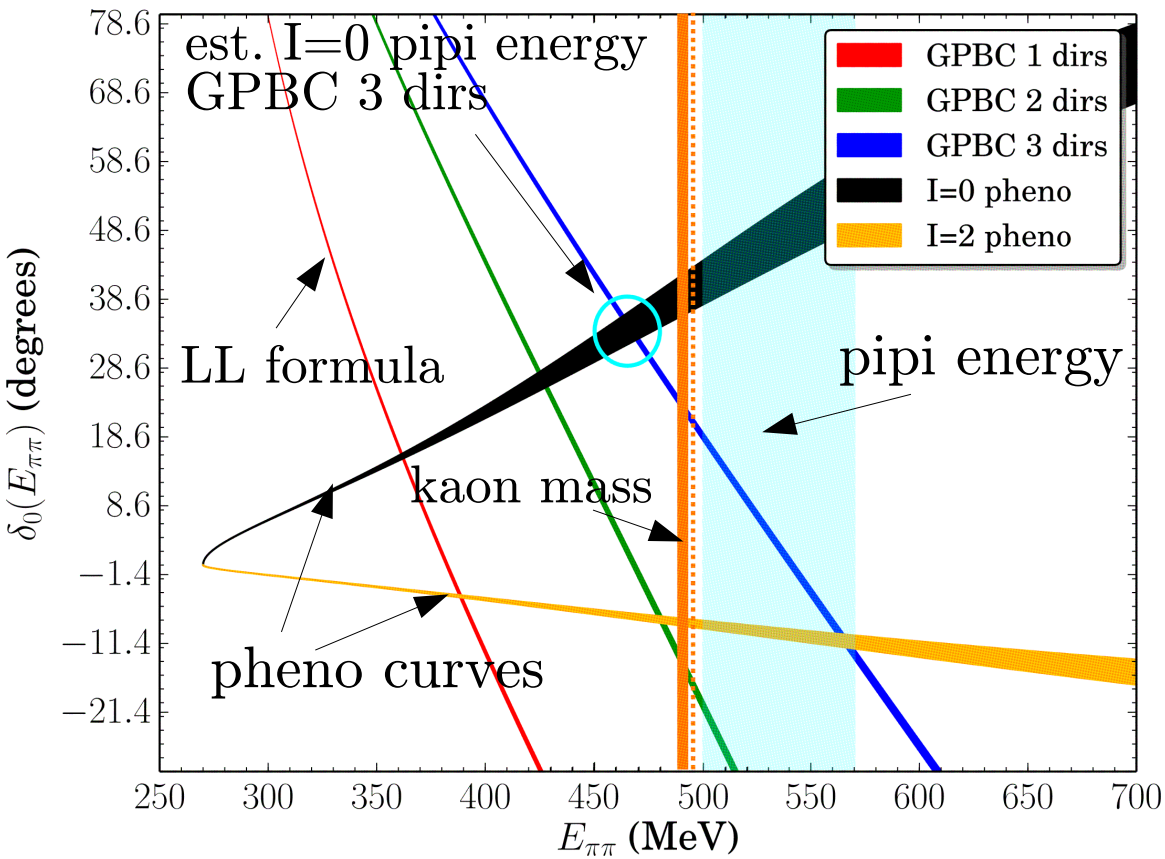

- For 32^3x64 a^{-1} ~1.38 GeV DWF+IDSDR β=1.75 close match with GPBC in 3 dirn.
- 4.6 fm^3 box.
- Measure (161 confs):

E_π=274.7(14) MeV

m_π~143.2(11) MeV

m_K=490.2(24) MeV

$E_{\pi\pi}$(I=0) = 534(34) MeV

$E_{\pi\pi}$(I=2) = 572(3) MeV

Effective Energies

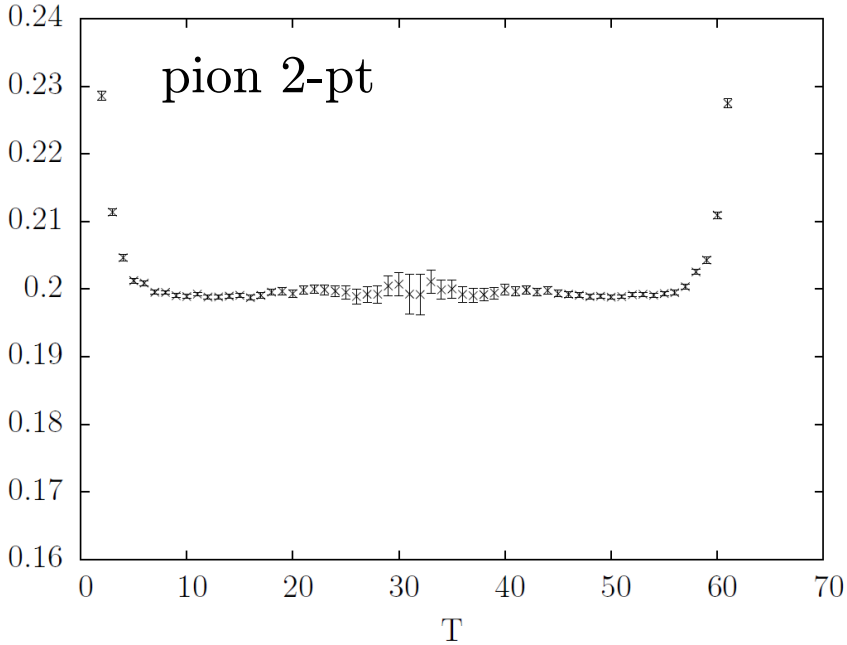

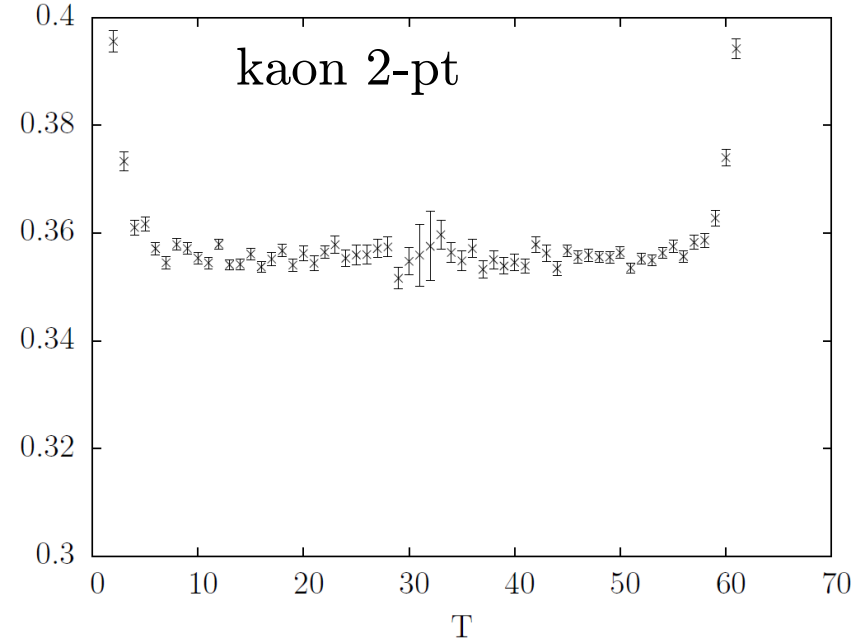

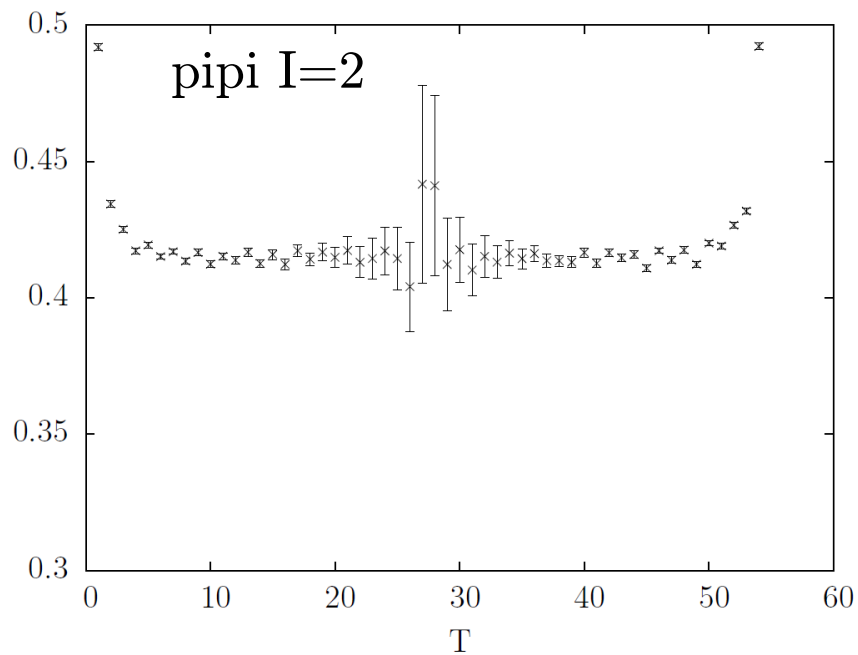

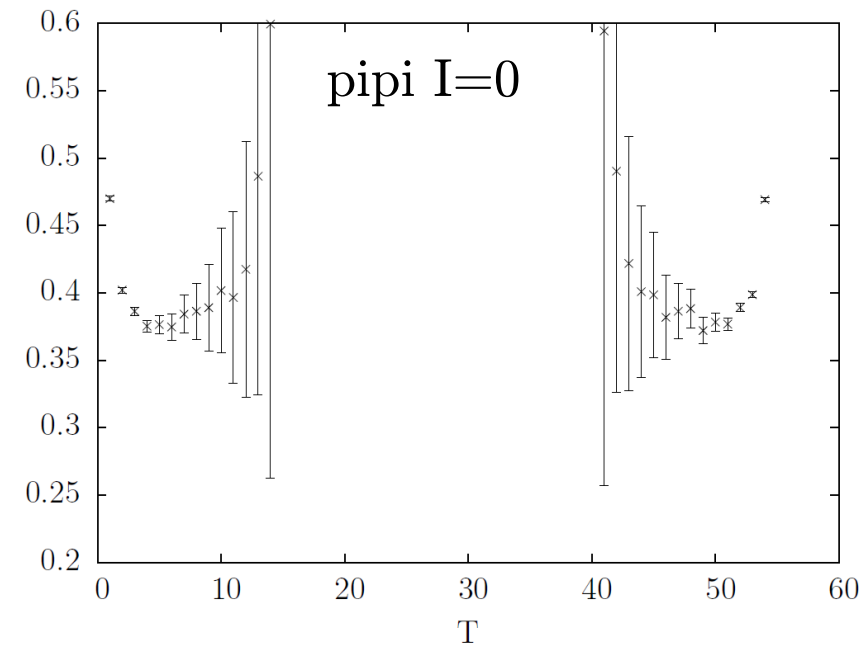

- Measure with K-pipi separations of 10,12 and 14.
- Currently measured 161 configurations.
- Error is completely dominated by disconnected diagrams.

$$\frac{\langle \pi\pi(t{=}12)|Q_2(t{=}T_{op})|K(t{=}0)\rangle}{Z_K Z_{\pi\pi} e^{-m_{\pi\pi}*12}}$$

[Dominant contribution to Re(A_0)]

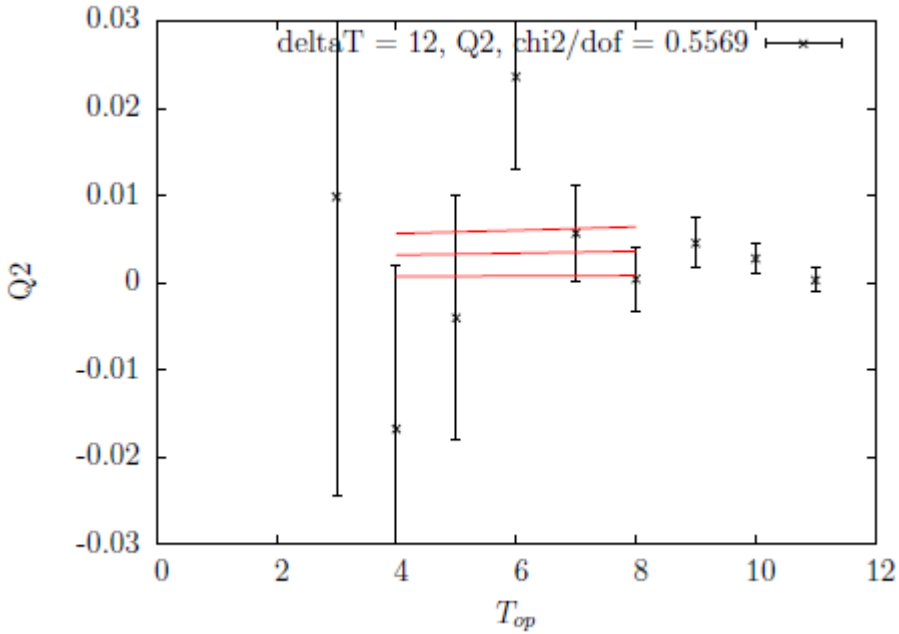

$$\frac{\langle \pi\pi(t{=}12)|Q_6(t{=}T_{op})|K(t{=}0)\rangle}{Z_K Z_{\pi\pi} e^{-m_{\pi\pi}*12}}$$

[Dominant contribution to Im(A_0)]

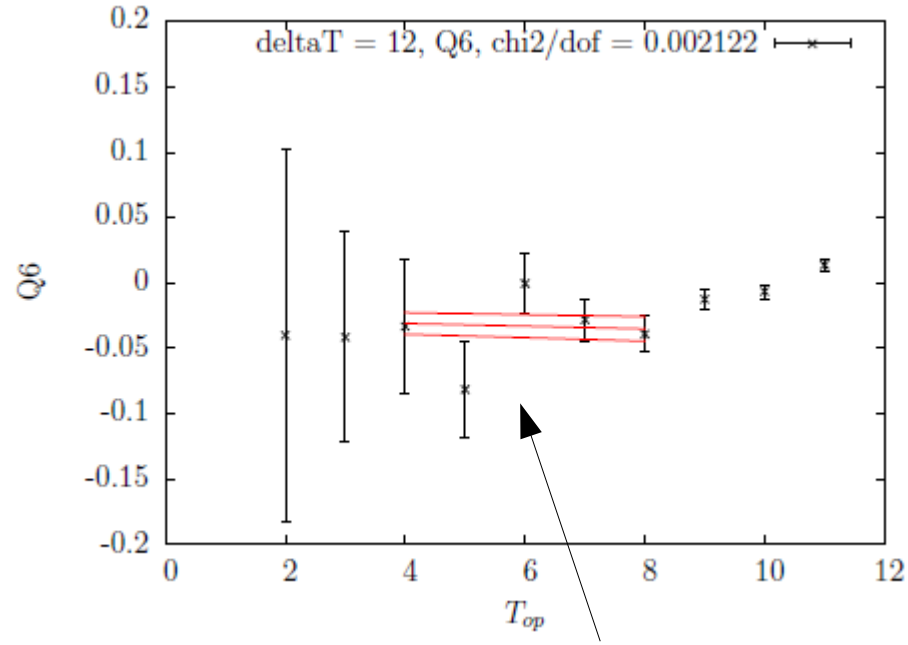

slight slope is due to small difference between kaon and pipi energies

- Currently obtain 35% errors on Im(A_0) and 30% on Re(A_0).
- Re(A_0) can be precisely determined in expt, so only Im(A_0) is important.
- Currently obtain stat error on ε' approx 2x experimental error if we use Re(A_0) from expt.

Systematic Errors

Two main sources of sys error:

- Discretization effects (~15%)
  - We currently measure using only one coarse lattice spacing.
  - Future calculations will need to be performed on multiple lattice spacings, like A_2 analysis.
- Wilson coefficients (unknown)
  - Unlike A_2, charm effects possibly play a significant role.
  - Our calculation is performed in the 3-flavor effective theory where the charm has been integrated out perturbatively.
  - Charm is light so it is not clear how reliable this is.
  - Ultimately we will need to perform a full 4-flavor dynamical calculation.
  - To estimate error we are looking into a direct comparison of a 3-flavor threshold calculation and a 4-flavor calculation on the same lattice (partially-quenched charm).

Conclusions

Conclusions and Outlook

- We have now measured A_2 with 2-3% stat error and 10% systematic.
- Sys. error is dominated by perturbative matching to MSbar and can be reduced by higher-order calculation or step-scaling to higher energies.

- A_0 calculation has begun using a single coarse lattice but with physical kinematics.
- Preliminary results from 161 meas give 35% stat errors on $\mathrm{Im}(A_0)$ and error on ε' about 2x expt. if we use $\mathrm{Re}(A_0)$ from expt.
- Sys. errors dominated by discretization effects and use of 3-flavor Wilson coeffs. Future calculations will need to be performed using multiple 4-flavor dynamical ensembles.

Subtraction term consistent with 0

$\frac{\langle\pi\pi(t{=}14)|\bar{s}\gamma_5 d(t{=}T_{op})|K(t{=}0)\rangle}{Z_K Z_{\pi\pi} e^{-m_{K^*}t_{op}-m_{\pi\pi^*}(14-t_{op})}}$ term depending on Kaon mass. Using 69 configurations

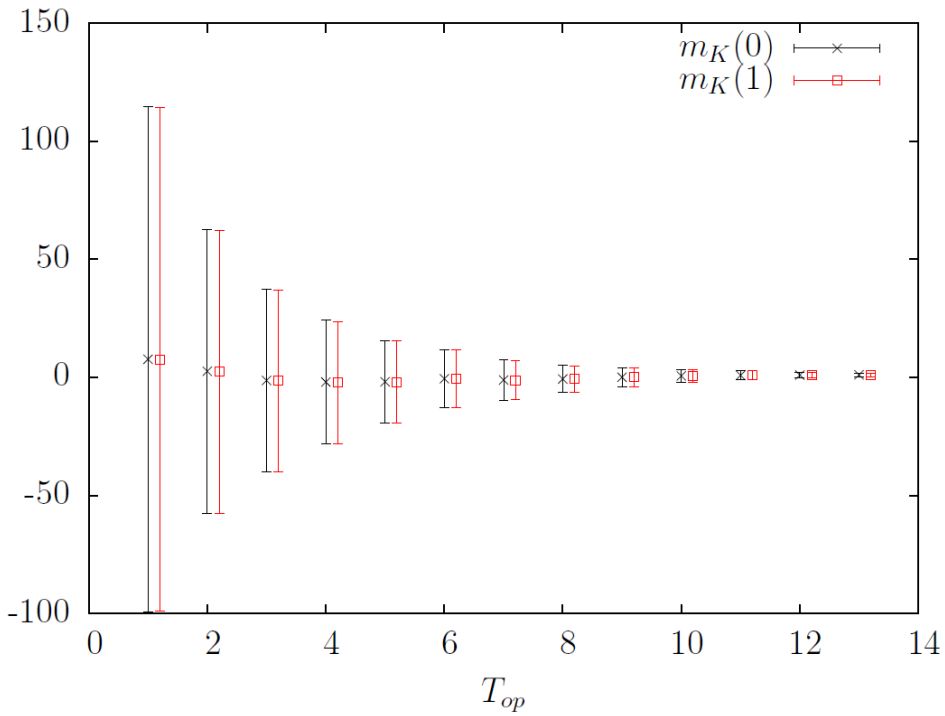

Significant effect on stat error

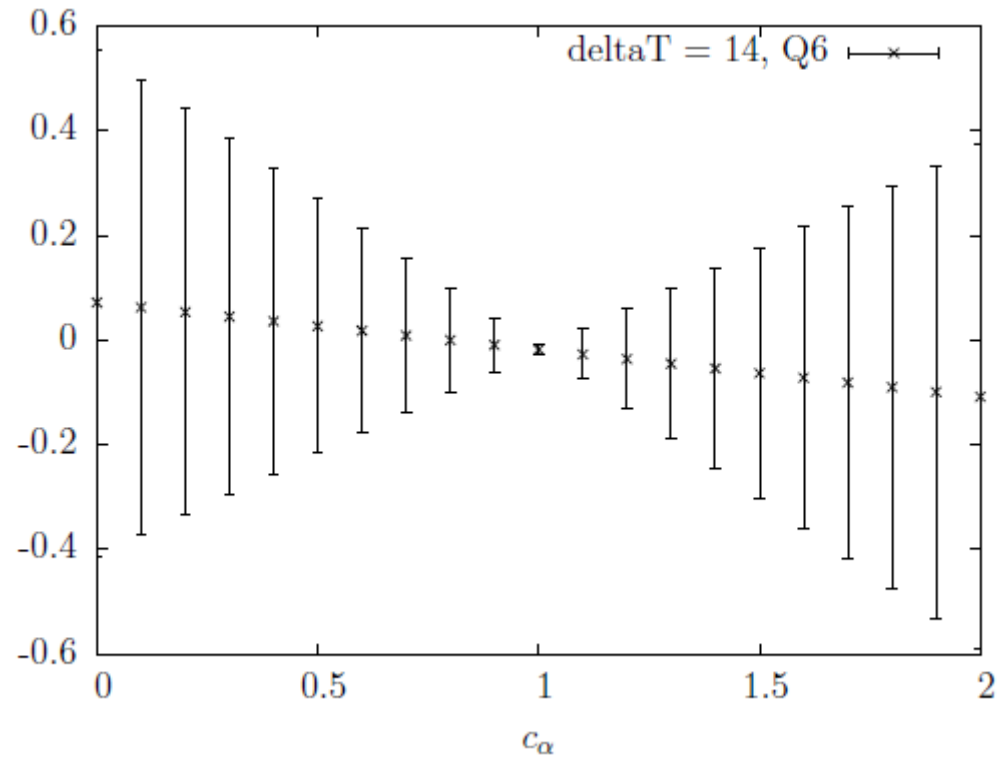

$$\frac{\langle\pi\pi(t{=}14)|Q_6(t{=}T_{op}){-}c_\alpha\alpha_i(t{=}T_{op})\bar{s}\gamma_5 d(t{=}T_{op})|K(t{=}0)\rangle}{Z_K Z_{\pi\pi} e^{-m_{\pi\pi^*}14}}.$$

Subtraction essential for signal to be obtained

G-parity BCs

- At quark level: $\hat{G}\begin{pmatrix} u \\ d \end{pmatrix} = \begin{pmatrix} -C\bar{d}^T \\ C\bar{u}^T \end{pmatrix}$ where $C = \gamma^2\gamma^4$. in our conventions
- Gauge invariance requires gauge field to obey charge conjugation (complex conjugate) boundary conditions.
- New ensembles needed (true for all modifications of BCs due to disconnected diagrams).
- For stationary kaon eigenstates we must introduce a fictional partner to the strange quark; s'

$$|\tilde{K}^0\rangle = \left(|\bar{s}d\rangle + |\bar{u}s'\rangle\right)/\sqrt{2} \quad \text{is G-parity even}$$

- Must take root of s/s' determinant to remove it from action; introduces non-locality that vanishes exponentially in L.

Implementation

- Dirac operator applied simultaneously to two fermion fields that mix at the global lattice boundary.
- Naively expect factor of 2 in cost due to two flavors. However fields are intrinsically two-flavor; use of $M^\dagger M$ in HMC to ensure positive-definite matrix requires square-root of light determinant (fourth-root for s/s')

RHMC needed throughout

- Standard double-precision multi-shift solver is quite slow due to linear algebra overheads coupled with finite BG/Q memory bandwidth.
- Developed optimized mixed-precision multi-shift inverter for RHMC in BFM/Bagel to optimize memory bandwidth usage on BG/Q.
- Alternative solution might be to use TWQCD's single-flavor action to avoid RHMC for light quarks.

Summary of code changes

- HMC and basic measurement code written in CPS, with modified BFM/Bagel solvers for BG/Q.
- Complex conjugate BCs on gauge fields required changes to virtually all aspects of the codebase:

  - Gauge fixing algorithms
  - Plaquette and rectangle, plus staples.
  - Momentum field CC BCs, gauge force.
  - Memory layout reordering code.
  - Modified CPS+BFM/Bagel Dirac ops: Shamir DWF, Mobius DWF, twisted mass (for DSDR).
  - Fermion forces.
  - Eigenvalue algorithms: Ritz, Lanczos.
  - CPS propagator code.
  - Standard measurements: two-point correlators, B_K, Wilson flow, residual mass.
  - Multi-shift optimization

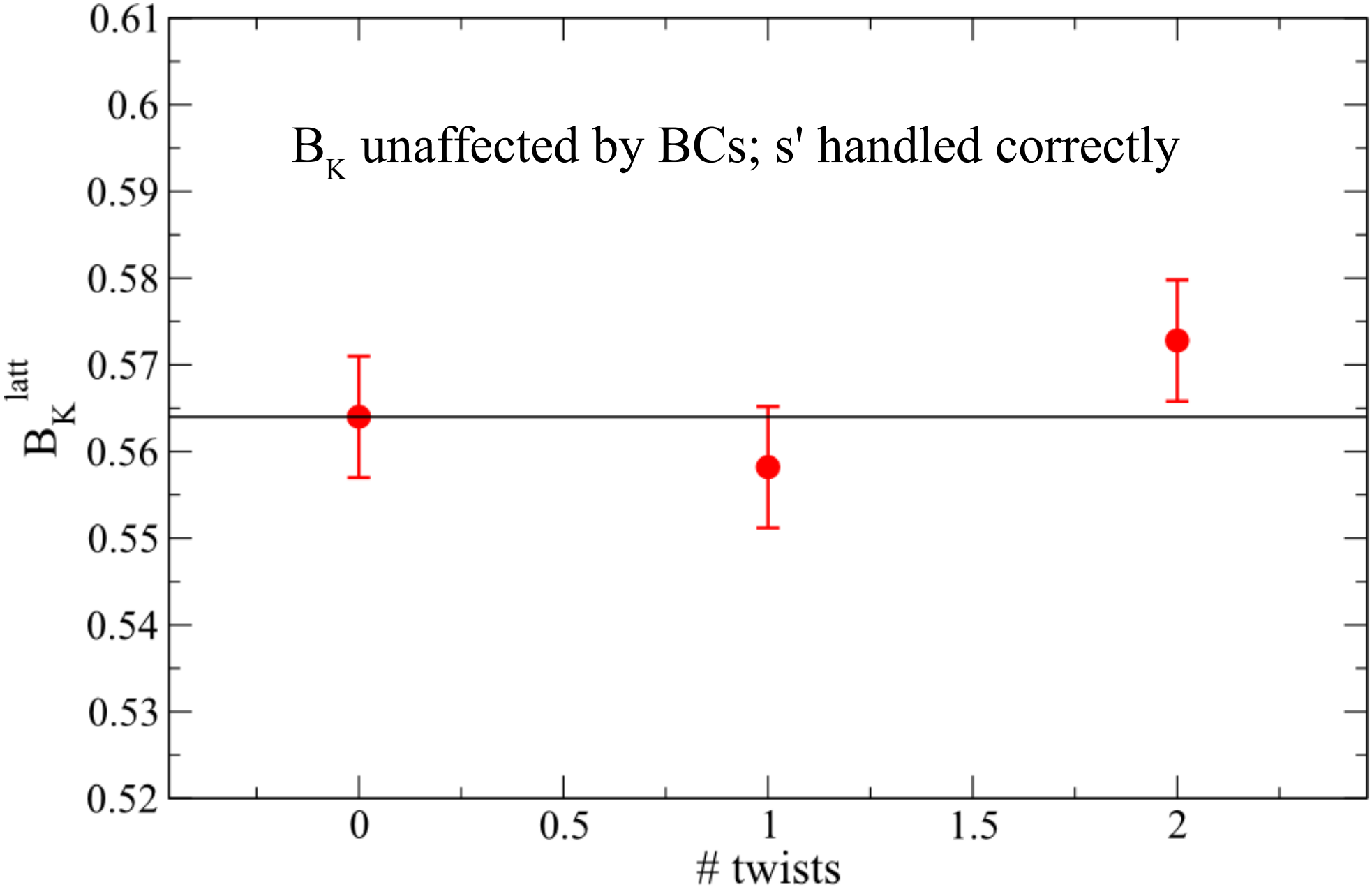
B_K unaffected by BCs; s' handled correctly
B_K^{latt}
0.61
0.6
0.59
0.58
0.57
0.56
0.55
0.54
0.53
0.52
0
0.5
1
1.5
2
twists

Ensemble Generation

- Ensemble generated on USQCD 512-node BGQ machine at BNL.
  - ~660 configurations to date.
  - Approx 400 thermalized.
  - 6.8 hours per configuration.
  - 89% Metropolis acceptance (88% theor.)

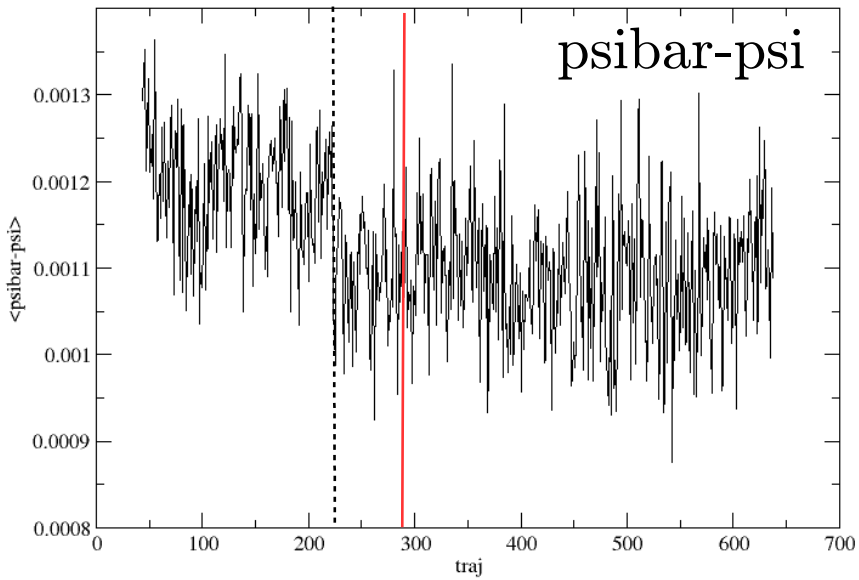

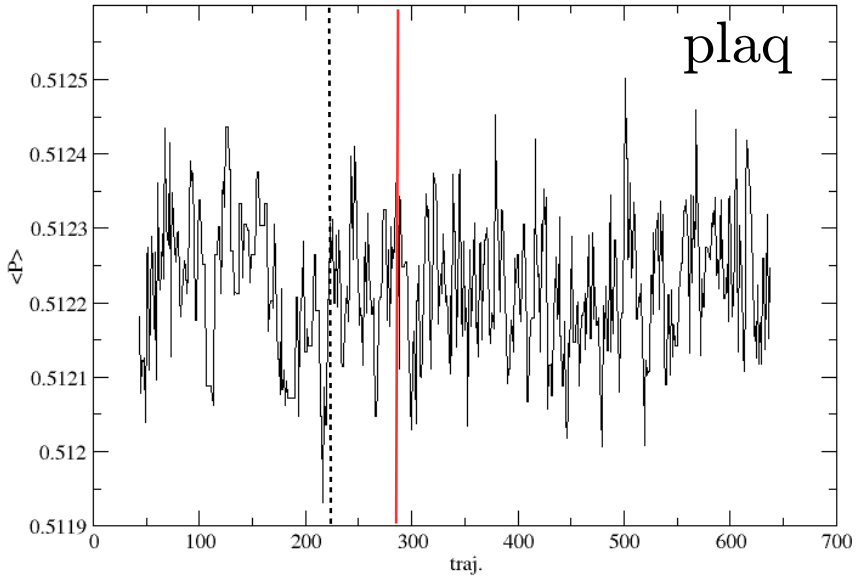

Dashed line: reduced quark mass
Red line: measurements begin (286)

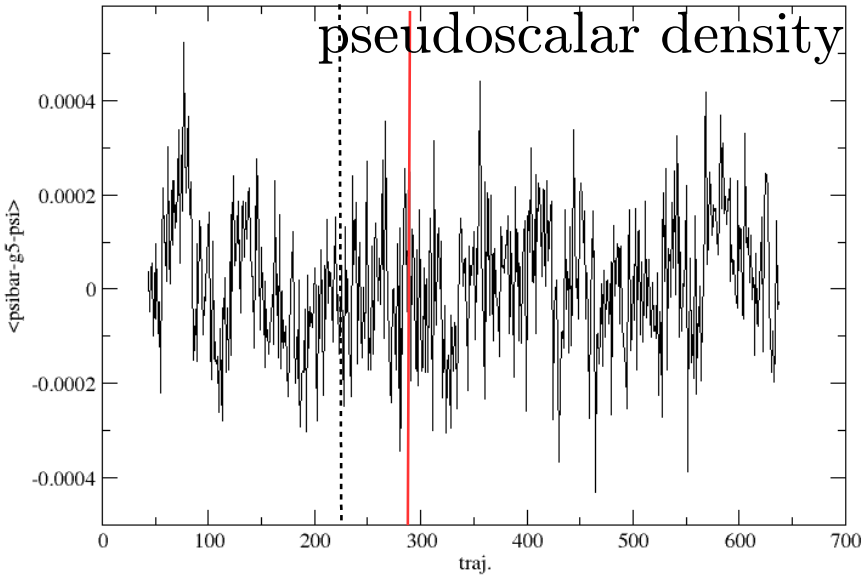

ΔI=1/2 Decay

- Must measure $K^0 \to \pi^+\pi^-$ and $K^0 \to \pi^0\pi^0$ with I=0 final state. Boundary conditions must therefore:
  - Conserve isospin such that I=0 state can be isolated.
  - Give momentum to both charged and neutral pions.
- Conventional application of twisted BCs to the d-quark breaks both of these.
- Instead, we use G-parity:

$$\hat{G} = \hat{C} e^{i\pi \hat{I}_y} \quad : \qquad \hat{G}|\pi^\pm\rangle = -|\pi^\pm\rangle$$
$$\hat{G}|\pi^0\rangle = -|\pi^0\rangle$$

- As a boundary condition:

$$\pi^i(x+L) = \hat{G}\pi^i(x) = -\pi^i(x)$$

Discretized lattice momenta

$$|p| \in (\pi/L,\, 3\pi/L,\, 5\pi/L \ldots)$$

Moving ground-state

Baryogenesis

$$\eta = \frac{n_B - n_{\bar{B}}}{n_\gamma} = 6.14(25) \times 10^{-10}$$

- The Universe is matter dominated, but why?
- Most likely explanation is existence of baryogenesis mechanism.
- Sackarov conditions (1967):
  - B-number violation
  - Non-thermal interactions (e.g. during a phase transition)
  - C and CP violation.
- Why C *and* CP? Because C-breaking $\Gamma(X \to Y + B) \neq \Gamma(\bar{X} \to \bar{Y} + \bar{B})$ but allows

$$\Gamma(X \to q_L q_L) + \Gamma(X \to q_R q_R) = \Gamma(\bar{X} \to \bar{q}_L \bar{q}_L) + \Gamma(\bar{X} \to \bar{q}_R \bar{q}_R)$$

CP-violation prevents this.

- Amount of CP-violation in Standard Model far too small to account for observed value.
- Most BSM theories introduce additional direct CP-violation but a precise SM value does not yet exist which could be compared to experiment.

Charmed-strange and bottom-strange positive parity mesons from Lattice QCD

Daniel Mohler

Fermilab Theory Group
Batavia, IL, USA

BNL,
February 2015

Fermilab

Collaborators: C. B. Lang, L. Leskovec, S. Prelovsek, R. M. Woloshyn

Phys. Rev. Lett. 111 (2013) 22, 222001;
Phys. Rev. **D**90 (2014) 3, 034510;
arXiv:1501.01646

Outline

1. Motivation & Methods
   - Motivation
   - Lattices used
   - Heavy quarks with the Fermilab method
2. Positive parity D_s mesons
   - $D^{(*)}K$ scattering and $D^*_{s0}(2317)$, $D_{s1}(2460)$
3. Positive parity B_s mesons
   - $B^{(*)}K$ scattering and $J^P = 0^+, 1^+$ B_s mesons
4. Conclusions & outlook

Motivation: Experimental D_s spectrum

- Established states:
  - D_s ($J^P = 0^-$) and D_s^* (1^-)
  - $D_{s0}^*(2317)$ (0^+), $D_{s1}(2460)$ (1^+), $D_{s1}(2536)$ (1^+), $D_{s2}^*(2573)$ (2^+)
- More recent discoveries:
  - $D_{s1}^*(2700)$ seen by BaBar, Belle, LHCb (1^-)
  - $D_{sJ}^*(2860)$ seen by BaBar
    LHCb overlapping 1^- and 3^- states
  - $D_{sJ}^*(3040)$ seen by BaBar (1^+?,2^-?)
  - questionable $D_{sJ}^*(2632)$ seen by SELEX (1^-?)
- $j = \frac{1}{2}$ doublet almost mass-degenerate with non-strange states
- Some models suggest a tetraquark/molecular interpretations for controversial states
- (Most) lattice studies using single hadron ($c\bar{s}$) interpolators get too large or badly determined masses
- Large m_π: $D_{s0}^*(2317)$ below DK threshold;
  Small m_π: $D_{s0}^*(2317) \approx DK$ threshold

A previous attempt . . .

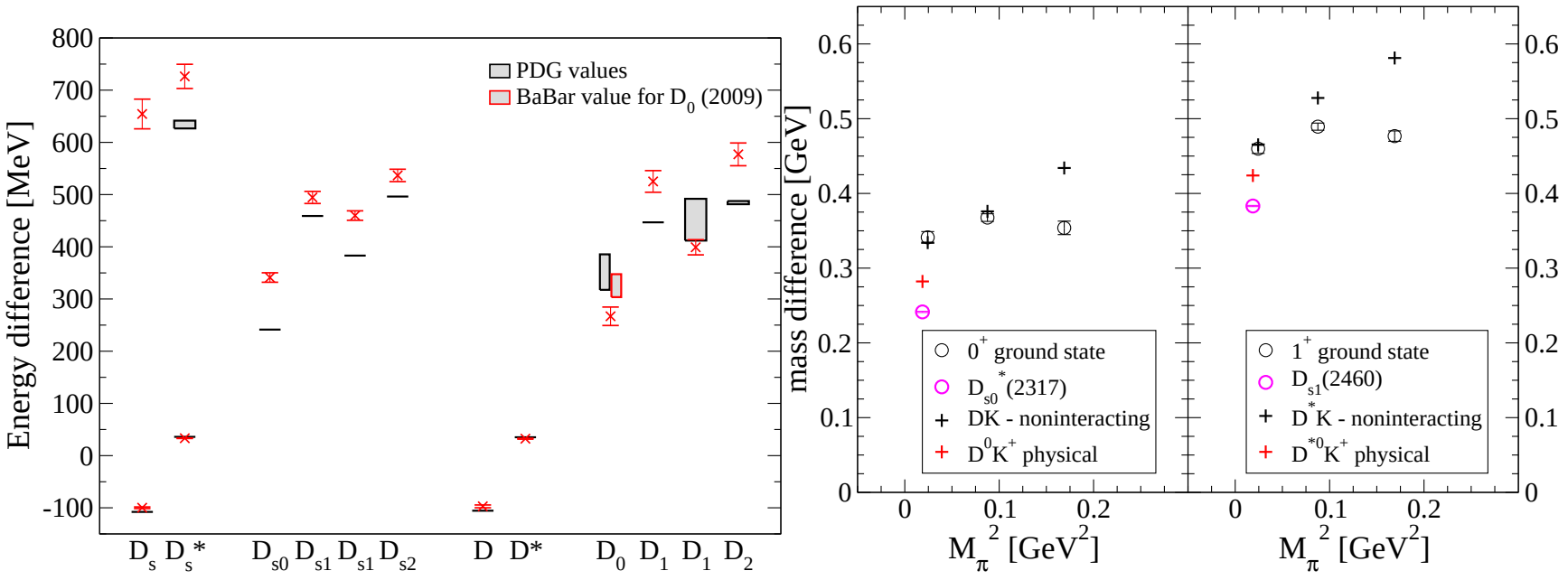

Mohler and Woloshyn, PRD 84 054503, 2011

- DK threshold turned out to be unphysical
- Even with light sea-quark masses the lowest states with $J^P = 0^+, 1^+$ remained unphysical
- Including the DK threshold explicitly might be vital

Technicalities: Lattices used

ID	$N_L^3 \times N_T$	N_f	a[fm]	L[fm]	#configs	m_π[MeV]	m_K[MeV]
(1)	$16^3 \times 32$	2	0.1239(13)	1.98	280/279	266(3)(3)	552(2)(6)
(2)	$32^3 \times 64$	2+1	0.0907(13)	2.90	196	156(7)(2)	504(1)(7)

- Ensemble (1) has 2 flavors of nHYP-smeared quarks

  Gauge ensemble from Hasenfratz et al. PRD 78 054511 (2008)

  Hasenfratz et al. PRD 78 014515 (2008)

- Ensemble (2) has 2+1 flavors of Wilson-Clover quarks

  PACS-CS, Aoki et al. PRD 79 034503 (2009)

- On the small volume we use distillation
  On the larger volume we use stochastic distillation

  Peardon et al. PRD 80, 054506 (2009);

  Morningstar et al. PRD 83, 114505 (2011)

Heavy quarks using the *Fermilab method*

El-Khadra et al., PRD 55,3933

- We tune κ for the spin averaged kinetic mass $(M_{\eta_c} + 3M_{J/\Psi})/4$ to assume its physical value
- General form for the dispersion relation

Bernard et al. PRD83:034503,2011

$$E(p) = M_1 + \frac{p^2}{2M_2} - \frac{a^3 W_4}{6} \sum_i p_i^4 - \frac{(p^2)^2}{8M_4^3} + \dots$$

- We compare results from three different fit strategies
- Energy splittings are expected to be close to physical
- For MeV values of masses

$$M = \Delta M + M_{sa,phys}$$

Testing our tuning: charm and light

	Ensemble (1)	Ensemble (2)	Experiment
m_π	266(3)(3)	156(7)(2)	139.5702(4)
m_K	552(1)(6)	504(1)(7)	493.677(16)
m_ϕ	1015.8(1.8)(10.7)	1018.4(2.8)(14.6)	1019.455(20)
m_{η_s}	732.3(0.9)(7.7)	692.9(0.5)(9.9)	688.5(2.2)*
$m_{J/\Psi} - m_{\eta_c}$	107.9(0.3)(1.1)	107.1(0.2)(1.5)	113.2(0.7)
$m_{D_s^*} - m_{D_s}$	120.4(0.6)(1.3)	142.1(0.7)(2.0)	143.8(0.4)
$m_{D^*} - m_D$	129.4(1.8)(1.4)	148.4(5.2)(2.1)	140.66(10)
$2m_{\overline{D}} - m_{\overline{\bar{c}c}}$	890.9(3.3)(9.3)	882.0(6.5)(12.6)	882.4(0.3)
$2M_{\overline{D_s}} - m_{\overline{\bar{c}c}}$	1065.5(1.4)(11.2)	1060.7(1.1)(15.2)	1084.8(0.6)
$m_{D_s} - m_D$	96.6(0.9)(1.0)	94.0(4.6)(1.3)	98.87(29)

- A single ensemble: Discrepancies due to discretization and unphysical light-quark masses expected

Low-lying charmonium spectrum

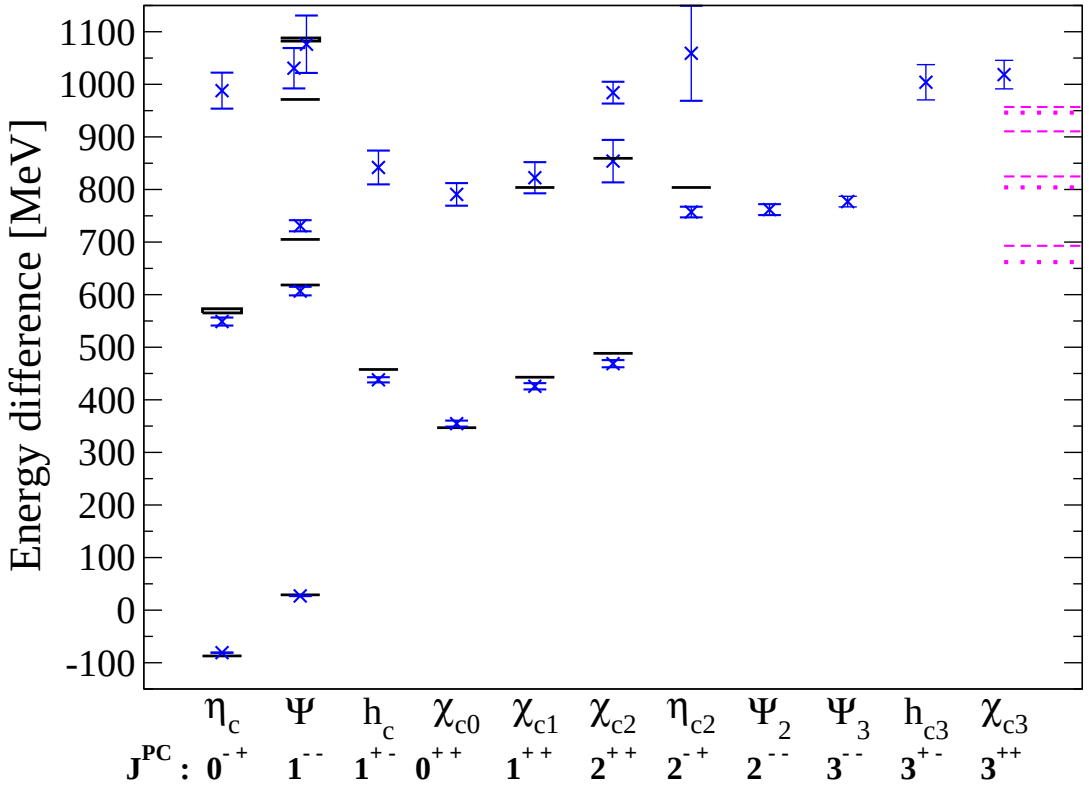

DM, S. Prelovsek, R. M. Woloshyn, PRD 87 034501 (2013);

- Serves as further confirmation of our heavy-quark approach
- Data from 1 ensemble; Errors statistical + scale setting

Revisiting the $D_{s0}^*(2317)$ and $D_{s1}(2460)$

- Use almost physical light quarks
- Work with a partially quenched strange quark
  - Use ϕ meson and η_s to set strange quark mass
  - We obtain $\kappa_s = 0.13666$
- Improve charm quark tuning used for Fermilab charm
  - Use Landau link for $c_{sw,c} = \frac{1}{u_0^3}$
  - Empirically this reduces discretization effects
- Explicitly include DK interpolators into the basis

Contractions

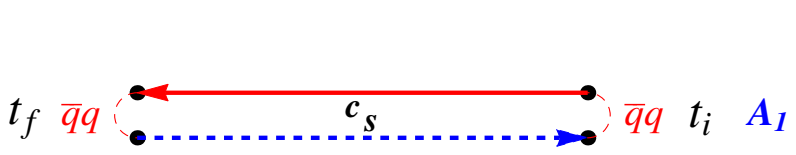

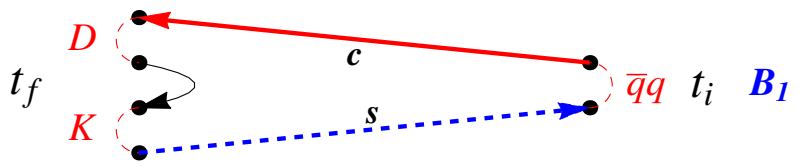

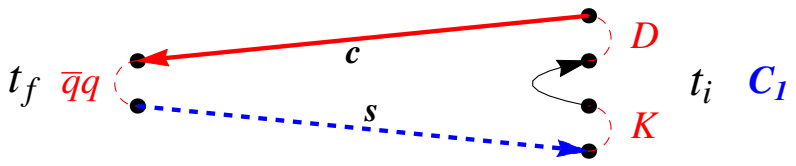

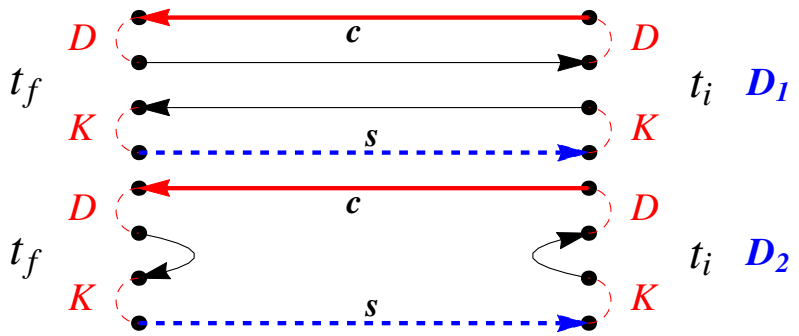

- Handled efficiently within the distillation method

Peardon et al. PRD 80, 054506 (2009)
Morningstar et al. PRD 83, 114505 (2011)

Energy levels for D_s with $J^P = 0^+$

DM, Lang, Leskovec, Prelovsek, Woloshyn, PRL 111 222001 (2013)

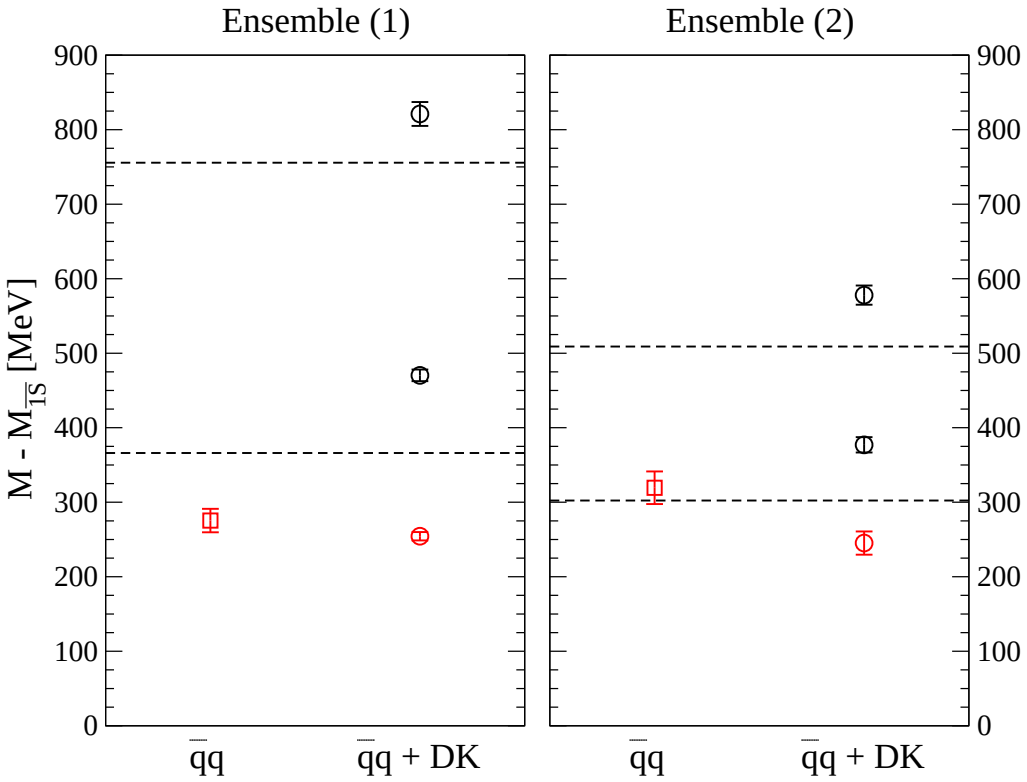

- With the combined basis we obtain a much better quality of the ground state plateau
- The variational method yields two low-lying levels and fits are unambiguous

Possible interpretations

(1) A sub-threshold state stable under the strong interaction

- We call this "bound state scenario"
- This is irrespective of the nature of the state
- One expects a negative scattering length in this case

See `Sasaki and Yamazaki, PRD 74 114507 (2006)` for details.

(2) A resonance in a channel with attractive interaction

- The lowest state corresponds to the scattering level shifted below threshold in finite volume
- The additional level would indicate a QCD resonance
- One expects a positive scattering length in this case

This is the situation for the $D_0^*(2400)$

`DM, Prelovsek, Woloshyn, PRD 87 034501 (2013).`

Using Lüscher's formula

- We can test the plausibility of these scenarios using Lüscher's formula and an effective range approximation

M. Lüscher Commun. Math. Phys. 105 (1986) 153; Nucl. Phys. B 354 (1991) 531; Nucl. Phys. B 364 (1991) 237.

$$K^{-1} = p\cot\delta(p) = \frac{2}{\sqrt{\pi}L} Z_{00}(1;q^2)\ ,$$
$$\approx \frac{1}{a_0} + \frac{1}{2} r_0 p^2\ ,$$

- Results for ensembles (1) and (2)

$$a_0 = -0.756 \pm 0.025\mathrm{fm} \qquad r_0 = 0.056 \pm 0.031\mathrm{fm} \qquad (1)$$
$$a_0 = -1.33 \pm 0.20\mathrm{fm} \qquad r_0 = 0.27 \pm 0.17\mathrm{fm} \qquad (2)$$

Results for the scattering length a_0

DM, Lang, Leskovec, Prelovsek, Woloshyn, PRL 111 222001 (2013)

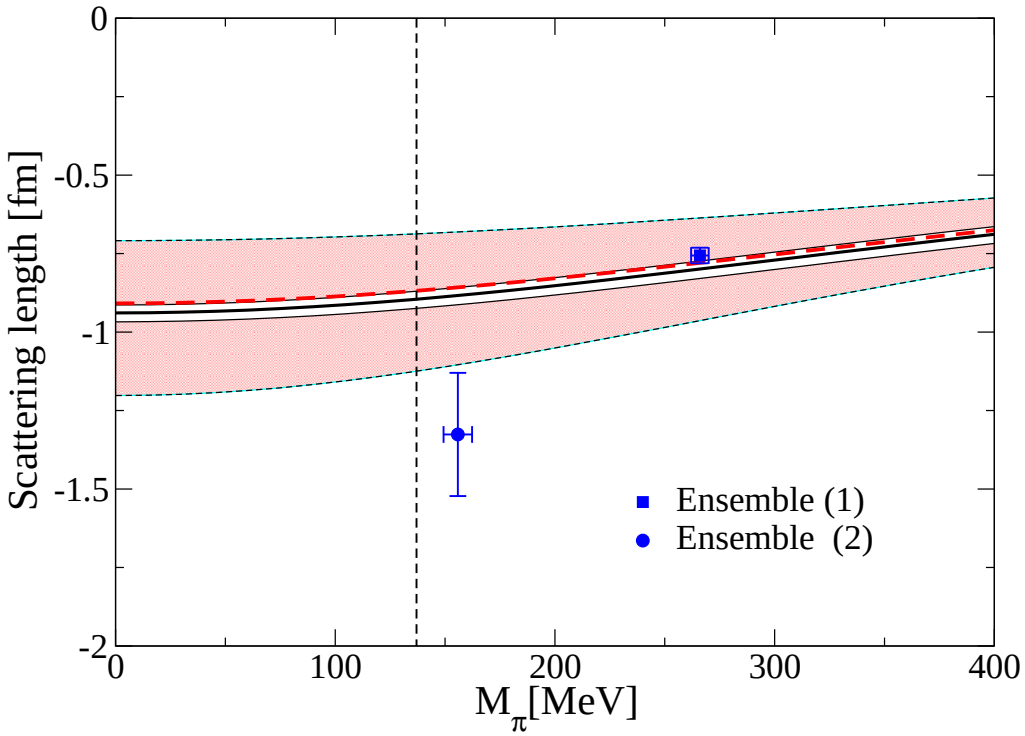

- We compare to the predictions from an indirect calculation

  Liu et al. PRD 87 014508 (2013).
- Our determination robustly leads to negative values.

Infinite volume bound states *vs.* experiment

- (Infinite volume)bound state: T-matrix pole for $\cot\delta(i|p_b|) = i$
- Using our a_0 and r_0 we can determine the binding momentum and calculate the corresponding Energy level

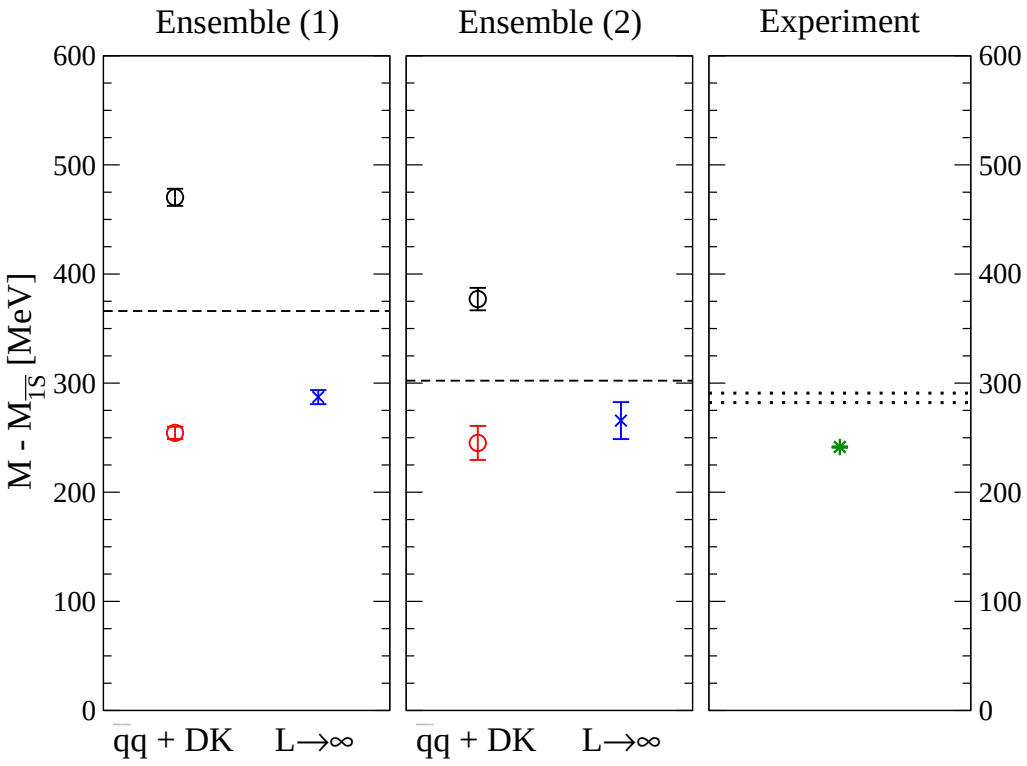

Extending our calculation to the $D_{s1}(2460)$

- Assume the heavy quark limit is a good approximation
  $\rightarrow$ $D_{s1}(2536)$ decays only in D-wave
  we extract just a naive energy level

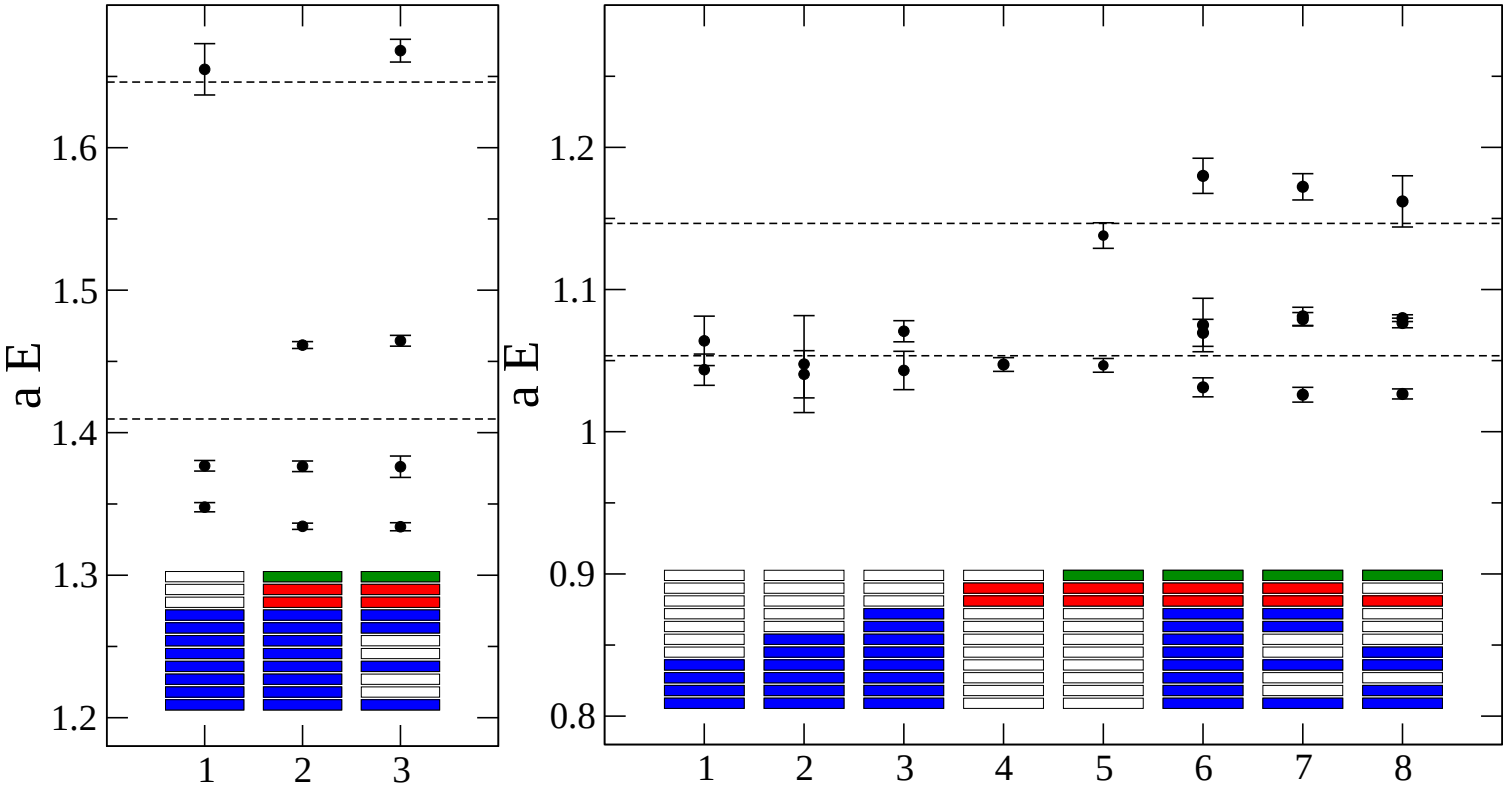

Results in T_1^+

set	$a_0^{D^*K}$ [fm]	$r_0^{D^*K}$ [fm]	$(ap_B)^2$	am_B	$m_K + m_{D^*} - m_B$ [MeV]	$m_B - \frac{1}{4}(m_{D_s} + 3m_{D_s^*})$ [MeV]
Ensemble (1)						
	-0.665(25)	-0.106(37)	-0.0301(15)	1.3511(35)	93.2(4.7)(1.0)	404.6(4.5)(4.2)
Ensemble (2)						
set 1	-1.15(19)	0.13(22)	-0.0071(22)	1.0336(60)	43.2(13.8)(0.6)	408(13)(5.8)
set 2	-1.11(11)	0.10(10)	-0.0073(16)	1.0331(41)	44.2(9.9)(0.6)	407.0(8.8)(5.8)
Experiment						
					44.7	383

set	$m_{D_{s1}(2536)} - \frac{1}{4}(m_{D_s} + 3m_{D_s^*})$ [MeV]	$m_{D_{s1}(2536)} - m_K - m_{D^*}$ [MeV]
Ensemble (1)		
	444(12)	-53(12)
Ensemble (2)		
set 1	507(10)	56(11)
set 2	501(8)	50(8)
Experiment		
	459	31

Resulting D_s P-wave spectrum

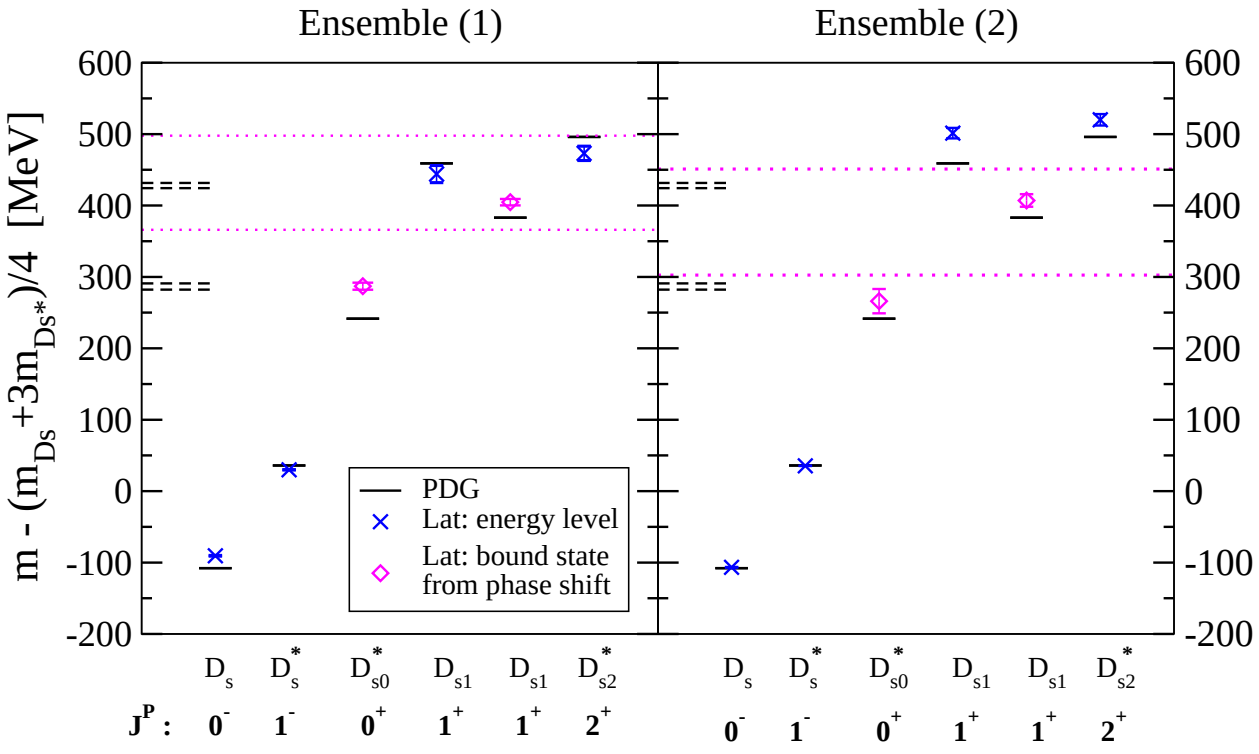

- Remaining discrepancies of the size of discretization uncertainties
- Many improvements possible

B_s states from experiment

- Two p-wave states known from experiment:
  $B_{s1}(5830)$ with $M = 5828.7(4)$ MeV
  $B^*_{s2}(5840)$ with $M = 5839.96(20)$ MeV and $\Gamma = 1.6(5)$ MeV
- Discovered in two body decays into $K^- B^+$ at CDF/D0 and also seen by LHCb
- Remaining B^*_{s0} and B_{s1} states not measured
  LHCb is working on this
- Could be seen in electromagnetic transitions, transitions with a single π^0 or transitions through a virtual σ with $\sigma \to 2\pi$.

Bardeen, Eichten, Hill, PRD 68 054024 (2003)

- What can we say?

Predictions for B_s states (models or model+EFT)

	0^+	1^+
Covariant (U)ChPT	5726(28)	5778(26)
NLO UHMChPT	5696(20)(30)	5742(20)(30)
LO UChPT	5725(39)	5778(7)
LO χ-SU(3)	5643	5690
Bardeen, Eichten, Hill	5718(35)	5765(35)
rel. quark model 1	5804	5842
rel. quark model 2	5833	5865
rel. quark model 3	5830	5858

For references see arXiv:1501.01646

- Relevant thresholds at ≈5773 MeV and ≈5819 MeV
- Unitarized ChPT variants: dynamically generated states below threshold
- Quark model predictions: above threshold

Previous lattice results

- NRQCD b quarks and staggered light quarks
  States predicted slightly below the $B^{(*)}K$ thresholds:

$$M_{B^*_{s0}} = 5752(16)(5)(25) \qquad M_{B_{s1}} = 5806(15)(5)(25)$$

Gregory et al. PRD 83 014506 (2011)

- Static-light mesons with the transition amplitude method

McNeile, Michael, Thompson, PRD 70 054501 (2004)

- Static-light mesons plus interpolation between static light states and experiment D_s states

Green et al. PRD 69 094505 (2004)

- Static-light states on quenched and 2 flavor lattices

Burch et al. PRD 79 014504 (2009)

Testing our tuning: charm and beauty

	Ensemble (1)	Ensemble (2)	Experiment
$m_{J/\psi} - m_{\eta_c}$	107.9(0.3)(1.1)	107.1(0.2)(1.5)	113.2(0.7)
$m_{D_s^*} - m_{D_s}$	120.4(0.6)(1.3)	142.1(0.7)(2.0)	143.8(0.4)
$m_{D^*} - m_D$	129.4(1.8)(1.4)	148.4(5.2)(2.1)	140.66(10)
$2m_{\overline{D}} - m_{\overline{\bar{c}c}}$	890.9(3.3)(9.3)	882.0(6.5)(12.6)	882.4(0.3)
$2M_{\overline{D_s}} - m_{\overline{\bar{c}c}}$	1065.5(1.4)(11.2)	1060.7(1.1)(15.2)	1084.8(0.6)
$m_{D_s} - m_D$	96.6(0.9)(1.0)	94.0(4.6)(1.3)	98.87(29)
$m_{B^*} - m_B$	-	46.8(7.0)(0.7)	45.78(35)
$m_{B_{s^*}} - m_{B_s}$	-	47.1(1.5)(0.7)	$48.7^{+2.3}_{-2.1}$
$m_{B_s} - m_B$	-	81.5(4.1)(1.2)	87.35(23)
$m_\Upsilon - m_{\eta_b}$	-	44.2(0.3)(0.6)	62.3(3.2)
$2m_{\overline{B}} - m_{\overline{\bar{b}b}}$	-	1190(11)(17)	1182.7(1.0)
$2m_{\overline{B_s}} - m_{\overline{\bar{b}b}}$	-	1353(2)(19)	1361.7(3.4)
$2m_{B_c} - m_{\eta_b} - m_{\eta_c}$	-	169.4(0.4)(2.4)	167.3(4.9)

- Errors statistical and scale setting only
- Bottom quark slightly to light

B^*_{so} and B_{s1}: Results

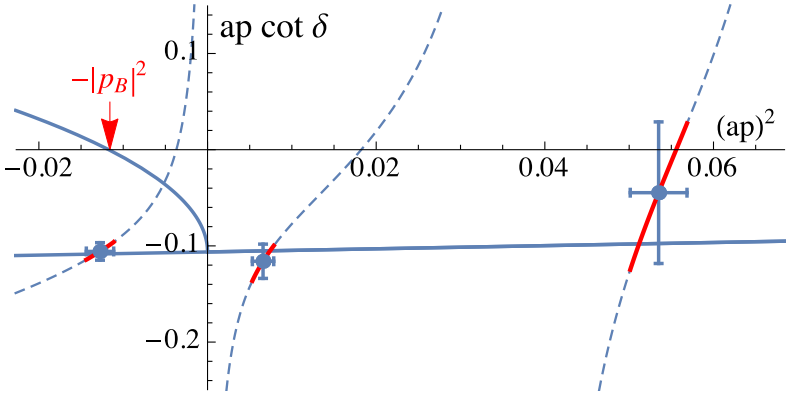

$$a_0^{BK} = -0.85(10)\,\mathrm{fm}$$
$$r_0^{BK} = 0.03(15)\,\mathrm{fm}$$
$$M_{B_{s0}} = 5.711(13)\,\mathrm{GeV}$$

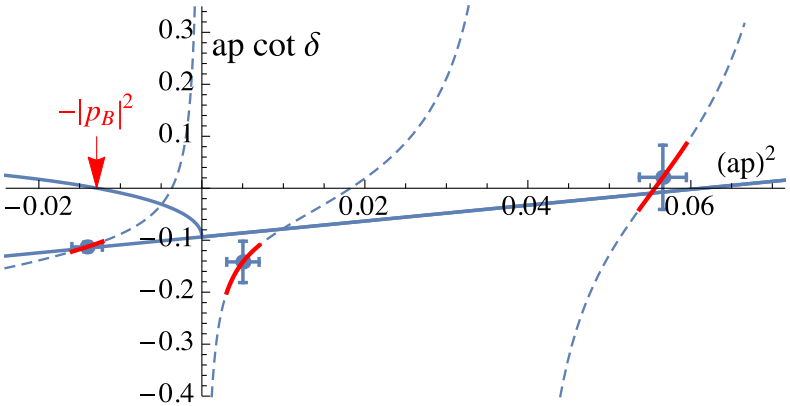

$$a_0^{B^*K} = -0.97(16)\,\mathrm{fm}$$
$$r_0^{B^*K} = 0.28(15)\,\mathrm{fm}$$
$$M_{B_{s0}} = 5.750(17)\,\mathrm{GeV}$$

- Energy from the difference to the $B^{(*)}K$ threshold

A further sanity check

- Discretization errors expected to be smaller than for D_s

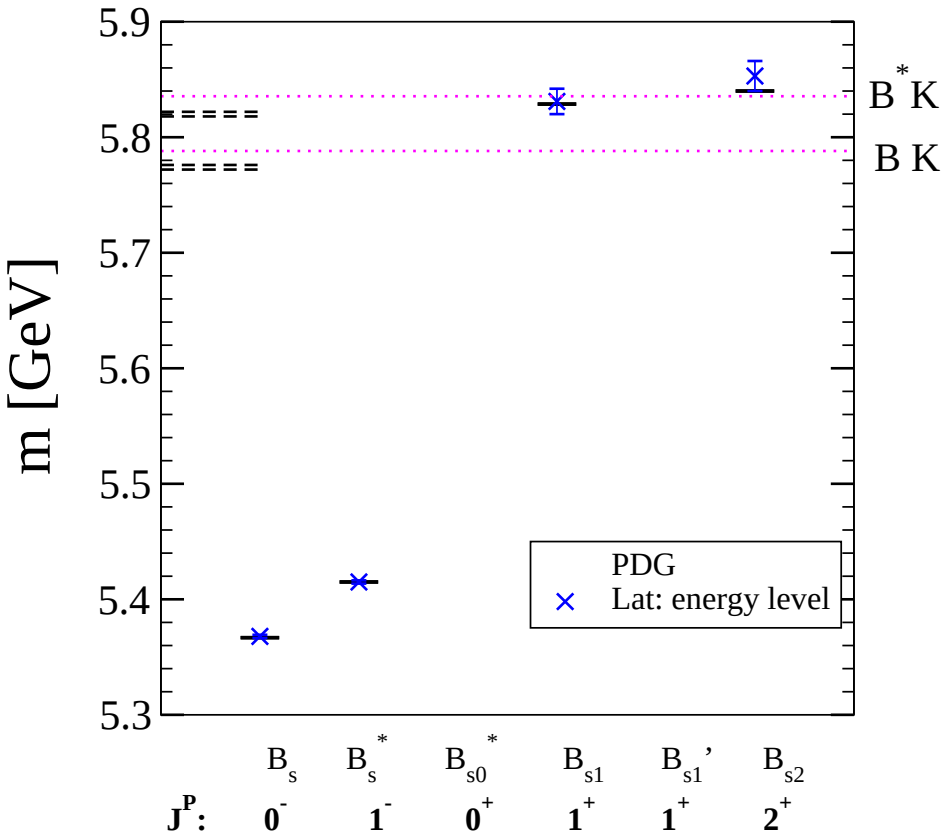

$$M_{B'_{s1}} = 5.831(9)(6)\,\mathrm{GeV}$$
$$M_{B_{s2}} = 5.853(11)(6)\,\mathrm{GeV}$$

- Uncertainties just statistics and scale setting

B^*_{so} and B_{s1}: Systematic uncertainties

source of uncertainty	expected size [MeV]
heavy-quark discretization	12
finite volume effects	8
unphysical Kaon, isospin & EM	11
b-quark tuning	3
dispersion relation	2
spin-average (experiment)	2
scale uncertainty	1
3 pt vs. 2 pt linear fit	2
total	19

- discretiation effects from HQET power counting also considering mass mismatches

  Oktay, Kronfeld Phys.Rev. D78 014504 (2008)

- Finite volume from difference between the energy level and the pole

Comparing to models

	0^+	1^+
Covariant (U)ChPT	5726(28)	5778(26)
NLO UHMChPT	5696(20)(30)	5742(20)(30)
LO UChPT	5725(39)	5778(7)
LO χ-SU(3)	5643	5690
Bardeen, Eichten, Hill	5718(35)	5765(35)
rel. quark model	5804	5842
rel. quark model	5833	5865
rel. quark model	5830	5858
HPQCD 2010	5752(16)(5)(25)	5806(15)(5)(25)
this work	5713(11)(19)	5750(17)(19)

Conclusions & outlook

- Determining the the QCD spectrum close to thresholds has just begun
- Meson and baryon states close to threshold(s) can be attacked
- Coupled channel results encouraging (see David Wilson)
- Many improvements to what I presented possible (stay tuned)
- LHCb, BelleII and $\overline{\mathrm{P}}$ANDA will gather a lot of data
  $\rightarrow$ I would like them to compare to QCD, not models!
- Extracting resonance parameters from lattice scattering phase shifts will need (some degree) of modeling, just like in experiment.

Thank you!

Backup slides

• • •

Composition of eigenstates

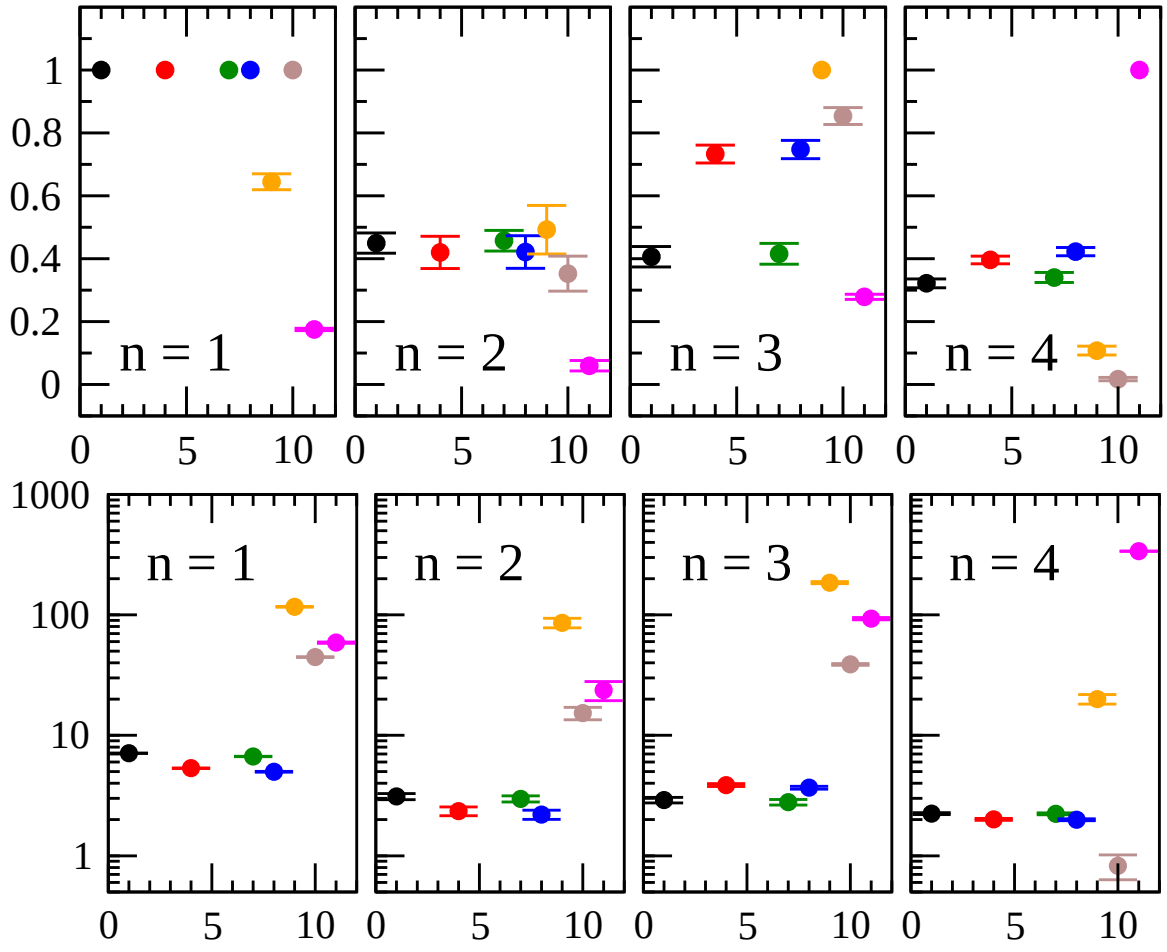

- Beware: Ambiguity in the normalization (eliminated by ratios)

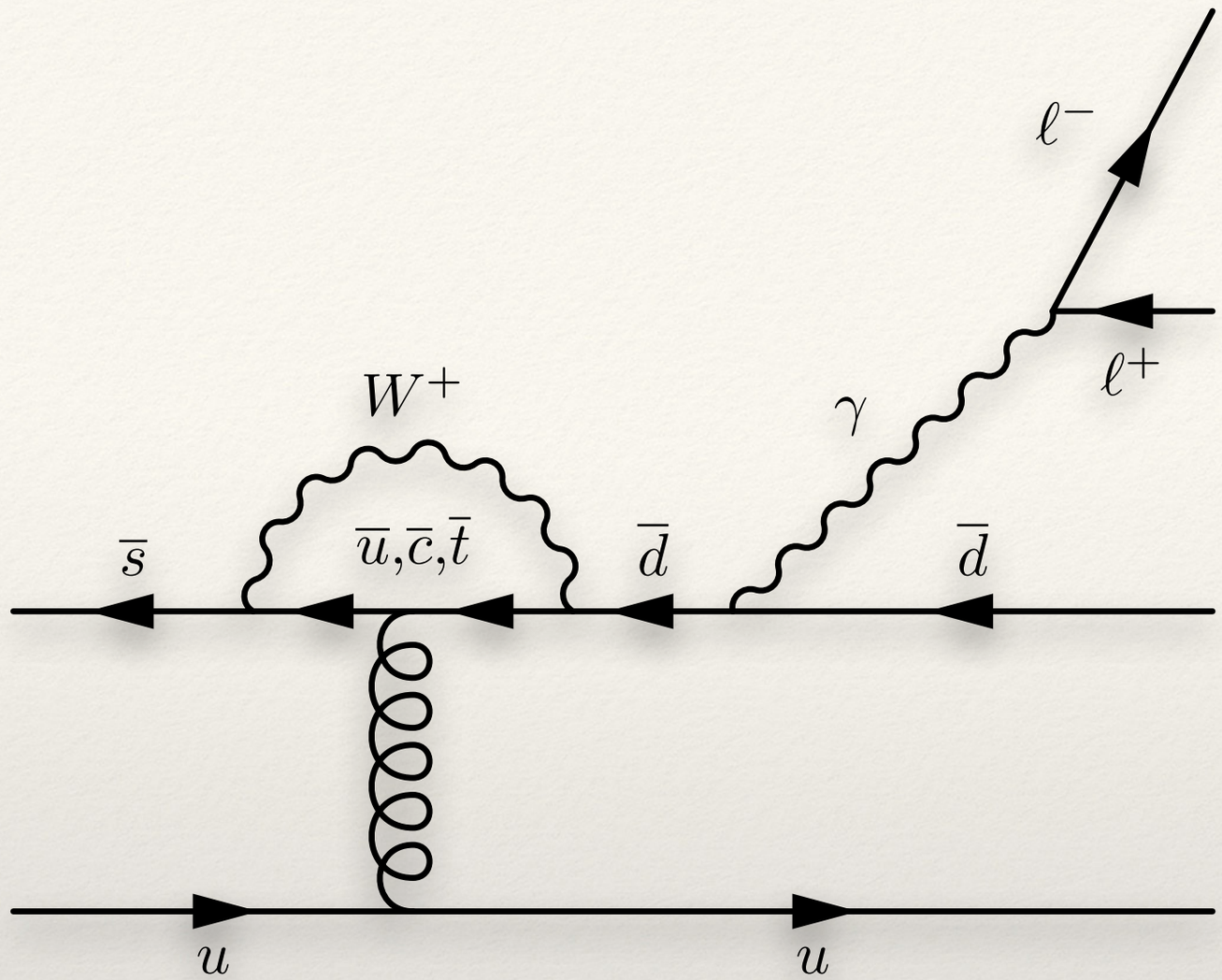

6th of February 2015 — MNME 2015 (BNL, USA)

$K \to \pi \ell^+ \ell^-$ decays on the lattice

UNIVERSITY OF Southampton

Antonin J. Portelli
(RBC-UKQCD collaborations)

Motivations

Motivations

- Rare kaons decays $K \to \pi \ell^+ \ell^-$ and $K \to \pi \overline{\nu} \nu$ are flavour changing neutral current processes (FCNC)

Motivations

- Rare kaons decays $K \to \pi \ell^+ \ell^-$ and $K \to \pi \bar{\nu} \nu$ are flavour changing neutral current processes (FCNC)
- They are heavily suppressed in the Standard Model and sensitive to New Physics

Motivations

- Rare kaons decays $K \to \pi \ell^+ \ell^-$ and $K \to \pi \overline{\nu} \nu$ are flavour changing neutral current processes (FCNC)
- They are heavily suppressed in the Standard Model and sensitive to New Physics
- Each type of process contains 3 decays: K^+, K_S^0 and K_L^0

Motivations

- Rare kaons decays $K \to \pi \ell^+ \ell^-$ and $K \to \pi \overline{\nu} \nu$ are flavour changing neutral current processes (FCNC)
- They are heavily suppressed in the Standard Model and sensitive to New Physics
- Each type of process contains 3 decays: K^+, K_S^0 and K_L^0
- $K \to \pi \overline{\nu} \nu$ will be discussed in the next talk (X. Feng)

Motivations

- Rare kaons decays $K \to \pi \ell^+ \ell^-$ and $K \to \pi \overline{\nu} \nu$ are flavour changing neutral current processes (FCNC)
- They are heavily suppressed in the Standard Model and sensitive to New Physics
- Each type of process contains 3 decays: K^+, K_S^0 and K_L^0
- $K \to \pi \overline{\nu} \nu$ will be discussed in the next talk (X. Feng)
- $K^+ \to \pi^+ \ell^+ \ell^-$: long-distance dominated

Motivations

- Rare kaons decays $K \to \pi \ell^+ \ell^-$ and $K \to \pi \bar{\nu} \nu$ are flavour changing neutral current processes (FCNC)
- They are heavily suppressed in the Standard Model and sensitive to New Physics
- Each type of process contains 3 decays: K^+, K_S^0 and K_L^0
- $K \to \pi \bar{\nu} \nu$ will be discussed in the next talk (X. Feng)
- $K^+ \to \pi^+ \ell^+ \ell^-$: long-distance dominated
- $K_{L/S}^0 \to \pi^0 \ell^+ \ell^-$: feature indirect/direct CP-violation interference

- Euclidean formulation
- Ultraviolet & infrared behaviour
- Preliminary lattice results
- Summary & perspectives

Euclidean formulation

Minkowski amplitude

$$\mathscr{A}_\mu^c(q^2) = \int \mathrm{d}^4x \, \langle \pi^c(\mathbf{p}) | \, \mathrm{T}[J_\mu(0) H_W(x)] \, | K^c(\mathbf{k}) \rangle$$

Minkowski amplitude

EM current (weak contribution negligible)

$$\mathscr{A}_\mu^c(q^2) = \int \mathrm{d}^4x \, \langle \pi^c(\mathbf{p}) | \, \mathrm{T}[J_\mu(0) H_W(x)] \, | K^c(\mathbf{k}) \rangle$$

Minkowski amplitude

EM current (weak contribution negligible)

$$\mathscr{A}_\mu^c(q^2) = \int \mathrm{d}^4x \, \langle \pi^c(\mathbf{p}) | \, \mathrm{T}[J_\mu(0) H_W(x)] \, | K^c(\mathbf{k}) \rangle$$

Effective $\Delta S = 1$ weak Hamiltonian

Minkowski amplitude

EM current (weak contribution negligible)

$$\mathscr{A}_\mu^c(q^2) = \int \mathrm{d}^4x \, \langle \pi^c(\mathbf{p}) | \, \mathrm{T}[J_\mu(0) H_W(x)] \, | K^c(\mathbf{k}) \rangle$$

Effective $\Delta S = 1$ weak Hamiltonian

Spectral representation:

$$\mathscr{A}_\mu^c(q^2) = i \int_0^{+\infty} \mathrm{d}E \, \frac{\rho(E)}{2E} \, \frac{\langle \pi^c(\mathbf{p}) | \, J_\mu(0) \, | E, \mathbf{k} \rangle \, \langle E, \mathbf{k} | \, H_W(0) \, | K^c(\mathbf{k}) \rangle}{E_K(\mathbf{k}) - E + i\varepsilon}$$

$$- i \int_0^{+\infty} \mathrm{d}E \, \frac{\rho_S(E)}{2E} \, \frac{\langle \pi^c(\mathbf{p}) | \, H_W(0) \, | E, \mathbf{p} \rangle \, \langle E, \mathbf{p} | \, J_\mu(0) \, | K^c(\mathbf{k}) \rangle}{E - E_\pi(\mathbf{p}) + i\varepsilon}$$

Euclidean correlation function

$$\Gamma_\mu^{(4)\,c}(x, \mathbf{k}, \mathbf{p}) = \langle \phi_{\pi^c}(t_\pi, \mathbf{p}) \mathrm{T}[J_\mu(0) H_W(x)] \phi_{K^c}(t_K, \mathbf{k})^\dagger \rangle$$

Euclidean correlation function

$$\Gamma_\mu^{(4)\,c}(x, \mathbf{k}, \mathbf{p}) = \langle \phi_{\pi^c}(t_\pi, \mathbf{p}) \mathrm{T}[J_\mu(0) H_W(x)] \phi_{K^c}(t_K, \mathbf{k})^\dagger \rangle$$

pion and kaon interpolating operators

Euclidean correlation function

$$\Gamma_\mu^{(4)\,c}(x,\mathbf{k},\mathbf{p}) = \langle \phi_{\pi^c}(t_\pi,\mathbf{p})\mathrm{T}[J_\mu(0)H_W(x)]\phi_{K^c}(t_K,\mathbf{k})^\dagger\rangle$$

pion and kaon interpolating operators

For $-t_\pi, t_K \to +\infty$:

$$\Gamma_\mu^{(4)\,c}(x,\mathbf{k},\mathbf{p}) = \underbrace{\frac{Z_\pi Z_K^\dagger e^{-t_\pi E_\pi(\mathbf{p})} e^{t_K E_K(\mathbf{k})}}{4E_\pi(\mathbf{p})E_K(\mathbf{k})}}\,\underbrace{\langle \pi^c(\mathbf{p})|\,\mathrm{T}[J_\mu^b(0)H_W(x)]\,|K^c(\mathbf{k})\rangle}$$

Euclidean correlation function

$$\Gamma_\mu^{(4)\,c}(x,\mathbf{k},\mathbf{p}) = \langle \phi_{\pi^c}(t_\pi,\mathbf{p})\mathrm{T}[J_\mu(0)H_W(x)]\phi_{K^c}(t_K,\mathbf{k})^\dagger\rangle$$

pion and kaon interpolating operators

For $-t_\pi, t_K \to +\infty$:

$$\Gamma_\mu^{(4)\,c}(x,\mathbf{k},\mathbf{p}) = \underbrace{\frac{Z_\pi Z_K^\dagger e^{-t_\pi E_\pi(\mathbf{p})} e^{t_K E_K(\mathbf{k})}}{4E_\pi(\mathbf{p})E_K(\mathbf{k})}}_{\text{can be obtained from 2-point functions}} \underbrace{\langle \pi^c(\mathbf{p})|\,\mathrm{T}[J_\mu^b(0)H_W(x)]\,|K^c(\mathbf{k})\rangle}$$

Euclidean correlation function

$$\Gamma_\mu^{(4)\,c}(x,\mathbf{k},\mathbf{p}) = \langle \phi_{\pi^c}(t_\pi,\mathbf{p})\mathrm{T}[J_\mu(0)H_W(x)]\phi_{K^c}(t_K,\mathbf{k})^\dagger\rangle$$

pion and kaon interpolating operators

For $-t_\pi, t_K \to +\infty$:

$$\Gamma_\mu^{(4)\,c}(x,\mathbf{k},\mathbf{p}) = \underbrace{\frac{Z_\pi Z_K^\dagger e^{-t_\pi E_\pi(\mathbf{p})} e^{t_K E_K(\mathbf{k})}}{4E_\pi(\mathbf{p})E_K(\mathbf{k})}}_{\text{can be obtained from 2-point functions}} \underbrace{\langle \pi^c(\mathbf{p})|\,\mathrm{T}[J_\mu^b(0)H_W(x)]\,|K^c(\mathbf{k})\rangle}_{\tilde{\Gamma}_\mu^{(4)\,c}(x,\mathbf{k},\mathbf{p})}$$

Quark Wick contractions

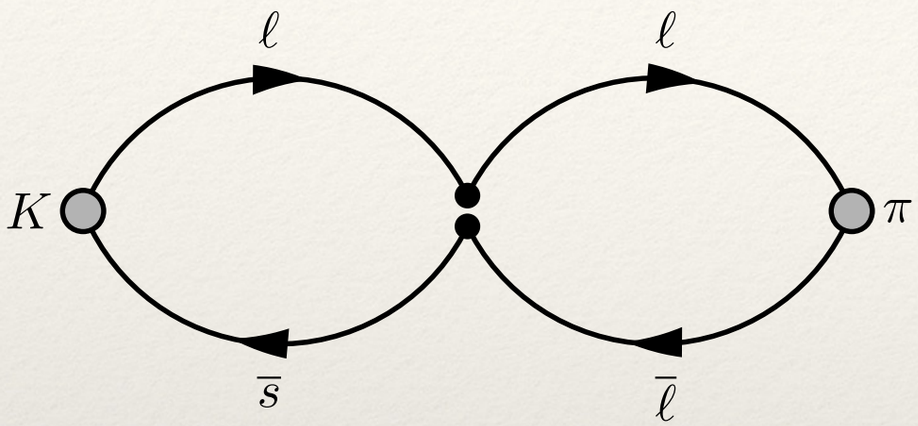

C: “Connected”

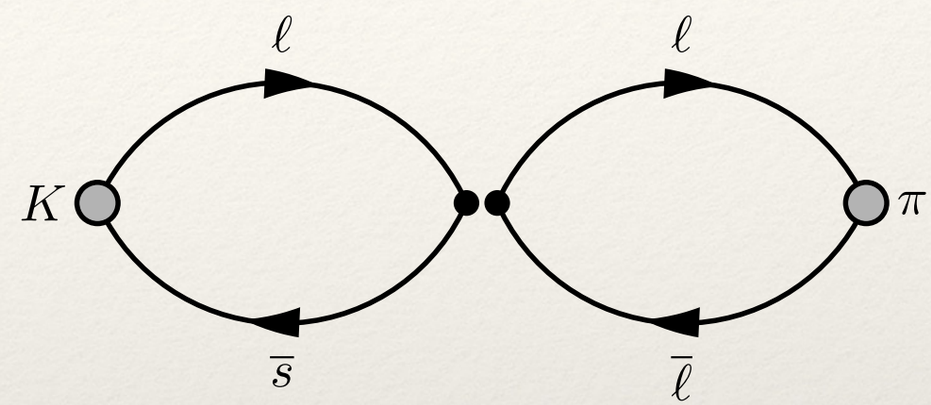

W: “Wing”

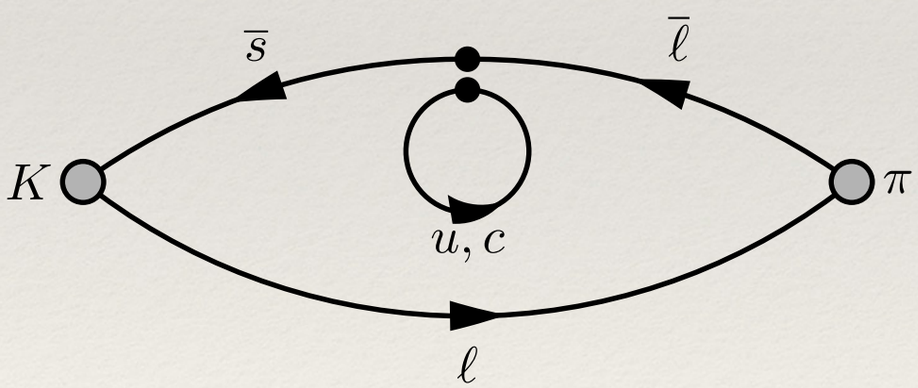

E: “Eye”

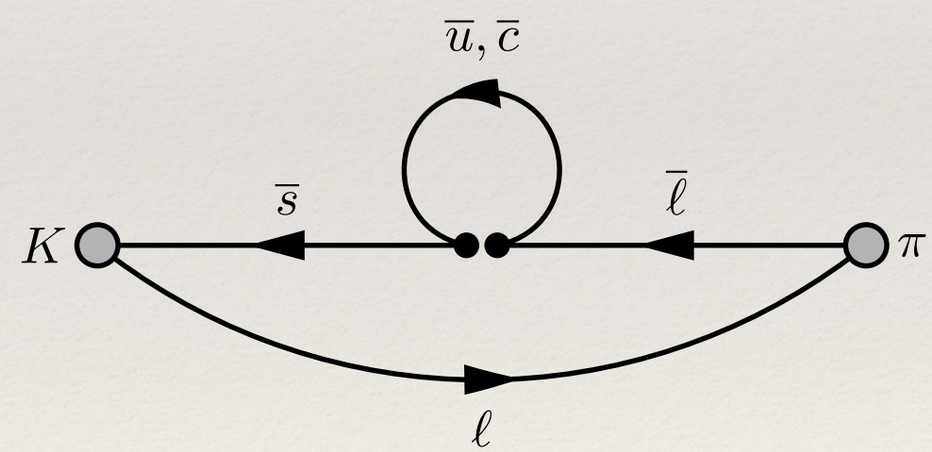

S: “Saucer”

Names: E. Goode

Quark Wick contractions

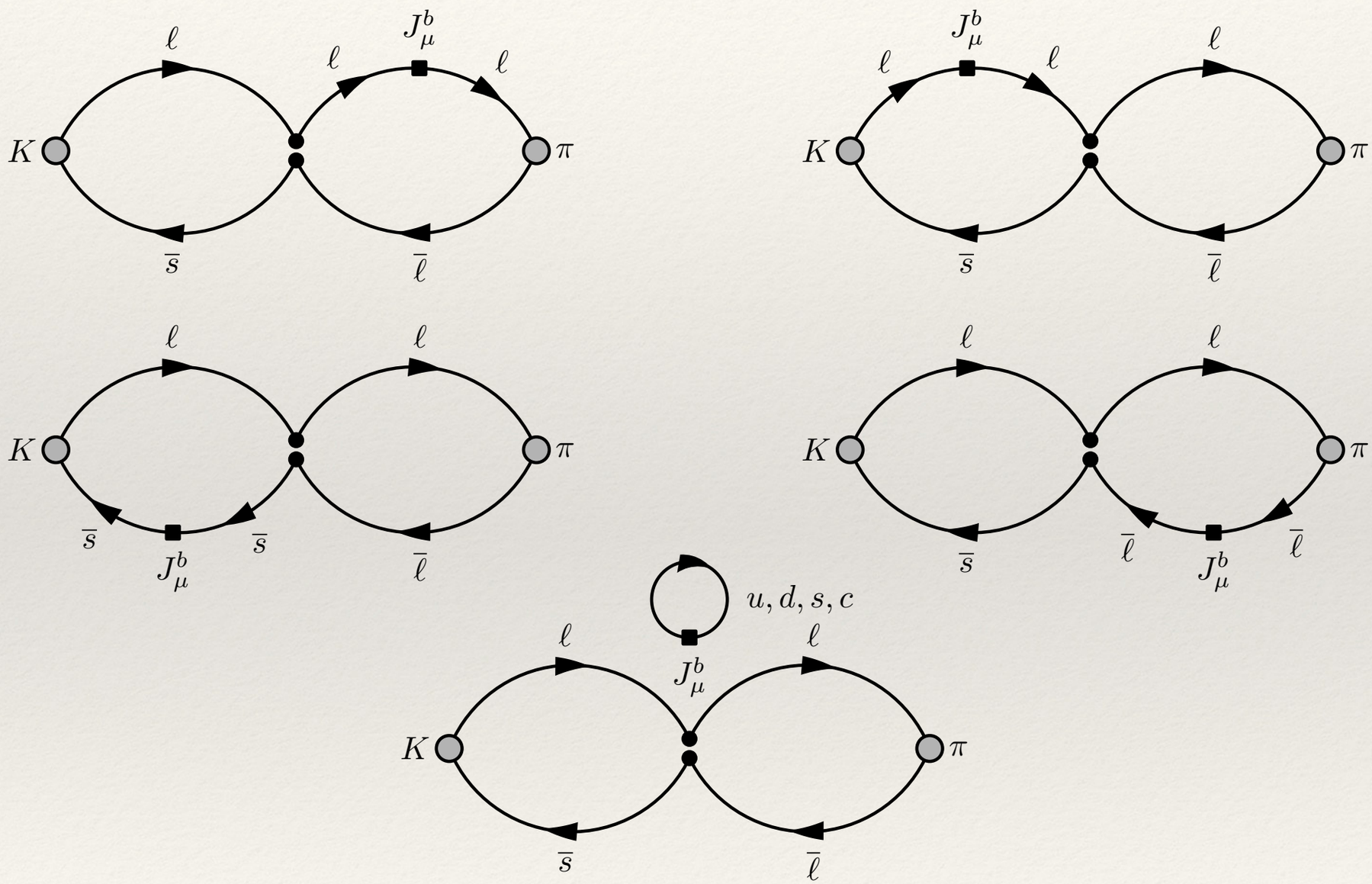

Quark Wick contractions

Neutral case additional diagrams:

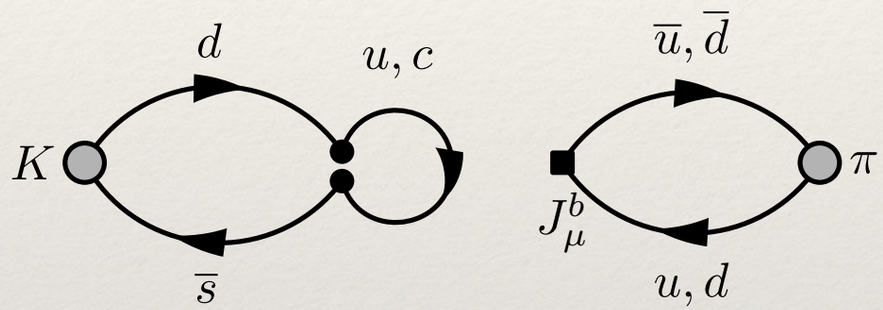

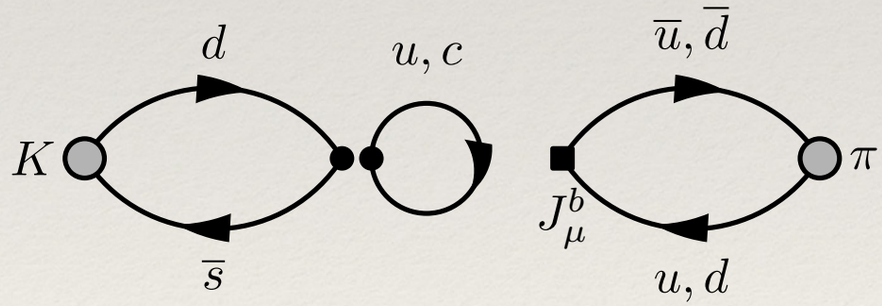

Euclidean spectral representation

Integrated correlator on a finite time interval $[-T_a, T_b]$:

$$\int \mathrm{d}^3\mathbf{x} \int_{-T_a}^{T_b} \mathrm{d}t\, \tilde{\Gamma}_\mu^{(4)\,c}(t, \mathbf{x}, \mathbf{k}, \mathbf{p}) = -\int_0^{+\infty} \mathrm{d}E\, \frac{\rho(E)}{2E} \frac{\langle \pi^c(\mathbf{p})|\, J_\mu(0)\, |E, \mathbf{k}\rangle \langle E, \mathbf{k}|\, H_W(0)\, |K^c(\mathbf{k})\rangle}{E_K(\mathbf{k}) - E}$$
$$\times \left(1 - e^{[E_K(\mathbf{k}) - E]T_a}\right)$$
$$+ \int_0^{+\infty} \mathrm{d}E\, \frac{\rho_S(E)}{2E} \frac{\langle \pi^c(\mathbf{p})|\, H_W(0)\, |E, \mathbf{p}\rangle \langle E, \mathbf{p}|\, J_\mu(0)\, |K^c(\mathbf{k})\rangle}{E - E_\pi(\mathbf{p})}$$
$$\times \left(1 - e^{-[E - E_\pi(\mathbf{p})]T_b}\right)$$

Euclidean spectral representation

Integrated correlator on a finite time interval $[-T_a, T_b]$:

$$\int \mathrm{d}^3\mathbf{x} \int_{-T_a}^{T_b} \mathrm{d}t\, \tilde{\Gamma}_\mu^{(4)\,c}(t, \mathbf{x}, \mathbf{k}, \mathbf{p}) = -\int_0^{+\infty} \mathrm{d}E\, \frac{\rho(E)}{2E} \frac{\langle \pi^c(\mathbf{p})|\, J_\mu(0)\, |E, \mathbf{k}\rangle \langle E, \mathbf{k}|\, H_W(0)\, |K^c(\mathbf{k})\rangle}{E_K(\mathbf{k}) - E} \times (1 - e^{[E_K(\mathbf{k}) - E]T_a})$$

$$+ \int_0^{+\infty} \mathrm{d}E\, \frac{\rho_S(E)}{2E} \frac{\langle \pi^c(\mathbf{p})|\, H_W(0)\, |E, \mathbf{p}\rangle \langle E, \mathbf{p}|\, J_\mu(0)\, |K^c(\mathbf{k})\rangle}{E - E_\pi(\mathbf{p})} \times (1 - e^{-[E - E_\pi(\mathbf{p})]T_b})$$

- growing exponential for $E < E_K(\mathbf{k})$

Euclidean spectral representation

Integrated correlator on a finite time interval $[-T_a, T_b]$:

$$\int \mathrm{d}^3\mathbf{x} \int_{-T_a}^{T_b} \mathrm{d}t\, \tilde{\Gamma}_\mu^{(4)\,c}(t, \mathbf{x}, \mathbf{k}, \mathbf{p}) = -\int_0^{+\infty} \mathrm{d}E\, \frac{\rho(E)}{2E} \frac{\langle \pi^c(\mathbf{p}) | J_\mu(0) | E, \mathbf{k}\rangle \langle E, \mathbf{k} | H_W(0) | K^c(\mathbf{k})\rangle}{E_K(\mathbf{k}) - E} \times (1 - e^{[E_K(\mathbf{k}) - E]T_a})$$
$$+ \int_0^{+\infty} \mathrm{d}E\, \frac{\rho_S(E)}{2E} \frac{\langle \pi^c(\mathbf{p}) | H_W(0) | E, \mathbf{p}\rangle \langle E, \mathbf{p} | J_\mu(0) | K^c(\mathbf{k})\rangle}{E - E_\pi(\mathbf{p})} \times (1 - e^{-[E - E_\pi(\mathbf{p})]T_b})$$

- growing exponential for $E < E_K(\mathbf{k})$
- need to be removed to obtain the Minkowski amplitude

Euclidean spectral representation

Integrated correlator on a finite time interval $[-T_a, T_b]$:

$$\int \mathrm{d}^3\mathbf{x} \int_{-T_a}^{T_b} \mathrm{d}t\, \tilde{\Gamma}_\mu^{(4)\,c}(t, \mathbf{x}, \mathbf{k}, \mathbf{p}) = -\int_0^{+\infty} \mathrm{d}E\, \frac{\rho(E)}{2E} \frac{\langle \pi^c(\mathbf{p}) | J_\mu(0) | E, \mathbf{k}\rangle \langle E, \mathbf{k} | H_W(0) | K^c(\mathbf{k})\rangle}{E_K(\mathbf{k}) - E} \times (1 - e^{[E_K(\mathbf{k}) - E]T_a})$$

$$+ \int_0^{+\infty} \mathrm{d}E\, \frac{\rho_S(E)}{2E} \frac{\langle \pi^c(\mathbf{p}) | H_W(0) | E, \mathbf{p}\rangle \langle E, \mathbf{p} | J_\mu(0) | K^c(\mathbf{k})\rangle}{E - E_\pi(\mathbf{p})} \times (1 - e^{-[E - E_\pi(\mathbf{p})]T_b})$$

- growing exponential for $E < E_K(\mathbf{k})$
- need to be removed to obtain the Minkowski amplitude
- generated by 1, 2 and 3-pion intermediate states

Removing the single-pion divergence

1. Reconstruct the divergent single-pion term by computing J_μ and H_W matrix elements for $\pi \to \pi\gamma^*$ and $K \to \pi$ transitions

Removing the single-pion divergence

1. Reconstruct the divergent single-pion term by computing J_μ and H_W matrix elements for $\pi \to \pi\gamma^*$ and $K \to \pi$ transitions
2. One can show that the physical amplitude is invariant under $H_W \mapsto H_W + c_S \bar{s} d$, c_S can be tuned to cancel the $K \to \pi$ matrix element

Two-pion intermediate states

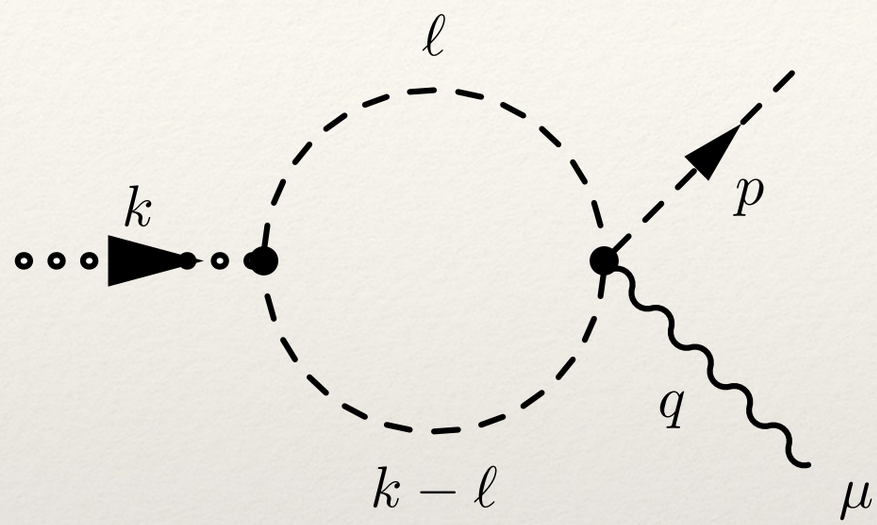

Two-pion intermediate states

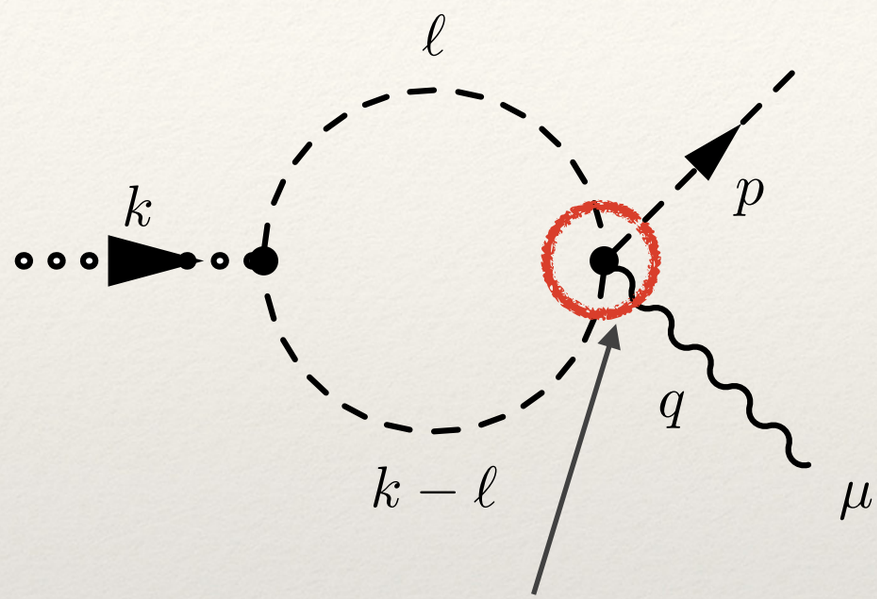

$$\varepsilon_{\mu\nu\rho\sigma} p_1^\nu p_2^\rho p_3^\sigma F(s,t,u)$$

Two-pion intermediate states

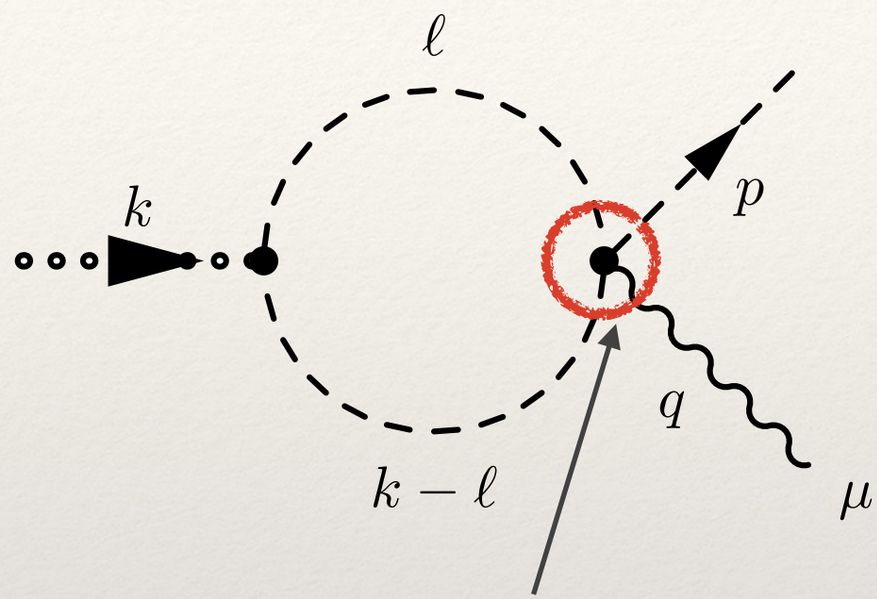

$$\varepsilon_{\mu\nu\rho\sigma} p_1^\nu p_2^\rho p_3^\sigma F(s,t,u)$$

After integrating ℓ, only two independent momenta.

Two-pion intermediate states

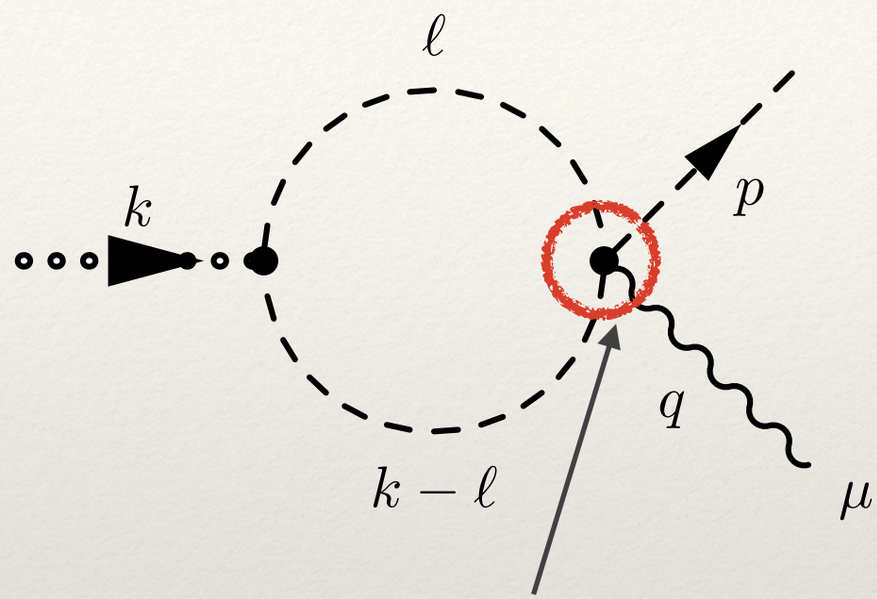

$$\varepsilon_{\mu\nu\rho\sigma} p_1^\nu p_2^\rho p_3^\sigma F(s,t,u)$$

After integrating ℓ, only two independent momenta.

No two-pion intermediate state

Removing the 3-pion divergence

- One needs $K \to \pi\pi\pi$ matrix elements

Removing the 3-pion divergence

- One needs $K \to \pi\pi\pi$ matrix elements
- On the lattice: unknown and probably very challenging

Removing the 3-pion divergence

- One needs $K \to \pi\pi\pi$ matrix elements
- On the lattice: unknown and probably very challenging
- [arXiv:1408.5933] proposed a theory for the quantisation of 3-pion states in a finite volume
  (*cf.* also S. Sharpe's talk yesterday)

Removing the 3-pion divergence

- One needs $K \to \pi\pi\pi$ matrix elements
- On the lattice: unknown and probably very challenging
- [arXiv:1408.5933] proposed a theory for the quantisation of 3-pion states in a finite volume
  (*cf.* also S. Sharpe's talk yesterday)
- Only a problem for pion masses less than ~165 MeV

Ultraviolet & infrared behaviour

Individual operator renormalisation

- The vector current is conserved and does not need renormalisation

Individual operator renormalisation

- The vector current is conserved and does not need renormalisation
- The renormalisation of the weak hamiltonian is also know and is much more simple with chiral fermions (*cf. e.g.* [Z. Bai, *et al*. PRL, 113(1), p. 112003, 2014]).

Short distance operator product

UV divergences may appear in loops between J_μ and H_W :

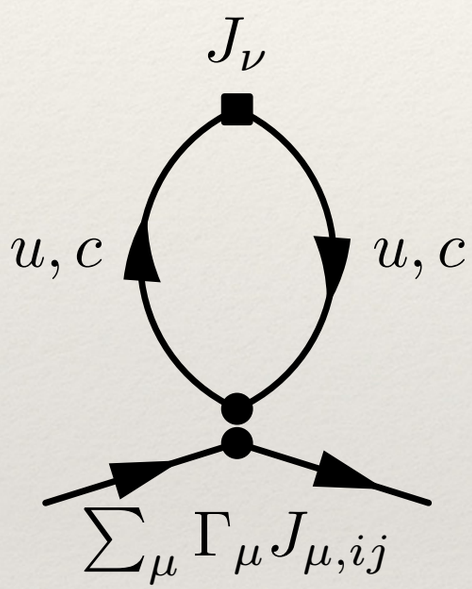

$$= \sum_\nu \Gamma_\nu [\Pi^u_{\mu\nu,ij}(q) - \Pi^c_{\mu\nu,ij}(q)]$$

$$\text{with } \Pi^f_{\mu\nu,ij}(q) = \sum_x \langle J^f_\mu(x) J^f_{\nu,ij}(0) \rangle \, e^{iq\cdot x}$$

Short distance operator product

UV divergences may appear in loops between J_μ and H_W :

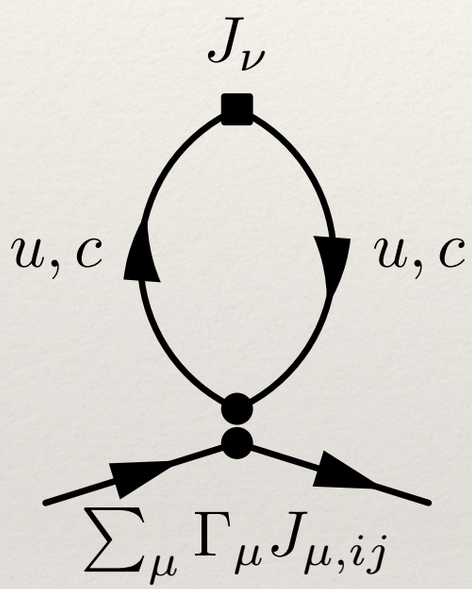

$$= \sum_\nu \Gamma_\nu [\Pi^u_{\mu\nu,ij}(q) - \Pi^c_{\mu\nu,ij}(q)]$$

$$\text{with } \Pi^f_{\mu\nu,ij}(q) = \sum_x \langle J^f_\mu(x) J^f_{\nu,ij}(0) \rangle \, e^{iq\cdot x}$$

Same divergence structure than HVP

Short distance operator product

OPE with lattice regularisation:

$$\Pi^f_{\mu\nu,ij}(q) \underset{a\to 0}{=} C^1_{\mu\nu,ij} + C^{\overline{f}f}_{\mu\nu,ij} \langle m_f \overline{f} f \rangle + \dots$$

Short distance operator product

OPE with lattice regularisation:

$$\Pi^f_{\mu\nu,ij}(q) \underset{a\to 0}{=} \underbrace{C^1_{\mu\nu,ij}}_{\text{dim 2}} + C^{\overline{f}f}_{\mu\nu,ij} \langle m_f \overline{f} f \rangle + \dots$$

Short distance operator product

OPE with lattice regularisation:

$$\Pi^f_{\mu\nu,ij}(q) \underset{a\to 0}{=} \underbrace{C^1_{\mu\nu,ij}}_{\text{dim 2}} + \underbrace{C^{\overline{f}f}_{\mu\nu,ij}}_{\text{dim -2}} \langle m_f \overline{f} f \rangle + \dots$$

Short distance operator product

OPE with lattice regularisation:

$$\Pi^f_{\mu\nu,ij}(q) \underset{a\to 0}{=} \underbrace{C^1_{\mu\nu,ij}}_{\text{dim 2}} + \underbrace{C^{\overline{f}f}_{\mu\nu,ij}}_{\text{dim -2}} \langle m_f \overline{f} f \rangle + \underbrace{\ldots}_{\text{irrelevant}}$$

Short distance operator product

OPE with lattice regularisation:

$$\Pi^f_{\mu\nu,ij}(q) \underset{a\to 0}{=} \underbrace{C^1_{\mu\nu,ij}}_{\text{dim 2}} + \underbrace{C^{\overline{f}f}_{\mu\nu,ij}}_{\text{dim -2}} \langle m_f \overline{f} f \rangle + \underbrace{\ldots}_{\text{irrelevant}}$$

- vector case: WI lower dimensions by 2: mass independent logarithmic divergence

Short distance operator product

OPE with lattice regularisation:

$$\Pi^f_{\mu\nu,ij}(q) \underset{a\to 0}{=} \underbrace{C^1_{\mu\nu,ij}}_{\text{dim 2}} + \underbrace{C^{\overline{f}f}_{\mu\nu,ij}}_{\text{dim -2}} \langle m_f \overline{f} f \rangle + \underbrace{\ldots}_{\text{irrelevant}}$$

- vector case: WI lower dimensions by 2: mass independent logarithmic divergence
- GIM subtraction cancels mass independent divergences

Finite-size effects

- Cuts in diagram: power-law finite volume effects (*cf. e.g.* S. Sharpe's talk yesterday)

Finite-size effects

- Cuts in diagram: power-law finite volume effects (*cf. e.g.* S. Sharpe's talk yesterday)
- Possible with 3-pion on-shell intermediate states:

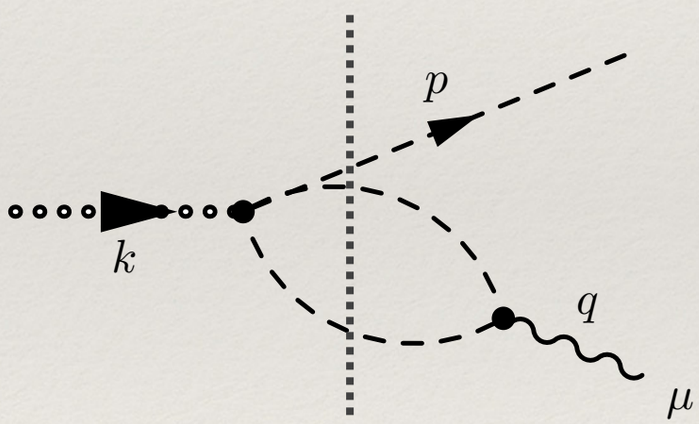

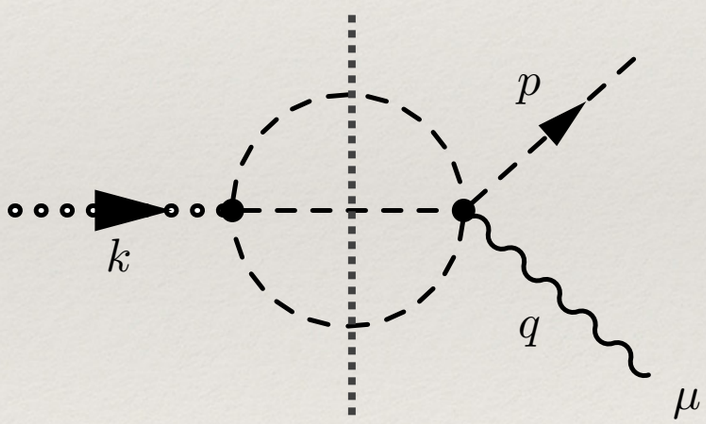

Finite-size effects

- Cuts in diagram: power-law finite volume effects (*cf. e.g.* S. Sharpe's talk yesterday)
- Possible with 3-pion on-shell intermediate states:

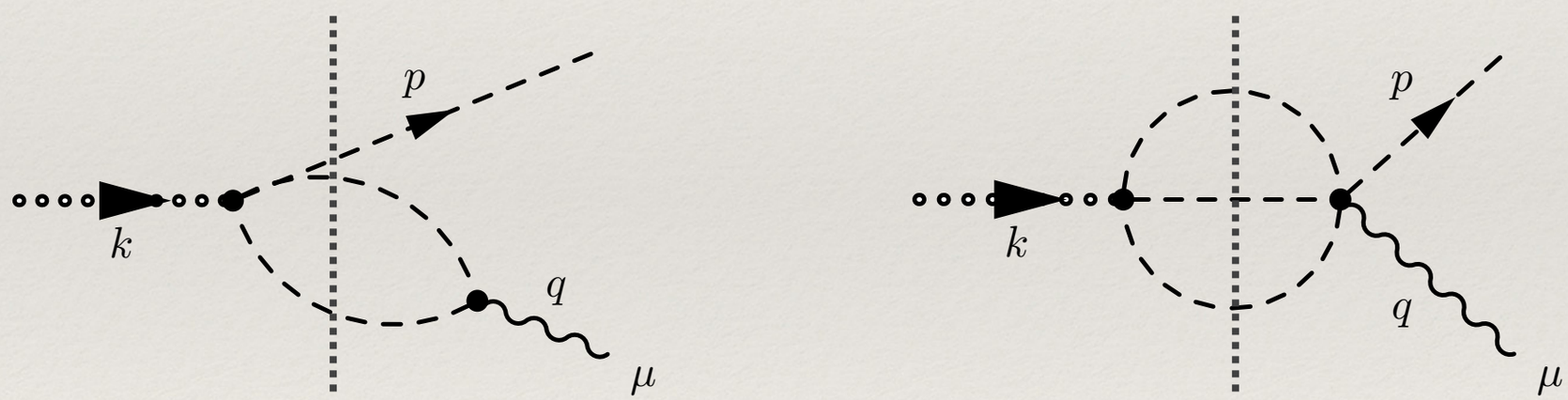

- All other finite-size effects: exponentially suppressed

Preliminary lattice results

Lattice setup

- DWF action, 64×24^3 lattice with spacing ~0.12 fm

Lattice setup

- DWF action, 64×24^3 lattice with spacing ~0.12 fm
- $N_f = 2 + 1$, $M_\pi \simeq 420$ MeV and $M_K \simeq 600$ MeV

Lattice setup

- DWF action, 64×24^3 lattice with spacing ~0.12 fm
- $N_f = 2 + 1$, $M_\pi \simeq 420$ MeV and $M_K \simeq 600$ MeV
- $K(2\pi/L, 0, 0) \to \pi(0, 0, 0)$, $q^2 \simeq -0.09$ GeV^2

Lattice setup

- DWF action, 64×24^3 lattice with spacing ~0.12 fm
- $N_f = 2 + 1$, $M_\pi \simeq 420$ MeV and $M_K \simeq 600$ MeV
- $K(2\pi/L, 0, 0) \to \pi(0, 0, 0)$, $q^2 \simeq -0.09$ GeV^2
- only W and C connected diagrams

Lattice setup

- DWF action, 64×24^3 lattice with spacing ~0.12 fm
- $N_f = 2 + 1$, $M_\pi \simeq 420$ MeV and $M_K \simeq 600$ MeV
- $K(2\pi/L, 0, 0) \to \pi(0, 0, 0)$, $q^2 \simeq -0.09$ GeV^2
- only W and C connected diagrams
- gauge fixed wall sources, sequential current insertion

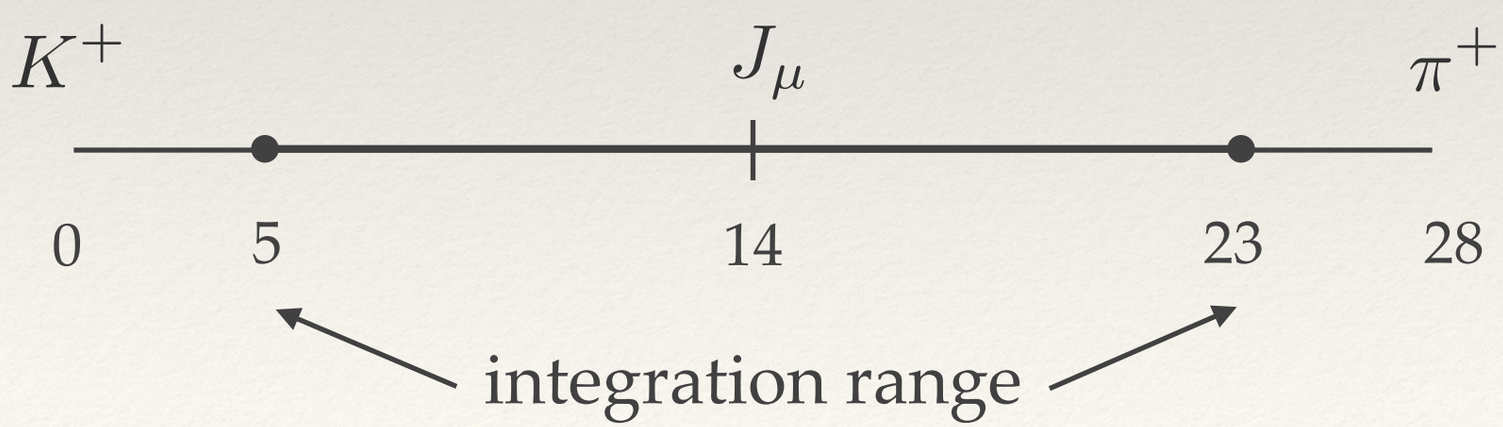

2-point function fit

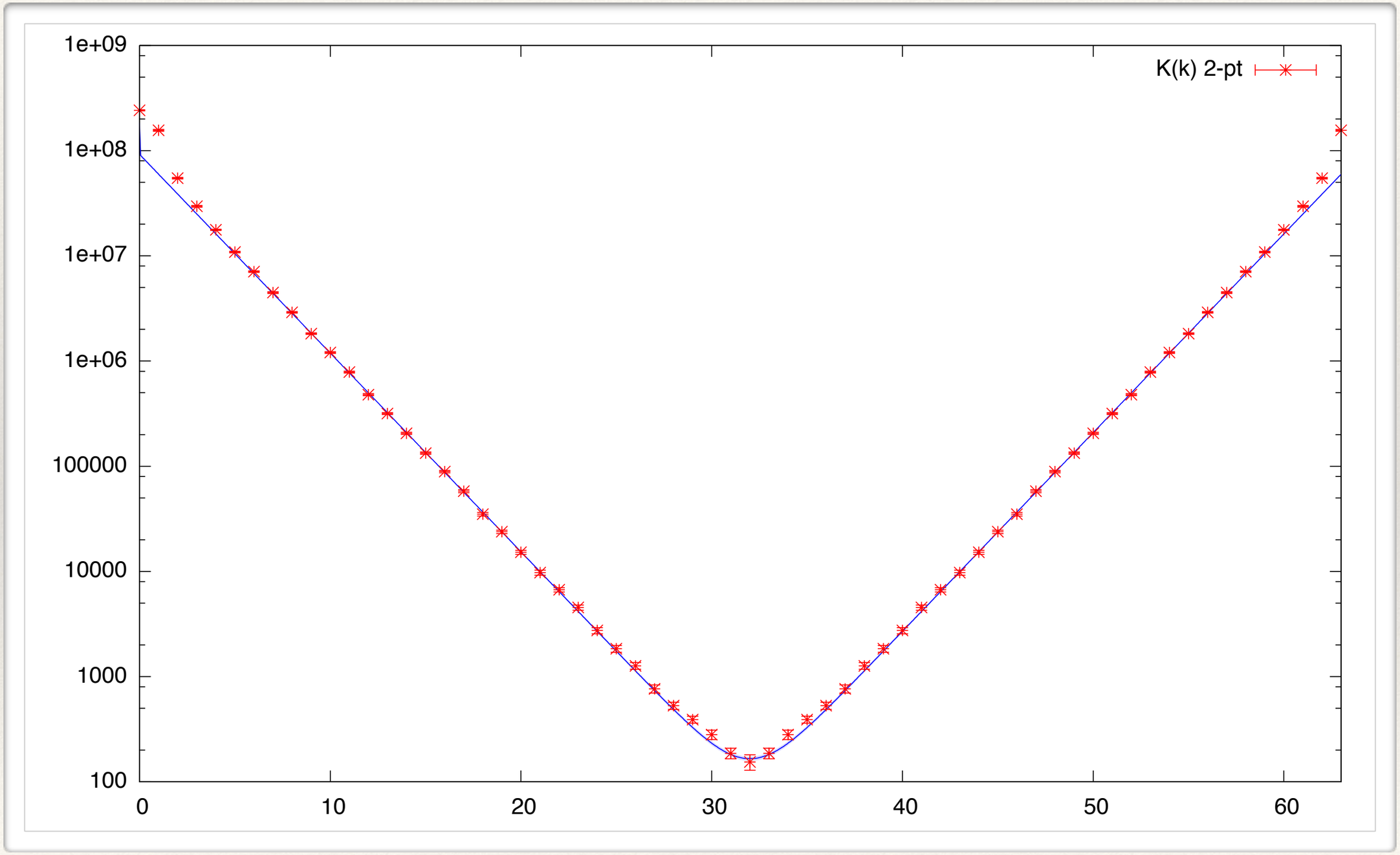

EM current matrix element

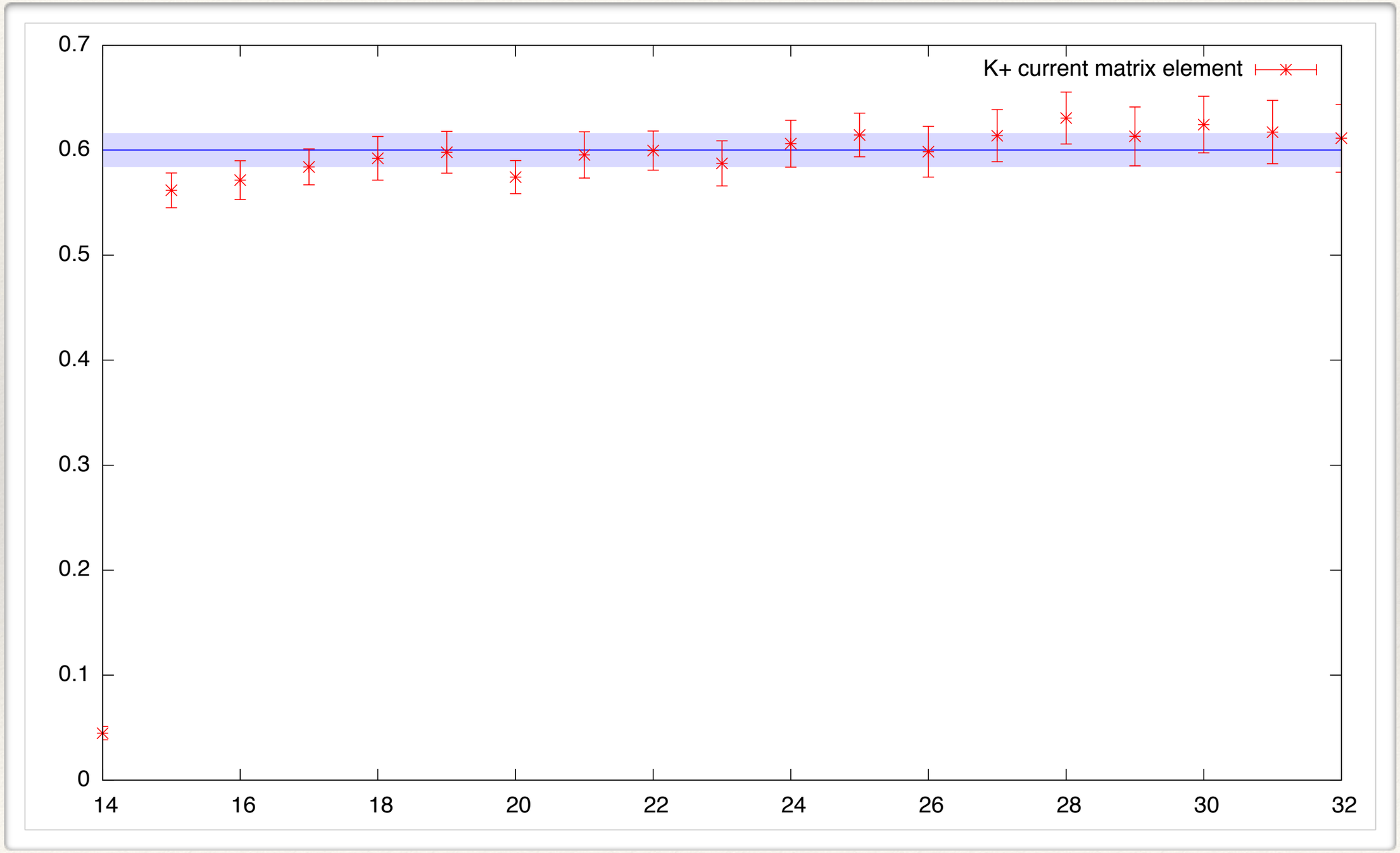

Weak Hamiltonian matrix element

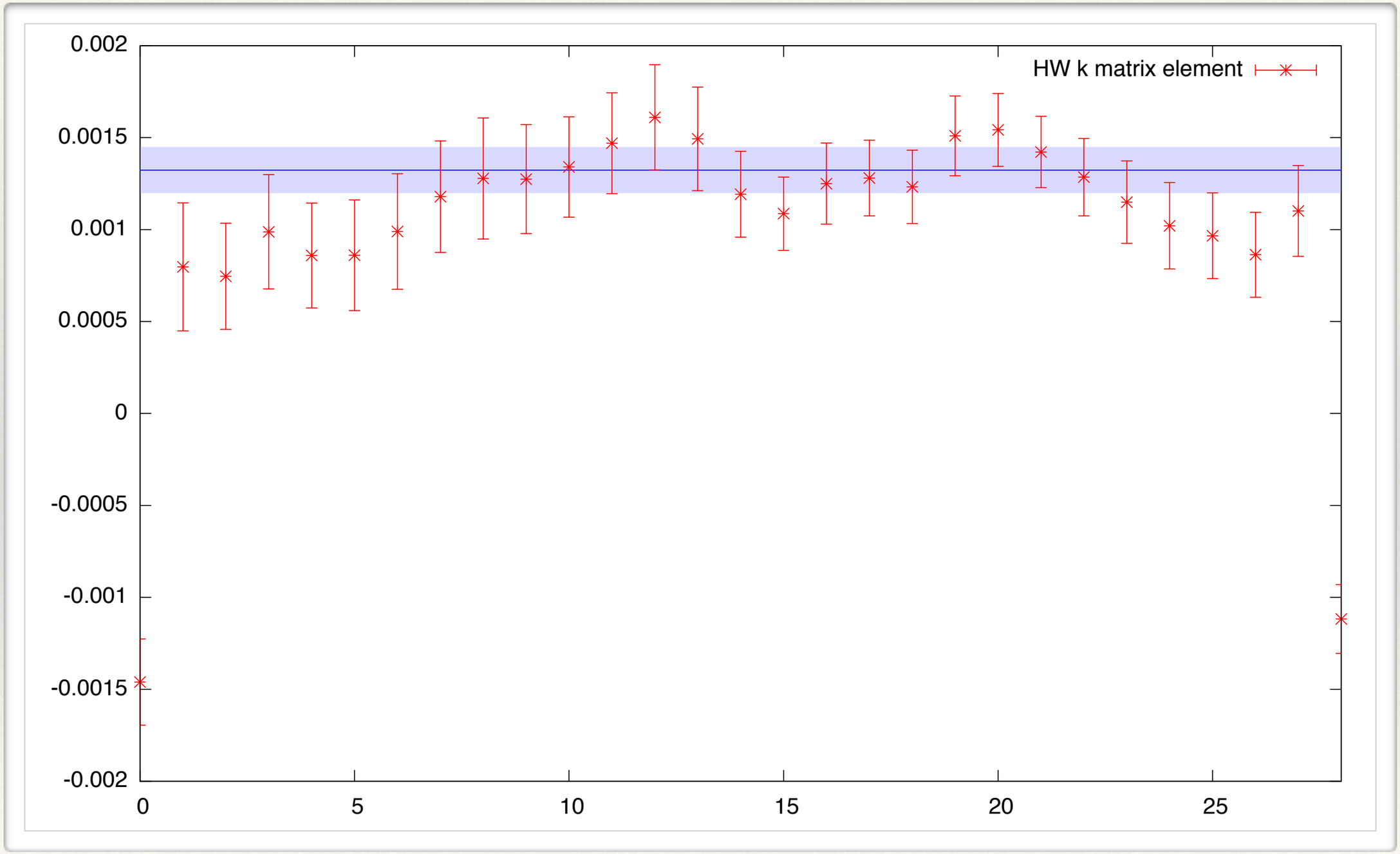

c_S determination

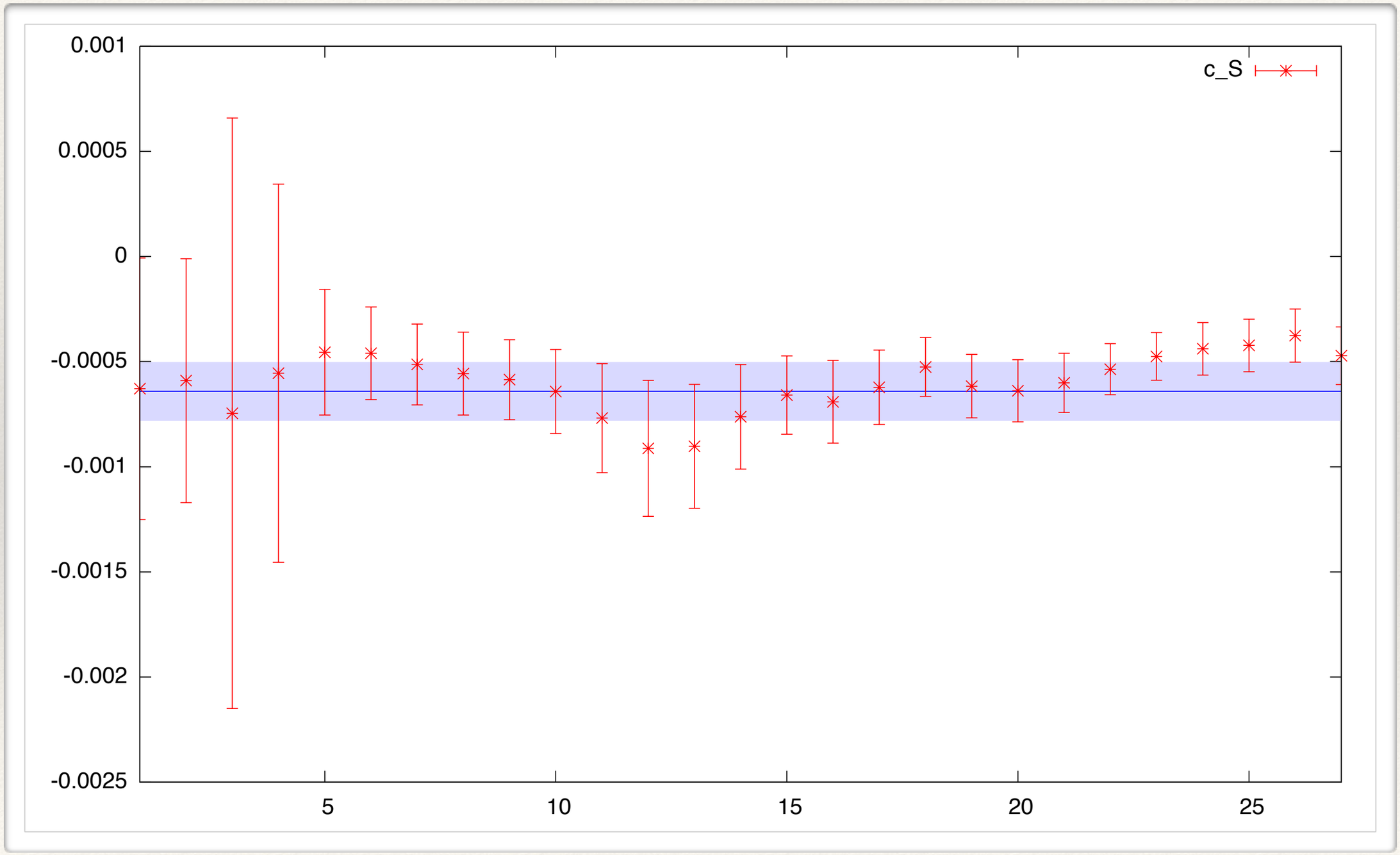

Rare kaon decay correlation function

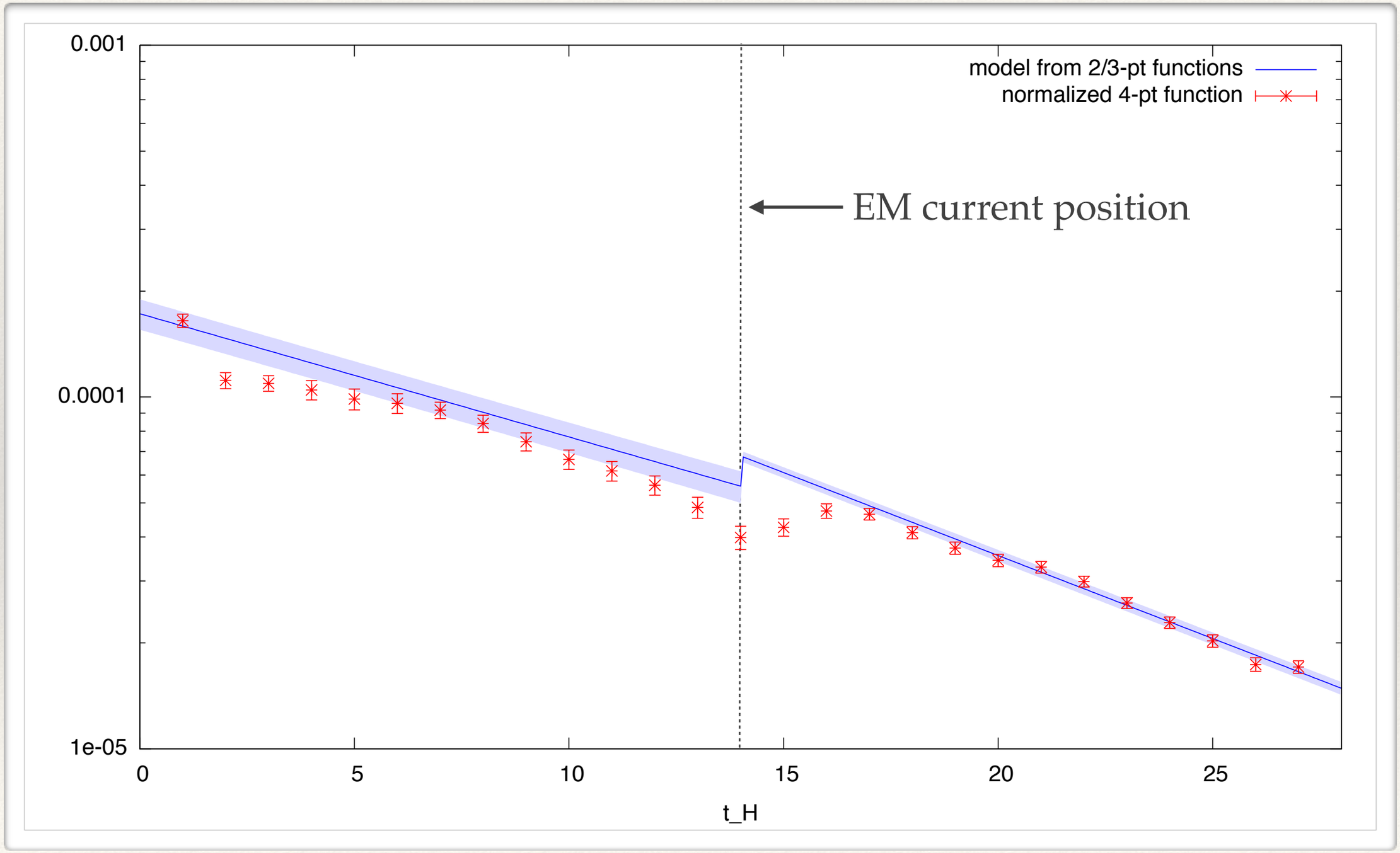

Rare kaon decay correlation function

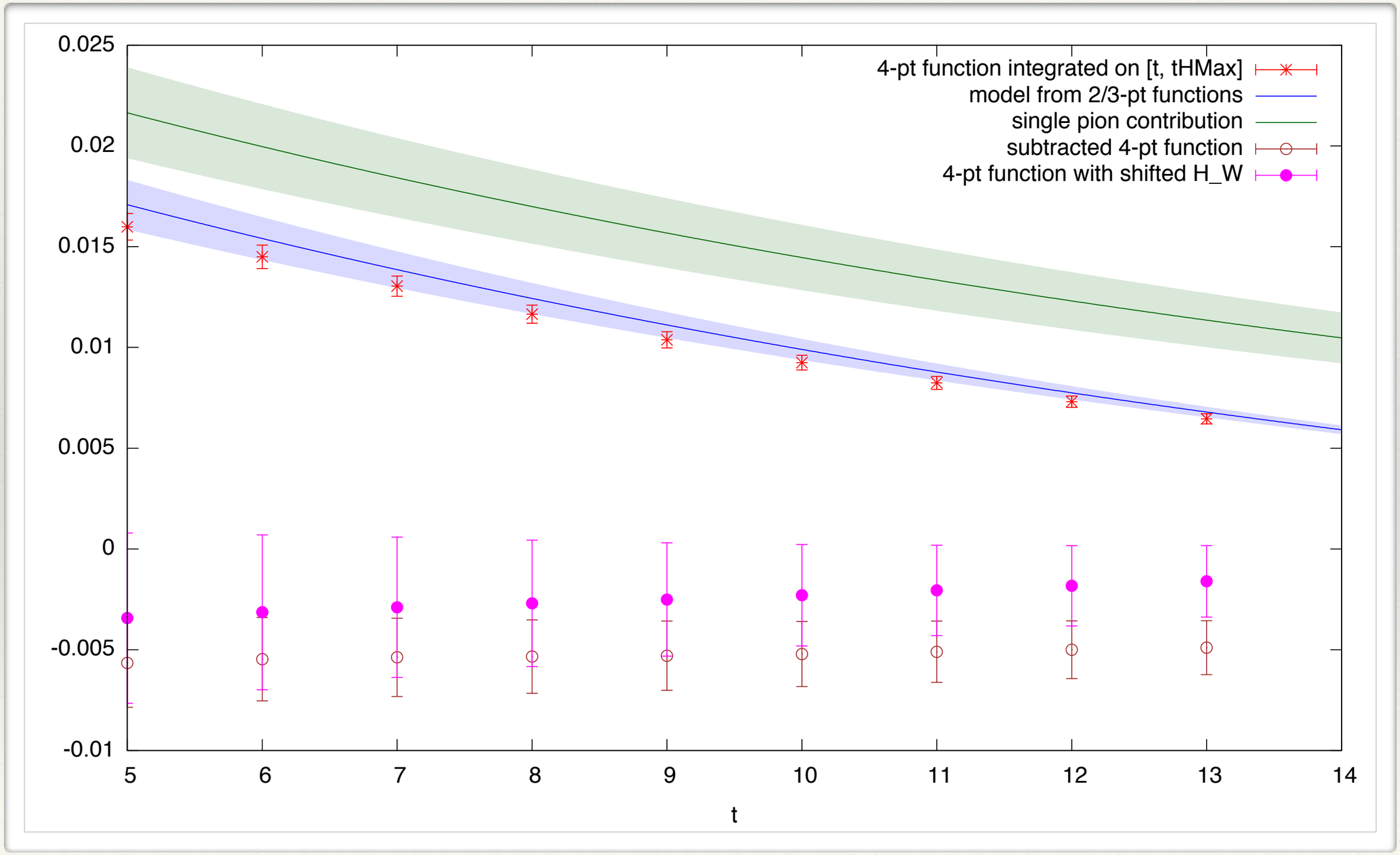

Summary & outlook

Summary

Summary

- We know how to define the di-lepton rare kaon decay matrix element in Euclidean space-time

Summary

- We know how to define the di-lepton rare kaon decay matrix element in Euclidean space-time
- Intermediate states with energy less than the kaon one have to be subtracted: possibly 1,2 or 3-pion states

Summary

- We know how to define the di-lepton rare kaon decay matrix element in Euclidean space-time
- Intermediate states with energy less than the kaon one have to be subtracted: possibly 1,2 or 3-pion states
- Two methods for the single-pion state

Summary

- We know how to define the di-lepton rare kaon decay matrix element in Euclidean space-time
- Intermediate states with energy less than the kaon one have to be subtracted: possibly 1,2 or 3-pion states
- Two methods for the single-pion state
- No 2-pion intermediate state

Summary

- We know how to define the di-lepton rare kaon decay matrix element in Euclidean space-time
- Intermediate states with energy less than the kaon one have to be subtracted: possibly 1,2 or 3-pion states
- Two methods for the single-pion state
- No 2-pion intermediate state
- Short-distance behaviour completely regulated by GIM mechanism and gauge-invariance

Summary

- We know how to define the di-lepton rare kaon decay matrix element in Euclidean space-time
- Intermediate states with energy less than the kaon one have to be subtracted: possibly 1,2 or 3-pion states
- Two methods for the single-pion state
- No 2-pion intermediate state
- Short-distance behaviour completely regulated by GIM mechanism and gauge-invariance
- If no on-shell 3-pion intermediate state: exponentially suppressed finite-size effects

Summary

- We know how to define the di-lepton rare kaon decay matrix element in Euclidean space-time
- Intermediate states with energy less than the kaon one have to be subtracted: possibly 1,2 or 3-pion states
- Two methods for the single-pion state
- No 2-pion intermediate state
- Short-distance behaviour completely regulated by GIM mechanism and gauge-invariance
- If no on-shell 3-pion intermediate state: exponentially suppressed finite-size effects
- Preliminary lattice calculations agree with theory

Outlook

Outlook

- Try different kinematics, time positions

Outlook

- Try different kinematics, time positions
- How to include efficiently S, E and disconnected diagrams?

Outlook

- Try different kinematics, time positions
- How to include efficiently S, E and disconnected diagrams?
- Aim at lighter quark masses

Outlook

- Try different kinematics, time positions
- How to include efficiently S, E and disconnected diagrams?
- Aim at lighter quark masses
- How to deal with the 3-pion intermediate state at the physical point?

Thank you!

Extract collinear parton distributions from lattice QCD calculations

Jianwei Qiu

Brookhaven National Laboratory

Stony Brook University

Based on work done with

Tomomi Ishikawa, Yan-Qing Ma, Shinsuke Yoshida, …

arXiv:1404.6860, 1412.2688, …

RBRC workshop on "Multi-hadron and nonlocal matrix elements in lattice QCD"

Brookhaven National Lab, Upton, NY, February 5-6, 2015

Outline

- Why Parton distribution functions (PDFs)?

  No PDFs, no predictions for Higgs production x-sections, …

- PDFs from lattice QCD calculations

- Our proposal – QCD collinear factorization

- Case study – Extract PDFs from quasi PDFs

- Summary and outlook

QCD factorization: PDFs

- **One hadron:** $\ell + h(p) \to \ell' + X$

$\sigma_{\text{tot}}^{\text{DIS}}$:

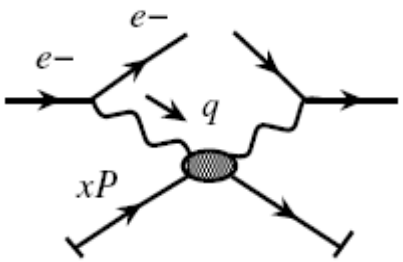

$\otimes$

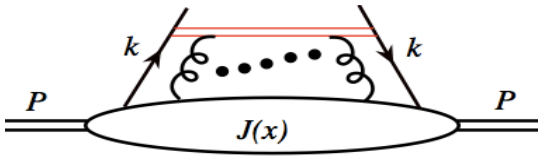

$+ O\left(\frac{1}{QR}\right)$

Hard-part
Probe

Parton-distribution
Structure

Power corrections
Approximation

QCD factorization: PDFs

- **One hadron:** $\ell + h(p) \to \ell' + X$

$\sigma_{\text{tot}}^{\text{DIS}}$:

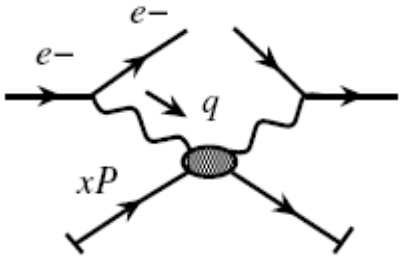

$\otimes$

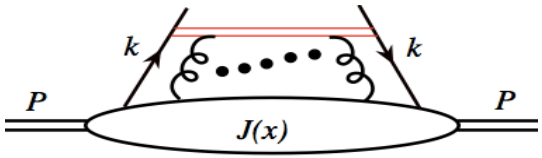

$+ O\left(\frac{1}{QR}\right)$

Hard-part
Probe

Parton-distribution
Structure

Power corrections
Approximation

- **Two hadrons:**

$h(p) + h'(p') \to V(\gamma^*, Z^0, \ldots) + X$

$\sigma_{\text{tot}}^{\text{DY}}$:

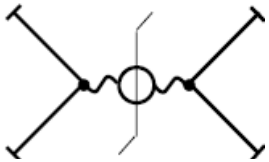

$\otimes$

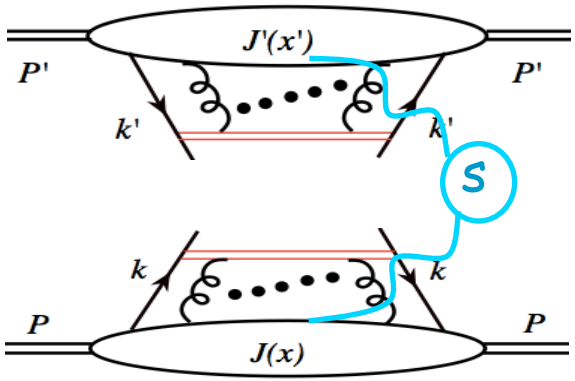

$+ O\left(\frac{1}{QR}\right)$

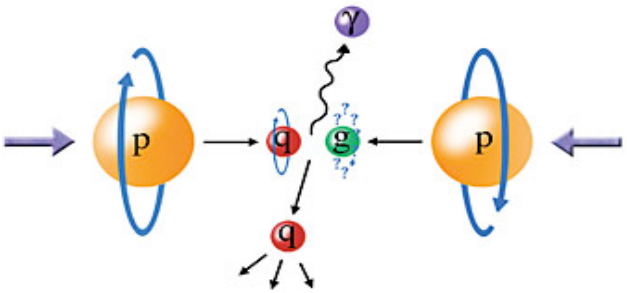

Predictive power:
Universal Parton Distributions

Operator definition of PDFs

- **Quark distribution (spin-averaged):**

$$q(x,\mu^2) = \int \frac{d\xi_-}{4\pi} e^{-ix\xi_- P_+} \langle P|\overline{\psi}(\xi_-)\gamma_+ \exp\left\{-ig\int_0^{\xi_-} d\eta_- A_+(\eta_-)\right\}\psi(0)|P\rangle \; + \text{UVCT}$$

- **Cut-vertex notation:**

$$\longleftarrow \frac{\gamma\cdot n}{2P\cdot n}\,\delta\left(x-\frac{k\cdot n}{P\cdot n}\right)\frac{d^4k}{(2\pi)^4}$$

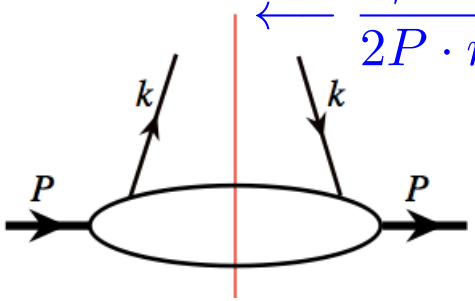

+ UVCT

PDFs are not direct physical observables, such as cross sections!
But, well-defined in QCD and process independent!

Operator definition of PDFs

- **Quark distribution (spin-averaged):**

$$q(x,\mu^2) = \int \frac{d\xi_-}{4\pi} e^{-ix\xi_- P_+} \langle P|\overline{\psi}(\xi_-)\gamma_+ \exp\left\{-ig\int_0^{\xi_-} d\eta_- A_+(\eta_-)\right\}\psi(0)|P\rangle \; + \text{UVCT}$$

- **Cut-vertex notation:**

$$\longleftarrow \frac{\gamma\cdot n}{2P\cdot n}\,\delta\left(x-\frac{k\cdot n}{P\cdot n}\right)\frac{d^4k}{(2\pi)^4}$$

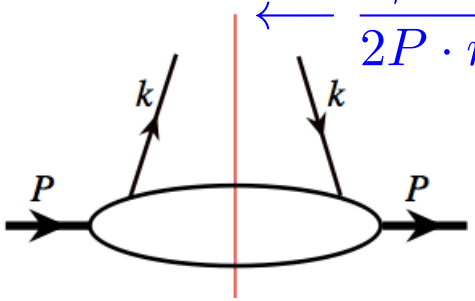

+ UVCT

PDFs are not direct physical observables, such as cross sections!
But, well-defined in QCD and process independent!

- **Parton interpretation emerges in *n.A = 0* gauge**
- **Independent of hadron momentum *P***
- **Simplest of all parton correlation functions of the hadron**

Global QCD analyses – a successful story

- World data with "Q" > 2 GeV

+ Factorization:

DIS: $$F_2(x_B, Q^2) = \Sigma_f C_f(x_B/x, \mu^2/Q^2) \otimes f(x, \mu^2)$$

H-H: $$\frac{d\sigma}{dy dp_T^2} = \Sigma_{ff'} f(x) \otimes \frac{d\hat{\sigma}_{ff'}}{dy dp_T^2} \otimes f'(x')$$

+ DGLAP Evolution:

$$\frac{\partial f(x, \mu^2)}{\partial \ln \mu^2} = \Sigma_{f'} P_{ff'}(x/x') \otimes f'(x', \mu^2)$$

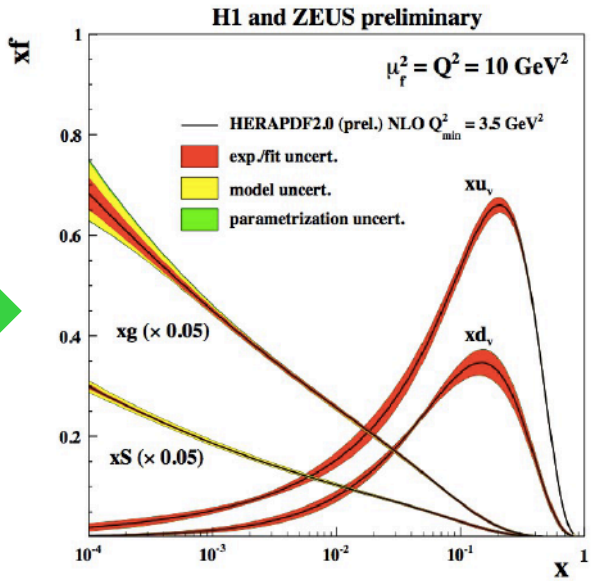

Global QCD analyses – a successful story

- **World data with "Q" > 2 GeV**

+ Factorization:

DIS: $$F_2(x_B, Q^2) = \Sigma_f C_f(x_B/x, \mu^2/Q^2) \otimes f(x, \mu^2)$$

H-H: $$\frac{d\sigma}{dy dp_T^2} = \Sigma_{ff'} f(x) \otimes \frac{d\hat{\sigma}_{ff'}}{dy dp_T^2} \otimes f'(x')$$

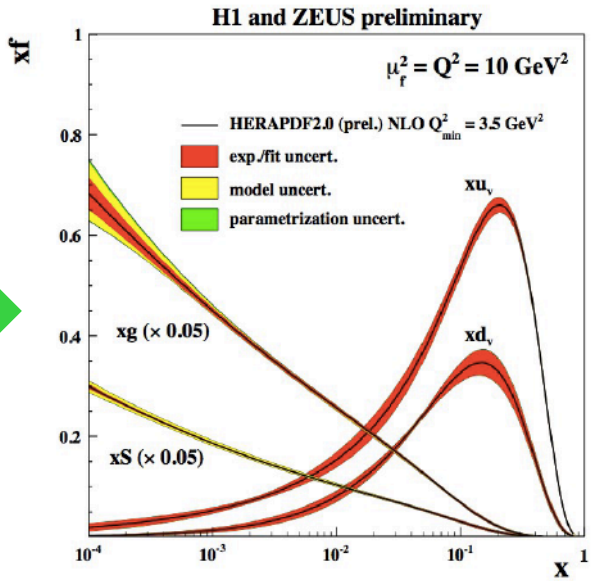

+ DGLAP Evolution:

$$\frac{\partial f(x, \mu^2)}{\partial \ln \mu^2} = \Sigma_{f'} P_{ff'}(x/x') \otimes f'(x', \mu^2)$$

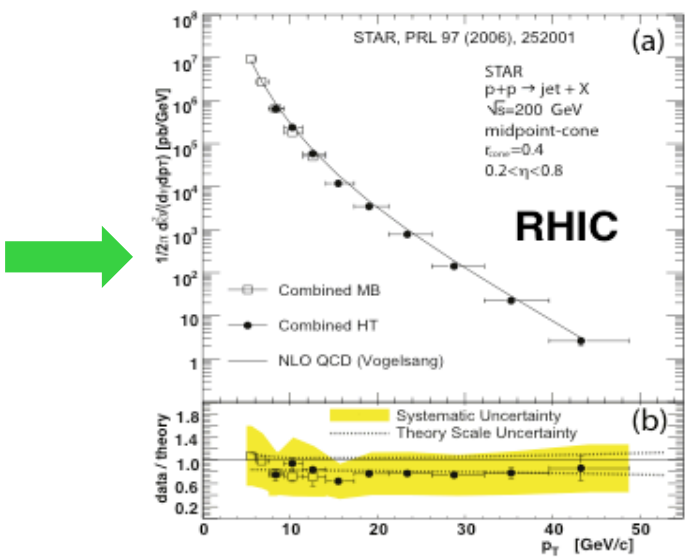

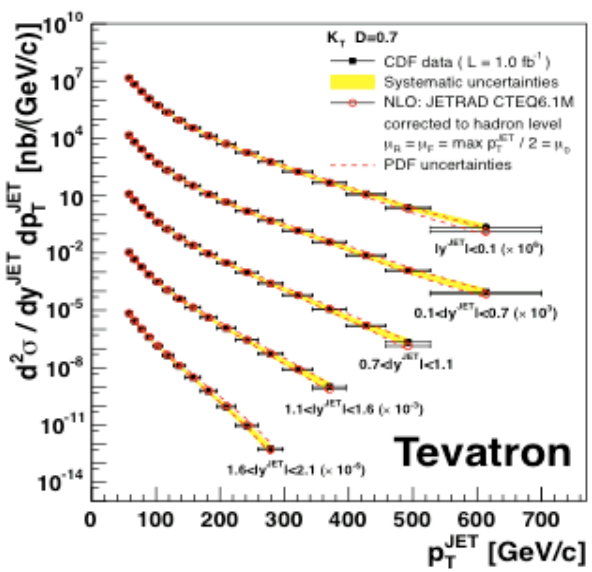

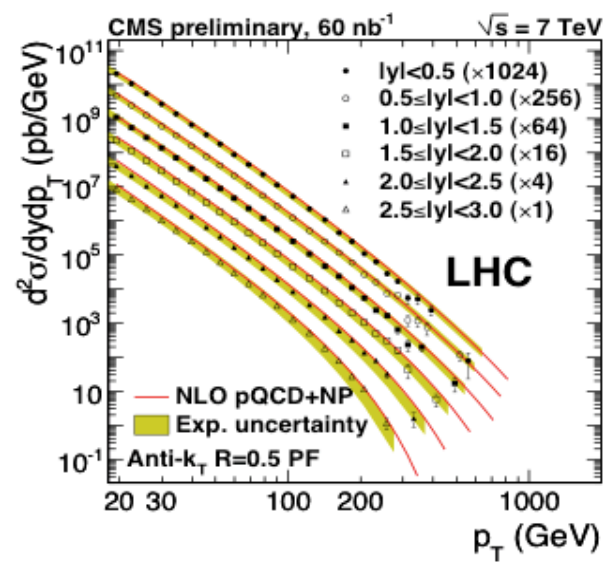

Uncertainties of PDFs

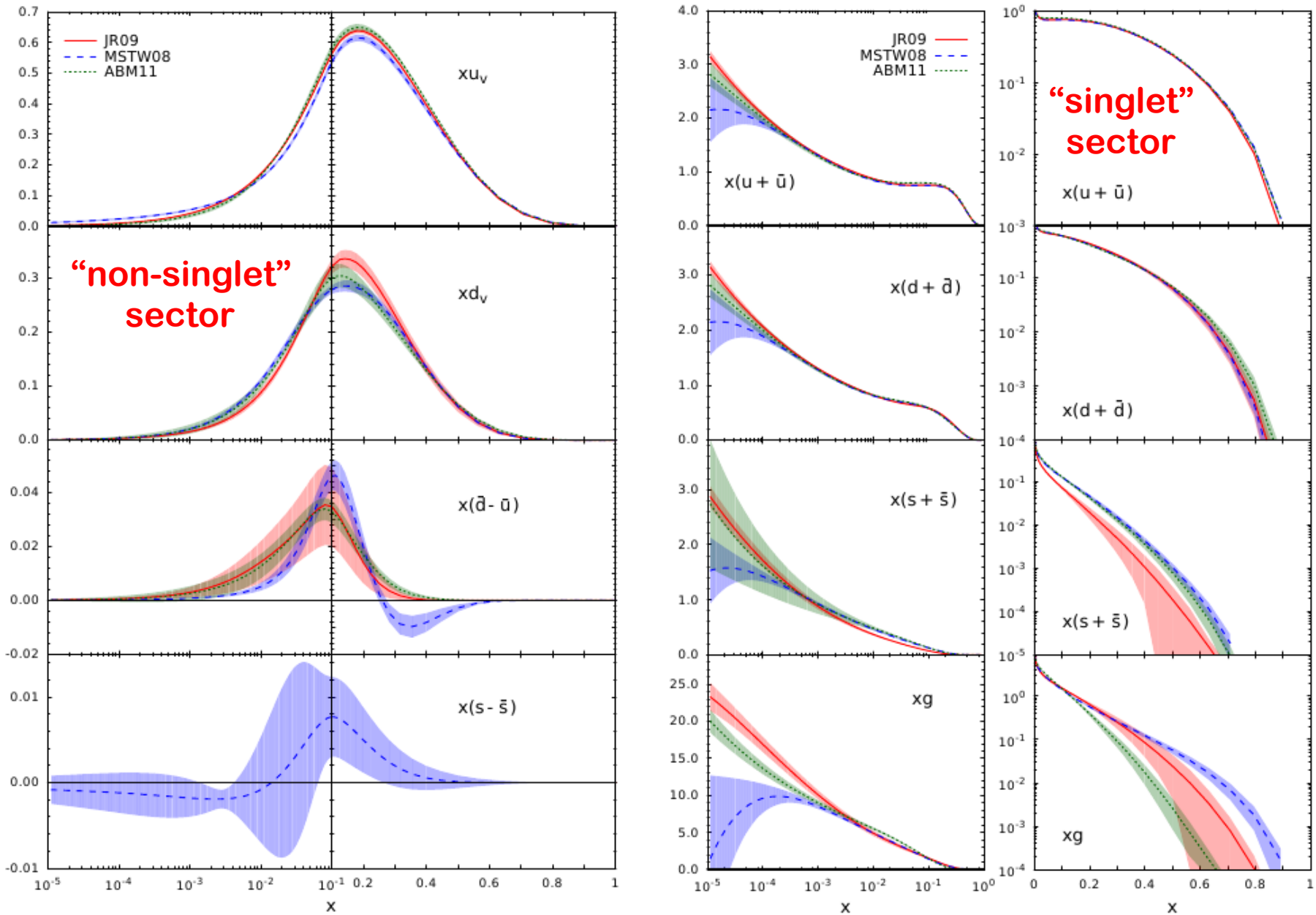

Partonic luminosities

q - qbar

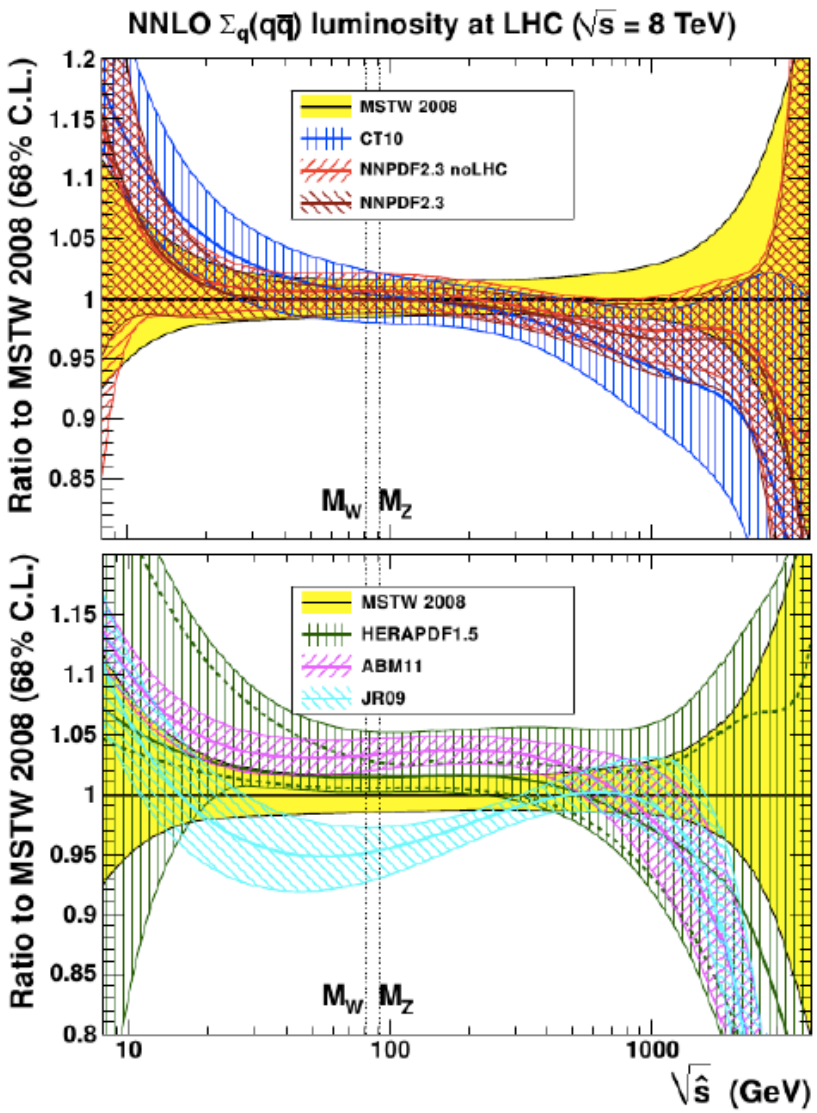

g - g

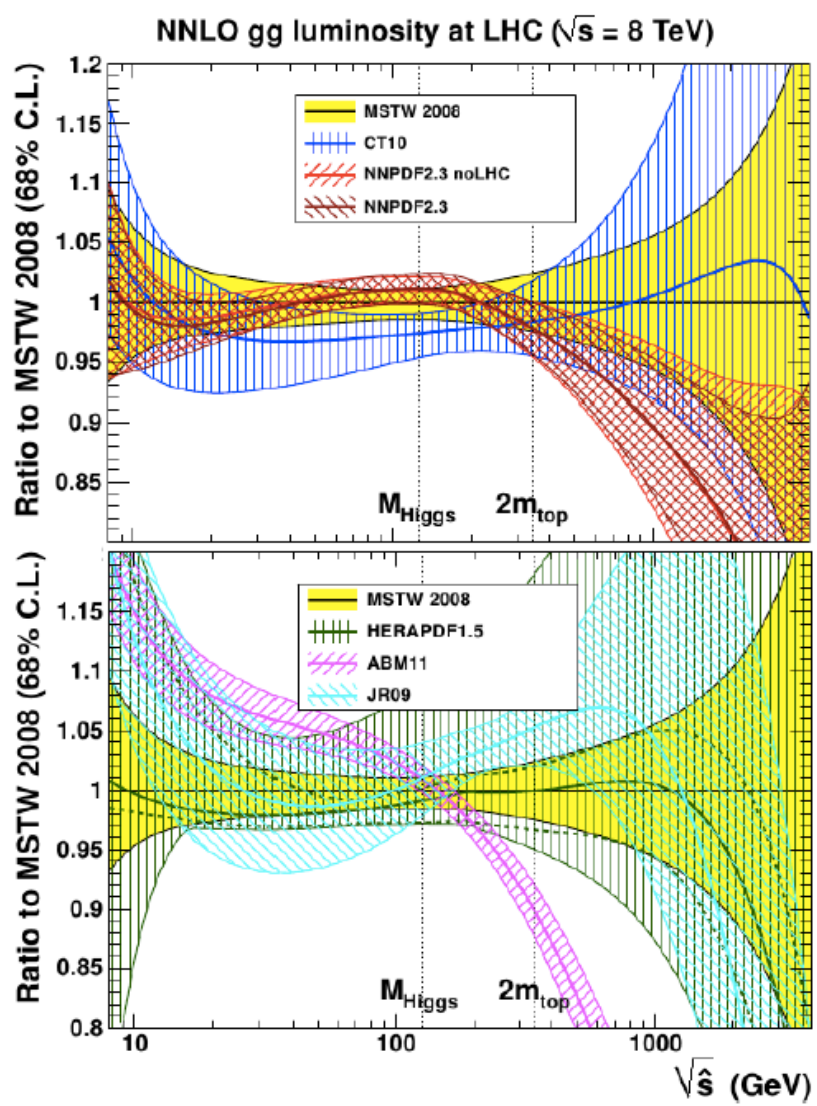

PDFs at large x

- Testing ground for hadron structure at x → 1:

  - $d/u \to 1/2$ — SU(6) Spin-flavor symmetry
  - $d/u \to 0$ — Scalar diquark dominance
  - $d/u \to 1/5$ — pQCD power counting
  - $d/u \to \dfrac{4\mu_n^2/\mu_p^2 - 1}{4 - \mu_n^2/\mu_p^2} \approx 0.42$ — Local quark-hadron duality

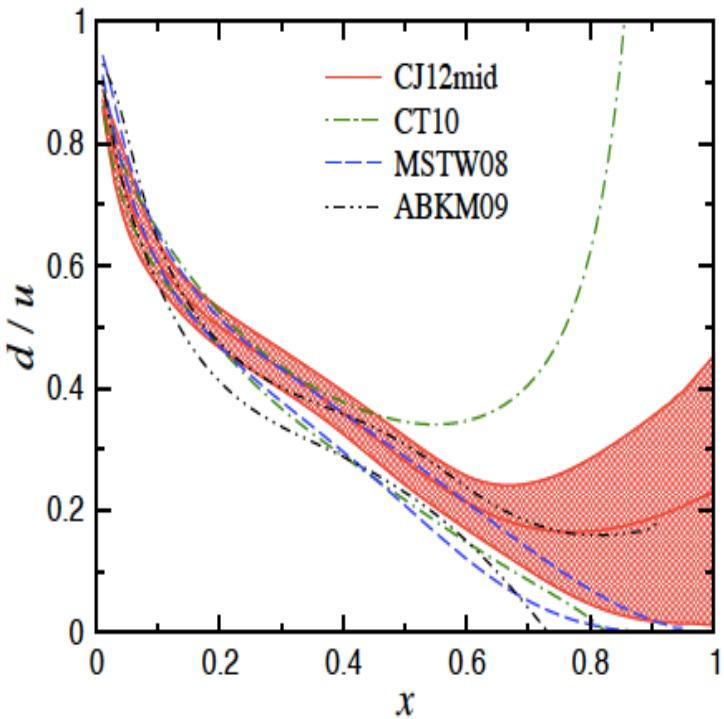

PDFs at large x

- Testing ground for hadron structure at x → 1:

✧ $d/u \to 1/2$	SU(6) Spin-flavor symmetry	✧ $\Delta u/u \to 2/3$ $\Delta d/d \to -1/3$
✧ $d/u \to 0$	Scalar diquark dominance	✧ $\Delta u/u \to 1$ $\Delta d/d \to -1/3$
✧ $d/u \to 1/5$	pQCD power counting	✧ $\Delta u/u \to 1$ $\Delta d/d \to 1$
✧ $d/u \to \dfrac{4\mu_n^2/\mu_p^2 - 1}{4 - \mu_n^2/\mu_p^2} \approx 0.42$	Local quark-hadron duality	✧ $\Delta u/u \to 1$ $\Delta d/d \to 1$

Can lattice QCD help?

Lattice QCD

- The main non-perturbative approach to solve QCD

- Hadron mass spectrum:

Predict the spectrum
with limited inputs

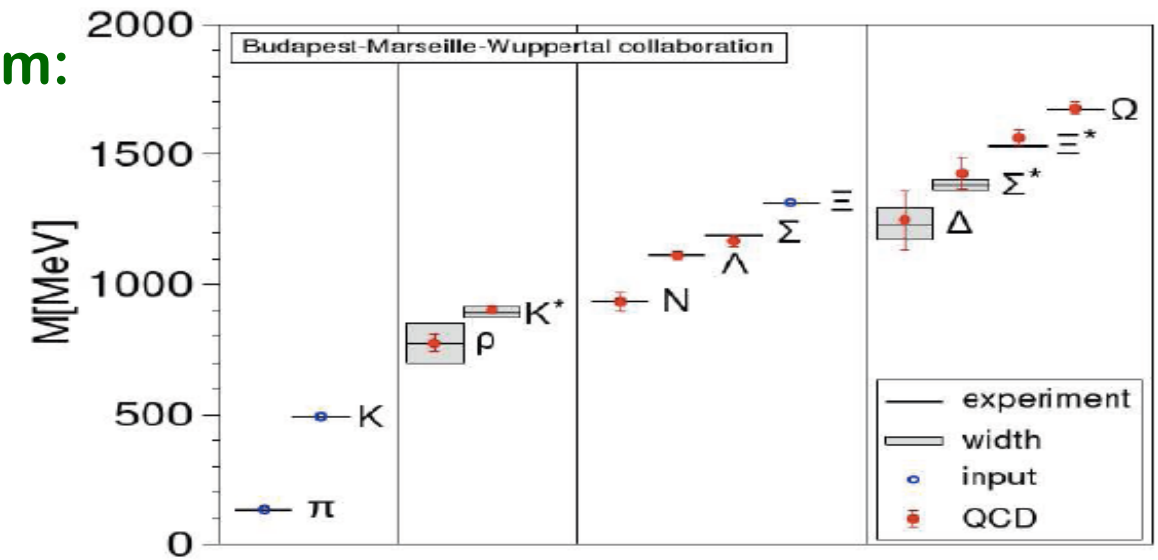

Lattice QCD

- The main non-perturbative approach to solve QCD

- Hadron mass spectrum:

Predict the spectrum with limited inputs

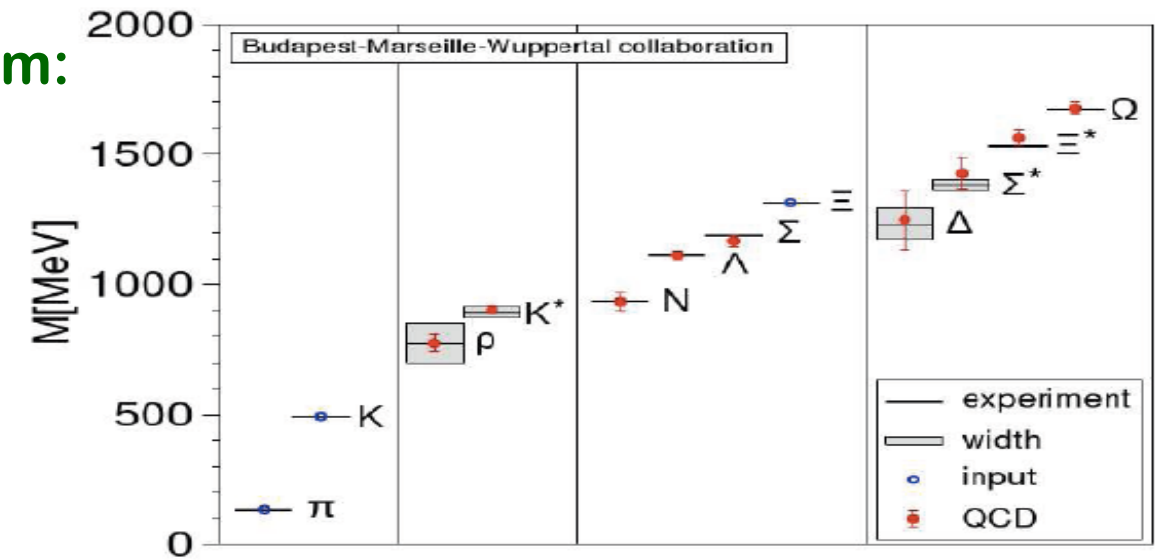

- An intrinsically Euclidean approach:
  - Lattice "time" is Euclidean: $\tau = i\,t$
  - No direct implementation of physical time

Cannot calculate PDFs directly, whose operators are time-dependent

PDFs from lattice QCD

- Moments of PDFs – matrix elements of local operators

$$\langle x^n(\mu^2)\rangle_q \equiv \int_0^1 dx\, x^n\, q(x,\mu^2)$$

- Works, but, hard and limited moments:

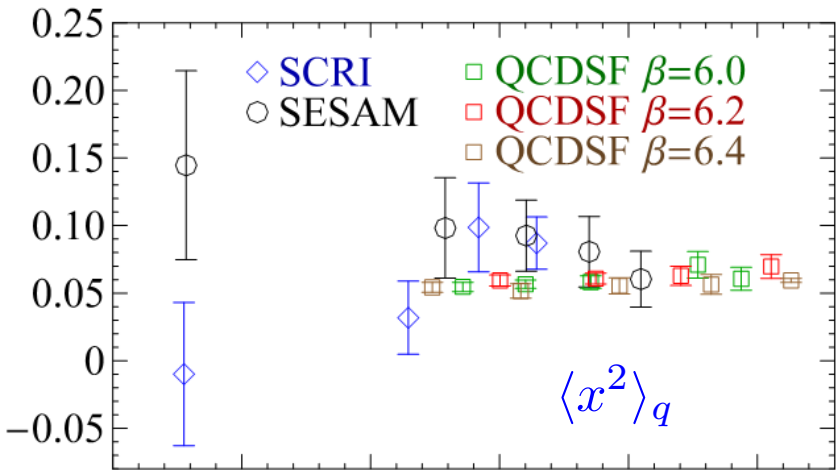

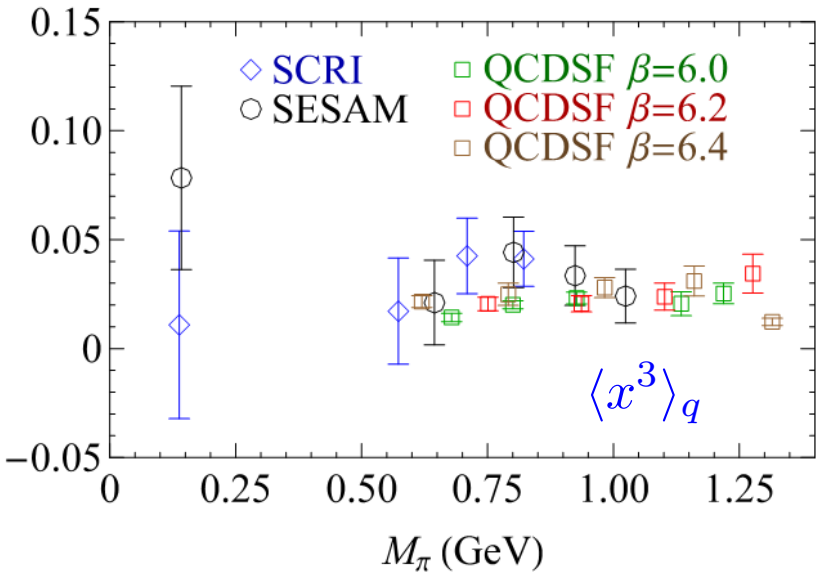

Dolgov et al., hep-lat/0201021

Gockeler et al., hep-ph/0410187

Limited moments – hard to get the full x-dependent distributions!

From quasi-PDFs to PDFs (Ji's idea)

Ji, arXiv:1305.1539

❑ "Quasi" quark distribution (spin-averaged):

$$\tilde{q}(x,\mu^2,P_z) \equiv \int \frac{d\xi_z}{4\pi} e^{-ixP_z\xi_z} \langle P|\overline{\psi}(\xi_z)\gamma_z \exp\left\{-ig\int_0^{\xi_z} d\eta_z A_z(\eta_z)\right\}\psi(0)|P\rangle + \mathrm{UVCT}(\mu^2)$$

❑ Features:

- Quark fields separated along the z-direction – not boost invariant!
- Perturbatively UV power divergent: $\propto (\mu/P_z)^n$ with $n > 0$ - renormalizable?
- Quasi-PDFs ➔ *Normal PDFs when $P_z \to \infty$*
- Quasi-PDFs could be calculated using standard lattice method

❑ Proposed matching:

Ji, arXiv:1305. 1539

$$\tilde{q}(x,\mu^2,P_z) = \int_x^1 \frac{dy}{y} Z\left(\frac{x}{y},\frac{\mu}{P_z}\right) q(y,\mu^2) + \mathcal{O}\left(\frac{\Lambda^2}{P_z^2},\frac{M^2}{P_z^2}\right)$$

- Size of $O(1/P_z^2)$ terms
- UV renormalization of power divergence, and potential operator mixing, …

Our observation

- QCD factorization of single-hadron cross section:

Momentum transfer

CO Factorization

PDFs

$$\sigma^{\rm DIS}(x, Q^2; \sqrt{s}) \propto$$

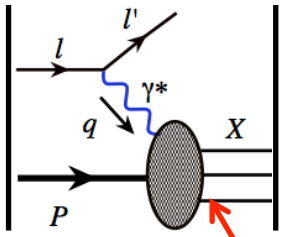

$$^2 \approx \sum_f \mathcal{C}_f(x, \frac{Q^2}{\mu^2}, \sqrt{s}) \otimes f_i(x, \mu^2) + \mathcal{O}\left[\frac{1}{Q^2}\right]$$

Collision energy

Single hadron Matrix elements

Perturbative coefficients

Power corrections

- ✧ PDFs are UV and IR finite, but, absorb perturbative CO divergence!
- ✧ With a large momentum transfer, PDFs completely cover all leading power CO divergence of single hadron matrix elements

Our observation

- **QCD factorization of single-hadron cross section:**

Momentum transfer

CO Factorization

PDFs

$$\sigma^{\rm DIS}(x, Q^2; \sqrt{s}) \propto$$

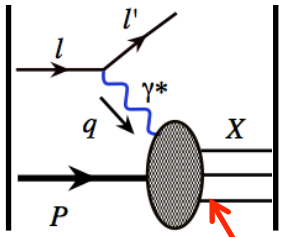

$$^2 \approx \sum_f \mathcal{C}_f(x, \frac{Q^2}{\mu^2}, \sqrt{s}) \otimes f_i(x, \mu^2) + \mathcal{O}\left[\frac{1}{Q^2}\right]$$

Collision energy

Single hadron Matrix elements

Perturbative coefficients

Power corrections

- ✧ **PDFs are UV and IR finite, but, absorb perturbative CO divergence!**
- ✧ **With a large momentum transfer, PDFs completely cover all leading power CO divergence of single hadron matrix elements**

- **Collinear divergences are from the region when $k_T \to 0$:**

Leading power perturbative CO divergences of single hadron matrix elements are logarithmic, $\propto \int dk_T^2/k_T^2$ **, and**

are the same for both Minkowski and Euclidean time

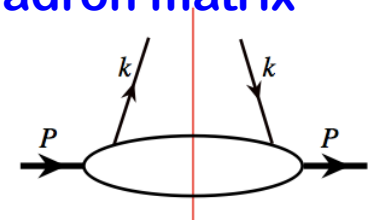

Our ideas

- **Lattice QCD can calculate "single" hadron matrix elements:**

$$\langle 0|\,\mathcal{O}(\overline{\psi},\psi,A)\,|0\rangle = \frac{1}{Z}\int \mathcal{D}A\mathcal{D}\overline{\psi}\mathcal{D}\psi\; e^{iS(\overline{\psi},\psi,A)}\mathcal{O}(\overline{\psi},\psi,A)$$

$$\sum_{P'}|P'\rangle\langle P'| \quad \sum_{P}|P\rangle\langle P| \quad \Rightarrow \quad \langle P_z|\mathcal{O}(\overline{\psi},\psi,A)|P_z\rangle$$

Ma and Qiu, arXiv:1404.6860 1412.2688

With an Euclidean time

- ✧ **Operators made of conserved currents – Physical – No need for UVCT**

  Need a large scale, μ^2, e.g., the offshellness of the current(s)

- ✧ **Operators lead to perturbative UV divergence – Renormalizable!**

$$\widetilde{\sigma}(\tilde{x},P_z;\mu^2)_{\rm E} \equiv \text{ F.T. of } \langle P_z|\mathcal{O}(\overline{\psi},\psi,A)(\delta_z)|P_z\rangle + \text{UVCT}(\mu^2)$$

quasi-PDFs

Our ideas

- **Lattice QCD can calculate "single" hadron matrix elements:**

$$\langle 0|\,\mathcal{O}(\overline{\psi},\psi,A)\,|0\rangle = \frac{1}{Z}\int \mathcal{D}A\mathcal{D}\overline{\psi}\mathcal{D}\psi\; e^{iS(\overline{\psi},\psi,A)}\mathcal{O}(\overline{\psi},\psi,A)$$

$$\sum_{P'}|P'\rangle\langle P'| \quad \sum_{P}|P\rangle\langle P| \quad \Rightarrow \quad \langle P_z|\mathcal{O}(\overline{\psi},\psi,A)|P_z\rangle$$

Ma and Qiu, arXiv:1404.6860 1412.2688

With an Euclidean time

✧ Operators made of conserved currents – Physical – No need for UVCT

Need a large scale, μ^2, e.g., the offshellness of the current(s)

✧ Operators lead to perturbative UV divergence – Renormalizable!

$$\widetilde{\sigma}(\tilde{x},P_z;\mu^2)_{\rm E} \equiv \text{ F.T. of } \langle P_z|\mathcal{O}(\overline{\psi},\psi,A)(\delta_z)|P_z\rangle + \text{UVCT}(\mu^2)$$

quasi-PDFs

- **Collinear factorization:**

Normal PDFs

$$\widetilde{\sigma}(\tilde{x},P_z;\mu^2)_{\rm E} = \Sigma_f \int_0^1 \frac{dx}{x}\,\mathcal{C}_f\left(\frac{\tilde{x}}{x},\frac{\bar{\mu}^2}{\mu^2},\alpha_s;P_z\right) f(x,\bar{\mu}^2) + \mathcal{O}\left[\frac{1}{\mu^\alpha}\right]$$

✧ Perturbatively, $\widetilde{\sigma}(\tilde{x},P_z;\mu^2)_{\rm E}$ and $f(x,\bar{\mu}^2)$ have the same CO divergence

✧ Matching coefficients, $\mathcal{C}_f$, are IR safe and perturbatively calculable

Extract PDFs from lattice "cross sections"

❑ Lattice "cross section":

$$\tilde{\sigma}_{\rm E}^{\rm Lat}(\tilde{x}, 1/a, P_z) \propto \text{F.T. of } \langle P_z|\mathcal{O}(\overline{\psi}, \psi, A)|P_z\rangle + \text{UVCT}(1/a)$$

- ✧ Its continuum limit is UV renormalizable
- ✧ It is calculable in lattice QCD with an Euclidean time, "E"
- ✧ It is infrared (IR) safe, calculated in lattice perturbation theory
- ✧ All CO divergences of its continuum limit ($a \to 0$) can be factorized into the normal PDFs with perturbatively calculable hard coefficients

  "Collision energy" $P_z \sim$ "$\sqrt{s}$" ***"rapidity"*** $\tilde{x} \sim$ "y"

  "Hard momentum transfer" $1/a \sim \tilde{\mu} \sim$ "Q"

❑ UV renormalization:

- ✧ No UVCT needed if $\mathcal{O}(\overline{\psi}, \psi, A)$ is made of conserved currents
- ✧ The quasi-PDFs are not made of conserved currents – UVCT needed

❑ CO Factorization – IR safe matching coefficients:

$$\tilde{\sigma}_{\rm E}^{\rm Lat}(\tilde{x}, \frac{1}{a}, P_z) \approx \sum_i \int_0^1 \frac{dx}{x} f_{i/h}(x, \mu^2)\, \tilde{\mathcal{C}}_i(\frac{\tilde{x}}{x}, \frac{1}{a}, \mu^2, P_z)$$

QCD Global analysis of lattice data

Differences between Ji's approach and ours

❑ For the quasi-PDFs:

✧ **Ji's approach – high P_z effective field theory:**

Ji, arXiv:1305.1539
1404.6680

$$\tilde{q}(x,\mu^2,P_z) = \int_x^1 \frac{dy}{y} Z\left(\frac{x}{y},\frac{\mu}{P_z}\right) q(y,\mu^2) + \mathcal{O}\left(\frac{\Lambda^2}{P_z^2},\frac{M^2}{P_z^2}\right)$$

✧ **Our approach – QCD collinear factorization:**

Ma and Qiu,
arXiv:1404.6860
1412.2688

$$\tilde{q}(x,\mu^2,P_z) = \sum_f \int_0^1 \frac{dy}{y} \mathcal{C}_f\left(\frac{x}{y},\frac{\mu^2}{\bar{\mu}^2},P_z\right) f(y,\bar{\mu}^2) + \mathcal{O}\left(\frac{1}{\mu^2}\right)$$

Parameter like $\sqrt{s}$

Factorization scale

High twist Power corrections

$$\sigma^{\rm DIS}(x,Q^2;\sqrt{s}) \propto$$

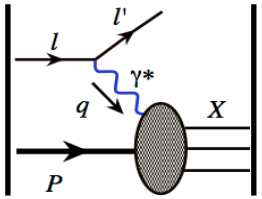

$$^2 \approx \sum_f \mathcal{C}_f(x,\frac{Q^2}{\mu^2},\sqrt{s}) \otimes f_i(x,\mu^2) + \mathcal{O}\left[\frac{1}{Q^2}\right]$$

Differences between Ji's approach and ours

❑ For the quasi-PDFs:

✧ **Ji's approach – high P_z effective field theory:**

Ji, arXiv:1305.1539
1404.6680

$$\tilde{q}(x,\mu^2,P_z) = \int_x^1 \frac{dy}{y} Z\left(\frac{x}{y},\frac{\mu}{P_z}\right) q(y,\mu^2) + \mathcal{O}\left(\frac{\Lambda^2}{P_z^2},\frac{M^2}{P_z^2}\right)$$

✧ **Our approach – QCD collinear factorization:**

Ma and Qiu,
arXiv:1404.6860
1412.2688

$$\tilde{q}(x,\mu^2,P_z) = \sum_f \int_0^1 \frac{dy}{y} \mathcal{C}_f\left(\frac{x}{y},\frac{\mu^2}{\bar{\mu}^2},P_z\right) f(y,\bar{\mu}^2) + \mathcal{O}\left(\frac{1}{\mu^2}\right)$$

Parameter like $\sqrt{s}$ | **Factorization scale** | **High twist Power corrections**

$$\sigma^{\rm DIS}(x,Q^2;\sqrt{s}) \propto$$

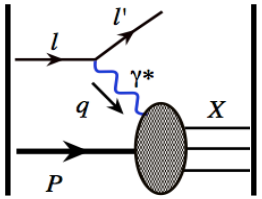

$$^2 \approx \sum_f \mathcal{C}_f(x,\frac{Q^2}{\mu^2},\sqrt{s}) \otimes f_i(x,\mu^2) + \mathcal{O}\left[\frac{1}{Q^2}\right]$$

❑ Beyond quasi-PDFs:

Lattice "cross-sections" – *lattice calculable single hadron matrix elements*

UV and IR safe with a large momentum transfer, CO factorized into PDFs

Case study – factorization of quasi-PDFs

- **The "Quasi-quark" distribution, as an example:**

Ma and Qiu, arXiv:1404.6860 1412.2688

$$\tilde{q}(\tilde{x},\tilde{\mu}^2,P_z) = \int \frac{dy_z}{4\pi} e^{i\tilde{x}P_z y_z} \langle P|\overline{\psi}(y_z)\gamma_z \exp\left\{-ig\int_0^{y_z} dy_z' A_z(y_z')\right\}\psi(0)|P\rangle$$

✧ **Feynman diagram representation:** $\Phi_{n_z}^{(f,a)}(\{\xi_z,0\}) = \Phi_{n_z}^{\dagger(f,a)}(\{\infty,\xi_z\})\,\Phi_{n_z}^{(f,a)}(\{\infty,0\})$

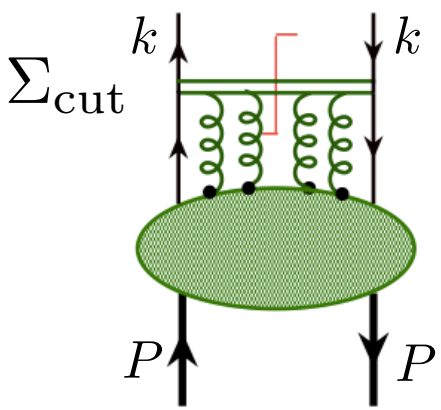

$$\longleftarrow \quad \frac{\gamma_z}{2P_z}\,\delta\left(\tilde{x}-\frac{k_z}{P_z}\right)$$

$$P_z \sim \text{“}\sqrt{s}\text{”} \sim \tilde{\mu}/\tilde{x}$$ ***Sufficiently large***

$$P^2 \sim 0$$

Case study – factorization of quasi-PDFs

- **The "Quasi-quark" distribution, as an example:**

Ma and Qiu, arXiv:1404.6860 1412.2688

$$\tilde{q}(\tilde{x},\tilde{\mu}^2,P_z) = \int \frac{dy_z}{4\pi} e^{i\tilde{x}P_z y_z} \langle P|\overline{\psi}(y_z)\gamma_z \exp\left\{-ig\int_0^{y_z} dy_z' A_z(y_z')\right\}\psi(0)|P\rangle$$

- **Feynman diagram representation:** $\Phi_{n_z}^{(f,a)}(\{\xi_z,0\}) = \Phi_{n_z}^{\dagger(f,a)}(\{\infty,\xi_z\})\,\Phi_{n_z}^{(f,a)}(\{\infty,0\})$

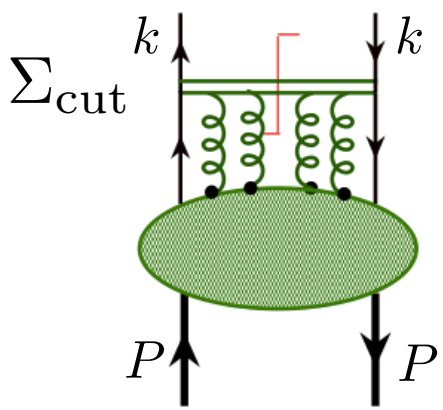

$$\longleftarrow \quad \frac{\gamma_z}{2P_z}\,\delta\left(\tilde{x}-\frac{k_z}{P_z}\right)$$

$$P_z \sim \text{“}\sqrt{s}\text{”} \sim \tilde{\mu}/\tilde{x}$$ ***Sufficiently large***

$$P^2 \sim 0$$

- **Like PDFs, it is IR finite**
- **Like PDFs, it is UV divergent, but, worse (linear UV divergence)**

  Potential trouble! - mixing with the Log UV of PDFs?

- **Like PDFs, it is CO divergent – factorizes CO divergence into PDFs**

  Show to all orders in perturbation theory

All order QCD factorization of CO divergence

Ma and Qiu, arXiv:1404.6860

❑ Generalized ladder decomposition in a physical gauge

$$n \cdot A = A^+ = 0$$

Mueller, PRD 1974

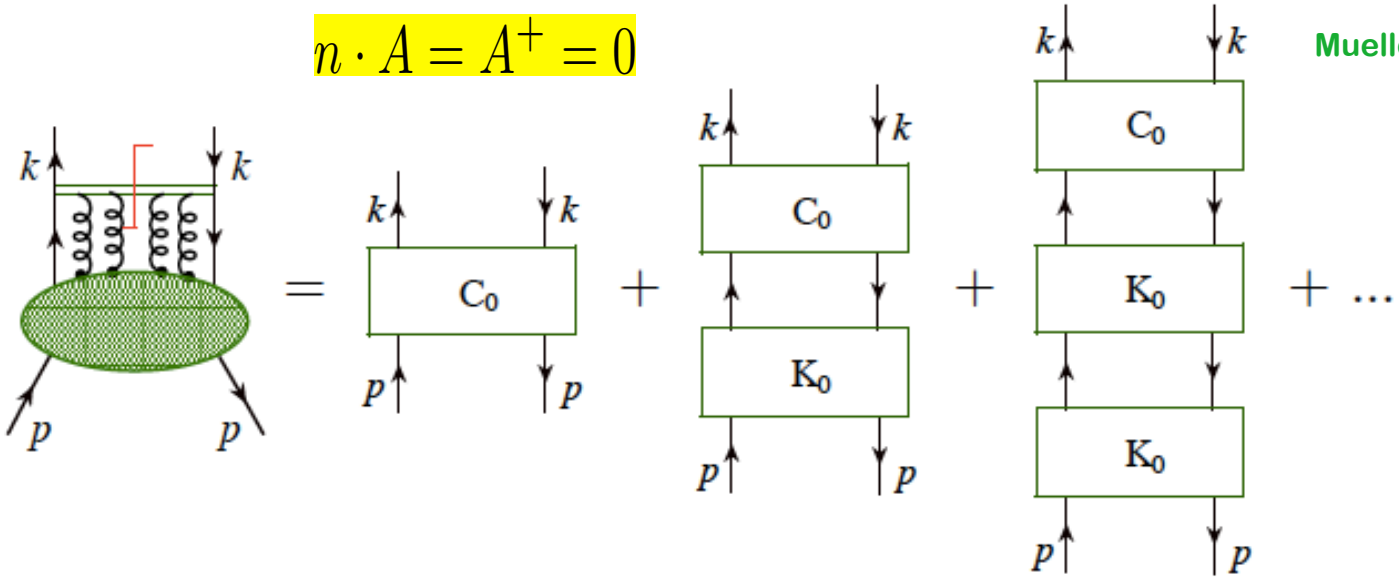

❑ $C_0,\ K_0$:2PI kernels

✧ Only process dependence:

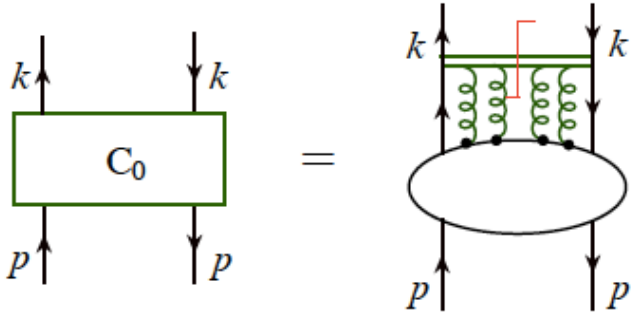

✧ 2PI are finite in a physical gauge for fixed *k* and *p*:

Ellis, Georgi, Machacek, Politzer, Ross, 1978, 1979

All order QCD factorization of CO divergence

❑ 2PI kernels – Diagrams:

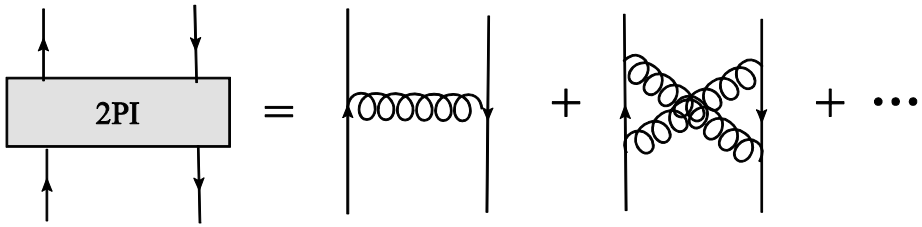

❑ Ordering in virtuality: $P^2 \ll k^2 \lesssim \tilde{\mu}^2$ – Leading power in $\frac{1}{\tilde{\mu}}$

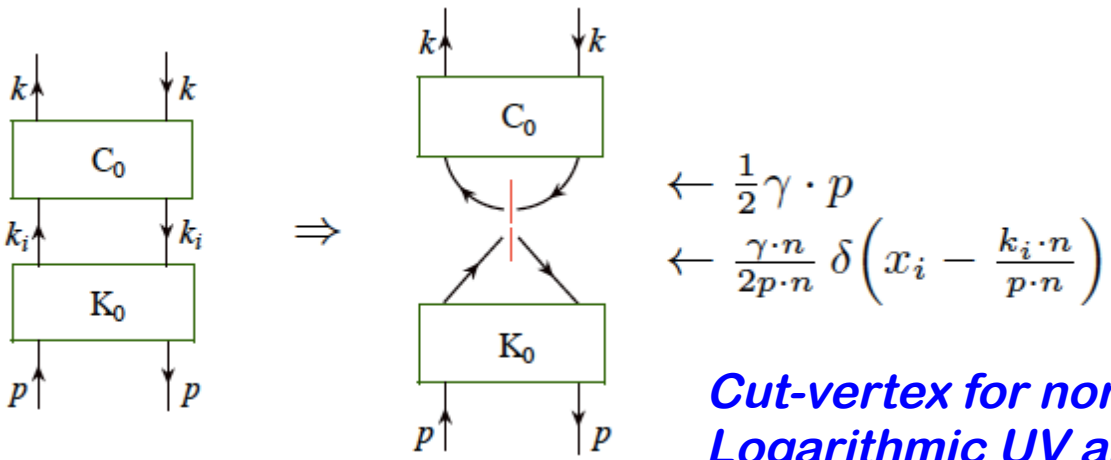

+ power suppressed

Cut-vertex for normal quark distribution
Logarithmic UV and CO divergence

❑ Renormalized kernel - parton PDF:

$$K \equiv \int d^4k_i\, \delta\left(x_i - \frac{k^+}{p^+}\right) \mathrm{Tr}\left[\frac{\gamma\cdot n}{2p\cdot n} K_0 \frac{\gamma\cdot p}{2}\right] + \mathrm{UVCT}_{\mathrm{Logarithmic}}$$

All order QCD factorization of CO divergence

- **Projection operator for CO divergence:**

$\widehat{\mathcal{P}}\,K$ Pick up the logarithmic CO divergence of *K*

- **Factorization of CO divergence:**

$$\tilde{f}_{q/p} = \lim_{m\to\infty} C_0 \sum_{i=0}^{m} K^i + \mathrm{UVCTs}$$

$$= \lim_{m\to\infty} C_0 \left[1 + \sum_{i=0}^{m-1} K^i (1-\widehat{\mathcal{P}})K\right]_{\mathrm{ren}} + \tilde{f}_{q/p}\,\widehat{\mathcal{P}}\,K$$

$$= \lim_{m\to\infty} C_0 \left[1 + \sum_{i=1}^{m} \left[(1-\widehat{\mathcal{P}})K\right]^i\right]_{\mathrm{ren}} + \tilde{f}_{q/p}\,\widehat{\mathcal{P}}\,K$$

$$\tilde{f}_{q/P} = \left[C_0 \frac{1}{1-(1-\widehat{\mathcal{P}})K}\right]_{\mathrm{ren}} \left[\frac{1}{1-\widehat{\mathcal{P}}K}\right]$$

CO divergence free

Normal Quark distribution

All CO divergence of quasi-quark distribution

All order QCD factorization of CO divergence

- **Projection operator for CO divergence:**

$\widehat{\mathcal{P}}\, K$ Pick up the logarithmic CO divergence of *K*

- **Factorization of CO divergence:**

$$\tilde{f}_{q/p} = \lim_{m\to\infty} C_0 \sum_{i=0}^{m} K^i + \text{UVCTs}$$

$$= \lim_{m\to\infty} C_0 \left[1 + \sum_{i=0}^{m-1} K^i (1-\widehat{\mathcal{P}})K\right]_{\text{ren}} + \tilde{f}_{q/p}\,\widehat{\mathcal{P}}\,K$$

$$= \lim_{m\to\infty} C_0 \left[1 + \sum_{i=1}^{m} \left[(1-\widehat{\mathcal{P}})K\right]^i\right]_{\text{ren}} + \tilde{f}_{q/p}\,\widehat{\mathcal{P}}\,K$$

$$\tilde{f}_{q/P} = \left[C_0 \frac{1}{1-(1-\widehat{\mathcal{P}})K}\right]_{\text{ren}} \left[\frac{1}{1-\widehat{\mathcal{P}}K}\right]$$

Normal Quark distribution

CO divergence free

All CO divergence of quasi-quark distribution

$$\tilde{\sigma}_{\text{M}}(\tilde{x}, \tilde{\mu}^2, P_z) \approx \sum_i \int_0^1 \frac{dx}{x} f_{i/h}(x, \mu^2)\, \mathcal{C}_i\left(\frac{\tilde{x}}{x}, \tilde{\mu}^2, \mu^2, P_z\right)$$

UV finite?

UV renormalization

Ma and Qiu, arXiv:1404.6860, …

❑ UV divergences (difference in gauge link):

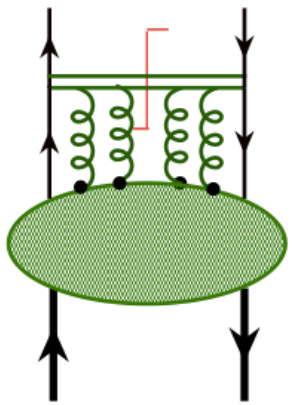

$n_z^2 = -1$ $\qquad$ $\frac{1}{2}\gamma^z$

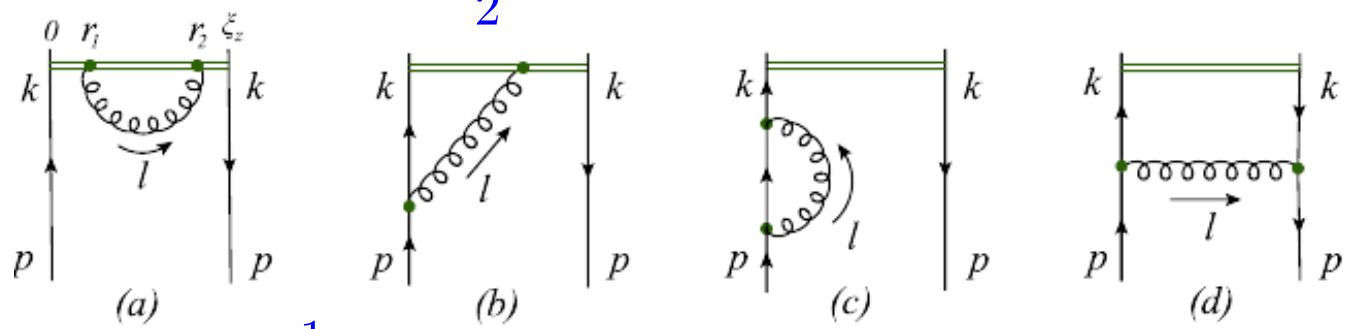

$$\frac{1}{2}\gamma\cdot p \propto \left[\gamma^0 - \gamma^z\right]$$

❑ Renormalization:

$$\left[C_0 \frac{1}{1-(1-\hat{\mathcal{P}})K}\right]_{\text{ren}} \equiv C_0 \frac{1}{1-(1-\hat{\mathcal{P}})K} + \text{UVCTs}$$

In coordinate space: ξ_z Independence!

✧ **Power divergence:** **Diagram (a) – independent of ξ_z**

Removed by "mass" renormalization of a test particle – the gauge link

✧ **Left-over log divergence:** Dotsenko and Vergeles NPB, (1980)

Dimensional regularization – ξ_z independence of $1/\varepsilon$ – finite CTs

✧ **Log(ξ_z) – term:** **Artifact of dimensional regularization**

One-loop example: quark ➔quark

Ma and Qiu, arXiv:1404.6860

- Expand the factorization formula:

$$\tilde{f}^{(1)}_{q/q}(\tilde{x}) = f^{(0)}_{q/q}(x) \otimes \mathcal{C}^{(1)}_{q/q}(\tilde{x}/x) + f^{(1)}_{q/q}(x) \otimes \mathcal{C}^{(0)}_{q/q}(\tilde{x}/x)$$

$$\Rightarrow \quad \mathcal{C}^{(1)}_{q/q}(t, \tilde{\mu}^2, \mu^2, P_z) = \tilde{f}^{(1)}_{q/q}(t, \tilde{\mu}^2, P_z) - f^{(1)}_{q/q}(t, \mu^2)$$

- Feynman diagrams:

Same diagrams for both

$\tilde{f}_{q/q}$ and $f_{q/q}$

But, in different gauge

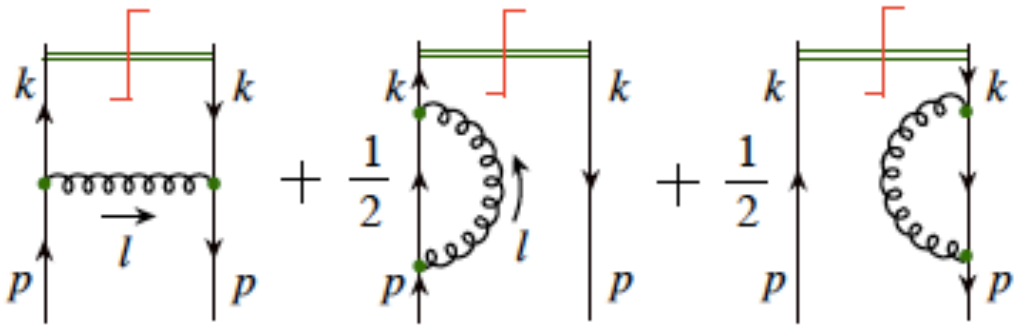

- Gauge choice:

$$n_z \cdot A = 0 \quad \text{for} \quad \tilde{f}_{q/q} \qquad\qquad n \cdot A = 0 \quad \text{for} \quad f_{q/q}$$

Gluon propagator:

$$\tilde{d}^{\alpha\beta}(l) = -g^{\alpha\beta} + \frac{l^\alpha n_z^\beta + n_z^\alpha l^\beta}{l_z} - \frac{n_z^2\, l^\alpha l^\beta}{l_z^2}$$

with $n_z^2 = -1$

One-loop "quasi-quark" distribution in a quark

Ma and Qiu, arXiv:1404.6860

❑ Real + virtual contribution:

$$\tilde{f}^{(1)}_{q/q}(\tilde{x},\tilde{\mu}^2,P_z) = C_F \frac{\alpha_s}{2\pi}\frac{(4\pi)^\epsilon}{\Gamma(1-\epsilon)}\int_0^{\tilde{\mu}^2}\frac{dl_\perp^2}{l_\perp^{2+2\epsilon}}\int_{-\infty}^{+\infty}\frac{dl_z}{P_z}\left[\delta(1-\tilde{x}-y)-\delta(1-\tilde{x})\right]\left\{\frac{1}{y}\left(1-y+\frac{1-\epsilon}{2}y^2\right)\right.$$
$$\left.\times\left[\frac{y}{\sqrt{\lambda^2+y^2}}+\frac{1-y}{\sqrt{\lambda^2+(1-y)^2}}\right]+\frac{(1-y)\lambda^2}{2y^2\sqrt{\lambda^2+y^2}}+\frac{\lambda^2}{2y\sqrt{\lambda^2+(1-y)^2}}+\frac{1-\epsilon}{2}\frac{(1-y)\lambda^2}{[\lambda^2+(1-y)^2]^{3/2}}\right\}$$

where $y = l_z/P_z,\ \lambda^2 = l_\perp^2/P_z^2,\ C_F = (N_c^2-1)/(2N_c)$

❑ Cancelation of CO divergence:

$$\frac{y}{\sqrt{\lambda^2+y^2}}+\frac{1-y}{\sqrt{\lambda^2+(1-y)^2}} = 2\theta(0<y<1)-\left[\mathrm{Sgn}(y)\frac{\sqrt{\lambda^2+y^2}-|y|}{\sqrt{\lambda^2+y^2}}+\mathrm{Sgn}(1-y)\frac{\sqrt{\lambda^2+(1-y)^2}-|1-y|}{\sqrt{\lambda^2+(1-y)^2}}\right]$$

Only the first term is CO divergent for 0 < y < 1, which is the same as the divergence of the normal quark distribution – necessary!

One-loop "quasi-quark" distribution in a quark

Ma and Qiu, arXiv:1404.6860

❑ Real + virtual contribution:

$$\tilde{f}^{(1)}_{q/q}(\tilde{x},\tilde{\mu}^2,P_z) = C_F \frac{\alpha_s}{2\pi}\frac{(4\pi)^\epsilon}{\Gamma(1-\epsilon)}\int_0^{\tilde{\mu}^2}\frac{dl_\perp^2}{l_\perp^{2+2\epsilon}}\int_{-\infty}^{+\infty}\frac{dl_z}{P_z}\left[\delta(1-\tilde{x}-y)-\delta(1-\tilde{x})\right]\left\{\frac{1}{y}\left(1-y+\frac{1-\epsilon}{2}y^2\right)\right.$$
$$\left.\times\left[\frac{y}{\sqrt{\lambda^2+y^2}}+\frac{1-y}{\sqrt{\lambda^2+(1-y)^2}}\right]+\frac{(1-y)\lambda^2}{2y^2\sqrt{\lambda^2+y^2}}+\frac{\lambda^2}{2y\sqrt{\lambda^2+(1-y)^2}}+\frac{1-\epsilon}{2}\frac{(1-y)\lambda^2}{[\lambda^2+(1-y)^2]^{3/2}}\right\}$$

where $y = l_z/P_z,\ \lambda^2 = l_\perp^2/P_z^2,\ C_F = (N_c^2-1)/(2N_c)$

❑ Cancelation of CO divergence:

$$\frac{y}{\sqrt{\lambda^2+y^2}}+\frac{1-y}{\sqrt{\lambda^2+(1-y)^2}} = 2\theta(0<y<1)-\left[\mathrm{Sgn}(y)\frac{\sqrt{\lambda^2+y^2}-|y|}{\sqrt{\lambda^2+y^2}}+\mathrm{Sgn}(1-y)\frac{\sqrt{\lambda^2+(1-y)^2}-|1-y|}{\sqrt{\lambda^2+(1-y)^2}}\right]$$

Only the first term is CO divergent for $0 < y < 1$, which is the same as the divergence of the normal quark distribution – necessary!

❑ UV renormalization:

Different treatment for the upper limit of $l_\perp^2$ integration - "scheme"

Here, a UV cutoff is used – other scheme is discussed in the paper

One-loop coefficient functions

Ma and Qiu, arXiv:1404.6860

- $\overline{\text{MS}}$ scheme for $f_{q/q}(x,\mu^2)$:

$$\mathcal{C}^{(1)}_{q/q}(t,\tilde{\mu}^2,\mu^2,P_z) = \tilde{f}^{(1)}_{q/q}(t,\tilde{\mu}^2,P_z) - f^{(1)}_{q/q}(t,\mu^2)$$

$$\frac{\mathcal{C}^{(1)}_{q/q}(t)}{C_F\frac{\alpha_s}{2\pi}} = \left[\frac{1+t^2}{1-t}\ln\frac{\tilde{\mu}^2}{\mu^2}+1-t\right]_+ + \left[\frac{t\Lambda_{1-t}}{(1-t)^2}+\frac{\Lambda_t}{1-t}+\frac{\mathrm{Sgn}(t)\Lambda_t}{\Lambda_t+|t|}\right.$$
$$\left.-\frac{1+t^2}{1-t}\left[\mathrm{Sgn}(t)\ln\left(1+\frac{\Lambda_t}{2|t|}\right)+\mathrm{Sgn}(1-t)\ln\left(1+\frac{\Lambda_{1-t}}{2|1-t|}\right)\right]\right]_N$$

where $\Lambda_t = \sqrt{\tilde{\mu}^2/P_z^2+\underline{t^2}}-|t|$, $\mathrm{Sgn}(t)=1$ if $t\geq 0$, and -1 otherwise.

$t=\tilde{x}/x$

- Generalized "+" description:

$$\int_{-\infty}^{+\infty} dt\left[g(t)\right]_N h(t) = \int_{-\infty}^{+\infty} dt\, g(t)\left[h(t)-h(1)\right]$$

For a testing function $h(t)$

- Explicit verification of the factorization at one-loop:

Coefficient functions for all partonic channels are IR safe and finite!

$$\mathcal{C}^{(1)}_{i/j}(t,\tilde{\mu}^2,\mu,P_z) \quad \text{with } i,j=q,\bar{q},g$$

From Lattice quasi-PDFs to PDFs

- **BNL – RBRC efforts:**

$$\tilde{f}^{\mathrm{Latt.}}_{i/h}(\tilde{x}, \frac{1}{a}, P_z)_{\mathrm{E}} \xleftrightarrow[\text{Tomomi's talk}]{\text{One-loop Perturbative Matching}} \tilde{f}^{\mathrm{Cont.}}_{j/h}(\tilde{x}, \mu^2, P_z)_{\mathrm{E}}$$

$$\updownarrow \quad \text{Same}$$

$$f_{i/h}(x, \bar{\mu}^2)_{\mathrm{M}} \xleftrightarrow[\text{This talk}]{\text{One-loop Perturbative Matching}} \tilde{f}^{\mathrm{Cont.}}_{j/h}(\tilde{x}, \mu^2, P_z)_{\mathrm{M}}$$

From Lattice quasi-PDFs to PDFs

- **BNL – RBRC efforts:**

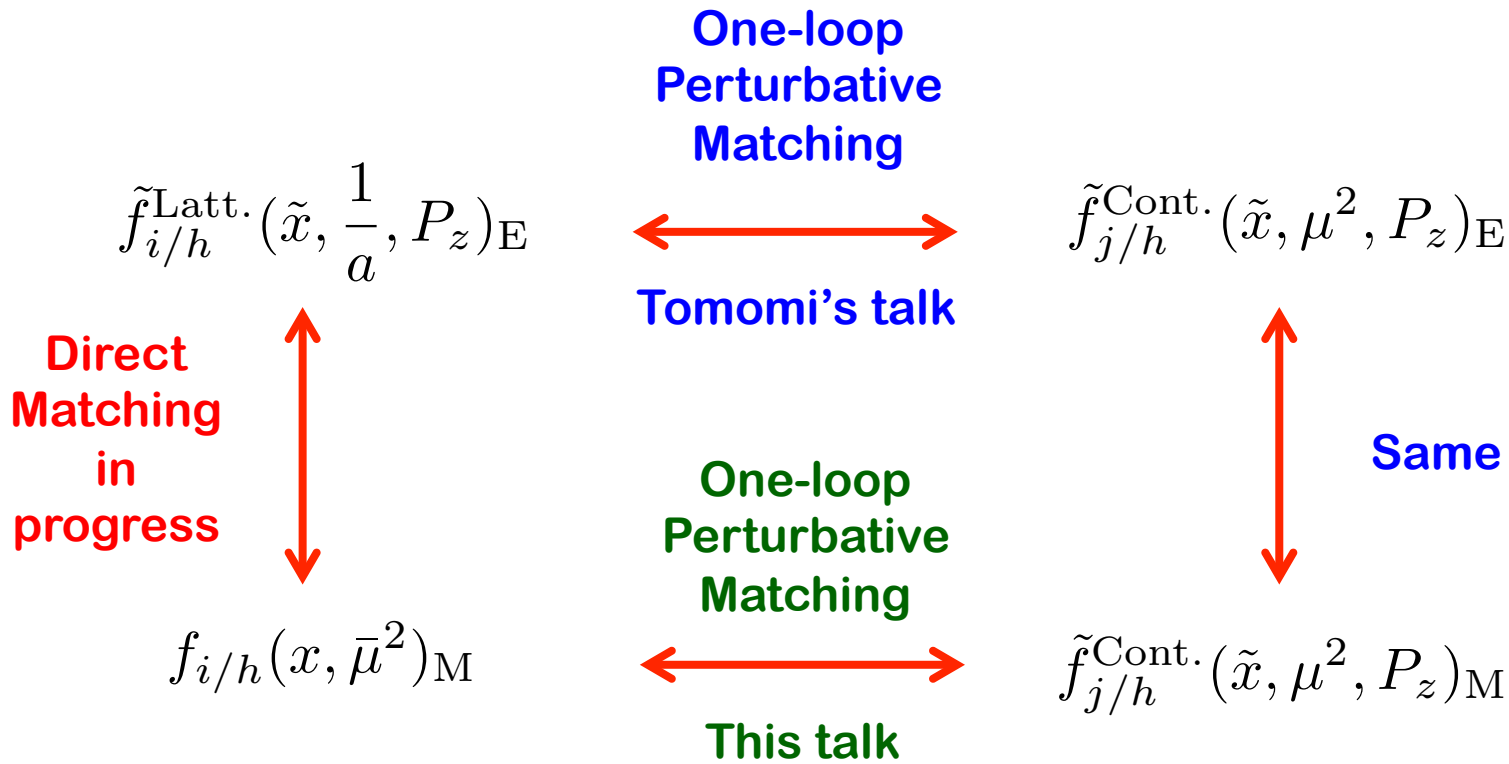

- **To do list:**
  - ✧ Matching with more realistic lattice fermion (no principle difficulty)
  - ✧ Lattice numerical simulations of the quasi-PDFs
  - ✧ First physics project: d(x)/u(x) at large x

Summary and outlook

- "lattice cross sections" = single hadron matrix elements calculable in Lattice QCD and factorizable in QCD

  Key difference from Ji's idea:

  Expansion in $1/\mu$ instead of that in $1/P_z$

- Extract PDFs by global analysis of data on "Lattice cross sections". Same should work for other distributions

$$\tilde{\sigma}_{\rm E}^{\rm Lat}(\tilde{x}, \frac{1}{a}, P_z) \approx \sum_i \int_0^1 \frac{dx}{x} f_{i/h}(x, \mu^2) \tilde{C}_i(\frac{\tilde{x}}{x}, \frac{1}{a}, \mu^2, P_z)$$

- Conservation of difficulties – complementarity:

  High energy scattering experiments

  – less sensitive to large x parton distribution/correlation

  "Lattice factorizable cross sections"

  – more suited for large x PDFs, and more: PDFs of meson?

- Lattice QCD can calculate PDFs, but, more works are needed!

Thank you!

BACKUP SLIDES

Nucleon's internal structure

- Our understanding of the nucleon evolves

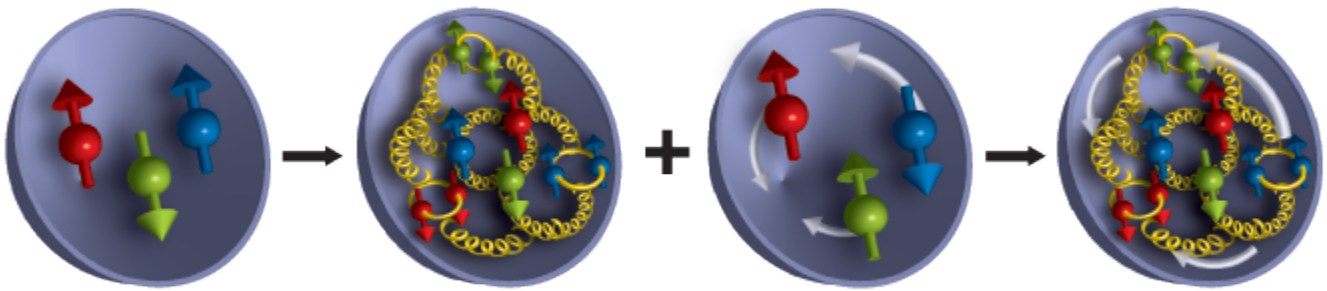

1970s 1980s/2000s Now

Nucleon is a strongly interacting, relativistic bound state of quarks and gluons

- QCD bound states:
  - Neither quarks nor gluons appear in isolation!
  - Understanding such systems completely is still beyond the capability of the best minds in the world

- The great intellectual challenge:

Probe nucleon structure without "seeing" quarks and gluons?

PDFs from lattice QCD

- How to get x-dependent PDFs with a limited moments?
  - Assume a smooth functional form with some parameters
  - Fix the parameters with the lattice calculated moments

$$xq(x) = a\,x^b(1-x)^c(1+\epsilon\sqrt{x}+\gamma\,x)$$

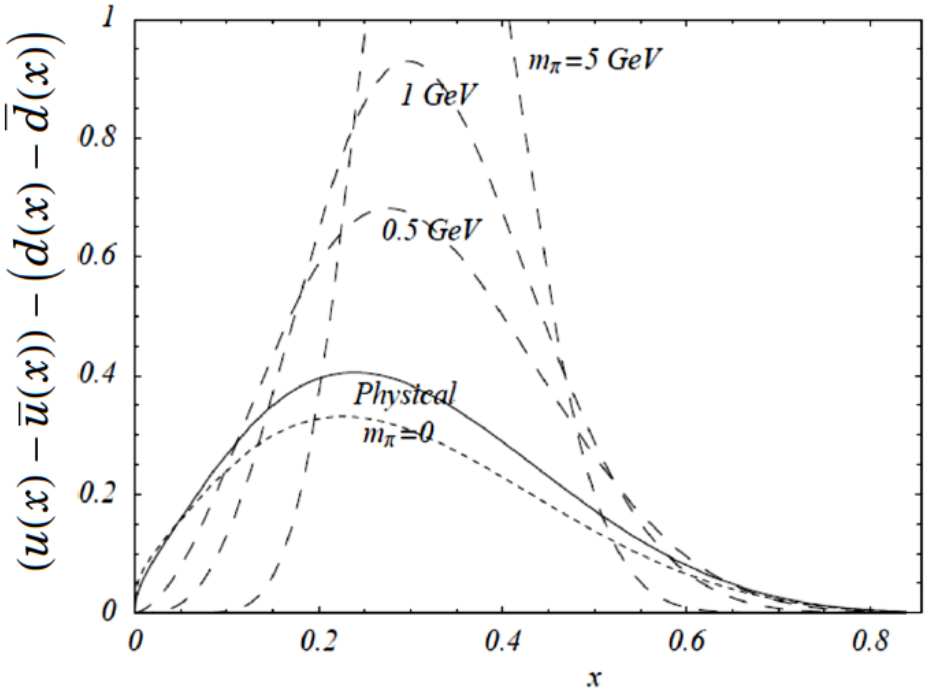

W. Dermold et al., Eur.Phys.J.direct C3 (2001) 1-15

Cannot distinguish valence quark contribution from sea quarks

"Quasi-PDFs" have no parton interpretation

- **Normal PDFs conserve parton momentum:**

$$
\begin{aligned}
M &= \sum_q \left[\int_0^1 dx\, x f_q(x) + \int_0^1 dx\, x f_{\bar{q}}(x) \right] + \int_0^1 dx\, x f_g(x) \\
&= \sum_q \int_{-\infty}^{\infty} dx\, x f_q(x) + \frac{1}{2} \int_{-\infty}^{\infty} dx\, x f_g(x) \\
&= \frac{1}{2(P^+)^2} \langle P | T^{++}(0) | P \rangle = \text{constant}
\end{aligned}
$$

$T^{\mu\nu}$

Energy-momentum tensor

- **"Quasi-PDFs" do not conserve "parton" momentum:**

$$
\begin{aligned}
\widetilde{\mathcal{M}} &= \sum_q \left[\int_0^{\infty} d\tilde{x}\, \tilde{x} \tilde{f}_q(\tilde{x}) + \int_0^{\infty} d\tilde{x}\, \tilde{x} \tilde{f}_{\bar{q}}(\tilde{x}) \right] + \int_0^{\infty} d\tilde{x}\, \tilde{x} \tilde{f}_g(\tilde{x}) \\
&= \sum_q \int_{-\infty}^{\infty} d\tilde{x}\, \tilde{x} \tilde{f}_q(\tilde{x}) + \frac{1}{2} \int_{-\infty}^{\infty} d\tilde{x}\, \tilde{x} \tilde{f}_g(\tilde{x}) \\
&= \frac{1}{2(P_z)^2} \langle P | \left[T^{zz}(0) - g^{zz}(\ldots) \right] | P \rangle \neq \text{constant}
\end{aligned}
$$

Note: "Quasi-PDFs" are not boost invariant

The first try

§ Exploratory study

Lin *et al.*, arXiv:1402.1462

$$\int \frac{dz}{4\pi} e^{-izk_z} \left\langle P \left| \bar{\psi}(z)\, \gamma_z \exp\left(-ig \int_0^z dz'\, A_z(z')\right) \psi(0) \right| P \right\rangle$$

$P_z \in \{1, 2, 3\}\, {}^{2\pi}/_{L}$

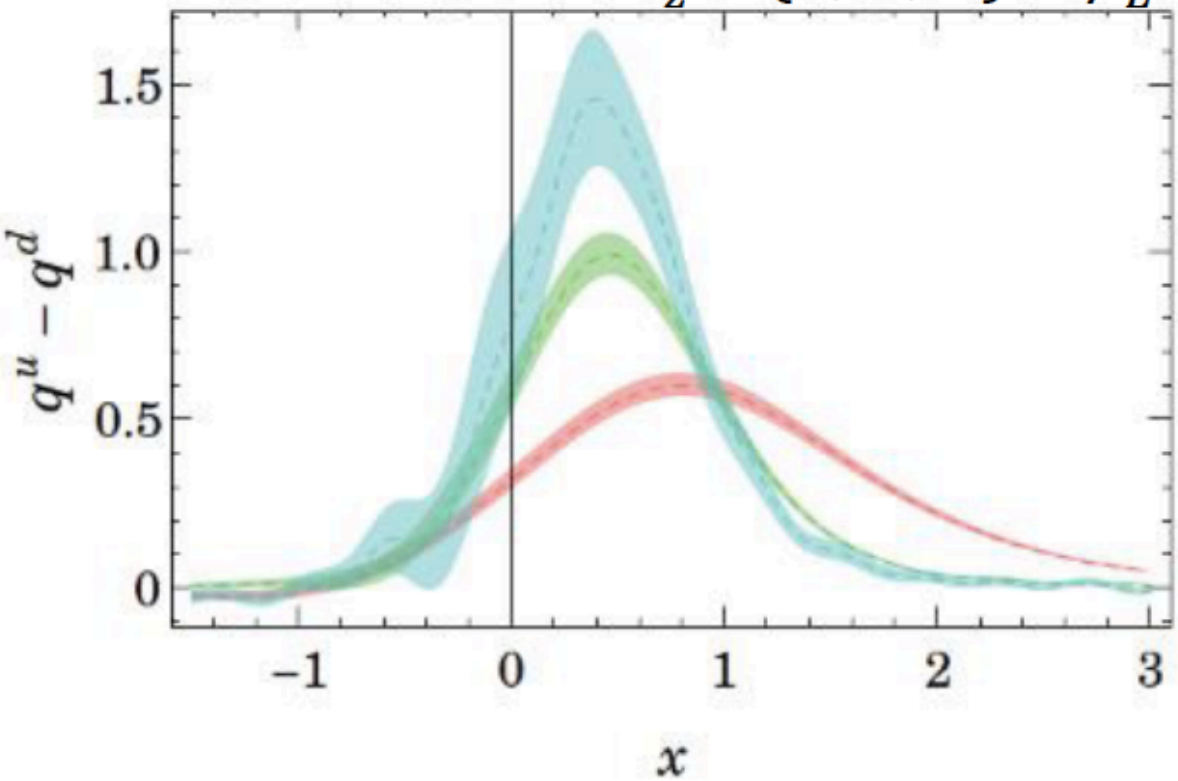

Distribution gets sharper as P_z increases

Artifacts due to finite P_z on the lattice

Improvement?

Work out leading-P_z corrections

QED Corrections to Hadronic Processes in Lattice QCD

Chris Sachrajda

School of Physics and Astronomy
University of Southampton
Southampton SO17 1BJ
UK

Multi Hadron and Nonlocal Matrix Elements in Lattice QCD

Brookhaven National Laboratory
5 - 6 February 2015

UNIVERSITY OF Southampton
School of Physics and Astronomy

UNIVERSITY OF Southampton
School of Physics and Astronomy

N.Carrasco, V.Lubicz, G.Martinelli, CTS, N.Tantalo, C.Tarantino, M.Testa
(arXiv:1502.00257)

- Electromagnetic corrections to hadronic masses are now being calculated. For a review see A.Portelli at Lattice 2014.
- The results of (some) weak matrix elements obtained from lattice QCD are now being quoted with $O(1\%)$ precision e.g. FLAG Collaboration, arXiv:1310.8555

f_π	f_K	f_D	f_{D_s}	f_B	f_{B_s}
130.2(1.4)	156.3(0.8)	209.2(3.3)	248.6(2.7)	190.5(4.2)	227.7(4.5)

(results given in MeV)

- We therefore need to start considering electromagnetic (and other isospin breaking) effects if we are to use these results to extract CKM matrix elements at a similar precision.
- For illustration, we consider f_π but the discussion is general. we do not use ChPT. For a ChPT based discussion of f_π, see J.Gasser & G.R.S.Zarnauskas, arXiv:1008.3479
- At $O(\alpha^0)$

$$\Gamma(\pi^+ \to \ell^+ \nu_\ell) = \frac{G_F^2 \, |V_{ud}|^2 f_\pi^2}{8\pi} \, m_\pi \, m_\ell^2 \left(1 - \frac{m_\ell^2}{m_\pi^2}\right)^2 .$$

Infrared Divergences

- At $O(\alpha)$ infrared divergences are present and we have to consider

$$\begin{aligned}\Gamma(\pi^+ \to \ell^+ \nu_\ell(\gamma)) &= \Gamma(\pi^+ \to \ell^+ \nu_\ell) + \Gamma(\pi^+ \to \ell^+ \nu_\ell \gamma) \\ &\equiv \Gamma_0 + \Gamma_1 \,,\end{aligned}$$

  where the suffix denotes the number of photons in the final state.
- Each of the two terms on the rhs is infrared divergent, the divergences cancel in the sum.
- The cancelation of infrared divergences between contributions with virtual and real photons is an old and well understood issue.

  F.Bloch and A.Nordsieck, PR 52 (1937) 54
- The question for our community is how best to combine this understanding with lattice calculations of non-perturbative hadronic effects.
- This is a generic problem if em corrections are to be included in the evaluation of a decay process.

Lattice computations of $\Gamma(\pi^+ \to \ell^+ \nu_\ell(\gamma))$ at $O(\alpha)$

- In principle, particularly as techniques and resources improve in the future, it may be better to compute Γ_1 nonperturbatively over a larger range of photon energies.
- At present we do not propose to compute Γ_1 nonperturbatively. Rather we consider only photons which are sufficiently soft for the point-like (pt) approximation to be valid.
  - A cut-off ΔE of $O(10\text{-}20\,\mathrm{MeV})$ appears to be appropriate both experimentally and theoretically.

    F.Ambrosino et al., KLOE collaboration, hep-ex/0509045; arXiv:0907.3594
- We now write

$$\boxed{\Gamma_0 + \Gamma_1(\Delta E) = \lim_{V\to\infty}(\Gamma_0 - \Gamma_0^{\rm pt}) + \lim_{V\to\infty}(\Gamma_0^{\rm pt} + \Gamma_1(\Delta E))\,.}$$

  - The second term on the rhs can be calculated in perturbation theory. It is infrared convergent, but does contain a term proportional to $\log \Delta E$.
  - The first term is also free of infrared divergences.
  - Γ_0 is calculated nonperturbatively and $\Gamma_0^{\rm pt}$ in perturbation theory. The subtraction in the first term is performed for each momentum and then the sum over momenta is performed (see below).

Outline of Talk

$$\boxed{\Gamma_0 + \Gamma_1(\Delta E) = \lim_{V\to\infty}(\Gamma_0 - \Gamma_0^{\rm pt}) + \lim_{V\to\infty}(\Gamma_0^{\rm pt} + \Gamma_1(\Delta E))\,.}$$

1 Introduction
2 What is G_F at $O(\alpha)$?
3 Proposed calculation of $\Gamma_0 - \Gamma_0^{\rm pt}$
4 Calculation of $\Gamma_0^{\rm pt} + \Gamma_1(\Delta E)$
5 Estimates of structure dependent contributions to $\Gamma_1(\Delta E)$
6 Summary and Conclusions

2. What is G_F at $O(\alpha)$?

1. The results for the widths are expressed in terms of G_F, the Fermi constant ($G_F = 1.16632(2) \times 10^{-5}\,\mathrm{GeV}^{-2}$). This is obtained from the muon lifetime:

$$\frac{1}{\tau_\mu} = \frac{G_F^2 m_\mu^5}{192\pi^3}\left[1 - \frac{8m_e^2}{m_\mu^2}\right]\left[1 + \frac{\alpha}{2\pi}\left(\frac{25}{4} - \pi^2\right)\right].$$

S.M.Berman, PR 112 (1958) 267; T.Kinoshita and A.Sirlin, PR 113 (1959) 1652

- This expression can be viewed as the definition of G_F. Many EW corrections are absorbed into the definition of G_F; the explicit $O(\alpha)$ corrections come from the following diagrams in the effective theory:

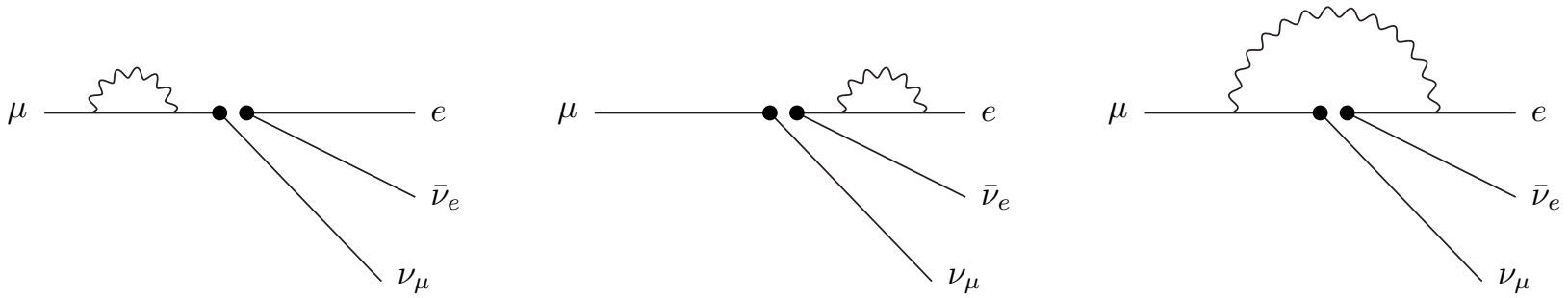

together with the diagrams with a real photon.

- These diagrams are evaluated in the W-regularisation in which the photon propagator is modified by:

A.Sirlin, PRD 22 (1980) 971

$$\frac{1}{k^2} \to \frac{M_W^2}{M_W^2 - k^2}\,\frac{1}{k^2}\,. \qquad \left(\frac{1}{k^2} = \frac{1}{k^2 - M_W^2} + \frac{M_W^2}{M_W^2 - k^2}\,\frac{1}{k^2}\right)$$

W-regularization (cont)

- The $\gamma - W$ box diagram:

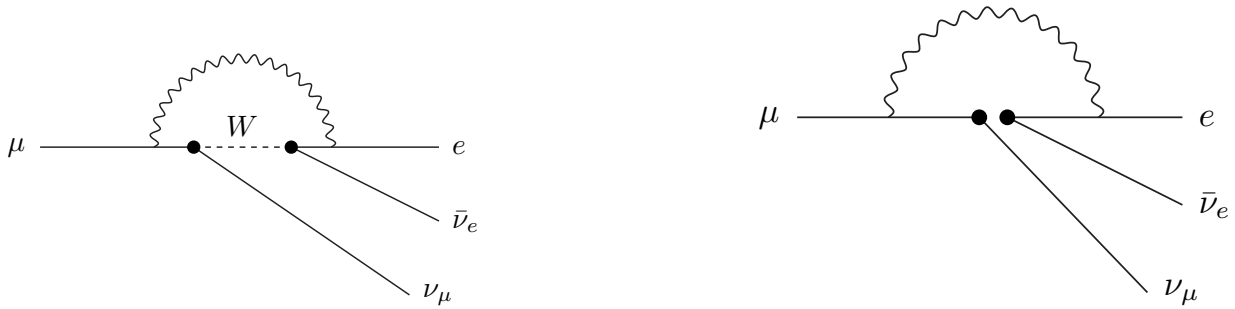

As an example providing some evidence & intuition that the W-regularization is useful consider the $\gamma - W$ box diagram.

- In the standard model (left-hand diagram) it contains both the γ and W propagators.
- In the effective theory this is preserved with the W-regularization where the photon propagator is proportional to

$$\frac{1}{k^2}\frac{1}{k^2 - M_W^2}$$

and the two diagrams are equal up to terms of $O(q^2/M_W^2)$, where q is the momentum of the e and ν_e.

3. Proposed calculation of $\Gamma_0 - \Gamma_0^{\mathbf{pt}}$

- Most (but not all) of the EW corrections which are absorbed in G_F are common to other processes (including pion decay) $\Rightarrow$ factor in the amplitude of $(1 + 3\alpha/4\pi(1 + 2\bar{Q}) \log M_Z/M_W)$, where $\bar{Q} = \frac{1}{2}(Q_u + Q_d) = 1/6$.

  A.Sirlin, NP B196 (1982) 83; E.Braaten & C.S.Li, PRD 42 (1990) 3888

- We therefore need to calculate the pion-decay diagrams in the effective theory with

$$H_{\rm eff} = \frac{G_F}{\sqrt{2}} V_{ud}^* \left(1 + \frac{\alpha}{\pi} \log \frac{M_Z}{M_W}\right) (\bar{d}_L \gamma^\mu u_L)(\bar{\nu}_{\ell,L} \gamma_\mu \ell_L)$$

  in the W-regularization.

- Thus for example, with the Wilson action for both the gluons and fermions:

$$\begin{aligned} O_1^{\rm W-reg} &= \left(1 + \frac{\alpha}{4\pi}\left(2\log a^2 M_W^2 - 15.539\right)\right) O_1^{\rm bare} + \frac{\alpha}{4\pi}\left(0.536\, O_2^{\rm bare}\right. \\ &\quad \left. +1.607\, O_3^{\rm bare} - 3.214\, O_4^{\rm bare} - 0.804\, O_5^{\rm bare}\right) , \end{aligned}$$

where

$$O_1 = (\bar{d}\gamma^\mu(1-\gamma^5)u)\,(\bar{\nu}_\ell\gamma_\mu(1-\gamma^5)\ell) \qquad O_2 = (\bar{d}\gamma^\mu(1+\gamma^5)u)\,(\bar{\nu}_\ell\gamma_\mu(1-\gamma^5)\ell)$$

$$O_3 = (\bar{d}(1-\gamma^5)u)\,(\bar{\nu}_\ell(1+\gamma^5)\ell) \qquad O_4 = (\bar{d}(1+\gamma^5)u)\,(\bar{\nu}_\ell(1+\gamma^5)\ell)$$

$$O_5 = (\bar{d}\sigma^{\mu\nu}(1+\gamma^5)u)\,(\bar{\nu}_\ell\sigma_{\mu\nu}(1+\gamma^5)\ell)\,.$$

Proposed calculation of $\Gamma_0 - \Gamma_0^{\mathbf{pt}}$ (Cont)

Consider now the evaluation of Γ_0.

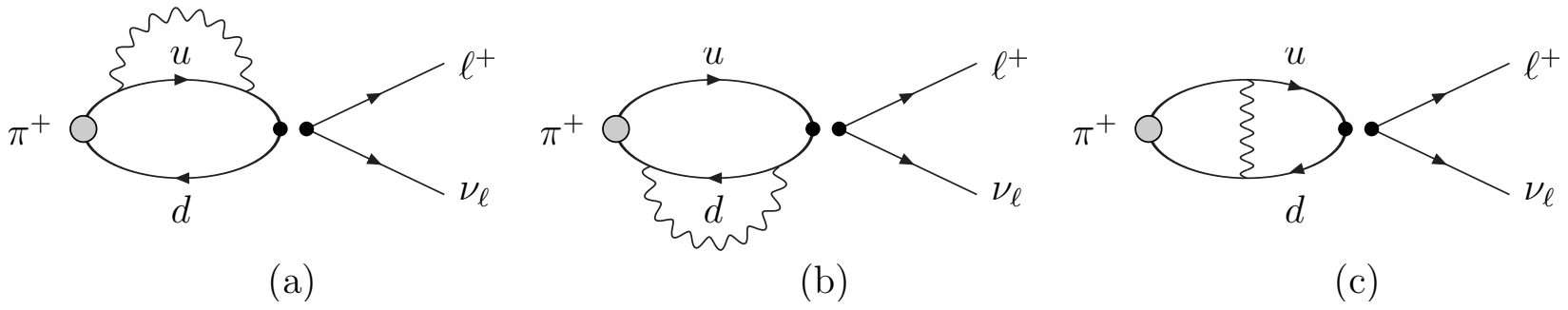

- The correlation function for this set of diagrams is of the form:

$$C_1(t) = -\frac{1}{2}\int d^3\vec{x}\, d^4x_1\, d^4x_2\, \langle 0|T\{J_W^\nu(0)\, j_\mu(x_1) j_\mu(x_2)\phi^\dagger(\vec{x},-t)\}\,|\,0\rangle\ \Delta(x_1,x_2)\,,$$

  where $j_\mu(x) = \sum_f Q_f \bar{f}(x)\gamma_\mu f(x)$, J_W is the weak current, ϕ is an interpolating operator for the pion and Δ is the photon propagator.

- Combining C_1 with the lowest order correlator:

$$C_0(t) + C_1(t) \simeq \frac{e^{-m_\pi t}}{2m_\pi} Z^\phi \,\langle\, 0\,|J_W^\nu(0)\,|\,\pi^+\rangle\,,$$

  where now $O(\alpha)$ terms are included.

- $e^{-m_\pi t} \simeq e^{-m_\pi^0 t}\,(1-\delta m_\pi\, t)$ and Z^ϕ is obtained from the two-point function.

Proposed calculation of $\Gamma_0 - \Gamma_0^{\mathbf{pt}}$ (Cont)

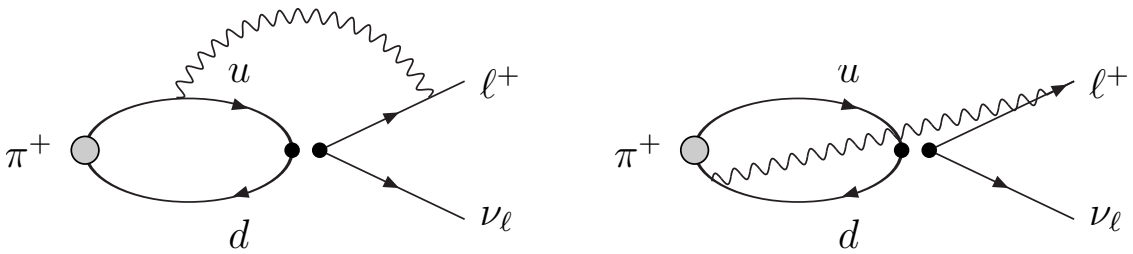

(e) (f)

$$\bar{C}_1(t)_{\alpha\beta} = -\int d^3\vec{x}\, d^4x_1\, d^4x_2\, \langle 0|T\{J_W^\nu(0)\, j_\mu(x_1)\phi^\dagger(\vec{x},-t)\}|\,0\rangle\, \Delta(x_1,x_2) \times \left(\gamma_\nu(1-\gamma^5)S(0,x_2)\gamma_\mu\right)_{\alpha\beta} e^{E_\ell\, t_2} e^{-i\vec{p}_\ell\cdot\vec{x}_2}$$

$$\simeq Z_0^\phi\, \frac{e^{-m_\pi^0 t}}{2m_\pi^0}\, (\bar{M}_1)_{\alpha\beta}$$

- Corresponding contribution to the amplitude is $\bar{u}_\alpha(p_{\nu_\ell})(\bar{M}_1)_{\alpha\beta}v_\beta(p_\ell)$.
- Diagrams (e) and (f) are not simply generalisations of the evaluation of f_π.
- The lepton's wave function renormalisation cancels in the difference $\Gamma_0 - \Gamma_0^{\mathrm{pt}}$.
- We have to be able to isolate the finite-volume ground state (pion).
- The Minkowski $\leftrightarrow$ Euclidean continuation can be performed (the time integrations are convergent).

Convergence of the t_2 integration

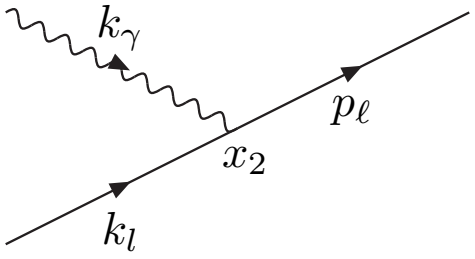

- For every term in the $\vec{k}_\gamma$ integration, $\omega_\gamma + \omega_l > E_l$ so the t_2 behaviour, $\exp[-(\omega_k + \omega_l - E_l)t_2]$ is convergent.

There are also disconnected diagrams to be evaluated.

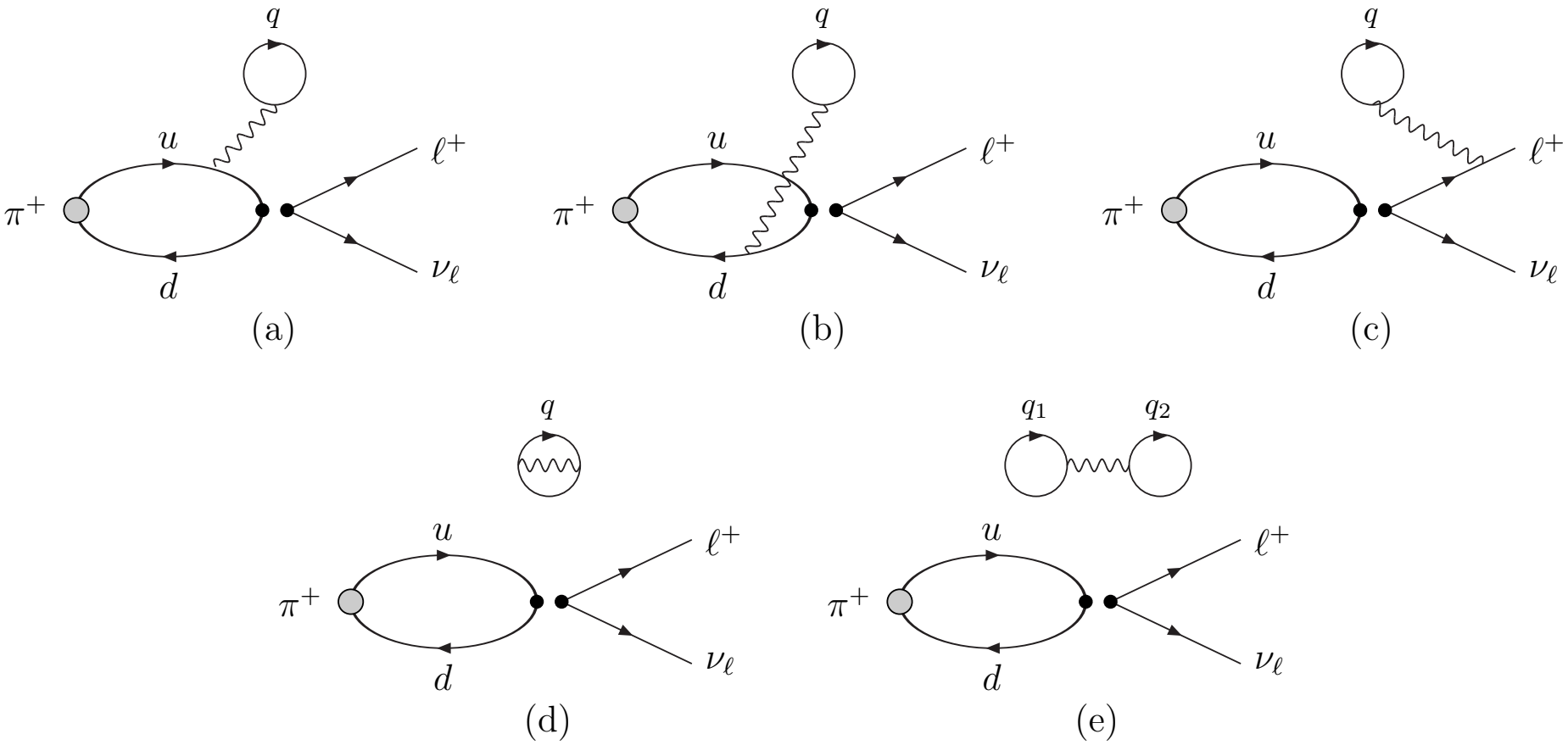

4. Calculation of $\Gamma^{\mathbf{pt}} = \Gamma_0^{\mathbf{pt}} + \Gamma_1^{\mathbf{pt}}$

- The total width, $\Gamma^{\rm pt}$ was calculated in 1958/9 using a Pauli-Villars regulator for the UV divergences and m_γ for the infrared divergences.

  S.Berman, PR **112** (1958) 267, T.Kinoshita, PRL **2** (1959) 477

  - This is a useful check on our perturbative calculation.

- In the perturbative calculation we use the following Lagrangian for the interaction of a point-like pion with the leptons:

$$\mathcal{L}_{\pi\text{-}\ell\text{-}\nu_\ell} \quad = \quad i\,G_F f_\pi V_{ud}^* \;\{(\partial_\mu - ieA_\mu)\pi\}\left\{\bar{\psi}_{\nu_\ell}\frac{1+\gamma_5}{2}\gamma^\mu\psi_\ell\right\} + \text{H.C.}\,.$$

The corresponding Feynman rules are:

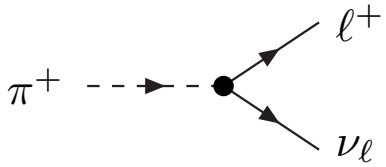

$$= -iG_F f_\pi V_{ud}^* p_\pi^\mu \tfrac{1+\gamma^5}{2}\gamma_\mu$$

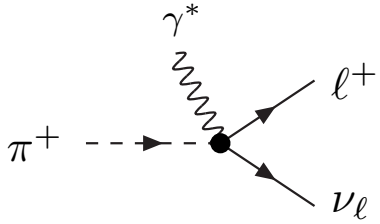

$$= ie\,G_F f_\pi V_{ud}^* g^{\mu\nu} \tfrac{1+\gamma^5}{2}\gamma_\mu$$

Diagrams to be evaluated

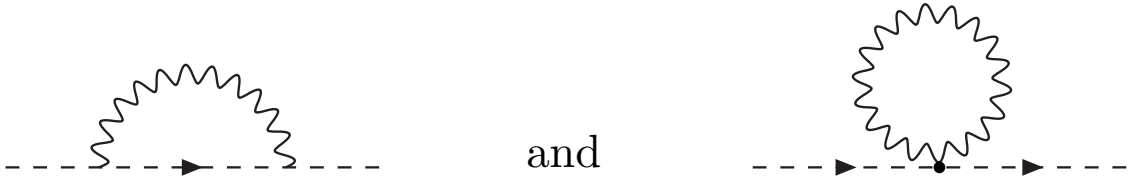

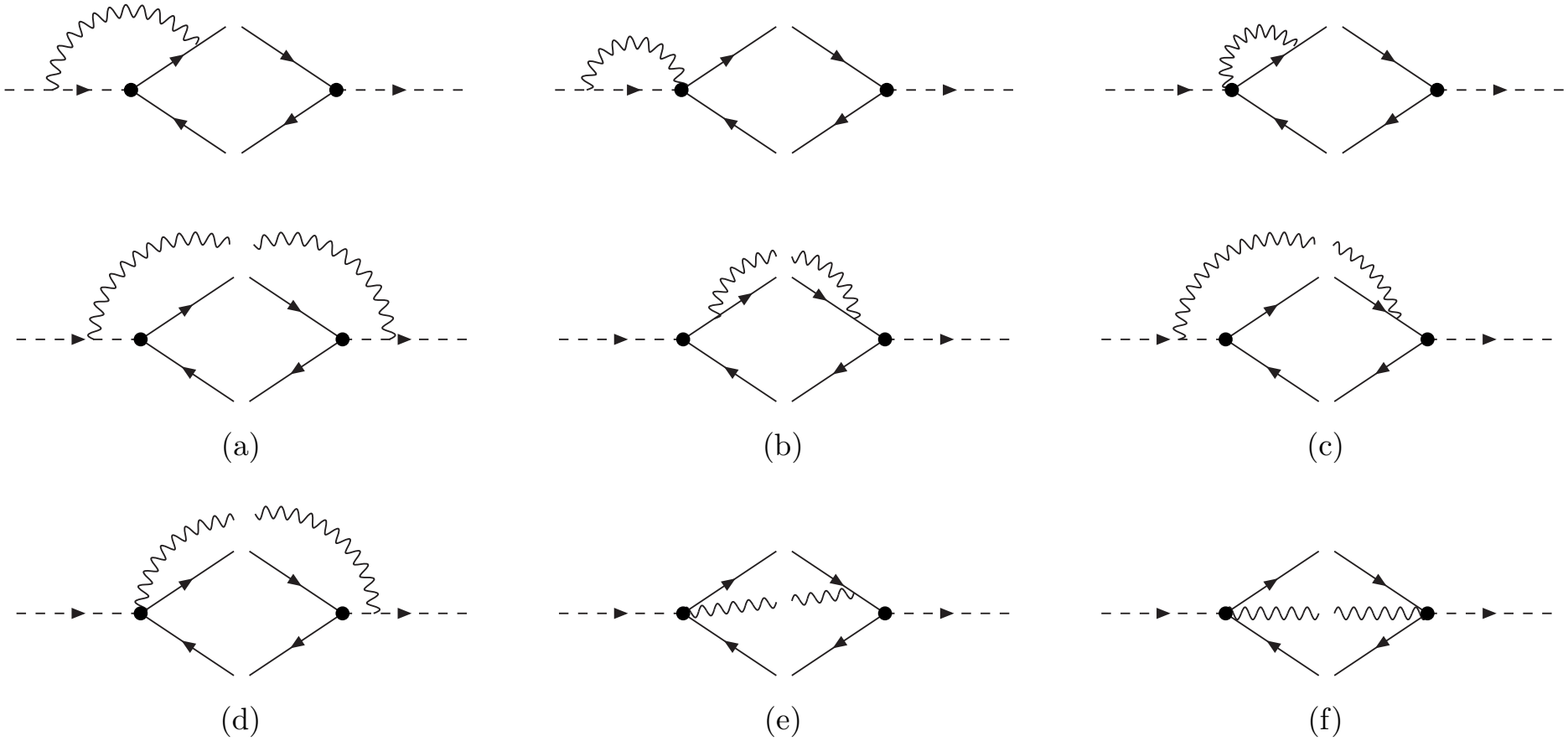

4. Calculation of $\Gamma^{\mathbf{pt}} = \Gamma_0^{\mathbf{pt}} + \Gamma_1^{\mathbf{pt}}$ (cont)

- We find, for $E_\gamma < \Delta E$

$$\begin{aligned}\Gamma^{\rm pt}(\Delta E) \quad = \quad \Gamma_0^{\rm tree} \times \Bigg(1 + \frac{\alpha}{4\pi}\Bigg\{ & 3\log\left(\frac{m_\pi^2}{M_W^2}\right) + \log\left(r_\ell^2\right) - 4\log(r_E^2) + \frac{2-10r_\ell^2}{1-r_\ell^2}\log(r_\ell^2) \\ & -2\frac{1+r_\ell^2}{1-r_\ell^2}\log(r_E^2)\log(r_\ell^2) - 4\frac{1+r_\ell^2}{1-r_\ell^2}\,\mathrm{Li}_2(1-r_\ell^2) - 3 \\ & +\Bigg[\frac{3+r_E^2-6r_\ell^2+4r_E(-1+r_\ell^2)}{(1-r_\ell^2)^2}\log(1-r_E) + \frac{r_E(4-r_E-4r_\ell^2)}{(1-r_\ell^2)^2}\log(r_\ell^2) \\ & -\frac{r_E(-22+3r_E+28r_\ell^2)}{2(1-r_\ell^2)^2} - 4\frac{1+r_\ell^2}{1-r_\ell^2}\,\mathrm{Li}_2(r_E)\Bigg]\Bigg\}\Bigg) \ ,\end{aligned}$$

where $r_E = 2\Delta E/m_\pi$ and $r_\ell = m_\ell/m_\pi$.

- We believe that this is a new result.

4. Calculation of $\Gamma^{\mathbf{pt}} = \Gamma_0^{\mathbf{pt}} + \Gamma_1^{\mathbf{pt}}$ (cont)

- The total rate is readily computed by setting r_E to its maximum value, namely $r_E = 1 - r_\ell^2$, giving

$$\Gamma^{\rm pt} = \Gamma_0^{\rm tree} \times \left\{ 1 + \frac{\alpha}{4\pi} \left(3\log\left(\frac{m_\pi^2}{M_W^2}\right) - 8\log(1-r_\ell^2) - \frac{3r_\ell^4}{(1-r_\ell^2)^2}\log(r_\ell^2) \right.\right.$$
$$\left.\left. -8\frac{1+r_\ell^2}{1-r_\ell^2}\,\mathrm{Li}_2(1-r_\ell^2) + \frac{13-19r_\ell^2}{2(1-r_\ell^2)} + \frac{6-14r_\ell^2-4(1+r_\ell^2)\log(1-r_\ell^2)}{1-r_\ell^2}\,\log(r_\ell^2) \right) \right\}.$$

- This result agrees with the well known results in literature providing an important check of our calculation.

4. Calculation of $\Gamma^{\mathbf{pt}} = \Gamma_0^{\mathbf{pt}} + \Gamma_1^{\mathbf{pt}}$ (cont)

- It is of course possible instead to impose a cut-off on the energy of the final-state lepton, requiring it to be close to its maximum value $E_\ell^{\max} = \frac{m_\pi}{2}(1 + r_\ell^2)$.
- We also give, up to $O(\Delta E_\ell)$, the distribution for $\Gamma^{\rm pt}(\Delta E_\ell)$ defined as

$$\Gamma^{\rm pt}(\Delta E_\ell) = \int_{E_\ell^{max} - \Delta E_\ell}^{E_\ell^{max}} dE'_\ell \, \frac{d\Gamma^{\rm pt}}{dE'_\ell} \, ,$$

where $0 \leq \Delta E_\ell \leq (m_\pi - m_\ell)^2/(2m_\pi)$;

$$\Gamma^{\rm pt}(\Delta E_\ell) = \Gamma_0^{\rm tree} \times \left\{ 1 + \frac{\alpha}{4\pi} \left[3 \log\left(\frac{m_\pi^2}{M_W^2}\right) + 8 \log\left(1 - r_\ell^2\right) - 7 \right.\right.$$
$$+ \log\left(r_\ell^2\right) \frac{3 - 7r_\ell^2 + 8\Delta E_\ell + 4\left(1 + r_\ell^2\right) \log\left(1 - r_\ell^2\right)}{1 - r_\ell^2}$$
$$\left.\left. + \log\left(2\Delta E_\ell\right) \left(-8 - 4 \frac{1 + r_\ell^2}{1 - r_\ell^2} \log\left(r_\ell^2\right) \right) \right] \right\} .$$

- Summary: The perturbative calculation of $\Gamma_0^{\rm pt} + \Gamma_1(\Delta E)$ is done.

5. Estimates of structure dependent contributions to $\Gamma_1(\Delta E)$

- For sufficiently small ΔE the structure dependent contributions to Γ_1 can be neglected.
- How big might they be for experimentally accessible values of ΔE?
  To estimate this for f_π and f_K we use Chiral Perturbation Theory.

  J.Bijnens, G.Ecker and J.Gasser, hep-ph/9209261,
  J.Bijnens, G.Colangelo, G.Ecker and J.Gasser, hep-ph/9411311.
  V. Cirigliano and I. Rosell, arXiv:0707.3439 [hep-ph]],
  L. Ametller, J. Bijnens, A. Bramon and F. Cornet, hep-ph/9302219.
- We define

$$R_1^A(\Delta E) = \frac{\Gamma_1^A(\Delta E)}{\Gamma_0^{\alpha,\mathrm{pt}} + \Gamma_1^{\mathrm{pt}}(\Delta E)} \ , \qquad A = \{\mathrm{SD,INT}\} \ ,$$

  where SD and INT refer to the structure dependent and interference (between SD and pt) contributions respectively.
  - Note that the notation I am using here differs from that in the paper.

5. Estimates of structure dependent contributions to $\Gamma_1(\Delta E)$ (cont)

- Start with a decomposition in terms of Lorenz invariant form factors of the hadronic matrix element

$$H^{\mu\nu}(k,p_\pi) \quad = \quad \int d^4x\, e^{ikx}\, T\langle 0|j^\mu(x)J_W^\nu(0)|\pi(p_\pi)\rangle$$

and separate the contribution corresponding to the approximation of a point-like pion $H^{\mu\nu}_{\rm pt}$, from the structure dependent part $H^{\mu\nu}_{\rm SD}$,

$$H^{\mu\nu} = H^{\mu\nu}_{\rm SD} + H^{\mu\nu}_{\rm pt} \ .$$

- $H^{\mu\nu}_{\rm pt}$ is simply given by

$$H^{\mu\nu}_{\rm pt} = f_\pi \left[g^{\mu\nu} - \frac{(2p_\pi - k)^\mu (p_\pi - k)^\nu}{(p_\pi - k)^2 - m_\pi^2} \right] .$$

- The structure dependent component can be parametrised by four independent invariant form factors which we define as

$$\begin{aligned} H^{\mu\nu}_{\rm SD} \quad = \quad & H_1 \left[k^2 g^{\mu\nu} - k^\mu k^\nu \right] + H_2 \left\{ \left[(k\cdot p_\pi - k^2) k^\mu - k^2 (p_\pi - k)^\mu \right] (p_\pi - k)^\nu \right\} \\ & -i \frac{F_V}{m_\pi} \epsilon^{\mu\nu\alpha\beta} k_\alpha p_{\pi\,\beta} + \frac{F_A}{m_\pi} \left[(k\cdot p_\pi - k^2) g^{\mu\nu} - (p_\pi - k)^\mu k^\nu \right] \ . \end{aligned}$$

5. Estimates of structure dependent contributions to $\Gamma_1(\Delta E)$ (cont)

- For the decay into a real photon, only F_V and F_A contribute.
- At $O(p^4)$ in chiral perturbation theory,

$$F_V = \frac{m_P}{4\pi^2 f_\pi} \quad \text{and} \quad F_A = \frac{8m_P}{f_\pi}\left(L_9^r + L_{10}^r\right),$$

  where $P = \pi$ or K and L_9^r, L_{10}^r are Gasser-Leutwyler coefficients.
- The numerical values of these constants have been taken from the review by M.Bychkov and G.D'Ambrosio in the PDG. F_V and F_A are 0.0254 and 0.0119 for the pion and 0.096 and 0.042 for the Kaon (for the pion these values of the form factors, obtained from direct measurements, can be found in the supplement to the PDG.)

5. Estimates of structure dependent contributions to $\Gamma_1(\Delta E)$ (cont)

Pion

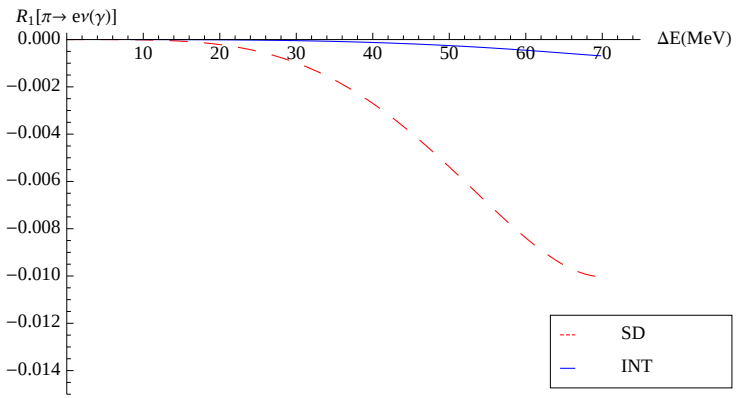

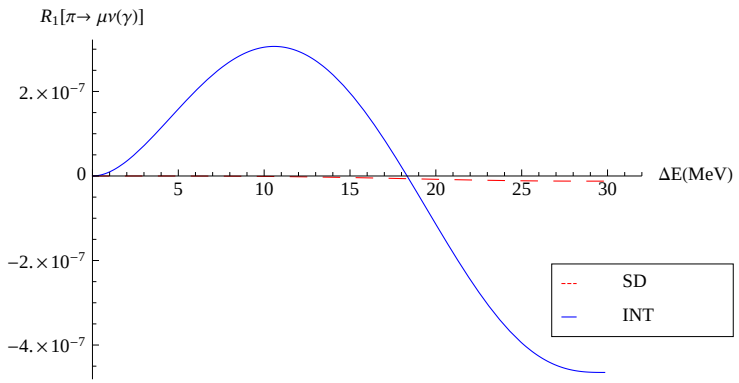

Kaon

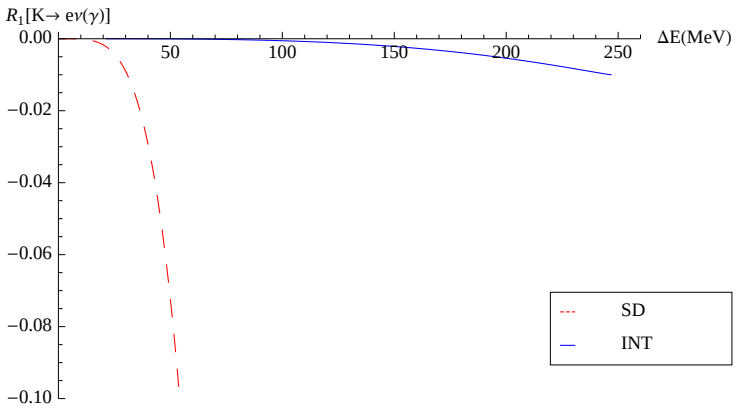

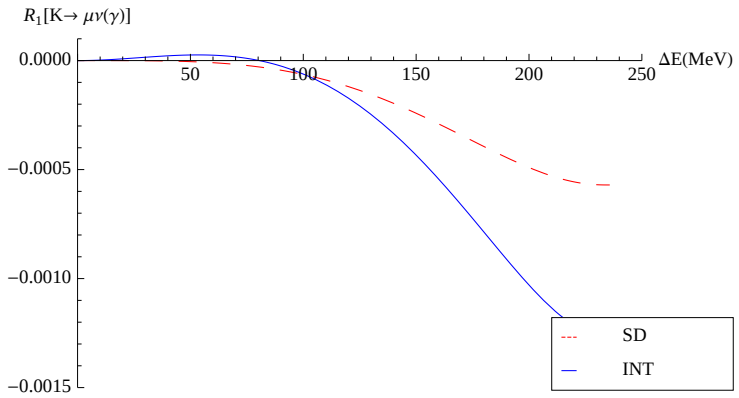

5. Estimates of structure dependent contributions to $\Gamma_1(\Delta E)$ (cont)

- For heavy-light mesons we don't have such ChPT calculations.
- For the B-meson in particular we have another small scale $< \Lambda_{\rm QCD}$, $m_{B^*} - m_B \simeq 45\,$MeV so that we may expect that we will have to go to smaller ΔE in order to be able to neglect SD effects.
- Calculations based on the extreme approximation of single pole dominance suggest that this is likely to be the case.

  D. Becirevic, B. Haas and E. Kou, arXiv:0907.1845 [hep-ph]
- To be investigated further!

6. Summary and Conclusions

- Lattice calculations of some physical quantities are approaching $O(1\%)$ precision $\Rightarrow$ we need to include isospin-breaking effects, including electromagnetic effects, to make the tests of the SM even more stringent.
- For decay widths and scattering cross sections including em effects introduces infrared divergences.
- In this work we propose a method for dealing with these divergences, illustrating the procedure by a detailed study of the leptonic (and semileptonic) decays of pseudoscalar mesons.
- Although challenging, the method is within reach of present simulations and we will now implement the procedure in an actual numerical computation.
  - Power-like FV corrections, $O(1/(L\Lambda_{\rm QCD})^n)$, to be evaluated.
  - $O(\alpha\alpha_s)$ matching factors to be studied.
- In the future one can envisage relaxing the condition $\Delta E \ll \Lambda_{\rm QCD}$, including the emission of real photons with energies which do resolve the structure of the initial hadron. Such calculations can be performed in Euclidean space under the same conditions as above, i.e. providing that there is a mass gap.
  - The natural extension of the present proposal is to subtract and add $\Gamma_1^{\rm pt}(\Delta E)$ to determine $\Gamma_1(\Delta E) - \Gamma_1^{\rm pt}(\Delta E)$, so that our calculation of $\Gamma_0^{\rm pt} + \Gamma_1^{\rm pt}(\Delta E)$ will still be useful.

Finite volume quantization conditions for multiparticle states

Steve Sharpe
University of Washington

The fundamental issue

- Lattice simulations are done in finite volumes
- Experiments are not

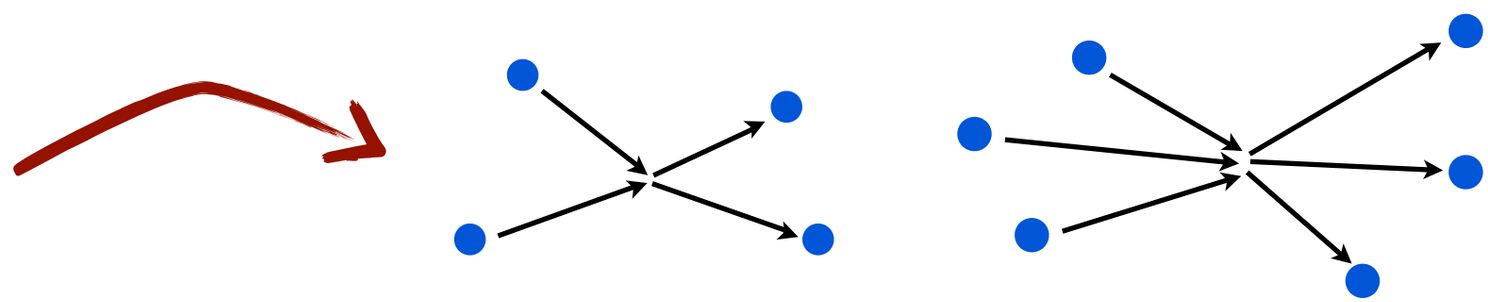

How do we connect these?

The fundamental issue

- Lattice simulations are done in finite volumes
- Experiments are not

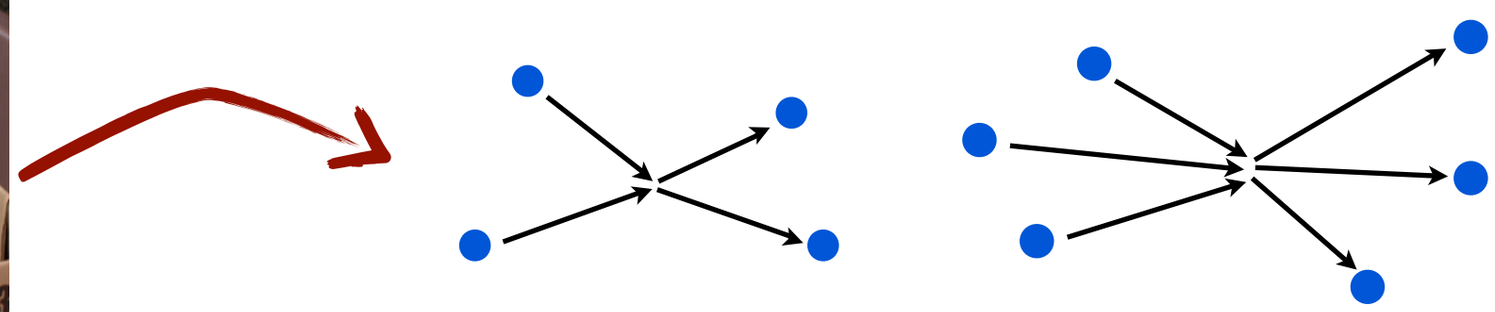

How do we connect these?

The fundamental issue

- Lattice QCD can calculate energy levels of multiple particle systems in a box
- How are these related to scattering amplitudes?

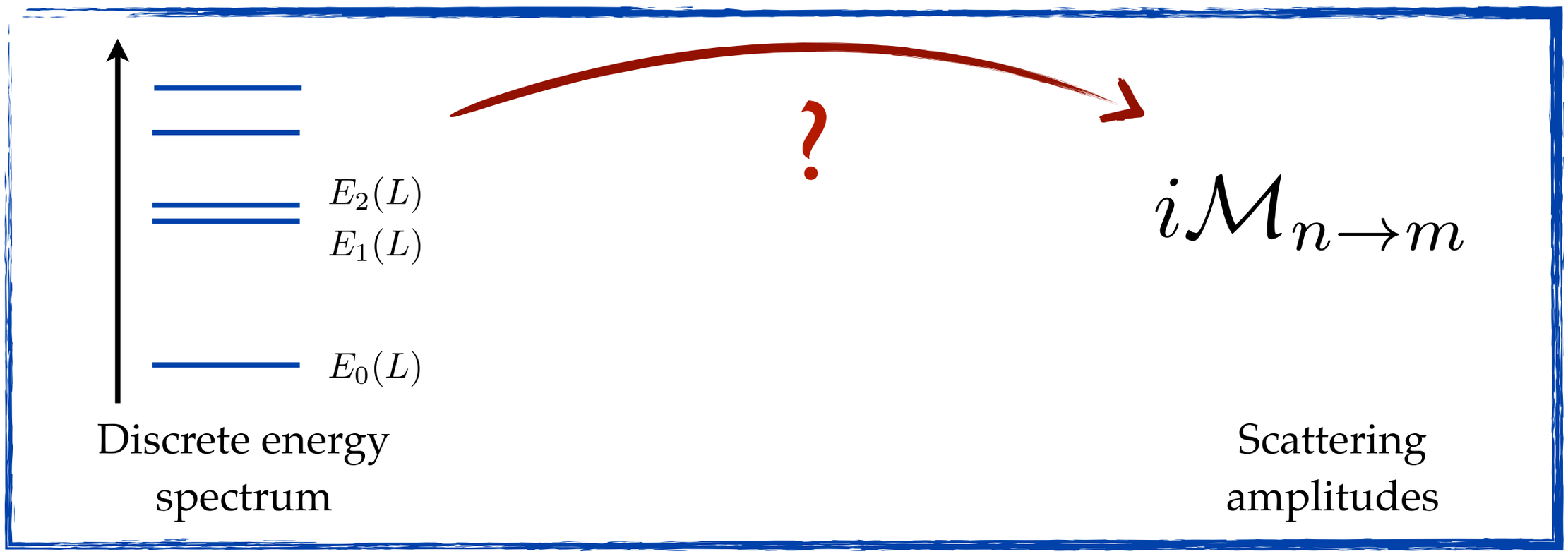

When is spectrum related to scattering amplitudes?

✘

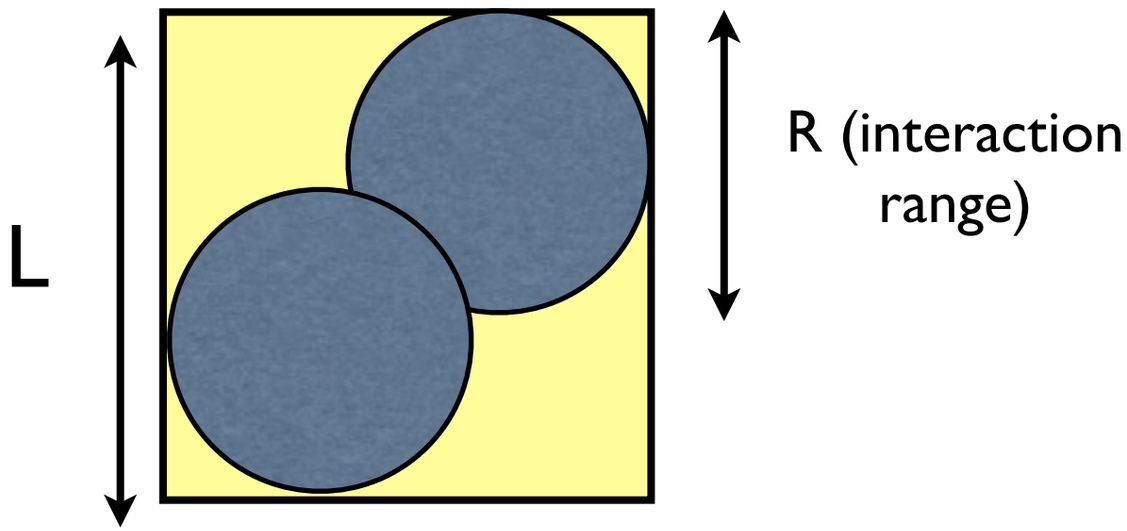

L<2R
No "outside" region.
Spectrum NOT related to scatt. amps.
Depends on finite-density properties

✔

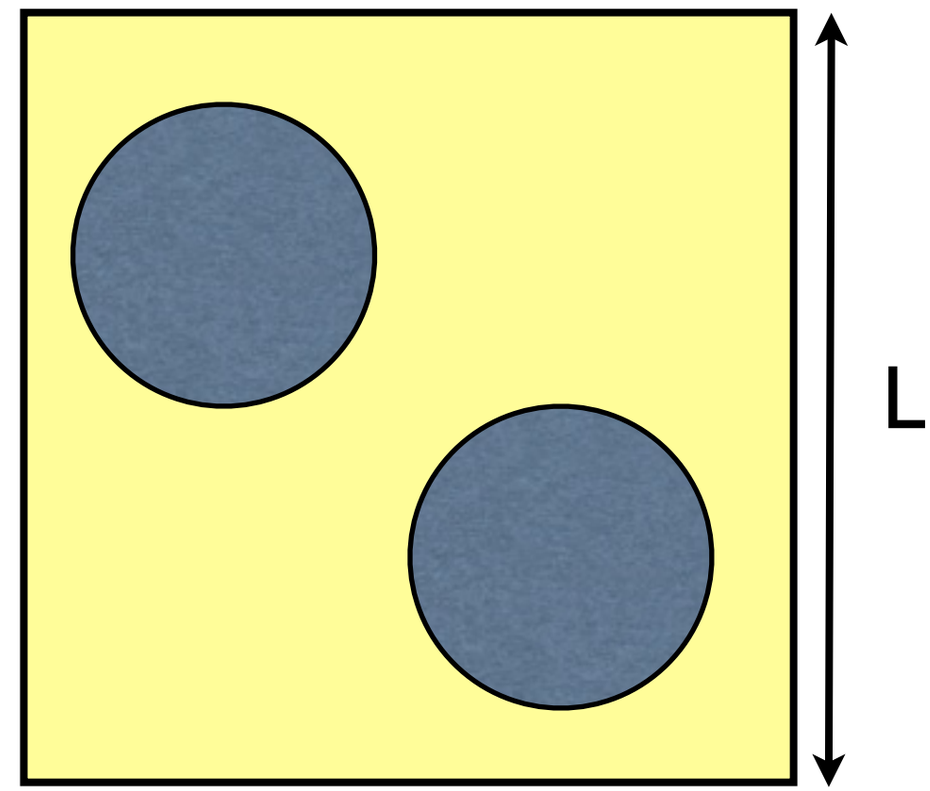

L>2R
There is an "outside" region.
Spectrum IS related to scatt. amps.
up to corrections proportional to
$e^{-M_\pi L}$
[Lüscher]

Systems considered today

Quantization conditions

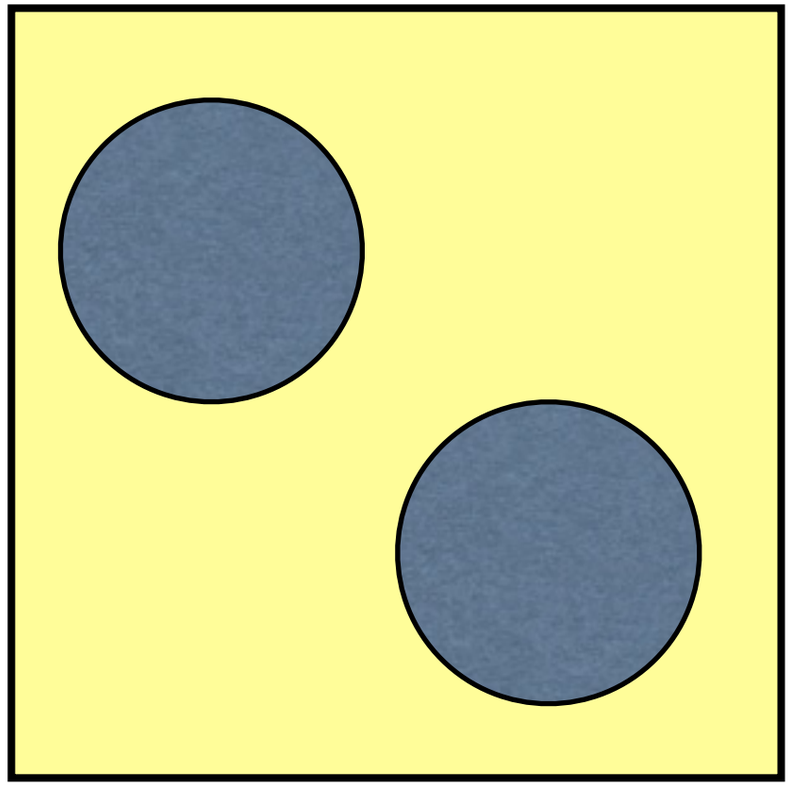

Theoretically understood;
numerical implementations mature

[Mohler, Wilson]

What about including QED?

[Beane, Davoudi]

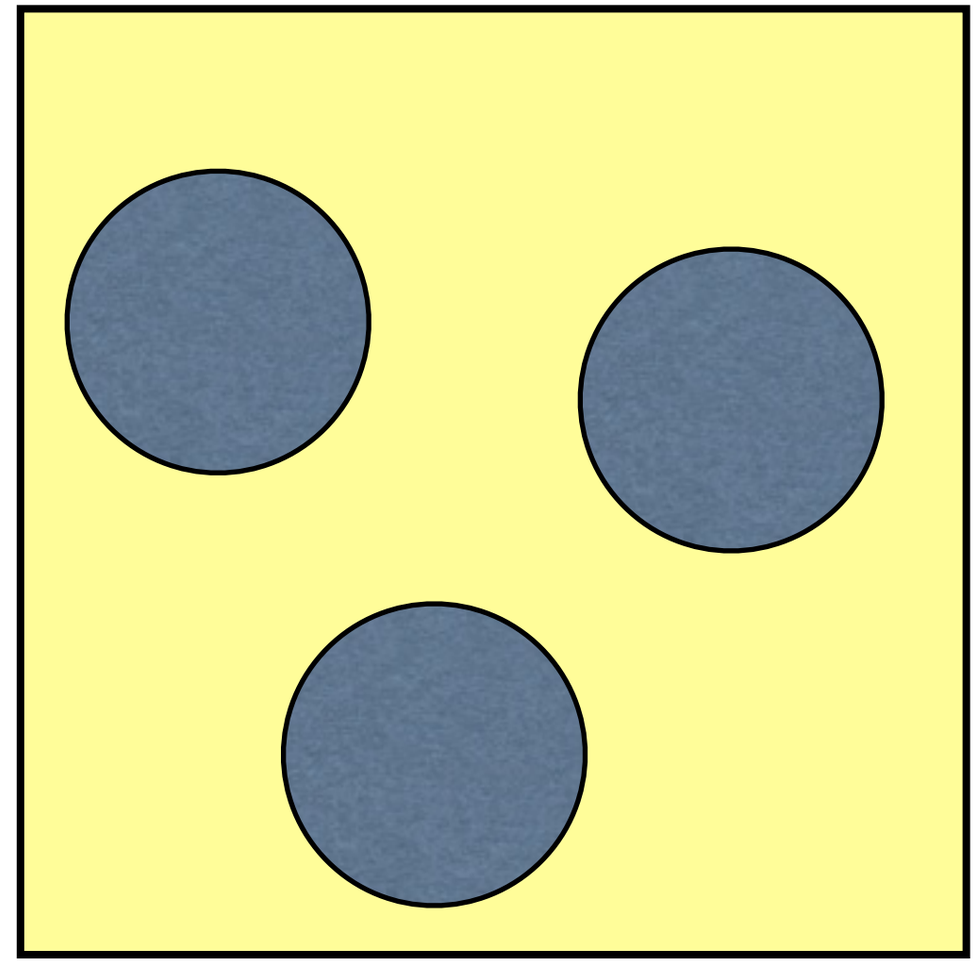

Formalism under development

[Hansen]

How implement numerically?

[Doi]

Systems considered today

Transition amplitudes

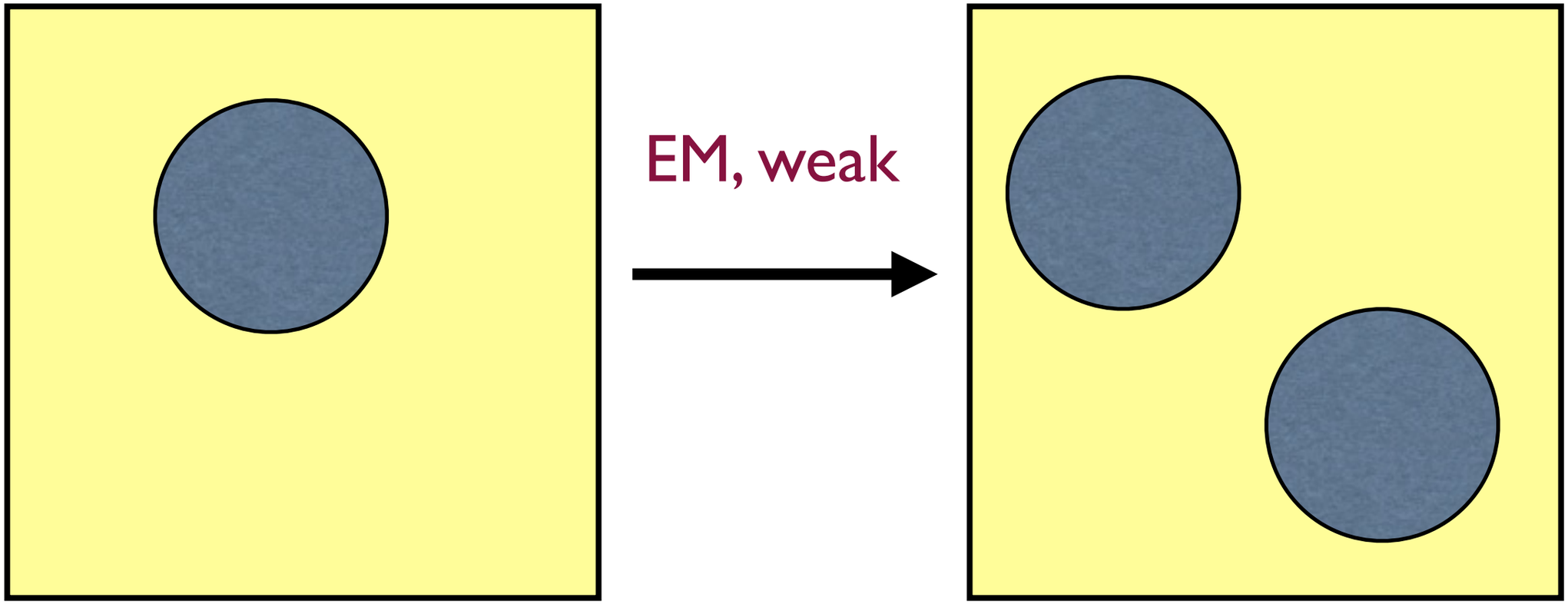

Theoretically understood; [Agadjanov, Briceño]

numerical implementations expanding [Ishizuka, Kelly, Shultz]

Outline

- Motivation
- Theoretical status
- Key theoretical ingredients
- 2-particle quantization condition
- Future directions & challenges

Studying resonances

- Most hadrons are resonances
  - Resonances are not asymptotic states; show up in behavior of scatt. amplitudes
  - FV methods determine scattering amplitudes indirectly

Studying resonances

- Most hadrons are resonances
  - Resonances are not asymptotic states; show up in behavior of scatt. amplitudes
  - FV methods determine scattering amplitudes indirectly

ρ resonance in ππ phase shift

[Dudek et al., 2013]

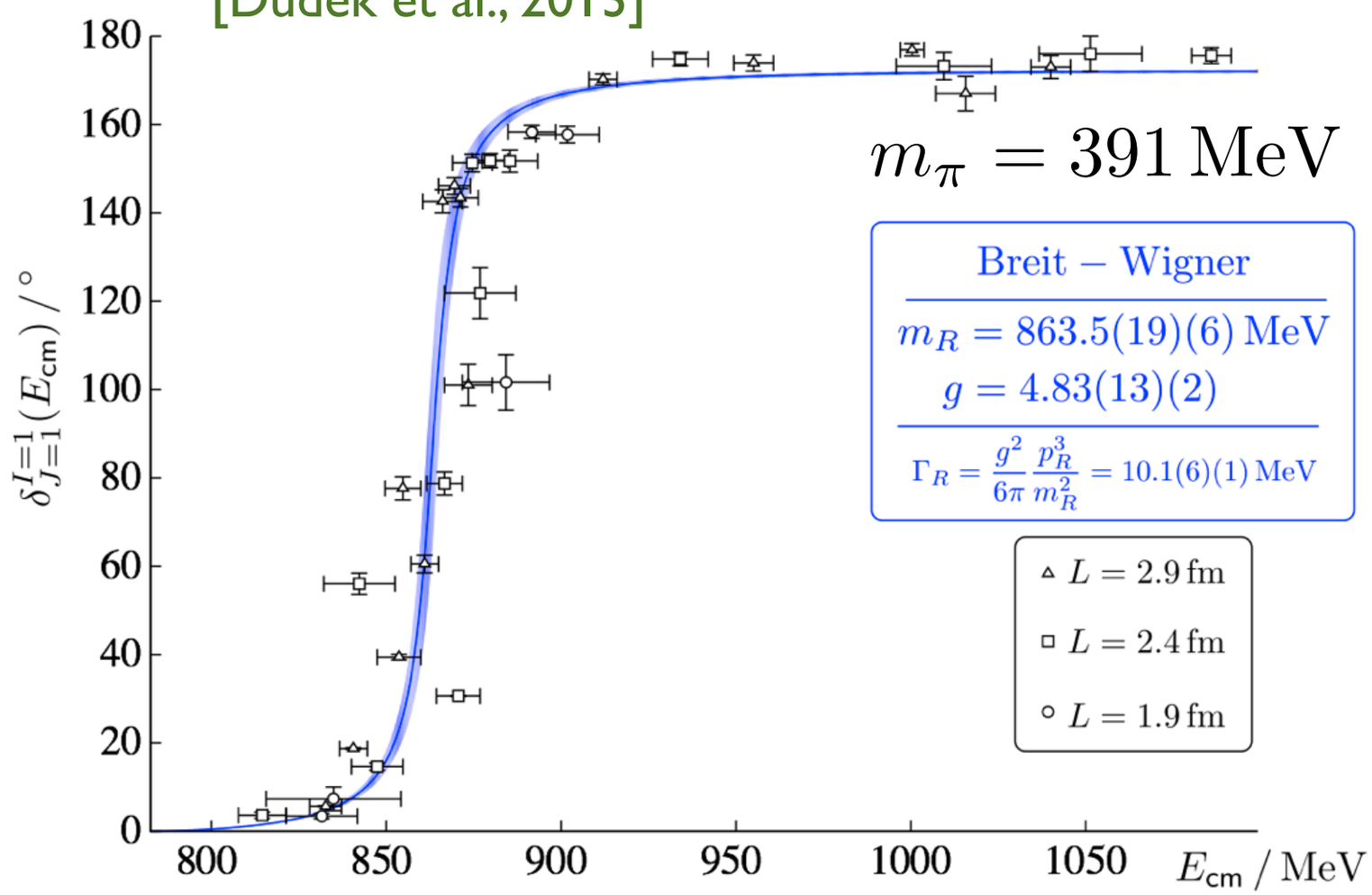

Studying resonances

- Most hadrons are resonances
  - Resonances are not asymptotic states; show up in behavior of scatt. amplitudes
  - FV methods aim to determine scattering amplitudes indirectly
- Many resonances have three particle decay channels

$$\omega(782) \to \pi\pi\pi \qquad K^* \longrightarrow K\pi\pi \quad N(1440) \to N\pi\pi$$

Studying resonances

- Most hadrons are resonances
  - Resonances are not asymptotic states; show up in behavior of scatt. amplitudes
  - FV methods aim to determine scattering amplitudes indirectly
- Many resonances have three particle decay channels

$$\omega(782) \to \pi\pi\pi \qquad K^* \longrightarrow K\pi\pi \quad N(1440) \to N\pi\pi$$

- Most resonances have multiple decay channels

$$a_0(980) \longrightarrow \eta\pi, K\overline{K} \qquad f_0(980) \longrightarrow \pi\pi, K\overline{K}$$

Determining interactions

- For nuclear physics need NN <u>and</u> NNN interactions
  - Input for effective field theory treatments of larger nuclei & nuclear matter

- Meson interactions needed for understanding pion & kaon condensates
  - $\pi\pi$, $K\overline{K}$, $\pi\pi\pi$, $\pi K\overline{K}$, etc.

Calculating decay amplitudes

- Weak decay amplitudes allow tests of SM
  - $K \to \pi\pi, \pi\pi\pi$
  - $D \to \pi\pi, K\bar{K}, \eta\eta, 4\pi, \ldots.$
  - $B \to K\pi$ (+ $\ell^+ \ell^-$)
  - ...
- EM transition amplitudes probe hadron structure

$$\rho \longrightarrow \pi\gamma^* \qquad\qquad N\gamma^* \longrightarrow \Delta \longrightarrow N\pi$$

Theoretical status

Status for 2 particles

- Long understood in NRQM [Huang & Yang 57, ...]
- Quantization formula in QFT for energies below inelastic threshold converted into NRQM problem and solved by [Lüscher 86 & 91]
- Solution generalized to arbitrary total momentum **P**, multiple (2 body) channels, general BCs and arbitrary spins [Rummukainen & Gottlieb 85; Kim, Sachrajda & SS 05; Bernard, Lage, Meißner & Rusetsky 08; Hansen & SS 12; Briceño & Davoudi 12; …]
- Relation between finite volume $1\to 2$ weak amplitude (e.g. $K\to\pi\pi$) and infinite volume decay amplitude determined [Lellouch & Lüscher 00]
- LL formula generalized to general **P**, to multiple (2 body) channels, and to arbitrary currents and general BCs (e.g. $\gamma^*\pi\to\rho\to\pi\pi$, $\gamma^*N\to\Delta\to\pi N$, $\gamma D\to NN$) [Kim, Sachrajda & SS 05; Christ, Kim & Yamazaki 05; Meyer 12; Hansen & SS 12; Briceño & Davoudi 12; Agadjanov, Bernard, Meißner & Rusetsky 14; Briceño, Hansen & Walker-Loud 14; …]
- Leading order QED effects on quantization condition determined [Beane & Savage 14]

Status for 3 particles

- [Beane, Detmold & Savage 07 and Tan 08] derived threshold expansion for n particles in NRQM, and argued it applied also in QFT
- [Polejaeva & Rusetsky 12] showed in NREFT that 3 body spectrum determined by infinite-volume scattering amplitudes, using integral equation
- [Briceño & Davoudi 12] used a dimer approach in NREFT, with s-wave interactions only, to determine relation between spectrum and a finite volume quantity, itself related to infinite-volume amplitudes by an integral equation
- [Hansen & SS 14, 15] derived quantization condition in (fairly) general, relativistic QFT relating spectrum and $\mathcal{M}_2$ and 3-body scattering *quantity* $K_{df,3}$; relation between $K_{df,3}$ & $\mathcal{M}_3$ via integral equations now known
- [Meißner, Rios & Rusetsky 14] determined volume dependence of 3-body bound state in unitary limit

Some key theoretical ingredients

Following method of [Kim, Sachrajda & SS 05]

Set-up

- Work in continuum (assume that LQCD can control discretization errors)

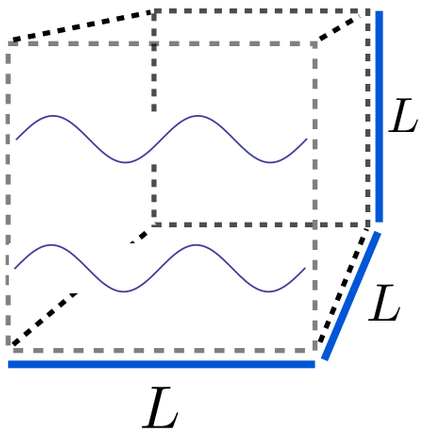

- Cubic box of size L with periodic BC, and infinite (Minkowski) time
  - Spatial loops are sums: $\frac{1}{L^3}\sum_{\vec{k}}$ $\quad \vec{k} = \frac{2\pi}{L}\vec{n}$
  - Easily extend to other BC (e.g. twisted)

- Consider general QFT with arbitrary vertices

Methodology

- Calculate (for some $\mathbf{P}=2\pi\mathbf{n}_P/L$)

CM energy is $E^*=\sqrt{(E^2-P^2)}$

$$C_L(E,\vec{P}) \equiv \int_L d^4x \; e^{-i\vec{P}\cdot\vec{x}+iEt} \langle\Omega| T\sigma(x)\sigma^\dagger(0)|\Omega\rangle_L$$

- Poles in C_L occur at energies of finite-volume spectrum
- For 2 & 3 particle states, $\sigma \sim \pi^2$ & π^3, respectively
- Use all-orders diagrammatic expansion, e.g.

$C_L(E,\vec{P}) =$

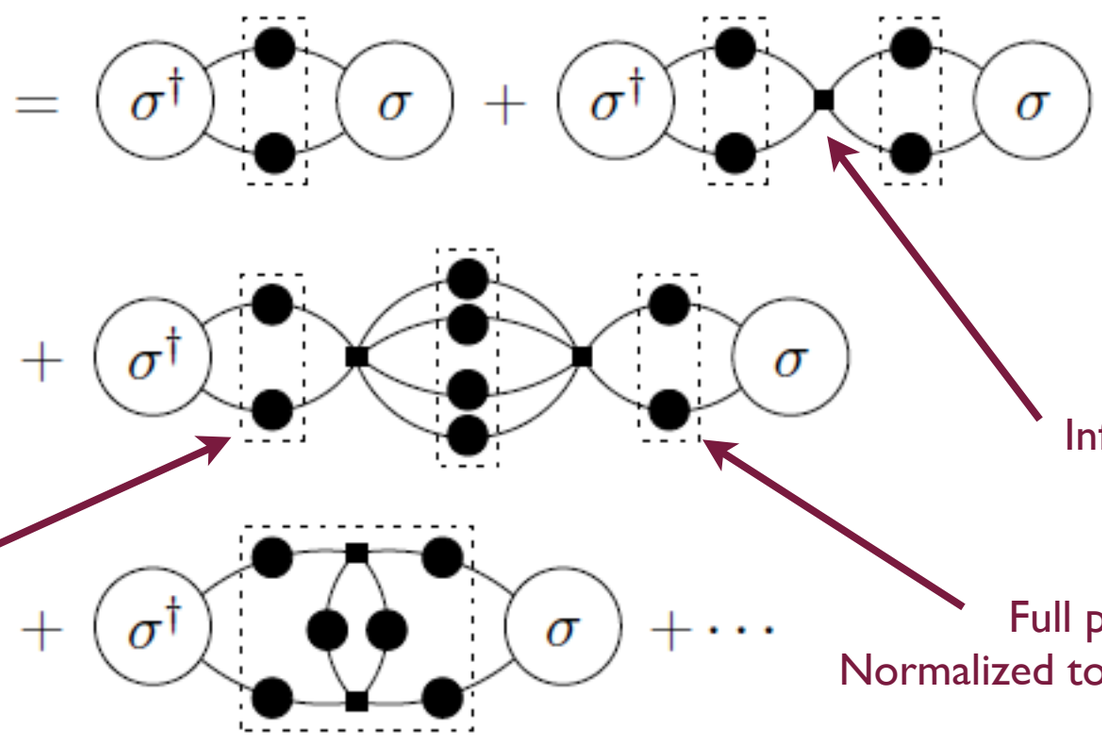

Infinite-volume vertices

Boxes indicated summation over finite-volume momenta

Full propagators Normalized to unit residue at pole

Key step 1

- Replace loop sums with integrals where possible
  - Drop exponentially suppressed terms (~e^{-ML}, $e^{-(ML)^2}$, etc.) while keeping power-law dependence

$$\frac{1}{L^3}\sum_{\vec{k}} g(\vec{k}) = \int \frac{d^3k}{(2\pi)^3} g(\vec{k}) + \sum_{\vec{l}\neq\vec{0}} \int \frac{d^3k}{(2\pi)^3} e^{iL\vec{l}\cdot\vec{k}} g(\vec{k})$$

Key step 1

- Replace loop sums with integrals where possible
  - Drop exponentially suppressed terms (~e^{-ML}, $e^{-(ML)^2}$, etc.) while keeping power-law dependence

$$\frac{1}{L^3}\sum_{\vec{k}} g(\vec{k}) = \int \frac{d^3k}{(2\pi)^3} g(\vec{k}) + \cancel{\sum_{\vec{l}\neq\vec{0}} \int \frac{d^3k}{(2\pi)^3} e^{iL\vec{l}\cdot\vec{k}} g(\vec{k})}$$

Exp. suppressed if g(k) is smooth and scale of derivatives of g is ~1/M

Key step 2

- Use "sum=integral + [sum-integral]" if integrand has pole, with [KSS]

$$\left(\int \frac{dk_0}{2\pi}\frac{1}{L^3}\sum_{\vec{k}} - \int \frac{d^4k}{(2\pi)^4}\right) f(k)\frac{1}{k^2-m^2+i\epsilon}\frac{1}{(P-k)^2-m^2+i\epsilon}g(k)$$

$$= \int d\Omega_{q^*}\, d\Omega_{q^{*\prime}}\, f^*(\hat{q}^*)\mathcal{F}\quad(q^*, q^{*\prime})g^*(\hat{q}^{*\prime}) \quad + \text{exp. suppressed}$$

q^* is relative momentum of pair on left in CM

Kinematic function

f & g evaluated for ON-SHELL momenta
Depend only on direction in CM

- Example

$P = (E, \vec{P})$ →

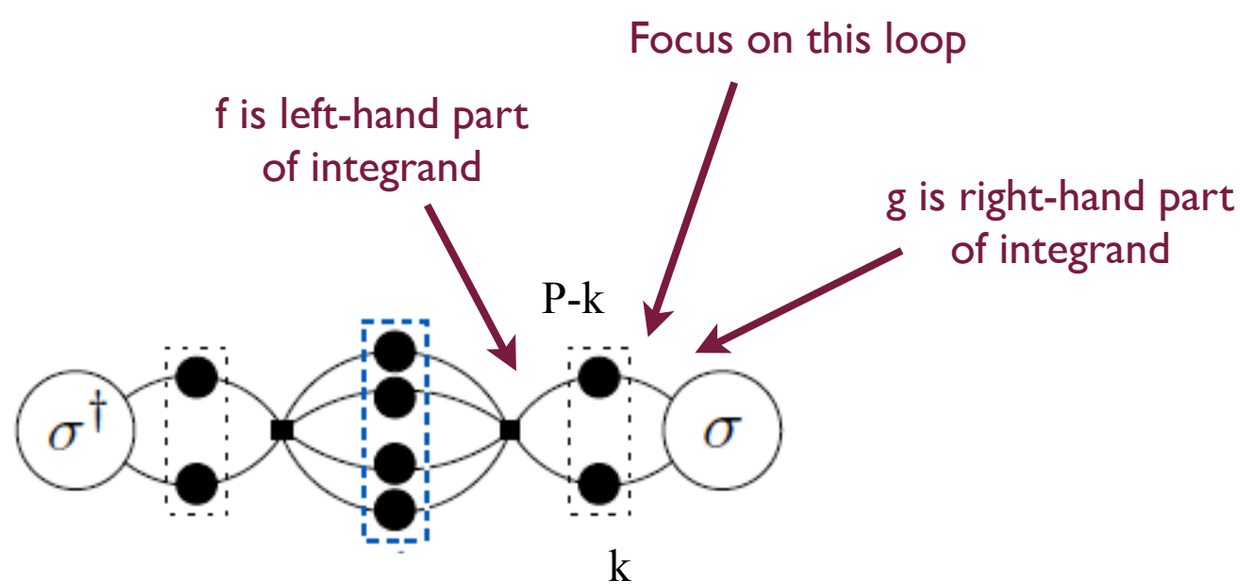

Key step 2

- Use "sum=integral + [sum-integral]" where integrand has pole, with [KSS]

$$\left(\int \frac{dk_0}{2\pi}\frac{1}{L^3}\sum_{\vec{k}} - \int \frac{d^4k}{(2\pi)^4}\right) f(k)\frac{1}{k^2-m^2+i\epsilon}\frac{1}{(P-k)^2-m^2+i\epsilon}g(k)$$
$$= \int d\Omega_{q^*}\, d\Omega_{q^{*\prime}}\, f^*(\hat{q}^*)\mathcal{F}\quad(q^*, q^{*\prime})g^*(\hat{q}^{*\prime})$$

- Decomposed into spherical harmonics, $\mathcal{F}$ becomes

$$F_{\ell_1,m_1;\ell_2,m_2} \equiv \quad \eta\left[\frac{\mathrm{Re}q^*}{8\pi E^*}\delta_{\ell_1\ell_2}\delta_{m_1m_2} + \frac{i}{2\pi EL}\sum_{\ell,m} x^{-\ell}\,\mathcal{Z}^P_{\ell m}[1;x^2]\int d\Omega\, Y^*_{\ell_1,m_1}Y^*_{\ell,m}Y_{\ell_2,m_2}\right]$$

$x \equiv q^*L/(2\pi)$ and $\mathcal{Z}^P_{\ell m}$ is a generalization of the zeta-function

Key step 2

- Use "sum=integral + [sum-integral]" where integrand has pole, with [KSS]

$$\left(\int \frac{dk_0}{2\pi}\frac{1}{L^3}\sum_{\vec{k}} - \int \frac{d^4k}{(2\pi)^4}\right) f(k)\frac{1}{k^2-m^2+i\epsilon}\frac{1}{(P-k)^2-m^2+i\epsilon}g(k)$$
$$= \int d\Omega_{q^*}\, d\Omega_{q^{*\prime}}\, f^*(\hat{q}^*)\mathcal{F}\quad (q^*, q^{*\prime})g^*(\hat{q}^{*\prime})$$

- Diagrammatically

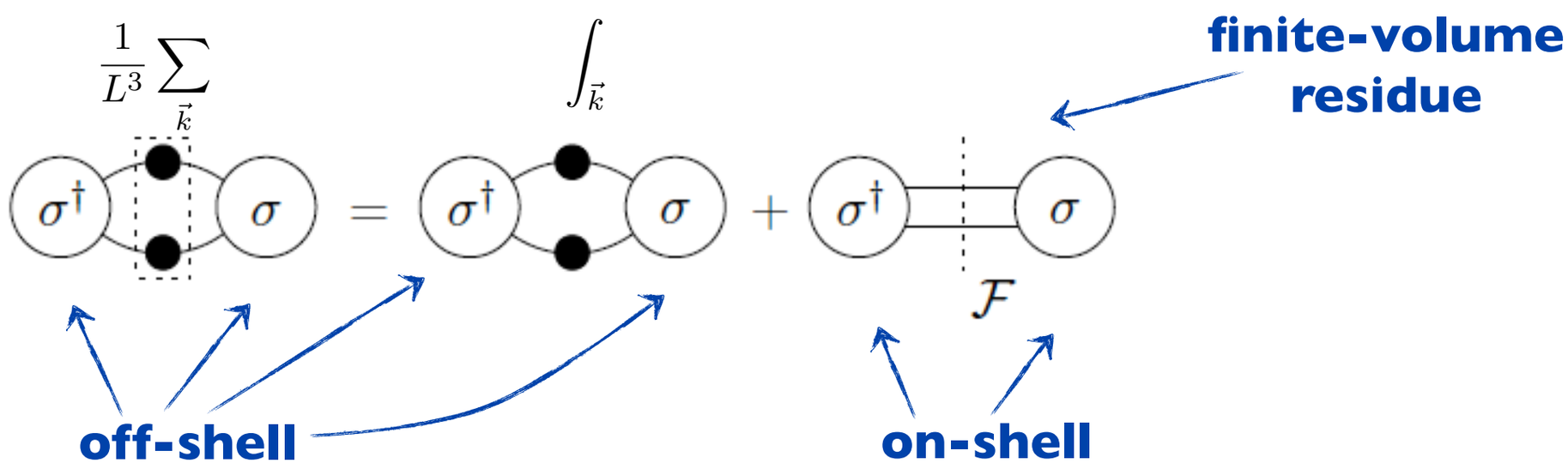

Variant of key step 2

- For generalization to 3 particles use (modified) PV prescription instead of iε

$$\left(\int \frac{dk_0}{2\pi} \frac{1}{L^3} \sum_{\vec{k}} \overset{\widetilde{PV}}{-\!\!\!\!\!\!\int} \frac{d^4k}{(2\pi)^4} \right) f(k) \frac{1}{k^2 - m^2 + \cancel{i\epsilon}} \frac{1}{(P-k)^2 - m^2 + \cancel{i\epsilon}} g(k)$$

$$= \int d\Omega_{q^*} d\Omega_{q^{*\prime}} f^*(\hat{q}^*) \mathcal{F}_{\widetilde{PV}}(q^*, q^{*\prime}) g^*(\hat{q}^{*\prime})$$

- Key properties of F_{PV} : real and no unitary cusp at threshold [see Max's talk]

Key step 3

- Identify potential singularities: can use time-ordered PT (i.e. do k_0 integrals)
- Example

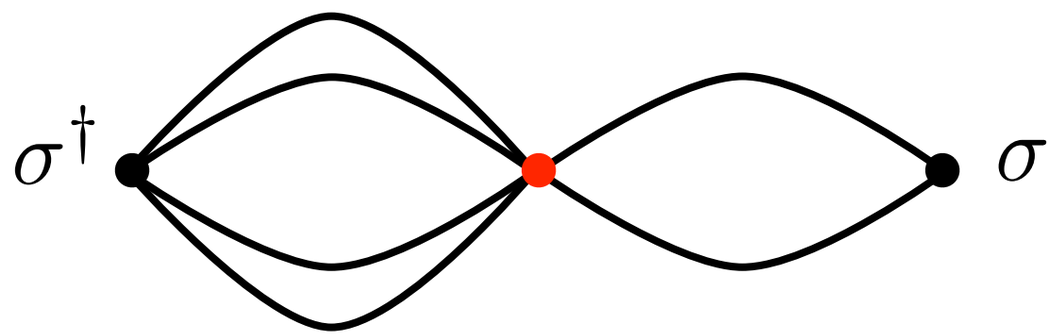

Key step 3

- 2 out of 6 time orderings:

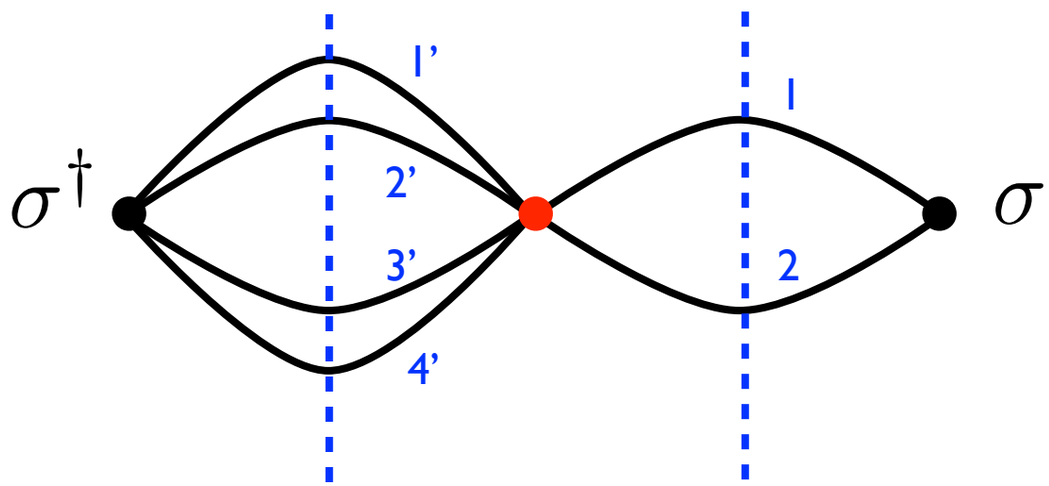

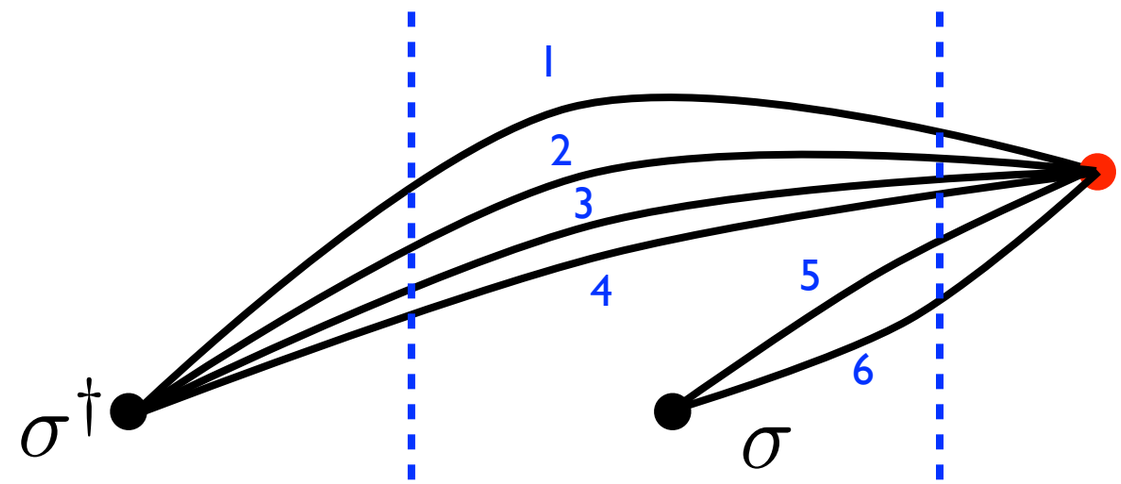

$$\frac{1}{E-\omega_1'-\omega_2'-\omega_3'-\omega_4'} \qquad \frac{1}{E-\omega_1-\omega_2} \qquad \frac{1}{E-\omega_1-\omega_2-\omega_3-\omega_4} \qquad \frac{1}{\sum_{j=1,6}\omega_j}$$

On-shell energy $\omega_j = \sqrt{\vec{k}_j^2 + M^2}$

Key step 3

- 2 out of 6 time orderings:

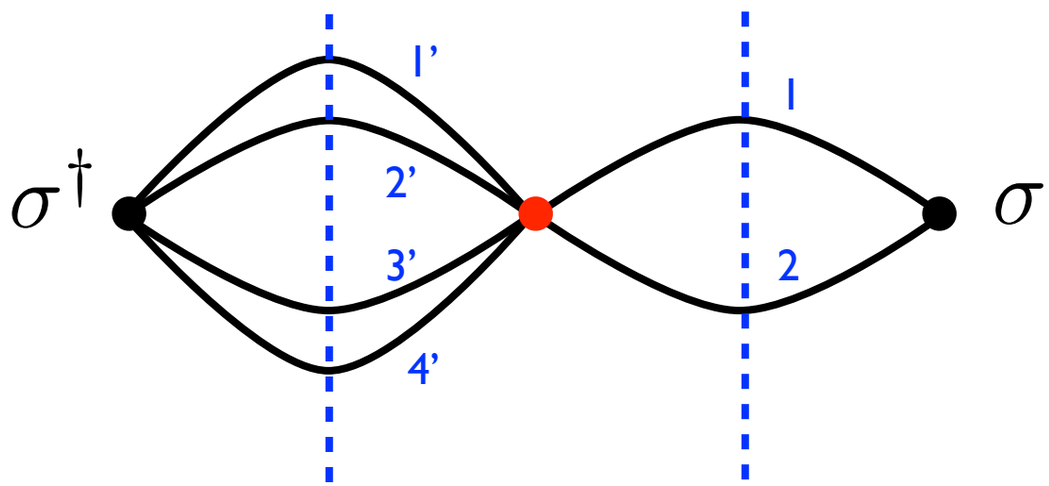

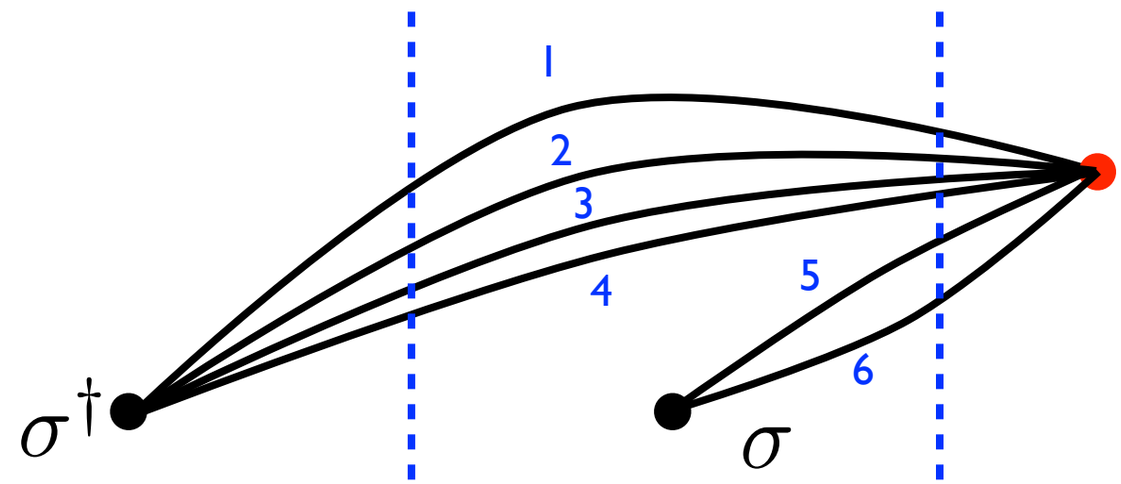

$$\frac{1}{E-\omega_1'-\omega_2'-\omega_3'-\omega_4'} \qquad \frac{1}{E-\omega_1-\omega_2} \qquad \frac{1}{E-\omega_1-\omega_2-\omega_3-\omega_4} \qquad \frac{1}{\sum_{j=1,6}\omega_j}$$

- If restrict $0 < E^* < 4M$ then only 2-particle "cuts" have singularities, and these occur only when both particles go on-shell

Combining key steps 1-3

- For each diagram, determine which momenta must be summed, and which can be integrated
- In our example, find:

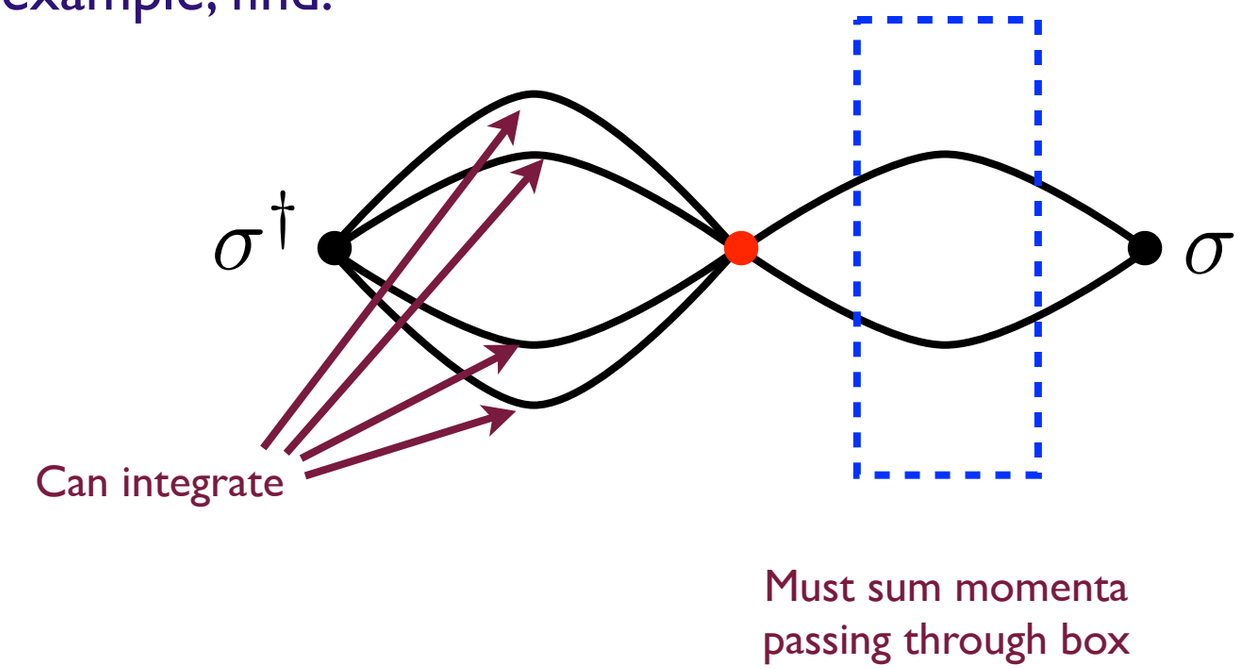

Combining key steps 1-3

- For each diagram, determine which momenta must be summed, and which can be integrated

- In our example, find:

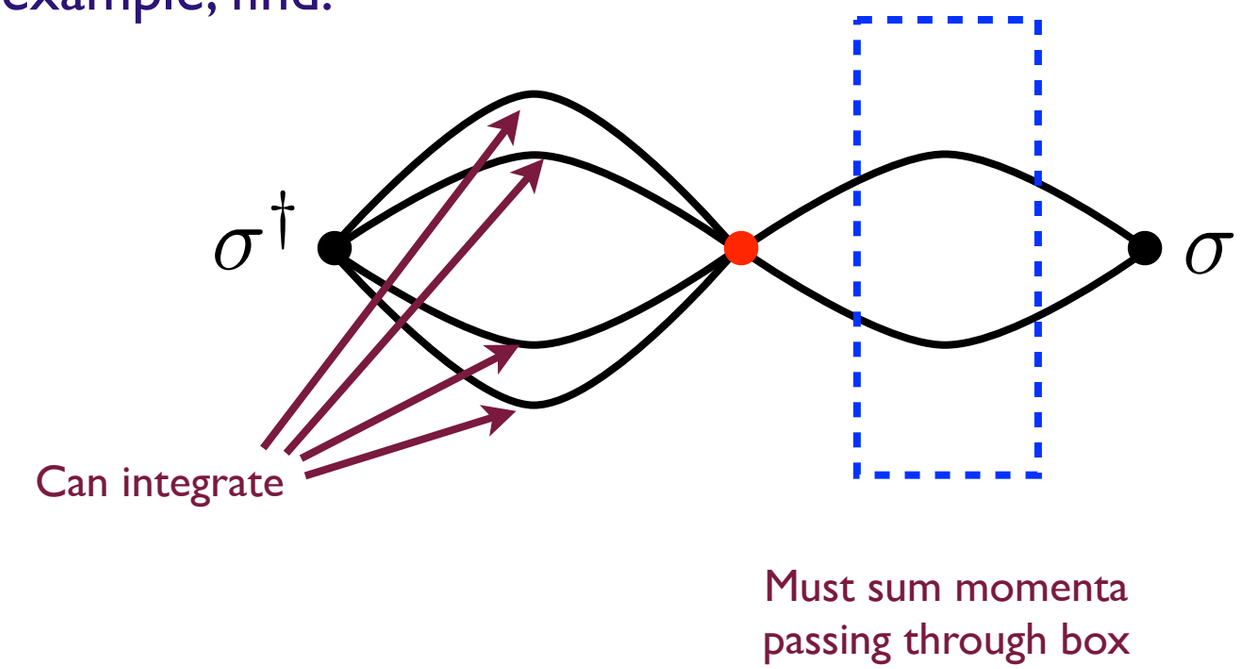

- Then repeatedly use sum=integral + "sum-integral" to simplify

2-particle quantization condition

Following method of [Kim, Sachrajda & SS 05]

- Apply previous analysis to 2-particle correlator ($0 < E^* < 4M$)

$$C_L(E,\vec{P}) =$$

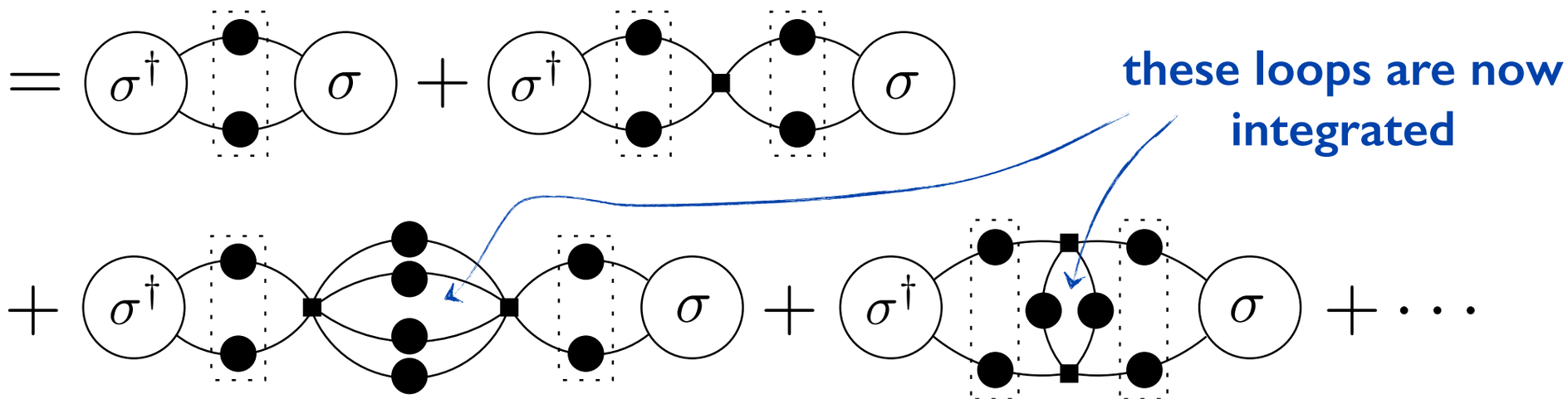

- Collect terms into infinite-volume Bethe-Salpeter kernels

$$C_L(E,\vec{P}) =$$

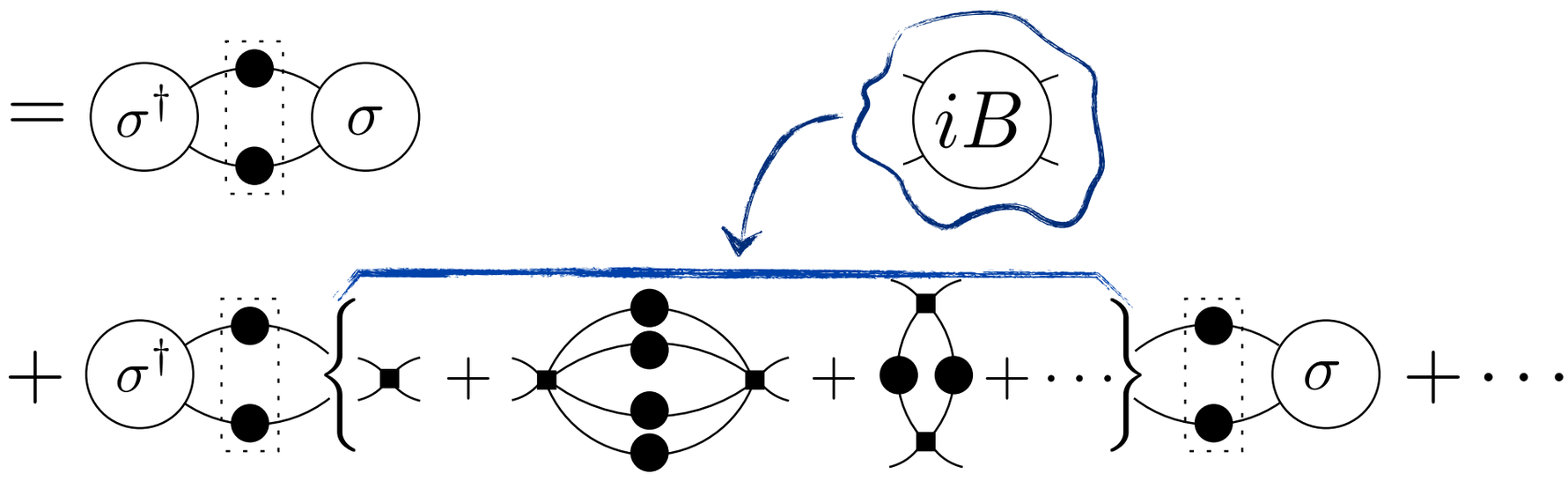

- Apply previous analysis to 2-particle correlator
- Collect terms into infinite-volume Bethe-Salpeter kernels

$C_L(E,\vec{P}) =$

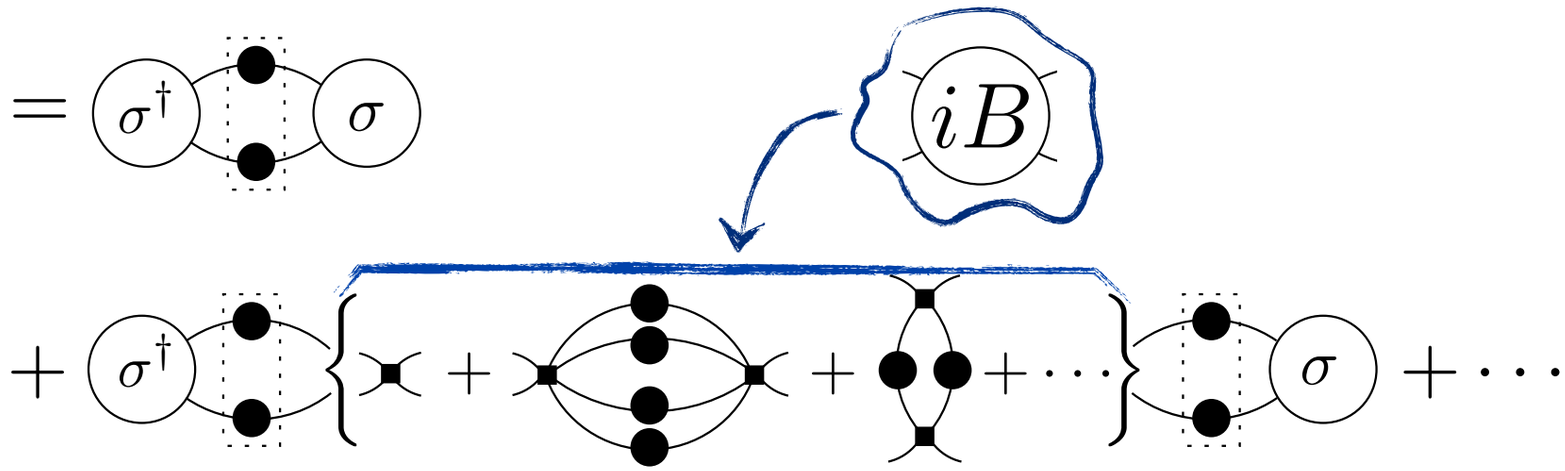

- Leading to

$C_L(E,\vec{P}) =$

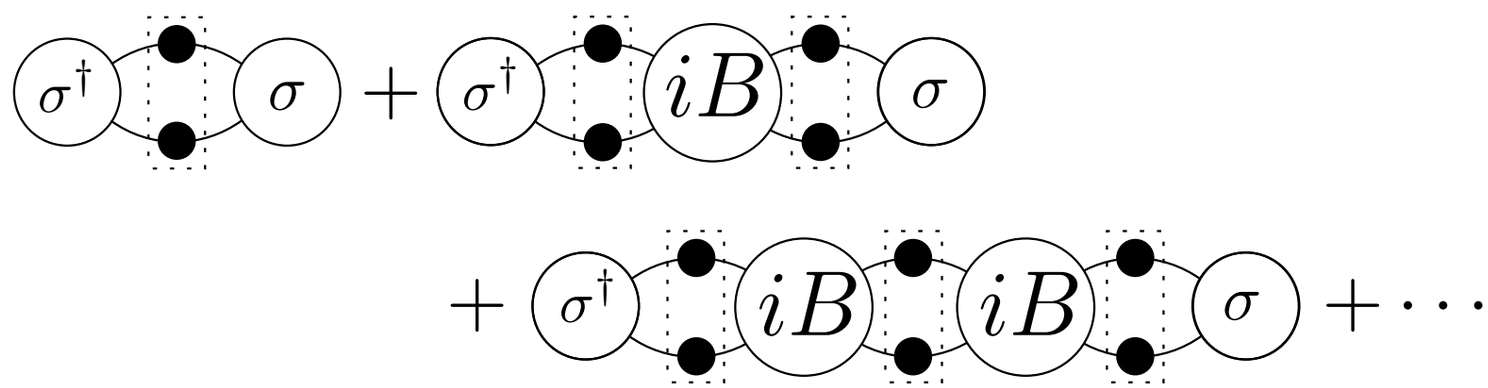

- Next use sum identity

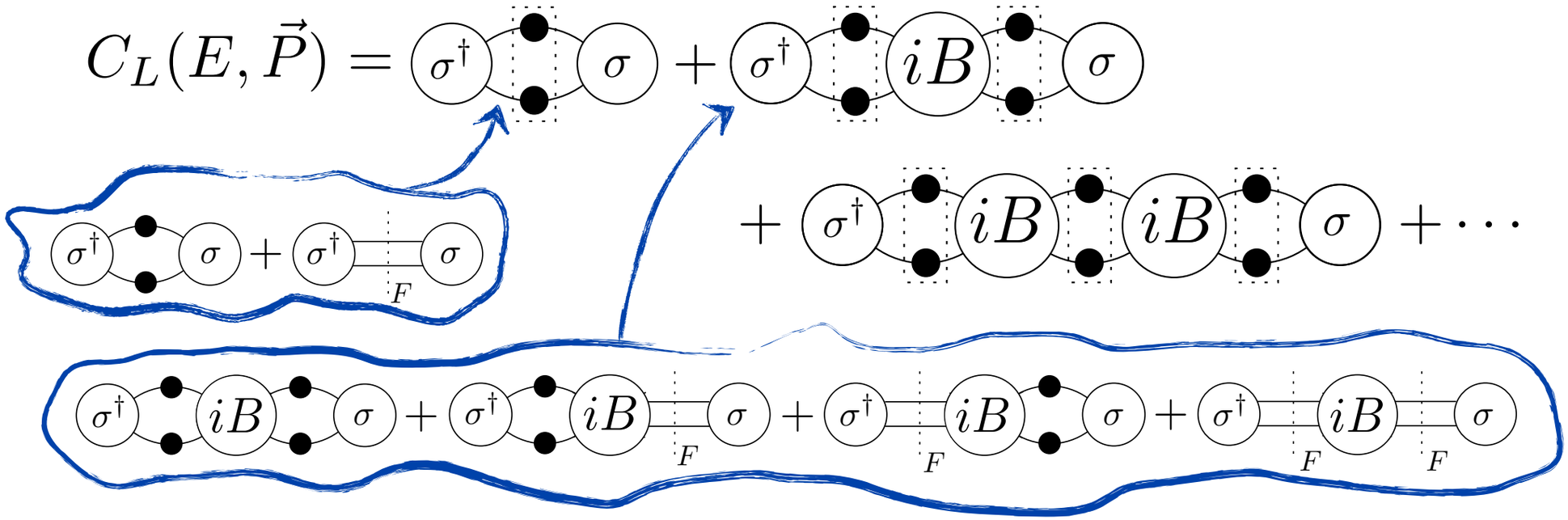

- And regroup according to number of "F cuts"

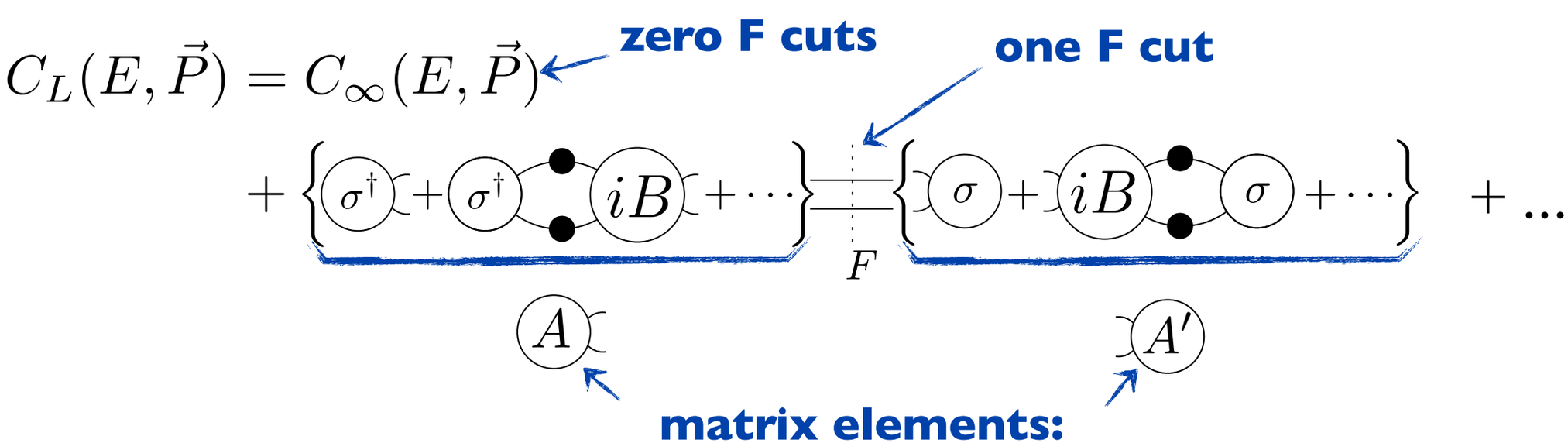

- Next use sum identity

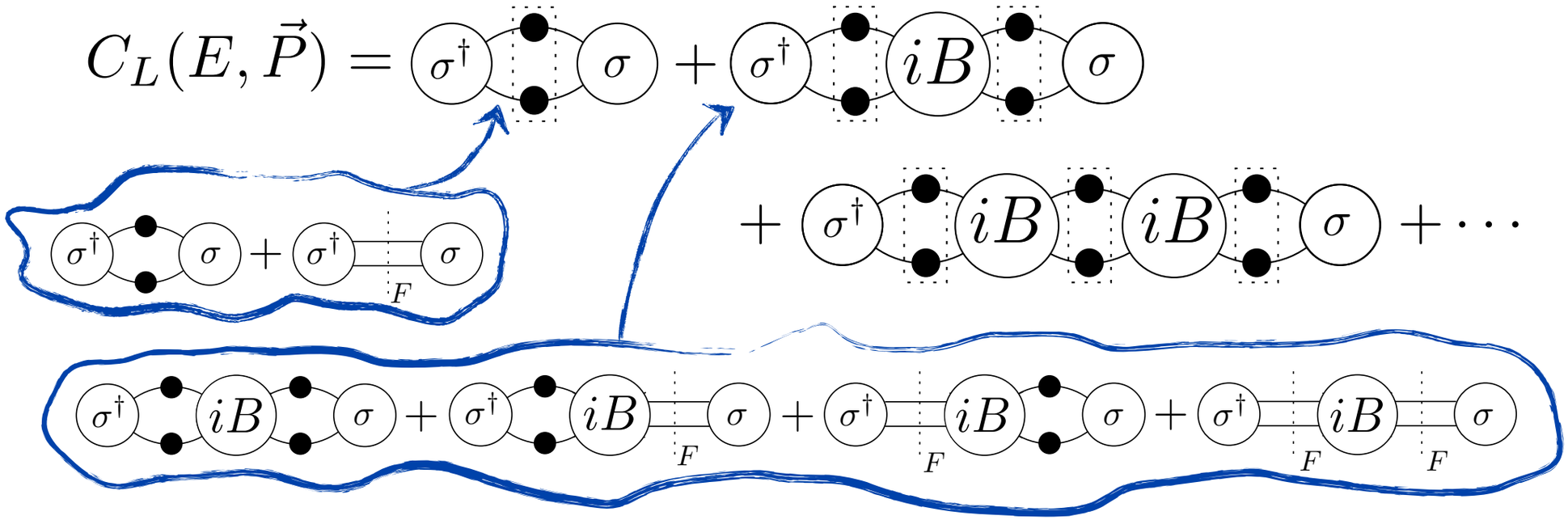

- And keep regrouping according to number of "F cuts"

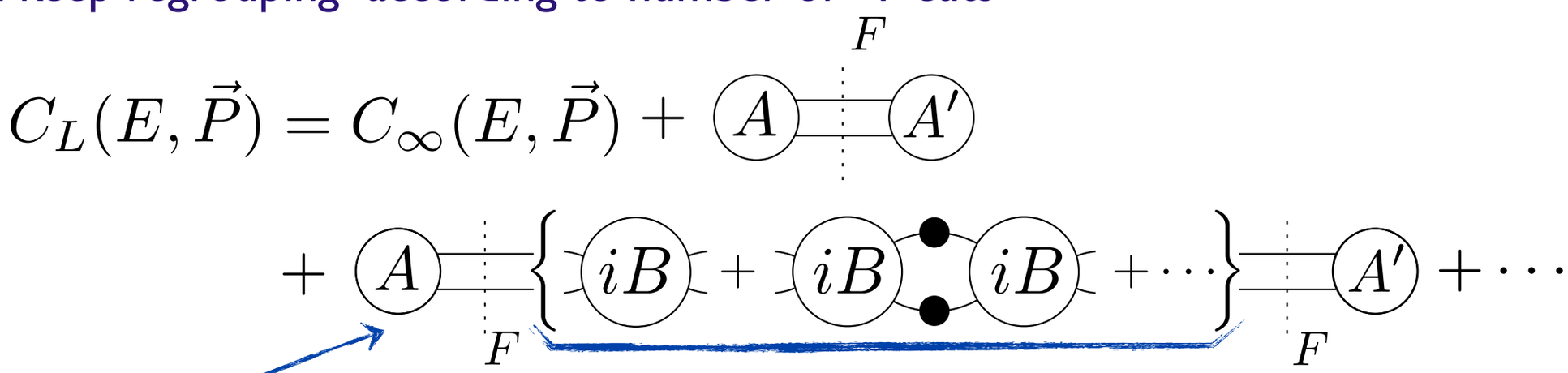

two F cuts

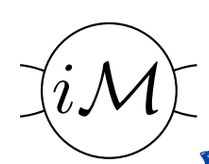

the infinite-volume, on-shell 2→2 scattering amplitude

- Next use sum identity

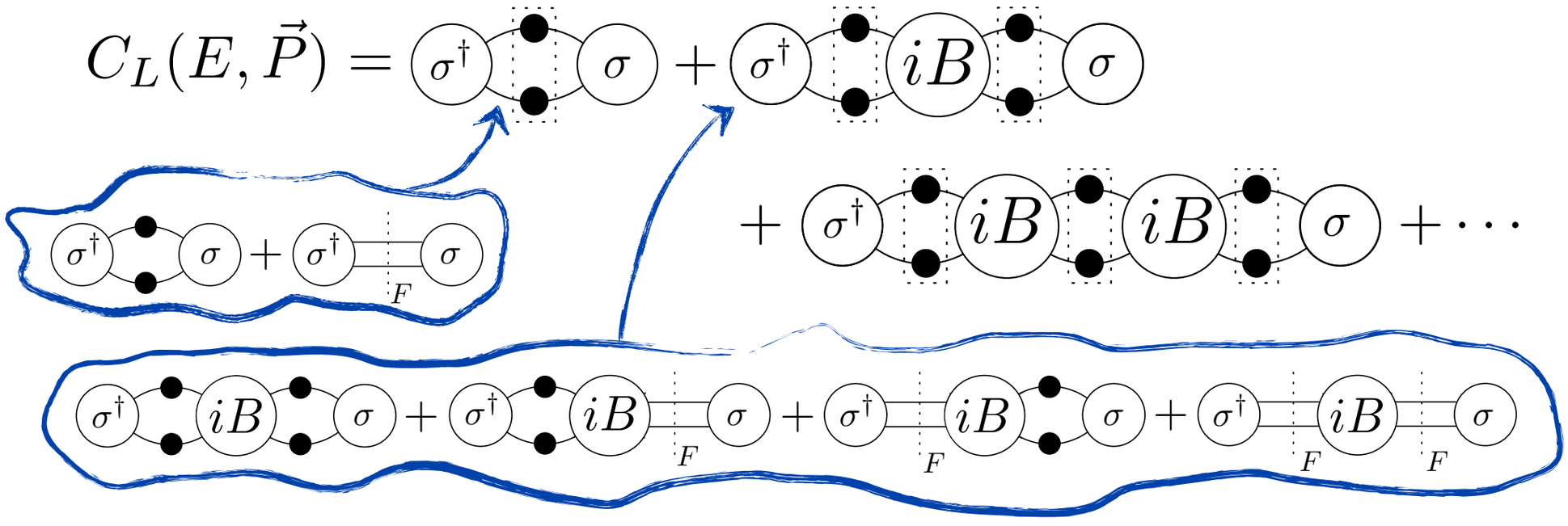

- Alternate form if use PV-tilde prescription:

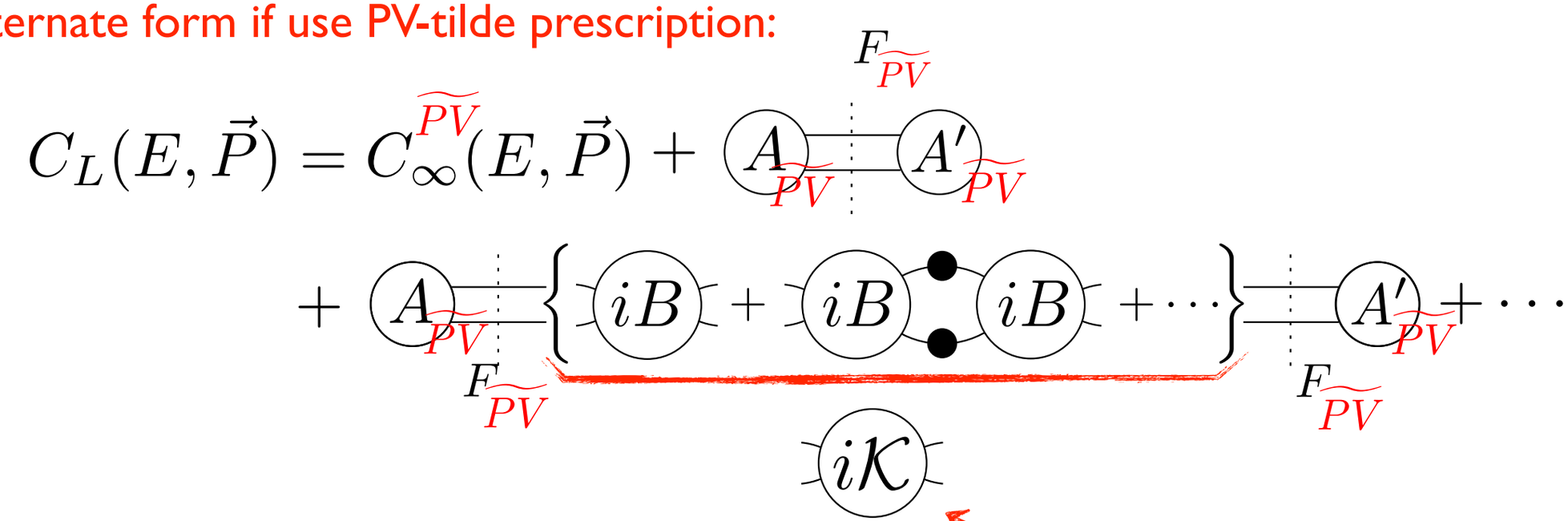

the infinite-volume, on-shell 2→2 K-matrix

- Final result:

$$C_L(E,\vec{P}) = C_\infty(E,\vec{P})$$

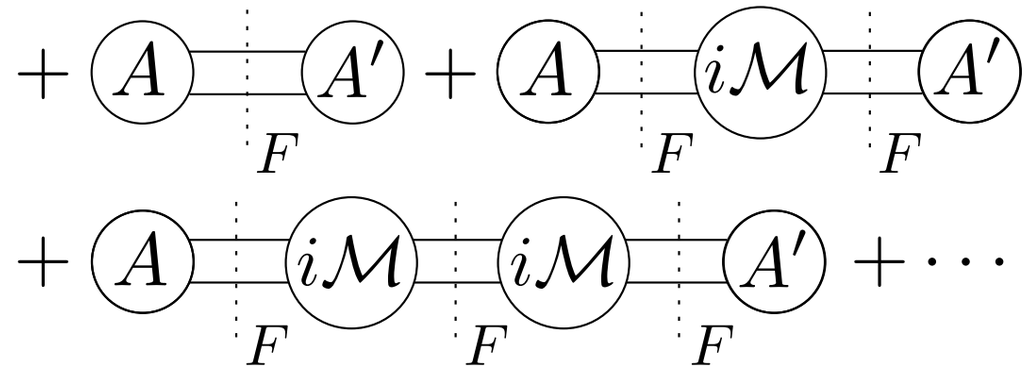

$$+ \cdots$$

- $$C_L(E,\vec{P}) = C_\infty(E,\vec{P}) + \sum_{n=0}^{\infty} A' iF [i\mathcal{M}_{2\to 2} iF]^n A$$

- Correlator is expressed in terms of infinite-volume, physical quantities and kinematic functions encoding the finite-volume effects

- Final result:

$$C_L(E,\vec{P}) = C_\infty(E,\vec{P})$$

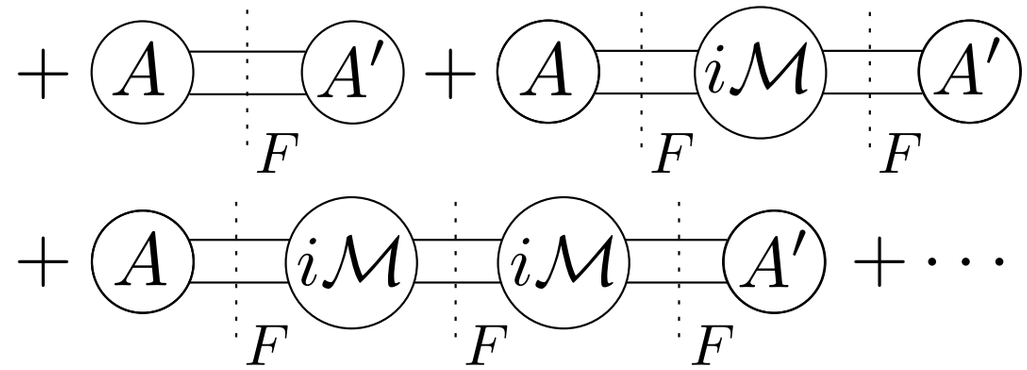

- $$C_L(E,\vec{P}) = C_\infty(E,\vec{P}) + \sum_{n=0}^{\infty} A' iF [i\mathcal{M}_{2\to 2} iF]^n A$$

- $$C_L(E,\vec{P}) = C_\infty(E,\vec{P}) + A' iF \frac{1}{1 - i\mathcal{M}_{2\to 2} iF} A$$

no poles, only cuts

no poles, only cuts

matrices in l,m space

- $C_L(E,\vec{P})$ diverges whenever $iF \dfrac{1}{1 - i\mathcal{M}_{2\to 2} iF}$ diverges

2-particle quantization condition

$$C_L(E,\vec{P}) = C_\infty(E,\vec{P}) + A' iF \frac{1}{1 - i\mathcal{M}_{2\to 2} iF} A$$

- At fixed L & **P**, the finite-volume spectrum E_1, E_2, ... is given by solutions to

$$\Delta_{L,\vec{P}}(E) = \det\left[(iF)^{-1} - i\mathcal{M}_{2\to 2}\right] = 0$$

- $\mathcal{M}$ is diagonal in *l,m*: $i\mathcal{M}_{2\to 2;\ell',m';\ell,m} \propto \delta_{\ell,\ell'}\delta_{m,m'}$
- F is off-diagonal, since the box violates rotation symmetry
- To make useful, truncate by assuming that $\mathcal{M}$ vanishes above l_{max}
- For example, if l_{max}=0, obtain

$$i\mathcal{M}_{2\to 2;00;00}(E_n^*) = [iF_{00;00}(E_n,\vec{P},L)]^{-1}$$

Generalization of s-wave Lüscher equation to moving frame [Rummukainen & Gottlieb]

Equivalent K-matrix form

$$C_L(E,\vec{P}) = C_\infty(E,\vec{P}) + A' i F_{\widetilde{\mathrm{PV}}} \frac{1}{1+\mathcal{K}_2 F_{\widetilde{\mathrm{PV}}}} A$$

- At fixed L & **P**, the finite-volume spectrum E_1, E_2, ... is given by solutions to

$$\Delta_{L,\vec{P}}(E) = \det\left[(F_{\widetilde{PV}})^{-1} + \mathcal{K}_2\right] = 0$$

- $\mathcal{K}_2$ is diagonal in *l,m*
- F_{PV} is off-diagonal, since the box violates rotation symmetry
- To make useful, truncate by assuming that $\mathcal{K}_2$ vanishes above l_{max}
- For example, if l_{max}=0, obtain

$$i\mathcal{K}_{2;00;00}(E_n^*) = \left[iF_{\widetilde{PV};00;00}(E_n,\vec{P},L)\right]^{-1}$$

Future directions & challenges

Many challenges remain!

- Extend $1\to2$ work to include arbitrary spin particles (so can use for N)
  - First step in NREFT taken for $\gamma^*N\to\Delta\to\pi N$ [Agadjanov et al. 14]
- Develop general formalism for $2\to2$ *transitions* (e.g. resonance form factors)
- Fully develop 3 body formalism
  - Allow two particle sub channels to be resonant
  - Extend to non-identical particles, particles with spin
  - Generalize LL factors to $1\to3$ decay amplitudes (e.g. for $K\to\pi\pi\pi$)
  - ....
- Develop models of amplitudes so that new results can be implemented in simulations (e.g. following $K\pi$, $K\eta$ coupled channel analysis of [Dudek, Edwards, Thomas & Wilson 14])

Many challenges remain!

- Onwards to 4 particles?!?

Thank you!
Questions?

Backup Slides

3-particle correlator

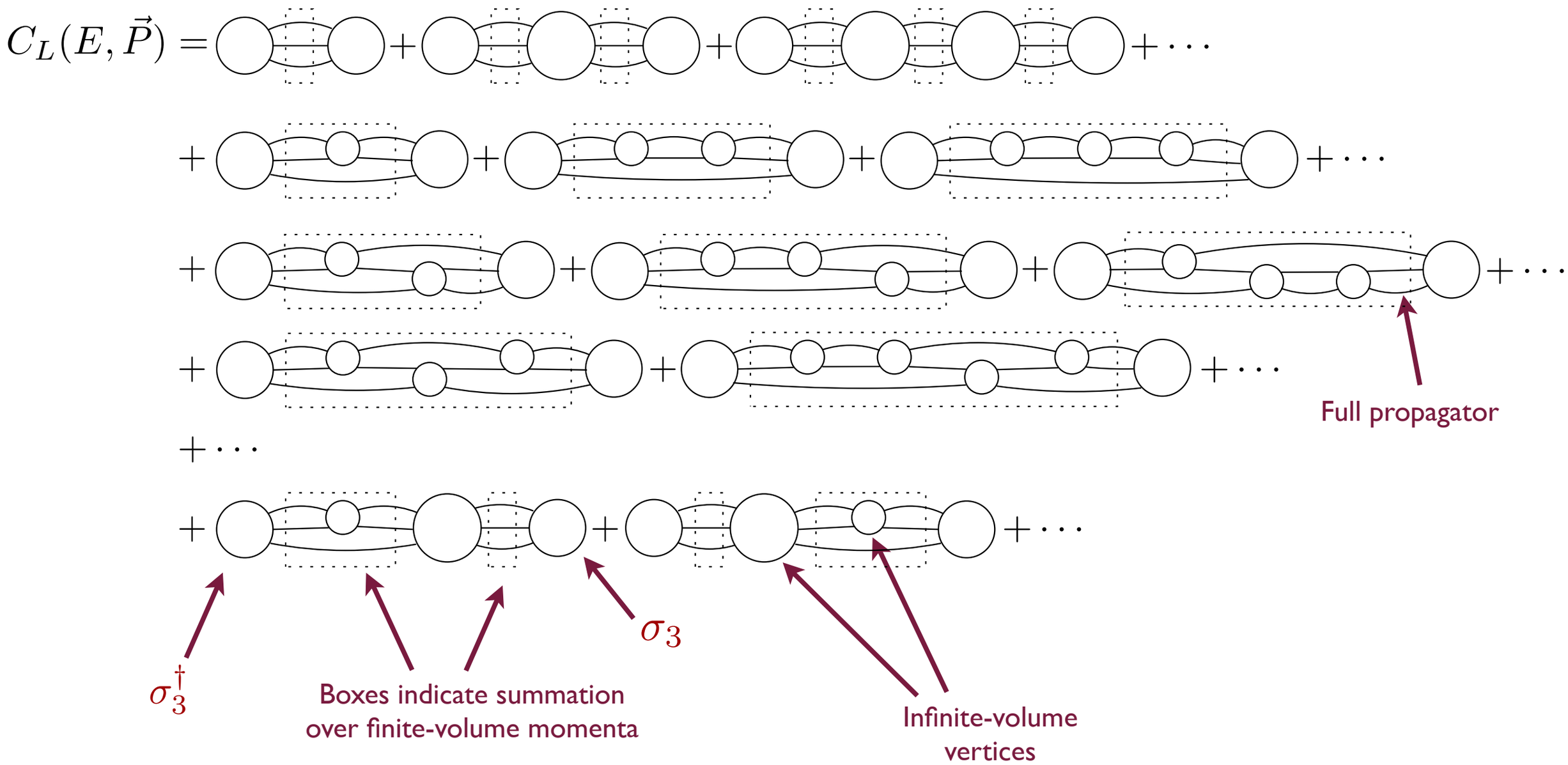

Excited meson radiative transition matrix elements using distillation

Christian Shultz
Old Dominion University

with Jo Dudek and Robert Edwards

arXiv:1501.07457

Framing The Problem

what do we want?

what do we have?

Vector Current Matrix Elements

$$\langle n; p'\lambda' | j^\mu | m; p\lambda \rangle$$

$$j^\mu = \sum_q e_q \bar{\psi}_q \gamma^\mu \psi_q$$

Distillation

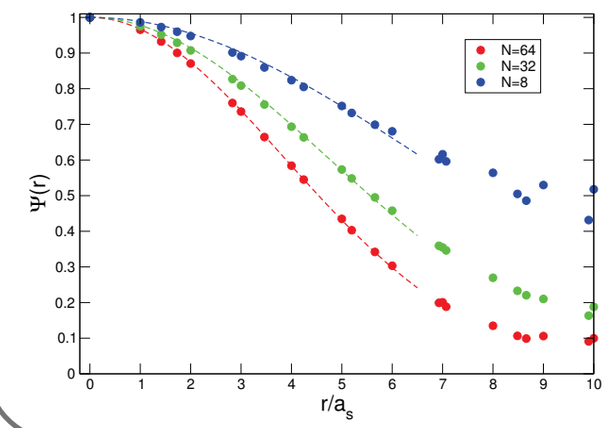

HSC, Phys.Rev. D80 (2009) 054506

Optimized Operators

$$\Omega_n^\dagger \sim v_i \mathcal{O}_i^\dagger$$

Variational Method

$$C(t)V = C(t_0)V\Lambda$$

Large Basis of Interpolators

$$\mathcal{O}^{J\lambda} \sim \bar{\psi}\Gamma_a \overleftrightarrow{D}_b \overleftrightarrow{D}_c \cdots \psi \times \mathrm{CG}(a, b, c \to J\lambda)$$

spectroscopy

Spectroscopy

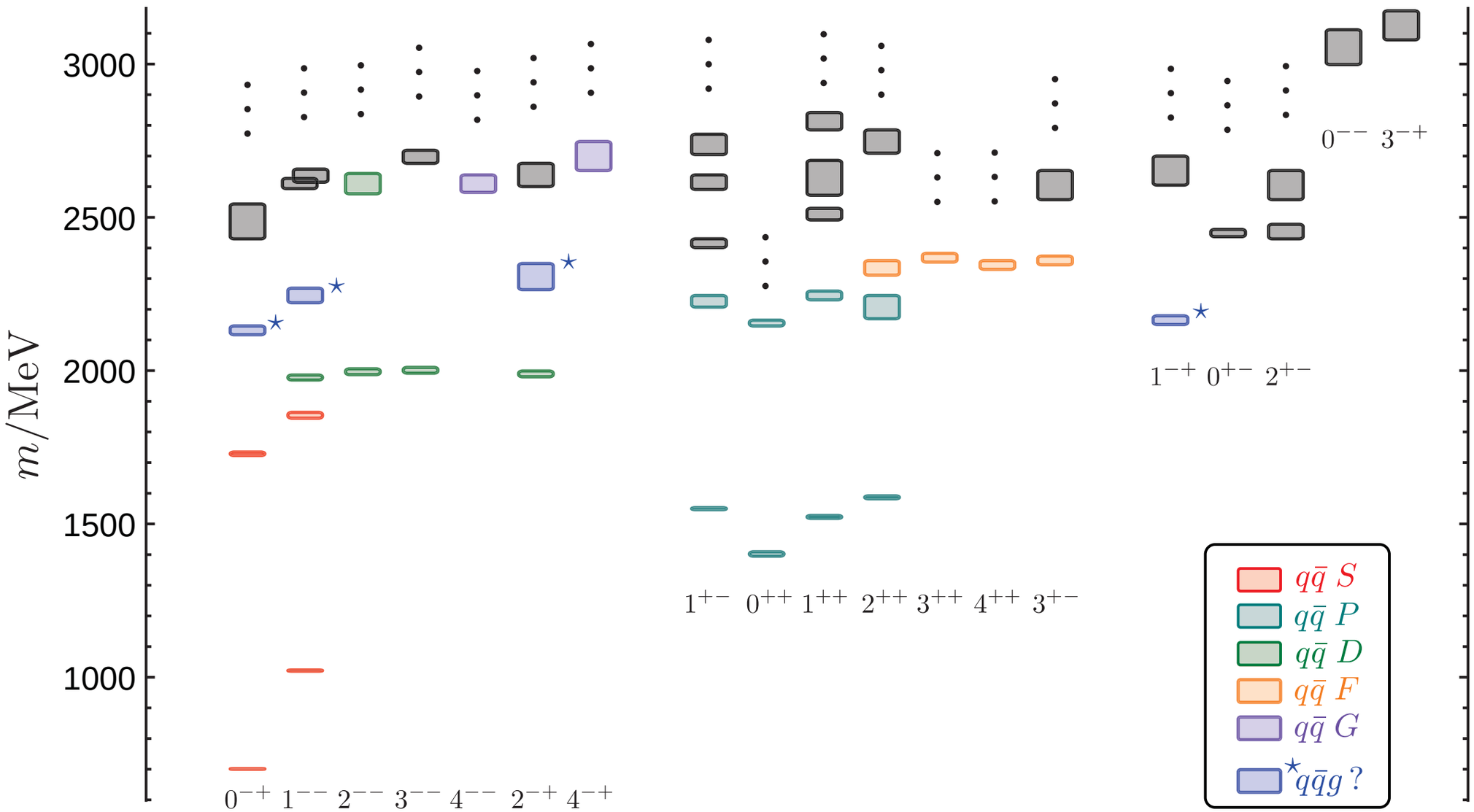

$m_\pi \sim 700\mathrm{MeV}$

JJDudek, Phys.Rev. D84 (2011) 074023

Spectroscopy

Two Point Function

$$C_{\mathcal{O}}(t) = \langle 0|\mathcal{O}(t)\mathcal{O}^\dagger(0)|0\rangle$$
$$= \sum_{\mathfrak{n}} \frac{e^{-E_{\mathfrak{n}} t}}{2E_{\mathfrak{n}}} |\langle 0|\mathcal{O}(0)|\mathfrak{n}\rangle|^2$$

Isolate a single state

What if $|\langle 0|\mathcal{O}(0)|\mathfrak{n}\rangle|^2$ is small (zero) ?

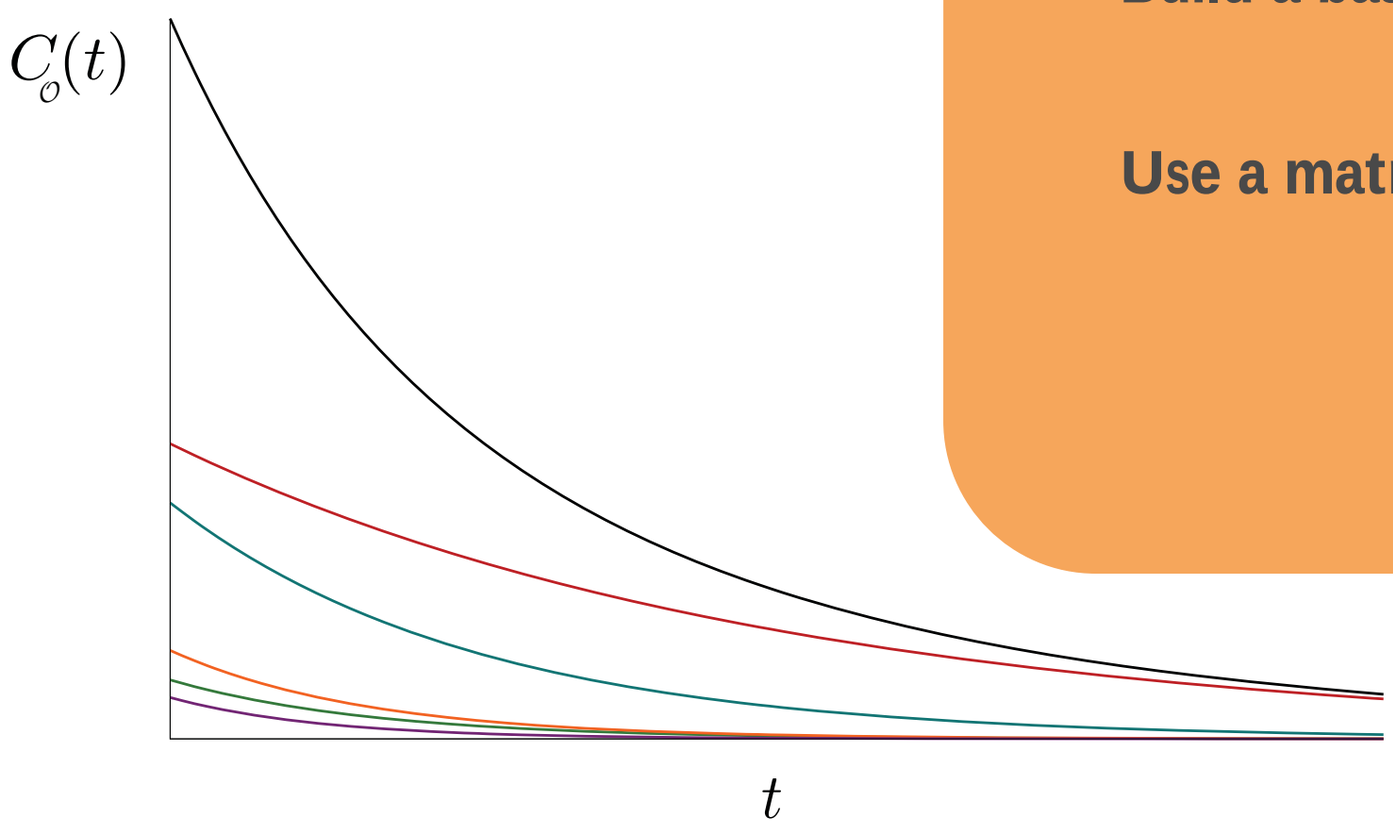

Solution:

Build a basis of operators

$$\mathcal{O}^{J\lambda} \sim \bar{\psi}\Gamma_a \overleftrightarrow{D}_b \overleftrightarrow{D}_c \cdots \psi \times \mathrm{CG}(a,b,c \to J\lambda)$$

Use a matrix of correlators

$$C(t)v^{(\mathfrak{n})} = \lambda_{\mathfrak{n}}(t) C(t_0) v^{(\mathfrak{n})}$$

Diagonalize the matrix

Projected Ops

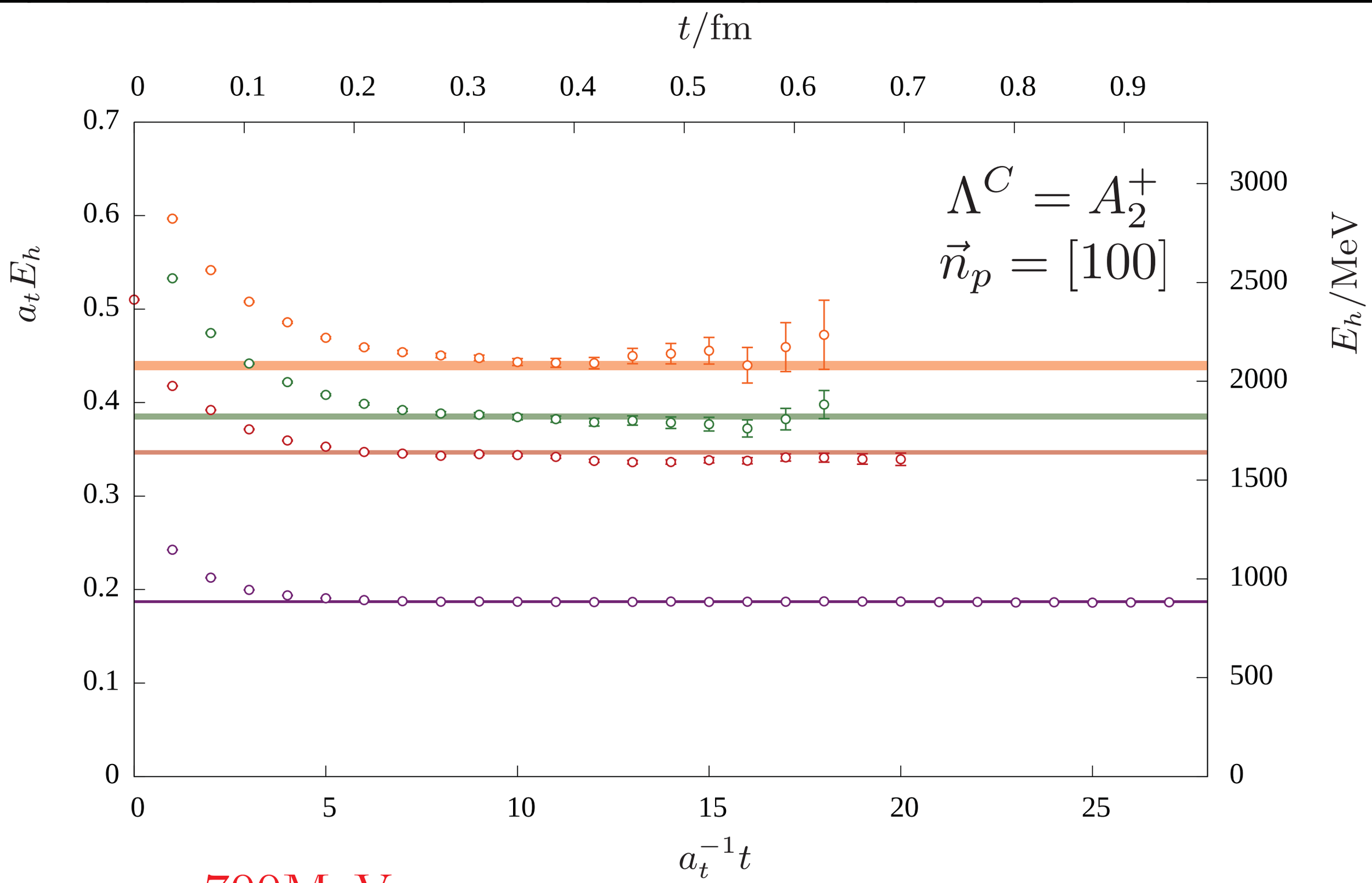

$m_\pi \sim 700\mathrm{MeV}$

Matrix Elements

Matrix elements 'hide' in 3-pt functions

$$j^\mu = \sum_q e_q \bar{\psi}_q \gamma^\mu \psi_q$$

$$C^\mu_{\mathbf{nm}} = \langle 0 | \Omega_{\mathbf{n}}(t) j^\mu(t_\gamma) \Omega^\dagger_{\mathbf{m}}(0) | 0 \rangle$$

$$= \sum_{\mathbf{n}'\mathbf{m}'} \langle \mathbf{n}' | j^\mu | \mathbf{m}' \rangle e^{-E_{\mathbf{n}'}(t-t_\gamma)} e^{-E_{\mathbf{m}'} t_\gamma}$$

sum over everything

need to isolate

$$\times \frac{\langle 0 | \Omega_{\mathbf{n}}(0) | \mathbf{n}' \rangle}{2E_{\mathbf{n}'}} \frac{\langle \mathbf{m}' | \Omega^\dagger_{\mathbf{m}}(0) | 0 \rangle}{2E_{\mathbf{m}'}}$$

Matrix Elements

Matrix elements 'hide' in 3-pt functions

$$j^\mu = \sum_q e_q \bar{\psi}_q \gamma^\mu \psi_q$$

$$C^\mu_{\mathbf{nm}} = \langle 0 | \Omega_{\mathbf{n}}(t) j^\mu(t_\gamma) \Omega^\dagger_{\mathbf{m}}(0) | 0 \rangle$$

$$= \sum_{\mathbf{n}'\mathbf{m}'} \langle \mathbf{n}' | j^\mu | \mathbf{m}' \rangle e^{-E_{\mathbf{n}'}(t-t_\gamma)} e^{-E_{\mathbf{m}'} t_\gamma}$$

$$\times \frac{\langle 0 | \Omega_{\mathbf{n}}(0) | \mathbf{n}' \rangle}{2E_{\mathbf{n}'}} \frac{\langle \mathbf{m}' | \Omega^\dagger_{\mathbf{m}}(0) | 0 \rangle}{2E_{\mathbf{m}'}}$$

sum over everything

need to isolate

"diagonalize" the sum?

3-pt Functions

$$C^{\mu}_{n,m}(\delta t, t_\gamma) = \langle 0|\Omega_n(\delta t) j^{\mu}(t_\gamma)\Omega^{\dagger}_m(0)|0\rangle$$

Optimized Operators

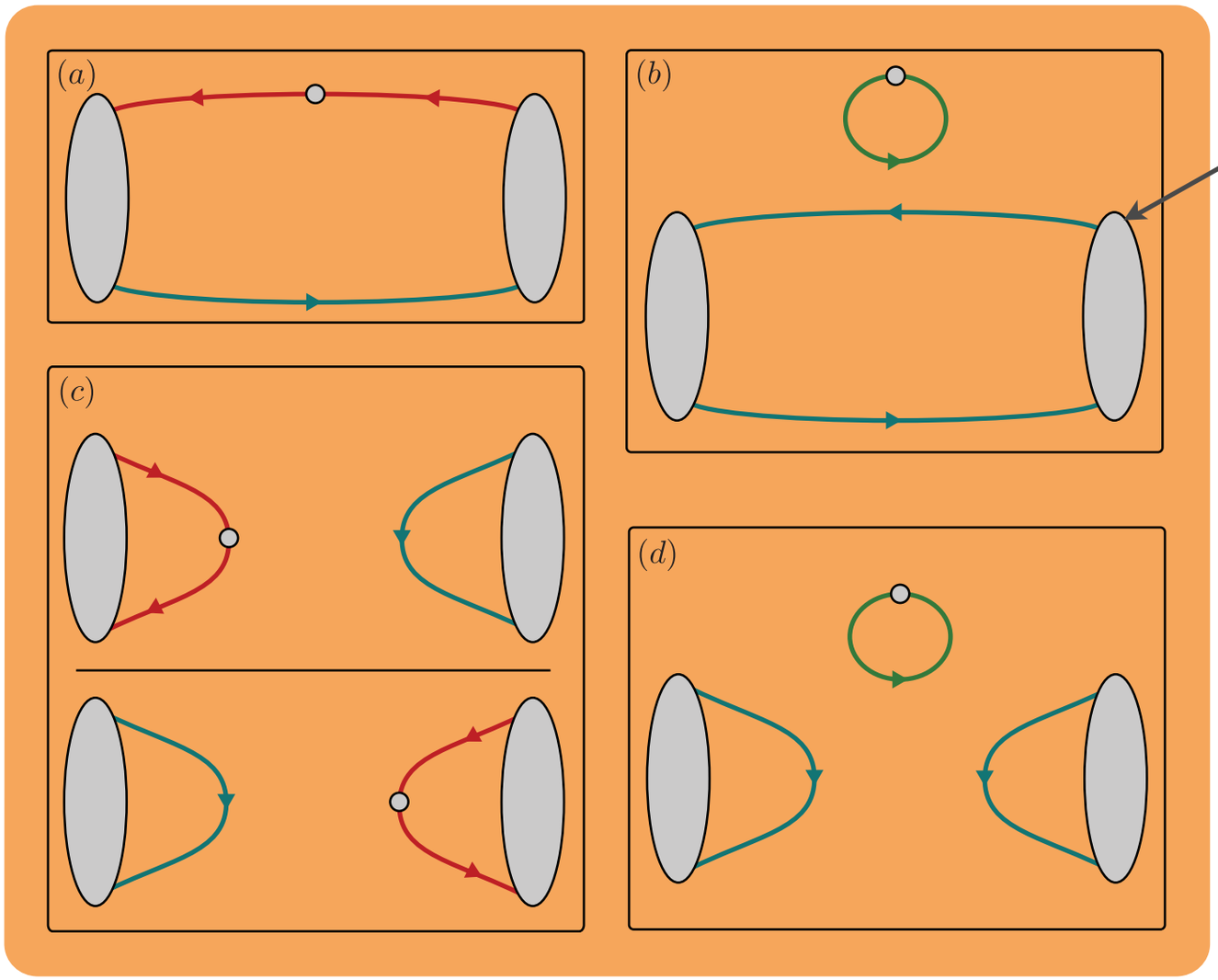

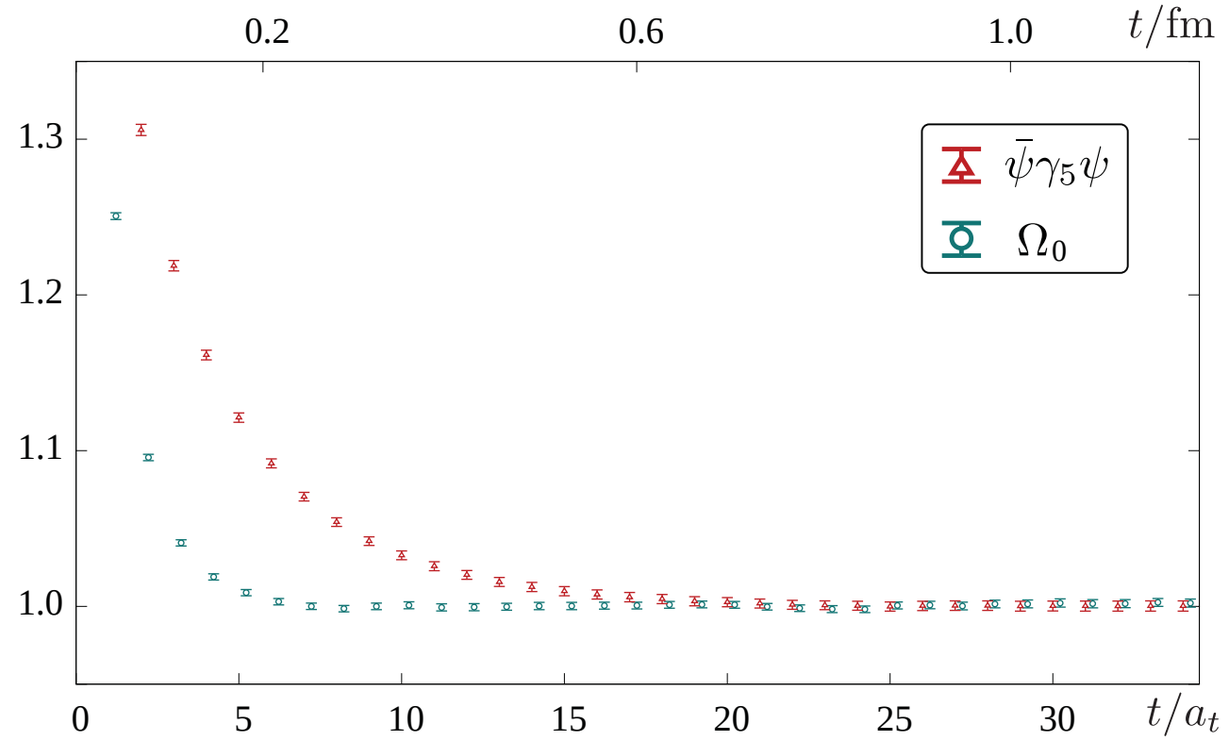

The Linear System

Optimized Operators
'relax' quickly

pollution term

$$C^{\mu}_{n,m}(\delta t, t_\gamma) \sim \frac{e^{-E_n(\delta t - t_\gamma)}}{2E_n}\frac{e^{-E_m t_\gamma}}{2E_m}\langle n|j^\mu|m\rangle + f(\delta t, t_\gamma)$$

Matrix Element Decompositions

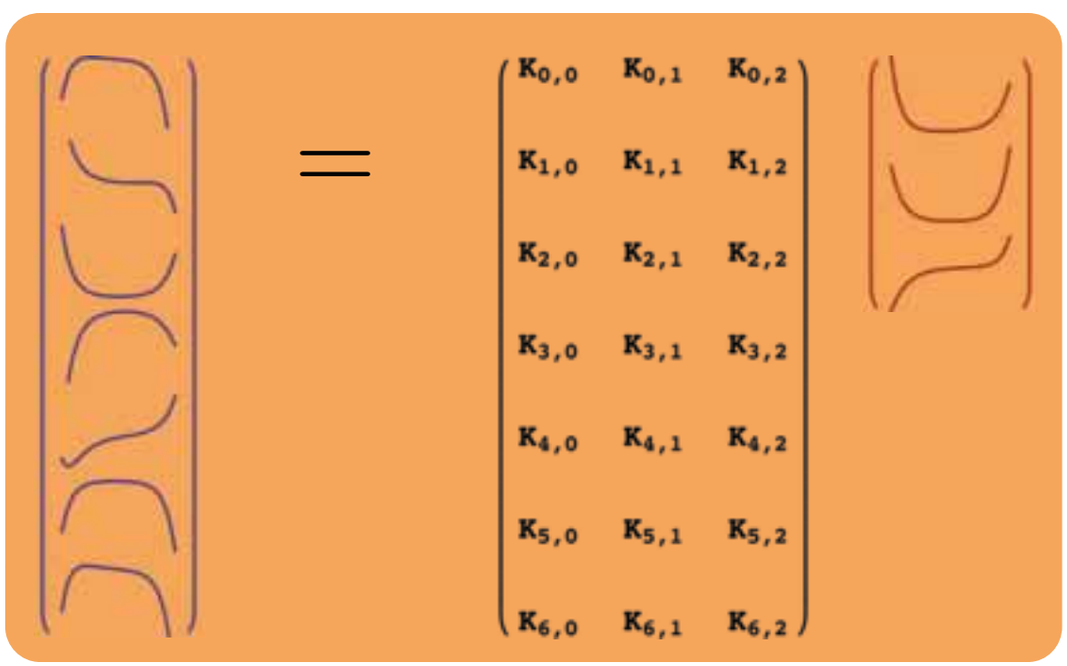

Kinematic Factor

Form Factor

$$\langle n|j^\mu|m\rangle = \sum_k K^\mu_k(n,m) F_k(Q^2)$$

Some Examples

$$\langle \pi, p'|j^\mu|\pi, p\rangle = (p' + p)^\mu F_\pi(Q^2)$$

$$\langle \pi, p'|j^\mu|\rho, p\lambda\rangle = \frac{2}{m_\rho + m_\pi}\epsilon^{\mu\nu\sigma\eta} p'_\nu p_\sigma \varepsilon_\eta(p,\lambda) F_{\rho\pi}(Q^2)$$

Signal Isolation

$$C^{\mu}_{\mathfrak{n}\mathfrak{m}} = \langle 0|\Omega_{\mathfrak{n}}(t) j^{\mu}(t_\gamma)\Omega^{\dagger}_{\mathfrak{m}}(0)|0\rangle$$
$$= \sum_{\mathfrak{n}'\mathfrak{m}'} \langle \mathfrak{n}'|j^{\mu}|\mathfrak{m}'\rangle e^{-E_{\mathfrak{n}'}(t-t_\gamma)} e^{-E_{\mathfrak{m}'}t_\gamma}$$

$$\times \frac{\langle 0|\Omega_{\mathfrak{n}}(0)|\mathfrak{n}'\rangle}{2E_{\mathfrak{n}'}} \frac{\langle \mathfrak{m}'|\Omega^{\dagger}_{\mathfrak{m}}(0)|0\rangle}{2E_{\mathfrak{m}'}}$$

How well does it work?

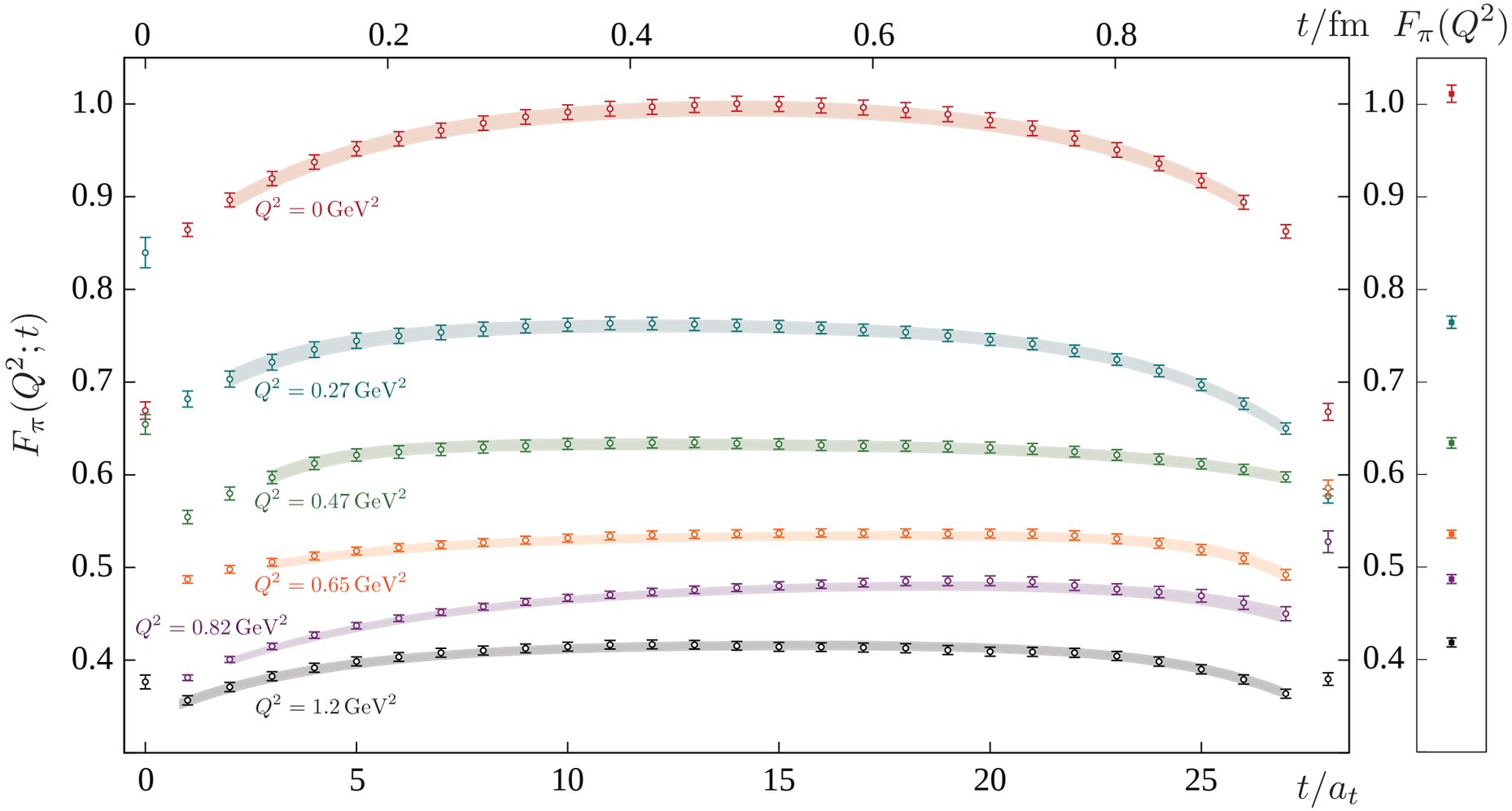

$$\Omega^{\dagger}_{\pi} \sim \sum_i v_i^{(\pi)} \mathcal{O}^{\dagger}_i$$

Time Dependence

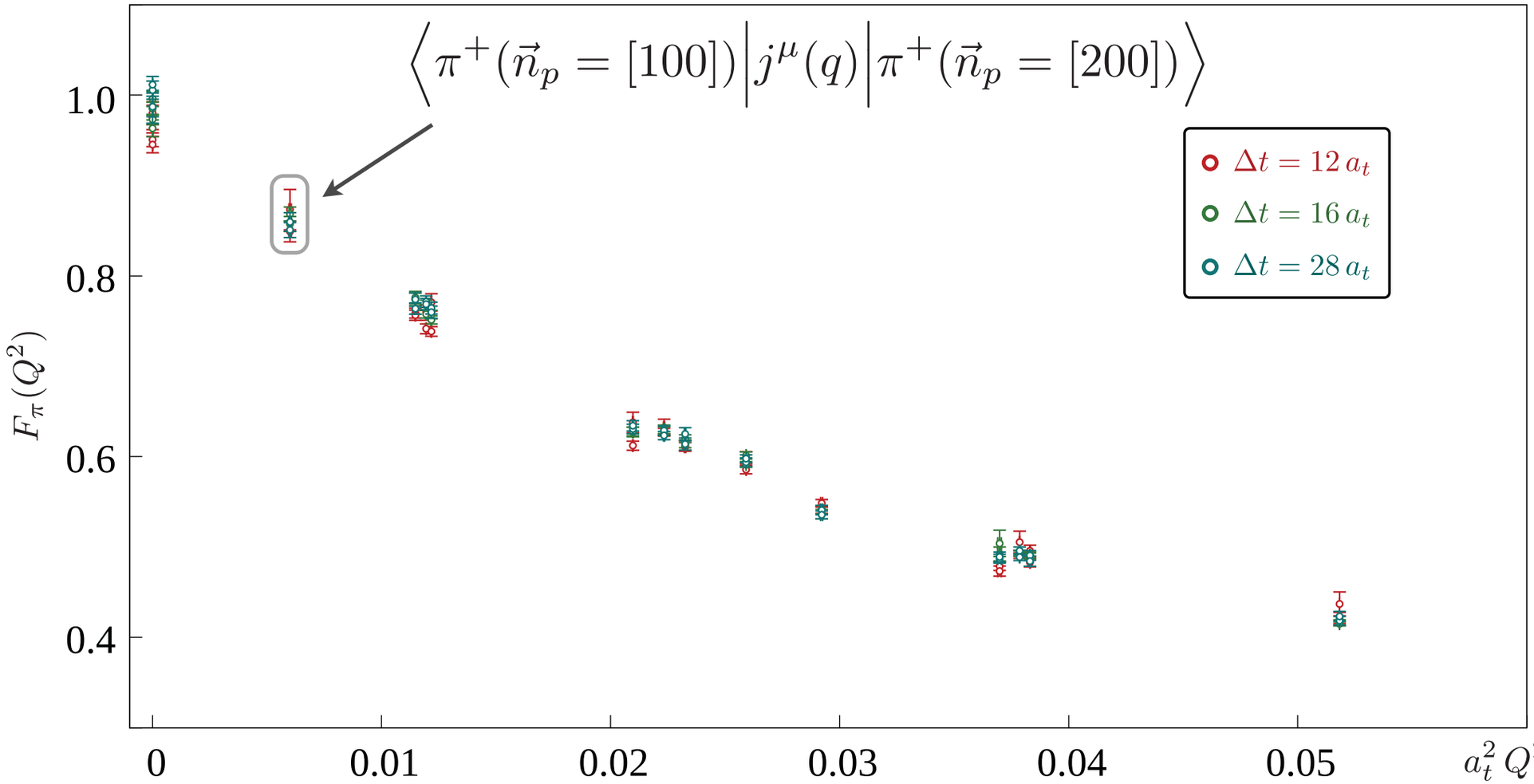

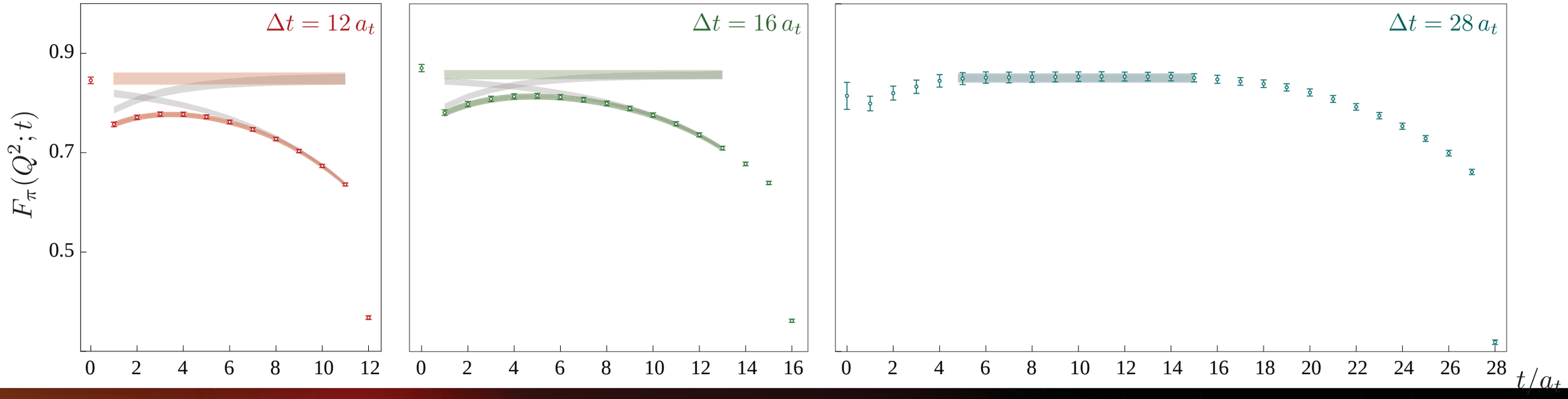

A Lattice Artifact

$\pi \to \pi\gamma$

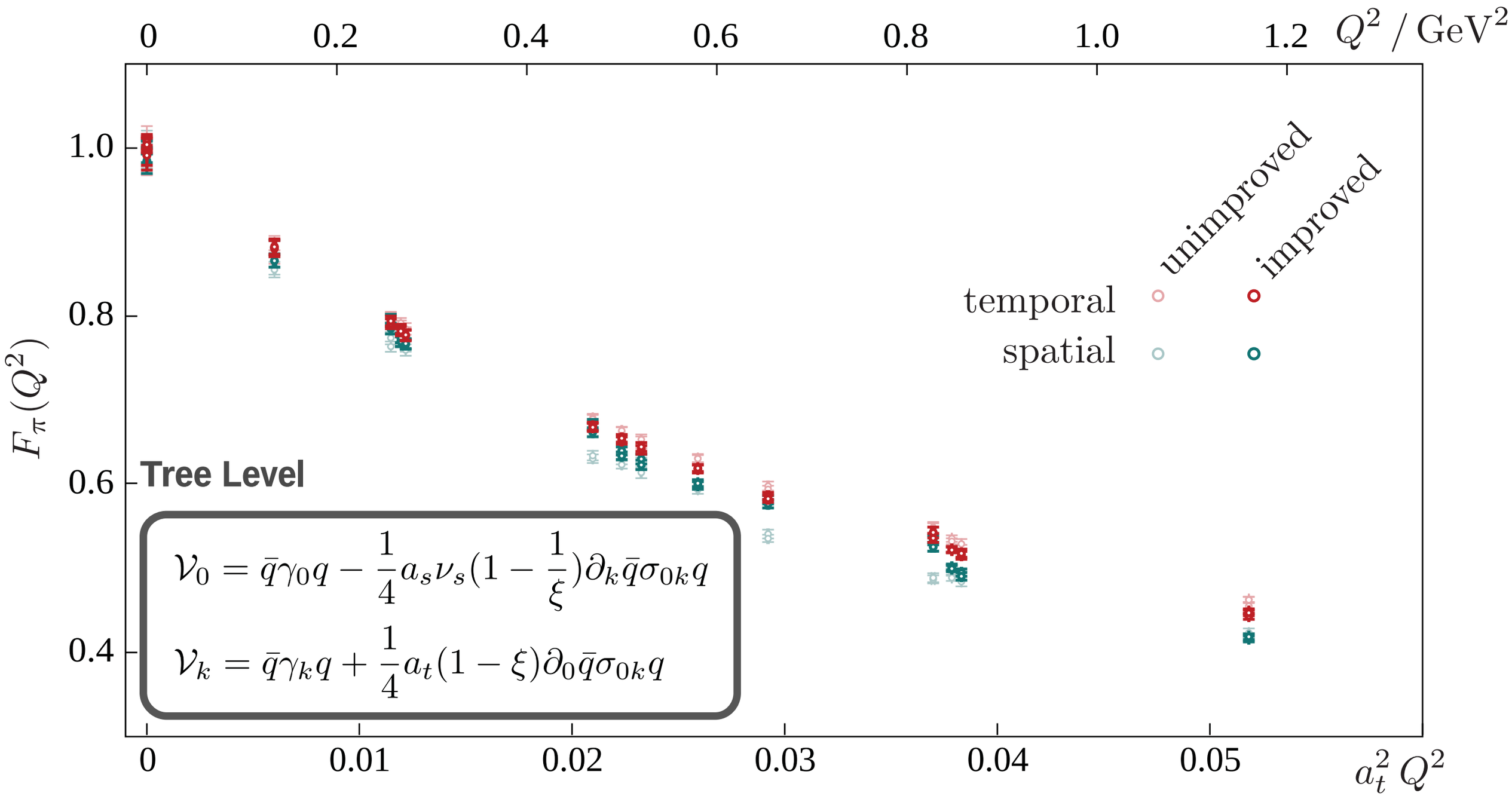

The Calculation

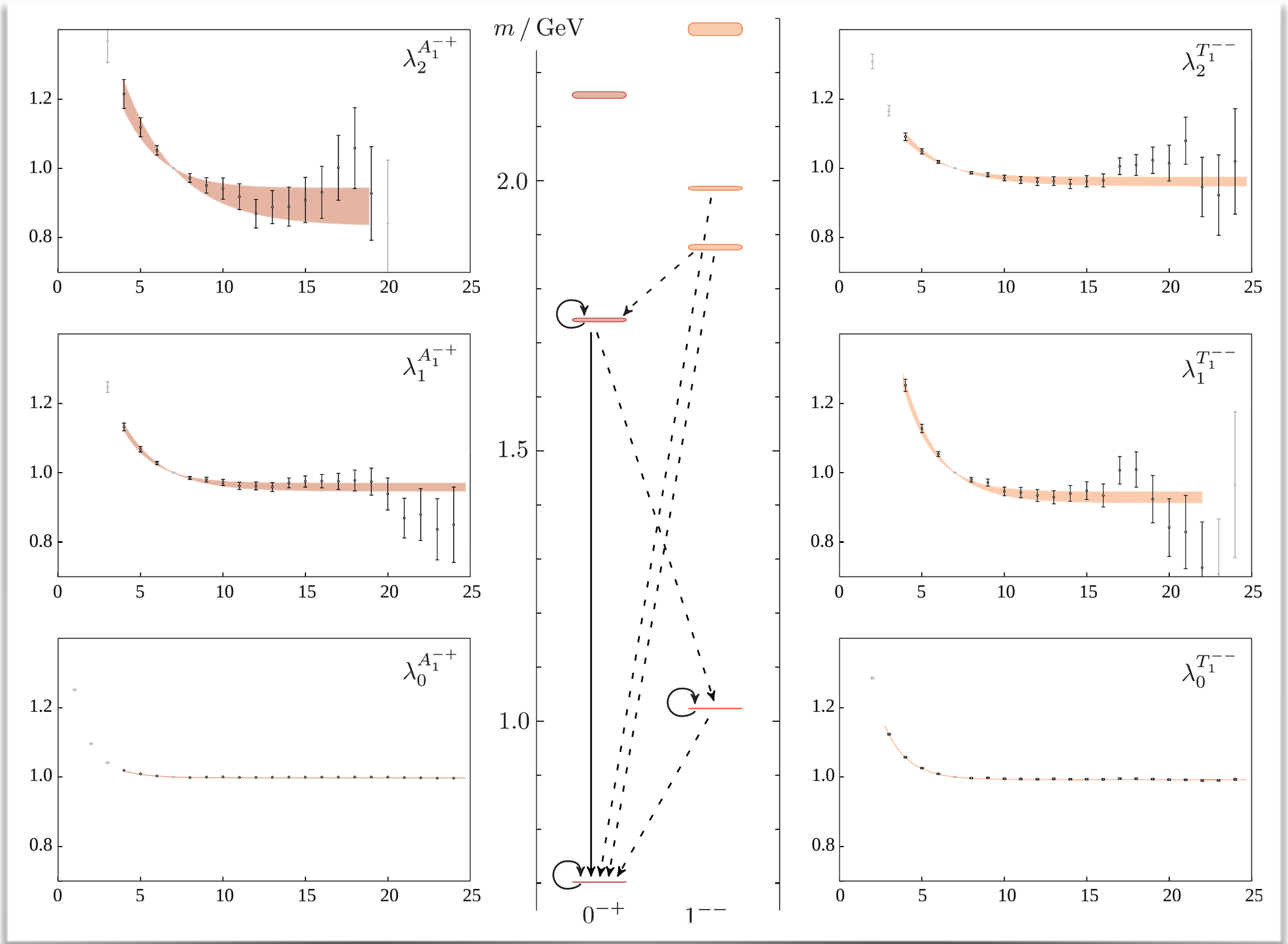

Pion Form-factor

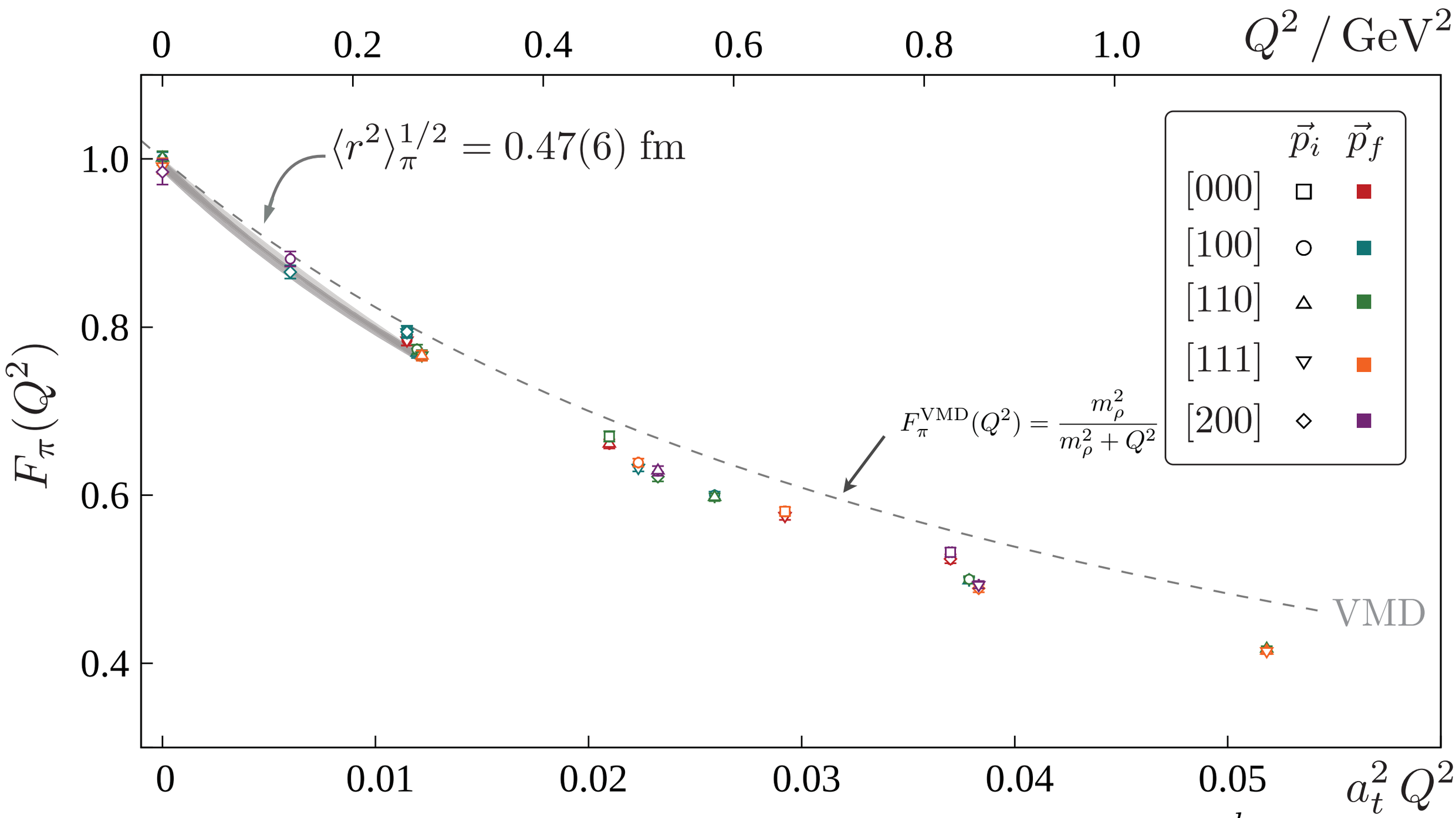

$$\langle r^2 \rangle = -6 \frac{d}{dQ^2} F(Q^2)|_{Q^2=0}$$

Rho Form-factors

$\rho \to \rho\gamma$

linear combinations of multipoles

$$\langle \rho, p'\lambda' | j^\mu | \rho, p\lambda \rangle = -(p'+p)^\mu \epsilon^*_\alpha(p'\lambda')\epsilon^\alpha(p\lambda) G_1(Q^2)$$
$$+ \left[\epsilon^\mu(p\lambda)\epsilon^*_\alpha(p'\lambda')p^\alpha + \epsilon^{\mu *}(p'\lambda')\epsilon^\alpha(p\lambda)p'_\alpha\right] G_2(Q^2)$$
$$- (p'+p)^\mu \epsilon^*_\alpha(p'\lambda')p^\alpha \epsilon^\beta(p\lambda)p'_\beta \frac{G_3(Q^2)}{2m_\rho^2}$$

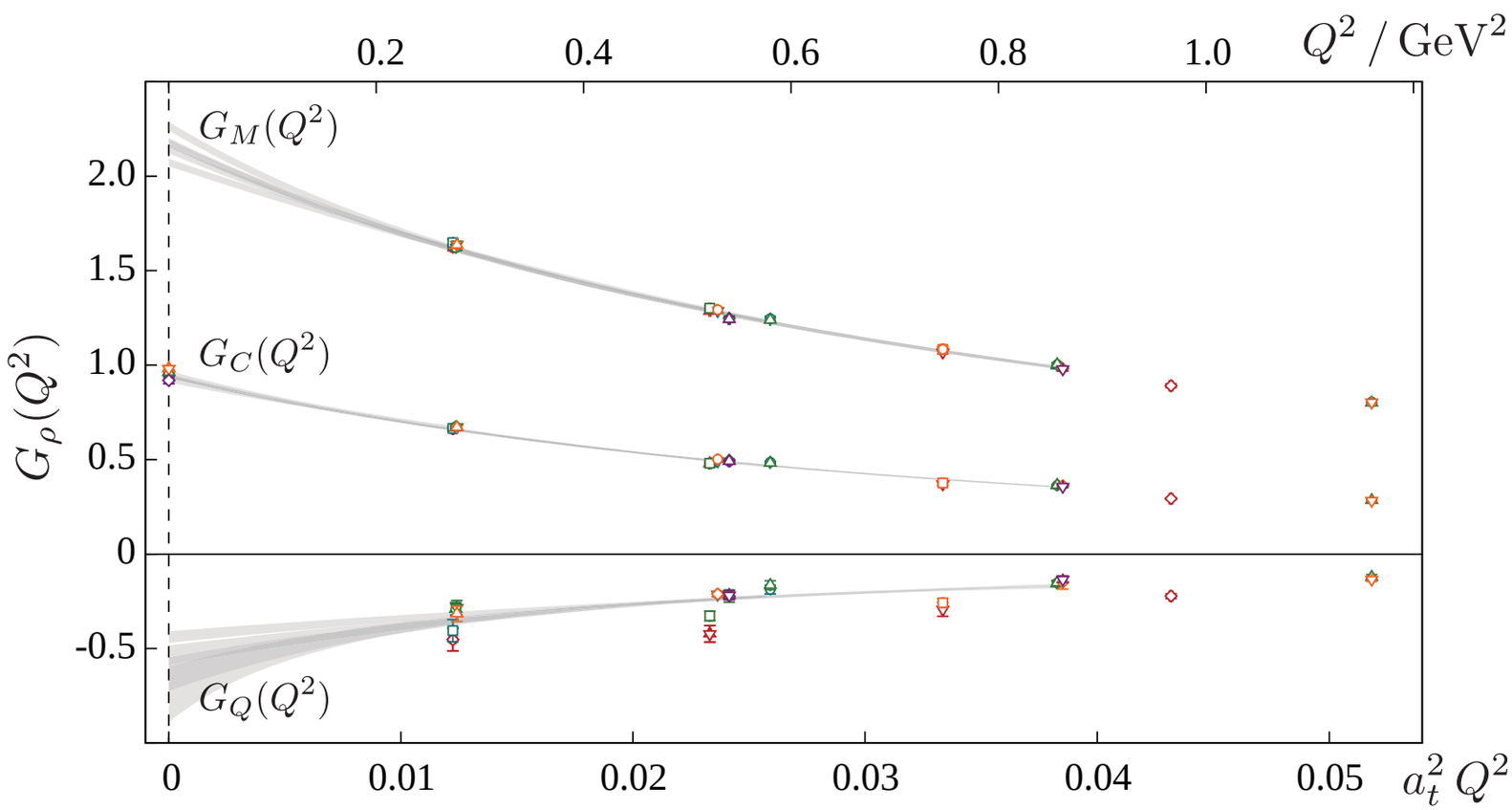

Rho Form-factors

$\rho \to \rho\gamma$

linear combinations of multipoles

$$\langle \rho, p'\lambda' | j^\mu | \rho, p\lambda \rangle = -(p'+p)^\mu \epsilon^*_\alpha(p'\lambda')\epsilon^\alpha(p\lambda) G_1(Q^2)$$
$$+ [\epsilon^\mu(p\lambda)\epsilon^*_\alpha(p'\lambda')p^\alpha + \epsilon^{\mu *}(p'\lambda')\epsilon^\alpha(p\lambda)p'_\alpha] G_2(Q^2)$$
$$- (p'+p)^\mu \epsilon^*_\alpha(p'\lambda')p^\alpha \epsilon^\beta(p\lambda)p'_\beta \frac{G_3(Q^2)}{2m_\rho^2}$$

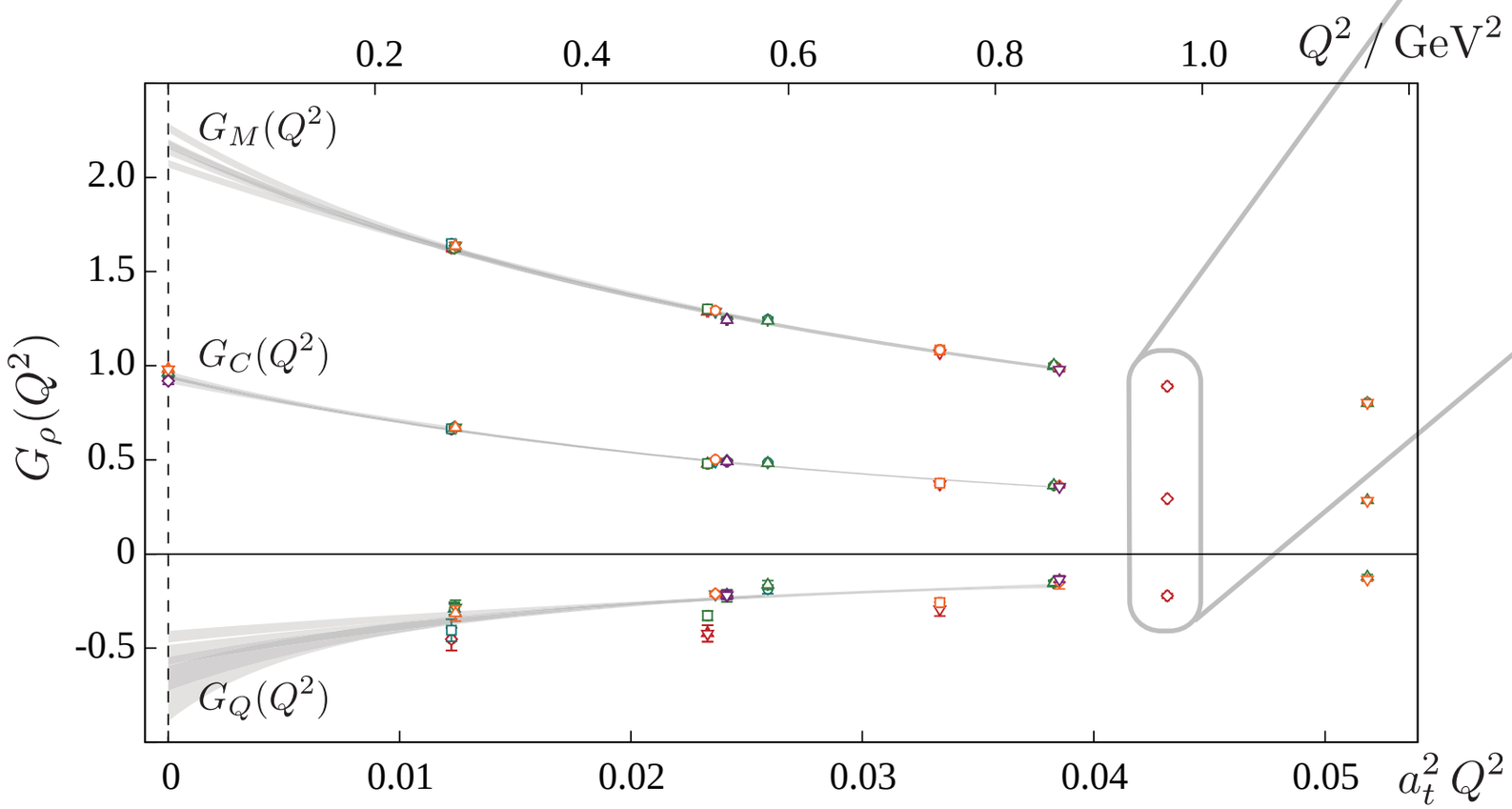

solved simultaneously

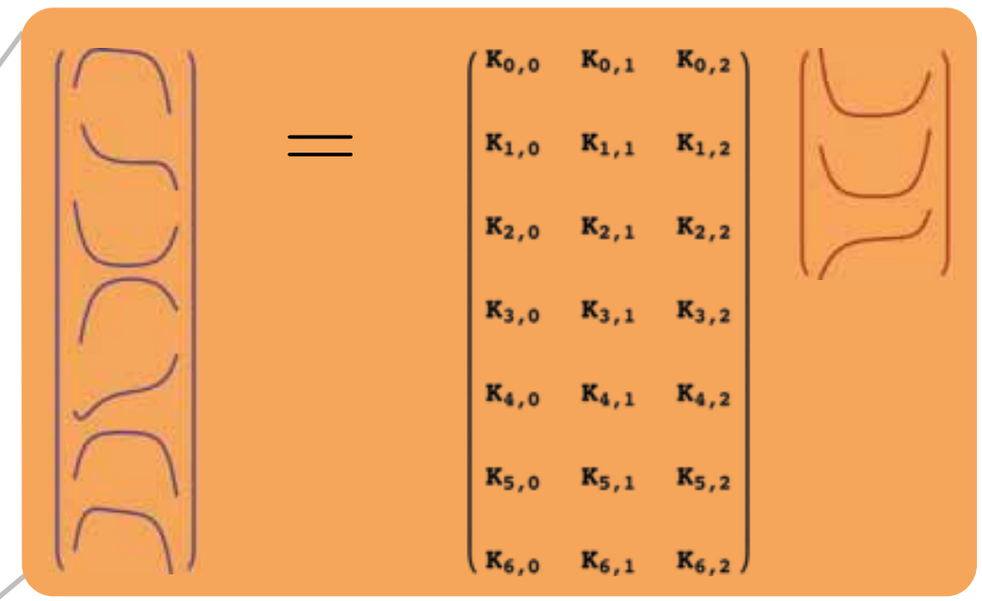

$$\langle n | j^\mu | m \rangle = \sum_k K^\mu_k(n,m) F_k(Q^2)$$

Kinematic Factor

Form Factor

Transitions

$\rho \to \pi\gamma$

$$\langle \rho; p'\lambda | j^\mu | \pi; p \rangle = \frac{2F(Q^2)}{m_\rho + m_\pi} \epsilon^{\mu\nu\eta\sigma} p'_\nu p_\eta \varepsilon^*_\sigma(p', \lambda)$$

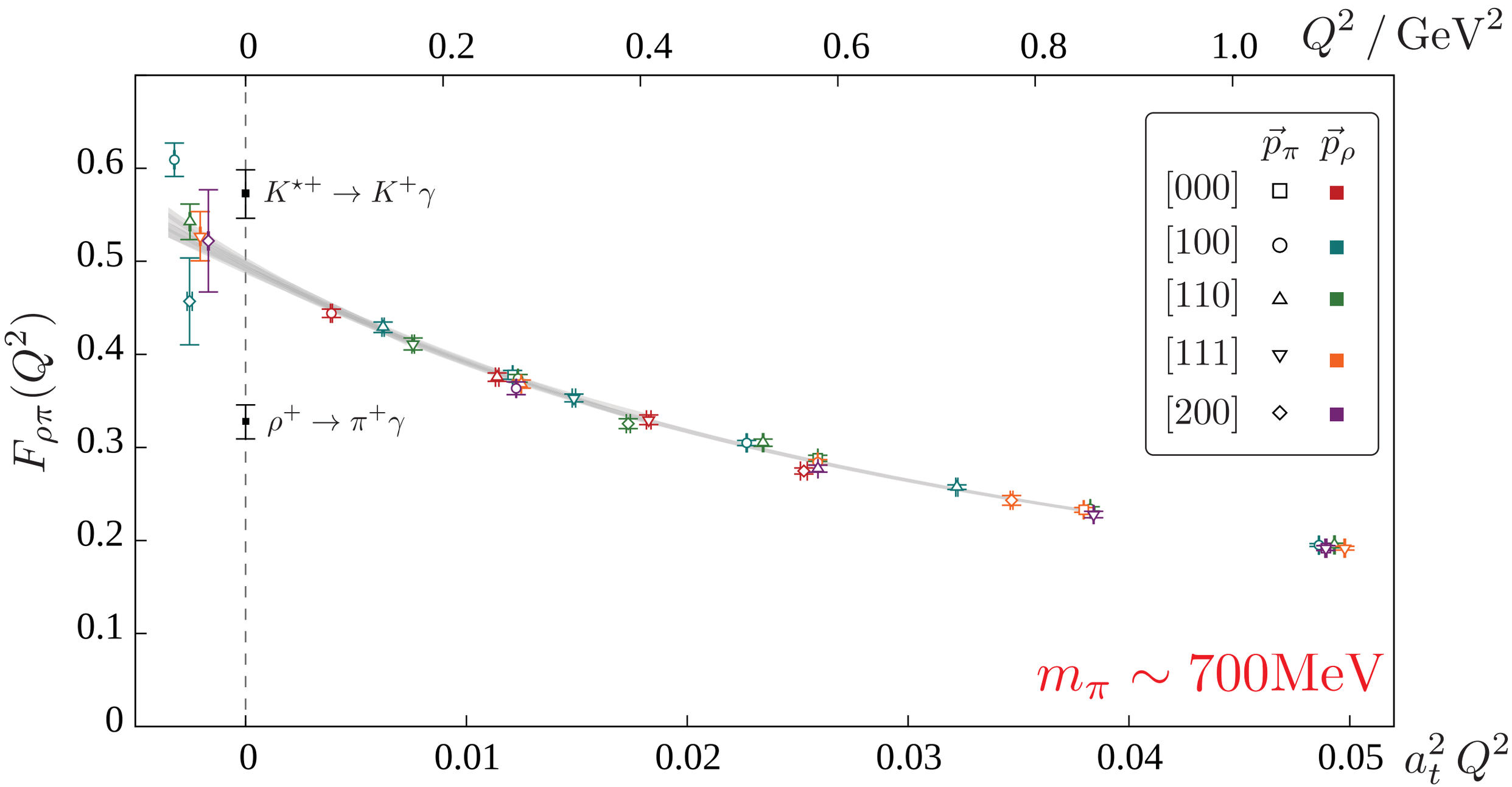

The 'Illegal Stuff'

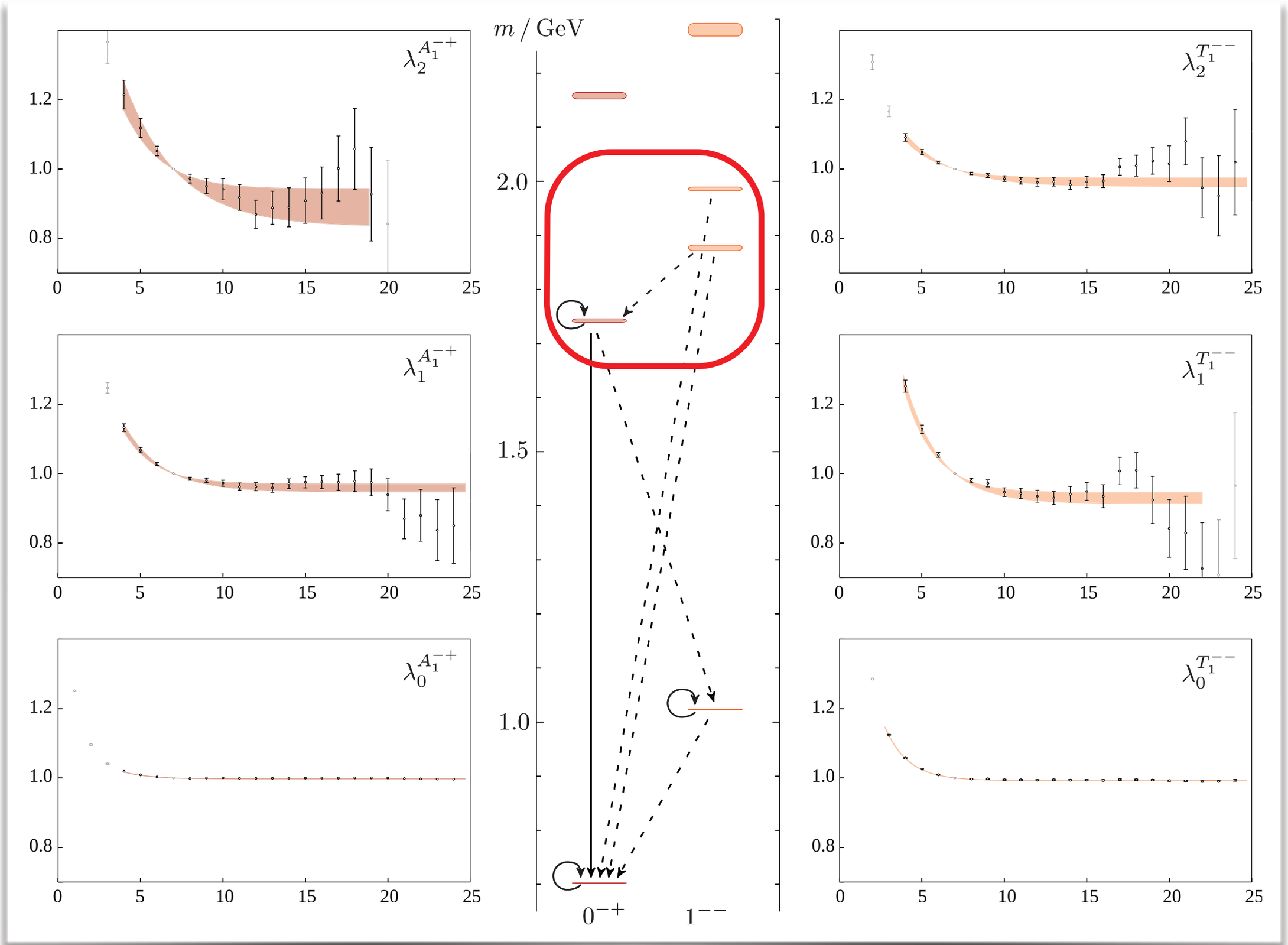

Something New

$\pi' \to \pi'\gamma$

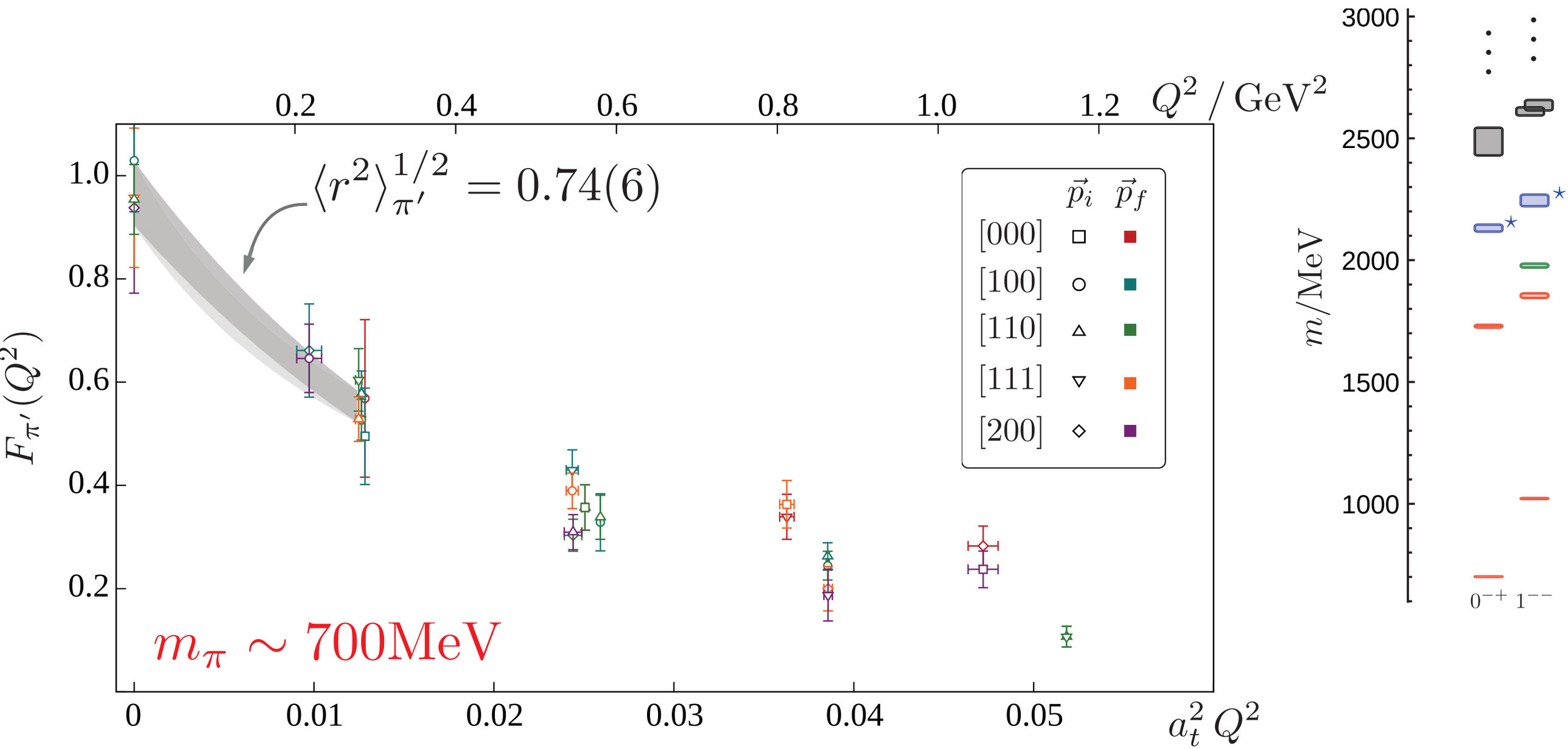

A Look 'Under the Hood'

$$C^{\mu}_{\mathfrak{n}\mathfrak{m}} = \langle 0|\Omega_{\mathfrak{n}}(t) j^{\mu}(t_\gamma)\Omega^{\dagger}_{\mathfrak{m}}(0)|0\rangle$$

$$= \sum_{\mathfrak{n}'\mathfrak{m}'} \langle \mathfrak{n}'|j^{\mu}|\mathfrak{m}'\rangle e^{-E_{\mathfrak{n}'}(t-t_\gamma)} e^{-E_{\mathfrak{m}'}t_\gamma}$$

$$\times \frac{\langle 0|\Omega_{\mathfrak{n}}(0)|\mathfrak{n}'\rangle}{2E_{\mathfrak{n}'}} \frac{\langle \mathfrak{m}'|\Omega^{\dagger}_{\mathfrak{m}}(0)|0\rangle}{2E_{\mathfrak{m}'}}$$

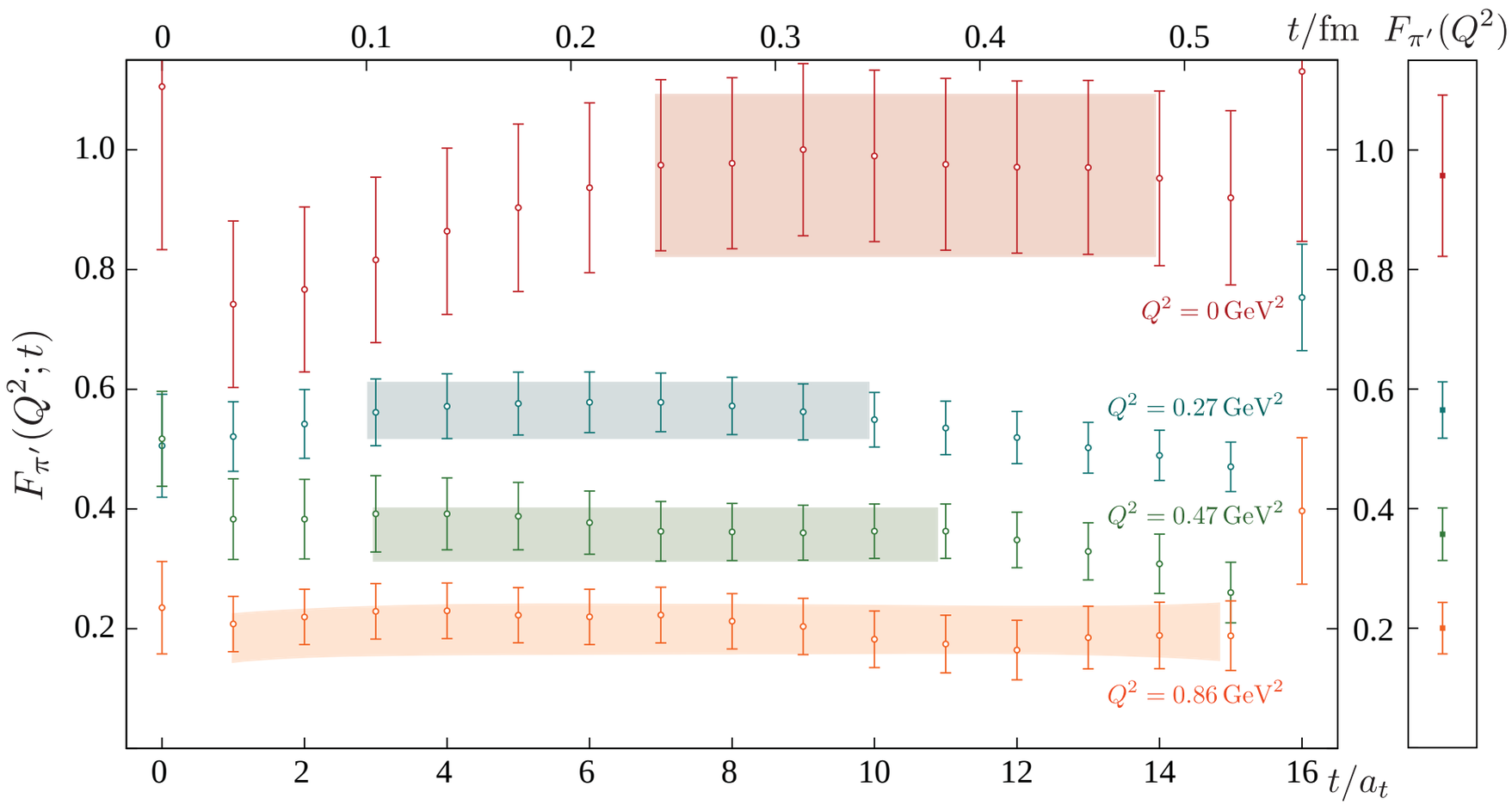

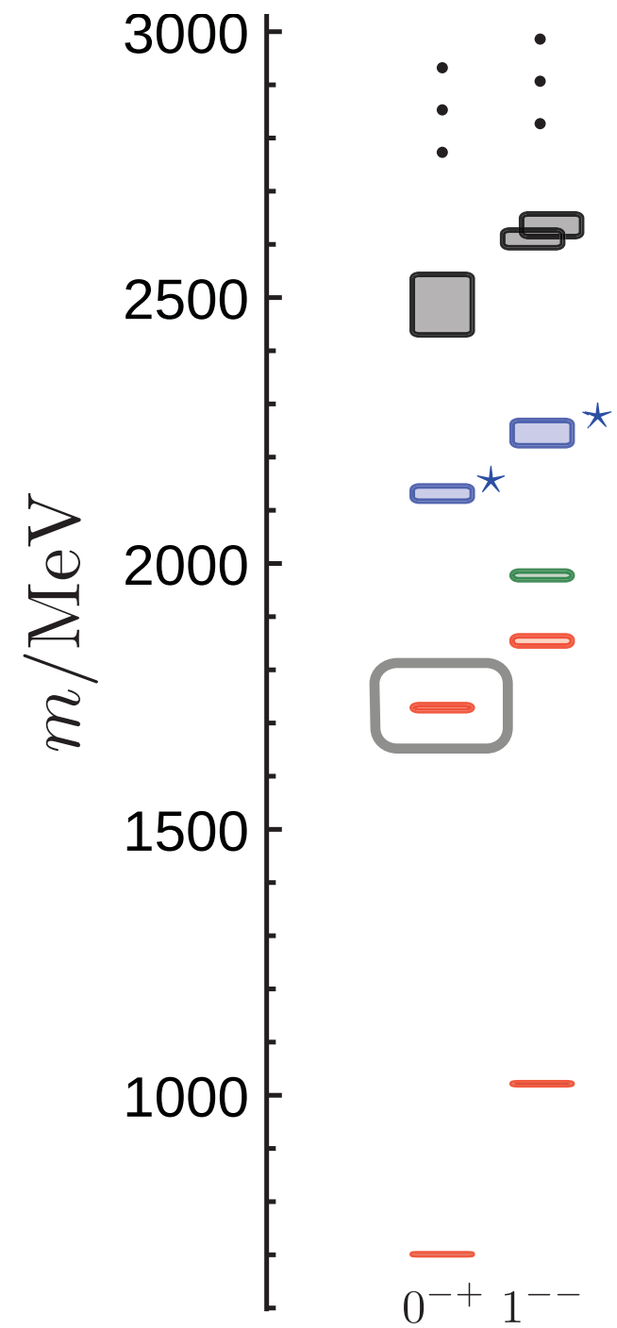

A Look 'Under the Hood'

$$C^{\mu}_{\mathfrak{n}\mathfrak{m}} = \langle 0|\Omega_{\mathfrak{n}}(t) j^{\mu}(t_\gamma)\Omega^{\dagger}_{\mathfrak{m}}(0)|0\rangle$$
$$= \sum_{\mathfrak{n}'\mathfrak{m}'} \langle \mathfrak{n}'|j^{\mu}|\mathfrak{m}'\rangle e^{-E_{\mathfrak{n}'}(t-t_\gamma)} e^{-E_{\mathfrak{m}'}t_\gamma}$$
$$\times \frac{\langle 0|\Omega_{\mathfrak{n}}(0)|\mathfrak{n}'\rangle}{2E_{\mathfrak{n}'}} \frac{\langle \mathfrak{m}'|\Omega^{\dagger}_{\mathfrak{m}}(0)|0\rangle}{2E_{\mathfrak{m}'}}$$

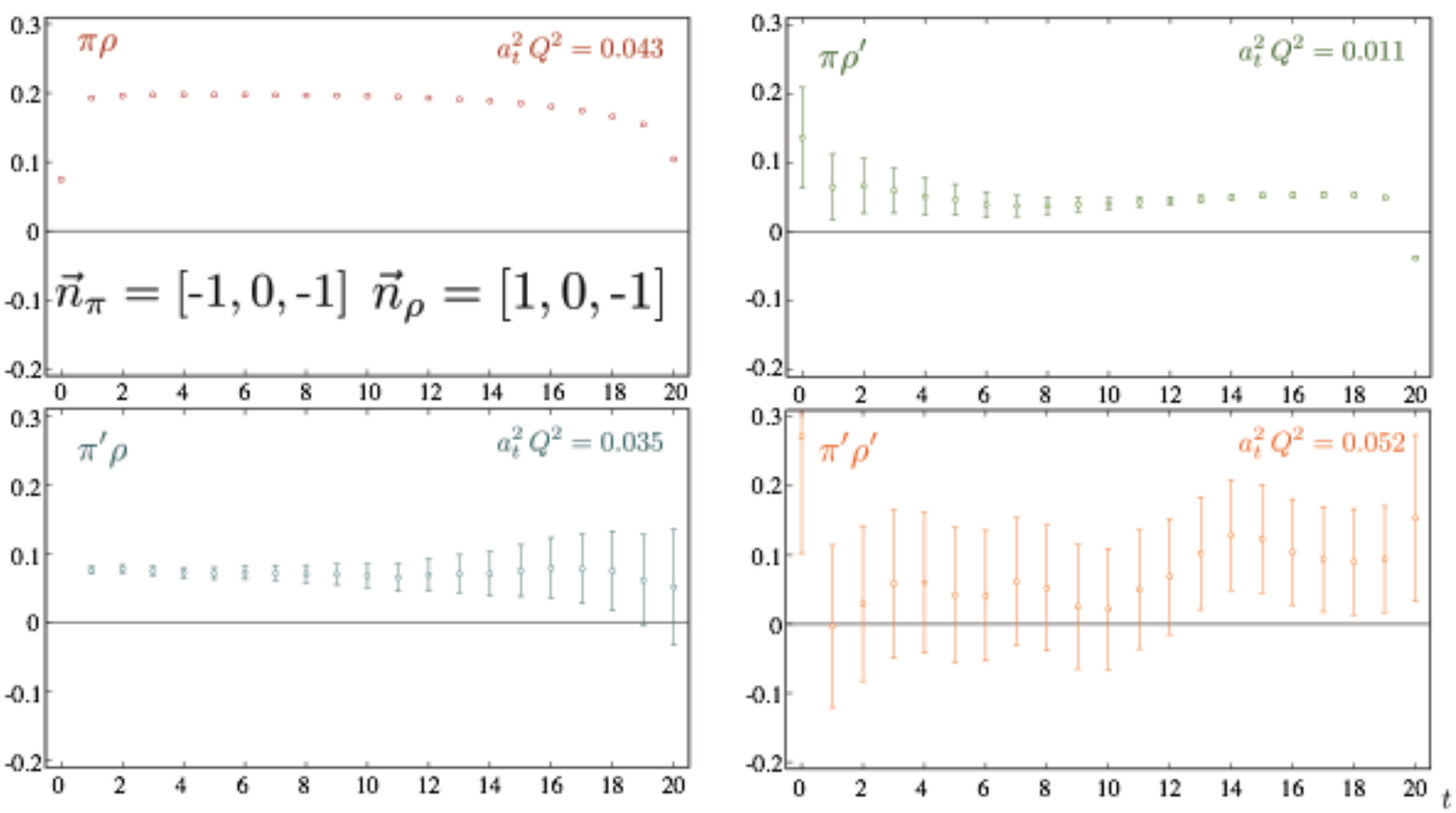

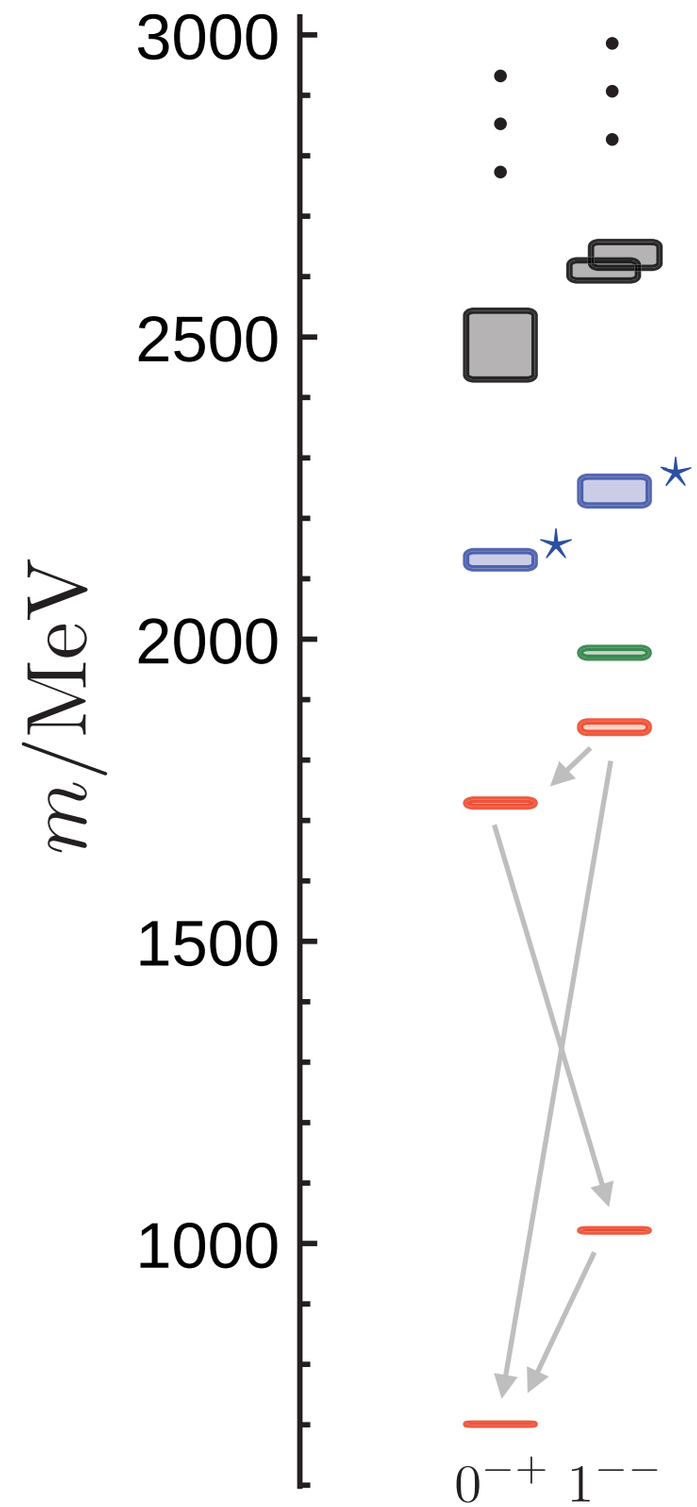

‘Hindered’ Transitions

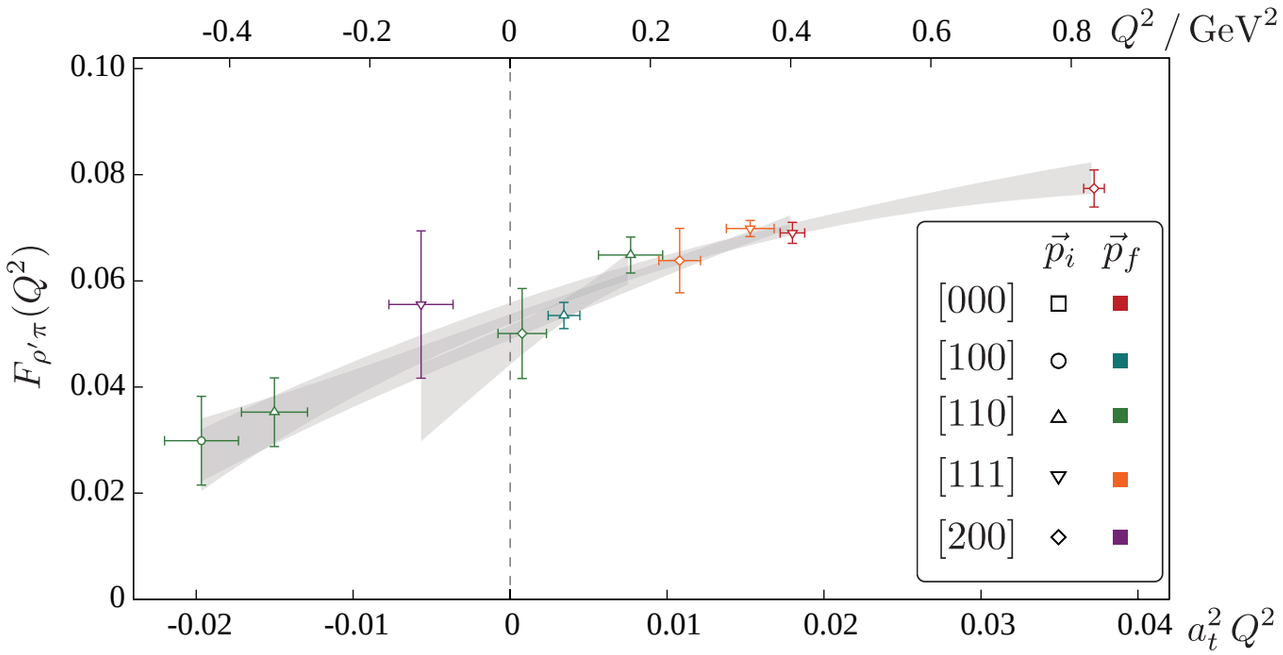

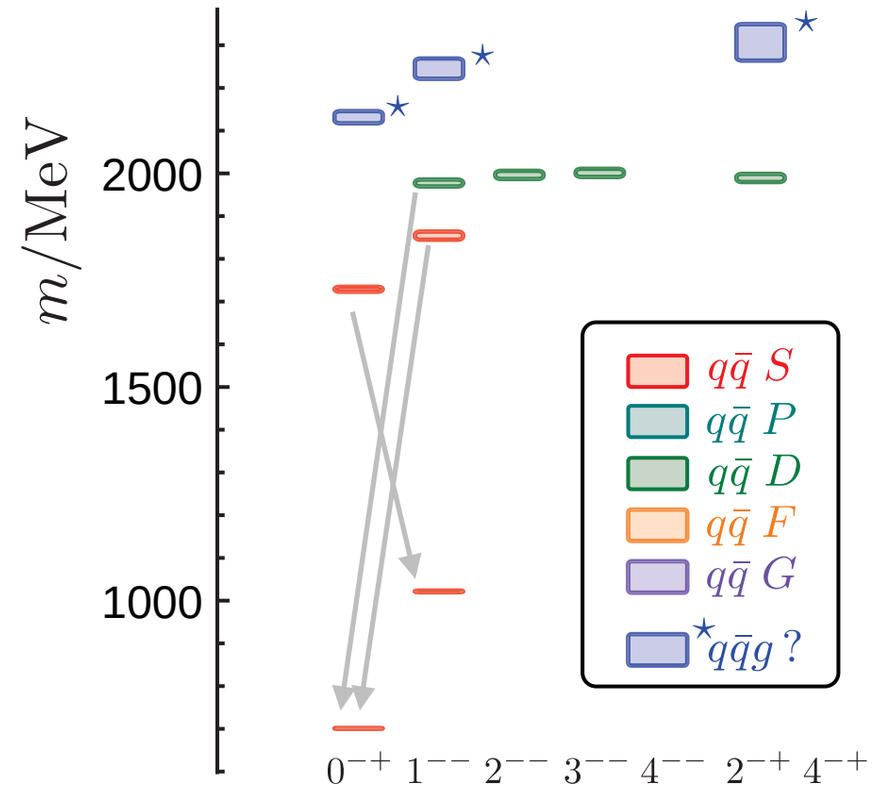

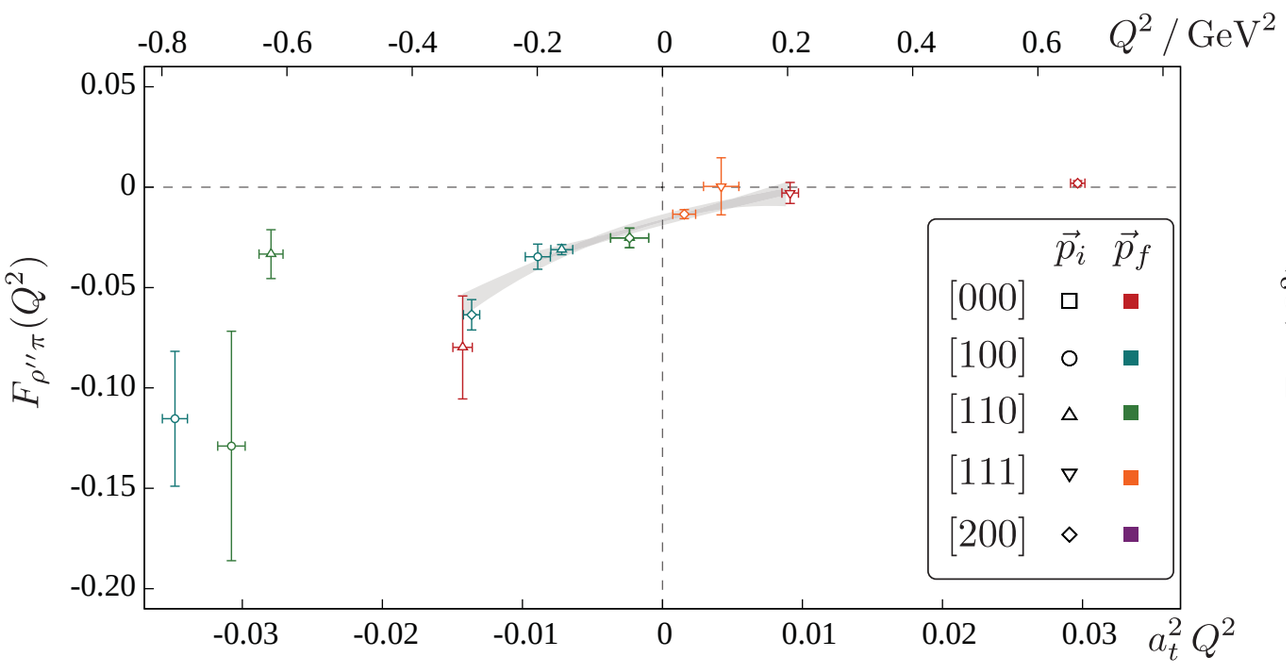

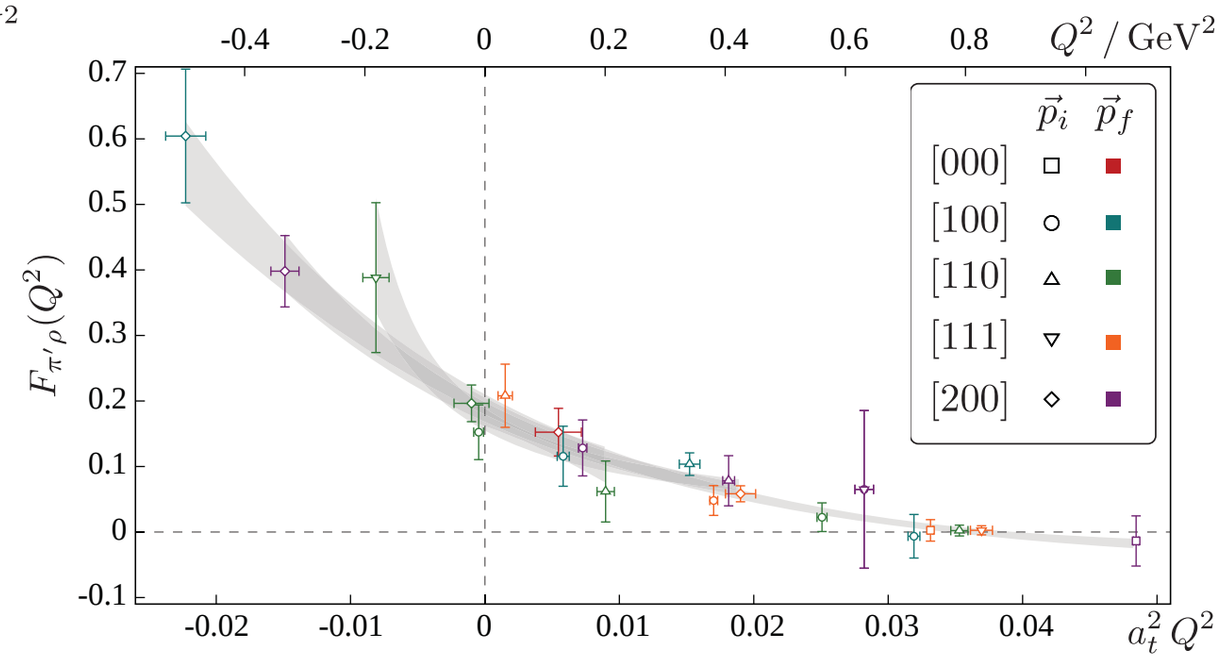

Excited to Excited Transition

$\rho' \to \pi' \gamma$

$$\langle \rho; p'\lambda | j^\mu | \pi; p \rangle = \frac{2F(Q^2)}{m_\rho + m_\pi} \epsilon^{\mu\nu\eta\sigma} p'_\nu p_\eta \varepsilon^*_\sigma(p', \lambda)$$

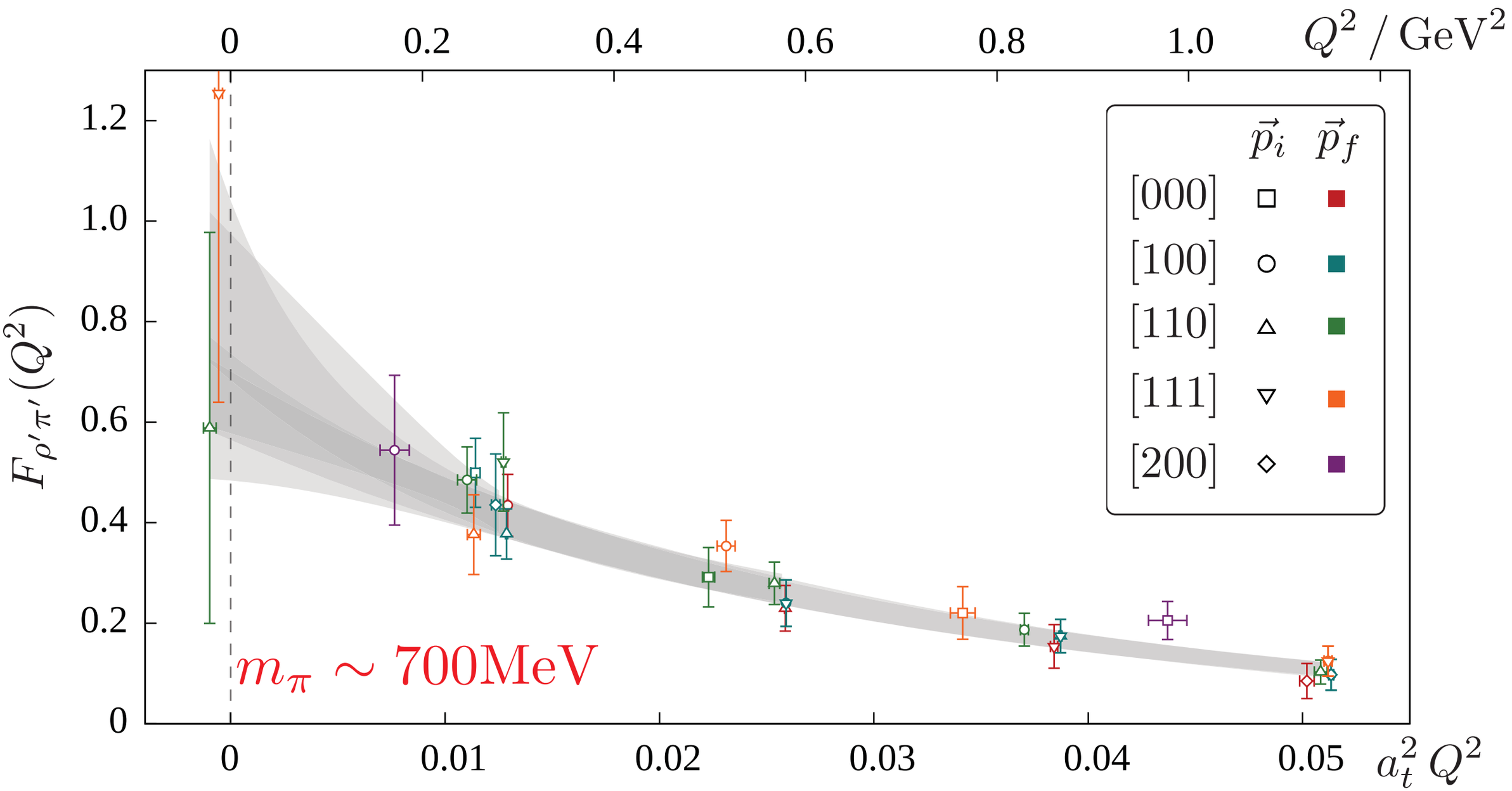

The Future

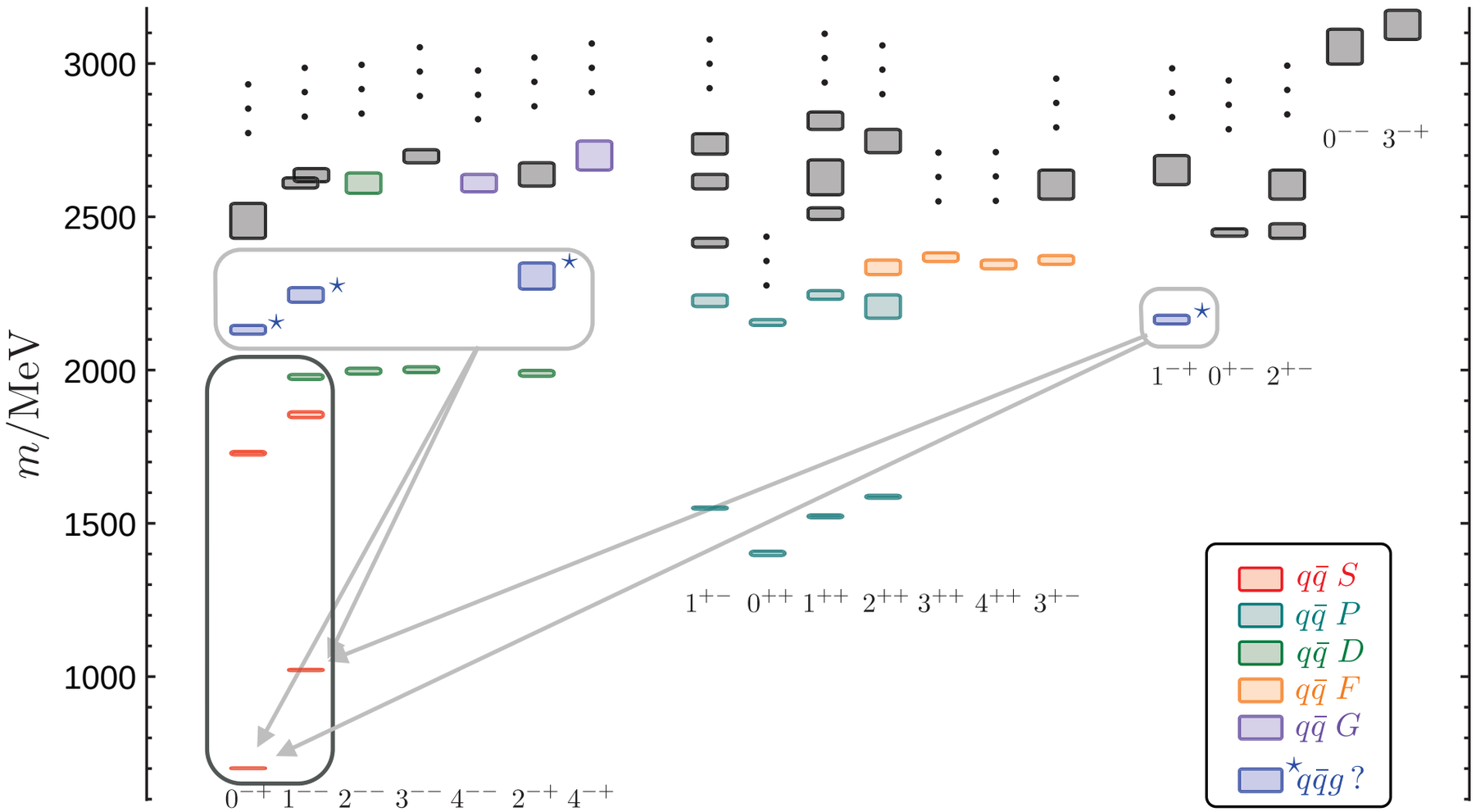

what have we done?

- implemented the formalism
- moved beyond ground states
- explored systematics
- seen real physics

In the works

- explore more of the spectrum
- unstable to stable transition

other directions

- charm, tetraquarks, baryons?

Correlator Construction

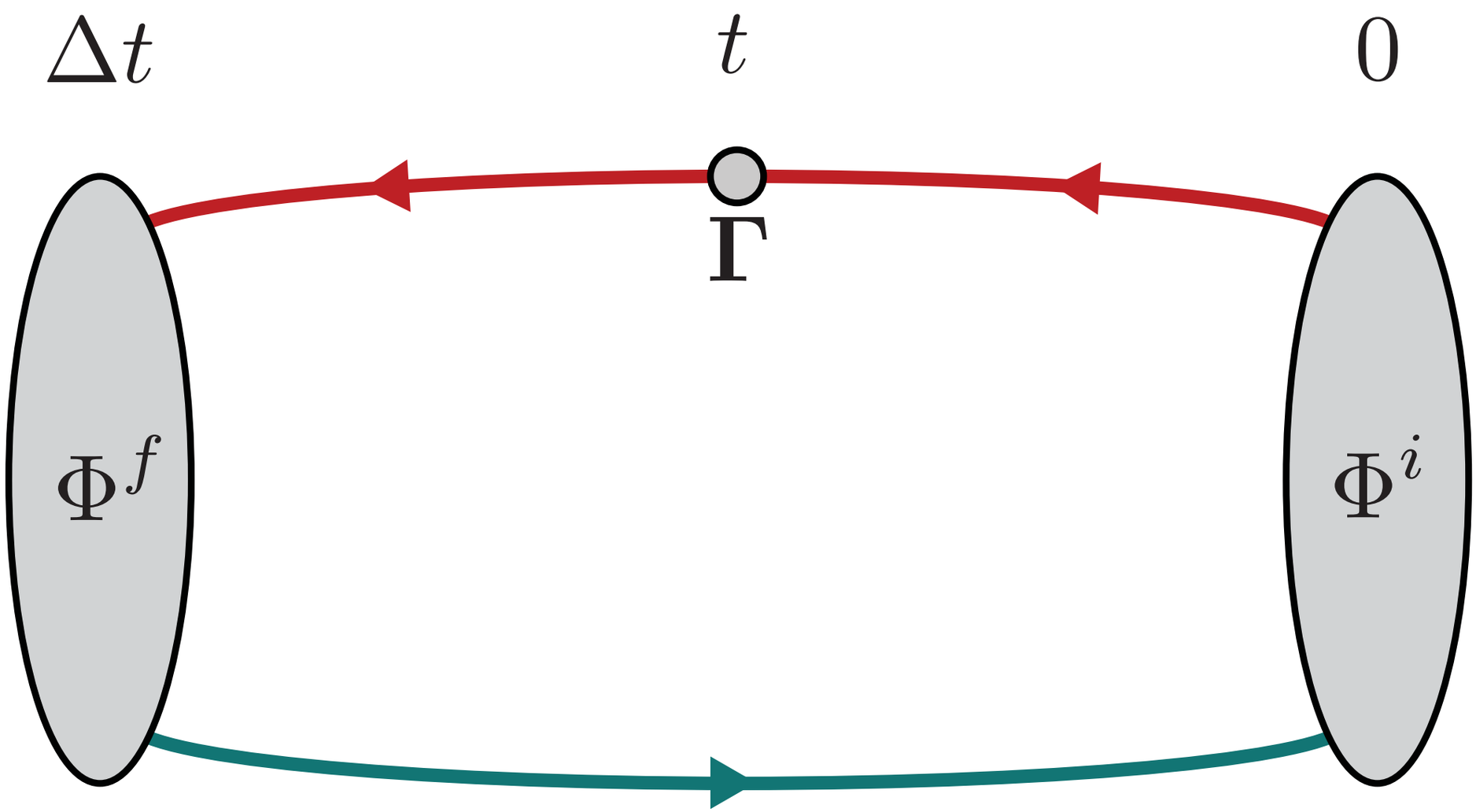

Clover Action

Add irrelevant operators

$$S_C \equiv a_t a_s^3 \sum_x \bar{\psi}(x) \left[m_0 + \nu_t \not{D}_t^W + \nu_s \sum_i \not{D}_s^W - \frac{a_s}{2} \left(c_t \sum_i \sigma_{4i} F_{4i} - c_s \sum_{i<i'} \sigma_{ii'} F_{ii'} \right) \right] \psi(x)$$

$$S_C = \bar{\psi} \overleftarrow{\Omega} \left[m + \not{\nabla} \right] \overrightarrow{\Omega} \psi$$

$$\overrightarrow{\Omega} = 1 + a_t \Omega_m m + a_t \Omega_t \overrightarrow{\not{\nabla}}_t + a_s \Omega_s \sum_i \overrightarrow{\not{\nabla}}_i$$

Redefine QED fields

$$\tilde{V}^\mu = \bar{\psi} \overleftarrow{\Omega} \gamma^\mu \overrightarrow{\Omega} \psi$$

Tree Level

$$\mathcal{V}_0 = \bar{\psi}\gamma_0\psi - \frac{1}{4} a_s \nu_s (1 - \frac{1}{\xi}) \partial_k \bar{\psi} \sigma_{0k} \psi$$

$$\mathcal{V}_k = \bar{\psi}\gamma_k\psi - \frac{1}{4} a_t \left(1 - \xi\right) \partial_0 \bar{\psi} \sigma_{0k} \psi$$

Phys. Rev. D 64, 034509

Renormalization

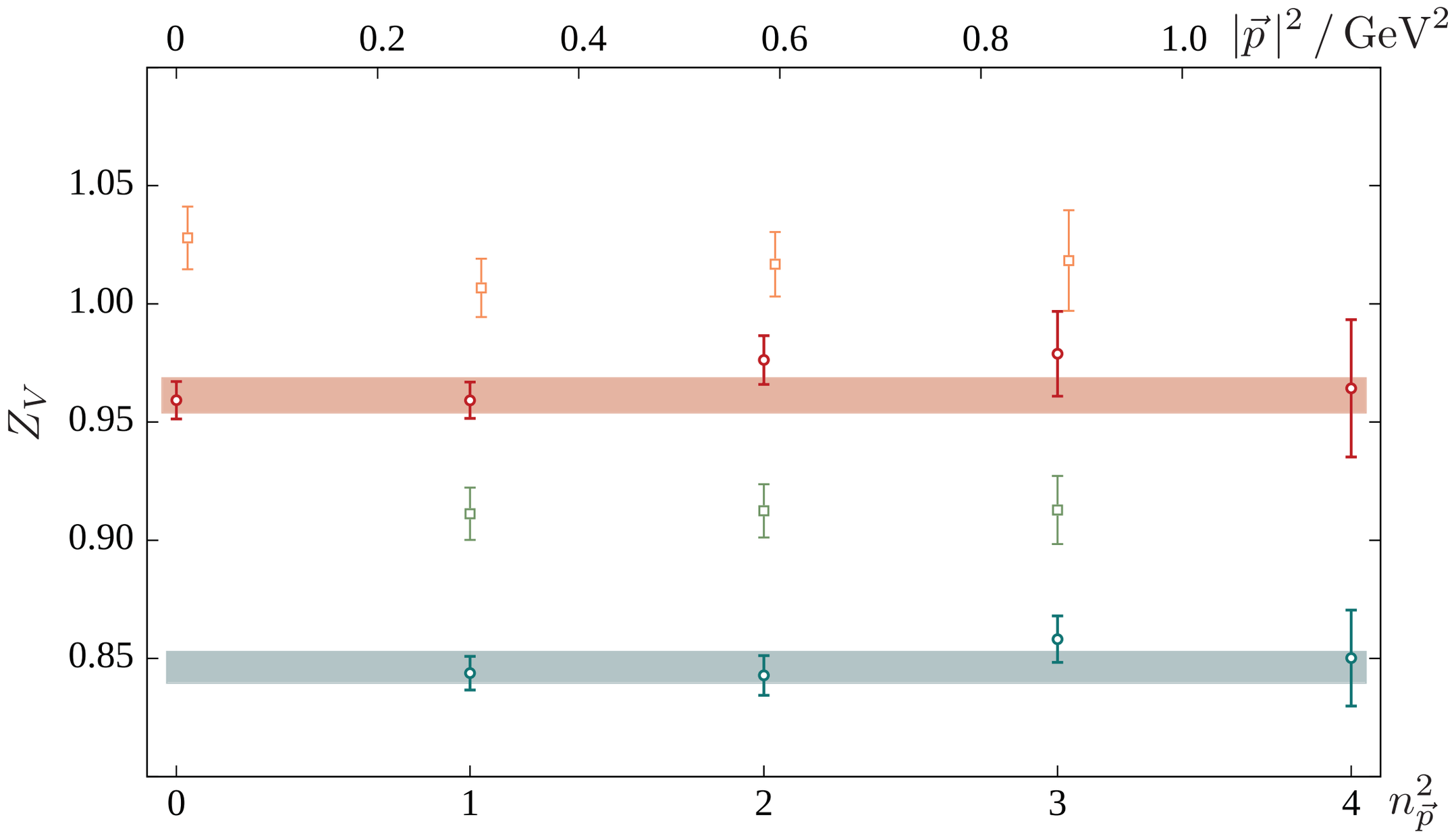

Dispersion

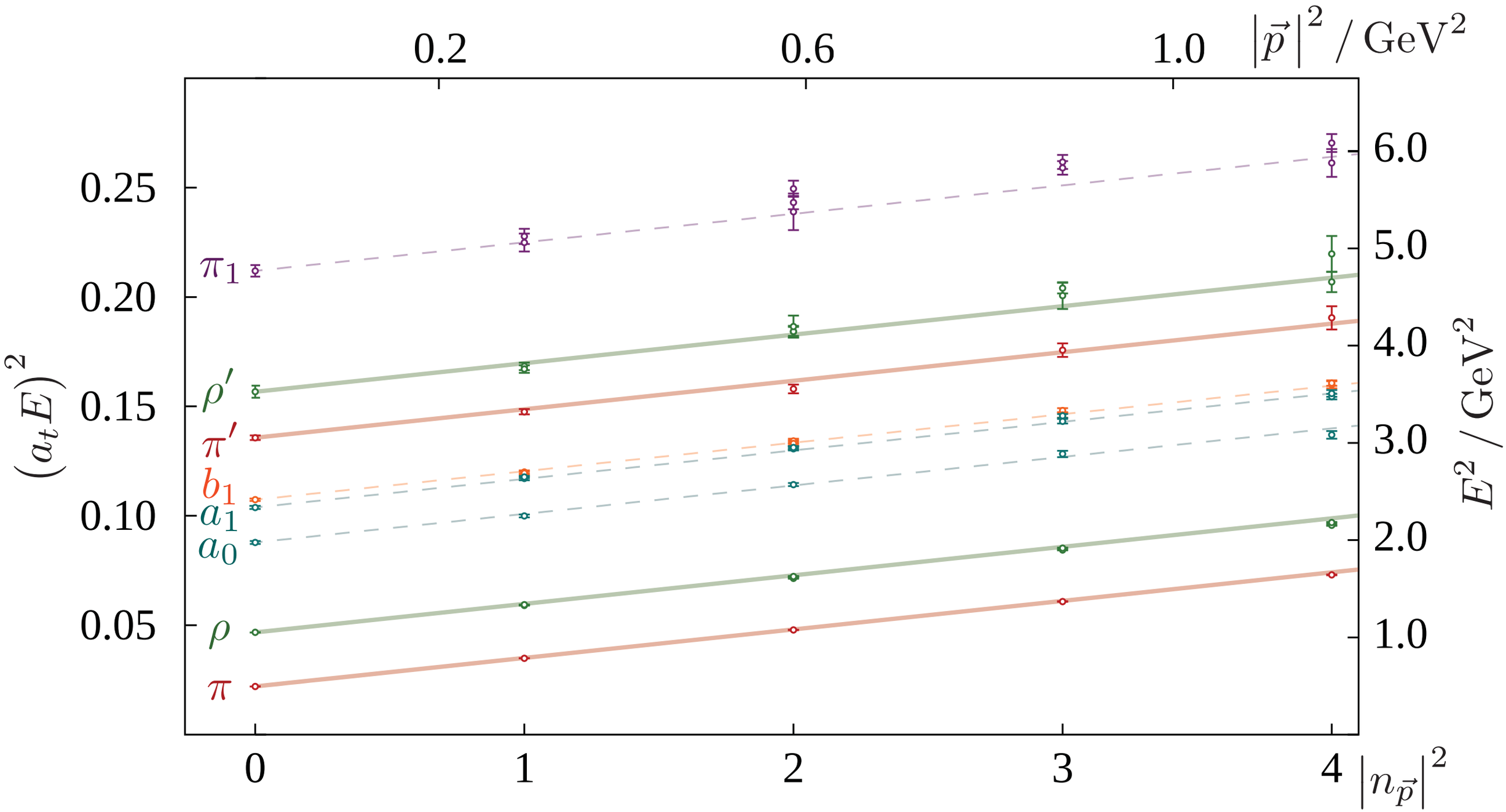
0.2
0.6
1.0
$|\vec{p}|^2$ / GeV^2
0.25
0.20
0.15
0.10
0.05
$(a_t E)^2$
6.0
5.0
4.0
3.0
2.0
1.0
E^2 / GeV^2
π_1
ρ'
π'
b_1
a_1
a_0
ρ
π
0
1
2
3
4
$|n_{\vec{p}}|^2$

Rotational Symmetry

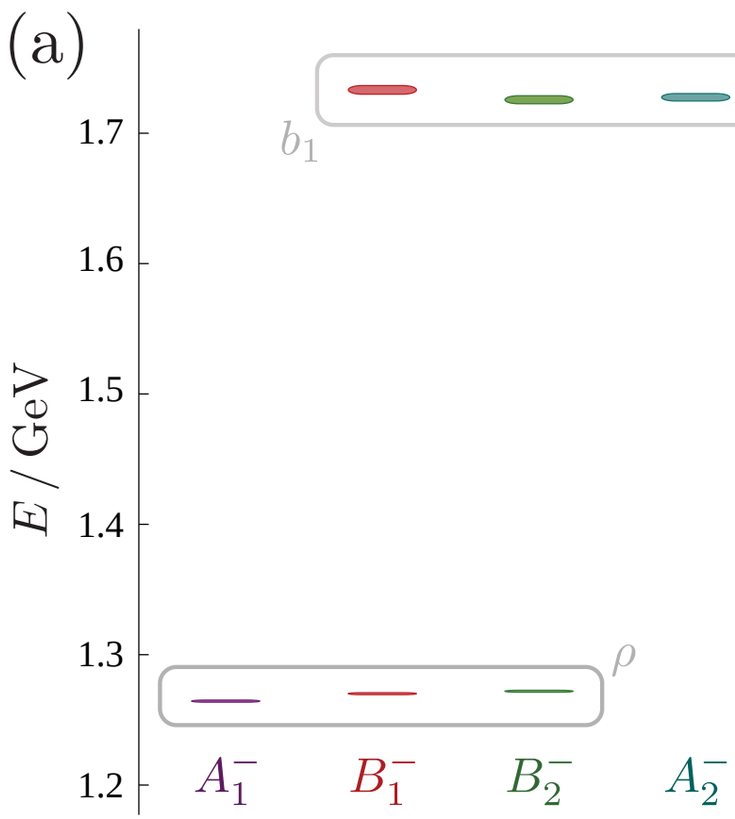

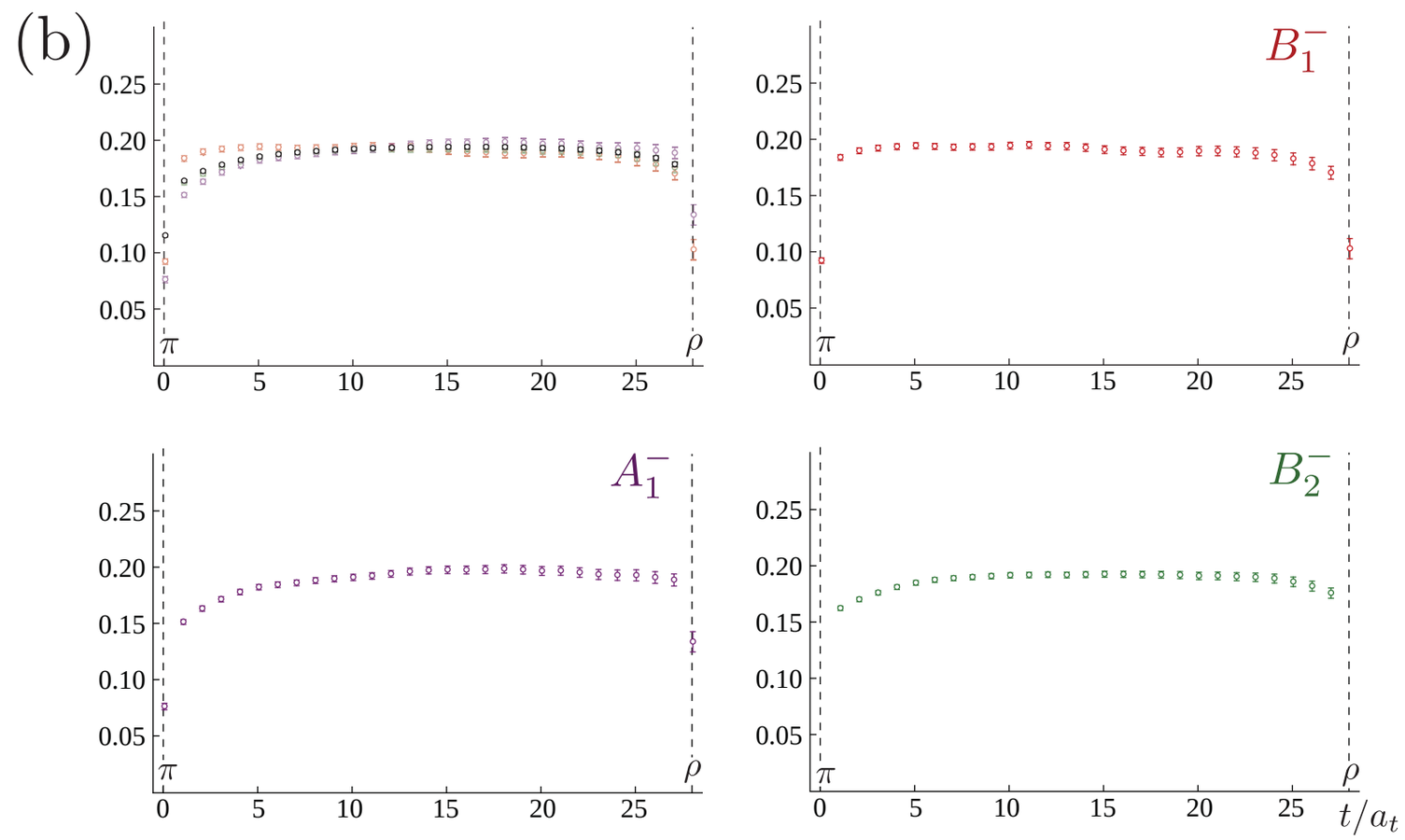

$$\vec{n}_p = [110]$$

$$\langle 0|\Omega_\rho^{(\Lambda)}(28,\vec{p}\,')j^{\mu(E_2)}(t,\vec{q})\Omega_\pi^\dagger(0,\vec{p})|0\rangle$$

$$\vec{n}_{p'} = [0,1,1] \qquad \vec{n}_p = [0,\text{-}1,1]$$

Reconstruction

$$C^{\mu}_{\mathfrak{n}\mathfrak{m}} = \langle 0|\Omega_{\mathfrak{n}}(t) j^{\mu}(t_\gamma)\Omega^{\dagger}_{\mathfrak{m}}(0)|0\rangle$$

$$= \sum_{\mathfrak{n}'\mathfrak{m}'} \langle \mathfrak{n}'|j^{\mu}|\mathfrak{m}'\rangle e^{-E_{\mathfrak{n}'}(t-t_\gamma)} e^{-E_{\mathfrak{m}'}t_\gamma}$$

$$\times \frac{\langle 0|\Omega_{\mathfrak{n}}(0)|\mathfrak{n}'\rangle}{2E_{\mathfrak{n}'}} \frac{\langle \mathfrak{m}'|\Omega^{\dagger}_{\mathfrak{m}}(0)|0\rangle}{2E_{\mathfrak{m}'}}$$

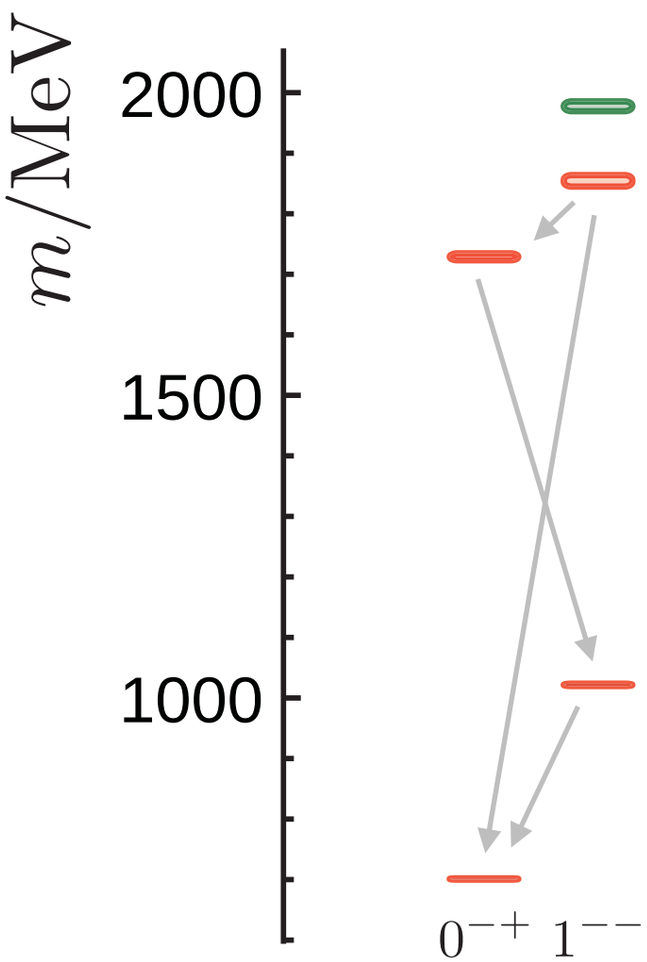

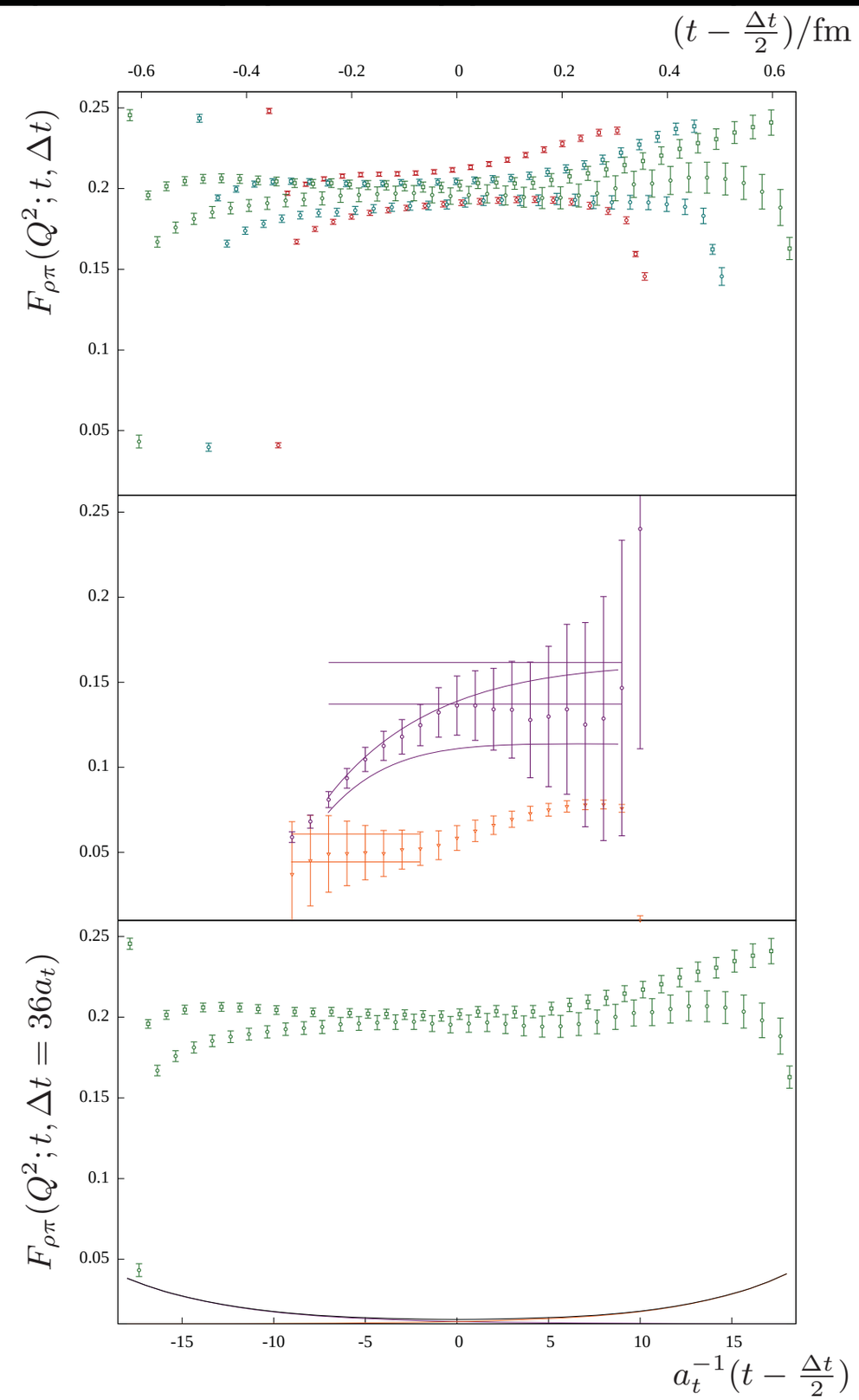

Resonances in coupled-channel scattering from lattice QCD

David Wilson

Old Dominion University

Based on work in collaboration with J.J. Dudek, R.G. Edwards and C.E. Thomas.

Multi-Hadron and Nonlocal Matrix Elements in Lattice QCD
Brookhaven National Laboratory
5-6 February 2015.

Resonances from QCD

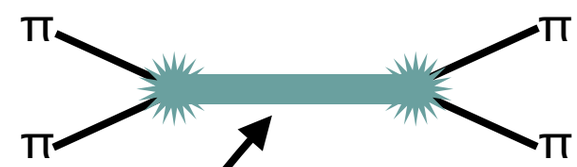

$$\sim \frac{1}{\rho(s)} \frac{s^{\frac{1}{2}}\Gamma(s)}{m_R^2 - s - i s^{\frac{1}{2}}\Gamma(s)}$$

$$\Gamma(s) = \frac{g_R^2}{6\pi} \frac{k_{cm}^3}{E_{cm}^2}$$

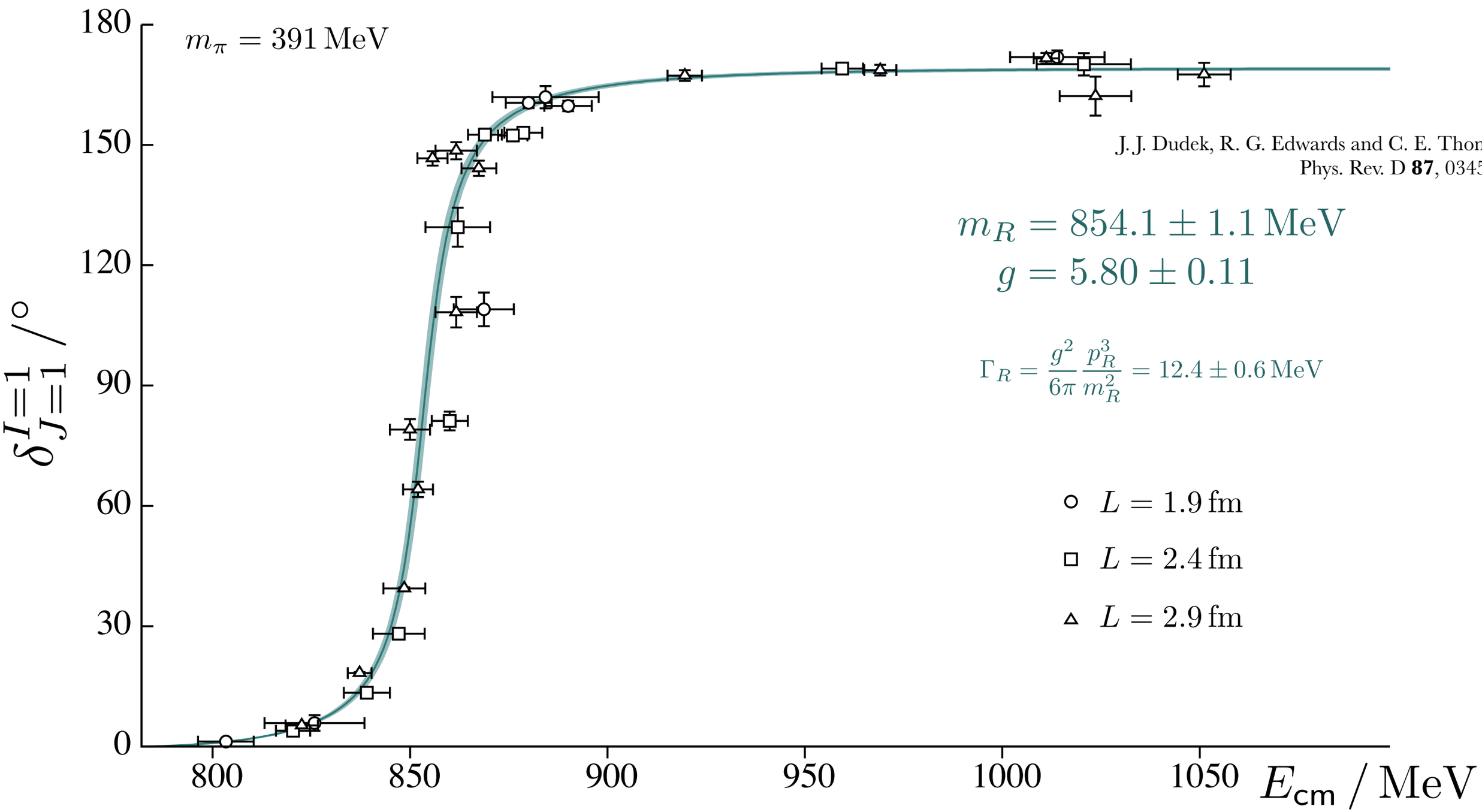

J. J. Dudek, R. G. Edwards and C. E. Thomas
Phys. Rev. D **87**, 034505

Coupled-channel scattering

- The ρ meson is a nice starting point but what about other states?
- Most physical resonances couple to multiple channels.
- To understand the physical spectrum, applying coupled-channel methods will be essential.
- We consider here **πK**, where **ηK** can also contribute in I=1/2.
- The physical amplitudes have resonances in several partial waves:

$\mathcal{J}^P=0^+$	$\kappa(700)$, $K_0^\star(1430)$, ...
$\mathcal{J}^P=1^-$	$K^\star(892)$, ...
$\mathcal{J}^P=2^+$	$K_2^\star(1430)$, ...

Coupled-channel scattering

Main ingredients to obtain the finite volume spectra:

- Anisotropic lattices - finer temporal spacing.
- Distillation.
- A large basis of $\bar{q}q$-like constructions.
- Pairs of optimised meson operators.
- Variational method to obtain the spectrum.

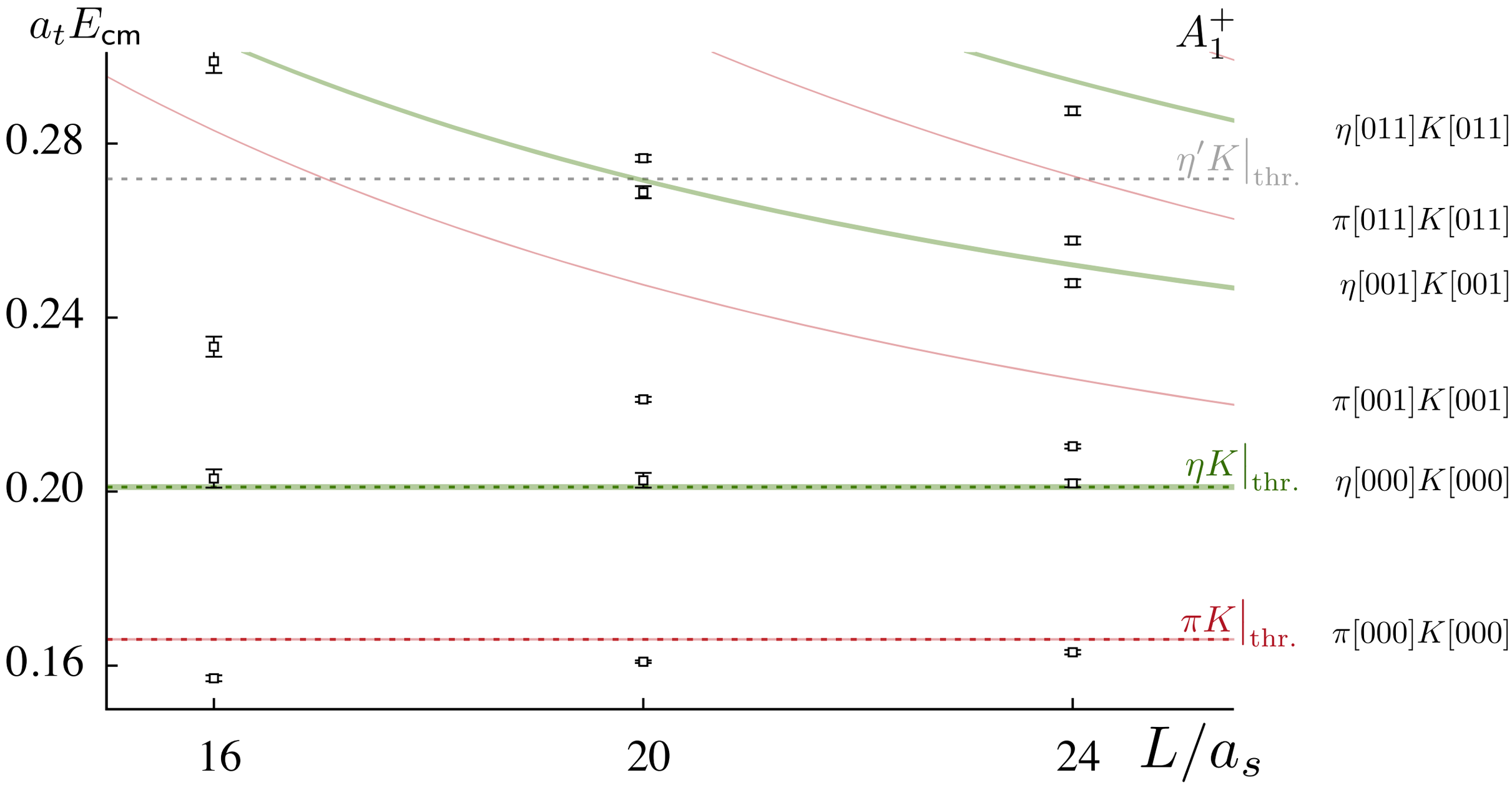

Coupled-channel scattering

Main ingredients to obtain the finite volume spectra:

- Anisotropic lattices - finer temporal spacing.
- Distillation.
- A large basis of $\bar{q}q$-like constructions.
- Pairs of optimised meson operators.
- Variational method to obtain the spectrum.

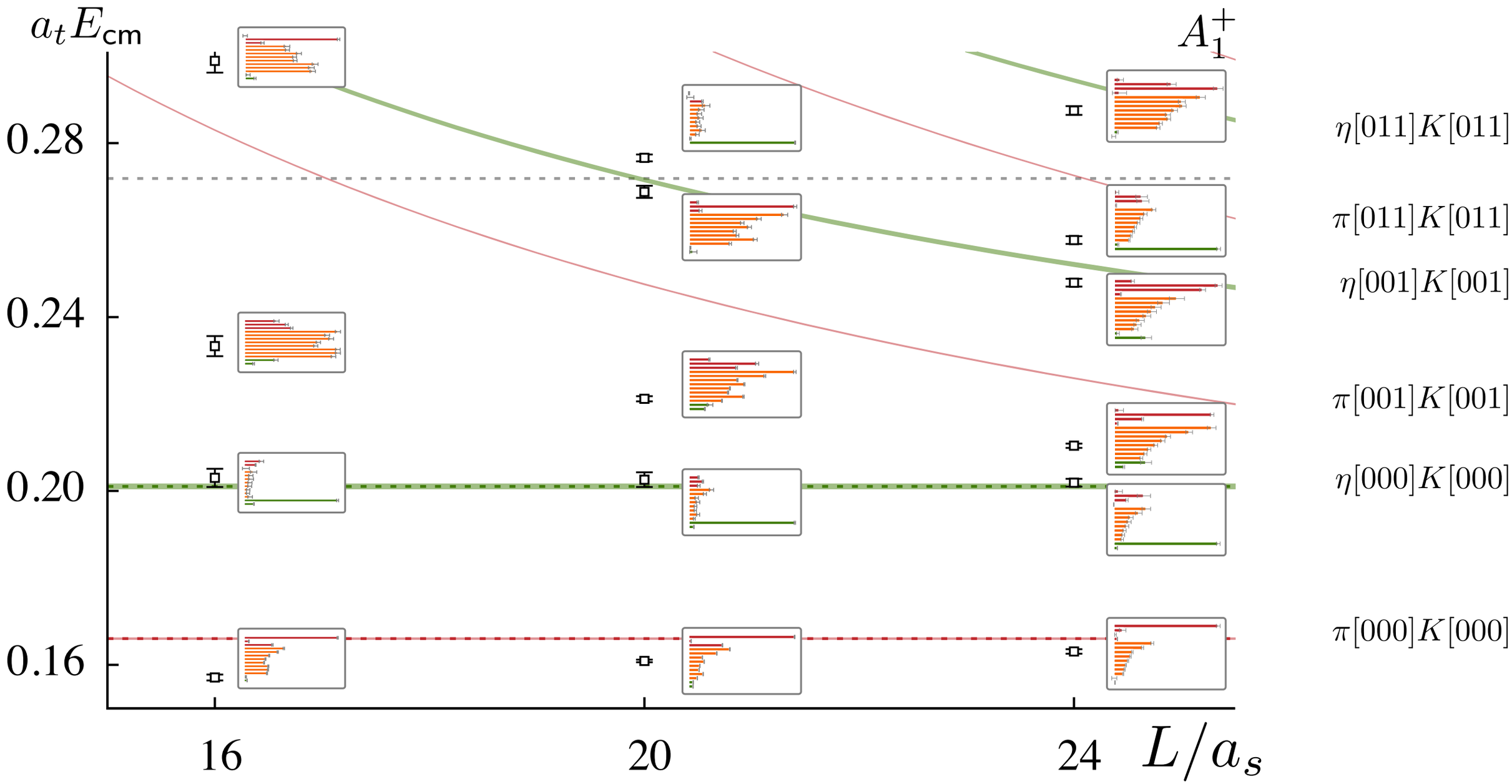

Coupled-channel extensions of Lüscher's method

$$\det\left[\delta_{ij}\delta_{\ell\ell'}\delta_{nn'} + i\rho_i t_{ij}^{(\ell)}\left(\delta_{\ell\ell'}\delta_{nn'} + i\mathcal{M}^{\vec{d},\Lambda}_{ij,\,\ell n,\,\ell' n'}\right)\right] = 0$$

Many contributors:
Lüscher
Gottlieb & Rummukainen
Christ, Kim, & Yamazaki
Kim, Sachrajda & Sharpe
He, Feng & Liu
Bernard, Lage, Meissner, and Rusetsky
Leskovec & Prelovsek
Briceño & Davoudi
Hansen & Sharpe
Gockeler *et al*
Guo, Dudek, Edwards & Szczepaniak
Briceño, Davoudi, Luu
+ ...

Coupled-channel extensions of Lüscher's method

$$S_{ij} = \delta_{ij} + 2i\,(\rho_i \rho_j)^{\frac{1}{2}}\, t_{ij}$$

Angular momentum

scattering t-matrix

momentum boost vector

lattice irrep

$$\det\left[\delta_{ij}\delta_{\ell\ell'}\delta_{nn'} + i\rho_i t_{ij}^{(\ell)}\left(\delta_{\ell\ell'}\delta_{nn'} + i\mathcal{M}^{\vec{d},\Lambda}_{ij,\,\ell n,\,\ell' n'}\right)\right] = 0$$

Channels:
eg πK, ηK

phase space

$$\rho_i = \frac{2k_i^{(cm)}}{E_{cm}}$$

finite volume object - contains generalised Lüscher Zeta functions

$$\mathcal{M} \sim \frac{1}{\gamma}\sum_{\text{spins}}(\text{CGs})\sum_{\vec{r}}\frac{r^\ell Y_{\ell m}(\hat{\vec{r}})}{r^2 - q^2}$$

Symmetry of the volume mixes partial waves - *M* mixes partial waves.
t-matrix is diagonal in partial waves, but can couple scattering channels: $\pi K \rightarrow \eta K$

Coupled-channel extensions of Lüscher's method

$$S_{ij} = \delta_{ij} + 2i\,(\rho_i \rho_j)^{\frac{1}{2}}\, t_{ij}$$

Angular momentum

momentum boost vector

lattice irrep

scattering t-matrix

$$\det\left[\delta_{ij}\delta_{\ell\ell'}\delta_{nn'} + i\rho_i t_{ij}^{(\ell)}\left(\delta_{\ell\ell'}\delta_{nn'} + i\mathcal{M}^{\vec{d},\Lambda}_{ij,\,\ell n,\,\ell' n'}\right)\right] = 0$$

Channels:
eg πK, ηK

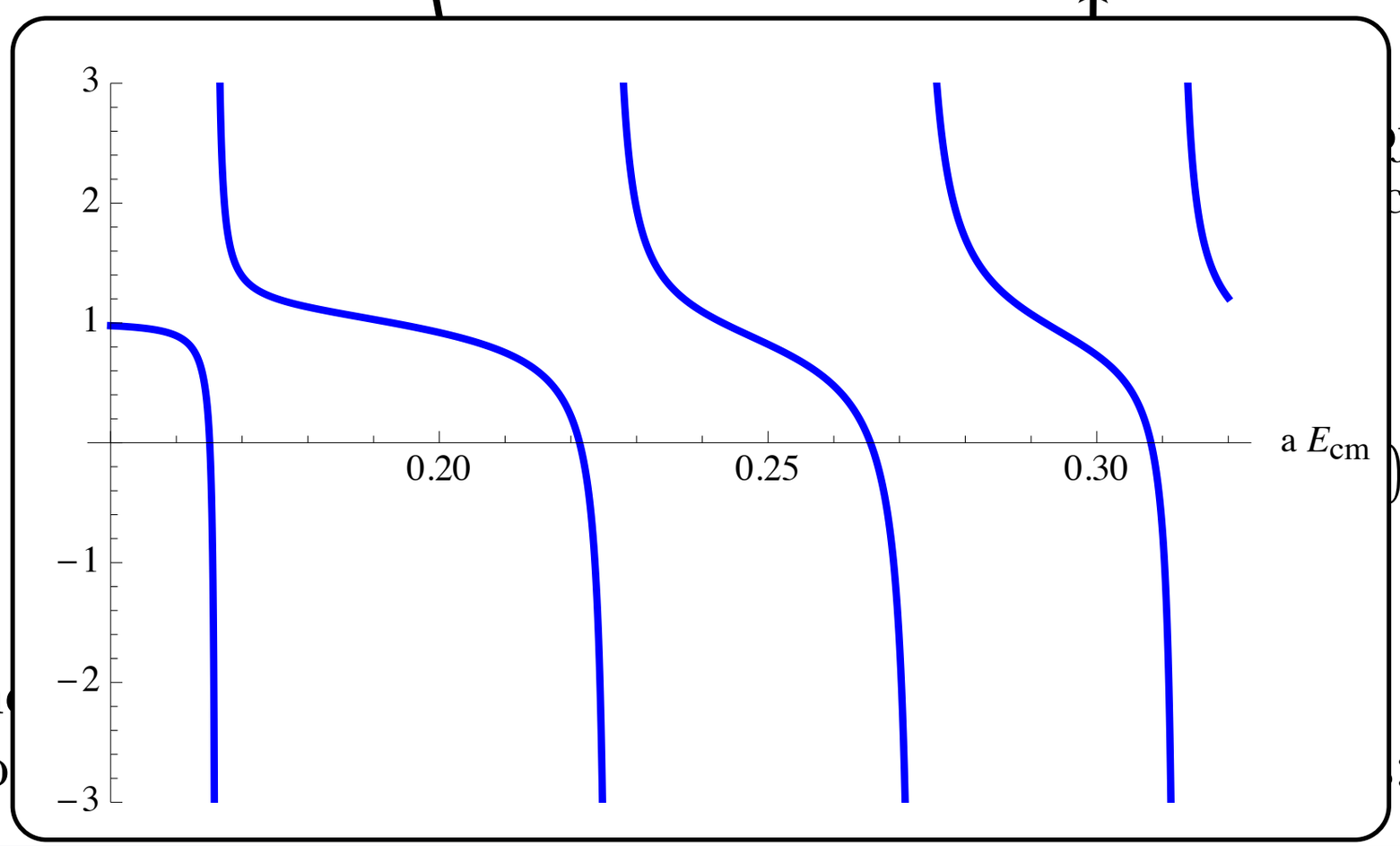

ject - contains
cher Zeta functions

$$\sum_{\vec{r}} \frac{r^{\ell} Y_{\ell m}(\hat{\vec{r}})}{r^2 - q^2}$$

Symmetry of th
t-matrix is diago

: $\pi K \rightarrow \eta K$

Resonances from QCD

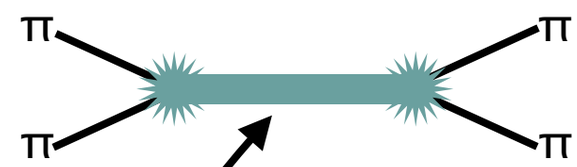

$$\sim \frac{1}{\rho(s)} \frac{s^{\frac{1}{2}}\Gamma(s)}{m_R^2 - s - i s^{\frac{1}{2}}\Gamma(s)}$$

$$\Gamma(s) = \frac{g_R^2}{6\pi} \frac{k_{cm}^3}{E_{cm}^2}$$

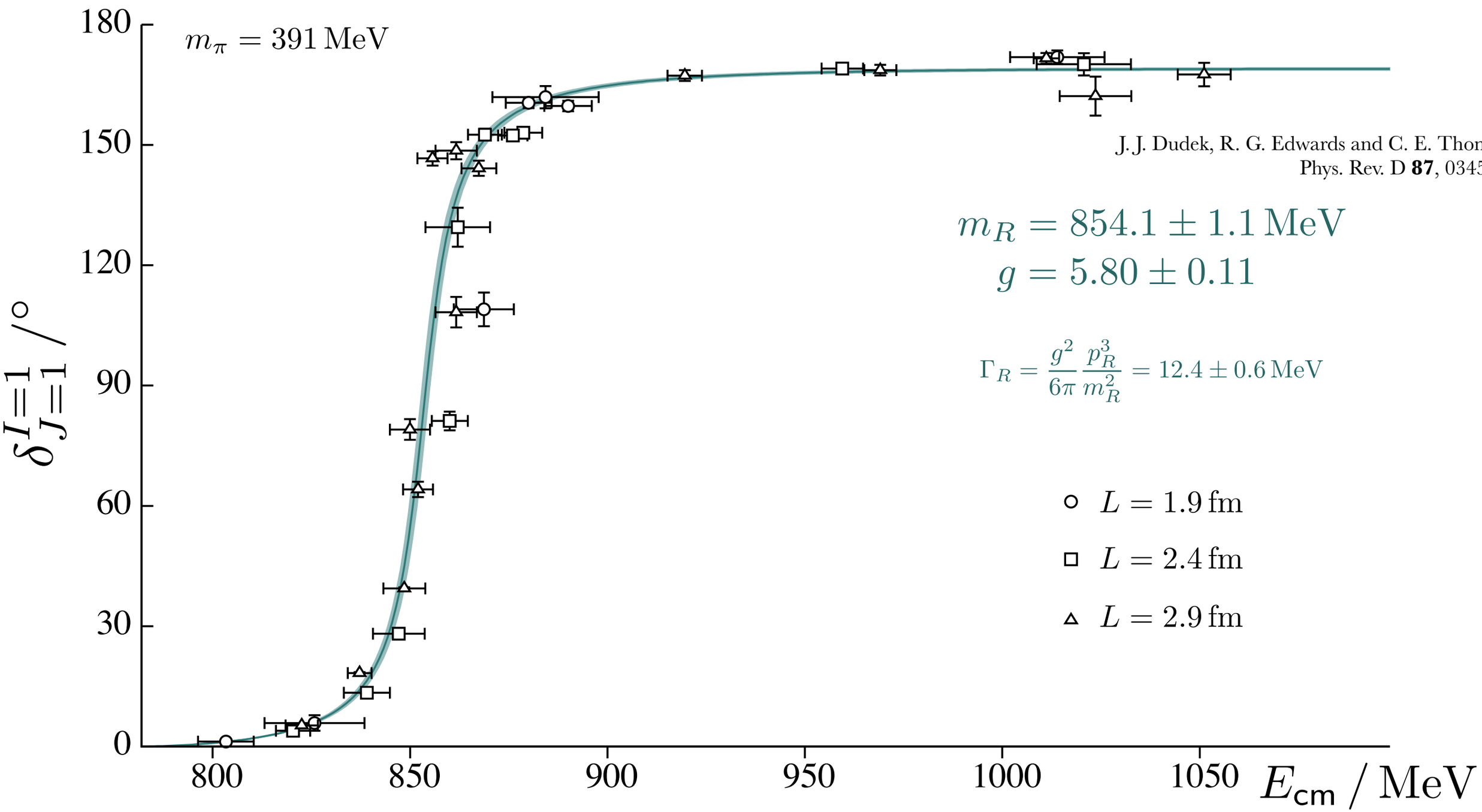

J. J. Dudek, R. G. Edwards and C. E. Thomas
Phys. Rev. D **87**, 034505

Coupled-channel scattering

Problem: Three or more unknowns for each energy level, eg: $\eta(E_{cm})$, $\delta_1(E_{cm})$, $\delta_2(E_{cm})$
(...and even more with higher partial waves)

$$t_{ij} = \begin{cases} \frac{\eta\, e^{2i\delta_i} - 1}{2i\,\rho_i} & (i = j) \\ \frac{\sqrt{1-\eta^2}\, e^{i(\delta_i+\delta_j)}}{2\sqrt{\rho_i\,\rho_j}} & (i \neq j) \end{cases}$$

2x2 complex matrix (or more) but only one equation.
No direct relation from energy levels to amplitudes

$$\det\left[\delta_{ij}\delta_{\ell\ell'}\delta_{nn'} + i\rho_i t_{ij}^{(\ell)}\left(\delta_{\ell\ell'}\delta_{nn'} + i\mathcal{M}^{\vec{d},\Lambda}_{ij,\,\ell n,\,\ell' n'}\right)\right] = 0$$

Finite volume energy levels

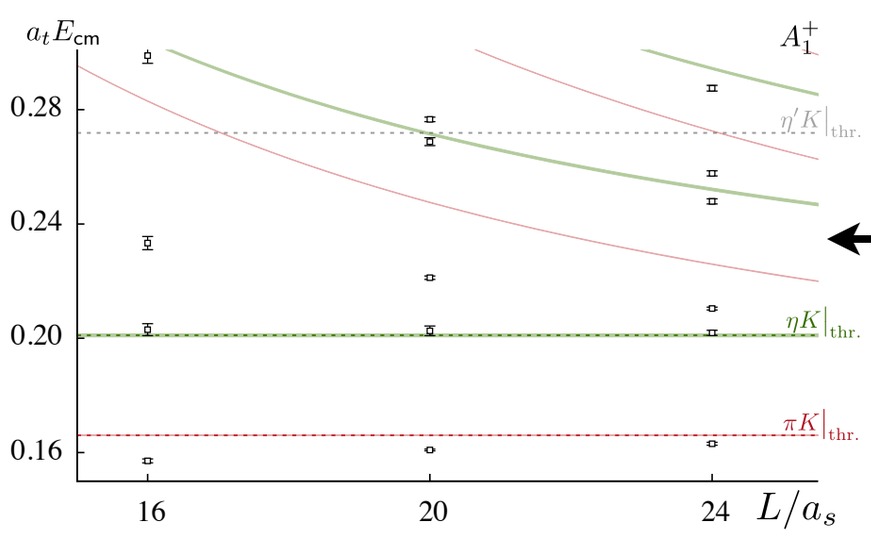

?

Extensions of Lüscher's method

Scattering Amplitudes

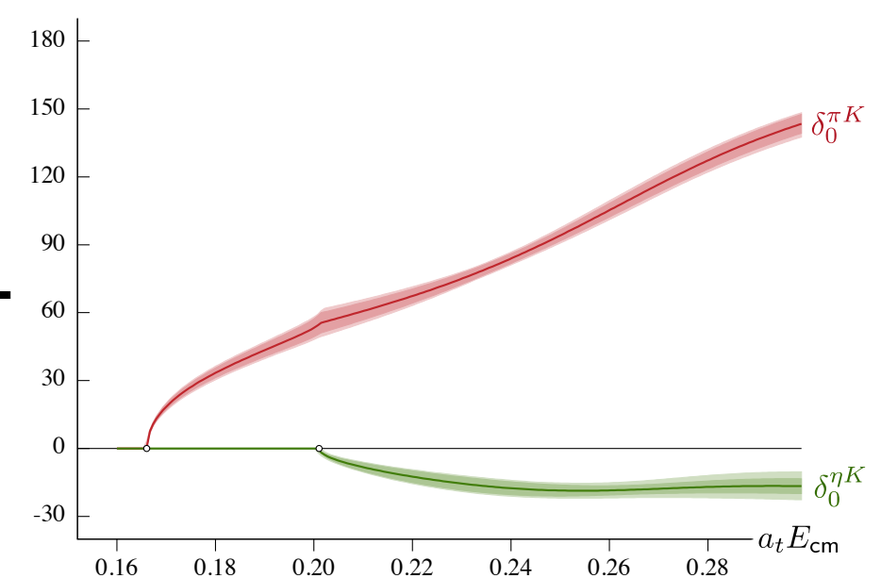

Coupled channel scattering

Solution: Parameterise *t*-matrix, constrain parameters using many energy levels
E.g.: *K*-matrix (it's essential that we preserve unitarity)

$$S_{ij} = \delta_{ij} + 2i\,(\rho_i \rho_j)^{\frac{1}{2}}\, t_{ij}$$

$$[S^\dagger S]_{ij} = \delta_{ij}$$

$$\rightarrow \mathrm{Im}[t^{-1}]_{ij} = -\rho_i \delta_{ij}$$

- *K*-matrix contains everything not constrained by unitarity

$$t_{ij}^{-1}(s) = K_{ij}^{-1}(s) - i\delta_{ij}\rho_i(s)$$

- *K* must be real for real *s*. One option for two channel scattering:

$$K = \frac{1}{m^2 - s}\begin{bmatrix} g_{\pi K}^2 & g_{\pi K}\, g_{\eta K} \\ g_{\pi K}\, g_{\eta K} & g_{\eta K}^2 \end{bmatrix} + \begin{bmatrix} \gamma_{\pi K,\pi K} & \gamma_{\pi K,\eta K} \\ \gamma_{\pi K,\eta K} & \gamma_{\eta K,\eta K} \end{bmatrix}$$

- *m*, *g*, *γ* are real free parameters. Simple to add more - more poles, or a polynomial in *s*.
- Simple to generalise to scattering with non-zero angular momentum.
- Can improve model by adding extra physically motivated properties - eg: Chew-Mandelstam phase space.

Coupled-channel scattering

- Describe t-matrix using K-matrix in S-wave only → obtain model spectra.
- Minimise a χ^2 to obtain the best agreement between the K-matrix and lattice energies.

$$K = \frac{1}{m^2 - s}\begin{bmatrix} g_{\pi K}^2 & g_{\pi K}\, g_{\eta K} \\ g_{\pi K}\, g_{\eta K} & g_{\eta K}^2 \end{bmatrix} + \begin{bmatrix} \gamma_{\pi K,\pi K} & \gamma_{\pi K,\eta K} \\ \gamma_{\pi K,\eta K} & \gamma_{\eta K,\eta K} \end{bmatrix}.$$

$$\chi^2/N_{\rm dof} = \frac{6.40}{15-6} = 0.71$$

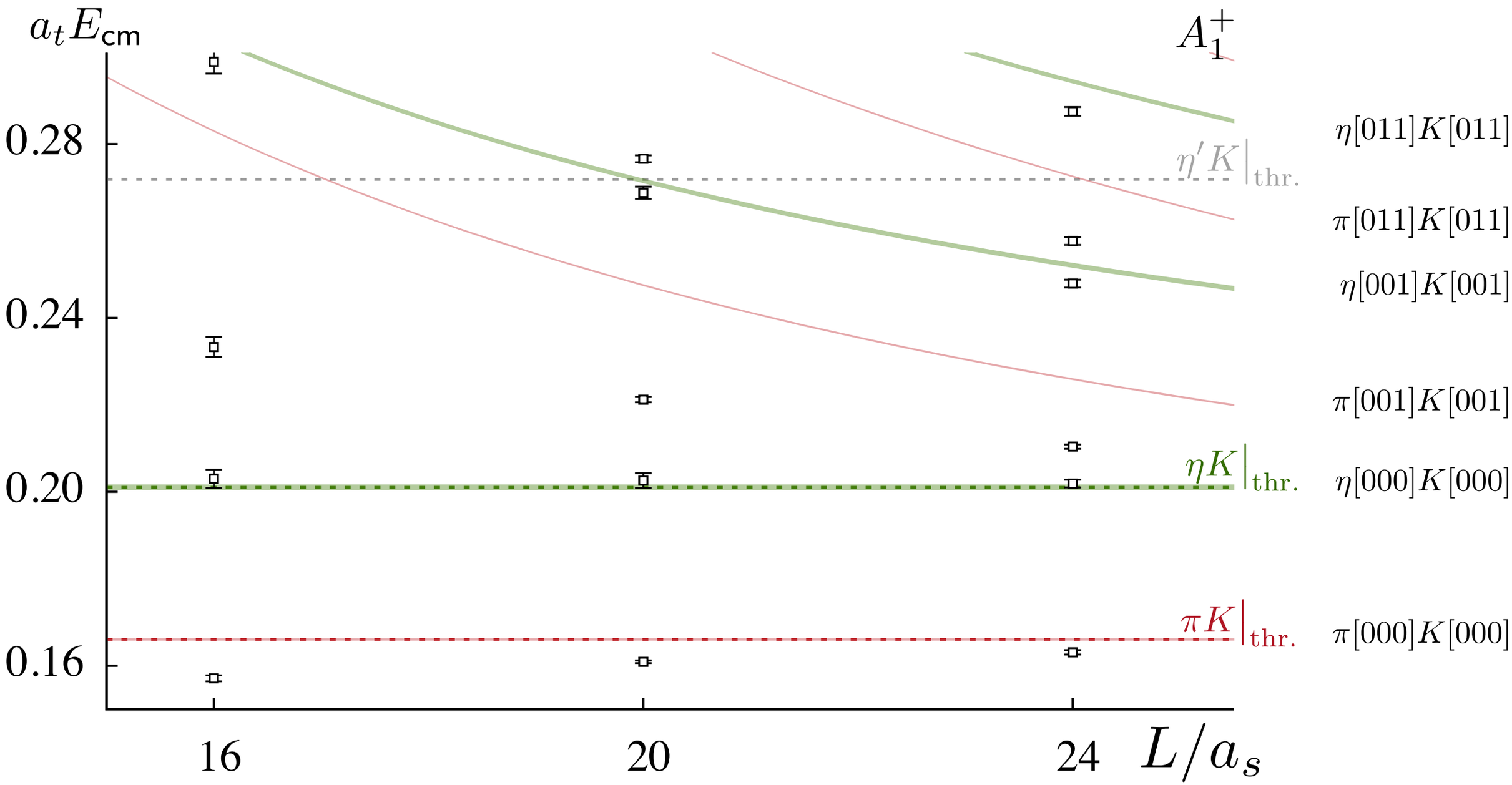

Coupled-channel scattering

- Describe t-matrix using K-matrix in S-wave only → obtain model spectra.
- Minimise a χ^2 to obtain the best agreement between the K-matrix and lattice energies.

$$K = \frac{1}{m^2 - s}\begin{bmatrix} g_{\pi K}^2 & g_{\pi K}\, g_{\eta K} \\ g_{\pi K}\, g_{\eta K} & g_{\eta K}^2 \end{bmatrix} + \begin{bmatrix} \gamma_{\pi K,\pi K} & \gamma_{\pi K,\eta K} \\ \gamma_{\pi K,\eta K} & \gamma_{\eta K,\eta K} \end{bmatrix}.$$

$$\chi^2/N_{\rm dof} = \frac{6.40}{15-6} = 0.71$$

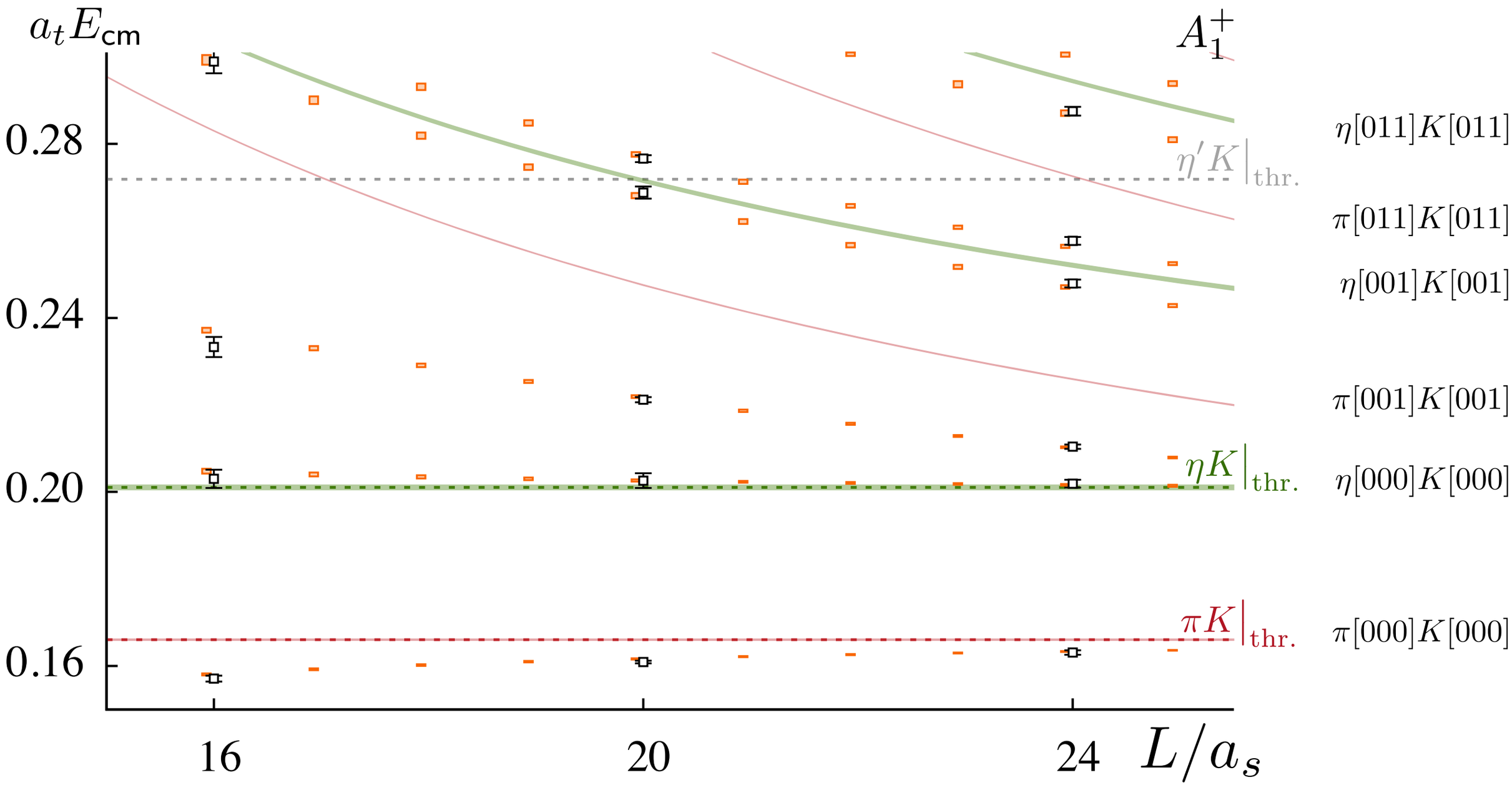

S-wave amplitudes

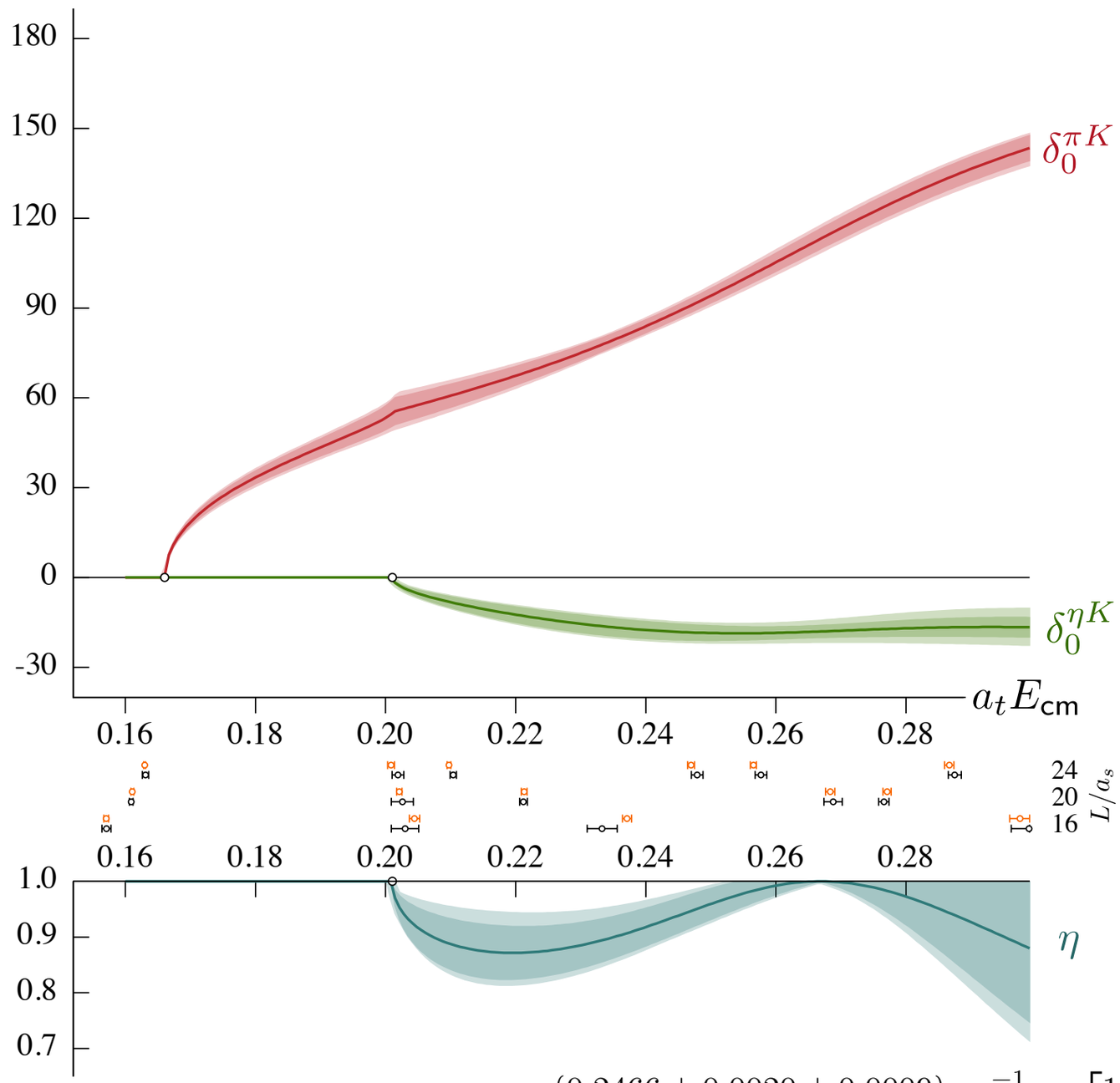

$$t_{ij} = \begin{cases} \dfrac{\eta\, e^{2i\delta_i} - 1}{2i\,\rho_i} & (i = j) \\ \dfrac{\sqrt{1-\eta^2}\, e^{i(\delta_i+\delta_j)}}{2\sqrt{\rho_i\,\rho_j}} & (i \neq j) \end{cases}$$

- Broad resonance in *S*-wave πK.
- ηK coupling is small.
- 3 subthreshold points, naturally included in an energy-level fit.

$$\begin{aligned} m &= (0.2466 \pm 0.0020 \pm 0.0009) \cdot a_t^{-1} \\ g_{\pi K} &= (0.165 \pm 0.006 \pm 0.002) \cdot a_t^{-1} \\ g_{\eta K} &= (0.033 \pm 0.010 \pm 0.003) \cdot a_t^{-1} \\ \gamma_{\pi K,\pi K} &= 0.184 \pm 0.054 \pm 0.030 \\ \gamma_{\pi K,\eta K} &= -0.52 \pm 0.20 \pm 0.06 \\ \gamma_{\eta K,\eta K} &= -0.37 \pm 0.07 \pm 0.05 \end{aligned}$$

$$\begin{bmatrix} 1 & 0.35 & -0.38 & 0.17 & 0.27 & -0.19 \\ & 1 & -0.05 & -0.16 & 0.85 & 0.08 \\ & & 1 & 0.26 & -0.11 & 0.64 \\ & & & 1 & 0.10 & 0.25 \\ & & & & 1 & 0.05 \\ & & & & & 1 \end{bmatrix}$$

$$\chi^2/N_{\rm dof} = \frac{6.40}{15-6} = 0.71\,.$$

More energy levels

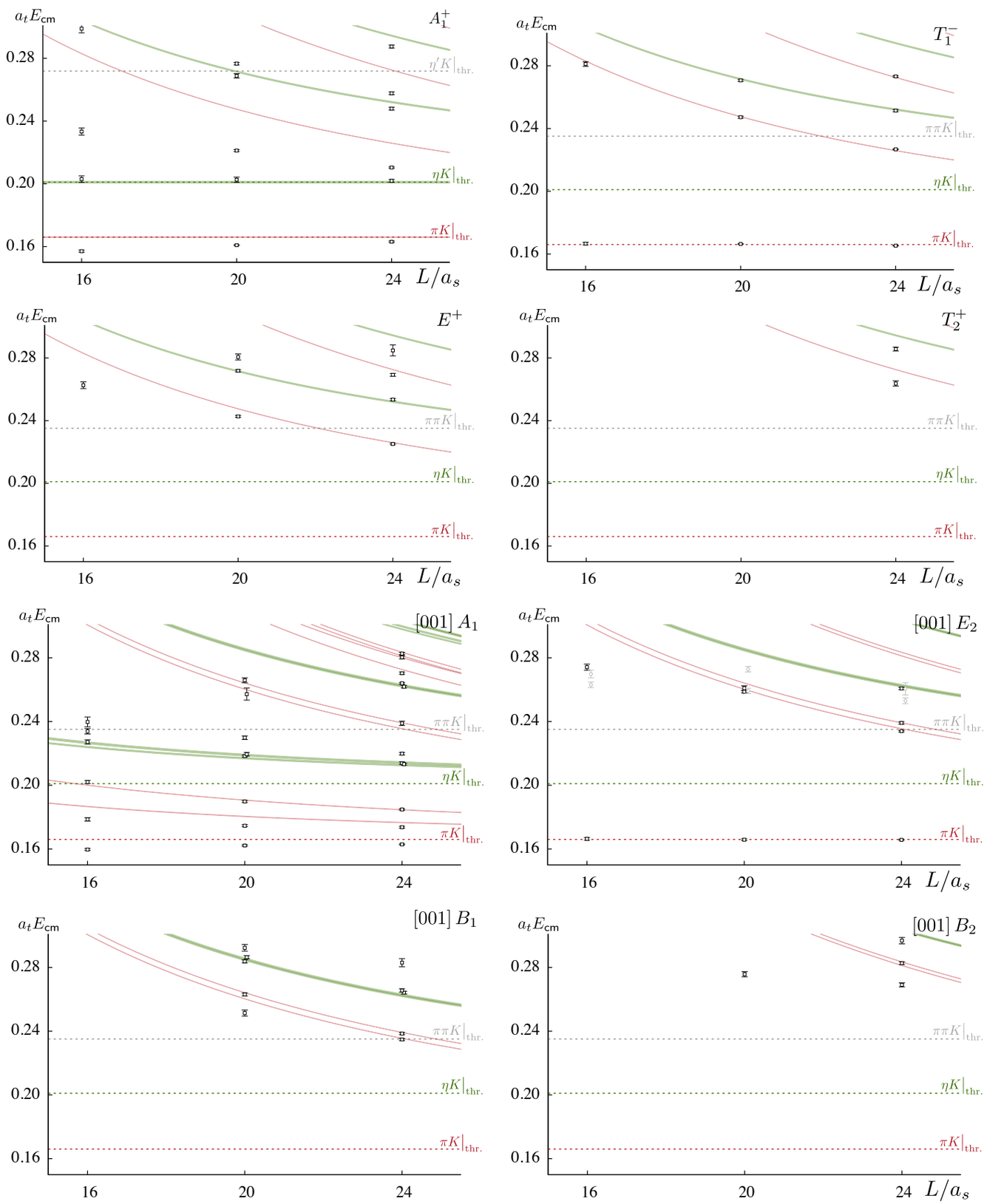

- Many more energy levels from irreps where the mesons are **moving with respect to the lattice**.
- Less symmetry. More **mixing of partial waves**.
- Requires simultaneous knowledge.

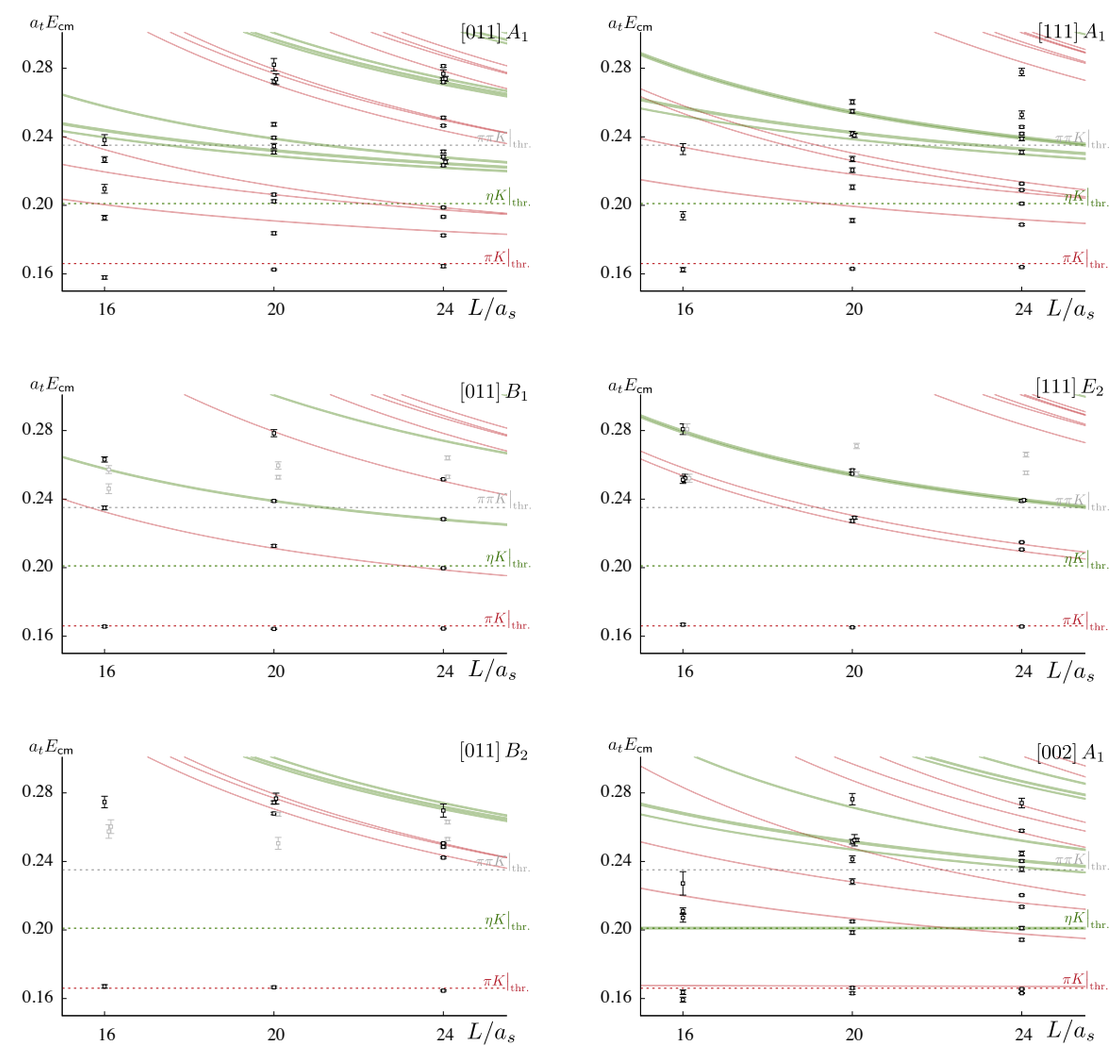

$[011]A_1$

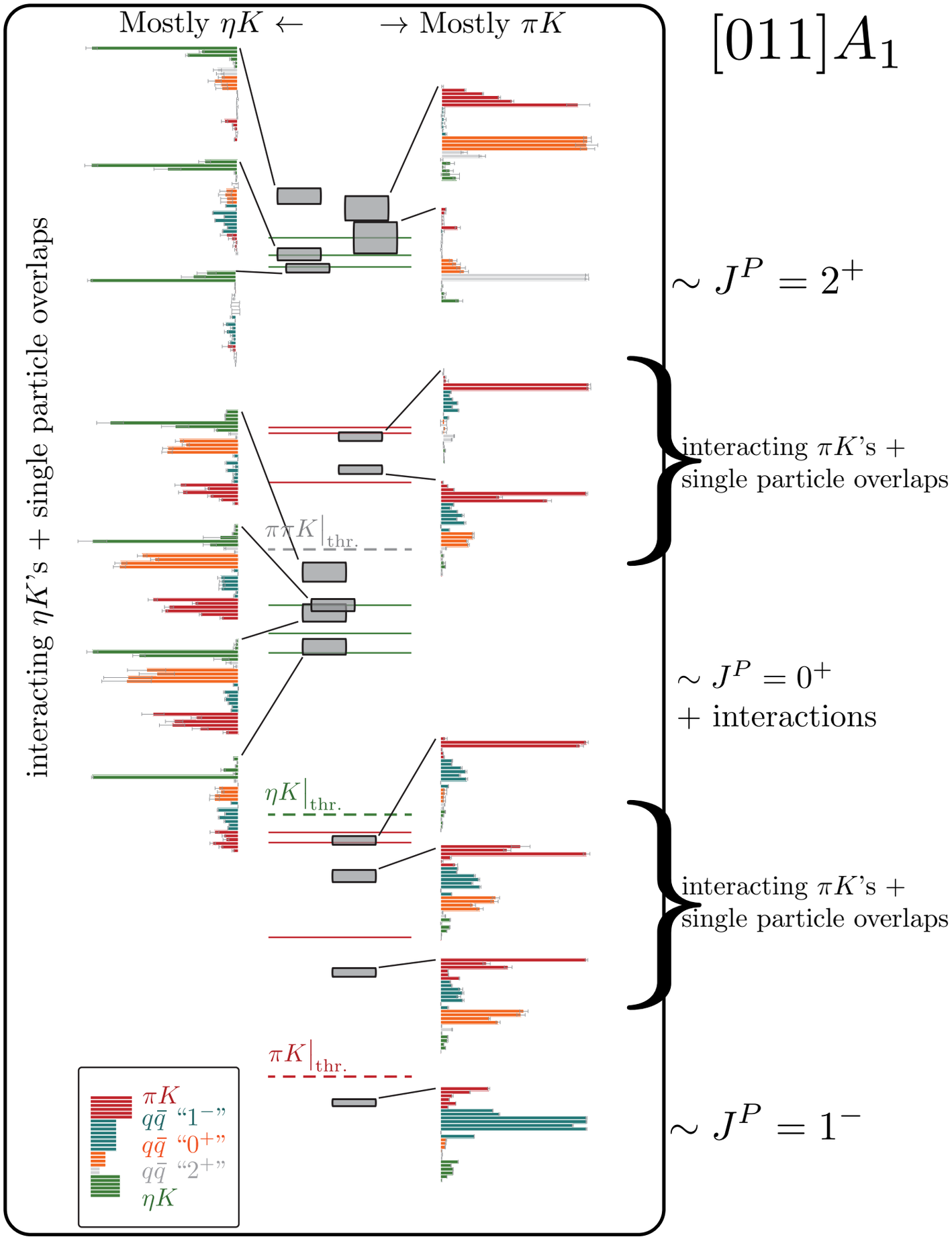

- Overlaps ~ guide to resonant content $Z_i^{\mathfrak{n}} = \langle \mathfrak{n} | \mathcal{O}_i^\dagger | 0 \rangle$
- Shifted πK-like and ηK-like states
- $\mathcal{J}^P$=1⁻ state near to πK threshold, $\mathcal{J}^P$=2⁺ state, extra $\mathcal{J}^P$=0⁺.
- Considerable partial-wave mixing. [011] A_1 contains $\mathcal{J}^P$=0⁺, 1, 2, ...

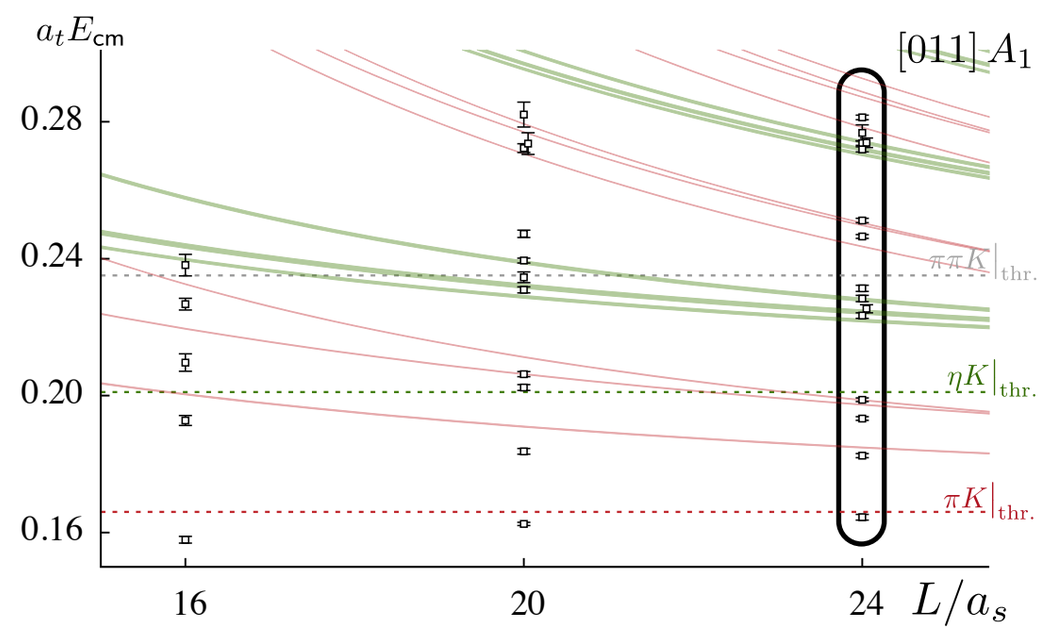

P-wave near-threshold state

Elastic scattering just above πK threshold, no ηK to consider.

The irreps with *P*-wave overlap:

T_1^-, [001] A_1, [001] E_2, [011] A_1, [011] $B_{1,2}$, [111] A_1, [111] E_2, [002] A_1

all have an "extra" level near πK threshold.

Fitting the energy levels using an elastic Breit-Wigner in πK:

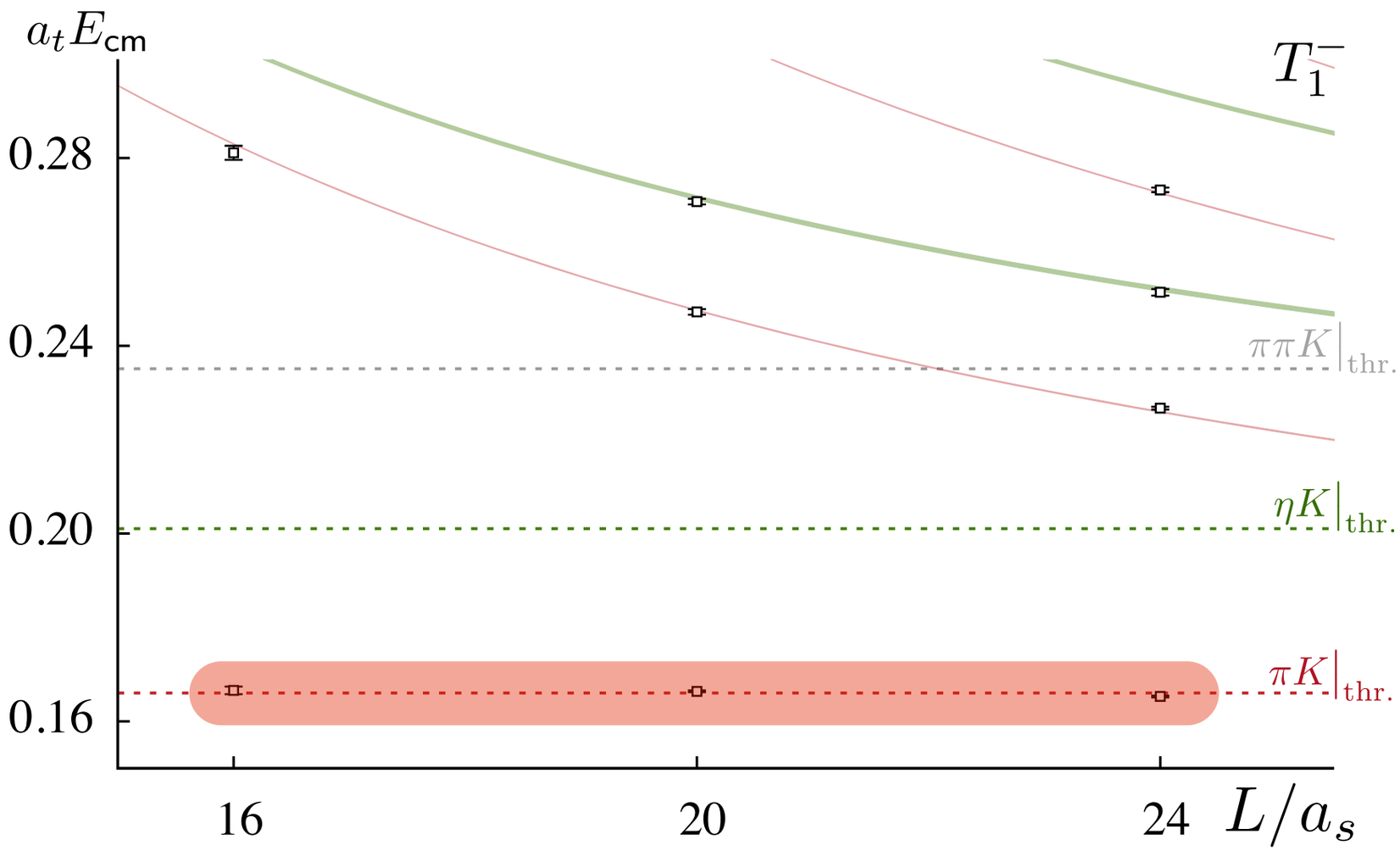

P-wave near-threshold state

$$t = \frac{1}{\rho(s)} \frac{s^{\frac{1}{2}}\Gamma(s)}{m_R^2 - s - i s^{\frac{1}{2}}\Gamma(s)}$$

$$\Gamma(s) = \frac{g_R^2}{6\pi} \frac{k_{cm}^3}{E_{cm}^2}$$

Elastic scattering just above πK threshold, no ηK to consider.

The irreps with *P*-wave overlap:

$\mathcal{T}_1^-$, [001] A_1, [001] E_2, [011] A_1, [011] $B_{1,2}$, [111] A_1, [111] E_2, [002] A_1

all have an "extra" level near πK threshold.

$$k^3 \cot \delta_1 = (m_R^2 - s) \frac{6\pi s^{\frac{1}{2}}}{g_R^2}$$

Fitting the energy levels using an elastic Breit-Wigner in πK:

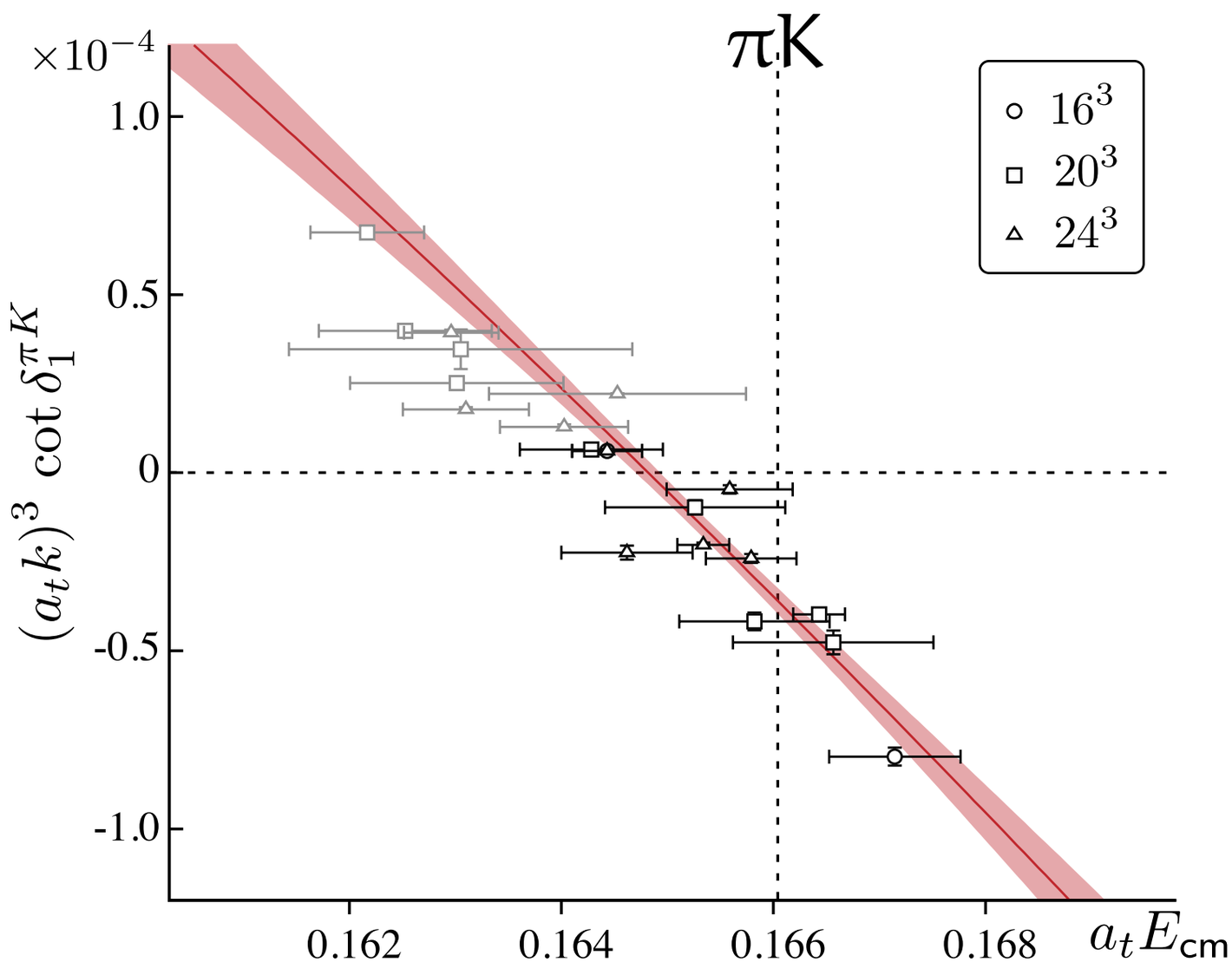

In t there is a pole on the real axis just below πK threshold:

Bound state in $\mathcal{J}^P = 1^-$

S+P-waves from 80 energy levels

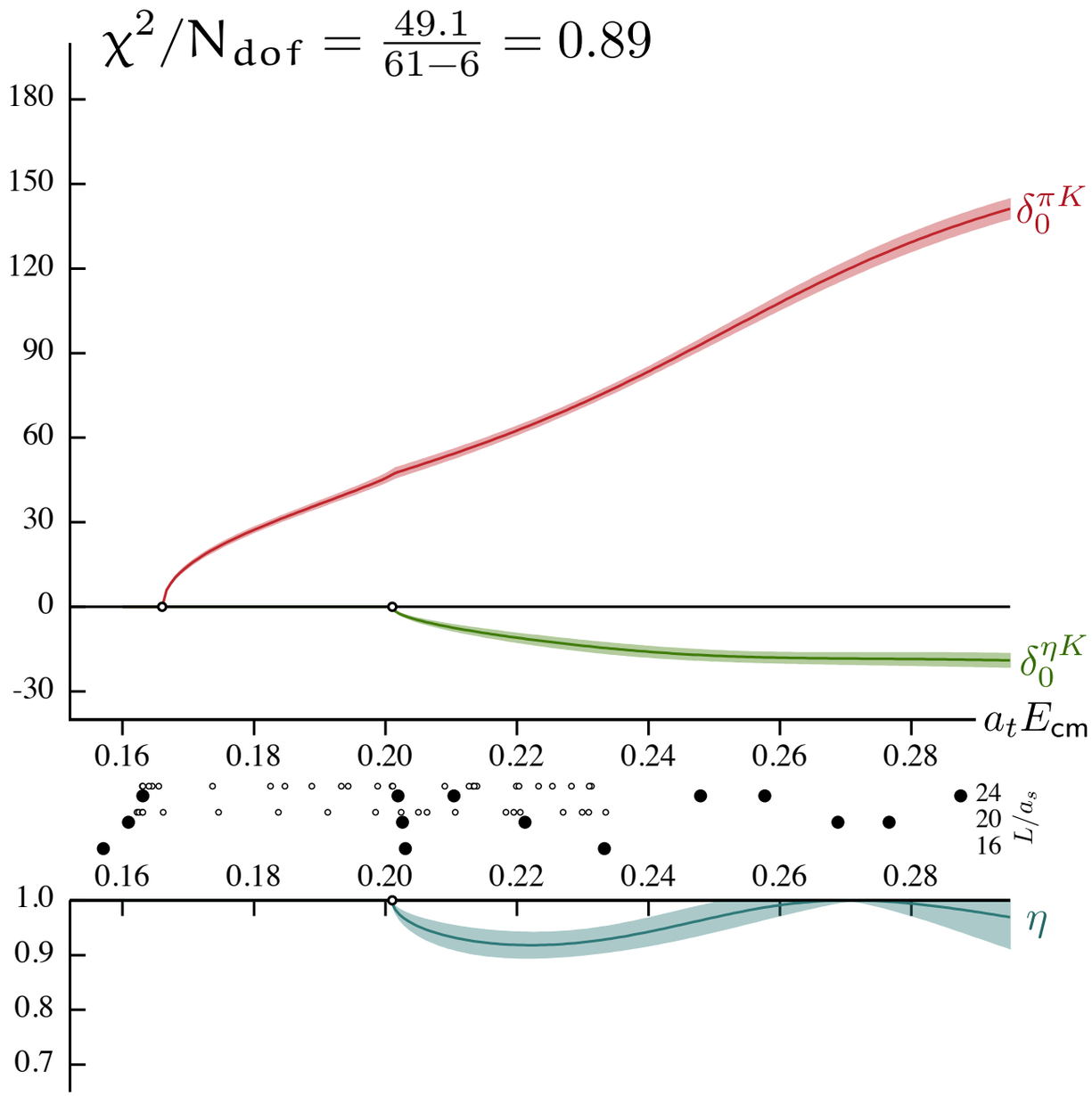

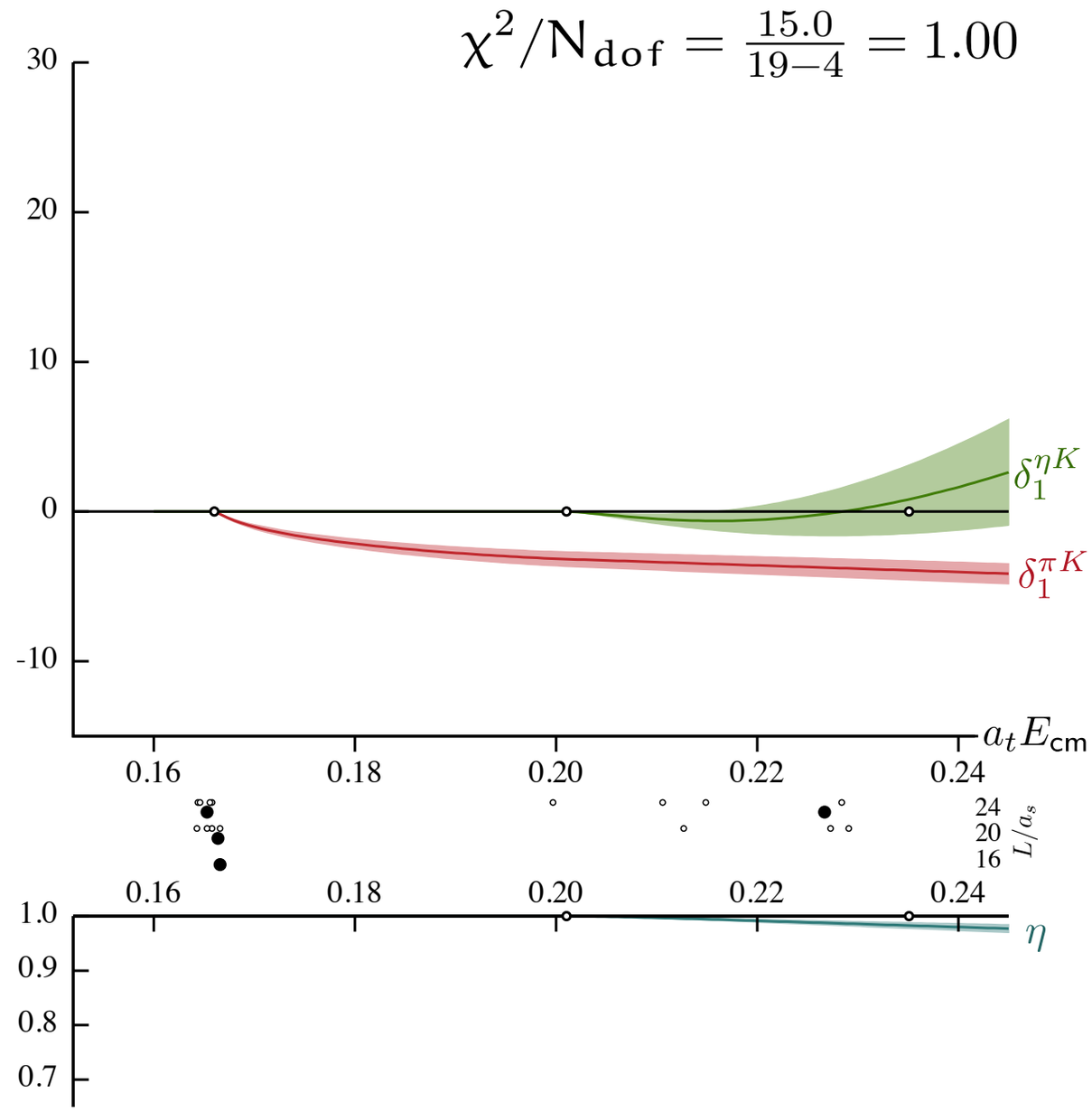

- Simple K-matrix parameterisations in S and P wave.
- Separate fits and global fits yield consistent results.
- D-wave is negligible in this region.

Parameterisation variation

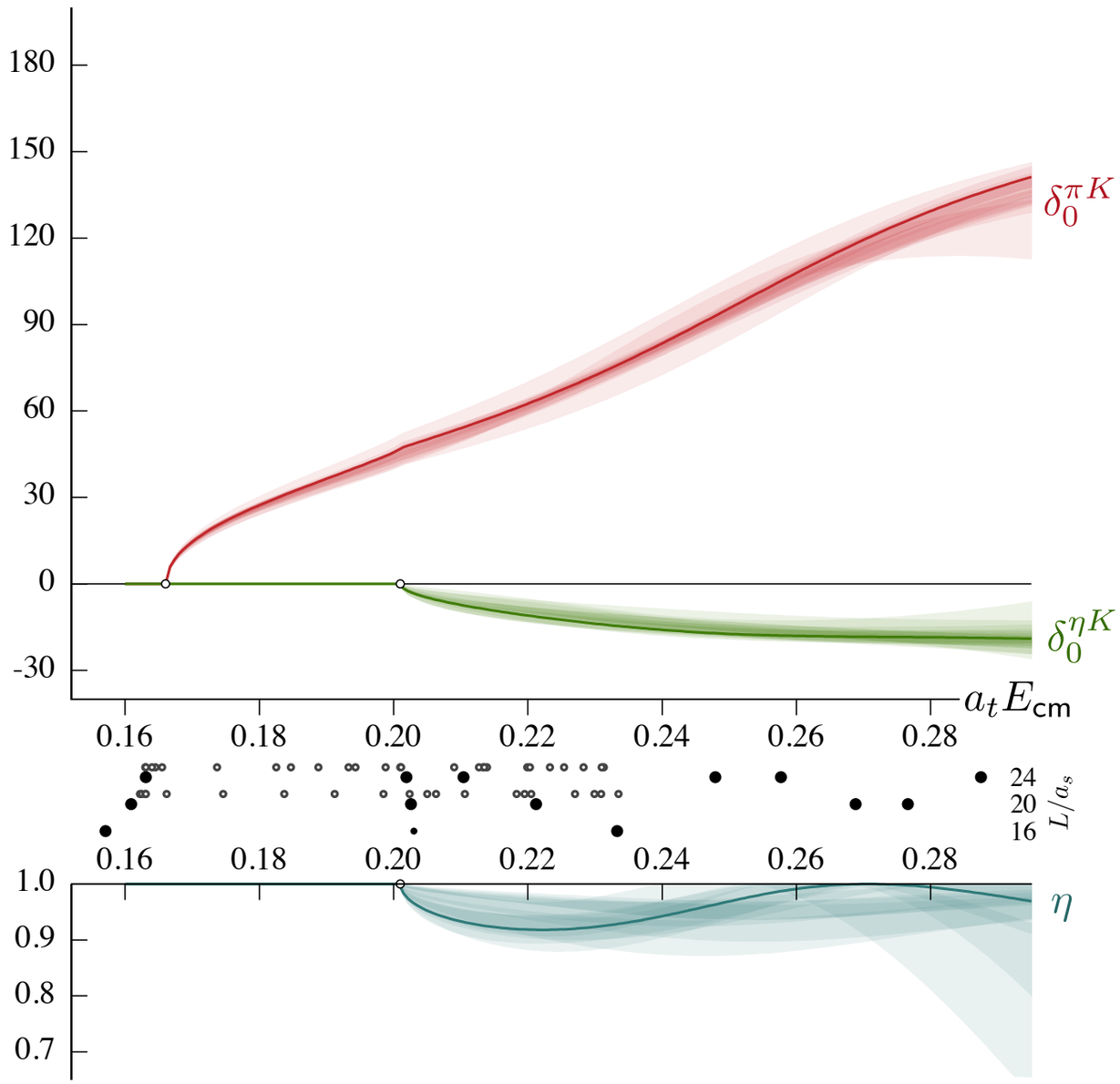

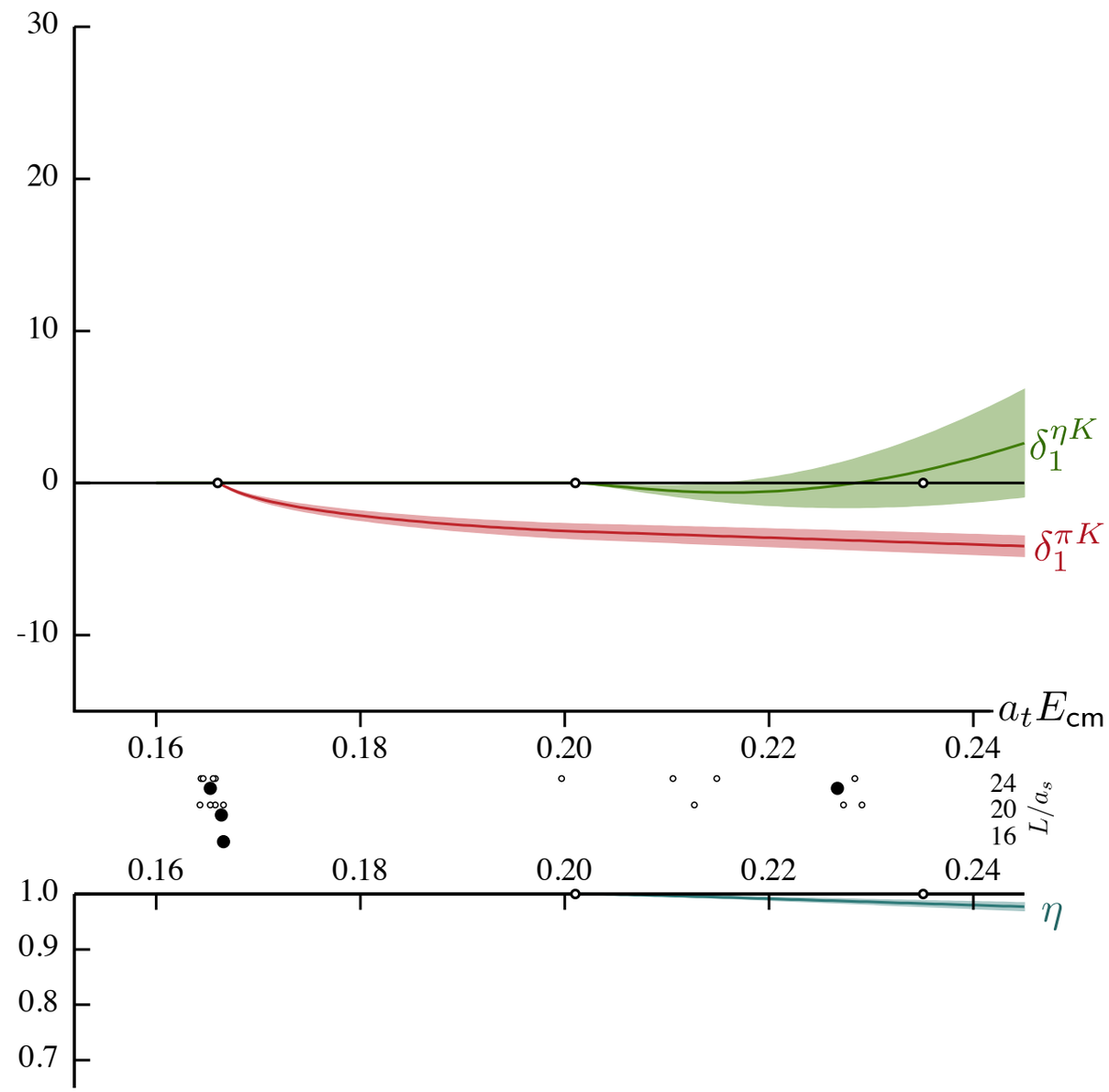

- Simple K-matrix parameterisations in S and P wave.
- Separate fits and global fits yield consistent results.
- D-wave is negligible in this region.

Narrow *D*-wave resonance

- Many other energy levels containing scattering amplitude information.
- Using only irreps with $\mathcal{J}$=2 and higher (E^+, T_2^+, [100]$B_{1,2}$) we find a narrow resonance:
- Fit to energies. Discrete points obtained in η→1 limit.
- In $\mathcal{J}\geq 1$ scattering the lowest threshold is $\pi\pi K$ at $a_t E_{cm}$=0.235.
- Ideally requires 3-body formalism. Although not strictly rigorous, we can apply the 2→2 formalism anyway.

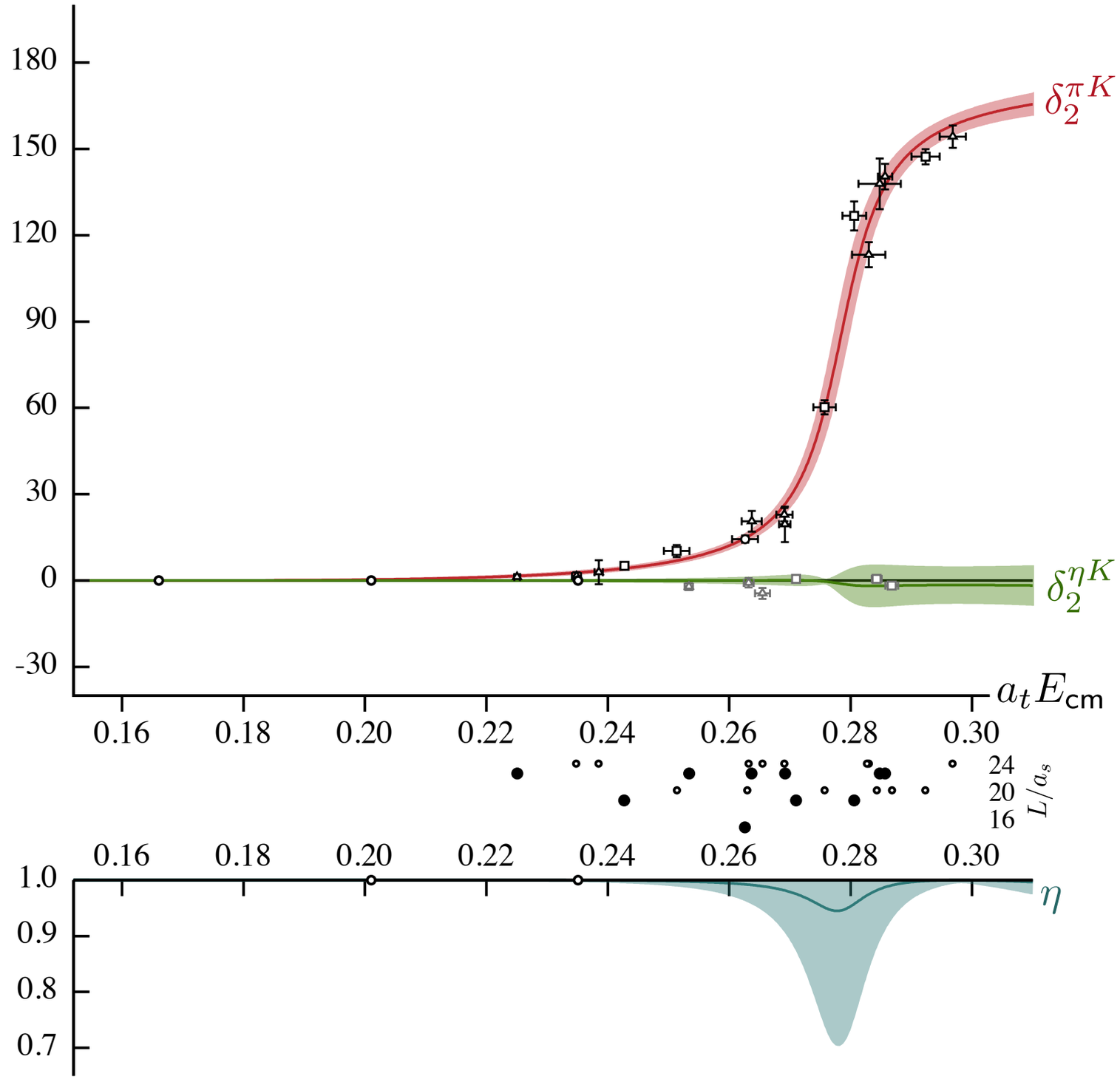

$$\chi^2/N_{\rm dof} = 1.31$$

Poles

Multi-sheeted complex plane due to square-root branch cuts at each threshold, in single channel case for now:

$$k_{cm} = \pm\frac{1}{2}\left(E_{cm}^2 - 4m^2\right)^{\frac{1}{2}}$$

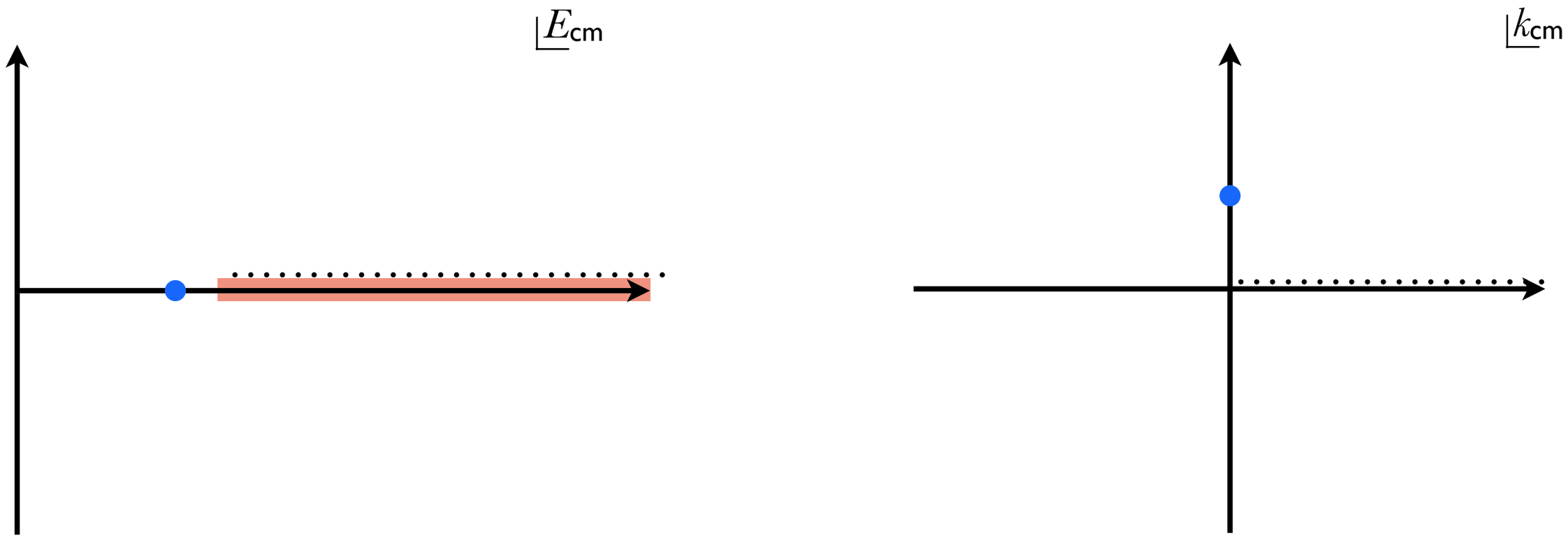

Bound state

Poles

Multi-sheeted complex plane due to square-root branch cuts at each threshold, in single channel case for now:

$$k_{cm} = \pm\frac{1}{2}\left(E_{cm}^2 - 4m^2\right)^{\frac{1}{2}}$$

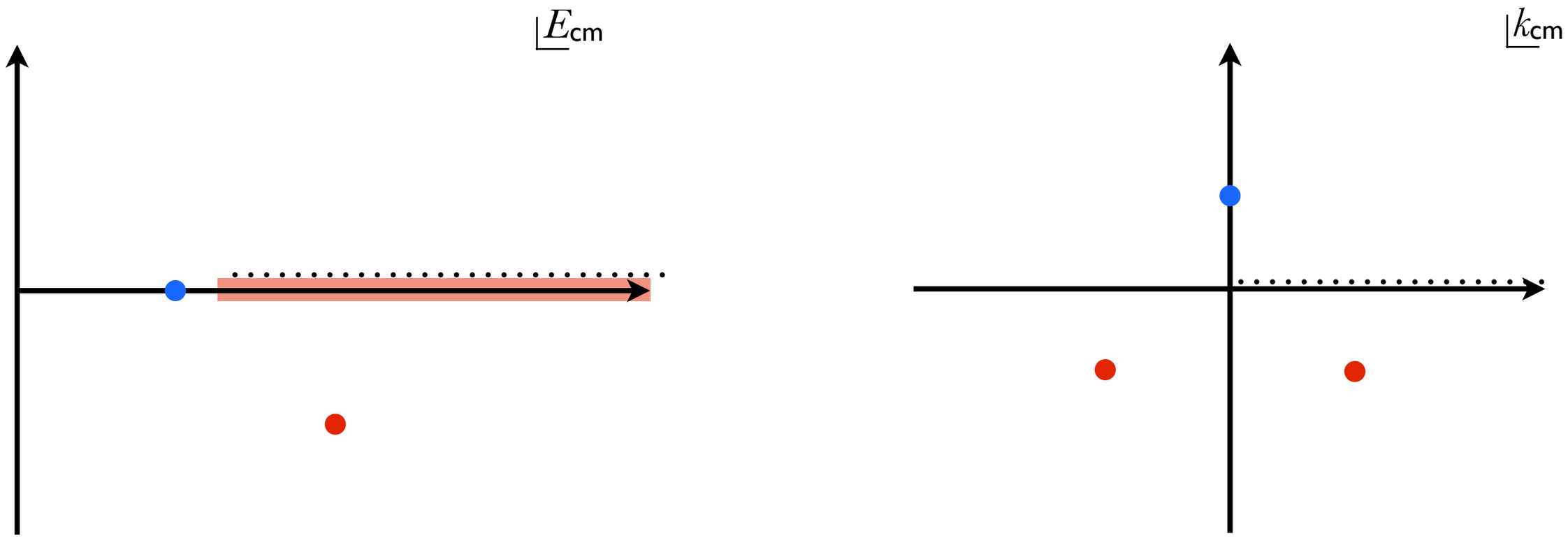

Bound state

Resonance

Poles

Multi-sheeted complex plane due to square-root branch cuts at each threshold, in single channel case for now:

$$k_{cm} = \pm\frac{1}{2}\left(E_{cm}^2 - 4m^2\right)^{\frac{1}{2}}$$

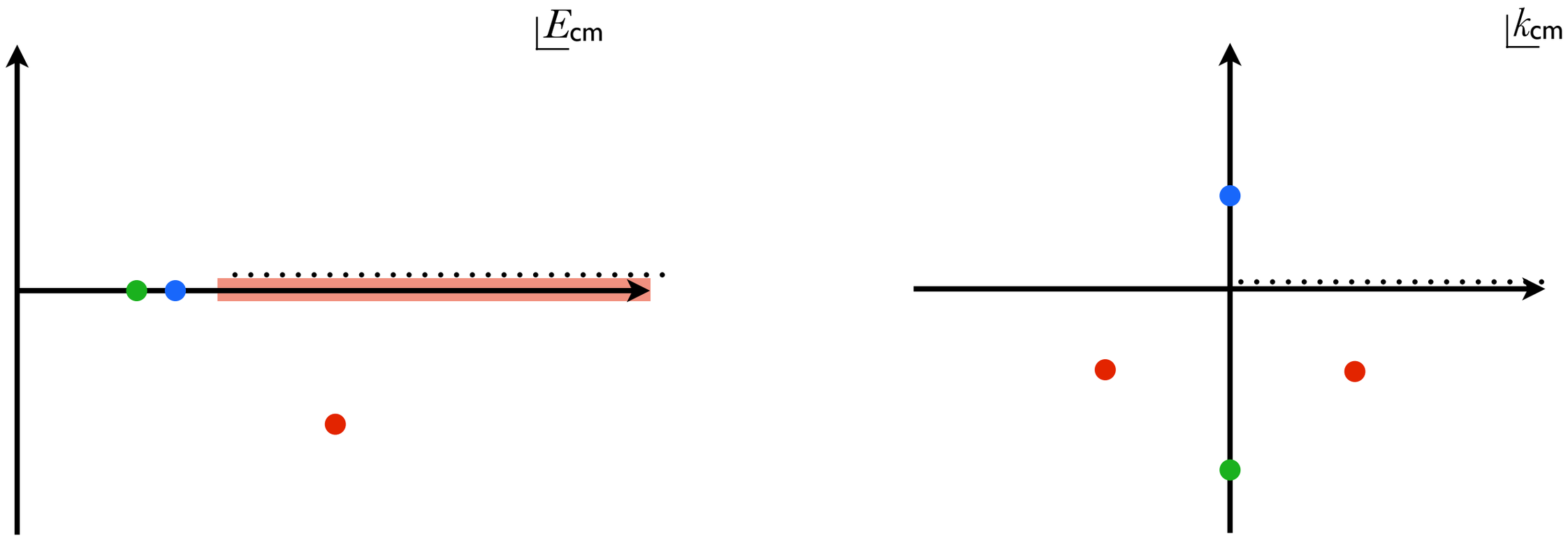

Bound state

Resonance

Virtual Bound state

S-matrix poles

Actual situation: Unequal masses and an extra pair of sheets due to ηK scattering

→ Poles and residues on multiple sheets.

$$k_{cm} = \pm\frac{1}{2}\left(E_{cm}^2 - 2\left(m_1^2 + m_2^2\right) + \frac{(m_1^2 - m_2^2)^2}{E_{cm}^2}\right)^{\frac{1}{2}}$$

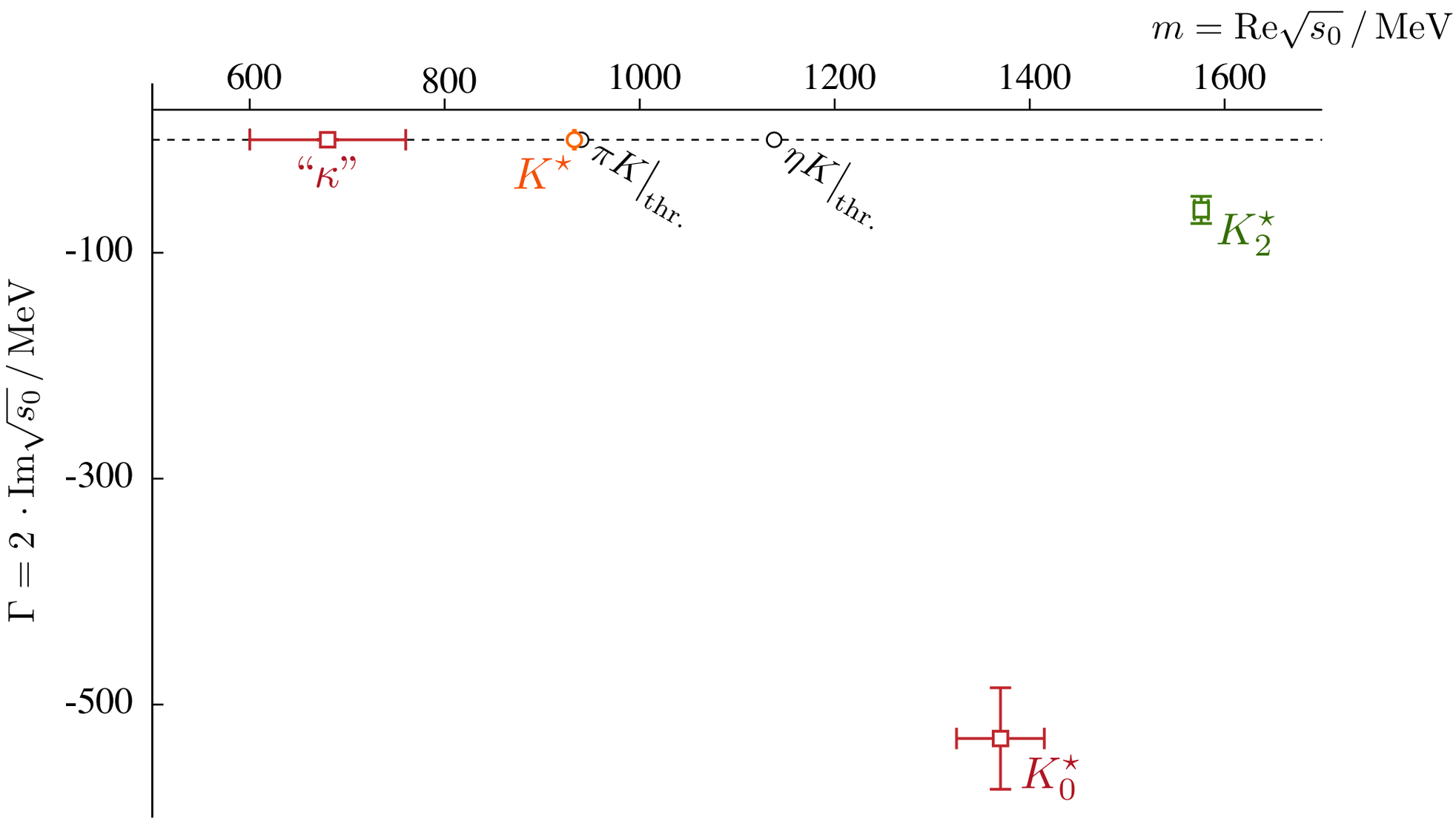

S-matrix poles

Actual situation: Unequal masses and an extra pair of sheets due to ηK scattering

→ Poles and residues on multiple sheets.

$$k_{cm} = \pm\frac{1}{2}\left(E_{cm}^2 - 2\left(m_1^2 + m_2^2\right) + \frac{(m_1^2 - m_2^2)^2}{E_{cm}^2}\right)^{\frac{1}{2}}$$

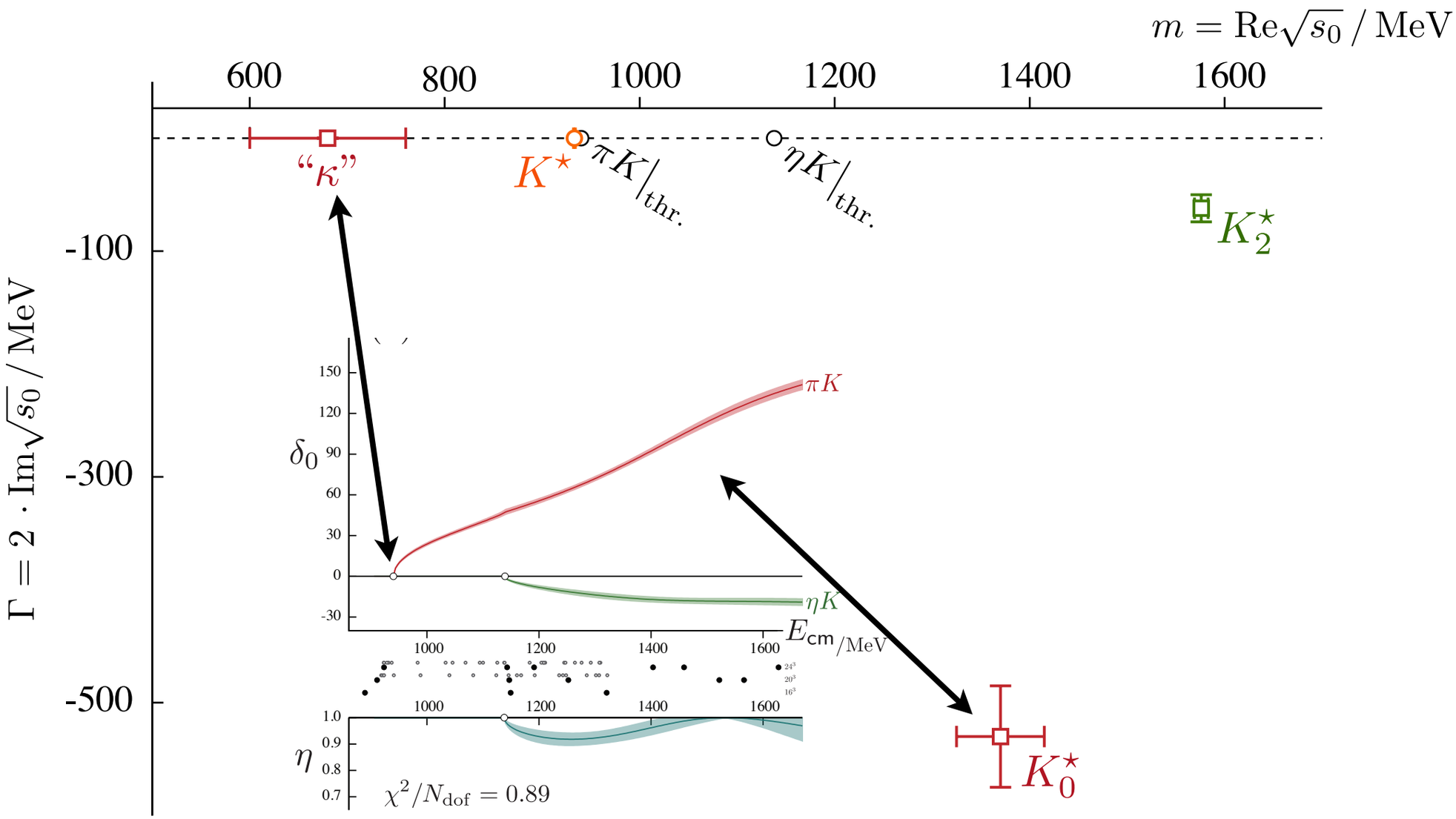

S-matrix poles

Actual situation: Unequal masses and an extra pair of sheets due to ηK scattering

→ Poles and residues on multiple sheets.

$$k_{cm} = \pm\frac{1}{2}\left(E_{cm}^2 - 2\left(m_1^2 + m_2^2\right) + \frac{(m_1^2 - m_2^2)^2}{E_{cm}^2}\right)^{\frac{1}{2}}$$

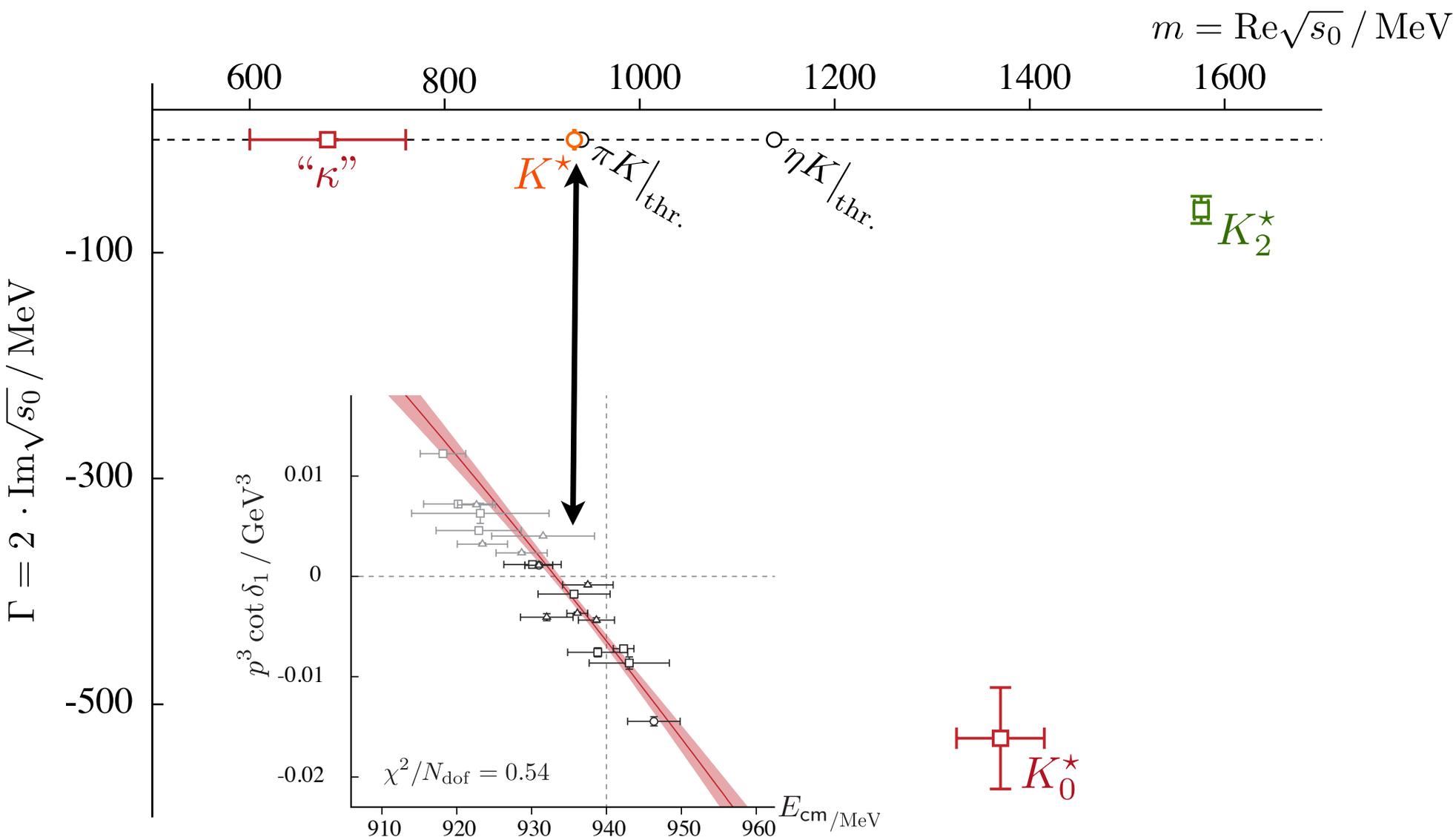

S-matrix poles

Actual situation: Unequal masses and an extra pair of sheets due to ηK scattering

→ Poles and residues on multiple sheets.

$$k_{cm} = \pm\frac{1}{2}\left(E_{cm}^2 - 2\left(m_1^2 + m_2^2\right) + \frac{(m_1^2 - m_2^2)^2}{E_{cm}^2}\right)^{\frac{1}{2}}$$

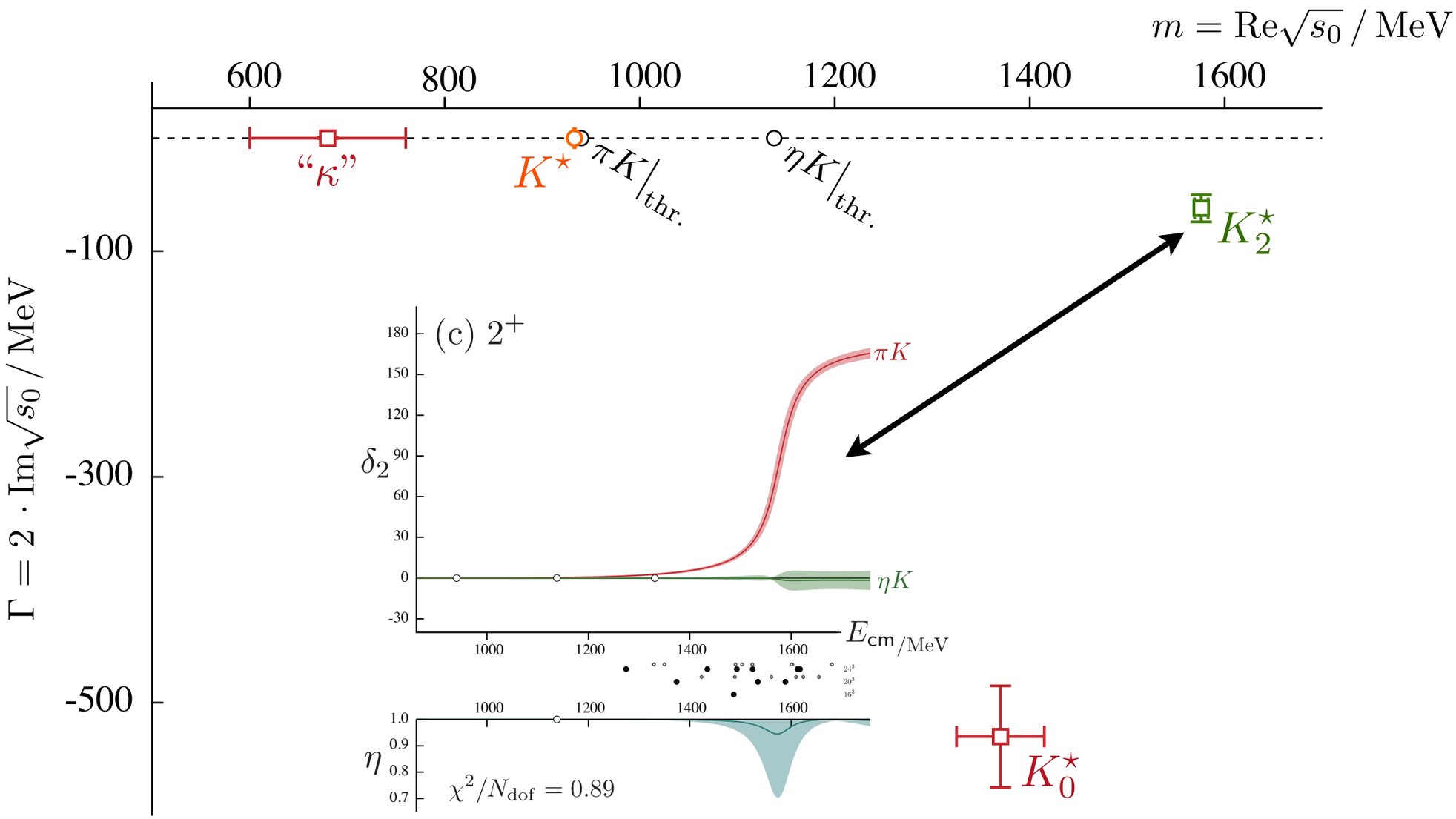

Summary

- Coupled-channel scattering amplitudes can be obtained from QCD using lattice methods.
- Using extensions of Lüscher's method, we were able to connect finite volume energy levels to infinite volume scattering amplitudes.
- There are many exciting possibilities for future calculations using similar methods:

  Strongly coupled systems like the $a_0(980)$ and $f_0(980)$ are under investigation.

  Investigations into $\pi\gamma \rightarrow \pi\pi$ and similar processes are underway.

  Channels involving charm quarks are also under investigation by European collaborators.
- Further in the future: $\pi N \rightarrow \pi N$, $\gamma N \rightarrow \pi N$. Multiparticle scattering, exotics.

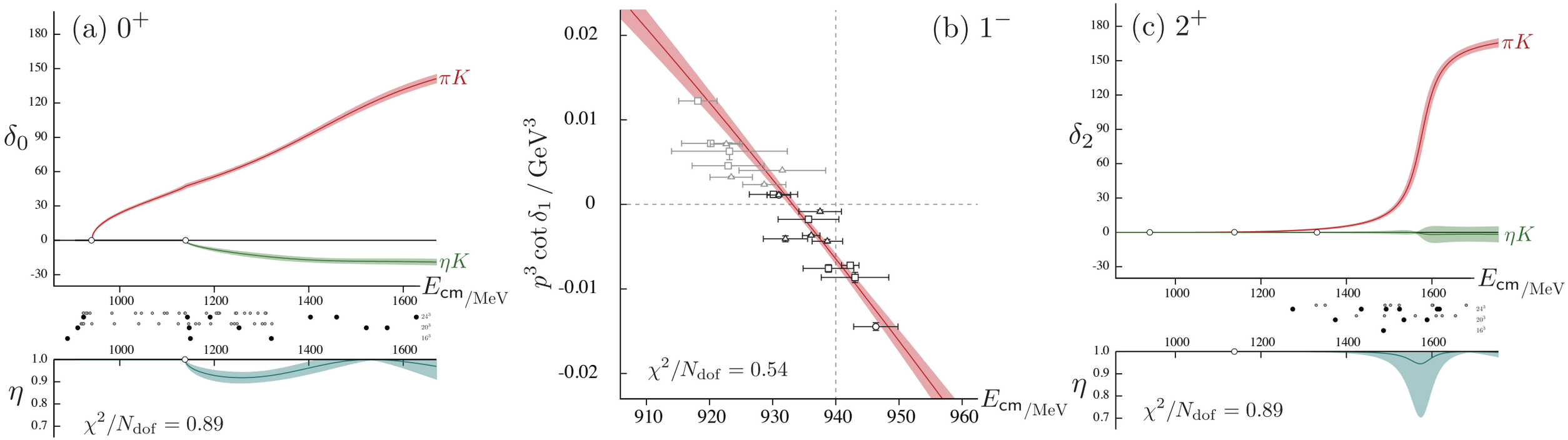

Light nuclei from lattice QCD

Takeshi Yamazaki

University of Tsukuba

K.-I. Ishikawa, Y. Kuramashi, and A. Ukawa

Refs: PRD81:111504(R)(2010); PRD84:054506(2011); PRD86:074514(2012)

Multi-Hadron and Nonlocal Matrix Elements in Lattice QCD

RIKEN BNL Research Center Workshop

@ Brookhaven National Laboratory, February 5–6 2015

Outline

1. Introduction
2. Problems of nuclei in lattice QCD
3. Simulation parameters
4. (Preliminary) Results
   - ^{4}He and ^{3}He channels
   - NN channels
5. Summary and future work

Introduction

$$\text{Binding force} \begin{cases} \text{protons and neutrons} \rightarrow \text{nuclei} \\ \text{quarks and gluons} \rightarrow \text{protons and neutrons} \end{cases}$$

both from fundamental strong interaction of quark and gluon

well known in experiment

Spectrum of nuclei

success of Shell model: Jensen and Mayer (1949)

degrees of freedom of protons and neutrons

Spectrum of proton and neutron (nucleons)

success of non-perturbative calculation of QCD

such as lattice QCD

degrees of freedom of quarks and gluons

$$\underbrace{\text{quarks and gluons} \rightarrow \overbrace{\text{protons and neutrons}}^{\text{Shell model}}}_{\text{lattice QCD}} \rightarrow \text{nuclei}$$

Introduction

$$\text{Binding force} \begin{cases} \text{protons and neutrons} \rightarrow \text{nuclei} \\ \text{quarks and gluons} \rightarrow \text{protons and neutrons} \end{cases}$$

both from fundamental strong interaction of quark and gluon

well known in experiment

Spectrum of nuclei

success of Shell model: Jensen and Mayer (1949)

degrees of freedom of protons and neutrons

Spectrum of proton and neutron (nucleons)

success of non-perturbative calculation of QCD

such as lattice QCD

degrees of freedom of quarks and gluons

goal: quantitatively understand property of nuclei from QCD

$$\underbrace{\text{quarks and gluons} \rightarrow \overbrace{\text{protons and neutrons} \rightarrow \text{nuclei}}^{\text{Shell model}}}_{\text{lattice QCD}}$$

Ultimate goal of lattice QCD

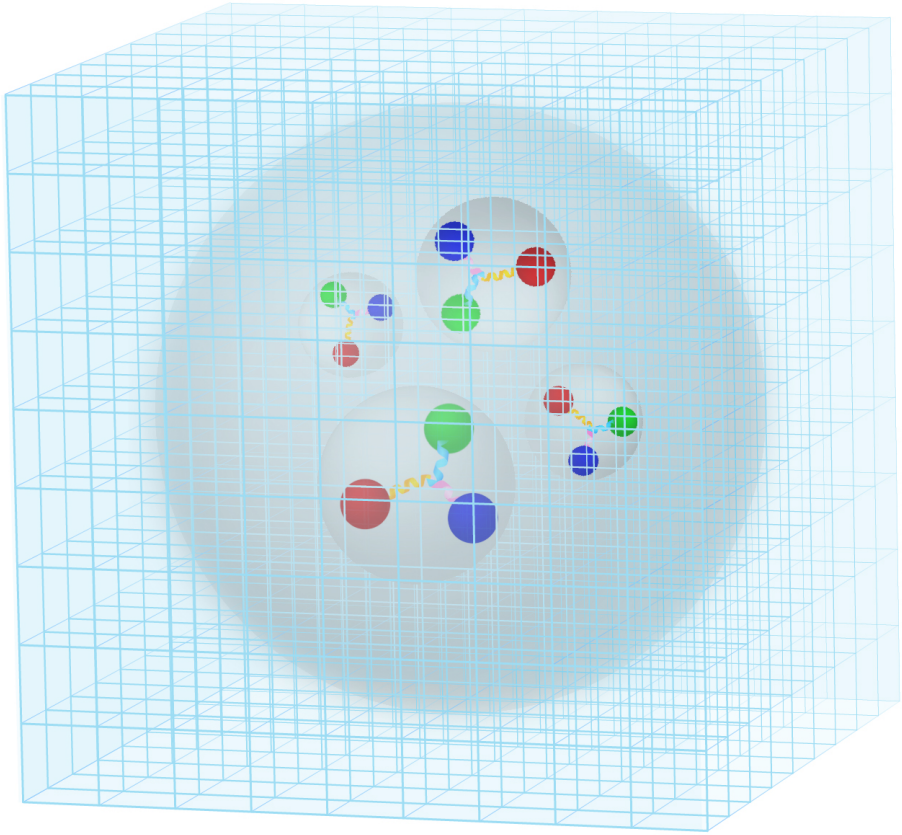

http://www.jicfus.jp/jp/promotion/pr/mj/2014-1/

quantitatively understand property of nuclei

from first principle of strong interaction

Introduction

Motivation :

Understand property of nuclei from QCD

If we can study nuclei from QCD, we may be able to

1. reproduce spectrum of nuclei
2. predict property of nuclei hard to calculate or observe

such as neutron rich nuclei

So far not so many works for multi-baryon bound states.
Before studying such difficult problems, we should study

$\rightarrow$ Can we reproduce known binding energy in light nuclei?

Multi-baryon bound state from lattice QCD

Not observed before '09 (except H-dibaryon '88 Iwasaki *et al.*)

1. ^{4}He and ^{3}He

   '10 PACS-CS $N_f = 0$ $m_\pi = 0.8$ GeV PRD81:111504(R)(2010)

Exploratory study of three- and four-nucleon systems

PACS-CS Collaboration, PRD81:111504(R)(2010)

Identification of bound state from volume dependence of ΔE

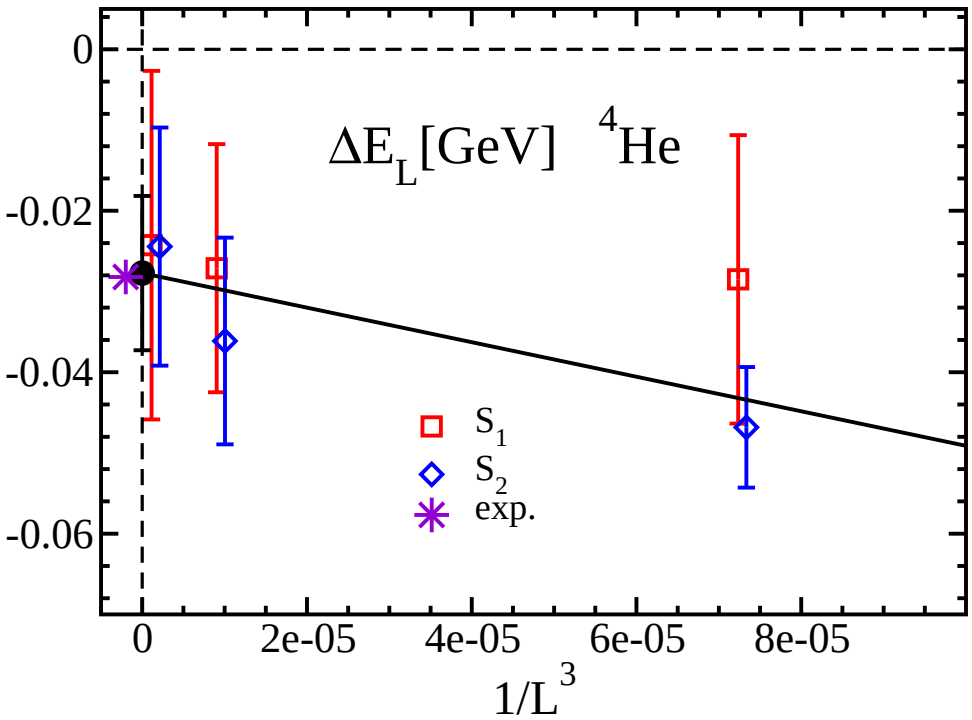

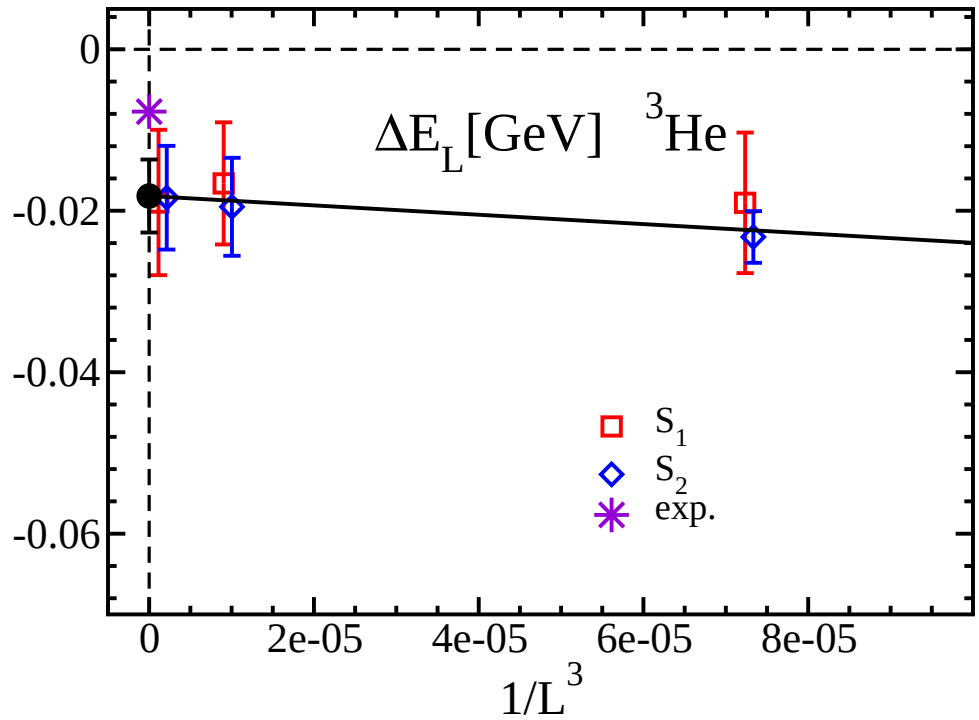

$\Delta E_{^4\mathrm{He}} = 27.7(7.8)(5.5)$ MeV $\qquad$ $\Delta E_{^3\mathrm{He}} = 18.2(3.5)(2.9)$ MeV

1. Observe bound state in both channels
2. Same order of ΔE to experiment

Several systematic errors included, e.g., $N_f = 0$, $m_\pi = 0.8$ GeV

Multi-baryon bound state from lattice QCD

Not calculated before '09 (except H-dibaryon '88 Iwasaki *et al.*)

1. ^{4}He and ^{3}He

   '10 PACS-CS $N_f = 0$ $m_\pi = 0.8$ GeV PRD81:111504(R)(2010)

   '12 HALQCD $N_f = 3$ $m_\pi = 0.47$ GeV, $m_\pi > 1$ GeV ^{4}He

   '12 NPLQCD $N_f = 3$ $m_\pi = 0.81$ GeV

   '12 TY *et al.* $N_f = 2 + 1$ $m_\pi = 0.51$ GeV PRD86:074514(2012)

2. H dibaryon in ΛΛ channel (S=−2, I=0)

   '11 NPLQCD $N_f = 2 + 1$ $m_\pi = 0.39$ GeV

   '11 HALQCD $N_f = 3$ $m_\pi = 0.67$–1.02 GeV

   '11 Luo et al. $N_f = 0$ $m_\pi = 0.5$–1.3 GeV

   '12 NPLQCD $N_f = 3$ $m_\pi = 0.81$ GeV

3. NN

   '11 PACS-CS $N_f = 0$ $m_\pi = 0.8$ GeV PRD84:054506(2011)

   '12 NPLQCD $N_f = 2 + 1$ $m_\pi = 0.39$ GeV (Possibility)

   '12 NPLQCD $N_f = 3$ $m_\pi = 0.81$ GeV

   '12 TY *et al.* $N_f = 2 + 1$ $m_\pi = 0.51$ GeV PRD86:074514(2012)

Other states: ΞΞ, '12 NPLQCD; spin-2 $N\Omega$, ^{16}O and ^{40}Ca, '14 HALQCD

Extend our works to $N_f = 2 + 1$ QCD with smaller m_π

Problems of multi-nucleon bound state

Traditional method for example ^{4}He channel

$$\langle 0|O_{^4\mathrm{He}}(t)O^\dagger_{^4\mathrm{He}}(0)|0\rangle = \sum_n \langle 0|O_{^4\mathrm{He}}|n\rangle\langle n|O^\dagger_{^4\mathrm{He}}|0\rangle e^{-E_n t} \xrightarrow[t\gg 1]{} A_0\, e^{-E_0 t}$$

Difficulties for multi-nucleon calculation

1. Statistical error

Statistical error $\propto \exp\left(N_N\left[m_N - \frac{3}{2}m_\pi\right]t\right)$

2. Calculation cost

Wick contraction for ^{4}He $= p^2n^2 = (udu)^2(dud)^2$: 518400

proton $= p = (udu)$: 2

3. Identification of bound state on finite volume

Finite volume effect of attractive scattering state

$$\Delta E_L = E_0 - N_N m_N = O(L^{-3}) < 0 \leftrightarrow \text{binding energy}$$

Problems of multi-nucleon bound state

Traditional method for example ^{4}He channel

$$\langle 0|O_{^4\mathrm{He}}(t)O^\dagger_{^4\mathrm{He}}(0)|0\rangle = \sum_n \langle 0|O_{^4\mathrm{He}}|n\rangle\langle n|O^\dagger_{^4\mathrm{He}}|0\rangle e^{-E_n t} \xrightarrow[t\gg 1]{} A_0\, e^{-E_0 t}$$

Difficulties for multi-nucleon calculation

1. Statistical error

Statistical error $\propto \exp\left(N_N\left[m_N - \frac{3}{2}m_\pi\right]t\right)$

2. Calculation cost

Wick contraction for ^{4}He $= p^2n^2 = (udu)^2(dud)^2$: 518400

proton $= p = (udu)$: 2

Most severe problem before '09: (every t)$\times N_{\mathrm{meas}} \sim O(10^6)$

3. Identification of bound state on finite volume

Finite volume effect of attractive scattering state

$$\Delta E_L = E_0 - N_N m_N = O(L^{-3}) < 0 \leftrightarrow \text{binding energy}$$

Problems of multi-nucleon bound state

Traditional method for example ^{4}He channel

$$\langle 0|O_{^4\mathrm{He}}(t)O^\dagger_{^4\mathrm{He}}(0)|0\rangle = \sum_n \langle 0|O_{^4\mathrm{He}}|n\rangle\langle n|O^\dagger_{^4\mathrm{He}}|0\rangle e^{-E_n t} \xrightarrow[t\gg 1]{} A_0\, e^{-E_0 t}$$

Difficulties for multi-nucleon calculation

1. Statistical error

Statistical error $\propto \exp\left(N_N\left[m_N - \frac{3}{2}m_\pi\right]t\right)$

$\rightarrow$ heavy quark $m_\pi = 0.8$–0.3 GeV + large # of measurements

2. Calculation cost PACS-CS PRD81:111504(R)(2010)

Wick contraction for ^{4}He $= p^2n^2 = (udu)^2(dud)^2$: 518400 $\rightarrow$ 1107

$\rightarrow$ reduction using $p(n) \leftrightarrow p(n)$ $p \leftrightarrow n$, $u(d) \leftrightarrow u(d)$ in $p(n)$

Multi-meson: '10 Detmold and Savage

Multi-baryon: '12 Doi and Endres; Detmold and Orginos; '13 Günther et al.

3. Identification of bound state on finite volume

attractive scattering state $\Delta E_L = E_0 - N_N m_N = O(L^{-3}) < 0$

'86,'91 Lüscher, '07 Beane *et al.*

$\rightarrow$ Volume dependence of $\Delta E_L \rightarrow \Delta E_\infty \neq 0 \rightarrow$ bound state

Spectral weight: '04 Mathur *et al.*, Anti-PBC '05 Ishii *et al.*

Problems of multi-nucleon bound state

Traditional method for example ^{4}He channel

$$\langle 0|O_{^4\mathrm{He}}(t)O^\dagger_{^4\mathrm{He}}(0)|0\rangle = \sum_n \langle 0|O_{^4\mathrm{He}}|n\rangle\langle n|O^\dagger_{^4\mathrm{He}}|0\rangle e^{-E_n t} \xrightarrow[t\gg 1]{} A_0\, e^{-E_0 t}$$

Difficulties for multi-nucleon calculation

1. Statistical error

Statistical error $\propto \exp\left(N_N\left[m_N - \frac{3}{2}m_\pi\right]t\right)$

Most severe problem

2. Calculation cost

Wick contraction for ^{4}He $= p^2n^2 = (udu)^2(dud)^2$: 518400

proton $= p = (udu)$: 2

Used to be most severe problem

3. Identification of bound state on finite volume

Finite volume effect of attractive scattering state

$$\Delta E_L = E_0 - N_N m_N = O(L^{-3}) < 0 \leftrightarrow \text{binding energy}$$

Simulation parameters

$N_f = 2 + 1$ QCD

Iwasaki gauge action at $\beta = 1.90$

$a^{-1} = 2.194$ GeV with $m_\Omega = 1.6725$ GeV '10 PACS-CS

non-perturbative $O(a)$-improved Wilson fermion action

$m_\pi = 0.51$ GeV and $m_N = 1.32$ GeV PRD86:074514(2012)

$m_\pi = 0.30$ GeV and $m_N = 1.05$ GeV arXiv:150X.XXXX

$m_s \sim$ physical strange quark mass

^{4}He, ^{3}He, NN($^3S_1$ and $^1S_0$)

		$m_\pi = 0.5$ GeV		$m_\pi = 0.3$ GeV		R
L	L [fm]	N_{conf}	N_{meas}	N_{conf}	N_{meas}	
32	2.9	200	192			
40	3.6	200	192			
48	4.3	200	192	400	1152	12
64	5.8	190	256	160	1536	5

$R = (N_{\text{conf}} \cdot N_{\text{meas}})_{0.3\text{GeV}} / (N_{\text{conf}} \cdot N_{\text{meas}})_{0.5\text{GeV}}$

Computational resources

PACS-CS, T2K-Tsukuba, HA-PACS, COMA at Univ. of Tsukuba

T2K-Tokyo and FX10 at Univ. of Tokyo, and K at AICS

Results

Effective mass of nucleon on $L = 5.8$ fm

$$\text{Effective } m_N = \log\left(\frac{C_N(t)}{C_N(t+1)}\right)$$

$m_\pi = 0.5$ GeV

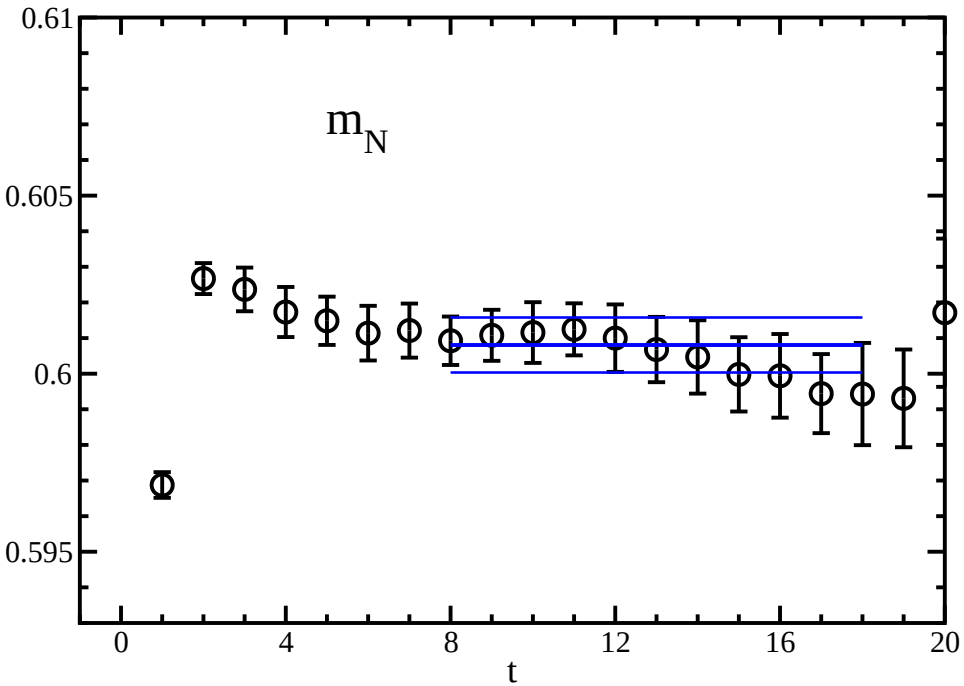

$m_\pi = 0.3$ GeV

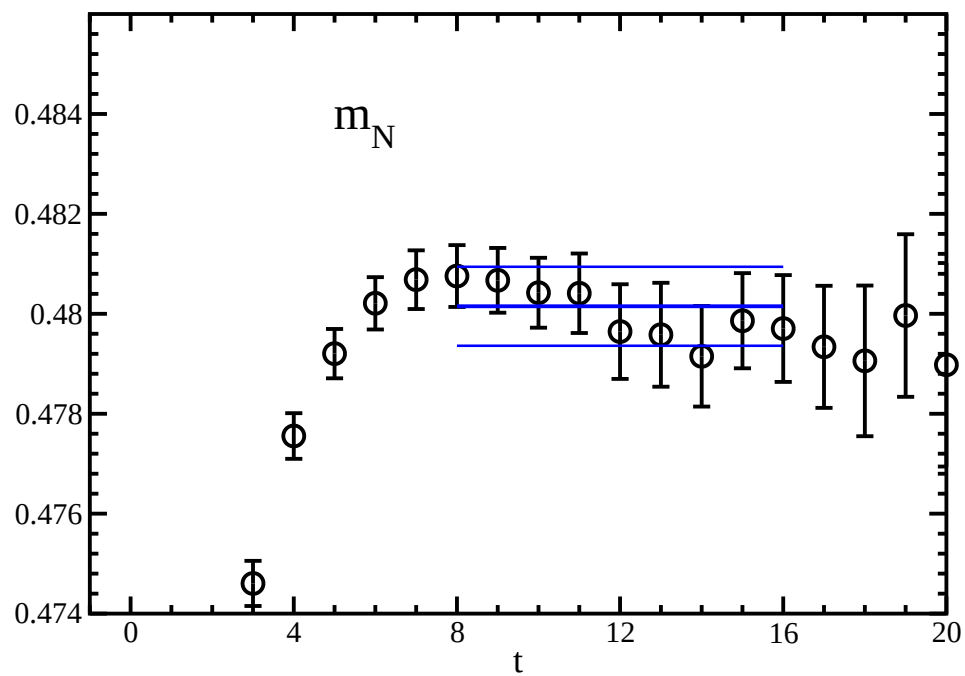

- Good plateau $t \gtrsim 7$
- Statistical error $< 0.2\%$

$\Delta E_L = E_0 - N_N m_N$ in ^{4}He and ^{3}He channels

at $m_\pi = 0.5$ GeV on $L = 5.8$ fm

TY *et al.*, PRD86:074514(2012)

$$\Delta E_L = \log\left(\frac{R_{^4\mathrm{He}}(t)}{R_{^4\mathrm{He}}(t+1)}\right) \text{ with } R_{^4\mathrm{He}}(t) = \frac{C_{^4\mathrm{He}}(t)}{(C_N(t))^4}$$

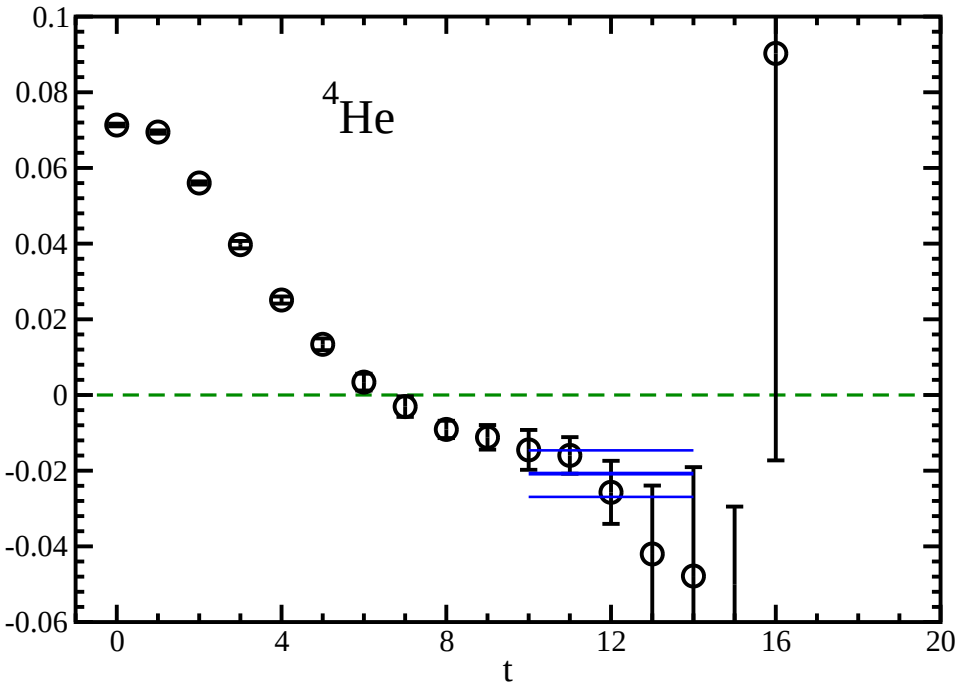

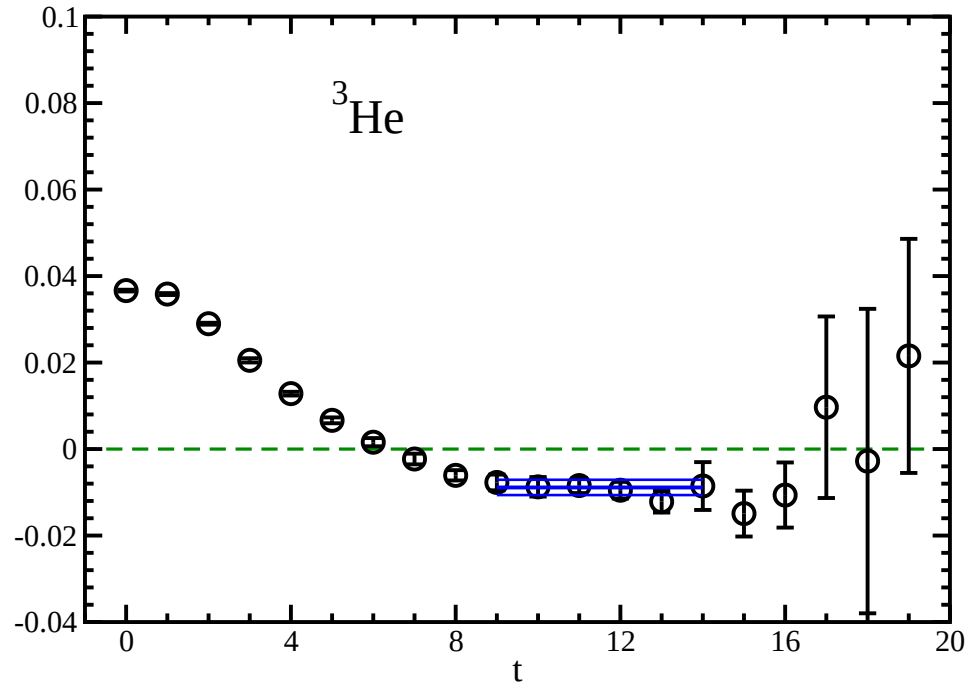

- Larger error in ^{4}He channel
- Statistical error under control in $t < 12$
- Negative ΔE_L in both channels

^{4}He and ^{3}He channels $\Delta E_L = E_0 - N_N m_N$ at $m_\pi = 0.5$ GeV

TY *et al.*, PRD86:074514(2012)

Identification of bound state from volume dependence of ΔE

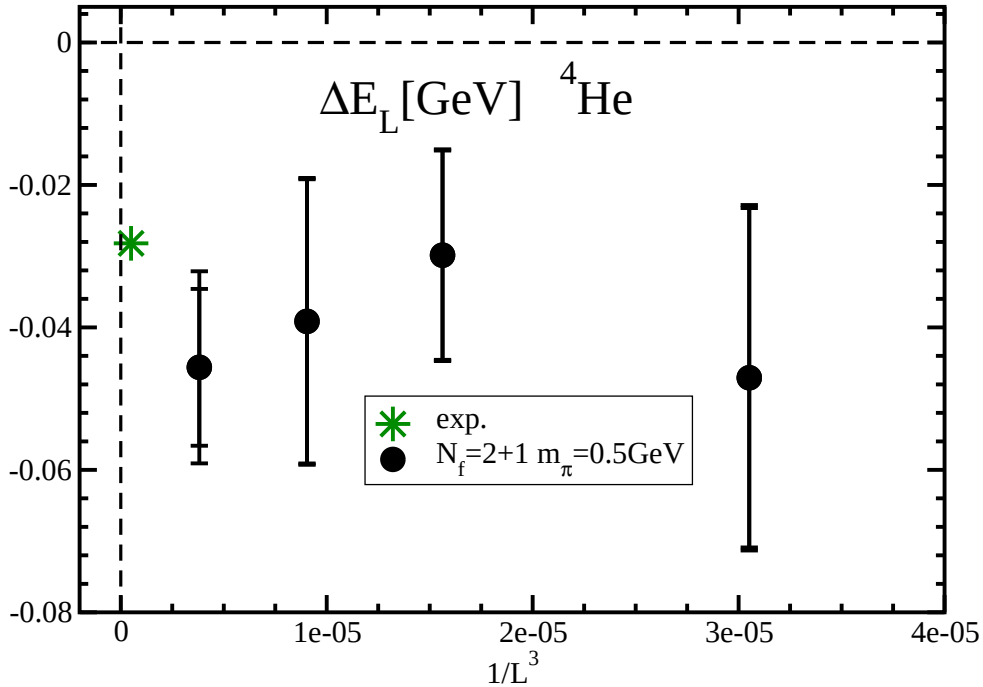

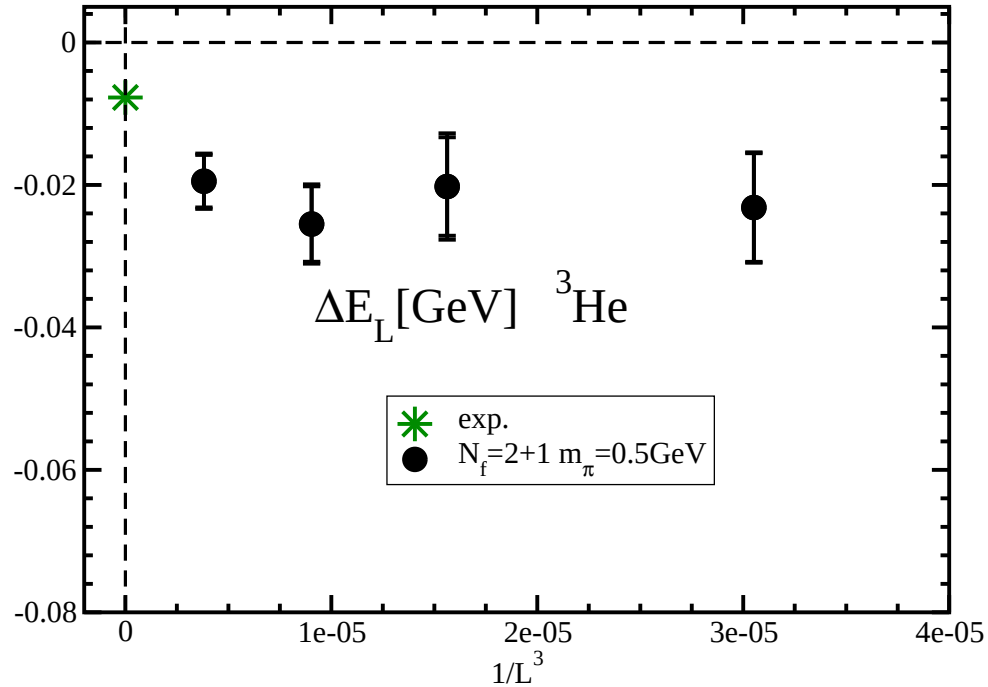

- $\Delta E_L < 0$ and mild volume dependence
- Infinite volume extrapolation with $\Delta E_L = -\Delta E_{\text{bind}} + C/L^3$

^{4}He and ^{3}He channels $\Delta E_L = E_0 - N_N m_N$ at $m_\pi = 0.5$ GeV

TY *et al.*, PRD86:074514(2012)

Identification of bound state from volume dependence of ΔE

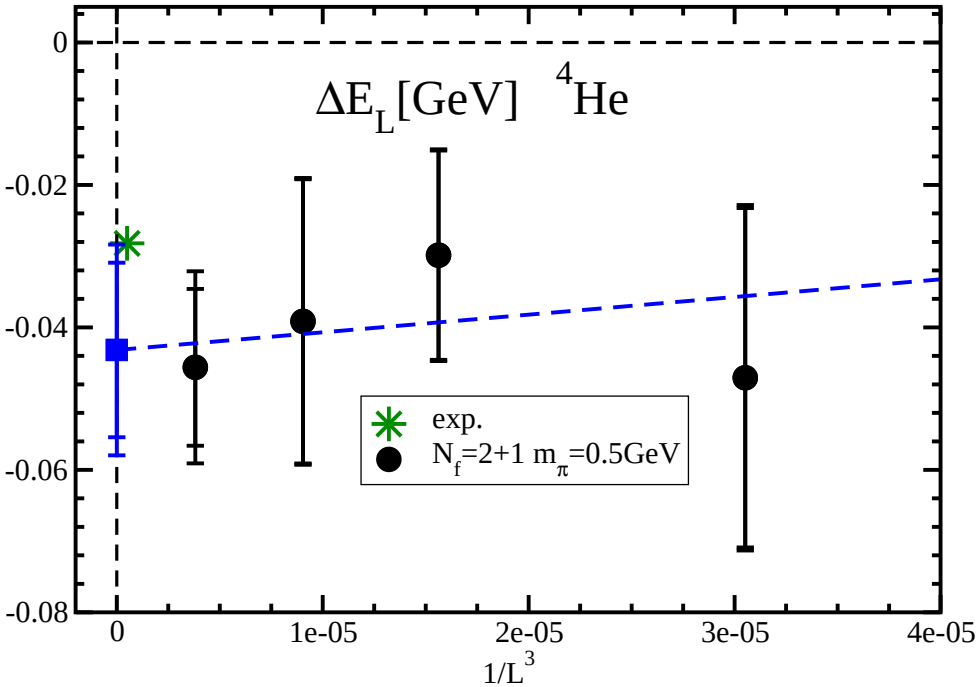

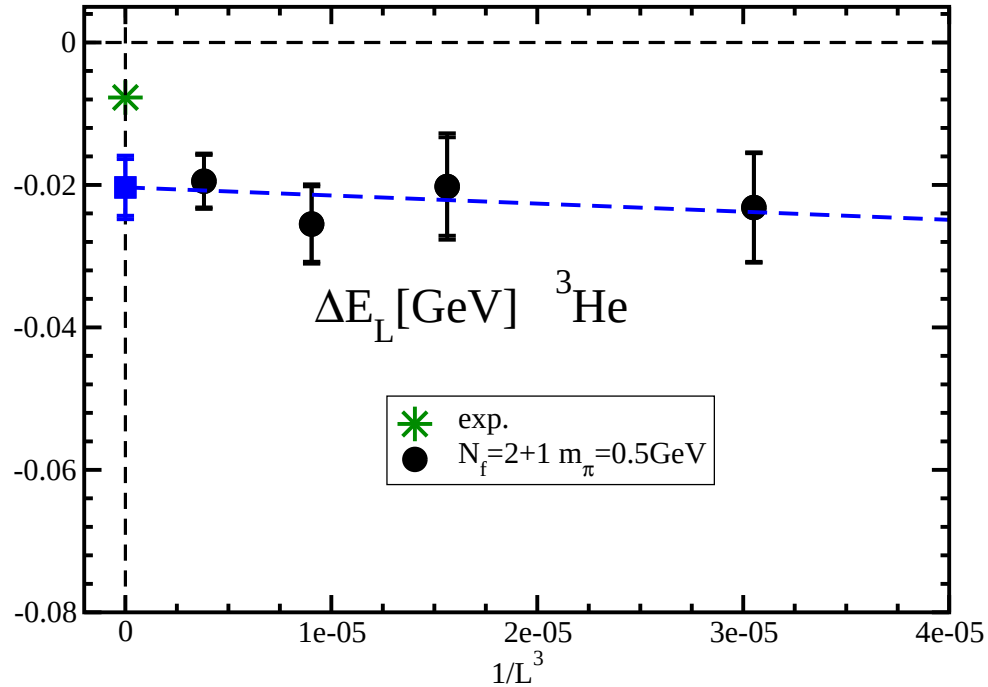

$\Delta E_{^4\mathrm{He}} = 43(12)(8)$ MeV

$\Delta E_{^3\mathrm{He}} = 20.3(4.0)(2.0)$ MeV

Observe bound state in both channels

ΔE_L in 2-nucleon channels at $m_\pi = 0.5$ GeV on $L = 5.8$ fm

TY *et al.*, PRD86:074514(2012)

$$\Delta E_L = \log\left(\frac{R_{\rm NN}(t)}{R_{\rm NN}(t+1)}\right) \text{ with } R_{\rm NN}(t) = \frac{C_{\rm NN}(t)}{(C_N(t))^2}$$

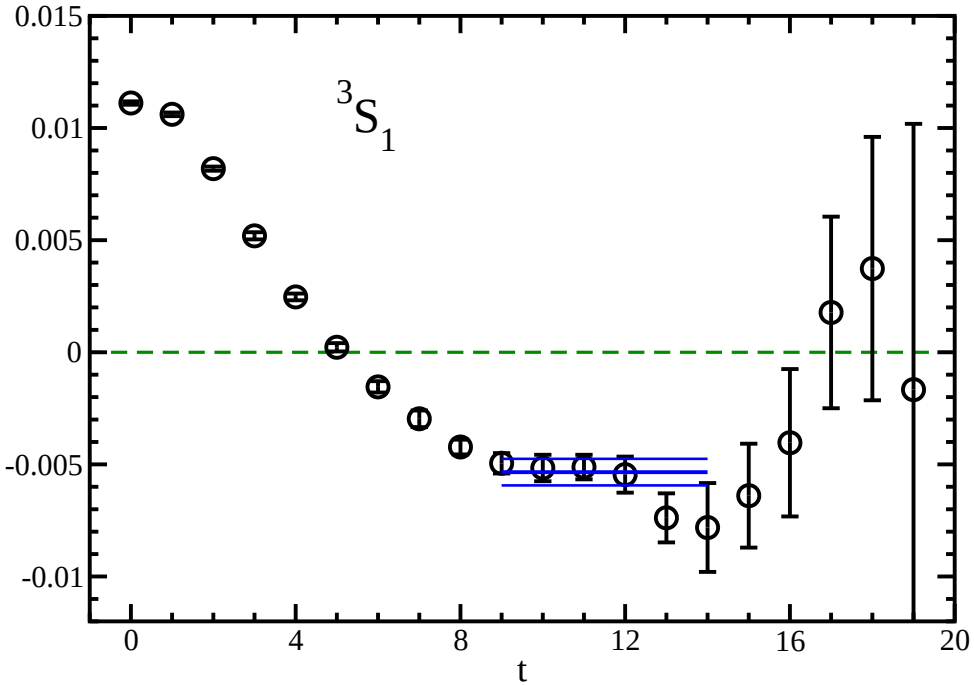

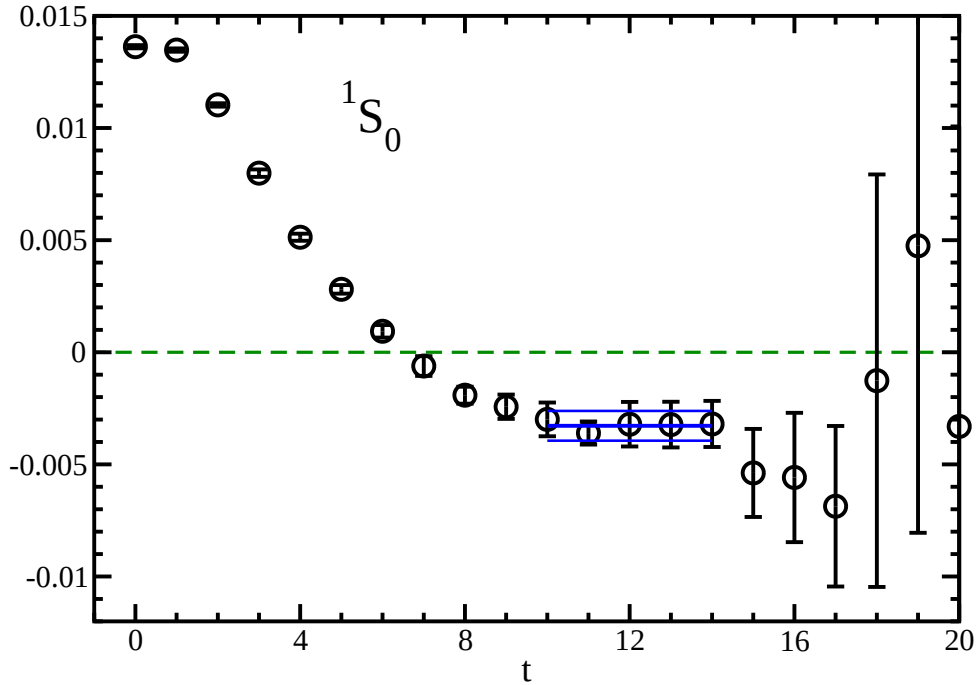

- Statistical error under control in $t \leq 12$
- Smaller error than ^{4}He and ^{3}He channels
- Negative ΔE_L in both channels

NN ($^3S_1$ and $^1S_0$) channels $\Delta E_L = E_0 - 2m_N$ at $m_\pi = 0.5$ GeV

TY *et al.*, PRD86:074514(2012)

Identification of bound state from volume dependence of ΔE

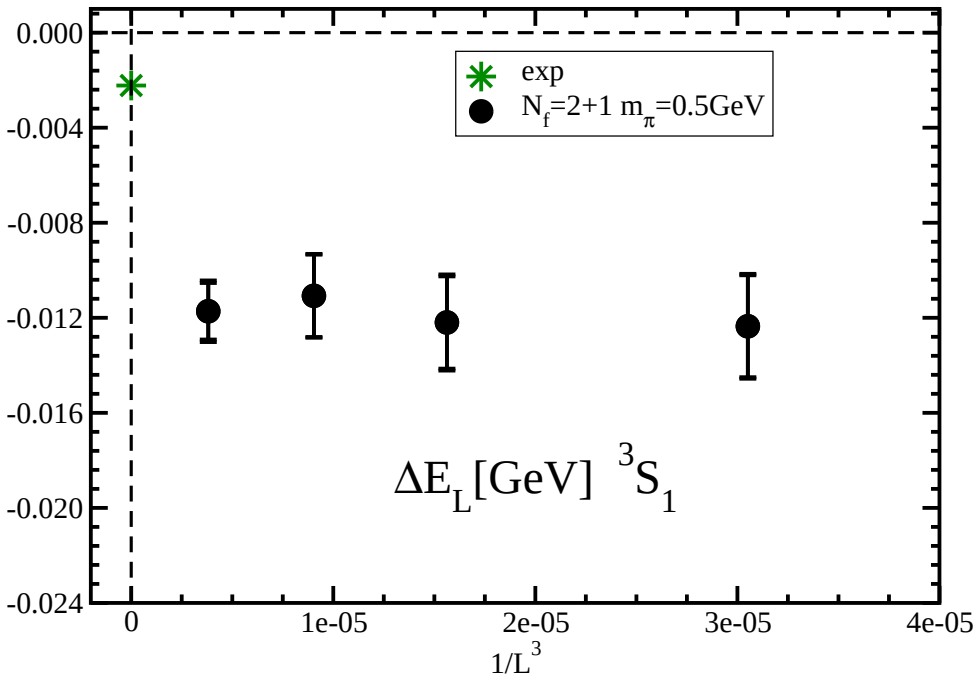

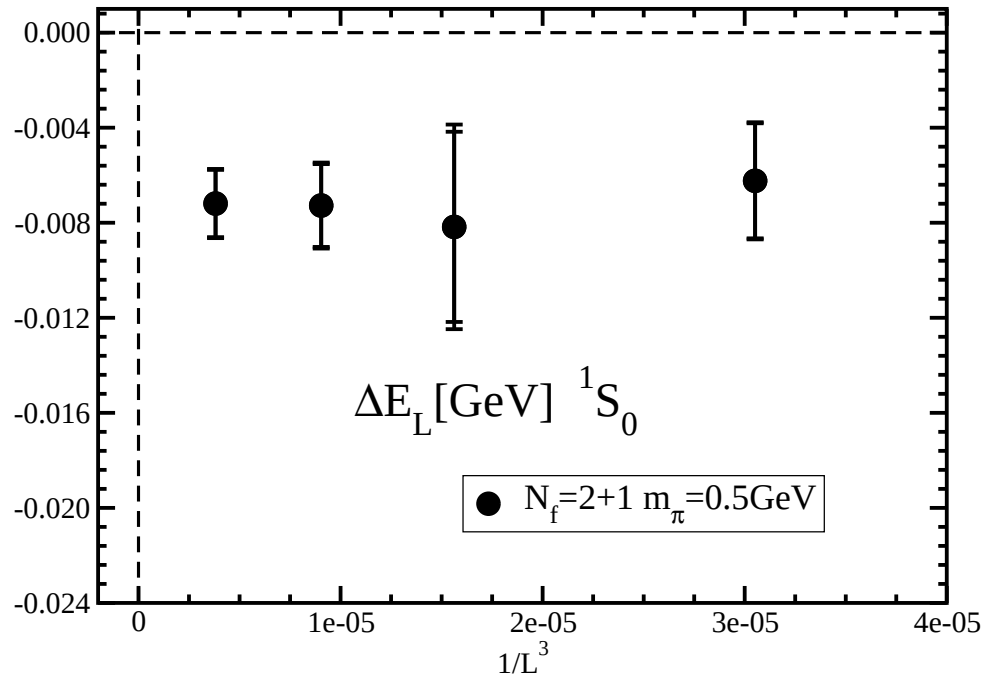

- Negative ΔE_L
- Infinite volume extrapolation of ΔE_L '04 Beane *et al.*, '06 Sasaki & TY

$$\Delta E_L = -\frac{\gamma^2}{m_N}\left\{1 + \frac{C_\gamma}{\gamma L}\sum_{\vec{n}}{}' \frac{\exp(-\gamma L\sqrt{\vec{n}^2})}{\sqrt{\vec{n}^2}}\right\}, \quad \Delta E_{\text{bind}} = \frac{\gamma^2}{m_N}$$

based on Lüscher's finite volume formula

NN ($^3S_1$ and $^1S_0$) channels $\Delta E_L = E_0 - 2m_N$ at $m_\pi = 0.5$ GeV

TY *et al.*, PRD86:074514(2012)

Identification of bound state from volume dependence of ΔE

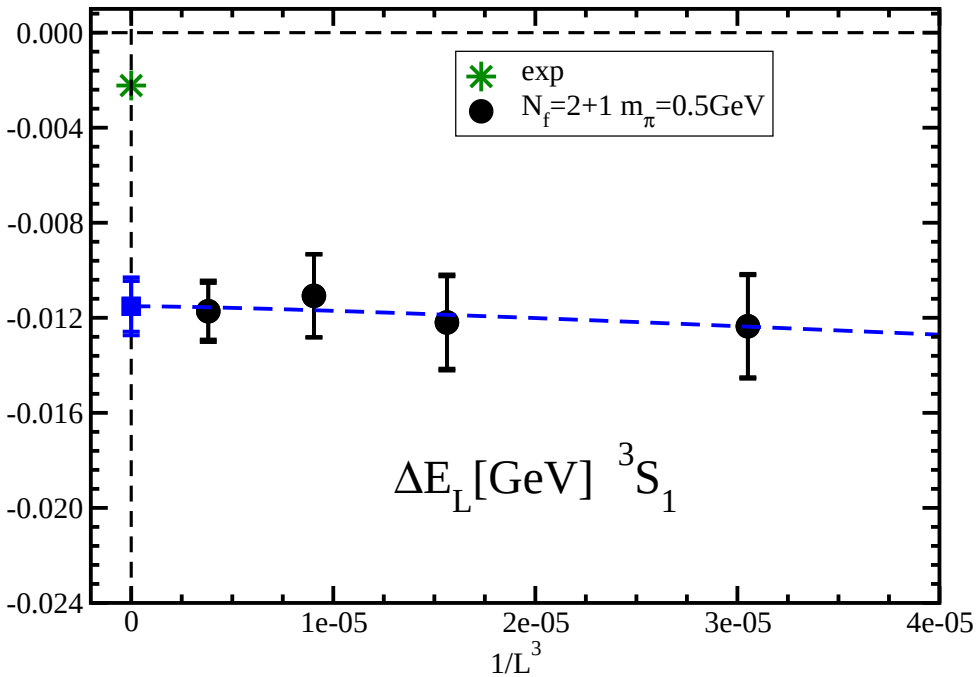

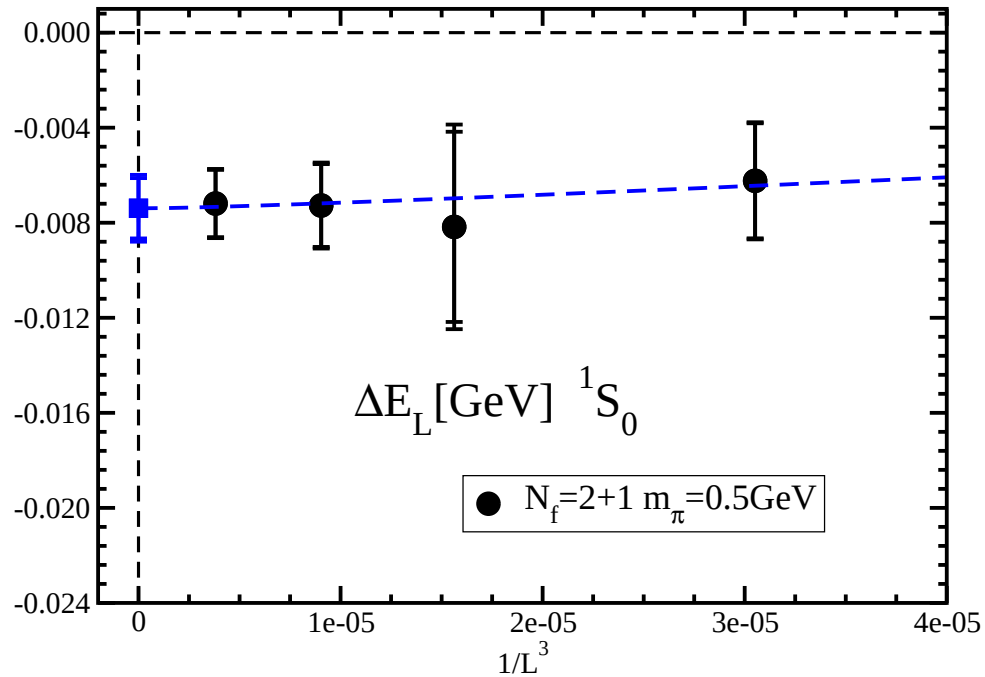

Bound state in both channels ← different from experiment

$\Delta E_{^3S_1} = 11.5(1.1)(0.6)$ MeV $\qquad$ $\Delta E_{^1S_0} = 7.4(1.3)(0.6)$ MeV

Preliminary results at $m_\pi = 0.3$GeV with two volumes

TY *et al.*, arXiv:150X.XXXX

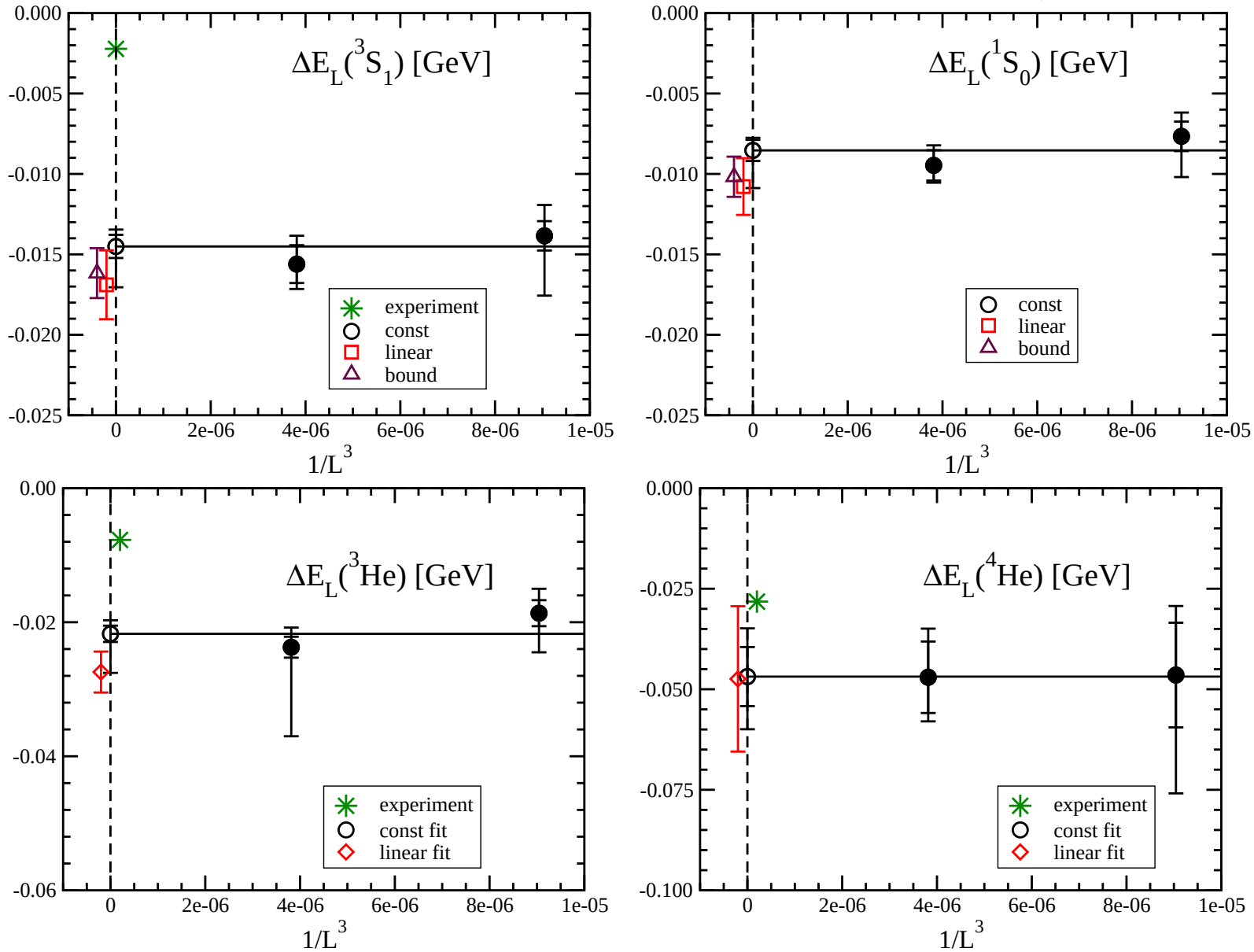

Comparison of ^{3}He and ^{4}He nuclei with preliminary results

PACS-CS, PRD81:111504(R)(2010); TY *et al.*, PRD86:074514(2012); NPLQCD, PRD87:034506(2013)

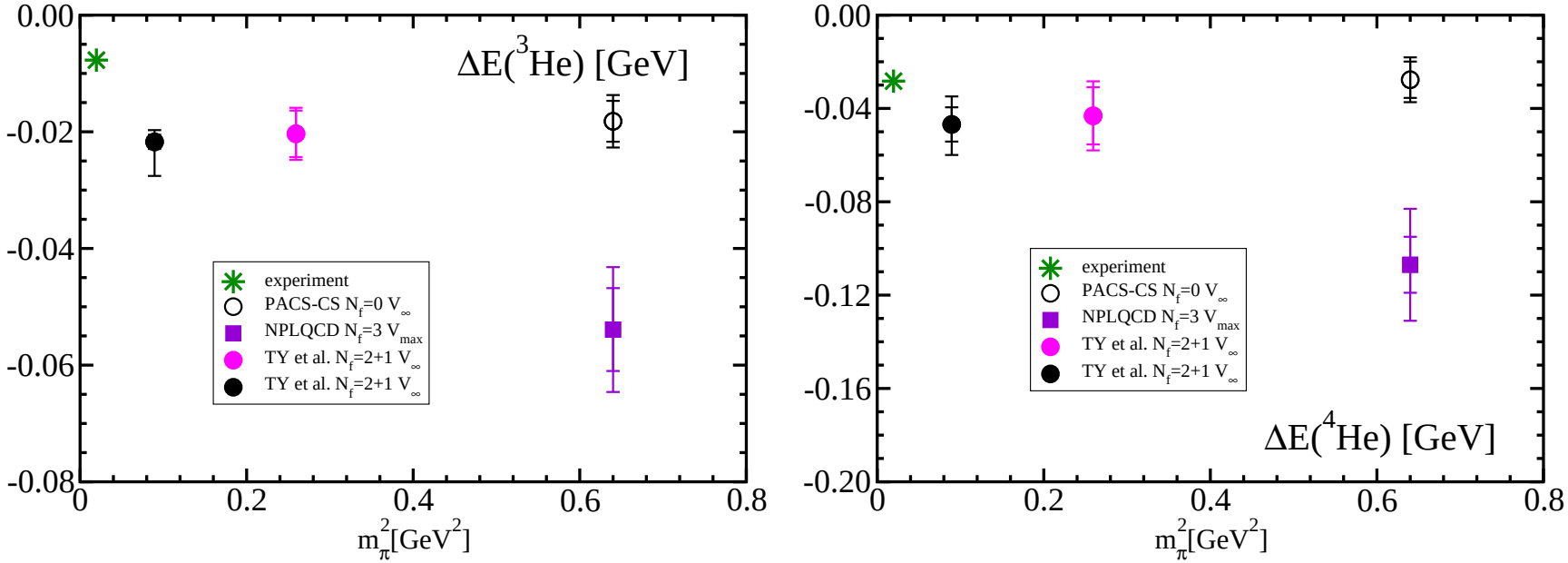

$L^3 \to \infty$ results only

Light nuclei likely formed in 0.3 GeV $\leq m_\pi \leq$ 0.8 GeV

Same order of ΔE to experiments

Comparison of ^{3}He and ^{4}He nuclei with preliminary results

PACS-CS, PRD81:111504(R)(2010); TY *et al.*, PRD86:074514(2012); NPLQCD, PRD87:034506(2013)

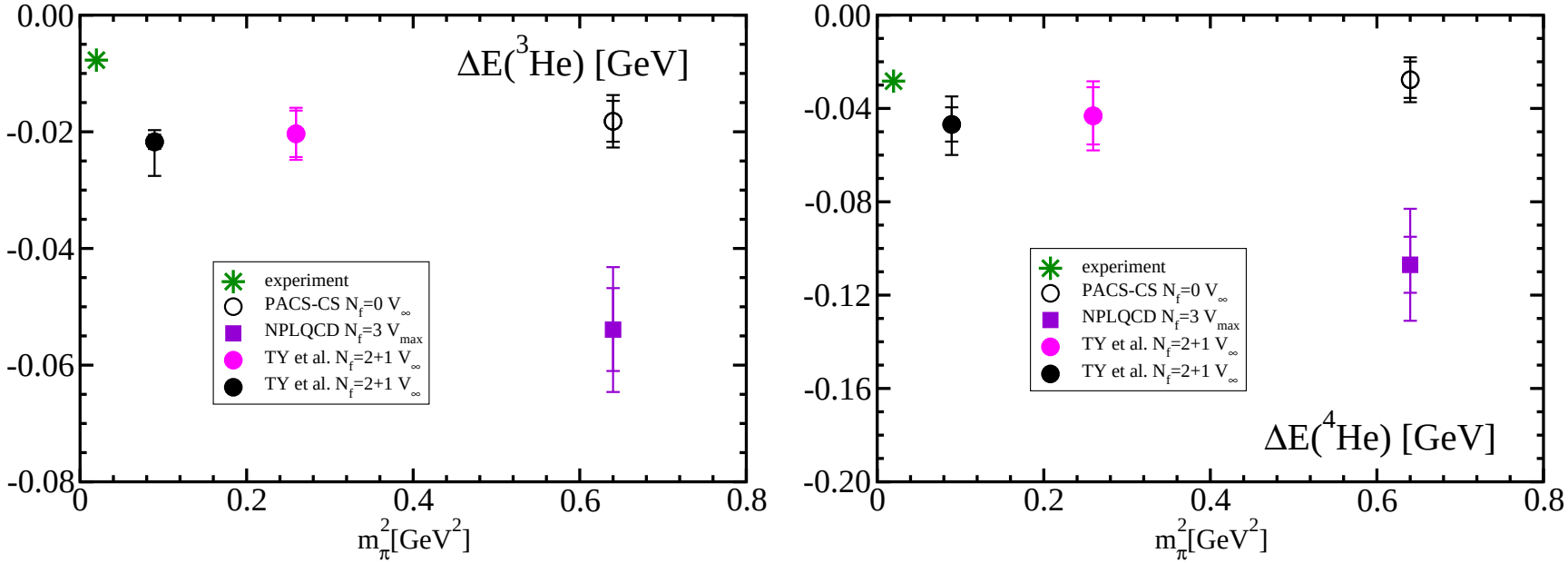

$L^3 \to \infty$ results only

Light nuclei likely formed in 0.3 GeV $\leq m_\pi \leq$ 0.8 GeV

Same order of ΔE to experiments $\to$ relatively easier than NN

large $|\Delta E|$ makes less V dependence at physical m_π

touchstone of quantitative understanding of nuclei from lattice QCD

Investigations of m_π dependence $\to$ $m_\pi =$ 0.14 GeV on $L \sim$ 8 fm

Comparison of NN channels with preliminary results

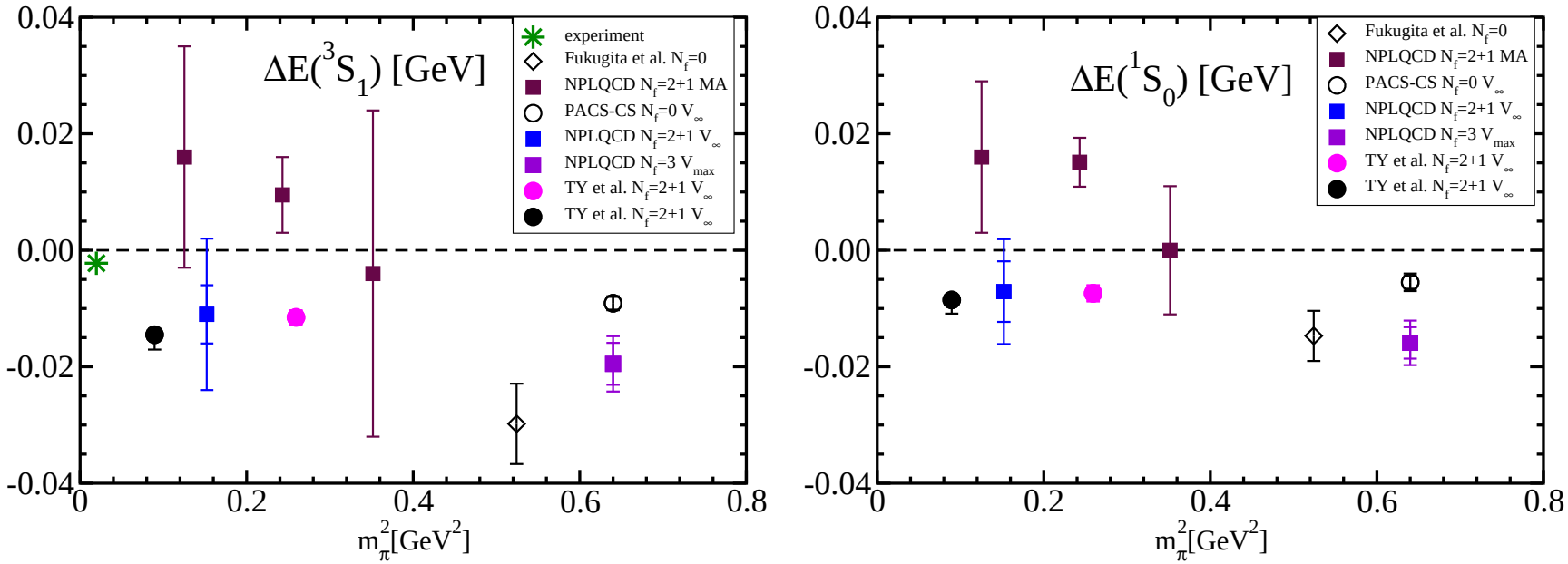

Volume dependence of ΔE_L in recent works

Comparison of NN channels with preliminary results

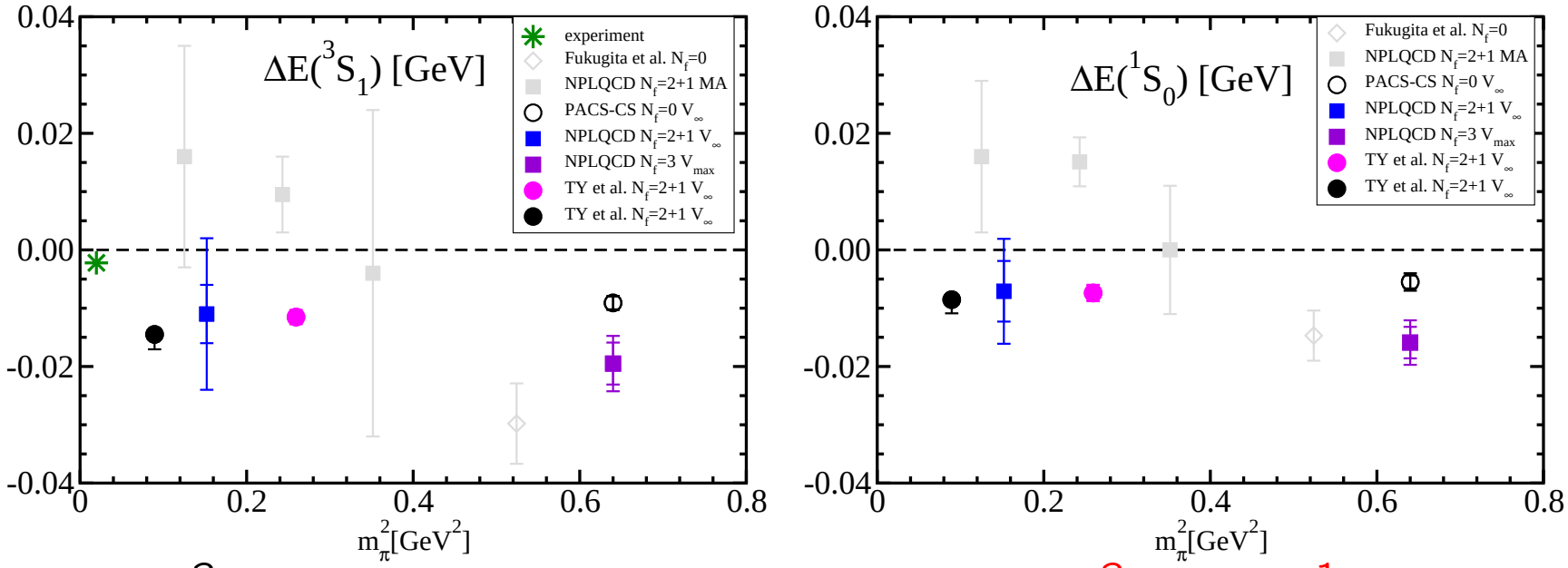

$L^3 \to \infty$: existence of bound states in $^3S_1$ and $^1S_0$

inconsistent with experiment due to larger m_π

Investigations of m_π dependence $\to$ $m_\pi = 0.14$ GeV on $L \sim 8$ fm

Comparison of NN channels with preliminary results

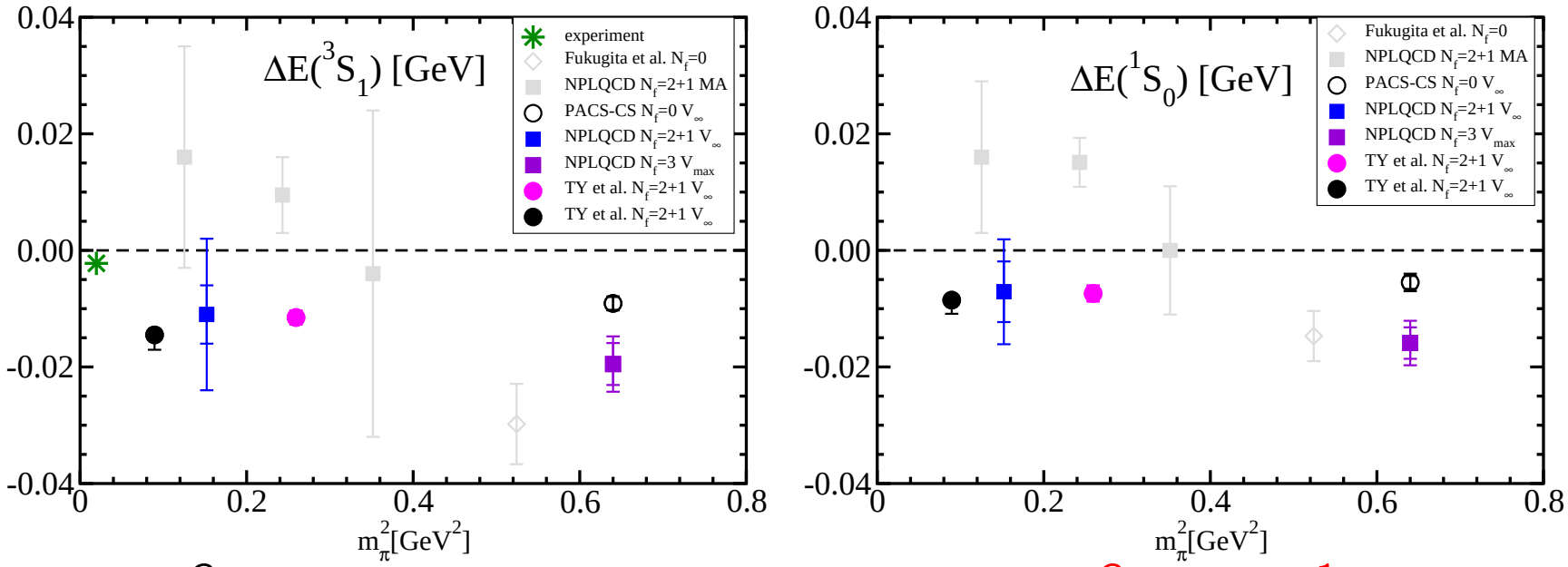

$L^3 \to \infty$: existence of bound states in $^3S_1$ and $^1S_0$

inconsistent with experiment due to larger m_π

Investigations of m_π dependence $\to m_\pi = 0.14$ GeV on $L \sim 8$ fm

Large finite volume effect expected even on $L \sim 8$ fm '86 Lüscher, '04 Beane

$^3S_1$: $\Delta E_{\text{exp}} = 2.2$ MeV

$$\Delta E_L = -\left(\Delta E_{\text{exp}} + \mathcal{O}(\exp(-L\sqrt{m_N \Delta E_{\text{exp}}}))\right) \sim -4 \text{ MeV}$$

$^1S_0$: $a_0^{\text{exp}} = 23.7$ fm

$$\Delta E_L = -\frac{4\pi a_0^{\text{exp}}}{m_N L^3} + \mathcal{O}(1/L^4) \sim -2 \text{ MeV}$$

Summary

$N_f = 2 + 1$ lattice QCD at $m_\pi = 0.5$ and 0.3 GeV

- Volume dependence of ΔE

  $\Delta E \neq 0$ of 0th state in infinite volume limit

  $\rightarrow$ bound state in ^{4}He, ^{3}He, ^{3}S$_1$ and ^{1}S$_0$ at $m_\pi = 0.5$ and 0.3 GeV

- ΔE larger than experiment and small m_π dependence
- Bound state in ^{1}S$_0$ not observed in experiment

  Deep bound state in $N_f = 3$ at $m_\pi = 0.8$ GeV ('12 NPLQCD)

- No bound state in HALQCD method

Need further investigations *e.g.* quark mass dependence

$N_f = 2 + 1$ $m_\pi \sim 0.14$ GeV on $L \sim 8$ fm calculation is ongoing.

Very preliminary results of $\Delta E = E_0 - N_N m_N$

at $m_\pi \sim 0.14$ GeV on $L \sim 8$ fm

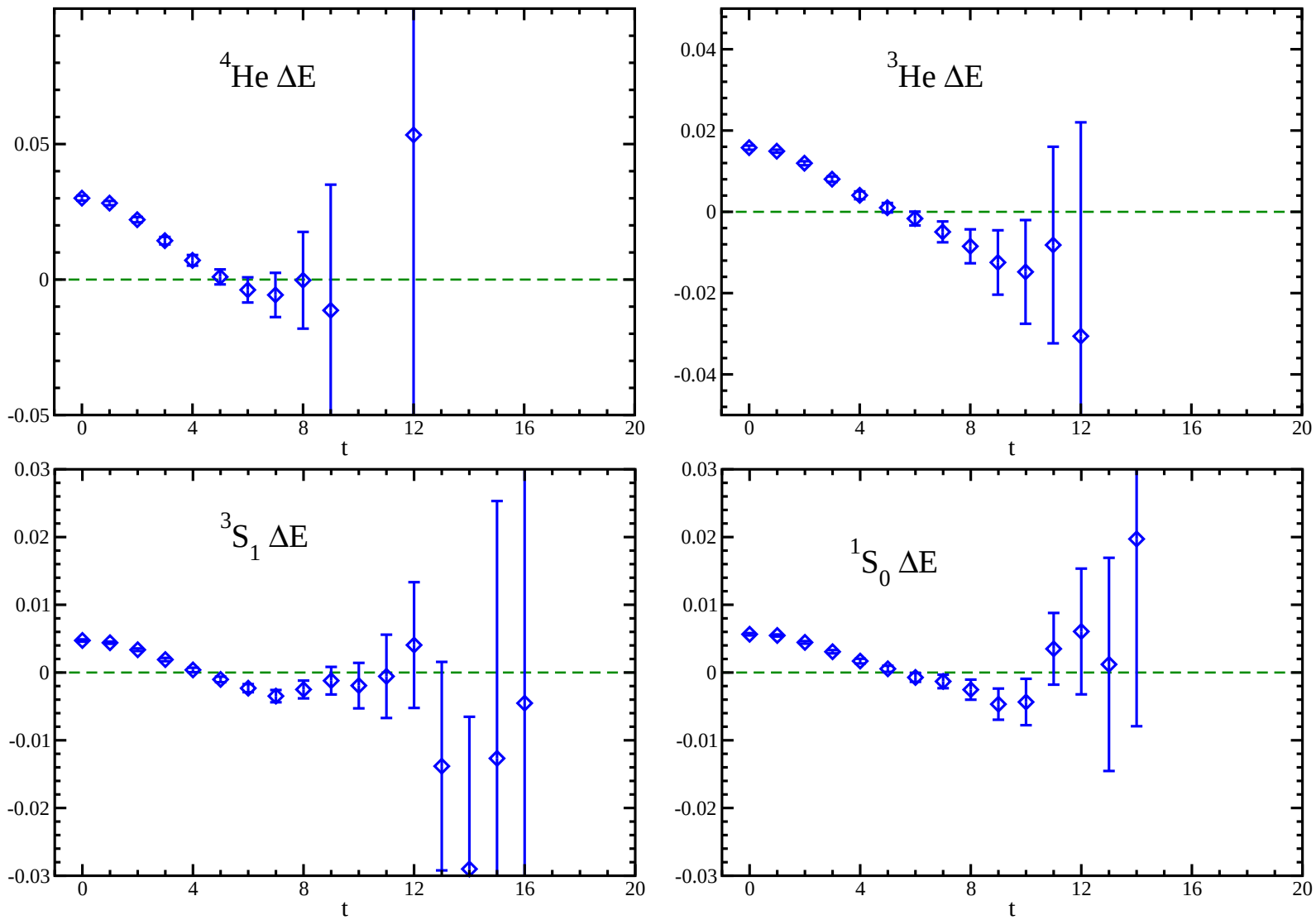

Back up

Uncertainty of Lüscher's method

TY *et al.* and NPLQCD

Lüscher's method $\sim \Delta E$ of 0th state and $L^3 \to \infty$

$\to$ same as traditional method to obtain hadron mass

current study: smeared quark field + $C_{NN}(t)/(C_N(t))^2$ in large t

$\Delta E(t)$ from + to − $\to$ plateau $\to$ large statistical fluctuation

TY *et al.*, $N_f = 2+1$ $m_\pi = 0.5$ GeV

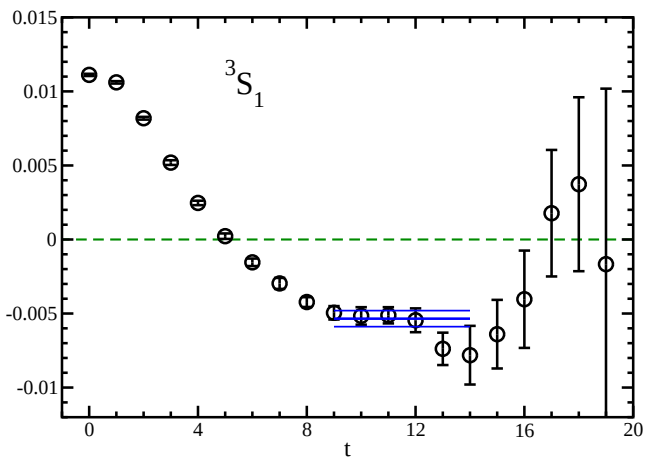

PRD86:074514(2012)

NPLQCD, $N_f = 3$ $m_\pi = 0.8$ GeV

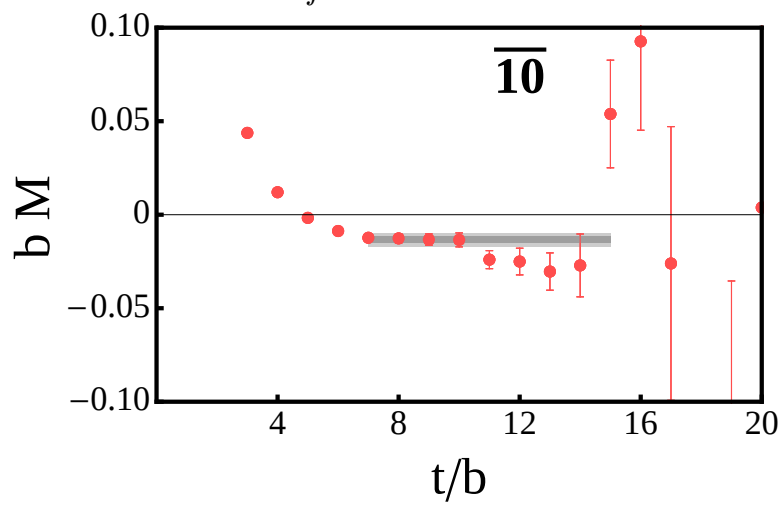

PRD87:034506(2013)

- 0th state energy from variational method

Uncertainty of Lüscher's method

TY *et al.* and NPLQCD

Lüscher's method $\sim \Delta E$ of 0th state and $L^3 \to \infty$

$\to$ same as traditional method to obtain hadron mass

- 0th state energy from variational method

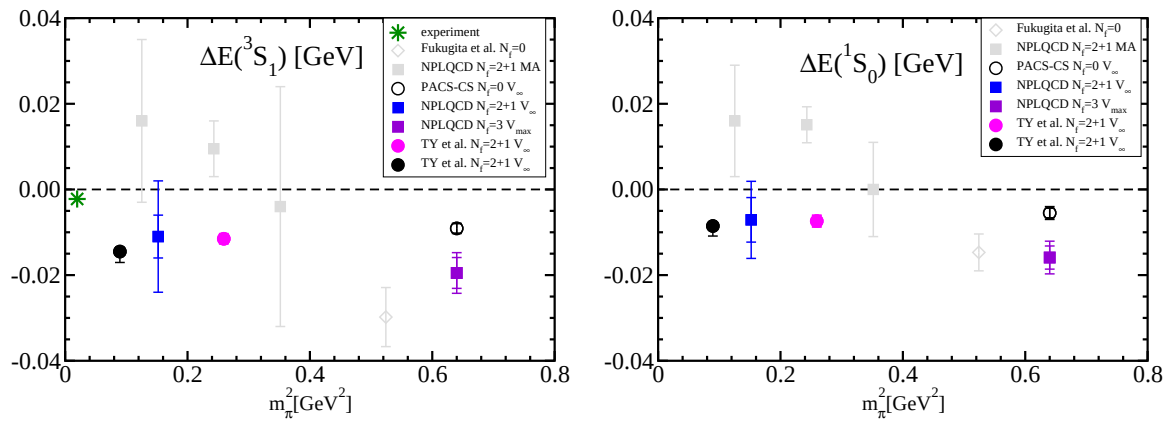

- 2.9σ difference of ΔE at $m_\pi = 0.8$ GeV ($N_f = 0$ and $N_f = 3$)

- Investigation of m_π dependence

Bound state in $^1S_0$ vanishes at physical m_π?

3. Preliminary results

Effective nucleon mass at $L = 5.8$ fm

$$m_N = \log\left(\frac{C_{\mathrm{N}}(t)}{C_{\mathrm{N}}(t+1)}\right)$$

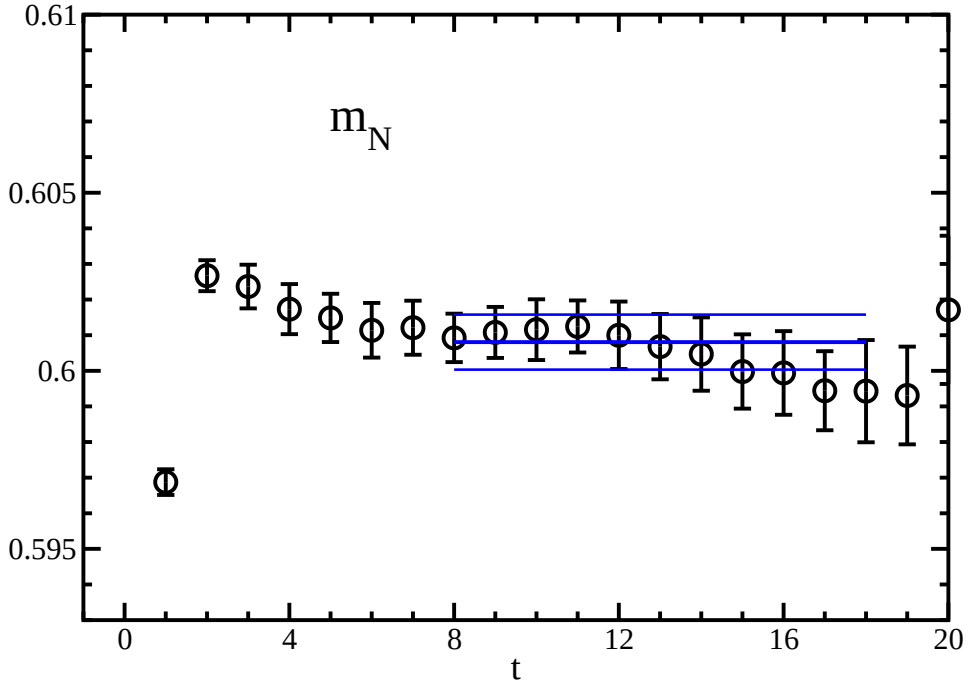

3. Preliminary results

Effective energy in ^{4}He and ^{3}He channels at $L = 5.8$ fm

$$E_0 = \log\left(\frac{C_{^4\mathrm{He}}(t)}{C_{^4\mathrm{He}}(t+1)}\right)$$

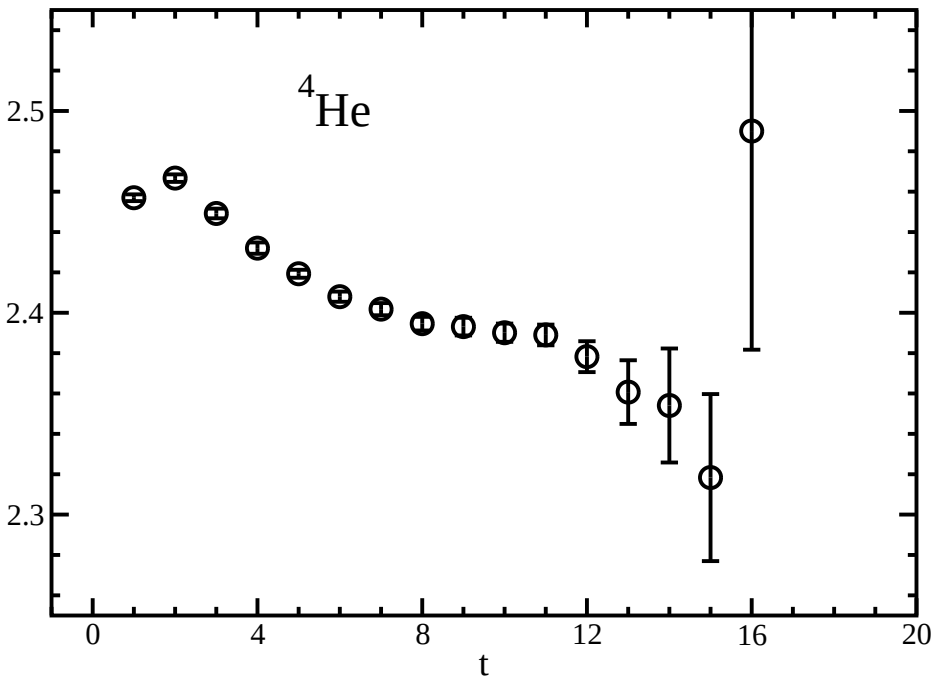

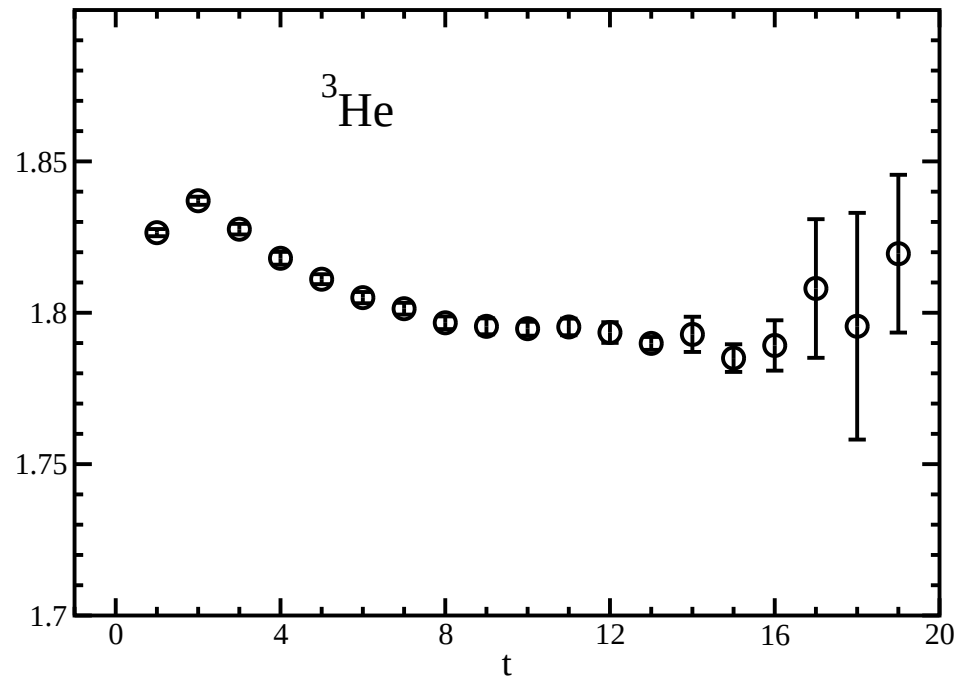

3. Preliminary results

Effective energy in NN channels at $L = 5.8$ fm

$$E_0 = \log\left(\frac{C_{\mathrm{NN}}(t)}{C_{\mathrm{NN}}(t+1)}\right)$$

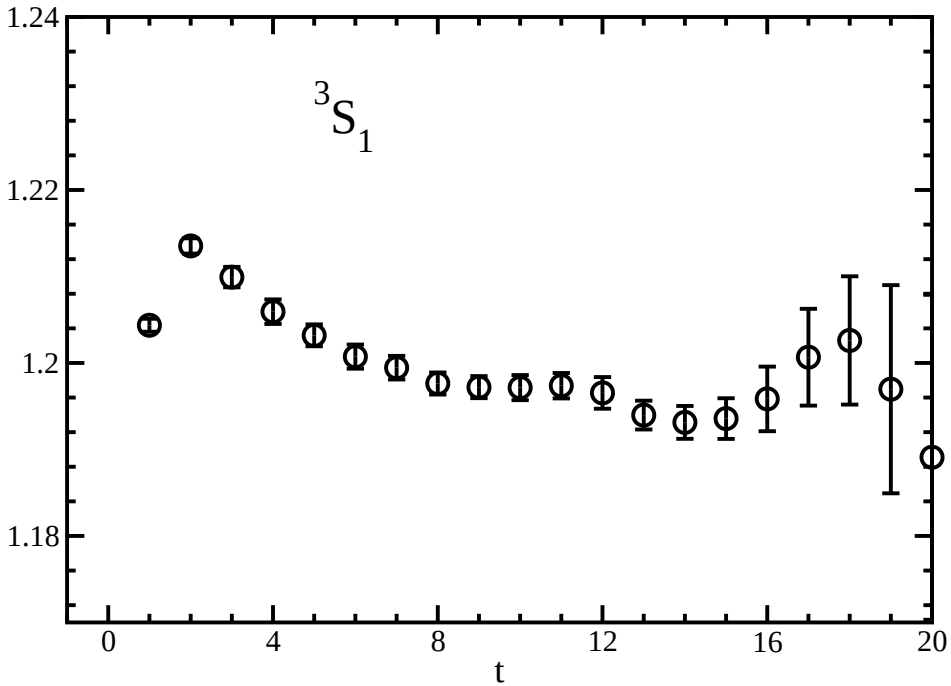

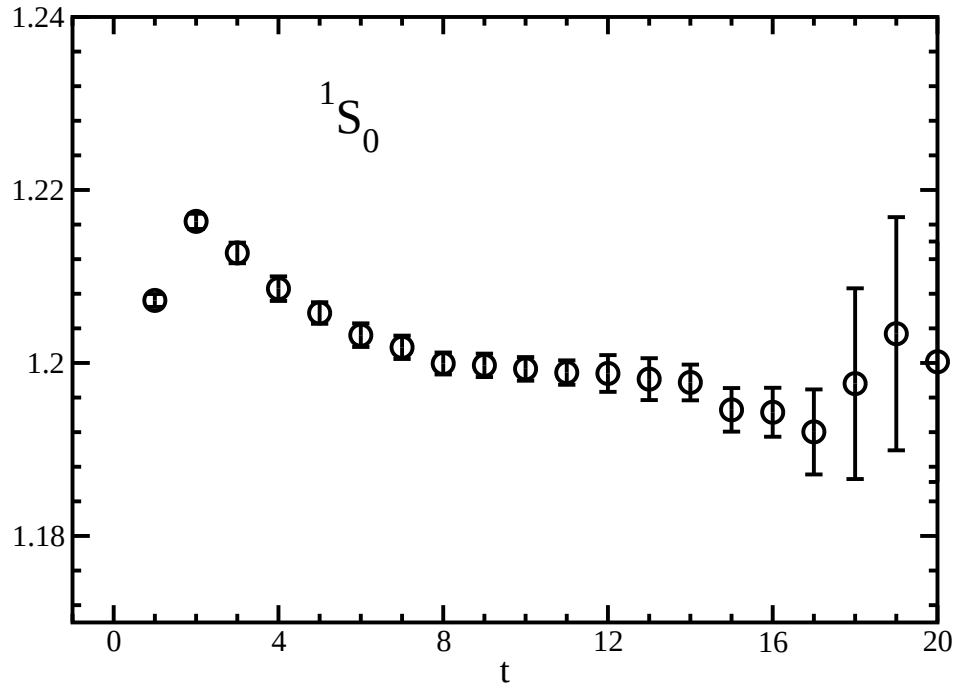

Effective mass @ $m_\pi = 0.3$GeV

Preliminary result of $N_f = 2 + 1$ TY *et al.*

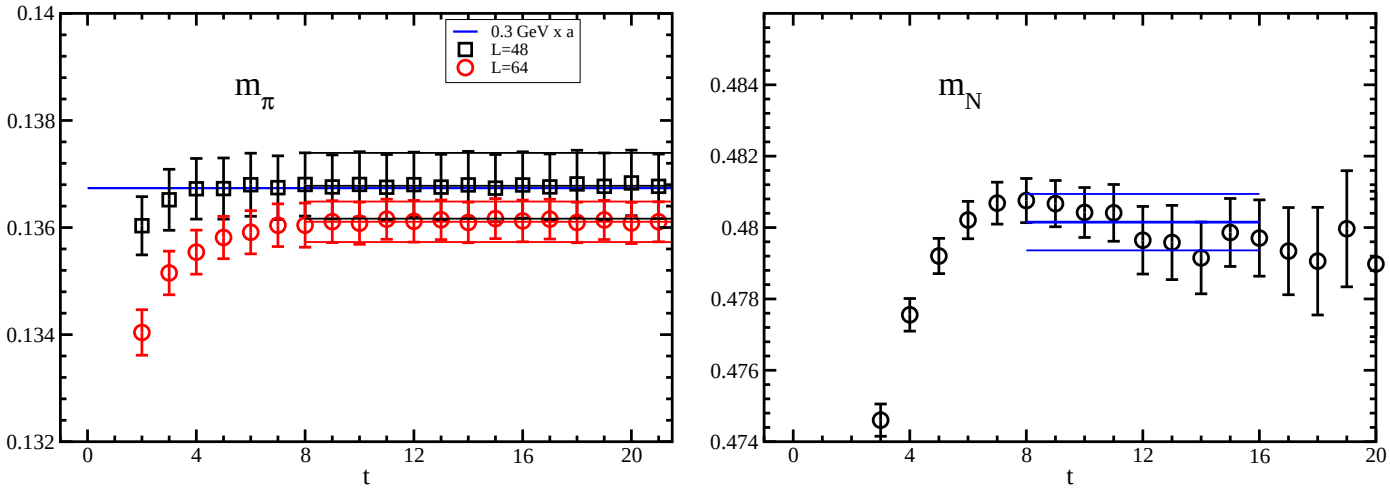

effective ΔE_L @ $m_\pi = 0.3$GeV on $L = 48$

Preliminary result of $N_f = 2 + 1$ TY *et al.*

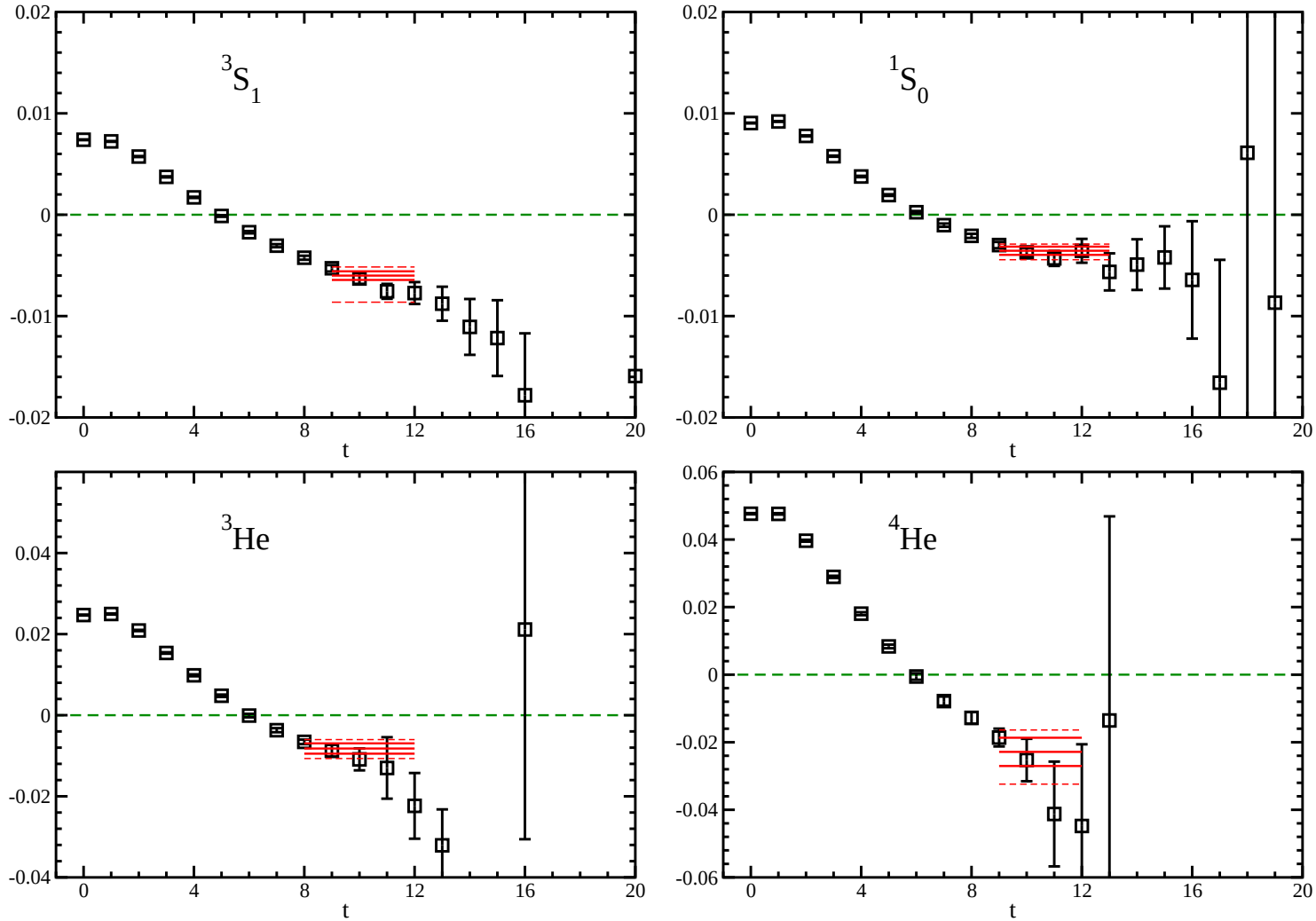

Current status of NN channels

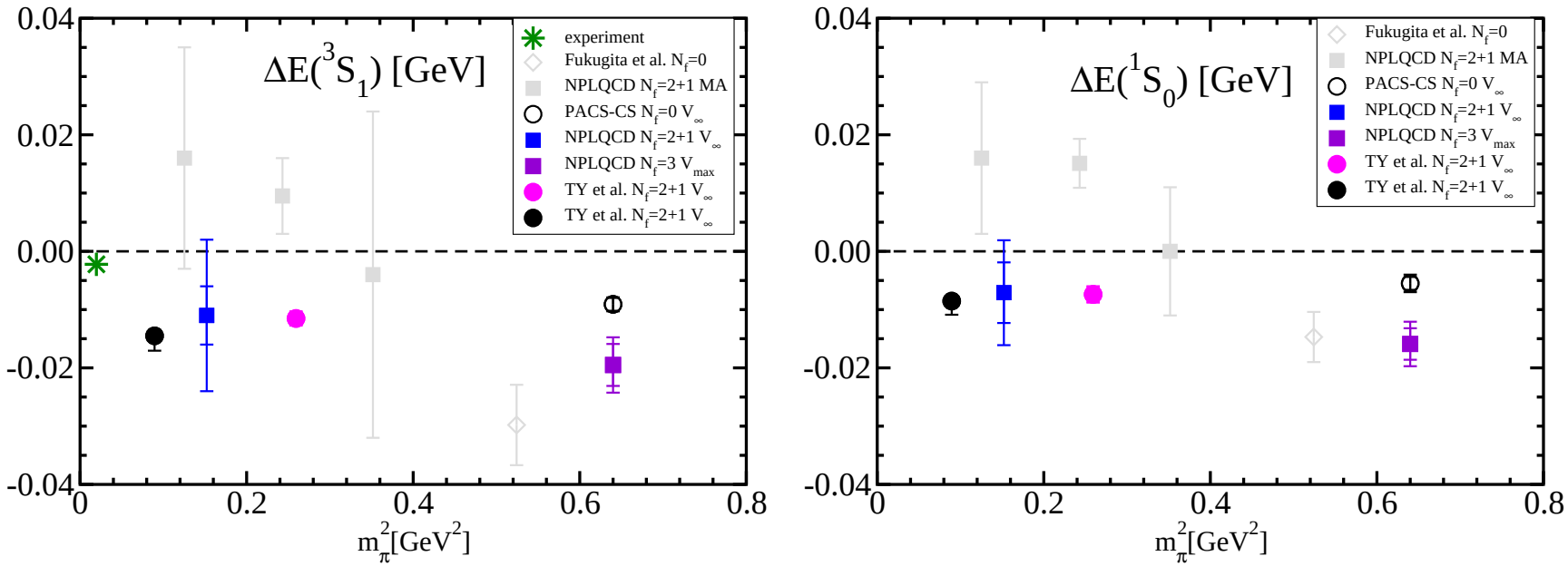

$L^3 \to \infty$: existence of bound states in $^3S_1$ and $^1S_0$

inconsistent with experiment due to larger m_π

$a_0 < 0$ at $m_\pi = 0.8$ GeV $\to$ bound state in each channel

c.f. Beane *et al.*, PLB585:106(2004); Sasaki and TY, PRD74:114507(2006)

	PACS-CS, $N_f = 0^*$	NPLQCD, $N_f = 3$
$a_0^{^3S_1}$[fm]	$-1.05(24)\,(^{5}_{65})$	$-1.82\,(^{14}_{13})\,(^{17}_{12})$
$a_0^{^1S_0}$[fm]	$-1.62(24)\,(^{1}_{75})$	$-2.33\,(^{19}_{17})\,(^{27}_{20})$

* from $L = 6.1$ fm PACS-CS, PRD84:054506(2011)

NPLQCD, PRD87:034506(2013)

Expectation of large quark mass dependence

radii from form factors F_1 and F_2

Constantinou, Lat14 plenary

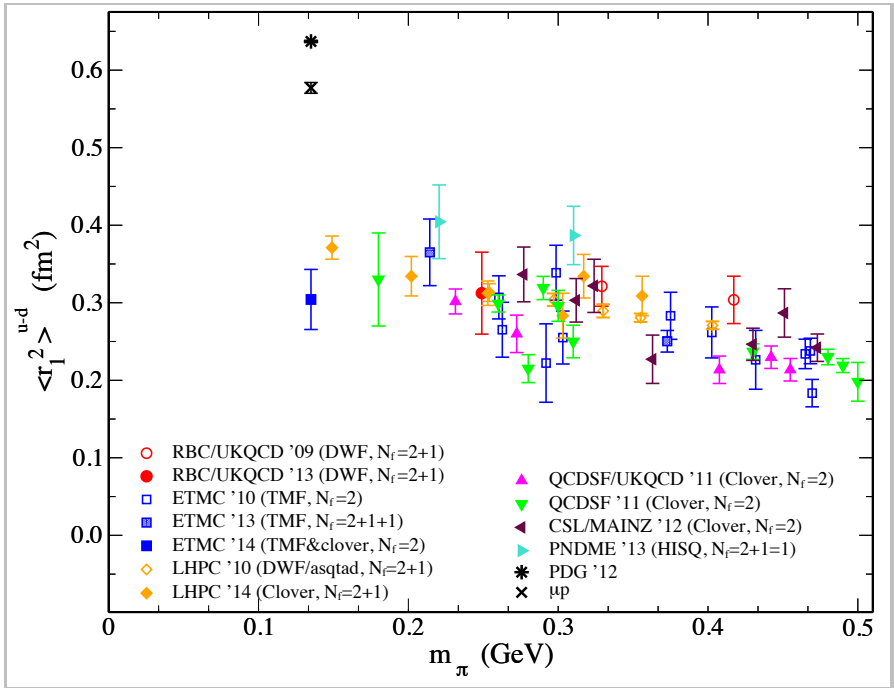

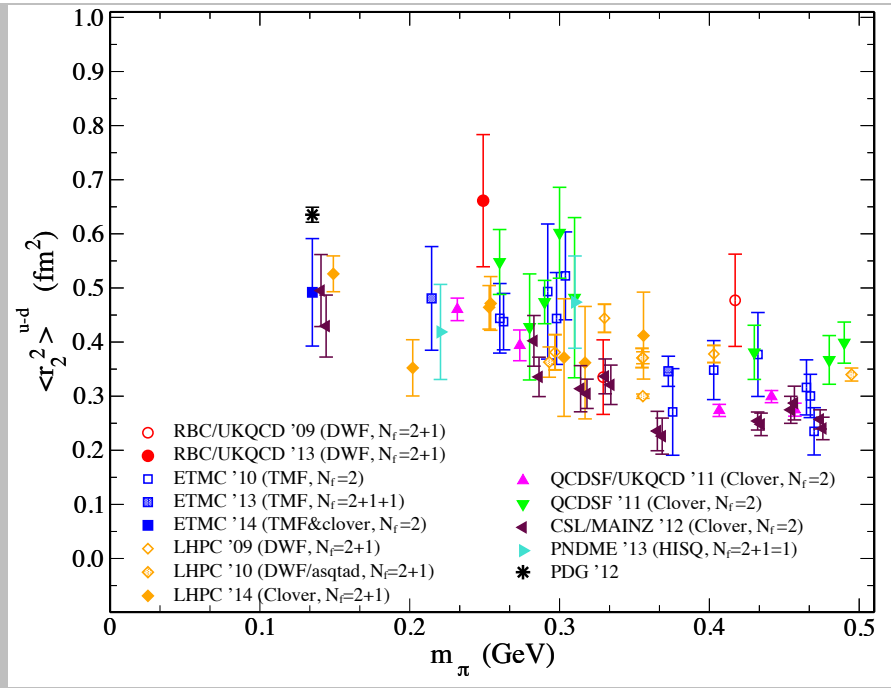

Expectation of large quark mass dependence

rms radii from form factors F_1 and F_2

'09 RBC+UKQCD

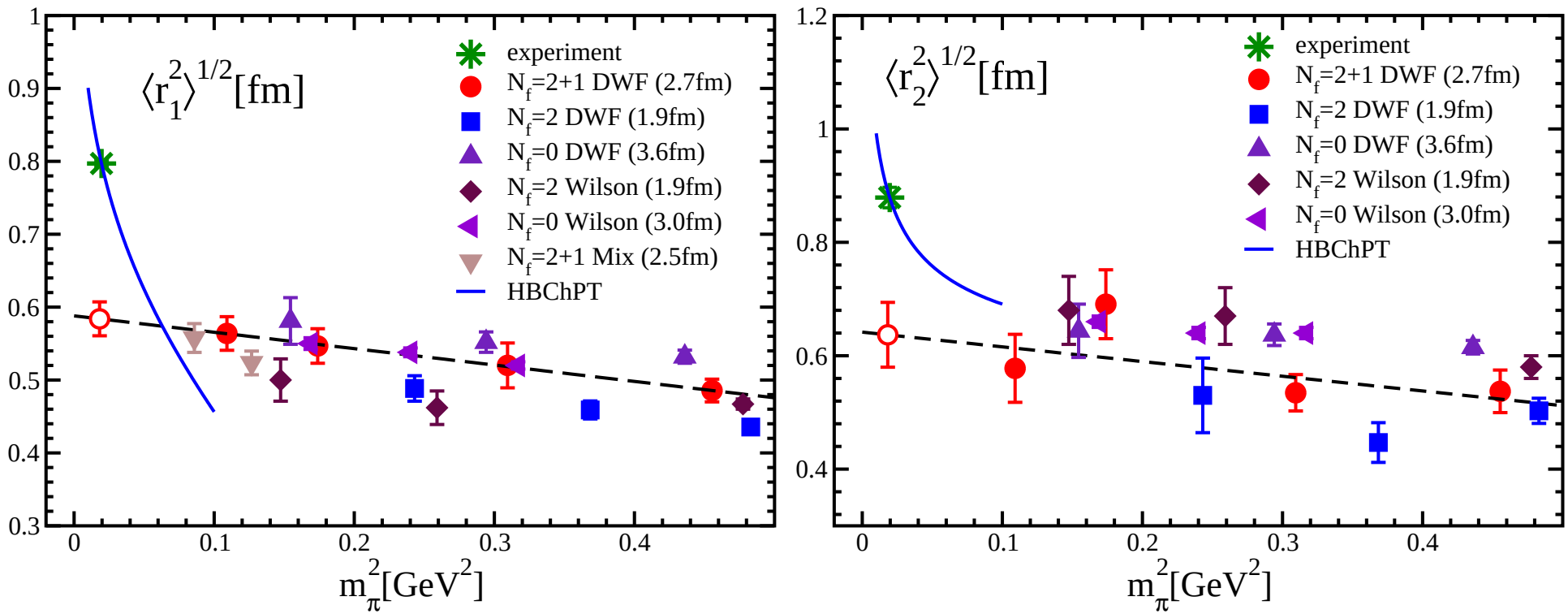

Multi-Hadron and Nonlocal Matrix Elements in Lattice QCD

February 5-6, 2015
Instrumentation, Bldg 535, Large Seminar Room

Thursday, February 5, 2015

08:30-08:55 **REGISTRATION**

08:55-09:00 **WELCOME**

09:00-10:30 FINITE-VOLUME QUANTIZATION CONDITIONS (Chair: Prof. Stefan Meinel)

09:00 **Finite volume quantization conditions for multi-particle states**
Prof. Stephen Sharpe (University of Washington)

09:30 **Three particles in a box: Relating the finite-volume spectrum to three-to-three scattering**
Dr. Maxwell Hansen (University of Mainz)

10:00 **Single-hadron states in a finite volume in the presence of QED interactions**
Dr. Zohreh Davoudi (Massachusetts Institute of Technology)

10:30-11:00 **COFFEE BREAK**

11:00-11:30 FINITE-VOLUME QUANTIZATION CONDITIONS (Chair: Prof. Ethan Neil)

11:00 **Charged particles scattering in a finite volume**
Prof. Silas Beane (University of Washington)

11:30-12:30 HADRON RESONANCES (Chair: Prof. Ethan Neil)

11:30 **Resonances in coupled pi-K eta-K scattering from lattice QCD**
Dr. David Wilson (Old Dominion University)

12:00 **Charmed-strange and bottom-strange positive parity mesons from Lattice QCD**
Dr. Daniel Mohler (Fermilab)

12:30-14:00 **LUNCH BREAK**

14:00-15:15 NONLOCAL MATARIX ELEMENTS (Chair: Dr. William Detmold)

14:00 **Aspects of Lattice QCD calculations of transverse momentum-dependent parton distributions (TMDs)**
Prof. Michael Engelhardt (New Mexico State University)

14:30 **Extract collinear parton distribution functions from lattice QCD calculations**
Prof. Jianwei Qiu (BNL)

15:00 **Perturbative matching for quasi-PDFs between continuum and lattice**
Dr. Tomomi Ishikawa (RIKEN BNL Research Center)

15:15-16:00 **COFFEE BREAK**

16:00-18:00 MULTI-HADRON MATRIX ELEMENTS (Chair: Dr. Zohreh Davoudi)

16:00 **Resonance form factors in lattice QCD**
Mr. Andria Agadjanov (University of Bonn)

16:30 **Hadronic transition processes in a finite volume**
Dr. Raul Briceno (Jefferson Lab)

17:00 **Excited meson radiative transition matrix elements using distillation**
Mr. Christian Shultz (Old Dominion University)

17:30 **K -> pi pi decay amplitudes from improved Wilson fermion**
Prof. Naruhito Ishizuka (University of Tsukuba)

Back to Contents

Friday, February 6, 2015

09:00-09:30 MULTI-HADRON MATRIX ELEMENTS (Chair: Prof. Chris Sachrajda)

09:00 **Progress towards an ab initio, Standard Model calculation of direct CP-violation in K decays**
Dr. Christopher Kelly (RIKEN BNL Research Center)

09:30-10:30 NONLOCAL MATRIX ELEMENTS (Chair: Prof. Chris Sachrajda)

09:30 **Computing the long-distance contribution to the K_L-K_S mass difference**
Prof. Norman Christ (Columbia University)
10:00 **Lattice calculation of long distance contribution to epsilon_K**
Mr. Ziyuan Bai (Columbia University)

10:30-11:00 **COFFEE BREAK**

11:00-12:30 NONLOCAL MATRIX ELEMENTS (Chair: Dr. Amarjit Soni)

11:00 **K -> pi l+ l- decays on the lattice**
Dr. Antonin Portelli (University of Southampton)
11:30 **K -> pi nu nubar decays on the lattice**
Dr. Xu Feng (Columbia University)
12:00 **QED corrections to hadronic processes in lattice QCD**
Prof. Christopher Sachrajda (University of Southampton)

12:30-13:45 **LUNCH BREAK**

13:45-14:15 NONLOCAL MATRIX ELEMENTS (Chair: Prof. Norman Christ)

13:45 **Lattice calculation of the hadronic light by light contributions to the muon anomalous magnetic moment**
Mr. Luchang Jin (Columbia University)

14:15-15:15 NUCLEI (Chair: Prof. Norman Christ)

14:15 **HAL QCD method for hadron interactions on the lattice**
Dr. Takumi Doi (RIKEN)
14:45 **Light nuclei from lattice QCD**
Prof. Takeshi Yamazaki (University of Tsukuba)

15:15-16:00 **COFFEE BREAK**

16:00-17:15 NUCLEI (Chair: Dr. Taku Izubuchi)

16:00 **QCD calculations of nuclear matrix elements**
Prof. William Detmold (Massachusetts Institute of Technology)
16:30 **Ongoing search for the H-dibaryon in two-flavor lattice QCD**
Dr. Anthony Francis (University of Mainz)
16:45 **Structure of charmed tetraquarks from LQCD**
Dr. Yoichi Ikeda (RIKEN)

Back to Contents

Multi-Hadron and Nonlocal Matrix Elements in Lattice QCD

February 5-6, 2105

List of Participants

Name	Affiliation	e-Mail Address
Andria Agadjanov	University of Bonn	aagadjanov@hiskp.uni-bonn.de
Ziyuan Bai	Columbia University	zb2174@columbia.edu
Silas Beane	University of Washington	silas@uw.edu
Raul Briceno	Thomas Jefferson National Accelerator Facility	rbriceno@jlab.org
Norman Christ	Columbia University	nhc@phys.columbia.edu
Michael Creutz	Brookhaven National Laboratory	mike@latticeguy.net
Zohreh Davoudi	Massachusetts Institute of Technology	davoudi@mit.edu
William Detmold	Massachusetts Institute of Technology	wdetmold@mit.edu
Takumi Doi	RIKEN	doi@ribf.riken.jp
Michael Engelhardt	New Mexico State University	engel@nmsu.edu
Xu Feng	Columbia University	pkufengxu@gmail.com
Anthony Francis	York University	afrancis@uni-mainz.de
Maxwell Hansen	University of Mainz	hansen@kph.uni-mainz.de
Yoichi Ikeda	RIKEN	yikeda@riken.jp
Tomomi Ishikawa	RIKEN BNL Research Center	tomomi@quark.phy.bnl.gov
Naruhito Ishizuka	University of Tsukuba	ishizuka@ccs.tsukuba.ac.jp
Taku Izubuchi	Brookhaven National Laboratory & RBRC	izubuchi@bnl.gov
Luchang Jin	Columbia University	lj2289@columbia.edu
Christopher Kelly	RIKEN BNL Research Center	ckelly@quark.phy.bnl.gov
Meifeng Lin	Brookhaven National Laboratory	mlin@bnl.gov
Simonetta Liuti	University of Virginia	sl4y@virginia.edu
Stefan Meinel	University of Arizona & RBRC	smeinel@email.arizona.edu
Daniel Mohler	Fermilab	dmohler@fnal.gov
David Murphy	Columbia University	dmurphy@phys.columbia.edu
Ethan Neil	University of Colorado & RBRC	ethan.neil@colorado.edu
Antonin Portelli	University of Southampton	antonin.portelli@me.com
Manju Prakash	Hofstra University	prakashmanju169@gmail.com
Jianwei Qiu	Brookhaven National Laboratory	jqiu@bnl.gov
Christopher Sachrajda	University of Southampton	cts@phys.soton.ac.uk
Stephen Sharpe	University of Washington	srsharpe@uw.edu
Christian Shultz	Old Dominion University	christian.shultz@gmail.com
David Wilson	Old Dominion University	djwilson@jlab.org
Takeshi Yamazaki	University of Tsukuba	yamazaki@het.ph.tsukuba.ac.jp
Daiqian Zhang	Columbia University	dz2203@columbia.edu

Back to Contents

RIKEN BNL Research Center Proceedings

Volume 119 – Thermal Photons and Dileptons in Heavy-Ion Collisions, August 20-22, 2014 – BNL-106066-2014
Volume 118 – The Approach to Equilibrium in Strongly Interacting Matter, April 2-4, 2014 – BNL-104423-2014
Volume 117 – Lattice Meets Experiment 2013: Beyond the Standard Model, December 5-6, 2013 – BNL-103493-2013
Volume 116 – RBRC Scientific Review Committee Meeting, October 31 - November 1, 2013 – BNL-102596-2013
Volume 115 – Jet Quenching at RHIC vs LHC in Light of Recent dAu vs pPb Controls, April 15-17, 2013 – BNL-100766-2013
Volume 114 – The Physics of p↑+A Collisions at RHIC, January 7-9, 2013 – BNL-99107-2013
Volume 113 – Thermal Radiation Workshop, December 5-7, 2012 – BNL-99088-2013
Volume 112 – RBRC Scientific Review Committee Meeting, November 6-8, 2012 – BNL-99621-2013
Volume 111 – Forward Physics at RHIC, July 30-Aug 1, 2012 – BNL-98400-2012
Volume 110 – P- and CP-odd Effects in Hot and Dense Matter, June 25-27, 2012 – BNL-98398-2012
Volume 109 – New Horizons for Lattice Computations with Chiral Fermions, May 14-18, 2012 – BNL-98392-2012
Volume 108 – Hyperon-Hyperon Interactions and Searches for Exotic Di-Hyperons in Nuclear Collisions, February 29 – March 2, 2012 – BNL-97035-2012
Volume 107 – Future Directions in High Energy QCD, October 20-22, 2011 – BNL-98119-2011
Volume 106 – Fluctuations, Correlations and RHIC Low Energy Runs, October 3-5, 2011 – BNL-96514-2011
Volume 105 – Opportunities for Polarized He-3 in RHIC and EIC, September 28-30, 2011 – BNL-96418-2011
Volume 104 – Brookhaven Summer Program on Quarkonium Production in Elementary and Heavy Ion Collisions, June 6-18, 2011 – BNL-96171-2011
Volume 103 – Opportunities for Drell-Yan Physics at RHIC, May 11-13, 2011 – BNL-95236-2011
Volume 102 – Initial State Fluctuations and Final-State Particle Correlations, February 2-4, 2011 – BNL-94704-2011
Volume 101 – RBRC Scientific Review Committee Meeting, October 27-29, 2010 – BNL-94589-2011
Volume 100 – Summer Program on Nucleon Spin Physics, July 14-27, 2010 – BNL-96163-2011
Volume 99 – The Physics of W and Z Bosons, June 24-25, 2010 – BNL-94287-2010
Volume 98 – Saturation, the Color Glass Condensate and the Glasma: What Have We Learned from RHIC? – May 10-12, 2010 – BNL-94271-2010
Volume 97 – RBRC Scientific Review Committee Meeting, October 21-22, 2009 – BNL-90674-2009
Volume 96 – P- and CP-Odd Effects in Hot and Dense Matter, April 26-30, 2010 – BNL-94237-2010
Volume 95 – Progress in High-pT Physics at RHIC, March 17-19, 2010 – BNL-94214-2010
Volume 94 – Summer Program on Nucleon Spin Physics at LBL, June 1-12, 2009
Volume 93 – PHENIX Spinfest School 2009 at BNL - July 1-31, 2009 – BNL-90343-2009
Link: PHENIXSpinfestSchool2009@BNL
Volume 92 – PKU-RBRC Workshop on Transverse Spin Physics, June 30 - July 4, 2008, Beijing, China – BNL-81685-2008
Volume 91 – RBRC Scientific Review Committee Meeting, November 17-18, 2008 – BNL-81556-2008
Volume 90 – PHENIX Spinfest School 2008 at BNL, August 4-8, 2008 – BNL-81478-2008
Volume 89 – Understanding QGP through Spectral Functions and Euclidean Correlators, April 23-25, 2008 – BNL-81318-2008
Volume 88 – Hydrodynamics in Heavy Ion Collisions and QCD Equation of State, April 21-22, 2008 – BNL-81307-2008
Volume 87 – RBRC Scientific Review Committee Meeting, November 5-6, 2007 – BNL-79570-2007
Volume 86 – Global Analysis of Polarized Parton Distributions in the RHIC Era, October 8, 2007 – BNL-79457-2007
Volume 85 – Parity-Violating Spin Asymmetries at RHIC-BNL, April 26-27, 2007 – BNL-79146-2007
Volume 84 – Domain Wall Fermions at Ten Years, March 15-17, 2007 – BNL 77857-2007
Volume 83 – QCD in Extreme Conditions, July 31 - August 2, 2006 – BNL-76933-2006

Back to Contents

Volume 82 – RHIC Physics in the Context of the Standard Model, June 18-23, 2006 – BNL-76863-2006
Volume 81 – Parton Orbital Angular Momentum (Joint RBRC/University of New Mexico Workshop) February 24-26, 2006 – BNL-75937-2006
Volume 80 – Can We Discover the QCD Critical Point at RHIC?, March 9-10, 2006 – BNL-75692-2006
Volume 79 – Strangeness in Collisions, February 16-17, 2006 – BNL-79763-2008
Volume 78 – Heavy Flavor Productions and Hot/Dense Quark Matter, December 12-14, 2005 – BNL-76915-2006
Volume 77 – RBRC Scientific Review Committee Meeting, October 10-12, 2005 – BNL-52649-2005
Volume 76 – Odderon Searches at RHIC, September 27-29, 2005 – BNL-75092-2005
Volume 75 – Single Spin Asymmetries, June 1-3, 2005 – BNL-74717-2005
Volume 74 – RBRC QCDOC Computer Dedication and Symposium on RBRC QCDOC, May 26, 2005 – BNL-74813-2005
Volume 73 – Jet Correlations at RHIC, March 10-11, 2005 – BNL-73910-2005
Volume 72 – RHIC Spin Collaboration Meetings XXXI, XXXII, XXXIII – BNL-73866-2005
Volume 71 – Classical and Quantum Aspects of the Color Glass Condensate – BNL-73793-2005
Volume 70 – Strongly Coupled Plasmas: Electromagnetic, Nuclear & Atomic – BNL-73867-2005
Volume 69 – RBRC Scientific Review Committee Meeting, November 16-17, 2004 – BNL-73546-2004
Volume 68 – Workshop on the Physics Programme of the RBRC and UKQCD QCDOC Machines – BNL-73604-2004
Volume 67 – High Performance Computing with BlueGene/L and QCDOC Architectures, October 27-28, 2004
Volume 66 – RHIC Spin Collaboration Meeting XXIX, Torino Italy – BNL-73534-2004
Volume 65 – RHIC Spin Collaboration Meetings XXVII, XXVIII, XXX – BNL-73506-2004
Volume 64 – Theory Summer Program on RHIC Physics – BNL-73263-2004
Volume 63 – RHIC Spin Collaboration Meetings XXIV, XXV, XXVI – BNL-72397-2004
Volume 62 – New Discoveries at RHIC, May 14-15, 2004 – BNL-72391-2004
Volume 61 – RIKEN-TODAI Mini Workshop on "Topics in Hadron Physics at RHIC", March 23-24, 2004 – BNL-72336-2004
Volume 60 – Lattice QCD at Finite Temperature and Density – BNL-72083-2004
Volume 59 – RHIC Spin Collaboration Meetings XXI, XXII, XXIII – BNL-72382-2004
Volume 58 – RHIC Spin Collaboration Meeting XX – BNL-71900-2004
Volume 57 – High pt Physics at RHIC, December 2-6, 2003 – BNL-72069-2004
Volume 56 – RBRC Scientific Review Committee Meeting, November 20-21, 2003 – BNL-71899-2003
Volume 55 – Collective Flow and QGP Properties – BNL-71898-2003
Volume 54 – RHIC Spin Collaboration Meetings XVII, XVIII, XIX – BNL-71751-2003
Volume 53 – Theory Studies for Polarized pp Scattering – BNL-71747-2003
Volume 52 – RIKEN School on QCD "Topics on the Proton" – BNL-71694-2003
Volume 51 – RHIC Spin Collaboration Meetings XV, XVI – BNL-71539-2003
Volume 50 – High Performance Computing with QCDOC and BlueGene – BNL-71147-2003
Volume 49 – RBRC Scientific Review Committee Meeting, November 21-22, 2002 – BNL-52679
Volume 48 – RHIC Spin Collaboration Meeting XIV – BNL-71300-2003
Volume 47 – RHIC Spin Collaboration Meetings XII, XIII – BNL-71118-2003
Volume 46 – Large-Scale Computations in Nuclear Physics using the QCDOC – BNL-52678
Volume 45 – Summer Program: Current and Future Directions at RHIC – BNL-71035
Volume 44 – RHIC Spin Collaboration Meetings VIII, IX, X, XI – BNL-71117-2003
Volume 43 – RIKEN Winter School – Quark-Gluon Structure of the Nucleon and QCD – BNL-52672
Volume 42 – Baryon Dynamics at RHIC – BNL-52669
Volume 41 – Hadron Structure from Lattice QCD – BNL-52674
Volume 40 – Theory Studies for RHIC-Spin – BNL-52662

Back to Contents

Volume 39 – RHIC Spin Collaboration Meeting VII – BNL-52659
Volume 38 – RBRC Scientific Review Committee Meeting, November 29-30, 2001 – BNL-52649
Volume 37 – RHIC Spin Collaboration Meeting VI (Part 2) – BNL-52660
Volume 36 – RHIC Spin Collaboration Meeting VI – BNL-52642
Volume 35 – RIKEN Winter School – Quarks, Hadrons and Nuclei – QCD Hard Processes and the Nucleon Spin – BNL-52643
Volume 34 – High Energy QCD: Beyond the Pomeron – BNL-52641
Volume 33 – Spin Physics at RHIC in Year-1 and Beyond – BNL-52635
Volume 32 – RHIC Spin Physics V – BNL-52628
Volume 31 – RHIC Spin Physics III & IV Polarized Partons at High Q^2 Region – BNL-52617
Volume 30 – RBRC Scientific Review Committee Meeting, September 28-29, 2000 – BNL-52603
Volume 29 – Future Transversity Measurements – BNL-52612
Volume 28 – Equilibrium & Non-Equilibrium Aspects of Hot, Dense QCD – BNL-52613
Volume 27 – Predictions and Uncertainties for RHIC Spin Physics & Event Generator for RHIC Spin Physics III – Towards Precision Spin Physics at RHIC – BNL-52596
Volume 26 – Circum-Pan-Pacific RIKEN Symposium on High Energy Spin Physics – BNL-52588
Volume 25 – RHIC Spin – BNL-52581
Volume 24 – Physics Society of Japan Biannual Meeting Symposium on QCD Physics at RIKEN BNL Research Center – BNL-52578
Volume 23 – Coulomb and Pion-Asymmetry Polarimetry and Hadronic Spin Dependence at RHIC Energies – BNL-52589
Volume 22 – OSCAR II: Predictions for RHIC – BNL-52591
Volume 21 – RBRC Scientific Review Committee Meeting, May 27-28, 1999 – BNL-52568
Volume 20 – Gauge-Invariant Variables in Gauge Theories – BNL-52590
Volume 19 – Numerical Algorithms at Non-Zero Chemical Potential – BNL-52573
Volume 18 – Event Generator for RHIC Spin Physics – BNL-52571
Volume 17 – Hard Parton Physics in High-Energy Nuclear Collisions – BNL-52574
Volume 16 – RIKEN Winter School - Structure of Hadrons - Introduction to QCD Hard Processes – BNL-52569
Volume 15 – QCD Phase Transitions – BNL-52561
Volume 14 – Quantum Fields In and Out of Equilibrium – BNL-52560
Volume 13 – Physics of the 1 Teraflop RIKEN-BNL-Columbia QCD Project First Anniversary Celebration – BNL-66299
Volume 12 – Quarkonium Production in Relativistic Nuclear Collisions – BNL-52559
Volume 11 – Event Generator for RHIC Spin Physics – BNL-66116
Volume 10 – Physics of Polarimetry at RHIC – BNL-65926
Volume 9 – High Density Matter in AGS, SPS and RHIC Collisions – BNL-65762
Volume 8 – Fermion Frontiers in Vector Lattice Gauge Theories – BNL-65634
Volume 7 – RHIC Spin Physics – BNL-65615
Volume 6 – Quarks and Gluons in the Nucleon – BNL-65234
Volume 5 – Color Superconductivity, Instantons and Parity (Non?)-Conservation at High Baryon Density – BNL-65105
Volume 4 – Inauguration Ceremony and Non-Equilibrium Many Body Dynamics – BNL-64912
Volume 3 – Hadron Spin-Flip at RHIC Energies – BNL-64724
Volume 2 – Perturbative QCD as a Probe of Hadron Structure – BNL-64723
Volume 1 – Open Standards for Cascade Models for RHIC – BNL-64722

Back to Contents

Li Keran

Nuclei as heavy as bulls
Through collision
Generate new states of matter.
T.D. Lee

©CCASTA

Organizers
Stefan Meinel (U of AZ / RBRC)
Taku Izubuchi (BNL / RBRC)

RIKEN BNL Research Center
Bldg. 510A, Brookhaven National Laboratory
Upton, NY 11973-5000, USA

February 2015